

**STATE OF NEW MEXICO
SECRETARY OF THE DEPARTMENT OF ENVIRONMENT**

**IN THE MATTER OF THE
APPLICATION OF THE
SANDOVAL COUNTY PUBLIC
WORKS DEPARTMENT FOR A
SOLID WASTE FACILITY PERMIT
FOR THE SANDOVAL COUNTY
LANDFILL**

**APPLICATION FOR PERMIT RENEWAL AND MODIFICATION
SANDOVAL COUNTY LANDFILL**

APRIL 2015 (UPDATED FEBRUARY 2016)

**VOLUME III:
LANDFILL ENGINEERING CALCULATIONS**

Prepared For:

**Sandoval County Public Works Department
2708 Iris N.E.
Rio Rancho, NM 87144
505.867.0814**

Submitted To:

**New Mexico Environment Department
Solid Waste Bureau - Permit Section
P.O. Box 5469
Santa Fe, NM 87502-5469**

Prepared By:

**Gordon Environmental Inc.
213 S. Camino del Pueblo
Bernalillo, NM 87004
505.867.6990**

**APPLICATION FOR PERMIT RENEWAL AND MODIFICATION
SANDOVAL COUNTY LANDFILL**

APRIL 2015 (UPDATED FEBRUARY 2016)

TABLE OF CONTENTS

CERTIFICATION OF SERVICE	i
CERTIFICATION OF APPLICATION	ii
TABLE OF CONTENTS	iii

Section	Title
VOLUME I	PERMIT APPLICATION TEXT
1	Introduction and Project Description
2	Solid Waste Management General Requirements
3	Solid Waste Facility Permits and Registrations
4	Solid Waste and Registered Facility Maximum Size, Siting Criteria, and Design Criteria
5	Solid Waste Facility and Registered Facility Operating Requirements
6	Solid Waste Facility and Composting Facility Closure and Post-Closure Requirements
7	Solid Waste Facility and Registered Facility Operator Certification
8	Special Waste Requirements
9	Solid Waste Facility Ground Water Monitoring System Plan and Ground Water Monitoring Plan; Corrective Action
10	Financial Assurance
VOLUME II	LANDFILL MANAGEMENT PLANS
1	Permit Plans
2	Plan of Operations
3	Contingency Plan
4	Construction Quality Assurance (CQA) Plan
5	Closure/Post-Closure Plan
6	Landfill Gas Management Plan
7	Leachate Management Plan

**APPLICATION FOR PERMIT RENEWAL AND MODIFICATION
SANDOVAL COUNTY LANDFILL**

APRIL 2015 (UPDATED FEBRUARY 2016)

8	Special Waste Disposal Management Plans
9	Transportation Plan
10	Waste Screening and Inspection Plan
11	Composting Plan of Operations

VOLUME III LANDFILL ENGINEERING CALCULATIONS

1	Volumetrics
2	Settlement Calculations
3	Slope Stability Analysis
4	Compatibility Documentation
5	Pipe Loading Calculations
6	Erosion Calculations
7	Geosynthetic Tensile Stress and Stability Analysis
8	Drainage Calculations
9	Geotextile Filter Fabric Analysis
10	HELP Model

VOLUME IV SITING AND LAND USE

1	Siting Criteria
2	Land Use

VOLUME V HYDROGEOLOGY AND GROUNDWATER

1	Hydrogeology
2	Groundwater Monitoring Plan

VOLUME VI SUPPORTING DOCUMENTATION

1	Financial Assurance
2	Public Notification
3	Disclosure

**APPLICATION FOR PERMIT RENEWAL AND MODIFICATION
SANDOVAL COUNTY LANDFILL**

APRIL 2015 (UPDATED FEBRUARY 2016)

LIST OF PERMIT PLANS

Sheet No.	Title
1	Cover Sheet and Drawing Index
2	Site Plan - Existing Site Conditions
3	Site Development Plan
4	Site Development Plan - Unit IV
5	Base Grading Plan – Unit IV
6	Liner Details
7	Liner & Leachate Collection System Details
8	Leachate Collection System Plan
9	Leachate Collection System Details
10	Final Grading Plan
11	Final Drainage Plan
12	Drainage Details
13	Cross-Sections

**APPLICATION FOR PERMIT RENEWAL AND MODIFICATION
SANDOVAL COUNTY LANDFILL**

**VOLUME III: LANDFILL ENGINEERING CALCULATIONS
SECTION 1: VOLUMETRIC CALCULATIONS**

TABLE OF CONTENTS

1.0	INTRODUCTION	III.1-1
2.0	LANDFILL VOLUMETRIC CALCULATIONS	III.1-1

LIST OF TABLES

Table No.	Title	Page
III.1.1	CAPACITY ANALYSIS	III.1-3
III.1.2	SOIL REQUIREMENTS	III.1-4

APPLICATION FOR PERMIT RENEWAL AND MODIFICATION SANDOVAL COUNTY LANDFILL

VOLUME III: LANDFILL ENGINEERING CALCULATIONS SECTION 1: VOLUMETRIC CALCULATIONS

1.0 INTRODUCTION

The Sandoval County Landfill (SCLF) is an existing solid waste facility operating in compliance with its current Permits, SWM-050304 and SWM-050304 (SP), and the New Mexico Environment Department (NMED) Solid Waste Rules (20.9.2-2.9.10 NMAC). SCLF is located at 2708 Iris Road NE in Rio Rancho, New Mexico (NM), and occupies 178.3 acres \pm . SCLF is publicly owned and operated by the County of Sandoval (“the County”), and is currently permitted to accept municipal solid waste (MSW), including construction and demolition debris (C&D) and tires, and two special wastes: petroleum contaminated soils (PCS) and sludge.

2.0 LANDFILL VOLUMETRIC CALCULATIONS

Landfill volumetric calculations were completed for SCLF corresponding to the design shown on the **Permit Plans (Volume II.1)**. Landfill volumetric calculations included waste capacity analysis, and the soil material balance.

As shown in **Table III.1.1** (Capacity Analysis), the approximate in-place waste and soil fill was estimated for Units I, II, and III, based on the most recent aerial photography for the site (January 2014); and the total estimated in-place waste is 8,430,000 cubic yards (cy). The remaining gross airspace for Units III and IV is 11,643,000 cy \pm ; and the remaining waste capacity for these Units is 8,376,517 cy \pm (i.e., 4,607,084 tons \pm @ 1,100 lbs/cy). SCLF has a projected longevity of approximately 44 years at waste receipts of 350 tons per day (tpd), and 34 years at waste receipts of 450 tpd. Currently, based on waste receipts for 2014, SCLF averages 412 tpd.

As shown in **Table III.1.2** (Soil Requirements), the soil requirements were estimated for the landfill to identify the necessary soils/waste ratio and is presented in **Table III.1.2** (i.e., Total Cover). On-site stockpiles consist of approximately 750,000 cy, which is sufficient to complete closure of Units I and II. SCLF plans to import additional suitable soils from County Public Works Projects to supplement on-site resources as necessary. The vegetation layer for the landfill cap

will be comprised of select on-site and imported materials that have been stockpiled from topsoil stripped from the surface of new areas being developed, and may be enhanced with compost and/or wood chips. Daily, intermediate, and final cover soils are derived from on-site borrow sources, and existing stockpiles, as all cell excavations are complete. SCLF is currently using a tarping system as a very effective means of reducing the lost capacity associated with soil as daily cover, and plans to implement additional alternative daily cover technologies as well (see **Volume II.2**).

**APPLICATION FOR PERMIT RENEWAL AND MODIFICATION
SANDOVAL COUNTY LANDFILL**

**VOLUME III: LANDFILL ENGINEERING CALCULATIONS
SECTION 1: VOLUMETRICS**

**TABLE III.1.1
Capacity Analysis**

Description	Fill Area (acres) ±	Approximate In-Place Waste and Soil Fill (yd ³) ¹	Remaining Gross Airspace (yd ³)	Total Cover (yd ³) ²	Remaining Waste Capacity Airspace (yd ³) ^{3,4}	Remaining Waste Capacity Airspace (tons) ⁵	Remaining Longevity Estimate (years) ^{6,7}	
							@ 350 tons/day	@ 450 tons/day
Landfill								
Unit I	29.4	3,500,000	0	87,604	0	0	0	0
Unit II	19.5	2,000,000	0	64,372	0	0	0	0
Unit III	63.6	2,930,000	5,091,000	992,388	4,098,612	2,254,237	21	17
Unit IV	10.0	0	6,552,000	1,849,095	4,277,905	2,352,848	22	17
Landfill Total	122.5	8,430,000	11,643,000	2,993,459	8,376,517	4,607,084	44	34

Notes:

1. Approximate in-place waste and soil reported for Units I, II, and III as of the January 2014 aerial topography. Volumes for Units I and II are geometric estimates.
2. Includes protective soil cover, daily cover, intermediate cover, and final cover and approximately 425,000 cy structural fill to attain Unit IV base grades. For Units I and II, only final cover is considered over the sideslope areas. Total cover volumes are summarized in **Table III.1.2**.
3. Total Waste Capacity for Unit III = Remaining Gross Airspace - Total Cover; Total Waste Capacity for Unit IV = Remaining Gross Airspace - (Total Cover - 425,000 cy of Structural Fill).
4. Total Waste Capacity for Unit IV = Remaining Gross Airspace - Total Cover - 425,000 cy of Structural Fill.
5. Waste density assumed to be 1,100 lbs/cy.
6. 350 tons/day = 105,700 tons/yr based on 302 operating days/year.
7. 450 tons/day = 135,900 tons/yr based on 302 operating days/year.

**APPLICATION FOR PERMIT RENEWAL AND MODIFICATION
SANDOVAL COUNTY LANDFILL**

**VOLUME III: LANDFILL ENGINEERING CALCULATIONS
SECTION 1: VOLUMETRICS**

**TABLE III.1.2
Soil Requirements**

Description	Area (acres) ±	Soil Required (yd³)					Total Soil Required (yd³)
		Structural Fill	Protective Cover¹	Daily Cover²	Intermediate Cover³	Final Cover⁴	
Landfill							
Unit I	18.1	0	0	0	0	87,604	87,604
Unit II	13.3	0	0	0	0	64,372	64,372
Unit III	60.4	0	101,317	723,284	41,947	125,840	992,388
Unit IV	30.7	425,000	99,059	904,924	105,028	315,084	1,849,095
Landfill Total	122.5	425,000	200,376	1,628,209	146,975	592,900	2,993,459

Notes:

- Protective Soil Layer volume assumes 2.0 foot soil depth over lined areas in Unit III; Cells 4C, 5B, 6B and 7 (31.4 acres±) and Unit IV (30.7 acres±).
- Daily cover assumes soil usage @ 15% of effective airspace in Unit III (intermediate grades) and Unit IV.
- Intermediate cover assumes 1-foot soil depth over entire fill area; Unit III = 26 acres± and Unit IV = 65.1 acres±. Units I and II have sufficient intermediate cover placed.
- Final cover assumes 3-foot depth over entire fill areas:
Unit I = 18.1 acres±
Unit II = 13.3 acres±
Unit III = 26.0 acres±
Unit IV = 65.1 acres±
- Approximately 750,000 cy of on-site soils available in existing stockpiles.
- Tarping and other ADC initiatives are underway to reduce proportion of daily cover soils.

**APPLICATION FOR PERMIT RENEWAL AND MODIFICATION
SANDOVAL COUNTY LANDFILL**

**VOLUME III: ENGINEERING DESIGN AND CALCULATIONS
SECTION 2: SETTLEMENT CALCULATIONS**

TABLE OF CONTENTS

1.0	INTRODUCTION	III.2-1
2.0	DESIGN CRITERIA	III.2-1
3.0	FOUNDATION SOILS SETTLEMENT	III.2-1
4.0	WASTE SETTLEMENT CALCULATIONS	III.2-8
5.0	SOIL COVER SETTLEMENT CALCULATIONS.....	III.2-13
6.0	CONCLUSION.....	III.2-21

LIST OF FIGURES

Figure No.	Title	Page
III.2.1	SETTLEMENT POINTS.....	III.2-3

LIST OF TABLES

Table No.	Title	Page
III.2.1	SETTLEMENT AND ANGULAR DISTORTION OF FOUNDATION SOILS BETWEEN POINTS, CROSS SECTION A-A'	III.2-5
III.2.2	SETTLEMENT AND ANGULAR DISTORTION OF FOUNDATION SOILS BETWEEN POINTS, CROSS SECTION B-B'	III.2-6
III.2.3	SETTLEMENT AND ANGULAR DISTORTION OF FOUNDATION SOILS BETWEEN POINTS, CROSS SECTION C-C'	III.2-7
III.2.4	WASTE SETTLEMENT AND ANGULAR DISTORTION BETWEEN POINTS, CROSS SECTION A-A'	III.2-10
III.2.5	WASTE SETTLEMENT AND ANGULAR DISTORTION BETWEEN POINTS, CROSS SECTION B-B'	III.2-11
III.2.6	WASTE SETTLEMENT AND ANGULAR DISTORTION BETWEEN POINTS, CROSS SECTION C-C'	III.2-12
III.2.7	SETTLEMENT AND ANGULAR DISTORTION OF SOILS BETWEEN POINTS, CROSS SECTION A-A'	III.2-15
III.2.8	SETTLEMENT AND ANGULAR DISTORTION OF SOILS BETWEEN POINTS, CROSS SECTION B-B'	III.2-16
III.2.9	SETTLEMENT AND ANGULAR DISTORTION OF SOILS	

**APPLICATION FOR PERMIT RENEWAL AND MODIFICATION
SANDOVAL COUNTY LANDFILL**

**VOLUME III: ENGINEERING DESIGN AND CALCULATIONS
SECTION 2: SETTLEMENT CALCULATIONS**

	BETWEEN POINTS, CROSS SECTION C-C'	III.2-17
III.2.10	TOTAL SETTLEMENT AND ANGULAR DISTORTION BETWEEN POINTS, CROSS SECTION A-A'	III.2-18
III.2.11	TOTAL SETTLEMENT AND ANGULAR DISTORTION BETWEEN POINTS, CROSS SECTION B-B'	III.2-19
III.2.12	TOTAL SETTLEMENT AND ANGULAR DISTORTION BETWEEN POINTS, CROSS SECTION C-C'	III.2-20

LIST OF ATTACHMENTS

Attachment No.	Title
III.2.A	SUMMARY OF GEOTECHNICAL LABORATORY TESTING RESULTS
III.2.B	QIAN, XUEDE; KOERNER, ROBERT M.; AND GRAY, DONALD H. 2002. <i>GEOTECHNICAL ASPECTS OF LANDFILL DESIGN AND CONSTRUCTION</i> . NEW YORK: PRENTICE HALL.
III.2.C	CODUTO, DONALD P. 1998. <i>GEOTECHNICAL ENGINEERING PRINCIPLES AND PRACTICES</i> . NEW JERSEY: PRENTICE HILL.
III.2.D	SHARMA, HARI .D. AND SANGEETA P. LEWIS. 1994. <i>WASTE CONTAINMENT SYSTEMS, WASTE STABILIZATION AND LANDFILLS: DESIGN AND EVALUATION</i> . NEW YORK: JOHN WILEY AND SONS.
III.2.E	STEPHENS, DANIEL B.; HSU, KUO-CHIN; PRIEKSAT, MARK A.; ANKENY, MARK D.; BLANDFORD, NEIL; ROTH, TRACY L.; KELSEY, JAMES A.; WHITWORTH, JULIA R. 1997. A COMPARISON OF ESTIMATED AND CALCULATED EFFECTIVE POROSITY. <i>HYDROGEOLOGY JOURNAL</i> (1998) 6:156–165.
III.2.F	CARTER, M. AND BENTLEY, S.P. 1991. <i>CORRELATIONS OF SOIL PROPERTIES</i> LONDON: PENTECH PRESS

APPLICATION FOR PERMIT RENEWAL AND MODIFICATION SANDOVAL COUNTY LANDFILL

VOLUME III: ENGINEERING DESIGN AND CALCULATIONS SECTION 2: SETTLEMENT CALCULATIONS

1.0 INTRODUCTION

The Sandoval County Landfill (SCLF) is an existing solid waste facility operating in compliance with its current Permits, SWM-050304 and SWM-050304 (SP), and the New Mexico Environment Department (NMED) Solid Waste Rules (20.9.2-2.9.10 NMAC). SCLF is located at 2708 Iris Road NE in Rio Rancho, New Mexico (NM), and occupies 178.3 acres \pm . SCLF is publicly owned and operated by the County of Sandoval (“the County”), and is currently permitted to accept municipal solid waste (MSW), including construction and demolition debris (C&D) and tires, and two special wastes: petroleum contaminated soils (PCS) and sludge.

2.0 DESIGN CRITERIA

The slope of the final cover, liner, and leachate collection piping after settlement must be consistent with the performance specifications for leachate collection and stormwater control. That is, the final cover and leachate collection system must allow adequate stormwater to runoff to the management controls, and to convey generated leachate such that the head on the high density polyethylene (HDPE) flexible membrane liner (FML) does not exceed 12 inches.

3.0 FOUNDATION SOILS SETTLEMENT

The methodology for estimating floor potential settlement involves selecting key points on the surface of the landfill floor, computing the settlement at each point, and evaluating the resultant change in surface elevation. Points were conservatively selected from a cross-section where the waste and fill material is thickest. Qian et al. (2002), present a method to determine landfill foundation settlement that evaluates elastic, primary, and secondary settlement. Geotechnical analyses of on-site soils indicate that the soils available at the SCLF site consist primarily of a mixture of sand with varying amounts of silt (SP-SM, sand with varying amounts of silt). **Attachment III.2.A** provides a summary of the laboratory testing results compiled from samples collected at the SWRL site during construction of Cells 4C, 5B, 6A and 7. Since the foundation soils consist of sands with varying amounts of silt, elastic settlement is conservatively assumed for this calculation. The elastic settlement is estimated using the equation:

$$Z_e = \left(\frac{\Delta\sigma}{M_s} \right) H_o$$

Equation 12.20, Attachment III.2.B, p. 469

Where:

- Z_e = elastic settlement of soil layer (ft)
- H_o = initial thickness of soil layer (ft)
- $\Delta\sigma$ = increment of vertical effective stress, lb/ft²
- M_s = constrained modulus of soil, lb/ft²

The constrained modulus is provided in equation:

$$M_s = \frac{E_s(1 - \nu_s)}{(1 + \nu_s)(1 - 2\nu_s)}$$

Equation 12.21, Attachment III.2.B, p. 470

Where:

- M_s = constrained modulus of soil, lb/ft²
- E_s = elastic modulus of soil (lb/ft²) **Attachment III.2.B, p. 310**
 E_s was interpolated from the data from Table 9.5, p. 310 (**Attachment III.2.B**) for GM, SM, ML, and GC, SC with < 20% fines soils between 85% and 95% standard Proctor dry density to determine E_s for 90% as specified in the subgrade soils. $E_s = (1,000 \text{ psi} + 4,100 \text{ psi})/2 = 2,550 \text{ psi} \times 144 \text{ in}^2/\text{ft}^2 = 367,200 \text{ lb/ft}^2$
- ν_s = Poisson's ratio for soil = 0.38, which was found using the same method to estimate the elastic modulus of soil

Settlement is estimated at the select locations (Points A1 through A19, Points B1 through B21 and Points C1 through C20) shown on the landfill cross-sections (**Figure III.2.1**). An example calculation is demonstrated at point A9 on Cross Section A-A', with a total overburden depth of 179.88 ft. (final cover + intermediate cover + waste + protective soil layer).

Point A9

Elastic Foundation Soil Settlement

Thickness of Waste = 173.88 ft. (assume entire thickness of waste from intermediate cover to top of protective soil layer; providing a conservative analysis)

Unit Weight of Soil = 115 lb/ft³ Dry Density

Unit Weight of Waste = 65 lb/ft³

$\Delta\sigma$ = (waste effective stress) + (protective soil layer effective stress) + (intermediate cover effective stress) + (final cover effective stress)

$$\Delta\sigma = (173.88 \text{ ft})(65 \text{ lb/ft}^3) + (2 \text{ ft})(115 \text{ lb/ft}^3) + (1 \text{ ft})(115 \text{ lb/ft}^3) + (3 \text{ ft})(115 \text{ lb/ft}^3) = 11,918.75 \text{ lb/ft}^2$$

$$M_s = \frac{367,200 \text{ lb} / \text{ft}^2 (1 - 0.38)}{(1 + 0.38)(1 - 2 * 0.38)} = 687,391.30 \text{ lb} / \text{ft}^2$$

H_o = 173.88 ft. the full thickness of the compressible GM, SM, ML, and GC, SC with < 20% fines soils; the compressible soil is considered incompressible at the depth of 50 ft.

$$Z_e = \left(\frac{11,992.20}{687,391.30} \right) 50 \text{ ft} = 0.872 \text{ ft}$$

Settlement between points A9 and A8 = 0.87 ft – 0.86 ft = 0.01 ft

Change in slope of base grade:

Updated elevation of base grade at point A8 = Approximately 5,381.82 ft.

Updated elevation of base grade at point A9 = 5,377.49 ft. – 0.87 ft. = 5,376.62 ft.

$$\text{Updated base grade slope} = \frac{(5,382.82 \text{ ft} - 5,376.62 \text{ ft})}{100 \text{ ft}} \times 100 = 3.95\%$$

Change in base grade slope = 3.96% - 3.95% = 0.01%

The angular distortion between points A9 and A8 is determined as follows:

$$\text{Distortion} = \frac{(\text{Settlement}_{A13} - \text{Settlement}_{A14})}{\text{distance}} * 100$$

$$\text{Distortion} = \frac{(0.87 \text{ ft} - 0.86 \text{ ft})}{100 \text{ ft}} * 100 = -0.01\%$$

A summary of potential foundation soils settlement is provided in **Tables III.2.1, III.2.2 and III.2.3** for cross sections A-A', B-B' and C-C', respectively. The angular distortion between each point is calculated as above. The maximum angular distortion of the foundation soils on the floor of Units III and IV (i.e., settlement points A2 to A19, B3 to B20 and C3 to C19) is - 0.078% between points B9 and B10 on Cross-Section B-B'; and - 0.027% between points C8 and C9. The minimum slope on the landfill floor; perpendicular to the leachate collection pipe, is approximately 1.51% in Unit III and 3.36% in Unit IV; following settlement. Additionally, the minimum slope of the leachate collection pipe is 3.86% to the leachate collection sump in Unit IV (Section A-A'). These slopes are adequate, and ensure that the design and performance standards for the leachate collection system are met.

TABLE III.2.1
Settlement and Angular Distortion of Foundation Soils Between Points
Cross Section A-A'
Sandoval County Landfill

Point Location	Total Depth	$\Delta\sigma$	Total Settlement (feet)	Distance Between Points (feet)	Angular Distortion (%)	Distortion Direction	Design Base Grade Elevation (feet)	Design Slope Between Point Locations (%)	Updated Base Grade Elevation (feet)	Updated Slope Between Point Locations (%)
A1	28.78	2,170.70	0.16	100	-0.152	▲	5,413.02	6.31	5,412.86	6.46
A2	60.84	4,254.60	0.31	100	-0.134	▲	5,406.71	4.01	5,406.40	4.14
A3	89.08	6,090.20	0.44	100	-0.143	▲	5,402.70	3.99	5,402.26	4.13
A4	119.29	8,053.85	0.59	100	-0.130	▲	5,398.71	3.93	5,398.12	4.06
A5	146.74	9,838.10	0.72	100	-0.075	▲	5,394.78	4.10	5,394.06	4.17
A6	162.60	10,869.00	0.79	100	-0.036	▲	5,390.68	3.98	5,389.89	4.02
A7	170.28	11,368.20	0.83	100	-0.037	▲	5,386.70	4.02	5,385.87	4.06
A8	178.04	11,872.60	0.86	100	-0.009	▲	5,382.68	5.19	5,381.82	5.20
A9	179.88	11,992.20	0.87	100	0.005	▼	5,377.49	3.96	5,376.62	3.95
A10	178.75	11,918.75	0.87	100	0.058	▼	5,373.53	4.04	5,372.66	3.98
A11	166.51	11,123.15	0.81	100	0.092	▼	5,369.49	4.05	5,368.68	3.96
A12	147.00	9,855.00	0.72	100	0.098	▼	5,365.44	3.96	5,364.72	3.86
A13	126.22	8,504.30	0.62	100	0.093	▼	5,361.48	4.03	5,360.86	3.94
A14	106.55	7,225.75	0.53	100	0.051	▼	5,357.45	3.96	5,356.92	3.91
A15	95.81	6,527.65	0.47	100	0.083	▼	5,353.49	4.04	5,353.02	3.96
A16	78.17	5,381.05	0.39	100	0.080	▼	5,349.45	5.85	5,349.06	5.77
A17	61.18	4,276.70	0.31	100	0.073	▼	5,343.60	5.85	5,343.29	5.78
A18	45.79	3,276.35	0.24	100	0.102	▼	5,337.75	-7.49	5,337.51	7.59
A19	24.15	1,869.75	0.14				5,345.24		5,345.10	

Notes:

Points Correspond to **Figure III.2.1**

Elevations based on NM State Plan Coordinate System

Variables and values used in equations listed in the test:

Es 367200
vs 0.38
Ho 50
Ms 687391.3

TABLE III.2.2
Settlement and Angular Distortion of Foundation Soils Between Points
Cross Section B-B'
Sandoval County Landfill

Point Location	Total Depth	$\Delta\sigma$	Total Settlement (feet)	Distance Between Points (feet)	Angular Distortion (%)	Distortion Direction	Design Base Grade Elevation (feet)	Design Slope Between Point Locations (%)	Updated Base Grade Elevation (feet)	Updated Slope Between Point Locations (%)
B1	128.05	8,623.25	0.63	100	-0.143	▲	5,286.00	0.00	5,285.37	0.14
B2	148.76	10,595.40	0.77	100	-0.117	▲	5,286.00	0.00	5,285.23	0.12
B3	173.05	12,203.25	0.89	100	-0.094	▲	5,286.00	0.00	5,285.11	0.09
B4	196.20	13,495.00	0.98	100	0.127	▼	5,286.00	31.89	5,285.02	32.02
B5	169.81	11,751.65	0.85	100	0.229	▼	5,317.89	38.33	5,317.04	38.56
B6	122.74	8,608.60	0.63	100	0.131	▼	5,356.22	5.83	5,355.59	5.96
B7	100.13	6,808.45	0.50	100	-0.024	▲	5,362.05	7.67	5,361.55	7.69
B8	102.75	7,140.75	0.52	100	-0.033	▲	5,354.38	3.89	5,353.86	3.92
B9	110.05	7,596.25	0.55	100	-0.078	▲	5,350.49	11.34	5,349.94	11.42
B10	128.83	8,673.95	0.63	100	-0.039	▲	5,339.15	1.47	5,338.52	1.51
B11	137.17	9,216.05	0.67	100	-0.031	▲	5,337.68	0.26	5,337.01	0.23
B12	143.76	9,644.40	0.70	100	-0.019	▲	5,337.94	2.32	5,337.24	2.30
B13	147.77	9,905.05	0.72	100	-0.015	▲	5,340.26	0.90	5,339.54	0.92
B14	150.97	10,113.05	0.74	100	-0.015	▲	5,339.36	3.34	5,338.62	3.35
B15	154.10	10,316.50	0.75	100	0.033	▼	5,336.02	4.51	5,335.27	4.54
B16	147.16	9,865.40	0.72	100	0.068	▼	5,340.53	4.57	5,339.81	4.64
B17	132.83	8,933.95	0.65	100	0.083	▼	5,345.10	0.87	5,344.45	0.79
B18	115.29	7,793.85	0.57	100	0.093	▼	5,344.23	1.89	5,343.66	1.80
B19	95.66	6,517.90	0.47	100	0.127	▼	5,342.34	1.89	5,341.87	2.02
B20	68.82	4,773.30	0.35	100	0.174	▼	5,344.23	11.77	5,343.88	11.94
B21	32.01	2,380.65	0.17				5,356.00		5,355.83	

Notes:

Points Correspond to **Figure III.2.1**

Elevations based on NM State Plan Coordinate System

Variables and values used in equations listed in the test:

E_s 367200
 ν_s 0.38
 H_o 50
 M_s 687391.3

TABLE III.2.3
Settlement and Angular Distortion of Foundation Soils Between Points
Cross Section C-C'
Sandoval County Landfill

Point Location	Total Depth	$\Delta\sigma$	Total Settlement (feet)	Distance Between Points (feet)	Angular Distortion (%)	Distortion Direction	Design Base Grade Elevation (feet)	Design Slope Between Point Locations (%)	Updated Base Grade Elevation (feet)	Updated Slope Between Point Locations (%)
C1	155.850	10,430.25	2.36	100	1.461	▼	5,286.00	0.00	5,283.64	1.46
C2	179.050	12,431.25	0.90	100	-0.111	▲	5,286.00	0.00	5,285.10	0.11
C3	204.110	13,960.15	1.02	100	-0.050	▲	5,286.00	10.24	5,284.98	10.19
C4	216.980	14,650.20	1.07	100	0.093	▼	5,296.24	33.33	5,295.17	33.42
C5	200.200	13,370.00	0.97	100	0.006	▼	5,329.57	33.34	5,328.60	33.35
C6	188.330	13,284.95	0.97	100	0.170	▼	5,362.91	33.33	5,361.94	33.50
C7	159.640	10,954.10	0.80	100	-0.059	▲	5,396.24	11.67	5,395.44	11.73
C8	174.590	11,763.85	0.86	100	-0.027	▼	5,384.57	3.33	5,383.71	3.36
C9	181.210	12,132.15	0.88	100	-2.524	▲	5,381.24	5.56	5,380.36	8.08
C10	186.320	12,567.80	3.41	100	-0.801	▲	5,375.68	25.00	5,372.27	25.80
C11	208.640	13,861.60	4.21	100	0.037	▼	5,350.68	3.07	5,346.47	3.03
C12	207.720	13,801.80	4.17	100	0.155	▼	5,347.61	0.22	5,343.44	0.06
C13	203.770	13,545.05	4.02	100	0.459	▼	5,347.39	2.00	5,343.37	2.46
C14	191.630	12,755.95	3.56	100	0.844	▼	5,349.39	2.00	5,345.83	2.84
C15	167.070	11,159.55	2.71	100	0.755	▼	5,351.39	1.91	5,348.68	2.66
C16	141.600	9,504.00	1.96	100	0.596	▼	5,353.30	0.43	5,351.34	0.17
C17	117.720	7,951.80	1.36	100	0.509	▼	5,352.87	2.46	5,351.51	2.97
C18	92.670	6,323.55	0.85	100	0.716	▼	5,355.33	3.13	5,354.48	3.85
C19	35.800	2,627.00	0.14	100	0.045	▼	5,358.46	15.08	5,358.32	15.13
C20	28.860	2,175.90	0.09				5,373.54		5,373.45	

Notes:

Points Correspond to **Figure III.2.1**

Elevations based on NM State Plan Coordinate System

Variables and values used in equations listed in the test:

Es 367200
vs 0.38
Ho 50
Ms 687391.3

4.0 WASTE SETTLEMENT CALCULATIONS

The methodology to estimate waste settlement involves selecting key points on the final cover surface, computing the settlement at each point, and evaluating the resultant change in surface elevation. Points were selected from Cross-Sections A-A', B-B' and C-C' (**Figure III.2.1**). Qian et al. (2002; **Attachment III.2.B**) refine a method developed by Sowers (1973) for determining settlement in landfills. This method is based on developed soils consolidation theory, which relates settlement to layer thickness and changes in void ratio.

The primary settlement is estimated using equation:

$$\Delta H_c = C_c \frac{H_0}{1 + e_0} \log \frac{\sigma_i}{\sigma_o} \quad \text{Equation 12.4, Attachment III.2.B, p. 449}$$

Where:

- ΔH_c = Primary settlement
- C_c = Primary compression index = 0.05 (**Attachment III.2.B, Figure 6.10, p. 202**)
- H_0 = Initial thickness of the waste layer before settlement (assume entire thickness of waste from intermediate cover to the top of protective soil layer; this provides a conservative analysis) [**Figure III.2.1**] = 90.34 *ft*
- e_o = Waste void ratio before settlement = 2.03 (**Attachment III.2.B, p. 188**)
- σ_o = Previously applied pressure in waste layer (assumed to equal the compaction pressure = 1,000 *lbs/ft²*)
- σ_i = Total overburden pressure applied at the mid-level of the waste layer (*lbs/ft²*)

Long-term secondary settlement is estimated by equation:

$$\Delta H_s = C_\alpha \frac{H_0}{1 + e_0} \log \frac{t_2}{t_1} \quad \text{Equation 12.7, Attachment III.2.B, p.450}$$

Where:

- ΔH_s = Secondary settlement
- C_α = Secondary compression index (Arid Climate, Conditions are Unfavorable for decomposition) = 0.03(e_o) if $e_o = 2.03$ then $(0.03)(2.03) = 0.0609$ (**Attachment III.2.B, Figure 6.11, p. 203**)
- H_0 = Waste thickness at start of secondary settlement = $H - H_c$ (**Figure III.2.1**)
- e_o = Waste void ratio = 2.03 (**Attachment III.2.B, p. 188**)
- t_1 = Starting time of secondary settlement (1 month = 0.0833 years)
- t_2 = Ending time of secondary settlement = Assume 30 years (conservative as the site must maintain the final cover and landfill for a minimum of 30 years)

Settlement is estimated at the key locations (Points A1 through A19, Points B1 through B21 and Points C1 through C20) shown on the landfill Cross-Sections A-A', B-B' and C-C' (**Figure III.2.1**). An example calculation is demonstrated at point A9 on Cross-Sections A-A'.

Point A9

Primary Waste Settlement

Maximum Thickness of Waste = 173.88 ft.

$$\Delta H_c = C_c \frac{H_0}{1 + e_0} \log \frac{\sigma_i}{\sigma_o}$$

Where:

$$\begin{aligned} C_c &= \text{Primary compression index} = 0.05 \text{ (Attachment III.2.B, Figure 6.10, p. 202)} \\ H_0 &= 173.88 \text{ ft} \\ e_o &= 2.03 \text{ (Attachment III.2.B, p. 188)} \\ \sigma_o &= 1,000 \text{ lbs/ft}^2 \text{ (Typical compaction of waste as found in New Mexico)} \\ \sigma_i &= 0.5[(173.88 \text{ ft})(65 \text{ lbs/ft}^3) + (6 \text{ ft})(115 \text{ lbs/ft}^2)] = 5,996.10 \text{ lbs/ft}^2 \end{aligned}$$

$$\Delta H_c = 0.05 \frac{173.88}{1 + 2.03} \log \frac{5,996.10 \frac{\text{lbs}}{\text{ft}^2}}{1,000 \frac{\text{lbs}}{\text{ft}^2}}$$

$$\Delta H_c = 2.23 \text{ ft}$$

Secondary Waste Settlement

$$H_o = 173.88 \text{ ft} - 2.23 \text{ ft} = 171.65 \text{ ft}$$

$$\Delta H_s = 0.0609 \frac{171.65}{1 + 2.03} \log \frac{30 \text{ years}}{0.0833 \text{ years}}$$

$$\Delta H_s = 8.82 \text{ ft}$$

$$\text{Total waste settlement} = 2.23 \text{ ft.} + 8.82 \text{ ft.} = 11.05 \text{ ft.}$$

The maximum final settlement of waste is the sum of primary and secondary settlement at point A9. The waste settlement is 2.23 ft. + 8.82 ft. = 11.05 ft, which has nominal impact on the corresponding calculations for slope, runoff, etc. A summary of potential waste settlement is provided in **Tables III.2.4, III.2.4** and **III.2.6** for cross sections A-A', B-B' and C-C', respectively.

TABLE III.2.4
Waste Settlement and Angular Distortion Between Points
Cross Section A-A'
Sandoval County Landfill

Point Location	Total Depth (feet)	Waste Depth (feet)	σ_i	Primary Settlement (feet)	New Waste depth (feet)	Secondary Settlement (feet)	Total Settlement (feet)	Distance Between Points (feet)	Angular Distortion (%)	Distortion Direction
A1	28.78	22.78	1,085.35	0.01	22.77	1.17	1.18	100	-1.92	▲
A2	60.84	54.84	2,127.30	0.30	54.54	2.80	3.10	100	-1.80	▲
A3	89.08	83.08	3,045.10	0.66	82.42	4.23	4.90	100	-2.00	▲
A4	119.29	113.29	4,026.93	1.13	112.16	5.76	6.89	100	-1.86	▲
A5	146.74	140.74	4,919.05	1.61	139.13	7.15	8.76	100	-1.09	▲
A6	162.60	156.60	5,434.50	1.90	154.70	7.95	9.85	100	-0.53	▲
A7	170.28	164.28	5,684.10	2.05	162.23	8.34	10.38	100	-0.54	▲
A8	178.04	172.04	5,936.30	2.20	169.84	8.73	10.92	100	-0.13	▲
A9	179.88	173.88	5,996.10	2.23	171.65	8.82	11.05	100	0.08	▼
A10	178.75	172.75	5,959.38	2.21	170.54	8.76	10.97	100	0.85	▼
A11	166.51	160.51	5,561.58	1.97	158.54	8.15	10.12	100	1.35	▼
A12	147.00	141.00	4,927.50	1.61	139.39	7.16	8.77	100	1.41	▼
A13	126.22	120.22	4,252.15	1.25	118.97	6.11	7.36	100	1.32	▼
A14	106.55	100.55	3,612.88	0.93	99.62	5.12	6.04	100	0.71	▼
A15	95.81	89.81	3,263.83	0.76	89.05	4.58	5.34	100	1.14	▼
A16	78.17	72.17	2,690.53	0.51	71.66	3.68	4.19	100	1.07	▼
A17	61.18	55.18	2,138.35	0.30	54.88	2.82	3.12	100	0.94	▼
A18	45.79	39.79	1,638.18	0.14	39.65	2.04	2.18	100	1.25	▼
A19	24.15	18.15	934.88	-0.01	18.16	0.93	0.92			

Notes:

Points Correspond to **Figure III.2.1**

Elevations based on NM State Plan Coordinate System

Variables and values used in equations listed in the text:

C_c 0.05
 e_0 2.03
 σ_o 1030
 C_α 0.0609

TABLE III.2.5
Waste Settlement and Angular Distortion Between Points
Cross Section B-B'
Sandoval County Landfill

Point Location	Total Depth (feet)	Waste Depth (feet)	σ_i	Primary Settlement (feet)	New Waste Depth (feet)	Secondary Settlement (feet)	Total Settlement (feet)	Distance Between Points (feet)	Angular Distortion (%)	Distortion Direction
B1	128.05	122.05	4,311.63	1.28	120.77	6.21	7.48	100	-0.68	▲
B2	148.76	130.24	5,297.70	1.56	128.68	6.61	8.17	100	-1.63	▲
B3	173.05	153.95	6,101.63	2.00	151.95	7.81	9.80	100	-1.87	▲
B4	196.20	181.36	6,747.50	2.48	178.88	9.19	11.67	100	1.81	▼
B5	169.81	155.53	5,875.83	1.97	153.56	7.89	9.86	100	3.11	▼
B6	122.74	110.13	4,304.30	1.15	108.98	5.60	6.75	100	1.13	▼
B7	100.13	94.13	3,404.23	0.83	93.30	4.79	5.62	100	0.01	▲
B8	102.75	93.51	3,570.38	0.85	92.66	4.76	5.61	100	-0.50	▲
B9	110.05	101.19	3,798.13	0.97	100.22	5.15	6.12	100	-1.42	▲
B10	128.83	122.83	4,336.98	1.29	121.54	6.24	7.54	100	-0.57	▲
B11	137.17	131.17	4,608.03	1.44	129.73	6.67	8.10	100	-0.45	▲
B12	143.76	137.76	4,822.20	1.55	136.21	7.00	8.55	100	-0.27	▲
B13	147.77	141.77	4,952.53	1.63	140.14	7.20	8.83	100	-0.22	▲
B14	150.97	144.97	5,056.53	1.68	143.29	7.36	9.05	100	-0.22	▲
B15	154.10	148.10	5,158.25	1.74	146.36	7.52	9.26	100	0.48	▼
B16	147.16	141.16	4,932.70	1.61	139.55	7.17	8.78	100	0.98	▼
B17	132.83	126.83	4,466.98	1.36	125.47	6.45	7.81	100	1.18	▼
B18	115.29	109.29	3,896.93	1.07	108.22	5.56	6.63	100	1.30	▼
B19	95.66	89.66	3,258.95	0.76	88.90	4.57	5.33	100	1.73	▼
B20	68.82	62.82	2,386.65	0.39	62.43	3.21	3.60	100	2.23	▼
B21	32.01	26.01	1,190.33	0.03	25.98	1.33	1.37			

Notes:

Points Correspond to **Figure III.2.1**

Elevations based on NM State Plan Coordinate System

Variables and values used in equations listed in the text:

C_c 0.05
 e_0 2.03
 σ_o 1030
 C_a 0.0609

TABLE III.2.6
Waste Settlement and Angular Distortion Between Points
Cross Section C-C'
Sandoval County Landfill

Point Location	Total Depth (feet)	Waste Depth (feet)	σ_i	Primary Settlement (feet)	New Waste depth (feet)	Secondary Settlement (feet)	Total Settlement (feet)	Distance Between Points (feet)	Angular Distortion (%)	Distortion Direction
C1	155.85	149.85	5,215.13	1.77	148.08	7.61	9.38	100	-1.03	▼
C2	179.05	163.19	6,215.63	2.14	161.05	8.28	10.41	100	-1.88	▼
C3	204.11	190.25	6,980.08	2.65	187.60	9.64	12.29	100	-1.09	▼
C4	216.98	206.05	7,325.10	2.94	203.11	10.44	13.38	100	0.96	▲
C5	200.20	193.06	6,685.00	2.63	190.43	9.78	12.41	100	1.65	▲
C6	188.33	167.46	6,642.48	2.27	165.19	8.49	10.76	100	1.44	▲
C7	159.64	148.09	5,477.05	1.80	146.29	7.52	9.32	100	-1.23	▲
C8	174.59	166.28	5,881.93	2.11	164.17	8.44	10.55	100	-0.54	▲
C9	181.21	174.14	6,066.08	2.25	171.89	8.83	11.08	100	-0.24	▲
C10	186.32	177.18	6,283.90	2.33	174.85	8.98	11.32	100	-1.76	▲
C11	208.64	202.64	6,930.80	2.81	199.83	10.27	13.08	100	0.07	▼
C12	207.72	201.72	6,900.90	2.79	198.93	10.22	13.01	100	0.28	▲
C13	203.77	197.77	6,772.53	2.71	195.06	10.02	12.73	100	0.86	▲
C14	191.63	185.63	6,377.98	2.46	183.17	9.41	11.88	100	1.72	▼
C15	167.07	161.07	5,579.78	1.98	159.09	8.17	10.16	100	1.75	▼
C16	141.60	135.60	4,752.00	1.51	134.09	6.89	8.40	100	1.62	▼
C17	117.72	111.72	3,975.90	1.11	110.61	5.68	6.79	100	1.66	▼
C18	92.67	86.67	3,161.78	0.72	85.95	4.42	5.13	100	3.55	▼
C19	35.80	29.80	1,313.50	0.06	29.74	1.53	1.59	100	0.40	▼
C20	28.86	22.86	1,087.95	0.01	22.85	1.17	1.19			

Notes:

Points Correspond to **Figure III.2.1**

Elevations based on NM State Plan Coordinate System

Variables and values used in equations listed in the text:

C_c 0.05
 e_0 2.03
 σ_o 1030
 C_a 0.0609

5.0 SOIL COVER SETTLEMENT CALCULATIONS

The final cover soil layer consisting of vegetative, barrier, intermediate cover layers; and protective soil layer and structural fill soils will also experience nominal consolidation due to its own weight and overburden, as applicable. An example calculation is demonstrated at point A9 on Cross-Sections A-A'. The method for evaluating settlement of the soil cover and cushion layers is based on equation:

Point A9

Primary Soil Settlement

$$\Delta H_p = C_c \frac{H_p}{1 + e_s} \log \frac{P_o + \Delta P}{P_o} \quad \text{Equation B.2, Attachment III.2.D, p. 569}$$

e_s = Soil void ratio = 0.83 based on a porosity of 0.453 (**Attachment III.2.E, p.161**)

$$e_s = \frac{0.453}{1 - 0.453}$$

Thickness of Soil = H = 3 feet of final cover + 1 foot of intermediate cover soil + 2 feet of protective soil layer = 6.0 ft

Unit Weight of Soil = 115 lb/ft³ Dry Density

$$H_p = 6.0 \text{ ft}$$

$C_c = 0.30 (e_o - 0.27) = 0.16$ (for inorganic, cohesive soil; silt, some clay; silty clay; clay) [**Attachment III.2.F**]

$$\Delta P = (3.0 \text{ ft.}) (115 \text{ lb/ft}^3) + (1 \text{ ft}) (115 \text{ lb/ft}^3) + (2.0 \text{ ft.}) (115 \text{ lb/ft}^3) = 690.0 \text{ lb/ft}^2$$

$$P_o = \frac{H}{2} (115 \text{ lb/ft}^3) = 3.0(115) = 345.0 \text{ lb/ft}^2$$

$$\Delta H_p = (0.16) \left(\frac{6.0 \text{ ft}}{1 + 0.83} \right) \log \left(\frac{345.0 \frac{\text{lbs}}{\text{ft}^2} + 690.0 \frac{\text{lbs}}{\text{ft}^2}}{345.0 \frac{\text{lbs}}{\text{ft}^2}} \right)$$

$$\Delta H_p = 0.25 \text{ ft}$$

Secondary Soil Cover Settlement

$$\Delta H_s = C_s \frac{H_o}{1 + e_s} \log \frac{t_2}{t_1}$$

C_s = Secondary compression index = 5-10% (C_c) [**Attachment III.2.F**]

Assume $C_s = 0.10$ (C_c)

$$C_s = 0.10 (0.16) = 0.016$$

$$H_o = 6.5 \text{ ft.} - 0.25 \text{ ft.} = 5.75 \text{ ft}$$

$$e_s = 0.83$$

$$t_2 = 30 \text{ years}$$

$$t_1 = 0.0833 \text{ years (1 month)}$$

$$\Delta H_s = 0.016 \left(\frac{5.75 \text{ ft}}{1 + 0.83} \right) \log \frac{30 \text{ years}}{0.0833 \text{ years}} = 0.13 \text{ ft}$$

The maximum settlement of the final cover is the sum of primary and secondary settlement at point A14. The soil final cover layer settlement is equal to 0.25 ft. + 0.13 ft. = 0.38 ft. A summary of potential waste settlement is provided in **Tables III.2.7, III.2.8** and **III.2.9** for cross sections A-A', B-B' and C-C', respectively.

The total settlement and angular distortion for the foundation soils, waste and cover soils between the points on cross sections A-A', B-B' and C-C' are provided in **Tables III.2.10, III.2.11** and **III.2.12**, respectively

TABLE III.2.7
Settlement and Angular Distortion of Soils Between Points
Cross Section A-A'
Sandoval County Landfill

Point Location	Total Soil Depth (feet)	AP	P _o	Primary Settlement (feet)	New Soil Depth (feet)	Secondary Settlement (feet)	Total Settlement (feet)	Distance Between Points (feet)	Angular Distortion (%)	Distortion Direction
A1	6.00	690.00	345.00	0.25	5.75	0.13	0.38	100	0.00	▼
A2	6.00	690.00	345.00	0.25	5.75	0.13	0.38	100	0.00	▼
A3	6.00	690.00	345.00	0.25	5.75	0.13	0.38	100	0.00	▼
A4	6.00	690.00	345.00	0.25	5.75	0.13	0.38	100	0.00	▼
A5	6.00	690.00	345.00	0.25	5.75	0.13	0.38	100	0.00	▼
A6	6.00	690.00	345.00	0.25	5.75	0.13	0.38	100	0.00	▼
A7	6.00	690.00	345.00	0.25	5.75	0.13	0.38	100	0.00	▼
A8	6.00	690.00	345.00	0.25	5.75	0.13	0.38	100	0.00	▼
A9	6.00	690.00	345.00	0.25	5.75	0.13	0.38	100	0.00	▼
A10	6.00	690.00	345.00	0.25	5.75	0.13	0.38	100	0.00	▼
A11	6.00	690.00	345.00	0.25	5.75	0.13	0.38	100	0.00	▼
A12	6.00	690.00	345.00	0.25	5.75	0.13	0.38	100	0.00	▼
A13	6.00	690.00	345.00	0.25	5.75	0.13	0.38	100	0.00	▼
A14	6.00	690.00	345.00	0.25	5.75	0.13	0.38	100	0.00	▼
A15	6.00	690.00	345.00	0.25	5.75	0.13	0.38	100	0.00	▼
A16	6.00	690.00	345.00	0.25	5.75	0.13	0.38	100	0.00	▼
A17	6.00	690.00	345.00	0.25	5.75	0.13	0.38	100	0.00	▼
A18	6.00	690.00	345.00	0.25	5.75	0.13	0.38	100	0.00	▼
A19	6.00	690.00	345.00	0.25	5.75	0.13	0.38	100	0.00	▼

Notes:

Points Correspond to **Figure III.2.1**

Elevations based on NM State Plan Coordinate System

Variables and Values used in Equations in text:

C_c 0.16
 e_s 0.83
 C_s 0.016

TABLE III.2.8
Settlement and Angular Distortion of Soils Between Points
Cross Section B-B'
Sandoval County Landfill

Point Location	Total Soil Depth (feet)	AP	P _o	Primary Settlement (feet)	New Soil Depth (feet)	Secondary Settlement (feet)	Total Settlement (feet)	Distance Between Points (feet)	Angular Distortion (%)	Distortion Direction
B1	6.00	690.00	345.00	0.25	5.75	0.13	0.38	100	-0.79	▲
B2	18.52	2,129.80	1,064.90	0.77	17.75	0.40	1.17	100	-0.04	▲
B3	19.11	2,197.65	1,098.83	0.80	18.31	0.41	1.21	100	0.27	▼
B4	14.84	1,706.60	853.30	0.62	14.22	0.32	0.94	100	0.04	▼
B5	14.28	1,642.20	821.10	0.60	13.68	0.31	0.90	100	0.11	▼
B6	12.61	1,450.15	725.08	0.53	12.08	0.27	0.80	100	0.42	▼
B7	6.00	690.00	345.00	0.25	5.75	0.13	0.38	100	-0.14	▲
B8	8.24	947.60	473.80	0.34	7.90	0.18	0.52	100	-0.04	▲
B9	8.86	1,018.90	509.45	0.37	8.49	0.19	0.56	100	0.18	▼
B10	6.00	690.00	345.00	0.25	5.75	0.13	0.38	100	0.00	▼
B11	6.00	690.00	345.00	0.25	5.75	0.13	0.38	100	0.00	▼
B12	6.00	690.00	345.00	0.25	5.75	0.13	0.38	100	0.00	▼
B13	6.00	690.00	345.00	0.25	5.75	0.13	0.38	100	0.00	▼
B14	6.00	690.00	345.00	0.25	5.75	0.13	0.38	100	0.00	▼
B15	6.00	690.00	345.00	0.25	5.75	0.13	0.38	100	0.00	▼
B16	6.00	690.00	345.00	0.25	5.75	0.13	0.38	100	0.00	▼
B17	6.00	690.00	345.00	0.25	5.75	0.13	0.38	100	0.00	▼
B18	6.00	690.00	345.00	0.25	5.75	0.13	0.38	100	0.00	▼
B19	6.00	690.00	345.00	0.25	5.75	0.13	0.38	100	0.00	▼
B20	6.00	690.00	345.00	0.25	5.75	0.13	0.38	100	0.00	▼
B21	6.00	690.00	345.00	0.25	5.75	0.13	0.38	100	0.00	▼

Notes:

Points Correspond to **Figure III.2.1**

Elevations based on NM State Plan Coordinate System

Variables and Values used in Equations in text:

C_c 0.16
 e_s 0.83
 C_s 0.016

TABLE III.2.9
Settlement and Angular Distortion of Soils Between Points
Cross Section C-C'
Sandoval County Landfill

Point Location	Total Soil Depth (feet)	AP	P _o	Primary Settlement (feet)	New Soil Depth (feet)	Secondary Settlement (feet)	Total Settlement (feet)	Distance Between Points (feet)	Angular Distortion (%)	Distortion Direction
C1	6.00	690.00	345.00	0.25	5.75	0.13	0.38	100	-0.62	▲
C2	15.86	1,823.90	911.95	0.66	15.20	0.34	1.00	100	0.13	▼
C3	13.86	1,593.90	796.95	0.58	13.28	0.30	0.88	100	0.18	▼
C4	10.93	1,256.95	628.48	0.46	10.47	0.23	0.69	100	0.24	▼
C5	7.14	821.10	410.55	0.30	6.84	0.15	0.45	100	-0.87	▼
C6	20.87	2,400.05	1,200.03	0.87	20.00	0.45	1.32	100	0.59	▼
C7	11.55	1,328.25	664.13	0.48	11.07	0.25	0.73	100	0.20	▼
C8	8.31	955.65	477.83	0.35	7.96	0.18	0.52	100	0.08	▼
C9	7.07	813.05	406.53	0.29	6.78	0.15	0.45	100	-0.13	▼
C10	9.14	1,051.10	525.55	0.38	8.76	0.20	0.58	100	0.20	▼
C11	6.00	690.00	345.00	0.25	5.75	0.13	0.38	100	0.00	▼
C12	6.00	690.00	345.00	0.25	5.75	0.13	0.38	100	0.00	▼
C13	6.00	690.00	345.00	0.25	5.75	0.13	0.38	100	0.00	▼
C14	6.00	690.00	345.00	0.25	5.75	0.13	0.38	100	0.00	▼
C15	6.00	690.00	345.00	0.25	5.75	0.13	0.38	100	0.00	▼
C16	6.00	690.00	345.00	0.25	5.75	0.13	0.38	100	0.00	▼
C17	6.00	690.00	345.00	0.25	5.75	0.13	0.38	100	0.00	▼
C18	6.00	690.00	345.00	0.25	5.75	0.13	0.38	100	0.00	▼
C19	6.00	690.00	345.00	0.25	5.75	0.13	0.38	100	0.00	▼
C20	6.00	690.00	345.00	0.25	5.75	0.13	0.38	100	0.00	▼

Notes:

Points Correspond to **Figure III.2.1**

Elevations based on NM State Plan Coordinate System

Variables and Values used in Equations in text:

C_c 0.16

e_s 0.83

C_s 0.016

TABLE III.2.10
Total Settlement and Angular Distortion Between Points
Cross Section A-A'
Sandoval County Landfill

Point Location	Total Settlement (feet)	Distance Between Points (feet)	Angular Distortion (%)	Distortion Direction	Design Final Grade Elevation (feet)	Design Slope Between Point Locations (%)	Updated Final grade Elevation (feet)	Updated Slope Between Point Locations (%)
A1	1.72	100	-2.86	▲	5441.80	25.75	5440.08	22.89
A2	4.58	100	-1.97	▲	5467.55	24.23	5462.97	22.26
A3	6.55	100	-1.87	▲	5491.78	26.22	5485.23	24.35
A4	8.42	100	-1.96	▲	5518.00	23.52	5509.58	21.56
A5	10.37	100	-1.06	▲	5541.52	11.76	5531.15	10.70
A6	11.44	100	-0.15	▲	5553.28	3.70	5541.84	3.55
A7	11.59	100	-0.72	▲	5556.98	3.74	5545.39	3.02
A8	12.31	100	-0.18	▲	5560.72	2.95	5548.41	3.13
A9	12.48	100	0.26	▼	5557.77	5.49	5545.29	5.23
A10	12.22	100	0.91	▼	5552.28	16.28	5540.06	15.37
A11	11.31	100	1.44	▼	5536.00	24.00	5524.69	22.56
A12	9.87	100	1.51	▼	5512.00	24.30	5502.13	22.79
A13	8.36	100	1.41	▼	5487.70	23.70	5479.34	22.29
A14	6.95	100	0.76	▼	5464.00	14.70	5457.05	13.94
A15	6.19	100	1.23	▼	5449.30	21.68	5443.11	20.45
A16	4.96	100	1.15	▼	5427.62	22.84	5422.66	21.69
A17	3.81	100	1.02	▼	5404.78	16.24	5400.97	15.22
A18	2.80	100	1.36	▼	5388.54	19.15	5385.74	17.79
A19	1.44				5369.39		5367.95	

Notes:

Points Correspond to **Figure III.2.1**

Elevations based on NM State Plan Coordinate System

TABLE III.2.11
Total Settlement and Angular Distortion Between Points
Cross Section B-B'
Sandoval County Landfill

Point Location	Total Settlement (feet)	Distance Between Points (feet)	Angular Distortion (%)	Distortion Direction	Design Final grade Elevation (feet)	Design Slope Between Point Locations (%)	Updated Final grade Elevation (feet)	Updated Slope Between Point Locations (%)
B1	8.49	100	-1.451	▼	5414.05	20.71	5405.56	19.26
B2	9.94	100	-1.626	▼	5434.76	24.29	5424.82	22.66
B3	11.57	100	-1.778	▼	5459.05	23.15	5447.48	21.37
B4	13.34	100	2.175	▲	5482.20	5.50	5468.86	7.67
B5	11.17	100	2.474	▲	5487.70	8.74	5476.53	6.27
B6	8.70	100	1.850	▲	5478.96	16.78	5470.26	14.93
B7	6.85	100	0.187	▲	5462.18	5.05	5455.33	4.86
B8	6.66	100	-0.458	▲	5457.13	3.41	5450.47	2.95
B9	7.12	100	-1.628	▲	5460.54	7.44	5453.42	5.81
B10	8.74	100	-0.407	▲	5467.98	6.87	5459.24	6.46
B11	9.15	100	-0.481	▼	5474.85	6.85	5465.70	6.37
B12	9.63	100	-0.294	▲	5481.70	6.33	5472.07	6.04
B13	9.93	100	-0.235	▲	5488.03	2.30	5478.10	2.07
B14	10.16	100	-0.230	▲	5490.33	0.21	5480.17	0.44
B15	10.39	100	0.510	▼	5490.12	2.43	5479.73	1.92
B16	9.88	100	1.045	▼	5487.69	9.76	5477.81	8.71
B17	8.84	100	1.264	▼	5477.93	18.41	5469.09	17.15
B18	7.57	100	1.392	▼	5459.52	21.52	5451.95	20.13
B19	6.18	100	1.855	▼	5438.00	24.95	5431.82	23.10
B20	4.33	100	4.325	▼	5413.05	25.04	5408.72	20.71
B21	0.00				5388.01		5388.01	

Notes:

Points Correspond to **Figure III.2.1**

Elevations based on NM State Plan Coordinate System

TABLE III.2.12
Total Settlement and Angular Distortion Between Points
Cross Section C-C'
Sandoval County Landfill

Point Location	Total Settlement (feet)	Distance Between Points (feet)	Angular Distortion (%)	Distortion Direction	Design Final grade Elevation (feet)	Design Slope Between Point Locations (%)	Updated Final grade Elevation (feet)	Updated Slope Between Point Locations (%)
C1	12.13	100	-0.192	▼	5441.85	23.20	5429.72	23.01
C2	12.32	100	-1.861	▼	5465.05	25.06	5452.73	23.20
C3	14.18	100	-0.953	▼	5490.11	23.11	5475.93	22.16
C4	15.13	100	1.296	▼	5513.22	16.55	5498.09	17.85
C5	13.84	100	0.793	▼	5529.77	21.47	5515.93	22.26
C6	13.04	100	2.197	▼	5551.24	4.64	5538.20	6.84
C7	10.85	100	-1.080	▲	5555.88	3.28	5545.03	2.20
C8	11.93	100	-0.484	▲	5559.16	3.34	5547.23	2.86
C9	12.41	100	-2.891	▲	5562.50	0.50	5550.09	3.39
C10	15.30	100	-2.364	▲	5562.00	2.68	5546.70	5.04
C11	17.67	100	0.102	▼	5559.32	3.99	5541.65	3.89
C12	17.56	100	0.436	▲	5555.33	4.17	5537.77	3.73
C13	17.13	100	1.317	▲	5551.16	10.14	5534.03	8.82
C14	15.81	100	2.561	▼	5541.02	22.56	5525.21	20.00
C15	13.25	100	2.509	▼	5518.46	23.56	5505.21	21.05
C16	10.74	100	2.211	▼	5494.90	24.31	5484.16	22.10
C17	8.53	100	2.166	▼	5470.59	22.59	5462.06	20.42
C18	6.36	100	4.261	▼	5448.00	23.74	5441.64	19.48
C19	2.10	100	0.444	▼	5424.26	23.86	5422.16	23.42
C20	1.66				5400.40		5398.74	

Notes:

Points Correspond to **Figure III.2.1**

Elevations based on NM State Plan Coordinate System

6.0 CONCLUSION

Settlement projections have been calculated for the landfill foundation, the waste mass and for the landfill final soil cover. Settlement estimates include elastic deformation and both, primary and secondary consolidation in the foundations soils, in the waste, and in the cover materials. The value of projected settlement in both the foundation soils, the waste and cover soils occurs where the waste thickness is greatest. In Unit IV; and occurs at point A9 on Cross-Section A-A'.

The maximum final settlement of the landfill foundation, waste mass and cover soils is the sum of primary and secondary settlement at point A9. The foundation soil settlement is equal to 0.87 ft; the waste settlement is equal to 11.05 ft and for cover soils is equal to 0.38 ft for a total settlement equal to 12.48 ft. Maximum total settlement that could occur on the final cover of the landfill is the sum of the foundation soil, waste, and cover settlement (i.e., 12.48 ft). The methodology used to determine settlement at point A9 was used to find the settlement of points A1-A19 for Cross-Section A-A', points B1-B21 for Cross-Section B-B' and C1-C20 for Cross Section C-C'.

The maximum settlement of the landfill cover is 1.06% between points A6 and A10. The minimum slope of the landfill cover after settlement is 3.02%. The slope of the final cover, liner and leachate collection pipe after settlement is adequate; and consistent with the performance specifications for the leachate collection system and stormwater controls.

**APPLICATION FOR PERMIT RENEWAL AND MODIFICATION
SANDOVAL COUNTY LANDFILL**

**VOLUME III: ENGINEERING DESIGN AND CALCULATIONS
SECTION 2: SETTLEMENT CALCULATIONS**

ATTACHMENT III.2.A

SUMMARY OF GEOTECHNICAL LABORATORY TESTING RESULTS

PSL LABORATORY ANALYSIS RESULTS SUMMARY

PROJECT INFORMATION			
PROJECT NAME:	Cell 4C Construction	PROJECT NO:	211.14.03
OWNER:	Sandoval County	CONTACTOR:	H R Construction, Inc.
PROJECT LOCATION:	Sandoval County Landfill		

SAMPLE ID	PERCENT FINER THAN BY WEIGHT - U.S. STANDARD SIEVE NUMBER							C.U. (d ₆₀ /d ₁₀)
	3/4"	1/2"	3/8"	4	10	40	200	
	19 mm	12.5 mm	9.5 mm	4.75 mm	2.0 mm	0.425 mm	0.075 mm	
1434024	100	100.0	99.0	97.0	94.0	84.0	5.1	2.61
1432025	100	99.0	99.0	97.0	95.0	86.0	4.8	2.53
1434026	97	97.0	96.0	95.0	92.0	83.0	5.1	2.64
1434027	100	99.0	98.0	96.0	94.0	84.0	5.1	2.62
1434028	100	98.0	98.0	96.0	93.0	84.0	4.7	2.59
1434029	100	99.0	97.0	95.0	92.0	81.0	3.5	2.70
1434030	100	96.0	94.0	93.0	90.0	81.0	5.3	2.73
1434031	100	99.0	97.0	95.0	92.0	82.0	4.2	2.67
1434032	100	97.0	97.0	96.0	93.0	84.0	5.1	2.60
1434033	97	96.0	94.0	92.0	90.0	80.0	3.4	2.74
1434034	100	100.0	100.0	98.0	95.0	85.0	5.4	2.58
1434035	100	99.0	99.0	96.0	93.0	83.0	5.0	2.65
1434036	100	99.0	99.0	97.0	93.0	83.0	4.4	2.63
1434037	100	97.0	96.0	93.0	90.0	76.0	3.2	2.97
1434038	100	100.0	99.0	97.0	94.0	84.0	4.6	2.60
1434039	100	98.0	97.0	95.0	92.0	83.0	4.7	2.63
1434040	100	99.0	98.0	96.0	93.0	83.0	5.0	2.65
1434041	100	100.0	99.0	98.0	95.0	85.0	4.7	2.56
1434042	100	99.0	98.0	96.0	94.0	84.0	5.0	2.61
1434043	100	99.0	99.0	97.0	94.0	83.0	4.2	2.64
AVERAGE:	100	98.5	97.7	95.8	92.9	82.9	4.6	2.65



(505) 867-6990

GORDON ENVIRONMENTAL, INC.

213 S. Camino del Pueblo

(505) 867-6991 Fax

Consulting Engineers

Bernalillo, New Mexico 87004

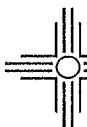
PSL LABORATORY ANALYSIS RESULTS SUMMARY

PROJECT INFORMATION			
PROJECT NAME:	Cell 6B Construction	PROJECT NO:	211.14.03
OWNER:	Sandoval County Public Works	CONTACTOR:	H R Construction, Inc.
PROJECT LOCATION:	Sandoval County Landfill		

SAMPLE ID	PERCENT FINER THAN BY WEIGHT - U.S. STANDARD SIEVE NUMBER							C.U. (d_{60}/d_{10})
	3/4"	1/2"	3/8"	4	10	40	200	
	19 mm	12.5 mm	9.5 mm	4.75 mm	2.0 mm	0.425 mm	0.075 mm	
1434044	100	100.0	99.0	96.0	93.0	86.0	6.2	2.54
1434045	100	100.0	99.0	96.0	94.0	86.0	6.2	2.55
1434046	100	100.0	99.0	98.0	96.0	89.0	7.1	2.46
1434047	100	96.0	96.0	93.0	90.0	84.0	6.7	2.62
1434048	100	99.0	98.0	95.0	92.0	86.0	6.3	2.54
1434049	100	99.0	97.0	95.0	92.0	89.0	6.6	2.42
1434050	100	100.0	99.0	96.0	94.0	88.0	6.8	2.48
1434051	100	100.0	100.0	97.0	95.0	88.0	6.5	2.49
1434052	97	96.0	96.0	93.0	90.0	84.0	4.3	2.56
1434053	100	99.0	97.0	95.0	92.0	85.0	5.7	2.56
1434054	100	99.0	98.0	96.0	94.0	88.0	6.8	2.48
1434055	100	100.0	98.0	96.0	94.0	88.0	6.7	2.48
1434056	100	99.0	97.0	95.0	92.0	85.0	4.9	2.54
1434057	100	99.0	97.0	95.0	92.0	85.0	4.9	2.54
1434058	100	99.0	98.0	94.0	89.0	82.0	5.5	2.67
1434059	100	100.0	100.0	96.0	93.0	86.0	5.5	2.53
1434060	100	100.0	99.0	97.0	95.0	88.0	5.1	2.45
1434061	100	99.0	99.0	97.0	94.0	87.0	6.4	2.51
1434062	100	98.0	97.0	95.0	92.0	86.0	5.8	2.52
1434063	100	100.0	100.0	99.0	96.0	89.0	4.9	2.41
1434064	100	100.0	99.0	97.0	94.0	88.0	5.9	2.46
1434065	100	100.0	100.0	98.0	96.0	90.0	5.9	2.40
1434066	100	100.0	99.0	97.0	95.0	88.0	5.5	2.46
1434067	100	100.0	100.0	98.0	95.0	88.0	6.3	2.48
1434068	100	100.0	100.0	98.0	97.0	90.0	5.8	2.41
1434069	100	98.0	97.0	96.0	94.0	87.0	4.9	2.48
1434070	100	97.0	96.0	95.0	92.0	86.0	5.3	2.51
1434071	100	100.0	99.0	97.0	95.0	88.0	5.4	2.46
1434072	100	100.0	100.0	98.0	96.0	89.0	6.7	2.46
1434073	100	100.0	100.0	99.0	97.0	90.0	5.3	2.39
AVERAGE:	100	99.2	98.4	96.2	93.7	87.1	5.9	2.50

REVIEWED BY: _____

SHEET 1 OF 1



(505) 867-6990

GORDON ENVIRONMENTAL, INC.

213 S. Camino del Pueblo

(505) 867-6991 Fax

Consulting Engineers

Bernalillo, New Mexico 87004

PSL LABORATORY ANALYSIS RESULTS SUMMARY

PROJECT INFORMATION	
PROJECT NAME: Cell 7 Construction	PROJECT NO: 211.14.03
OWNER: Sandoval County Public Works	CONTACTOR: H R Construction, Inc.
PROJECT LOCATION: Sandoval County Landfill	

SAMPLE ID	PERCENT FINER THAN BY WEIGHT - U.S. STANDARD SIEVE NUMBER							C.U. (d_{60}/d_{10})
	3/4"	1/2"	3/8"	4	10	40	200	
	19 mm	12.5 mm	9.5 mm	4.75 mm	2.0 mm	0.425 mm	0.075 mm	
1434076	100	99.0	99.0	99.0	98.0	94.0	4.3	2.25
1434077	100	100.0	100.0	99.0	99.0	96.0	5.7	2.23
1434078	100	100.0	100.0	100.0	99.0	96.0	5.9	2.23
1434079	100	99.0	99.0	98.0	97.0	94.0	5.5	2.27
1434080	100	99.0	99.0	99.0	98.0	95.0	6.7	2.26
1434081	100	100.0	100.0	99.0	98.0	95.0	6.4	2.26
1434082	100	100.0	100.0	99.0	98.0	95.0	5.6	2.25
1434083	100	100.0	100.0	99.0	98.0	95.0	4.7	2.23
1434084	100	100.0	100.0	99.0	98.0	85.0	3.7	2.57
1434085	100	100.0	99.0	99.0	97.0	88.0	4.0	2.44
1434086	100	100.0	100.0	99.0	98.0	84.0	4.0	2.63
1434087	100	100.0	100.0	99.0	99.0	95.0	5.3	2.25
1434088	100	100.0	100.0	99.0	98.0	89.0	4.9	2.43
1434089	100	100.0	100.0	99.0	98.0	81.0	3.5	2.76
1434090	100	100.0	100.0	99.0	98.0	95.0	5.3	2.24
1434091	100	100.0	100.0	100.0	99.0	96.0	5.3	2.22
1434092	100	100.0	100.0	100.0	99.0	96.0	6.0	2.23
1434093	100	100.0	100.0	99.0	98.0	88.0	4.1	2.46
1434094	100	100.0	100.0	100.0	99.0	95.0	5.2	2.24
1434095	100	100.0	100.0	99.0	98.0	94.0	4.0	2.25
1434096	100	100.0	100.0	99.0	99.0	95.0	6.1	2.26
1434097	100	100.0	100.0	99.0	98.0	85.0	4.6	2.60
1434098	100	100.0	100.0	99.0	99.0	96.0	5.6	2.21
1434099	100	100.0	100.0	99.0	98.0	95.0	5.5	2.24
1434100	100	100.0	100.0	100.0	98.0	95.0	4.3	2.22
1434101	100	100.0	100.0	99.0	98.0	93.0	4.8	2.29
1434102	100	100.0	99.0	98.0	97.0	94.0	5.7	2.27
1434103	100	100.0	100.0	99.0	98.0	83.0	4.5	2.69
1434104	100	100.0	100.0	100.0	99.0	96.0	6.5	2.24
1434105	100	100.0	100.0	99.0	98.0	95.0	5.8	2.25
AVERAGE:	100	99.9	99.8	99.1	98.2	92.4	5.1	2.33

REVIEWED BY: 

SHEET 1 OF 1

GRAIN SIZE DISTRIBUTION TEST DATA

3/24/2015

Client: Sandoval County Landfill**Project:** Application for Permit Modification**Project Number:** 211.00.01**Location:** Sandoval County Landfill**Depth:** Excavated Soils**Sample Number:** 1**Material Description:** Sandoval County Landfill Cells 4C, 5B, 6B, and 7 PSL soil evaluation.**Date:** 03/24/15**PL:** NP**LL:** NV**USCS Classification:** SP-SM**AASHTO Classification:** A-3**Sieve Test Data**

Dry Sample and Tare (grams)	Tare (grams)	Cumulative Pan Tare Weight (grams)	Sieve Opening Size	Cumulative Weight Retained (grams)	Percent Finer
530.00	30.00	0.00	3/4"	0.00	100.0
			1/2"	4.00	99.2
			3/8"	7.00	98.6
			#4	15.00	97.0
			#10	25.50	94.9
			#40	62.50	87.5
			#200	474.00	5.2

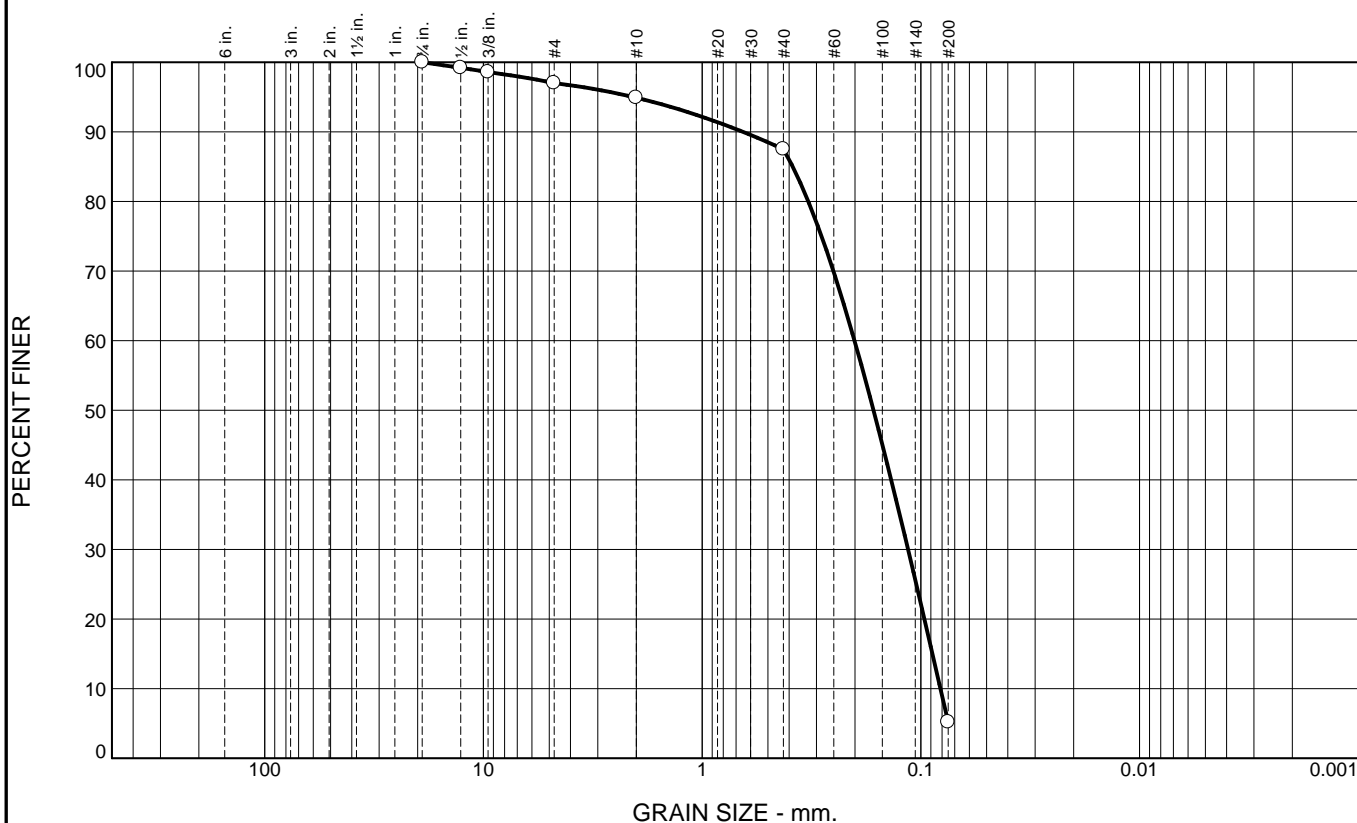
Fractional Components

Cobbles	Gravel			Sand				Fines		
	Coarse	Fine	Total	Coarse	Medium	Fine	Total	Silt	Clay	Total
0.0	0.0	3.0	3.0	2.1	7.4	82.3	91.8			5.2

D ₁₀	D ₁₅	D ₂₀	D ₃₀	D ₅₀	D ₆₀	D ₈₀	D ₈₅	D ₉₀	D ₉₅
0.0813	0.0885	0.0963	0.1144	0.1646	0.2010	0.3269	0.3852	0.6506	2.0627

Fineness Modulus	C _u	C _c
1.04	2.47	0.80

Particle Size Distribution Report



% +3"	% Gravel		% Sand			% Fines	
	Coarse	Fine	Coarse	Medium	Fine	Silt	Clay
0.0	0.0	3.0	2.1	7.4	82.3	5.2	

SIEVE SIZE	PERCENT FINER	SPEC.* PERCENT	PASS? (X=NO)
3/4"	100.0		
1/2"	99.2		
3/8"	98.6		
#4	97.0		
#10	94.9		
#40	87.5		
#200	5.2		

* (no specification provided)

<u>Soil Description</u>		
Sandoval County Landfill Cells 4C, 5B, 6B, and 7 PSL soil evaluation.		
<u>Atterberg Limits</u>		
PL= NP	LL= NV	PI=
<u>Coefficients</u>		
D ₉₀ = 0.6506	D ₈₅ = 0.3852	D ₆₀ = 0.2010
D ₅₀ = 0.1646	D ₃₀ = 0.1144	D ₁₅ = 0.0885
D ₁₀ = 0.0813	C _u = 2.47	C _c = 0.80
<u>Classification</u>		
USCS= SP-SM	AASHTO= A-3	
<u>Remarks</u>		

Source of Sample: Sandoval County Landfill
Sample Number: 1

Depth: Excavated Soils

Date: 03/24/15



Client: Sandoval County Landfill
Project: Application for Permit Modification

Project No: 211.00.01

Figure 1

**APPLICATION FOR PERMIT RENEWAL AND MODIFICATION
SANDOVAL COUNTY LANDFILL**

**VOLUME III: ENGINEERING DESIGN AND CALCULATIONS
SECTION 2: SETTLEMENT CALCULATIONS**

ATTACHMENT III.2.B

**QIAN, XUEDE; KOERNER, ROBERT M.; AND GRAY, DONALD H. 2002.
GEOTECHNICAL ASPECTS OF LANDFILL DESIGN AND CONSTRUCTION.
NEW YORK: PRENTICE HALL.**

GEOTECHNICAL ASPECTS OF LANDFILL DESIGN AND CONSTRUCTION

Xuede Qian

*Geotechnical Engineering Specialist
Michigan Department of Environmental Quality*

Robert M. Koerner

*H. L. Bowman Professor of Civil Engineering, Drexel University
Director, Geosynthetic Research Institute*

Donald H. Gray

*Professor of Civil and Environmental Engineering
The University of Michigan*



PRENTICE HALL
Upper Saddle River, New Jersey 07458

TABLE 6.5 Index Properties of Solid Waste

Source	Unit Weight		Volumetric Moisture Content	Porosity	Void Ratio
	lb/ft ³	kN/m ³			
Rovers and Farquhar (1973)	59	9.3	0.16	—	—
Fungaroli (1979)	63	9.9	0.05	—	—
Wigh (1979)	73	11.5	0.08	—	—
Walsh and Kinman (1979)	90	14.1	0.17	—	—
Walsh and Kinman (1981)	89	14.0	0.17	—	—
Schroeder et al. (1984a, b)	—	—	0.28	0.52	1.08
Owels et al. (1990)	40 to 90	6.3 to 14.1	0.10 to 0.20	0.40 to 0.50	0.67 to 1.0
Schroeder et al. (1994a, b)	—	—	0.29	0.67	2.03
Zornberg et al. (1999)	64 to 95	10 to 15	0.30	0.49 to 0.62	1.02 to 1.65

Based on its constituent composition the average moisture content of the solid waste shown in Table 6.4 can be calculated as follows:

$$\begin{aligned}
 w_d &= [(60.0)(10.4) + (50.0)(19.1) + (20.0)(34.6) + (10.0)(6.0) + (15.0)(5.0) \\
 &\quad + (15.0)(9.5) + (2.0)(4.0) + (2.0)(7.2) + (8.0)(2.8) + (3.0)(1.4)]/100 \\
 &= (624 + 955 + 692 + 60 + 75 + 142.5 + 8 + 14.4 + 22.4 + 4.2)/100 \\
 &= 2597.5/100 \\
 &= \underline{26.0\%}
 \end{aligned}$$

Thus, the average dry gravimetric moisture content of the solid waste shown in Table 6.4 is 26.0%.

More information about the moisture content of solid waste can be found in Table 6.5. It should be noted that the values of moisture content listed in Table 6.5 are calculated on a volume basis and differ from those calculated on a weight basis, which is more common to geotechnical analyses.

6.4 POROSITY OF MUNICIPAL SOLID WASTE

Porosity is defined as the ratio of the volume of voids to the total volume occupied by a solid waste or soil. Void ratio is defined as the ratio of the volume of voids to the volume of solids. Porosity can be related to the void ratio by using the relationships

$$n = \frac{e}{1 + e} \quad (6.7)$$

and

$$e = \frac{n}{1 - n} \quad (6.8)$$

where n = porosity of solid waste; and
 e = void ratio of solid waste.

The porosity of MSW varies typically from 0.40 to 0.67 depending on the compaction and composition of the waste. For comparison, a typical compacted clay liner material will have a porosity of about 0.40. Table 6.5 shows a summary of the index properties of municipal solid waste, which includes initial volumetric moisture content, initial porosity, initial void ratio and unit weight data.

6.5 HYDRAULIC CONDUCTIVITY OF MUNICIPAL SOLID WASTE

Proper assessment of the hydraulic conductivity of municipal solid waste is important in the design of leachate collection systems and in leachate recirculation planning particularly for bioreactor landfills (see Chapter 15). The hydraulic conductivity can be measured using a field leachate pumping test and a large-scale percolation test in test pits or by using large-diameter permeameters in the laboratory.

Hydraulic conductivity measured in test pits at several landfills in Canada by Landva and Clark (1990) is plotted against unit weight in Figure 6.3. The values shown are based on an intermediate stage of water level recession, after the flow had stabilized and before any debris could clog the voids. The measured coefficients of hydraulic conductivity (1.0×10^{-3} to 4.0×10^{-2} cm/sec) correspond to those associated with clean sand and gravel. Qian (1994) used three-year field data from an active landfill in the state of Michigan to develop a relationship between precipitation and leachate volume from a primary leachate collection system with time. With this information, the hydraulic conductivity of the waste can be calculated based on the water travel time, hydraulic gradient, and waste thickness. The hydraulic conductivity calculated in this way was estimated to be about 9.2×10^{-4} to 1.1×10^{-3} cm/sec. Table 6.6 summarizes the hydraulic conductivity of different types of MSW taken from the

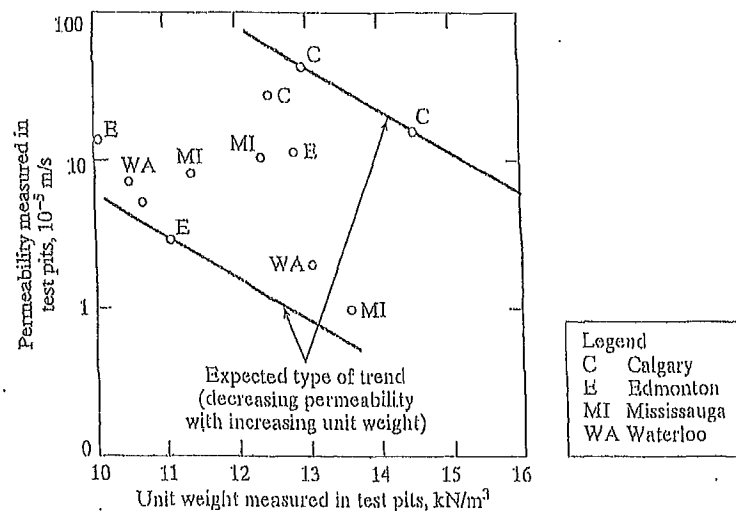
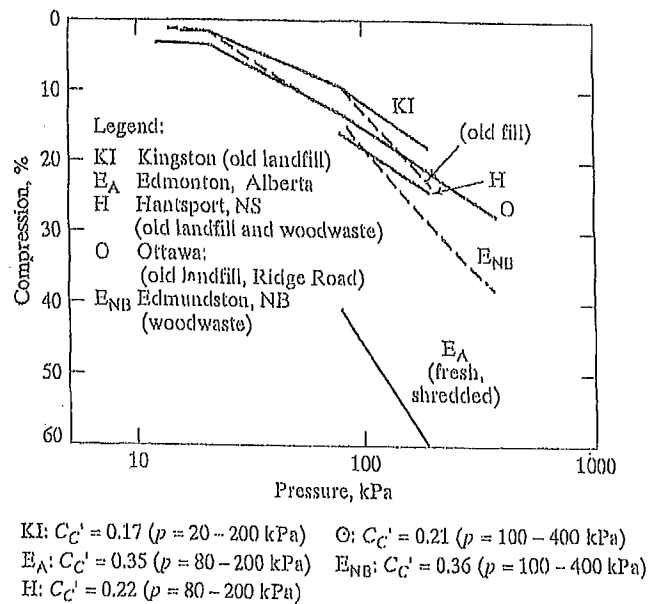


FIGURE 6.3 Unit Weight and Permeability (from Percolation) as Measured in Landfill Test Pits (Landva and Clark, 1990)

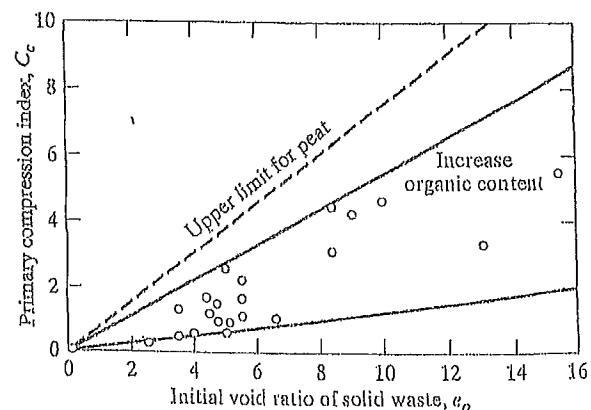
FIGURE 6.9 Compressive Strain versus Log Pressure for Various Landfills in Canada (Landva and Clark, 1990)



cans; the lower values are for the less resilient materials. The maximum C_c for peat is about one-third greater than the maximum observed for waste fills.

Landva and Clark (1990) found that the coefficient of secondary consolidation, C_{α} (the gradient of the compression versus log time relationship) was in the range 0.2 to 3.0 percent per log cycle time, depending on the type of waste involved. Field testing results using a settlement platform (Keene, 1977) showed that the coefficient of secondary consolidation, C_{α} , varies between 0.014 and 0.034. Too few tests have been carried out for any firm relationship to be established between the value of C_{α} and the type of waste, but it does appear that C_{α} increases with increasing organic content. Sowers (1973) pointed out that the coefficient of secondary consolidation, C_{α} , is also a

FIGURE 6.10 Compressibility of MSW Landfills (Sowers, 1973)



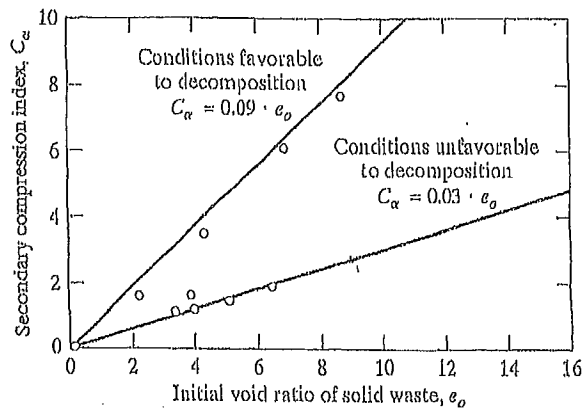


FIGURE 6.11 Secondary Compression of MSW Landfills (Sowers, 1973)

function of the void ratio, as shown in Figure 6.11. For any given void ratio, there is a large range in C_α , related to the potential for physico-chemical and bio-chemical decay. The value is high if the organic content subject to decay is large and the environment is favorable; namely, warm, moist, with fluctuating water table that pumps fresh air into the fill. The value is low for more inert materials and an unfavorable environment. More research and data are necessary before this relationship can be defined more closely.

The most widely reported compressibility parameter is the modified secondary compression index (C'_α). The reported values of C'_α range from 0.001 to 0.59. The lowest value represents the compressibility of a landfill that had been subjected to dynamic compaction. For typical landfills the lower limit of C'_α is generally around 0.01 to 0.03. This compares to 0.005 to 0.02 for common clays (Holtz and Kovacs, 1981). Fassett et al. (1994) observed that the typical upper limit of C'_α appears to be approximately 0.1.

According to Yen and Scanlon (1975), the settlement rate of waste increases with depth, hence larger values of C'_α should be associated with thicker fills. They observed that this effect leveled off at about 90 ft. and suggested that conditions within the landfill at great depths limit the biological activity to anaerobic decomposition, which is much slower than the aerobic decomposition believed to occur in shallower fills.

The values of C_α and C'_α , like C_c and C'_c , are dependent on the values used for e_0 or H_0 . The value of C'_α is also dependent on stress level, time, and on how the origin of time is selected. The waste placement or filling period for landfills is often long and should be taken into consideration for settlement rate analyses (Yen and Scanlon, 1975). The zero time selection has a large impact on C'_α particularly during earlier phases of a landfill (Fassett et al., 1994).

An additional problem with determining C'_α is the fact that this parameter is generally not constant. Edgers (1992) presents settlement log-time data from 22 case histories (shown in Figure 6.12). The majority of the curves show a relatively flat slope (i.e. low C'_α values) at small times, but at larger times the slope greatly increases (Figure 6.13). They attributed the higher slopes in the later stages of compression to increasing decomposition, but it may simply be an artifact of the log-time scale. It is

d = diameter of perforated hole or width of perforated slot on the pipe, in or m; and

n = number of perforated holes or slots per row per foot of pipe.

Pipe stiffness is measured according to ASTM D2412 (Standard Test Method for External Loading Properties of Plastic Pipe by Parallel-Plate Loading). The elastic modulus of the pipe material depends on the type of resin and formulation being used. Three formulas that can be used to calculate pipe stiffness are

$$PS = \frac{E \cdot I}{0.149 \cdot r^3} \quad (9.24)$$

$$PS = 0.559 \cdot E \cdot (t/r)^3 \quad (9.25)$$

and

$$PS = 4.47 \cdot \frac{E}{(SDR - 1)^3} \quad (9.26)$$

where PS = pipe stiffness, lb/in² or kN/m²;

E = elastic modulus of the pipe material, lb/in² or kN/m²;

I = moment of inertia of the pipe wall per unit length,

$I = t^3/12$, in⁴/in = in³ or m⁴/m = m³;

r = mean radius of pipe, in or m;

t = wall thickness of pipe, in or m; and

SDR = standard dimension ratio, the same as the dimension ratio.

The allowable deflection ratios for a typical commercial polyethylene pipe are listed in Table 9.4.

Deflections of buried flexible pipe are commonly calculated using Equation 9.16 or 9.21. These equations use the soil reaction modulus, E' , as a surrogate parameter for soil stiffness. It should be noted that the values of E' in Table 9.3 only apply for soil fills of less than 50 ft (15 m). However, megafills built over leachate collection pipes often exceed 150 ft (46 m) in height. The soil reaction modulus is not a directly measurable soil parameter; instead it must be determined by back-calculation using observed pipe deflections. Research by Selig (1990) showed that E' is a function of the bedding condition and overburden pressure. Selig's studies were carried out to seek a correlation between the soil reaction modulus and soil stiffness parameters such as

TABLE 9.4 Allowable Deflection Ratio of Polyethylene Pipe

SDR	Allowable Deflection Ratio
11	2.7%
13.5	3.4%
15.5	3.9%
17	4.2%
19	4.7%
21	5.2%
26	6.5%
32.5	8.1%

Young's modulus of soil, E_s , and the constrained modulus of soil, M_s , where E_s and D_s are related through Poisson's ratio of soil, ν_s , by

$$M_s = \frac{E_s \cdot (1 - \nu_s)}{(1 + \nu_s)(1 - 2 \cdot \nu_s)} \quad (9.27)$$

where M_s = constrained modulus of soil, lb/ft² or kN/m²;
 E_s = elastic modulus of soil, lb/ft² or kN/m²; and
 ν_s = Poisson's ratio of soil.

The studies and analyses by Neilson (1967), Allgood and Takahashi (1972), and Hartely and Duncan (1987) indicated that for

$$E' = k \cdot M_s \quad (9.28)$$

the value of k may vary from 0.7 to 2.3. Using $k = 1.5$ as a representative value and $\nu_s = 0.3$, in addition to combining Equations 9.27 and 9.28 yields the following relationship between the elastic modulus of the pipe and soil (Selig, 1990):

$$E' = 2 \cdot E_s \quad (9.29)$$

The values of elastic parameters, E_s and ν_s , can be found in Table 9.5 according to different percents of density from a standard Proctor compaction test (ASTM D698).

TABLE 9.5 Elastic Soil Parameters (Selig, 1990)

Soil Type	Stress Level		85% Standard Density			95% Standard Density		
			E_s			E_s		
	psi	kPa	psi	MPa	ν_s	psi	MPa	ν_s
SW, SP, GW, GP	1	7	1,300	9	0.26	1,600	11	0.40
	5	35	2,100	14	0.21	4,100	28	0.29
	10	70	2,600	18	0.19	6,000	41	0.24
	20	140	3,300	23	0.19	8,600	59	0.23
	40	280	4,100	28	0.23	13,000	90	0.25
	60	420	4,700	32	0.28	16,000	110	0.29
GM, SM, ML, and GC, SC with < 20% fines	1	7	600	4	0.25	1,800	12	0.34
	5	35	700	5	0.24	2,500	17	0.29
	10	70	800	6	0.23	2,900	20	0.27
	20	140	850	6	0.30	3,200	22	0.29
	40	280	900	6	0.38	3,700	25	0.32
	60	420	1,000	7	0.41	4,100	28	0.35
CL, MH, GC, SC	1	7	100	1	0.33	400	3	0.42
	5	35	250	2	0.29	800	6	0.35
	10	70	400	3	0.28	1,100	8	0.32
	20	140	600	4	0.25	1,300	9	0.30
	40	280	700	5	0.35	1,400	10	0.35
	60	420	800	6	0.40	1,500	10	0.38

Table 12.2 Comparison of Settlement and Construction Period (Yen and Scanlon, 1975)

Range of Fill Depth H_0 , feet, (meter)	Average Construction Period, t_c (month)	Total Time Required for Construction and Settlement (months)	Approximate Time Required for Settlement to Complete (month)
40 to 80 (12 to 24)	12	113	101
40 to 80 (12 to 24)	72	324	252
80 to 100 (24 to 30)	12	245	233
80 to 100 (24 to 30)	72	310	238

Used with permission of ASCE.

12.4 ESTIMATION OF LANDFILL SETTLEMENT

The usual laboratory tests for soil consolidation testing are not well suited for obtaining accurate consolidation parameters for solid waste that has a heterogeneous composition and extremely large particle sizes. By analyzing the field settlement data from some large-scale pilot landfill cells, Sowers (1973) proposed an alternative method to estimate the amount of the landfill settlement. In recent years, this method has been revised and refined several times by other investigators.

The settlement of solid waste includes primary settlement and long-term secondary compression. The total amount of settlement is given by the expression

$$\Delta H = \Delta H_c + \Delta H_\alpha \quad (12.3)$$

where ΔH = total settlement of solid waste;

ΔH_c = primary settlement of solid waste;

ΔH_α = long-term secondary settlement of solid waste.

12.4.1 Settlement of New Solid Waste

Based on the procedure proposed by Sowers (1973), the equations that follow can be used to calculate the settlement for new landfilled solid waste. The *Initial primary settlement* is given by

$$\Delta H_c = C_c \cdot \frac{H_0}{1 + e_0} \cdot \log \frac{\sigma_1}{\sigma_0} \quad (12.4)$$

or

$$\Delta H_c = C'_c \cdot H_0 \cdot \log \frac{\sigma_1}{\sigma_0} \quad (12.5)$$

where ΔH_c = primary settlement;

e_0 = initial void ratio of the waste layer before settlement;

H_0 = initial thickness of the waste layer before settlement;

C_c = primary compression index (recall Figure 6.10);

C'_c = modified primary compression index, $C'_c = 0.17 \sim 0.36$;

σ_0 = previously applied pressure in the waste layer (assumed equal to the compaction pressure, $\sigma_0 = 1,000 \text{ lb/ft}^2$ or 48 kN/m^2);

σ_1 = total overburden pressure applied at the mid level of the waste layer.

The previous compaction pressure applied on the solid waste layer during placement with compaction equipment is assumed to be 1,000 lb/ft² (48 kN/m²) based on 1973 compaction efforts for municipal solid waste landfills. In other words, the waste that has been placed in the landfill is essentially incompressible at normal pressure below 1,000 lb/ft² (48 kN/m²) due to the preconsolidation effect caused by previous compaction of the material. The value of the previously applied pressure, σ_o , should be changed during estimation of settlement if the compaction effort is much lower or higher than 1,000 lb/ft² (48 kN/m²) for a specific landfill project. Indeed, current practices of using waste compactors in the 100 to 150 U.S. tons (900 to 1,300 kN) range will significantly increase the value of σ_o .

The *long-term secondary settlement* can be obtained from

$$\Delta H_\alpha = C_\alpha \cdot \frac{H_o}{1 + e_o} \cdot \log \frac{t_2}{t_1} \quad (12.6)$$

or

$$\Delta H_\alpha = C'_\alpha \cdot H_o \cdot \log \frac{t_2}{t_1} \quad (12.7)$$

where ΔH_α = long-term secondary settlement;

e_o = initial void ratio of the waste layer before settlement;

H_o = initial thickness of the waste layer before settlement;

C_α = secondary compression index (recall Figure 6.11);

C'_α = modified secondary compression index, $C'_\alpha = 0.03 \sim 0.1$;

t_1 = starting time of the time period for which long-term settlement of the layer is desired, $t_1 = 1$ month;

t_2 = ending time of the time period for which long-term settlement of the layer is desired.

Because a standard consolidation test method for solid waste has not yet been developed, the selection of waste compression indices are mainly based on experience and limited field data. The value of the primary compression index C_c can be selected from Figure 6.10 based on the initial void ratio and organic content of the solid waste. The value of the secondary compression index C_α can be selected from Figure 6.11 based on the initial void ratio of the waste and the decomposition conditions.

Generally, the initial void ratio of municipal solid waste placed in a landfill after compaction is quite difficult to determine, and hence the values of the primary compression index C_c and the secondary compression index C_α cannot be estimated readily for settlement analysis. Accordingly, an alternative approach has been used in engineering practice—namely, the use of a “modified” primary compression index C'_c and a “modified” secondary compression index C'_α . Based on experience, the value of the modified primary compression index C'_c varies from 0.17 to 0.36, and the value of the modified secondary compression index C'_α varies from 0.03 to 0.1 for municipal solid waste (depending on the initial compaction effort and composition of the solid waste). The value of the modified secondary compression index C'_α for common clay ranges from 0.005 to 0.02. Therefore, the secondary settlement for municipal solid waste is approximately five to six times that of common clay.

12.4.2 Settlement of Existing Solid Waste

The following equations can be used to calculate the settlement of an existing solid waste landfill caused by vertical expansion (Chapter 14) or other additional extra loading, such as a light structure on a raft foundation.

The *primary settlement* is obtained by

$$\Delta H_e = C_e \cdot \frac{H_o}{1 + e_o} \cdot \log \frac{\sigma_o + \Delta \sigma}{\sigma_o} \quad (12.8)$$

or

$$\Delta H_e = C'_e \cdot H_o \cdot \log \frac{\sigma_o + \Delta \sigma}{\sigma_o} \quad (12.9)$$

where ΔH_e = primary settlement;
 e_o = initial void ratio of the waste layer before settlement;
 H_o = initial thickness of the waste layer of the existing landfill;
 C_e = primary compression index;
 C'_e = modified primary compression index, $C'_e = 0.17 \sim 0.36$;
 σ_o = existing overburden pressure acting at the mid level of the waste layer;
 $\Delta \sigma$ = increment of overburden pressure due to vertical expansion or other extra load.

The *long-term secondary settlement* is given by

$$\Delta H_\alpha = C_\alpha \cdot \frac{H_o}{1 + e_o} \cdot \log \frac{t_2}{t_1} \quad (12.10)$$

or

$$\Delta H_\alpha = C'_\alpha \cdot H_o \cdot \log \frac{t_2}{t_1} \quad (12.11)$$

where ΔH_α = secondary settlement;
 e_o = initial void ratio of the waste layer before starting secondary settlement;
 H_o = initial thickness of the waste layer before starting secondary settlement;
 C_α = secondary compression index;
 C'_α = modified secondary compression index, $C'_\alpha = 0.03 \sim 0.1$;
 t_1 = starting time of the secondary settlement. It is assumed to be equal to the age of the existing landfill for vertical expansion project;
 t_2 = ending time of the secondary settlement.

(e.g., temperature within landfill and oxygen reaching the waste) still is not entirely clear. These functions should be used with caution in engineering practice and should be supported by additional testing data and research.

12.7 ESTIMATION OF LANDFILL FOUNDATION SETTLEMENT

If the landfill is underlain by a soil layer, particularly a thick layer of soft, fine-grained soil, consolidation settlements may be large. In these cases, design analyses should consider settlement of the foundation clay layer. Both primary consolidation and long-term secondary settlement should be considered. Calculations are performed using conventional equations from soil mechanics theory and a time frame at least equal to the active life and postclosure care period of the landfill.

Excessive settlement of an underlying foundation clay layer will affect the performance of a landfill liner and leachate collection system. The purposes of analyzing the settlement of a foundation clay layer and overlying landfill liner and leachate collection/removal system are as follows:

- (i) Tensile strain induced in the liner system and leachate collection and removal system must be limited to a minimum allowable tensile strain for the components of these two systems. The compacted clay liner usually has the smallest allowable tensile strain value between 0.1% and 1.0% and an average allowable tensile strain of 0.5%.
- (ii) Post-settlement grades of the landfill cell subbase and the leachate collection pipes must be sufficient to maintain leachate performance to prevent grade reversal and leachate ponding in accordance with the rule requirements.

12.7.1 Total Settlement of Landfill Foundation

The total settlement of landfill foundation soil can be divided into three portions: elastic settlement, primary consolidation settlement, and secondary consolidation settlement. The settlement of sandy soils includes only elastic settlement. The settlement of clayey soils includes all three types of settlements. The total settlement of clayey soil is equal to the sum of the elastic settlement and the primary and secondary settlements. Because the permeability of clay is quite low, it takes a long time to complete the whole process of consolidation settlement. The settlement of clayey soil is usually much larger than the settlement of sandy soils.

Because the settlement of sandy soils includes only elastic settlement, the settlement of sand layer can be calculated from the Elastic Settlement equation, which is

$$Z_e = (\Delta\sigma/M_s)H_o \quad (12.20)$$

where Z_e = elastic settlement of soil layer, ft or m;
 H_o = initial thickness of soil layer, ft or m;
 $\Delta\sigma$ = increment of vertical effective stress, lb/ft² or kN/m²;
 M_s = constrained modulus of soil, lb/ft² or kN/m².

The constrained modulus is given by

$$M_s = \frac{E_s \cdot (1 - v_s)}{(1 + v_s)(1 - 2 \cdot v_s)} \quad (12.21)$$

where M_s = constrained modulus of soil, lb/ft² or kN/m²;
 E_s = elastic modulus of soil, see Table 9.5, lb/ft² or kN/m²;
 v_s = Poisson's ratio of soil, see Table 9.5.

The *primary consolidation settlement* is given by

$$Z_c = C_r \cdot \frac{H_{oi}}{1 + e_{oi}} \cdot \log \frac{p_c}{\sigma_o} + C_c \cdot \frac{H_o}{1 + e_{oi}} \cdot \log \frac{\sigma_o + \Delta\sigma}{p_c} \quad (12.22)$$

where Z_c = primary consolidation settlement of clay layer, ft or m;
 H_o = initial thickness of clay layer, ft or m; $\approx 2 \text{ m}$
 e_{oi} = initial void ratio of clay layer;
 C_r = recompression index;
 C_c = primary compression index.
 σ_o = initial vertical effective stress, lb/ft² or kN/m²;
 p_c = preconsolidation pressure, lb/ft² or kN/m²;
 $\Delta\sigma$ = increment of vertical effective stress, lb/ft² or kN/m².

The *secondary compression settlement* is given by

$$Z_\alpha = C_\alpha \cdot \frac{H_{os}}{1 + e_{os}} \cdot \log \frac{t_2}{t_1} \quad (12.23)$$

where Z_α = long-term secondary compression settlement, ft or m;
 e_{os} = initial void ratio of clay layer before starting secondary consolidation settlement;
 C_α = secondary consolidation compression index;
 H_{os} = initial thickness of clay layer before starting secondary consolidation settlement, ft or m;
 t_1 = starting time of the time period for which long-term settlement of the layer is desired;
 t_2 = ending time of the time period for which long-term settlement of the layer is desired.

The total settlement of clay layer includes three portions: elastic settlement, primary consolidation settlement, and secondary consolidation settlement. These three types of settlement for clayey soil layers can be calculated from Equations 12.20, 12.22, and 12.23, respectively. The total settlement of clayey soil at point i can be determined from the equation

$$Z_i = (Z_a)_i + (Z_c)_i + (Z_\alpha)_i \quad (12.24)$$

where Z_i = total settlement of points i ;
 $(Z_a)_i$ = elastic settlement of point i ;
 $(Z_c)_i$ = primary consolidation settlement of point i ;
 $(Z_\alpha)_i$ = secondary consolidation settlement of point i .

**APPLICATION FOR PERMIT RENEWAL AND MODIFICATION
SANDOVAL COUNTY LANDFILL**

**VOLUME III: ENGINEERING DESIGN AND CALCULATIONS
SECTION 2: SETTLEMENT CALCULATIONS**

ATTACHMENT III.2.C

CODUTO, DONALD P. 1998.

GEOTECHNICAL ENGINEERING PRINCIPLES AND PRACTICES.

NEW JERSEY: PRENTICE HALL.

Geotechnical Engineering

Principles and Practices

Donald P. Coduto

*Professor of Civil Engineering
California State Polytechnic University, Pomona*

PRENTICE HALL, Upper Saddle River, NJ 07458

where:

$(N_1)_{60}$ = corrected SPT N -value, as defined in Chapter 3

C_p = grain size correction factor

C_A = aging correction factor

C_{OCR} = overconsolidation correction factor

D_{50} = grain size at which 50 percent of the soil is finer (mm) as defined in Section 4.4

t = age of soil (time since deposition in years). If no age information data is available, use $t = 100$ yr.

OCR = overconsolidation ratio, as defined in Chapter 11. If no information is available to assess the OCR, use a value of 2.

q_c = cone resistance (kg/cm^2 or ton/ft^2), as defined in Chapter 3

Q_c = compressibility factor

= 0.91 for highly compressible sands

= 1.00 for moderately compressible sands

= 1.09 for slightly compressible sands

For purposes of solving this formula, a sand with a high fines content or a high mica content is "highly compressible," whereas a pure quartz sand is "slightly compressible."

σ'_v = vertical effective stress (lb/ft^2 ; kPa), as defined in Chapter 10

Many people confuse relative density with relative compaction. The latter is defined in Chapter 6. Although the names are similar, and they measure similar properties, these two parameters are numerically different. In addition, some people in other professions use the term "relative density" to describe what we call specific gravity! Geotechnical engineers should never use the term in this way.

Table 4.5 presents typical values of e_{min} and e_{max} for various sandy soils. These are not intended to be used in lieu of laboratory or in-situ tests, but could be used to check test results or for preliminary analyses.

TABLE 4.5 TYPICAL VALUES OF e_{min} AND e_{max} (Hough, 1969; Adapted by permission of John Wiley and Sons, Inc.)

Soil Description	e_{min} (dense)	e_{max} (loose)
Equal spheres (theoretical values)	0.35	0.92
Clean, poorly graded medium sand (Ottawa, Illinois)	0.50	0.80
Clean, fine-to-medium sand	0.40	1.0
Uniform inorganic silt	0.40	1.1
Silty sand	0.30	0.90
Clean fine-to-coarse sand	0.20	0.95
Micaceous sand	0.40	1.2
Silty sand and gravel	0.14	0.85

TABLE 11.3 TYPICAL CONSOLIDATION PROPERTIES OF SATURATED NORMALLY CONSOLIDATED SANDY SOILS AT VARIOUS RELATIVE DENSITIES (Adapted from Burmister, 1962)

Soil Type	$C_c / (1+e_0)$					
	$D_r = 0\%$	$D_r = 20\%$	$D_r = 40\%$	$D_r = 60\%$	$D_r = 80\%$	$D_r = 100\%$
Medium to coarse sand, some fine gravel (SW)	-	-	0.005	-	-	-
Medium to coarse sand (SW/SP)	0.010	0.008	0.006	0.005	0.005	0.002
Fine to coarse sand (SW)	0.011	0.009	0.007	0.005	0.004	0.002
Fine to medium sand (SW/SP)	0.012	0.010	0.008	0.006	0.004	0.003
Fine sand (SP)	0.015	0.013	0.010	0.008	0.005	0.003
Fine sand with trace fine to coarse silt (SP-SM)	-	-	0.011	-	-	-
Fine sand with little fine to coarse silt (SM)	0.017	0.014	0.012	0.009	0.006	0.003
Fine sand with some fine to coarse silt (SM)	-	-	0.014	-	-	-

For saturated overconsolidated sands, $C_c / (1+e_0)$ is typically about one-third of the values listed in Table 11.3, which makes such soils nearly incompressible. Compacted fills can be considered to be overconsolidated, as can soils that have clear geologic evidence of preloading, such as glacial tills. Therefore, many settlement analyses simply consider the compressibility of such soils to be zero. If it is unclear whether a soil is normally consolidated or overconsolidated, it is conservative to assume it is normally consolidated.

Very few consolidation tests have been performed on gravelly soils, but the compressibility of these soils is probably equal to or less than those for sand, as listed in Table 11.3.

Another characteristic of sands and gravels is their high hydraulic conductivity, which means any excess pore water drains very quickly. Thus, the rate of consolidation is very fast, and typically occurs nearly as fast as the load is applied. Thus, if the load is due to a fill, the consolidation of these soils may have little practical significance.

However, there are at least two cases where consolidation of coarse-grained soils can be very important and needs more careful consideration:

1. Loose sandy soils subjected to dynamic loads, such as those from an earthquake. They can experience very large and irregular settlements that can cause serious damage. Kramer (1996) discusses methods of evaluating this problem.

**APPLICATION FOR PERMIT RENEWAL AND MODIFICATION
SANDOVAL COUNTY LANDFILL**

**VOLUME III: ENGINEERING DESIGN AND CALCULATIONS
SECTION 2: SETTLEMENT CALCULATIONS**

ATTACHMENT III.2.D

**SHARMA, HARI .D. AND SANGEETA P. LEWIS. 1994.
*WASTE CONTAINMENT SYSTEMS, WASTE STABILIZATION
AND LANDFILLS: DESIGN AND EVALUATION.*
NEW YORK: JOHN WILEY AND SONS.**

WASTE CONTAINMENT SYSTEMS, WASTE STABILIZATION, AND LANDFILLS: DESIGN AND EVALUATION

HARI D. SHARMA, PH.D., P.E.

Chief Engineer and Director
EMCON Associates
San Jose, California

SANGEETA P. LEWIS, P.E.

Project Manager
CH₂M Hill
Oakland, California



A Wiley-Interscience Publication

JOHN WILEY & SONS, INC.

New York / Chichester / Toronto / Brisbane / Singapore

APPENDIX B

SETTLEMENT ANALYSES

Landfill settlement analyses include both foundation and refuse settlements. Foundation settlements are important in designing appropriately graded LCRSs, since these are typically gravity-flow systems. Refuse settlements are important in final cover design and estimating final landfill capacity. Estimating refuse settlements has also been critical in designing vertical landfill expansions and structures constructed on closed landfills.

Foundation settlement analyses for landfills follow the same principle as traditional geotechnical engineering settlement analyses. In this appendix we therefore focus on refuse settlements. For ease in reference, however, a brief discussion of foundation settlements is provided. The reader is referred to introductory geotechnical engineering textbooks if explanation is required on soil settlement and consolidation theories.

B.1 FOUNDATION SETTLEMENT

B.1.1 Mechanisms

For cohesive soils, settlement is characterized by the following three mechanisms:

- Immediate settlement following load application
- Consolidation settlements, which occur gradually as excess pore pressure caused by the applied loads are dissipated
- Secondary compression of the soil skeleton

Consolidation and secondary compression occur over several years and are theoretically never complete.

For granular soils, settlement is caused primarily by the compression of the soil skeleton as the particles rearrange due to the applied loads. Due to the relatively high permeability of granular soils, excess pore pressures induced by the applied load are assumed to dissipate in a very short period of time, and settlement is assumed to occur within a short period following load application; this is sometimes called immediate settlement.

B.1.2 Calculation of Settlement

For cohesive soils the total amount of consolidation settlement can be calculated using the following equation:

$$s = \Delta H = \frac{\Delta e}{1 + e_0} H_t \quad (\text{B.1})$$

where s = settlement

ΔH = change in height of layer

Δe = change in void ratio

e_0 = initial void ratio

H_t = layer thickness

Equation (B.1) can be modified as follows to suit the parameters obtained from a consolidation test:

$$s = \Delta H = \frac{C_c H_t}{1 + e_0} \left(\log \frac{P_0 + \Delta P}{P_0} \right) \quad (\text{B.2})$$

where C_c = consolidation index or compression index

P_0 = initial stress

ΔP = change in stress

For an infinite layer of soil, the change in stress is relatively easy to calculate and is typically equal to the change in applied load or overburden. However, since most aboveground landfills may be considered embankment loads, the subsurface stress distribution may be calculated using the influence chart shown in Figure B.1 for embankments of infinite length (Osterberg, 1957; U.S. Dept. of the Navy, 1982).

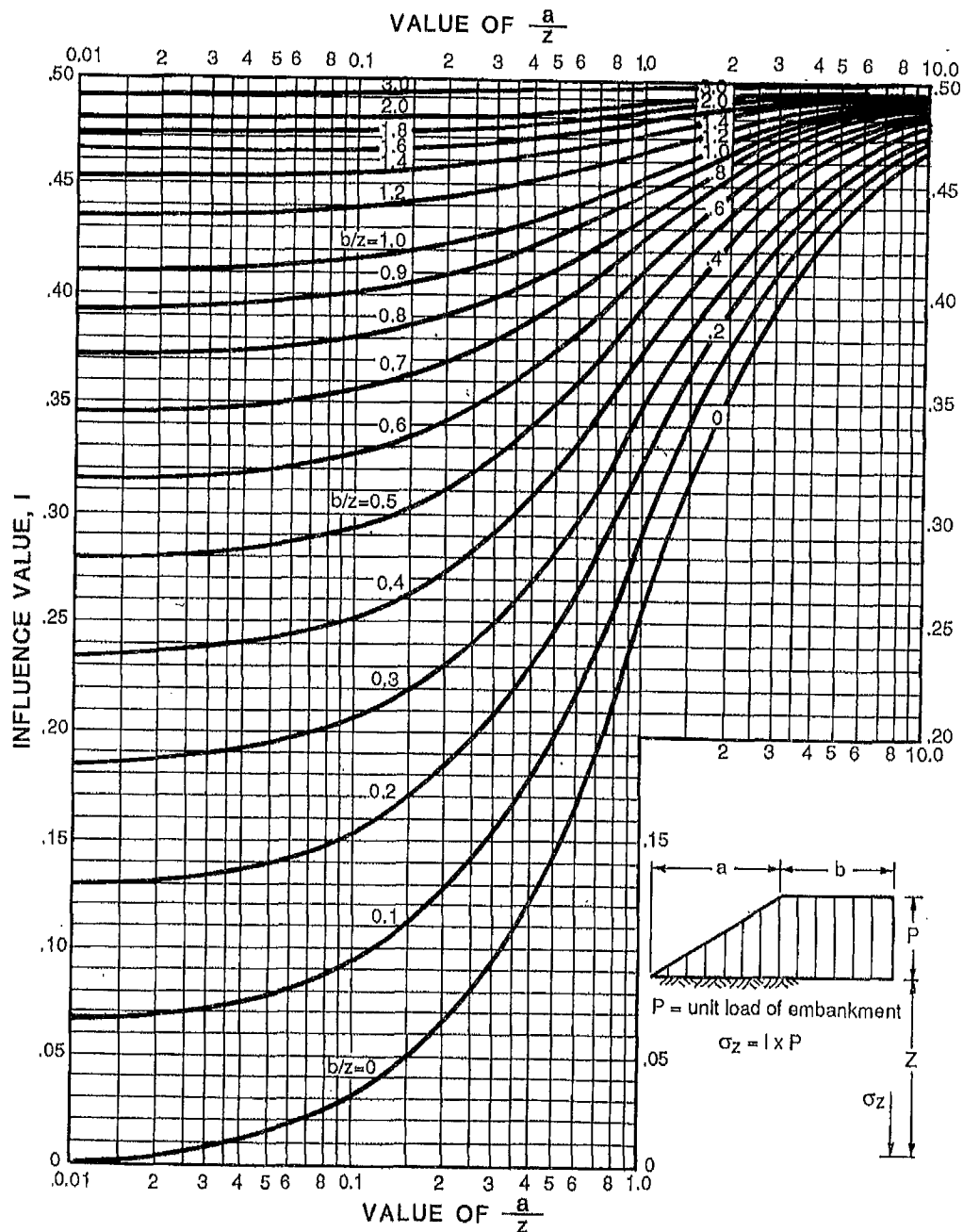


Figure B.1 Influence value for vertical stress under embankment load of infinite length. (From U.S. Dept. of the Navy, 1982.)

B.1.3 Liquefaction

B.1.3.1 Liquefaction Potential. In seismic regions, significant foundation settlements may also occur due to liquefaction of loose to medium-dense saturated cohesionless soils. Liquefaction is defined as a process where high shear deformations, typically induced by seismic activity, results in a progressive buildup of pore pressure. With limited drainage during the short period that the shear load is in-

**APPLICATION FOR PERMIT RENEWAL AND MODIFICATION
SANDOVAL COUNTY LANDFILL**

**VOLUME III: ENGINEERING DESIGN AND CALCULATIONS
SECTION 2: SETTLEMENT CALCULATIONS**

ATTACHMENT III.2.E

STEPHENS, DANIEL B.; HSU, KUO-CHIN; PRIEKSAT, MARK A.; ANKENY, MARK D.; BLANDFORD, NEIL; ROTH, TRACY L.; KELSEY, JAMES A.; WHITWORTH, JULIA R. 1997. A COMPARISON OF ESTIMATED AND CALCULATED EFFECTIVE POROSITY. *HYDROGEOLOGY JOURNAL* (1998) 6:156–165.

A comparison of estimated and calculated effective porosity

Daniel B. Stephens · Kuo-Chin Hsu
Mark A. Prieksat · Mark D. Ankeny
Neil Blandford · Tracy L. Roth · James A. Kelsey
Julia R. Whitworth

Abstract Effective porosity in solute-transport analyses is usually estimated rather than calculated from tracer tests in the field or laboratory. Calculated values of effective porosity in the laboratory on three different textured samples were compared to estimates derived from particle-size distributions and soil-water characteristic curves. The agreement was poor and it seems that no clear relationships exist between effective porosity calculated from laboratory tracer tests and effective porosity estimated from particle-size distributions and soil-water characteristic curves. A field tracer test in a sand-and-gravel aquifer produced a calculated effective porosity of approximately 0.17. By comparison, estimates of effective porosity from textural data, moisture retention, and published values were approximately 50–90% greater than the field calibrated value. Thus, estimation of effective porosity for chemical transport is highly dependent on the chosen transport model and is best obtained by laboratory or field tracer tests.

Résumé La porosité effective dans les analyses de transport de soluté est habituellement estimée, plutôt que calculée à partir d'expériences de traçage sur le terrain ou au laboratoire. Les valeurs calculées de la porosité effective au laboratoire sur trois échantillons de textures différentes ont été comparées aux estimations provenant de distributions de taille de particules et de courbes caractéristiques sol-eau. La concordance était plutôt faible et il semble qu'il n'existe aucune relation claire entre la porosité effective calculée à partir des expériences de traçage au laboratoire et la porosité effective estimée à partir des distributions de taille de parti-

cules et de courbes caractéristiques sol-eau. Une expérience de traçage de terrain dans un aquifère de sables et de graviers a fourni une porosité effective calculée d'environ 0,17. En comparaison, les estimations de porosité effective de données de texture, de teneur en eau et les valeurs publiées étaient environ 50 à 90% plus fortes que la valeur calibrée sur le terrain. Ainsi, l'estimation de la porosité effective pour le transport en solution dépend fortement du modèle de transport utilisé et est préférable lorsqu'elle est obtenue à partir d'expériences de traçage de laboratoire ou de terrain.

Resumen La porosidad efectiva en el análisis del transporte de solutos se suele estimar, en lugar de calcularse a partir de ensayos de trazadores en el campo o el laboratorio. Los valores calculados de la porosidad efectiva en el laboratorio en tres muestras de distintas texturas se compararon con las estimaciones realizadas a partir de las distribuciones de tamaño de partículas y de las curvas características suelo-agua. El ajuste fue bastante pobre y parece que no existe una relación clara entre los valores de la porosidad efectiva calculados mediante los tres métodos. Un ensayo de trazadores en el campo, en un acuífero formado por arenas y gravas, dio lugar a un valor de porosidad efectiva calculado de 0.17. Las estimaciones realizadas a partir de los datos de textura, humedad retenida y valores publicados eran entre un 50–90 por ciento mayores que el valor calibrado en el ensayo de campo. Así, la estimación del valor de la porosidad efectiva para el transporte químico depende mucho del modelo de transporte seleccionado y es mejor si se obtiene a partir de ensayos de laboratorio o de campo.

Key words laboratory experiments measurements · tracer tests · unconsolidated sediments · numerical modeling

Introduction

Modeling the transport of contaminants in groundwater has become a common and sometimes routine task for many practitioners in the field of hydrogeology over the past 15 years. Usually, hydraulic conductivity, and to a much lesser extent dispersivity, are the focus of field and laboratory data-collection efforts for models

Received, March 1997
Revised, August 1997
Accepted, August 1997

Daniel B. Stephens (✉) · Kuo-Chin Hsu · Mark A. Prieksat
Mark D. Ankeny · Neil Blandford · Tracy L. Roth
James A. Kelsey
Daniel B. Stephens and Associates, Inc., 6020 Academy Road
NE, Albuquerque, New Mexico 87109, USA
Fax: +505-822-8877
e-mail: dbsteph@dbstephens.com

Julia R. Whitworth
New Mexico Institute of Mining and Technology, Socorro,
New Mexico 87801, USA

that are based on the advection–dispersion equation (ADE). A third hydraulic parameter required for transport modeling is effective porosity. For aquifer simulations, it has become common practice to estimate effective porosity from one's experience or the literature.

Effective porosity is generally defined for solute transport as that portion of the soil or rock through which chemicals move, or that portion of the media that contributes to flow (Fetter 1993; Domenico and Schwartz 1990). Horton et al. (1987) added some confusion by defining effective porosity as that part of the pore space where velocity is greater than the average fluid velocity. However, its in simplest and traditional form, effective porosity n_e is

$$n_e = \frac{q}{v} \quad (1)$$

where v is the mean velocity of a conservative tracer and q is the specific discharge, or Darcy velocity (e.g., Bear and Verruijt 1987). It is well recognized that effective porosity is less than the total porosity, because, even if the medium is fully saturated, not all of the water-filled pores are interconnected or contribute to flow. Therefore, terms such as mobile and immobile water or dead-end pores are also used in reference to the definition of effective porosity. In fact, Luckner and Schestakow (1991) equate effective porosity and mobile water content. In this paper we review some of the methods to derive effective porosity in the laboratory and field and assess their validity.

Determining effective porosity from tracer tests is not common practice. Field tracer tests are rare because of their expense, duration, and the impacts of the tracer on the aquifer may not be tolerated by regulators. Laboratory tracer tests are uncommon because the core samples are small and potentially unrepresentative of the aquifer at the scale of interest. Furthermore, laboratory cores are almost always vertical and perpendicular to the bedding, whereas aquifer flow and transport are predominantly horizontal; consequently, column tracer tests may poorly reproduce field conditions. Another reason that effective porosity is not often evaluated is that it has a small range of variability compared with hydraulic conductivity and dispersivity. Nevertheless, in the application of transport models, which in practice is often driven by environmental regulation and litigation, a need exists to justify the data that go into transport models with some type of measurement.

For the above reasons, effective porosity is most often obtained from other measured parameters, such as specific yield, or total porosity minus specific retention or residual water content. For example, Bear (1972, p. 484) defines effective porosity as the drainable porosity or the total porosity minus the field capacity. He indicates that for conditions of homogeneous soils and deep water tables, specific yield and effective porosity are identical. Practitioners in hydrogeology have been

attracted to this apparent identity, and they estimate effective porosity from the convenient relationship between particle size and specific yield, shown in *Figure 1*, that is included in most standard textbooks. Although effective porosity has been assigned two different definitions, many assume that the resulting two values are numerically equivalent. Unfortunately, many appear to have forgotten the caution issued by Bear (1972, p. 8) not to confuse effective porosity defined in the context of transport with effective porosity that pertains to drainage and capillary processes. Despite the obvious distinction, effective porosity defined by the latter is often used in simulating groundwater contamination and seems to have gained acceptance as a surrogate for the transport effective porosity without much challenge. For example, Boutwell et al. (1986) state “Most transport equations use effective porosity which does not include dead-end and unconnected pores. Effective porosity approximately equals specific yield.”

The purpose of this article is to evaluate the reliability of methods in estimating effective porosity from drainage and capillary measurements as well as particle size. Column tracer experiments were conducted in the laboratory to determine effective porosity, and these results were compared with estimates of effective porosity derived from soil–water characteristic curves and particle size. The second part of this article compares results of a field tracer test, where effective porosity was obtained by model calibration, to estimates of effective porosity derived from soil–water characteristic curves and particle size.

Calculating Effective Porosity for Transport

Effective porosity as required in groundwater transport models can be determined by laboratory and field techniques. Approaches to making these determinations are presented here, but the scope of the article precludes a comprehensive historical review or critique of

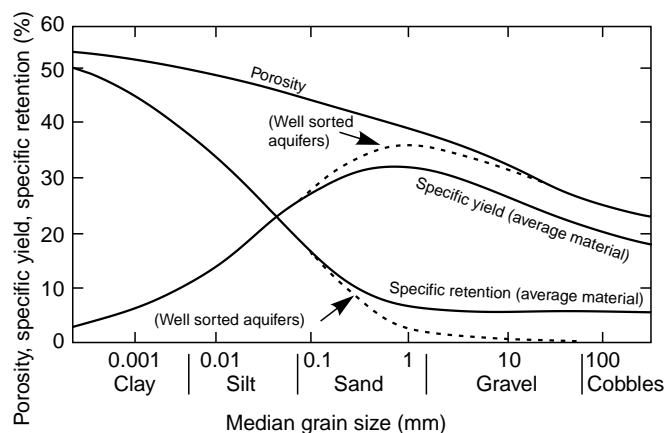


Fig. 1 Relationship between median grain size and water-storage properties of alluvium

all methods available. Such a thorough review has not been published to our knowledge, although excellent discussions of effective porosity in transport processes are in Norton and Knapp (1977), de Marsily (1986), Peyton et al. (1985), and elsewhere.

Laboratory Methods

For traditional solute-transport modeling, effective porosity (n_e) can be defined as the ratio between Darcy flux and seepage velocity, where q is experimental Darcy flux and v is seepage velocity (Eq. (1)). Laboratory apparatus for evaluating transport consists of a column packed with the media to be tested, fittings to maintain a constant flow rate through the column, fittings to inject tracers into the upstream end of the column, and a means to collect samples of outflow periodically for chemical analyses. Darcy flux can be calculated directly from the steady flow rate and column diameter, but seepage velocity depends on the conceptual transport model chosen.

If it is assumed that transport is a chemical and physical equilibrium process, solute transport can be modeled with a single porosity model described by the ADE

$$R \frac{\partial c}{\partial t} + v_i \frac{\partial c}{\partial x_i} = \frac{\partial}{\partial x_i} \left(D_{ij} \frac{\partial c}{\partial x_j} \right) \quad i, j = 1, 2, 3 \quad (2)$$

where R is the retardation factor, c is the solute concentration, v_i is the seepage velocity component in the x_i direction, and D_{ij} is the component of the dispersion coefficient tensor. This model assumes that degradation and chemical production are not significant. The mobile-flow pore space is represented by a single effective porosity and is used to estimate seepage velocity. Advective and diffusive processes are active within the pore space designated as effective porosity.

If it is assumed that there is no retardation, then the traditional column-testing approach can utilize the analytical solution of a one-dimensional version of Eq. (2) with constant inlet concentration, c_0 , and zero initial concentration

$$\frac{c}{c_0} = \frac{1}{2} \left[1 \pm \operatorname{erf} \left(\frac{x - vt}{2\sqrt{Dt}} \right) \right] \quad (3)$$

where erf is the error function. The relative concentration point ($c/c_0 = 0.5$) describes solute moving at the average velocity and for a nonreactive tracer $c/c_0 = 0.5$ should occur when one pore volume of solution has flowed from the column. Using the measured elapse time, $t_{0.5}$ at $c/c_0 = 0.5$, the known column length, L , and experimental Darcy flux, q , the effective porosity can be calculated as

$$n_e = \frac{L}{t_{0.5} q} \quad (4)$$

This approach is similar to determining n_e with Eq. (1), because $L/t_{0.5}$ is essentially the average solute velocity

eluting from the column. Luckner and Schestakow (1991) describe a three-step tracer test in short columns designed explicitly to quantify effective porosity.

Shackelford (1995) proposed a cumulative mass approach to derive effective porosity from breakthrough curves. A cumulative mass ratio (CMR) is calculated from

$$\text{CMR} = \frac{\sum \Delta m}{V_p c_0} = \frac{R_d}{2 P_L} [(\xi_4 - \xi_2) \operatorname{erfc}(\xi_1) + (\xi_4 + \xi_2) \exp(\xi_2) \operatorname{erfc}(\xi_3)] \quad (5)$$

where

$$\xi_1 = \frac{R_d - T}{2 \sqrt{\frac{TR_d}{P_L}}}; \quad \xi_2 = P_L; \quad \xi_3 = \frac{R_d + T}{2 \sqrt{\frac{TR_d}{P_L}}};$$

and $\xi_4 = \frac{TP_L}{R_d}$ (6)

T is the number of pore volumes of flow, R_d is the retardation factor, and P_L is the column Péclet number. The CMR is plotted vs T and the slope of the plot during steady-state transport is unity, given by

$$\lim_{T \rightarrow \infty} \frac{d(\text{CMR})}{dT} = \lim_{T \rightarrow \infty} \frac{1}{2} [\operatorname{erfc}(\xi_1) + \exp(\xi_2) \operatorname{erfc}(\xi_3)] = 1 \quad (7)$$

The unit slope is plotted to determine the x -axis intercept and is designated as T_0 representing the retardation factor R_d . The measured value of T_0 for a nonreactive tracer ($R_d = 1$) represents the ratio of n_e/n . Thus, effective porosity is derived by multiplying this ratio by the total porosity.

Kinetic adsorption and heterogeneous flow regions cause chemical and physical non-equilibrium, respectively. Two-site/two-region transport models (van Genuchten and Wagenet 1989) have been proposed to describe non-equilibrium phenomenon. The two-site/two-region model can be described in dimensionless form as

$$\beta R \frac{\partial C_1}{\partial T} + \frac{\partial C_1}{\partial Z} = \frac{1}{P} \frac{\partial^2 C_1}{\partial Z^2} + \omega(C_1 - C_2) \quad (8)$$

$$(1 - \beta) R \frac{\partial C_2}{\partial T} = \omega(C_1 - C_2) \quad (9)$$

where β is the partition coefficient, P is the Péclet number (defined as vL/D), C_1 is the concentration at equilibrium site, C_2 is the concentration at non-equilibrium site, and ω is a dimensionless mass transfer coefficient. For the two-region model when $R = 1$, β is the ratio of the mobile-water region to total porosity. The pore space is divided into two parts, the mobile-water region, where equilibrium processes occur, and the immobile region, where non-equilibrium processes occur. Both advection and diffusion occur in the mobile region, but only first-order kinetic processes occur in the immobile region. Toride et al. (1995) present a versatile

software program, CXTFIT, for evaluating solute breakthrough curves. The program optimizes the parameters by fitting curves to measured data for a range of conceptual models, including the mobile/immobile water model presented in Eqs. (8) and (9).

Breakthrough curves obtained from laboratory column tests can be described by a one-dimensional version of Eq. (2), where v and D are viewed as constants or by Eqs. (8) and (9). The decision to apply the equilibrium or non-equilibrium model may be judged using selection criteria presented by Carrera et al. (1990). The complex non-equilibrium model may be more representative of the soil system, but the equilibrium model is generally easier to use.

However, extrapolation of column-test results to field scales is still viewed with some skepticism. Therefore, several methods for determining effective porosity from field solute-transport experiments are presented.

Field Methods

Effective porosity can be obtained from field-scale well-tracer tests, in which a tracer is injected into a well and is pumped back from either the same injection well or from another well. For example, Hall et al. (1991) propose a method to estimate effective porosity in a homogeneous confined aquifer dominated by steady-state horizontal advective transport with a constant hydraulic gradient. They use Darcy's equation, with an added effective-porosity term from Eq. (1).

$$V = \frac{KI}{n_e} \quad (10)$$

and a version of the equation for the drift and pump-back test described by Leap and Kaplan (1988).

$$V = \frac{(Qt/\pi n_e b)^{1/2}}{d} \quad (11)$$

where K is the horizontal hydraulic conductivity; I is the horizontal hydraulic gradient; Q is pumping rate during recovery of tracer, t is the time elapsed from the start of pumping until the center of mass of the tracer is recovered; b is the aquifer thickness; and d is the time elapsed from the injection of tracer until the center of the mass of tracer is recovered. From Eqs. (11) and (12), effective porosity can be calculated as

$$n_e = \frac{\pi b K^2 I^2 d^2}{Qt} \quad (12)$$

A single-well borehole dilution test (Drost et al. 1968; Halevy et al. 1967; Grisak et al. 1977) can be conducted by injection and subsequent withdrawal of a tracer in a single well through a zone isolated by dual packers. Seepage velocity v can be calculated as

$$v = -\frac{V}{\beta A t} \ln\left(\frac{c}{c_0}\right) \quad (13)$$

where V is volume of the borehole interval with verti-

cal cross-sectional area A , β is a geometric factor ranging from 0.5–4.0, t is time, c is recovered tracer concentration, and c_0 is the concentration of introduced tracer. Effective porosity can then be calculated from Eq. (1) if specific discharge can be calculated from hydraulic conductivity K and hydraulic gradient I .

Two-well tests can be performed in both confined and unconfined aquifers (Gaspar and Oncescu 1972). One well is pumped at a constant flow rate Q , and when the flow rate is at a quasi-steady state, a tracer is injected into the other well at distance L from the pumping well. The concentration recovered from the pumping well is recorded over time. For a horizontal confined aquifer with thickness D , the effective porosity is calculated as

$$n_e = \frac{Qt_i}{\pi L^2 D} \quad (14)$$

where t_i is the travel time of the tracer between the injection and pumping wells. For an unconfined aquifer with negligible natural gradient, effective porosity can be calculated as

$$n_e = \frac{Qt_i}{\pi L^2 \left(h - \frac{Q}{4\pi k h} \right)} \quad (15)$$

where h is the hydraulic head in the well where the tracer was introduced. This method is effective if the wells span the thickness of the aquifer layer and if $L \gg h$ (Halevy and Nir 1962).

Another approach is to use solute-breakthrough data obtained from field tracer tests to calibrate the transport parameters of the model. However, since the numerical solution to most field-scale problems of non-reactive transport is non-unique (Molson and Frind 1990), the information obtained from model calibration may be valid only for the conceptual model used during calibration. Effective porosity is then a calibrated value that gives the best fit to measured solute breakthrough.

Laboratory Tracer Tests

Three soil materials (sand, silica flour, and a mixture of 75% fine sand and 25% silica flour) were chosen for testing. The sand, silica flour, and mixture columns were hand packed in the laboratory. Soil columns for the solute-breakthrough tests and hydraulic-properties tests were packed concurrently into a column comprised of brass cylinders to ensure that both columns would have similar physical and hydrologic characteristics.

Brass cylinders approximately 5 cm in diameter were cut to lengths of approximately 5 and 10 cm. The columns were prepared by securing one 5-cm-length and one 10-cm-length of brass cylinder together, end to end, using tape. The air-dry soil material was then poured

into the cylinder while gently tapping and shaking the cylinder, to insure uniform settling and packing, until the column was full. The cylinders were separated and trimmed flat on the ends. The 10-cm section was used for the solute-transport and breakthrough analysis, and the 5-cm portion was used for hydraulic-properties testing.

The repacked samples were placed in permeameters, and saturated hydraulic conductivities, K_s , were determined using constant and falling-head methods. Values of K_s are shown in Table 1. Soil-water characteristics for drainage were determined using hanging-column, pressure-plate, and thermocouple psychrometer analysis. Data from the moisture-retention analyses, shown in Figure 2, were fit using the RETC computer code (van Genuchten et al. 1991), and the results are shown in Table 1. The total porosity is equal to the saturated water content, θ_s , and is very close to the calculated porosity value obtained using the dry bulk density and an assumed particle density of 2.65 g/cm^3 .

Recognizing that the pressure potential used to determine residual moisture content will affect the moisture-retention analysis (Stephens and Rehfeldt 1985; Corey 1994), residual water contents (θ_r) were determined by using pressure potentials of -0.33 bar (Ahuja 1989) and -15 bar (Table 1).

Solute breakthrough tests, using a tritium tracer, were performed on the 10-cm-long repacked soil columns; results are shown in Table 2. The columns were oriented vertically and the flow direction was upward. A 0.05-M calcium sulfate–water solution was delivered from a reservoir to the columns using a peristaltic pump. The soil columns were periodically removed from the system and weighed to determine the extent of saturation. When the column weights were constant, the columns were considered to be saturated. Outflow solution was collected, using fraction collectors, for several days to determine column fluxes. After column fluxes had been determined, a tritium solute was then introduced into the influent solution. Activity of outflow samples and samples of the influent solutions were determined using a scintillation counter.

Solute-breakthrough data were analyzed using the CXTFIT (version 2.0) code (Toride et al. 1995). Both equilibrium and non-equilibrium models were fit to the tritium-breakthrough results. Effluent samples were assumed to represent flux-averaged concentrations. Because tritium approximates a conservative tracer, the retardation factor was set to 1 for all fitting procedures. The program was allowed to fit all other parameters, i.e., in the equilibrium model, mean pore velocity and dispersion are fitted, and in the non-equilibrium model two additional parameters, β and ω , are fitted. Measured data and fitted curves are shown in Figure 3. Calculated values of pore velocity and dispersion coefficient determined by fitting the equilibrium and non-equilibrium models are shown in Table 3. For the non-equilibrium model, $v = v_m$, the velocity through the mobile pores.

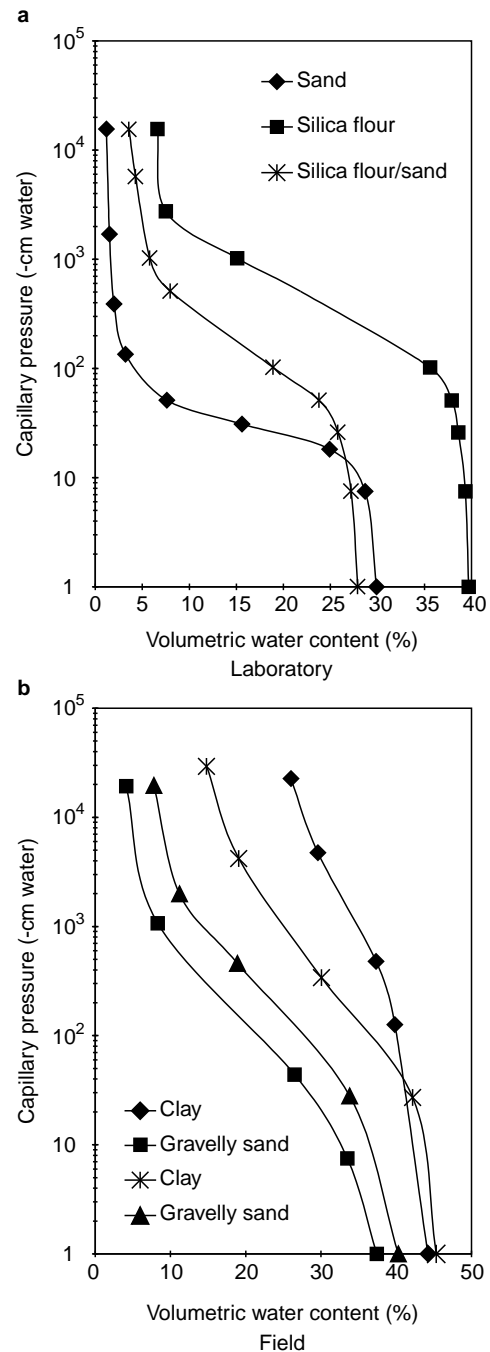


Fig. 2a,b Curves of soil-water characteristics

Effective porosity is calculated from Eq. (1) knowing q from the experimental flow rate (Table 2) and v obtained by analyses of the breakthrough curve using the CXTFIT program (Table 3). For the non-equilibrium model, one could presume that β , the mobile water content/porosity ratio, multiplied by the total porosity would also represent effective porosity.

Cumulative effluent solute mass was also measured for each column and the data were analyzed to compute effective porosity with Shackleford's cumulative-mass approach (Eqs. (5)–(7)).

Table 1 Laboratory hydraulic properties of soils used in the laboratory tracer tests and soils from the field site

Soil type	ρ_b (g/cm ³)	K_s (cm/sec)	θ_r (-1/3 bar) (cm ³ /cm ³)	θ_r (-15 bar) (cm ³ /cm ³)	θ_s (cm ³ /cm ³)	d_{50} (mm)
Sand	1.86	5.2×10^{-3}	0.024	0.011	0.300	0.13
Silica	1.60	1.6×10^{-5}	0.263	0.066	0.397	0.024
Sand/Silica Mixture	1.94	4.6×10^{-5}	0.124	0.036	0.279	0.091
Field 1 – Clay	1.48	2.0×10^{-8}	0.387	0.279	0.442	0.0065
Field 2 – Gravelly Sand	1.66	1.6×10^{-3}	0.157	0.046	0.374	8.7
Field 3 – Sandy Clay	1.45	2.3×10^{-6}	0.307	0.163	0.453	0.038
Field 4 – Gravelly Sand	1.58	4.7×10^{-4}	0.215	0.093	0.403	2.7

ρ_b : Bulk density
 K_s : Saturated hydraulic conductivity
 θ_r : Residual water content
 θ_s : Saturated water content
 d_{50} : Median grain size
 Porosity

Table 2 Laboratory tracer test conditions

Soil Type	Flow rate, Q (cm ³ /hr)	Inlet Pulse Duration (hr)	Column Cross Section, A (cm ²)	Column Length, L (cm)	Darcy flux, q (cm/hr)
Sand	24.40	12.35	42.21	10.045	0.578
Silica	19.79	21.5	42.21	9.124	0.469
Sand/Silica Mixture	16.89	13.1	42.21	9.737	0.400

Table 3 Transport parameters from laboratory experiments

Soil Type	Equilibrium Model		Non-Equilibrium Model			
	v (cm/hr)	D (cm ² /hr)	v (cm/hr)	D (cm ² /hr)	β	ω
Sand	1.339	7.76	5.621	2.24	0.2665	1.556
Silica	1.139	12.29	1.674	6.60	0.3221	0.1612
Sand/Silica Mixture	1.15	2.197	18.67	6.6×10^{-3}	0.068	6.16

v = Pore-water velocity
 D = Hydrodynamic dispersion coefficient
 $\beta = \theta_m/\theta$, where θ_m is the volumetric water content of mobile liquid phase and θ is total water content
 $\omega = \alpha L/\theta v$, where L is characteristic length, and α is a first-order kinetic rate coefficient

Table 4 Estimated and calculated effective porosity in soil columns

Soil Type	Calculated			Estimated		
	Equilibrium Model	Non-Equilibrium Model	Cumulative Mass Approach	Particle Size	$n-\theta_r$ (0.3b)	$n-\theta_r$ (15b)
Sand	0.431	0.102	0.248	0.32	0.276	0.289
Silica	0.412	0.280	0.159	0.20	0.134	0.331
Sand/Silica Mixture	0.348	0.021	0.261	0.30	0.155	0.243

Table 4 summarizes the laboratory measured and estimated effective-porosity results. The equilibrium-model parameters resulted in effective porosity values that were greater than the total porosity (Table 1) for each soil and were deemed to be unreasonable. The non-equilibrium model gave the best fit to the experimental breakthrough data. However, the calculated effective porosity represented only approximately 33, 70, 7% of the saturated water content for the sand, silica,

and sand/silica mix, respectively. The cumulative-mass approach provided estimates of effective porosity that appear intuitively more reasonable, inasmuch as the effective porosity comprises approximately 83, 40, and 93% of the saturated water content for the sand, silica, and sand/silica mix.

The β parameter from the non-equilibrium model (Table 3), when multiplied by total porosity, θ_s (Table 1), gives θ_m , the mobile water content. The respec-

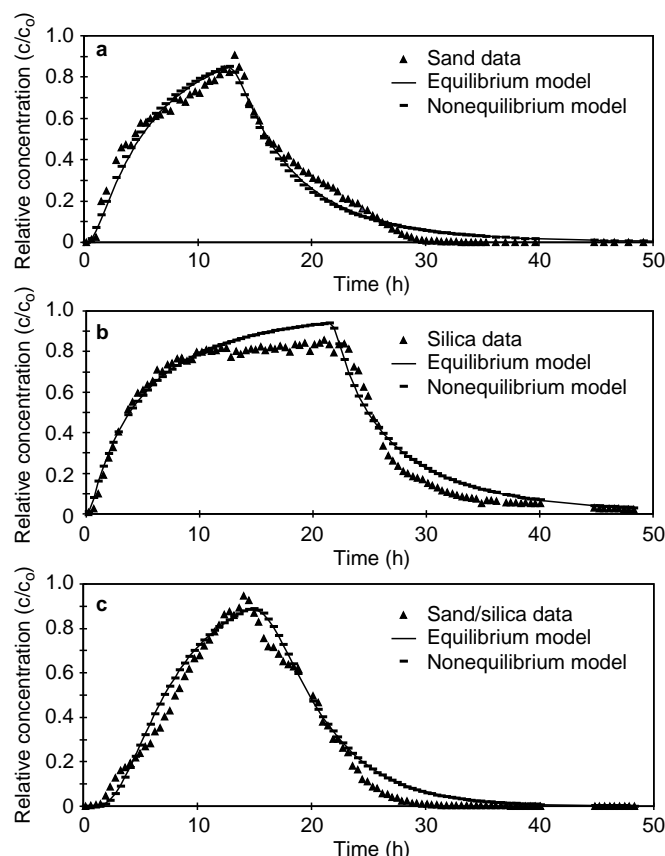


Fig. 3 Observed and fitted tritium breakthrough concentration for fine sand, silica flour, and sand/silica mixture

tive values of θ_m are 0.08 for sand, 0.128 for silica, and 0.02 for the sand/silica mix. The mobile water content is similar to the effective porosity calculated by *Eq. (1)*, except for silica. The reason for the poor agreement for silica is not clear.

Among the methods to estimate effective porosity of a specific soil, significant variability is evident. The estimated effective porosity from particle size (i.e., *Fig. 1*) tends to be most similar to effective porosity calculated by the cumulative-mass approach. The estimated effective porosity based on porosity minus the 0.33-bar water content gives reasonable agreement with calculated values from cumulative-mass approach, except for the sand/silica mix. The estimated effective porosity calculated as porosity minus the 15-bar water content gives fair agreement to effective porosity calculated for the sand and the sand/silica mix from the cumulative-mass approach; but for silica, porosity minus 15-bar water content overestimates the values from cumulative-mass approach by more than 100% and is actually closer to the effective porosity calculated the from non-equilibrium model.

Due to the scatter in calculated values of effective porosity for each soil, it is not possible to discern which model provided the most accurate estimate of effective porosity. The value of effective porosity appears to be

dependent on the conceptual model chosen for transport. Wide scatter also exists in the estimated values of effective porosity. Consequently, it is not possible based on these experiments to establish any relationship between estimated and calculated effective porosity, even for homogeneous soil.

Sources of uncertainty also exist in the analysis of the tracer experiments. For example, at the low Péclet numbers (0.9–5.2) in these short-column tests, the breakthrough curves are probably sensitive to boundary conditions. In the usual application of the equilibrium models, instead of obtaining v by fitting, one assumes that v is known from q/θ_s (Parker 1984). However, this would preclude us from obtaining effective porosity from *Eq. (1)*. Likewise, the velocity can be specified in the non-equilibrium model and effective porosity calculated from $\beta\theta_s$. Unfortunately, without constraints on more parameters, the calculated values of effective porosity from the popular code CXTFIT vary considerably. Perhaps special tracer tests, such as those described by Luckner and Schestakow (1991), would provide more definitive calculations of effective porosity in the laboratory.

Field Tracer Test

A groundwater reclamation system constructed to remediate contamination at the Tucson International Airport Superfund site (in Arizona, USA) afforded an opportunity to determine effective porosity in the field. The reclamation well field, which began operation in 1987, consists of extraction wells that pump contaminated water to a treatment plant where sulfuric acid is added to the treated water prior to reinjection. Sulfate in excess of background concentrations was considered as a conservative tracer in groundwater. Groundwater monitor wells were sampled periodically as part of the routine system performance assessment. A portion of the reclamation system consisting of the area near injection well R-5 and monitor well M-6 was used for analyzing the breakthrough data. This area and a geologic cross section are shown in *Figure 4*.

Effective porosity was obtained by calibrating a numerical flow and transport model. The flow code MODFLOW (McDonald and Harbaugh 1988) was used to generate the transient hydraulic-head field in two dimensions in the plan view (*Fig. 4*). The mesh consisted of grid blocks of 37 rows \times 31 columns having dimensions of 25 \times 25 feet. The injection-rate history is known from available metering records; rates ranged from 50–392 gpm. Hydraulic conductivity is 40 feet/day throughout this local domain and is consistent with the regional-scale conductivity field generated by geostatistical analysis of numerous well tests in the area. The storage coefficient is 0.25. The comparison of the model predicted and measured hydraulic head in the monitor well M-6 is presented in *Figure 5*.

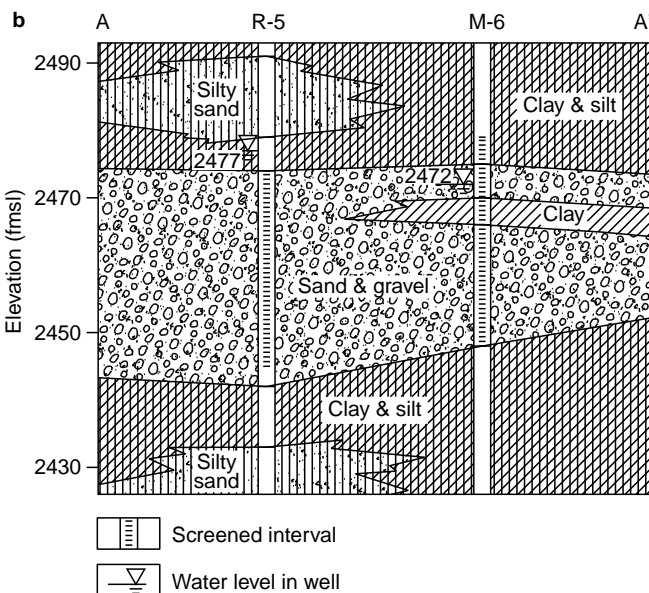
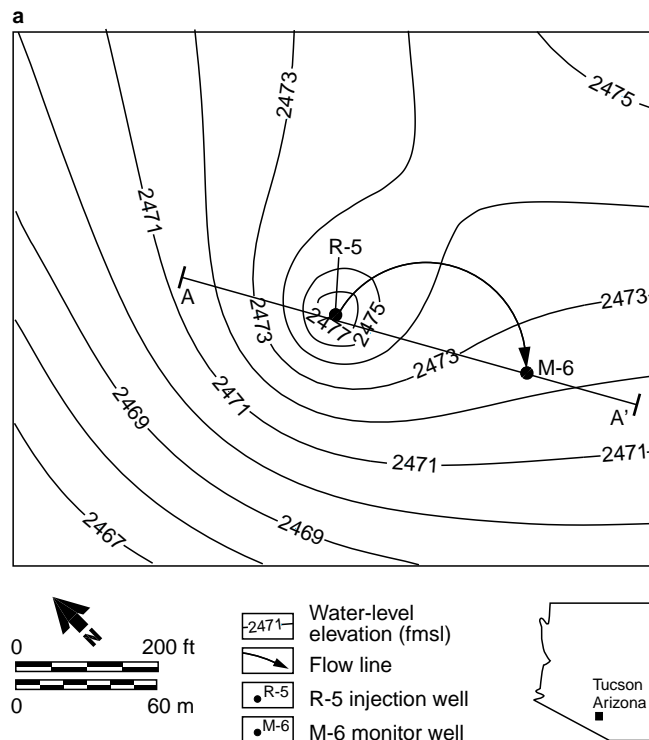


Fig. 4 **a** Water-level elevations and **b** geologic cross section through recharge well R-5 and monitor well M-6, Tucson International Airport Superfund Site, Arizona, USA

For transport, the solute-transport code SURFACT (Hydrogeologic, Inc. 1996) was used which accepted as input the velocity field produced by MODFLOW. Effective porosity was obtained in a trial-and-error process by adjusting the model-assigned effective porosity until a best fit to observed sulfate data was obtained. As part of the calibration process, longitudinal and

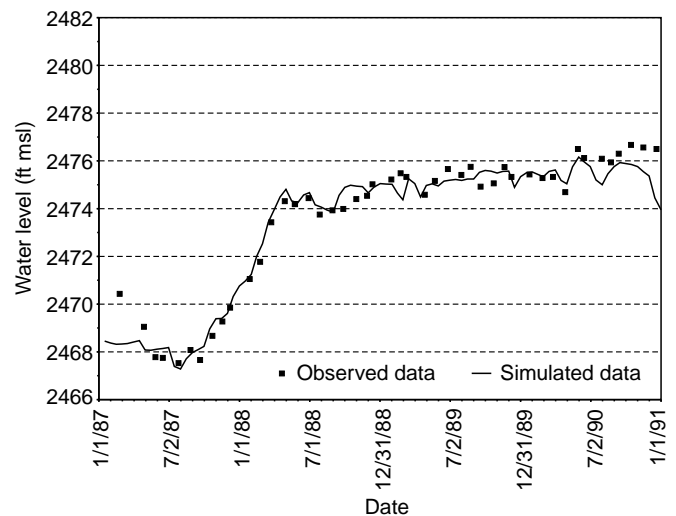


Fig. 5 Observed and predicted water levels in monitor well M-6

transverse dispersivity were also adjusted. The calibration criterion was the minimization of the root mean squared error in concentration

$$\text{RMS} = \left[\frac{1}{n} \sum_{i=1}^n (c_m - c_s)_i^2 \right]^{0.5} \quad (16)$$

where n is the number of monitoring data, c_m is the measured concentration, and c_s is the simulated concentration. The results are shown in *Figure 6*, which demonstrates that there is no unique solution, that the breakthrough curves are much more sensitive to effective porosity than dispersivity ratio, and that the best fit

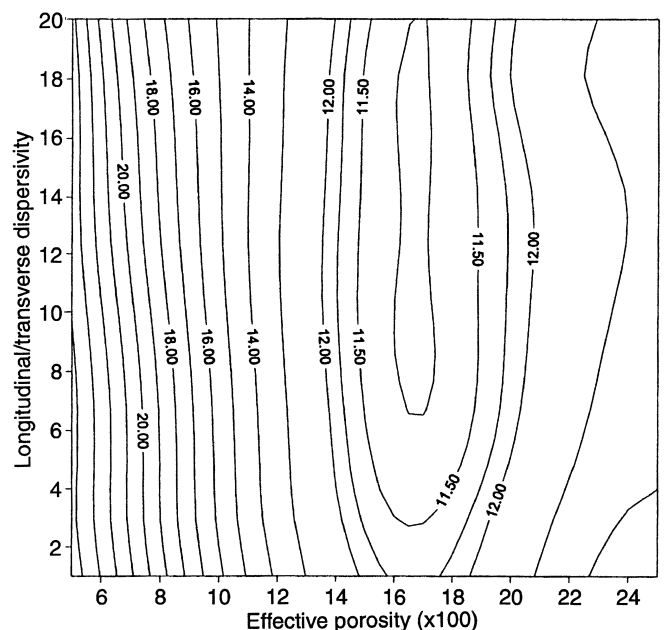


Fig. 6 RMS error from numerical simulation of sulfate breakthrough

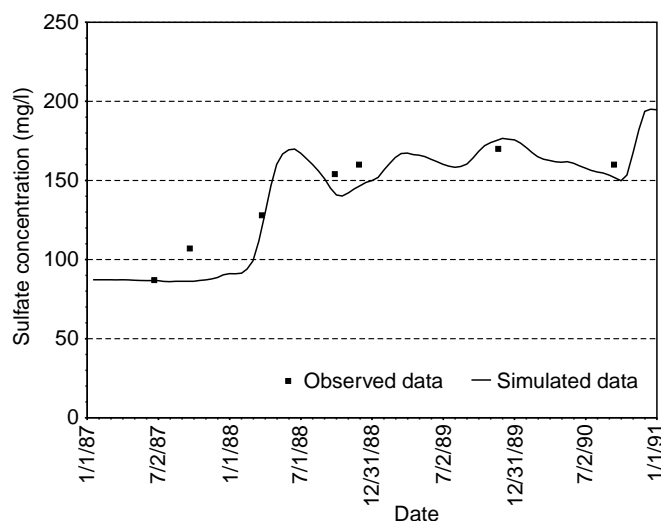


Fig. 7 Observed and predicted sulfate concentrations

to the measured concentration occurs when effective porosity is approximately 0.17. *Figure 7* shows the observed and simulated concentration history for the monitor well.

For comparison, the effective porosity also was inferred using *Figure 1* and estimated median particle size, based on geologic logs of the injection well. The aquifer consists of alluvium that is predominantly sand and gravel, with some layers of silt and clay (*Fig. 4*). Assuming transport occurs primarily in the gravelly sand, the effective porosity is estimated to be 0.32, based on a qualitative evaluation of soil texture. Measured physical properties from two core samples of similar gravelly sand field soils are given in *Table 1*. The measured median particle size by sieve analysis was used in *Figure 1* to determine specific yield. The estimated effective porosity is approximately 0.31.

The effective porosity was also estimated from measured soil–water characteristic curves on two samples of similar sand-and-gravel aquifer material from nearby borings (*Table 1*). For these samples effective porosity, estimated as porosity minus the 15-bar water content, ranges from 0.30–0.32. These values are consistent with effective porosity estimated from the specific yield determined with *Figure 1*, based on soil texture characterized both qualitatively from the geologic description and quantitatively from sieve analysis.

Groundwater models have also been constructed to simulate the regional transport of organic solvents over an area that encompasses this field tracer study area, as well as a plume one mile wide and five miles long. Each of the modelers estimated the effective porosity as 0.25, using professional judgment applied to the predominantly gravelly sand composition of the aquifer (Hargis and Montgomery 1982; Mock 1985; CH2M Hill 1987).

Table 5 summarizes the effective porosity values obtained at the field site. The estimates are approximately 50–90% greater than the measurements obtained from

Table 5 Estimated and calculated effective porosity at field site

Method		Effective Porosity
Calculated	Field Tracer Test	0.17
Estimated	Geologic Logs	0.32
	Measured Particle Size	0.31
	$n-\theta_r$ (15b)	0.32
	Mock (1985)	0.25
	CH2M Hill (1987)	0.25
	Hargis (1982)	0.25

the field tracer test. One practical implication of this result is that the predicted length of the regional TCE plume by the regional transport model using the smaller effective porosity would be at least 1.5 times longer than a plume predicted with the estimated, larger effective porosity.

Conclusion

A comparison of estimated and calculated effective porosity was done in this study. Calculated effective porosity from tracer tests in the laboratory is highly dependent on the chosen conceptual transport model and fitting approach. No consistent agreement was observed between estimated effective porosity and values calculated from laboratory tracer tests. Estimation methods tend to overestimate the transport effective porosity in a field tracer test conducted in a layered aquifer composed predominantly of gravelly sand. Effective porosity for transport cannot be reliably estimated from particle size and specific yield or from measurements of soil–water retention.

Field tracer tests provide the most direct method for obtaining effective porosity, but often they are relatively expensive and time-consuming. However, as in the case study here, model calibration may be a cost-effective approach to determine effective porosity using existing monitor-well time-series data.

Acknowledgment We are grateful to R. Bowman, Geoscience Department, New Mexico Institute of Mining Technology, Socorro, New Mexico, for conducting the laboratory tracer-breakthrough experiments and for his helpful suggestions in the interpretation of data.

References

- Ahuja LR, Cassel DK, Bruce RR, Barnes BB (1989) Evaluation of spatial distribution of hydraulic conductivity using effective porosity data. *Soil Sci Soc Am J* 148:404–411
- Bear J (1972) *Dynamics of fluids in porous media*. Elsevier, New York
- Bear J, Verruijt A (1987) *Modeling groundwater flow and pollution*. Reidel, Dordrecht

- Boutwell SH, Brown SM, Roberts BR, Atwood DF (1986) Modeling remedial actions at uncontrolled hazardous waste sites. Neyes Publications, Park Ridge, New Jersey
- CH2M-Hill (1987) Draft: assessment of the relative contribution to groundwater contamination from potential sources in the Tucson Airport area, Tucson, Arizona, EPA contract no. 68-01-7251, CH2M Hill, Santa Ana, California
- Carrera J, Samper J, Galarza G, Medina A (1990) An approach to process identification: application to solute transport through clays. In: ModelCARE 90: calibration and reliability in groundwater modeling. IAHS Publ 195:231–240
- Corey AT (1994) Mechanics of immiscible fluids in porous media. Water Resource Publication, Fort Collins, Colorado
- Marsily G de (1986) Quantitative hydrogeology: groundwater hydrology for engineers. Academic Press, San Diego, California
- Domenico PA, Schwartz FW (1990) Physical and chemical hydrogeology. Wiley, New York
- Drost W, Klotz D, Koch A, Moser M, Neumaier F, Rauert W (1968) Point dilution methods of investigating groundwater flow by means of radioisotopes. Water Resour Res 4:125–146
- Fetter CW (1993) Contaminant hydrogeology. MacMillan, New York
- Gaspar E, Oncescu M (1972) Radioactive tracers in hydrology. Elsevier, New York
- Grisak GE, Merriott WF, Williams DW (1977) A fluoride borehole dilution apparatus for groundwater velocity measurements. Can Geotech J 14:554–561
- Halevy E, Nir A (1962) The determination of aquifer parameters with the aid of radioactive tracers. J Geophys Res 67 (6): 403
- Halevy E, Moser H, Zellhofer O, Zuber A (1967) Borehole dilution techniques: a critical review. In: Isotopes in Hydrology, IAEA Proc Series, IAEA, Vienna
- Hall SH, Luttrell SP, Cronin WE (1991) A method for estimating effective porosity and ground-water velocity. Ground Water 29:171–174
- Hargis and Montgomery (1982) Digital simulation of contaminant transport in the regions aquifer systems, Tucson Report no. TR-C.4
- Horton R, Thompson ML, McBride JF (1987) Method of estimating the travel time of noninteracting solutes through compacted soil material. Soil Sci Soc Am J 51:48–53
- Hydrogeologic, Inc. (1996) MS-VNS users manual
- Leap DI, Kaplan PG (1988) A single-well tracing method for estimating regional advective velocity in a confined aquifer: theory and preliminary laboratory verification. Water Resour Res 24 (3): 993–998
- Luckner L, Schestakow WM (1991) Migration processes in the soil and groundwater zone. Lewis Publishers, Chelsea, Michigan
- McDonald MG, Harbaugh AW (1988) A modular three-dimension finite-difference groundwater flow model. USGS Open File Rep 83–875
- Mock PA, Travers BC, Williams CK (1985) Results of the Tucson Airport area remedial investigation, phase I, vol II. Tucson Report TR-B.1., pp 88–89
- Molson JW, Frind EO (1990) Perspectives on non-uniqueness in three-dimension transport simulations of biodegrading organic contaminants. In: ModelCARE 90: calibration and reliability in groundwater modeling. IAHS Publ 195:341–350
- Norton D, Knapp R (1977) Transport phenomena in hydrothermal systems: the nature of porosity. Am J Sci 277:913–936
- Parker JC (1984) Analysis of solute transport in column tracer studies. Soil Sci Soc Am J 48 (4): 719
- Peyton GR, Gibb JR, LeFaivre MH, Ritchey JD (1985) On the concept of effective porosity and its measurement in saturated fine-grained porous materials. In: Proc 2nd Canadian/American Conference of Hydrology, National Water Well Association, Dublin, Ohio
- Shackelford CD (1995) Cumulative mass approach for column testing. J Geotech Eng: 696–703
- Stephens DB, Rehfeldt KR (1985) Evaluation of closed-form analytical models to calculate conductivity in a fine sand. Soil Sci Soc Am J 49:12–19
- Toride N, Leij FJ, van Genuchten MTh (1995) The CXTFIT code for estimating transport parameters from laboratory and field tracer experiments. Version 2.0. U.S. Salinity Laboratory Research Rep no. 137
- van Genuchten MTh, Wagenet RJ (1989) Two-site/two-region models for pesticide transport and degradation: theoretical development and analytical solutions. Soil Sci Soc Am J 53:1303–1310
- van Genuchten MTh, Leij FJ, Yates SR (1991) The RETC code for quantifying the hydraulic functions of unsaturated soils. U.S. Salinity Laboratory Research Rep, 83 pp

**APPLICATION FOR PERMIT RENEWAL AND MODIFICATION
SANDOVAL COUNTY LANDFILL**

**VOLUME III: ENGINEERING DESIGN AND CALCULATIONS
SECTION 2: SETTLEMENT CALCULATIONS**

**ATTACHMENT III.2.F
CORRELATIONS OF SOIL PROPERTIES
CARTER, M. AND BENTLEY, S.P. 1991
LONDON: PENTECH PRESS**

Table 5.3 SOME PUBLISHED CORRELATIONS FOR COMPRESSION INDICES (AFTER AZZOUZ ET AL. 1976)

Equation	Regions of applicability
$C_c = 0.007 (LL - 7)$	Remoulded clays
$C_{cr} = 0.208e_0 + 0.0083$	Chicago clays
$C_c = 17.66 \times 10^{-3} w_n^2 + 5.93 \times 10^{-3} w_n - 1.35 \times 10^{-1}$	Chicago clays
$C_c = 1.15(e_0 - 0.35)$	All clays
$C_c = 0.30(e_0 - 0.27)$	Inorganic, cohesive soil; silt, some clay; silty clay; clay
$C_c = 1.15 \times 10^{-2} w_n$	Organic soils-meadow mats, peats, and organic silt and clay
$C_c = 0.75(e_0 - 0.50)$	Soils of very low plasticity
$C_{cr} = 0.156e_0 + 0.0107$	All clays
$C_u = 0.01 w_n$	Chicago clays

As summarized by Azzouz, Krizek, and Corotis (1976).
Note: w_n = natural water content.

clays:

$$C_c = 0.007(LL - 10).$$

Terzaghi and Peck (1967) proposed a similar relationship, based on research with clays of low and medium sensitivity:

$$C_c = 0.009(LL - 10).$$

This relationship has a reliability range of $\pm 30\%$ and is valid for inorganic clays of sensitivity up to 4 (see Chapter 6) and liquid limit up to 100. Based on the work of Skempton and Northey (1952) and Roscoe *et al.* (1958), Wroth and Wood (1978) used critical state soil mechanics considerations to deduce a relationship between compression index and plasticity index (PI) for remoulded clays:

$$C_c = \frac{1}{2} PI \cdot G_s$$

where G_s is the specific gravity of the soil solids. Table 5.3 produced by Azzouz *et al.* (1976) gives a summary of a number of published correlations.

The recompression index, C_{cr} , is defined in the same way as C_c except that it applies to the unloading phase of the consolidation test. Typical values of C_{cr} range from 0.015 to 0.35 (Roscoe *et al.* 1958) and are often assumed to be 5-10% of C_c .

5.1.5 Settlement corrections

If the results of oedometer tests are used directly to calculate settlements, the values obtained tend to over-estimate the settlements

**APPLICATION FOR PERMIT RENEWAL AND MODIFICATION
SANDOVAL COUNTY LANDFILL**

**VOLUME III: LANDFILL ENGINEERING CALCULATIONS
SECTION 3: SLOPE STABILITY ANALYSIS**

TABLE OF CONTENTS

1.0	LANDFILL DESCRIPTION AND LOCATION	III.3.1
2.0	PURPOSE	III.3.1
3.0	SLOPE SLABILITY DEISGN CRITERIA.....	III.3.4
3.1	Static Slope Stability.....	III.3.4
3.2	Seismic Slope Stability	III.3.6
3.3	Critical Cross Section – Landfill Configuration	III.3.6
4.0	SCLF SITE CHARACTERIZATION	III.3.8
4.1	Subsurface Conditions	III.3.8
4.2	Groundwater Elevation	III.3.8
5.0	LANDFILL LINER SYSTEM AND FINAL COVER DATA AND ASSUMPTIONS	III.3.9
5.1	Material Parameters	III.3.9
6.0	SLOPE STABILITY ANALYSES CALCULATIONS	III.3.13
6.1	Existing Landfill Waste – Units I and III.....	III.3.13
6.2	Excavated Slopes and Foundation Soils Before Waste Placement.....	III.3.15
6.3	Liner System Along Sideslopes With In-Place Waste Placed	III.3.15
6.4	Liner System Under Interim Fill Conditions	III.3.16
6.5	Final Slopes At Final Closure Conditions	III.3.17
7.0	SUMMARY AND CONCLUSIONS	III.3.18
8.0	RECOMMENDATIONS	III.3.21
9.0	REFERENCES	III.3.21

LIST OF FIGURES

Figure No.	Title	Page
III.3.1	SITE LOCATION MAP	III.3-3
III.3.2	LANDFILL CROSS SECTIONS	III.3-5
III.3.3	SEISMIC IMPACT ZONE MAP	III.3-7

**APPLICATION FOR PERMIT RENEWAL AND MODIFICATION
SANDOVAL COUNTY LANDFILL**

**VOLUME III: LANDFILL ENGINEERING CALCULATIONS
SECTION 3: SLOPE STABILITY ANALYSIS**

LIST OF TABLES

Table No.	Title	Page
III.3.1	SLOPE STABILITY ANALYSES SUMMARY	III.3-2
III.3.2	TARGET STATIC SLOPE STABILITY FACTORS OF SAFETY –CRITICAL CROSS SECTIONS.....	III.3-4
III.3.3	TARGET SEISMIC SLOPE STABILITY FACTORS OF SAFETY –CRITICAL CROSS SECTIONS.....	III.3-5
III.3.4	SCLF SLOPE STABILITY SLOPE STABILITY ANALYSES CRITICAL CROSS SECTIONS PRESENTED ON FIGURE III.3.2.....	III.3-7
III.3.5	FOUNDATION SOILS INTERNAL ANGLE OF FRICTION AND COHESION	III.3-10
III.3.6	GEOSYNTHETIC INTERFACE FRICTION ANGLES AND ADHESION-UNIT IV FLOOR LINER SYSTEM	III.3-11
III.3.7	GEOSYNTHETIC INTERFACE FRICTION ANGLES AND ADHESION-UNIT IV SIDESLOPE LINER SYSTEM	III.3-12
III.3.8	WASTE INTERNAL ANGLE OF FRICTION AND COHESION.....	III.3-13
III.3.9	FINAL COVER SYSTEM COMPONENTS (FROM TOP TO BOTTOM)	III.3-13
III.3.10	SCLF EXISTING LANDFILL INTERMEDIATE WASTE SLOPE COMPONENTS – SLOPE STABILITY INPUT PARAMETER SUMMARY ..	III.3-14
III.3.11	SCLF FOUNDATION SOILS – SLOPE STABILITY INPUT PARAMETER SUMMARY.....	III.3-15
III.3.12	UNIT IV SIDESLOPE LINER SYSTEM SLOPE STABILITY ANALYSIS – SIMPLIFIED LINER SYSTEM CHARACTERISTICS FOR MODELING	III.3-16
III.3.13	UNIT IV FLOOR LINER SYSTEM SLOPE STABILITY ANALYSIS – SIMPLIFIED LINER SYSTEM CHARACTERISTICS FOR MODELING	III.3-17
III.3.14	FINAL SLOPES AND FOUNDATION SOILS AT FINAL CLOSURE CONDITIONS SLOPE STABILITY ANALYSIS – SIMPLIFIED LANDFILL SYSTEM CHARACTERISTICS FOR MODELING	III.3-18
III.3.15	SUMMARY OF CALCULATED FACTOR OF SAFETY	III.3-19

**APPLICATION FOR PERMIT RENEWAL AND MODIFICATION
SANDOVAL COUNTY LANDFILL**

**VOLUME III: LANDFILL ENGINEERING CALCULATIONS
SECTION 3: SLOPE STABILITY ANALYSIS**

LIST OF ATTACHMENTS

Attachment No.	Title
III.3.A	THIEL, RICHARD. <i>PEAK VS RESIDUAL STRENGTH FOR LANDFILL STABILITY ANALYSIS</i> . THIEL ENGINEERING: OREGON HOUSE, CA, USA
III.3.B	GORDON ENVIRONMENTAL, INC. AUGUST 2005. <i>VOLUME V: HYDROGEOLOGY, SECTION 1: HYDROGEOLOGY</i> . SANDOVAL COUNTY LANDFILL APPLICATION FOR PERMIT.
III.3.C	KOERNER, ROBERT M. AND KOERNER, GEORGE R. SEPTEMBER 2007. <i>INTERPRETATION(S) OF LABORATORY GENERATED INTERFACE SHEAR STRENGTH DATA FOR GEOSYNTHETIC MATERIALS WITH EMPHASIS ON THE ADHESION VALUE</i> . GEOSYNTHETIC INSTITUTE.
III.3.D	ACS LABORATORY AND FIELD SERVICES. GEOTECHNICAL LABORATORY ANALYSIS OF ON-SITE SOILS. 2005 AND 2014.
III.3.E	“SLIDE®” ANALYSIS INFORMATION – SCENARIO 1 THROUGH 18
III.3.E-1	SCENARIO 1: SECTION A-A’; CIRCULAR, STATIC
III.3.E-1	SCENARIO 2: SECTION A-A’; CIRCULAR, SEISMIC
III.3.E-2	SCENARIO 3: SECTION A-A’, CIRCULAR, STATIC
III.3.E.2	SCENARIO 4: SECTION A-A’ CIRCULAR, SEISMIC
III.3.E-3	SCENARIO 5: SECTION A-A’; BLOCK, STATIC
III.3.E-3	SCENARIO 6: SECTION A-A’; BLOCK, SEISMIC
III.3.E-4	SCENARIO 7: SECTION A-A’, CIRCULAR, STATIC
III.3.E-4	SCENARIO 8: SECTION A-A’, CIRCULAR, SEISMIC
III.3.E-5	SCENARIO 9: SECTION A-A’, CIRCULAR, STATIC
III.3.E-5	SCENARIO 10: SECTION A-A’, CIRCULAR, SEISMIC
III.3.E-6	SCENARIO 11: SECTION A-A’, BLOCK, STATIC
III.3.E-6	SCENARIO 12: SECTION A-A’, BLOCK, SEISMIC
III.3.E-7	SCENARIO 13: SECTION C-C’; CIRCULAR, STATIC
III.3.E-7	SCENARIO 14: SECTION C-C’; CIRCULAR, SEISMIC
III.3.E-8	SCENARIO 15: SECTION C-C’; CIRCULAR, STATIC
III.3.E-8	SCENARIO 16: SECTION C-C’; CIRCULAR, SEISMIC
III.3.E-9	SCENARIO 17: SECTION C-C’; CIRCULAR, STATIC
III.3.E-9	SCENARIO 18: SECTION C-C’; CIRCULAR, SEISMIC

APPLICATION FOR PERMIT RENEWAL AND MODIFICATION SANDOVAL COUNTY LANDFILL

VOLUME III: LANDFILL ENGINEERING CALCULATIONS SECTION 3: SLOPE STABILITY ANALYSIS

1.0 LANDFILL DESCRIPTION AND LOCATION

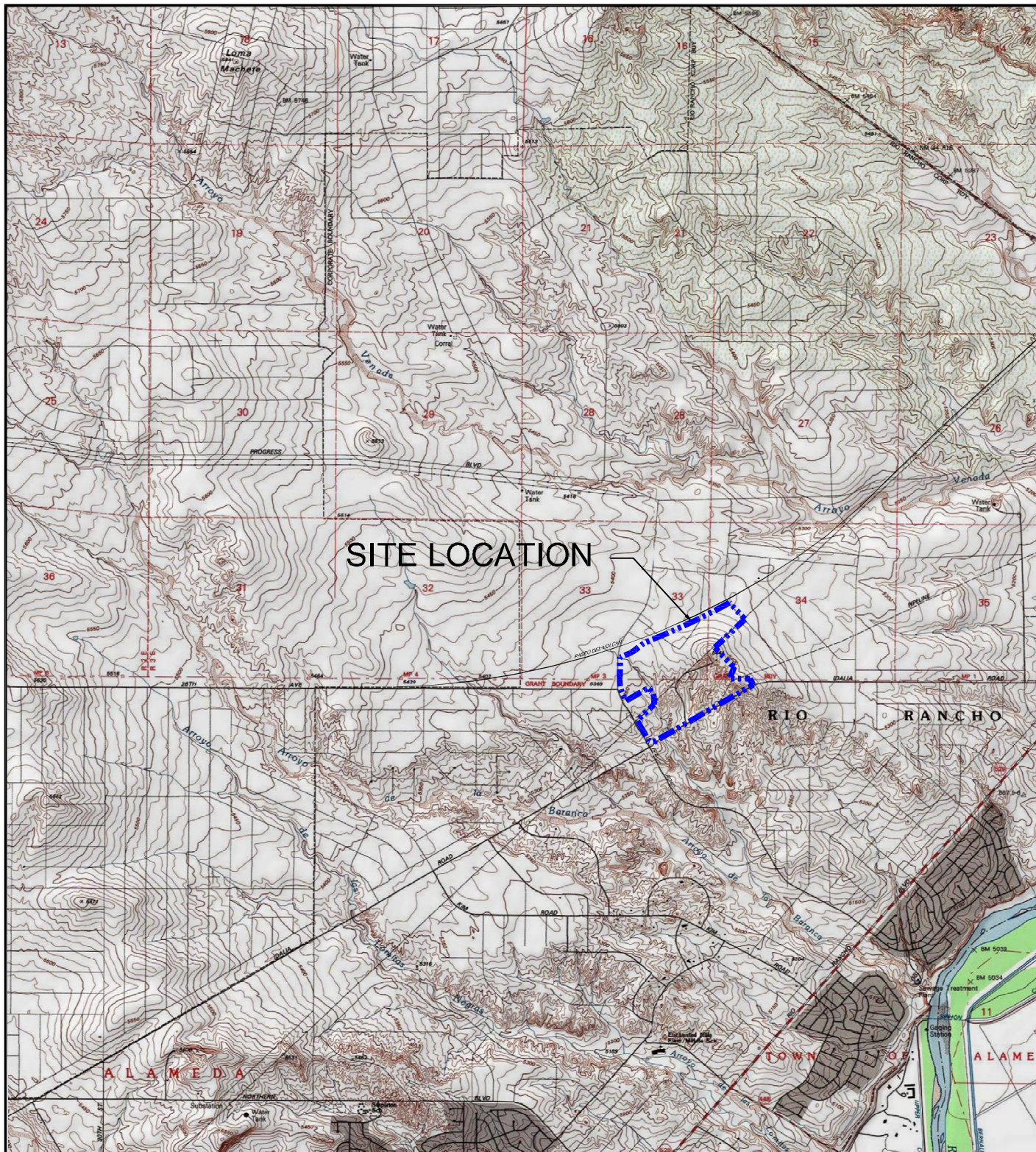
The Sandoval County Landfill (SCLF) is an existing solid waste disposal facility operating in compliance with its current Permits, SWM-050304 and SWM-050304 (SP), and the New Mexico Environment Department (NMED) Solid Waste Rules (20.9.2-2.9.10 NMAC). SCLF is located at 2708 Iris Road NE in Rio Rancho, New Mexico (NM), and occupies 178.3 acres \pm (**Figure III.3.1**). SCLF is publicly owned and operated by the County of Sandoval, and is currently permitted to accept municipal solid waste (MSW), construction and demolition debris (C&D), and two special wastes: petroleum contaminated soils (PCS) and sludge. The approximate geographic coordinates for the center of the landfill site are **Latitude 35.3092° North** and **Longitude 106.6198° West**.

2.0 PURPOSE

The purpose of these calculations is to demonstrate that the static and seismic slope stability analyses for the SCLF located in Sandoval County, New Mexico are in compliance with the Rules and accepted engineering standards. The slope stability analyses were performed for the scenarios listed in **Table III.3.1**.

TABLE III.3.1
Slope Stability Analyses Summary
Sandoval County Landfill

Slope Stability Analysis	Landfill Configuration	Type of Analysis
Intermediate Grading – Cell 8A Waste Slopes – Foundation Analysis	Cell 8A 3H:1V Interim Waste Slope	Circular – Static Circular – Seismic
Intermediate Grading – Cell 8A Waste Slopes – In-Place Waste Analysis	Cell 8A 3H:1V Interim Waste Slope	Circular – Static Circular – Seismic
Intermediate Grading – Cell 8A Liner System Analysis	Cell 8A Interim Fill Grades and Liner System	Block – Static Block - Seismic
Final Grading – Cells 8A, 8B and 8C Foundation Analysis	Cells 8A, 8B and 8C Final Fill Grades	Circular – Static Circular – Seismic
Final Grading – Cells 8A, 8B and 8C In-Place Waste Analysis	Cells 8A, 8B and 8C Final Fill Grades	Circular – Static Circular – Seismic
Final Grading – Cells 8A, 8B and 8C Liner System Analysis	Cells 8A, 8B and 8C Final Fill Grades and Liner System	Block – Static Block - Seismic
Intermediate Grading in Unit III and Unit IV Waste Analysis	Intermediate Fill Grades Unit III and Unit IV	Circular – Static Circular – Seismic
Intermediate Grading in Unit III and Unit IV Waste Analysis	Intermediate Fill Grades Unit III and Unit IV	Circular – Static Circular – Seismic
Final Grading – Waste Analysis	Final Grading Unit III and Unit IV	Circular – Static Circular – Seismic



LEGEND

--- SITE BOUNDARY

NOTES:

1. GEOGRAPHIC COORDINATES FOR THE CENTER OF THE SITE:
35.3092°N, 106.6198°W.
2. MAP REFERENCES:
MAP BASE FROM USA TOPO MAPS, 1:24000
USA TOPOGRAPHIC SERVICES, TOPOI MAP
3. SITE BOUNDARY FROM THE 2014 VACATION PLAT 093013
RRE BOOK 25 PAGE 65 SANDOVAL COUNTY LANDFILL

Drawing: P:\acad 2003\211.00.01\PERMIT FIGURES\SITE LOC MAP.dwg

Date/Time: Apr. 10, 2015-13:30:11 ; LAYOUT: A (P)

Copyright © All Rights Reserved, Gordon Environmental, Inc. 2015



SITE LOCATION MAP

SANDOVAL COUNTY LANDFILL
RIO RANCHO, NEW MEXICO



Gordon Environmental, Inc.

Consulting Engineers

213 S. Camino del Pueblo
Bernalillo, New Mexico, USA
Phone: 505-867-6990
Fax: 505-867-6991

DATE: 03/24/2015

CAD: SITE LOC MAP.dwg

PROJECT #: 211.00.01

DRAWN BY: DMI

REVIEWED BY: DRT

FIGURE III.3.1

APPROVED BY: IKG

gel@gordonenvironmental.com

3.0 SLOPE SLABILITY DEISGN CRITERIA

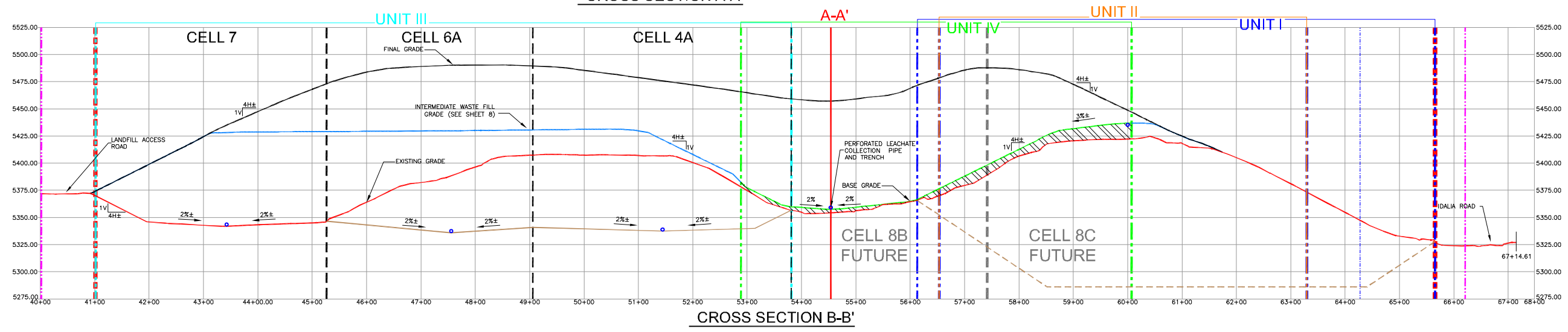
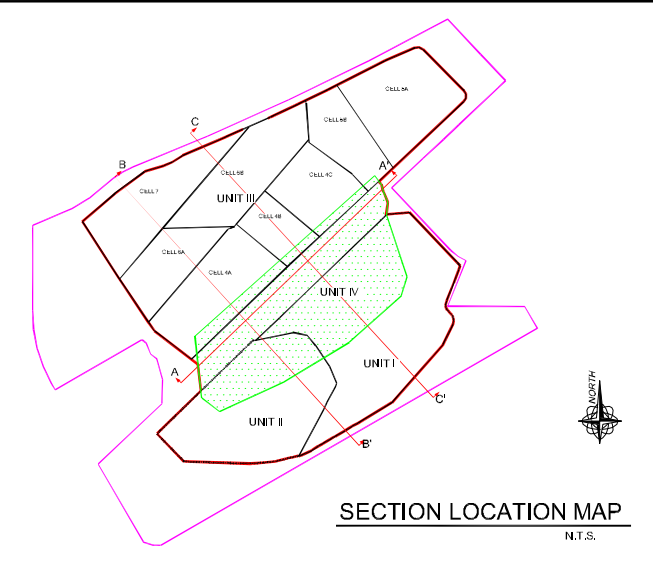
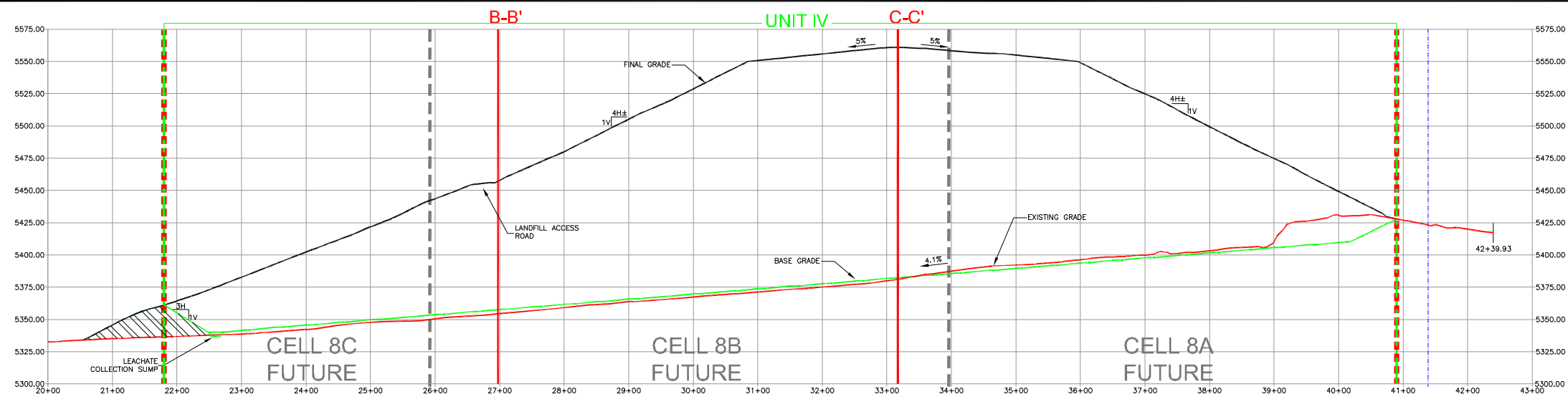
The SLIDE© (Rocscience Inc., 1989 – 2003) computer program for slope stability calculations is used to assess mass stability for the landfill for the configurations listed in **Table III.3.1**. Both circular and non-circular (block) failure planes are considered as listed in **Table III.3.1**.

3.1 Static Slope Stability

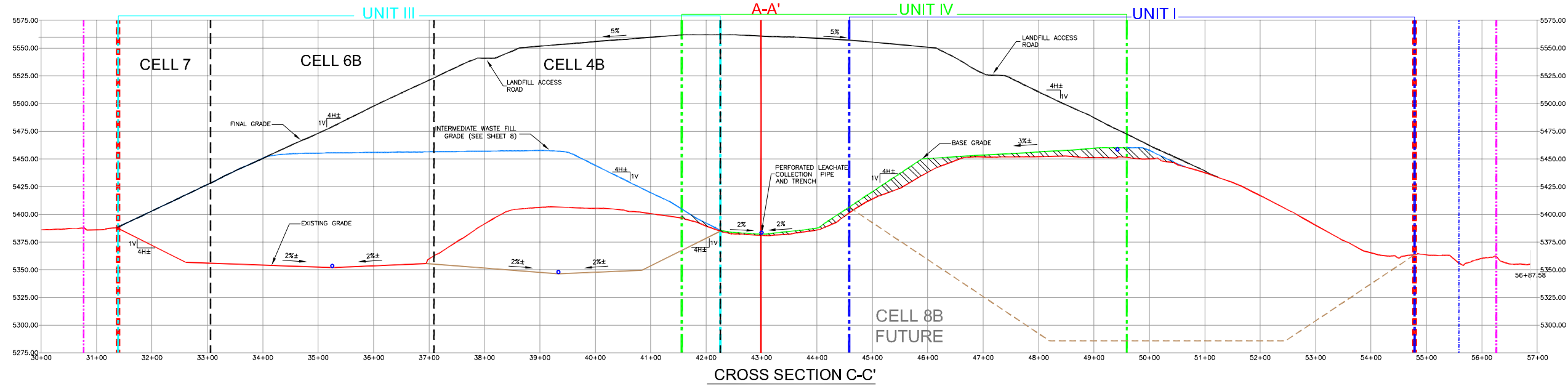
The static slope stability factor of safety (FS) is based on generally accepted values in both the geotechnical and solid waste industries; and presented in a number of the references presented in Section 9.0 in this demonstration. The use of peak shear strengths versus large-displacement (residual) shear strength parameters is discussed in depth in **Attachment III.3.A**. The static slope stability FS is evaluated for cross-sections (**Figure III.3.2**) that represent critical or near-critical combinations of the landfill's geometry and shear strength. Minimum acceptable FS for landfill slope stability depend on the landfill's specific condition being evaluated. The targeted calculated FS for interim conditions; i.e., liner system and interim waste fill slopes during operations is 1.5 using peak shear strengths. A FS of 1.5 using large-displacement shear strengths (residual shear strength parameters) is used for geosynthetic interfaces for the liner system. The target calculated FS for final landfill slopes at closure is 1.5 using peak shear strengths. The target static FS values to be used for the SCLF are listed in **Table III.3.2**.

TABLE III.3.2
Target Static Slope Stability Factors of Safety – Critical Cross Sections
Sandoval County Landfill

Landfill Configuration	Target Factor of Safety
Interim Landfill Waste Fill Slopes	1.5
Geosynthetic Interface Analysis	1.5
Final Landfill Build-Out including Final Cover Installation	1.5

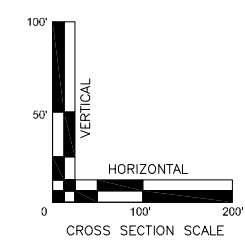



- LEGEND**
- FINAL GRADE
 - INTERMEDIATE WASTE FILL GRADE
 - EXISTING GRADE
 - UNIT IV COMPOSITE LINER GRADE
 - STRUCTURAL FILL SOIL COMPACTED TO 90% STANDARD PROCTOR DENSITY
 - AS-BUILT BASE GRADE BASED ON COMPLETED COA REPORTS
 - INTERPOLATED UNIT I AND UNIT II BASE GRADES
 - UNIT I BOUNDARY
 - UNIT II BOUNDARY
 - UNIT III BOUNDARY
 - UNIT IV BOUNDARY
 - CELL BOUNDARY
 - LIMIT OF WASTE BOUNDARY
 - PROPERTY BOUNDARY



NOT FOR CONSTRUCTION

Drawing: P:\acad 2003\211.00.01\PERMIT\FIGURES\13 X-SEC.dwg
Date/Time: Apr. 16, 2015-16:46:21 - LAYOUT: FIGURE 13
Copyright © All Rights Reserved, Gordon Environmental, Inc., 2012



LANDFILL CROSS SECTIONS		
SANDOVAL COUNTY LANDFILL RIO RANCHO, NEW MEXICO		
 Gordon Environmental, Inc. Consulting Engineers		
213 S. Camino del Pueblo Bernalillo, New Mexico, USA Phone: 505-867-6990 Fax: 505-867-6991	DATE: 04/16/2015 DRAWN BY: DMI APPROVED BY: IKG	CAD: 13 X-SEC.dwg REVIEWED BY: MRH gk@gordonenvironmental.com
PROJECT #: 211.00.01		FIGURE III.3.2

3.2 Seismic Slope Stability

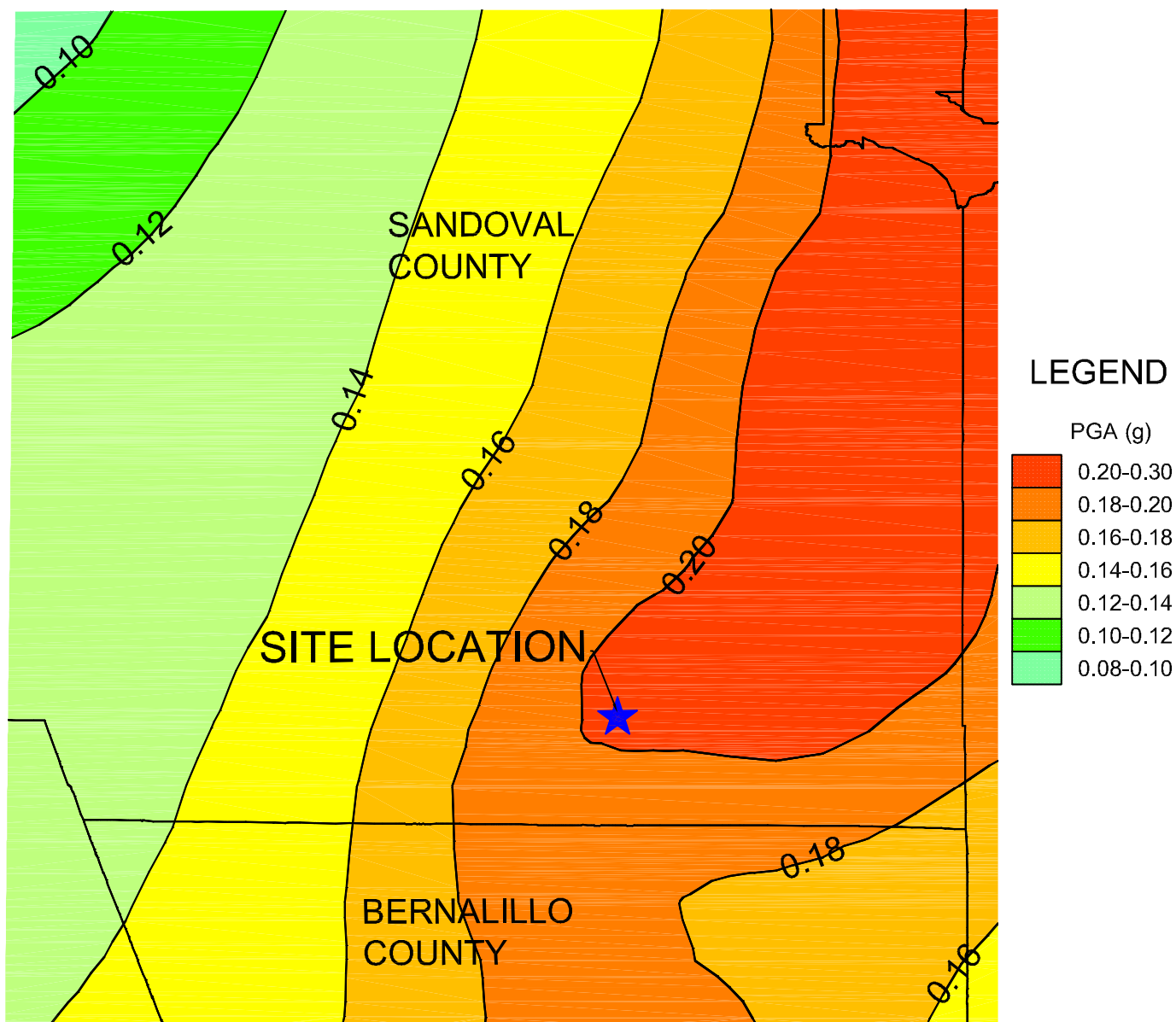
The seismic slope stability FS is evaluated for critical cross sections (**Figure III.3.2**) subjected to the peak horizontal ground acceleration that has a 10% probability of being exceeded in 250 years [New Mexico Environment Department (NMED), Solid Waste Rules (Rules), 20.9.3.4a New Mexico Administrative Code (NMAC)]. Values of maximum horizontal ground acceleration (MHA) having a certain probability of exceedance, (P_e), are derived from the United States Geologic Survey (USGS) National Seismic Hazard Maps (<http://earthquake.usgs.gov/research/hazmaps/design/>). Current National Seismic Hazard Maps for the landfill's latitude and longitude of Latitude 35.3092° North and Longitude 106.6198° West for 10% probability of being exceeded in 250 years is 0.2044 (**Figure III.3.3**). A peak horizontal ground acceleration equal to 0.2044g (i.e., 0.1044 above the regulatory standard) is used in the analyses of the critical cross sections for the landfill. The target seismic FS value to be used for the SCLF are listed in **Table III.3.3**.

TABLE III.3.3
Target Seismic Slope Stability Factors of Safety – Critical Cross Sections
Sandoval County Landfill

Landfill Configuration	Target Factor of Safety
Interim Landfill Waste Fill Slopes	1.0
Geosynthetic Interface Analysis	1.0
Final Landfill Build-Out including Final Cover Installation	1.0

3.3 Critical Cross Section – Landfill Configuration

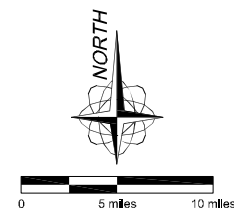
Slope stability analyses were performed for specific cross-sections to evaluate the critical configurations of the various components of the Landfill for each potential sliding scenario. The cross-sections used in the analyses are presented on **Figure III.3.2**, and listed in **Table III.3.4**.



Peak Horizontal Ground Acceleration (g) with 10% Probability of Exceedence in 250 Years

NOTES:

1. SEISMIC DATA FROM: USGS NATIONAL HAZARD MAPPING PROJECT GIS DATA and Petersen, Mark D., Frankel, Arthur D., Harmsen, Stephen C., Mueller, Charles S., Haller, Kathleen M., Wheeler, Russell L., Wesson, Robert L., Zeng, Yuehua, Boyd, Oliver S., Perkins, David M., Luco, Nicolas, Field, Edward H., Wills, Chris J., and Rukstales, Kenneth S., 2008, Documentation for the 2008 Update of the United States National Seismic Hazard Maps: U.S. Geological Survey Open-File Report 2008-1128, 61.
2. GEOGRAPHIC COORDINATES FOR THE CENTER OF THE SITE:
35.3092° N, 106.6198° W
3. PEAK HORIZONTAL GROUND ACCELERATION (g) with 10% PROBABILITY OF EXCEEDENCE IN 250 YEARS FOR THE SITE = 0.2044 g



SEISMIC IMPACT ZONE MAP

SANDOVAL COUNTY LANDFILL
RIO RANCHO, NEW MEXICO



Gordon Environmental, Inc.
Consulting Engineers

213 S. Camino del Pueblo
Bernalillo, New Mexico, USA
Phone: 505-867-6990
Fax: 505-867-6991

DATE: 03/31/2015	CAD: SEISMIC SANDOVAL.dwg	PROJECT #: 211.00.01
DRAWN BY: DMI	REVIEWED BY: DRT	
APPROVED BY: IKG	gel@gordonenvironmental.com	FIGURE III.3.3

TABLE III.3.4
SCLF Slope Stability Analyses Critical Cross Sections Presented on Figure III.3.2
Sandoval County Landfill

Landfill Configuration Slope Stability Analysis	Critical Cross Section Identification
Intermediate Grading – Cell 8A Waste Slopes and Liner System – Foundation Analysis	Cross Section A-A’
Intermediate Grading – Cell 8A Waste Slopes and Liner System – In-Place Waste Analysis	Cross Section A-A’
Intermediate Grading - Liner System Analysis	Cross Section A-A’
Final Grading – Cells 8A, 8B and 8C Foundation Analysis	Cross Section A-A’
Final Grading – Cells 8A, 8B and 8C In-Place Waste Analysis	Cross Section A-A’
Intermediate Grading in Unit III and Unit IV – Unit I Analysis	Cross Section C-C’
Intermediate Grading in Unit III and Unit IV Analysis	Cross Section C-C’
Final Grading – Waste Analysis	Cross Section C-C’

4.0 SCLF SITE CHARACTERIZATION

4.1 Subsurface Conditions

A hydrogeologic evaluation of the Landfill was conducted by John Schumaker & Associates, Inc. as part of the 1994 Application for Permit. The evaluation found that the site generally consists of *“The upper 60 feet of soil profile is comprised primarily of very fine to medium calcareous silty sands, with thin (i.e., a few inches thick) interbedded gravel, silt and clay lenses”*. Geotechnical borings completed as part of the 2005 Application for Permit are provided in **Attachment III.3.B** and recent soil testing results are included as **Attachment III.3.D**.

4.2 Groundwater Elevation

Groundwater elevation measurements have been conducted at the SCLF for at least 10 years. Monitoring wells MW-2, 3, 5, 6, and 7 are installed at depths appropriate to yield groundwater

samples from the uppermost water-bearing zone at each location. Completions of the site's monitoring wells (including decommissioned well MW-4) relative to the unconfined, uppermost water-bearing unit are depicted in the geologic cross sections provided in **Volume V.2**. Based on depth to groundwater measurements, the uppermost water-bearing zone beneath the site is significantly greater than 100' below base grade design elevations for Units II and III, as well as the projected floor elevations for Unit I. Based on the 100+ feet to groundwater, the slope stability analyses completed for the Landfill does not include a "water table" parameter in the analyses.

5.0 LANDFILL LINER SYSTEM AND FINAL COVER DATA AND ASSUMPTIONS

Data variables and assumptions for the Landfill liner and final cover systems are summarized in this section. The most critical input data variables, aside from the geometric coordinates of the landfill components that are determined from the critical cross-section, are fill unit weights (density), cohesion; and friction and adhesion of the landfill components. Internal angle of friction

and cohesion is considered for soil landfill components including the final cover; the waste (modeled to behave as a soil layer); and earthen components of the liner systems including the protective soil layer, compacted subgrade; and *in-situ* and re-compacted foundation soil. Interface friction is considered for the synthetic components of the liner including: textured high-density polyethylene liner (HDPE) liner, geosynthetic clay liner (GCL), double-sided geocomposite and the structural geogrid.

5.1 Material Parameters

5.1.1 Foundation Soils

The foundation soils at the site consist of "*primarily of very fine to medium calcareous silty sands, with thin (i.e., a few inches thick) interbedded gravel, silt and clay lenses*" (**Attachment III.3.B**). The hydrogeologic evaluation completed as part of the August 2005 Application for Permit did not include any geotechnical parameters (i.e., shear strength, etc.). Based on the type of soils present, GEI estimated the internal angle of friction for the foundation soils. The estimations are based literature review; Section 9.0 of this calculation package, and on similar soils encountered at New Mexico Landfills. Geotechnical parameters used in the analyses are summarized in **Table III.3.5**.

TABLE III.3.5
Foundation Soils Internal Angle of Friction and Cohesion^{1,2}
Sandoval County Landfill

Soil Material	Unit Weight	Internal Angle of Friction (Φ)	Cohesion ² [Assumed]
Foundation Soils (<i>in-situ</i> Relative Density; Dense)	115.0 lbs/ft ³	33°	0 lbs/ft ²

Notes:

1. Values reported for Φ and Cohesion are based on review of available literature and are used to predict the performance of landfill components.
2. Geotechnical laboratory testing of on-site soils show predominately silty-sands with sands (SP-SM) soils. For the purposes of these slope stability calculations, no cohesion was assumed providing an additional factor of safety.

5.1.2 Liner System Components

The liner system for Unit IV consists of the components listed in **Table III.3.6** on the floor; and on the sideslope, the components listed in **Table III.3.7**. Interface friction angles for the floor geosynthetics are reported as peak shear strength values; and large-displacement (residual) shear strength values for the sideslopes, as recommended in **Attachment III.3.A**. Documented interface friction angles were adopted from tests by Martin et al. (1984); Williams and Houlihan (1996); Koerner et al. (1986), Shark et al. (1998); and manufacturer's literature. The literature references are provided in **Section 9.0** of this calculation package.

TABLE III.3.6
Geosynthetic Interface Friction Angles and Adhesion¹ – Unit IV Floor Liner System
Sandoval County Landfill

Geosynthetic to Geosynthetic Interface	Normal Stresses lbs/in ²	Mohr-Coulomb Failure Envelope ³	
		Φ	Adhesion
HDPE Geogrid to Structural Fill Soils (SM) [undrained]	Reference 3	35°	0 lbs/ft ²
Nonwoven Geotextile of Geocomposite to HDPE Geogrid	14.1 28.3 56.5	21.4°	279 lbs/ft ²
Nonwoven Geotextile of Geocomposite to Woven Geotextile of GCL	13.9 55.6 83.3	19.7°	0 lbs/ft ²
Nonwoven Geotextile of GCL to 60-mil Double-Sided Textured HDPE FML	13.9 27.8 55.6	18.1°	70.5 lbs/ft ²
Protective Soil Layer (SM) to 60-mil Double-Sided Textured HDPE FML	56	24°	0 lbs/ft ²

Notes:

1. Values reported for Φ and Adhesion are based on review of available literature and are used to predict the performance of the liner system.
2. Geotechnical laboratory testing of on-site soils show predominately silty sands (i.e., SP-SM) soils. For the purposes of these calculations, it was assumed these soils would behave similar to SM soils that have no cohesion; providing an additional factor of safety.
3. As recommended in **Attachment III.3.A**, the values for Φ and Adhesion (when available in the literature) represent “Peak Shear Strength” values.

TABLE III.3.7
Geosynthetic Interface Friction Angles and Adhesion¹ – Unit IV Sideslope Liner System
Sandoval County Landfill

Geosynthetic to Geosynthetic Interface	Normal Stresses lbs/in ²	Mohr-Coulomb Failure Envelope ³	
		Φ	Adhesion
HDPE Geogrid to Structural Fill Soils (SM) [undrained]	Reference 3	30°	0 lbs/ft ²
Nonwoven Geotextile of Geocomposite to HDPE Geogrid	20.0 45.0 90.0	15.3°	243 lbs/ft ²
Nonwoven Geotextile of Geocomposite to Woven Geotextile of GCL	27.7 55.6 104.2	19°	50 lbs/ft ²
Nonwoven Geotextile of GCL to 60-mil Double-Sided Textured HDPE FML	27.7 55.6 104.2	19°	20 lbs/ft ²
Protective Soil Layer (SP-SM) to 60-mil Double-Sided Textured HDPE FML	55.6	21°	0 lbs/ft ²

Notes:

1. Values reported for Φ and Adhesion are based on review of available literature and are used to predict the performance of the liner system.
2. Geotechnical laboratory testing of on-site soils show predominately silty sands (i.e., SP-SM) soils. For the purposes of these calculations, it was assumed these soils would behave similar to SM soils that have no cohesion; providing an additional factor of safety.
3. As recommended in **Attachment III.3.A**, the values for Φ and Adhesion (when available in the literature) represent “Residual Shear Strength” values.

5.1.3 Waste

The municipal solid waste component has the properties as listed in **Table III.3.8** and is representative of typical of State of New Mexico municipal solid waste; and used in previous slope stability analyses completed for State of New Mexico Landfills.

TABLE III.3.8
Waste Internal Angle of Friction and Cohesion^{1,2}
Sandoval County Landfill

Soil Material	Unit Weight	Internal Angle of Friction (Φ)	Cohesion [Assumed]
Municipal Solid Waste (Compacted); Moderately Dense	65 lbs/ft ³	33°	0 lbs/ft ²

Notes:

1. Values reported for Φ and Cohesion are based on review of available literature and are used to predict the performance of landfill components.
2. For the purposes of these slope stability calculations, no cohesion was assumed providing an additional factor of safety.

5.1.4 Final Cover System

The final cover system cross section consists of the components listed in **Table III.3.9**. Geotechnical properties for the compacted barrier (infiltration) on-site soil layer are listed in **Table III.3.9**; and are based on laboratory geotechnical testing conducted by a New Mexico Soils Laboratory (**Attachment III.3.D**).

TABLE III.3.9
Final Cover System Components (From Top to Bottom)^{1,2}
Sandoval County Landfill

Final Cover System Component	Thickness	Unit Weight	Internal Angle of Friction (Φ)	Cohesion [Assumed]
Erosion/Vegetative Layer	6 inches	115.0 lbs/ft ³	33°	0 lbs/ft ²
Infiltration/Barrier Layer	3 feet	115.0 lbs/ft ³	33°	0 lbs/ft ²

Notes:

1. Values reported for Φ and Cohesion are based on review of available literature and are used to predict the performance of the compacted final cover system soils.
2. Geotechnical laboratory testing of on-site soils show predominately silty sands (i.e., SP-SM) soils. For the purposes of these calculations, it was assumed these soils would behave similar to SM soils that have no cohesion; providing an additional factor of safety.

6.0 SLOPE STABILITY ANALYSES CALCULATIONS

6.1 Existing Landfill Waste – Units I and III

A slope stability analysis was completed on the 4H:1V \pm slopes that currently exist on the Landfill for both static and seismic conditions. The parameters used in the analyses for the in-place soil and waste are as listed in **Table III.3.10**. The critical cross section C-C' on **Figure III.3.2** was used to evaluate the stability of the existing waste and soil sideslope. The existing sideslopes were evalu-

ated using Circular (static and seismic) configurations; and the FS reported for the Bishop Simplified and Spencer stability methods. The computed FS are presented in **Section 7.0** of these calculations.

TABLE III.3.10
SCLF Existing Landfill Intermediate Waste Slope Components –
Slope Stability Input Parameter Summary^{1,2}
Sandoval County Landfill

Component	Approximate Thickness	Unit Weight	Internal Angle of Friction (Φ)	Interface Friction Angle (Φ)	Cohesion [Assumed]
Intermediate Cover	12 inches	115.0 lbs/ft ³	33°	----	0 lbs/ft ²
In-Place Compacted Waste ³	Varies	65 lbs/ft ³	33°	----	0 lbs/ft ²
Protective Soil Layer	2 feet	115.0 lbs/ft ³	33°	----	0 lbs/ft ²
Protective Soil Layer to HDPE Textured FML	2 feet	115.0 lbs/ft ³	----	15.3° for landfill sideslopes and 18.1° for the floor	0 lbs/ft ²
Textured HDPE FML GCL	60-mil	59.4 lbs/ft ³	----	21.0° for landfill sideslopes and 24.0° for the floor	0 lbs/ft ²
GCL to Geocomposite	0.04 feet	97.4 lbs/ft ³	----	19.0° for landfill sideslopes and 18.1° for the floor	0 lbs/ft ²
Geocomposite to HDPE Structural Geogrid	0.02 feet	1 lbs/ft ³	----	15.3° for landfill sideslopes and 21.4° for the floor	0 lbs/ft ²
Geogrid to Structural Fill Soils	0.01	1 lbs/ft ³	----	35° for landfill sideslopes and 21.4° for the floor	0 lbs/ft ²

Notes:

1. *Values reported for Φ and Cohesion are based on review of available literature and are used to predict the performance of landfill components.*
2. *Geotechnical laboratory testing of on-site soils show predominately silty sands (i.e., SP-SM) soils. For the purposes of these calculations, it was assumed these soils would behave similar to SM soils that have no cohesion; providing an additional factor of safety.*
3. *Depth of in-place compacted waste based on the approximate base grade of Unit I and III as obtained from the Permit Plans.*

6.2 Excavated Slopes and Foundation Soils Before Waste Placement

Cross section A-A' on **Figure III.3.2** depicts the critical excavation slope in Cells 8A, 8B and 8C. The parameters used in the excavated slope evaluation are listed in **Table III.3.11**. The critical cross section A-A' on **Figure III.3.2** was used to evaluate the stability of the excavated sideslope. The excavated and structural fill sideslopes were evaluated using Circular (static and seismic) and the FS is reported for the Bishop Simplified and Spencer stability methods. The computed FS are presented in **Section 7.0** of these calculations.

TABLE III.3.11
SCLF Foundation Soils – Slope Stability Input Parameter Summary^{1,2}
Sandoval County Landfill

Component	Approximate Thickness	Unit Weight	Internal Angle of Friction (Φ)	Cohesion [Assumed]
Foundation Soils	50 feet	115 lbs/ft ³	33°	0 lbs/ft ²

Notes:

1. Values reported for Φ and Cohesion are based on review of available literature and are used to predict the performance of landfill components.
2. Geotechnical laboratory testing of on-site soils show predominately silty sands (i.e., SP-SM) soils. For the purposes of these calculations, it was assumed these soils would behave similar to SM soils that have no cohesion; providing an additional factor of safety.

6.3 Liner System Along Sideslopes With In-Place Waste Placed

For the purposes of simplifying the liner section for modeling, the GCL was removed as a geometric component of the liner system. The geocomposite is the layer within the liner system with the lowest interface friction againsts the HDPE geogrid. The other geosynthetics have high interface friction compared to the geocomposite to the geogrid. Therefore, the characteristics of geocomposite alone has been used as a conservative representation of the combined geosynthetic liner components of the system. The simplified liner section, for the purposes of modeling, is presented in **Table III.3.12**; from top to bottom. The critical interface friction between the HDPE geocomposite and the HDPE geogrid was used in this evaluation; and considered as the liner system in the analyses. The liner system along the sideslopes was evaluated using Block (static and seismic) configurations and the FS is reported for the Bishop Simplified and Spencer stability methods. The computed FS are presented in **Section 7.0** of these calculations.

TABLE III.3.12
Unit IV Sideslope Liner System Slope Stability Analysis - Simplified Liner System Charac-
teristics for Modeling^{1,2}
Sandoval County Landfill

Component	Unit Weight	Cohesion/Adhesion [Assumed]	Internal Angle of Friction	Interface Friction Angle
Protective Soil Layer	115 lbs/ft ³	0 lbs/ft ³	33°	----
Geocomposite Liner System	95.5 lbs/ft ³	0 lbs/ft ³	----	15.3°
Compacted Subgrade or Structural Fill	115 lbs/ft ³	0 lbs/ft ³	33°	----
Foundation Soils	115 lbs/ft ³	0 lbs/ft ³	33°	----

Notes:

1. Values reported for Φ and Adhesion/Cohesion are based on review of available literature and are used to predict the performance of landfill components.
2. Geotechnical laboratory testing of on-site soils show predominately silty sands (i.e., SP-SM) soils. For the purposes of these calculations, it was assumed these soils would behave similar to SM soils that have no cohesion; providing an additional factor of safety.

6.4 Liner System Under Interim Fill Conditions

The liner system evaluation under interim fill conditions for the Landfill has four soil components; intermediate cover, protective soil, structural soil fill and foundation soils. The liner system also is comprised of four geosynthetic components; a double-sided textured HDPE FML, a GCL, a geocomposite and a HDPE structural geogrid. The shear strength parameters for the soils and geosynthetics are listed in **Table III.3.13**. The liner system was evaluated using Block (static and seismic) configurations and the FS is reported for the Bishop Simplified and Spencer stability methods. The computed FS are presented in **Section 7.0** of these calculations.

TABLE III.3.13
Unit IV Floor Liner System Slope Stability Analysis – Simplified Liner System
Characteristics for Modeling^{1,2}
Sandoval County Landfill

Component	Unit Weight	Cohesion/Adhesion [Assumed]	Internal Angle of Friction	Interface Friction Angle
Intermediate Cover	115 lbs/ft ³	0 lbs/ft ²	33°	----
Waste	65 lbs/ft ³	0 lbs/ft ²	33°	----
Protective Soil Layer	115 lbs/ft ³	0 lbs/ft ²	33°	----
Geocomposite Composite Liner System	95.5 lbs/ft ³	0 lbs/ft ²	----	18.1°
Compacted Subgrade	115 lbs/ft ³	0 lbs/ft ²	33°	----
Foundation Soils	115 lbs/ft ³	0 lbs/ft ²	33°	----

Notes:

1. Values reported for Φ and Adhesion/Cohesion are based on review of available literature and are used to predict the performance of landfill components.
2. Geotechnical laboratory testing of on-site soils show predominately silty sands (i.e., SP-SM) soils. For the purposes of these calculations, it was assumed these soils would behave similar to SM soils that have no cohesion; providing an additional factor of safety.

6.5 Final Slopes At Final Closure Conditions

This slope stability analysis refers to the overall stability of the landfill including final cover side-slopes and foundation; when constructed to final conditions. The final slopes and foundation soils were evaluated using Circular (static and seismic) configurations and the FS is reported for the Bishop Simplified and Spencer stability methods. The computed FS are presented in **Section 7.0** of these calculations.

TABLE III.3.14
Final Slopes and Foundation Soils at Final Closure Conditions Slope Stability Analysis -
Simplified Landfill System Characteristics for Modeling^{1,2}
Sandoval County Landfill

Component	Unit Weight	Cohesion/Adhesion [Assumed]	Internal Angle of Friction	Interface Friction Angle
Final Cover	115 lbs/ft ³	0 lbs/ft ³	33°	----
Waste	65 lbs/ft ³	0 lbs/ft ³	33°	----
Protective Soil Layer	115 lbs/ft ³	0 lbs/ft ³	33°	----
Geosynthetic Composite Liner System	95.5 lbs/ft ³	0 lbs/ft ³	----	18.1°
Compacted Subgrade	115 lbs/ft ³	0 lbs/ft ³	33°	----
Foundation Soils	155 lbs/ft ³	0 lbs/ft ³	33°	----

Notes:

1. Values reported for Φ and Adhesion/Cohesion are based on review of available literature and are used to predict the performance of landfill components.
2. Geotechnical laboratory testing of on-site soils show predominately silty sands (i.e., SP-SM) soils. For the purposes of these calculations, it was assumed these soils would behave similar to SM soils that have no cohesion; providing an additional factor of safety.

7.0 SUMMARY AND CONCLUSIONS

The slope stability results are presented in **Table III.3.15**. The SLIDE® output and figures illustrating each of the critical failure surfaces for each scenario are presented in **Attachment III.3.E** of this calculation package. As shown in **Table III.3.15** the calculated FS for each scenario and shear surface for the Landfill configurations evaluated are greater than or equal to the target minimum FS.

TABLE III.3.15
Summary of Calculated Factor of Safety's
Sandoval County Landfill

Scenario	Landfill Configuration Description	Static Factor of Safety	Seismic Factor of Safety	Target Factor of Safety	Attachment
1	Intermediate Grading – Cell 8A Waste Slopes – Foundation Analysis	3.26		1.25	III.3.E-1 - Scenario 1: Section A-A'; Circular, Static
2			1.65	1.0	III.3.E-1 - Scenario 2: Section A-A'; Circular, Seismic
3	Intermediate Grading – Cell 8A Waste Slopes – Foundation Analysis	2.39		1.5	III.3.E-2 - Scenario 3: Section A-A'; Circular, Static
4			1.34	1.0	III.3.E-2 - Scenario 4: Section A-A'; Circular, Seismic
5	Intermediate Grading – Cell 8A Liner System Analysis	1.71		1.5	III.3.E-3 - Scenario 5: Section A-A', Block, static
6			1.09	1.0	III.3.E-3 - Scenario 6: Section A-A' Block, Seismic
7	Final Grading – Cells 8A, 8B and 8C Foundation Analysis	3.35		1.5	III.3.E-4 - Scenario 7: Section A-A'; Circular, Static
8			1.63	1.0	III.3.E-4 - Scenario 8: Section A-A'; Circular, Seismic
9	Final Grading – Cells 8A, 8B and 8C In-Place Waste Analysis	3.15		1.5	III.3.E-5 - Scenario 9: Section A-A'; Circular, Static
10			1.37	1.0	III.3.E-5 - Scenario 10: Section A-A'; Circular, Seismic
11	Final Grading – Cells 8A, 8B and 8C Liner System Analysis	2.14		1.5	III.3.E-6 - Scenario 11: Section A-A'; Block, Static
12			1.04	1.0	III.3.E-6 - Scenario 12: Section A-A'; Block, Seismic

TABLE III.3.15
Summary of Calculated Factor of Safety's
Sandoval County Landfill

Scenario	Landfill Configuration Description	Static Factor of Safety	Seismic Factor of Safety	Target Factor of Safety	Attachment
13	Intermediate Grading in Unit III and Unit IV Waste Analysis	4.74		1.5	III.3.E-7 - Scenario 13: Section C-C'; Circular, Static
14			2.00	1.0	III.3.E-7 - Scenario 14: Section C-C'; Circular, seismic
15	Intermediate Grading in Unit III and Unit IV Waste Analysis	3.88		1.5	III.3.E-8 - Scenario 15: Section C-C'; Circular, Static
16			1.97	1.0	III.3.E-8 - Scenario 16: Section C-C'; Circular, Seismic
17	Final Grading – Waste Analysis	2.87		1.5	III.3.E-9 - Scenario 17: Section C-C'; Circular, Static
18			1.55	1.0	III.3.E-9 - Scenario 18: Section C-C'; Circular, Seismic

8.0 RECOMMENDATIONS

The following recommendations are made regarding testing prior to additional construction of the SCLF:

- A. The simplified modeling assumes an interface friction value of 15.3° and 18.1° for the liner system on the sideslopes and floor, respectively. Specific laboratory testing should be conducted on representative samples of the proposed geosynthetics to be used in the liner system and representative soil materials at interface with the geosynthetics to confirm the validity of the values used in the model.
- B. The modeling used assumed values for the soil materials located at the SCLF based on other similar soils encountered at New Mexico landfills and review of available literature. It is recommended that appropriate laboratory testing be conducted on representative samples of the in-situ and re-compacted soil materials used in the construction of the foundation, structural fill, protective soil layer, compacted subgrade, and final cover soils.

9.0 REFERENCES

1. Kavazanjian (Kavazanjian, E. N. Matesovic, R. Bonapart, and G. R. Schmertmann). "Evaluation of MSW Properties for Seismic Analysis" Proceedings of Geoenvironment 2000: Characterization, Containment, Remediation, and Performance in Environmental Geotechnics, New Orleans, Louisiana. February 24-26, 1995, Edited by Yalcin B. Acar and David E. Daniel, Geotechnical Special Publication No. 46.
2. Hough, B.K., 1969. "Basic Soils Engineering". Ronald Press Company.
3. Hunt R.E. 1984. "Geotechnical Engineering Investigation Manual".
4. Koerner, R. M., 2005. "Designing with Geosynthetics", 5th Edition.
5. Richardson, G.N., and E. Kavazanjian Jr., 1995. "RCRA Subtitle D (258) Seismic Design Guidance for Municipal Solid Waste Landfill Facilities", EPA/600/R-95/051. Office of Research and Development, Washington, D.C. April 1995.
6. Richardson, G.N., 2002. "Slope Stability Considerations for Lined Landfills", Geotechnical Fabrics Report, May 2002.
7. Sharma and Lewis (Sharma H. D. and S. P. Lewis, 1994). "Waste Containment Systems, Waste Stabilization, and Landfills: Design and Evaluation", John Wiley and Sons, New York, New York.
8. Sharma (Sharma H. D., D. E. Hullings, and F. R. Greguras, 1997). "Interface Strength Tests and Application to Landfill Design", Geosynthetics '97: Conference Proceedings of Geosynthetics Conference in Long Beach, California, V.2.
9. Terzaghi and Peck (Terzaghi, K. and R. Peck, 1967). "Soil Mechanics in Engineering Practice", John Wiley and Sons, Inc., New York, New York.
10. Bentomat® GCL Direct Shear Database (TR-114BM), CETCO® Lining Technologies, 2009.
11. Koerner, Robert M. and Koerner, George R. 2007. *Interpretation(s) of Laboratory Generated Interface Shear Strength Data for Geosynthetic Materials with Emphasis on the Adhesion Value*. GRI White Paper #11. Geosynthetic Institute.
12. Thiel, Richard. *A Technical Note Regarding Interpretation of Cohesion (or Adhesion) and Friction Angle in Direct Shear Tests*. Geosynthetics, April May 2009 Volume 27: Pages 10-19.

13. Thiel, Richard. Peak vs Residual Shear Strength for Landfill Bottom Liner Stability Analyses. Thiel Engineering, Oregon House, CA, USA.
14. Rocscience, Inc., 1989-2003. "SLIDE©" Toronto, Ontario.
15. Naval Facilities Engineering Command. *Soil Mechanics Design Manual 7.1*, NAVFAC DM-7.1, May 1982 Print.
16. Bray, J.D., Rathje, E.M., and Merry, S.M. *Simplified Seismic Design Procedure for Geosynthetic-Lined, Solid Waste Landfills*, Geosynthetics International, Volume 5, No. 1-2. Pages 203-235.
17. Duncan, J. M., Horz, R. C., and Yang, T. L. 1989. *Shear Strength Correlations for Geotechnical Engineering*. Virginia Tech, Department of Civil Engineering.
18. Koerner, R. M. and Koerner, G. R. 1986. *Shear Strength Parameters Between Geomembranes and Cohesive Soils*. Geotextiles and Geomembranes, Vol. 4, No. 1, Pages 21-30.
19. Martin, J. P., Koerner, R. M., and Whitty, J.E. 1984. *Experimental Friction Evaluation of Slippage Between Geomembranes, Geotextiles, and Soils*. Proceedings: International Conference on Geomembranes. Denver, Colorado. Pages 191-196.
20. Williams, N. D. and Houlihan, M. F. 1987. *Evaluation of Interface Friction Properties Between Geosynthetics and Soils*. Geosynthetics '87 Conference, New Orleans, LA. Pages 616-627.

**APPLICATION FOR PERMIT RENEWAL AND MODIFICATION
SANDOVAL COUNTY LANDFILL**

**VOLUME III: LANDFILL ENGINEERING CALCULATIONS
SECTION 3: SLOPE STABILITY ANALYSIS**

ATTACHMENT III.3.A

**THIEL, RICHARD. *PEAK VS RESIDUAL STRENGTH FOR LANDFILL STABILITY
ANALYSIS*. THIEL ENGINEERING: OREGON HOUSE, CA, USA**

PEAK VS RESIDUAL SHEAR STRENGTH FOR LANDFILL BOTTOM LINER STABILITY ANALYSES

Richard Thiel

Thiel Engineering, Oregon House, CA, USA

ABSTRACT

The decision whether to use peak or residual shear strengths for a stability analysis must be made in the context of a specific design situation. Yet even when the specific situation is defined, the decision of whether to use peak or residual shear strength is often unclear. In general, if there are potential construction, operation, or design conditions that might cause relative displacement between layers, then a post-peak or residual shear strength for the layer having the lowest peak strength is appropriate. If seismic analyses predict deformation on a given interface, then the design should use the post-peak or residual shear strength for that interface. For bottom liner systems, where stress distribution along the liner system is very complex, it is advisable to verify that the slope stability has a factor of safety greater than unity for residual shear strength conditions along the critical interface.

INTRODUCTION

This paper is concerned with the forces that support a landfill on its liner system, and the shear strength of geosynthetic interfaces that keep the mass from sliding. Figure 1 schematically portrays the shear forces that work to keep the waste mass from sliding. If sliding occurs, the surface along which sliding would occur is called the critical surface, or potential slip plane. Bottom liner systems that use geosynthetics often have their critical surface along one of the geosynthetic interfaces. The shear strength of these interfaces can usually be measured by means of laboratory testing. These interfaces often realize their peak shear strength within a small amount of relative displacement (on the order of 25 mm), after which their shear strength decreases. Typically, after 50 to 300 mm of relative displacement, the shear strength is reduced to a steady minimum value, which is called the residual shear strength of that interface. Figure 2 shows a typical shear stress-displacement curve for a geosynthetic interface.

Over the life of a landfill the following activities occur: the liner system is built; waste is placed; settlement occurs; a final cover system is installed; and settlement and degradation of the waste continues. Each of these phases of the landfill's life produces different combinations of normal and shear stresses on the liner system. Landfill leachate and gas, which can create destabilizing pore pressures, are by-products of the landfill, and are removed with varying degrees of efficiency. The primary questions addressed in this paper are:

- Should a designer use peak or residual shear strengths, something in between, or a combination of peak and residual strengths, when evaluating a landfill design?
- What does the profession really know about the mobilized shear stresses? (This paper will focus on bottom liner systems.)
- Should the same choice whether to use peak or residual shear strengths be applied along the entire lining system, or should slopes and base liners be treated differently?
- Is there a preferred design approach?
- What factors of safety are appropriate for design?

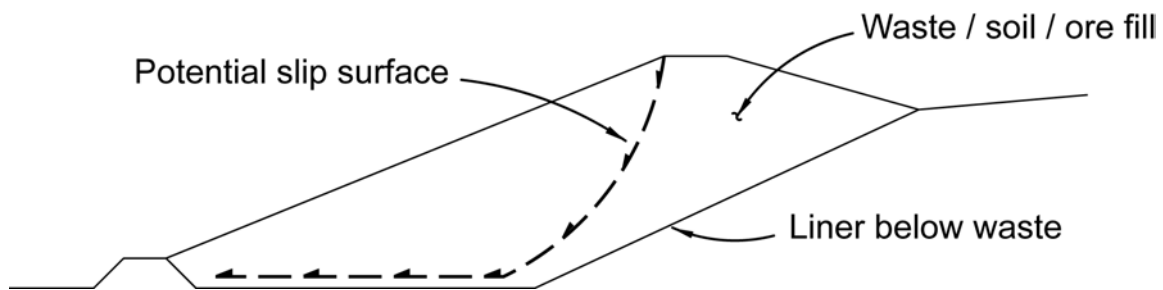


Figure 1 – Schematic of Shear Forces Along Critical Slip Plane

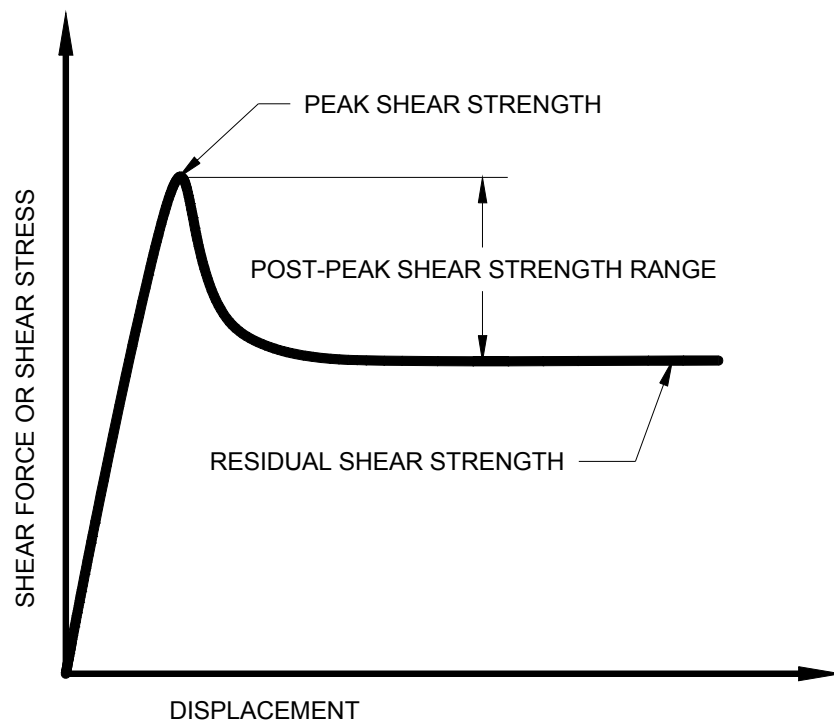


Figure 2 – Example Graph of Shear Force vs. Deformation for Geosynthetic Interface

ORGANIZATION OF THIS PAPER

Part 1 of the paper describes general considerations in performing slope stability analyses. It begins with a discussion of different types of slope stability analyses, including limit equilibrium, finite element, and 2-dimensional (2-D) vs. 3-dimensional (3-D) analyses. Understanding how the state-of-the-practice has developed, and the limitations of the analytical approach, both contribute strongly to making the right selection of appropriate shear strengths and factors of safety.

2-D limit-equilibrium analyses are by far the most common approach for evaluating slope stability. Part 1 discusses practical guidelines and common pitfalls that affect the results of these analyses, especially the selection of the critical shear plane on which the peak or residual shear strength will be modeled. Part 1 also discusses how pore pressures might cause a surface to exceed its peak shear strength and induce progressive failure. Selecting the appropriate shear strength requires an understanding of the effective normal stress range. Also, commissioning direct shear testing from a laboratory requires that one understand the proper testing parameters needed to obtain appropriate peak and/or residual shear strength values.

Part 2 of the paper directly addresses the question of peak vs. residual shear strength, and begins by discussing ductile vs. brittle behavior. Progressive failure, which occurs with brittle materials, then emerges as the chief concern of this paper. The discussion that follows considers conditions that could cause a brittle material to exceed its peak strength in the context of a landfill bottom liner, followed by a brief summary of field observations in this regard.

Part 3 discusses possible design approaches in terms of the selection of peak strength, residual strength, and hybrid approaches, and then considers the appropriate factors of safety for these different approaches.

Part 4 then presents conclusions reached from the preceding discussions. It also provides recommendations for practical design approaches based on the author's experience, as well as recommendations for further research.

This paper surveys the key considerations one employs when deciding whether to use peak or residual shear strength for bottom liner systems in landfills. It does not presume to make that decision, but rather seeks to outline and discuss all considerations that are necessary and pertinent to that process. Although many of the considerations this paper presents may be general enough to apply to cover (veneer) systems, it has been written solely with bottom liner systems in mind, and does not consider the long-term issues related to cover systems.

PART 1 – GENERAL CONSIDERATIONS

LIMIT-EQUILIBRIUM VS FINITE-ELEMENT ANALYSES

Limit-equilibrium analyses, whether 2-D or 3-D, are the most common methods of assessing slope stability. These methods can be performed by hand or, more commonly, by using a computer program. Such analyses evaluate the force and moment equilibrium of a slope on an assumed slip plane given assumed shear strength, unit weight, and pore pressure parameters. The result of these analyses is then presented as a factor of safety (*FS*) defined as:

$$FS = \frac{\text{Shear strength along the slip surface}}{\text{Shear stress along the slip surface}}$$

One defining characteristic of the limit-equilibrium approach is that it presumes that the factor of safety is the same everywhere along the slip plane. Therefore, the mobilized shear stress distribution along the slip plane is simplistically assumed to be a constant ratio of the shear strength along that plane. Such analyses also do not take into account elastic or plastic deformation. These are both significant considerations when deciding whether to use peak or residual shear strength.

Finite-element analyses attempt to calculate the stress distribution and deformations in a soil mass. In addition to considering force and moment equilibrium, these analyses also typically consider the materials' elastic modulus and Poisson's ratio, and some models can also calculate the change in shear strength with displacement for various materials. The result of these analyses is usually presented as a distribution of mobilized shear stress and displacements.

At first glance it would seem that finite-element analyses offer more of what we wish from a slope stability analysis as opposed to limit-equilibrium analyses. So much so, that we might even ask ourselves why we continue to bother with limit-equilibrium analyses. The fact remains, however, that the limit-equilibrium approach has been and will continue to be the basis of standard practice in the industry. The reasons for this, some of which also appear in the next section that considers 2-D vs. 3-D, are:

- Limit-equilibrium approaches have been performed and “calibrated” through industry experience for the past 80 years. Properly performed limit-equilibrium analyses have been proven to be adequate.
- Finite-element analyses are sophisticated and complicated to perform. The average design practitioner often is not adequately trained to perform such analyses, and the low frequency of projects that require their use do not justify the

resources needed to keep an engineer qualified to perform them on every landfill-design firm's staff.

- In the past few years the author has peer-reviewed a number of slope stability analyses. On four major landfill projects for which calculations had been prepared by separate reputable nationwide and local design firms, the author found fundamental errors in 2-D limit-equilibrium analyses. Some of these projects had already been built and were, in the author's opinion, at serious risk of large-scale failure. If such fundamental errors continue to be made with analyses as simple as 2-D limit-equilibrium, the prospects of universalizing a finite-element approach for the solid waste industry is not very promising. Finite-element analyses epitomize the expression "garbage-in garbage-out", so strict quality control and quality assurance is in order whenever they are employed.

2-D vs. 3-D ANALSYES

One issue that is periodically debated in the literature and at professional gatherings is the use of 2-D as opposed to 3-D analyses. Soong et al. (1998) question whether 2-D analyses are appropriate for landfills, and suggest it would be more appropriate to use 3-D analyses with residual strengths. From a pragmatic point of view, the everyday stability analysis has been, and will continue to be, 2-D in actual practice. There are three main reasons for this, clearly laid out by Duncan (1996):

- **Inherent Conservatism.** Properly performed 2-D analyses always give a factor of safety that is equal to or less than those given by 3-D analyses. 2-D analyses, therefore, are more conservative.
- **Ease of Application.** The average professional consulting engineer is interested in the amount of time it will take to arrive at an answer, the frequency of projects that will require special attention, and the effort it will take to organize the results in a final report. 3-D applications are simply not as easy to use as 2-D.
- **Avoidance of Errors.** As illustrated above, analyses are prone to errors, and 3-D analyses are more complicated than 2-D analyses. The author believes that the emphasis in the profession needs to be on performing solid, fundamental engineering, rather than on increased sophistication that invites more errors.

3-D analyses have mostly been used for forensic studies, and for those few complex situations that involve a very unusual geometry and/or distribution of shear strengths in the potential sliding mass. Examples of these can be found in Stark and Eid (1998). In the author's 16 years of experience performing stability analyses on dams, embankments, cut slopes, and landfills, there were only three situations where a 3-D analysis was warranted during design, and all three were satisfactorily accomplished using multiple 2-D sections. One of these projects was given as an example in the Stark

and Eid (1998) paper. In that case Stark and Eid (1998) felt that a 2-D slope stability analysis could not anticipate the combined effects of the project's complicated geometry and shear strength zones. After discussion of the project's complexity, they reported a minimum 3-D factor of safety of 1.65 using a 3-D analysis program. In fact, the original design team, of which the author was a part, had two years earlier calculated a factor of safety of 1.60 using weighted averages of several 2-D cross-sections. Thus, even in this circumstance that had unusually complicated geometry and shear strength conditions, a modified-2-D approach gave results one would expect relative to the 3-D analysis results.

Notwithstanding the reservations given above, 3-D analyses will well serve those who have the time and budget to perform them.

To summarize, the refinements in accuracy offered by 3-D analyses are rarely matched by the average practitioner's understanding of basic slope stability mechanics, much less the level of confidence ordinarily offered by assumed shear-strength and pore-pressure parameters. Most often, the differences in shear strength and pore-pressure assumptions made by different engineers will substantially outweigh the refinements obtained by favoring 3-D over 2-D analyses. Compare, for example, the different conclusions reached by Schmucker and Hendron (1998) versus Stark et al. (2000) regarding the cause of a major landfill failure; or the difference in 2-D vs. 3-D comparisons for a landfill failure described by Soong et al. (1998), from those made by Stark et al. (1998). These case histories, recently published by experienced professionals, do not provide a compelling argument that 3-D analyses should be preferred. They do, however, reinforce the notion that the major factors contributing to uncertainty in a slope's performance are shear strengths and fluid pressures, and that this is where our attention should be focused. The purpose of this paper is to focus specifically on one of these issues, namely, when it is appropriate to use residual vs. peak shear strength for geosynthetic interfaces at the base of a waste containment facility.

GENERAL DISCUSSION OF 2-D ANALYSIS APPROACH

Method of Analysis

Slope stability analyses are most commonly assessed using computer programs that evaluate the limit equilibrium of a 2-D cross-section. Less sophisticated limit equilibrium analyses can be performed using hand-calculation methods or charts. Hand calculations are an effective analysis tool because they often provide a clearer understanding of the critical aspects of the problem, and mistakes in geometry and assumed failure planes are less likely. A common approach is to perform a hand check on the most critical surface that has been analyzed by a computer program. A good summary of slope stability approaches using hand calculations is provided by Abramson et al. (1996).

Limit-equilibrium analyses of varying complexity that have been developed are available to design practitioners. One of the first approaches was the Ordinary Method of Slices developed by Fellenius. Later refinements were presented by Bishop, Janbu, Morgenstern and Price, Spencer, and others. A review of these methods is beyond the scope of this paper, and the reader is referred to Abramson et al. (1996) and Duncan (1996) as a starting place for a comparison of the various limit-equilibrium methods. The author would, however, offer three points from his own practice as to which method to use for performing stability analyses of bottom liner systems:

- The Bishop method is generally not applicable when analyzing bottom liner system geometries because it was developed for circular failure surfaces. The critical slip plane for liner systems is often a translational block that is non-circular.
- Spencer's method, which is now commonly available in computer codes, is considered more rigorous and complete in its analysis than the simplified Janbu method, which is commonly used for block analyses. Spencer's method is computationally more intensive, however, and may be difficult to use for random searches for a critical failure surface, even with modern computers. It is also less stable and can yield incorrect results unless the line of thrust results are checked by the user. Therefore, a good practice is to search for the critical surface using Janbu's simplified approach, and then perform a final check on the stability using Spencer's method. Usually, but not always, Janbu's method will result in a slightly higher factor of safety.
- The approach developed by NAVFAC (1982) for translational block analyses is often a good and appropriate method for performing a hand-check on the computer results for a 2-D translational block failure along a bottom liner system.

Identification of Critical Slip Plane

The most typical requirement for static stability is to meet a specified factor of safety. Just what constitutes an appropriate factor of safety will be discussed later in this paper. The idea is that if the stability analysis is performed correctly with the proper input variables, the factor of safety should provide a level of confidence that the slope will in fact be stable.

The essential operative words in the above paragraph relating to stability analyses is that they are "*performed correctly*". The safety margin in a factor of safety exists to account for unknown or unpredicted deviations from the original design assumptions. It is not, however, supposed to account for errors in the analysis, or incorrect geometric and material property assumptions.

When performing a correct analysis the critical slip plane for analysis must be identified correctly. An experienced geotechnical engineer is usually required in order to

select the critical cross-sections for analysis of a slope. Even for experienced practitioners, though, it is not always obvious which section is the most critical, and several trials generally need to be performed. For very complicated geometries, as described in the previous section, multiple 2-D sections may need to be weighted in order to simulate a 3-D analysis, or the more complex 3-D analysis can actually be performed.

In addition to selecting the proper cross-section, it is also important to search for and select the correct critical slip plane within that cross-section. In peer-reviewing slope stability analyses performed by others, the author has found errors in which the designer had correctly identified the critical cross-section, but incorrectly identified the critical slip plane within that cross-section. He found others, too, in which the designer had conceptually identified the correct slip plane, but failed to code the computer program to correctly place the slip plane at the correct interface within the liner system. The effects of such errors was to drop from an ignorantly-blissful factor of safety of 2 to 3, to an uncomfortable factor of safety of less than 1.1.

When the critical slip plane is along the liner system, the critical surface is always the one that has the lowest peak strength. If residual strengths are used in the analysis, they should reflect the surface that has the lowest peak shear strength, because that is the one that will govern deformations.

Pore Pressures

Next to gravity, pore pressures (most pervasively those caused by liquid as opposed to gas) are the single most prevalent factor contributing to slope stability failures. They are also among the most overlooked elements in slope stability analyses. Schmucker and Hendron (1998) illuminate this problem when they state that “Very little is known at this time regarding the generation and distribution of pore pressures in MSW landfills.”

The one area where evaluating the influence of pore pressures on slope stability has been well focused has been in the design of dams. For this reason there have been few dam failures due to the neglect of pore pressures, with dam failures in the past century generally being caused by other factors (e.g. liquefaction or piping). Pore pressures are not commonly included in landfill analyses. Yet most (or at least many) of the dramatic landfill failures reported in the industry can be attributed to pore pressures that built up either in the foundation, due to waste loading, or in the waste itself, due to leachate buildup or leachate injection. Examples are the Rumpke landfill failure (see Schmucker and Hendron, 1998, who attributed the failure in part to leachate buildup caused by an ice dam at the toe), and the Dona Juana landfill failure (see Hendron et al., 1999, who attributed the failure to high-pressure leachate injection).

When performing slope stability analyses, designers should consider the potential for unanticipated pore pressures. Unanticipated conditions may occur in landfills due to clogging of the leachate collection systems, or aggressive leachate recirculation in the waste mass. Additional discussion of this issue is provided by Koerner and Soong (2000). Further discussion later in this paper describes how pore pressures could lead to a localized exceedence of peak strength, leading ultimately to a progressive failure.

Selecting and Measuring Material Shear Strengths

Shear Strength Definition. Figure 3 illustrates a non-linear shear strength envelope, which is typical for many soil and geosynthetic interfaces. Sometimes the non-linearity is slight, and a straight-line approximation over the entire load range under consideration can be valid. This is often true for very narrow load ranges such as those considered for cover veneer systems. At other times this non-linearity is quite significant, especially when shear strength characteristics are evaluated over the broad range of normal loads indicative of bottom lining systems.

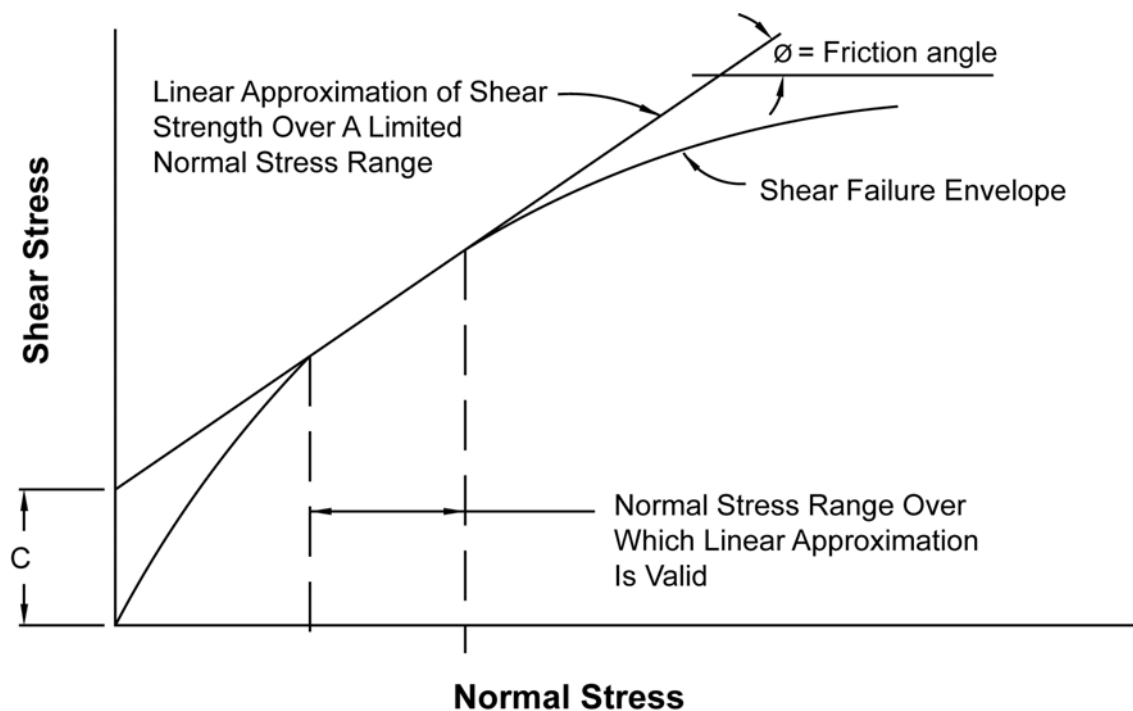


Figure 3 - Typical Shear Failure Envelope for Soil and Geosynthetic Materials.

If the shear strength curve of the evaluated materials is non-linear with respect to normal load, then special consideration should be given to defining the shear strength parameters within a specific normal load range. Many computer programs only allow the input of linear shear strength parameters. These parameters are normally identified as a friction parameter (ϕ) and a cohesion (or adhesion) parameter (c). It is useful to

recognize that these are often only mathematical parameters that describe the shear strength of a material or interface over a specific normal load range. The shear strength parameters are demonstrated in Figure 3.

Draft European Standards, and other publications (e.g. Koerner and Daniel, 1997) suggest that the apparent cohesion of a shear strength envelope can be ignored. As stated by Jones and Dixon (1998): “This assumption can have a significant effect in that the shear strength for any particular normal stress will be quoted as being lower than measured... It is possible that the failure envelope may curve to the origin at very low normal stresses, in which case ignoring the apparent cohesion will result in over conservative results.” If we recognize that the values of the parameters ϕ and c are only mathematical tools used to describe the measured or estimated shear strength over a given normal load range, we can discount statements that advocate that cohesion can be ignored.

The friction parameter (ϕ) is related to the slope of the line (slope = $\tan\phi$), the cohesion parameter (c) is the y-intercept, and the normal load range is the abscissa range over which the straight-line approximation of the shear strength envelope is valid. Use of the shear strength parameters outside of the normal load range for which they were defined is generally non-conservative, as illustrated in Figure 3.

If the computer program only allows the consideration of linear shear strength envelopes, the shear strength envelope for non-linear materials should be discretized into a series of straight-line approximations for different normal load ranges. Furthermore, where the critical slip surface runs through a material or interface that exhibits a non-linear strength envelope, the designer should either use a computer code that allows input of a non-linear shear strength envelope, or assign different strength parameters to different zones of the material or interface according to the normal loading it theoretically experiences. For computer codes that do not allow non-linear shear strength envelopes, the delineation of different normal-load zones for non-linear materials is usually calculated by hand. This procedure is outlined in detail by Thiel et al. (2001).

Shear Strength Measurement. For geosynthetic lining systems, the internal and interface shear strength is normally determined by using the direct shear test in accordance with ASTM D 5321. For GCL internal and interface shear strength evaluation, direct shear testing is conducted in accordance with ASTM D 6243. In these direct shear tests, the geosynthetic material and one or more contact surfaces, such as soil or other geosynthetics, are placed within a direct shear box. The specimens are hydrated, consolidated, and placed under a constant normal load in accordance with the ASTM procedures, along with any project-specific testing clarifications/instructions from the design engineer. A tangential (shear) force is applied to the materials, causing one section of the box to move in relation to the other section. The shear force needed to cause movement is recorded as a function of horizontal displacement.

The test is normally performed for several different normal loads. Typically a series of at least three individual tests are performed at specified normal load conditions. The normal load and shear forces are converted to stresses by the given area over which shear occurred, typically a 12 in x 12 in (300 mm x 300 mm) sample. The peak and post-peak (or residual, if deformation is taken far enough) shear strengths are plotted on a graph, and a best-fit straight line or curve is fit through the data to represent the shear strength envelope. Several factors can influence the interface shear strength of geosynthetics. The most important of these are discussed below.

Valid Testing Technique. While not offering any endorsements, the author can state that he trusts very few laboratories in the nation to provide high quality direct shear test data. Initial ASTM round-robin testing of even the most simple interface (nonwoven geotextile against a smooth HDPE geomembrane) produced a shot-gun scatter of results with very poor correlation. Unless the initial test data has integrity, most of the further considerations offered in this paper become meaningless. It is imperative that the designer screen the testing laboratory in order to obtain test data of assured accuracy.

Rate of Shear Displacement. The typical default shear rate for direct shear testing with geosynthetics as presented in ASTM D 5321 is 0.04 in/min (1.0 mm/min). For testing hydrated GCLs, ASTM D 6243 provides guidance on attaining consolidated drained conditions that should preclude the build-up of excess pore pressures.

In general the rate of shear displacement affects peak strength more than residual strength. Depending on the interface being tested, the strain rate of the test should be slow enough to give results representative of long-term (slow) shear conditions.

Hydration. The moisture content, degree of saturation, and degree of consolidation of adjacent soils and geosynthetics can all exert an influence on the shear strength results. It is important to direct the testing laboratory as to the sequence of hydration and consolidation. With clay soils adjacent to geosynthetics, it is generally more conservative to hydrate under low normal loads before consolidating. Thus far, the type of hydrating fluid has not been reported in the literature as affecting shear strength results, especially in regard to typical landfill leachates.

Normal Stress. The most common strength-related errors in computer slope stability analyses stem from using strength parameters that do not correspond to the normal load conditions at the surface being analyzed (Lambe et al., 1989). It is generally unconservative to extrapolate linear strength envelopes beyond the limits for which they were defined. It is, therefore, important that shear test data be acquired under normal loading conditions that are representative of the conditions being analyzed. For base liners this is zero to full height of the waste mass.

Utilization of Representative Materials. Designers often tend to use either published literature values or previously obtained test results for shear strengths. In such cases, their experience and judgment may assist them in selecting shear strength parameters for the purposes of preliminary design. It is highly recommended, however, that material-specific testing be performed to assist in preparing the final construction specifications, and/or to verify the actual materials delivered as part of a CQA program. The reason for this is that the variation in geosynthetic manufacturing parameters from job to job can have a significant effect on shear strength. The most significant of these is the degree of texturing on coextruded geomembranes. Figure 4 presents a graph showing the difference in peak and post-peak shear strengths obtained with two different degrees of texturing. Designers can use this concept to their advantage, as will be discussed later. Designers unaware of this issue may test a manufacturer's sample and obtain passing results, and then use GRI-GM 13 as a texturing specification. This would provide an extremely low-level requirement for texturing that may not achieve the same interface shear strength as the nice sample provided for initial testing by the manufacturer. The same principle may hold for geotextile-based products, whose fiber denier size, fiber type, degree of needling, etc. can influence its interface shear strength properties. The only way to be sure is to test the actual materials provided for construction.

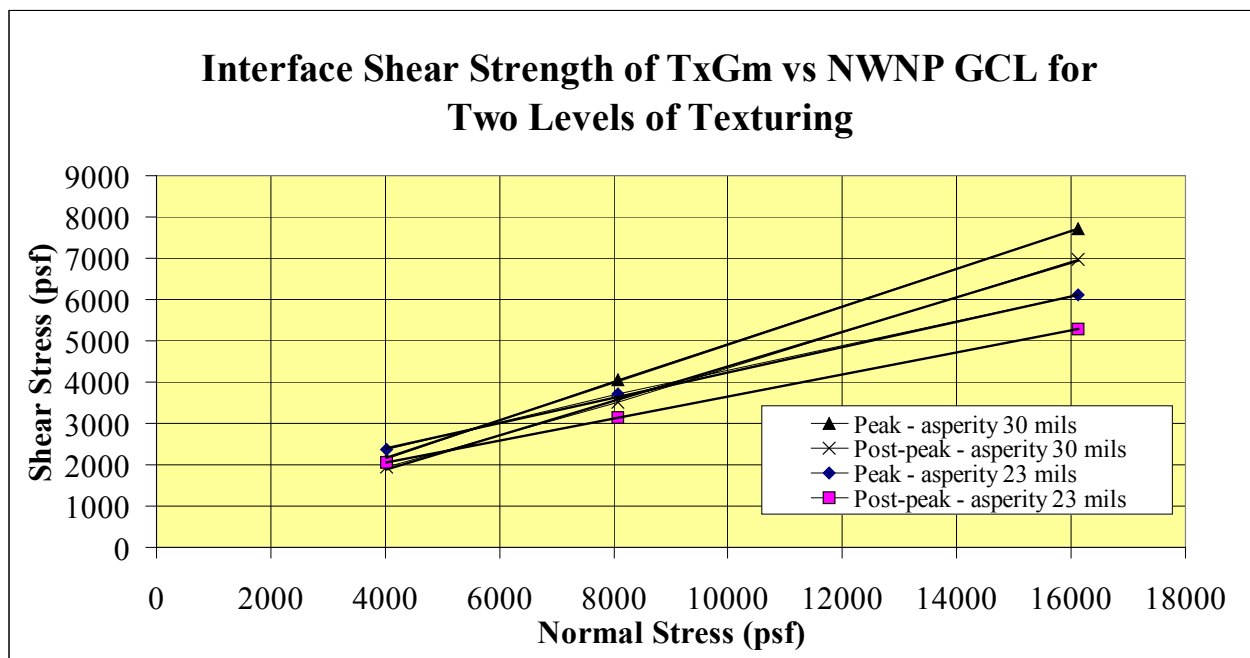


Figure 4 – Variation of Interface Shear Strength with Different Degrees of Geomembrane Texturing

Adjacent Materials and Consolidation Time. Using representative materials for direct shear testing refers not just to the materials for the interface being tested, but also to the adjacent materials. The use of realistic adjacent soil materials will typically provide slightly higher interface shear strengths than will, for example, the use of steel plates. In

the same vein, Breitenbach and Swan (1999) show that longer load consolidation times result in a significant increase in interface shear strengths, apparently due to micro-scale load-induced deformation of the interface materials. Jones and Dixon (1998) question the use of the ring-shear apparatus for testing, because the narrow specimen of limited surface area on hard, smooth boundaries may not be representative of field conditions. These factors can affect both the peak and post-peak shear strength results.

Peak vs. Post-Peak vs. Residual Shear Strength. The highest level of shear strength measured in a direct shear test under a given normal load is defined as the peak strength. With continued shear displacement there is typically a loss of strength. The shear strength at any given displacement past the point of peak strength is referred to as “post-peak strength”. The strength at which there is no further strength loss with continued displacement is called the “residual strength”. Many of the most common direct shear devices do not allow enough displacement to occur that would enable true residual strength to be measured (e.g., see Stark et al., 1996). Therefore, in some cases it is not technically correct to refer to end-of-test conditions as representing the “residual” strength, but rather, to refer to “post-peak” strength while also specifying the amount of displacement. For the purposes of this paper, the lowest expected shear strength after significant deformation (typically more than 3-6 inches [70-150 mm]) is described as the residual shear strength. Shear strengths between the peak and residual shear strength are referred to as post-peak. This brings us then, to the main focus of this paper, which is whether it is appropriate to use peak or residual shear strengths (or something in between).

PART 2 – PEAK vs. RESIDUAL: THEORETICAL AND PRACTICAL CONSIDERATIONS

BACKGROUND DISCUSSION ON BRITTLE MATERIALS AND PROGRESSIVE FAILURE

Many, but not all, geosynthetic interfaces are strain softening. This highlights the essence of the peak vs. residual question. With a relatively short amount of deformation (typically less than 25 mm), the materials pass beyond peak strength into a lower post-peak shear strength, ultimately becoming what we call residual. In geotechnical engineering these shear strength characteristics are also sometimes called ‘brittle’ – brittle meaning that the material substantially decreases in strength after it is “broken”, that is, has gone past peak strength. (Note that this has nothing to do with the tensile behavior of the material.) This behavior is in contrast to a ductile shear interface, which continues to deform after reaching its peak strength, but retains its strength close to the peak. An example of a brittle geosynthetic interface is an HDPE textured geomembrane against a geotextile, which produces a dramatic drop in strength after the peak strength is

exceeded. An example of a ductile geosynthetic interface is a smooth PVC geomembrane against a geotextile (see data published by Hillman and Stark, 2001). Also, MSW waste is generally considered a ductile material in terms of shear strength (Kavazanjian, 2001).

As a progressive failure develops, the shear stresses are redistributed within the slope. This often involves the slow deformation of the failing mass over time, followed by an abrupt slide. If the critical plane supporting a slope is brittle, and for some reason part of it is stressed past its peak strength, then that part quickly becomes significantly weaker, which means it can carry less of the load. That in turn puts more of the load on other parts of the critical plane, which may in turn cause another part of that plane to become overstressed and exceed its peak strength. The continuation of this process is called progressive failure. At some point the entire system becomes overstressed and an abrupt failure occurs. This is the concern when there is a brittle interface.

Progressive failures have been characteristically noted for stiff clays, as described by LaRochelle (1989): “We have come to realize that we cannot count on the peak strength in this strain-softening material either for short- or long-term stability.” Past landfill failures have been attributed to this same phenomenon (Schmucker and Hendron, 1998; Mazzucato et al., 1999; Stark et al., 2000), which holds significant potential for future failures (Gilbert and Byrne, 1996).

POTENTIAL CONDITIONS THAT MAY LEAD TO PROGRESSIVE FAILURE

Several reasons are provided below which explain why the peak strength of a bottom liner interface might unexpectedly be exceeded.

Non-Uniform Stress Distribution and Strain Incompatibility

Perhaps one of the most compelling reasons to be concerned about progressive failure in liner systems is that the stress distribution along the liner interface is not known. “It is impossible to obtain all of the necessary information in most cases” to perform a rigorous analysis of a progressive failure process (Tiande et al. 1999). “It is difficult to determine the available shear resistance along an interface exhibiting strain-softening behavior. It may be unsafe to assume that peak strength is available, while it may be excessively conservative and costly to assume that only the residual strength is available” (Gilbert and Byrne, 1996).

The complexities of stress distribution are affected by the type of loading and by pore pressures. According to Li and Lam (2001) “.. the development of progressive failure will also be different depending on whether failure is triggered by a rise in water table [*insert by author: namely, leachate*] or an increase in external loading [*insert by author: namely, continued waste stacking*]”.

Reddy et al. (1996) present a most interesting finite-element modeling study that evaluates the stress distribution and deformations along a landfill liner system for an assumed landfill geometry. Their study compares smooth and textured interfaces for different stiffnesses of waste. Although their analysis did not model strain-softening behavior of the interfaces, the results provide valuable insight into stress and strain distribution. Some of the conclusions from their study are:

- The stiffness of the waste influences the distribution of interface stress and shear displacements. Stiffer waste puts more stress and strain on side slopes (especially the lower part of the slope). Softer (more compressible) waste puts more stress on the base liner below the highest part of the waste, and more strain accumulation towards the toe. The overall factor of safety, however, is not affected by the waste stiffness, assuming that no strain-softening of the interface shear strength occurs.
- The smooth interface with 11° friction reached its peak strength in a number of places along the interface in their example, even though the global factor of safety was 1.5. The textured interface did not approach its peak strength anywhere along the interface in their example, but had a factor of safety of over 4. This means that a typical stability evaluation that results in a factor of safety of 1.5 may actually result in areas of the critical interface achieving their peak strength and possibly going into a reduced post-peak strength.

A finite element study was performed by Filz et al. (2001) who reached conclusions similar to those obtained by Reddy et al. (1996). Filz et al. (2001) provided a compelling demonstration that a smooth clay-geomembrane interface exhibiting strain-softening characteristics might be inappropriate to analyze based on peak shear strengths. They showed that the distribution of mobilized shear stresses was not uniform along the base and side slope, and would result in progressive exceedence of peak strength. Their comparative analyses demonstrated that whereas a limit-equilibrium analysis based on peak strengths might result in $FS = 1.6$, the finite-element analysis would suggest impending failure (i.e. $FS = 1.0$). The same problems analyzed using residual shear strengths in limit-equilibrium analyses resulted in an average $FS = 0.94$. Furthermore, for a finite-element analysis to show $FS = 1.5$, the limit-equilibrium analysis based on peak strengths needed to show a FS of about 2.2, and the limit-equilibrium analyses using residual shear strength resulted in $FS = 1.3$.

Differences in the relative stiffnesses of the overlying waste as compared to that of the liner interface are also cited by Gilbert and Byrne (1996) as a significant potential cause of deformations along the liner interface that could lead to residual shear strengths.

Similar suppositions are made by Stark et al. (2000), who postulate that strain incompatibility between MSW and underlying interfaces can lead to progressive failure, as they believe was the underlying cause of the Rumpke landfill failure. The weaker lower interfaces may achieve post-peak strengths before the MSW ever achieves peak

strength. After peak strength of the interfaces is achieved, the peak strength of the MSW may be mobilized at a time when the strength of the interfaces is reduced to the residual value. They state: “The greater the difference between the stress-strain characteristics of the MSW and the foundation soil or geosynthetic interfaces, the smaller the percentage of [peak] strength mobilized in the MSW and underlying materials.”¹

Unexpected Increases in Pore Pressure

The typical effect of pore pressures is to decrease the effective normal stress, which in turn decreases the effective shear strength, even as the shear stress that is driving instability remains unchanged. When pore pressures are introduced, the effective shear strength may be reduced to the point that the peak shear strength at that location is exceeded, at which point progressive failure can begin. This was what Schmucker and Hendron (1998) concluded was the triggering mechanism for the Rumpke landfill failure.

Seismic Loading

With seismic loading there is certainly the potential for deformation to occur along the critical failure plane, which can reduce the strength of the critical interface below its peak strength. In this regard the design practitioner needs to assess the potential for this type of deformation and, if the design earthquake is expected to produce deformation greater than about 20 mm, then the residual strength of that interface must be considered.

Construction Deformation

Construction conditions frequently result in temporary stability conditions with lower factors of safety than the completed fill scenario. To the author’s knowledge, the effect of preliminary interface deformation at low normal loads on the subsequent shear strength at higher normal loads has only been documented in one recent study by Esterhuizen et al. (2001). They showed that for a smooth clay-geomembrane interface, deformations at low normal loads would partially, but not fully, reduce the peak strength of the interface at higher normal loads. They provide a very interesting “work-softening” model to describe this behavior in a manner that can be used in a finite-element analysis. Although their model fits the data very well, it is only applicable to the specific clay and geomembrane used for their study, and it is not known at this time how well their approach would work for other interfaces. This is an area for further research.

¹ For years now the author has heard the statement that the strain incompatibility between waste and liner systems could be a major consideration in selecting appropriate shear strengths. It is interesting, however, that some of the literature reports surprisingly low amounts of deformation required to reach the peak strength of the waste; on the order of only 40 mm for rigid-body deformation. See, for example, Eid et al. (2000), Stark et al. (1998), Mazzucato et al. (1999). Also Kavazanjian (2001) states his belief that strain compatibility with MSW is not nearly as significant an issue as has generally been supposed, based on direct- and simple-shear test results that show that the strains and deformations required to reach peak strength are comparable to those required for most soils.

Waste and Foundation Settlement

Over time there is substantial deformation and settlement of the waste that may cause unknown redistribution of stresses. The settlement of waste adjacent to a sideslope has often been noted as a source of downdrag forces, which may become great enough to exceed the peak strength of one of the slope liner interfaces. This phenomenon was cited by Stark and Poeppel (1994) as a mechanism contributing to the Kettleman Hills landfill failure, and is echoed in Gilbert and Byrne's (1996) theoretical study: "...it is more likely that the residual strength will be mobilized along the side slope rather than the buttress [bottom liner]", and they even go so far as to say "...it is unlikely that an average stress greater than the residual value could be mobilized along a typical side slope in a containment system." Likewise, foundation settlement has the potential to cause differential movements of the liner system.

Aging and Creep

Geosynthetic durability has been the subject of many papers and studies which address the ability of geosynthetics to maintain their physical properties as containment barriers, and to some extent as tensile reinforcement. Little has been published, however, regarding the long-term durability of shear interfaces such as, for example, the long-term dependence on the strength of geotextile fibers at interfaces with textured geomembranes, or within reinforced GCLs. Quantitative predictions regarding the long-term aging and creep potential of geosynthetic interfaces are certainly beyond the author's capacity, but are noted as an additional potential mechanism whereby the assumed peak strength of an interface might be reduced.

FIELD OBSERVATIONS

From the author's experience and his informal polling of industry representatives, two general field observations that have been made regarding deformations along geosynthetic interfaces on slopes:

- Slopes that were designed with robust interfaces using textured geomembrane or granular materials against geosynthetics, have not been observed to undergo tension or deformation.
- Slopes that had less brittle, but also less strong interfaces, such as a geotextile over a smooth geomembrane, have been observed to result in tension in the upper geosynthetic, presumably due to slippage along the interface which occurred as a result of downdrag forces.

It is worthwhile to note in the Gilbert and Byrne (1996) model that strain softening on the slope would generally only occur if the slope angle was greater than the peak friction angle of the lining material. Although unverified by the author, this may be a

general guideline for estimating whether or not peak or residual shear strength would occur on a slope (excluding seismic forces). For example, on a 3(H):1(V) slope, perhaps a peak interface strength of 18° or more would maintain its peak strength, and an interface strength of less than that would have a higher potential for going into residual.

Given the large number of landfills constructed with geosynthetic bottom liner systems, it is quite surprising how few failures have actually been reported. Furthermore, none of the reported failures, to the author's knowledge, involved the progressive failure of a substantially brittle geosynthetic interface. Most of those failures have involved soil (including bentonite failures associated with unreinforced GCLs, which are ductile relative to shear strength). The best example of a pure geosynthetic failure that involved some degree of strain softening is the notorious Kettleman Hills failure, but the interfaces in that failure were fairly weak to begin with (all against smooth HDPE), and the initial factor of safety, even assuming peak strengths of the interfaces as they existed, was low, and below standard industry guidelines.

The conclusion of industry observations is that actual industry experience has not shown degradation of peak strength (i.e. progressive failure) to be a pervasive problem. Nonetheless, it definitely presents a potential problem that has on occasion bloomed into an unfortunate reality. It is, therefore, worth taking it into account by means of design and analysis considerations, which are discussed in the next section.

PART 3 - DESIGN APPROACHES

THE PEAK vs. RESIDUAL ISSUE IN THE CONTEXT OF THE DESIGN PROCESS

Many elements of a landfill are not designed, per se, but are largely dictated either by the owner's desires or by regulatory constraints. For example, the geometry of a landfill (boundaries, slopes, height, etc.) is often governed by an attempt to maximize the resource (i.e. volume) while meeting the constraints presented by conditional use permits, property line setbacks, maximum slope regulations and the like. Furthermore, the liner system is usually prescribed by regulation, at least in its fundamental requirements, and oftentimes by a default regulatory configuration.

In many cases then, the two major elements that influence a stability analysis are largely predetermined. That is, both the preferred landfill geometry and the liner system are more or less given to the "designer", who is charged with producing the "final design". From the point of view of slope stability, what is there left to do? Obviously the slope stability should be checked and verified. What does this mean and how is it done?

The first step in performing a slope stability analysis is to define the basis of the analysis. This is often documented in the project files as a Design Basis Memorandum (DBM), in which the following kinds of determinations are made:

- Will the analysis look at only the final configuration, or at interim operational configurations as well? (The latter option is highly recommended for risk management.)
- What unit weight will be assumed for the waste?
- What material strength values will be assumed for the different materials, and how will they be determined?
- Which pore-pressure scenarios will be evaluated?
- What will be the minimum acceptable factors of safety?
- Are seismic analyses required? If so, what approach will be used? How is the design earthquake defined? If a deformation approach is used, what is the maximum allowable deformation?

The results of the slope stability analyses will be:

- A static factor of safety (for each configuration analyzed).
- If a seismic analysis is required, the results will present either a potential magnitude of deformation along the critical slip plane, or a factor of safety for a simplified pseudo-static analysis.
- A description of the minimum required interface shear strength properties for the liner system construction.

It is this last point that makes slope stability analyses a design function rather than a mere geotechnical engineering exercise. It is essential that a clear linkage be made between the slope stability calculations and the ultimate project specifications, to ensure that the proper materials are provided during construction to meet the slope stability requirements. If the analysis results do not meet expectations, iterations of laboratory testing and/or alterations in slope geometry and/or liner materials may be required in order to achieve an acceptable design that can be adequately specified.

The design aspect of slope stability analyses becomes even more interesting when an additional constraint is put on the design criteria, namely to position the critical slip surface above the primary geomembrane. This is a common practice in Germany that is also employed by several design practitioners in the United States (and likely in other places as well, given the author's limited knowledge of practices worldwide). This design approach helps to ensure that, if for any reason slippage does occur, the barrier liner system will remain intact. Ensuring that the slip plane is above the primary geomembrane is not necessarily a simple matter; laboratory shear testing programs and

iterations of slope stability analyses are often required in order to achieve acceptable results.

Implicit in the slope stability design and analysis process is the need to decide whether peak or residual shear strengths should be used. Though this is not generally an issue for waste materials, which are usually considered ductile, it is often a significant issue for liner system interfaces. This decision will significantly influence the calculated factor of safety. For seismic analyses, the influence is often less significant, because if the seismic analysis indicates deformation will occur, a prudent designer will use a post-peak shear strength (even as the question remains whether to use a deformation-based post-peak strength, or a true residual strength).

WHAT IS AN APPROPRIATE FACTOR OF SAFETY?

The author previously co-authored a paper whose title posed this same question concerning cover systems (Liu et al., 1997). That paper discussed assessing the degree of confidence in each of the variables that went into assessing the factor of safety, and assessing the potential risk and cost of a failure. This approach is espoused by Gilbert (pers. comm.) who believes that the factor of safety should be based on “uncertainties, assumptions, and the consequences of failure.”

It is common in the literature to see geotechnical references that reiterate the idea that the greatest degree of uncertainty in performing slope stability analyses is the shear strength of the materials (e.g. Liu et al, 1997; Stark and Poeppel, 1994; Duncan, 1996). Given that the factor of safety is a reflection of uncertainty, it should logically reflect the degree of uncertainty in the shear strength properties. This was clearly noted by Terzaghi and Peck (1948, pg. 106):

“The practical consequences of the observed differences between real soils and their ideal substitutes must be compensated by adequate factors of safety.”

A commonly accepted value for the factor of safety in geotechnical engineering slope stability analyses is $FS \geq 1.5$. Many engineers blindly accept this value while remaining ignorant of its basis. The origin of this value was the empirical result of analyzing the relative success and failure of dams that have been constructed over the past century. Experience proved that when an analysis was performed correctly, assuming reasonable and prudent material properties, an earthen structure with a factor of safety of 1.5 can be expected to remain stable even when some of its structural geometry and material properties have varied from those assumed in the analysis. Similarly, other values for an acceptable factor of safety have been established as general industry practice for other types of problems, such as bearing capacity (required FS generally between 2 and 5) or drainage applications (FS generally ranging from 1 to 20 depending on the problem).

It is also fundamental to the establishment of generally accepted factors of safety that analyses are performed correctly, and are based on prudent assumptions regarding material properties, geometry, unit weights, and pore pressures. Factors of safety are not intended to compensate for engineering errors or omissions. Indeed, the author has evaluated failures where the design factor of safety exceeded 1.5, which means that the original design neglected to take into account one or more critical factors.

With containment lining systems we meet a unique opportunity. We have a greater ability to know where the potential critical slip plane is, and can measure its shear strength characteristics more accurately than we can in a number of traditional geotechnical problems. We have far more knowledge of the geometry and shear strengths than when we are confronted with a natural slope, for example. Knowing where slippage is most likely to occur, we have to assess the implications for deformation. As described previously in this paper, we often don't really know if some deformation will occur, but experience from many analogous failures, along with the process of deduction, tells us that it *could* occur. Knowing this, we should at least be prepared to use the post-peak shear strength of the surface having the lowest peak strength.

SPECIFIC APPROACHES

Some specific design approaches, which the author has himself employed, are summarized below. This does not imply that others approaches do not exist, but simply that this paper is based on the author's experience.

1. The Most Conservative Approach – Force the Slip Plane Above the Geomembrane and Use Residual Shear Strengths Everywhere the Slip Plane Occurs in the Liner System. A simple and common way of achieving this objective is to use single-side textured geomembrane for the primary liner, and then cover it with a geotextile or geonet product. In nearly every case the author has been involved with (save a few inevitable exceptions), single-sided textured geomembrane (textured side down, of course) always caused whatever slippage occurred to take place on the top surface of the geomembrane, if it was covered with another geosynthetic. Even when directly covered by a granular material, it was often possible to make the bottom (textured) interface stronger than the smooth geomembrane/granular soil interface. In our experience there is often not a large difference between the peak and residual shear strength on smooth geomembrane interfaces with either other geosynthetics or granular soils, and these interfaces would not be considered very brittle. There may be some exceptions, such as a smooth HDPE geomembrane against a wet clay as described by Filz et al. (2001) for the Kettleman Hills failure analysis.

Some designs may need greater shear strength for interim construction and operational conditions than can be provided by a smooth geomembrane surface, so a double-sided textured geomembrane may be required. In this case the design condition of having the weak interface above the primary geomembrane may still be achieved by specifying a more aggressive texturing on the lower side of the geomembrane (see shear data presented in Figure 4).

If a designer is able to use the residual shear strength of the upper geomembrane interface and achieve acceptable factors of safety, this design can be very safe from the point of view of both stability and environmental containment. This approach is favored by Hullings and Sansome (1997), who recommend: “If possible, provide a slip plane and a stress-free geomembrane.”

If true residual shear strengths are used for the analysis, and those strengths are measured with a degree of confidence that they represent worst case for the liner system interfaces, it follows that a lower-than-typical factor of safety can be allowed. Gilbert and Byrne (1996) suggest that a factor of safety simply greater than unity may be an adequate design criterion for analyses that assume residual shear strengths are the only strengths mobilized along the entire slip surface. Part of Gilbert’s rationale (personal communication, 2001) is that even if a failure were induced for a slope analyzed with this criterion, things could not degenerate quickly, presuming the analysis were properly performed. The slope could subsequently be monitored and measures taken to reduce the deformation rate, if deemed necessary.

A similar recommendation is given by Stark et al. (1998): “...strain incompatibility can facilitate the development of slope instability because the geosynthetic interface may mobilize a post-peak or residual strength while the waste is mobilizing a strength that is significantly below the peak strength. This can be incorporated into a design by assigning a residual strength to the critical interface or slip surface and requiring a factor of safety, $FS > 1$...Because field interface displacements and *effect(s) of progressive failure are not known [emphasis by author]*, a factor of safety, $FS > 1$ with a ring shear residual interface strength assigned to all potential slip surfaces should be satisfied in addition to meeting regulatory requirements.”

Filz et al. (2001) suggest that if true residual shear strengths are used for the analysis, then whatever factor of safety would normally be deemed appropriate for a given project could be reduced by the following reduction factor (RF):

$$RF = \tau_r / [\tau_r + 0.1(\tau_p - \tau_r)]$$

Where τ_r = residual shear strength, and τ_p = peak shear strength. They imply that the normally appropriate factor of safety would be determined based on considerations of uncertainty and consequences as described by Duncan (2000). Also, it should be noted that their discussion and recommendations were restricted to smooth-geomembrane/clay interfaces.

2. Safe Approach – Use Residual Shear Strength of the Interface with the Lowest Peak Strength. This approach could be the same as the above approach if the interface having the lowest shear strength happens to be above the primary geomembrane. If, due to overall slope stability constraints, the interface with the lowest peak strength is below the primary geomembrane (e.g. weak subgrade interface), this approach will still result in a very safe design relative to slope stability. It could, however, be less conservative in terms of environmental containment should deformation occur, causing a tear in the primary geomembrane. This approach is recommended by Gilbert and Byrne (1996) who “strongly recommended that the potential for instability be explored in a limit equilibrium analysis using residual strengths along all interfaces....It is strongly recommended that a factor of safety greater than one be achieved in all containment system slope designs, assuming residual strengths are mobilized along the entire slip surface.”

The same degree of factor of safety for this approach would apply as for Approach # 1 above. Holley et al. (1997) reported using residual shear strengths for a critical surface below the primary geomembrane in a steep canyon landfill, and obtaining operating factors of safety of 1.2 and an ultimate factor of safety of 1.4 for the final build-out. It is not clear if these were their minimum design criteria, or simply the results that they accepted.

3. Brute Strength Approach – This approach would employ very aggressive texturing to achieve high interface strengths, although the assumed strengths may be prorated by some factor to account for variability. The need to occasionally use this approach is suggested by Hullings and Sansome (1997): “Overall slope stability conditions often do not allow low interface strengths, so the interface strengths above the geomembrane cannot be much lower than the interface strength on the underside of the geomembrane.”

If the approach of high interface strength is used everywhere, and seismic analysis shows no deformation, an acceptable design basis may be to use peak shear strength with an adequately high factor of safety. How high is adequate is difficult to say, because the theoretical possibility of progressive failure still exists. The finite-element study performed by Filz et al. (2001) indicates that $FS > 2$ should be required for analyses based on peak strength of smooth-geomembrane/clay interfaces.

We have only the record of successful designs that were constructed based on peak strength to testify that the brute strength approach may be valid, but this does not demonstrate that it is conservative. The analysis should account for potential leachate build-up under worst case assumptions, for example after a post-closure maintenance period with substantial leachate still being generated, and the operations or leachate-collection layer completely clogged. Check that a submerged condition at the toe does not result in a reduction in shear strength (due to reduction in effective normal stresses) to the point that it fails the peak strength at the toe, which could lead to progressive failure through the rest of the fill (such as that discussed by Schmucker and Hendron, 1998).

4. Hybrid Approaches

- a) *Use Residual on the Side Slope and Peak on the Base.* To the author's knowledge, this approach was first documented in the literature by Stark and Poeppel (1994) in their review of the notorious Kettleman Hills failure. As they so aptly stated: "...it appears that peak and residual interface strengths should be assigned to the base and sideslopes, respectively, for design purposes." This was later echoed by Jones and Dixon (1998) from the U.K., who stated: "In some instances residual values may be appropriate on the side slope where large displacements are anticipated, used together with peak values on the base." In the author's opinion, this approach is a strong qualifier for accepting a traditional factor of safety in the range of 1.5 for ultimate build-out conditions (assuming unexpected pore-pressure scenarios are included in the evaluation), and 1.3 for operations.
- b) *Use Post-Peak Strength Values that Anticipate a Limited Amount of Deformation.* Shear strength reductions may occur due to relative deformations during construction, landfill operations, and waste settlement, but these deformations may be less than those which would lead to the minimum residual shear strength conditions. Also, based on their observation of numerous apparently successful facilities, design practitioners may consider peak shear strengths with an adequate factor of safety to be valid designs, while still wishing to incorporate an additional degree of conservatism by reducing the measured peak strength of the geosynthetic interfaces. These strength reductions would be applied to the side slope as well as the base. Use of this approach is suggested by Filz et al. (2001), who suggest using a mobilized strength that is higher than the residual by about 10% of the increment from residual to peak strength, and applying an appropriate factor of safety to this based on reliability concepts as described by Duncan (2000).

- c) *Use Lower Waste Shear Strengths.* From the observation of trends published in the literature, shear strengths of 30° or more are commonly used for municipal solid waste. This level of shear strength has been documented as being generally conservative (e.g. Kavazanjian, 2001), but may require some amount of strain to become fully mobilized. As an approach to stability analyses designers may wish to reduce the mobilized strength of the waste material to more closely match the strain compatibility of the liner system.

The author has used all the above approaches in his own practice, which over the years has been based on improved levels of understanding. Currently (subject to change!) the author employs a combination of Approach #1 and #4 as his standard practice. That is, he usually defines a “design condition” which he believes will be the actual long-term conditions that interface shear strengths will experience. The decision as to what long-term shear strengths he selects is project-specific (there are many variations), and a complete discussion of this is beyond the scope of this paper. Suffice it to say that the decision is usually related to the criteria described for Approach #4. Next, the author follows the advice of Gilbert and Byrne (1996) and checks that the stability under the worst-case shear strength conditions (e.g. hydrated residual shear strength) results in $FS > 1.0$. This latter test is often the more significant.

A good example of the above approach is for bottom liner designs that involve the encapsulation of unreinforced bentonite between two geomembranes. The design scenario argues that most of the bentonite will remain dry for at least several centuries, and the basic slope stability analysis is performed on this basis. A second analysis is performed, however, to verify that the stability factor of safety is greater than unity even when all of the bentonite is under fully hydrated residual shear strength conditions. This example is more fully described in Thiel et al. (2001).

PART 4 – CONCLUSIONS AND RECOMMENDATIONS

CONCLUSIONS

- Many geosynthetic interfaces are highly strain-softening (i.e. “brittle”). The most common example is a textured geomembrane against some form of geotextile (whether it be a cushion, part of a geonet composite, or a GCL).
- There are mechanisms that can lead to exceedence of peak strength even though a correctly-performed slope stability analysis predicts a factor of safety greater than one. Examples of these mechanisms include:
 - Non-uniform mobilized stress distribution.

- Relative differences in stiffness between waste and liner materials.
 - Unexpected pore pressures.
 - Seismic loading.
 - Deformation during construction.
 - Waste settlement.
 - Foundation settlement.
 - Aging and creep of the geosynthetics.
- Exceedence of peak strength in a brittle interface can result in progressive failure.
 - Based on field observation, most facilities designed with aggressive interface shear strengths are not experiencing post-peak shear strength, which means that the working shear stress is probably less than or equal to the peak strength. Only a few examples of progressive failure along geosynthetic interfaces have occurred in the industry, and these have not been along highly brittle interfaces, which means that the projects did not have high factors of safety to begin with, even assuming peak interface strengths.
 - Several design approaches have been used over the years and the standard-of-practice is evolving. In the United States a preferred approach has not yet clearly emerged.

RECOMMENDATIONS FOR PRACTICE

- Designers and CQA firms should conduct material-specific testing of interfaces to verify that the materials specified and/or supplied for a project are realistic and meet the design requirements. Whoever commissions the testing should possess a skilled familiarity with the design objectives as well as the testing technique.
- Designers should attempt to position the critical slip plane above the primary geomembrane to the extent feasible for a given project. If a double-sided textured geomembrane is required for construction or operational stability, attempt to specify more aggressive texturing on the under side of the geomembrane.
- Using peak shear strengths on the landfill base, and residual shear strengths on the side slopes appears to be a successful state-of-the-practice in many situations.
- Designers should consider evaluating all facilities for stability using the residual shear strength along the geosynthetic interface that has the lowest peak strength. This would be an advisable risk-management practice for designers, even if the FS under these conditions is simply greater than unity.

- Regardless of the design assumptions, specify soil spreading by pushing up-slope only, and require close monitoring of LCRS and operations soil placement on slopes during construction to verify that relative shear displacement does not occur during construction. Exceptions to this practice should be allowed only with field tests and CQA verification.
- If LCRS or operations soils are placed as part of landfill operations, designers should assume the worst and automatically assume residual side-slope shear strength conditions will occur (and extra leakage rates as well). The reason for this is that construction by landfill operators is usually not controlled and monitored closely.
- Check stability for a potential leachate buildup, especially near the toe of the landfill.

RECOMMENDATIONS FOR FURTHER RESEARCH

- More finite element analyses at an academic level, such as those performed by Reddy et al. (1996) and Filz et al. (2001) would be warranted, to gain a better understanding of the threshold beyond which localized stress distributions might cause exceedence of peak shear resistance. Refinements in the analyses would include modeling the strain-softening behavior of the geosynthetic interfaces, and checking different types of interfaces and geometries. The results of these analyses might prove useful for establishing guidelines as to when peak strengths might be exceeded and when they might be maintained. Ultimately, the author envisions correlations between the FS determined by limit equilibrium analyses, ratios of peak interface strengths to waste fill strengths, and relative stiffnesses (somewhat as proposed by Gilbert and Byrne (1996), but more specific and less general), being used to estimate when and where peak vs. post-peak strengths would be reached at the interfaces.
- The monitoring of slope deformation on geosynthetic interfaces that are being buried by waste is recommended. One fairly easy way to do this would be to use the simple tell-tale technique employed for the Cincinnati cover demonstration project (Koerner et al., 1996), though this would require participation by landfill owners and operators. This avenue of research echoes that suggested by Gilbert and Byrne (1996), who state: “Future research should focus on measuring deformations and mobilized shear resistances in existing waste containment facilities.”
- The monitoring of pore pressures in the LCRS above liner systems, with the reporting of the worst-case conditions, would provide valuable information regarding long term conditions in landfills. Unfortunately, any high pressures would likely result in a permit violation at many facilities, so it is improbable that

an existing owner will voluntarily monitor high pressures, much less report them. We are therefore left with only orphan or Superfund sites as a possible basis for monitoring. Because of this limitation, participation in international waste conferences is increasingly valuable.

- Additional laboratory testing, conducted on various types of interfaces, would be useful to assess the impact of interface deformations at low normal loads on the peak strength reductions at higher normal loads.

REFERENCES

Abramson, L.W., Lee, T.S., Sharma, S., and Boyce, G.M. (1996). Slope Stability and Stabilization Methods. John Wiley & Sons, Inc. New York.

Breitenbach, A.J. (1997) "Overview Study of Several Geomembrane Liner Failures Under High Fill Load Conditions." Proc. of Geosynthetics '97, IFAI, Vol. 2, pp. 1045-1061.

Breitenbach, A.J. and Swan, R.H. (1999) "Influence of High Load Deformations on Geomembrane Liner Interface Strengths." Proc. of Geosynthetics '99, IFAI, Vol. 1, pp. 517-529.

Brink, D., Day, P.W. and DuPreez, L. (1999) "Failure and Remediation of Bulbul Drive Landfill: Kwazulu-Natal, South Africa." Proc. Sardinia '99 Seventh International Waste Management and Landfill Symposium, CISA, Vol. III, pp. 555-562.

Duncan, J.M. (1996) "State of the Art: Limit Equilibrium and Finite-Element Analyses of Slopes." J. of Geotechnical Engineering, ASCE, Vol. 122, No. 7, May, pp. 577-596.

Duncan, J.M. (2000) "Factors of Safety and Reliability in Geotechnical Engineering" J. of Geotechnical and Geoenvironmental Engineering, ASCE, Vol. 126, No. 4, Apr., pp. 307-316.

Eid, H.T., Stark, T.D., Evans, W.D. and Sherry, P.E. (2000) "Municipal Solid Waste Slope Failure. I: Waste and Foundation Soil Properties." J. of Geotechnical and Geoenvironmental Engineering, ASCE, Vol. 126, No. 5, May, pp. 397-407.

Esterhuizen, J.B., Filz, G.M., and Duncan, J.M. (2001) "Constitutive Behavior of Geosynthetic Interfaces" J. of Geotechnical and Geoenvironmental Engineering, ASCE, Vol. 127, No. 10, Oct., pp. 834-840.

Filz, G.M., Esterhuizen, J.B., and Duncan, J.M. (2001) "Progressive Failure of Lined Waste Impoundments" J. of Geotechnical and Geoenvironmental Engineering, ASCE, Vol. 127, No. 10, Oct., pp. 841-848.

Gilbert, R.B. and Byrne, R.J. (1996) "Strain-Softening Behavior of Waste Containment System Interfaces." *Geosynthetics International*, IFAI, Vol. 3, No. 2, pp. 181-203.

Gilbert, R.B. (2001) Personal communication with the author.

Hendron, D.M., Fernandez, G., Prommer, P.J., Giroud, J.P., and Orozco, L.F. (1999) "Investigation of the Cause of the 27 September 1997 Slope Failure at the Dona Juana Landfill" *Proc. Sardinia '99 Seventh International Waste Management and Landfill Symposium*, CISA, Vol. III, pp. 545-554.

Hillman, R.P. and Stark, T.D. (2001) "Shear Strength Characteristics of PVC Geomembrance-Geosynthetic Interfaces." *Geosynthetics International*, IFAI, Vol. 8, No. 2, pp. 135-162.

Holley, K., Richardson, J., and Sadlier, M. (1997) "Design and Construction to Optimise Landfill Stability at the Nent Landfill, Hong Kong." *Proc. Sardinia '99 Seventh International Waste Management and Landfill Symposium*, CISA, Vol. III, pp. 565-574.

Hullings, D.E. and Sanome, L.J. (1997) "Geomembrane Anchor Trenches." *J. of Geotextiles and Geomembranes*, Elsevier, Vol. 15, Nos. 4-6, pp. 403-417.

Jones, D.R.V. and Dixon, N. (1998) "Shear Strength Properties of Geomembrane/Geotextile Interfaces." *J. of Geotextiles and Geomembranes*, Elsevier, Vol. 16, Nos. 1, pp. 45-71.

Kavazanjian, E. (2001) "Mechanical Properties of Solid Waste." *Proc. Sardinia '01 Eighth International Waste Management and Landfill Symposium*, CISA, Vol. III, pp. .

Koerner, R.M., Carson, D.A., Daniel, D.E., and Bonaparte, R. (1996) "Current Status of the Cincinnati GCL Test Plots" *Proceedings of the 10th GRI Conference, Field Performance of Geosynthetics and Geosynthetic Related Systems*. Geosynthetic Research Institute, Drexel University, Philadelphia, PA, pp. 147-175.

Koerner, R.M. and Daniel, D.E. (1997) Final Covers for Solid Waste Landfill and Abandoned Dumps. ASCE Press, Reston, VA.

Koerner, R.M. and Soong, T.Y. (2000) "Leachate in Landfills: The Stability Question." *Geotextiles and Geomembranes*, Elsevier, Vol. 18, pp. 293-309.

LaRochelle, P. (1989) "Problems of Stability: Progress and Hopes." The Art and Science of Geotechnical Engineering. Ed. by Corning et al., Prentice Hall, N.J., pp. 269-290.

Li, K.S. and Lam, J. (2001) Discussion of “Evolution of Progressive Failure of Landslides.” J. of Geotechnical and Geoenvironmental Engineering, ASCE, Vol. 127, No. 1, Jan., pg. 98.

Liu, C.N., Gilbert, R.B., Thiel, R.S., and Wright, S.G. (1997). “What is an Appropriate Factor of Safety for Landfill Cover Slopes?” Conference Proceedings from Geosynthetics '97. IFAI, Roseville, MN, pp. 481-496.

Mazzucato, A., Somonini, P. and Colombo, S. (1999) “Analysis of Block Slide in a MSW Landfill.” Proc. Sardinia '99 Seventh International Waste Management and Landfill Symposium, CISA, Vol. III, pp. 537-544.

NAVFAC (1982) Soil Mechanics. Design Manual 7.1, Department of the Navy, Naval Facilities Engineering Command, Alexandria, VA.

Reddy, K.R., Kosgi, S. and Motan, S. (1996) “Interface Shear Behavior of Landfill Composite Liner Systems: A Finite Element Analysis.” Geosynthetics International, IFAI, Vol. 3, No. 2, pp. 247-275.

Schmucker, B.O. and Hendron, D.M. (1998) “Forensic Analysis of the 9 March 1996 Landslide at the Rumpke Sanitary Landfill, Hamilton County, Ohio.” Proc. of the 12th GRI Conference, Lessons Learned from Geosynthetic Case Histories, Geosynthetic Institute, Folsom, PA, pp. 269-295.

Soong, T.Y., Hung, O., and Koerner, R.M. (1998) “Stability Analyses of Selected Landfill Failures by 2-D and 3-D Methods” Proc. of the 12th GRI Conference, Lessons Learned from Geosynthetic Case Histories, Geosynthetic Institute, Folsom, PA, pp. 296-329.

Stark, T.D. and Eid, H.T. (1998) “Performance of Three-Dimensional Slope Stability Methods in Practice” J. of Geotechnical and Geoenvironmental Engineering, ASCE, Vol. 124, No.11, Nov., pp. 1049-1060.

Stark, T.D., Arellano, D., Evans, W.D., Wilson, V.L., and Gonda, J.M. (1998) “Unreinforced Geosynthetic Clay Liner Case History.” Geosynthetics International, IFAI, Vol. 5, No. 5, pp. 521-544.

Stark, T.D., Eid, H.T., Evans, W.D. and Sherry, P.E. (2000) “Municipal Solid Waste Slope Failure. II: Stability Analyses.” J. of Geotechnical and Geoenvironmental Engineering, ASCE, Vol. 126, No. 5, May, pp. 408-419.

Stark, T.D., and Poeppel, A.R. (1994) “Landfill Liner Interface Strengths from Torsional Ring Shear Tests.” J. of Geotechnical Engineering, ASCE, Vol. 120, No. 3, March, pp. 597-615.

Terzaghi, K. and Peck, R. (1948) Soil Mechanics in Engineering Practice. John Wiley & Sons, New York, NY.

Thiel, R., Daniel, D.E., Erickson, R., Kavazanjian, E., and Giroud, J.P. (2001) *GundSeal GCL Design Manual*. Published by GSE, Houston, TX.

Tiande, M., Chongwu, M, and Shengzhi, W. (1999) “Evolution Model of Progressive Failure of Landslides.” J. of Geotechnical and Geoenvironmental Engineering, ASCE, Vol. 125, No. 10, Oct., pp. 827-831.

**APPLICATION FOR PERMIT RENEWAL AND MODIFICATION
SANDOVAL COUNTY LANDFILL**

**VOLUME III: LANDFILL ENGINEERING CALCULATIONS
SECTION 3: SLOPE STABILITY ANALYSIS**

ATTACHMENT III.3.B

**GORDON ENVIRONMENTAL, INC. AUGUST 2005. *VOLUME V: HYDROGEOLOGY,*
SECTION 1: HYDROGEOLOGY. SANDOVAL COUNTY LANDFILL
APPLICATION FOR PERMIT.**

**APPLICATION FOR PERMIT
SANDOVAL COUNTY LANDFILL**

**VOLUME V: HYDROGEOLOGY
SECTION 1: HYDROGEOLOGY**

TABLE OF CONTENTS

1.0	INTRODUCTION	1-1
2.0	REGIONAL GEOLOGY AND HYDROGEOLOGY	1-3
2.1	Physiographic Setting	1-3
2.2	Structural Setting	1-3
2.3	Regional Stratigraphy	1-7
2.3.1	Pre-Santa Fe Tertiary Deposits	1-7
2.3.2	Santa Fe Group Deposits	1-9
2.3.3	Post-Santa Fe Quaternary Deposits	1-10
2.4	Regional Hydrogeology	1-11
3.0	SITE GEOLOGY AND HYDROGEOLOGY	1-13
3.1	Summary of Previous Investigations	1-13
3.2	2003/2004 Drilling and Sampling	1-15
3.3	Borehole Plugging	1-17
3.4	Geotechnical Evaluation	1-17
3.5	Site Geology	1-18
3.5.1	Site Stratigraphy	1-18
3.5.2	Site Structure	1-23
3.6	Site Hydrogeology	1-23
4.0	BORE HOLE PLUGGING CERTIFICATION	1-26
5.0	REFERENCES	1-27

LIST OF FIGURES

Figure No.	Title	Page
V.1.1	SITE LOCATION MAP	1-2
V.1.2	PHYSIOGRAPHIC PROVINCES	1-4
V.1.3	ALBUQUERQUE BASIN	1-5
V.1.4	REGIONAL CROSS-SECTION OF NORTHERN ALBUQUERQUE BASIN	1-6
V.1.5	STRATIGRAPHIC COLUMN OF THE NORTHERN ALBUQUERQUE BASIN	1-8
V.1.6	REGIONAL GROUNDWATER ELEVATION CONTOUR MAP	1-12
V.1.7	BORING LOCATION MAP	1-14
V.1.8	GEOLOGIC MAP	1-20
V.1.9	SITE STRATIGRAPHIC COLUMN	1-21
V.1.10	SITE GEOLOGIC CROSS-SECTION A-A'	1-22
V.1.11	SITE MONITORING WELLS AND POTENTIOMETRIC CONTOURS	1-25

LIST OF TABLES

Table No.	Title	Page
V.1.1	SUMMARY OF EXPLORATORY DRILLING	1-15
V.1.2	SUMMARY OF GEOTECHNICAL TEST RESULTS	1-19

LIST OF ATTACHMENTS

Attachment No.	Title
V.1.A	BORING LOGS
V.1.B	WORKPLAN FOR MW-5 MONITORING WELL
V.1.C	NMED APPROVAL FOR MW-5
V.1.D	SUBMITTAL OF THE SANDOVAL COUNTY MW-5 MONITORING WELL INSTALLATION REPORT
V.1.E	PROPOSED LANDFILL EXPANSION SUBSURFACE INVESTIGATION WORKPLAN
V.1.F	NMED WORKPLAN APPROVAL
V.1.G	MONITORING WELL INSTALLATION REPORT FOR MW-6 AND MW-7
V.1.H	GEOTECHNICAL LABORATORY RESULTS
V.1.I	PHOTO LOG OF GEOLOGY AND 2004 DRILLING ACTIVITIES
V.1.J	ANNUAL GROUNDWATER MONITORING REPORT, MAY 2004
V.1.K	REQUEST FOR REDUCTION IN GROUNDWATER MONITORING REQUIREMENTS
V.1.L	NMED APPROVAL FOR REDUCTION
V.1.M	BASELINE GROUNDWATER MONITORING SYSTEM REPORT FOR SANDOVAL COUNTY LANDFILL

HYDROGEOLOGY

1.0 INTRODUCTION

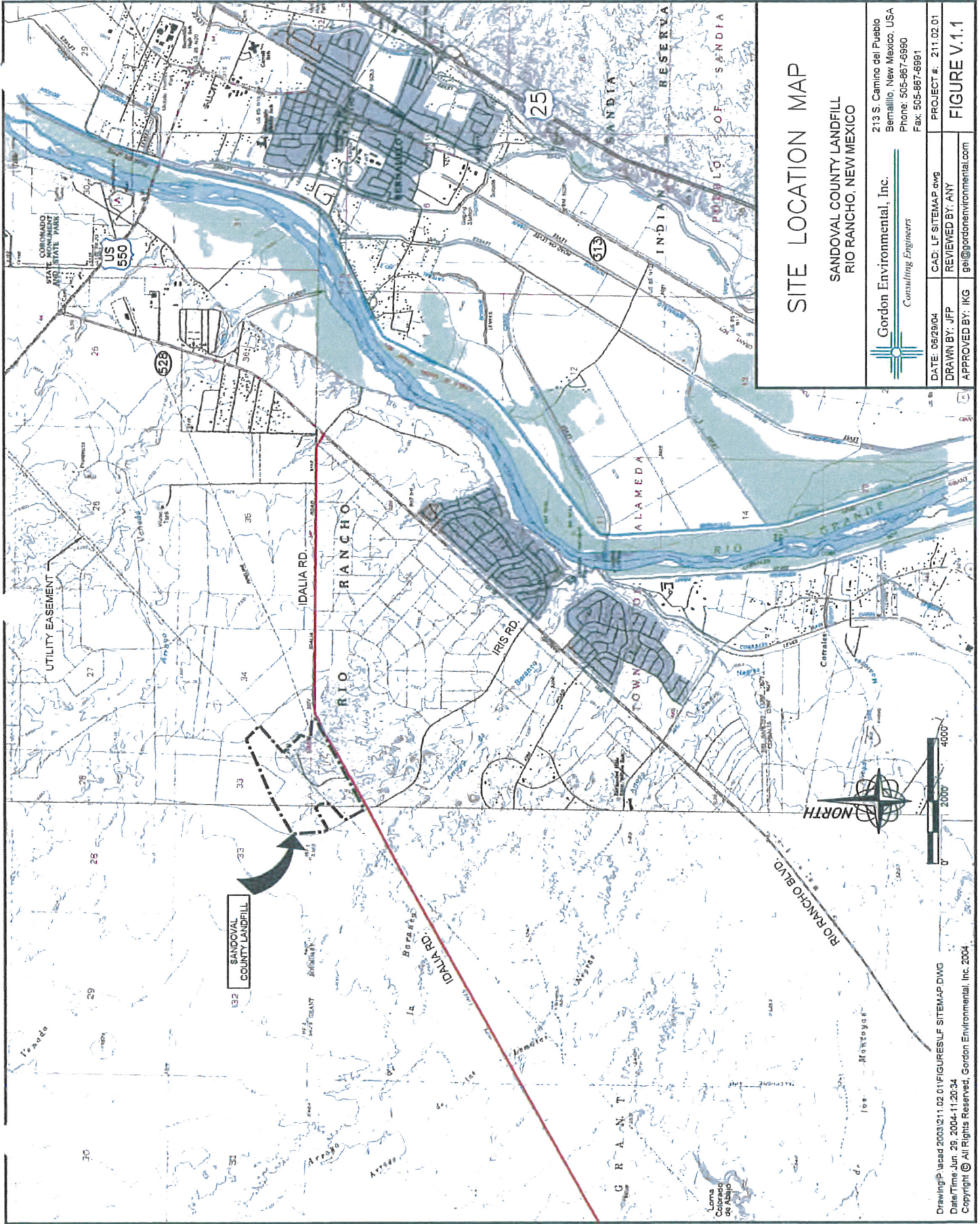
This hydrogeologic report was prepared by Gordon Environmental, Inc. (GEI) to demonstrate the suitability of a lateral expansion to the existing Sandoval County Landfill (SCLF). Specifically, this report provides geologic and hydrogeologic data developed in response to 20 NMAC 9.1, Section 202.7.

The data presented herein was compiled from published literature of the central New Mexico area and the results of on-site geologic investigations. The geologic investigation results correspond well with the published regional information. The SCLF is located in southern Sandoval County, within the city limits of Rio Rancho, New Mexico. The subsurface deposits are of the Upper Santa Fe Group and consist primarily of fine-grained, sandstones with interbedded mudstones and scattered lenses of gravels.

Groundwater has been encountered below the site at depths ranging from 330 to 440 feet below ground surface (fbgs) under unconfined conditions in sandstones in the Arroyo Ojito Formation. Due to the substantial depth to groundwater and the relative impermeability of the intervening deposits, the proposed site is an excellent setting for a municipal solid waste landfill.

The SCLF is a $177 \pm$ acre site that includes the current SCLF and adjacent property evaluated for a lateral expansion. The existing landfill, operating in compliance with NMED Permit No. SWM-050304, has been in operation since approximately 1983.

The SCLF is situated in southern Sandoval County, within the city limits of Rio Rancho, located about three miles southwest of the intersection of U.S. Highway 550 and State Highway 528 (**Figure V.1.1**).



SITE LOCATION MAP

SANDOVAL COUNTY LANDFILL
RIO RANCHO, NEW MEXICO



213 S. Camino del Pueblo
Bernalillo, New Mexico, USA
Phone: 505-867-6990
Fax: 505-867-6991

DATE: 05/29/04	CAD: LF SITEMAP.dwg	PROJECT #: 211.02.01
DRAWN BY: JFP	REVIEWED BY: ANY	FIGURE V.1.1
APPROVED BY: IKG	gel@gordonenvironmental.com	

2.0 REGIONAL GEOLOGY AND HYDROGEOLOGY

2.1 Physiographic Setting

The SCLF is located in the Albuquerque Basin of the northern Mexican Highland Section of the Basin and Range Physiographic Province (**Figure V.1.2**). This basin is situated in the Rio Grande Rift Zone, just outside the easternmost extent of the Colorado Plateau Province. The SCLF is located within the Rio Grande watershed, approximately 95 miles east of the continental divide.

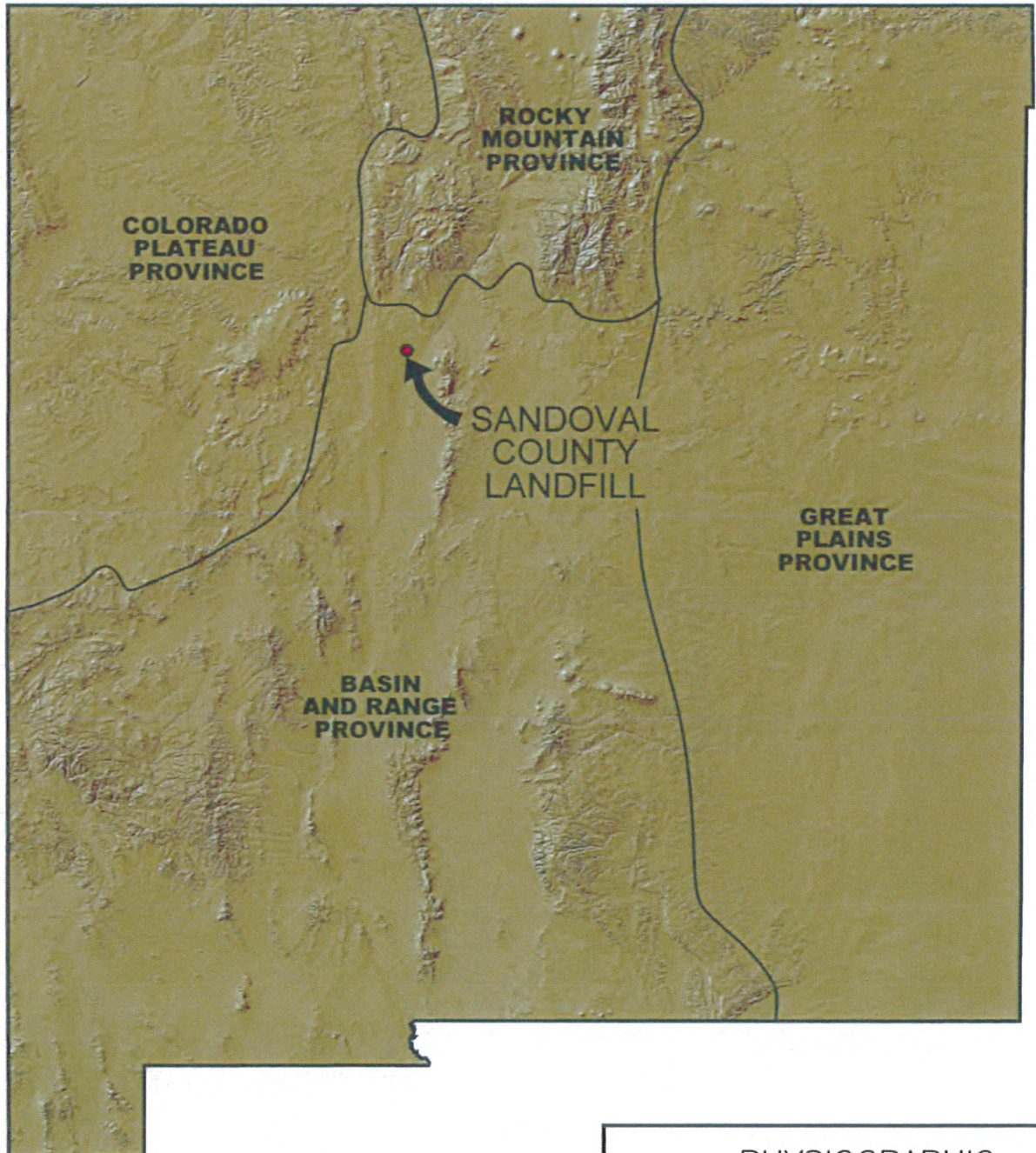
2.2 Structural Setting

The Albuquerque Basin is the largest of four en echelon structural basins that developed along the Rio Grande Rift. This north-south trending rift zone begins in south-central Colorado and extends to south-central New Mexico – a distance of approximately 350 miles. The Albuquerque Basin was formed through crustal extension occurring within the rift zone, resulting in elevated heat flows, faulting, volcanism and thick basin fill (up to 14,000 feet).

The Albuquerque Basin covers an area of approximately 2,700 square miles, and is approximately 90 miles long by 30 miles wide (Woodward, 1987). The Basin is structurally complex, with numerous major regional faults associated with rifting intersecting within and around the basin. Several of these faults bound major crustal blocks. Subsurface geophysical data indicate that the basin is divided into two half-grabens. The Tijeras Fault (**Figure V.1.3**), a major structural feature cross-cutting the rift south of Albuquerque, acted as a zone of accommodation for the two half-grabens. The presence of these two half-grabens allowed for the formation of two distinct sedimentary sub-basins with different sedimentary signatures: the Northern and Southern Albuquerque Basins.

The SCLF is located within the Northern Albuquerque Basin (**Figure V.1.3**), which displays about 1,150 feet of structural relief along its west side (SNL/NM, 1995). **Figure V.1.4** shows a regional west-east cross-section (Section A-A') through the Northern Albuquerque Basin that shows the subsurface geometry of the half-graben. The basin is a deep, sediment filled inner depression flanked by a series of faulted ramps along the margins (Hawley and Haase, 1992). This north-trending basin was subject to significant subsidence and northwest-southeast extension within the last 30 to 40 million years (Woodward, 1987; Lozinsky et al., 1991). Contemporaneous sedimentation derived from the erosion of newly emerging highlands and associated intermittent volcanic activity filled the basin during subsidence.

NEW MEXICO



PHYSIOGRAPHIC PROVINCES

SANDOVAL COUNTY LANDFILL
RIO RANCHO, NEW MEXICO

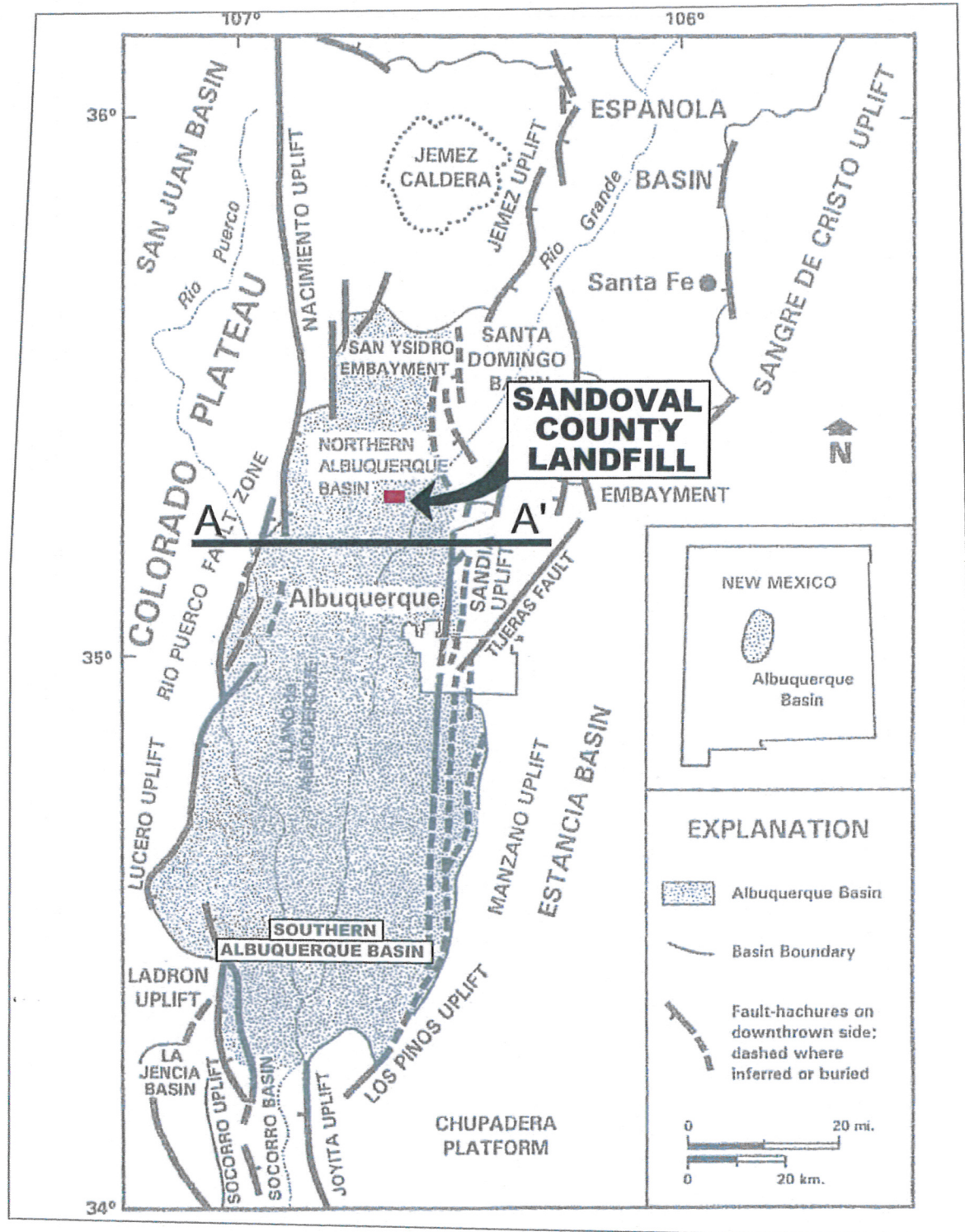


Gordon Environmental, Inc.
Consulting Engineers

213 S. Camino del Pueblo
Bernalillo, New Mexico, USA
Phone: 505-867-6990
Fax: 505-867-6991

Drawing: P:\acad 2003\211.02.01\FIGURES\SCLF PHYSIO.dwg
Date/Time: Jul. 09, 2004-13:24:14
Copyright © All Rights Reserved, Gordon Environmental, Inc. 2004

DATE: 06/29/04	CAD: SCLF PHYSIO.dwg	PROJECT #: 211.02.01
DRAWN BY: JFP	REVIEWED BY: JAB	
APPROVED BY: IKG	gei@gordonenvironmental.com	FIGURE V.1.2



SOURCE: LOZINSKY AND TEDFORD (1991)

Drawing P:\acad 2003\211.02.01\FIGURES\SCLF FAULTS.dwg
Date/Time: Jul. 09, 2004-13:25:10
Copyright © All Rights Reserved, Gordon Environmental, Inc. 2004

ALBUQUERQUE BASIN

SANDOVAL COUNTY LANDFILL
RIO RANCHO, NEW MEXICO



Gordon Environmental, Inc.
Consulting Engineers

213 S. Camino del Pueblo
Bernalillo, New Mexico, USA
Phone: 505-867-6990
Fax: 505-867-6991

DATE: 06/29/04

CAD: SCLF FAULTS.dwg

PROJECT #: 211.02.01

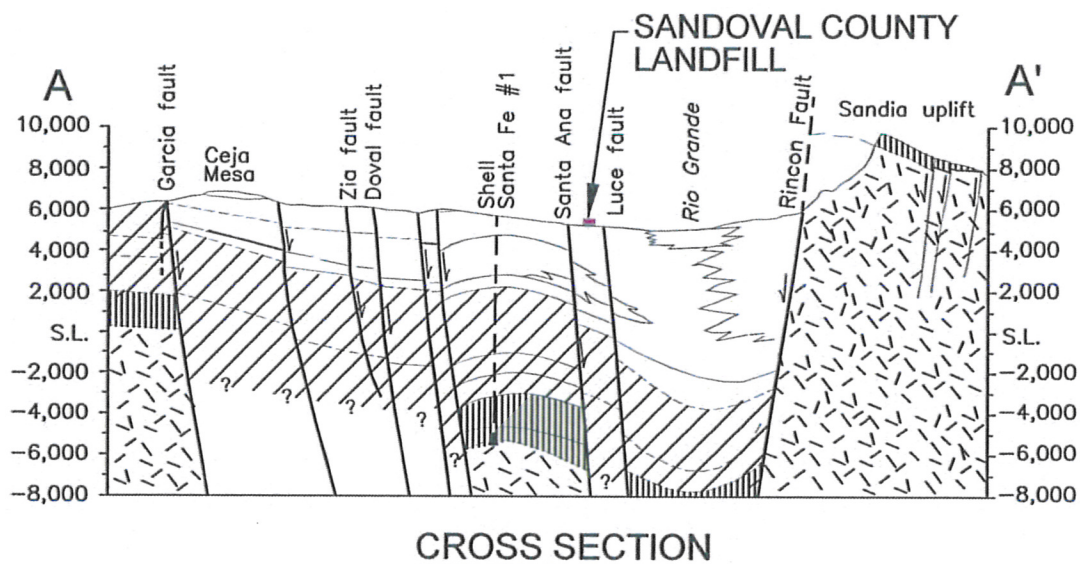
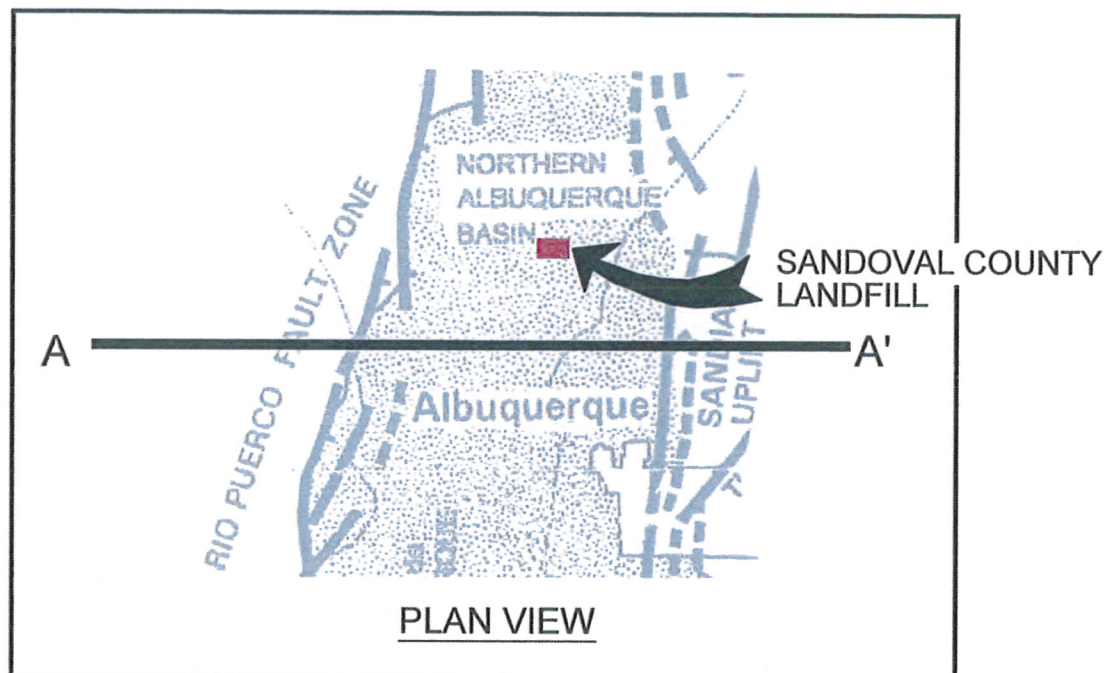
DRAWN BY: JFP

REVIEWED BY: JAB

APPROVED BY: IKG

gei@gordonenvironmental.com

FIGURE V.1.3



LEGEND



SOURCE: LOZINSKY AND TEDFORD (1991)

REGIONAL CROSS-SECTION OF NORTHERN ALBUQUERQUE BASIN

SANDOVAL COUNTY LANDFILL
RIO RANCHO, NEW MEXICO



Gordon Environmental, Inc.
Consulting Engineers

213 S. Camino del Pueblo
Bernalillo, New Mexico, USA
Phone: 505-867-6990
Fax: 505-867-6991

DATE: 06/29/04	CAD: SCLF GEOLOGIC.dwg	PROJECT #: 211.02.01
DRAWN BY: JFP	REVIEWED BY: JAB	
APPROVED BY: IKG	gei@gordonenvironmental.com	FIGURE V.1.4

2.3 Regional Stratigraphy

The Northern Albuquerque Basin occurs in an active tectonic zone (i.e., the Rio Grande Rift) that has been evolving and receiving sediment for at least the last 25 million years (late Oligocene to present). **Figure V.1.5** is a representative stratigraphic column for the Northern Albuquerque Basin.

Regional stratigraphy in the basin includes rocks ranging in age from Precambrian through Holocene (Kelley, 1977). The stratigraphic column is comprised of continental alluvial, fluvial, eolian, and lacustrine sediments, with minor inter-bedded mafic to intermediate volcanic rocks and detritus. For the purpose of this discussion, the stratigraphic record has been divided into three sections based on age and depositional environment: Pre-Santa Fe Tertiary deposits, Santa Fe Group Basin Fill deposits, and post-Santa Fe Quaternary deposits.

2.3.1 Pre-Santa Fe Tertiary Deposits

Along the eastern margin of the basin, where the Sandia uplift is exposed (see **Figure V.1.3**), the Santa Fe Group is underlain by Precambrian, Paleozoic, and Mesozoic rocks that outcrop in small marginal embayments, benches, and minor inliers. The extent to which pre-Santa Fe Group rocks are present at depth along the rift axis (i.e., the middle of the basin) is uncertain. These older sediments indicate that at least one depositional basin was present prior to the formation of the North Albuquerque Basin.

Four regional unconformities mark truncations in the pre-Santa Fe Group rock record (**Figure V.1.5**). The oldest unconformity is represented where the middle Pennsylvanian Sandia Formation rests directly on Precambrian basement rocks. The second unconformity occurs between the Upper Permian Glorieta Sandstone and the San Andreas Formation. The Glorieta Sandstone is comprised of medium to coarse-grained yellowish gray sandstone, while the San Andreas Formation is comprised of gray limestone with red shale interbeds.

The third unconformity occurs between the Upper Triassic Santa Rosa Sandstone and the overlying Eocene to Paleocene Baca/Galisteo Formations. The Santa Rosa Sandstone is comprised of buff to brown sandstone with abundant petrified wood. Erosion has removed most of the Cretaceous and Jurassic strata in the basin. However, deep oil test well data obtained from the Northern Albuquerque Basin indicates that the Santa Fe Group is locally underlain by Upper Cretaceous strata (Lozinsky, 1988; Cather, 1992).

ERA/SYSTEM/SERIES			UNIT/FORMATION		STRAT. COLUMN	DESCRIPTION
C E N O Z O I C	N E O G E N E	Holocene to Middle Pleistocene	Surficial Units			Cross-bedded, fine- to medium-grained eolian sand Poorly-sorted silty sandy cobble to boulder gravel
		Early Pleistocene to Early Miocene	Santa Fe Group	Upper Santa Fe Unit		Poorly-sorted silty sandy cobble to boulder gravel with relict and buried soils <i>Unconformity</i> <u>Caja Member, Arroyo Ojito Formation:</u> coarse grained sand and gravel <u>Loma Bordon Member, Arroyo Ojito Formation:</u> fine-grained silty sand with thin interbedded clay and gravel.
				Middle Santa Fe Unit		<u>Basinal:</u> medium- to fine-grained sandstone and mudstone; common buried soils <u>Marginal:</u> conglomeratic sandstone to pebbles and cobbles; common buried soils
				Lower Santa Fe Unit		<u>Basinal:</u> medium- to fine-grained sandstone, sandy mudstones <u>Marginal:</u> conglomeratic sandstone and mudstone <i>Unconformity</i>
	P A L E O G E N E	Oligocene	Unit of Isleta #2 Well			Fine- to coarse-grained sandstone; claystone, silt beds; volcanic detritus and ash-flow tuffs
		Eocene to Paleocene	Baca/ Galisteo Formations			Sandstone, variegated mudstone, and conglomerate
MESOZOIC		Upper Triassic	Santa Rosa Sandstone			<i>Unconformity</i> Buff brown sandstone, petrified wood
P A L E O Z O I C	Upper Permian	San Andres Formation			Gray limestone, separated by red shale	
		Glorieta Sandstone			<i>Unconformity</i> Medium- to coarse-grained yellowish gray sandstone	
	Lower Permian	Yeso Formation			<u>Upper:</u> gypsiferous sandstone, siltstone, and limestone <u>Lower:</u> fine-grained sandstone and siltstone	
		Abo Formation			Fine- to coarse-grained sandstone and conglomerate with interbedded siltstone	
		Madera Group	Bursum Fm.		Finely laminated silty mudstone	
	Upper to Middle Pennsylvanian		Wild Cow Formation		Rhythmically bedded sequence: conglomerate, sandstone, siltstone, shale, and limestone	
			Los Moyos Formation		Gray calcarenite with chert	
	Middle Pennsylvanian	Sandia Formation			Fining-upwards clastic sequence: conglomerate to calcareous siltstone <i>Unconformity</i>	
PRECAMBRIAN		Isleta Metasediments Tijeras Greenstone Complex Coyote Canyon Sequence Sandia Granite			Phyllite; meta-arkose; metaquartzite; greenstone; metarhyolite; quartzite; microcline and biotite granite	

ADAPED FROM SANDIA NATIONAL LABS/NEW MEXICO
1995 SITE-WIDE HYDROGEOLOGIC
CHARACTERIZATION PROJECT

STRATIGRAPHIC COLUMN OF THE NORTHERN ALBUQUERQUE BASIN

SANDOVAL COUNTY LANDFILL
RIO RANCHO, NEW MEXICO



Gordon Environmental, Inc.
Consulting Engineers

213 S. Camino del Pueblo
Bernalillo, New Mexico, USA
Phone: 505-867-6990
Fax: 505-867-6991

Drawing: P:\acad 2003\211.02.01\FIGURES\SCLF STRAT C.dwg
Date/Time: Jul. 09, 2004-13:26:46
Copyright © All Rights Reserved, Gordon Environmental, Inc. 2004

DATE: 08/29/04	CAD: SCFL STRAT C.dwg	PROJECT #: 211.02.01
DRAWN BY: JFP	REVIEWED BY: JAB	
APPROVED BY: IKG	gei@gordonenvironmental.com	

FIGURE V.1.5

The Eocene Baca/Galisteo Formations are generally less than 1,600 feet thick and were derived from non-volcanic, terrigenous sources. Sandstone, variegated mudstone and conglomerate are the principal rock types in the formation.

Finally, the fourth unconformity occurs between the Unit of Isleta #2 Well and the Miocene Lower Santa Fe Group and is represented in the central and eastern portions of the basin. The Oligocene Unit of Isleta #2 Well, estimated to reach thicknesses of about 7,000 feet locally, was derived primarily from non-volcanic terrigenous and intermediate composition volcanic source areas. Fine to coarse-grained sandstones, siltstones and claystones, and ash-flow tuffs are the dominant rock types in the unit. In the western part of the basin, the Santa Fe Group lies conformably upon the Unit of Isleta #2 Well.

2.3.2 Santa Fe Group Deposits

The Santa Fe Group is the major sedimentary unit in the North Albuquerque Basin. The Santa Fe Group ranges in age from about 25 million to 1 million years and was deposited prior to and during evolution of the Albuquerque Basin. The Santa Fe Group consists of alluvium derived from adjacent mountain highlands, with significant contributions from alluvial, fluvial, lacustrine and eolian sources (Ingarsoll et. al., 1990). The Santa Fe Group ranges from about 3,000 feet thick along the basin margins, to over 14,000 feet thick in the deeper axial portion of the basin (Lozinski, 1988; Russell and Snellson, 1990).

Hawley and Haase (1992) divided the Santa Fe Group into three units, the lower, middle and upper Santa Fe, based upon depositional environment and age. The Lower Santa Fe Unit is dominated by intercalated piedmont-slope, eolian, and fine-grained basin-floor deposits. Fan alluvium characterizes the piedmont deposits, while playa-margin alluvium and playa sediments form the major basin floor deposits. Conglomeritic sandstones are abundant. These deposits range in age from about 30 to 15 million years (middle Oligocene to middle Miocene).

The Middle Santa Fe Unit is dominated by piedmont-slope sediments with a strong fluvial contribution along the margins of the basin. Basinal medium to fine-grained sandstones and mudstones, and marginal conglomeritic sandstones and gravels are the dominant rock types. These sediments were deposited between about 15 million and 5 million years ago (middle Miocene to early Pliocene). The bulk of the Santa Fe Group was deposited during this time interval, when sedimentation and basin subsidence rates were the greatest. Detritus from the

adjacent highlands that were emerging to the northeast filled the Albuquerque Basin, covering the surface of the intrabasin divide (i.e., the Tijeras Fault). The new single topographic basin that was formed continued to aggrade through the early Quaternary.

The Upper Santa Fe Unit is characterized by intertonguing piedmont-slope and fluvial basin-floor deposits. Deposition occurred from about 5 million to 1 million years ago (upper Miocene to upper Pleistocene) and possibly as late as 0.5 million years ago (middle Pleistocene). Hawley and Haase (1992) split this unit into three subunits, two of which are present primarily in the western portion of the basin. One unit consists of poorly sorted, weakly stratified sand and conglomerates with an abundant silt-clay matrix derived from the emerging highlands to the east. This unit is not well represented in the western portion of the basin. A second subunit (Arroyo Ojito Formation) principally derived from the ancestral Rio Grande includes cross-stratified basin floor deposits characterized by thick zones of clean sand and pebble gravel. Fine to medium-grained overbank sediments were also deposited in areas where the ancestral Rio Grande, Rio San Jose, Rio Puerco and Rio Jemez merged into the Albuquerque Basin. A third subunit (Ceja Member of the Arroyo Ojito Formation) was derived primarily from basalts, andesites, rhyolite flows, and pyroclastic units to the northwest. Thickness of the Upper Santa Fe Unit locally attains 4,000 feet (Connell, 1995).

2.3.3 Post-Santa Fe Quaternary Deposits

Post-Santa Fe Quaternary units were deposited during river incision and partial backfilling episodes between about 0.5 million and 1 million years ago (middle Pleistocene). The Rio Grande and Rio Puerco drainage basins and nearby escarpments along the Llano de Albuquerque (the Cejita Blanca and Ceja del Rio Puerco) continued to evolve and supply sediment to the North Albuquerque Basin. Basin and valley fills include fan, pediment, inset-terrace, eolian, and floodplain deposits, as well as a mafic to intermediate volcanic rock contribution (Kelley and Kudo, 1978). Cross-bedded fine to medium-grained eolian sandstones and poorly-sorted silty sandy cobble to boulder gravels are abundant (Hawley and Haase, 1992). Eolian deposits are particularly abundant on the Llano de Albuquerque surface, with the largest dunes located along the western edge (Lambert, 1974; Kelley, 1977).

Fills related to cutting and partial backfilling of the Rio Grande and Rio Puerco Valleys during Middle to Late Quaternary glacial-interglacial cycles formed extensive terrace deposits that range in thickness from 30 to 200 feet. The latest cut-and-fill episode affecting

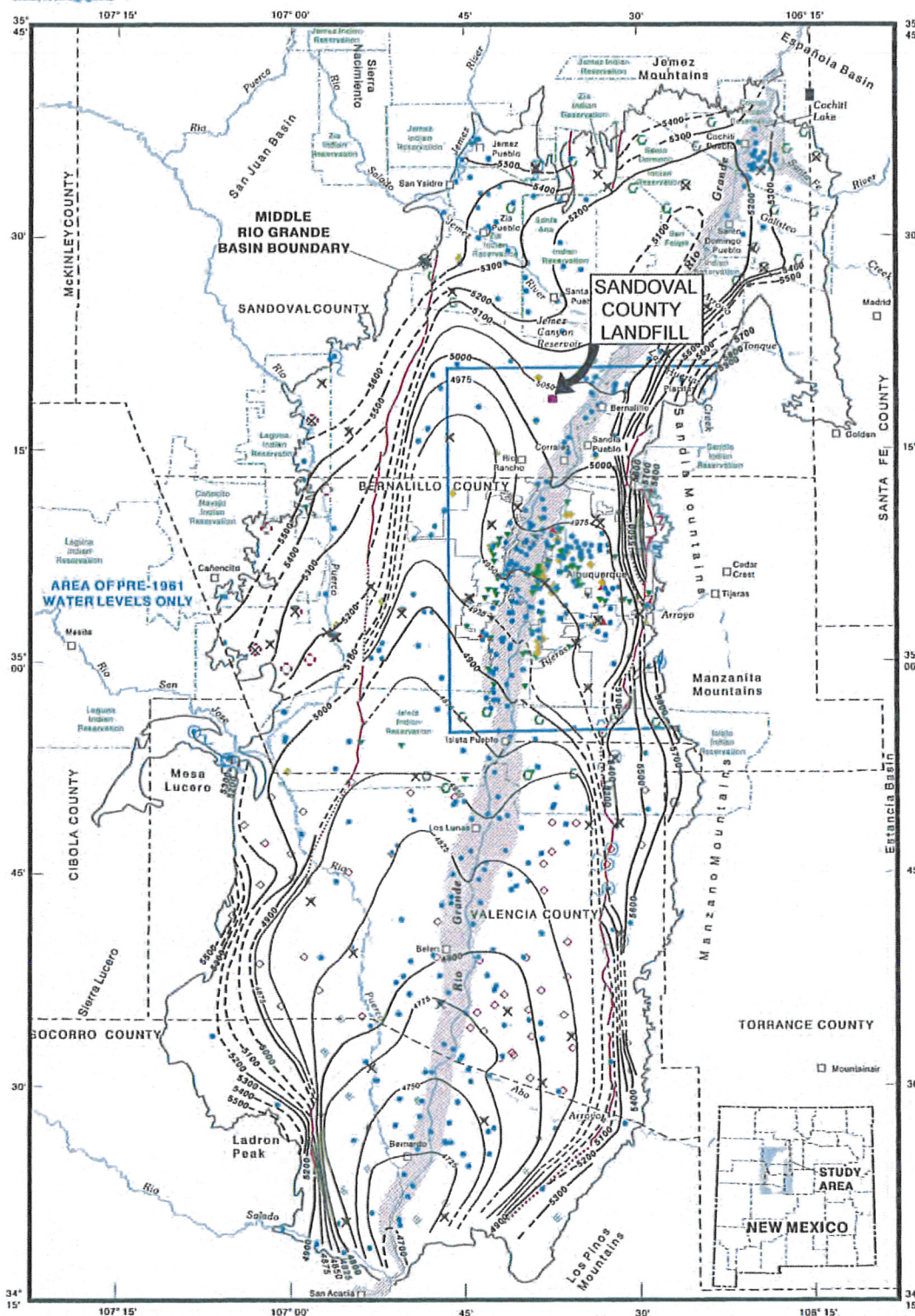
the Rio Grande - Rio Puerco system produced the channel and floodplain deposits of present inner-valley areas. During the last 10,000 to 15,000 years, the valleys have continued to aggrade as the relatively high rate of sedimentation has outpaced the ability of the Holocene drainages to remove detritus from the basin. This younger valley fill ranges up to 1,340 feet thick and forms the major shallow aquifer in the region (Hawley and Haase, 1992).

2.4 Regional Hydrogeology

Hawley and Haase (1992) developed a regional hydrologic framework of the Northern Albuquerque Basin. Groundwater flow in the Albuquerque-Belen Basin occurs through porous alluvial sediments comprising the Upper Santa Fe Unit (refer to Section 3.2.2). The major water-bearing units in the basin occur within the upper 2,000 feet of basin fill, primarily within the Arroyo Ojito Formation (Upper Santa Fe Unit). The aquifer matrix is generally comprised of unconsolidated to partially indurated sediments that were transported into the basin from the adjacent highlands, and from upstream areas along the Rio Grande Rift. These basin and fill deposits are of late Tertiary and Quaternary age (generally younger than 15 million years), locally derived, and have been reworked extensively by wind. The deposits also contain significant local volcanic and igneous sediments.





U.S. Geological Survey, Water-Resources Investigations Report (WRIR) 00-4249 contains a groundwater elevation contour map for the unconfined Santa Fe Group Aquifer in the middle Rio Grande Basin (Figure V.1.6). The vadose zone is generally 300-600 feet thick near the western portion of the Northern Albuquerque Basin. Recharge to the aquifer occurs through infiltration in the vadose zone. Precipitation enters the hydrologic system through the vadose zone as infiltrating rainfall and channel losses from flow in arroyos, and exits the system through evapotranspiration and recharge into the underlying aquifer.

The SCLF is situated two miles west of the Rio Grande in southern Sandoval County where the river transitions from a gaining reach to a losing reach. As a result, the groundwater flow pattern in southern Sandoval County fluctuates between southeasterly and southwesterly directions. The site-specific groundwater flow pattern may vary in a more complex fashion given the transition and the SCLF's location relative to this transition zone.



Base compiled from U.S. Geological Survey digital data, 1:100,000, 1977, 1978; and City of Albuquerque digital data, 1:2,400, 1994. Faults modified from Mark Hutton and Scott Minor, U.S. Geological Survey, written common, 1999.

EXPLANATION

-  **INNER VALLEY**
-  **WATER-LEVEL CONTOUR—Interval, in feet, is variable**
Dashed where inferred. Datum is sea level
-  **MAJOR FAULT LOCATED IN THE VICINITY OF A
LARGE HYDRAULIC DISCONTINUITY**
-  **AREA OF APPARENT HYDRAULIC DISCONTINUITY
NOT LOCATED NEAR A KNOWN FAULT**

- DATASOURCE:**
- National Water Information System
 - Meade (1949)
 - Ugrasik (1956)
 - Caprio (1960)
 - Bjorklund and Maxwell (1961)
 - Triss (1967)
 - Springel (1955)
 - Kerns (1998; written comments, 1995)
 - Risser and Lyford (1983)



REGIONAL GROUNDWATER ELEVATION CONTOUR MAP

SANDOVAL COUNTY LANDFILL
RIO RANCHO, NEW MEXICO

Gordon Environmental, Inc.
Consulting Engineers

213 S. Camino del Pueblo
Bernalillo, New Mexico, USA
Phone: 505-867-6990
Fax: 505-867-6991

DATE: 06/29/04	CAD: SCLF A REGIONAL_GW.dwg	PROJECT #: 211.02.01
DRAWN BY: JFP	REVIEWED BY: JAB	FIGURE V.1.6
APPROVED BY: IKG	gek@gordonenvironmental.com	

The Northern Albuquerque Basin is drained by two major stream drainage systems; the Rio Grande to the east and the Rio Puerco to the west. Both streams have cut into several hundred feet of former upper-basin fill, which is still preserved as the long sinuous mesa between these drainages known as Llano de Albuquerque.

3.0 SITE GEOLOGY AND HYDROGEOLOGY

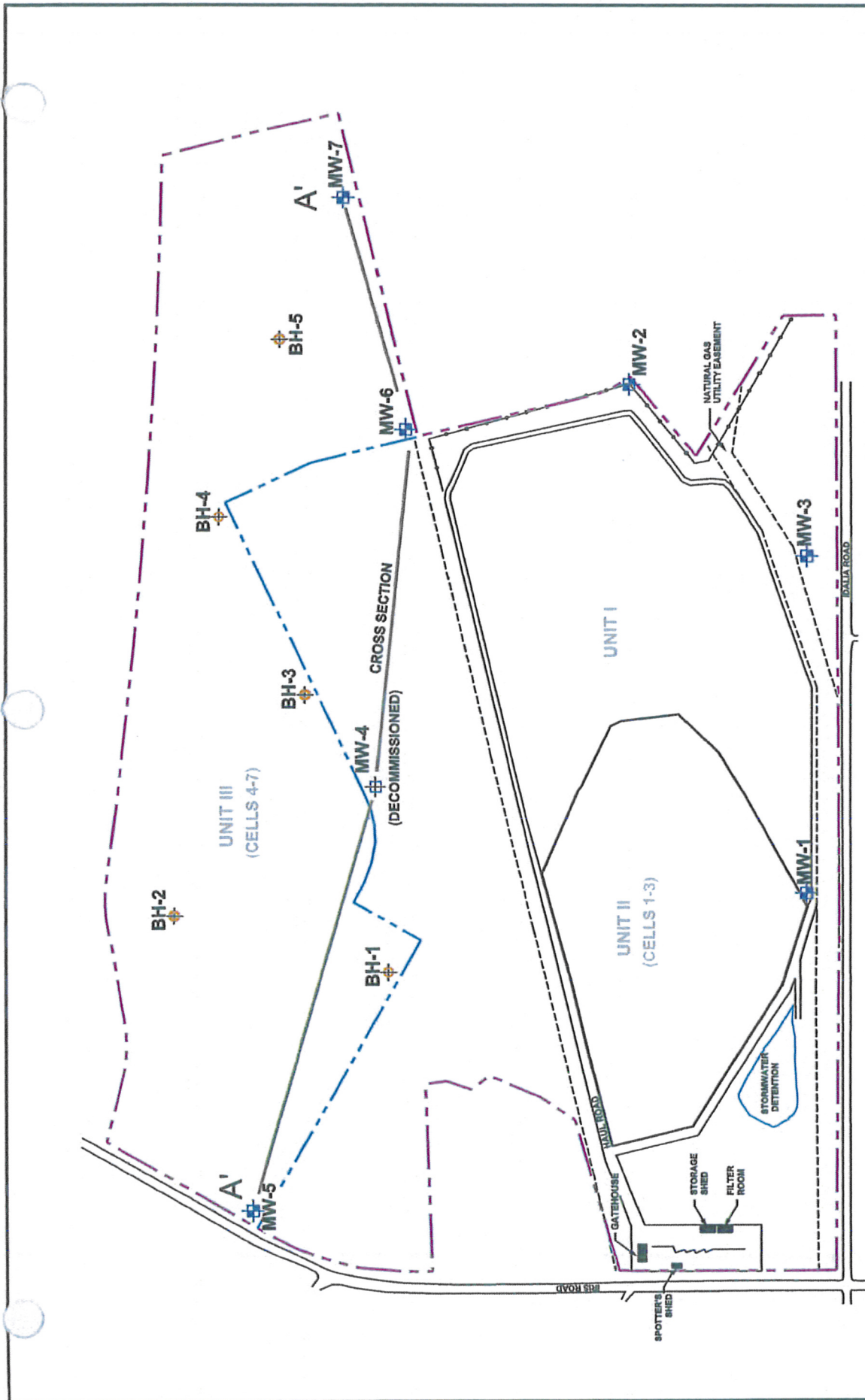
This section presents the geology and hydrogeology specific to the SCLF site, including investigative procedures, site stratigraphy and structure, and hydrogeology.

A substantial amount of information has been collected at the SCLF as part of both previous studies and more recent investigations. This section describes historical investigations at the site, and details of more recent studies to supplement the understanding of the site geology and hydrogeology in support of this permit application.

3.1 Summary of Previous Investigations

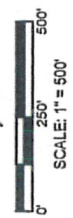
Prior to this Application for Permit, other site-specific studies were conducted to characterize the geology and hydrogeology and to document the suitability of the site for secure waste disposal. **Table V.1.1** summarizes recent subsurface investigations conducted at the SCLF, and the locations of soil borings and wells are shown on **Figure V.1.7**. Copies of boring logs from previous and recent investigations are provided in **Attachment V.1.A**.

The first site-specific hydrogeologic investigation was conducted in 1993 by SHB AGRA, Inc., of Albuquerque, NM. This initial investigation involved the completion of a boring located near the southern perimeter of the Unit II fill area. This boring was advanced to a depth of 102 fbs using a Failing F-10 hollow-stem auger rig. A Dresser T70W air-rotary casing hammer rig was used to complete to a depth of 340 fbs. Soil samples were collected to a depth of 300 fbs at 5-foot intervals by driving a 3-inch O.D. split-barrel ring sampler into the bottom of the boring. Soil samples were classified in accordance with the Unified Soil Classification System (ASTM D2487). These samples were predominately fine silty sands or poorly graded fine sand with silt, which are consistent with terrace or piedmont deposits. Water was encountered at a depth of approximately 320 fbs and the boring was completed as a monitoring well (MW-1). **Attachment V.1.A** includes the lithology log for this initial monitoring well.



LEGEND

- PROPERTY LINE
- FORMER PROPERTY LINE
- UTILITY EASEMENT
- FENCE LINE
- CROSS SECTION LOCATION: A-A'
- GROUNDWATER MONITORING WELL
- DECOMMISSIONED GROUNDWATER MONITORING WELL
- GEOTECHNICAL SOIL BORING
- PRK
- MW-1
- MW-4
- BH-1



BORING LOCATION MAP

SANDOVAL COUNTY LANDFILL
RIO RANCHO, NEW MEXICO

Gordon Environmental, Inc. <i>Consulting Engineers</i>		213 S. Camino del Pueblo Bernalillo, New Mexico, USA Phone: 505-867-6990 Fax: 505-867-6991
DATE: 02/17/05	CAD: SCLF BORELOC.dwg	PROJECT #: 211.02.01
DRAWN BY: JFP	REVIEWED BY: JAB	FIGURE V.1.7
APPROVED BY: IKG	ge@ GordonEnvironmental.com	

Table V.1.1
Summary of Exploratory Drilling
Sandoval County Landfill

Boring	Completion Date	Drilling Method	Surface Elevation (fmsl)	Total Depth (fbgs)	Depth-to-Water (fbgs)
MONITORING WELLS					
MW-1	06/10/93	Mud-Rotary	5319.53	340	330
MW-2	04/12/96	Mud-Rotary	5411.12	448	431
MW-3	04/21/96	Mud-Rotary	5371.27	410	392
MW-4	03/15/96	Mud-Rotary	5374.33	405	382
MW-5	08/11/03	Mud-Rotary	5362.58	384	362
MW-6	10/02/03	Mud-Rotary	5419.11	462	438
MW-7	10/22/03	Mud-Rotary	5360.39	404	378
2003 BORINGS					
BH-1	12/02/03	HSA	5349	60	ND
BH-2	12/02/03	HSA	5367	60	ND
BH-3	12/02/03	HSA	5384	60	ND
BH-4	12/02/03	HSA	5381	60	ND
BH-5	12/03/03	HSA	5378	60	ND

ND = not detected during drilling

fmsl = feet above mean sea level

fbgs = feet below ground surface

HSA = Hollow-Stem Auger

In April 1996, Roy F. Weston, Inc. completed three additional monitoring wells on the SCLF site. MW-2, MW-3 and MW-4 were completed to depths of 448 fbgs, 408 fbgs and 400 fbgs, respectively. An air-rotary casing hammer rig was used to complete and soil samples for testing were collected with a split-spoon sampler at 20-foot intervals. These additional monitoring wells encountered lithologies similar to those found in MW-1 and groundwater was encountered at depths ranging from approximately 380 to 430 fbgs. Lithology logs for these monitoring wells is provided in **Attachment IV.3.A**.

3.2 2003/2004 Drilling and Sampling

In accordance with the notification requirements of 20 NMAC 9.1, Section 802.D, GEI submitted a workplan to NMED in March 2003 to decommission MW-4 and install a replacement monitoring well (**Attachment V.1.B**). This workplan was approved by NMED on March 27, 2003 (**Attachment V.1.C**) and the approved replacement well (MW-5) was completed in July 2003. HydroGeologic Services, using an air rotary rig, completed this well to a depth of 384 fbgs. During rotary drilling, the drill cuttings returned to the surface were logged by a qualified GEI site representative. These cuttings were also selectively bagged and sealed for future laboratory testing. Samples were collected at 5-foot intervals and used

to construct a lithology log for this monitoring well (**Attachment V.1.A**). Groundwater was encountered at a depth of 362 fbs. A Monitoring Well Installation Report for MW-5 was submitted to NMED (**Attachment V.1.D**).

Additional hydrogeologic investigations were conducted in December 2003 and January 2004 to supplement the information collected during previous studies. A supplemental geologic investigation workplan for the site, as required by 20 NMAC 9.1 Section 202.A.7.b, was prepared by GEI (**Attachment V.1.E**) and approved by the NMED in August 2003 (**Attachment V.1.F**). As detailed in the work plan, the objectives of the subsurface investigation were to:

- Document the geologic suitability of the site to facilitate permitting of the 62 acre expansion area.
- Acquire detailed geologic and geotechnical data to support the detailed engineering design as required by 20 NMAC 9.1, Section 306.
- Characterize groundwater conditions for the expansion of a groundwater monitoring system in accordance with 20 NMAC 9.1, Section 801.

On December 2 and 3, 2003, Enviro-Drill, Inc. of Albuquerque, New Mexico, completed five Hollow-stem auger (HSA) borings within the central portion of the proposed expansion area (see **Figure V.1.7**). These holes were drilled using a portable CME 75 drill rig with 6-5/8-inch diameter augers to collect geotechnical data for the Unit III lateral expansion. These auger borings were each drilled to total depths of approximately 60 fbs and logged by a qualified GEI field representative. **Attachment V.1.A** includes the boring logs for the HSA borings. The logs include a visual field classification of the materials from each boring, as well as a graphical log of the materials; sample type; blow counts (per foot); laboratory measurements of dry density, moisture content (gravimetric), and soil classification; and any comments regarding the lithology or drilling activities.

In each of the borings, samples were collected at five-foot intervals using a standard 2-inch outside diameter (OD) split barrel sampler. Additionally, bulk samples (5-gallon buckets) were obtained at depths of 10 fbs and 40 fbs from three bore holes (BH-2, BH-3 and BH-5) for geotechnical analyses measurements. Split-spoon and bulk samples were evaluated for visual soil classification. Drilling, sample collection and sample shipping were conducted in accordance with standard operating procedures, and laboratory testing results for these samples is described in Section 3.4.

Field logging observations (see **Attachment V.1.A**) indicate that the soil profile in the proposed expansion area is consistent with samples collected from the approved Landfill area. The upper 60 feet of the soil profile is comprised primarily of very fine to medium calcareous silty sands, with thin (i.e., a few inches thick) interbedded gravel, silt and clay lenses.

Two down-gradient monitoring wells were drilled along the eastern portion of the expansion area (see **Figure V.1.7**). These wells were drilled and completed by Rodgers Environmental Services, Inc. using a mud-rotary rig. MW-6 was completed to a depth of 462 fbgs from January 20-22, 2004 and MW-7 was drilled to a depth of 404 fbgs from February 17-20, 2004. A GEI representative was on site and prepared lithology logs for these wells from drill hole cuttings gathered at 10-foot intervals. Unconfined groundwater was encountered at depths of 438 fbgs and 378 fbgs for MW-6 and MW-7, respectively. Copies of these lithology logs are provided in **Attachment V.1.A**, and a copy of the well installation report for these wells furnished in **Attachment V.1.H**.

3.3 Borehole Plugging

Upon completion, the boreholes were plugged in accordance with 20 NMAC 9.1 and the State Engineer's. In order to ensure that the abandoned bore holes will not provide a conduit for fluid migration into the Upper Santa Fe Unit and the underlying aquifer, all boreholes were backfilled with a cement-bentonite grout to the ground surface. This sixty feet of grout provides a seal with a permeability equal to or less than the natural formation across an interval that is below the planned landfill liner invert. The required Borehole Plugging Certification for this drilling program is provided in Section 4.0 in this text.

3.4 Geotechnical Evaluation

Numerous lithologic samples collected at the Facility during both previous studies and the 2003/2004 investigation have been tested in the laboratory for measurement of physical properties. Geotechnical testing on 57 soil samples collected during the completion of the initial boring was conducted by SHB AGRA in 1993. These samples consisted of sands, silty sands, silts and sandy clays. Tests included moisture content, density, particle size distributions, Atterberg Limits, and permeability. **Attachment V.1.H** presents the laboratory analyses from this testing program.

Ten samples from the 2003/2004 drilling program were selected for geotechnical testing for usage as potential drainage sand and final cover material. The samples were tested for some or all of the following physical properties: grain size distribution, Atterberg limits, moisture content, uniformity coefficient, specific gravity, porosity, dry density, and saturated hydraulic conductivity. **Table V.1.2** summarizes the results of these laboratory tests, including USCS Classification and sample depth.

3.5 Site Geology

The SCLF is underlain by a sequence of sediments consisting predominately of sandstones and gravels, with interbeds of siltstones and mudstones. These sediments belong to the Arroyo Ojito Formation (Connell, 1995) of the Upper Santa Fe Group and are of Pleistocene to Miocene in age. These are western basin-margin deposits, derived from the ancestral Rio Grande and the Colorado Plateau. Unconformably overlying the Arroyo Ojito Formation are Quaternary deposits of Pleistocene age (**Figure V.1.8**).

3.5.1 Site Stratigraphy

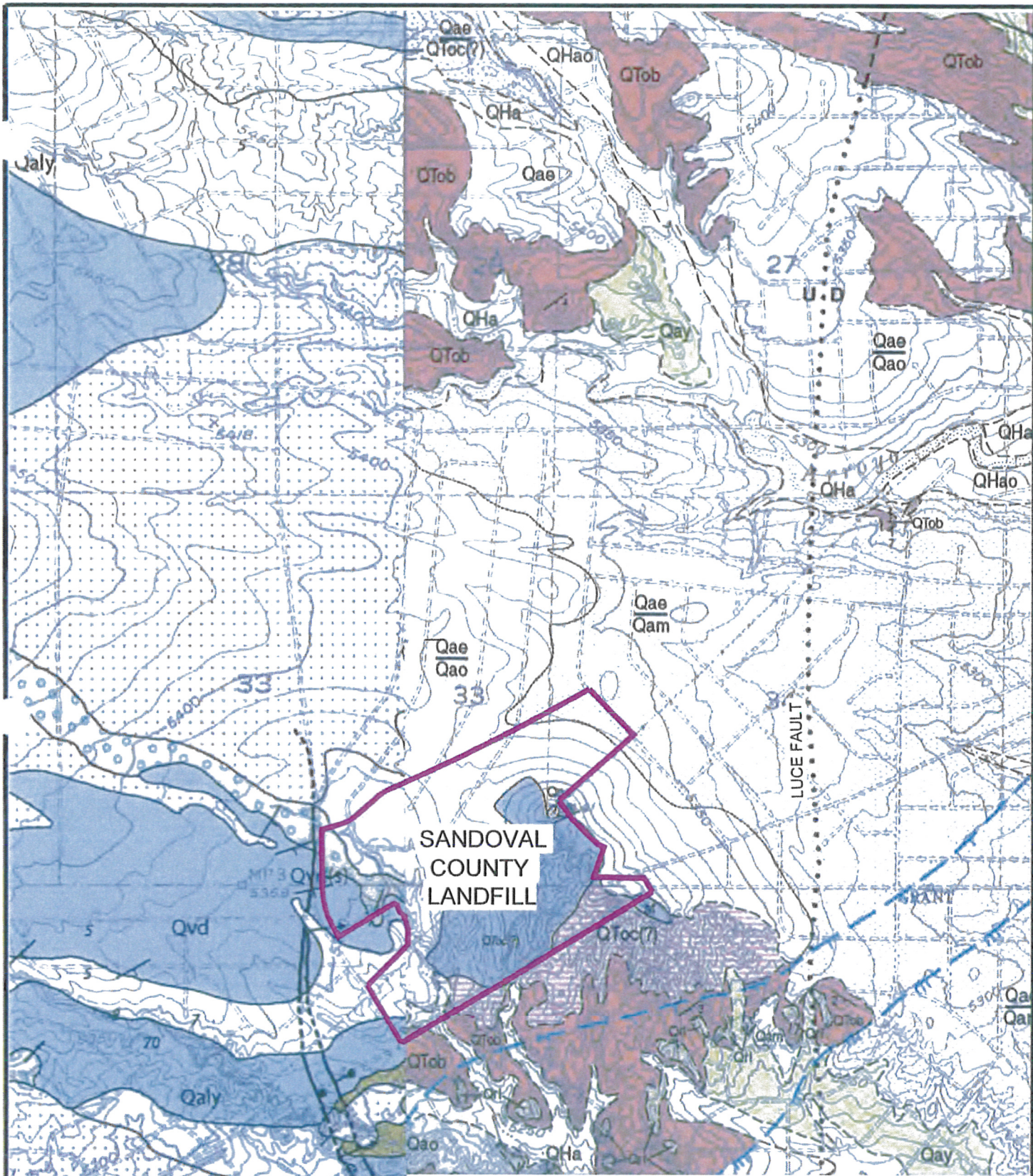
Figure V.1.9 shows the site-specific stratigraphy in the area of the SCLF. Information contained in this stratigraphic column is the result of mapping by the New Mexico Bureau of Mines and Mineral Resources, as well as on-site drilling and mapping activities by GEI.

Upper Santa Fe Group – The major stratigraphic unit underlying the Facility is the Upper Santa Fe Group. In this area, this Group is over 4,000 feet thick and is comprised of the Arroyo Ojito Formation, which consists of two members (the Loma Barbon and the Ceja). As shown in site photos, both members are exposed on an outcrop near the east-central portion of the property (**Attachment V.1.I**).

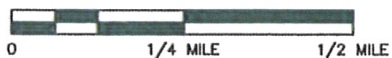
The Loma Barbon Member is the major unit within this formation and underlies the entire Facility. It consists of well-consolidated, fine-grained, yellow-brown to red-brown silty sandstones with interbedded mudstones and scattered lenses of coarse-grained sandstones and cobbly sandstones (see **Figure V.1.10**, Site Geologic Cross-Section A-A'). Cobbles are derived predominately from red granite, basalt and tuffs. Field mapping indicates a strike of N 10° E and a dip of 4° to the SE for this unit. It was deposited in a fluvial environment, thus, individual lenses of mudstones and coarse-grained facies are laterally discontinuous.

TABLE V.1.2
SUMMARY OF GEOTECHNICAL TEST RESULTS
SANDOVAL COUNTY LANDFILL

Sample Number	Sample Depth (fbgs)	USCS Class	Grain Size Distribution			Uniformity Coefficient	Natural Moisture (%)	Standard Proctor		Permeability (cm/sec)
			Pass #10 (%)	Pass #40 (%)	Pass #200 (%)			Max. Dry Density (PCF)	Optimum Moisture (%)	
BH-1	10	SP	88.5	77.6	4.7	3.05	2.5			
BH-1	20	SP-SM	95.5	80.9	7.4	3.04	3.9			
BH-1	35	SP-SM	99.3	91.3	5.4	2.61	4.0			
BH-1	40	SP	98.8	92.2	3.7	2.38	2.6			
BH-2	10	SP-SM	99.9	94.0	9.4	3.17	2.8			
BH-2	20	SP								9.88 E-06
BH-2	25	SP	99.6	95.6	2.6	1.90	3.7			
BH-2	30	SP	99.7	92.4	1.5	1.87	3.5			
BH-2	40	SP	99.7	92.1	1.9	1.85	3.4			
BH-2	40-45	SP						126.3	12.5	
BH-3	10	SP	97.5	89.4	1.6	1.84	2.5			
BH-3	15	SP								2.48 E-06
BH-3	20	SP	91.9	81.9	1.4	1.90	6.8			
BH-3	30	SP	99.1	90.6	1.0	1.80	3.5			
BH-3	35	SP	97.0	72.4	0.6	1.96	3.0			
BH-3	40-45	SP						129.7	10.5	
BH-4	10	SP	96.8	91.9	2.0	1.82	3.4			
BH-4	15	SP	99.8	95.8	1.4	1.79	3.7			
BH-4	20	SP	99.7	93.8	1.5	1.80	4.9			
BH-4	40	SP	99.2	95.2	1.0	1.77	2.8			
BH-5	10	SP	95.6	87.4	0.9	1.83	3.1			
BH-5	20	SP	99.0	95.3	2.0	1.79	2.7			
BH-5	30	SP	98.5	84.8	0.4	1.82	3.0			
BH-5	35	SP	99.9	92.5	0.4	1.77	3.9			
BH-5	40-45	SP						130.6	12.8	
Stockpile		SP	76.9	45.6	0.2	3.34				2.45 E-07



MAP ADAPTED FROM USGS MISCELLANEOUS FIELD STUDIES MAP
MF-2334 AND NMBMR OPEN FILE MAP SERIES OF-GM-16



GEOLOGIC MAP

SANDOVAL COUNTY LANDFILL
RIO RANCHO, NEW MEXICO



Gordon Environmental, Inc.
Consulting Engineers

213 S. Camino del Pueblo
Bernalillo, New Mexico, USA
Phone: 505-867-6990
Fax: 505-867-6991

DATE: 06/29/04

CAD: SCLF GEO.dwg

PROJECT #: 211 02.01

DRAWN BY: JFP

REVIEWED BY: JAB

APPROVED BY: IKG

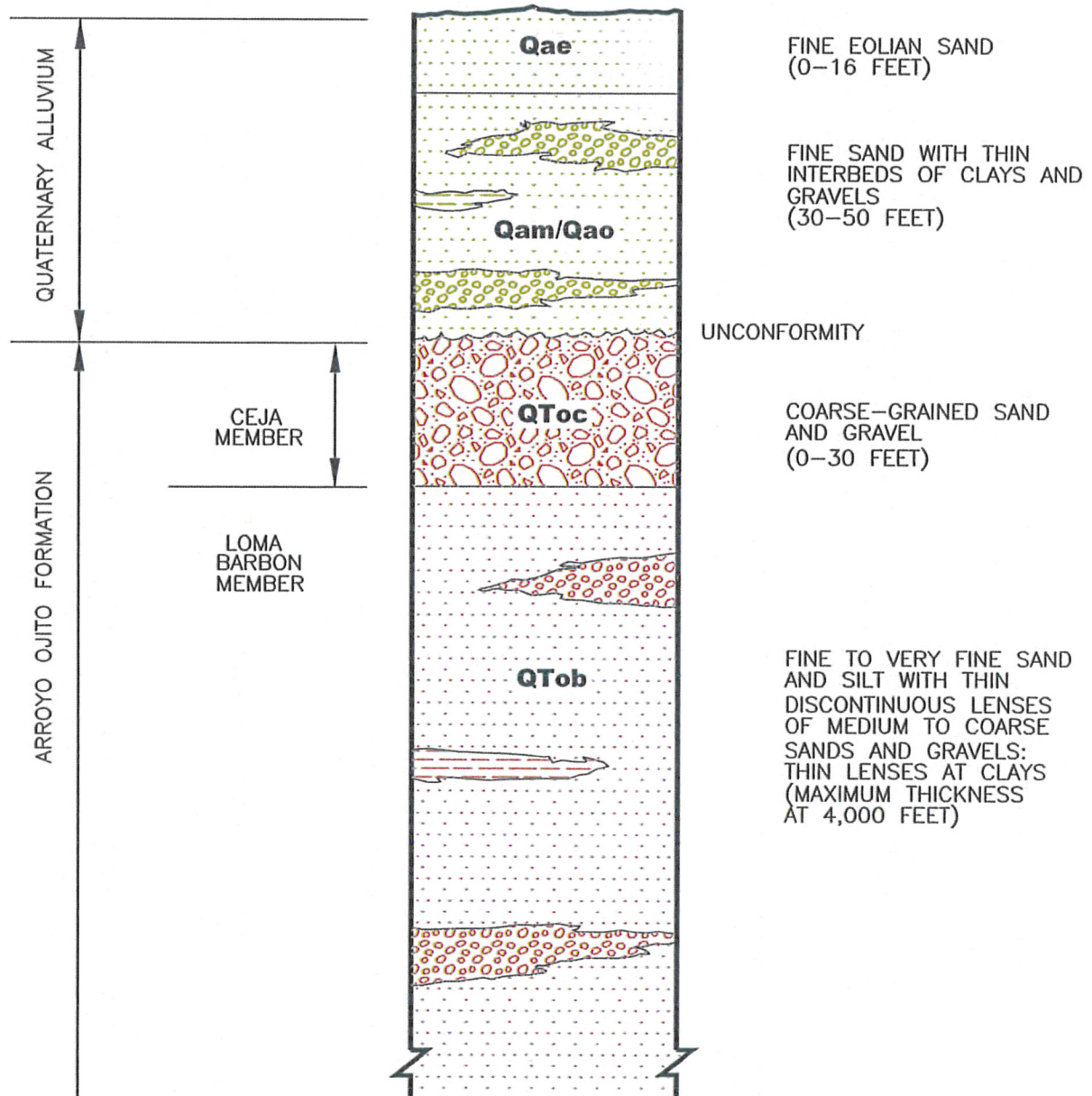
gei@gordonenvironmental.com

FIGURE V.1.8

Drawing P:\acad 2003\211 02.01\FIGURES\SCLF GEO.dwg

Date/Time: Jul. 12, 2004-08:11:30

Copyright © All Rights Reserved, Gordon Environmental, Inc. 2004



SITE STRATIGRAPHIC COLUMN

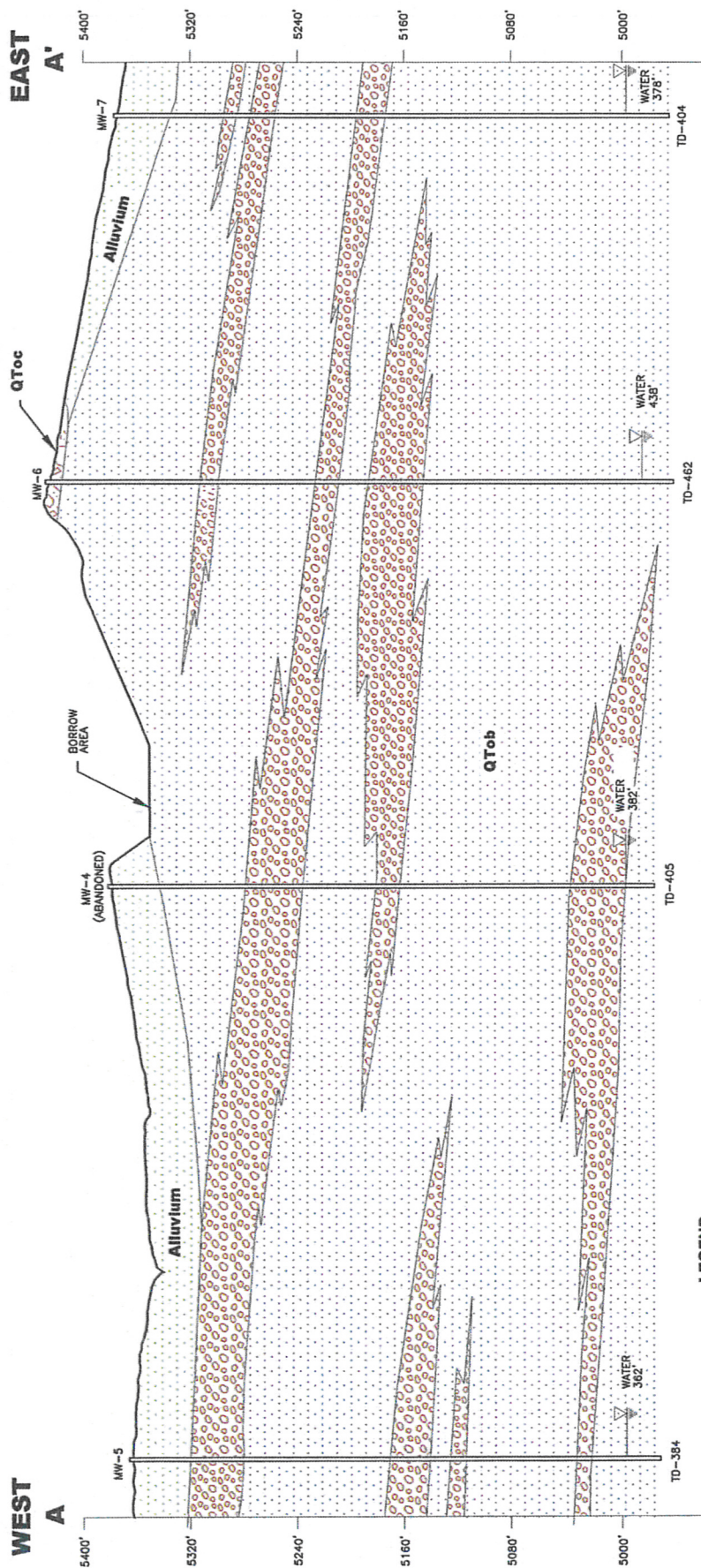
SANDOVAL COUNTY LANDFILL
RIO RANCHO, NEW MEXICO



Gordon Environmental, Inc.
Consulting Engineers

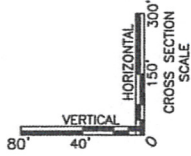
213 S. Camino del Pueblo
Bernalillo, New Mexico, USA
Phone: 505-867-6990
Fax: 505-867-6991

DATE: 06/29/04	CAD: SCLF STRAT.dwg	PROJECT #: 211.02.01
DRAWN BY: JFP	REVIEWED BY: JAB	
APPROVED BY: IKG	gei@gordonenvironmental.com	FIGURE V.1.9



LEGEND

- QUATERNARY ALLUVIUM
- QToC CEJA MEMBER
- QToB LOMA BARREN MEMBER
- COARSE-GRAINED FACIES LOMA BARREN MEMBER



SITE GEOLOGIC CROSS SECTION A-A'
SANDOVAL COUNTY LANDFILL
RIO RANCHO, NEW MEXICO

Gordon Environmental, Inc.
Consulting Engineers

213 S. Camino del Pueblo
Bernalillo, New Mexico, USA
Phone: 505-867-6990
Fax: 505-867-6991

DATE: 06/26/04	CAD: SCLF XSEC.dwg	PROJECT #: 211.02.01
DRAWN BY: JFP	REVIEWED BY: JAB	
APPROVED BY: HOG	gordone@environmental.com	

FIGURE V.1.10

**APPLICATION FOR PERMIT RENEWAL AND MODIFICATION
SANDOVAL COUNTY LANDFILL**

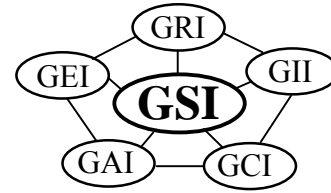
**VOLUME III: LANDFILL ENGINEERING CALCULATIONS
SECTION 3: SLOPE STABILITY ANALYSIS**

ATTACHMENT III.3.C

**KOERNER, ROBERT M. AND KOERNER, GEORGE R. SEPTEMBER 2007.
*INTERPRETATION(S) OF LABORATORY GENERATED INTERFACE SHEAR
STRENGTH DATA FOR GEOSYNTHETIC MATERIALS WITH EMPHASIS ON THE
ADHESION VALUE. GEOSYNTHETIC INSTITUTE***

Geosynthetic Institute

475 Kedron Avenue
Folsom, PA 19033-1208 USA
TEL (610) 522-8440
FAX (610) 522-8441



GRI White Paper #11

**Interpretation(s) of Laboratory Generated Interface Shear Strength
Data for Geosynthetic Materials With Emphasis on the Adhesion Value**

by

**Robert M. Koerner and George R. Koerner
Geosynthetic Institute
475 Kedron Avenue
Folsom, PA 19033 USA**

**Phone (610) 522-8440
Fax (610) 522-8441**

**E-mail:
robert.koerner@coe.drexel.edu
gkoerner@dca.net**

September 11, 2007

Interpretation(s) of Laboratory Generated Interface Shear Strength Data for Geosynthetic Materials With Emphasis on the Adhesion Value

The beginning point of this White Paper is based on the assumption that a designer has a credible set of laboratory generated shear stress versus shear displacement curves on the desired geosynthetic-to-geosynthetic or geosynthetic-to-soil interface tested per ISO 12957 or ASTM D5321, or ASTM D6243 if geosynthetic clay liners are involved. In this regard we are considering having such data as shown in Figure 1. It is clearly seen that many behavioral trends are possible.

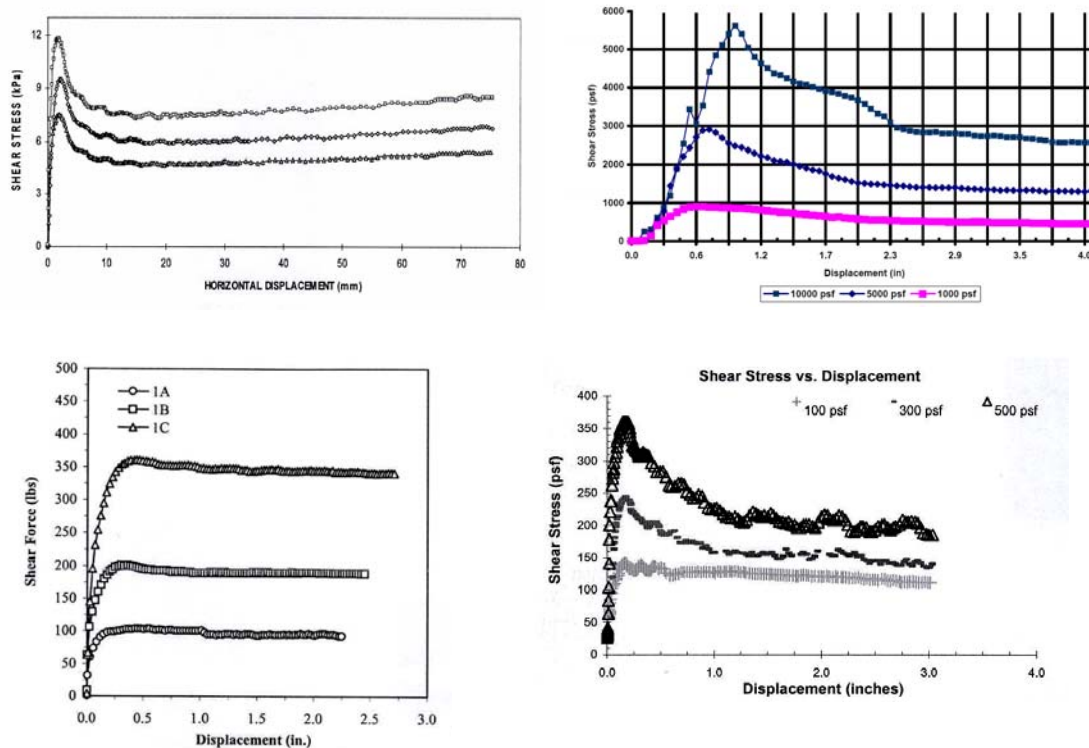


Figure 1 – Various stress versus displacement curves for different geosynthetic materials. (Data compliments of TRI, Golder, Precision and SGI Laboratories)

Either the designer or the testing laboratory will have to generate the Mohr-Coulomb failure envelope from these curves by selecting one point on each normal stress curve and plotting the results on a normal stress versus shear stress curve as shown in Figure 2a. A least squares fit of the data point produces the failure envelope. Even further, one might have more than one such failure envelopes; peak, large displacement and/or residual. Please note, however, that this White Paper is not about the selection of peak, large displacement or residual values and the technical literature is abundant on that subject.

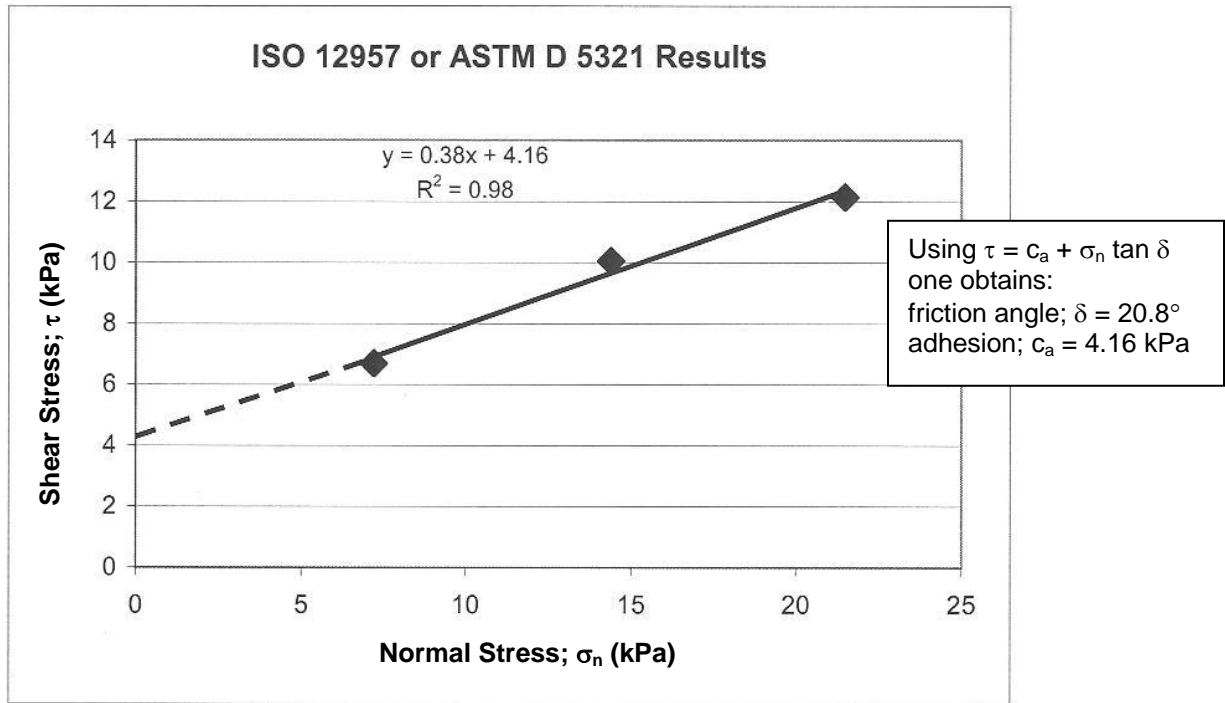


Figure 2a – Three point laboratory data leading to the drawing of a failure envelope and subsequent measurement of friction angle and shear strength intercept (or adhesion) values.

At any rate, to begin the present discussion on the interpretation of the selected failure envelope, the designer is confronted with something like that shown Figure 2a. Here the data points are clearly identified and the failure envelope is usually generated by a least squares fitting procedure. The dashed extension to the y-axis is often the general assumption particularly for low normal stresses as indicated. Note that there are indeed exceptions to this situation such as curved failure envelopes within the normal stress range tested, or zero normal stress tests. They are special cases and will be discussed later.

Interpretation #1 – Use of full “ c_a ” and full “ δ ” values

Assuming that the previous failure envelope is based on credible laboratory procedures, properly simulated insofar as representative samples, normal stress selection, moisture conditions, strain rate, etc., our recommended approach is to use the shear strength parameters directly in your slope stability analysis and, if found to be adequate, for your materials specification criteria as well. For landfill cover veneer stability problems all GSI Members and Associate Members should have our spreadsheet calculation program which is extremely easy to use. For others, there are many computer codes available. For a hypothetical veneer slope stability example using the two shear strength parameters (c_a and δ) from Figure 2a, the input information is as follows:

- cover soil thickness $h = 0.3$ m
- slope angle $\beta = 18.4^\circ$ (3-to-1)
- length of slope $L = 30.0$ m
- unit weight of cover soil $\gamma = 18.0$ kN/m³
- friction angle of cover soil $\phi = 30.0$ deg
- cohesion of cover soil $c = 0.0$ kN/m²
- friction angle of interface $\delta = 20.8$ deg
- adhesion of interface $c_a = 4.16$ kPa (= 87 psf)

By using the program just mentioned or similar procedure, the resulting slope factor-of-safety value is; $FS = 3.62$. This is a relatively high value and would generally be considered quite conservative. One point worth mentioning, however, is the strong influence of the adhesion value on factor-of-safety. To illustrate this, we now vary the c_a -value between zero and ten while holding everything else the same. This procedure results in the following table; clearly illustrating the sensitivity of the FS-value to this particular parameter.

Adhesion; " c_a "		Resulting FS-value
kPa	lb/ft ²	
0	0	1.18
2	42	2.35
4	84	3.53
6	125	4.70
8	167	5.80
10	209	7.05

Presented now is the heart of this White Paper concerning the *issue of how reliable is this laboratory generated c_a -value?* The ultimate decision is yours as the designer, but our opinions on different geosynthetic materials and related interfaces are as follows:

- For textured geomembranes against geotextiles or soil, the asperities (be they manufactured as structured, blown film, or impinged) are on the material giving rise to the high adhesion values, so we recommend using the adhesion value accordingly. Only by continuously rubbing the surfaces against one another can asperity reorientation occur and we feel this is an artifact of aggressive laboratory testing as has been done (and reported) using the ring shear testing device in particular. Alternatively, concern has been expressed when testing at very high normal stresses. The thought in both instances is that if you eliminate adhesion from textured geomembranes you are essentially assuming smooth geomembrane sheet. This is a designer's prerogative, but be prepared to have very gentle slopes in so doing.
- For smooth geomembranes against other geosynthetics or soil, a small adhesion is often observed. This is particularly the case for LLDPE, fPP, EPDM, and PVC. Each of these geomembranes are less hard than HDPE, and thus an indentation can be visualized (particularly dealing with soil) which is clearly a function of the

- applied normal stress. Assuming that the appropriate normal stresses were used in the direct shear test, we feel that one is generally justified in its use.
- (c) For geotextiles thermally bonded to geonets or other types of drainage cores, we feel that the full value of adhesion should be used. Most of these geocomposites can barely be “delaminated” in the conducting of the test and we have never heard of a field delamination problem from a properly manufactured geocomposite interface in this regard.
 - (d) For the internal shear strength of reinforced GCLs, the fibers would have to pull-out or break (or both) for a loss of adhesion. While you can force this to happen in the lab, we have no evidence of this occurring in the field. Test results invariably show high adhesion values. Furthermore, longevity (durability) of the fibers in a hydrated bentonite atmosphere promises 100-year lifetime, or longer. We have a creep-related paper in this regard. Thus, we see no reason not to use the laboratory generated value of adhesion for reinforced GCLs manufactured by either needlepunching or stitching. Of course, the upper and lower interfaces of the GCLs must be independently evaluated.
 - (e) For certain geosynthetic-to-soil interfaces, the interface shear behavior may force the failure plane into the soil. This results in the identification of the soil’s shear strength and if there is a shear strength intercept it is a cohesion value and can be used accordingly.

Thus, if adhesion from short-term testing is indicated by the failure envelope and the long-term permanence of the physical or mechanical mechanism giving rise to this adhesion is logical to anticipate, its use in a stability analysis and subsequent material’s specification is felt to be generally justified.

Interpretation #2 – Use of zero “ c_a ” and full “ δ ” value

For the situation where an adhesion is indicated by the failure envelope and you as the designer feel that its long-term existence is not justified, the most conservative approach you can take is to simply translate the entire failure envelope in a parallel manner down by the amount of adhesion indicated on the original data-generated graph; see Figure 2b.

The effect of this very conservative approach on the FS-value of the slope is substantial. The shear strength is now represented by a friction angle alone and the site-specific result will be very flat slopes. For example, the 3-to-1 slope in the hypothetical example given previously with an adhesion of zero, now has a FS = 1.18 using this approach. For the interfaces mentioned previously, we do not recommend this approach.

Alternatively, one could also decrease the adhesion slightly, but not entirely. That said, we really don’t know how to comment on this type of “compromise” situation?

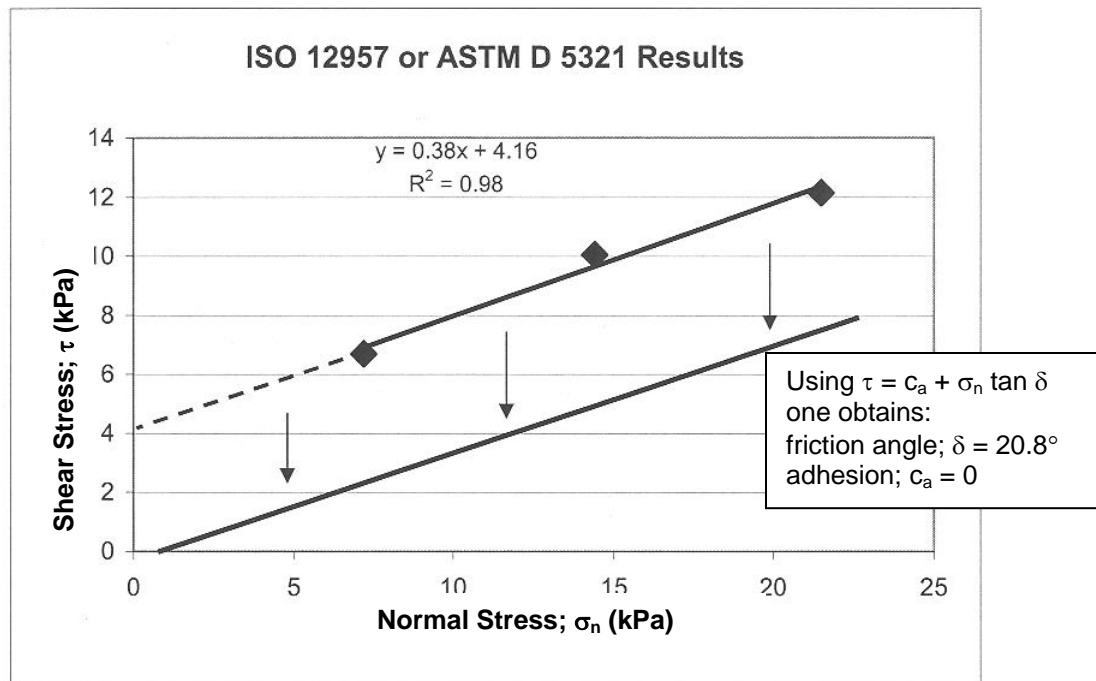


Figure 2b – Parallel translation downward of the entire laboratory generated failure envelope by an amount equal to the y-axis intercept, i.e., the adhesion.

Interpretation #3 – Use of zero “ c_a ” at zero normal stress only

A hybrid interpretation somewhere between the interpretations just presented is sometimes suggested, but its logic is somewhat difficult to fathom. In essence, the adhesion is lost only at zero normal stress but not at higher normal stresses. Thus, the failure envelope is forced through the origin but thereafter it is based on a least squares fit of the laboratory tested points as they were generated. Figure 3 illustrates the situation where the resulting friction angle is seen to be 32.2° . For our hypothetical example, this results in $FS = 1.93$. Alternatively, and equally difficult to fathom, is when only one laboratory point is generated and the failure envelope is forced through it and the origin. Both approaches are the least conservative of those mentioned in this White Paper giving rise to a rotation of the failure envelope and the highest friction angle possible. The angle resulting from this practice has been variously called “secant friction angle”, “secant angle”, or “modulus angle”. Of the group, secant angle is probably the best description for this interpretation since it shouldn’t be confused with the Mohr-Coulomb friction angle, and modulus brings with it completely other test procedures like tension testing.

We generally do not recommend such approaches for the reason that adhesion should be an intrinsic property of the interface involved and not be arbitrarily eliminated or used on the basis of a particular normal stress, or stresses. (That stated, if the interface is tested at

zero normal stress and found to have zero adhesion, the origin is a valid point and should then be used accordingly).

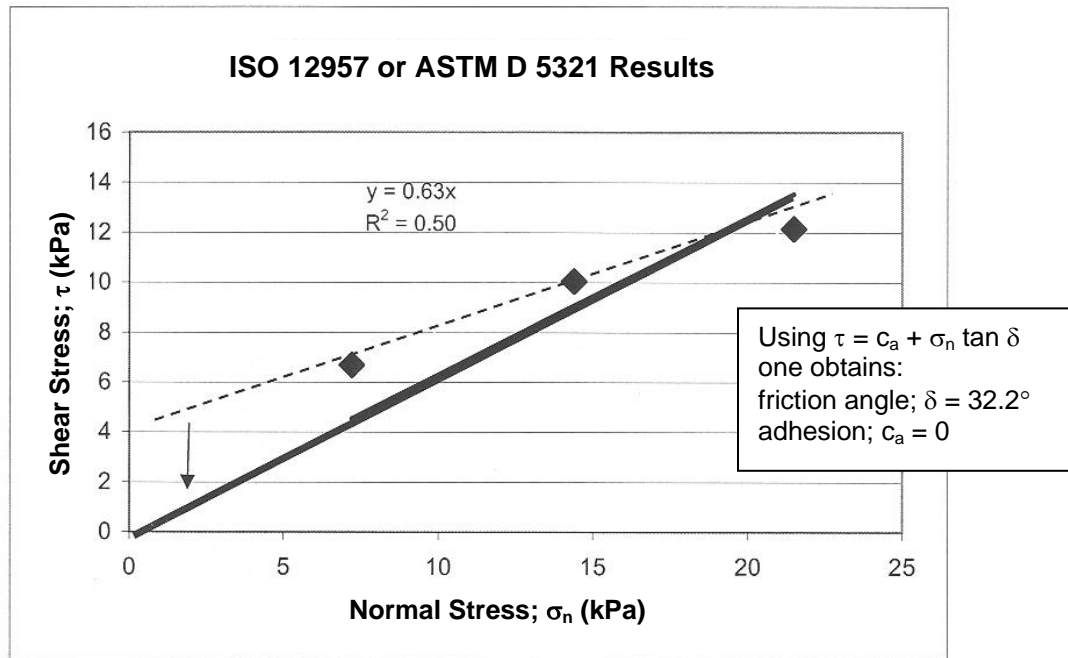


Figure 3 – Elimination of adhesion at zero normal stress but not at any of the three laboratory measured data points.

Interpretation #4 – Use of the total shear strength at a particular normal stress

A very straightforward approach to a specification value is to require a certain shear strength value at a particular normal stress. This is particularly the case if the failure envelope is curved as mentioned previously. In so doing, a specifier is requiring a single point to be taken from the failure envelope which is targeted at the expected field normal stress. Figure 4 suggests that if the field normal stress is 17.2 kPa it results in a required shear strength of 10.7 kPa, or greater. The shear strength value is thereby reflective of both a frictional component and adhesion, neither of which are specifically identified.

In so doing one avoids specifying individual “ c_a ” and “ δ ” values and much of the previous discussion is altogether avoided. The method can be extended to give two, or more, values of shear strength (or even the equation of the failure envelope) at different normal stresses in the form of a “required” table.

This approach has been used by a select few designers but is far from common practice. There is nothing of a fundamental nature which says it cannot be done and it would avoid some of the other complications inherent with different approaches.

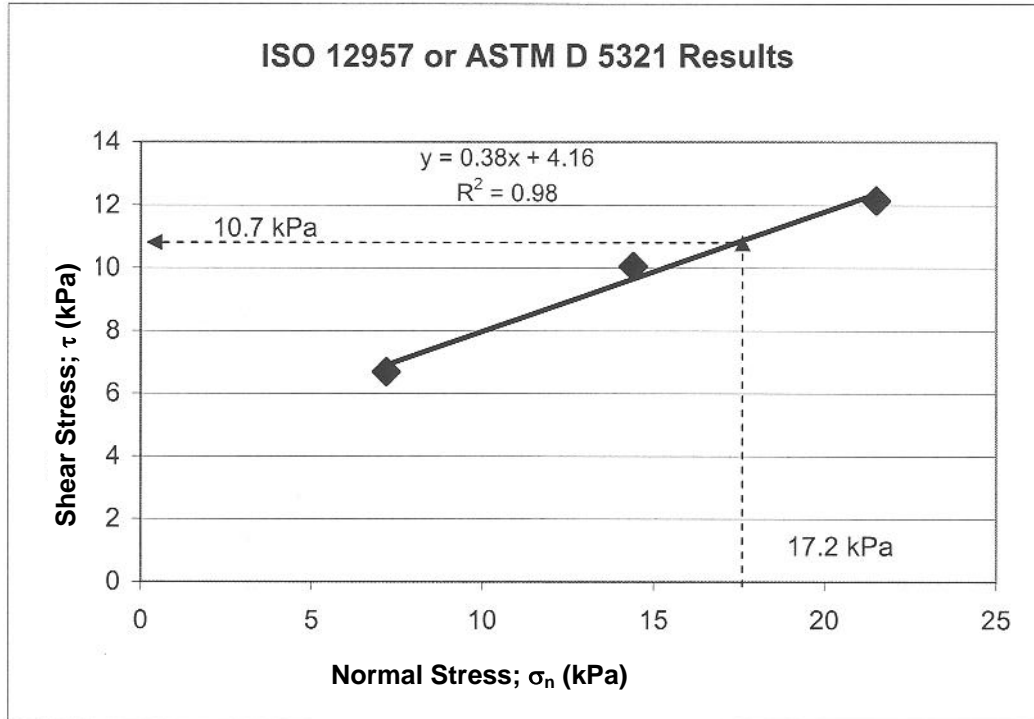


Figure 4 – Use of a laboratory generated failure envelope by specifying a site-specific normal stress and requiring a minimum value of shear strength taken directly off of the y-axis.

In summary, there are probably other or intermediate interpretations of an interface shear strength failure envelope for use in design and then a subsequent specification, but those presented here are felt to be the most common.

**APPLICATION FOR PERMIT RENEWAL AND MODIFICATION
SANDOVAL COUNTY LANDFILL**

**VOLUME III: LANDFILL ENGINEERING CALCULATIONS
SECTION 3: SLOPE STABILITY ANALYSIS**

ATTACHMENT III.3.D

**ACS LABORATORY AND FIELD SERVICES. GEOTECHNICAL LABORATORY
ANALYSIS OF ON-SITE SOILS. 2005 AND 2014.**

ATTACHMENT 1
SUMMARY OF GEOTECHNICAL TEST RESULTS
SANDOVAL COUNTY LANDFILL

Sample Number	Sample Depth (fbgs)	USCS Class	Grain Size Distribution			Uniformity Coefficient	Natural Moisture (%)	Standard Proctor		Permeability (cm/sec)
			Pass #10 (%)	Pass #40 (%)	Pass #200 (%)			Max. Dry Density (PCF)	Optimum Moisture (%)	
BH-1	10	SP	88.5	77.6	4.7	3.05	2.5			
BH-1	20	SP-SM	95.5	80.9	7.4	3.04	3.9			
BH-1	35	SP-SM	99.3	91.3	5.4	2.61	4.0			
BH-1	40	SP	98.8	92.2	3.7	2.38	2.6			
BH-2	10	SP-SM	99.9	94.0	9.4	3.17	2.8			
BH-2	20	SP								9.88 E-06
BH-2	25	SP	99.6	95.6	2.6	1.90	3.7			
BH-2	30	SP	99.7	92.4	1.5	1.87	3.5			
BH-2	40	SP	99.7	92.1	1.9	1.85	3.4			
BH-2	40-45	SP						126.3	12.5	
BH-3	10	SP	97.5	89.4	1.6	1.84	2.5			
BH-3	15	SP								2.48 E-06
BH-3	20	SP	91.9	81.9	1.4	1.90	6.8			
BH-3	30	SP	99.1	90.6	1.0	1.80	3.5			
BH-3	35	SP	97.0	72.4	0.6	1.96	3.0			
BH-3	40-45	SP						129.7	10.5	
BH-4	10	SP	96.8	91.9	2.0	1.82	3.4			
BH-4	15	SP	99.8	95.8	1.4	1.79	3.7			
BH-4	20	SP	99.7	93.8	1.5	1.80	4.9			
BH-4	40	SP	99.2	95.2	1.0	1.77	2.8			
BH-5	10	SP	95.6	87.4	0.9	1.83	3.1			
BH-5	20	SP	99.0	95.3	2.0	1.79	2.7			
BH-5	30	SP	98.5	84.8	0.4	1.82	3.0			
BH-5	35	SP	99.9	92.5	0.4	1.77	3.9			
BH-5	40-45	SP						130.6	12.8	
Stockpile		SP	76.9	45.6	0.2	3.34				2.45 E-07

DATE 01 08 15
CLIENT GORDON ENVIRONMENTAL
PROJECT Sandoval County LF

PERMIT
CONTRACT 211.14.03/01
JOB PSL: CELL 4-C
FILE 1543002

GORDON ENVIRONMENTAL, INC
213 South Camino Del Pueblo
Bernalillo, New Mexico 87004

ATTENTION: K. Gordon, PE
M. Heinsteins, PE

HYDRAULIC CONDUCTIVITY of GRANULAR SOILS
(Falling Head)

Specimen ID

Reference Reports:
1434 001

Orange-Brown SAND

CLASSIFICATION: USCS
Tested at: 101.3 lbs/ft³

% Passing # 200 Sieve :ASTM C 136

% Retained on 3/4" Sieve 0.0%

Maximum Dry Density 121.7 lbs/ft³

Optimum Moisture 8.9% of Dry Weight

% Compaction of Maximum Density 83.2%, Hydrated w/ deAired, distilled H₂O

COEFFICIENT OF PERMEABILITY, cm/sec: K 3.33×10^{-4}

Corrected Coefficient PERMEABILITY, cm/sec: K 3.16×10^{-4}
20°

DATE 01 08 15
CLIENT GORDON ENVIRONMENTAL
PROJECT Sandoval County LF

PERMIT
CONTRACT 211.14.03/01
JOB PSL
FILE 1534001

GORDON ENVIRONMENTAL, INC
213 South Camino Del Pueblo
Bernalillo, New Mexico 87004

ATTENTION: K. Gordon, PE
M. Heinstein, PE

HYDRAULIC CONDUCTIVITY of GRANULAR SOILS
(Falling Head)

Specimen ID

Reference Reports:
1434 074

Light Brown SAND

CLASSIFICATION: USCS
Tested at: 97.8 lbs/ft³

% Passing # 200 Sieve :ASTM C 136

% Retained on 3/4" Sieve 0.0%

Maximum Dry Density 113.9 lbs/ft³

Optimum Moisture 11.6% of Dry Weight

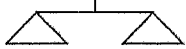
% Compaction of Maximum Density 85.9%, Hydrated w/ deAired, distilled H₂O

COEFFICIENT OF PERMEABILITY, cm/sec: K 8.90 X 10⁻⁴

Corrected Coefficient PERMEABILITY, cm/sec: K 9.77 X 10⁻⁴
20°

ACSPOB 1015
BERNALILLO NM 87004

505-867-6585



Laboratory & Field Testing Services

ACNM-NMSHTD & NICET Certified

DATE 06 30 14
CLIENT GORDON ENVIRONMENTAL
PROJECT Sandoval County LFPERMIT
CONTRACT 211.147.03
JOB PSL
FILE 1434021GORDON ENVIRONMENTAL, INC
213 South Camino Del Pueblo
Bernalillo, New Mexico 87004ATTENTION: K. Gordon, PE
M. Heinstein, PEHYDRAULIC CONDUCTIVITY of GRANULAR SOILS
(Falling Head)

Specimen ID	Moist: Source A
Reference Reports:	Orange-Tan SAND,
1434 001	With Silt, Trace Gravel
1434 003	CLASSIFICATION: USCS
	Tested at: 99.6 lbs/ft ³

% Passing # 200 Sieve :ASTM C 136	8.1%
% Retained on 3/4" Sieve	0.0%
Maximum Dry Density	121.7 lbs/ft ³
Optimum Moisture	8.9% of Dry Weight
% Compaction of Maximum Density	81.8%, Hydrated w/ deAired, distilled H ₂ O
COEFFICIENT OF PERMEABILITY, cm/sec: K	1.04×10^{-3}
Corrected Coefficient PERMEABILITY, cm/sec: K	8.97×10^{-4}

**APPLICATION FOR PERMIT RENEWAL AND MODIFICATION
SANDOVAL COUNTY LANDFILL**

**VOLUME III: LANDFILL ENGINEERING CALCULATIONS
SECTION 3: SLOPE STABILITY ANALYSIS**

ATTACHMENT III.3.E

“SLIDE®” ANALYSIS INFORMATION – SCENARIO 1 THROUGH 18

III.3.E-1	SCENARIO 1: SECTION A-A’; CIRCULAR, STATIC
III.3.E-1	SCENARIO 2: SECTION A-A’; CIRCULAR, SEISMIC
III.3.E-2	SCENARIO 3: SECTION A-A’, CIRCULAR, STATIC
III.3.E.2	SCENARIO 4: SECTION A-A’ CIRCULAR, SEISMIC
III.3.E-3	SCENARIO 5: SECTION A-A’; BLOCK, STATIC
III.3.E-3	SCENARIO 6: SECTION A-A’; BLOCK, SEISMIC
III.3.E-4	SCENARIO 7: SECTION A-A’, CIRCULAR, STATIC
III.3.E-4	SCENARIO 8: SECTION A-A’, CIRCULAR, SEISMIC
III.3.E-5	SCENARIO 9: SECTION A-A’, CIRCULAR, STATIC
III.3.E-5	SCENARIO 10: SECTION A-A’, CIRCULAR, SEISMIC
III.3.E-6	SCENARIO 11: SECTION A-A’, BLOCK, STATIC
III.3.E-6	SCENARIO 12: SECTION A-A’, BLOCK, SEISMIC
III.3.E-7	SCENARIO 13: SECTION C-C’; CIRCULAR, STATIC
III.3.E-7	SCENARIO 14: SECTION C-C’; CIRCULAR, SEISMIC
III.3.E-8	SCENARIO 15: SECTION C-C’; CIRCULAR, STATIC
III.3.E-8	SCENARIO 16: SECTION C-C’; CIRCULAR, SEISMIC
III.3.E-9	SCENARIO 17: SECTION C-C’; CIRCULAR, STATIC
III.3.E-9	SCENARIO 18: SECTION C-C’; CIRCULAR, SEISMIC

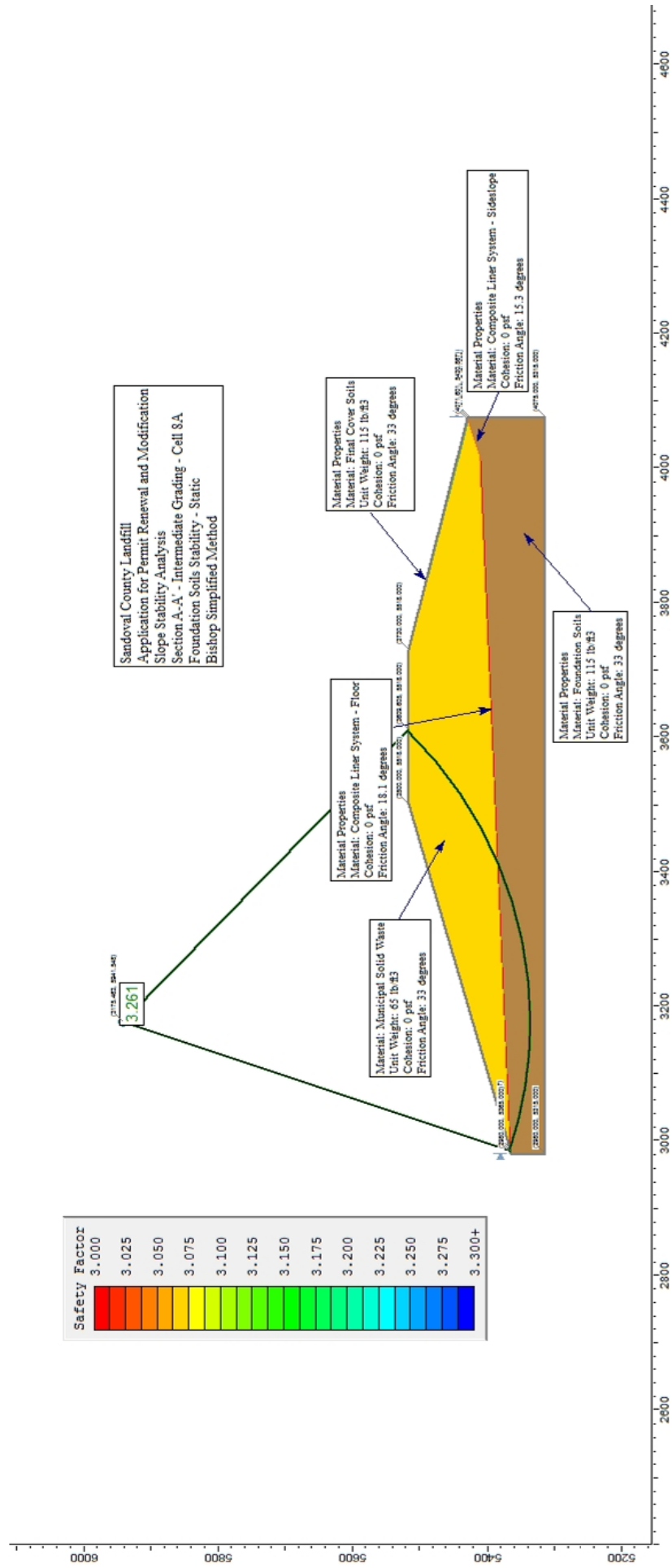
**APPLICATION FOR PERMIT RENEWAL AND MODIFICATION
SANDOVAL COUNTY LANDFILL**

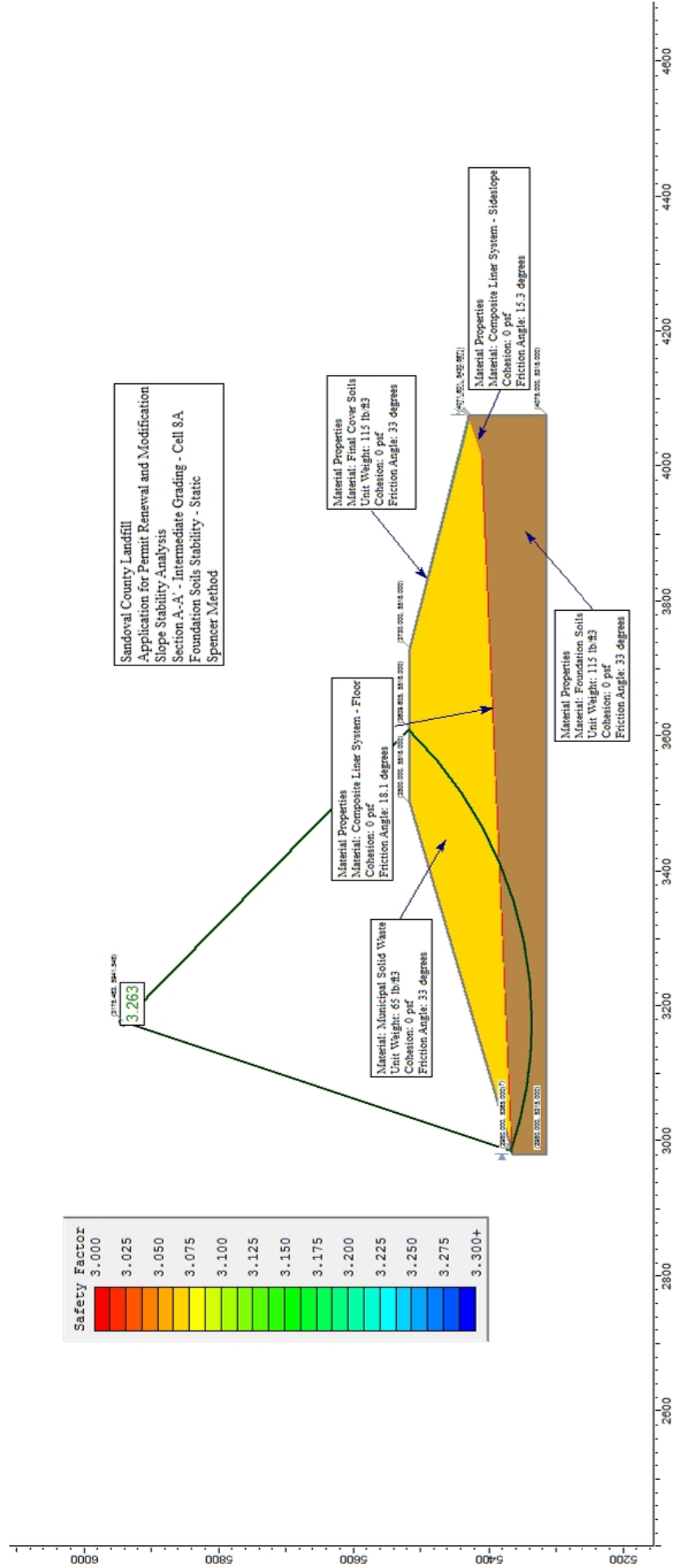
**VOLUME III: LANDFILL ENGINEERING CALCULATIONS
SECTION 3: SLOPE STABILITY ANALYSIS**

ATTACHMENT III.3.E-1

SCENARIO 1: SECTION A-A'; CIRCULAR, STATIC

SCENARIO 2: SECTION A-A'; CIRCULAR, SEISMIC





Sandoval County Landfill
Application for Permit Renewal and Modification
Slope Stability Analysis
Section A-A' - Intermediate Grading - Cell 8A
Foundation Soils Stability - Static
Spencer Method

Slide Analysis Information

Document Name

File Name: Section A-A' Intermediate Slope Circular Static - Foundation.sli

Project Settings

Project Title: Sandoval County Landfill - Permit Renewal and Modification

Failure Direction: Right to Left

Units of Measurement: Imperial Units

Pore Fluid Unit Weight: 62.4 lb/ft³

Groundwater Method: Water Surfaces

Data Output: Standard

Calculate Excess Pore Pressure: Off

Allow Ru with Water Surfaces or Grids: Off

Random Numbers: Pseudo-random Seed

Random Number Seed: 10116

Random Number Generation Method: Park and Miller v.3

Analysis Methods

Analysis Methods used:

Bishop simplified

Janbu simplified

Spencer

Number of slices: 25

Tolerance: 0.005

Maximum number of iterations: 50

Surface Options

Surface Type: Circular

Search Method: Grid Search

Radius increment: 10

Composite Surfaces: Enabled

Reverse Curvature: Create Tension Crack

Minimum Elevation: Not Defined

Minimum Depth: Not Defined

Material Properties

Material: Municipal Solid Waste

Strength Type: Mohr-Coulomb

Unit Weight: 65 lb/ft³

Cohesion: 0 psf

Friction Angle: 33 degrees

Water Surface: None

Material: Foundation Soils

Strength Type: Mohr-Coulomb

Unit Weight: 115 lb/ft³

Cohesion: 0 psf
Friction Angle: 33 degrees
Water Surface: None

Material: Final Cover Soils
Strength Type: Mohr-Coulomb
Unit Weight: 115 lb/ft³
Cohesion: 0 psf
Friction Angle: 33 degrees
Water Surface: None

Material: Composite Liner System - Floor
Strength Type: Mohr-Coulomb
Unit Weight: 115 lb/ft³
Cohesion: 0 psf
Friction Angle: 18.1 degrees
Water Surface: None

Material: Composite Liner System - Sideslope
Strength Type: Mohr-Coulomb
Unit Weight: 115 lb/ft³
Cohesion: 0 psf
Friction Angle: 15.3 degrees
Water Surface: None

Global Minimums

Method: bishop simplified
FS: 3.261320
Center: 3175.463, 5941.548
Radius: 606.529
Left Slip Surface Endpoint: 2983.768, 5366.109
Right Slip Surface Endpoint: 3609.611, 5518.000
Resisting Moment=1.49316e+009 lb-ft
Driving Moment=4.57839e+008 lb-ft

Method: janbu simplified
FS: 3.040680
Center: 3175.463, 5941.548
Radius: 606.529
Left Slip Surface Endpoint: 2983.768, 5366.109
Right Slip Surface Endpoint: 3609.611, 5518.000
Resisting Horizontal Force=2.32647e+006 lb
Driving Horizontal Force=765116 lb

Method: spencer
FS: 3.262500
Center: 3175.463, 5941.548
Radius: 606.529
Left Slip Surface Endpoint: 2983.768, 5366.109
Right Slip Surface Endpoint: 3609.611, 5518.000
Resisting Moment=1.4937e+009 lb-ft
Driving Moment=4.57839e+008 lb-ft
Resisting Horizontal Force=2.34044e+006 lb
Driving Horizontal Force=717376 lb

Valid / Invalid Surfaces

Method: bishop simplified

Number of Valid Surfaces: 1

Number of Invalid Surfaces: 0

Method: janbu simplified

Number of Valid Surfaces: 1

Number of Invalid Surfaces: 0

Method: spencer

Number of Valid Surfaces: 1

Number of Invalid Surfaces: 0

List of All Coordinates

Circular Failure Surface

3175.463 5941.548

2983.780 5366.112

3609.605 5518.000

Material Boundary

2987.976 5367.347

4010.000 5411.783

4015.000 5412.000

Material Boundary

2980.000 5365.000

4010.000 5409.783

Material Boundary

3730.000 5515.000

3730.000 5518.000

Material Boundary

3730.000 5515.000

4066.502 5429.167

4069.901 5428.300

4075.000 5427.000

Material Boundary

4010.000 5409.783

4010.000 5411.783

Material Boundary

4015.000 5412.000

4056.519 5425.840

4066.480 5429.160

4066.502 5429.167

4071.601 5430.867

Material Boundary

4010.000 5409.783

4015.000 5410.000

4069.901 5428.300

4075.000 5430.000

External Boundary

4075.000 5315.000

4075.000 5427.000

4075.000 5430.000

4071.601 5430.867

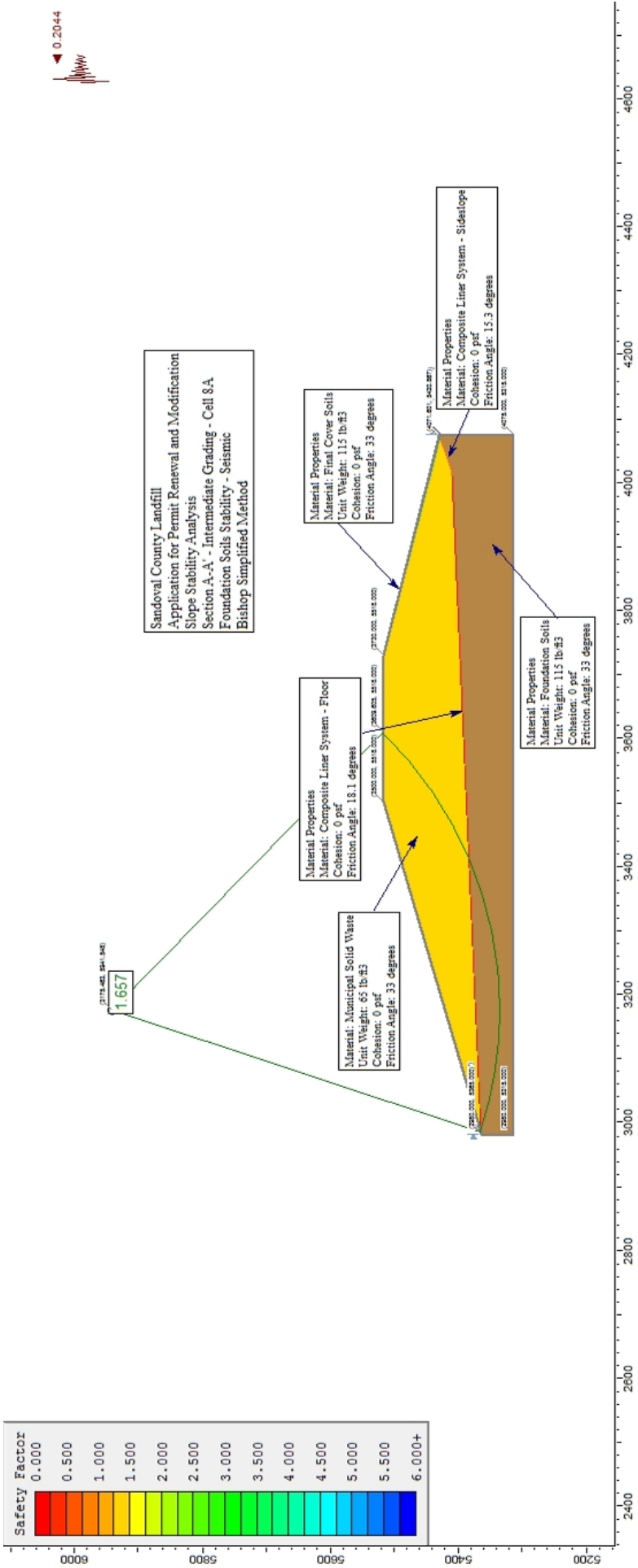
3730.000 5518.000

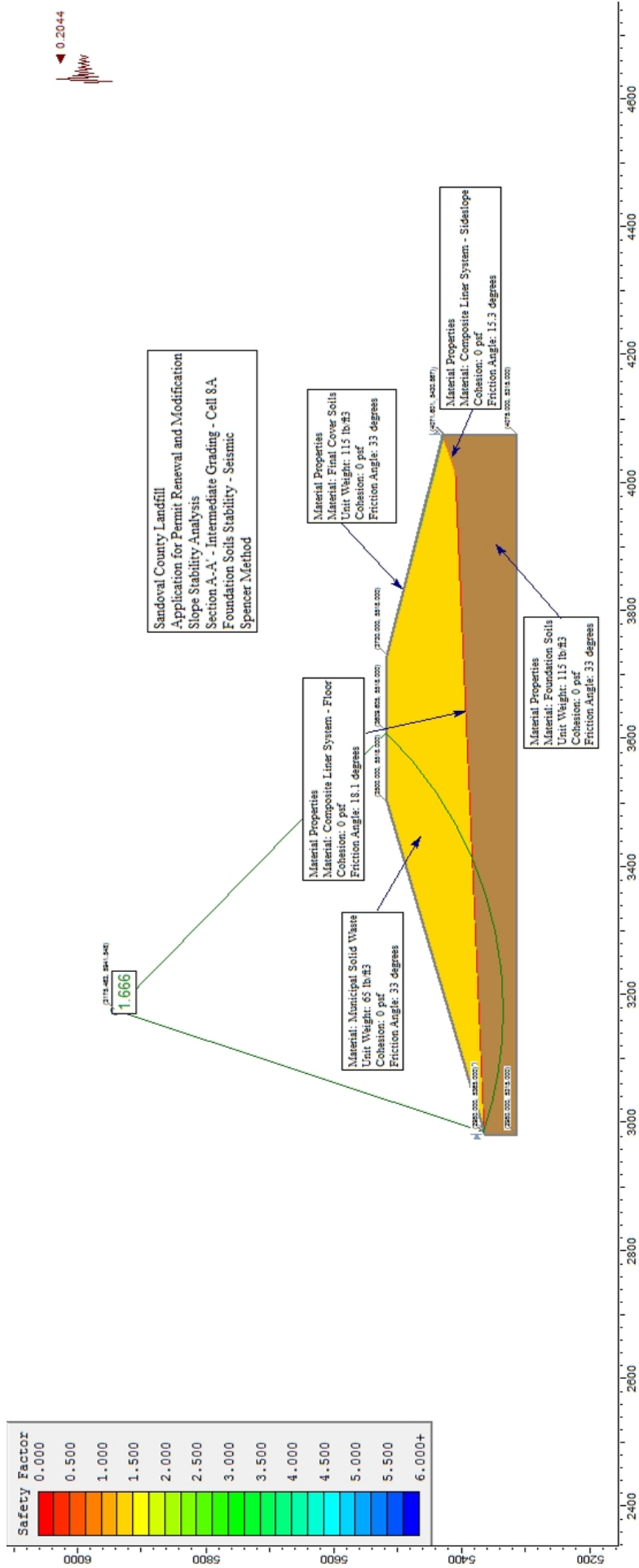
3500.000 5518.000

2987.976 5367.347

2980.000 5365.000

2980.000 5315.000





Slide Analysis Information

Document Name

File Name: Section A-A' Intermediate Slope Circular Seismic - Foundation.sli

Project Settings

Project Title: Sandoval County Landfill - Permit Renewal and Modification

Failure Direction: Right to Left

Units of Measurement: Imperial Units

Pore Fluid Unit Weight: 62.4 lb/ft³

Groundwater Method: Water Surfaces

Data Output: Standard

Calculate Excess Pore Pressure: Off

Allow Ru with Water Surfaces or Grids: Off

Random Numbers: Pseudo-random Seed

Random Number Seed: 10116

Random Number Generation Method: Park and Miller v.3

Analysis Methods

Analysis Methods used:

Bishop simplified

Janbu simplified

Spencer

Number of slices: 25

Tolerance: 0.005

Maximum number of iterations: 50

Surface Options

Surface Type: Circular

Search Method: Grid Search

Radius increment: 10

Composite Surfaces: Enabled

Reverse Curvature: Create Tension Crack

Minimum Elevation: Not Defined

Minimum Depth: Not Defined

Loading

Seismic Load Coefficient (Horizontal): 0.2044

Material Properties

Material: Municipal Solid Waste

Strength Type: Mohr-Coulomb

Unit Weight: 65 lb/ft³

Cohesion: 0 psf

Friction Angle: 33 degrees

Water Surface: None

Material: Foundation Soils

Strength Type: Mohr-Coulomb

Unit Weight: 115 lb/ft³

Cohesion: 0 psf

Friction Angle: 33 degrees

Water Surface: None

Material: Final Cover Soils

Strength Type: Mohr-Coulomb

Unit Weight: 115 lb/ft³

Cohesion: 0 psf

Friction Angle: 33 degrees

Water Surface: None

Material: Composite Liner System - Floor

Strength Type: Mohr-Coulomb

Unit Weight: 115 lb/ft³

Cohesion: 0 psf

Friction Angle: 18.1 degrees

Water Surface: None

Material: Composite Liner System - Sideslope

Strength Type: Mohr-Coulomb

Unit Weight: 115 lb/ft³

Cohesion: 0 psf

Friction Angle: 15.3 degrees

Water Surface: None

Global Minimums

Method: bishop simplified

FS: 1.657270

Center: 3175.463, 5941.548

Radius: 606.529

Left Slip Surface Endpoint: 2983.768, 5366.109

Right Slip Surface Endpoint: 3609.611, 5518.000

Resisting Moment=1.43938e+009 lb-ft

Driving Moment=8.68525e+008 lb-ft

Method: janbu simplified

FS: 1.536050

Center: 3175.463, 5941.548

Radius: 606.529

Left Slip Surface Endpoint: 2983.768, 5366.109

Right Slip Surface Endpoint: 3609.611, 5518.000

Resisting Horizontal Force=2.24388e+006 lb

Driving Horizontal Force=1.46081e+006 lb

Method: spencer

FS: 1.666060

Center: 3175.463, 5941.548

Radius: 606.529

Left Slip Surface Endpoint: 2983.768, 5366.109

Right Slip Surface Endpoint: 3609.611, 5518.000

Resisting Moment=1.44702e+009 lb-ft

Driving Moment=8.68525e+008 lb-ft
Resisting Horizontal Force=2.28261e+006 lb
Driving Horizontal Force=1.37006e+006 lb

Valid / Invalid Surfaces

Method: bishop simplified

Number of Valid Surfaces: 1

Number of Invalid Surfaces: 0

Method: janbu simplified

Number of Valid Surfaces: 1

Number of Invalid Surfaces: 0

Method: spencer

Number of Valid Surfaces: 1

Number of Invalid Surfaces: 0

List of All Coordinates

Circular Failure Surface

3175.463 5941.548

2983.780 5366.112

3609.605 5518.000

Material Boundary

2987.976 5367.347

4010.000 5411.783

4015.000 5412.000

Material Boundary

2980.000 5365.000

4010.000 5409.783

Material Boundary

3730.000 5515.000

3730.000 5518.000

Material Boundary

3730.000 5515.000

4066.502 5429.167

4069.901 5428.300

4075.000 5427.000

Material Boundary

4010.000 5409.783

4010.000 5411.783

Material Boundary

4015.000 5412.000

4056.519 5425.840

4066.480 5429.160

4066.502 5429.167

4071.601 5430.867

Material Boundary

4010.000 5409.783
4015.000 5410.000
4069.901 5428.300
4075.000 5430.000

External Boundary

4075.000 5315.000
4075.000 5427.000
4075.000 5430.000
4071.601 5430.867
3730.000 5518.000
3500.000 5518.000
2987.976 5367.347
2980.000 5365.000
2980.000 5315.000

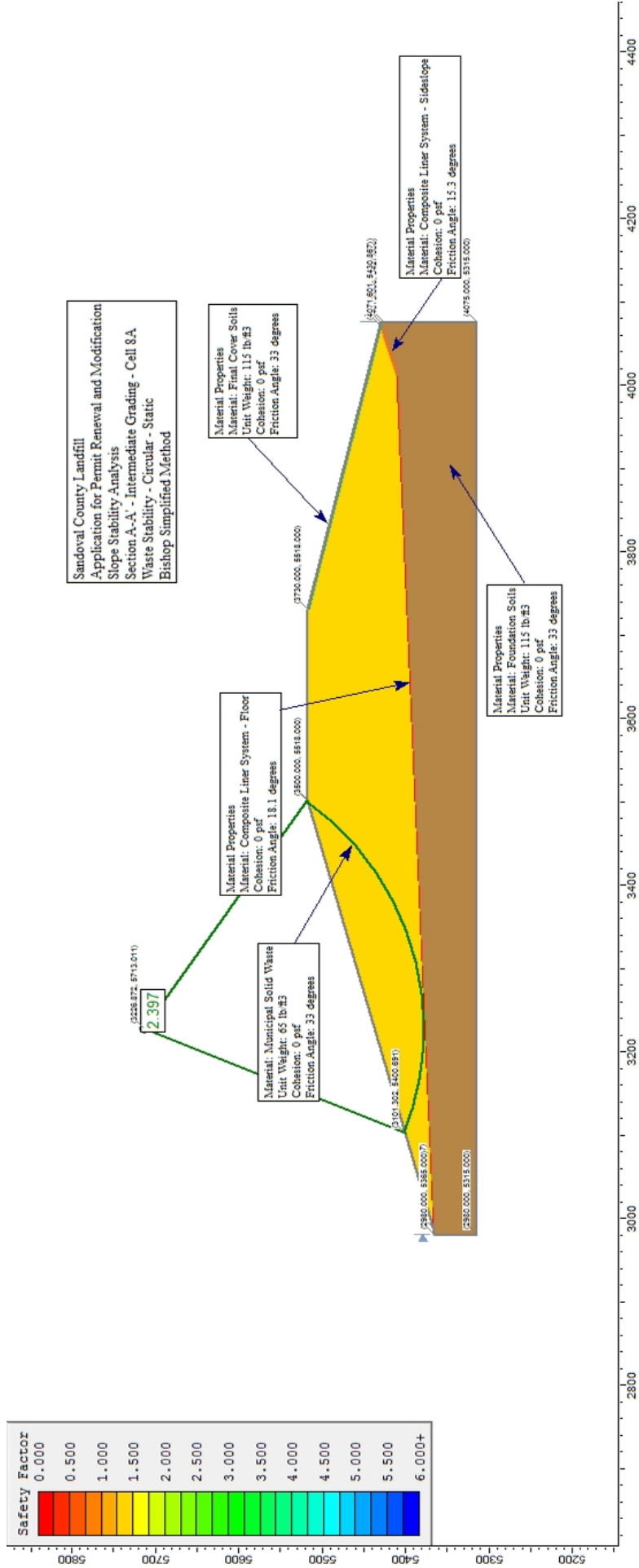
**APPLICATION FOR PERMIT RENEWAL AND MODIFICATION
SANDOVAL COUNTY LANDFILL**

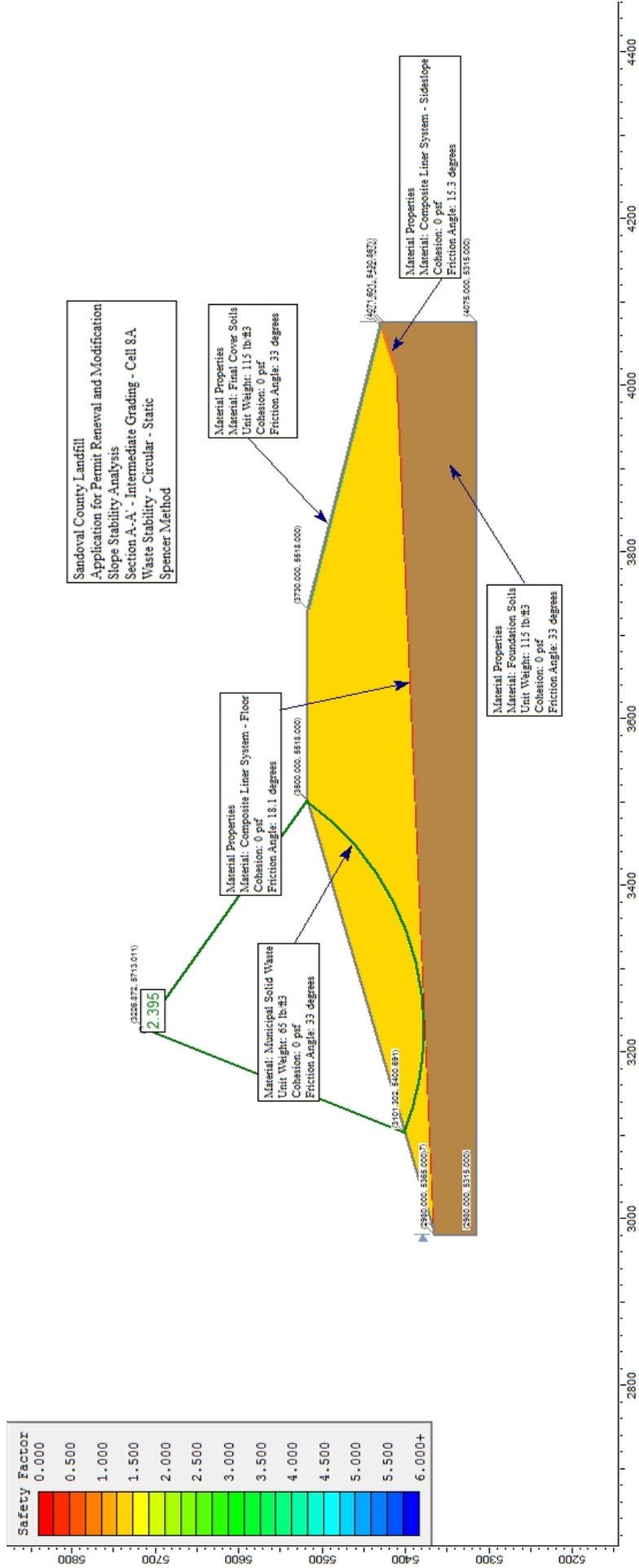
**VOLUME III: LANDFILL ENGINEERING CALCULATIONS
SECTION 3: SLOPE STABILITY ANALYSIS**

ATTACHMENT III.3.E-2

SCENARIO 3: SECTION A-A', CIRCULAR, STATIC

SCENARIO 4: SECTION A-A', CIRCULAR, SEISMIC





Slide Analysis Information

Document Name

File Name: Section A-A' Intermediate Slope Circular Static - Waste Stability.sli

Project Settings

Project Title: Sandoval County Landfill - Permit Renewal and Modification

Failure Direction: Right to Left

Units of Measurement: Imperial Units

Pore Fluid Unit Weight: 62.4 lb/ft³

Groundwater Method: Water Surfaces

Data Output: Standard

Calculate Excess Pore Pressure: Off

Allow Ru with Water Surfaces or Grids: Off

Random Numbers: Pseudo-random Seed

Random Number Seed: 10116

Random Number Generation Method: Park and Miller v.3

Analysis Methods

Analysis Methods used:

Bishop simplified

Janbu simplified

Spencer

Number of slices: 25

Tolerance: 0.005

Maximum number of iterations: 50

Surface Options

Surface Type: Circular

Search Method: Grid Search

Radius increment: 10

Composite Surfaces: Enabled

Reverse Curvature: Create Tension Crack

Minimum Elevation: Not Defined

Minimum Depth: Not Defined

Material Properties

Material: Municipal Solid Waste

Strength Type: Mohr-Coulomb

Unit Weight: 65 lb/ft³

Cohesion: 0 psf

Friction Angle: 33 degrees

Water Surface: None

Material: Foundation Soils

Strength Type: Mohr-Coulomb

Unit Weight: 115 lb/ft³

Cohesion: 0 psf
Friction Angle: 33 degrees
Water Surface: None

Material: Final Cover Soils
Strength Type: Mohr-Coulomb
Unit Weight: 115 lb/ft³
Cohesion: 0 psf
Friction Angle: 33 degrees
Water Surface: None

Material: Composite Liner System - Floor
Strength Type: Mohr-Coulomb
Unit Weight: 115 lb/ft³
Cohesion: 0 psf
Friction Angle: 18.1 degrees
Water Surface: None

Material: Composite Liner System - Sideslope
Strength Type: Mohr-Coulomb
Unit Weight: 115 lb/ft³
Cohesion: 0 psf
Friction Angle: 15.3 degrees
Water Surface: None

Global Minimums

Method: bishop simplified
FS: 2.397000
Center: 3226.872, 5713.011
Radius: 336.625
Left Slip Surface Endpoint: 3101.290, 5400.687
Right Slip Surface Endpoint: 3501.258, 5518.000
Resisting Moment=2.65633e+008 lb-ft
Driving Moment=1.10819e+008 lb-ft

Method: janbu simplified
FS: 2.194160
Center: 3226.872, 5713.011
Radius: 336.625
Left Slip Surface Endpoint: 3101.290, 5400.687
Right Slip Surface Endpoint: 3501.258, 5518.000
Resisting Horizontal Force=718911 lb
Driving Horizontal Force=327647 lb

Method: spencer
FS: 2.394610
Center: 3226.872, 5713.011
Radius: 336.625
Left Slip Surface Endpoint: 3101.290, 5400.687
Right Slip Surface Endpoint: 3501.258, 5518.000
Resisting Moment=2.65369e+008 lb-ft
Driving Moment=1.10819e+008 lb-ft
Resisting Horizontal Force=726023 lb
Driving Horizontal Force=303190 lb

Valid / Invalid Surfaces

Method: bishop simplified

Number of Valid Surfaces: 1

Number of Invalid Surfaces: 0

Method: janbu simplified

Number of Valid Surfaces: 1

Number of Invalid Surfaces: 0

Method: spencer

Number of Valid Surfaces: 1

Number of Invalid Surfaces: 0

List of All Coordinates

Circular Failure Surface

3226.872 5713.011

3101.302 5400.691

3501.257 5518.000

Material Boundary

2987.976 5367.347

4010.000 5411.783

4015.000 5412.000

Material Boundary

2980.000 5365.000

4010.000 5409.783

Material Boundary

3730.000 5515.000

3730.000 5518.000

Material Boundary

3730.000 5515.000

4066.502 5429.167

4069.901 5428.300

4075.000 5427.000

Material Boundary

4010.000 5409.783

4010.000 5411.783

Material Boundary

4015.000 5412.000

4056.519 5425.840

4066.480 5429.160

4066.502 5429.167

4071.601 5430.867

Material Boundary

4010.000 5409.783

4015.000 5410.000

4069.901 5428.300

4075.000 5430.000

External Boundary

4075.000 5315.000

4075.000 5427.000

4075.000 5430.000

4071.601 5430.867

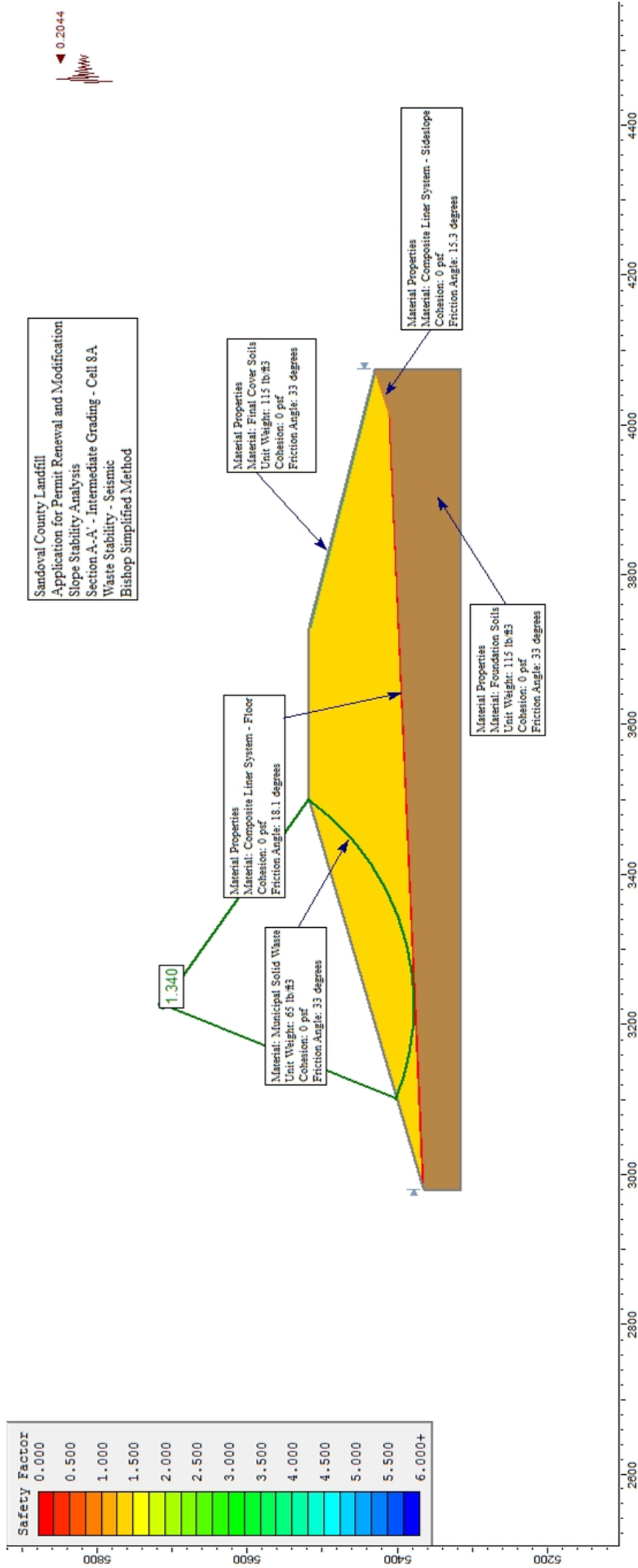
3730.000 5518.000

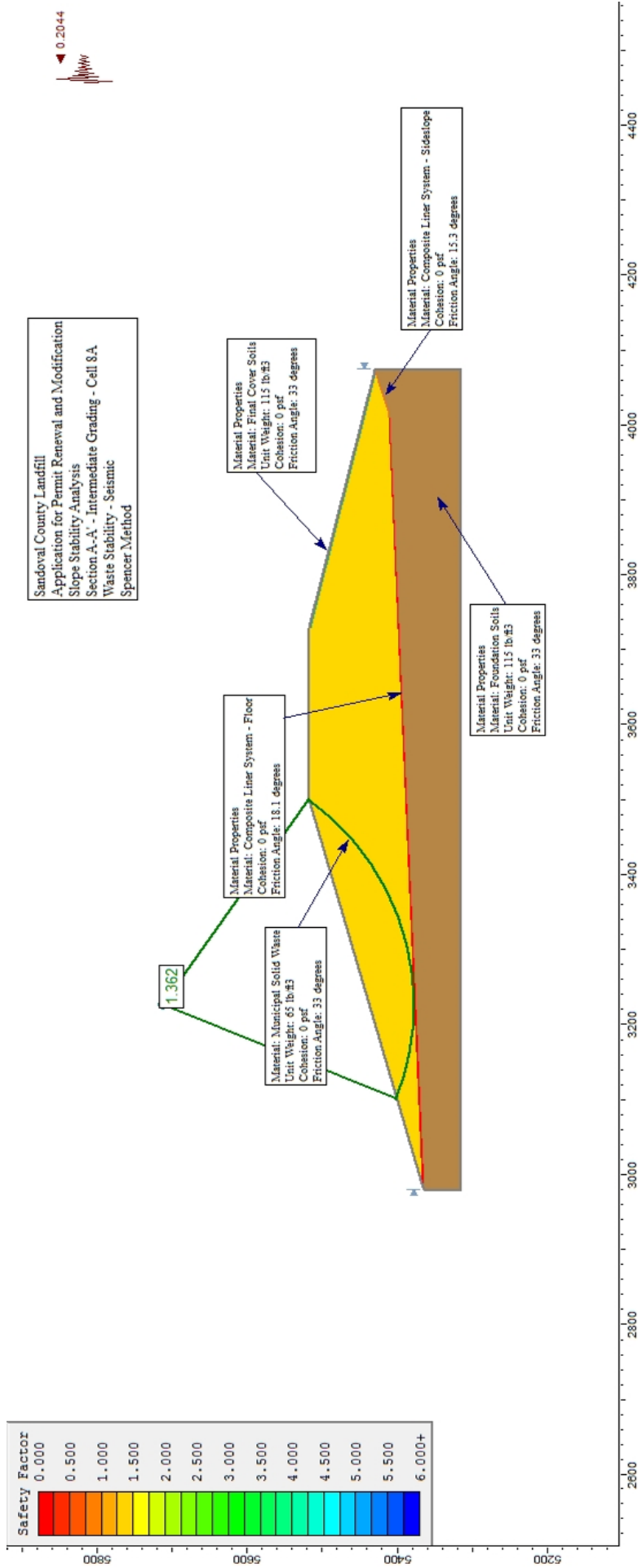
3500.000 5518.000

2987.976 5367.347

2980.000 5365.000

2980.000 5315.000





Slide Analysis Information

Document Name

File Name: Section A-A' Intermediate Slope Circular Seismic - Waste Stability.sli

Project Settings

Project Title: Sandoval County Landfill - Permit Renewal and Modification

Failure Direction: Right to Left

Units of Measurement: Imperial Units

Pore Fluid Unit Weight: 62.4 lb/ft³

Groundwater Method: Water Surfaces

Data Output: Standard

Calculate Excess Pore Pressure: Off

Allow Ru with Water Surfaces or Grids: Off

Random Numbers: Pseudo-random Seed

Random Number Seed: 10116

Random Number Generation Method: Park and Miller v.3

Analysis Methods

Analysis Methods used:

Bishop simplified

Janbu simplified

Spencer

Number of slices: 25

Tolerance: 0.005

Maximum number of iterations: 50

Surface Options

Surface Type: Circular

Search Method: Grid Search

Radius increment: 10

Composite Surfaces: Enabled

Reverse Curvature: Create Tension Crack

Minimum Elevation: Not Defined

Minimum Depth: Not Defined

Loading

Seismic Load Coefficient (Horizontal): 0.2044

Material Properties

Material: Municipal Solid Waste

Strength Type: Mohr-Coulomb

Unit Weight: 65 lb/ft³

Cohesion: 0 psf

Friction Angle: 33 degrees

Water Surface: None

Material: Foundation Soils

Strength Type: Mohr-Coulomb

Unit Weight: 115 lb/ft³

Cohesion: 0 psf

Friction Angle: 33 degrees

Water Surface: None

Material: Final Cover Soils

Strength Type: Mohr-Coulomb

Unit Weight: 115 lb/ft³

Cohesion: 0 psf

Friction Angle: 33 degrees

Water Surface: None

Material: Composite Liner System - Floor

Strength Type: Mohr-Coulomb

Unit Weight: 115 lb/ft³

Cohesion: 0 psf

Friction Angle: 18.1 degrees

Water Surface: None

Material: Composite Liner System - Sideslope

Strength Type: Mohr-Coulomb

Unit Weight: 115 lb/ft³

Cohesion: 0 psf

Friction Angle: 15.3 degrees

Water Surface: None

Global Minimums

Method: bishop simplified

FS: 1.340450

Center: 3226.872, 5713.011

Radius: 336.625

Left Slip Surface Endpoint: 3101.290, 5400.687

Right Slip Surface Endpoint: 3501.258, 5518.000

Resisting Moment=2.52107e+008 lb-ft

Driving Moment=1.88076e+008 lb-ft

Method: janbu simplified

FS: 1.215700

Center: 3226.872, 5713.011

Radius: 336.625

Left Slip Surface Endpoint: 3101.290, 5400.687

Right Slip Surface Endpoint: 3501.258, 5518.000

Resisting Horizontal Force=683410 lb

Driving Horizontal Force=562154 lb

Method: spencer

FS: 1.362040

Center: 3226.872, 5713.011

Radius: 336.625

Left Slip Surface Endpoint: 3101.290, 5400.687

Right Slip Surface Endpoint: 3501.258, 5518.000

Resisting Moment=2.56166e+008 lb-ft

Driving Moment=1.88076e+008 lb-ft
Resisting Horizontal Force=707365 lb
Driving Horizontal Force=519344 lb

Valid / Invalid Surfaces

Method: bishop simplified

Number of Valid Surfaces: 1

Number of Invalid Surfaces: 0

Method: janbu simplified

Number of Valid Surfaces: 1

Number of Invalid Surfaces: 0

Method: spencer

Number of Valid Surfaces: 1

Number of Invalid Surfaces: 0

List of All Coordinates

Circular Failure Surface

3226.872 5713.011

3101.302 5400.691

3501.257 5518.000

Material Boundary

2987.976 5367.347

4010.000 5411.783

4015.000 5412.000

Material Boundary

2980.000 5365.000

4010.000 5409.783

Material Boundary

3730.000 5515.000

3730.000 5518.000

Material Boundary

3730.000 5515.000

4066.502 5429.167

4069.901 5428.300

4075.000 5427.000

Material Boundary

4010.000 5409.783

4010.000 5411.783

Material Boundary

4015.000 5412.000

4056.519 5425.840

4066.480 5429.160

4066.502 5429.167

4071.601 5430.867

Material Boundary

4010.000 5409.783
4015.000 5410.000
4069.901 5428.300
4075.000 5430.000

External Boundary

4075.000 5315.000
4075.000 5427.000
4075.000 5430.000
4071.601 5430.867
3730.000 5518.000
3500.000 5518.000
2987.976 5367.347
2980.000 5365.000
2980.000 5315.000

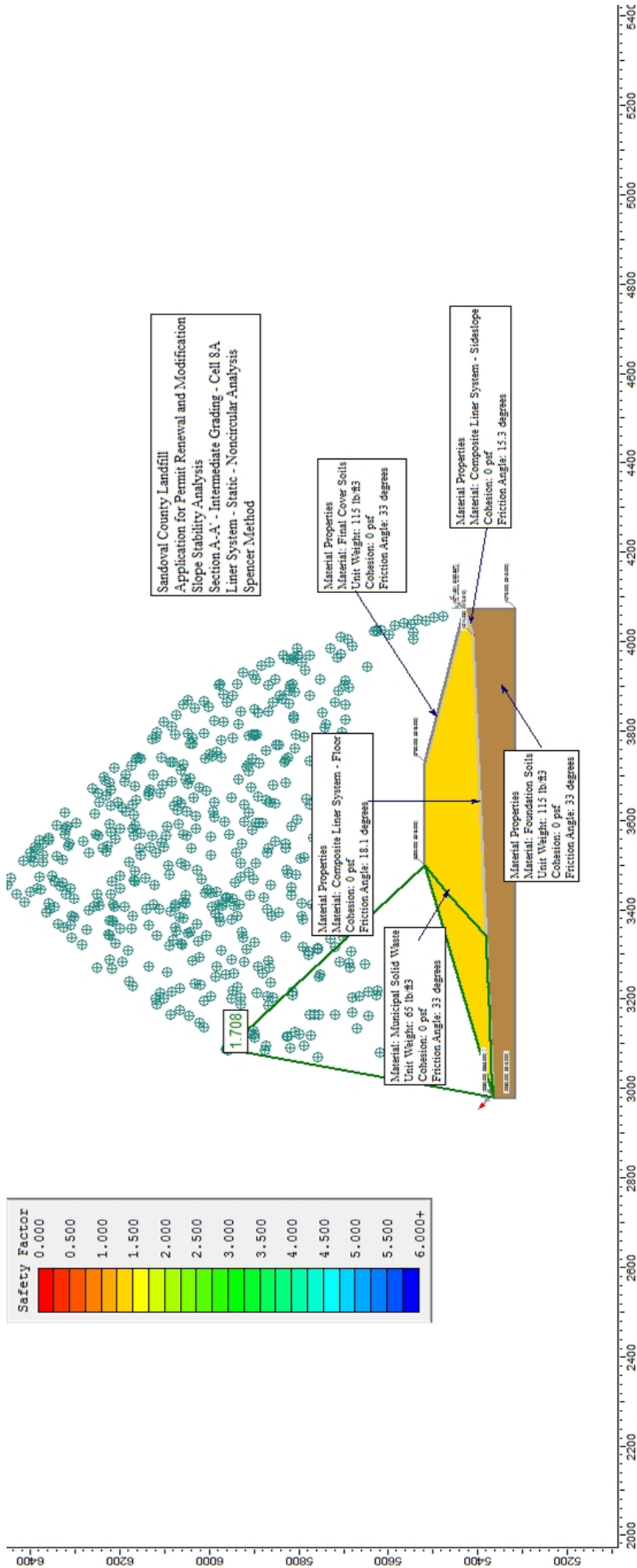
**APPLICATION FOR PERMIT RENEWAL AND MODIFICATION
SANDOVAL COUNTY LANDFILL**

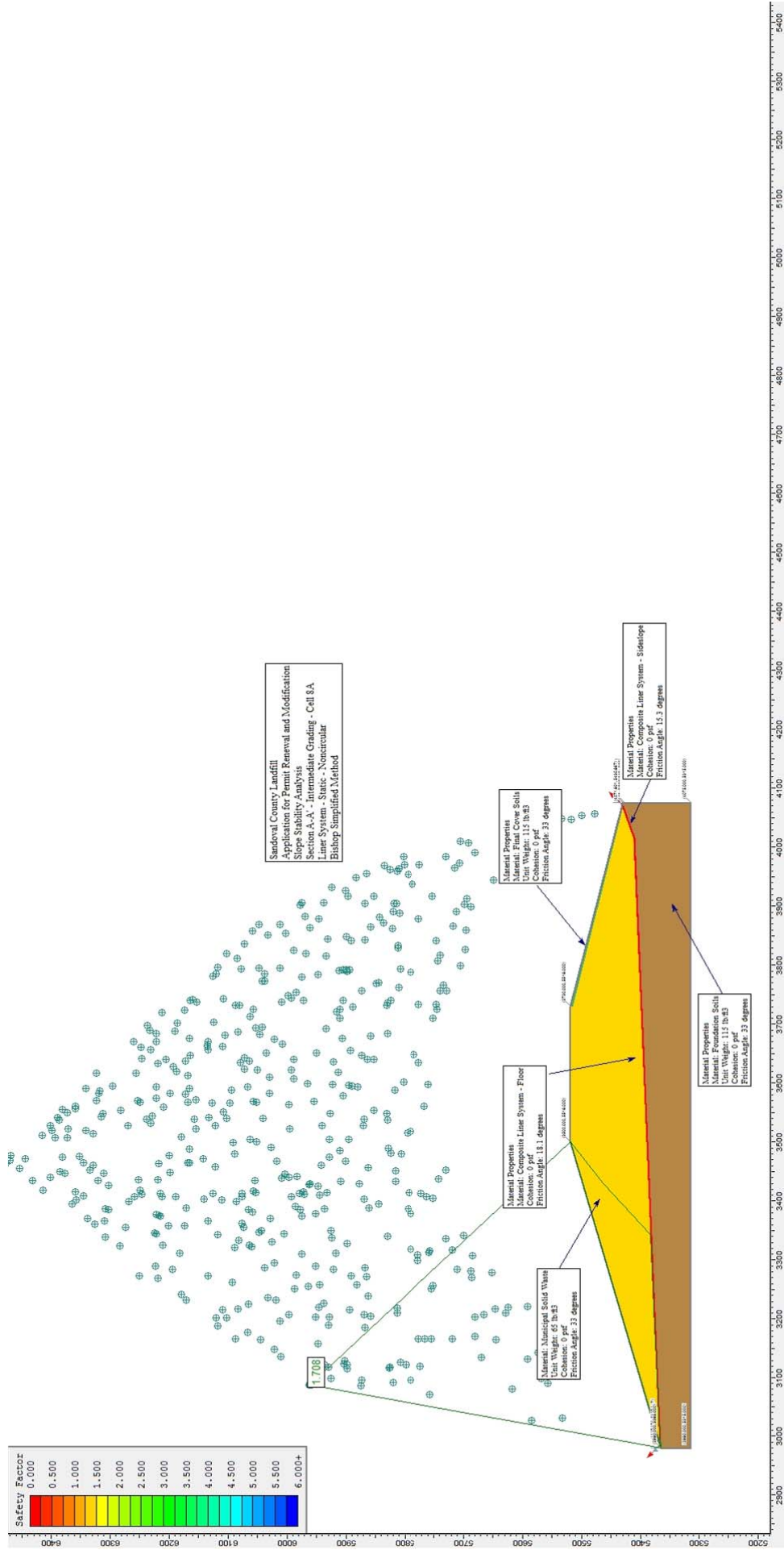
**VOLUME III: LANDFILL ENGINEERING CALCULATIONS
SECTION 3: SLOPE STABILITY ANALYSIS**

ATTACHMENT III.3.E-3

SCENARIO 5: SECTION A-A'; BLOCK, STATIC

SCENARIO 6: SECTION A-A'; BLOCK, SEISMIC





Slide Analysis Information

Document Name

File Name: Section A-A' Intermediate Slope Block Static - Waste Stability.sli

Project Settings

Project Title: Sandoval County Landfill - Permit Renewal and Modification

Failure Direction: Right to Left

Units of Measurement: Imperial Units

Pore Fluid Unit Weight: 62.4 lb/ft³

Groundwater Method: Water Surfaces

Data Output: Standard

Calculate Excess Pore Pressure: Off

Allow Ru with Water Surfaces or Grids: Off

Random Numbers: Pseudo-random Seed

Random Number Seed: 10116

Random Number Generation Method: Park and Miller v.3

Analysis Methods

Analysis Methods used:

Bishop simplified

Janbu simplified

Spencer

Number of slices: 25

Tolerance: 0.005

Maximum number of iterations: 50

Surface Options

Surface Type: Non-Circular Block Search

Number of Surfaces: 500

Pseudo-Random Surfaces: Enabled

Convex Surfaces Only: Disabled

Left Projection Angle (Start Angle): 135

Left Projection Angle (End Angle): 135

Right Projection Angle (Start Angle): 45

Right Projection Angle (End Angle): 45

Minimum Elevation: Not Defined

Minimum Depth: Not Defined

Material Properties

Material: Municipal Solid Waste

Strength Type: Mohr-Coulomb

Unit Weight: 65 lb/ft³

Cohesion: 0 psf

Friction Angle: 33 degrees

Water Surface: None

Material: Foundation Soils

Strength Type: Mohr-Coulomb

Unit Weight: 115 lb/ft³

Cohesion: 0 psf

Friction Angle: 33 degrees

Water Surface: None

Material: Final Cover Soils

Strength Type: Mohr-Coulomb

Unit Weight: 115 lb/ft³

Cohesion: 0 psf

Friction Angle: 33 degrees

Water Surface: None

Material: Composite Liner System - Floor

Strength Type: Mohr-Coulomb

Unit Weight: 115 lb/ft³

Cohesion: 0 psf

Friction Angle: 18.1 degrees

Water Surface: None

Material: Composite Liner System - Sideslope

Strength Type: Mohr-Coulomb

Unit Weight: 115 lb/ft³

Cohesion: 0 psf

Friction Angle: 15.3 degrees

Water Surface: None

Global Minimums

Method: bishop simplified

FS: 1.708080

Axis Location: 3087.000, 5961.500

Left Slip Surface Endpoint: 2980.000, 5365.000

Right Slip Surface Endpoint: 3500.000, 5518.000

Resisting Moment=3.64101e+008 lb-ft

Driving Moment=2.13163e+008 lb-ft

Method: janbu simplified

FS: 1.642390

Axis Location: 3086.489, 5958.648

Left Slip Surface Endpoint: 2980.000, 5365.000

Right Slip Surface Endpoint: 3497.514, 5517.269

Resisting Horizontal Force=558993 lb

Driving Horizontal Force=340353 lb

Method: spencer

FS: 1.738860

Axis Location: 3087.280, 5962.061

Left Slip Surface Endpoint: 2980.000, 5365.000

Right Slip Surface Endpoint: 3500.560, 5518.000

Resisting Moment=3.59576e+008 lb-ft

Driving Moment=2.06788e+008 lb-ft

Resisting Horizontal Force=544926 lb

Driving Horizontal Force=313382 lb

Valid / Invalid Surfaces

Method: bishop simplified

Number of Valid Surfaces: 318

Number of Invalid Surfaces: 186

Error Codes:

Error Code -107 reported for 185 surfaces

Error Code -108 reported for 1 surface

Method: janbu simplified

Number of Valid Surfaces: 309

Number of Invalid Surfaces: 194

Error Codes:

Error Code -107 reported for 185 surfaces

Error Code -108 reported for 1 surface

Error Code -111 reported for 8 surfaces

Method: spencer

Number of Valid Surfaces: 205

Number of Invalid Surfaces: 298

Error Codes:

Error Code -107 reported for 185 surfaces

Error Code -108 reported for 105 surfaces

Error Code -111 reported for 8 surfaces

Error Codes

The following errors were encountered during the computation:

-107 = Total driving moment or total driving force is negative. This will occur if the wrong failure direction is specified, or if high external or anchor loads are applied against the failure direction.

-108 = Total driving moment or total driving force < 0.1 . This is to limit the calculation of extremely high safety factors if the driving force is very small (0.1 is an arbitrary number).

-111 = safety factor equation did not converge

List of All Coordinates

Block Search Polyline

2985.360 5366.370

4014.932 5410.910

4072.668 5430.326

Material Boundary

2987.976 5367.347

4010.000 5411.783

4015.000 5412.000

Material Boundary

2980.000 5365.000
4010.000 5409.783

Material Boundary

3730.000 5515.000
3730.000 5518.000

Material Boundary

3730.000 5515.000
4066.502 5429.167
4069.901 5428.300
4075.000 5427.000

Material Boundary

4010.000 5409.783
4010.000 5411.783

Material Boundary

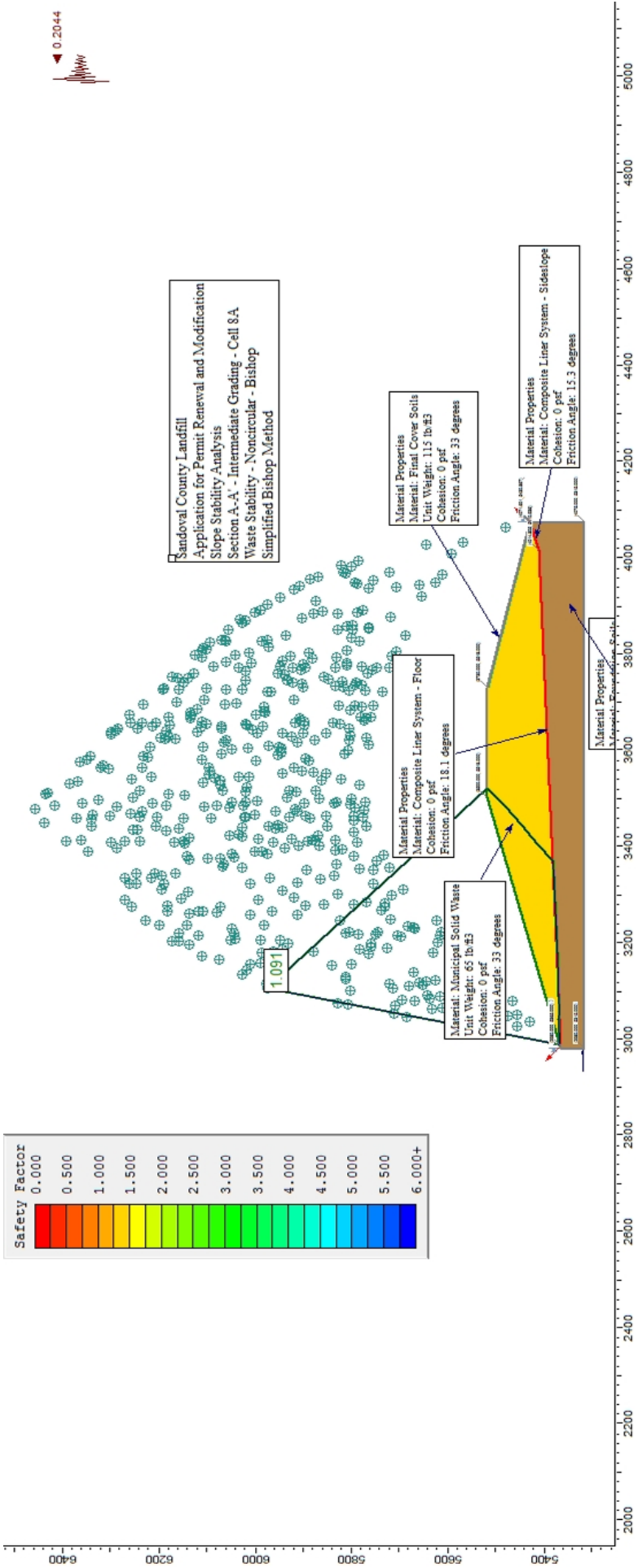
4015.000 5412.000
4056.519 5425.840
4066.480 5429.160
4066.502 5429.167
4071.601 5430.867

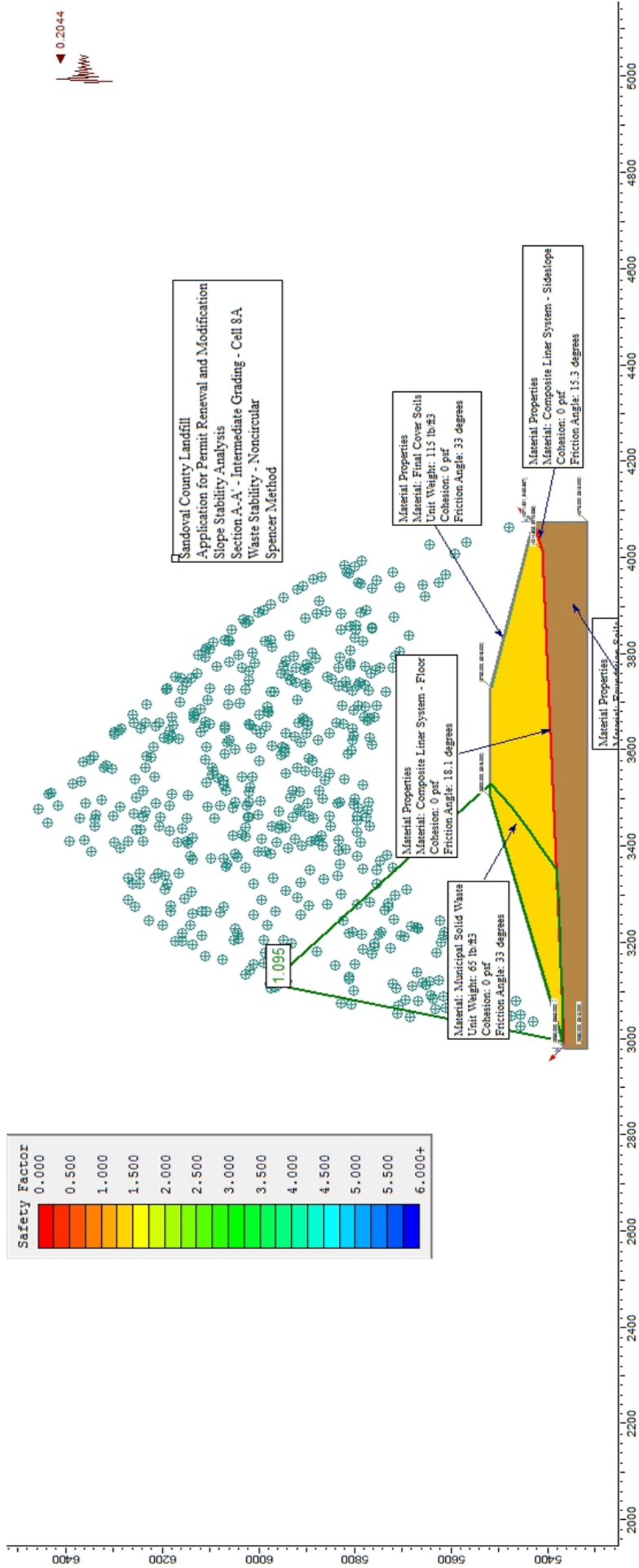
Material Boundary

4010.000 5409.783
4015.000 5410.000
4069.901 5428.300
4075.000 5430.000

External Boundary

4075.000 5315.000
4075.000 5427.000
4075.000 5430.000
4071.601 5430.867
3730.000 5518.000
3500.000 5518.000
2987.976 5367.347
2980.000 5365.000
2980.000 5315.000





Slide Analysis Information

Document Name

File Name: Section A-A' Intermediate Slope Block Seismic - Waste Stability.sli

Project Settings

Project Title: Sandoval County Landfill - Permit Renewal and Modification
Failure Direction: Right to Left
Units of Measurement: Imperial Units
Pore Fluid Unit Weight: 62.4 lb/ft³
Groundwater Method: Water Surfaces
Data Output: Standard
Calculate Excess Pore Pressure: Off
Allow Ru with Water Surfaces or Grids: Off
Random Numbers: Random Seed
Random Number Seed: 1428841297
Random Number Generation Method: Park and Miller v.3

Analysis Methods

Analysis Methods used:
Bishop simplified
Janbu simplified
Spencer

Number of slices: 25
Tolerance: 0.005
Maximum number of iterations: 50

Surface Options

Surface Type: Non-Circular Block Search
Number of Surfaces: 500
Pseudo-Random Surfaces: Enabled
Convex Surfaces Only: Disabled
Left Projection Angle (Start Angle): 135
Left Projection Angle (End Angle): 135
Right Projection Angle (Start Angle): 45
Right Projection Angle (End Angle): 45
Minimum Elevation: Not Defined
Minimum Depth: Not Defined

Loading

Seismic Load Coefficient (Horizontal): 0.2044

Back Analysis

Required Factor of Safety: 1.1
Reinforcement Load Elevation: 5318 ft

bishop simplified Active Force: 5090.21 lb
Center (3103.613, 5975.258) Radius 620.072

bishop simplified Passive Force: 5599.23 lb
Center (3103.613, 5975.258) Radius 620.072

janbu simplified Active Force: 45668.5 lb
Center (3114.005, 5961.098) Radius 607.027

janbu simplified Passive Force: 50235.4 lb
Center (3114.005, 5961.098) Radius 607.027

Material Properties

Material: Municipal Solid Waste
Strength Type: Mohr-Coulomb
Unit Weight: 65 lb/ft³
Cohesion: 0 psf
Friction Angle: 33 degrees
Water Surface: None

Material: Foundation Soils
Strength Type: Mohr-Coulomb
Unit Weight: 115 lb/ft³
Cohesion: 0 psf
Friction Angle: 33 degrees
Water Surface: None

Material: Final Cover Soils
Strength Type: Mohr-Coulomb
Unit Weight: 115 lb/ft³
Cohesion: 0 psf
Friction Angle: 33 degrees
Water Surface: None

Material: Composite Liner System - Floor
Strength Type: Mohr-Coulomb
Unit Weight: 95.5 lb/ft³
Cohesion: 279 psf
Friction Angle: 19 degrees
Water Surface: None

Material: Composite Liner System - Sideslope
Strength Type: Mohr-Coulomb
Unit Weight: 95.5 lb/ft³
Cohesion: 243 psf
Friction Angle: 19 degrees
Water Surface: None

Global Minimums

Method: bishop simplified
FS: 1.090960
Axis Location: 3103.522, 5975.076

Left Slip Surface Endpoint: 2987.974, 5367.346
Right Slip Surface Endpoint: 3520.377, 5518.000
Resisting Moment=4.92937e+008 lb-ft
Driving Moment=4.51839e+008 lb-ft

Method: janbu simplified

FS: 1.034890
Axis Location: 3103.522, 5975.076
Left Slip Surface Endpoint: 2987.974, 5367.346
Right Slip Surface Endpoint: 3520.377, 5518.000
Resisting Horizontal Force=730387 lb
Driving Horizontal Force=705760 lb

Method: spencer

FS: 1.094930
Axis Location: 3112.826, 5977.614
Left Slip Surface Endpoint: 2994.556, 5369.283
Right Slip Surface Endpoint: 3528.528, 5518.000
Resisting Moment=4.89415e+008 lb-ft
Driving Moment=4.46983e+008 lb-ft
Resisting Horizontal Force=741399 lb
Driving Horizontal Force=677121 lb

Valid / Invalid Surfaces

Method: bishop simplified

Number of Valid Surfaces: 467
Number of Invalid Surfaces: 36
Error Codes:
Error Code -107 reported for 19 surfaces
Error Code -108 reported for 17 surfaces

Method: janbu simplified

Number of Valid Surfaces: 445
Number of Invalid Surfaces: 58
Error Codes:
Error Code -107 reported for 19 surfaces
Error Code -108 reported for 20 surfaces
Error Code -111 reported for 19 surfaces

Method: spencer

Number of Valid Surfaces: 243
Number of Invalid Surfaces: 260
Error Codes:
Error Code -107 reported for 19 surfaces
Error Code -108 reported for 209 surfaces
Error Code -111 reported for 32 surfaces

Error Codes

The following errors were encountered during the computation:

-107 = Total driving moment or
total driving force is negative. This will occur
if the wrong failure direction is specified,

or if high external or anchor loads are applied against the failure direction.

-108 = Total driving moment
or total driving force < 0.1. This is to limit the calculation of extremely high safety factors if the driving force is very small (0.1 is an arbitrary number).

-111 = safety factor equation did not converge

List of All Coordinates

Block Search Polyline

2985.387 5366.508
4014.805 5410.936
4072.815 5430.376

Material Boundary

2987.976 5367.347
4010.000 5411.783
4015.000 5412.000

Material Boundary

2980.000 5365.000
4010.000 5409.783

Material Boundary

3730.000 5515.000
3730.000 5518.000

Material Boundary

3730.000 5515.000
4066.502 5429.167
4069.901 5428.300
4075.000 5427.000

Material Boundary

4010.000 5409.783
4010.000 5411.783

Material Boundary

4015.000 5412.000
4056.519 5425.840
4066.480 5429.160
4066.502 5429.167
4071.601 5430.867

Material Boundary

4010.000 5409.783
4015.000 5410.000
4069.901 5428.300
4075.000 5430.000

External Boundary

4075.000	5315.000
4075.000	5427.000
4075.000	5430.000
4071.601	5430.867
3730.000	5518.000
3500.000	5518.000
2987.976	5367.347
2980.000	5365.000
2980.000	5315.000

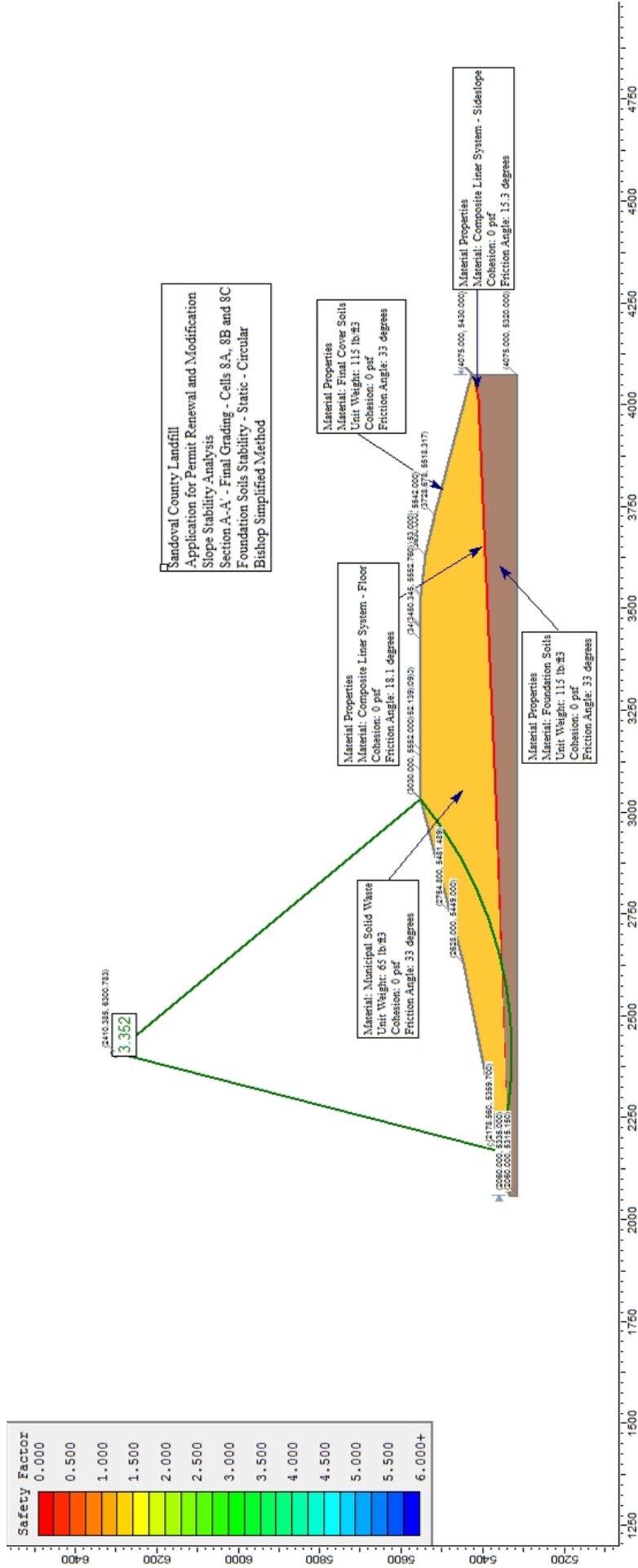
**APPLICATION FOR PERMIT RENEWAL AND MODIFICATION
SANDOVAL COUNTY LANDFILL**

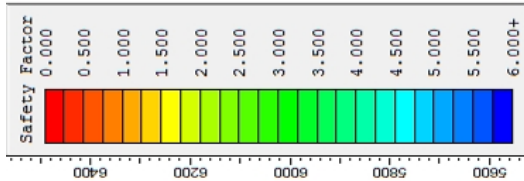
**VOLUME III: LANDFILL ENGINEERING CALCULATIONS
SECTION 3: SLOPE STABILITY ANALYSIS**

ATTACHMENT III.3.E-4

SCENARIO 7: SECTION A-A', CIRCULAR, STATIC

SCENARIO 8: SECTION A-A', CIRCULAR, SEISMIC





(2410.388, 8000.783)

3.352

Sandoval County Landfill
Application for Permit Renewal and Modification
Slope Stability Analysis
Section A-A' - Final Grading - Cells 8A, 8B and 8C
Foundation Soils Stability - Static - Circular
Spencer Method

Material Properties
Material: Final Cover Soils
Unit Weight: 115 lb/ft³
Cohesion: 0 psf
Friction Angle: 33 degrees

Material Properties
Material: Composite Linear System - Floor
Cohesion: 0 psf
Friction Angle: 18.1 degrees

Material: Municipal Solid Waste
Unit Weight: 65 lb/ft³
Cohesion: 0 psf
Friction Angle: 33 degrees

Material Properties
Material: Composite Linear System - Sideslope
Cohesion: 0 psf
Friction Angle: 15.3 degrees

Material Properties
Material: Foundation Soils
Unit Weight: 115 lb/ft³
Cohesion: 0 psf
Friction Angle: 33 degrees

(4075.000, 5430.000)

(4075.000, 5320.000)

(3403.000, 5810.317)

(3403.000, 5810.317)

(3403.000, 5810.317)

(3403.000, 5810.317)

(3403.000, 5810.317)

(3403.000, 5810.317)

(3403.000, 5810.317)

(3403.000, 5810.317)

(3403.000, 5810.317)

(3403.000, 5810.317)

(3403.000, 5810.317)

(3403.000, 5810.317)

(3403.000, 5810.317)

(3403.000, 5810.317)

(3403.000, 5810.317)

(3403.000, 5810.317)

(3403.000, 5810.317)

(3403.000, 5810.317)

(3403.000, 5810.317)

(3403.000, 5810.317)

(3403.000, 5810.317)

(3403.000, 5810.317)

(3403.000, 5810.317)

(3403.000, 5810.317)

(3403.000, 5810.317)

(3403.000, 5810.317)

(3403.000, 5810.317)

(3403.000, 5810.317)

(3403.000, 5810.317)

(3403.000, 5810.317)

(3403.000, 5810.317)

(3403.000, 5810.317)

(3403.000, 5810.317)

(3403.000, 5810.317)

(3403.000, 5810.317)

(3403.000, 5810.317)

(3403.000, 5810.317)

(3403.000, 5810.317)

(3403.000, 5810.317)

(3403.000, 5810.317)

(3403.000, 5810.317)

(3403.000, 5810.317)

(3403.000, 5810.317)

(3403.000, 5810.317)

(3403.000, 5810.317)

(3403.000, 5810.317)

(3403.000, 5810.317)

(3403.000, 5810.317)

(3403.000, 5810.317)

(3403.000, 5810.317)

(3403.000, 5810.317)

(3403.000, 5810.317)

(3403.000, 5810.317)

(3403.000, 5810.317)

(3403.000, 5810.317)

(3403.000, 5810.317)

(3403.000, 5810.317)

Slide Analysis Information

Document Name

File Name: Section A-A' Final Grading Static Block.sli

Project Settings

Project Title: SLIDE - An Interactive Slope Stability Program

Failure Direction: Right to Left

Units of Measurement: Imperial Units

Pore Fluid Unit Weight: 62.4 lb/ft³

Groundwater Method: Water Surfaces

Data Output: Standard

Calculate Excess Pore Pressure: Off

Allow Ru with Water Surfaces or Grids: Off

Random Numbers: Pseudo-random Seed

Random Number Seed: 10116

Random Number Generation Method: Park and Miller v.3

Analysis Methods

Analysis Methods used:

Bishop simplified

Janbu simplified

Spencer

Number of slices: 25

Tolerance: 0.005

Maximum number of iterations: 50

Surface Options

Surface Type: Non-Circular Block Search

Number of Surfaces: 500

Pseudo-Random Surfaces: Enabled

Convex Surfaces Only: Disabled

Left Projection Angle (Start Angle): 135

Left Projection Angle (End Angle): 135

Right Projection Angle (Start Angle): 45

Right Projection Angle (End Angle): 45

Minimum Elevation: Not Defined

Minimum Depth: Not Defined

Material Properties

Material: Final Cover Soils

Strength Type: Mohr-Coulomb

Unit Weight: 115 lb/ft³

Cohesion: 0 psf

Friction Angle: 33 degrees

Water Surface: None

Material: Composite Liner System, Floor

Strength Type: Mohr-Coulomb

Unit Weight: 95.5 lb/ft³

Cohesion: 0 psf

Friction Angle: 19 degrees

Water Surface: None

Material: Structural Fill Berm

Strength Type: Mohr-Coulomb

Unit Weight: 115 lb/ft³

Cohesion: 0 psf

Friction Angle: 33 degrees

Water Surface: None

Material: Municipal Solid Waste

Strength Type: Mohr-Coulomb

Unit Weight: 65 lb/ft³

Cohesion: 0 psf

Friction Angle: 33 degrees

Water Surface: None

Material: Foundation Soils

Strength Type: Mohr-Coulomb

Unit Weight: 115 lb/ft³

Cohesion: 0 psf

Friction Angle: 33 degrees

Water Surface: None

List of All Coordinates

Material Boundary

2060.0	5335.0
2249.7	5340.0
2249.7	5340.0
2249.8	5340.0
2249.8	5340.0
2249.8	5340.0
2250.0	5340.0
2250.2	5340.0
2250.2	5340.0

Material Boundary

2754.8	5481.5
2774.3	5486.4
3030.2	5551.5

Material Boundary

2181.8	5360.4
2181.8	5360.4
2181.8	5360.4
2187.3	5358.8

Material Boundary

2178.6	5359.7
2178.6	5359.7
2180.0	5359.3

2184.8	5358.0
2216.9	5349.1
2225.9	5346.6
2249.0	5340.2

Material Boundary

2187.3	5358.8
2188.1	5358.6
2215.7	5351.2
2218.8	5350.4
2250.0	5342.0

Material Boundary

2187.2	5358.9
2187.3	5358.8

Material Boundary

2181.9	5360.4
2188.3	5358.6
2215.7	5351.2
2217.3	5350.7
2218.8	5350.4
2250.0	5342.0
2980.3	5368.6
4015.3	5413.6
4075.0	5426.6

Material Boundary

2181.9	5360.4
2180.0	5360.0
2178.6	5359.7
2178.6	5359.7
2180.0	5359.3
2184.8	5358.0
2249.0	5340.2
2249.0	5340.2
2250.0	5340.0
2250.0	5340.0
2980.0	5365.0
4015.0	5410.0
4075.0	5423.0

Material Boundary

2628.0	5449.0
2774.3	5486.4
3030.4	5552.0
3130.0	5552.0
3134.7	5552.2

Material Boundary

3458.6	5552.9
3452.2	5552.8

Material Boundary

2180.0	5360.0
2180.0	5360.0

2180.0	5359.3
2180.0	5359.3
2180.0	5357.0
2184.8	5358.0
2184.8	5358.0
2188.1	5358.6
2188.3	5358.6
2628.0	5446.0
3030.2	5549.0
3130.0	5549.0
3189.1	5549.7
3458.8	5552.8

Material Boundary

3533.0	5549.0
3533.0	5549.0
3533.0	5549.0
3533.0	5549.0
3533.0	5549.0
3627.7	5539.3
3629.9	5539.0
3630.0	5539.0
3724.1	5516.2
3727.2	5515.5
3729.3	5515.0
4001.2	5445.8
4075.0	5427.1

Material Boundary

3450.3	5552.8
3189.1	5549.7
3129.6	5549.0
3530.2	5549.0
3533.0	5549.0
3533.0	5549.0
3533.0	5549.0
3533.0	5549.0
3533.0	5549.0
3533.0	5549.0
3530.0	5553.0
3627.7	5539.3
3630.0	5539.0
3630.0	5539.0
3727.0	5515.7
3730.0	5515.0
4001.2	5445.8
4075.0	5427.0

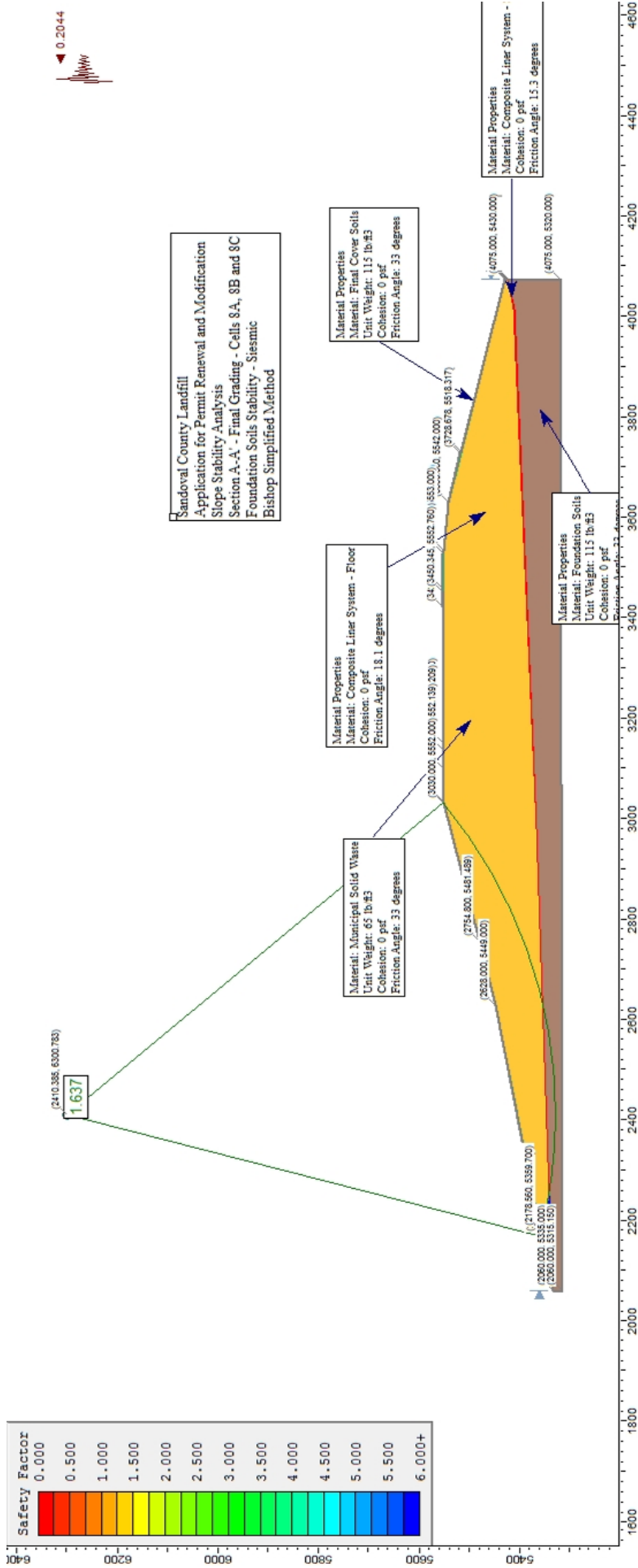
External Boundary

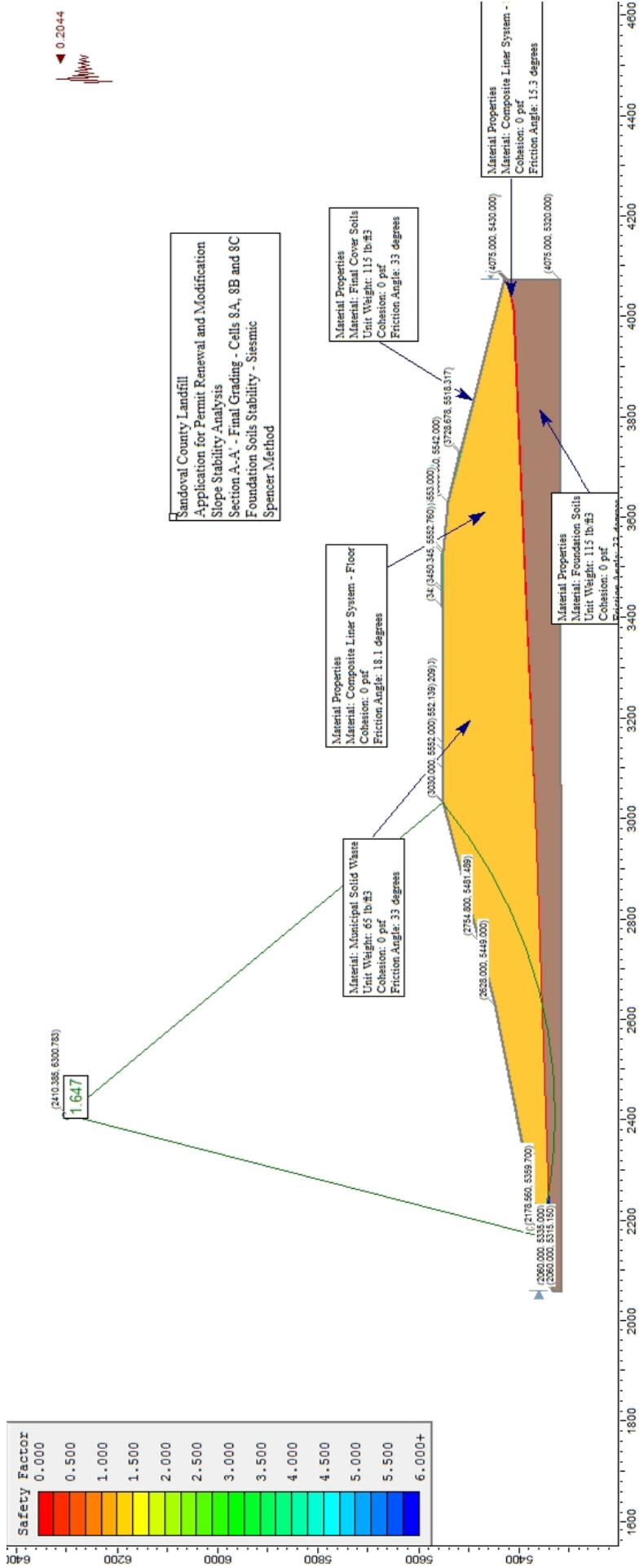
4075.0	5320.0
4075.0	5423.0
4075.0	5425.0
4075.0	5426.6
4075.0	5427.0
4075.0	5430.0
3730.0	5518.0
3728.7	5518.3

3630.0	5542.0
3534.9	5552.5
3530.0	5553.0
3458.6	5552.9
3420.7	5552.8
3452.2	5552.8
3458.8	5552.8
3450.3	5552.8
3150.0	5552.0
3134.7	5552.2
3099.6	5552.1
3030.0	5552.0
2754.8	5481.5
2628.0	5449.0
2181.9	5360.4
2181.8	5360.4
2181.8	5360.4
2180.0	5360.0
2178.6	5359.7
2060.0	5335.0
2060.0	5315.1

Block Search Polyline

2180.9	5360.0
2249.9	5340.9
4014.9	5411.8
4074.8	5424.7





Slide Analysis Information

Document Name

File Name: Section A-A' Final Grading Seismic Circular - Foundation.sli

Project Settings

Project Title: SLIDE - An Interactive Slope Stability Program

Failure Direction: Right to Left

Units of Measurement: Imperial Units

Pore Fluid Unit Weight: 62.4 lb/ft³

Groundwater Method: Water Surfaces

Data Output: Standard

Calculate Excess Pore Pressure: Off

Allow Ru with Water Surfaces or Grids: Off

Random Numbers: Pseudo-random Seed

Random Number Seed: 10116

Random Number Generation Method: Park and Miller v.3

Analysis Methods

Analysis Methods used:

Bishop simplified

Janbu simplified

Spencer

Number of slices: 25

Tolerance: 0.005

Maximum number of iterations: 50

Surface Options

Surface Type: Circular

Search Method: Grid Search

Radius increment: 10

Composite Surfaces: Disabled

Reverse Curvature: Create Tension Crack

Minimum Elevation: Not Defined

Minimum Depth: Not Defined

Loading

Seismic Load Coefficient (Horizontal): 0.2044

Material Properties

Material: Final Cover Soils

Strength Type: Mohr-Coulomb

Unit Weight: 115 lb/ft³

Cohesion: 0 psf

Friction Angle: 33 degrees

Water Surface: None

Material: Composite Liner System, Floor

Strength Type: Mohr-Coulomb

Unit Weight: 95.5 lb/ft³

Cohesion: 0 psf

Friction Angle: 19 degrees

Water Surface: None

Material: Structural Fill Berm

Strength Type: Mohr-Coulomb

Unit Weight: 115 lb/ft³

Cohesion: 0 psf

Friction Angle: 33 degrees

Water Surface: None

Material: Municipal Solid Waste

Strength Type: Mohr-Coulomb

Unit Weight: 65 lb/ft³

Cohesion: 0 psf

Friction Angle: 33 degrees

Water Surface: None

Material: Foundation Soils

Strength Type: Mohr-Coulomb

Unit Weight: 115 lb/ft³

Cohesion: 0 psf

Friction Angle: 33 degrees

Water Surface: None

List of All Coordinates

Material Boundary

2060.0	5335.0
2249.7	5340.0
2249.7	5340.0
2249.8	5340.0
2249.8	5340.0
2249.8	5340.0
2250.0	5340.0
2250.2	5340.0
2250.2	5340.0

Material Boundary

2754.8	5481.5
2774.3	5486.4
3030.2	5551.5

Material Boundary

2181.8	5360.4
2181.8	5360.4
2181.8	5360.4
2187.3	5358.8

Material Boundary

2178.6	5359.7
2178.6	5359.7

2180.0	5359.3
2184.8	5358.0
2216.9	5349.1
2225.9	5346.6
2249.0	5340.2

Material Boundary

2187.3	5358.8
2188.1	5358.6
2215.7	5351.2
2218.8	5350.4
2250.0	5342.0

Material Boundary

2187.2	5358.9
2187.3	5358.8

Material Boundary

2181.9	5360.4
2188.3	5358.6
2215.7	5351.2
2217.3	5350.7
2218.8	5350.4
2250.0	5342.0
2980.3	5368.6
4015.3	5413.6
4075.0	5426.6

Material Boundary

2181.9	5360.4
2180.0	5360.0
2178.6	5359.7
2178.6	5359.7
2180.0	5359.3
2184.8	5358.0
2249.0	5340.2
2249.0	5340.2
2250.0	5340.0
2250.0	5340.0
2980.0	5365.0
4015.0	5410.0
4075.0	5423.0

Material Boundary

2628.0	5449.0
2774.3	5486.4
3030.4	5552.0
3130.0	5552.0
3134.7	5552.2

Material Boundary

3452.2	5552.8
3458.6	5552.9

Material Boundary

2180.0	5360.0
--------	--------

2180.0	5360.0
2180.0	5359.3
2180.0	5359.3
2180.0	5357.0
2184.8	5358.0
2184.8	5358.0
2188.1	5358.6
2188.3	5358.6
2628.0	5446.0
3030.2	5549.0
3130.0	5549.0
3189.1	5549.7
3458.8	5552.8

Material Boundary

3533.0	5549.0
3533.0	5549.0
3533.0	5549.0
3533.0	5549.0
3533.0	5549.0
3627.7	5539.3
3629.9	5539.0
3630.0	5539.0
3724.1	5516.2
3727.2	5515.5
3729.3	5515.0
4001.2	5445.8
4075.0	5427.1

Material Boundary

3450.3	5552.8
3189.1	5549.7
3129.6	5549.0
3530.2	5549.0
3533.0	5549.0
3533.0	5549.0
3533.0	5549.0
3533.0	5549.0
3533.0	5549.0
3530.0	5553.0
3627.7	5539.3
3630.0	5539.0
3630.0	5539.0
3727.0	5515.7
3730.0	5515.0
4001.2	5445.8
4075.0	5427.0

External Boundary

4075.0	5320.0
4075.0	5423.0
4075.0	5425.0
4075.0	5426.6
4075.0	5427.0
4075.0	5430.0
3730.0	5518.0

3728.7	5518.3
3630.0	5542.0
3534.9	5552.5
3530.0	5553.0
3458.6	5552.9
3420.7	5552.8
3452.2	5552.8
3458.8	5552.8
3450.3	5552.8
3150.0	5552.0
3134.7	5552.2
3099.6	5552.1
3030.0	5552.0
2754.8	5481.5
2628.0	5449.0
2181.9	5360.4
2181.8	5360.4
2181.8	5360.4
2180.0	5360.0
2178.6	5359.7
2060.0	5335.0
2060.0	5315.1

Circular Failure Surface

2410.4	6300.8
2167.6	5357.4
3033.4	5552.0

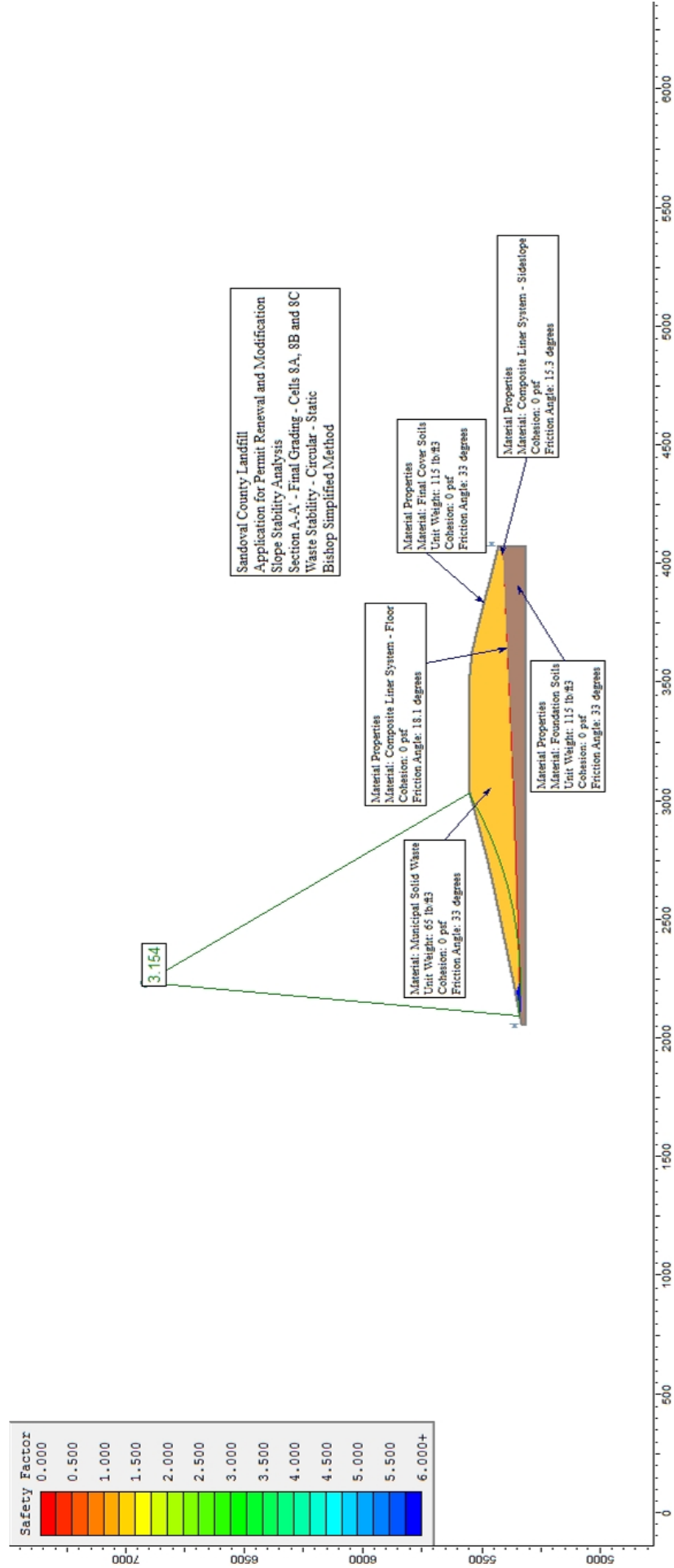
**APPLICATION FOR PERMIT RENEWAL AND MODIFICATION
SANDOVAL COUNTY LANDFILL**

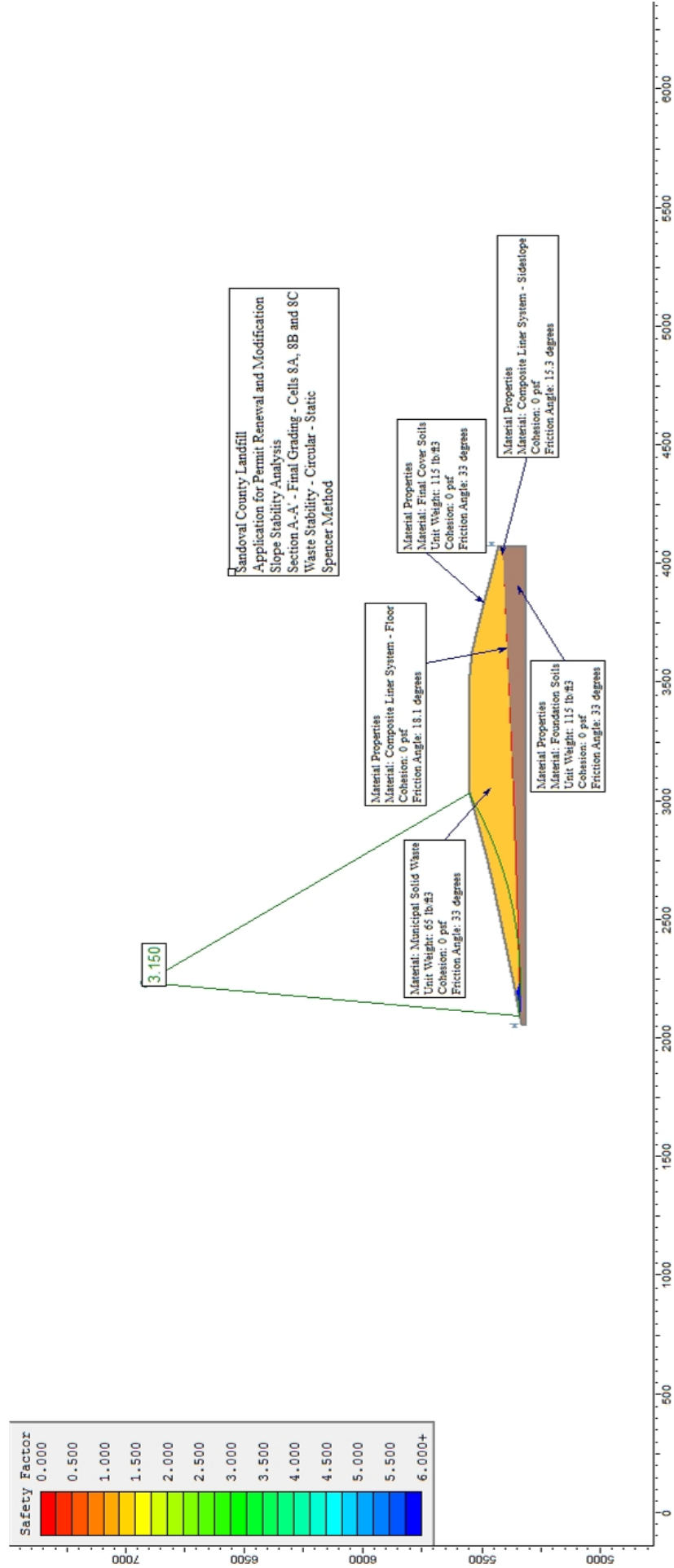
**VOLUME III: LANDFILL ENGINEERING CALCULATIONS
SECTION 3: SLOPE STABILITY ANALYSIS**

ATTACHMENT III.3.E-5

SCENARIO 9: SECTION A-A'; CIRCULAR, STATIC

SCENARIO 10: SECTION A-A', CIRCULAR, SEISMIC





Slide Analysis Information

Document Name

File Name: Section A-A' Intermediate Slope Circular Static - Waste Stability

Project Settings

Project Title: Sandoval County Landfill - Permit Renewal and Modification

Failure Direction: Right to Left

Units of Measurement: Imperial Units

Pore Fluid Unit Weight: 62.4 lb/ft³

Groundwater Method: Water Surfaces

Data Output: Standard

Calculate Excess Pore Pressure: Off

Allow Ru with Water Surfaces or Grids: Off

Random Numbers: Pseudo-random Seed

Random Number Seed: 10116

Random Number Generation Method: Park and Miller v.3

Analysis Methods

Analysis Methods used:

Bishop simplified

Janbu simplified

Spencer

Number of slices: 25

Tolerance: 0.005

Maximum number of iterations: 50

Surface Options

Surface Type: Circular

Search Method: Grid Search

Radius increment: 10

Composite Surfaces: Enabled

Reverse Curvature: Create Tension Crack

Minimum Elevation: Not Defined

Minimum Depth: Not Defined

Material Properties

Material: Municipal Solid Waste

Strength Type: Mohr-Coulomb

Unit Weight: 65 lb/ft³

Cohesion: 0 psf

Friction Angle: 33 degrees

Water Surface: None

Material: Foundation Soils

Strength Type: Mohr-Coulomb

Unit Weight: 115 lb/ft³

Cohesion: 0 psf
Friction Angle: 33 degrees
Water Surface: None

Material: Final Cover Soils
Strength Type: Mohr-Coulomb
Unit Weight: 115 lb/ft³
Cohesion: 0 psf
Friction Angle: 33 degrees
Water Surface: None

Material: Composite Liner System - Floor
Strength Type: Mohr-Coulomb
Unit Weight: 115 lb/ft³
Cohesion: 0 psf
Friction Angle: 18.1 degrees
Water Surface: None

Material: Composite Liner System - Sideslope
Strength Type: Mohr-Coulomb
Unit Weight: 115 lb/ft³
Cohesion: 0 psf
Friction Angle: 15.3 degrees
Water Surface: None

Global Minimums

Method: bishop simplified
FS: 2.397000
Center: 3226.872, 5713.011
Radius: 336.625
Left Slip Surface Endpoint: 3101.290, 5400.687
Right Slip Surface Endpoint: 3501.258, 5518.000
Resisting Moment=2.65633e+008 lb-ft
Driving Moment=1.10819e+008 lb-ft

Method: janbu simplified
FS: 2.194160
Center: 3226.872, 5713.011
Radius: 336.625
Left Slip Surface Endpoint: 3101.290, 5400.687
Right Slip Surface Endpoint: 3501.258, 5518.000
Resisting Horizontal Force=718911 lb
Driving Horizontal Force=327647 lb

Method: spencer
FS: 2.394610
Center: 3226.872, 5713.011
Radius: 336.625
Left Slip Surface Endpoint: 3101.290, 5400.687
Right Slip Surface Endpoint: 3501.258, 5518.000
Resisting Moment=2.65369e+008 lb-ft
Driving Moment=1.10819e+008 lb-ft
Resisting Horizontal Force=726023 lb
Driving Horizontal Force=303190 lb

Valid / Invalid Surfaces

Method: bishop simplified

Number of Valid Surfaces: 1

Number of Invalid Surfaces: 0

Method: janbu simplified

Number of Valid Surfaces: 1

Number of Invalid Surfaces: 0

Method: spencer

Number of Valid Surfaces: 1

Number of Invalid Surfaces: 0

List of All Coordinates

Circular Failure Surface

3226.872 5713.011

3101.302 5400.691

3501.257 5518.000

Material Boundary

2987.976 5367.347

4010.000 5411.783

4015.000 5412.000

Material Boundary

2980.000 5365.000

4010.000 5409.783

Material Boundary

3730.000 5515.000

3730.000 5518.000

Material Boundary

3730.000 5515.000

4066.502 5429.167

4069.901 5428.300

4075.000 5427.000

Material Boundary

4010.000 5409.783

4010.000 5411.783

Material Boundary

4015.000 5412.000

4056.519 5425.840

4066.480 5429.160

4066.502 5429.167

4071.601 5430.867

Material Boundary

4010.000 5409.783

4015.000 5410.000

4069.901 5428.300

4075.000 5430.000

External Boundary

4075.000 5315.000

4075.000 5427.000

4075.000 5430.000

4071.601 5430.867

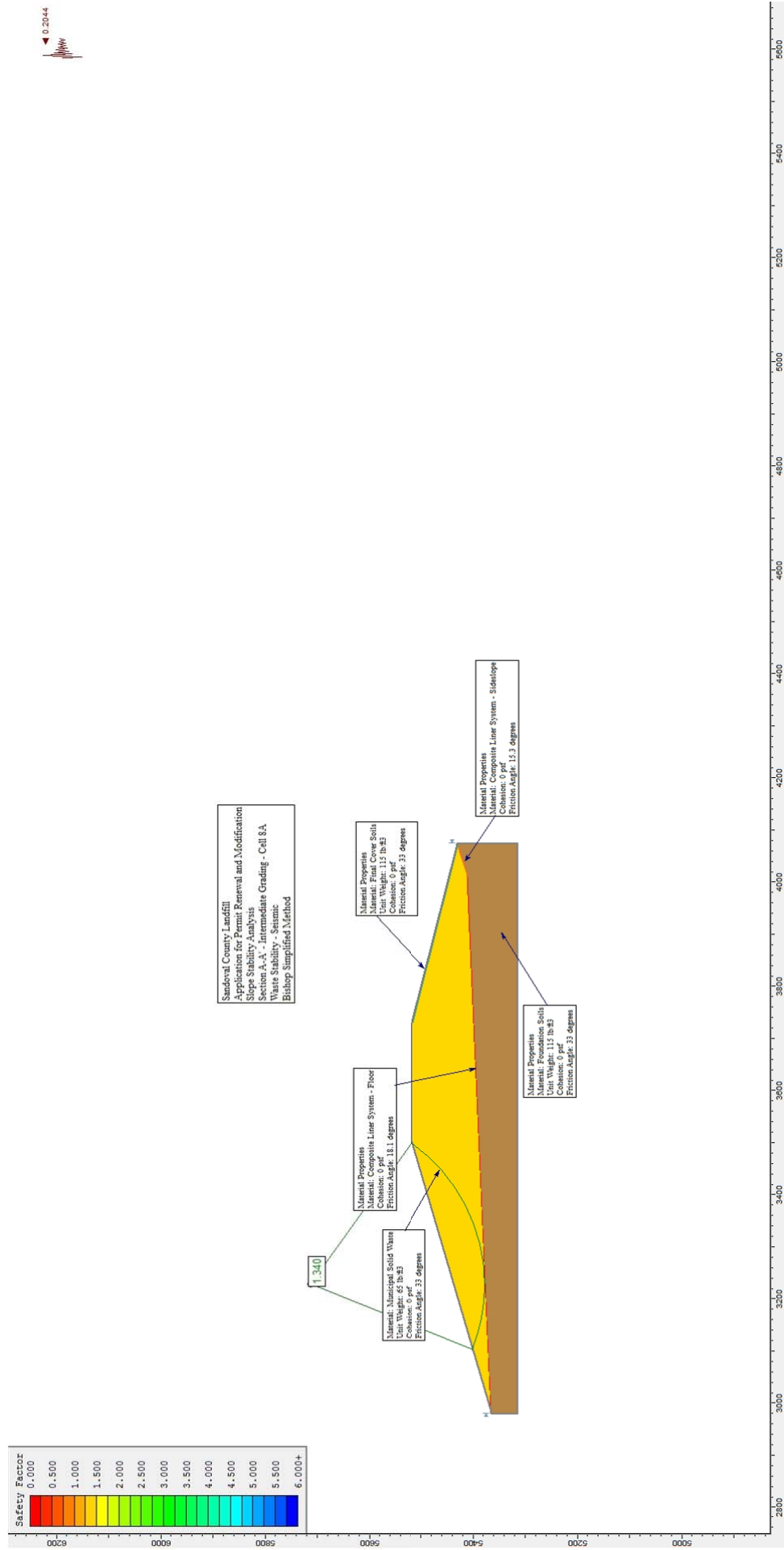
3730.000 5518.000

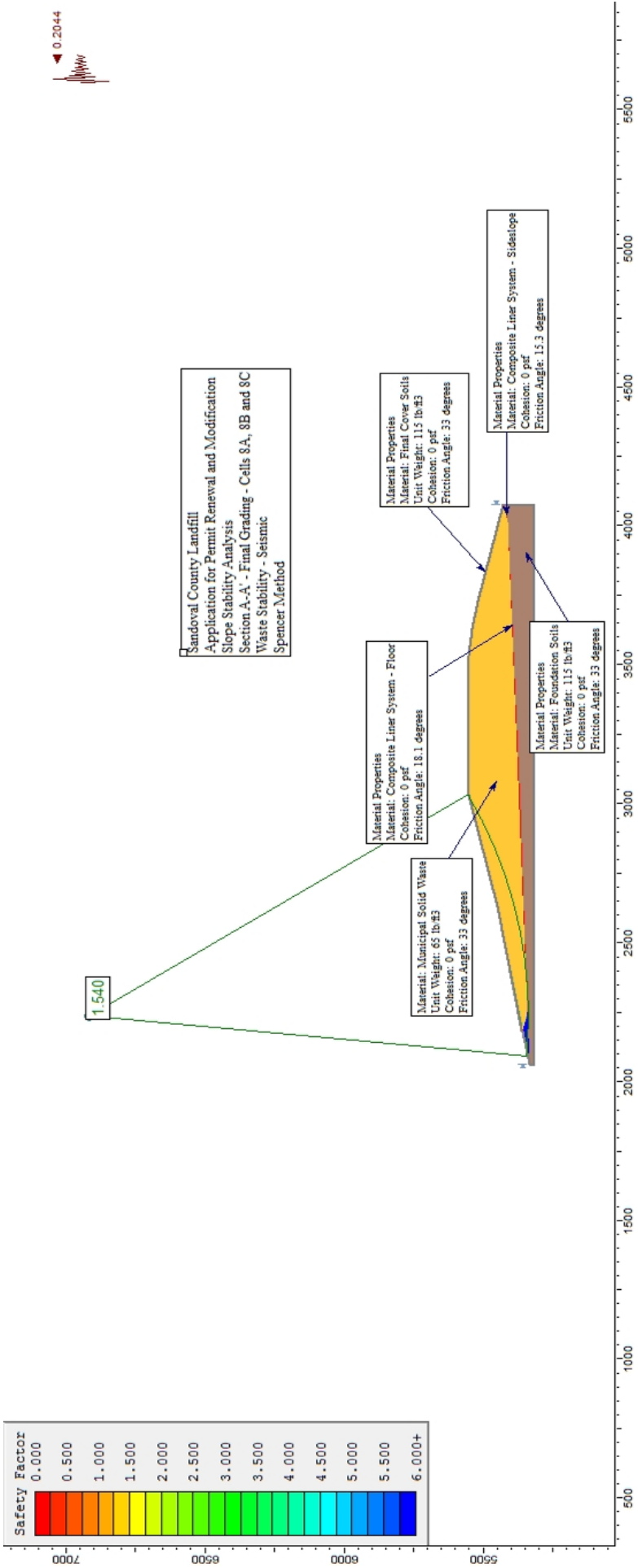
3500.000 5518.000

2987.976 5367.347

2980.000 5365.000

2980.000 5315.000





Slide Analysis Information

Document Name

File Name: Section A-A' Intermediate Slope Circular Seismic - Waste Stability

Project Settings

Project Title: Sandoval County Landfill - Permit Renewal and Modification

Failure Direction: Right to Left

Units of Measurement: Imperial Units

Pore Fluid Unit Weight: 62.4 lb/ft³

Groundwater Method: Water Surfaces

Data Output: Standard

Calculate Excess Pore Pressure: Off

Allow Ru with Water Surfaces or Grids: Off

Random Numbers: Pseudo-random Seed

Random Number Seed: 10116

Random Number Generation Method: Park and Miller v.3

Analysis Methods

Analysis Methods used:

Bishop simplified

Janbu simplified

Spencer

Number of slices: 25

Tolerance: 0.005

Maximum number of iterations: 50

Surface Options

Surface Type: Circular

Search Method: Grid Search

Radius increment: 10

Composite Surfaces: Enabled

Reverse Curvature: Create Tension Crack

Minimum Elevation: Not Defined

Minimum Depth: Not Defined

Loading

Seismic Load Coefficient (Horizontal): 0.2044

Material Properties

Material: Municipal Solid Waste

Strength Type: Mohr-Coulomb

Unit Weight: 65 lb/ft³

Cohesion: 0 psf

Friction Angle: 33 degrees

Water Surface: None

Material: Foundation Soils

Strength Type: Mohr-Coulomb

Unit Weight: 115 lb/ft³

Cohesion: 0 psf

Friction Angle: 33 degrees

Water Surface: None

Material: Final Cover Soils

Strength Type: Mohr-Coulomb

Unit Weight: 115 lb/ft³

Cohesion: 0 psf

Friction Angle: 33 degrees

Water Surface: None

Material: Composite Liner System - Floor

Strength Type: Mohr-Coulomb

Unit Weight: 115 lb/ft³

Cohesion: 0 psf

Friction Angle: 18.1 degrees

Water Surface: None

Material: Composite Liner System - Sideslope

Strength Type: Mohr-Coulomb

Unit Weight: 115 lb/ft³

Cohesion: 0 psf

Friction Angle: 15.3 degrees

Water Surface: None

List of All Coordinates

Material Boundary

2987.98 5367.35

4010.00 5411.78

4015.00 5412.00

Material Boundary

2980.00 5365.00

4010.00 5409.78

Material Boundary

3730.00 5515.00

3730.00 5518.00

Material Boundary

3730.00 5515.00

4066.50 5429.17

4069.90 5428.30

4075.00 5427.00

Material Boundary

4010.00 5409.78

4010.00 5411.78

Material Boundary

4015.00 5412.00

4056.52	5425.84
4066.48	5429.16
4066.50	5429.17
4071.60	5430.87

Material Boundary

4010.00	5409.78
4015.00	5410.00
4069.90	5428.30
4075.00	5430.00

External Boundary

4075.00	5315.00
4075.00	5427.00
4075.00	5430.00
4071.60	5430.87
3730.00	5518.00
3500.00	5518.00
2987.98	5367.35
2980.00	5365.00
2980.00	5315.00

Circular Failure Surface

3226.87	5713.01
3101.30	5400.69
3501.26	5518.00

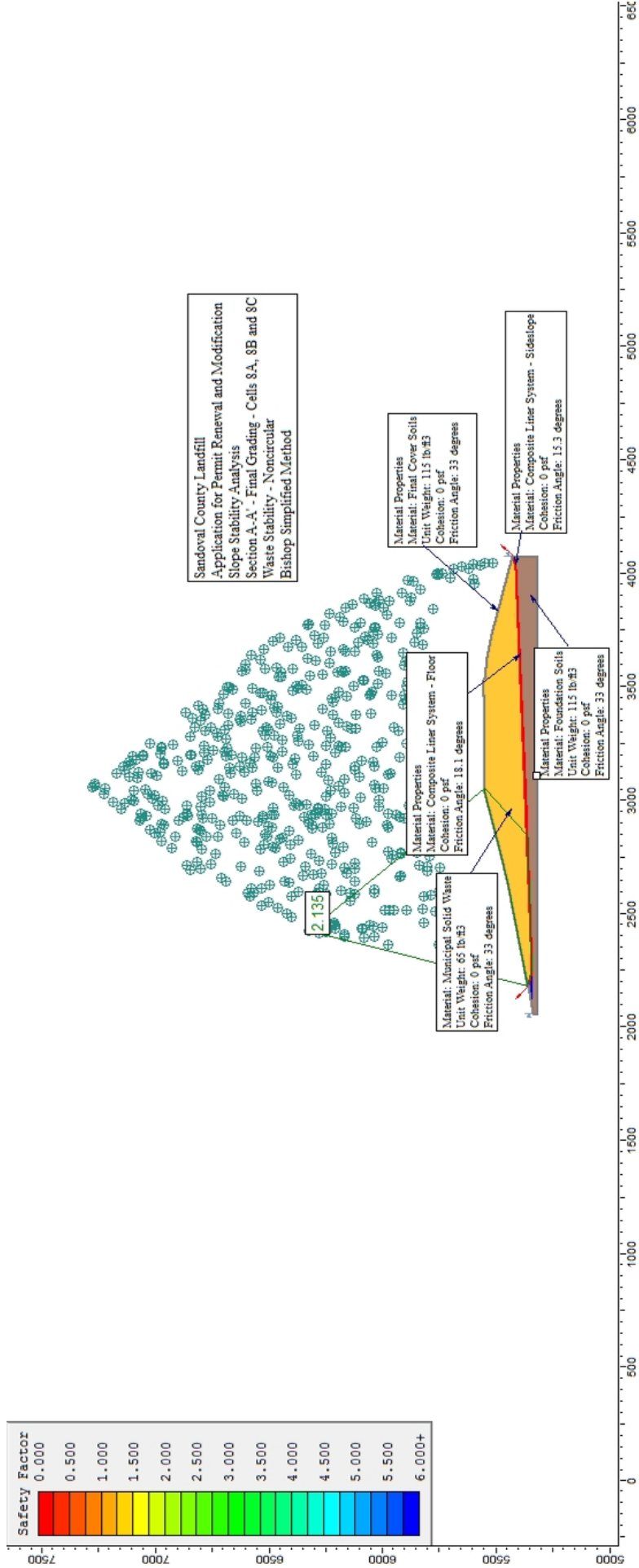
**APPLICATION FOR PERMIT RENEWAL AND MODIFICATION
SANDOVAL COUNTY LANDFILL**

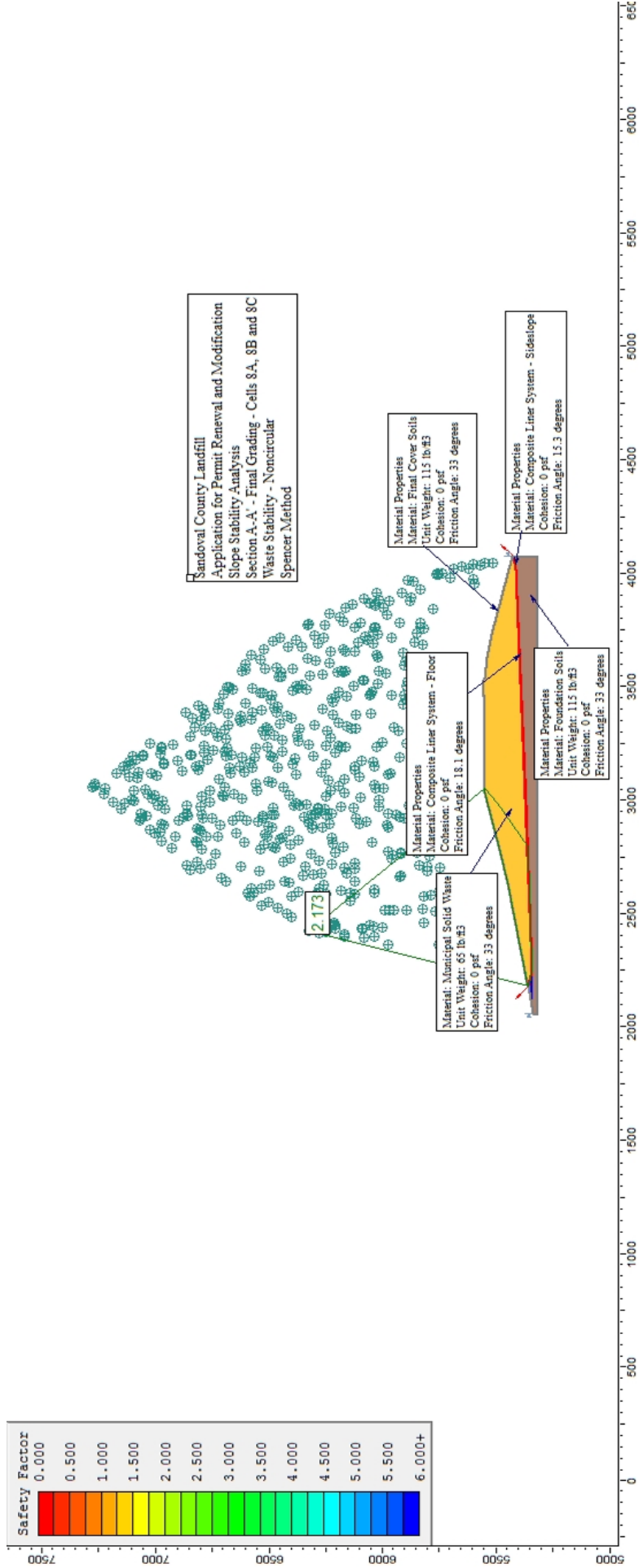
**VOLUME III: LANDFILL ENGINEERING CALCULATIONS
SECTION 3: SLOPE STABILITY ANALYSIS**

ATTACHMENT III.3.E-6

SCENARIO 11: SECTION A-A'; BLOCK, STATIC

SCENARIO 12: SECTION A-A', BLOCK, SEISMIC





Slide Analysis Information

Document Name

File Name: Section A-A' Final Grading Waste Fills Static Block.sli

Project Settings

Project Title: SLIDE - An Interactive Slope Stability Program

Failure Direction: Right to Left

Units of Measurement: Imperial Units

Pore Fluid Unit Weight: 62.4 lb/ft³

Groundwater Method: Water Surfaces

Data Output: Standard

Calculate Excess Pore Pressure: Off

Allow Ru with Water Surfaces or Grids: Off

Random Numbers: Pseudo-random Seed

Random Number Seed: 10116

Random Number Generation Method: Park and Miller v.3

Analysis Methods

Analysis Methods used:

Bishop simplified

Janbu simplified

Spencer

Number of slices: 25

Tolerance: 0.005

Maximum number of iterations: 50

Surface Options

Surface Type: Circular

Search Method: Grid Search

Radius increment: 10

Composite Surfaces: Disabled

Reverse Curvature: Create Tension Crack

Minimum Elevation: Not Defined

Minimum Depth: Not Defined

Material Properties

Material: Final Cover Soils

Strength Type: Mohr-Coulomb

Unit Weight: 115 lb/ft³

Cohesion: 0 psf

Friction Angle: 33 degrees

Water Surface: None

Material: Composite Liner System, Floor

Strength Type: Mohr-Coulomb

Unit Weight: 95.5 lb/ft³

Cohesion: 0 psf
Friction Angle: 19 degrees
Water Surface: None

Material: Structural Fill Berm
Strength Type: Mohr-Coulomb
Unit Weight: 115 lb/ft³
Cohesion: 0 psf
Friction Angle: 33 degrees
Water Surface: None

Material: Municipal Solid Waste
Strength Type: Mohr-Coulomb
Unit Weight: 65 lb/ft³
Cohesion: 0 psf
Friction Angle: 33 degrees
Water Surface: None

Material: Foundation Soils
Strength Type: Mohr-Coulomb
Unit Weight: 115 lb/ft³
Cohesion: 0 psf
Friction Angle: 33 degrees
Water Surface: None

List of All Coordinates

Material Boundary

2060.0	5335.0
2249.7	5340.0
2249.7	5340.0
2249.8	5340.0
2249.8	5340.0
2249.8	5340.0
2250.0	5340.0
2250.2	5340.0
2250.2	5340.0

Material Boundary

2754.8	5481.5
2774.3	5486.4
3030.2	5551.5

Material Boundary

2181.8	5360.4
2181.8	5360.4
2181.8	5360.4
2187.3	5358.8

Material Boundary

2178.6	5359.7
2178.6	5359.7
2180.0	5359.3
2184.8	5358.0
2216.9	5349.1
2225.9	5346.6

2249.0 5340.2

Material Boundary

2187.3 5358.8
2188.1 5358.6
2215.7 5351.2
2218.8 5350.4
2250.0 5342.0

Material Boundary

2187.2 5358.9
2187.3 5358.8

Material Boundary

2181.9 5360.4
2188.3 5358.6
2215.7 5351.2
2217.3 5350.7
2218.8 5350.4
2250.0 5342.0
2980.3 5368.6
4015.3 5413.6
4075.0 5426.6

Material Boundary

2181.9 5360.4
2180.0 5360.0
2178.6 5359.7
2178.6 5359.7
2180.0 5359.3
2184.8 5358.0
2249.0 5340.2
2249.0 5340.2
2250.0 5340.0
2250.0 5340.0
2980.0 5365.0
4015.0 5410.0
4075.0 5423.0

Material Boundary

2628.0 5449.0
2774.3 5486.4
3030.4 5552.0
3130.0 5552.0
3134.7 5552.2

Material Boundary

3452.2 5552.8
3458.6 5552.9

Material Boundary

2180.0 5360.0
2180.0 5360.0
2180.0 5359.3
2180.0 5359.3
2180.0 5357.0

2184.8	5358.0
2184.8	5358.0
2188.1	5358.6
2188.3	5358.6
2628.0	5446.0
3030.2	5549.0
3130.0	5549.0
3189.1	5549.7
3458.8	5552.8

Material Boundary

3533.0	5549.0
3533.0	5549.0
3533.0	5549.0
3533.0	5549.0
3533.0	5549.0
3627.7	5539.3
3629.9	5539.0
3630.0	5539.0
3724.1	5516.2
3727.2	5515.5
3729.3	5515.0
4001.2	5445.8
4075.0	5427.1

Material Boundary

3450.3	5552.8
3189.1	5549.7
3129.6	5549.0
3530.2	5549.0
3533.0	5549.0
3533.0	5549.0
3533.0	5549.0
3533.0	5549.0
3533.0	5549.0
3533.0	5549.0
3530.0	5553.0
3627.7	5539.3
3630.0	5539.0
3630.0	5539.0
3727.0	5515.7
3730.0	5515.0
4001.2	5445.8
4075.0	5427.0

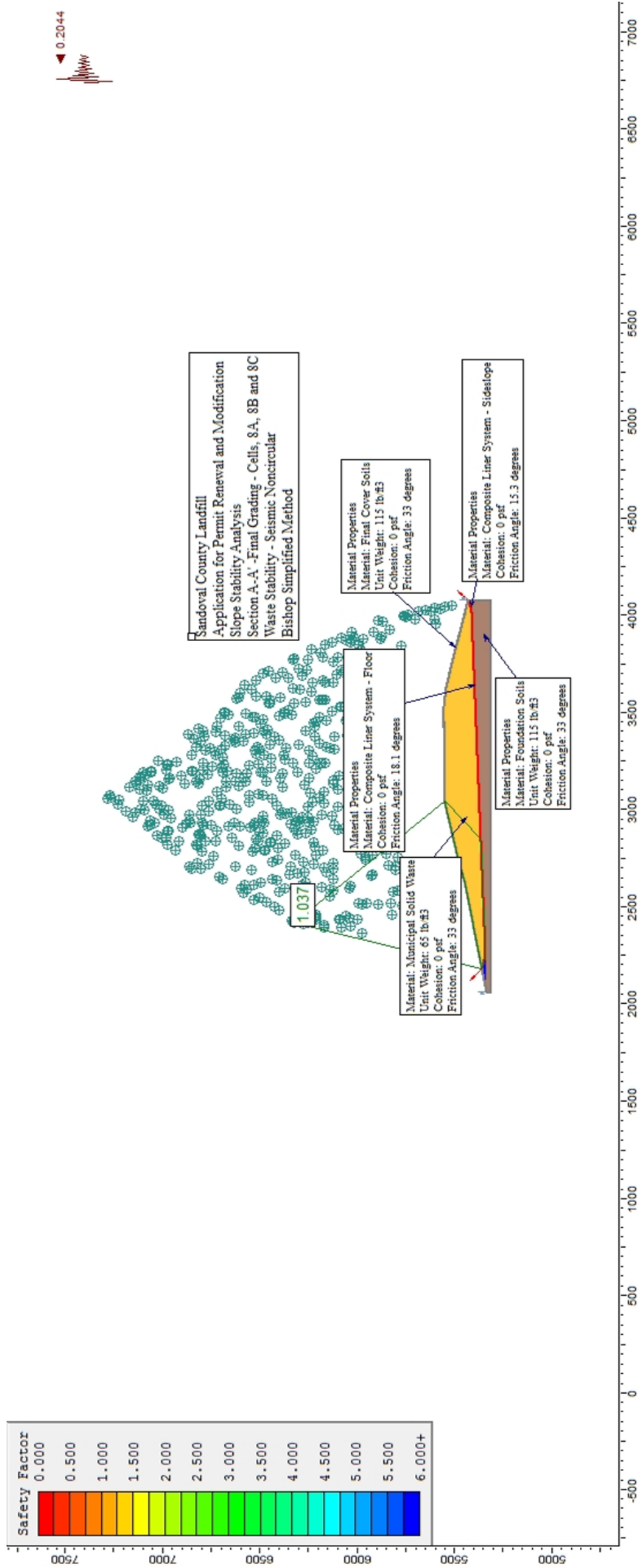
External Boundary

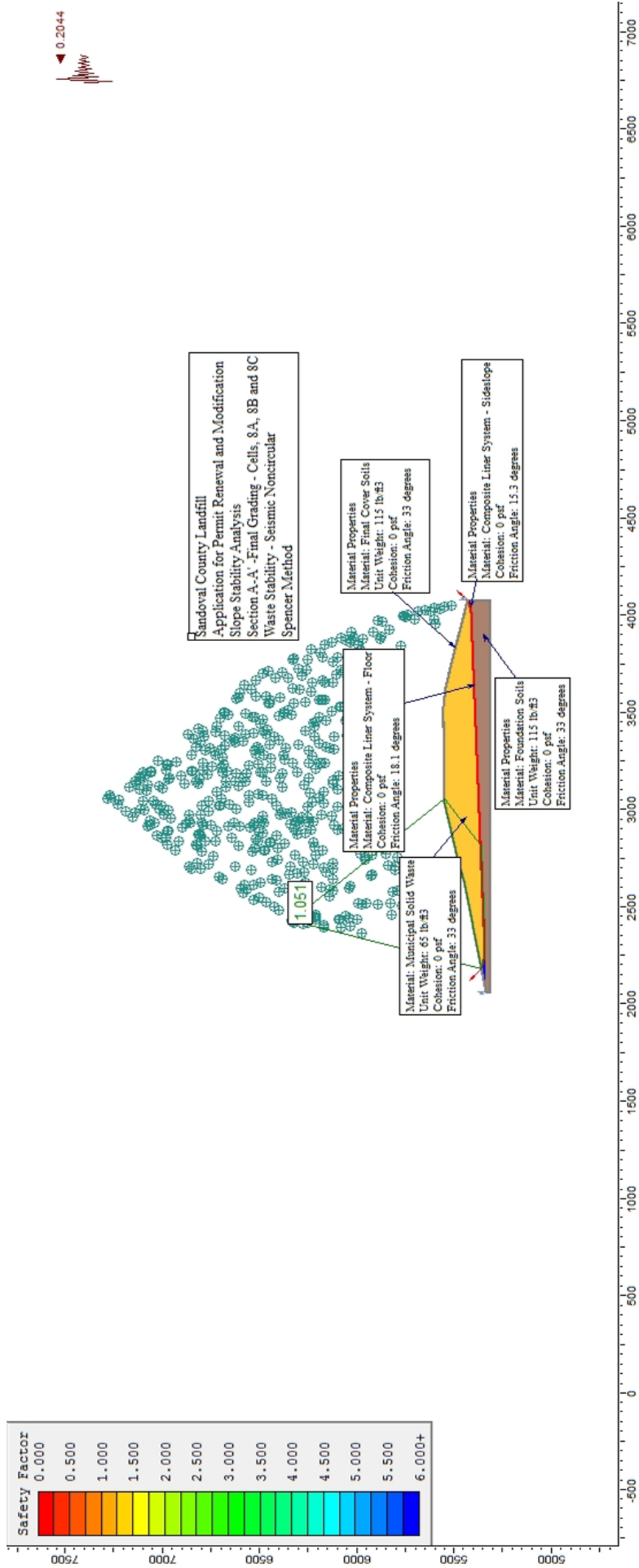
4075.0	5320.0
4075.0	5423.0
4075.0	5425.0
4075.0	5426.6
4075.0	5427.0
4075.0	5430.0
3730.0	5518.0
3728.7	5518.3
3630.0	5542.0
3534.9	5552.5
3530.0	5553.0

3458.6	5552.9
3420.7	5552.8
3452.2	5552.8
3458.8	5552.8
3450.3	5552.8
3150.0	5552.0
3134.7	5552.2
3099.6	5552.1
3030.0	5552.0
2754.8	5481.5
2628.0	5449.0
2181.9	5360.4
2181.8	5360.4
2181.8	5360.4
2180.0	5360.0
2178.6	5359.7
2060.0	5335.0
2060.0	5315.1

Circular Failure Surface

2232.9	6918.6
2090.0	5341.3
3033.4	5552.0





Slide Analysis Information

Document Name

File Name: Section A-A' Final Grading Waste Fills Seismic Block.sli

Project Settings

Project Title: SLIDE - An Interactive Slope Stability Program

Failure Direction: Right to Left

Units of Measurement: Imperial Units

Pore Fluid Unit Weight: 62.4 lb/ft³

Groundwater Method: Water Surfaces

Data Output: Standard

Calculate Excess Pore Pressure: Off

Allow Ru with Water Surfaces or Grids: Off

Random Numbers: Pseudo-random Seed

Random Number Seed: 10116

Random Number Generation Method: Park and Miller v.3

Analysis Methods

Analysis Methods used:

Bishop simplified

Janbu simplified

Spencer

Number of slices: 25

Tolerance: 0.005

Maximum number of iterations: 50

Surface Options

Surface Type: Non-Circular Block Search

Number of Surfaces: 500

Pseudo-Random Surfaces: Enabled

Convex Surfaces Only: Disabled

Left Projection Angle (Start Angle): 135

Left Projection Angle (End Angle): 135

Right Projection Angle (Start Angle): 45

Right Projection Angle (End Angle): 45

Minimum Elevation: Not Defined

Minimum Depth: Not Defined

Loading

Seismic Load Coefficient (Horizontal): 0.2044

Material Properties

Material: Final Cover Soils

Strength Type: Mohr-Coulomb

Unit Weight: 115 lb/ft³

Cohesion: 0 psf
Friction Angle: 33 degrees
Water Surface: None

Material: Composite Liner System, Floor

Strength Type: Mohr-Coulomb
Unit Weight: 95.5 lb/ft³
Cohesion: 0 psf
Friction Angle: 19 degrees
Water Surface: None

Material: Structural Fill Berm

Strength Type: Mohr-Coulomb
Unit Weight: 115 lb/ft³
Cohesion: 0 psf
Friction Angle: 33 degrees
Water Surface: None

Material: Municipal Solid Waste

Strength Type: Mohr-Coulomb
Unit Weight: 65 lb/ft³
Cohesion: 0 psf
Friction Angle: 33 degrees
Water Surface: None

Material: Foundation Soils

Strength Type: Mohr-Coulomb
Unit Weight: 115 lb/ft³
Cohesion: 0 psf
Friction Angle: 33 degrees
Water Surface: None

Global Minimums

Method: bishop simplified

FS: 1.037270
Axis Location: 2419.164, 6321.707
Left Slip Surface Endpoint: 2178.570, 5359.702
Right Slip Surface Endpoint: 3044.412, 5552.029
Resisting Moment=1.6815e+009 lb-ft
Driving Moment=1.62107e+009 lb-ft

Method: janbu simplified

FS: 0.989866
Axis Location: 2419.164, 6321.707
Left Slip Surface Endpoint: 2178.570, 5359.702
Right Slip Surface Endpoint: 3044.412, 5552.029
Resisting Horizontal Force=1.55826e+006 lb
Driving Horizontal Force=1.57422e+006 lb

Method: spencer

FS: 1.050510
Axis Location: 2425.716, 6335.115
Left Slip Surface Endpoint: 2178.467, 5359.681
Right Slip Surface Endpoint: 3057.714, 5552.055
Resisting Moment=1.69389e+009 lb-ft

Driving Moment=1.61244e+009 lb-ft
Resisting Horizontal Force=1.58285e+006 lb
Driving Horizontal Force=1.50674e+006 lb

Valid / Invalid Surfaces

Method: bishop simplified

Number of Valid Surfaces: 465

Number of Invalid Surfaces: 38

Error Codes:

Error Code -107 reported for 28 surfaces

Error Code -108 reported for 10 surfaces

Method: janbu simplified

Number of Valid Surfaces: 449

Number of Invalid Surfaces: 54

Error Codes:

Error Code -107 reported for 28 surfaces

Error Code -108 reported for 16 surfaces

Error Code -111 reported for 10 surfaces

Method: spencer

Number of Valid Surfaces: 264

Number of Invalid Surfaces: 239

Error Codes:

Error Code -107 reported for 28 surfaces

Error Code -108 reported for 183 surfaces

Error Code -111 reported for 28 surfaces

Error Codes

The following errors were encountered during the computation:

-107 = Total driving moment or total driving force is negative. This will occur if the wrong failure direction is specified, or if high external or anchor loads are applied against the failure direction.

-108 = Total driving moment or total driving force < 0.1. This is to limit the calculation of extremely high safety factors if the driving force is very small (0.1 is an arbitrary number).

-111 = safety factor equation did not converge

List of All Coordinates

Block Search Polyline

2180.939 5359.986

2249.882 5340.911

4014.867 5411.825

4074.759 5424.735

Material Boundary

2060.000 5335.000
2249.710 5340.004
2249.710 5340.004
2249.773 5340.005
2249.802 5340.006
2249.814 5340.006
2249.953 5340.010
2250.181 5340.016
2250.180 5340.016

Material Boundary

2754.800 5481.489
2774.285 5486.445
3030.224 5551.549

Material Boundary

2181.849 5360.367
2181.849 5360.368
2181.849 5360.367
2187.349 5358.831

Material Boundary

2178.560 5359.700
2178.595 5359.690
2180.000 5359.302
2184.843 5357.962
2216.939 5349.084
2225.927 5346.598
2249.035 5340.207

Material Boundary

2187.347 5358.831
2188.142 5358.617
2215.689 5351.217
2218.782 5350.386
2250.000 5342.000

Material Boundary

2187.213 5358.872
2187.349 5358.831

Material Boundary

2181.862 5360.368
2188.252 5358.639
2215.689 5351.217
2217.258 5350.713
2218.782 5350.386
2249.989 5341.998
2980.318 5368.629
4015.318 5413.629
4075.000 5426.560

Material Boundary

2181.864 5360.359

2180.000 5359.978
2178.595 5359.690
2178.568 5359.685
2180.000 5359.289
2184.819 5357.957
2249.035 5340.207
2249.041 5340.205
2249.953 5340.010
2250.000 5340.000
2980.000 5365.000
4015.000 5410.000
4075.000 5423.000

Material Boundary

2628.000 5449.000
2774.285 5486.445
3030.386 5552.000
3130.000 5552.000
3134.651 5552.209

Material Boundary

3452.155 5552.781
3458.571 5552.857

Material Boundary

2180.000 5359.992
2180.000 5359.978
2180.000 5359.302
2180.000 5359.289
2180.000 5357.000
2184.819 5357.957
2184.843 5357.962
2188.142 5358.617
2188.252 5358.639
2628.000 5446.000
3030.224 5549.000
3130.000 5549.000
3189.104 5549.680
3458.779 5552.781

Material Boundary

3532.978 5548.978
3532.986 5548.978
3532.995 5548.977
3532.992 5548.987
3533.009 5548.985
3627.688 5539.254
3629.863 5539.031
3629.984 5539.002
3724.060 5516.224
3727.245 5515.453
3729.301 5515.016
4001.184 5445.829
4074.953 5427.056

Material Boundary

3450.345	5552.760
3189.104	5549.680
3129.586	5548.978
3530.165	5548.978
3532.978	5548.978
3532.995	5548.977
3533.016	5548.976
3533.010	5548.984
3533.009	5548.985
3530.000	5553.000
3627.688	5539.254
3629.984	5539.002
3630.000	5539.000
3727.000	5515.720
3730.000	5515.000
4001.184	5445.829
4075.000	5427.000

External Boundary

4075.000	5320.000
4075.000	5423.000
4075.000	5425.000
4075.000	5426.560
4075.000	5427.000
4075.000	5430.000
3730.000	5518.000
3728.678	5518.317
3630.000	5542.000
3534.913	5552.460
3530.000	5553.000
3458.571	5552.857
3420.742	5552.781
3452.155	5552.781
3458.779	5552.781
3450.345	5552.760
3150.000	5552.000
3134.651	5552.209
3099.610	5552.139
3030.000	5552.000
2754.800	5481.489
2628.000	5449.000
2181.862	5360.368
2181.849	5360.367
2181.849	5360.367
2180.000	5359.992
2178.560	5359.700
2060.000	5335.000
2060.000	5315.150

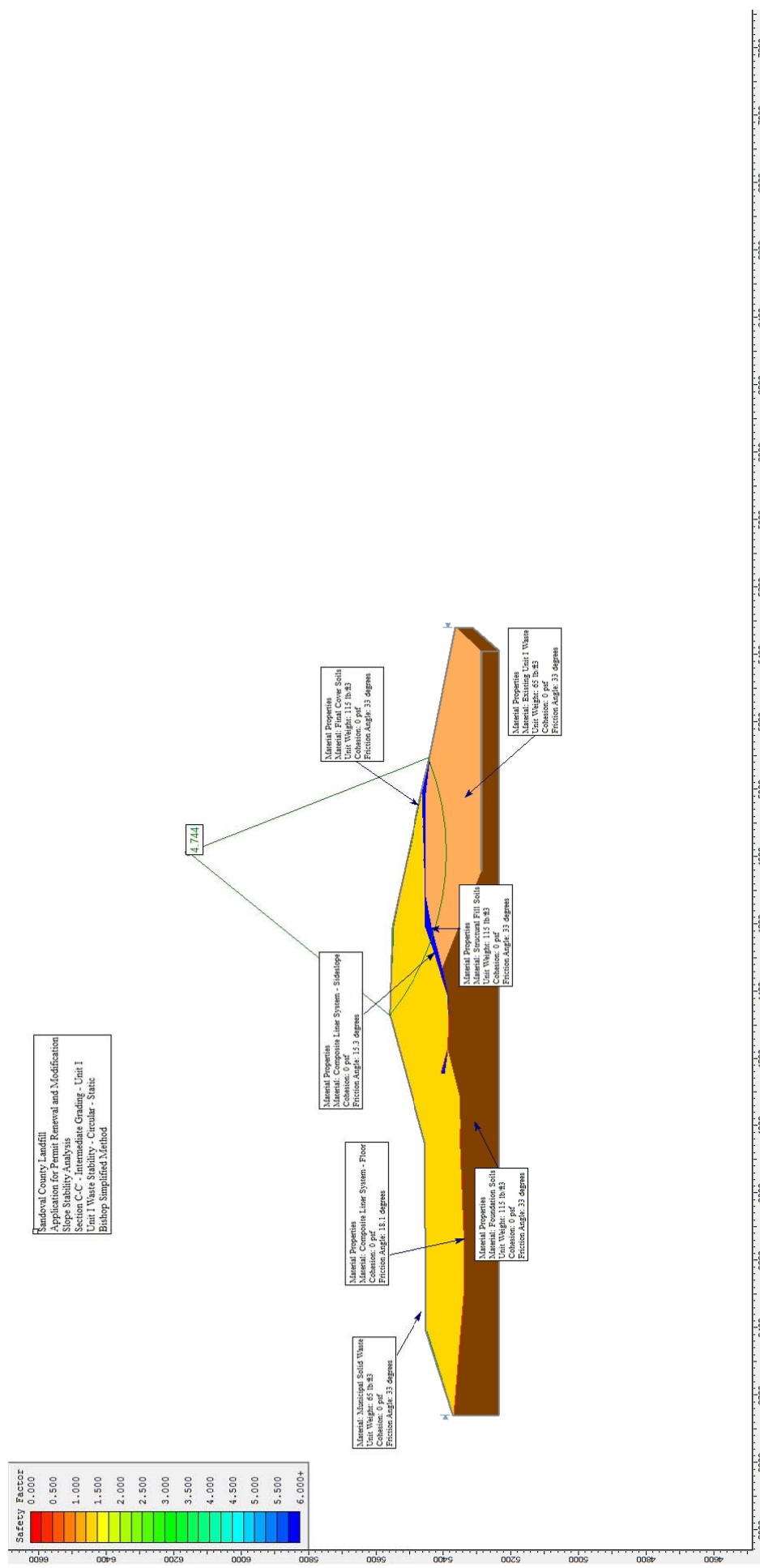
**APPLICATION FOR PERMIT RENEWAL AND MODIFICATION
SANDOVAL COUNTY LANDFILL**

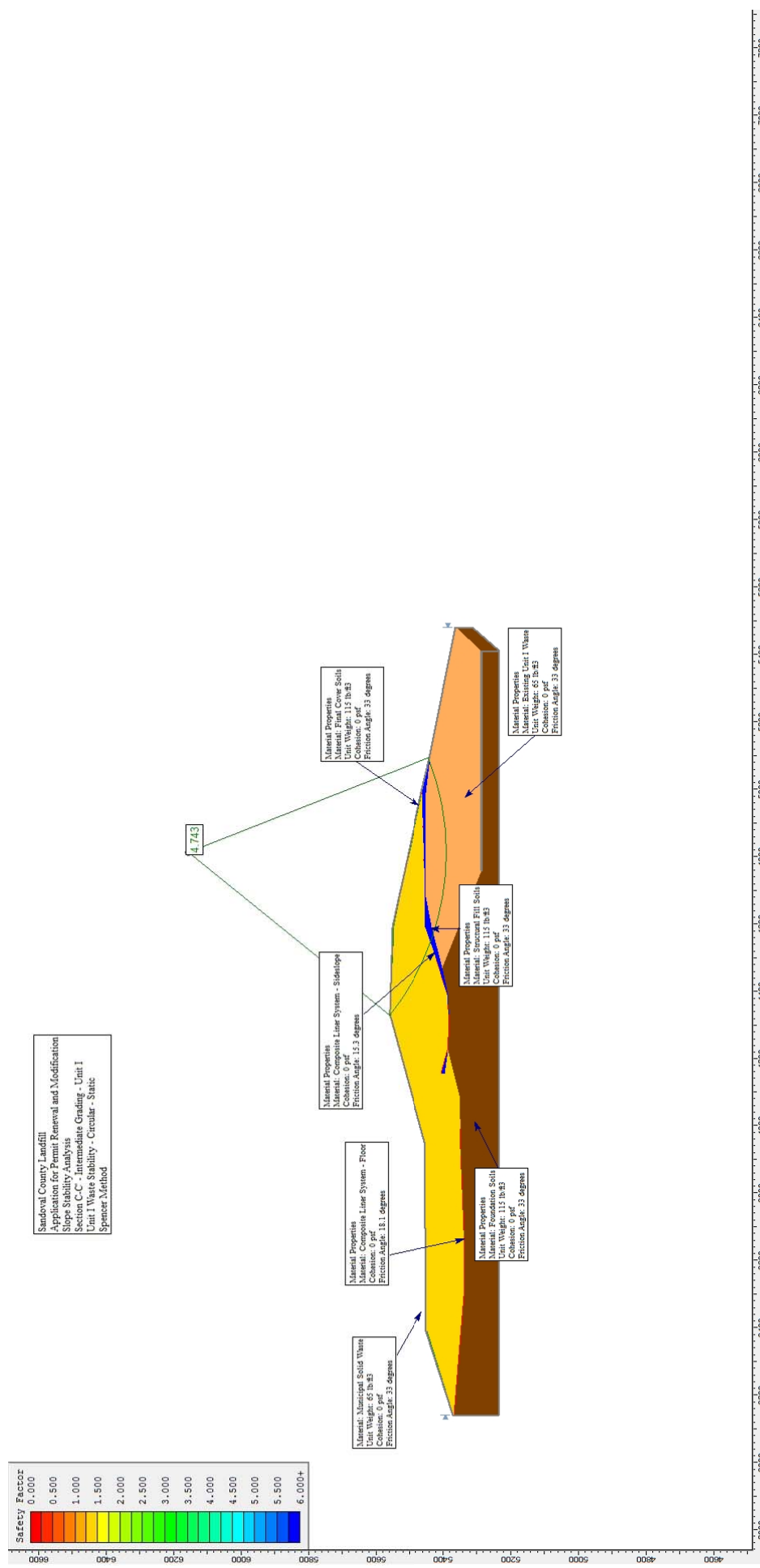
**VOLUME III: LANDFILL ENGINEERING CALCULATIONS
SECTION 3: SLOPE STABILITY ANALYSIS**

ATTACHMENT III.3.E-7

SCENARIO 13: SECTION C-C'; CIRCULAR, STATIC

SCENARIO 14: SECTION C-C', CIRCULAR, SEISMIC





Slide Analysis Information

Document Name

File Name: Section C-C' Unit IV-Unit III Intermediate Grading Circular Static Waste Unit I

Project Settings

Project Title: SLIDE - An Interactive Slope Stability Program

Failure Direction: Left to Right

Units of Measurement: Imperial Units

Pore Fluid Unit Weight: 62.4 lb/ft³

Groundwater Method: Water Surfaces

Data Output: Standard

Calculate Excess Pore Pressure: Off

Allow Ru with Water Surfaces or Grids: Off

Random Numbers: Pseudo-random Seed

Random Number Seed: 10116

Random Number Generation Method: Park and Miller v.3

Analysis Methods

Analysis Methods used:

Bishop simplified

Janbu simplified

Spencer

Number of slices: 25

Tolerance: 0.005

Maximum number of iterations: 50

Surface Options

Surface Type: Circular

Search Method: Grid Search

Radius increment: 10

Composite Surfaces: Enabled

Reverse Curvature: Create Tension Crack

Minimum Elevation: 5236

Minimum Depth: Not Defined

Material Properties

Material: Existing Unit I Waste

Strength Type: Mohr-Coulomb

Unit Weight: 65 lb/ft³

Cohesion: 0 psf

Friction Angle: 33 degrees

Water Surface: None

Material: Municipal Solid Waste

Strength Type: Mohr-Coulomb

Unit Weight: 65 lb/ft³

Cohesion: 0 psf
Friction Angle: 33 degrees
Water Surface: None

Material: Structural Fill Soils
Strength Type: Mohr-Coulomb
Unit Weight: 115 lb/ft³
Cohesion: 0 psf
Friction Angle: 33 degrees
Water Surface: None

Material: Composite Liner System
Strength Type: Mohr-Coulomb
Unit Weight: 95.5 lb/ft³
Cohesion: 0 psf
Friction Angle: 19 degrees
Water Surface: None

Material: Foundation Soils
Strength Type: Mohr-Coulomb
Unit Weight: 115 lb/ft³
Cohesion: 0 psf
Friction Angle: 33 degrees
Water Surface: None

Material: Final Cover Soils
Strength Type: Mohr-Coulomb
Unit Weight: 115 lb/ft³
Cohesion: 0 psf
Friction Angle: 33 degrees
Water Surface: None

Global Minimums

Method: bishop simplified
FS: 4.743520
Center: 4811.347, 6156.078
Radius: 768.484
Left Slip Surface Endpoint: 4327.241, 5559.245
Right Slip Surface Endpoint: 5093.558, 5441.288
Resisting Moment=2.39523e+009 lb-ft
Driving Moment=5.04947e+008 lb-ft

Method: janbu simplified
FS: 4.484110
Center: 4811.347, 6156.078
Radius: 768.484
Left Slip Surface Endpoint: 4327.241, 5559.245
Right Slip Surface Endpoint: 5093.558, 5441.288
Resisting Horizontal Force=2.99603e+006 lb
Driving Horizontal Force=668145 lb

Method: spencer
FS: 4.743200
Center: 4811.347, 6156.078
Radius: 768.484

Left Slip Surface Endpoint: 4327.241, 5559.245
Right Slip Surface Endpoint: 5093.558, 5441.288
Resisting Moment=2.39506e+009 lb-ft
Driving Moment=5.04947e+008 lb-ft
Resisting Horizontal Force=3.00255e+006 lb
Driving Horizontal Force=633022 lb

Valid / Invalid Surfaces

Method: bishop simplified

Number of Valid Surfaces: 1

Number of Invalid Surfaces: 0

Method: janbu simplified

Number of Valid Surfaces: 1

Number of Invalid Surfaces: 0

Method: spencer

Number of Valid Surfaces: 1

Number of Invalid Surfaces: 0

List of All Coordinates

Circular Failure Surface

4811.347 6156.078

4327.245 5559.246

5093.551 5441.290

Material Boundary

5408.842 5286.738

5480.000 5361.000

Material Boundary

4468.000 5403.000

4756.844 5286.738

Material Boundary

4330.082 5559.438

4346.250 5559.438

Material Boundary

4155.000 5405.000

4225.000 5386.000

Material Boundary

4990.000 5462.000

5090.000 5439.000

5480.000 5361.000

Material Boundary

4155.000 5404.686

4155.000 5395.000

4222.418 5385.369

4222.466 5385.362

4225.000 5385.000

4300.000 5380.000
4390.000 5385.000
4468.000 5403.000
4589.000 5435.000
4690.000 5452.000
4990.000 5450.000
5090.000 5439.000
4990.000 5463.000
4987.691 5462.942
4985.861 5462.897
4687.494 5455.456
4655.504 5454.658
4589.000 5453.000
4513.570 5427.580
4492.524 5420.488
4387.094 5384.958

Material Boundary

3950.000 5456.000
4330.082 5559.438
4584.679 5548.184
4585.526 5548.155
4590.000 5548.000
4593.921 5547.177
4690.000 5527.000
4826.869 5497.345
4985.861 5462.897
4990.000 5462.000
4690.000 5453.000

Material Boundary

4593.921 5547.177
4826.869 5497.345
4987.691 5462.942
4990.428 5462.357

Material Boundary

3140.000 5366.000
3262.000 5357.000
3525.014 5335.167
3525.083 5335.089
3674.218 5337.167
3690.052 5337.404
3911.467 5346.067
3932.000 5347.000
3948.694 5347.423
4090.000 5351.000
4225.000 5385.000
4225.000 5386.000
4222.418 5385.369
4090.000 5353.000
3932.000 5349.000
3689.923 5339.337
3524.899 5338.000
3262.000 5359.000
3140.000 5368.000

Material Boundary

3262.000 5359.000
3525.014 5335.167
3525.000 5335.000
3674.218 5337.167
3689.923 5339.337
3911.467 5346.067
3948.694 5347.423
3992.000 5349.000
4090.000 5353.000

Material Boundary

3140.000 5368.000
3389.968 5446.990
3390.000 5447.000

Material Boundary

4155.428 5407.551
4225.000 5388.000
4300.000 5383.000
4390.000 5389.000
4441.000 5404.000
4451.509 5407.091
4458.000 5409.000
4470.505 5413.295
4487.839 5419.250
4589.000 5454.000
4655.504 5454.658
4690.000 5455.000
4990.000 5462.000
4990.000 5460.000
4690.000 5453.000
4589.000 5452.000
4492.524 5420.488
4470.505 5413.295
4451.509 5407.091
4390.000 5387.000
4300.000 5382.000
4225.000 5386.000
4155.000 5404.686
4155.000 5405.000
4155.428 5407.551

Material Boundary

4225.000 5386.000
4300.000 5381.000
4390.000 5387.000
4441.000 5404.000
4450.000 5407.000
4487.839 5419.250
4513.570 5427.580
4589.000 5452.000

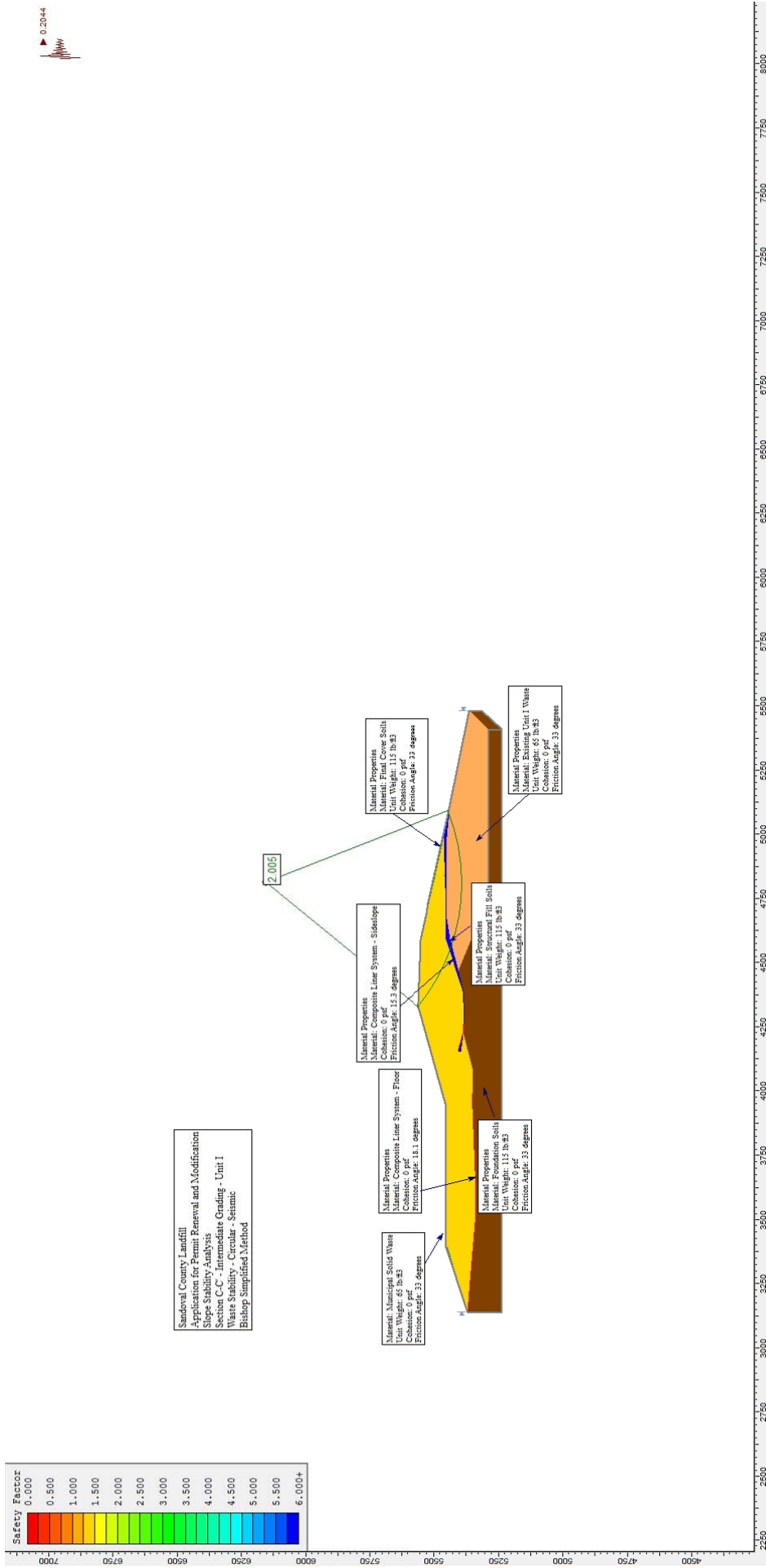
Material Boundary

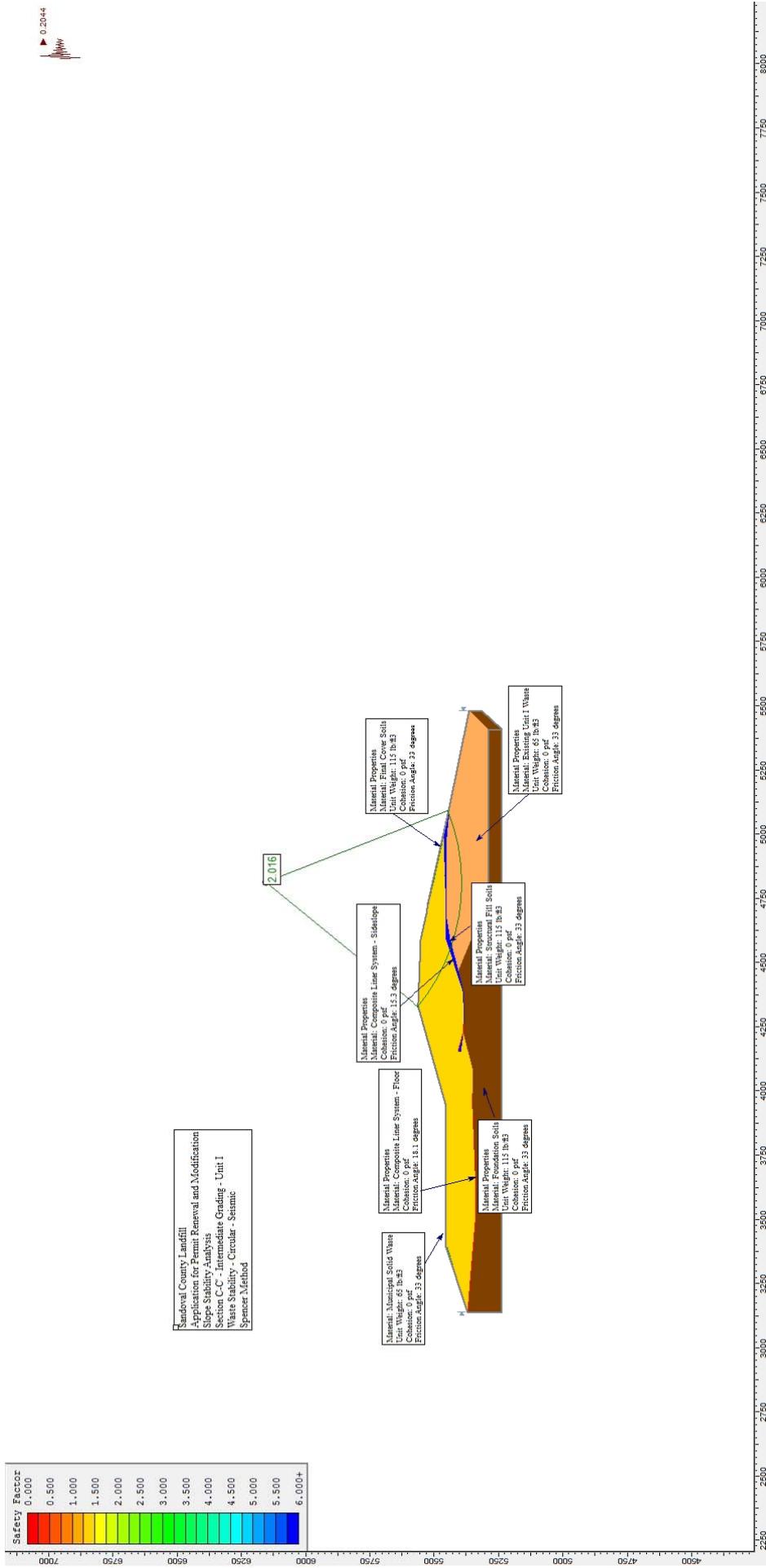
3391.150 5450.655

3391.233 5450.656
3440.436 5451.447

External Boundary

3140.000 5236.064
5408.768 5234.764
5407.588 5285.504
4756.844 5286.738
5408.842 5286.738
5408.842 5234.712
5480.000 5314.000
5480.000 5361.000
5480.000 5364.000
5090.000 5442.000
4990.000 5465.000
4732.674 5520.754
4690.000 5530.000
4590.026 5550.995
4590.042 5550.984
4590.036 5550.984
4590.026 5550.985
4588.244 5551.061
4588.154 5551.064
4588.106 5551.066
4587.290 5551.094
4422.057 5556.813
4346.250 5559.438
4330.000 5560.000
3950.000 5456.000
3440.436 5451.447
3390.008 5450.997
3390.008 5447.000
3390.000 5446.988
3390.000 5447.000
3390.000 5451.000
3140.000 5370.000
3140.000 5368.000
3140.000 5366.000





Slide Analysis Information

Document Name

File Name: Section C-C' Unit IV-Unit III Intermediate Grading Circular Seismic Waste Unit I

Project Settings

Project Title: SLIDE - An Interactive Slope Stability Program

Failure Direction: Left to Right

Units of Measurement: Imperial Units

Pore Fluid Unit Weight: 62.4 lb/ft³

Groundwater Method: Water Surfaces

Data Output: Standard

Calculate Excess Pore Pressure: Off

Allow Ru with Water Surfaces or Grids: Off

Random Numbers: Pseudo-random Seed

Random Number Seed: 10116

Random Number Generation Method: Park and Miller v.3

Analysis Methods

Analysis Methods used:

Bishop simplified

Janbu simplified

Spencer

Number of slices: 25

Tolerance: 0.005

Maximum number of iterations: 50

Surface Options

Surface Type: Circular

Search Method: Grid Search

Radius increment: 10

Composite Surfaces: Enabled

Reverse Curvature: Create Tension Crack

Minimum Elevation: 5236

Minimum Depth: Not Defined

Loading

Seismic Load Coefficient (Horizontal): 0.2044

Material Properties

Material: Existing Unit I Waste

Strength Type: Mohr-Coulomb

Unit Weight: 65 lb/ft³

Cohesion: 0 psf

Friction Angle: 33 degrees

Water Surface: None

Material: Municipal Solid Waste

Strength Type: Mohr-Coulomb

Unit Weight: 65 lb/ft³

Cohesion: 0 psf

Friction Angle: 33 degrees

Water Surface: None

Material: Structural Fill Soils

Strength Type: Mohr-Coulomb

Unit Weight: 115 lb/ft³

Cohesion: 0 psf

Friction Angle: 33 degrees

Water Surface: None

Material: Composite Liner System

Strength Type: Mohr-Coulomb

Unit Weight: 95.5 lb/ft³

Cohesion: 0 psf

Friction Angle: 19 degrees

Water Surface: None

Material: Foundation Soils

Strength Type: Mohr-Coulomb

Unit Weight: 115 lb/ft³

Cohesion: 0 psf

Friction Angle: 33 degrees

Water Surface: None

Material: Final Cover Soils

Strength Type: Mohr-Coulomb

Unit Weight: 115 lb/ft³

Cohesion: 0 psf

Friction Angle: 33 degrees

Water Surface: None

Global Minimums

Method: bishop simplified

FS: 2.004780

Center: 4811.347, 6156.078

Radius: 768.484

Left Slip Surface Endpoint: 4327.241, 5559.245

Right Slip Surface Endpoint: 5093.558, 5441.288

Resisting Moment=2.33733e+009 lb-ft

Driving Moment=1.16588e+009 lb-ft

Method: janbu simplified

FS: 1.870930

Center: 4811.347, 6156.078

Radius: 768.484

Left Slip Surface Endpoint: 4327.241, 5559.245

Right Slip Surface Endpoint: 5093.558, 5441.288

Resisting Horizontal Force=2.92348e+006 lb

Driving Horizontal Force=1.56258e+006 lb

Method: spencer

FS: 2.016090

Center: 4811.347, 6156.078

Radius: 768.484

Left Slip Surface Endpoint: 4327.241, 5559.245

Right Slip Surface Endpoint: 5093.558, 5441.288

Resisting Moment=2.35051e+009 lb-ft

Driving Moment=1.16588e+009 lb-ft

Resisting Horizontal Force=2.95363e+006 lb

Driving Horizontal Force=1.46503e+006 lb

Valid / Invalid Surfaces

Method: bishop simplified

Number of Valid Surfaces: 1

Number of Invalid Surfaces: 0

Method: janbu simplified

Number of Valid Surfaces: 1

Number of Invalid Surfaces: 0

Method: spencer

Number of Valid Surfaces: 1

Number of Invalid Surfaces: 0

List of All Coordinates

Circular Failure Surface

4811.347 6156.078

4327.245 5559.246

5093.551 5441.290

Material Boundary

5408.842 5286.738

5480.000 5361.000

Material Boundary

4468.000 5403.000

4756.844 5286.738

Material Boundary

4330.082 5559.438

4346.250 5559.438

Material Boundary

4155.000 5405.000

4225.000 5386.000

Material Boundary

4990.000 5462.000

5090.000 5439.000

5480.000 5361.000

Material Boundary

4155.000 5404.686

4155.000	5395.000
4222.418	5385.369
4222.466	5385.362
4225.000	5385.000
4300.000	5380.000
4390.000	5385.000
4468.000	5403.000
4589.000	5435.000
4690.000	5452.000
4990.000	5450.000
5090.000	5439.000
4990.000	5463.000
4987.691	5462.942
4985.861	5462.897
4687.494	5455.456
4655.504	5454.658
4589.000	5453.000
4513.570	5427.580
4492.524	5420.488
4387.094	5384.958

Material Boundary

3950.000	5456.000
4330.082	5559.438
4584.679	5548.184
4585.526	5548.155
4590.000	5548.000
4593.921	5547.177
4690.000	5527.000
4826.869	5497.345
4985.861	5462.897
4990.000	5462.000
4690.000	5453.000

Material Boundary

4593.921	5547.177
4826.869	5497.345
4987.691	5462.942
4990.428	5462.357

Material Boundary

3140.000	5366.000
3262.000	5357.000
3525.014	5335.167
3525.083	5335.089
3674.218	5337.167
3690.052	5337.404
3911.467	5346.067
3932.000	5347.000
3948.694	5347.423
4090.000	5351.000
4225.000	5385.000
4225.000	5386.000
4222.418	5385.369
4090.000	5353.000
3932.000	5349.000

3689.923 5339.337
3524.899 5338.000
3262.000 5359.000
3140.000 5368.000

Material Boundary

3262.000 5359.000
3525.014 5335.167
3525.000 5335.000
3674.218 5337.167
3689.923 5339.337
3911.467 5346.067
3948.694 5347.423
3992.000 5349.000
4090.000 5353.000

Material Boundary

3140.000 5368.000
3389.968 5446.990
3390.000 5447.000

Material Boundary

4155.428 5407.551
4225.000 5388.000
4300.000 5383.000
4390.000 5389.000
4441.000 5404.000
4451.509 5407.091
4458.000 5409.000
4470.505 5413.295
4487.839 5419.250
4589.000 5454.000
4655.504 5454.658
4690.000 5455.000
4990.000 5462.000
4990.000 5460.000
4690.000 5453.000
4589.000 5452.000
4492.524 5420.488
4470.505 5413.295
4451.509 5407.091
4390.000 5387.000
4300.000 5382.000
4225.000 5386.000
4155.000 5404.686
4155.000 5405.000
4155.428 5407.551

Material Boundary

4225.000 5386.000
4300.000 5381.000
4390.000 5387.000
4441.000 5404.000
4450.000 5407.000
4487.839 5419.250
4513.570 5427.580

4589.000 5452.000

Material Boundary

3391.150 5450.655

3391.233 5450.656

3440.436 5451.447

External Boundary

3140.000 5236.064

5408.768 5234.764

5407.588 5285.504

4756.844 5286.738

5408.842 5286.738

5408.842 5234.712

5480.000 5314.000

5480.000 5361.000

5480.000 5364.000

5090.000 5442.000

4990.000 5465.000

4732.674 5520.754

4690.000 5530.000

4590.026 5550.995

4590.042 5550.984

4590.036 5550.984

4590.026 5550.985

4588.244 5551.061

4588.154 5551.064

4588.106 5551.066

4587.290 5551.094

4422.057 5556.813

4346.250 5559.438

4330.000 5560.000

3950.000 5456.000

3440.436 5451.447

3390.008 5450.997

3390.008 5447.000

3390.000 5446.988

3390.000 5447.000

3390.000 5451.000

3140.000 5370.000

3140.000 5368.000

3140.000 5366.000

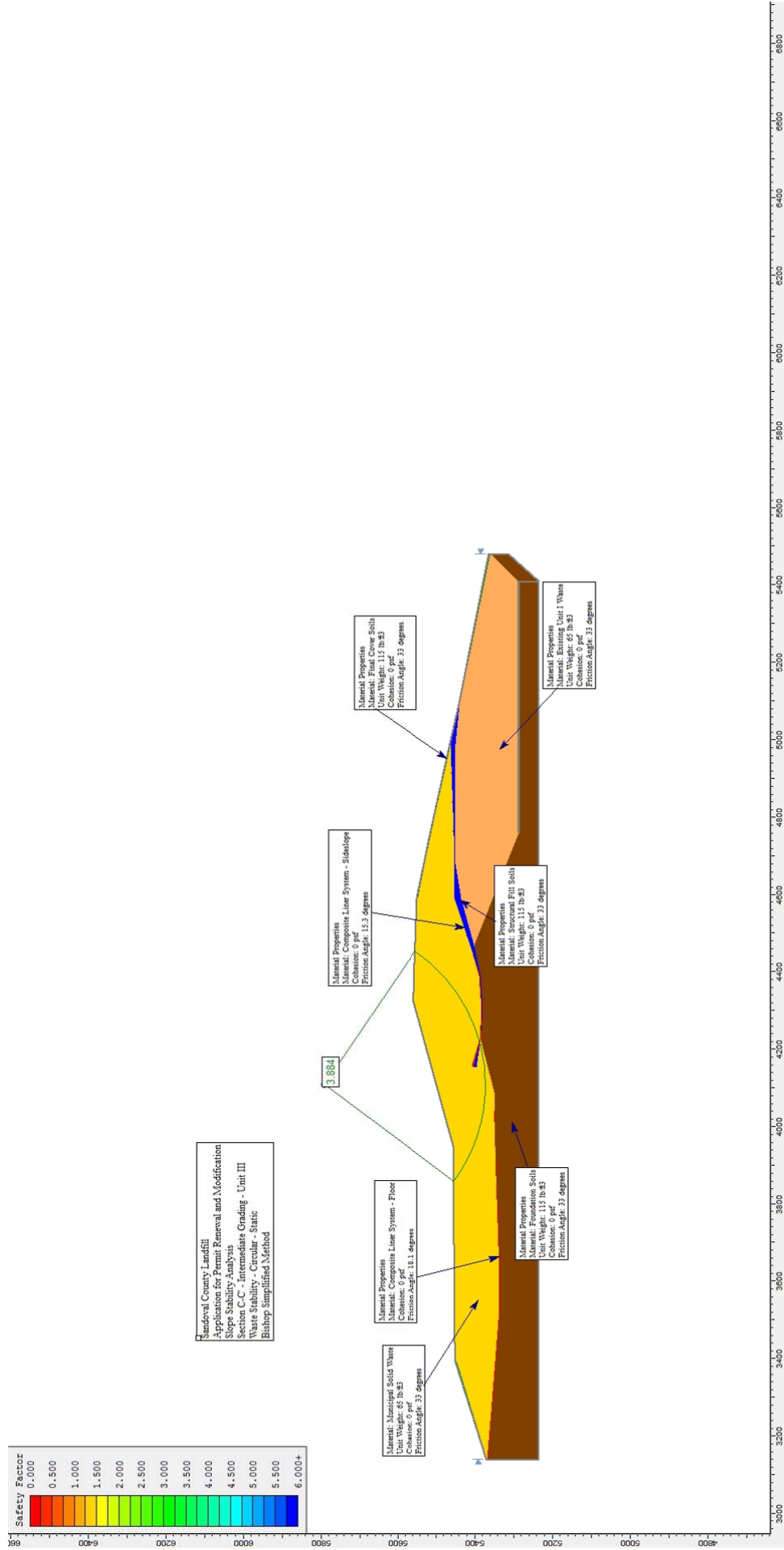
**APPLICATION FOR PERMIT RENEWAL AND MODIFICATION
SANDOVAL COUNTY LANDFILL**

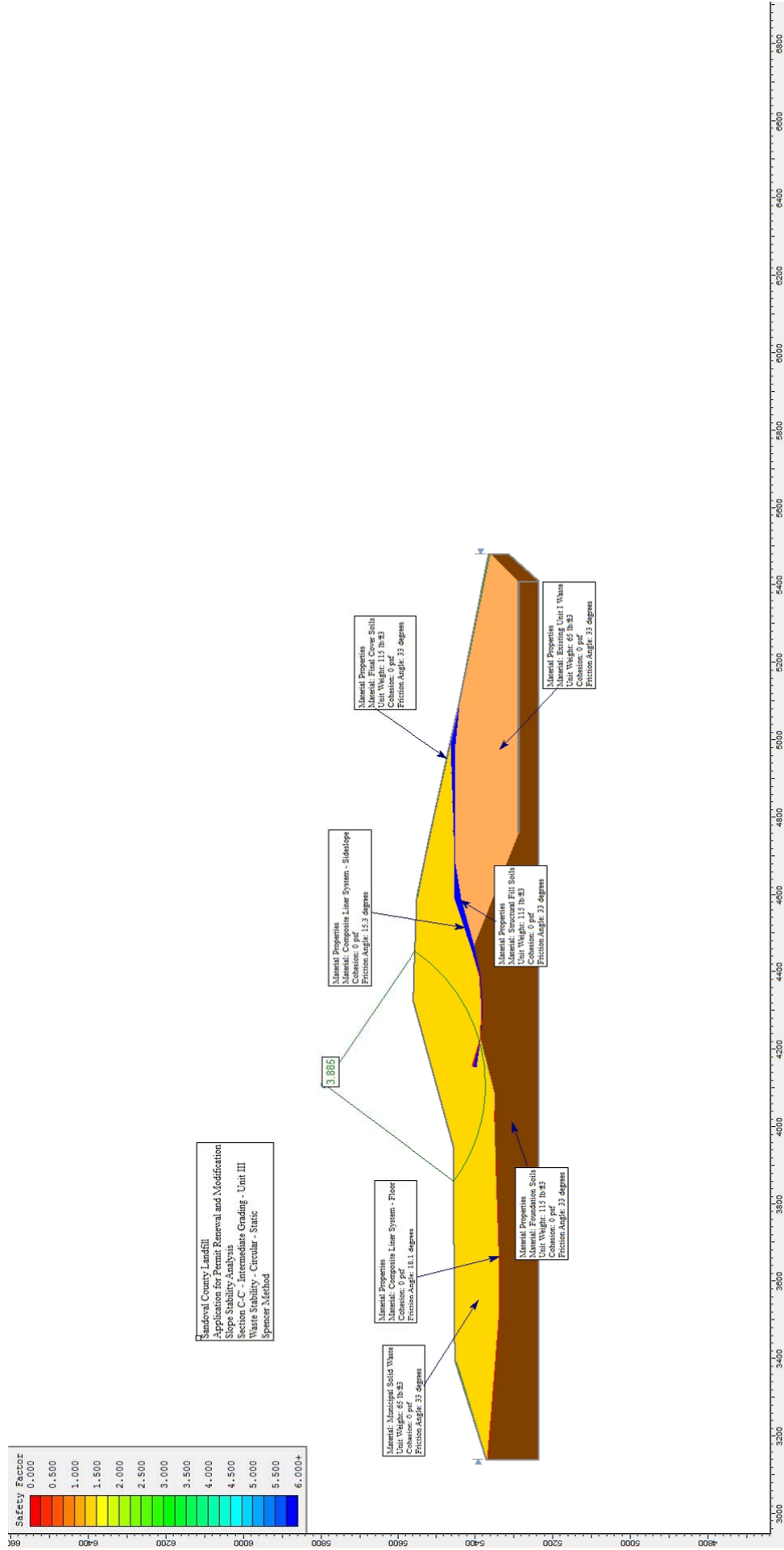
**VOLUME III: LANDFILL ENGINEERING CALCULATIONS
SECTION 3: SLOPE STABILITY ANALYSIS**

ATTACHMENT III.3.E-8

SCENARIO 15: SECTION C-C'; CIRCULAR, STATIC

SCENARIO 16: SECTION C-C', CIRCULAR, SEISMIC





Slide Analysis Information

Document Name

File Name: Section C-C' Unit IV-Unit III Intermediate Grading Circular Static Waste Unit III

Project Settings

Project Title: Sandoval County Landfill - Permit Renewal and Modification

Failure Direction: Right to Left

Units of Measurement: Imperial Units

Pore Fluid Unit Weight: 62.4 lb/ft³

Groundwater Method: Water Surfaces

Data Output: Standard

Calculate Excess Pore Pressure: Off

Allow Ru with Water Surfaces or Grids: Off

Random Numbers: Pseudo-random Seed

Random Number Seed: 10116

Random Number Generation Method: Park and Miller v.3

Analysis Methods

Analysis Methods used:

Bishop simplified

Janbu simplified

Spencer

Number of slices: 25

Tolerance: 0.005

Maximum number of iterations: 50

Surface Options

Surface Type: Circular

Search Method: Grid Search

Radius increment: 10

Composite Surfaces: Enabled

Reverse Curvature: Create Tension Crack

Minimum Elevation: 5236

Minimum Depth: Not Defined

Material Properties

Material: Existing Unit I Waste

Strength Type: Mohr-Coulomb

Unit Weight: 65 lb/ft³

Cohesion: 0 psf

Friction Angle: 33 degrees

Water Surface: None

Material: Municipal Solid Waste

Strength Type: Mohr-Coulomb

Unit Weight: 65 lb/ft³

Cohesion: 0 psf
Friction Angle: 33 degrees
Water Surface: None

Material: Structural Fill Soils
Strength Type: Mohr-Coulomb
Unit Weight: 115 lb/ft³
Cohesion: 0 psf
Friction Angle: 33 degrees
Water Surface: None

Material: Composite Liner System
Strength Type: Mohr-Coulomb
Unit Weight: 95.5 lb/ft³
Cohesion: 0 psf
Friction Angle: 19 degrees
Water Surface: None

Material: Foundation Soils
Strength Type: Mohr-Coulomb
Unit Weight: 115 lb/ft³
Cohesion: 0 psf
Friction Angle: 33 degrees
Water Surface: None

Material: Final Cover Soils
Strength Type: Mohr-Coulomb
Unit Weight: 115 lb/ft³
Cohesion: 0 psf
Friction Angle: 33 degrees
Water Surface: None

List of All Coordinates

Material Boundary
5408.84 5286.74
5480.00 5361.00

Material Boundary
4468.00 5403.00
4756.84 5286.74

Material Boundary
4330.08 5559.44
4346.25 5559.44

Material Boundary
4155.00 5405.00
4225.00 5386.00

Material Boundary
4990.00 5462.00
5090.00 5439.00
5480.00 5361.00

Material Boundary

4155.00	5404.69
4155.00	5395.00
4222.42	5385.37
4222.47	5385.36
4225.00	5385.00
4300.00	5380.00
4390.00	5385.00
4468.00	5403.00
4589.00	5435.00
4690.00	5452.00
4990.00	5450.00
5090.00	5439.00
4990.00	5463.00
4987.69	5462.94
4985.86	5462.90
4687.49	5455.46
4655.50	5454.66
4589.00	5453.00
4513.57	5427.58
4492.52	5420.49
4387.09	5384.96

Material Boundary

3950.00	5456.00
4330.08	5559.44
4584.68	5548.18
4585.53	5548.15
4590.00	5548.00
4593.92	5547.18
4690.00	5527.00
4826.87	5497.35
4985.86	5462.90
4990.00	5462.00
4690.00	5453.00

Material Boundary

4593.92	5547.18
4826.87	5497.35
4987.69	5462.94
4990.43	5462.36

Material Boundary

3140.00	5366.00
3262.00	5357.00
3525.01	5335.17
3525.08	5335.09
3674.22	5337.17
3690.05	5337.40
3911.47	5346.07
3932.00	5347.00
3948.69	5347.42
4090.00	5351.00
4225.00	5385.00
4225.00	5386.00
4222.42	5385.37
4090.00	5353.00

3932.00	5349.00
3689.92	5339.34
3524.90	5338.00
3262.00	5359.00
3140.00	5368.00

Material Boundary

3262.00	5359.00
3525.01	5335.17
3525.00	5335.00
3674.22	5337.17
3689.92	5339.34
3911.47	5346.07
3948.69	5347.42
3992.00	5349.00
4090.00	5353.00

Material Boundary

3140.00	5368.00
3389.97	5446.99
3390.00	5447.00

Material Boundary

4155.43	5407.55
4225.00	5388.00
4300.00	5383.00
4390.00	5389.00
4441.00	5404.00
4451.51	5407.09
4458.00	5409.00
4470.50	5413.30
4487.84	5419.25
4589.00	5454.00
4655.50	5454.66
4690.00	5455.00
4990.00	5462.00
4990.00	5460.00
4690.00	5453.00
4589.00	5452.00
4492.52	5420.49
4470.50	5413.30
4451.51	5407.09
4390.00	5387.00
4300.00	5382.00
4225.00	5386.00
4155.00	5404.69
4155.00	5405.00
4155.43	5407.55

Material Boundary

4225.00	5386.00
4300.00	5381.00
4390.00	5387.00
4441.00	5404.00
4450.00	5407.00
4487.84	5419.25

4513.57	5427.58
4589.00	5452.00

Material Boundary

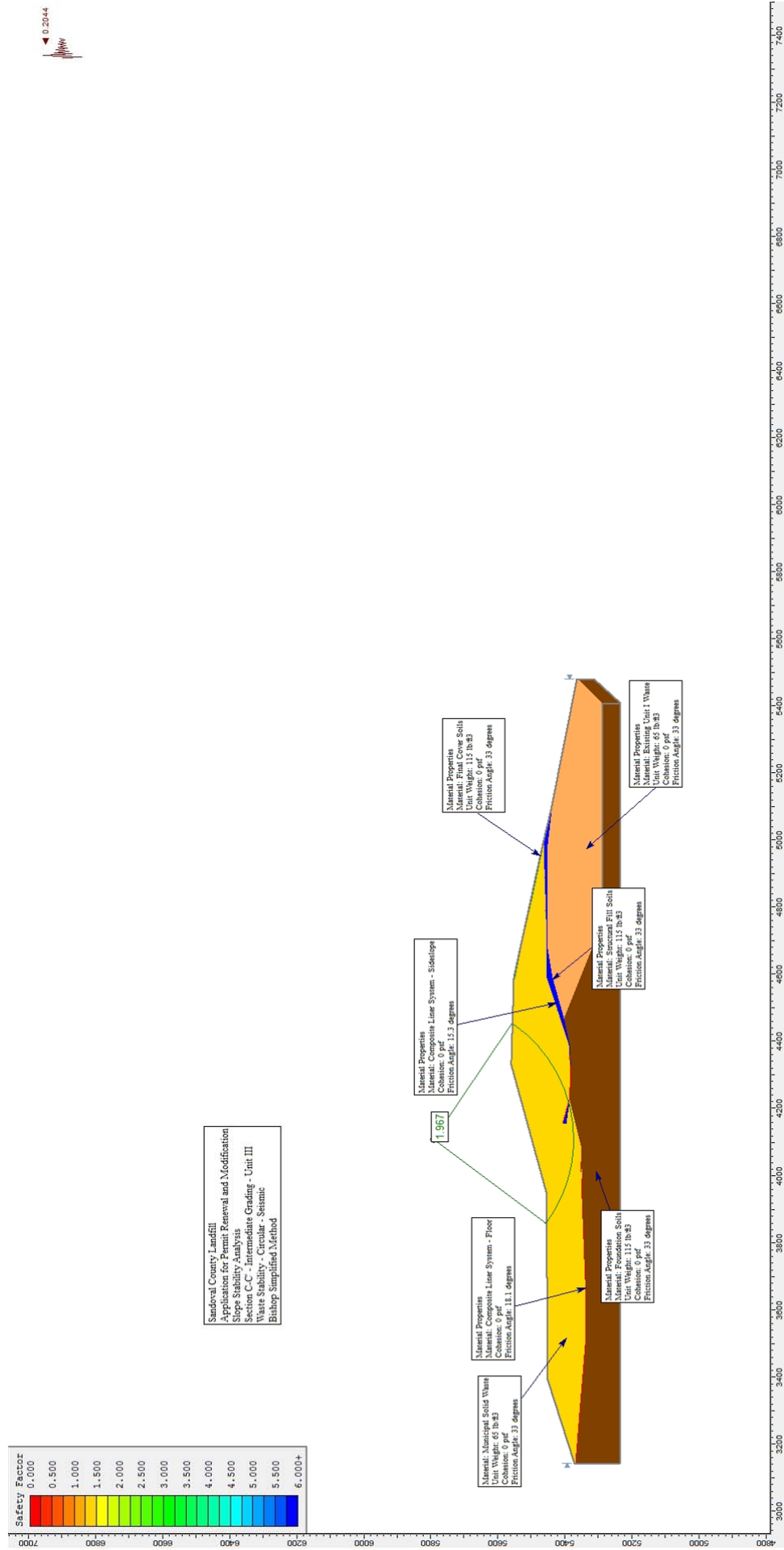
3391.15	5450.66
3391.23	5450.66
3440.44	5451.45

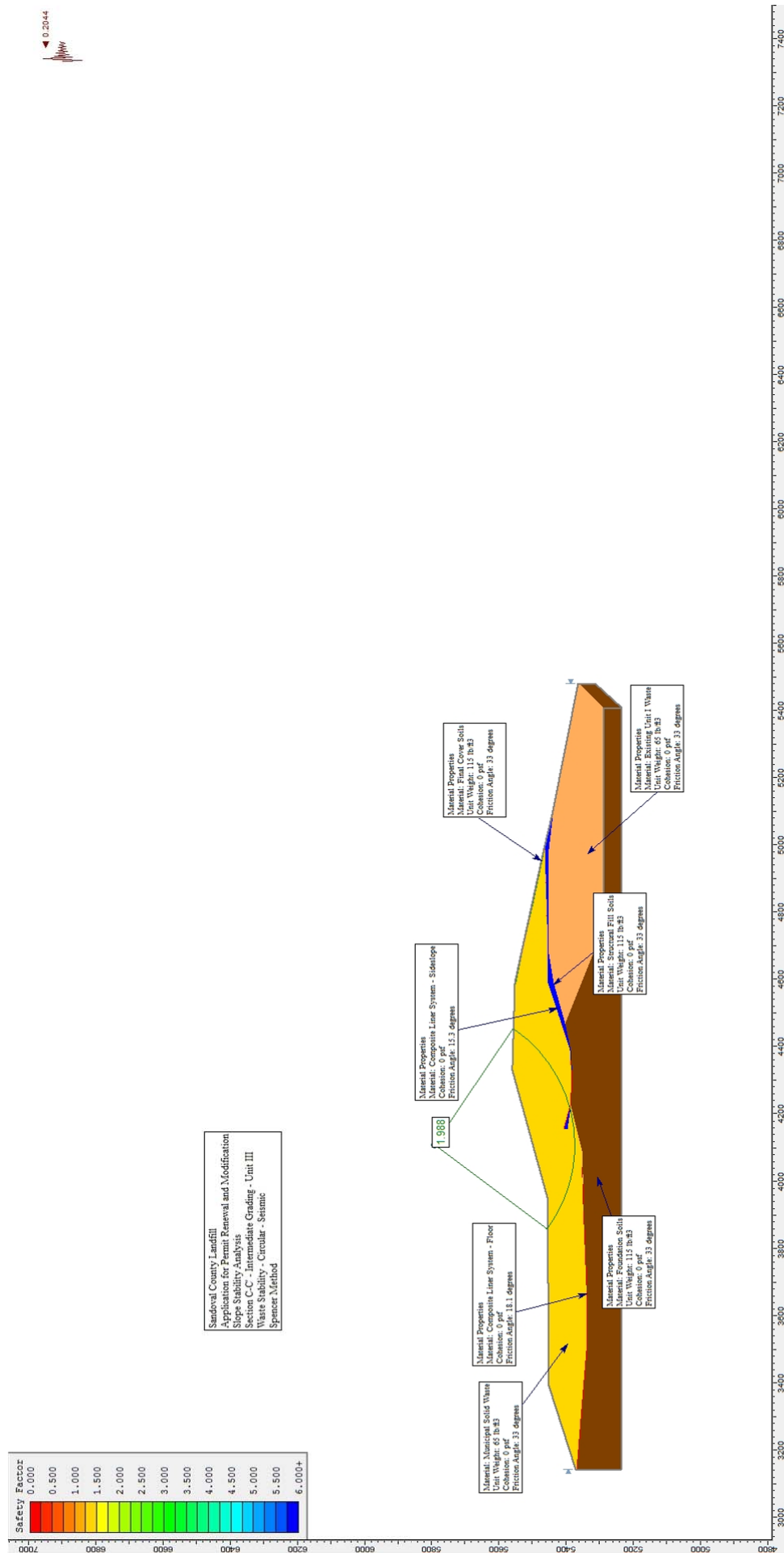
External Boundary

3140.00	5236.06
5408.77	5234.76
5407.59	5285.50
4756.84	5286.74
5408.84	5286.74
5408.84	5234.71
5480.00	5314.00
5480.00	5361.00
5480.00	5364.00
5090.00	5442.00
4990.00	5465.00
4732.67	5520.75
4690.00	5530.00
4590.03	5550.99
4590.04	5550.98
4590.04	5550.98
4590.03	5550.98
4588.24	5551.06
4588.15	5551.06
4588.11	5551.07
4587.29	5551.09
4422.06	5556.81
4346.25	5559.44
4330.00	5560.00
3950.00	5456.00
3440.44	5451.45
3390.01	5451.00
3390.01	5447.00
3390.00	5446.99
3390.00	5447.00
3390.00	5451.00
3140.00	5370.00
3140.00	5368.00
3140.00	5366.00

Circular Failure Surface

4108.11	5791.42
3857.06	5455.17
4455.24	5555.66





Slide Analysis Information

Document Name

File Name: Section C-C' Unit IV-Unit III Intermediate Grading Circular Seismic Waste Unit III

Project Settings

Project Title: Sandoval County Landfill - Permit Renewal and Modification

Failure Direction: Right to Left

Units of Measurement: Imperial Units

Pore Fluid Unit Weight: 62.4 lb/ft³

Groundwater Method: Water Surfaces

Data Output: Standard

Calculate Excess Pore Pressure: Off

Allow Ru with Water Surfaces or Grids: Off

Random Numbers: Pseudo-random Seed

Random Number Seed: 10116

Random Number Generation Method: Park and Miller v.3

Analysis Methods

Analysis Methods used:

Bishop simplified

Janbu simplified

Spencer

Number of slices: 25

Tolerance: 0.005

Maximum number of iterations: 50

Surface Options

Surface Type: Circular

Search Method: Grid Search

Radius increment: 10

Composite Surfaces: Enabled

Reverse Curvature: Create Tension Crack

Minimum Elevation: 5236

Minimum Depth: Not Defined

Loading

Seismic Load Coefficient (Horizontal): 0.2044

Material Properties

Material: Existing Unit I Waste

Strength Type: Mohr-Coulomb

Unit Weight: 65 lb/ft³

Cohesion: 0 psf

Friction Angle: 33 degrees

Water Surface: None

Material: Municipal Solid Waste

Strength Type: Mohr-Coulomb

Unit Weight: 65 lb/ft³

Cohesion: 0 psf

Friction Angle: 33 degrees

Water Surface: None

Material: Structural Fill Soils

Strength Type: Mohr-Coulomb

Unit Weight: 115 lb/ft³

Cohesion: 0 psf

Friction Angle: 33 degrees

Water Surface: None

Material: Composite Liner System

Strength Type: Mohr-Coulomb

Unit Weight: 95.5 lb/ft³

Cohesion: 0 psf

Friction Angle: 19 degrees

Water Surface: None

Material: Foundation Soils

Strength Type: Mohr-Coulomb

Unit Weight: 115 lb/ft³

Cohesion: 0 psf

Friction Angle: 33 degrees

Water Surface: None

Material: Final Cover Soils

Strength Type: Mohr-Coulomb

Unit Weight: 115 lb/ft³

Cohesion: 0 psf

Friction Angle: 33 degrees

Water Surface: None

Global Minimums

Method: bishop simplified

FS: 1.967030

Center: 4108.110, 5791.417

Radius: 419.635

Left Slip Surface Endpoint: 3857.048, 5455.170

Right Slip Surface Endpoint: 4455.262, 5555.664

Resisting Moment=1.03884e+009 lb-ft

Driving Moment=5.28126e+008 lb-ft

Method: janbu simplified

FS: 1.709770

Center: 4108.110, 5791.417

Radius: 419.635

Left Slip Surface Endpoint: 3857.048, 5455.170

Right Slip Surface Endpoint: 4455.262, 5555.664

Resisting Horizontal Force=2.27986e+006 lb

Driving Horizontal Force=1.33344e+006 lb

Method: spencer

FS: 1.987910

Center: 4108.110, 5791.417

Radius: 419.635

Left Slip Surface Endpoint: 3857.048, 5455.170

Right Slip Surface Endpoint: 4455.262, 5555.664

Resisting Moment=1.04987e+009 lb-ft

Driving Moment=5.28126e+008 lb-ft

Resisting Horizontal Force=2.33386e+006 lb

Driving Horizontal Force=1.17403e+006 lb

Valid / Invalid Surfaces

Method: bishop simplified

Number of Valid Surfaces: 1

Number of Invalid Surfaces: 0

Method: janbu simplified

Number of Valid Surfaces: 1

Number of Invalid Surfaces: 0

Method: spencer

Number of Valid Surfaces: 1

Number of Invalid Surfaces: 0

List of All Coordinates

Circular Failure Surface

4108.110 5791.417

3857.062 5455.170

4455.244 5555.665

Material Boundary

5408.842 5286.738

5480.000 5361.000

Material Boundary

4468.000 5403.000

4756.844 5286.738

Material Boundary

4330.082 5559.438

4346.250 5559.438

Material Boundary

4155.000 5405.000

4225.000 5386.000

Material Boundary

4990.000 5462.000

5090.000 5439.000

5480.000 5361.000

Material Boundary

4155.000 5404.686

4155.000	5395.000
4222.418	5385.369
4222.466	5385.362
4225.000	5385.000
4300.000	5380.000
4390.000	5385.000
4468.000	5403.000
4589.000	5435.000
4690.000	5452.000
4990.000	5450.000
5090.000	5439.000
4990.000	5463.000
4987.691	5462.942
4985.861	5462.897
4687.494	5455.456
4655.504	5454.658
4589.000	5453.000
4513.570	5427.580
4492.524	5420.488
4387.094	5384.958

Material Boundary

3950.000	5456.000
4330.082	5559.438
4584.679	5548.184
4585.526	5548.155
4590.000	5548.000
4593.921	5547.177
4690.000	5527.000
4826.869	5497.345
4985.861	5462.897
4990.000	5462.000
4690.000	5453.000

Material Boundary

4593.921	5547.177
4826.869	5497.345
4987.691	5462.942
4990.428	5462.357

Material Boundary

3140.000	5366.000
3262.000	5357.000
3525.014	5335.167
3525.083	5335.089
3674.218	5337.167
3690.052	5337.404
3911.467	5346.067
3932.000	5347.000
3948.694	5347.423
4090.000	5351.000
4225.000	5385.000
4225.000	5386.000
4222.418	5385.369
4090.000	5353.000
3932.000	5349.000

3689.923 5339.337
3524.899 5338.000
3262.000 5359.000
3140.000 5368.000

Material Boundary

3262.000 5359.000
3525.014 5335.167
3525.000 5335.000
3674.218 5337.167
3689.923 5339.337
3911.467 5346.067
3948.694 5347.423
3992.000 5349.000
4090.000 5353.000

Material Boundary

3140.000 5368.000
3389.968 5446.990
3390.000 5447.000

Material Boundary

4155.428 5407.551
4225.000 5388.000
4300.000 5383.000
4390.000 5389.000
4441.000 5404.000
4451.509 5407.091
4458.000 5409.000
4470.505 5413.295
4487.839 5419.250
4589.000 5454.000
4655.504 5454.658
4690.000 5455.000
4990.000 5462.000
4990.000 5460.000
4690.000 5453.000
4589.000 5452.000
4492.524 5420.488
4470.505 5413.295
4451.509 5407.091
4390.000 5387.000
4300.000 5382.000
4225.000 5386.000
4155.000 5404.686
4155.000 5405.000
4155.428 5407.551

Material Boundary

4225.000 5386.000
4300.000 5381.000
4390.000 5387.000
4441.000 5404.000
4450.000 5407.000
4487.839 5419.250
4513.570 5427.580

4589.000 5452.000

Material Boundary

3391.150 5450.655

3391.233 5450.656

3440.436 5451.447

External Boundary

3140.000 5236.064

5408.768 5234.764

5407.588 5285.504

4756.844 5286.738

5408.842 5286.738

5408.842 5234.712

5480.000 5314.000

5480.000 5361.000

5480.000 5364.000

5090.000 5442.000

4990.000 5465.000

4732.674 5520.754

4690.000 5530.000

4590.026 5550.995

4590.042 5550.984

4590.036 5550.984

4590.026 5550.985

4588.244 5551.061

4588.154 5551.064

4588.106 5551.066

4587.290 5551.094

4422.057 5556.813

4346.250 5559.438

4330.000 5560.000

3950.000 5456.000

3440.436 5451.447

3390.008 5450.997

3390.008 5447.000

3390.000 5446.988

3390.000 5447.000

3390.000 5451.000

3140.000 5370.000

3140.000 5368.000

3140.000 5366.000

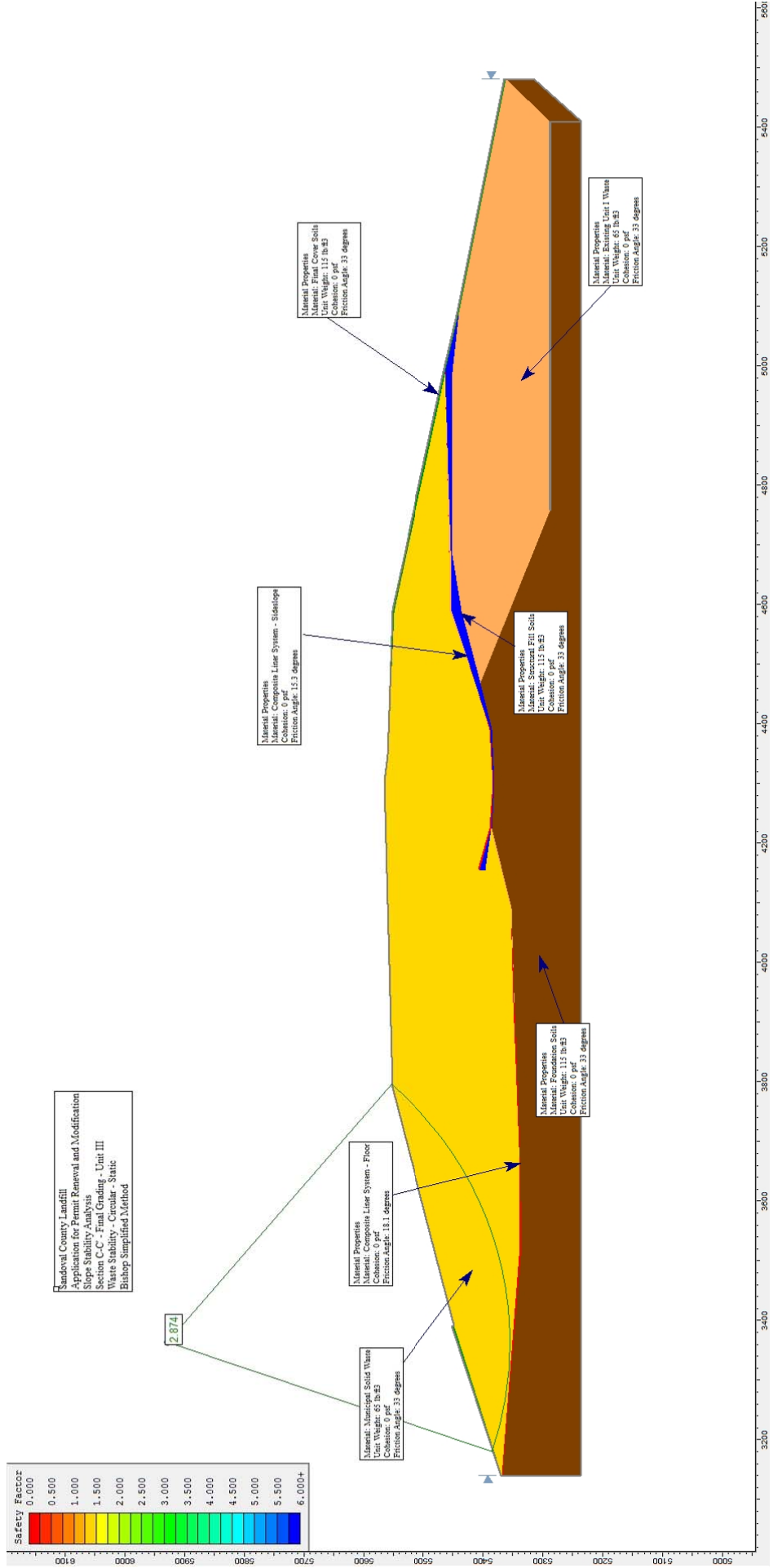
**APPLICATION FOR PERMIT RENEWAL AND MODIFICATION
SANDOVAL COUNTY LANDFILL**

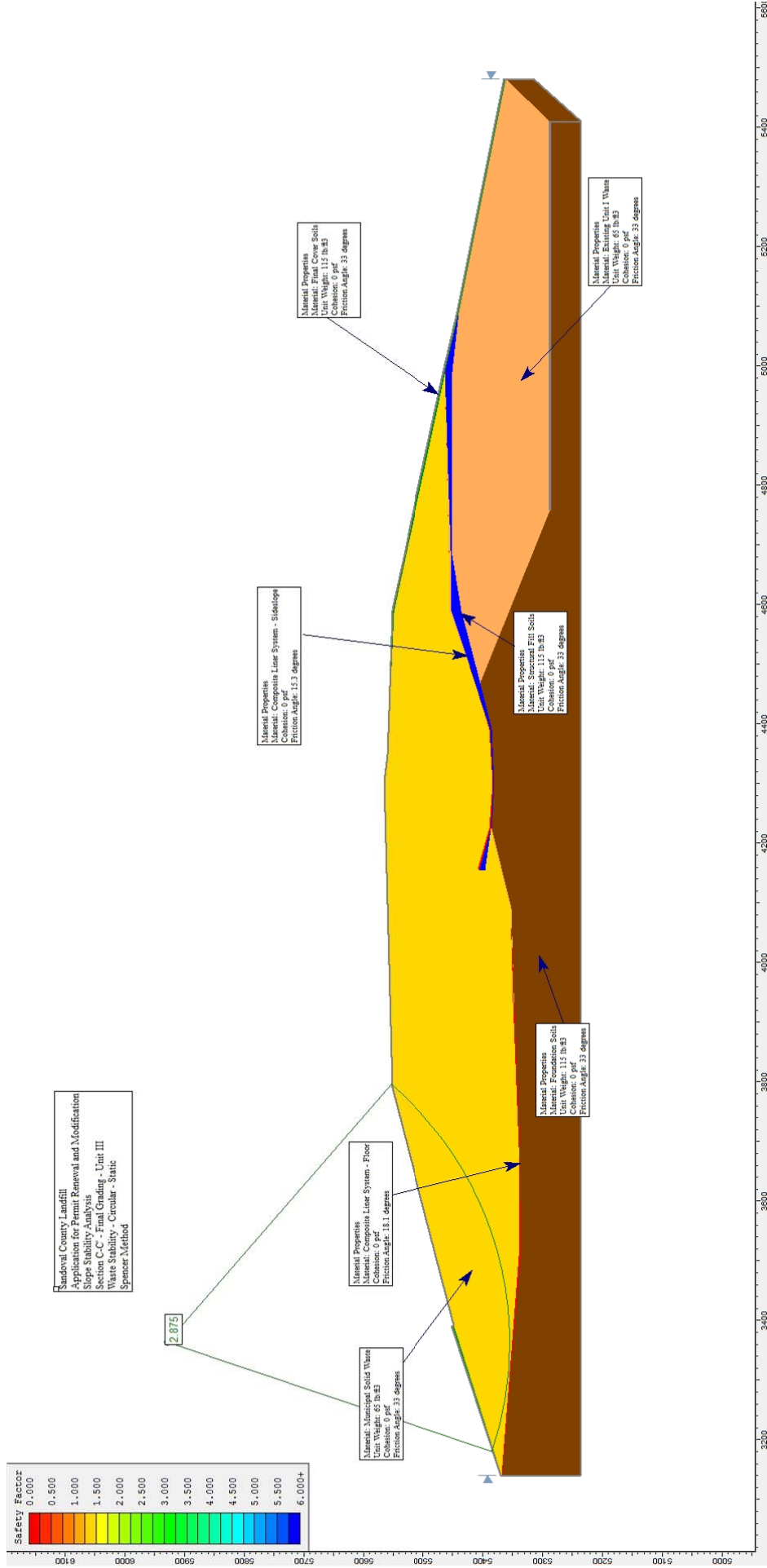
**VOLUME III: LANDFILL ENGINEERING CALCULATIONS
SECTION 3: SLOPE STABILITY ANALYSIS**

ATTACHMENT III.3.E-9

SCENARIO 17: SECTION C-C'; CIRCULAR, STATIC

SCENARIO 18: SECTION C-C', CIRCULAR, SEISMIC





Slide Analysis Information

Document Name

File Name: Section C-C' Unit IV-Unit III Final Grading Circular Static

Project Settings

Project Title: Sandoval County Landfill - Permit Renewal and Modification
Failure Direction: Right to Left
Units of Measurement: Imperial Units
Pore Fluid Unit Weight: 62.4 lb/ft³
Groundwater Method: Water Surfaces
Data Output: Standard
Calculate Excess Pore Pressure: Off
Allow Ru with Water Surfaces or Grids: Off
Random Numbers: Pseudo-random Seed
Random Number Seed: 10116
Random Number Generation Method: Park and Miller v.3

Analysis Methods

Analysis Methods used:

Bishop simplified
Janbu simplified
Spencer

Number of slices: 25
Tolerance: 0.005
Maximum number of iterations: 50

Surface Options

Surface Type: Circular
Search Method: Grid Search
Radius increment: 10
Composite Surfaces: Disabled
Reverse Curvature: Create Tension Crack
Minimum Elevation: Not Defined
Minimum Depth: Not Defined

Material Properties

Material: Existing Unit I Waste
Strength Type: Mohr-Coulomb
Unit Weight: 65 lb/ft³
Cohesion: 0 psf
Friction Angle: 33 degrees
Water Surface: None

Material: Municipal Solid Waste
Strength Type: Mohr-Coulomb
Unit Weight: 65 lb/ft³

Cohesion: 0 psf
Friction Angle: 33 degrees
Water Surface: None

Material: Structural Fill Soils
Strength Type: Mohr-Coulomb
Unit Weight: 115 lb/ft³
Cohesion: 0 psf
Friction Angle: 33 degrees
Water Surface: None

Material: Composite Liner System
Strength Type: Mohr-Coulomb
Unit Weight: 95.5 lb/ft³
Cohesion: 0 psf
Friction Angle: 19 degrees
Water Surface: None

Material: Foundation Soils
Strength Type: Mohr-Coulomb
Unit Weight: 115 lb/ft³
Cohesion: 0 psf
Friction Angle: 33 degrees
Water Surface: None

Material: Final Cover Soils
Strength Type: Mohr-Coulomb
Unit Weight: 115 lb/ft³
Cohesion: 0 psf
Friction Angle: 33 degrees
Water Surface: None

List of All Coordinates

Material Boundary
5408.84 5286.74
5480.00 5361.00

Material Boundary
4468.00 5403.00
4756.84 5286.74

Material Boundary
4155.00 5405.00
4225.00 5386.00

Material Boundary
4990.00 5462.00
5090.00 5439.00
5480.00 5361.00

Material Boundary
4155.00 5404.69
4155.00 5395.00
4222.42 5385.37
4222.47 5385.36

4225.00	5385.00
4300.00	5380.00
4390.00	5385.00
4468.00	5403.00
4589.00	5435.00
4690.00	5452.00
4990.00	5450.00
5090.00	5439.00
4990.00	5463.00
4987.69	5462.94
4985.86	5462.90
4687.49	5455.46
4655.50	5454.66
4589.00	5453.00
4513.57	5427.58
4492.52	5420.49
4387.09	5384.96

Material Boundary

4349.43	5559.33
4584.68	5548.18
4585.53	5548.15
4590.00	5548.00
4593.92	5547.18
4690.00	5527.00
4826.87	5497.35
4985.86	5462.90
4990.00	5462.00
4690.00	5453.00

Material Boundary

4593.92	5547.18
4826.87	5497.35
4987.69	5462.94
4990.43	5462.36

Material Boundary

3140.00	5366.00
3262.00	5357.00
3525.01	5335.17
3525.08	5335.09
3674.22	5337.17
3690.05	5337.40
3911.47	5346.07
3932.00	5347.00
3948.69	5347.42
4090.00	5351.00
4225.00	5385.00
4225.00	5386.00
4222.42	5385.37
4090.00	5353.00
3932.00	5349.00
3689.92	5339.34
3524.90	5338.00
3262.00	5359.00
3140.00	5368.00

Material Boundary

3262.00	5359.00
3525.01	5335.17
3525.00	5335.00
3674.22	5337.17
3689.92	5339.34
3911.47	5346.07
3948.69	5347.42
3992.00	5349.00
4090.00	5353.00

Material Boundary

3140.00	5368.00
3389.97	5446.99
3390.00	5447.00

Material Boundary

4155.43	5407.55
4225.00	5388.00
4300.00	5383.00
4390.00	5389.00
4441.00	5404.00
4451.51	5407.09
4458.00	5409.00
4470.50	5413.30
4487.84	5419.25
4589.00	5454.00
4655.50	5454.66
4690.00	5455.00
4990.00	5462.00
4990.00	5460.00
4690.00	5453.00
4589.00	5452.00
4492.52	5420.49
4470.50	5413.30
4451.51	5407.09
4390.00	5387.00
4300.00	5382.00
4225.00	5386.00
4155.00	5404.69
4155.00	5405.00
4155.43	5407.55

Material Boundary

4225.00	5386.00
4300.00	5381.00
4390.00	5387.00
4441.00	5404.00
4450.00	5407.00
4487.84	5419.25
4513.57	5427.58
4589.00	5452.00

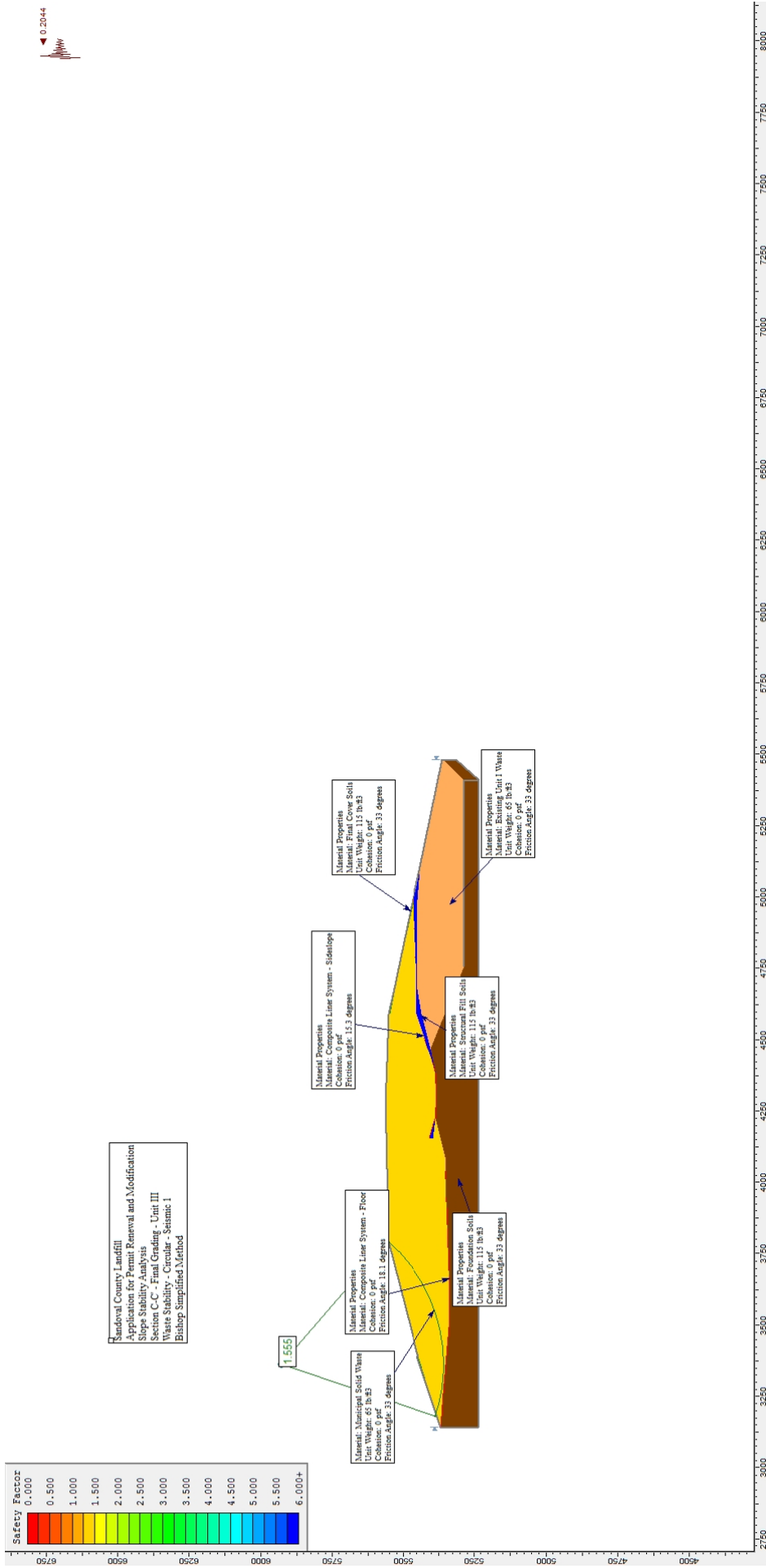
External Boundary

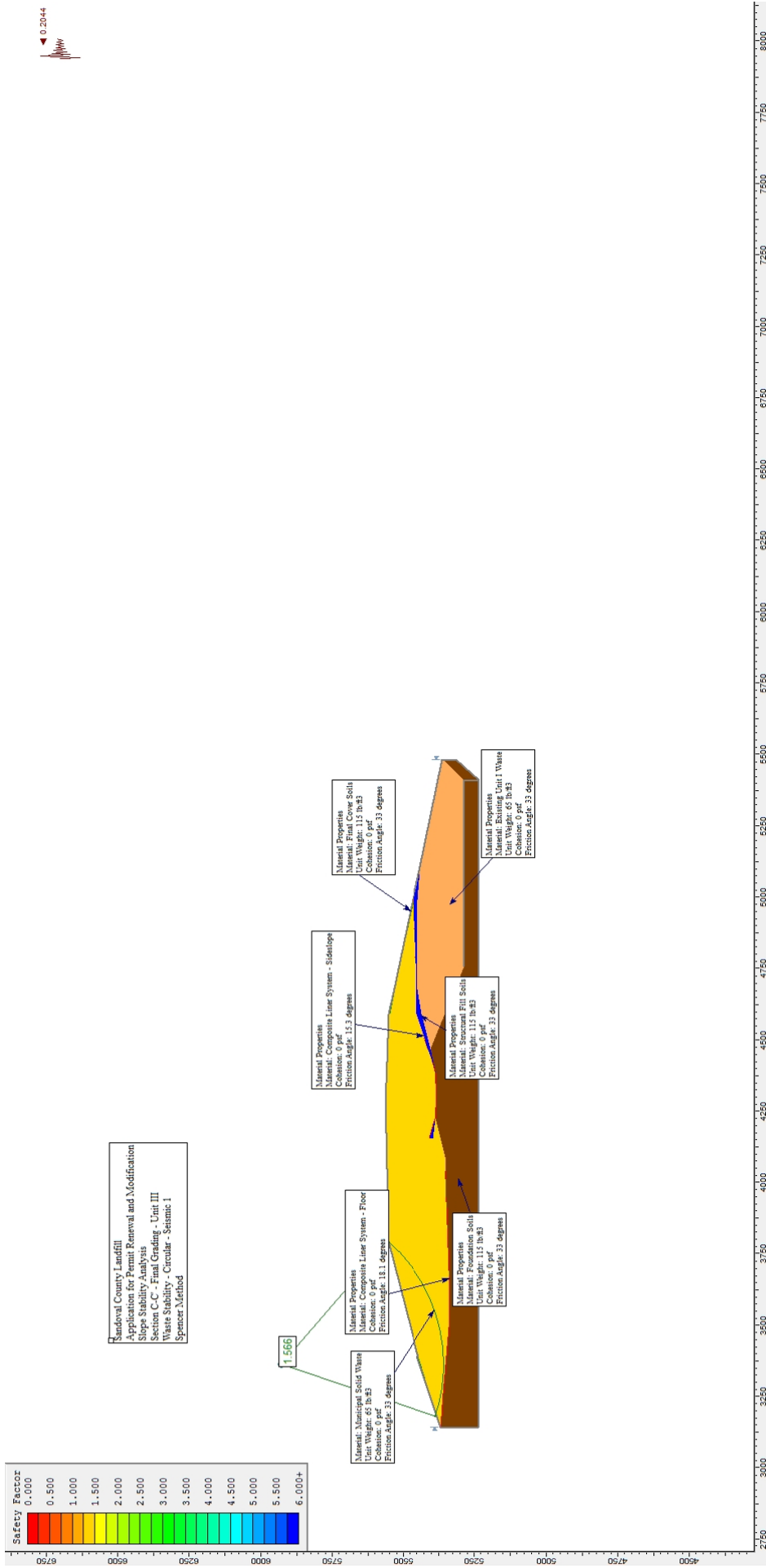
3140.00	5236.06
---------	---------

5408.77	5234.76
5407.59	5285.50
4756.84	5286.74
5408.84	5286.74
5408.84	5234.71
5480.00	5314.00
5480.00	5361.00
5480.00	5364.00
5090.00	5442.00
4990.00	5465.00
4732.67	5520.75
4690.00	5530.00
4590.03	5550.99
4590.04	5550.98
4590.04	5550.98
4590.03	5550.98
4588.24	5551.06
4588.15	5551.06
4588.11	5551.07
4587.29	5551.09
4422.06	5556.81
4349.43	5559.33
4346.25	5559.44
4346.94	5559.72
4346.13	5560.00
4301.75	5564.66
3790.28	5551.35
3404.87	5450.88
3390.01	5447.00
3390.00	5446.99
3390.00	5447.00
3390.00	5451.00
3140.00	5370.00
3140.00	5368.00
3140.00	5366.00

Circular Failure Surface

3362.64	5927.58
3179.59	5382.83
3797.21	5551.53





Slide Analysis Information

Document Name

File Name: Section C-C' Unit IV-Unit III Final Grading Circular Seismic

Project Settings

Project Title: Sandoval County Landfill - Permit Renewal and Modification
Failure Direction: Right to Left
Units of Measurement: Imperial Units
Pore Fluid Unit Weight: 62.4 lb/ft³
Groundwater Method: Water Surfaces
Data Output: Standard
Calculate Excess Pore Pressure: Off
Allow Ru with Water Surfaces or Grids: Off
Random Numbers: Pseudo-random Seed
Random Number Seed: 10116
Random Number Generation Method: Park and Miller v.3

Analysis Methods

Analysis Methods used:

Bishop simplified

Janbu simplified

Spencer

Number of slices: 25

Tolerance: 0.005

Maximum number of iterations: 50

Surface Options

Surface Type: Circular

Search Method: Grid Search

Radius increment: 10

Composite Surfaces: Disabled

Reverse Curvature: Create Tension Crack

Minimum Elevation: Not Defined

Minimum Depth: Not Defined

Loading

Seismic Load Coefficient (Horizontal): 0.2044

Material Properties

Material: Existing Unit I Waste

Strength Type: Mohr-Coulomb

Unit Weight: 65 lb/ft³

Cohesion: 0 psf

Friction Angle: 33 degrees

Water Surface: None

Material: Municipal Solid Waste

Strength Type: Mohr-Coulomb

Unit Weight: 65 lb/ft³

Cohesion: 0 psf

Friction Angle: 33 degrees

Water Surface: None

Material: Structural Fill Soils

Strength Type: Mohr-Coulomb

Unit Weight: 115 lb/ft³

Cohesion: 0 psf

Friction Angle: 33 degrees

Water Surface: None

Material: Composite Liner System

Strength Type: Mohr-Coulomb

Unit Weight: 95.5 lb/ft³

Cohesion: 0 psf

Friction Angle: 19 degrees

Water Surface: None

Material: Foundation Soils

Strength Type: Mohr-Coulomb

Unit Weight: 115 lb/ft³

Cohesion: 0 psf

Friction Angle: 33 degrees

Water Surface: None

Material: Final Cover Soils

Strength Type: Mohr-Coulomb

Unit Weight: 115 lb/ft³

Cohesion: 0 psf

Friction Angle: 33 degrees

Water Surface: None

List of All Coordinates

Material Boundary

5408.84 5286.74

5480.00 5361.00

Material Boundary

4468.00 5403.00

4756.84 5286.74

Material Boundary

4155.00 5405.00

4225.00 5386.00

Material Boundary

4990.00 5462.00

5090.00 5439.00

5480.00 5361.00

Material Boundary

4155.00	5404.69
4155.00	5395.00
4222.42	5385.37
4222.47	5385.36
4225.00	5385.00
4300.00	5380.00
4390.00	5385.00
4468.00	5403.00
4589.00	5435.00
4690.00	5452.00
4990.00	5450.00
5090.00	5439.00
4990.00	5463.00
4987.69	5462.94
4985.86	5462.90
4687.49	5455.46
4655.50	5454.66
4589.00	5453.00
4513.57	5427.58
4492.52	5420.49
4387.09	5384.96

Material Boundary

4349.43	5559.33
4584.68	5548.18
4585.53	5548.15
4590.00	5548.00
4593.92	5547.18
4690.00	5527.00
4826.87	5497.35
4985.86	5462.90
4990.00	5462.00
4690.00	5453.00

Material Boundary

4593.92	5547.18
4826.87	5497.35
4987.69	5462.94
4990.43	5462.36

Material Boundary

3140.00	5366.00
3262.00	5357.00
3525.01	5335.17
3525.08	5335.09
3674.22	5337.17
3690.05	5337.40
3911.47	5346.07
3932.00	5347.00
3948.69	5347.42
4090.00	5351.00
4225.00	5385.00
4225.00	5386.00
4222.42	5385.37
4090.00	5353.00
3932.00	5349.00

3689.92	5339.34
3524.90	5338.00
3262.00	5359.00
3140.00	5368.00

Material Boundary

3262.00	5359.00
3525.01	5335.17
3525.00	5335.00
3674.22	5337.17
3689.92	5339.34
3911.47	5346.07
3948.69	5347.42
3992.00	5349.00
4090.00	5353.00

Material Boundary

3140.00	5368.00
3389.97	5446.99
3390.00	5447.00

Material Boundary

4155.43	5407.55
4225.00	5388.00
4300.00	5383.00
4390.00	5389.00
4441.00	5404.00
4451.51	5407.09
4458.00	5409.00
4470.50	5413.30
4487.84	5419.25
4589.00	5454.00
4655.50	5454.66
4690.00	5455.00
4990.00	5462.00
4990.00	5460.00
4690.00	5453.00
4589.00	5452.00
4492.52	5420.49
4470.50	5413.30
4451.51	5407.09
4390.00	5387.00
4300.00	5382.00
4225.00	5386.00
4155.00	5404.69
4155.00	5405.00
4155.43	5407.55

Material Boundary

4225.00	5386.00
4300.00	5381.00
4390.00	5387.00
4441.00	5404.00
4450.00	5407.00
4487.84	5419.25
4513.57	5427.58

4589.00 5452.00

External Boundary

3140.00 5236.06
5408.77 5234.76
5407.59 5285.50
4756.84 5286.74
5408.84 5286.74
5408.84 5234.71
5480.00 5314.00
5480.00 5361.00
5480.00 5364.00
5090.00 5442.00
4990.00 5465.00
4732.67 5520.75
4690.00 5530.00
4590.03 5550.99
4590.04 5550.98
4590.04 5550.98
4590.03 5550.98
4588.24 5551.06
4588.15 5551.06
4588.11 5551.07
4587.29 5551.09
4422.06 5556.81
4349.43 5559.33
4346.25 5559.44
4346.94 5559.72
4346.13 5560.00
4301.75 5564.66
3790.28 5551.35
3404.87 5450.88
3390.01 5447.00
3390.00 5446.99
3390.00 5447.00
3390.00 5451.00
3140.00 5370.00
3140.00 5368.00
3140.00 5366.00

Circular Failure Surface

3362.64 5927.58
3179.59 5382.83
3797.21 5551.53

**APPLICATION FOR PERMIT RENEWAL AND MODIFICATION
SANDOVAL COUNTY LANDFILL**

**VOLUME III: LANDFILL ENGINEERING CALCULATIONS
SECTION 4: COMPATIBILITY DEMONSTRATION**

TABLE OF CONTENTS

1.0	SUMMARY	4-1
-----	---------------	-----

LIST OF TABLES

Table No.	Title	Page
III.4.1	GEOSYNTHETIC APPLICATIONS AND COMPATIBILITY DEMONSTRATION	4-2

LIST OF ATTACHMENTS

Attachment No.	Title
III.4.A	HDPE GEOMEMBRANES REFERENCE DOCUMENTATION
III.4.B	GEOSYNTHETIC CLAY LINER REFERENCE DOCUMENTATION
III.4.C	GEOTEXTILE REFERENCE DOCUMENTATION
III.4.D	HPDE GEONET REFERENCE DOCUMENTATION
III.4.E	HDPE GEOGRIDS REFERENCE DOCUMENTATION
III.4.F	HDPE PIPE REFERENCE DOCUMENTATION
III.4.G	PVC PIPE REFERENCE DOCUMENTATION

APPLICATION FOR PERMIT RENEWAL AND MODIFICATION SANDOVAL COUNTY LANDFILL

VOLUME III: LANDFILL ENGINEERING CALCULATIONS SECTION 4: COMPATIBILITY DEMONSTRATION

1.0 SUMMARY

Geosynthetics have a proven track record in a variety of civil engineering applications. Landfill construction provides a unique opportunity to incorporate a range of engineered materials that exceed the equivalent performance of soils. The design of the Sandoval County Landfill (SCLF) includes several examples of geosynthetics and “plastics” deployed for their superior characteristics, usually applied in conjunction with soil layers:

- Geomembranes (flexible membrane liners) provided as barrier layer in the liner system.
- Geotextiles serving as cushioning layers and as filters to maintain flow.
- Geosynthetic clay liners (GCLs) employed as secondary composite layers for liners.
- Geogrids used to enhance structural stability of the liner systems.
- Geonets, which include geotextile layers on both sides, to provide a preferred flow zone for landfill gas collection.
- The use of High Density Polyethylene (HDPE) and Polyvinyl Chloride (PVC) and piping systems.

Geosynthetics are selected in the design process for their demonstrated performance characteristics in the project’s environmental setting. These materials must be able to withstand the physical and chemical forces that they will experience, as documented in this section. **Attachment III.4.A** includes recent research results that indicate the functional longevity of HDPE liners in similar installations is in the hundreds of years.

This section provides demonstrations, as required by 20.9.4 NMAC that the geosynthetic components are compatible with the waste, contact water, and gases to be encountered within the landfill environment. The attached compatibility documentation includes published reports and test results; and is further endorsed by industry experience and proven installations by the design engineers. For the performance criteria of both soil and geosynthetic components to be achieved, they must be constructed in strict accordance with the **Permit Plans (Volume II.I)** and the Construction Quality Assurance (CQA) Plan (**Volume II.4**), of this Application for Permit.

Table III.4.1 is an index of compatibility data provided for each of the prescribed geosynthetic materials and their function in the engineering design.

TABLE III.4.1
Geosynthetic Applications and Compatibility Demonstration
Sandoval County Landfill

	MATERIAL	FUNCTION	ATTACHED REFERENCE DOCUMENTATION	
1	HDPE Geomembrane	Primary barrier layer for landfill liner.	III.4.A	<i>Geomembrane Lifetime Prediction: Unexposed and Exposed Conditions</i>
				<i>Chemical Compatibility of Poly-Flex Liners*</i>
				<i>Chemical Resistance Table Low Density and High Density Polyethylene*</i>
				<i>NSC, Contaminant Solutions for Industrial Waste; HDPE Geomembrane</i>
				<i>Liner Longevity Article: Geosynthetics Magazine, Oct/Nov 2008</i>
2	GCL	Secondary layer in composite liner.	III.4.B	<i>The Effects of Leachate on the Hydraulic Conductivity of Bentomat</i>
				<i>Bench-scale Hydraulic Conductivity Tests of Bentonitic Blanket Materials for Liner and Cover Systems (Thesis by Paula Estornell)</i>
3	Geotextile	Filter layer around leachate collection piping and filter for geocomposites.	III.4.C	<i>Amoco Technical Note No. 7, Chemical Resistance of Amoco Polypropylene Geotextiles</i>
				<i>Amoco Technical Note No. 14, Geotextile Polymers for Waste Applications</i>
4	HDPE Geonet	Landfill gas collection layer below cap (includes geotextiles on both sides).	III.4.D	<i>Professional Plastics, Inc. – HDPE and LDPE Resistance Chart by Chemical</i>
5	HDPE GeoGrids	Added structural support for liner system.	III.4.E	<i>Borealis – Chemical Resistance Table Polypropylene*</i>
				<i>Tensar – Structural Geogrid UX1100MSE Product Specification</i>
				<i>Tensar – TriAx® TX160 Geogrid Product Specification</i>
6	HDPE Pipe	Solid and slotted piping, leachate collection system and GCCS.	III.4.F	<i>Chemical Resistance of Plastics and Elastomers Used in Pipeline Construction</i>
				<i>Driscopipe Engineering Characteristics</i>
				<i>Plexco Chemical Resistance Information</i>
7	PVC Pipe	Solid and slotted piping, GCCS.	III.4.G	<i>Certainteed - PVC Chemical Resistance</i>

Acronyms used:

GCL: Geosynthetic Clay Liner
FML: Flexible Membrane Liner
GCCS: Gas collection and control system

PVC: Polyvinyl Chloride
HDPE: High Density Polyethylene

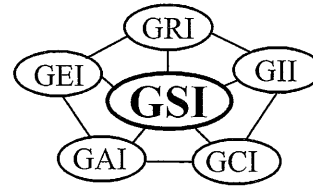
**APPLICATION FOR PERMIT RENEWAL AND MODIFICATION
SANDOVAL COUNTY LANDFILL**

**VOLUME III: LANDFILL ENGINEERING CALCULATIONS
SECTION 4: COMPATIBILITY DEMONSTRATION**

**ATTACHMENT III.4.A
HDPE GEOMEMBRANES REFERENCE DOCUMENTATION**

Geosynthetic Institute

475 Kedron Avenue
Folsom, PA 19033-1208 USA
TEL (610) 522-8440
FAX (610) 522-8441



GRI White Paper #6

- on -

**Geomembrane Lifetime Prediction:
Unexposed and Exposed Conditions**

by

**Robert M. Koerner, Y. Grace Hsuan and George R. Koerner
Geosynthetic Institute
475 Kedron Avenue
Folsom, PA 19033 USA**

**Phone (610) 522-8440
Fax (610) 522-8441**

**E-mails:
robert.koerner@coe.drexel.edu
grace.hsuan@coe.drexel.edu
gkoerner@dca.net**

June 7, 2005

Geomembrane Lifetime Prediction: Unexposed and Exposed Conditions

1.0 Introduction

Without any hesitation the most frequently asked question we have had over the past 25 years' is "how long will a particular geomembrane last".* The two-part answer to the question, largely depends on whether the geomembrane is covered in a timely manner or left exposed to the site-specific environment. Before starting, however, recognize that the answer to either covered or exposed geomembrane lifetime prediction is neither easy, nor quick, to obtain. Further complicating the answer is the fact that all geomembranes are formulated materials consisting of (at the minimum), (i) the resin from which the name derives, (ii) carbon black or colorants, (iii) short-term processing stabilizers, and (iv) long-term antioxidants. If the formulation changes (particularly the additives), the predicted lifetime will also change. See Table 1 for the most common types of geomembranes and their approximate formulations.

Table 1 - Types of commonly used geomembranes and their approximate formulations
(based on weight percentage)

Type	Resin	Plasticizer	Fillers	Carbon Black	Additives
HDPE	95-98	0	0	2-3	0.25-1
LLDPE	94-96	0	0	2-3	0.25-3
fPP	85-98	0	0-13	2-4	0.25-2
PVC	50-70	25-35	0-10	2-5	2-5
CSPE	40-60	0	40-50	5-10	5-15
EPDM	25-30	0	20-40	20-40	1-5

HDPE = high density polyethylene

PVC = polyvinyl chloride (plasticized)

LLDPE = linear low density polyethylene

CSPE = chlorsulfonated polyethylene

fPP = flexible polypropylene

EPDM = ethylene propylene diene terpolymer

* More recently, the same question has arisen but focused on geotextiles, geogrids, geopipe, fibers of GCLs, etc. This White Paper, however, is focused on geomembranes due to the general lack of information on the other geosynthetics.

The possible variations being obvious, one must also address the degradation mechanisms which might occur. They are as follows accompanied by some generalized commentary.

- Ultraviolet - occurs only when the geosynthetic is exposed; it will be the focus of the second part of this communication.
- Oxidation - this occurs in all polymers and is the major mechanism in polyolefins (polyethylene and polypropylene) under covered conditions.
- Ozone - this occurs in all polymers that are exposed to the environment. The site-specific environment is critical in this regard.
- Hydrolysis - this is the primary mechanism in polyesters and polyamides.
- Chemical - can occur in all polymers and can vary from water (least aggressive) to organic solvents (most aggressive).
- Radioactive - not a factor unless the polymer is exposed to radioactive materials of sufficiently high intensity to cause chain scission, e.g., high level radioactive waste materials.
- Biological - generally not a factor unless biologically sensitive additives (such as low molecular weight plasticizers) are included in the formulation.
- Stress State - a complicating factor which is site-specific and should be appropriately modeled in the incubation process.
- Temperature - clearly, the higher the temperature the more rapid the degradation of all of the above mechanisms; temperature is critical to lifetime and furthermore is the key to time-temperature-superposition which is the basis of the laboratory incubation methods which will be followed.

2.0 Lifetime Prediction: Unexposed Conditions

Lifetime prediction studies at GRI began at Drexel University under U. S. EPA contract from 1991 to 1997 and have continued under GSI consortium funding since that time. Focus to date has been on HDPE geomembranes beneath solid waste landfills due to its common use in this particular challenging application. Incubation of the coupons has been in landfill simulation cells (see Figure 1) maintained at 85, 75, 65 and 55°C. The specific conditions within these cells are oxidation beneath, chemical (water) from above, and the equivalent of 50 m of solid waste mobilizing compressive stress. Results have been forthcoming over the years insofar as three distinct lifetime stages; see Figure 2.

Stage A - Antioxidant Depletion Time

Stage B - Induction Time to Onset of Degradation

Stage C - Time to Reach 50% Degradation (Halflife)

2.1 Stage A - Antioxidant Depletion Time

The purposes of stabilizer antioxidants are to (i) prevent polymer degradation during processing, and (ii) prevent oxidation reactions from taking place during Stage A of service life, respectively. Obviously, there can only be a given amount of antioxidants in any formulation. Once the antioxidants are depleted, additional oxygen will begin to attack the polymer chains, leading to subsequent stages as shown in Figure 2. The duration of the antioxidant depletion stage depends on both the type and amount of antioxidants.

The depletion of antioxidants is the consequence of two processes: (i) chemical reactions with the oxygen diffusing into the geomembrane, and (ii) physical loss of antioxidants from the geomembrane. The chemical process involves two main functions; the scavenging of free radicals converting them into stable molecules, and the reaction with unstable hydroperoxide

(ROOH) forming a more stable substance. Regarding physical loss, the process involves the distribution of antioxidants in the geomembrane and their volatility and extractability to the site-specific environment.

Hence, the rate of depletion of antioxidants is related to the type and amount of antioxidants, the service temperature, and the nature of the site-specific environment. See Hsuan and Koerner (1998) for additional details.

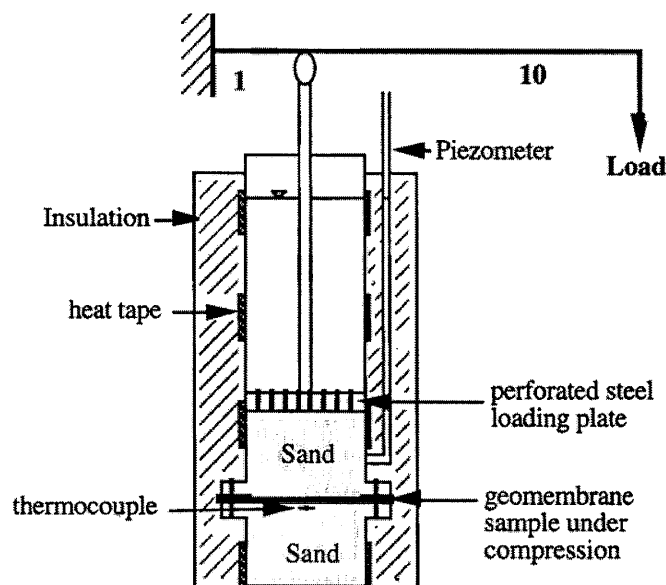


Figure 1. Incubation schematic and photograph of multiple cells maintained at various constant temperatures.

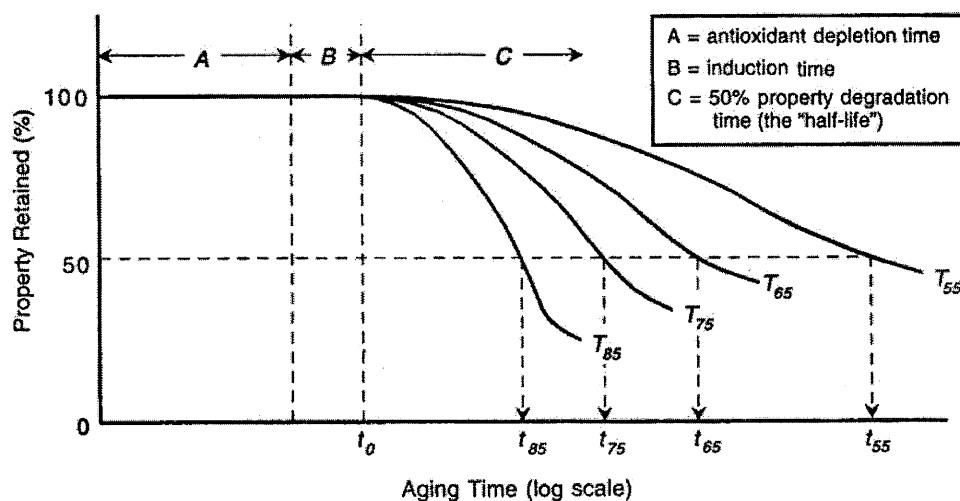


Figure 2. Three conceptual stages in chemical aging of polyolefin geomembranes.

2.2 Stage B - Induction Time to Onset of Degradation

In a pure polyolefin resin, i.e., one without carbon black and antioxidants, oxidation occurs extremely slowly at the beginning, often at an immeasurable rate. Eventually, oxidation occurs more rapidly. The reaction eventually decelerates and once again becomes very slow. This progression is illustrated by the S-shaped curve of Figure 3(a). The initial portion of the curve (before measurable degradation takes place) is called the induction period (or induction time) of the polymer. In the induction period, the polymer reacts with oxygen forming hydroperoxide (ROOH), as indicated in Equations (1)-(3). However, the amount of ROOH in this stage is very small and the hydroperoxide does not further decompose into other free radicals which inhibits the onset of the acceleration stage.

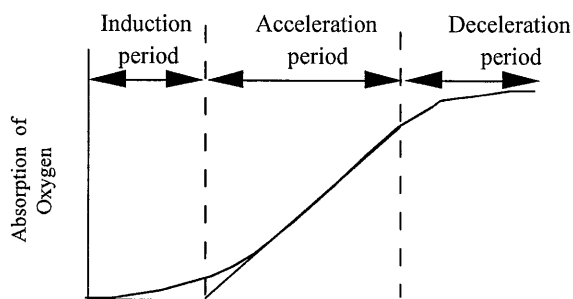
In a stabilized polymer such as one with antioxidants, the accelerated oxidation stage takes an even longer time to be reached. The antioxidants create an additional depletion time stage prior to the onset of the induction time, as shown in Figure 3(b).



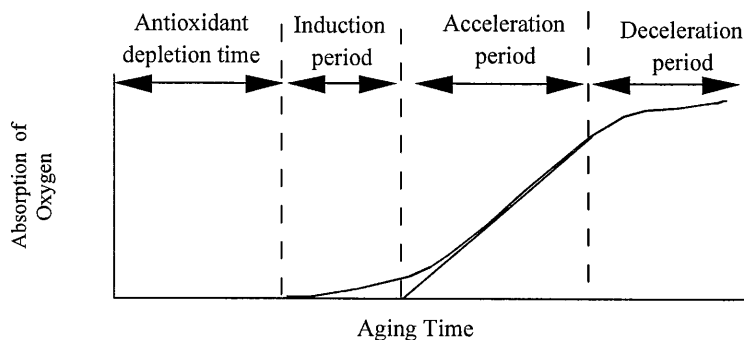
(aided by energy or catalyst residues in the polymer)



In the above, RH represents the polyethylene polymer chains; and the symbol “•” represents free radicals, which are highly reactive molecules.



(a) Pure unstabilized polyethylene

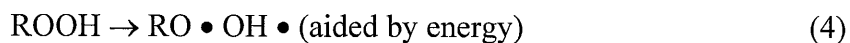


(b) stabilized polyethylene

Figure 3. Curves illustrating various stages of oxidation.

2.3 Stage C - Time to Reach 50% Degradation (Halflife)

As oxidation continues, additional ROOH molecules are being formed. Once the concentration of ROOH reaches a critical level, decomposition of ROOH begins, leading to a substantial increase in the amount of free radicals, as indicated in Equations (4) to (6). The additional free radicals rapidly attack other polymer chains, resulting in an accelerated chain reaction, signifying the end of the induction period, Rapoport and Zaikov (1986). This indicates that the concentration of ROOH has a critical control on the duration of the induction period.



A series of oxidation reactions produces a substantial amount of free radical polymer chains ($\text{R} \bullet$), called alkyl radicals, which can proceed to further reactions leading to either cross-linking or chain scission in the polymer. As the degradation of polymer continues, the physical and mechanical properties of the polymer start to change. The most noticeable change in physical properties is the melt index, since it relates to the molecular weight of the polymer. As for mechanical properties, both tensile break stress (strength) and break strain (elongation) decrease. Ultimately, the degradation becomes so severe that all tensile properties start to change (tear, puncture, burst, etc.) and the engineering performance is jeopardized. This signifies the end of the so-called “service life” of the geomembrane.

Although quite arbitrary, the limit of service life of polymeric materials is often selected as a 50% reduction in a specific design property. This is commonly referred to as the halflife time, or simply the “halflife”. It should be noted that even at halflife, the material still exists and

can function, albeit at a decreased performance level with a factor-of-safety lower than the initial design value.

2.4 Summary of Lifetime Research-to-Date

Stage A, that of antioxidant depletion for HDPE geomembranes as required in the GRI-GM13 Specification, has been well established by our own research and corroborated by others, e.g., Sangram and Rowe (2004). The GRI data for Standard and High Pressure Oxidative Induction Time (OIT) is given in Table 2. The values are quite close to one another. Also, as expected, the lifetime is strongly dependent on the service temperature; with the higher the temperature the shorter the lifetime.

Table 2 - Lifetime prediction of HDPE (nonexposed) at various field temperatures

In Service Temperature (°C)	Stage "A" (yrs.)		Stage "B" (yrs.)	Stage "C" (yrs.)		Total Lifetime (ave. values)
	Std OIT	HP-OIT	Field Data	(max.)	(min.)	
20	200	215	30	255	149	449
25	135	144	25	132	77	270
30	95	98	20	70	41	173
35	65	67	15	38	22	111
40	45	47	10	21	12	73

Notes: Stage "A" measured values from Hsuan and Guan (1997) research via GRI
 Stage "B" estimated values from field samples by GRI
 Stage "C" literature values from Gedde, et al. (1994)

Stage "B", that of induction time, has been obtained by comparing 30-year old polyethylene water and milk containers (containing no long-term antioxidants) with currently produced containers. The data shows that degradation is just beginning to occur as evidenced by slight changes in break strength and elongation, but not in yield strength and elongation. The lifetime for this stage is also given in Table 2.

Stage "C", the time for 50% change of mechanical properties is given in Table 2 as well. The data depends on the activation energy, or slope of the Arrhenius curve, which is very

sensitive to material and experimental techniques. The data is from Gedde, et al. (1994) which is typical of the HDPE resin used for gas pipelines.

Summarizing Stages A, B, and C, it is seen in Table 2 that the halflife of covered HDPE geomembranes (formulated according to the current GRI-GM13 Specification) is estimated to be 449-years at 20°C. This, of course, brings into question the actual temperature for a covered geomembrane such as beneath a solid waste landfill. Figure 4 presents multiple thermocouple monitoring data of a municipal waste landfill liner in Pennsylvania for over 10-years, Koerner and Koerner (2005). Note that for 6-years the temperature was approximately 20°C. At that time and for the subsequent 4-years the temperature increased to approximately 30°C. Thus, the halflife of this geomembrane is predicted to be from 270 to 449 years within this temperature range. The site is still being monitored, see Koerner and Koerner (2005).

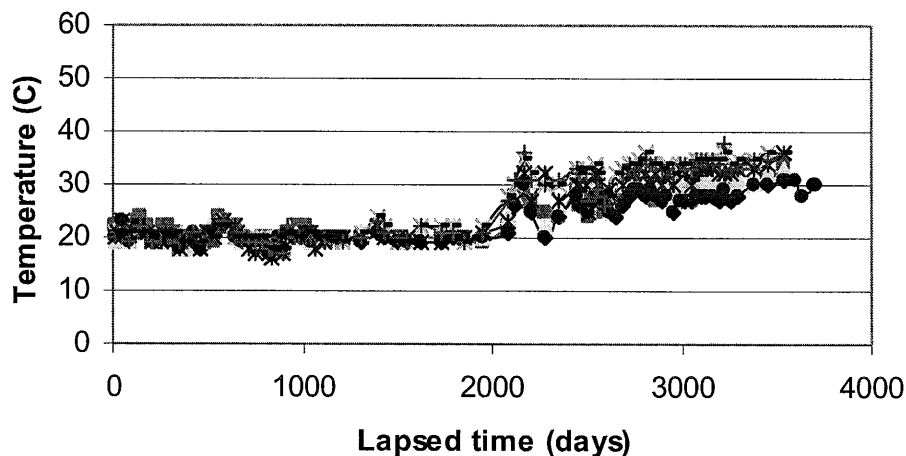


Figure 4. Long-term monitoring of an HDPE liner beneath a municipal solid waste landfill in Pennsylvania.

2.5 Lifetime of Other Covered Geomembranes

By virtue of its widespread use as liners for solid waste landfills, HDPE is by far the widest studied type of geomembrane. Note that in most countries (other than the U.S.), HDPE is the required geomembrane type for solid waste containment. Some commentary on other-than HDPE geomembranes (recall Table 1) follows:

2.5.1 Linear Low Density Polyethylene (LLDPE) geomembranes

The nature of the LLDPE resin and its formulation is very similar to HDPE. The fundamental difference is that LLDPE is a lower density, hence lower crystallinity, than HDPE; e.g., 10% versus 50%. This has the effect of allowing oxygen to diffuse into the polymer structure quicker, and likely decreases Stages A and C. How much is uncertain since no data is available, but it is felt that the lifetime of LLDPE will be somewhat reduced with respect to HDPE.

2.5.2 Plasticizer migration in PVC geomembranes

Since PVC geomembranes necessarily have plasticizers in their formulations so as to provide flexibility, the migration behavior must be addressed for this material. In PVC the plasticizer bonds to the resin and the strength of this bonding versus liquid-to-resin bonding is significant. One of the key parameters of a stable long-lasting plasticizer is its molecular weight. The higher the molecular weight of the plasticizer in a PVC formulation, the more durable will be the material. Conversely, low molecular weight plasticizers have resulted in field failures even under covered conditions. See Miller, et al. (1991), Hammon, et al. (1993), and Giroud and Tisinger (1994) for more detail in this regard.

2.5.3 Crosslinking in EPDM and CSPE geomembranes

The EPDM geomembranes mentioned in Table 1 are crosslinked thermoset materials. The oxidation degradation of EPDM takes place in either ethylene or propylene fraction of the co-polymer via free radical reactions, as expressed in Figure 5, which are described similarly by Equations (4) to (6).

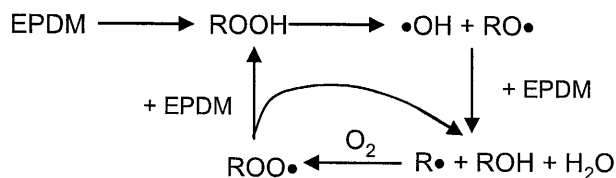


Figure 5. Oxidative degradation of crosslinked EPDM geomembranes, (Wang and Qu, 2003).

For CSPE geomembranes, the degradation mechanism is dehydrochlorination by losing chlorine and generating carbon-carbon double bonds in the main polymer chain, as shown in Figure 6. The carbon-carbon double bonds become the preferred sites for further thermodegradation or cross-linking in the polymer, leading to eventual brittleness of the geomembrane.

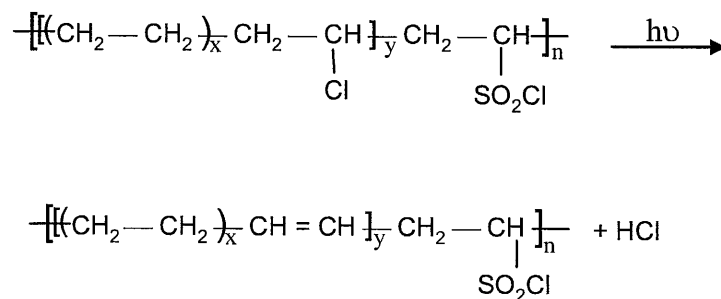


Figure 6. Dechlorination degradation of crosslinked CSPE geomembranes (Chailan, et al., 1995).

Neither EPDM nor CSPE has had a focused laboratory study of the type described for HDPE reported in the open literature. Most of lifetime data for these geomembranes is antidotal by virtue of actual field performance. Under covered conditions, as being considered in this section, there have been no reported failures by either of these thermoset polymers to our knowledge.

3.0 Lifetime Prediction: Exposed Conditions

Lifetime prediction of exposed geomembranes have taken two very different pathways; (i) prediction from anecdotal feedback and field performance, and (ii) from laboratory weathermometer predictions.

3.1 Field Performance

There is a large body of anecdotal information available on field feedback of exposed geomembranes. It comes from two quite different sources, i.e., dams in Europe and flat roofs in the USA.

Regarding exposed geomembranes in dams in Europe, the original trials were using 2.0 mm thick polyisobutylene bonded directly to the face of the dam. There were numerous problems encountered as described by Scuero (1990). Similar experiences followed using PVC geomembranes. In 1980, a geocomposite was first used at Lago Nero which had a 200 g/m² nonwoven geotextile bonded to the PVC geomembrane. This proved quite successful and led to the now-accepted strategy of requiring drainage behind the geomembrane. In addition to thick nonwoven geotextiles, geonets, and geonet composites have been successful. Currently over 50 concrete and masonry dams have been rehabilitated in this manner and are proving successful for over 30-years of service life. The particular type of PVC plasticized geomembranes used for these dams is proving to be quite durable. Tests by the dam owners on residual properties show only nominal changes in properties, Cazzuffi (1998). As indicated in Miller, et al. (1991) and Hammond, et al. (1993), however, different PVC materials and formulations result in very different behavior; the choice of plasticizer and the thickness both being of paramount importance.

Regarding exposed geomembranes in flat roofs, past practice in the USA is almost all with EPDM and CSPE and, more recently, with fPP. Manufacturers of these geomembranes regularly warranty their products for 20-years and such warrants appear to be justified. EPDM and CSPE, being thermoset or elastomeric polymers, can be used in dams without the necessity of having seams by using vertical attachments spaced at 2 to 4 m centers, see Scuero and Vaschetti (1996). Conversely, fPP can be seamed by a number of thermal fusion methods. All of these geomembrane types have good conformability to rough substrates as is typical of concrete and masonry dam rehabilitation. It appears as though experiences (both positive and negative) with geomembranes in flat roofs should be transferred to all types of waterproofing in civil engineering applications.

3.2 Laboratory Weatherometer Predictions

For an accelerated simulation of direct sunlight using a laboratory weatherometer one usually considers a worst-case situation which is the solar maximum condition. This condition consists of global, noon sunlight, on the summer solstice, at normal incidence. It should be recognized that the UV-A range is the target spectrum for a laboratory device to simulate the naturally occurring phenomenon, see Hsuan and Koerner (1993), and Suits and Hsuan (2001).

The Xenon Arc Weatherometer (ASTM G155) was introduced in Germany in 1954. There are two important features; the type of filters and the irradiance settings. Using a quartz inner and borosilicate outer filter (quartz/boro) results in excessive low frequency wavelength degradation. The more common borosilicate inner and outer filters (boro/boro) shows a good correlation with solar maximum conditions, although there is an excess of energy below 300 nm wavelength. Irradiance settings are important adjustments in shifting the response although they do not eliminate the portion of the spectrum below 300 nm frequency. Nevertheless, the Xenon

Arc weatherometer is commonly used method for exposed lifetime prediction of all types of geosynthetics.

UV Fluorescent Lamps (ASTM G154) are an alternative type of accelerated laboratory test device which became available in the early 1970's. They reproduce the ultraviolet portion of the sunlight spectrum but not the full spectrum as in Xenon Arc weatherometers. Earlier FS-40 and UVB-313 lamps give reasonable short wavelength output in comparison to solar maximum. The UVA-340 lamp was introduced in 1987 and its response is seen to reproduce ultraviolet light quite well. This device (as well as other types of weatherometers) can handle elevated temperature and programmed moisture on the test specimens.

Research at the Geosynthetic Institute (GSI) is actively pursuing both Xenon and UV Fluorescent devices on a wide range of geomembranes. Table 3 gives the geomembranes being incubated and the current number of hours of exposure.

Table 5 - Details of the GSI laboratory exposed weatherometer study on various types of geomembranes

Geomembrane Type	Thickness (mm)	UV Fluorescent Exposure*	Xenon Exposure*	Comment
1. HDPE (GM13)	1.50	8000 hrs.	6600 hrs.	Basis of GRI-GM13 Spec
2. LLDPE (GM17)	1.00	8000	6600	Basis of GRI-GM-17 Spec
3. PVC (No. Amer.)	0.75	8000	6600	Low Mol. Wt. Plasticizer
4. PVC (Europe)	2.50	7500	6600	High Mol. Wt. Plasticizer
5. fPP (BuRec)	1.00	2745**	4416**	Field Failure at 26 mos.
6. fPP-R (Texas)	0.91	100	100	Field Failure at 8 years
7. fPP (No. Amer.)	1.00	7500	6600	Expected Good Performance

*As of 12 July 2005 exposure is ongoing

**Light time to reach halflife of break and elongation

3.3 Laboratory Weatherometer Acceleration Factors

The key to validation of any laboratory study is to correlate results to actual field performance. For the nonexposed geomembranes of Section 2 such correlations will take hundreds of years for properly formulated products. For the exposed geomembranes of Section

3, however, the lifetimes are significantly shorter and such correlations are becoming possible. In particular, Geomembrane #5 (flexible polypropylene) of Table 3 was an admittedly poor geomembrane formulation which failed in 26 months of exposure at El Paso, Texas, USA. The reporting of this failure is available in the literature, Comer, et al. (1998). Note that for both UV Fluorescent and Xenon Arc laboratory testing of this material, failure (halflife to 50% reduction in strength and elongation) occurred at 2745 and 4416 hours, respectively. The comparative analysis of laboratory and field for this case history allows for the obtaining of acceleration factors for the two incubation devices.

3.3.1 Comparison between field and UV Fluorescent weatherometer

The light source used in the UV fluorescent weatherometer is UVA with wavelengths from 295-400 nm. In addition, the intensity of the radiation is controlled by the Solar Eye irradiance control system. The UV energy output throughout the test is 68.25 W/m^2 .

The time of exposure to reach 50% elongation at break

$$\begin{aligned} &= 2745 \text{ hr. of light} \\ &= 9,882,000 \text{ seconds} \end{aligned}$$

$$\begin{aligned} \text{Total energy in MJ/m}^2 &= 68.25 \text{ W/m}^2 \times 9,882,000 \\ &= 674.4 \text{ MJ/m}^2 \end{aligned}$$

The field site was located at El Paso, Texas. The UVA radiation energy (295-400 nm) at this site is estimated based on data collected by the South Florida Testing Lab in Arizona (which is a similar atmospheric location). For 26 months of exposure, the accumulated UV radiation energy is 724 MJ/m^2 which is very close to that generated from the UV fluorescent weatherometer. Therefore, direct comparison of the exposure time between field and UV fluorescent is acceptable.

Field time	vs.	Fluorescent UV light time:	Thus,	the acceleration factor is 6.8.
= 26 Months		= 3.8 Months		

3.3.2 Comparison between field and Xenon Arc weatherometer

The light source of the Xenon Arc weatherometer simulates almost the entire sunlight spectrum from 250 to 800 nm. Depending of the age of the light source and filter, the solar energy ranges from 340.2 to 695.4 W/m², with the average value being 517.8 W/m².

The time of exposure to reach 50% elongation at break

$$\begin{aligned} &= 4416 \text{ hr. of light} \\ &= 15,897,600 \text{ seconds} \end{aligned}$$

$$\begin{aligned} \text{Total energy in MJ/m}^2 &= 517.8 \text{ W/m}^2 \times 15,897,600 \\ &= 8232 \text{ MJ/m}^2 \end{aligned}$$

The solar energy in the field is again estimated based on data collected by the South Florida Testing Lab in Arizona. For 26 months of exposure, the accumulated solar energy (295-800 nm) is 15,800 MJ/m², which is much higher than that from the Xenon Arc weatherometer. Therefore, direct comparison of halflives obtained from the field and Xenon Arc weatherometer is not anticipated to be very accurate. However, for illustration purposes the acceleration factor based on Xenon Arc weatherometer would be as follows:

$$\begin{array}{lll} \text{Field} & \text{vs.} & \text{Xenon Arc} \\ = 26 \text{ Months} & & = 6.1 \text{ Months} \end{array} \quad \text{Thus, the acceleration factor is 4.3.}$$

4.0 Summary and Recommendations

This White Paper has described research on the geomembrane type which has had the majority of research effort, that being nonexposed HDPE used in landfill applications. While this material promises service lifetime of hundreds of years, the elevated temperatures of exposed or nearly exposed geomembranes in other applications (dams, canals, reservoirs, etc.) is expected to be greatly reduced. It was shown that HDPE decreases its predicted halflife from 449-years at 20°C, to 73-years at 40°C. Other geomembrane types (LLDPE, PVC, EPDM and CSPE) have had essentially no focused effort on lifetime prediction of the type described herein. All are candidates for additional research in this regard.

Exposed geomembrane lifetime was addressed from the perspective of field performance which is very unequivocal. Experience in Europe, mainly with relatively thick PVC containing high molecular weight plasticizers, has given 25-years of service and the geomembranes are still in use. Experience in the USA with exposed geomembranes on flat roofs, mainly with EPDM and CSPE, has given 20⁺-years of service. The newest geomembrane type in such applications is fPP which currently carries similar warranties. To be noted, however, is that degradation is a very slow process and every time a formulation changes there is uncertainty as to its long-time field performance versus the previous formulation.

Alternatively, exposed geomembrane lifetime can be addressed by using accelerating laboratory weatherometers. GSI is fully involved in such an activity using UV Fluorescent and Xenon Arc weatherometers. Two types of polyethylene, two PVCs, and three fPP geomembranes (seven in total) are being incubated for sufficient time to reach their respective lifetimes. One type of fPP has reached this level and correlation to actual field failure time is reasonable. Analysis of this (poorly formulated) geomembrane results in acceleration factors of 6.8 for UV Fluorescent, and 4.3 for Xenon Arc devices. Based on such acceleration factors, for 20-year lifetime exposed geomembranes typical laboratory weatherometer exposure will be 3-years, or longer. As noted in Table 2 such testing is ongoing and will be continued so as to report our findings at a future date. In this regard we are proceeding as follows so as to develop the required confidence needed for use of geomembranes in long-term, permanent, systems.

- (i) Extend HDPE laboratory studies on nonexposed geomembranes to other polymer types such as PVC, LLDPE, fPP, EPDM and CSPE.
- (ii) Evaluate, to the extent possible, various additives particularly antioxidants in polyolefins (HDPE, LLDPE and fPP) and plasticizers in PVC.

- (iii) Document and analyze geomembrane dam rehabilitation in Europe (and elsewhere) with particular emphasis on durability.
- (iv) Document and analyze geomembrane use in flat roofs and other exposed applications, e.g., pond and reservoir liners as well as canal liners.
- (v) Initiate a broad research program on lifetime prediction of exposed geomembranes (of all types and formulations) using laboratory weatherometers such as the ongoing study described herein.

Acknowledgements

The financial assistance of the member organizations of the Geosynthetic Institute and its related institutes for research, information, education, accreditation and certification is sincerely appreciated. Their identification and contact member information is available on the Institute's web site at <<geosynthetic-institute.org>>.

References

- Cazzuffi, D., "Long-Term Performance of Exposed Geomembranes on Dams in the Italian Alps," Proc. 6th Intl. Conf. on Geosynthetics, IFAI, 1998, pp. 1107-1114.
- Chailan, J.-F., Boiteux, C., Chauchard, J., Pinel, B. and Seytre, G., "Effect of Thermal Degradation on the Viscoelastic and Dielectric Properties of Chlorosulfonated Polyethylene (CSPE) Compounds," Journal of Polymer Degradation and Stability, Vol. 48, 1995, pp. 61-65.
- Comer, A. I., Hsuan, Y. G. and Konrath, L., "The Performance of Flexible Polypropylene Geomembranes in Covered and Exposed Environments," 6th International Conference on Geosynthetics, Atlanta, Georgia, USA, March, 1998, pp. 359-364.
- Gedde, U. W., Viebke, J., Leijstrom, H. and Ifwarson, M., "Long-Term Properties of Hot-Water Polyolefin Pipes - A Review," Polymer Engineering and Science, Vol. 34, No. 24, 1994, pp. 1773-1787.
- Giroud, J.-P. and Tisinger, L. G., "The Influence of Plasticizers on the Performance of PVC Geomembranes," PVC GRI-17 Conference, IFAI, Roseville, MN, 1994, pp. 169-196.
- Hammon, M., Hsuan, G., Levin, S. B. and Mackey, R. E., "The Re-examination of a Nine-Year-Old PVC Geomembrane Used in a Top Cap Application," 31st Annual SWANA Conference, San Jose, CA, 1993, pp. 93-108.
- Hsuan, Y. G. and Guan, Z., "Evaluation of the Oxidation Behavior of Polyethylene Geomembranes Using Oxidative Induction Time Tests," ASTM STP 1326, Riga and Patterson, Eds., ASTM, 1997, pp. 138-149.

- Hsuan, Y. G. and Koerner, R. M., "Can Outdoor Degradation be Predicted by Laboratory Acceleration Weathering?," GFR, November, 1993, pp. 12-16.
- Hsuan, Y. G. and Koerner, R. M., "Antioxidant Depletion Lifetime in High Density Polyethylene Geomembranes," Jour. Geotech. and Geoenviron. Engr., ASCE, Vol. 124, No. 6, 1998, pp. 532-541.
- Koerner, G. R. and Koerner, R. M., "In-Situ Temperature Monitoring of Geomembranes," Proc. GRI-18 Conf. at GeoFrontiers, Austin, TX, 2005, 6 pgs.
- Miller, L. V., Koerner, R. M., Dewyea, J. and Mackey, R. E., "Evaluation of a 30 mil PVC Liner and Leachate Collection System," Proc. 29th Annual GRCDA/SWANA Conf., Cincinnati, OH, 1991.
- Müeller, W. and Jakob, I., "Oxidative Resistance of High-Density Polyethylene Geomembranes," Jour. Polymer Degradation and Stability, Elsevier Publ. Co., No. 79, 2003, pp. 161-172.
- Rapoport, N. Y. and Zaikov, G. E., "Kinetics and Mechanisms of the Oxidation of Stressed Polymer," Developments in Polymer Stabilization—4, G. Scott, Ed., Applied Science Publishers Ltd., London, U.K., 1986, pp. 207-258.
- Sangam, H. P. and Rowe, R. K., "Effects of Exposure Conditions on the Depletion of Antioxidants from HDPE Geomembranes", Canadian Geotechnical Journal, Vol. 39, 2002, pp. 1221-1230.
- Scuero, A., "The Use of Geocomposites for the Rehabilitation of Concrete Dams," Proc. 4th Intl. Conf. on Geosynthetics, The Hague, Balkema Publ. Co., 1990, pg. 474.
- Scuero, A. M. and Vaschetti, G. L., "Geomembranes for Masonry and Concrete Dams: State-of-the-Art Report," Proc. Geosynthetics Applications, Design and Construction, M. B. deGroot, et al., Eds., A. A. Balkema, 1996, pp. 889-898.
- Suits, L. D. and Hsuan, Y. G., "Assessing the Photo Degradation of Geosynthetics by Outdoor Exposure and Laboratory Weatherometers," Proc. GRI-15 Conference, Hot Topics in Geosynthetics II, GII Publ., Folsom, PA, 2001, pp. 267-279.
- Wang, W. and Qu, B., "Photo and Thermo-Oxidative Degradation of Photocrosslinked Ethylene-Propylene-Diene Terpolymer," Journal of Polymer Degradation and Stability, Vol. 81, 2003, pp. 531-537.

CHEMICAL COMPATIBILITY OF POLY-FLEX LINERS

Chemical compatibility or resistance, as applied to geomembranes, is a relative term. Actual compatibility would mean that one material dissolves in the other such as alcohol in water or grease in gasoline. An example of incompatibility would be oil and water. In liners it is undesirable to have the chemicals dissolve in the liner, hence the term compatibility is the reverse of what is normally meant in the chemical industry. In the strictest sense and from a laboratory perspective, chemical compatibility, as the term applies to this industry, would imply that the chemical has no effect on the liner. On the other hand, from an engineering perspective, chemical compatibility means that a liner survives the exposure to a given chemical even though the chemical could have some effect on the performance of the liner, but not enough to cause failure. Therefore, one must understand and define chemical compatibility for a specific project.

Generally polyethylene is effected by chemicals in one of three ways.

1. No effect—This means that the chemical in question and the polyethylene do not interact. The polyethylene does not gain (lose) weight or swell, and the physical properties are not significantly altered.
2. Oxidizes (cross linking)—Chemicals classed as oxidizing agents cause the polyethylene molecules to cross link and cause irreversible changes to the physical properties of the liner. Basically they make the liner brittle.
3. Plasticizes—Chemicals in this classification are soluble in the polyethylene structure. They do not change the structure of the polyethylene itself but act as a plasticizer. In doing so, the liner experiences weight gain of 3-15%, may swell by up to 10%, and has measurable changes in physical properties (e.g. the tensile strength at yield may decrease by up to 20%). Even under these conditions the liner maintains its integrity and is not breached by liquids, provided the liner has not been subjected to any stress. These effects are reversible once the chemicals are removed and the liner has time to dry out.

Aside from the effect that chemicals have on a liner is the issue of vapor permeation through the liner. Vapor permeation is molecular diffusion of chemicals through the liner. Vapor transmission for a given chemical is dependent primarily on liner type, contact time, chemical solubility, temperature, thickness, and concentration gradient, but not on hydraulic head or pressure. Transmission through the liner can occur in as little as 1-2 days. Normally, a small amount of chemical is transmitted. Generally HDPE has the lowest permeation rate of the liners that are commercially available.

As stated above chemical compatibility is a relative term. For example, the use of HDPE as a primary containment of chlorinated hydrocarbons at a concentration of 100% may not be recommended, but it may be acceptable at 0.1% concentration for a limited time period or may be acceptable for secondary containment. Factors that go into assessment of chemical compatibility are type of chemical(s), concentration, temperature and the type of application. No hard and fast rules are available to make decisions on chemical compatibility. Even the EPA 9090 test is just a method to generate data so that an opinion on chemical compatibility can be more reliably reached.

A simplified table on chemical resistance is provided to act as a screening process for chemical containment applications.

CHEMICAL RESISTANCE INFORMATION

CHEMICAL CLASS	CHEMICAL EFFECT	PRIMARY CONTAINMENT (LONG TERM CONTACT)		SECONDARY CONTAINMENT (SHORT TERM CONTACT)	
		HDPE	LLDPE	HDPE	LLDPE
CARBOXYLIC ACID - Unsubstituted (e.g. Acetic acid) - Substituted (e.g. Lactic acid) - Aromatic (e.g. Benzoic Acid)	1	B A A	C B B	A A A	C A A
ALDEHYDES - Aliphatic (e.g. Acetaldehyde) - Hetrocyclic (e.g. Furfural)	3	B C	C C	B B	C C
AMINE - Primary (e.g. Ethylamine) - Secondary (e.g. Diethylamine) - Aromatic (e.g. Aniline)	3	B C B	C C C	B B B	C C C
CYANIDES (e.g. Sodium Cyanide)	1	A	A	A	A
ESTER (e.g. Ethyl acetate)	3	B	C	B	C
ETHER (e.g. Ethyl ether)		C	C	B	C
HYDROCARBONS - Aliphatic (e.g. Hexane) - Aromatic (e.g. Benzene) - Mixed (e.g. Crude oil)	3	C C C	C C C	B B B	C C C
HALOGENATED HYDROCARBONS - Aliphatic (e.g. Dichloroethane) +A4 - Aromatic (e.g. Chlorobenzene)	3	C C	C C	B B	C C
ALCOHOLS - Aliphatic (e.g. Ethyl alcohol) - Aromatic (e.g. Phenol)	1	A A	A C	A A	A B
INORGANIC ACID - Non-oxidizers (e.g. Hydrochloric acid) - Oxidizers (e.g. Nitric Acid)	1 2	A C	A C	A B	A C
INORGANIC BASES (e.g. Sodium hydroxide)	1	A	A	A	A
SALTS (e.g. Calcium chloride)	1	A	A	A	A
METALS (e.g. Cadmium)	1	A	A	A	A
KETONES (e.g. Methyl ethyl ketone)	3	C	C	B	C
OXIDIZERS (e.g. Hydrogen peroxide)	2	C	C	C	C

Chemical Effect (see discussion on Chemical Resistance)

1. No Effect—Most chemicals of this class have no or minor effect.
2. Oxidizer—Chemicals of this class will cause irreversible degradation.
3. Plasticizer—Chemicals of this class will cause a reversible change in physical properties.

Chart Rating

- A. Most chemicals of this class have little or no effect on the liner.
Recommended regardless of concentration or temperature (below 150° F).
- B. Chemicals of this class will affect the liner to various degrees.
Recommendations are based on the specific chemical, concentration and temperature.
Consult with Poly-Flex, Inc.
- C. Chemicals of this class at high concentrations will have significant effect on the physical properties of the liner.
Generally not recommended but may be acceptable at low concentrations and with special design considerations.
Consult with Poly-Flex, Inc.

The data in this table is provided for informational purposes only and is not intended as a warranty or guarantee. Poly-Flex, Inc. assumes no responsibility in connection with the use of this data. Consult with Poly-Flex, Inc. for specific chemical resistance information and liner selection.

Chemicals Resistance Table

Low Density and High Density Polyethylene

INTRODUCTION

The table in this document summarises the data given in a number of chemical resistance tables at present in use in various countries, derived from both practical experience and test results.

Source: ISO/TR 7472, 7474; Carlowitz: "Kunststofftabellen-3. Auflage".

The table contains an evaluation of the chemical resistance of a number of fluids judged to be either aggressive or not towards low and high density polyethylene. This evaluation is based on values obtained by immersion of low and high density polyethylene test specimens in the fluid concerned at 20 and 60°C and atmospheric pressure, followed in certain cases by the determination of tensile characteristics.

A subsequent classification will be established with respect to a restricted number of fluids deemed to be technically or commercially more important, using equipment which permits testing under pressure and the determination of the coefficient of chemical resistance for each fluid. These tests will thus furnish more complete indications on the use of low and high density polyethylene products for the transport of stated fluids, including their use under pressure.

SCOPE AND FIELD APPLICATION

This document establishes a provisional classification of the chemical resistance of low and high density polyethylene with respect to about 300 fluids. It is intended to provide general guidelines on the possible utilisation of low and high density polyethylene:

- at temperatures up to 20 and 60°C
- in the absence of internal pressure and external mechanical stress
(for example flexural stresses, stresses due to thrust, rolling loads etc).

DEFINITIONS, SYMBOLS AND ABBREVIATIONS

The criteria of classification, definitions, symbols and abbreviations adopted in this document are as follows:

S = Satisfactory

The chemical resistance of low or high density polyethylene exposed to the action of a fluid is classified as "satisfactory" when the results of test are acknowledged to be satisfactory by the majority of the countries participating in the evaluation.

L = Limited

The chemical resistance of low or high density polyethylene exposed to the action of a fluid is classified as "limited" when the results of tests are acknowledged to be "limited" by the majority of the countries participating in the evaluation.

Also classified as "limited" are the resistance to the action of chemical fluids for which judgements "S" and "NS" or "L" are pronounced to an equal extent.

NS = Not satisfactory

The chemical resistance of low or high density polyethylene exposed to the action of a fluid is classified as "not satisfactory" when the results of tests are acknowledged to be "not satisfactory" by the majority of the countries participating in the evaluation.

Also classified as "not satisfactory" are materials for which judgements "L" and "NS" are pronounced to an equal extent.

Sat.sol Saturated aqueous solution, prepared at 20°C

Sol Aqueous solution at a concentration higher than 10 %, but not saturated

Dil.sol Dilute aqueous solution at a concentration equal to or lower than 10 %

Work.sol Aqueous solution having the usual concentration for industrial use

Solution concentrations reported in the text are expressed as a percentage by mass.
The aqueous solutions of sparingly soluble chemicals are considered, as far as chemical action towards low or high density polyethylene is concerned, as saturated solutions.

In general, common chemical names are used in this document.

The table is made as a first guideline for user of polyethylene. If a chemical compound is not to be found or if there is an uncertainty on the chemical resistance in an application, please contact Borealis for advise and proposal on testing.

**Chemical resistance of low density and high density polyethylene,
not subjected to mechanical stress, to various fluids at 20 and 60°C**

Chemical or product	Concentration	LD °C		HD °C	
		20	60	20	60
Acetaldehyde	100 %	L	NS	S	L
Acetanilide	—			S	S
→ Acetic acid	10 %	S	S	S	S
→ Acetic acid	60 %	S	L	S	S
Acetic acid, glacial	Greater than 96 %	L	NS	S	L
Acetic anhydride	100 %	L	NS	S	L
Acetone	100 %	L	NS	L	L
Acrylnitrile	—	S	S	S	S
Acetylsilicacid	—	S	S	S	S
Adipic acid	Sat.sol	S	S	S	S
→ After shave	—	NS	NS	NS	NS
Aliphatic hydrocarbons	—	L	NS	L	L
Allyl acetate	—	S	L	S	L
Allyl alcohol	100 %	L	NS	—	—
Allyl alcohol	96 %	—	—	S	S
Allyl chloride	—	L	NS	L	NS
Aluminium chloride	Sat.sol	S	S	S	S
Aluminium fluoride	Sat.sol	S	S	S	S
Aluminium hydroxide	Sat.sol	S	S	S	S
Aluminium nitrate	Sat.sol	S	S	S	S
Aluminium oxychloride	Sat.sol	S	S	S	S
Al/potassium sulphate	Sat.sol	S	S	S	S
Aluminium sulphate	Sat.sol	S	S	S	S
Alums	Sol	S	S	S	S
Aminobenzoic acid	—	S	S	S	S
Ammonia, dry gas	100 %	S	S	S	S
→ Ammonia, liquid	100 %	L	L	S	S
Ammonia, aqueous	Dil.sol	S	S	S	S
Ammonium acetate	—	S	S	S	S
Ammonium carbonate	Sat.sol	S	S	S	S
→ Ammonium chloride	Sat.sol	S	S	S	S
Ammonium fluoride	Sol	S	—	S	S
Ammonium hexafluorosilicate	Sat.sol	S	S	S	S
Ammonium hydrogen carbonate	Sat.sol	S	S	S	S
Ammonium hydroxide	10 %	S	S	S	S
Ammonium hydroxide	30 %	S	S	S	S

Chemical or product	Concentration	LD °C		HD °C	
		20	60	20	60
Ammonium metaphosphate	Sat.sol	S	S	S	S
Ammonium nitrate	Sat.sol	S	S	S	S
Ammonium oxalate	Sat.sol	S	S	S	S
Ammonium phosphate	Sat.sol	S	S	S	S
Ammonium persulphate	Sat.sol	S	S	S	S
Ammonium sulphate	Sat.sol	S	S	S	S
Ammonium sulphide	Sol	S	S	S	S
Ammonium thiocyanate	Sat.sol	S	S	S	S
Amyl acetate	100 %	NS	NS	L	L
Amyl alcohol	100 %	L	L	S	L
Amyl chloride	100 %	NS	NS	—	—
Amyl phthalate	—	L	L	S	L
Aniline	100 %	NS	NS	S	L
Anilinchlorohydrate	—	L	—	—	—
Antimony (III) chloride	90 %	—	—	S	S
Antimony (III) chloride	Sat.sol	S	S	S	S
Antimony trichloride	Sol	S	S	S	S
→ Apple juice	Sol	—	—	S	L
Aqua regia	HCl/HNO ₃ = 3/1	NS	NS	NS	NS
Aromatic hydrocarbons	—	NS	NS	NS	NS
Arsenic acid	Sat.sol	S	S	S	S
Asorbic acid	10 %	S	S	S	S
Barium bromide	Sat.sol	S	S	S	S
Barium carbonate	Sat.sol	S	S	S	S
Barium chloride	Sat.sol	S	S	S	S
Barium hydroxide	Sat.sol	S	S	S	S
Barium sulphate	Sat.sol	S	S	S	S
Barium sulphide	Sat.sol	S	S	S	S
→ Beer	—	S	S	S	S
Benzaldehyde	100 %	L	NS	S	L
Benzene	100 %	NS	NS	L	L
Benzoic acid	Sat.sol	S	S	S	S
Benzoylchloride	—	S	L	S	L
Benzyl alcohol	—	S	L	S	S
Benzylsulphonic acid	10 %	S	S	S	S
Bismuth carbonate	Sat.sol	S	S	S	S
Bitumen	—	S	L	S	S
→ Bleach lye	10 %	S	S	S	S

Chemical or product	Concentration	LD °C		HD °C	
		20	60	20	60
Borax	Sat.sol	S	S	S	S
Boric acid	Sat.sol	S	S	S	S
Boron trifluoride	—	L	NS	L	NS
Brake fluid	—	L	NS	L	NS
Brine	—	S	S	S	S
Bromine, dry gas	100 %	NS	NS	NS	NS
Bromine, liquid	100 %	NS	NS	NS	NS
Bromoform	100 %	NS	NS	NS	NS
Butandiol	10 %	S	S	S	S
Butandiol	60 %	S	S	S	S
Butandiol	100 %	S	S	S	S
Butane, gas	100 %	—	—	S	S
Butanol	100 %	S	L	S	S
→ Butter	—	S	S	S	S
Butyl acetate	100 %	S	L	S	L
Butyl alcohol	100 %	S	S	S	S
Butyl chloride	—	S	—	S	—
Butylene glycol	10 %	S	S	S	S
Butylene glycol	60 %	S	S	S	S
Butylene glycol	100 %	S	S	S	S
Butyraldehyde	—	—	—	S	L
Butyric acid	100 %	L	L	S	L
Calcium arsenate	—	S	S	S	S
Calcium benzoate	—	S	S	S	S
Calcium bisulphide	—	S	S	S	S
Calcium bromate	10 %	S	S	S	S
Calcium bromide	Sat.sol	S	S	S	S
Calcium carbonate	Sat.sol	S	S	S	S
Calcium chlorate	Sat.sol	S	S	S	S
→ Calcium chloride	Sat.sol	S	S	S	S
Calcium chromate	40 %	S	S	S	S
Calcium cyanide	—	S	S	S	S
Calcium hydrosulphide	Sol	S	S	S	S
Calcium hydroxide	Sat.sol	S	S	S	S
Calcium hypochlorite	Sol	S	S	S	S
Calcium nitrate	Sat.sol	S	S	S	S
Calcium oxide	Sat.sol	S	S	S	S
Calcium perchlorate	1 %	S	—	S	S

Chemical or product	Concentration	LD °C		HD °C	
		20	60	20	60
Calcium permanganate	20 %	S	S	S	S
Calcium persulphate	Sol	S	S	S	S
Calcium sulphate	Sat.sol	S	S	S	S
Calcium sulphide	Dil.sol	—	—	L	L
Camphor oil	—	NS	NS	L	L
Carbon dioxide, dry gas	100 %	—	—	S	S
Carbon dioxide, wet	—	S	S	S	S
Carbon disulphide	100 %	NS	NS	L	NS
Carbon monoxide	100 %	S	S	S	S
Carbon tetrachloride	100 %	NS	NS	L	NS
Carbonic acid	—	S	S	S	S
→ Castor oil	Sol	S	S	S	S
Chlorine, water	2 % Sat.sol	L	L	S	S
Chlorine, aqueous	Sat.sol	NS	NS	L	NS
Chlorine, dry gas	100 %	NS	NS	L	NS
Chloroacetic acid	Sol	—	—	S	S
Chlorobenzene	100 %	NS	NS	NS	NS
Chloroethanol	100 %	S	S	S	S
Chloroform	100 %	NS	NS	NS	NS
Chloromethane, gas	100 %	L	—	L	—
Chlorosulphonic acid	100 %	NS	NS	NS	NS
Chloropropene	—	NS	—	L	—
Chrome alum	Sol	S	S	S	S
Chromic acid	Sat.sol	S	S	—	—
Chromic acid	20 %	—	—	S	L
Chromic acid	50 %	—	—	S	L
Chromium VI oxide	Sat.sol	S	S	S	S
→ Cider	—	S	S	S	S
Citric acid	Sat.sol	S	S	S	S
Citric acid	10 %	S	S	S	S
Citric acid	25 %	S	S	S	S
Coconut oil alcoholic	—	S	S	S	S
→ Coffee	—	S	S	S	S
Copper (II) chloride	Sat.sol	S	S	S	S
Copper cyanide	Sat.sol	S	S	S	S
Copper (II) fluoride	Sat.sol	S	S	S	S
Copper (II) fluoride	2 %	S	S	S	S
Copper (II) nitrate	Sat.sol	S	S	S	S
Copper (II) sulphate	Sat.sol	S	S	S	S

Chemical or product	Concentration	LD °C		HD °C	
		20	60	20	60
→ Corn oil	—	S	S	S	S
→ Cottonseed oil	—	S	S	S	S
Cresylic acid	Sat.sol	—	—	L	—
Crotonaldehyde	Sat.sol	L	—	—	—
Cyclanone	—	S	S	S	S
Cyclohexane	—	NS	NS	NS	NS
Cyclohexanol	Sat.sol	L	NS	—	—
Cyclohexanol	100 %	—	—	S	S
Cyclohexanone	100 %	NS	NS	S	L
Decahydronaphthalene	100 %	L	NS	S	L
Decane	—	NS	NS	L	NS
Decalin	100 %	—	—	S	L
→ Detergents, synthetic	—	S	S	S	S
Developers (photographic)	Work.conc	—	—	S	S
Dextrin	Sol	S	S	S	S
Dextrose	Sol	S	S	S	S
Diacetone alcohol	—	L	L	L	L
Diazo salts	—	S	S	S	S
Dibutyl amine	—	NS	NS	L	NS
Dibutyl ether	—	NS	NS	L	—
Dibutylphthalate	—	L	L	S	L
Dichlorobenzene	—	NS	NS	NS	NS
Dichloroethylene	—	NS	NS	NS	NS
Dichloropropylene	—	NS	NS	NS	NS
→ Diesel oil	—	S	NS	S	L
Diethyl ether	100 %	NS	NS	L	—
Diethyl ketone	—	L	NS	L	L
Diethylene glycol	—	S	S	S	S
Diglycolic acid	—	S	S	S	S
Diisobutylketone	100 %	S	L	S	L
Dimethyl amine	100 %	NS	NS	—	—
Dimethyl formamid	—	S	L	S	S
Diethyl phthalate	100 %	L	NS	S	L
Dioxan	100 %	—	—	S	S
Dipentene	—	NS	NS	NS	NS
Disodium phosphate	—	S	S	S	S
→ Drano, plumbing cleaner	—	S	S	S	S

Chemical or product	Concentration	LD °C		HD °C	
		20	60	20	60
Emulsions, photographic	—	S	S	S	S
Ethandiol	100 %	S	S	S	S
Ethanol	40 %	S	L	S	L
Ethanol	96 %	L	L	—	—
Ethyl acetate	100 %	L	NS	S	NS
Ethyl acrylate	100 %	NS	NS	L	NS
Ethyl alcohol	35 %	S	S	S	S
Ethyl alcohol	100 %	S	S	S	S
Ethyl benzene	—	NS	NS	NS	NS
Ethyl chloride	100 %	NS	NS	NS	NS
Ethylene chloride	100 %	NS	NS	NS	NS
Ethylene diamine	100 %	S	L	S	S
Ethyl ether	—	NS	NS	NS	NS
Ethylene glycol	100 %	S	S	S	S
Ethyl mercaptan	—	NS	NS	NS	NS
Ferric chloride	Sat.sol	S	S	S	S
Ferric nitrate	Sat.sol	S	S	S	S
Ferric sulphate	Sat.sol	S	S	S	S
Ferrous chloride	Sat.sol	S	S	S	S
Ferrous sulphate	Sat.sol	S	S	S	S
→ Fish solubles	Sol	S	S	S	S
Fluoboric acid	—	S	S	S	S
Fluorine gas	100 %	L	NS	NS	NS
Fluorine gas, dry	100 %	NS	NS	NS	NS
Fluorine gas, wet	100 %	NS	NS	NS	NS
Fluorosilic acid	Conc	S	L	S	L
Fluorosilic acid	40 %	S	S	S	S
Formaldehyde	40 %	S	S	S	S
Formic acid	40 %	S	S	S	S
Formic acid	98 to 100 %	S	S	S	S
→ Fructose	Sat.sol	S	S	S	S
→ Fruit pulps	Sol	S	S	S	S
Furfural	100 %	NS	NS	NS	NS
Furfuryl alcohol	100 %	L	NS	S	L
Gallic acid	Sat.sol	S	S	S	S
Gasoline, petrol	—	L	NS	L	L
Gelatine	—	S	S	S	S

Chemical or product	Concentration	LD °C		HD °C	
		20	60	20	60
Glucose	Sat.sol	S	S	S	S
→ Glycerine	100 %	S	S	S	S
Glycerol	100 %	S	S	S	S
Glycolic acid	30 %	S	L	—	—
Glycolic acid	Sol	—	—	S	S
n-Heptane	100 %	NS	NS	L	NS
Hexachlorobenzene	—	S	S	S	L
Hexachlorophene	—	NS	NS	L	L
Hexamethylenetriamine	40 %	S	—	S	—
Hexane	—	S	L	S	L
Hexanol, tertiary	—	S	S	S	S
Hydrobromic acid	50 %	S	S	S	S
Hydrobromic acid	Up to 100 %	S	S	S	S
Hydrochloric acid	Up to 36 %	S	S	S	S
Hydrochloric acid	Conc	S	S	S	S
Hydrochlorous acid	Conc	S	S	S	S
Hydrocyanic acid	10 %	S	S	S	S
Hydrocyanic acid	Sat.sol	S	S	S	S
Hydrofluoric acid	40 %	S	S	S	S
Hydrofluoric acid	60 %	S	L	S	L
Hydrogen	100 %	S	S	S	S
Hydrogen chloride	Dry gas	S	S	S	S
Hydrogen peroxide	30 %	S	L	S	S
Hydrogen peroxide	90 %	S	NS	S	NS
Hydrogen sulphide gas	100 %	S	S	S	S
Hydroquinone	Sat.sol	S	S	—	—
Hydroxylamine	up to 12 %	S	S	S	S
→ Inks	—	S	S	S	S
Iodine (in potassium sol)	—	L	NS	NS	NS
Iodine (in alcohol)	—	NS	NS	NS	NS
Iron (II) chloride	Sat.sol	S	S	S	S
Iron (II) sulphate	Sat.sol	S	S	S	S
Iron (III) chloride	Sat.sol	S	S	S	S
Iron (III) nitrate	Sol	S	S	S	S
Iron (III) sulphate	Sat.sol	S	S	S	S
Iso octane	100 %	S	NS	S	L
Iso pentane	—	NS	NS	NS	NS

Chemical or product	Concentration	LD °C		HD °C	
		20	60	20	60
Isopropanol	—	S	S	S	S
Isopropyl amine	—	NS	NS	NS	NS
Isopropyl ether	100 %	L	NS	S	NS
Kerosene	—	NS	NS	NS	NS
→ Lactic acid	10 %	S	S	S	S
Lactic acid	28 %	S	S	S	S
Lactic acid	up to 100 %	S	S	S	S
→ Latex	—	S	S	S	S
Lead acetate	Dil.sol	S	S	S	S
Lead acetate	Sat.sol	S	S	S	S
Lead arsenate	—	S	S	S	S
Lubricating oil	—	S	S	S	S
Lysol	—	NS	NS	L	NS
Magnesium carbonate	Sat.sol	S	S	S	S
Magnesium chloride	Sat.sol	S	S	S	S
Magnesium hydroxide	Sat.sol	S	S	S	S
Magnesium nitrate	Sat.sol	S	S	S	S
Magnesium sulphate	Sat.sol	S	S	S	S
Maleic acid	Sat.sol	S	S	S	S
Mercury	—	S	S	S	S
Mercury (I) nitrate	Sol	S	S	S	S
Mercury (II) chloride	Sat.sol	S	S	S	S
Mercury (II) cyanide	Sat.sol	S	S	S	S
Mercury	100 %	S	S	S	S
Methanol	100 %	S	L	S	S
Methyl alcohol	100 %	S	L	S	S
Methyl benzoic acid	Sat.sol	NS	NS	L	—
Methyl bromide	100 %	NS	NS	NS	NS
Methyl chloride	100 %	NS	NS	NS	NS
Methylcyclohexane	—	L	NS	L	NS
Methyl ethyl ketone	100 %	—	—	S	L
Methylene chloride	—	NS	NS	NS	NS
Methoxybutanol	100 %	S	L	S	L
→ Milk	—	S	S	S	S
Milk of Magnesia	—	S	L	S	L
→ Mineral oils	—	L	NS	S	L

Chemical or product	Concentration	LD °C		HD °C	
		20	60	20	60
→ Molasses	Work.conc	S	S	S	S
Motor oil	–	S	L	S	S
Naphtha	–	L	NS	L	NS
Naphtahalene	–	NS	NS	L	–
Nickel chloride	Sat.sol	S	S	S	S
Nickel nitrate	Sat.sol	S	S	S	S
Nickel sulphate	Sat.sol	S	S	S	–
Nicotine	Dil.sol	S	S	S	S
Nicotinic acid	Dil.sol	L	L	S	–
Nitric acid	25 %	S	S	S	S
Nitric acid	50 %	S	L	S	L
Nitric acid	70 %	S	L	S	L
Nitric acid	95 %	NS	NS	NS	NS
Nitric acid	100 %	NS	NS	NS	NS
Nitrobenzene	100 %	NS	NS	NS	NS
Nitroethane	100 %	S	NS	S	NS
Nitromethane	100 %	S	–	S	–
Nitrotoluene	–	NS	NS	NS	NS
n-Octane	–	S	S	S	S
Octyl alcohol	–	S	NS	S	NS
→ Oil and fats		L	NS	S	L
Oleic acid	100 %	L	NS	S	S
Oleum (H ₂ SO ₄ + 10 % SO ₃)		NS	NS	NS	NS
Oleum (H ₂ SO ₄ + 50 % SO ₃)		NS	NS	NS	NS
→ Olive oil	–	S	NS	S	NS
Orthophosphoric acid	50 %	S	S	S	S
Orthophosphoric acid	95 %	S	L	S	L
Oxalic acid	Sat.sol	S	S	S	S
Oxygen	100 %	S	–	S	L
Ozone	100 %	NS	NS	L	NS
Paraffin oil	–	S	L	S	S
n-Pentane	–	NS	NS	NS	NS
Pentane-2	–	NS	NS	NS	NS
Perchloric acid	20 %	S	S	S	S
Perchloric acid	50 %	S	L	S	L
Perchloric acid	70 %	S	NS	S	NS

Chemical or product	Concentration	LD °C		HD °C	
		20	60	20	60
Perchloroethylene	—	NS	NS	NS	NS
Phenol	Sol	L	NS	S	S
Phosphine	100 %	S	S	S	S
Phosphoric acid	up to 25 %	S	S	S	S
Phosphoric acid	25 to 50 %	S	S	S	S
Phosphoric (III) chloride	100 %	S	L	S	L
Phosphorous (II) chloride	100 %	—	—	S	L
Phosphorous pentoxide	100 %	S	S	S	S
Phosphorous trichloride	100 %	S	L	S	L
Photographic solutions	—	S	S	S	S
Phtalic acid	50 %	S	S	S	S
Picric acid	Sat.sol	S	L	S	—
Plating solutions	—	S	S	S	S
Potassium acetate	—	S	S	S	S
Potassium aluminium sulphate	Sat.sol	S	S	S	S
Potassium benzoate	—	S	S	S	S
Potassium bicarbonate	Sat.sol	S	S	S	S
Potassium borate	Sat.sol	S	S	S	S
Potassium bromate	Sat.sol	S	S	S	S
Potassium bromide	Sat.sol	S	S	S	S
Potassium carbonate	Sat.sol	S	S	S	S
Potassium chlorate	Sat.sol	S	S	S	S
Potassium chloride	Sat.sol	S	S	S	S
Potassium chromate	Sat.sol	S	S	S	S
Potassium cyanide	Sol	S	S	S	S
Potassium dichromate	Sat.sol	S	S	S	S
Potassium fluoride	Sat.sol	S	S	S	S
Potassium hexacyanoferrate (III)	Sat.sol	S	S	S	S
Potassium hexacyanoferrate (II)	Sat.sol	S	S	S	S
Potassium hexafluorosilicate	Sat.sol	S	S	S	S
Potassium hydrogen carbonate	Sat.sol	S	S	S	S
Potassium hydrogen sulphate	Sat.sol	S	S	S	S
Potassium hydrogen sulphide	Sol	—	—	S	S
Potassium hydroxide	10 %	S	S	S	S
Potassium hydroxide	Sol	S	S	S	S
Potassium hypochlorite	Sol	S	L	S	L
Potassium iodate	10 %	S	S	S	S
Potassium iodide	Sat.sol	S	S	S	S
Potassium nitrate	Sat.sol	S	S	S	S

Chemical or product	Concentration	LD °C		HD °C	
		20	60	20	60
Potassium orthophosphate	Sat.sol	S	S	S	S
Potassium oxalate	Sat.sol	S	S	S	S
Potassium perchlorate	Sat.sol	S	S	S	S
Potassium permanganate	20 %	S	S	S	S
Potassium persulphate	Sat.sol	S	S	S	S
Potassium phosphate	Sat.sol	S	S	S	S
Potassium sulphate	Sat.sol	S	S	S	S
Potassium sulphide	Sol	S	S	S	S
Potassium sulphite	Sat.sol	S	S	—	—
Potassium thiocyanate	Sat.sol	S	S	S	S
Potassium thiosulphate	Sat.sol	S	S	S	S
Propargul alcohol	—	S	S	S	S
n-Propyl alcohol	—	S	S	S	S
Propionic acid	50 %	—	—	S	S
Propionic acid	100 %	—	—	S	L
Propylene dichloride	100 %	NS	NS	NS	NS
Propylene glycol	—	S	S	S	S
Pyridine	100 %	—	—	S	L
Quinol (hydroquinone)	Sat.sol	S	S	S	S
Resorcinol	Sat.sol	S	S	S	S
Salicylic acid	Sat.sol	S	S	S	S
Sea water	—	S	S	S	S
Selenic acid	—	S	S	S	S
Silicon oil	—	S	S	S	S
Silver acetate	Sat.sol	S	S	S	S
Silver cyanide	Sat.sol	S	S	S	S
Silver nitrate	Sat.sol	S	S	—	—
Soap solution	100 %	S	S	S	S
Sodium acetate	Sat.sol	S	S	—	—
Sodium antimonate	Sat.sol	S	S	S	S
Sodium arsenite	Sat.sol	S	S	S	S
Sodium benzoate	Sat.sol	S	S	S	S
Sodium bicarbonate	Sat.sol	S	S	S	S
Sodium bisulphate	Sat.sol	S	S	S	S
Sodium bisulphite	Sat.sol	S	S	S	S
Sodium borate	—	S	S	S	S
Sodium bromide	Sat.sol	S	S	S	S
Sodium carbonate	Sat.sol	S	S	S	S

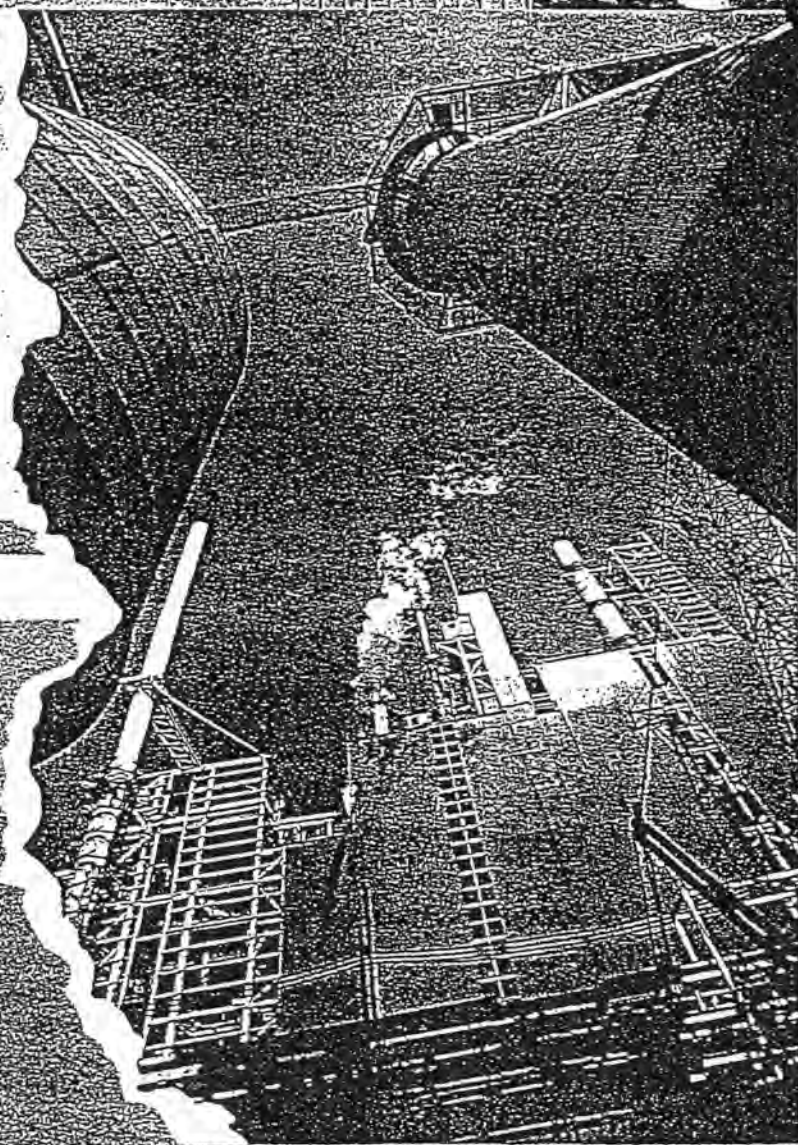
Chemical or product	Concentration	LD °C		HD °C	
		20	60	20	60
Sodium chlorate	Sat.sol	S	S	S	S
Sodium chloride	Sat.sol	S	S	S	S
Sodium chlorite	Sat.sol	L	—	—	—
Sodium cyanide	Sat.sol	S	S	S	S
Sodium dichromate	Sat.sol	S	S	S	S
Sodium fluoride	Sat.sol	S	S	S	S
Sodium hexacyanoferrate (III)	Sat.sol	—	—	S	S
Sodium hexacyanoferrate (II)	Sat.sol	—	—	S	S
Sodium hexafluorosilicate	Sat.sol	S	S	S	S
Sodium hydrogen carbonate	Sat.sol	S	S	S	S
Sodium hydrogen sulphate	Sat.sol	S	S	S	S
Sodium hydrogen sulphite	Sol	S	S	S	S
Sodium hydroxide	40 %	S	S	S	S
Sodium hydroxide	Sol	—	—	S	S
Sodium hypochloride	—	L	NS	S	S
Sodium hypochlorite	15 %	—	—	S	S
	available Cl	—	—	S	S
Sodium iodate	10 %	S	S	S	S
Sodium iodide	Sat.sol	S	S	S	S
Sodium nitrate	Sat.sol	S	S	S	S
Sodium nitrite	Sat.sol	S	S	S	S
Sodium orthophosphate	Sat.sol	S	S	S	S
Sodium oxalate	Sat.sol	S	S	S	S
Sodium phosphate	Sat.sol	S	S	S	S
Sodium silicate	Sol	S	S	S	S
Sodium sulphate	Sat.sol	S	S	S	S
Sodium sulphide	Sat.sol	S	S	S	S
Sodium sulphite	Sat.sol	S	S	S	S
Sodium thiocyanate	Sat.sol	S	S	S	S
Stannic chloride	Sat.sol	S	S	S	S
Stannous chloride	Sat.sol	S	S	S	S
Starch solution	Sat.sol	S	S	S	S
Stearic acid	Sat.sol	S	L	S	—
Styrene	Sol	L	NS	L	NS
Sulphur dioxide, dry	100 %	S	S	S	S
Sulphur trioxide	100 %	NS	NS	NS	NS
Sulphur acid	10 to 50 %	S	S	S	S
Sulphuric acid	10 %	S	S	S	S
Sulphuric acid	50 %	S	S	S	S

Chemical or product	Concentration	LD °C		HD °C	
		20	60	20	60
Sulphuric acid	70 %	S	L	S	L
Sulphuric acid	80 %	S	NS	S	NS
Sulphuric acid	98 %	L	NS	S	NS
Sulphuric acid	Fuming	NS	NS	NS	NS
Sulphurous acid	30 %	S	S	S	S
Sulphurous acid	Sol	S	S	S	S
→ Tallow	—	S	L	S	L
Tannic acid	Sol	S	S	S	S
Tartaric acid	Sat.sol	S	S	S	S
Tartaric acid	Sol	—	—	S	S
Tetrachloroethylene	100 %	NS	NS	NS	NS
Tetrachloromethane	100 %	NS	NS	L	NS
Tetradecane	—	NS	NS	NS	NS
Tetrahydrofuran	—	NS	NS	NS	NS
Tetrahydronaphthalene	100 %	L	NS	S	L
Thionyl chloride	100 %	NS	NS	NS	NS
Tin (II) chloride	Sat.sol	S	S	S	S
Tin (IV) chloride	Sol	S	S	S	S
Tin (IV) chloride	Sat.sol	—	—	S	S
Titanium tetrachloride	Sat.sol	NS	NS	NS	NS
Toluene	100 %	NS	NS	L	NS
Tribromomethane	—	NS	NS	NS	NS
Trichloroacetaldehyde	—	S	—	S	—
Trichlorobenzene	—	NS	NS	—	—
Trichloroethylene	100 %	NS	NS	NS	NS
Triethanolamine	100 %	S	—	S	—
Triethanolamine	Sol	—	—	S	L
Triethylene glycol	—	S	S	S	S
Trisodium phosphate	Sat.sol	S	S	—	—
Turpentine	—	NS	NS	NS	NS
Urea	up to 30 %	S	S	S	S
Urea	Sol	S	S	S	S
Urine	—	S	S	S	S
Vanilla extract	—	S	S	S	S
Vaseline	—	S	L	S	S
→ Vegetables oils	—	S	L	S	S
→ Vinegar	—	S	S	S	S
→ Water	—	S	S	S	S
Wetting agents	—	S	S	S	S
→ Wines and spirits	—	S	S	S	S
Chemical or product	Concentration	LD °C		HD °C	
		20	60	20	60

Xylene	100 %	NS	NS	L	NS
Yeast	Sol	S	S	S	S
Zinc bromide	Sat.sol	S	S	S	S
Zinc carbonate	Sat.sol	-	-	S	S
Zinc chloride	Sat.sol	S	S	S	S
Zinc oxide	Sat.sol	S	S	S	S
Zinc stearate	-	S	S	S	S
Zinc sulphate	Sat.sol	S	S	S	S
o-Zylene		NS	NS	NS	NS
p-Zylene	-	NS	NS	NS	NS

CONTAINMENT SOLUTIONS FOR INDUSTRIAL WASTE

Dike raising
Sludge caps
Sludge ponds
Secondary
containment
Landfill linings
Landfill caps
Floating covers



NOC

HIGH DENSITY POLYETHYLENE (HDPE) GEOMEMBRANE

Over the past five years, the geomembrane industry has experienced numerous changes. Factors such as the increased concern for the environment; new products in the marketplace; and the push for tighter governmental control over the environment have all played a significant role in revolutionizing the geosynthetic industry.

Today, the most widely used geomembrane in the waste management industry is High Density Polyethylene (HDPE). HDPE offers superior performance by maintaining the highest standards of durability.

FEATURES AND BENEFITS

National Seal Company's HDPE geomembrane is manufactured on a computer controlled, flat sheet extruder using virgin, first quality, high molecular weight polyethylene. This process guarantees a material thickness of $\pm 5\%$ from target, the most stringent quality control available in the industry. NSC also guarantees the minimum average thickness of our liner will be greater than or equal to the nominal thickness. HDPE is available in 40 (1.0mm), 50 (1.25mm), 60 (1.5mm), 80 (2.0mm), and 100 (2.5mm) mil thicknesses.

★ Chemical Resistance - Often the chemical resistance of the liner is the most critical aspect of the design process. HDPE is the most chemically resistant of all geomembranes. Typical landfill leachates pose no threat to a liner made of HDPE.

Low Permeability - The low permeability of HDPE provides assurance that groundwater will not penetrate the liner; rainwater will not infiltrate a cap; and methane gas will not migrate away from the gas venting system.

Ultraviolet Resistance - HDPE has excellent resistance to ultraviolet degradation. NSC adds carbon black which provides UV protection. Plasticizers are never used in NSC's geomembranes so there is never a concern about volatilization of the plasticizer which can be caused by UV exposure.

APPLICATIONS:

Landfill (primary and secondary containment) Landfill caps Lagoon liners Pond liners Floating covers Secondary containment for above ground storage tanks	Retention ponds for mining applications Wastewater treatment facilities Potable water reservoirs Tank linings Canal linings Heap leach pads
--	--

HDPE GEOMEMBRANE PHYSICAL PROPERTIES

60 mil

The properties on this page are not part of NSC's Manufacturing Quality Control program and are not included on the material certifications. Seam testing is the responsibility of the installer and/or CQA personnel.

PROPERTIES	METHOD	UNITS	MINIMUM ¹	TYPICAL
Multi-Axial Tensile Elongation	GRI, GM-4	percent	20.0	28.0
Critical Cone Height	GRI, GM-3, NSC mod.	cm	1.0	1.5
Wide Width Tensile	ASTM D 4885			
Stress at Yield		psi	2000	2110
Strain at Yield		%	15.0	20.0
Brittleness Temp. by Impact ²	ASTM D 746	°C	-75	<-90
Coef. of Linear Thermal Exp. ²	ASTM D 696	°C ⁻¹	1.5×10^{-4}	1.2×10^{-4}
ESCR, Bent Strip	ASTM D 1693	hours	1500	>10,000
Hydrostatic Resistance	ASTM D 751	psi	450	510
Modulus of Elasticity	ASTM D 638	psi	80,000	135,000
Ozone Resistance	ASTM D 1149, 168 hrs	P/F	P	P
Permeability ²	ASTM E 96	cm/sec · Pa	2.3×10^{-14}	8.1×10^{-15}
Puncture Resistance	FTMS 101, method 2065	ppi	1300	1700
		lbs	78	105
Soil Burial Resistance ²	ASTM D 3083, NSF mod.	% change	10	0
Tensile Impact	ASTM D 1822	ft lbs/in ²	250	420
Volatile Loss ²	ASTM D 1203, A	percent	0.10	0.06
Water Absorption ²	ASTM D 570, 23°C	percent	0.10	0.04
Water Vapor Transmission ²	ASTM E 96	g/day · m ²	0.024	0.009

SEAM PROPERTIES	METHOD	UNITS	MINIMUM ¹	TYPICAL
Shear Strength	ASTM D 4437, NSF mod.	psi	2000	2700
		ppi	120	166
Peel Strength	ASTM D 4437, NSF mod.	psi	1500	1870
(hot wedge fusion)		ppi	90	115
Peel Strength	ASTM D 4437, NSF mod.	psi	1300	1590
(fillet extrusion)		ppi	78	98

STANDARD ROLL DIMENSIONS

Length	1110 feet	Area	16,650 ft ²
Width	15 feet	Weight	5,000 lbs

This information contained herein has been compiled by National Seal Company and is, to the best of our knowledge, true and accurate. All suggestions and recommendations are offered without guarantee. Final determination of suitability for use based on any information provided, is the sole responsibility of the user. There is no implied or expressed warranty of merchantability of fitness of the product for the contemplated use.

NSC reserves the right to update the information contained herein in accordance with technological advances in the material properties.

6H-0893

NSC

NATIONAL SEAL COMPANY

245 Corporate Blvd. • Suite 300

Aurora, IL 60504

(708) 898-1161 • (800) 323-3820

Fax: (708) 898-3461



HDPE GEOMEMBRANE QUALITY CONTROL SPECIFICATIONS

60 mil

National Seal Company's High Density Polyethylene (HDPE) Geomembranes are produced from virgin, first quality, high molecular weight resins and are manufactured specifically for containment in hydraulic structures. NSC HDPE geomembranes have been formulated to be chemically resistant, free of leachable additives and resistant to ultraviolet degradation.

The following properties are tested as a part of NSC's quality control program. Certified test results for properties on this page are available upon request. Refer to NSC's Quality Control Manual for exact test methods and frequencies.

All properties meet or exceed NSF Standard Number 54.

RESIN PROPERTIES	METHOD	UNITS	MINIMUM ¹	TYPICAL
Melt Flow Index ²	ASTM D 1238	g/10 min	0.50	0.25
Oxidative Induction Time	ASTM D 3895, Al pan, 200°C, 1 atm O ₂	minutes	100	120

SHEET PROPERTIES	METHOD	UNITS	MINIMUM ¹	TYPICAL
Thickness	ASTM D 751, NSF mod.			
Average		mils	60.0	61.5
Individual		mils	57.0	59.7
Density	ASTM D 1505	g/cm ³	0.940	0.948
Carbon Black Content	ASTM D 1603	percent	2.0-3.0	2.35
Carbon Black Dispersion	ASTM D 3015, NSF mod.	rating	A1, A2, B1	A1
Tensile Properties	ASTM D 638			
Stress at Yield		psi	2200	2550
		ppi	132	157
Stress at Break		psi	3800	4850
		ppi	228	298
Strain at Yield	1.3" gage length (NSF)	percent	13.0	16.9
Strain at Break	2.0" gage or extensometer	percent	700	890
	2.5" gage length (NSF)	percent	560	710
Dimensional Stability ²	ASTM D 1204, NSF mod.	percent	1.5	0.4
Tear Resistance	ASTM D 1004	ppi	750	860
		lbs	45	53
Puncture Resistance	ASTM D 4833	ppi	1800	2130
		lbs	108	131
Constant Load ESCR, Single Point	GRI, GM-5a	hours	200	> 400

¹ This value represents the minimum acceptable test value for a roll as tested according to NSC's Manufacturing Quality Control Manual. Individual test specimen values are not addressed in this specification except thickness.

² Indicates Maximum Value

NSC

NATIONAL SEAL COMPANY
1245 Corporate Blvd. • Suite 300
Aurora, IL 60504
(708) 898-1161 • (800) 323-3820
Fax: (708) 898-3461

How long will my liner last?

| What is the remaining service life of my HDPE geomembrane?

By Ian D. Peggs, P.E., P.Eng., Ph.D.

Introduction

In his keynote lecture at the GeoAmericas-2008 conference last March, Dr. Robert Koerner (et al., 2008) of the Geosynthetic Institute (GSI) reported the ongoing Geosynthetic Research Institute (GRI) work to make the first real stab at assessing the service lives of high-density polyethylene (HDPE), linear low-density polyethylene (LLDPE), reinforced PE, ethylene propylene diene terpolymer (EPDM), and flexible polypropylene (fPP) exposed geomembranes.

The selected environment simulated that of Texas, USA, in sunny ambient temperatures between ~7°C (45°F) and 35°C (95°F). Of course, an exposed black HDPE geomembrane in the sun will achieve much higher temperatures, probably in excess of 80°C (176°F).

I do not know what the temperature would be at 150-300mm above the liner (for those still specifying this parameter), but it is quite immaterial. The only temperature of concern is the actual geomembrane temperature.

The lifetimes are shown in **Table 1**, but it must be recognized that these data are for specific manufactured products with specific formulations. The “greater than” notation indicates that laboratory exposures (incubations) are still on-going, not

that some samples have failed after the indicated time period. The PE-R-1 material is a thin LLDPE, so it might be expected to be the first to reach the defined end of life; the half-life—the time to loss of 50% of uniaxial tensile properties.

It is interesting to note that HDPE-1 and LLDPE-1 are proceeding apace, but it would be expected that the LLDPE-1 would reach its half-life earlier than HDPE-1. However, this does not automatically follow. With adequate additive formulations, perhaps LLDPE could be left exposed and demonstrate more weathering resistance than some HDPEs. This demonstrates the fact that all PEs, whether HD or LLD, are not identical—they can have different long-term performances dependent on the PE resin used and the formulation of the stabilizer package. However, such differences are not evident in the conventional mechanical properties such as tensile strength/elongation, puncture and tear resistances, and so on.

The two fPPs are performing well. However, there had also been an fPP-1, one of the first PP geomembranes that did not perform well. This was due to a totally inappropriate stabilizer formulation. That particular product lasted 1.5 years in service. In

Final Inspection continued on page 44

	Type	Specification	Predicted Lifetime in Texas, USA
	HDPE-1	GRI-GM13	>28 years (Incubation ongoing)
	LLDPEE-1	GRI-GM17	>28 years (Incubation ongoing)
	EPDM-1	GRI-GM21	>20 years (Incubation ongoing)
	PE-R-1	GRI-GM22	≈17 years (reached halflife)
	fPP-2	GRI-GM18 (temp. susp.)	>27 years (Incubation ongoing)
	fPP-3	GRI-GM18 (temp. susp.)	>17 years (Incubation ongoing)

Table 1 | Estimated exposed geomembrane lifetimes

| Ian Peggs is president of I-CORP International Inc. and is a member of *Geosynthetics* magazine's Editorial Advisory Committee.

Final Inspection continued from page 56

the QUV weatherometer, it lasted 1,800 light hours at 70°C (158°F). Therefore, the lab/field correlation is that 1,000 QUV light hours is equivalent to a 0.83yr service life under those specific environmental conditions.

At another location in Texas, Korrner/GRI found 1,000hr of QUV exposure was equivalent to 1.1 year actual field exposure. Consequently, for Texas exposures GRI is using a correlation of 1000hr QUV exposure as equivalent to 1yr of in-service exposure. Clearly, the correlation would be different in less sunny and colder environments.

The failed fPP-1 liner was replaced with a correctly stabilized fPP that, subsequently, performed well.

So how can we evaluate the condition of our exposed liners in a simple and practical manner to ensure they will continue to provide adequate service lifetimes and to get sufficient warning of impending expiration?

For each installation, a baseline needs to be established, and changes from that baseline need to be monitored.

A liner lifetime evaluation program

Rather than be taken by surprise when a liner fails or simply expires, it should be possible to monitor the condition of the liner to obtain a few years of notice for impending expiration. One can then plan for a timely replacement without the potential for accidental environmen-

values that generally significantly exceed the specification.

A final option for the baseline would be to use the values at the time of the first liner assessment.

The first liner condition assessment would consist of a site visit during which a general visual examination would be done together with a mechanical probing of the edges of welds. A visual examination would include the black/gray shades of different panels that might indicate low carbon contents.

A closer examination should be done using a loupe (small magnifier) on suspect areas such as wrinkle peaks, the tops and edges of multiple extrusion weld beads, and the apex-down creases of round die-manufactured sheet.

The last detail is significant because the combination of oxidizing surface and exposed surface tension when the liner contracts at low temperatures and the crease is pulled flat can be one of the first locations to crack. The apex-up creases do not fail at the same time because the oxidized exposed surface is under compression (or less tension) when the crease is flattened out.

Appropriate samples for detailed laboratory testing will be removed.

It may be appropriate to do a water lance electrical integrity survey on the exposed sideslopes, but this would only be effective on single liners, and on double liners with a composite primary liner, a conductive geomembrane, or a geocomposite with a conductive geotextile on top.

A sampling and testing regime

A liner lifetime evaluation program should be simple, meaningful, and cost-effective.

While it will initially require expert polymer materials science/engineering input to analyze the test data and to define the critical parameters, it should ultimately be possible to use an expert system to automatically make predictions using the input test data.

Small samples will be taken from deep in the anchor trench and from appropriate

... it should be possible to monitor the condition of the liner to obtain a few years of notice for impending expiration.

While estimated correlations might be made for other locations using historical weather station sunshine and temperature data, there is no question that the best remaining lifetime assessments will be obtained using samples removed from the field installation of interest.

A lifetime in excess of 28yr, demonstrated for a recently-made HDPE geomembrane, is comparable to the present actual service periods of as long as 30-35yr. However, actual lifetimes of as low as ~15yr have also been experienced.

Do service lifetimes now exceeding 30yr mean that we might expect to see another round of stress cracking failures as exposed liners finally oxidize sufficiently on the surface to initiate stress cracking?

This would be frustrating after resolving the early 1980s problems with stress cracking failures at welds and stone protrusions when the liners contracted at low temperatures, but it is the way end-of-life will become apparent. And will that be soon or in another 5-20 years? It would be useful to know.

tal damage and undesirable publicity. A program of periodic liner-condition assessment is proposed.

For baseline data, it would be useful to have some archive material to test, but that is not usually available. Manufacturers often discard retained samples after about 5 years. Perhaps facility owners should be encouraged to keep retained samples at room temperature and out of sunlight. The next best thing is to use material from the anchor trench or elsewhere that has not experienced extremes in temperature and that has not been exposed to UV radiation or to expansion/contraction stresses.

Less satisfactory options are to use the original NSF 54 specifications, the manufacturer's specifications, or the GRI-GM13 specifications at the appropriate time of liner manufacturing. The concern with using these specifications is that while aged material may meet them, there is no indication of whether the measured values have significantly decreased from the actual as-manufactured

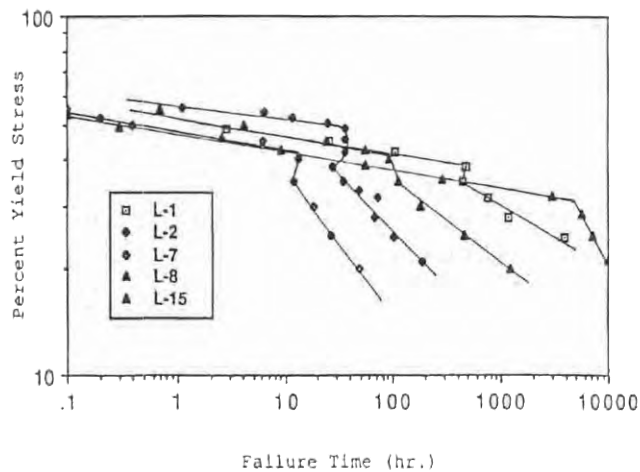


Figure 1 | Standard stress rupture curves for five HDPE geomembranes (Hsuan, et al. 1992)

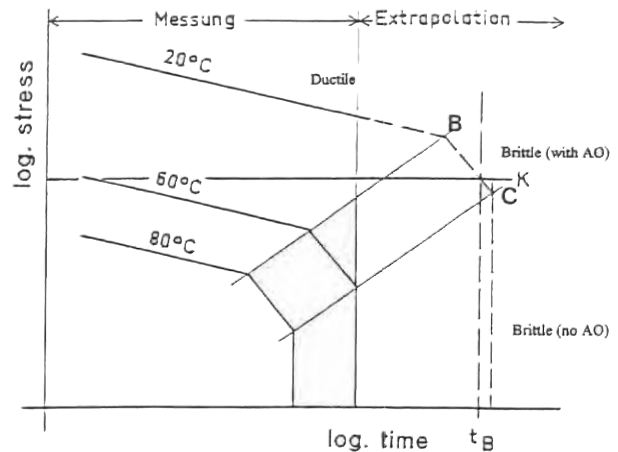


Figure 2 | Stress rupture curves showing third stage (Brittle no AO) oxidized limit. (Gaubert, et al. 1985)

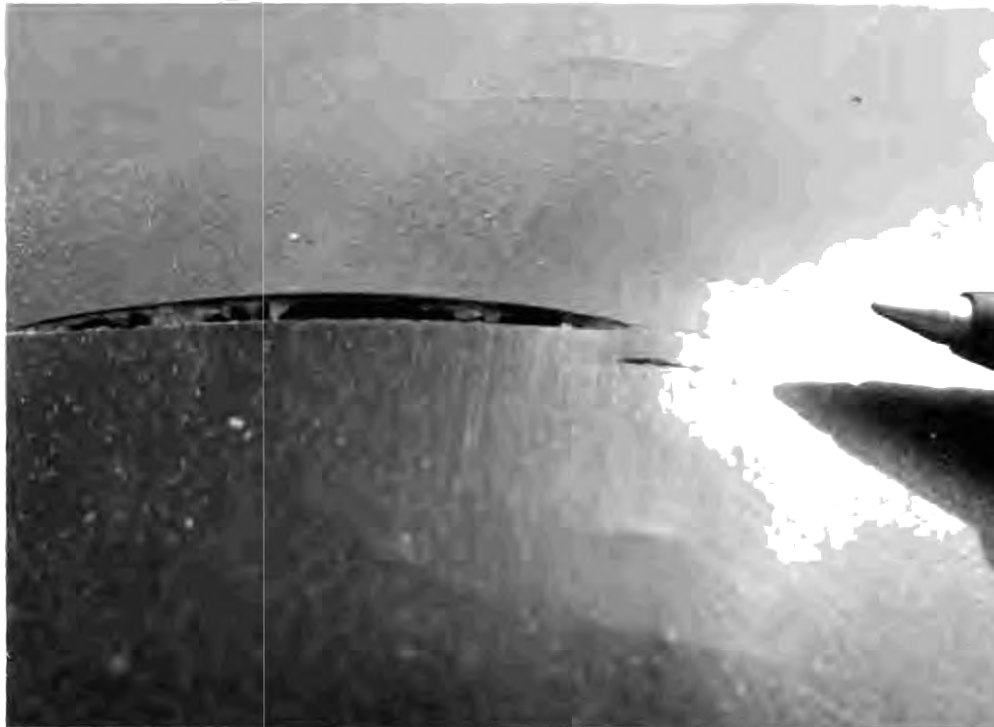


Figure 3 | Stress crack initiated by extruder die line at stone protrusion

exposed locations. Potential sites for future sample removal by the facility owner for future testing will be identified and marked by the expert during the first site visit.

The baseline sample(s) will be tested as follows:

- Single-point stress cracking resistance (SCR) on a molded plaque by ASTM D5397

- High-pressure oxidative induction time (HP-OIT) by ASTM D5885
- Fourier transform infrared spectroscopy (FTIR-ATR) on upper surface to determine carbonyl index (CI) on nonarchive samples only
- Oven aging/HP-OIT (GRI-GM13)
- UV resistance/HP-OIT (GRI-GM13)

The exposed samples will be tested as follows:

- Carbon content (ASTM D1603)
- Carbon dispersion (ASTM D5596)
- Single-point SCR on molded plaque (ASTM D5397)
- Light microscopy of exposed surface, through-thickness cross sections, and thin microsections (~15 μm thick) as necessary
- HP-OIT on 0.5-mm-thick exposed surface layers from basic sheet and from sheet at edge of extruded weld bead (ASTM D5885), preferably at a double-weld bead
- FTIR-ATR on exposed surface to determine CI
- Oven aging/HP-OIT on 0.5mm surface layer (GRI-GM13)
- UV resistance/HP-OIT on 0.5 mm surface layer (GRI-GM13)

Carbon content is done to ensure adequate basic UV protection. Carbon dispersion is done to ensure uniform surface UV protection and to evaluate agglomerates that might act as initiation sites for stress cracking.

HP-OIT is used to assess the remaining amount of stabilizer additives, both in the liner panels and in the sheet adjacent to an extrusion weld. Most stress cracking is observed at the edges of extrusion

weld beads in the lower sheet, so it is important to monitor this location.

While standard OIT (ASTM D3895 at 200°C) better assesses the relevant stabilizers effective at processing (melting) and welding temperatures, the relevant changes in effective stabilizer content during continued service, including in the weld zone, will be provided by measurement of HP-OIT. There will be no future high temperature transient where knowledge of S-OIT will be useful. It is expected that the liner adjacent to the weld bead will be more deficient in stabilizer than the panel itself. Therefore, S-OIT is not considered in this program.

Note that HP-OIT is measured on a thin surface layer because the surface layer may be oxidized while the body of the geomembrane may not. If material

from the full thickness of the geomembrane is used it could show a significant value of OIT, implying that there is still stabilizer present and that oxidation is far from occurring. However, the surface layer could be fully oxidized with stress cracks already initiated and propagating. A crack will then propagate more easily through unoxidized material than would initiation and propagation occur in unoxidized material.

The fact that the HP-OIT meets a certain specification value in the as-manufactured condition provides no guarantee that thermo- and photo-oxidation protection will be provided for a long time. Stabilizers might be consumed quickly or slowly while providing protection. They may also be consumed quickly to begin with, then more slowly, or vice versa.

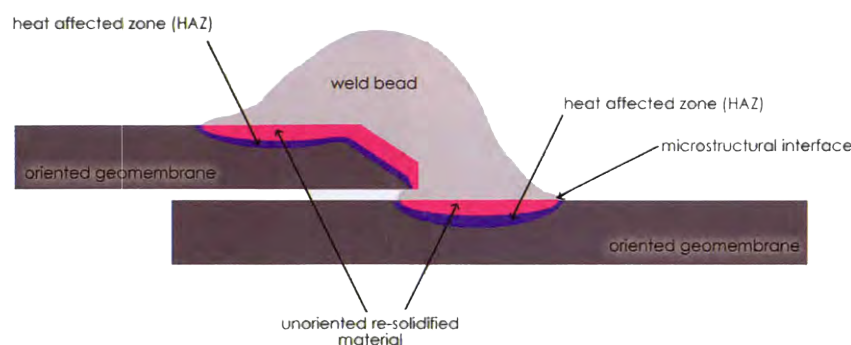


Figure 4 | Schematic of microstructure at extrusion weld

Hence, the need for continuing oven (thermal) aging and UV resistance tests. These two parameters, assessed by measuring retained HP- OIT, are critical to the assessment of remaining service life.

Oven (thermal) aging and UV resistance tests performed in this program will provide an extremely valuable data base that relates laboratory testing to in-service performance and that will further aid in more accurately projecting in-service performance from laboratory testing results.

Special considerations

Because we do not know, by OIT measurements alone, whether the surface layer is or is not oxidized (unless OIT is zero), and since we do not yet know at what level of OIT loss there might be an oxidized surface layer (the database has not yet been generated), FTIR directly on the surface of the geomembrane is performed using the attenuated total reflectance (ATR) technique to deny or confirm the presence of oxidation products (carbonyl groups).

Following the practice of Broutman, et al. (1989) and Duvall (2002) on HDPE pipes, if the ratio of the carbonyl peak at wave number 1760 cm^{-1} and the C-H stretching (PE) peak at wave number 1410 cm^{-1} is more than 0.10, there is a sufficiently oxidized surface layer that

stress cracking might be initiated. For those familiar with the two slope stress rupture curve (**Figure 1**) where the brittle stress cracking region is the steeper segment below the knee, there is a third vertical part of the curve (**Figure 2**) where the material is fully oxidized and fracture occurs at the slightest stress. This is what will happen at the end of service life. But first note the times to initiation of stress cracking (the knees in the curves) in **Figure 1**—they range from $\sim 10/\text{hr}$ to

$\sim 5,000/\text{hr}$ —clearly confirming that all HDPEs are not the same. Some are far more durable than others.

At the end of service life, at some level of OIT, there will be a critically oxidized surface layer that when stressed, such as at low temperatures by an upwards protruding stone, or by flexing due to wind uplift, will initiate a stress crack on the surface that will propagate downward through the geomembrane, as shown by the crack in **Figure 3**.

This crack, initiated at a stress concentrating surface die mark, occurred when the liner contracted at low temperatures, and tightened over an upwardly protruding stone. The straight morphology of the crack, and the ductile break at the bottom surface as the stress in the remaining ligament rose above the knee in the stress rupture curve, are typical of a stress crack. Note the shorter stress cracks initiated along other nearby die marks.

Stress cracks are preferentially initiated along the edges of welds because the adjacent geomembrane has been more depleted of stabilizers during the high temperature welding process. Thus, under further oxidizing service conditions, it will become the first location to

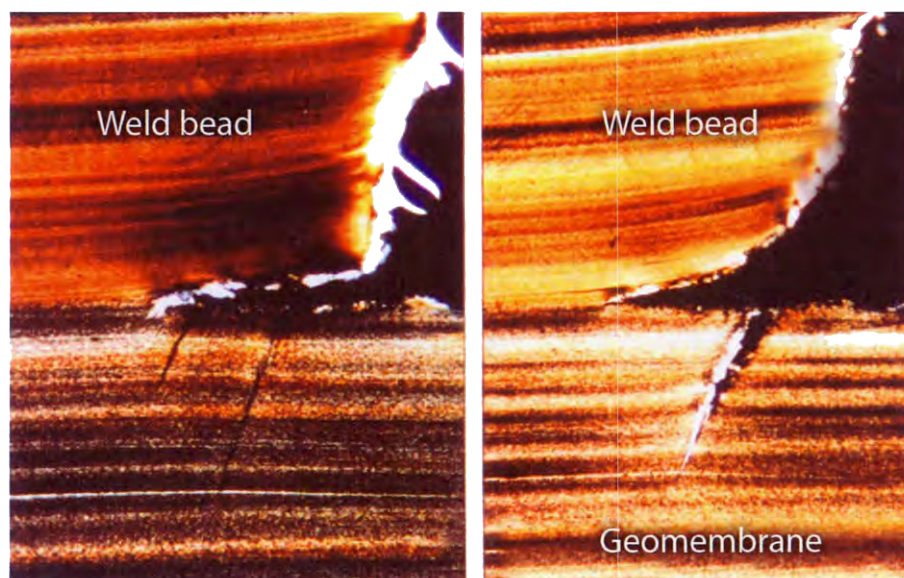


Figure 5 | Typical off-normal angle of precursor crazes (left) and stress crack (right) at edge of extrusion weld.

Type	Specification	Predicted Lifetime in Texas, USA
Side wall exposed	54	5
Side wall concrete side	81	71
Lower launder exposed	16	3
Lower launder concrete side	145	1

Table 2 | S-OIT values on solution and concrete liner surfaces (Peggs, 2008).

be oxidized to the critical level at which stress cracks will be initiated under any applied stress. In addition, the geometrical notches at grinding gouges and at the edges of the bead increase local stresses to critical levels for SC to occur.

I also believe that an internal microstructural flaw exists between the originally oriented geomembrane structure and the pool of more isotropic melted and resolidified material at the edge of the weld zone, as shown schematically in **Figure 4**. Most stress cracks occur at an off-normal angle at the edge of the weld bead that may be related to the angle of this molten-pool to oriented-structure interface (**Figure 5**). It is also known that stress increases the extraction of stabilizers from polyolefin materials.

With all of these agencies acting synergistically, it is not surprising that stress cracking often first occurs adjacent to extrusion welds.

Looking ahead

With the first field assessment test results available to us, and the extent of changes from the baseline sample known, removal of a second set of samples by the facility owner (at locations previously identified and marked by the initial surveyor), will be planned for a future time, probably in 2 or 3 years.

Why 2 or 3 years? In an extreme chemical environment, extensive reductions in

S-OIT of studded HDPE concrete protection liners in mine solvent extraction facilities using kerosene/aromatic hydrocarbon/sulfuric acid process solutions at 55°C (131°F) have been observed on the solution and concrete sides of the liner (**Table 2**) within 1 year (Peggs 2008). But it is unlikely that such rapid decreases will be observed in air-exposed material.

With this second set of field samples, and with three sets of data points, practically reliable extrapolations of remaining lifetime can start to be made.

It is expected that a few years of notice for impending failures will be possible.

The key point to note in making these condition assessments is that, while all HDPE geomembranes have very similar conventional index properties, they can have widely variable photo-oxidation, thermal-oxidation, and stress-cracking resistances. Therefore, some HDPEs are more durable than others.

Thus, while one HDPE geomembrane manufactured in 1990 failed after 15 years in 2005, another HDPE geomembrane made in 1990 from a different HDPE resin (or more correctly a medium-density polyethylene [MDPE] resin), and with a better stabilizer additive package, could still have a remaining lifetime of 5, 20, or 30 years.

So, keep a close eye on those exposed liners and we'll learn a great deal more about liner performance and get notice of

the end of service lifetime. And if owners can retain some archive material from new installations, so much the better.

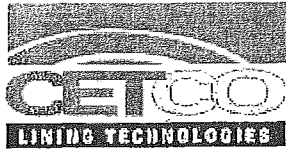
References

- Broutman L.J., Duvall, D.E., So, P.K. (1989). "Fractographic Study of a Polyethylene Sewer Pipe Failure." SPE Antec, pp 1599-1602.
- Duvall, D.E. (2002). "Analyses of Large Diameter Polyethylene Piping Failures." Proceedings of the Society of Plastics Engineers, 60th Annual Technical Conference.
- Gaube, E., Gebler, H., Müller, W., and Gondro, C. (1985). "Creep Rupture Strength and Aging of HDPE Pipes 30 Years Experience in Testing of Pipes." *Kunststoffe* 74 7, pp 412-415.
- Koerner, R.M., Hsuan, Y.G., Koerner, G. (2008). "Freshwater and Geosynthetics: A Perfect Marriage." Keynote Lecture at GeoAmericas 2008, IFAI, Roseville, Minn., USA.
- Hsuan, Y.G., Koerner, R.M., Lord, A.E., Jr., (1992). "The Notched Constant Tensile Load (NCTL) Test to Evaluate Stress Cracking Resistance." 6th GRI Seminar, MQC/MQA and CQC/CQA of Geosynthetics, Folsom, Pa., USA, pp 244-256.
- Peggs, I.D., (2008). "The Performance of Concrete Protection Liners in Mine SX/EW Mixers and Settlers: The Need for Chemical Resistance Testing." Proceedings of GeoAmericas 2008, IFAI, Roseville, Minn., USA. **G**

**APPLICATION FOR PERMIT RENEWAL AND MODIFICATION
SANDOVAL COUNTY LANDFILL**

**VOLUME III: LANDFILL ENGINEERING CALCULATIONS
SECTION 4: COMPATIBILITY DEMONSTRATION**

**ATTACHMENT III.4.B
GEOSYNTHETIC CLAY LINER REFERENCE DOCUMENTATION**



Laboratory Data Reports

THE EFFECTS OF LEACHATE ON THE HYDRAULIC CONDUCTIVITY OF BENTOMAT®

Compatibility testing was performed to determine the effects of solid waste landfill leachate on the permeability of Bentomat over a prescribed time period. Testing was performed in accordance with United States Environmental Protection Agency (USEPA) Method 9100, as provided in SW846.

Hydration of specimens was conducted using de-aired tap water for approximately 48 hours. Saturation was also conducted using de-aired tap water until a minimum B value of 0.95 was achieved. Following hydration and saturation, baseline hydraulic conductivity was performed using water. After the baseline hydraulic conductivity was established, the permeant was switched to leachate. Testing continued for an additional 30 days to allow a sufficient number of pore volumes to permeate the specimen to establish a hydraulic conductivity with leachate.

Results show that the hydraulic conductivity of Bentomat ^{was} unaffected when permeated with this leachate.

TR-101A
Revised 12/00

1500 W. Shure Drive • Arlington Heights, IL 60004 • USA • (847) 392-5800 • FAX (847) 577-5571 /www.CETCO.com
A wholly owned subsidiary of AMCOL International

The information and data contained herein are believed to be accurate and reliable. CETCO makes no warranty of any kind and accepts no responsibility for the results obtained through application of this information.

FINAL REPORT
LABORATORY TESTING OF BENTOMAT

Prepared for

American Colloid Company
One North Arlington
1500 West Shure Drive
Arlington Heights, Illinois 60004-1434

Prepared by

GeoSyntec Consultants
Geomechanics and Environmental Laboratory
1600 Oakbrook Drive, Suite 565
Norcross, Georgia 30093

GeoSyntec Consultants Project Number: GL1614

31 July 1991

2. TEST PROCEDURES

2.1 Task 1: EPA 9100 Compatibility Testing

Compatibility testing on the Bentomat was performed to measure the effect of leachate on the hydraulic conductivity of the mat product over a prescribed period of time. Testing was performed in accordance with the United States Environmental Protection Agency (USEPA) Method 9100 SW-846, Revision 1, 1987. The test conditions for Task 1 were as follows:

- Testing was conducted using flexible-wall triaxial permeameters, as shown in Photograph 2.1-1.
- Three replicate samples of the Bentomat were tested.
- Each sample was trimmed to a diameter of 2.8 in. (70 mm) and assembled in the following test configuration (from bottom to top): porous stone/filter paper/sand layer/Bentomat/sand layer/filter paper/porous stone.
- Hydration and saturation of the samples using de-aired tap water was conducted at an effective stress of 2.0 psi (14 kPa) for a time period of approximately 48 hours. Saturation was defined as a minimum Skempton's B-parameter of 0.95.
- Consolidation of the saturated test samples was performed at an effective stress of 5.0 psi (35 kPa). Pore-water displacement was monitored until primary consolidation was complete.
- To determine the baseline hydraulic conductivity, the samples were permeated using de-aired tap water. The average hydraulic gradient used for baseline permeation was approximately 50. For this testing program, initial hydration and saturation was

conducted using de-aired tap water. Hydration with leachate may or may not yield different results.

- After establishing the baseline hydraulic conductivity, the permeant was switched to the leachate. Because of the slow permeation rates and the objective to increase the volume of leachate in contact with the Bentomat, the sand layer was replaced on all samples by an Amoco 4516 geotextile after approximately three weeks of testing. Permeation of the samples with the leachate continued for an additional 30 days. The hydraulic conductivity of the sample was monitored and reported daily during this period.
- Permeation of the test specimens with the leachate was initially conducted at an average hydraulic gradient of approximately 50. In order to increase flow through the Bentomat during the prescribed time period, the average hydraulic gradient was increased to approximately 160.
- Because the final hydrated thickness of the Bentomat is unknown until the completion of testing and for comparison of the test data, the hydraulic conductivity was calculated using 0.4 in. (1.0 cm) for the Bentomat. These values were used in all calculations of hydraulic conductivity in Tasks 1 through 7.

TABLE 3.1-1

EPA 9100 COMPATIBILITY TESTING
BENTOMAT SPECIMEN CONDITIONS

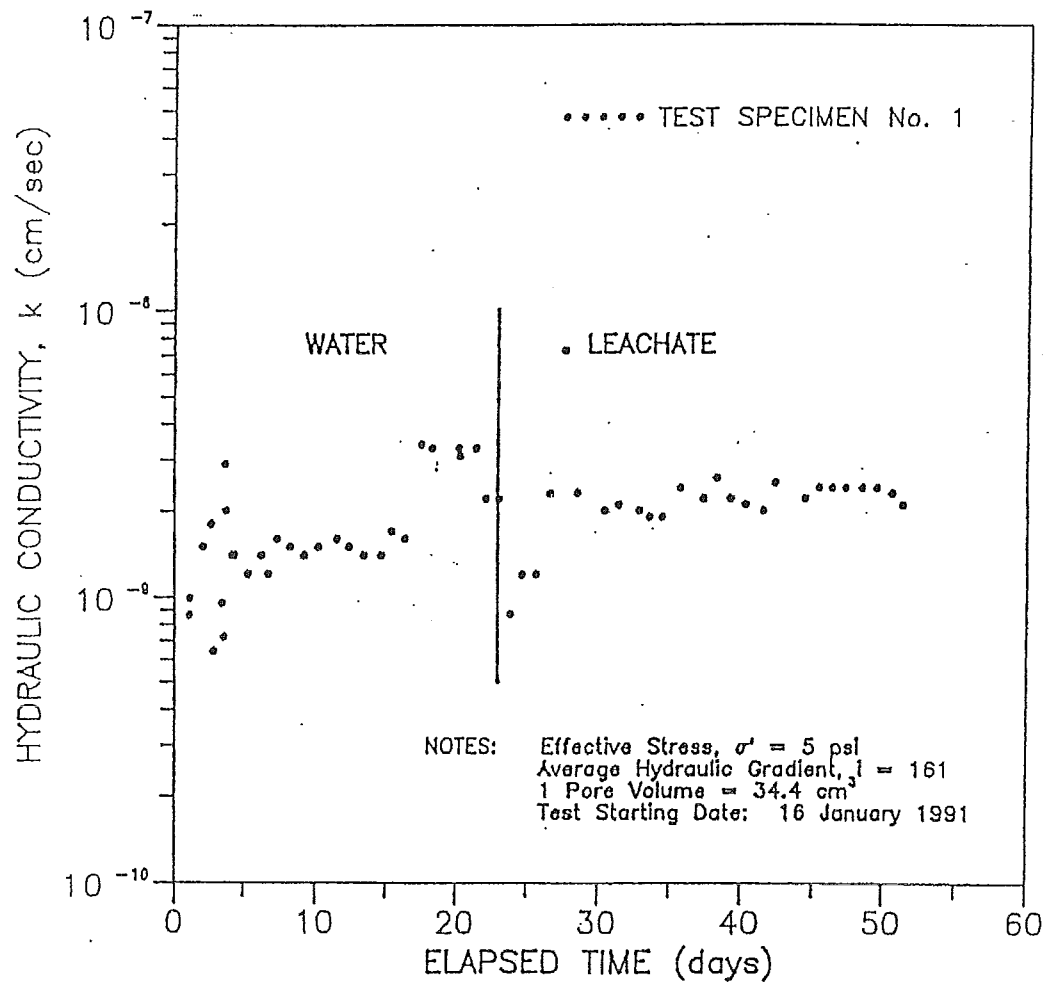
American Colloid Company

Parameters	Specimen No. 1		Specimen No. 2		Specimen No. 3	
	Initial	Final	Initial	Final	Initial	Final
Thickness, in.	0.29	0.39	0.33	0.43	0.28	0.36
Diameter, in.	3.01	3.14	3.19	3.30	3.11	3.18
¹ Dry Mass, g	30.8	24.4	38.3	31.4	34.4	26.1
² Mass/Area, lb/ft ²	1.37	1.00	1.54	1.16	1.44	1.05
Water Content, %	18.8	170.1	15.7	169.4	10.9	167.4

Notes: ¹ The dry mass includes the dry weight of the bentonite and the geotextiles bonded to the specimen.

² The mass/area is determined using the dry mass of the material normalized with respect to the cross-sectional area of the test specimen before drying.

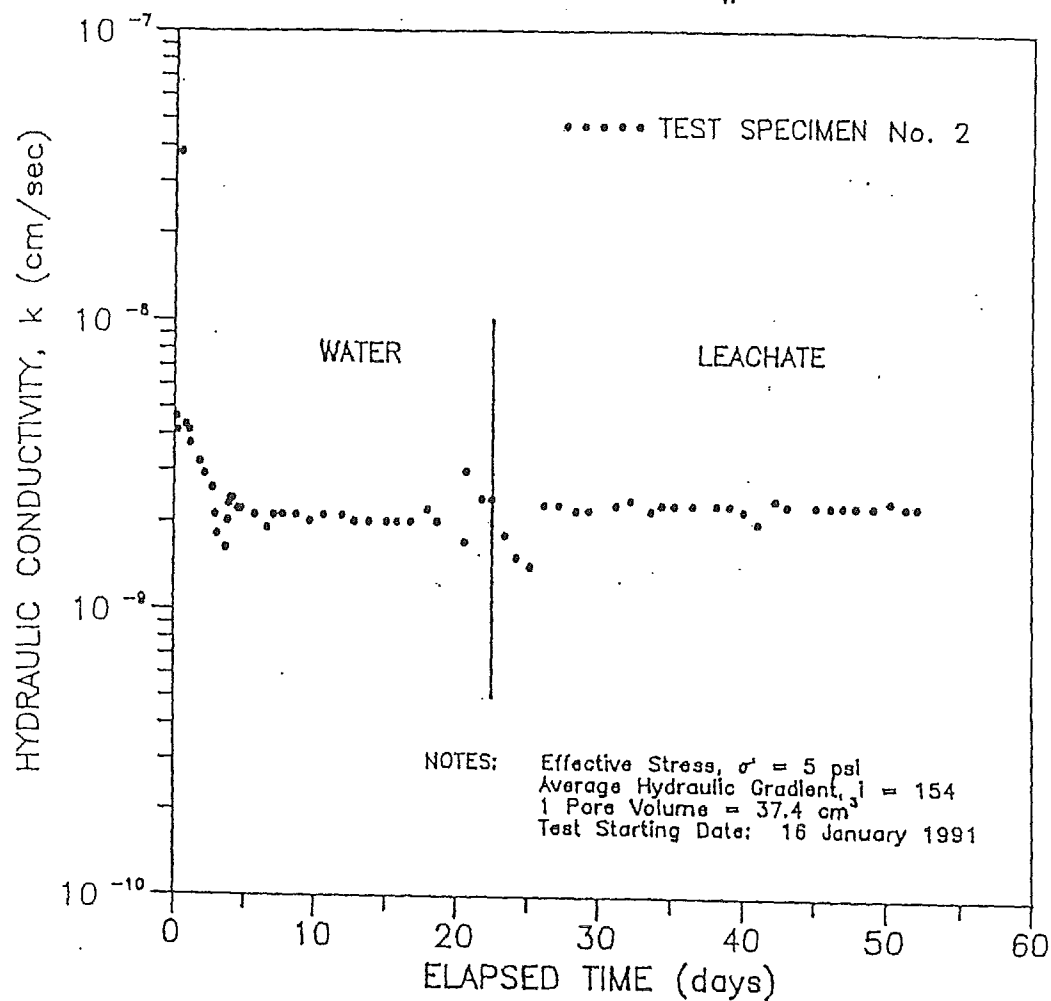
EPA 9100. COMPATIBILITY TESTING
BENTOMAT SAMPLE #ELO05



GEOSYNTEC CONSULTANTS
GEOMECHANICS AND ENVIRONMENTAL LABORATORY

FIGURE NO.	3.1-1
PROJECT NO.	GL1614
DOCUMENT NO.	GEL91066
PAGE NO.	

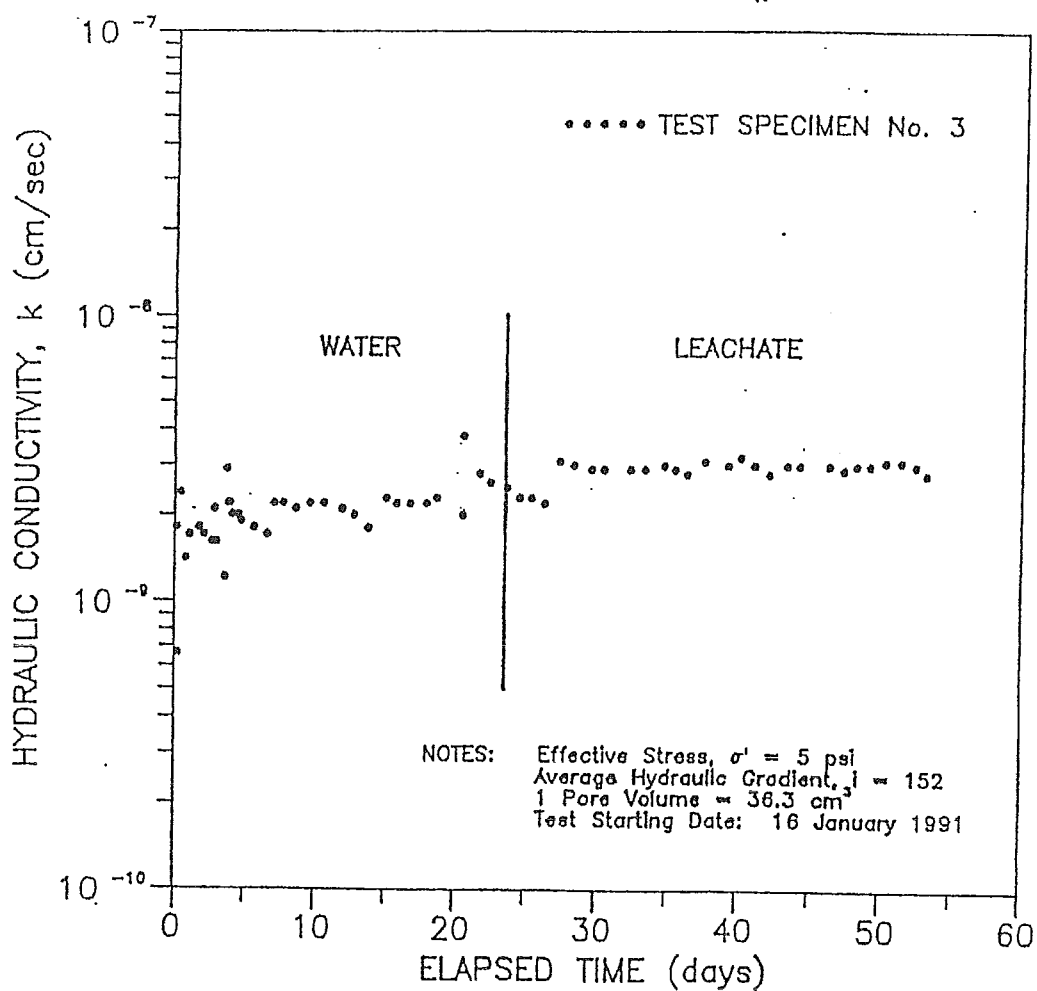
EPA 9100 COMPATIBILITY TESTING BENTOMAT SAMPLE #EL005



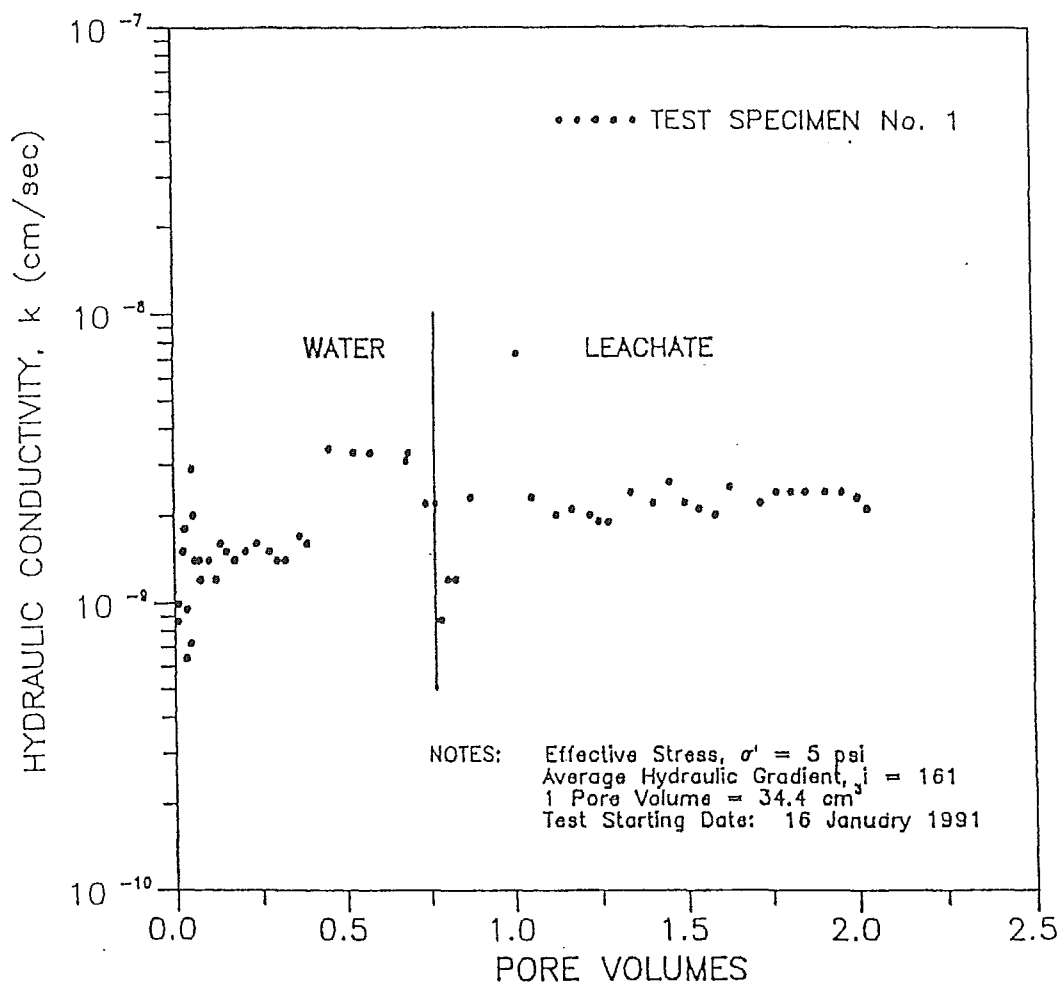
GEOSYNTEC CONSULTANTS
GEOMECHANICS AND ENVIRONMENTAL LABORATORY

FIGURE NO.	3.1-2
PROJECT NO.	GL1614
DOCUMENT NO.	GEL91066
PAGE NO.	

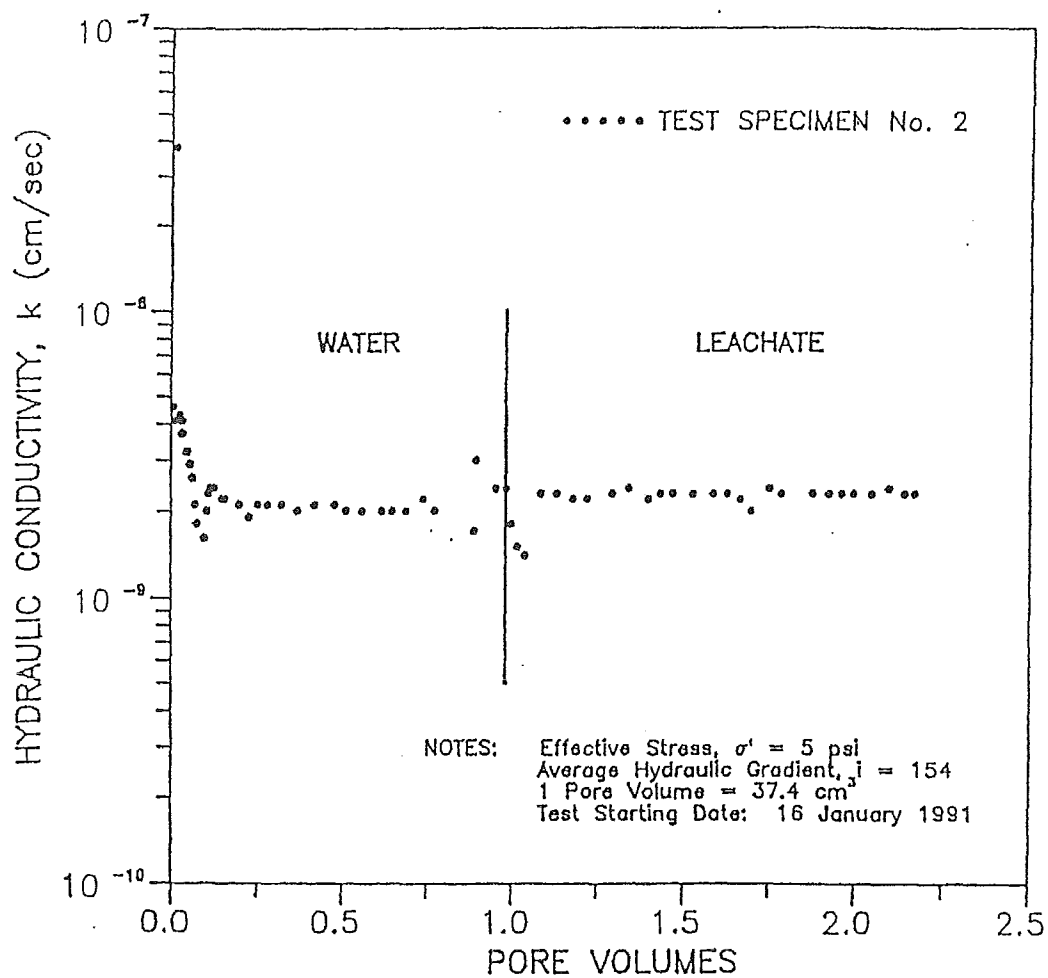
EPA 9100 COMPATIBILITY TESTING BENTOMAT SAMPLE #ELO05



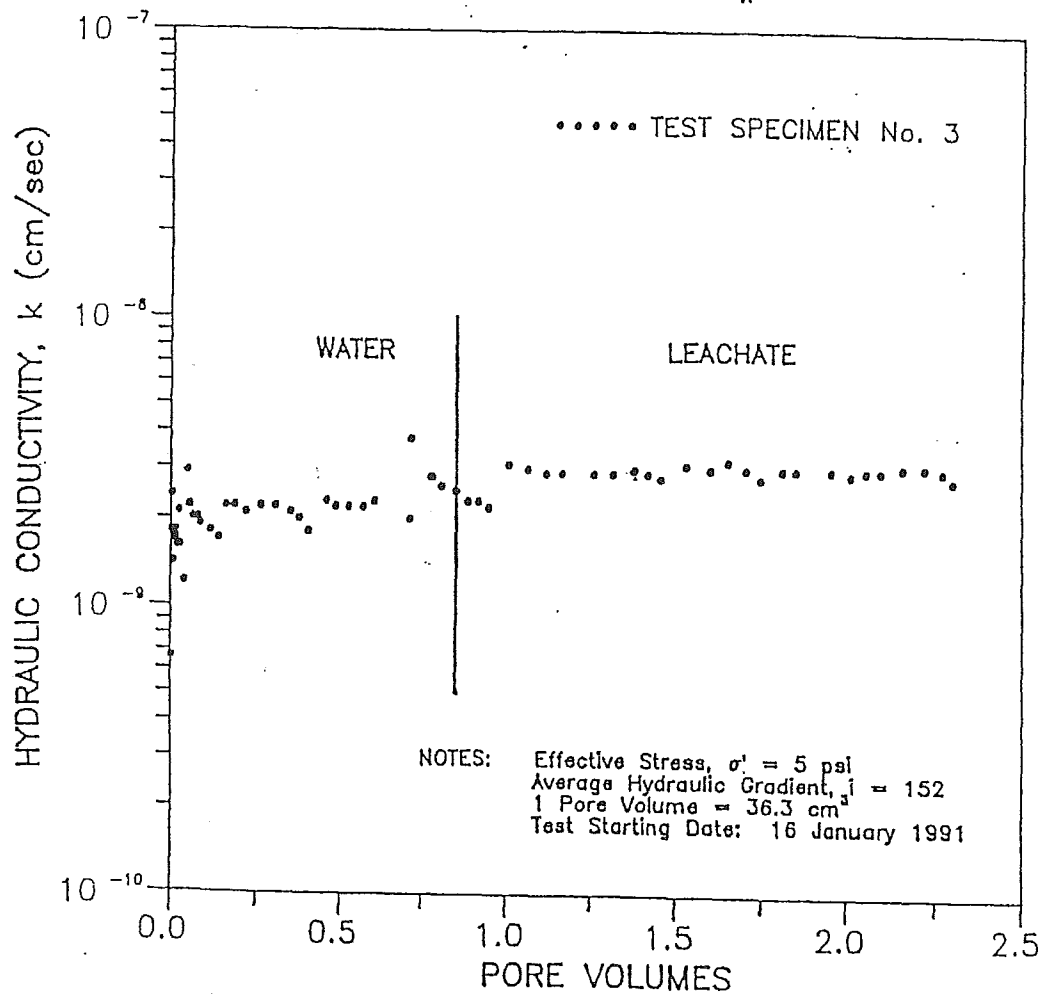
EPA 9100 COMPATIBILITY TESTING BENTOMAT SAMPLE #ELO05



EPA 9100 COMPATIBILITY TESTING BENTOMAT SAMPLE #ELO05



EPA 9100 COMPATIBILITY TESTING BENTOMAT SAMPLE #EL005



GEOSYNTEC CONSULTANTS
GEOMECHANICS AND ENVIRONMENTAL LABORATORY

FIGURE NO.	3.1-6
PROJECT NO.	GL1614
DOCUMENT NO.	GEL91066
PAGE NO.	

3.1 Task 1: EPA 9100 Compatibility Testing

3.1.1 Test Results

The physical conditions of the three Bentomat specimens, measured before and after the tests, are summarized in Table 3.1-1. Graphical presentations of the hydraulic conductivity as a function of elapsed time are presented in Figures 3.1-1, 2, and 3. Graphical presentations of the hydraulic conductivity as a function of the volume of liquid passed through the specimens (i.e., pore volumes) are presented in Figures 3.1-4, 5, and 6.

3.1.2 Observations

Because of the low hydraulic conductivity of the bentonite mat, and in order to maximize the volume of leachate through the mat, the sand layer in each test was replaced by an Amoco 4516 geotextile during that test. This generally occurred shortly before the permeant was switched from water to leachate. In many cases the data indicated erratic behavior for a short time after the switch, but the hydraulic conductivities eventually became consistent.

All specimens were initially permeated at a hydraulic gradient of 50. The resulting hydraulic conductivity measurements were somewhat variable. The hydraulic gradient was subsequently increased to 160 after approximately five days of testing. The test results tended to stabilize after the gradient increase. The average hydraulic gradients that were used for the remainder of each test after the initial increase gradient is indicated on each figure.

In all cases, the data presented in the tables show that each specimen swelled in thickness and in diameter, and that each specimen experienced an apparent loss of mass. The effluent water however, was not visibly cloudy in any of the tests.

In each figure, a transition from water to leachate is indicated. The variability in the test results near this transition is likely the result of disturbance due to leachate injection and removal of the sand layer. Within a short period of time, the test results stabilized.

BENCH-SCALE HYDRAULIC CONDUCTIVITY TESTS
OF BENTONITIC BLANKET MATERIALS
FOR LINER AND COVER SYSTEMS

by

PAULA ESTORNELL, B.S.C.E.

THESIS

Presented to the Faculty of the Graduate School of
The University of Texas at Austin
in Partial Fulfillment
of the Degree of
MASTER OF SCIENCE IN ENGINEERING

THE UNIVERSITY OF TEXAS AT AUSTIN

August, 1991

aid in maintaining a 6- to 9-in-wide overlap during installation.

2.1.2 Available Laboratory Test Data of the Hydraulic Properties of Bentomat®

2.1.2.1 Bentomat® Permeation with Water

J & L Testing Company (1990) conducted flexible-wall hydraulic conductivity tests on 6-in (150-mm) diameter samples of Bentomat® containing either untreated granular bentonite ("CS" grade) or high-contaminant-resistant bentonite ("SS" grade). Test conditions and results are summarized in Table 2.2. The duration of the tests was not reported. Figure 2.2 presents the relationship between hydraulic conductivity and maximum effective stress. Hydraulic conductivities ranged from 6×10^{-10} cm/s to 6×10^{-9} cm/s.

2.1.2.2 Bentomat® Permeation with Chemical Leachates

GeoSyntec Consultants (1991a) performed compatibility tests on Bentomat® in flexible-wall permeameters in order to measure the effect of landfill leachate on the alternative barrier material. Three 2.8-in (70-mm) diameter replicate samples were permeated first with de-aired water (under an effective stress of 2.0 psi (14 kPa) and a hydraulic gradient of about 50) and then with leachate (under an effective stress of

Table 2.2 Summary of Results of Hydraulic Conductivity Tests on Bentomat® (J&L Testing Company, 1990)

<u>Grade of Bentonite</u>	<u>Stress (psi)</u>				<u>Hydraulic Conductivity (cm/s)</u>
	<u>Cell</u>	<u>Headwater</u>	<u>Tailwater</u>	<u>Maximum Effective</u>	
High-Contaminant-Resistant ("SS")	50	42.2	41.8	8.2	2.1×10^{-9}
	50	44.6	39.4	10.6	7.5×10^{-10}
	50	47.2	36.8	13.2	5.8×10^{-10}
Untreated Granular Bentonite ("CS")	50	42.2	41.8	8.2	5.6×10^{-9}
	50	44.6	39.4	10.6	1.1×10^{-9}
	50	47.2	36.8	13.2	9.8×10^{-10}

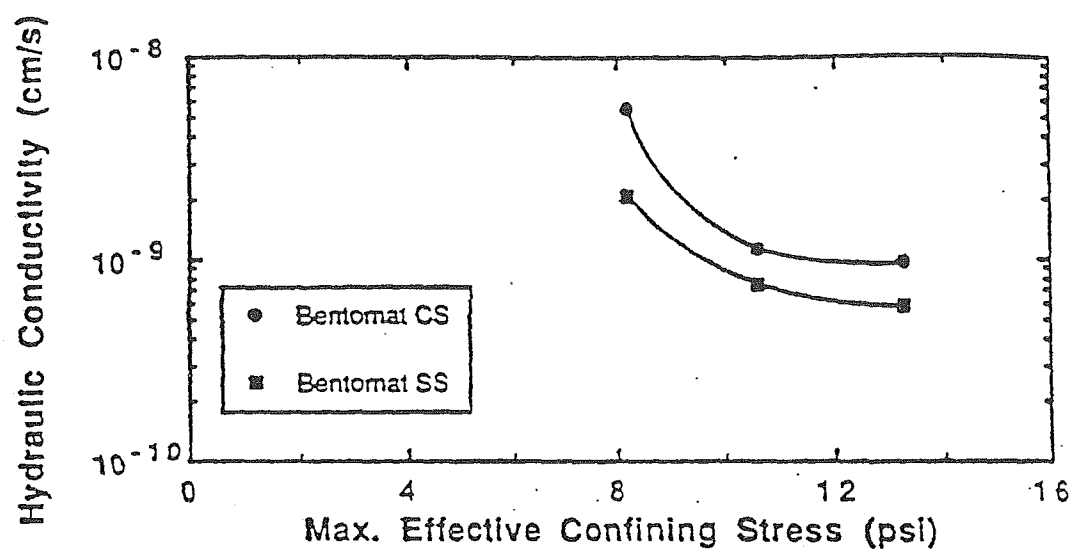


Fig. 2.2 Results of Flexible-Wall Hydraulic Conductivity Tests on Bentomat® (J&L Testing Company, 1990)

5.0 psi (35 kPa) and an average hydraulic gradient of approximately 160). The steady-state hydraulic conductivity, after two months of testing and 2.3 pore volumes of flow, was approximately 2×10^{-9} cm/s using the de-aired water and approximately 2.5×10^{-9} cm/s using the landfill leachate. The results seem to indicate that Bentomat® samples that have been hydrated first with de-aired water will have very little increase in hydraulic conductivity after the introduction of landfill leachate.

2.1.2.3 Effects of Desiccation on Bentomat®

GeoSyntec Consultants (1991a) conducted a flexible-wall hydraulic conductivity test on a 2.8-in (70-mm) sample of Bentomat® that had undergone 4 desiccation cycles. Each cycle involved first permeating the sample with de-aired water (using an effective stress of 5.0 psi (34 kPa) and an average hydraulic gradient of approximately 25) then desiccating the sample for two weeks in a 40°C (104°F) oven. This procedure was repeated 4 times. The steady-state hydraulic conductivity, measured after each cycle, ranged sporadically between 1×10^{-9} cm/s and 3×10^{-9} cm/s. The results show little effect of desiccation on the hydraulic conductivity of Bentomat®.

2.2.2 Available Laboratory Test Data on the Hydraulic Properties of Claymax®

2.2.2.1 Claymax® Permeation with Water

Literature published by the James Clem Corporation lists 2×10^{-10} cm/s as the hydraulic conductivity of Claymax® permeated with de-aired water. A summary of published measurements of the hydraulic conductivity of Claymax® to water is given in Table 2.4. Results are plotted in Fig. 2.5 in terms of hydraulic conductivity versus effective confining stress. The results show that the hydraulic conductivity to water varies from just under about 1×10^{-8} cm/s at low effective stress to just above 1×10^{-10} cm/s at high effective stress.

2.2.2.2 Claymax® Permeation with Various Liquid and Chemical Leachates

The information available concerning hydraulic conductivity of Claymax® permeated with liquids other than water is summarized in Table 2.5. All of the test specimens that were hydrated with water and then permeated with chemicals maintained a hydraulic conductivity $\leq 1 \times 10^{-8}$ cm/s, even for compounds such as diesel fuel and heptane that would normally be very aggressive to soil liner materials. Brown, Thomas, and Green (1984), for example, found that the

Table 2.4 Results of Hydraulic Conductivity Tests on Claymax® Permeated with Water

Source of Information	Permeameter	Backpressure Saturation?	Permeant/ Water	Diameter of Sample (in.)	Effective Stress (psf)	Hydraulic Conductivity (cm/s)
Clem Corp. Literature	- -	- -	Deaired Water	- -	- -	2×10^{-10}
Chen-Northern (1988)	Flex. Wall	Yes	- -	2.5	3.5	2×10^{-9}
GeoServices (1988a)	Flex. Wall	Yes	Deaired Tap Water	2.8	29	4×10^{-10}
GeoServices (1989c)	Flex. Wall	Yes	Deaired Tap Water	2.8	30	8×10^{-10}
GeoServices (1989c)	Flex. Wall	Yes	Deaired Tap Water	2.8	30	8×10^{-10}
GeoServices (1989c)	Flex. Wall	Yes	Deaired Tap Water	2.8	30	3×10^{-10}
GeoServices (1989c)	Flex. Wall	Yes	Deaired Tap Water	2.8	30	7×10^{-10}
Shan (1990)	Flex. Wall	No	Distilled Water	4.0	2	2×10^{-9}
Shan (1990)	Flex. Wall	No	Tap Water	4.0	2	2×10^{-9}
Shan (1990)	Flex. Wall	No	Distilled Water	4.0	5	1×10^{-9}
Shan (1990)	Flex. Wall	No	Tap Water	4.0	5	8×10^{-10}
Shan (1990)	Flex. Wall	No	Distilled Water	4.0	10	6×10^{-10}
Shan (1990)	Flex. Wall	No	Distilled Water	4.0	20	3×10^{-10}
Shan (Unpub.)	Flex. Wall	Yes	Tap Water	12	2	2×10^{-9}
GeoServices (1990b)	Flex. Wall	Yes	Deaired Water	- -	30	3×10^{-10}
GeoSyntec (1990a)	Flex. Wall	Yes	Deaired Water	- -	1.0	2×10^{-9}
GeoSyntec (1990a)	Flex. Wall	Yes	Deaired Water	- -	1.5	4×10^{-9}

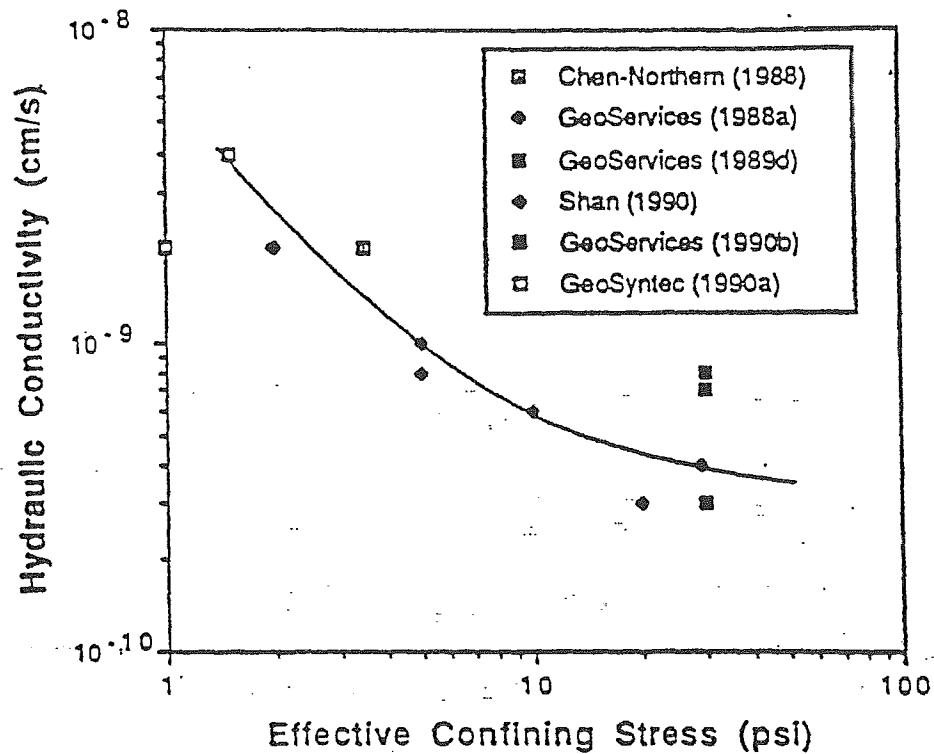


Fig. 2.5 Results of Hydraulic Conductivity Tests on Claymax® Permeated with Water

Table 2.5 Hydraulic Conductivity of Claymax® Permeated with Various Liquids

Source of Information	Permeant Liquid	Hydrallon Liquid	Pore Volumes of Flow	Effective		Hydraulic Conductivity (cm/s)
				Stress (psi)	Stress	
STS Consultants (1988b)	Sewage Leachate	Sewage Leachate	-	-	-	8×10^{-10}
STS Consultants (1988c)	Paper Pulp Sludge	Paper Pulp Sludge	-	-	-	2×10^{-10}
GeoServices (1988b)	Simulated Seawater	Simulated Seawater	-	30	30	2×10^{-10}
STS Consultants (1989a)	Landfill Leachate	Landfill Leachate	-	-	-	4×10^{-10}
STS Consultants (1989b)	Ash-Fill Leachate	Ash-Fill Leachate	-	-	-	1×10^{-10}
GeoServices (1989c)	Diesel Fuel	Water	1.5	30	30	9×10^{-10}
GeoServices (1989c)	Jet Fuel	Water	2.5	30	30	9×10^{-10}
GeoServices (1989c)	Unleaded Gasoline	Water	1.6	30	30	3×10^{-10}
Shan (1990)	50% (Vol) Methanol	Water	2.2	5	5	9×10^{-10}
Shan (1990)	Heptane	Water	0.2	5	5	1×10^{-10}
Shan (1990)	Sulfuric Acid	Water	3.1	5	5	6×10^{-11}
Shan (1990)	0.01 N CaSO ₄	Water	2.2	5	5	1×10^{-9}
Shan (1990)	0.5 N CaCl ₂	Water	2.4	5	5	8×10^{-9}
Shan (Unpublished)	50% (Vol) Methanol	50% Methanol	4	5	5	5×10^{-6}
Shan (Unpublished)	Methanol	Methanol	5.4	5	5	3×10^{-5}
Shan (Unpublished)	Heptane	Heptane	4.3	5	5	5×10^{-5}
GeoServices (1990a)	Methyl Tertiary Butyl Ether	Deaired Water	1.6	30	30	7×10^{-10}
Klohn Leonoff (1990)	Solution from Goldmine	Solution from Goldmine	1.8	17.4	17.4	2×10^{-10}
GeoSyntec (1991b)	Landfill Leachate	Deaired Water	1.7	5	5	3×10^{-9}

hydraulic conductivity of a compacted, micaceous soil was 1 to 4 orders of magnitude higher to kerosene, diesel fuel, and gasoline than it was to water. The inconsistency of results reported in Table 2.5 to the research conducted by Brown and his co-workers may be related to either a small cumulative pore volumes of flow in the tests on Claymax® or application of a high compressive stress to the test specimens. The cumulative pore volumes of flow of permeant liquid was not reported in many of the test referenced in Table 2.5; in many cases, there was probably an insufficient quantity of flow to determine the full effects of the permeant liquids. In some tests, a large effective confining stress was used. Broderick and Daniel (1990) found that one compacted clay was vulnerable to significant alterations in hydraulic conductivity when compressive stresses were $\leq 5 - 10$ psi (34 - 69 kPa) but did not undergo an increase in hydraulic conductivity when the specimens were permeated with compressive stresses larger than 5 to 10 psi (34 to 69 kPa). Brown and his co-workers applied no compressive stress to their test specimens.

Tests on specimens of Claymax® that were hydrated with the same liquid as the eventual permeant liquid (rather than water) showed mixed results. For leachates, a paper pulp sludge, and simulated seawater, the hydraulic conductivity was found to be $< 1 \times 10^{-9}$ cm/s. However, the significance of

these results is questionable because the duration of the tests was short, the cumulative pore volumes of flow was not reported, and the applied compressive stress was not reported. In as-yet unpublished tests by Shan, markedly different results were obtained when Claymax® was not prehydrated with water. Shan found that when dry Claymax® was permeated directly with a 50% mixture of water and methanol, with pure methanol, or with heptane, the bentonite did not hydrate even after several pore volumes of flow, and the hydraulic conductivity did not drop below 1×10^{-6} cm/s. Shan used a compressive stress of 5 psi (34 kPa). Thus, with concentrated organic liquids, the conditions of hydration appear to play an important role in determining the ability of the bentonitic blanket to resist the deleterious action of organic chemicals. The bentonite appears to be more chemically resistant if hydrated with fresh water before exposure to concentrated organic chemicals.

2.2.2.3 Effects of Desiccation on Claymax®

The effects of desiccation were investigated by GeoServices (1989d). Three hydrated samples of Claymax® were placed in a temperature- and humidity-controlled chamber. The chambers operated on a timed cycle to simulate day and night conditions. The temperature and humidity during

thick HDPE geomembrane, was the material tested during this study.

2.3.2 Available Laboratory Test Data of the Hydraulic Properties of Paraseal and Gundseal

2.3.2.1 Paraseal Permeation with Water

Pittsburgh Testing Laboratory (1985) conducted a hydraulic conductivity test on a 2.5-in (64-mm) diameter sample of Paraseal. A 15-ft (4.6-m) head of water was applied to the sample, which was soaked for 5 days prior to permeation. A single, falling-head test was performed, which yielded a hydraulic conductivity reported to be 4×10^{-10} cm/s. Further details of the test procedures are not available. However, because the direction of flow was apparently through the HDPE membrane, the test may have provided a measure of sidewall leakage rather than flow through the material.

2.3.2.2 Gundseal Permeation with Chemical Leachates

The hydraulic conductivity of Gundseal permeated with landfill leachate was measured by GeoSyntec Consultants (1991c). A grid of 0.12-in (3-mm) diameter holes on 0.3 in (0.75 cm) centers were drilled into the Gundseal test samples in order to effectively test the bentonite portion of the Gundseal product. Three 2.8-in (70-mm) diameter samples

were placed in flexible-wall permeameters and subjected to an effective stress of 5.0 psi (35 kPa). The test specimens were permeated, first with de-aired water then with leachate. The average hydraulic gradient applied during permeation with de-aired water was 50. The hydraulic gradient was increased to 230 during permeation with the leachate in order to increase flow through the Gundseal. The average hydraulic conductivity of the punctured Gundseal specimens was 1×10^{-9} cm/s for both the de-aired water and the leachate after approximately 1.2 pore volumes of flow. The hydraulic conductivity of the prehydrated bentonite appeared unaffected by the introduction of the leachate.

2.3.2.3 Effects of Desiccation on Gundseal

GeoSyntec Consultants (1991c) measured the hydraulic conductivity of a sample of Gundseal that had undergone 4 desiccation cycles. The 2.8-in (70-mm) diameter sample was punctured with small holes in the same grid pattern as the samples described previously. The test sample was permeated with de-aired water in a flexible-wall permeameter under an effective stress of 5.0 psi (34 kPa) and an average hydraulic gradient of 215 in order to determine hydraulic conductivity. The sample was removed from the permeameter, subjected to a 0.4 psi (3 kPa) confining stress, and placed in an oven for two

2.5 Summary of Hydraulic Properties of Bentomat®, Claymax®, and Paraseal/Gundseal

Table 2.10 is an abridged summary of the hydraulic conductivity data of Bentomat®, Claymax®, and Paraseal/Gundseal. The table includes results from tests conducted by GeoSyntec (1991a,b,c), GeoSyntec (1990b), and Shan (1990). Results from hydraulic conductivity tests conducted by other laboratories have not been included in Table 2.10 in order to present the information in a simplified and concise form.

Table 2.10 Summary of Hydraulic Conductivity Tests on Bentomax®, Claymax®, and Paraseal/Gundseal

Sample	Bentomax®			Claymax®			Paraseal/Gundseal		
	Reference	Effective Stress (psf)	Hydraulic Conductivity (cm/s)	Reference	Effective Stress (psf)	Hydraulic Conductivity (cm/s)	Reference	Effective Stress (psf)	Hydraulic Conductivity (cm/s)
Sample Permeated with Deaired Water	GeoSynTec (1991a)	2.0	2.0×10^{-9}	GeoSynTec (1991b)	2.0	1.8×10^{-9}	GeoSynTec (1991c)	5.0	1×10^{-9}
★ Sample Permeated with Landfill Leachate	GeoSynTec (1991a)	5.0	2.5×10^{-9}	GeoSynTec (1991b)	5.0	2.8×10^{-9}	GeoSynTec (1991c)	5.0	1×10^{-9}
	GeoSynTec (1991a)	5.0	1.0×10^{-9} to 3.0×10^{-9}	Shan (1990)	2.0	2.0×10^{-9}	GeoSynTec (1991c)	5.0	2.0×10^{-9}
Desaturated Sample	GeoSynTec (1991a)	5.0	1.0×10^{-9} to 3.0×10^{-9}	Shan (1990)	2.0	2.0×10^{-9}	GeoSynTec (1991c)	5.0	2.0×10^{-9}
Freeze-Thaw Sample	GeoSynTec (1991a)	5.0	1.0×10^{-9} to 6.0×10^{-9}	Shan (1990)	2.0	2.2×10^{-9}	GeoSynTec (1991c)	5.0	1.0×10^{-9}
Damaged Sample	GeoSynTec (1991a)	5.0	1.3×10^{-4}	Shan (1990)	2.0	5.0×10^{-9}	GeoSynTec (1991c)	5.0	1.0×10^{-3}
	GeoSynTec (1991a)	5.0	1.7×10^{-4}	Shan (1990)	2.0	5.0×10^{-9}	GeoSynTec (1991c)	5.0	1.0×10^{-3}
	GeoSynTec (1991a)	5.0	3.0×10^{-5}	Shan (1990)	2.0	5.0×10^{-9}	GeoSynTec (1991c)	5.0	1.0×10^{-3}
Composite Sample	GeoSynTec (1991a)	5.0	3.0×10^{-9}	Shan (1990)	2.0	4.0×10^{-9}	GeoSynTec (1991c)	5.0	2.0×10^{-9}
Overlapped Seam Sample	GeoSynTec (1991a)	5.0	6.0×10^{-7} to 2.0×10^{-5}	GeoSynTec (1990b)	1.0	2.0×10^{-9}	GeoSynTec (1991c)	5.0	8.0×10^{-8}

(1) The damaged Claymax® sample tested by Shan (1990) was punctured with 3 - 1 inch diameter holes.

Report

Project

HYDRAULIC CONDUCTIVITY AND
COMPATIBILITY TESTING OF CLAYMAX
BALTIMORE COUNTY LANDFILL PROJECT
TOWNSON, MARYLAND

Client

CLEM ENVIRONMENTAL CORPORATION
444 NORTH MICHIGAN AVENUE, SUITE 1610
CHICAGO, IL 60611

Project # 25868-XH

Date MAY 11, 1989



STS Consultants Ltd.
Consulting Engineers
111 Plimston Road

HYDRAULIC CONDUCTIVITY AND COMPATIBILITY TESTING OF CLAYMAX
BALTIMORE COUNTY LANDFILL PROJECT
TOWNSON, MARYLAND

SCOPE OF SERVICES

STS was to perform two hydraulic conductivity tests on sections of Claymax liner material in conjunction with a six inch sand layer utilizing leachates as the hydration medium and the permeants. The Claymax specimens were supplied to STS by Clem Environmental and the leachate specimens were obtained from L.A. Solamen, Inc. All testing materials were delivered to our Northbrook Testing Facility.

Test Equipment

The equipment used in the compatibility study was a triaxial compression permeameter. This equipment incorporates the use of a flexible membrane, preventing sidewall seepage. back pressure to facilitate specimen saturation small diameter burettes making measurement of small volumes of collected permeant possible and the system is closed preventing the permeant from being exposed to the surrounding air.

Specimen Construction

Each of the specimens, utilized throughout the testing program, consisted of an approximately six inch cylindrical column of silica sand on top of which a circular section of Claymax was placed. The orientation of the Claymax to the sand provided for permeant flow initiated through the sand followed by the Claymax section. The directional flow of the permeant, is similar to those conditions found in the field applications.

Once the specimens were assembled, a flexible rubber membrane was used to encase the specimens while sealed in the triaxial permeameter chamber.

Test Procedures

After its initial construction and placement in a triaxial compression permeameter each of the specimens is backpressure saturated. To aide in specimen saturation, carbon dioxide gas was allowed to flow freely through the test specimen, inundating the voids in the sand and dry Claymax. The use of this carbon dioxide gas has been accepted as a procedure to aide in specimen saturation. The carbon dioxide gas will go into solution more readily than normal atmospheric air. Once it was determined that the carbon dioxide gas had completely inundated the voids of the test specimen, the permeants were allowed to free flow through the test specimen first saturating the silica sand and then the Claymax section. For this study, the leachates were utilized both as a set hydrating medium and as the actual permeant for the hydraulic conductivity determination.

Two leachates were used during the study. The first was labeled Parkton Landfill and the second labeled as Eastern Sanitary Landfill. It is the understanding of STS Consultants that the two leachates were a municipal landfill leachate and contained such things as heavy metals, phenals, cyanide, copper, phosphorus and other substances.

Once the leachate had fully hydrated the test specimen, the specimen was allowed to stand for a 24 hour hydration period. Following the hydration period, the backpressure saturation techniques were implemented to complete the saturation procedures. This was accomplished by simultaneously increasing the cell and back pressures in increments while maintaining a pressure differential of 0.125 kilograms per square centimeter (KSC). Pressures were incrementally increased until obtaining testing pressures of 4.125 KSC cell pressure and 4.00 KSC back pressure.

Clem Environmental Corporation
STS Project No. 25868-XH
May 11, 1989

Specimen saturation was considered complete when a Skempton's Pore Pressure B-parameter of 0.95 or greater was obtained. The "B" parameter is simply a ratio of an increase in pore water pressure to a simultaneous increase in confining pressure. When full specimen saturation was determined, permeant flow was initiated through the bottom of the test specimen, allowed to flow through the top of the test specimen and collect in a calibrated burette. The test was performed utilizing two separate gradients. The initial gradient consisted of an application of a hydraulic head of one foot. The second gradient was applied as a hydraulic head equivalent to 35 feet.

During the entire test, permeant volume versus time measurements were recorded and the hydraulic conductivity of the test specimen at the two gradients was determined. The test was allowed to continue until it had been determined that a minimum of three pore volumes of pore fluid had passed through the test specimen. Once this had occurred and steady state flow had been established, the test was terminated.

Laboratory Test Results

As a result of the testing as outlined above, the Claymax section utilizing the Parkton Landfill Leachate, as the permeant, obtained hydraulic conductivity values of 2×10^{-10} centimeters per second (cm/sec) for a hydraulic head of one foot and 4×10^{-10} cm/sec for a hydraulic head of 35 feet. The Claymax section exposed to the Eastern Sanitary Landfill leachate obtain hydraulic conductivity values of 3×10^{-10} cm/sec utilizing a hydraulic head of 1 foot and 4×10^{-10} cm/sec utilizing a hydraulic head of 35 feet. A summary of specific specimen characteristics and final hydraulic conductivity values is attached to this report.



STS Consultants Ltd.

STS PROJECT NO. 25868-XH

PROJECT Baltimore County

Landfill Project

DATE 4-24-89

SUMMARY OF HYDRAULIC CONDUCTIVITY TESTS

Permeant	Parkton Landfill	Eastern Sanitary Landfill
Sample No.	1	2
Classification	Claymax with 6" Silica Sand	Claymax with 6" Silica Sand
Unit Weight (pcf)	51.6	62.5
Water Content (%)	Dry	Dry
Diameter (cm)	7.028	7.026
Length (cm)	0.568	0.616
Saturation B Value	0.97	0.99
Hydraulic Conductivity k (cm/sec)	1 ft. 2×10^{-10} 35 ft. 4×10^{-10}	1 ft. 3×10^{-10} 35 ft. 4×10^{-10}



Dennis F. Rasmussen
County Executive

BALTIMORE COUNTY
WASTEWATER MONITORING AND ANALYSIS DIVISION
INDUSTRIAL DISCHARGE CONTROL PROGRAM

Rev: 12/87

SAMPLING/ANALYSIS FORM

Sample No.: 9 01110

Industry Name: EASTERN SANITARY LANDFILL Facility No.:
Address: Days Cove Road
Telephone: Requested by: P. Phillips
Sampling Site Location: Leachate pit
Special Instructions: STD 5, metals, Total alkalinity & Chlorides

FIELD

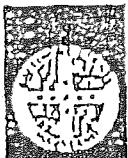
Date and Time of Sampling: Start 1/18/89 10:20 a.m. Finish
Sampled by: P. Phillips, T.E. Ryan
Type of Sample: Grab
Sampler Settings: N/A
Sample Characteristics: 1 quart; dark gray; 1 quart; dark brown
Preservatives Added: Cooled with ice
Comments and Observations:
Delivered to Lab by: PP, TER Date: 1/18/89 Time: 11:50 a.m.

LABORATORY

Sample received by: WP Date: 1/18/89 Time: 11:50 a.m.
Characteristics of Note:
(Origin of Seed: Polysand)

ANALYTICAL RESULTS

Code	BDL	Parameter	Conc. (mg/L)	Code	BDL	Parameter	Conc. (mg/L)
		pH	6.3	3011	0.05	Ni (Nickel)	BDL
		BOD	122 mg/L	3015	0.01	Zn (Zinc)	0.05 mg/L
		COD	148 mg/L	3130		Phenols	
		TSS	125 mg/L	3013	0.01	Silver	BDL
5012		FOG - A&V					
5013		FOG - Petr		*		GRAB pH	
2026		P (Phosphorus)	2.52 mg/L				
3006	0.01	Cd (Cadmium)	BDL			Total Fe	3.88 mg/L
3007	0.03	Cr (Chromium)	BDL			Total alkalinity	350 mg/L
3008	0.02	Cu (Copper)	0.04 mg/L			Chloride	80 mg/L
4		Cn (Cyanide)					
3009	0.10	Pb (Lead)	0.36 mg/L				



BALTIMORE COUNTY
WASTEWATER MONITORING AND ANALYSIS DIVISION
INDUSTRIAL DISCHARGE CONTROL PROGRAM

Rev: 12/87

Dennis F. Rasmussen
County Executive

SAMPLING/ANALYSIS FORM

Sample No.: 9 02104

Industry Name: PARKTON Facility No.: _____
Address: _____
Telephone: _____ Requested by: R. Much
Sampling Site Location: Cell #3
Special Instructions: pH, BOD, COD, TSS, Alkalinity, Chloride, Metals

FIELD

Date and Time of Sampling: Start 2/9/89 Finish _____
Sampled by: R. Much, R. Kramer
Type of Sample: Grab
Sampler Settings: _____
Sample Characteristics: _____
Preservatives Added: _____
Comments and Observations: _____
Delivered to Lab by: BK, RM Date: 2/9/89 Time: 2:20 P.M.

LABORATORY

Sample received by: WP Date: 2/9/89 Time: 2:20 P.M.
Characteristics of Note: _____

(Origin of Seed: Polyseed)

ANALYTICAL RESULTS

Code	BDL	Parameter	Conc. (mg/L)	Code	BDL	Parameter	Conc. (mg/L)
		pH	6.1	3011	0.05	Ni (Nickel)	1.44 mg/L
		BOD	38,888 mg/L	3015	0.01	Zn (Zinc)	5.45 mg/L
		COD	60,831 mg/L	3130		Phenols	
		TSS	691 mg/L	3013	0.01	Silver	0.03 mg/L
012		FOG - A&V					
013		FOG - Petr		*		GRAB pH	
026		P (Phosphorus)	Interference				
006	0.01	Cd (Cadmium)	0.10 mg/L			Total Fe	736.00 mg/L
007	0.05	Cr (Chromium)	0.22 mg/L			Total alkalinity	15,000 mg/L
008	0.02	Cu (Copper)	0.17 mg/L			Chloride	1,500 mg/L
002		Cn (Cyanide)					
009	0.10	Pb (Lead)	0.60 mg/L				

**APPLICATION FOR PERMIT RENEWAL AND MODIFICATION
SANDOVAL COUNTY LANDFILL**

**VOLUME III: LANDFILL ENGINEERING CALCULATIONS
SECTION 4: COMPATIBILITY DEMONSTRATION**

**ATTACHMENT III.4.C
GEOTEXTILES REFERENCE DOCUMENTATION**

Technical Note No. 7

Chemical Resistance of Amoco Polypropylene Geotextiles

Amoco woven and nonwoven geotextiles are manufactured from polypropylene with ultra violet stabilizing additives. The excellent chemical resistance of Amoco polypropylene geotextiles is one of the qualities which has established Amoco as a leading producer of geotextiles for use in the waste containment industry. This technical note addresses the chemical resistance of polypropylene with a focus on recent testing programs which have clearly demonstrated the durability of Amoco fabrics in a variety of chemical environments.

Are polypropylene geotextiles durable in the chemical environment of landfill leachates?

Yes. Of the polymers used to manufacture geotextiles, polypropylene exhibits the greatest resistance to chemical attack. In fact, polypropylene is the polymer of choice for such commonly used products as landfill liners, synthetic grass for athletic fields, outdoor carpeting, battery cases, bleach bottles, antifreeze jugs, washing machine agitators, and thousands of other commonly used items that are routinely exposed to chemical environments. Polypropylene is stable within a pH range of 2 to 13, making one of the most stable polymers.

Polypropylene geotextiles have been found to be durable in a wide range of chemical environments (Bell, et. al., 1980; Haxo, 1978, 1983; Pucetas, et.al., 1991; Tisinger, et. al., 1989). Research has found both woven and nonwoven polypropylene geotextiles to be non-biodegradable and resistant to commonly encountered soil-bound chemicals, landfill leachates, mildew, and insects.

How is the chemical resistance of polypropylene geotextiles determined?

Numerous laboratory test programs have subjected polypropylene to severe chemical environ-

ments such as solutions of organic solvents, oils, organic acids, and inorganic acids. The laboratory tests are generally performed in accordance with ASTM D 543, "Standard Test Method for Resistance of Plastics to Chemical Reagents." These test programs have found polypropylene to exhibit superb chemical resistance.

In the ASTM D 543 procedure, the specimens are immersed in a concentrated chemical solution at a specified temperature for a specified exposure period. This test method exposes the polypropylene to extremely harsh conditions which are considerably more severe than those encountered in most civil engineering applications.

The chemical compatibility of geotextiles with leachates is determined by EPA Test Method 9090 (EPA 9090), "*Compatibility Test for Wastes and Membrane Liners*." This was the laboratory method used in the Amoco geotextile test programs reported in this technical note. Geotextile samples are immersed in a constant temperature leachate bath for four months. At the end of each month samples of the fabric are removed and subjected to physical testing. Changes in properties may indicate chemically imposed degradation.

Have Amoco geotextiles been proven to be chemically resistant?

Four laboratory testing programs have been performed to evaluate the chemical compatibility of Amoco geotextiles with landfill leachates. The tests exposed both Amoco woven and nonwoven products to hazardous and municipal waste leachates.

In all testing programs there was no indication of geotextile degradation due to exposure to landfill leachates. The test results are summarized in the remainder of this technical note.

Hazardous waste leachate

A laboratory testing program was performed in 1989 to evaluate the chemical compatibility of Amoco geotextiles with a hazardous waste leachate. The program included EPA 9090 testing of 4 oz/yd² and 8 oz/yd² nonwoven specimens. The testing exposed the geotextiles to leachate in both the laboratory and in a leachate collection sump at a hazardous waste landfill. Test evaluation incorporated detailed microstructural analyses which are not typically incorporated into chemical resistance testing programs. Methods included differential scanning calorimetry, thermal gravimetric analysis, and infrared spectrophotometry. These analyses were performed to identify any changes in the microstructure of the geotextile due to immersion in the leachate.

The results of this testing program found the geotextile microstructure remained intact, stable, and unchanged (Tisinger, et. al., 1989).

Municipal waste leachate

The chemical resistance of Amoco geotextiles to municipal solid waste leachate was evaluated in three laboratory testing programs. The first program, completed in 1990, included EPA 9090 testing of 16 oz/yd² nonwoven geotextile specimens. The second test program, performed in 1992, tested specimens of 8 oz/yd² nonwoven geotextile. The third program, completed in 1993, evaluated the chemical resistance of a high strength woven geotextile. The testing programs evaluated changes in physical properties of the specimens, including specimen dimensions, thickness, grab tensile strength and elongation, puncture resistance, burst strength, and tear strength. In all cases there were no measurable changes in physical properties of the specimens after exposure to the leachate.

Are the results of these tests applicable to Amoco geotextiles which have not been similarly tested?

Yes. All Amoco geotextiles are equally resistant to chemical degradation because they are all manufactured using the same polymer and additives. This conclusion is supported by the test results, which demonstrated no difference in chemical resistance for different types of Amoco geotextiles. The information in this technical note, therefore, is considered to be applicable to all Amoco geotextiles regardless of weight, thickness, or strength.

References

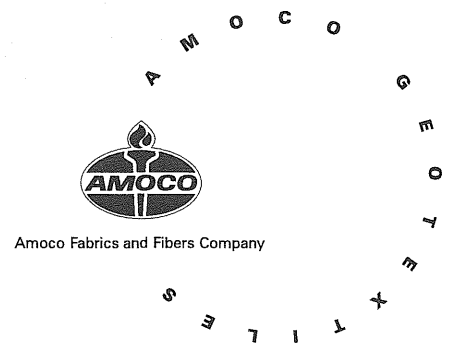
- Bell, J.R., et. al., "Evaluation of Test Methods and Use Criteria for Geotechnical Fabrics in Highway Applications," Federal Highway Administration, FHWA/RD-80-021, 1980, 202 p.
- EPA Method 9090, "Compatibility Test for Wastes and Membrane Liners,"
- Test Methods for Evaluating Solid Waste, Physical/Chemical Methods, US Environmental Protection Agency, EPA 530/SW-646, 1988.
- Haxo, R.S., "Chemical Resistance of Lining Materials with Different Waste Fluids," *Proceedings of the Colloque sur l'Etancheite Superficielle des Bassins, Barrages et Canaux*, Paris, France, 1983, pp. 13-20.
- Haxo, R.S., "Interaction of Selected Lining Materials with Various Hazardous Wastes," *Proceedings of the Fourth Annual Research Symposium on Land Disposal of Hazardous Wastes*, EPA-600/9-78-016, Southwest Research Institute, US Environmental Protection Agency, Solid and Hazardous Waste Research Division, San Antonio, TX, 1978, pp. 256-273.
- Pucetas, R.C., Verschoor, K.L., Allen, S.R., and Sprague, C.J., "The Chemical Resistance of Geotextiles to be Used in Secondary Containment Systems for Underground Storage Tanks," *Geosynthetics '91 Conference Proceedings*, Atlanta, GA, published by the Industrial Fabrics Association International, St. Paul, MN, 1991, pp. 311-314.
- Tisinger, L.G. and Dudzik, B.E., "An Evaluation of Chemical Resistance Test Results of Nonwoven, Needle-Punched Polypropylene Geotextile Exposed to Hazardous Waste Landfill Leachate," *Sardinia '89 2nd International Landfill Symposium*, 1989.

Note: This technical note is believed to be an accurate representation of information available from public sources; however, because the conditions in which such information may be used are beyond the control of Amoco Fabrics and Fibers Company, Amoco does not guarantee the suggestions and recommendations contained herein. Amoco assumes no responsibility for the use of information presented herein and hereby disclaims all liabilities which may arise in connection with such use. Final determination of the suitability of information and suggested uses is the sole responsibility of the user.

Amoco Fabrics and Fibers Company
260 The Bluffs
Austell, GA 30168
770-984-4444 800-445-7732
770-944-4584 • fax
email address: geotextiles@bp.com
http://geotextile.com
Part of the BP Amoco Group

Copyright 1996, Amoco Fabrics and Fibers Company
Code 94-097/3,000/12-97

Technical Note No. 14



Geotextile Polymers for Waste Applications

What types of polymers are used to manufacture geotextiles?

Virtually all geotextile fibers are made from either polypropylene or polyester polymers.

Are these polymers used in a 100% pure form?

The manufacture of geosynthetics usually includes the addition of stabilizers and other additives that are blended with the base polymer. The additives constitute a minor fraction of the polymer mixture.

Additives are used primarily to counteract the effects of oxidation, to which many synthetic polymers are sensitive. Oxidation can cause a reduction in material properties such as strength and elasticity. The main sources of oxidation are heat/temperature (thermal oxidation) and ultra violet (UV) radiation from sunlight (photo-oxidation). Manufacturers of geosynthetics add a variety of proprietary additives during production to make the polymers more stable against thermal and UV degradation (see Amoco Technical Note No. 9).

Should the designer specify polypropylene or polyester for geotextiles to be used in waste applications?

The type of polymer used in the fabrication of the geotextile is not a relevant design parameter. The specifications should be developed to focus on the required physical properties of the geotextile relative to strength, hydraulic performance, and chemical compatibility and durability. These elements are addressed in detail in the Amoco Waste-Related Geotextile Guide Specifications.

Does the type of base polymer affect the chemical resistance of geotextiles used in landfills?

Geotextiles in landfills are exposed to leachates, which are generally dilute solutions of chemicals. The geotextile must be resistant to degrading in this chemical environment. Chemical resistance of geotextiles to leachates is evaluated in the laboratory using EPA Test Method 9090 (EPA 9090). The results of such testing on polypropylene and polyester have proved both polymers to be relatively inert and durable in various chemical environments of hazardous and nonhazardous waste landfills (refer to Amoco Technical Note No. 7).

Of the polymers used to manufacture geotextiles, polypropylene exhibits the greatest resistance to chemical attack. Polypropylene is inert to most chemicals except for some highly concentrated solvents. Geotextiles are not expected to be exposed to such solvents in waste applications, where the associated leachates typically contain only trace to very low concentrations of solvent constituents.

Polyester exhibits comparable chemical compatibility. However, unlike polypropylene, polyester is subject to hydrolysis in aqueous environments such as landfill leachates. Hydrolysis is a process in which water-based solvents or water alone causes the polymer chains to break. This can result in a reduction in the mechanical properties of the polymer. Despite this characteristic, the results of EPA 9090 testing on polyester do not show an impact from hydrolysis.

What effect does polymer type have on the UV resistance of geotextiles used in landfills?

There are only slight differences in the UV stability of various geotextile polymers. From a construction perspective, these differences have no impact on the selection of geotextiles for landfill applications. Regardless of the polymer type, it is important to limit exposure of the geotextile to potentially damaging UV radiation.

In landfill applications, geotextiles are usually covered by soil layers and waste soon after construction. Their exposure to UV radiation therefore generally occurs only during construction. Regardless of polymer type, exposure of the fabrics to sunlight during installation should be limited in accordance with the project specifications (see Amoco Waste-Related Geotextile Guide Specifications).

On some landfill side slopes, the geotextile might be left exposed for an extended time before being covered with soil. In these cases, the geotextile must be protected from UV radiation by alternative methods, regardless of whether the fabric is manufactured of polypropylene or polyester. Alternatives include covering the geotextile with a sacrificial geotextile layer or opaque plastic sheet. The sacrificial layer would be removed prior to placing soil cover.

Has the performance of Amoco geotextiles in landfill applications been verified?

Yes. In fact, the excellent chemical resistance of Amoco polypropylene geotextiles is one of the qualities that has established Amoco as a leading supplier of fabrics to the waste containment industry.

Laboratory testing programs have been performed specifically to evaluate the chemical compatibility of Amoco polypropylene geotextiles with landfill leachates. In all test cases there were no measurable changes in the physical properties of the Amoco geotextiles after exposure to leachates. Also, unlike polyester, polypropylene does not undergo hydrolysis. Amoco Technical Note No. 7 provides detailed information regarding the chemical compatibility test conditions, procedures, and results.

References

Amoco Fabrics and Fibers Company, *Technical Note No. 7, Chemical Resistance of Amoco Polypropylene Geotextiles*.

Amoco Fabrics and Fibers Company, *Technical Note No. 9, Ultra Violet Light Degradation*.

Amoco Fabrics and Fibers Company, *Technical Note No. 12, Staple Fiber and Continuous Filament Polypropylene Geotextiles: A Comparison*.

Amoco Fabrics and Fibers Company, *Waste-Related Geotextile Guide Specifications*.

EPA Method 9090, "Compatibility Test for Wastes and Membrane Liners," *Test Methods for Evaluating Solid Waste, Physical/Chemical Methods, Environmental Protection Agency*, EPA 530/SW-846, 1988.

GeoSyntec Consultants, Correspondence to Amoco Fabrics and Fibers Company, Atlanta, GA, July 1993.

Note: This technical note is believed to be an accurate representation of information available from public sources; however, because the conditions in which such information may be used are beyond the control of Amoco Fabrics and Fibers Company, Amoco does not guarantee the suggestions and recommendations contained herein. Amoco assumes no responsibility for the use of information presented herein and hereby disclaims all liabilities which may arise in connection with such use. Final determination of the suitability of information and suggested uses is the sole responsibility of the user.

**APPLICATION FOR PERMIT RENEWAL AND MODIFICATION
SANDOVAL COUNTY LANDFILL**

**VOLUME III: LANDFILL ENGINEERING CALCULATIONS
SECTION 4: COMPATIBILITY DEMONSTRATION**

**ATTACHMENT III.4.D
GEONET REFERENCE DOCUMENTATION**

HDPE and LDPE Resistance Chart by Chemical

LDPE & HDPE resistance listed by chemical

1,4-dioxane	LDPE and HDPE at 20C° show little or no damage after 30 days of constant exposure. LDPE at 50C° shows some effect after 7 days of constant exposure.
Acetaldehyde	LDPE and HDPE at 20C° show little or no damage after 30 days of constant exposure. HDPE at 50C° shows some effect after 7 days of constant exposure. LDPE - immediate damage may occur.
Acetic Acid 5 %	LDPE and HDPE at 20C°-50C° show little or no damage after 30 days of constant exposure.
Acetic Acid, glacial 50%	LDPE and HDPE at 20C° show little or no damage after 30 days of constant exposure. LDPE at 50 C° - immediate damage may occur.
Acetone	LDPE and HDPE at 20C°-50C° - damage may occur. Not recommended for continuous use.
Allyl Alcohol	LDPE and HDPE at 20C°-50C° show little or no damage after 30 days of constant exposure.
Aluminum salts	LDPE and HDPE at 20C°-50C° show little or no damage after 30 days of constant exposure.
Amino acids	LDPE and HDPE at 20C°-50C° show little or no damage after 30 days of constant exposure.
Ammonia	LDPE and HDPE at 20C°-50C° show little or no damage after 30 days of constant exposure.
Ammonium carbonate, saturated	LDPE and HDPE at 20C°-50C° show little or no damage after 30 days of constant exposure.
Ammonium phosphate	LDPE and HDPE at 20C°-50C° show little or no damage after 30 days of constant exposure.
Ammonium sulphate	LDPE and HDPE at 20C°-50C° show little or no damage after 30 days of constant exposure.
Amyl chloride	HDPE at 20C° shows some effect after 7 days of constant exposure. HDPE at 50C° and LDPE at 20C°-50C° - immediate damage may occur. Not recommended for continuous use.
Aniline	LDPE and HDPE at 20C° show little or no damage after 30 days of constant exposure. HDPE at 50C° shows some effect after 7 days of constant exposure.
Benzene	LDPE and HDPE at 20C°-50C° - damage may occur. Not recommended for continuous use.
Benzyl alcohol	LDPE and HDPE at 50C° - immediate damage may occur. HDPE at 20C° shows some effect after 7 days of constant exposure.
Boric acid	LDPE and HDPE at 20C°-50C° show little or no damage after 30 days of constant exposure.
Bromine	LDPE and HDPE at 50C° - immediate damage may occur. HDPE at 20C° shows some effect after 7 days of constant exposure.
Butyric acid	LDPE and HDPE at 50C° - immediate damage may occur. HDPE at 20C° shows some effect after 7 days of constant exposure.
Calcium chloride	LDPE and HDPE at 20C°-50C° show little or no damage after 30 days of constant exposure.
Calcium hydroxide saturated	LDPE and HDPE at 20C°-50C° show little or no damage after 30 days of constant exposure.
Calcium sulphate	No data is available at this time.
Carbon tetrachloride	HDPE at 20C° shows little or no damage after 30 days. LDPE at 20C° and HDPE at 50C° show some effect after 7 days of constant exposure. LDPE at 50C° not recommended.
Chlorobenzene	Immediate damage may occur. Not recommended for continuous use.
Chloroform	HDPE and LDPE at 20C° show some effect after 7 days. At -50C° - immediate damage may occur. Not recommended for continuous use.
Chlorine 10% in water	HDPE and LDPE at 20C° shows little or no damage after 30 days. LDPE at 50C° shows damage and is not recommended.
Chromic acid 10%	LDPE and HDPE at 20C°-50C° show little or no damage after 30 days of constant exposure.
Chromic acid 50%	LDPE and HDPE at 20C°-50C° show little or no damage after 30 days of constant exposure.
Citric acid 10%	LDPE and HDPE at 20C°-50C° show little or no damage after 30 days of constant exposure.
Cresol	HDPE at 20C° shows some effect after 7 days. LDPE at 20C°-50C° and HDPE at 50C° show immediate damage and are not recommended for continuous use.
Cyclohexane	LDPE and HDPE at 50C° - immediate damage may occur. HDPE and LDPE at 20C° show some effect after 7 days of constant exposure.
Diethyl ketone	LDPE and HDPE at 20C°-50C° - damage may occur. Not recommended for continuous use.
Dimethylsulfoxide	LDPE and HDPE at 20C°-50C° show little or no damage after 30 days of constant exposure.
Ethanol 95%	LDPE and HDPE at 20C°-50C° show little or no damage after 30 days of constant exposure.

Ethyl acetate	LDPE and HDPE at 20C°-50C° show little or no damage after 30 days of constant exposure.
Ethyl benzene	HDPE at 20C° shows some effect after 7 days. LDPE at 20C°-50C° and HDPE at 50C° show immediate damage and are not recommended for continuous use.
Ethylene glycol	LDPE and HDPE at 20C°-50C° show little or no damage after 30 days of constant exposure.
Ethylene oxide	HDPE at 20C° shows little or no damage after 30 days of constant exposure. LDPE at 20C° and LDPE/ HDPE at 50C° show some effect after 7 days.
Ferric chloride	LDPE and HDPE at 20C°-50C° show little or no damage after 30 days of constant exposure.
Fluoride	LDPE and HDPE at 20C°-50C° show little or no damage after 30 days of constant exposure.
Fluorine	HDPE at 20C° shows little or no damage after 30 days of constant exposure. LDPE at 20C° shows some effect after 7 days. Neither HDPE or LDPE are recommended at 50C°.
Formaldehyde 10%	LDPE and HDPE at 20C°-50C° show little or no damage after 30 days of constant exposure.
Formaldehyde 40%	LDPE and HDPE at 20C°-50C° show little or no damage after 30 days of constant exposure.
Glycerol	LDPE and HDPE at 20C°-50C° show little or no damage after 30 days of constant exposure.
Heating oil	No further data is available at this time.
Hexane	HDPE at 20C° shows little or no damage after 30 days continuous use and at 50 C° shows some effect after 7 days. LDPE not recommended at any temperature.
Hydrochloric acid 5%	LDPE and HDPE at 20C°-50C° show little or no damage after 30 days of constant exposure.
Hydrochloric acid 20%	LDPE and HDPE at 20C°-50C° show little or no damage after 30 days of constant exposure.
Hydrochloric acid 35%	LDPE and HDPE at 20C°-50C° show little or no damage after 30 days of constant exposure.
Hydrocyanic acid	LDPE and HDPE at 20C°-50C° show little or no damage after 30 days of constant exposure.
Hydrofluoric acid	LDPE and HDPE at 20C°-50C° show little or no damage after 30 days of constant exposure.
Hydrofluoric acid 4%	LDPE and HDPE at 20C°-50C° show little or no damage after 30 days of constant exposure.
Hydrofluoric acid 48%	LDPE and HDPE at 20C°-50C° show little or no damage after 30 days of constant exposure.
Hydrogen peroxide 3%	LDPE and HDPE at 20C°-50C° show little or no damage after 30 days of constant exposure.
Hydrogen peroxide 30%	LDPE and HDPE at 20C°-50C° show little or no damage after 30 days of constant exposure.
Isobutyl alcohol	LDPE and HDPE at 20C°-50C° show little or no damage after 30 days of constant exposure.
Isopropyl acetate	No data is available at this time.
Isopropyl alcohol	LDPE and HDPE at 20C°-50C° show little or no damage after 30 days of constant exposure.
Kerosene	LDPE and HDPE at 20C° show some effect after 7 days. HDPE and LDPE not recommended at 50C°, as immediate damage may occur.
Lactic Acid 10 %	LDPE and HDPE at 20C°-50C° show little or no damage after 30 days of constant exposure.
Lactic Acid 90 %	LDPE and HDPE at 20C°-50C° show little or no damage after 30 days of constant exposure.
Lead acetate	LDPE and HDPE at 20C°-50C° show little or no damage after 30 days of constant exposure.
Metallic salts, dissolved	No data is available at this time.
Methanoic acid 100%	No data is available at this time.
Methanol	LDPE and HDPE at 20C°-50C° show little or no damage after 30 days of constant exposure.
Methyl ethyl ketone	Immediate damage may occur. Not recommended for continuous use.
Methyl propyl ketone	HDPE at 20C° shows some effect after 7 days. LDPE at 20C°-50C° and HDPE at 50C° - Immediate damage may occur. Not recommended for continuous use.
Methylene chloride	HDPE at 20C° shows some effect after 7 days. LDPE at 20C°-50C° and HDPE at 50C° - Immediate damage may occur. Not recommended for continuous use.
Mineral oil	LDPE and HDPE at 20C° show little or no damage after 30 days of constant exposure. LDPE at 50C° may show immediate damage and is not recommended.
n-amyl acetate	LDPE and HDPE at 20C° show little or no damage after 30 days of constant exposure. LDPE at 50C° shows some effect after 7 days or constant exposure.
n-butyl alcohol	LDPE and HDPE at 20C°-50C° show little or no damage after 30 days of constant exposure.
n-octane	LDPE and HDPE at 20C°-50C° show little or no damage after 30 days of constant exposure.
Nitric acid 50 %	LDPE at 20C° shows little or damage after 30 days. HDPE at 20C° and LDPE at 50C° show effect after 7 days. HDPE at 50C° shows immediate damage and is not recommended.
Nitric acid 70 %	HDPE and LDPE at 20C° show some effect after 7 days. Both at 50C° show immediate damage and are not recommended.
Oleic acid	HDPE at 20C°-50C° show little or no damage after 30 days of constant exposure. LDPE at 20C°-50C° shows immediate damage and is not recommended.
Oxalic acid	LDPE at 20C° shows some effect after 7 days. HDPE at 20C° and both HDPE and LDPE at 50C° show little or no damage after 30 days.
Ozone	HDPE and LDPE at 20C° show little or no damage after 30 days of constant exposure. HDPE and LDPE at 50C° show immediate damage and are not recommended.
Perchloric acid	HDPE and LDPE at 20C° show little or no damage after 30 days of constant exposure. HDPE and LDPE at

	50C° show immediate damage and are not recommended.
Perchloric ethylene	HDPE and LDPE at 20C°-50C° show immediate damage and are not recommended.
Phenol	HDPE and LDPE at 20C°-50C° show immediate damage and are not recommended.
Phosphoric acid 10%	LDPE and HDPE at 20C°-50C° show little or no damage after 30 days of constant exposure.
Phosphoric acid 85%	HDPE and LDPE at 20C° show little or no damage after 30 days of constant exposure. LDPE at 50C° shows immediate damage and is not recommended.
Phosphorous trichloride	HDPE and LDPE at 20C° show little or no damage after 30 days of constant exposure. LDPE at 50C° has no data available. HDPE at 50C° shows some effect after 7 days.
Potassium acetate	No data is available at this time.
Potassium bromide	No data is available at this time.
Potassium carbonate	LDPE and HDPE at 20C°-50C° show little or no damage after 30 days of constant exposure.
Potassium hydroxide 5 %	LDPE and HDPE at 20C°-50C° show little or no damage after 30 days of constant exposure.
Potassium hydroxide concentrated	LDPE and HDPE at 20C°-50C° show little or no damage after 30 days of constant exposure.
Potassium permanganate	LDPE and HDPE at 20C°-50C° show little or no damage after 30 days of constant exposure.
Propylene glycol	LDPE and HDPE at 20C°-50C° show little or no damage after 30 days of constant exposure.
Pyridine	Immediate damage may occur. Not recommended for continuous use.
Salicylic acid, saturated	LDPE and HDPE at 20C°-50C° show little or no damage after 30 days of constant exposure.
Silver acetate	LDPE and HDPE at 20C°-50C° show little or no damage after 30 days of constant exposure.
Silver nitrate	LDPE and HDPE at 20C°-50C° show little or no damage after 30 days of constant exposure.
Sodium carbonate	LDPE and HDPE at 20C°-50C° show little or no damage after 30 days of constant exposure.
Sodium chloride, saturated	LDPE and HDPE at 20C°-50C° show little or no damage after 30 days of constant exposure.
Sodium dichromate	LDPE and HDPE at 20C°-50C° show little or no damage after 30 days of constant exposure.
Sodium hydroxide 1%	LDPE at 20C°-50C° shows little or no damage after 30 days of constant exposure. HDPE at 20C°-50C° shows some effect after 7 days.
Sodium hydroxide 50%	LDPE and HDPE at 20C°-50C° show little or no damage after 30 days of constant exposure.
Sodium hypochlorite 15%	HDPE at 20C°-50C° show little or no damage after 30 days of constant exposure. LDPE at 20C° is suitable but at 50C° shows some effect after 7 days.
Sodium nitrate	LDPE and HDPE at 20C°-50C° show little or no damage after 30 days of constant exposure.
Sodium sulphate	LDPE and HDPE at 20C°-50C° show little or no damage after 30 days of constant exposure.
Sucrose	LDPE and HDPE at 20C°-50C° show little or no damage after 30 days of constant exposure.
Sulphide	No additional information is available at this time.
Sulfuric acid 6%	LDPE and HDPE at 20C°-50C° show little or no damage after 30 days of constant exposure.
Sulfuric acid 20%	LDPE and HDPE at 20C°-50C° show little or no damage after 30 days of constant exposure.
Sulfuric acid 60%	LDPE and HDPE at 20C°-50C° show little or no damage after 30 days of constant exposure.
Sulfuric acid 98%	LDPE at 20C°-50C° shows little or no damage after 30 days of constant exposure. HDPE at 20C° shows effect after 7 days and is not recommended for use at 50C°.
Tannic acid	LDPE and HDPE at 20C°-50C° show little or no damage after 30 days of constant exposure.
Tetrahydrofuran	HDPE and LDPE at 20C° show some effect after 7 day of constant exposure. HDPE and LDPE at 50C° show immediate damage and are not recommended.
Toluene	LDPE at 20C° show some effect after 7 day of constant exposure. HDPE at 20C°-50C° and LDPE at 50C° show immediate damage and are not recommended.
Trichloroacetic acid	HDPE and LDPE at 20C° show some effect after 7 day of constant exposure. HDPE and LDPE at 50C° show immediate damage and are not recommended.
Trichlorethane	Immediate damage may occur. Not recommended for continuous use.
Turpentine oil	HDPE and LDPE at 20C° show some effect after 7 day of constant exposure. HDPE and LDPE at 50C° show immediate damage and are not recommended.
Urea	LDPE and HDPE at 20C°-50C° show little or no damage after 30 days of constant exposure.
Xylene	HDPE at 20C° shows some effect after 7 day of constant exposure. LDPE at 20-50C° and HDPE at 50C° show immediate damage and are not recommended.
Zinc chloride	LDPE and HDPE at 20C°-50C° show little or no damage after 30 days of constant exposure.

Call Professional Plastics at (888) 995-7767 or
E-Mail sales@proplas.com
Order Online at www.professionalplastics.com

**APPLICATION FOR PERMIT RENEWAL AND MODIFICATION
SANDOVAL COUNTY LANDFILL**

**VOLUME III: LANDFILL ENGINEERING CALCULATIONS
SECTION 4: COMPATIBILITY DEMONSTRATION**

**ATTACHMENT III.4.E
HPDE GEOGRIDS REFERENCE DOCUMENTATION**



Polypropylene Chemical Resistance Table Polypropylene

Introduction

The table in this document summarises the data given in a number of polypropylene chemical resistance tables at present in use in various countries, derived from both practical experience and test results.

Source: ISO/TR 10358

The table contains an evaluation of the chemical resistance to a number of fluids judged to be either aggressive or not towards polypropylene. This evaluation is based on values obtained by immersion of polypropylene test specimens in the fluid concerned at 20, 60 and 100°C and atmospheric pressure, followed in certain cases by the tensile characteristics.

A subsequent classification will be established with respect to a restricted number of fluids deemed to be technically or commercially more important, using equipment which permits testing under pressure and the determination of the "coefficient of chemical resistance" for each fluid. These tests will thus furnish more complete indications on the use of polypropylene piped for the transport of stated fluids, including their use under pressure.

Scope and Field Application

This document establishes a provisional classification of the chemical resistance of polypropylene with respect to about 180 fluids. It is intended to provide general guidelines on the possible utilisation of polypropylene piping for the conveyance of fluids:

- at temperatures up to 20, 60 and 100°C
- in the absence of internal pressure and external mechanical stress
(for example flexural stresses, stresses due to thrust, rolling loads etc).

Definitions, Symbols and Abbreviations

The criteria of classifications, definitions, symbols and abbreviations adopted in this document are as follows:

S = Satisfactory

The chemical resistance of polypropylene exposed to the action of a fluid is classified as "satisfactory" when the results of test are acknowledged to be "satisfactory" by the majority of the countries participating in the evaluation.

L = Limited



Polypropylene

Chemical Resistance Table Polypropylene

The chemical resistance of polypropylene exposed to the action of fluid is classified as "limited" when the results of tests are acknowledged to be "limited" by the majority of the countries participating in the evaluation.

Also classified as "limited" are the resistances to the action of chemical fluids for which judgements "S" and "NS" or "L" are pronounced to an equal extent.

NS = Not satisfactory

The chemical resistance of polypropylene exposed to the action of a fluid classified as "not satisfactory" when the results of test are acknowledged to be "not satisfactory" by the majority of the countries participating in the evaluation.

Also classified as "not satisfactory" are materials for which judgement "L" and "NS" are pronounced to an equal extent.

Sat.sol Saturated aqueous solution, prepared at 20°C

Sol Aqueous solution at a concentration higher than 10 % but not saturated

Dil.sol Dilute aqueous solution at a concentration equal to or lower than 10 %

Work.sol Aqueous solution having the usual concentration for industrial use

Solution concentrations reported in the text are expressed as a percentage by mass. The aqueous solutions of sparingly soluble chemicals are considered, as far as chemical action towards polypropylene is concerned, as saturated solutions.

In general, common chemical names are used in this document.

The table is made as a first guideline for user of polypropylene. If a chemical compound is not to be found or if there is an uncertainty on the chemical resistance in an application, please contact Borealis for advise and proposal on testing.



Polypropylene

Chemical Resistance Table Polypropylene

Chemical Resistance of Polypropylene, Not Subjected to Mechanical Stress, to Various Fluids at 20, 60 and 100°C

Chemical or Product	Concentration	Temperature °C		
		20	60	100
Acetic acid	Up to 40 %	S	S	-
Acetic acid	50 %	S	S	L
Acetic acid, glacial	> 96 %	S	L	NS
Acetic anhydride	100 %	S	-	-
Acetone	100 %	S	S	-
Acetophenone	100 %	S	L	-
Acrylonitrile	100 %	S	-	-
Air		S	S	S
Allyl alcohol	100 %	S	S	-
Almond oil		S	-	-
Alum	Sol	S	S	-
Ammonia, aqueous	Sat.sol	S	S	-
Ammonia, dry gas	100 %	S	-	-
Ammonia, liquid	100 %	S	-	-
Ammonium acetate	Sat. sol	S	S	-
Ammonium chloride	Sat.sol	S	S	-
Ammonium fluoride	Up to 20 %	S	S	-
Ammonium hydrogen carbonate	Sat.sol	S	S	-
Ammonium metaphosphate	Sat.sol	S	S	S
Ammonium nitrate	Sat.sol	S	S	S
Ammonium persulphate	Sat.sol	S	S	-
Ammonium phosphate	Sat.sol	S	-	-
Ammonium sulphate	Sat.sol	S	S	S
Ammonium sulphide	Sat.sol	S	S	-
Amyl acetate	100 %	L	-	-
Amyl alcohol	100 %	S	S	S
Aniline	100 %	S	S	-
Apple juice		S	-	-
Aqua regia	HCl/HNO ₃ =3/1	NS	NS	NS
Barium bromide	Sat.sol	S	S	S
Barium carbonate	Sat.sol	S	S	S
Barium chloride	Sat.sol	S	S	S



Polypropylene

Chemical Resistance Table Polypropylene

Chemical or Product	Concentration	Temperature °C		
		20	60	100
Barium hydroxide	Sat.sol	S	S	S
Barium sulphide	Sat.sol	S	S	S
Beer		S	S	-
Benzene	100 %	L	NS	NS
Benzoic acid	Sat.sol	S	S	-
Benzyl alcohol	100 %	S	L	-
Borax	Sol	S	S	-
Boric acid	Sat.sol	S	-	-
Boron trifluoride	Sat.sol	S	-	-
Bromine, gas		NS	NS	NS
Bromine, liquid	100 %	NS	NS	NS
Butane, gas	100 %	S	-	-
Butanol	100 %	S	L	L
Butyl acetate	100 %	L	NS	NS
Butyl glycol	100 %	S	-	-
Butyl phenols	Sat.sol	S	-	-
Butyl phthalate	100 %	S	L	L
Calcium carbonate	Sat.sol	S	S	S
Calcium chlorate	Sat.sol	S	S	-
Calcium chloride	Sat.sol	S	S	S
Calcium hydroxide	Sat.sol	S	S	S
Calcium hypochlorite	Sol	S	-	-
Calcium nitrate	Sat.sol	S	S	-
Camphor oil		NS	NS	NS
Carbon dioxide, dry gas		S	S	-
Carbon dioxide, wet gas		S	S	-
Carbon disulphide	100 %	S	NS	NS
Carbon monoxide, gas		S	S	-
Carbon tetrachloride	100 %	NS	NS	NS
Castor oil	100 %	S	S	-
Caustic soda	Up to 50 %	S	L	L
Chlorine, aqueous	Sat.sol	S	L	-
Chlorine, dry gas	100 %	NS	NS	NS
Chlorine, liquid	100 %	NS	NS	NS
Chloroacetic acid	Sol	S	-	-



Polypropylene

Chemical Resistance Table Polypropylene

Chemical or Product	Concentration	Temperature °C		
		20	60	100
Chloroethanol	100 %	S	-	-
Chloroform	100 %	L	NS	NS
Chlorosulphonic acid	100 %	NS	NS	NS
Chrome alum	Sol	S	S	-
Chromic acid	Up to 40 %	S	L	NS
Citric acid	Sat.sol	S	S	S
Coconut oil		S	-	-
Copper (II) chloride	Sat.sol	S	S	-
Copper (II) nitrate	Sat.sol	S	S	S
Copper (II)	Sat.sol	S	S	-
Corn oil		S	L	-
Cottonseed oil		S	S	-
Cresol	Greater than 90 %	S	-	-
Cyclohexane	100 %	S	-	-
Cyclohexanol	100 %	S	L	-
Cyclohexanone	100 %	L	NS	NS
Decalin (decahydronaphthalene)	100 %	NS	NS	NS
Dextrin	Sol	S	S	-
Dextrose	Sol	S	S	S
Dibutyl phthalate	100 %	S	L	NS
Dichloroacetic acid	100 %	L	-	-
Dichloroethylene (A and B)	100 %	L	-	-
Diethanolamine	100 %	S	-	-
Diethyl ether	100 %	S	L	-
Diethylene glycol	100 %	S	S	-
Diglycolic acid	Sat.sol	S	-	-
Diisooctyl	100 %	S	L	-
Dimethyl amine, gas		S	-	-
Dimethyl formamide	100 %	S	S	-
Diocetyl phthalate	100 %	L	L	-
Dioxane	100 %	L	L	-
Distilled water	100 %	S	S	S
Ethanolamine	100 %	S	-	-
Ethyl acetate	100 %	L	NS	NS

Borealis A/S

Parallelsvej 16,
DK-2800 Kongens Lyngby (Denmark)
Telephone: +45 45 96 60 00
Fax : +45 45 96 61 23
www.borealisgroup.com





Polypropylene

Chemical Resistance Table Polypropylene

Chemical or Product	Concentration	Temperature °C		
		20	60	100
Ethyl alcohol	Up to 95 %	S	S	S
Ethyl chloride, gas		NS	NS	NS
Ethylene chloride (mono and di)		L	L	-
Ethyl ether	100 %	S	L	-
Ethylene glycol	100 %	S	S	S
Ferric chloride	Sat.sol	S	S	S
Formaldehyde	40 %	S	-	-
Formic acid	10 %	S	S	L
Formic acid	85 %	S	NS	NS
Formic acid, anhydrous	100 %	S	L	L
Fructose	Sol	S	S	S
Fruit juice		S	S	S
Gasoline, petrol (aliphatic hydrocarbons)		NS	NS	NS
Gelatine		S	S	-
Glucose	20 %	S	S	S
Glycerine	100 %	S	S	S
Glycolic acid	30 %	S	-	-
Heptane	100 %	L	NS	NS
Hexane	100 %	S	L	-
Hydrobromic acid	Up to 48 %	S	L	NS
Hydrochloric acid	Up to 20 %	S	S	S
Hydrochloric acid	30 %	S	L	L
Hydrochloric acid	From 35 to 36 %	S	-	-
Hydrofluoric acid	Dil.sol	S	-	-
Hydrofluoric acid	40 %	S	-	-
Hydrogen	100 %	S	-	-
Hydrogen chloride, dry gas	100 %	S	S	-
Hydrogen peroxide	Up to 10 %	S	-	-
Hydrogen peroxide	Up to 30 %	S	L	-
Hydrogen sulphide, dry gas	100 %	S	S	-
Iodine, in alcohol		S	-	-
Isoctane	100 %	L	NS	NS



Polypropylene

Chemical Resistance Table Polypropylene

Chemical or Product	Concentration	Temperature °C		
		20	60	100
Isopropyl alcohol	100 %	S	S	S
Isopropyl ether	100 %	L	-	-
Lactic acid	Up to 90 %	S	S	-
Lanoline		S	L	-
Linseed oil		S	S	S
Magnesium carbonate	Sat.sol	S	S	S
Magnesium chloride	Sat.sol	S	S	-
Magnesium hydroxide	Sat.sol	S	S	-
Magnesium sulphate	Sat.sol	S	S	-
Maleic acid	Sat.sol	S	S	-
Mercury (II) chloride	Sat.sol	S	S	-
Mercury (II) cyanide	Sat.sol	S	S	-
Mercury (I) nitrate	Sol	S	S	-
Mercury	100 %	S	S	-
Methyl acetate	100 %	S	S	-
Methyl alcohol	5 %	S	L	L
Methyl amine	Up to 32 %	S	-	-
Methyl bromide	100 %	NS	NS	NS
Methyl ethyl ketone	100 %	S	-	-
Methylene chloride	100 %	L	NS	NS
Milk		S	S	S
Monochloroacetic acid	>85 %	S	S	-
Naphtha		S	NS	NS
Nickel chloride	Sat.sol	S	S	-
Nickel nitrate	Sat.sol	S	S	-
Nickel sulphate	Sat.sol	S	S	-
Nitric acid	Up to 30 %	S	NS	NS
Nitric acid	From 40 to 50 %	L	NS	NS
Nitric acid, fuming (with nitrogen dioxide)		NS	NS	NS
Nitrobenzene	100%	S	L	-
Oleic acid	100 %	S	L	-
Oleum (sulphuric acid with 60 % of SO ₃)		S	L	-

Borealis A/S

Parallelsvej 16,
 DK-2800 Kongens Lyngby (Denmark)
 Telephone: +45 45 96 60 00
 Fax : +45 45 96 61 23
 www.borealisgroup.com





Polypropylene

Chemical Resistance Table Polypropylene

Chemical or Product	Concentration	Temperature °C		
		20	60	100
Olive oil	Sat.sol	S	S	L
Oxalic acid		S	L	NS
Oxygen, gas		S	-	-
Paraffin oil (FL65)	(2 N) 20 %	S	L	NS
Peanut oil		S	S	-
Peppermint oil		S	-	-
Perchloric acid	5 %	S	-	-
Petroleum ether (ligroine)		L	L	-
Phenol		S	S	-
Phenol	90 %	S	-	-
Phosphine, gas	Up.to 85 %	S	S	-
Phosphoric acid		S	S	S
Phosphorus oxychloride		L	-	-
Picric acid	Sat.sol	S	-	-
Potassium bicarbonate	Sat.sol	S	S	S
Potassium borate	Sat.sol	S	S	-
Potassium bromate	Up to 10 %	S	S	-
Potassium bromide	Sat.sol	S	S	-
Potassium carbonate	Sat.sol	S	S	-
Potassium chlorate	Sat.sol	S	S	-
Potassium chlorite	Sat.sol	S	S	-
Potassium chromate	Sat.sol	S	S	-
Potassium cyanide	Sol	S	-	-
Potassium dichromate	Sat.sol	S	S	S
Potassium ferricyanide	Sat.sol	S	S	-
Potassium fluoride	Sat.sol	S	S	-
Potassium hydroxide	Up to 50 %	S	S	S
Potassium iodide	Sat.sol	S	-	-
Potassium nitrate	Sat.sol	S	S	-
Potassium perchlorate	10 %	S	S	-
Potassium permanganate	(2 N) 30 %	S	-	-
Potassium persulphate	Sat.sol	S	S	-
Potassium sulphate	Sat.sol	S	S	-
Propane, gas	100 %	S	-	-
Propionic acid	>50 %	S	-	-



Polypropylene

Chemical Resistance Table Polypropylene

Chemical or Product	Concentration	Temperature °C		
		20	60	100
Pyridine	100 %	L	-	-
Seawater		S	S	S
Silicon oil		S	S	S
Silver nitrate	Sat.sol	S	S	L
Sodium acetate	Sat.sol	S	S	S
Sodium benzoate	35 %	S	L	-
Sodium bicarbonate	Sat.sol	S	S	S
Sodium carbonate	Up to 50 %	S	S	L
Sodium chlorate	Sat.sol	S	S	-
Sodium chloride	Sat.sol	S	S	-
Sodium chlorite	2 %	S	L	NS
Sodium chlorite	20 %	S	L	NS
Sodium dichromate	Sat.sol	S	S	S
Sodium hydrogen carbonate	Sat.sol	S	S	S
Sodium hydrogen sulphate	Sat.sol	S	S	-
Sodium hydrogen sulphite	Sat.sol	S	-	-
Sodium hydroxide	1 %	S	S	S
Sodium hydroxide	From 10 to 60 %	S	S	S
Sodium hypochlorite	5 %	S	S	-
Sodium hypochlorite	10 % - 15 %	S	-	-
Sodium hypochlorite	20 %	S	L	-
Sodium metaphosphate	Sol	S	-	-
Sodium nitrate	Sat.sol	S	S	-
Sodium perborate	Sat.sol	S	S	-
Sodium phosphate (neutral)		S	S	S
Sodium silicate	Sol	S	S	-
Sodium sulphate	Sat.sol	S	S	-
Sodium sulphide	Sat.sol	S	-	-
Sodium sulphite	40 %	S	S	S
Sodium thiosulphate (hypo)	Sat.sol	S	-	-
Soybean oil		S	L	-
Succinic acid	Sat.sol	S	S	-
Sulphuric acid	Up to 10 %	S	S	S
Sulphuric dioxide, dry or wet	100 %	S	S	-

Borealis A/S

Parallevej 16,
 DK-2800 Kongens Lyngby (Denmark)
 Telephone: +45 45 96 60 00
 Fax : +45 45 96 61 23
 www.borealisgroup.com





Polypropylene

Chemical Resistance Table Polypropylene

Chemical or Product	Concentration	Temperature °C		
		20	60	100
Sulphur acid	From 10 to 30 %	S	S	-
Sulphuric acid	50 %	S	L	L
Sulphuric acid	96 %	S	L	NS
Sulphuric acid	98 %	L	NS	NS
Sulphurous acid	Up to 30 %	S	-	-
Tartaric acid	Sat.sol	S	S	-
Tetrahydrofuran	100 %	L	NS	NS
Tetralin	100 %	NS	NS	NS
Thiophene	100 %	S	L	-
Tin (IV) chloride	Sol	S	S	-
Tin (II) chloride	Sat.sol	S	S	-
Toluene	100 %	L	NS	NS
Trichloroacetic acid	Up to 50 %	S	S	-
Trichloroethylene	100 %	NS	NS	NS
Triethanolamine	Sol	S	-	-
Turpentine		NS	NS	NS
Urea	Sat.sol	S	S	-
Vinegar		S	S	-
Water brackish, mineral, potable		S	S	S
Whiskey		S	S	-
Wines		S	S	-
Xylene	100 %	NS	NS	NS
Yeast	Sol	S	S	S
Zinc chloride	Sat.sol	S	S	-
Zinc sulphate	Sat.sol	S	S	-



Polypropylene

Chemical Resistance Table Polypropylene

Disclaimer

The information contained herein is to our knowledge accurate and reliable as of the date of publication. Borealis extends no warranties and makes no representations as to the accuracy or completeness of the information contained herein, and assumes no responsibility regarding the consequences of its use or for any printing errors.

Our products are intended for sale to industrial and commercial customers. It is the customer's responsibility to inspect and test our products in order to satisfy himself as to the suitability of the products for the customer's particular purpose. The customer is also responsible for the appropriate, safe and legal use, processing and handling of our products. Nothing herein shall constitute any warranty (express or implied, of merchantability, fitness for a particular purpose, compliance with performance indicators, conformity to samples or models, non-infringement or otherwise), nor is protection from any law or patent to be inferred. No statement herein shall be construed as an endorsement of any product or process.

Insofar as products supplied by Borealis or its subsidiary companies are used in conjunction with third party materials, it is the responsibility of the customer to obtain all necessary information relating to the third party materials and ensure that Borealis' products when used together with these materials are suitable for the customer's particular purpose. No liability can be accepted in respect of the use of Borealis' products in conjunction with other materials. The information contained herein relates exclusively to our products when not used in conjunction with any third party materials.

Borealis emphasises that the data for the chemical resistance of polyethylene and polypropylene displayed in the chemical resistance wizard on this web site is based on data from multiple sources. Borealis does not guarantee the accuracy and correctness of such data, and does not accept any responsibility for any loss or damage that result from the use, inability to use or the results of use of this web site wizard by customers or by any third parties to whom such data may be transmitted. You are required to carry out the appropriate tests to ensure the suitability and safety of the products for the envisaged use in accordance with all applicable regulations.

Borealis A/S

Parallelsvej 16,
DK-2800 Kongens Lyngby (Denmark)
Telephone: +45 45 96 60 00
Fax : +45 45 96 61 23
www.borealisgroup.com



Product Specification - Structural Geogrid UX1100MSE

Tensar International Corporation reserves the right to change its product specifications at any time. It is the responsibility of the specifier and purchaser to ensure that product specifications used for design and procurement purposes are current and consistent with the products used in each instance.

Product Type: Integrally Formed Structural Geogrid
Polymer: High Density Polyethylene
Load Transfer Mechanism: Positive Mechanical Interlock
Recommended Applications: MESA System (Segmental Block Walls), SierraScape System (Welded Wire Walls)

Product Properties

Index Properties	Units	MD Values ¹
▪ Tensile Strength @ 5% Strain ²	kN/m (lb/ft)	27 (1,850)
▪ Ultimate Tensile Strength ²	kN/m (lb/ft)	58 (3,970)
▪ Junction Strength ³	kN/m (lb/ft)	54 (3,690)
▪ Flexural Stiffness ⁴	mg-cm	500,000
Durability		
▪ Resistance to Long Term Degradation ⁵	%	100
▪ Resistance to UV Degradation ⁶	%	95
Load Capacity		
▪ Maximum Allowable Strength for 120-year Design Life ⁷	kN/m (lb/ft)	21.2 (1,450)
Recommended Allowable Strength Reduction Factors⁷		
▪ Minimum Reduction Factor for Installation Damage (RF _{ID}) ⁸		1.05
▪ Reduction Factor for Creep for 120-year Design Life (RF _{CR}) ⁹		2.60
▪ Minimum Reduction Factor for Durability (RF _D)		1.00

Dimensions and Delivery

The structural geogrid shall be delivered to the jobsite in roll form with each roll individually identified and nominally measuring 1.33 meters (4.36 feet) in width and 76.2 meters (250.0 feet) in length. A typical truckload quantity is 432 rolls.

Notes:

1. Unless indicated otherwise, values shown are minimum average roll values determined in accordance with ASTM D4759-02. Brief descriptions of test procedures are given in the following notes.
2. True resistance to elongation when initially subjected to a load measured via ASTM D6637-10 Method A without deforming test materials under load before measuring such resistance or employing "secant" or "offset" tangent methods of measurement so as to overstate tensile properties.
3. Load transfer capability determined in accordance with ASTM D7737-11.
4. Resistance to bending force determined in accordance with ASTM D7748-12, using one meter (minimum) long specimen.
5. Resistance to loss of load capacity or structural integrity when subjected to chemically aggressive environments in accordance with EPA 9090 immersion testing.
6. Resistance to loss of load capacity or structural integrity when subjected to 500 hours of ultraviolet light and aggressive weathering in accordance with ASTM D4355-05.
7. Reduction factors are used to calculate the geogrid strength available for resisting force in long-term load bearing applications. Allowable Strength (T_{allow}) is determined by reducing the ultimate tensile strength (T_{ult}) by reduction factors for installation damage (RF_{ID}), creep (RF_{CR}) and chemical/biological durability (RF_D = RF_{CD}·RF_{BD}) per GRI-GG4-05 [$T_{allow} = T_{ult}/(RF_{ID} \cdot RF_{CR} \cdot RF_D)$]. Recommended minimum reduction factors are based on product-specific testing. Project specifications, standard public agency specifications and/or design code requirements may require higher reduction factors. Design of the structure in which the geogrid is used, including the selection of appropriate reduction factors and design life, is the responsibility of the outside licensed professional engineer providing the sealed drawings for the project.
8. Minimum value is based on Installation Damage Testing in Sand, Silt, and Clay soils. Coarser soils require increased RF_{ID} values.
9. Reduction Factor for Creep determined for 120-year design life and in-soil temperature of 20°C using standard extrapolation techniques to creep rupture data obtained following the test procedure in ASTM D5262-04. Actual design life of the completed structure may differ.

Tensar International Corporation warrants that at the time of delivery the geogrid furnished hereunder shall conform to the specification stated herein. Any other warranty including merchantability and fitness for a particular purpose, are hereby excluded. If the geogrid does not meet the specifications on this page and Tensar is notified prior to installation, Tensar will replace the geogrid at no cost to the customer.

This product specification supersedes all prior specifications for the product described above and is not applicable to any products shipped prior to February 1, 2013.

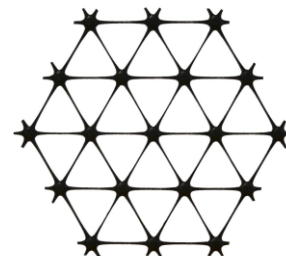
Product Specification - TriAx® TX160 Geogrid

Tensar International Corporation reserves the right to change its product specifications at any time. It is the responsibility of the person specifying the use of this product and of the purchaser to ensure that product specifications relied upon for design or procurement purposes are current and that the product is suitable for its intended use in each instance.

Tensar TriAx® Geogrid

General

1. The geogrid is manufactured from a punched polypropylene sheet, which is then oriented in three substantially equilateral directions so that the resulting ribs shall have a high degree of molecular orientation, which continues at least in part through the mass of the integral node.
2. The properties contributing to the performance of a mechanically stabilized layer include the following:



Index Properties	Longitudinal	Diagonal	Transverse	General
▪ Rib pitch ⁽²⁾ , mm (in)	40 (1.60)	40 (1.60)	-	
▪ Mid-rib depth ⁽²⁾ , mm (in)	-	1.6 (0.06)	1.4 (0.06)	
▪ Mid-rib width ⁽²⁾ , mm (in)	-	1.0 (0.04)	1.2 (0.05)	
▪ Rib shape				Rectangular
▪ Aperture shape				Triangular

Structural Integrity

▪ Junction efficiency ⁽³⁾ , %	93
▪ Radial stiffness at low strain ⁽⁴⁾ , kN/m @ 0.5% strain (lb/ft @ 0.5% strain)	300 (20,580)

Durability

▪ Resistance to chemical degradation ⁽⁵⁾	100%
▪ Resistance to ultra-violet light and weathering ⁽⁶⁾	70%

Dimensions and Delivery

The TX geogrid shall be delivered to the jobsite in roll form with each roll individually identified and nominally measuring 3.0 meters (9.8 feet) and/or 4.0 meters (13.1feet) in width and 75 meters (246 feet) in length.

Notes

1. Unless indicated otherwise, values shown are minimum average roll values determined in accordance with ASTM D4759-02. Brief descriptions of test procedures are given in the following notes.
2. Nominal dimensions.
3. Load transfer capability determined in accordance with ASTM D6637-10 and ASTM D7737-11 and expressed as a percentage of ultimate tensile strength.
4. Radial stiffness is determined from tensile stiffness measured in any in-plane axis from testing in accordance with ASTM D6637-10.
5. Resistance to loss of load capacity or structural integrity when subjected to chemically aggressive environments in accordance with EPA 9090 immersion testing.
6. Resistance to loss of load capacity or structural integrity when subjected to 500 hours of ultraviolet light and aggressive weathering in accordance with ASTM D4355-05.

**APPLICATION FOR PERMIT RENEWAL AND MODIFICATION
SANDOVAL COUNTY LANDFILL**

**VOLUME III: LANDFILL ENGINEERING CALCULATIONS
SECTION 4: COMPATIBILITY DEMONSTRATION**

**ATTACHMENT III.4.F
HDPE PIPE REFERENCE DOCUMENTATION**

Chemical Resistance of Plastics and Elastomers Used in Pipeline Construction

1. Introduction

It is now inconceivable to construct pipelines without the use of plastics. Pipes made from plastics are used not only for drinking water, water for general use and waste water, but also for the conveyance of aggressive liquids and gases. Expensive pipe materials such as lined metal, ceramic or glass, have been largely superseded by plastic pipes. It is, however, important that the most suitable plastic material is selected for each application. This "Chemical Resistance List" serves as a useful guide in this respect. The list is periodically revised to include the latest findings. It contains all plastics and elastomers in the George Fischer product range which can come into direct contact with the media.

The information is based on experiments, immersion and, when available, on data from tests which include temperature and pressure as stress factors. The results achieved in immersion experiments cannot be applied without reservation to pipes under stress, i.e. internal pressure, as the factor "stress corrosion cracking" is not taken into consideration. In certain cases it can be of advantage to test the suitability under the planned working conditions. The tests referred to have been carried out partly by George Fischer and partly by the International Standardization Organization (ISO) or national standards organizations.

Pure chemicals were used for the tests. If a mixture of chemicals is to be conveyed in practice this may affect the chemical resistance of the plastic. It is possible in special cases to carry out appropriate tests with the specific mixture. Suitable test equipment is available at George Fischer for this purpose, which we regard as part of our service to the customer. It goes without saying that we are willing to give individual advice at any time. In this connection it is worth mentioning that George Fischer already possesses information concerning the behavior towards plastics of a number of chemicals or mixtures of chemicals which are

not yet included in this list. The "Chemical Resistance List" gives valuable assistance in the planning of plastic pipelines. Please refer to the following instructions, which are important for the application and evaluation of this list.

2. Instructions for the Use of the Chemical Resistance List

2.1 General

As stated in the introduction, the "Chemical Resistance List" is only intended as a guide. Changes in the composition of the medium or special working conditions could lead to deviations. If there is any doubt, it is advisable to test the behavior of the material under the specific working conditions, by means of a pilot installation. No guarantees can be given in respect of the information contained in this booklet. The data shown is based upon information available at the time of printing, but it may, however, be revised from time to time in the light of subsequent research and experience.

2.2 Classification

The customary classifications: **resistant**, **conditionally resistant** and **not recommended** are depicted by the signs: +, O, and -, which allow simple presentation and application. These classifications are defined as:

Resistant: +

Within the acceptable limits of pressure and temperature the material is unaffected or only insignificantly affected.

Conditionally Resistant: O

The medium can attack the material or cause swelling. Restrictions must be made in regard to pressure and/or temperature, taking the expected service life into account. The service life of the installation can be noticeably shortened. Further consultation with George Fischer is recommended.

Not recommended: -

The material cannot be used with the medium at all, or only under special conditions.

(Courtesy George Fischer Engineering Handbook)

2.3 Pipe Joints

2.3.1 Solvent Cement Joints (PVC)

Solvent cement joints made with standard PVC cement and primer systems are generally as resistant as the PVC material itself. The following chemicals are, however, an exception:

- Sulphuric acid H_2SO_4 in concentrations above 70 percent
- Hydrochloric acid HCl in concentrations above 25 percent
- Nitric acid HNO_3 in concentrations above 20 percent

Hydrofluoric acid in any concentration in conjunction with the above media the solvent cement joining is classified as "conditionally resistant". Previously recommended solvent cement (Dytex, by Henkel, Germany) used for pipe and fittings to carry concentrated acids, can no longer be brought into the United States because of its methylene chloride solvent system being classified as a carcinogen. There is no known domestically available substitute. Special consideration should be given to the possible attack of the cemented joints by these concentrated acids.

2.3.2 Fusion Joints

In the case of PE, PP, and PVDF (ISYGEF®) heat fusion joints have practically the same chemical resistance as the respective material. In conjunction with media which could cause stress cracking, the fused joints can be subjected to an increased risk due to residual stress from the joining process.

2.4 Sealing Materials

Depending upon the working conditions and the stress involved, the life span of the sealing materials can differ from that of the pipeline material. Seals in PTFE, which are not included in this list, are resistant to all the chemicals indicated. The greater permeability of PTFE should, however, be considered. Under certain working conditions, for example when conveying highly aggressive media such as hydrochloric acid, this material characteristic must be taken into account.

(Courtesy George Fischer Engineering Handbook)

2.5 General Summary and Limits of Application

The following table includes all the materials contained in the George Fischer product range, and their abbreviations. The summary gives preliminary information regarding the general behavior of the materials and the temperature limits.

2.6 Standards

This list has been compiled with reference to the following ISO standards:

ISO/TR 7473

Unplasticized polyvinyl chloride pipes and fittings – Chemical resistance with respect to fluids.

ISO/TR 7474

High density polyethylene pipes and fittings – Chemical resistance with respect to fluids to be conveyed.

ISO/TR 7471

Polypropylene (PP) pipes and fittings – Chemical resistance with respect to fluids.

ISO TR 10358

Plastic pipes and fittings – Combined chemical resistance classification table.

DVS 2205 Part I

Calculations for thermoplastic containers and appliances.

DIN 8080 Supplement 1 «Pipes of chlorinated polyvinyl chloride (PVC-C), PVC-C 250 – Chemical Resistance».

Material	Abbreviation	Remarks	Maximum Permissible Temperature (Water) °C	
			Constant	Short Term
Polyvinyl Chloride	PVC	Resistant to most solutions of acids, alkalis and salts and to organic compounds miscible with water. Not resistant to aromatic and chlorinated hydrocarbons.	60*	60*
Chlorinated Polyvinyl Chloride	CPVC	Can be used similarly to PVC but at higher temperatures. Consult factory for specific applications.	90*	110*
High-density Polyethylene	PE 50	Resistant to hydrous solutions of acids, alkalis and salts as well as to a large number of organic solvents. Unsuitable for concentrated oxidizing acids.	60*	60*
Polypropylene, heat stabilized	PP	Chemical resistance similar to that of PE but suitable for higher temperatures.	90*	110*
Polyvinylidene Fluoride	PVDF (KALIF®)	Resistant to acids, solutions of salts, aliphatic, aromatic and chlorinated hydrocarbons, alcohols and halogens. Conditionally suitable for ketones, esters, organic bases and oil-line solutions.	140*	150*
Polybutylene 1	PB	Similar to PE 50, but can be used up to 90°C.	90*	100*
Polycarbonate	PCMA	Resistant to most solvents and hydrous alkalis. Unsuitable for acids.	60*	80*
Polytetrafluoroethylene (e.g. Teflon®)	PTTF	Resistant to all chemicals in this list.	250*	300*
Nitrile Rubber	NBR	Good resistance to oil and petrol. Unsuitable for oxidizing media.	90*	120*
Butyl Rubber Ethylene Propylene Rubber	BR EPDM	Good resistance to ozone and weather. Especially suitable for aggressive chemicals. Unsuitable for oils and fats.	90*	120*
Chloroprene Rubber (e.g. Neoprene®)	CR	Chemical resistance very similar to that of PVCU and between that of Nitrile and Butyl rubber.	80*	110*
Fluorine Rubber (e.g. Viton®)	FPM	Has best chemical resistance to solvents of all elastomers.	150*	200*
Chlorine Sulphonyl Polyethylene (e.g. Hypalon®)	CSM	Chemical resistance similar to that of EPDM.	100*	140*

*Registered trade name

The abbreviations listed below are found throughout the listings and have the following definition:

Q/E (Quellung/Erweichung) = swelling/softening
D/P (Diffusion/Permeation) = diffusion/permeation
SpkB (Spannungsrisbildung) = environmental stress cracking

(Courtesy George Fischer Engineering Handbook)

Aggressive Media				Chemical Resistance											
Medium	Formula	Boiling point °C	Concentration	Temperature °C	PVC	CPVC	ABS	PE	PP-H	PVDF (S/GFR)	EFDM	FFM	NBR	CR	CSM
Acetaldehyde	CH ₃ -CHO (C ₂ H ₄ O)	21	technically pure	20 40 60 80 100 120 140	-	-	-	+	+	+	+	+	+	+	+
Acetaldehyde			40% aqueous solution	20 40 60 80 100 120 140	+	+	-	+	+	+	+	+	+	+	+
Acetic acid (SpR)	CH ₃ COOH	118	technically pure, glacial	20 40 60 80 100 120 140	+	+	-	+	+	+	+	+	+	+	+
Acetic acid (SpR)	CH ₃ COOH		10% aqueous	20 40 60 80 100 120 140	+	+	+	+	+	+	+	+	+	+	+
Acetic acid (SpR)			50% aqueous	20 40 60 80 100 120 140	+	+	+	+	+	+	+	+	+	+	+
Acetic acid (SpR)	CH ₃ COOH		60%	20 40 60 80 100 120 140	+	-	-	+	+	+	+	+	+	+	+
Acetic acid (SpR)		118	98%	20 40 60 80 100 120 140	-	-	-	+	+	+	+	+	+	+	+
Acetic acid anhydride (SpR)	(CH ₃ -CO) ₂ O	139	technically pure	20 40 60 80 100 120 140	-	-	-	+	+	+	+	+	+	+	+

(Courtesy George Fischer Engineering Handbook)

Aggressive Media					Chemical Resistance										
Medium	Formula	Boiling point °C	Concentration	Temperature °C	PVC	CPVC	ABS	PE	PP-H	PVDF (SYGEL)	EPDM	TFM	NBR	CR	CSM
Acetic acid isobutyl ester	$(CH_3)_2CHCH_2CH_2CO_2H$		technically pure	20 40 60 80 100 120 140	-	-	-	-	-	-	-	-	-	-	-
Acetone	CH_3CO-CH_3	56	technically pure	20 40 60 80 100 120 140	-	-	-	++	++	-	++	-	-	-	0/0/0
Acetone			up to 10%, aqueous	20 40 60 80 100 120 140	-	-	0	++	++	0/0/0	++	0/0	-	0+	0/0/0
Acetonitrile	CH_3CN	81.6	100%	20 40 60 80 100 120 140	-	-	-	-	-	-	-	-	-	-	-
Acetophenone	$CH_3CO-C_6H_5$		100 %	20 40 60 80 100 120 140	-	-	-	-	-	-	+	-	-	-	-
Acrylic acid methyl ester	$CH_2=CHCOOCH_3$	80.3	technically pure	20 40 60 80 100 120 140	-	-	-	-	+	-	0	-	-	-	-
Acrylic ester	$CH_2=CH-COO-CH_2CH_3$	100	technically pure	20 40 60 80 100 120 140	-	-	-	-	-	-	0	-	-	0	+
Acrylonitrile	$CH_2=CH-CN$	77	technically pure	20 40 60 80 100 120 140	-	-	-	++	++	-	++	0/0	-	++	0/0/0

(Courtesy George Fischer Engineering Handbook)

Aggressive Medio					Chemical Resistance										
Medium	Formula	Boiling point °C	Concentration	Temperature °C	PVC	CPVC	ABS	PE	PP-H	PVDF (KRYGEL)	EPDM	FRM	NBR	CR	CSM
Adipic acid	HOOC-(CH ₂) ₄ -COOH	fp 153	saturated, aqueous	20 40 60 80 100 120 140	+	+	-	+	+	+	+	+	+	+	+
Alum	see Potassium/ aluminium sulphate														
Alcoholic spirits (Gin, Whisky, etc.)			approx. 40% ethyl alcohol	20 40 60 80 100 120 140	+	O	-	+	+	+	+	+	+	+	+
Allyl alcohol	H ₂ C=CH-CH ₂ -OH	97	98%	20 40 60 80 100 120 140	O	O	-	+	+	+	O	O	+	O	+
Aluminium chloride	AlCl ₃		10%, aqueous	20 40 60 80 100 120 140	+	+	+	+	+	+	+	+	+	+	+
Aluminium chloride	AlCl ₃	115	saturated	20 40 60 80 100 120 140	+	+	+	+	+	+	+	+	+	+	+
Aluminium fluoride	AlF ₃		saturated	20 40 60 80 100 120 140	+	+	+	+	+	+	+	+	+	+	+
Aluminium hydroxide	Al(OH) ₃		Suspension	20 40 60 80 100 120 140	+	+	+	+	+	+	+	+	+	+	+
Aluminium nitrate	Al(NO ₃) ₃		saturated	20 40 60 80 100 120 140	+	+	+	+	+	+	+	+	+	+	+

(Courtesy George Fischer Engineering Handbook)

Aggressive Media				Chemical Resistance											
Medium	Formula	Boiling point °C	Concentration	Temperature °C	PVC	CPVC	ABS	PE	PPH	PVDF (KALOREX)	EPDM	FRP	NBR	CR	CSM
Aluminium sulphate	Al ₂ (SO ₄) ₃		10%, aqueous	20 40 60 80 100 120 140	+	+	+	+	+	+	+	+	+	+	+
Aluminium sulphate			cold saturated, aqueous	20 40 60 80 100 120 140	+	+	+	+	+	+	+	+	+	+	+
Ammonia (Sp88)	NH ₃	-32	gaseous, technically pure	20 40 60 80 100 120 140	+	+	+	+	+	+	+	+	+	+	+
Ammonium acetate	CH ₃ COONH ₄		aqueous, all	20 40 60 80 100 120 140	+	+	+	+	+	+	+	+	+	+	+
Ammonium aluminium sulfate				20 40 60 80 100 120 140	+	+	+	+	+	+	+	+	+	+	+
Ammonium bromide				20 40 60 80 100 120 140	+	+	+	+	+	+	+	+	+	+	+
Ammonium carbonate	(NH ₄) ₂ CO ₃		50%, aqueous	20 40 60 80 100 120 140	+	+	+	+	+	+	+	+	+	+	+
Ammonium chloride	NH ₄ Cl	115	aqueous, cold saturated	20 40 60 80 100 120 140	+	+	+	+	+	+	+	+	+	+	+

(Courtesy George Fischer Engineering Handbook)

Aggressive Media					Chemical Resistance										
Medium	Formula	Boiling point °C	Concentration	Temperature °C	PVC	CPVC	ABS	PE	PP-H	PVDF (STGF)	EPDM	FPM	NBR	CR	CSM
Ammonium chlorate				20 40 60 80 100 120 140	++ ++ ++ ++ ++ ++ ++					++ ++ ++ ++ ++ ++ ++					
Ammonium dichromate	$(\text{NH}_4)_2 \text{Cr}_2 \text{O}_7$		saturated	20 40 60 80 100 120 140		+++ +++ +++ +++ +++ +++ +++									
Ammonium dihydrogenphosphate				20 40 60 80 100 120 140	++ ++ ++ ++ ++ ++ ++			++ ++ ++ ++ ++ ++ ++							
Ammonium fluoride	NH_4F			20 40 60 80 100 120 140	++ ++ ++ ++ ++ ++ ++	+		++ ++ ++ ++ ++ ++ ++							
Ammonium formate				20 40 60 80 100 120 140						++ ++ ++ ++ ++ ++ ++					
Ammonium hexafluoroarsenate				20 40 60 80 100 120 140						++ ++ ++ ++ ++ ++ ++					
Ammonium hydrogen fluoride	NH_4HF_2		50%, aqueous	20 40 60 80 100 120 140	++ ++ ++ ++ ++ ++ ++	+		++ ++ ++ ++ ++ ++ ++		+	+				
Ammonium hydrogencarbonate				20 40 60 80 100 120 140	++ ++ ++ ++ ++ ++ ++			++ ++ ++ ++ ++ ++ ++							

(Courtesy George Fischer Engineering Handbook)

Aggressive Media					Chemical Resistance										
Medium	Formula	Boiling point °C	Concentration	Temperature °C	PVC	CPVC	ABS	PE	PPH	PVDF (S/G/EF)	EPDM	IFM	NBR	CR	CSM
Ammonium hydrogenphosphate				20 40 60 80 100 120 140	++ ++ ++ ++ ++ ++ ++			++ ++ ++ ++ ++ ++ ++							
Ammonium hydrogensulfite				20 40 60 80 100 120 140					++ ++ ++ ++ ++ ++ ++						
Ammonium hydroxide	NH ₄ OH		aqueous, cold saturated	20 40 60 80 100 120 140	++ ++ ++ ++ ++ ++ ++		++ ++ ++ ++ ++ ++ ++		++ ++ ++ ++ ++ ++ ++	++ ++ ++ ++ ++ ++ ++		++ ++ ++ ++ ++ ++ ++	++ ++ ++ ++ ++ ++ ++	++ ++ ++ ++ ++ ++ ++	++ ++ ++ ++ ++ ++ ++
Ammonium nitrate	NH ₄ NO ₃	112	aqueous, saturated	20 40 60 80 100 120 140	++ ++ ++ ++ ++ ++ ++		++ ++ ++ ++ ++ ++ ++		++ ++ ++ ++ ++ ++ ++	++ ++ ++ ++ ++ ++ ++	++ ++ ++ ++ ++ ++ ++	++ ++ ++ ++ ++ ++ ++	++ ++ ++ ++ ++ ++ ++	++ ++ ++ ++ ++ ++ ++	++ ++ ++ ++ ++ ++ ++
Ammonium oxalate	H ₂ NOOC-COONH ₄			20 40 60 80 100 120 140					++ ++ ++ ++ ++ ++ ++	++ ++ ++ ++ ++ ++ ++					
Ammonium persulphate	(NH ₄) ₂ S ₂ O ₈			20 40 60 80 100 120 140		++ ++ ++ ++ ++ ++ ++			++ ++ ++ ++ ++ ++ ++						
Ammonium phosphate	(NH ₄) ₃ PO ₄		saturated	20 40 60 80 100 120 140	++ ++ ++ ++ ++ ++ ++	++ ++ ++ ++ ++ ++ ++	++ ++ ++ ++ ++ ++ ++	++ ++ ++ ++ ++ ++ ++	++ ++ ++ ++ ++ ++ ++	++ ++ ++ ++ ++ ++ ++	++ ++ ++ ++ ++ ++ ++	++ ++ ++ ++ ++ ++ ++	++ ++ ++ ++ ++ ++ ++	++ ++ ++ ++ ++ ++ ++	++ ++ ++ ++ ++ ++ ++
Ammonium sulphate	(NH ₄) ₂ SO ₄		aqueous, saturated	20 40 60 80 100 120 140	++ ++ ++ ++ ++ ++ ++	++ ++ ++ ++ ++ ++ ++	++ ++ ++ ++ ++ ++ ++	++ ++ ++ ++ ++ ++ ++	++ ++ ++ ++ ++ ++ ++	++ ++ ++ ++ ++ ++ ++	++ ++ ++ ++ ++ ++ ++	++ ++ ++ ++ ++ ++ ++	++ ++ ++ ++ ++ ++ ++	++ ++ ++ ++ ++ ++ ++	++ ++ ++ ++ ++ ++ ++

(Courtesy George Fischer Engineering Handbook)

Aggressive Media				Chemical Resistance											
Medium	Formula	Boiling point °C	Concentration	Temperature °C	PVC	CPVC	ABS	PE	PP-H	PVDF (STGFI)	EPDM	FRM	NBR	CR	CSM
Ammonium sulphide	NH ₄ ₂ S		aqueous, oil	20 40 60 80 100 120 140	+	+	+	+	+	+	+	+	+	+	+
Ammonium tetrafluoroborate				20 40 60 80 100 120 140	+	+	+	+	+	+	+	+	+	+	+
Ammonium thiocyanate	NH ₄ SCN		saturated	20 40 60 80 100 120 140	+	+	+	+	+	+	+	+	+	+	+
Amyl acetate	CH ₃ CH ₂ CH ₂ COOCH ₃	141	technically pure	20 40 60 80 100 120 140	-	-	-	+	+	+	+	+	+	+	+
Amyl alcohol (SpR3)	CH ₃ CH ₂ CH ₂ CH ₂ OH	137	technically pure	20 40 60 80 100 120 140	+	+	+	+	+	+	+	+	+	+	+
Aniline	C ₆ H ₅ NH ₂	182	technically pure	20 40 60 80 100 120 140	-	-	-	+	+	+	+	+	+	+	+
Aniline hydrochloride	C ₆ H ₅ NH ₂ +HCl	245	aqueous, saturated	20 40 60 80 100 120 140	+	+	+	+	+	+	+	+	+	+	+
Antimony thiocyanate				20 40 60 80 100 120 140	+	+	+	+	+	+	+	+	+	+	+

(Courtesy George Fischer Engineering Handbook)

Aggressive Media				Chemical Resistance											
Medium	Formula	Boiling point °C	Concentration	Temperature °C	PVC	CPVC	ABS	PE	PP-H	PVDF (SYGEE)	EPDM	FRM	NBR	CR	CSM
Antimony trichloride (SpRb)	SbCl ₃		90% aqueous	20 40 60 80 100 120 140	+	+	-	+	+	+	+	+	-	+	+
Aqua regia (SpRb)	HNO ₃ +HCl			20 40 60 80 100 120 140	O	+	-	-	-	O	-	O	-	-	O
Arsenic acid	H ₃ AsO ₄		80% aqueous	20 40 60 80 100 120 140	+	+	+	+	+	+	+	+	+	+	+
Barium carbonate	BaCO ₃			20 40 60 80 100 120 140	+	+	+	+	+	+	+	+	+	+	+
Barium chloride	BaCl ₂		saturated	20 40 60 80 100 120 140	+	+	+	+	+	+	+	+	+	+	+
Barium hydroxide	Ba(OH) ₂	102	aqueous, saturated	20 40 60 80 100 120 140	+	+	+	+	+	-	+	+	+	+	+
Barium salts			aqueous, all	20 40 60 80 100 120 140	+	+	+	+	+	+	+	+	+	+	+
Barium sulfate	BaSO ₄			20 40 60 80 100 120 140	+	+	+	+	+	+	+	+	+	+	+

(Courtesy George Fischer Engineering Handbook)

Aggressive Media					Chemical Resistance										
Medium	Formula	Boiling point °C	Concentration	Temperature °C	PVC	CPVC	ABS	PE	PPH	PVDF (STGEF)	EPDM	FPM	NBR	CR	CSM
Barium sulfide	BaS		suspension	20 40 60 80 100 120 140	++ ++ ++ ++ ++ ++ ++			++ ++ ++ ++ ++ ++ ++			++ ++ ++ ++ ++ ++ ++				
Battery acid	see Sulphuric acid 40%														
Beef tallow emulsion, sulphonated (Sp88)			usual commercial	20 40 60 80 100 120 140	+ + + + + + +	o o o o o o o	+ + + + + + +	+ + + + + + +			- + + + + + +	+ + + + + + +	+ + + + + + +	+ + + + + + +	+ + + + + + +
Beer			usual commercial	20 40 60 80 100 120 140	++ ++ ++ ++ ++ ++ ++		++ ++ ++ ++ ++ ++ ++	++ ++ ++ ++ ++ ++ ++	++ ++ ++ ++ ++ ++ ++			+ + + + + + +	+ + + + + + +	+ + + + + + +	+ + + + + + +
Benzaldehyde	C ₆ H ₅ -CHO	180	saturated, aqueous	20 40 60 80 100 120 140	- - - - - - -	- - - - - - -	- - - - - - -	+ + + + + + +	+ + + + + + +	o o o o o o o	+ + + + + + +	+ + + + + + +	o o o o o o o	- - - - - - -	- - - - - - -
Benzene	C ₆ H ₆	80	technically pure	20 40 60 80 100 120 140	- - - - - - -	- - - - - - -	- - - - - - -	o o o o o o o	o o o o o o o	+ + + + + + +	- - - - - - -	+ + + + + + +	o o o o o o o	- - - - - - -	- - - - - - -
Benzenesulfonic acid	C ₆ H ₅ SO ₃ H		technically pure	20 40 60 80 100 120 140						+ + + + + + +		+ + + + + + +			
Benzoic acid	C ₆ H ₅ -COOH	Fp., 122	aqueous, oil	20 40 60 80 100 120 140	+ + + + + + +	+ + + + + + +	+ + + + + + +	+ + + + + + +	+ + + + + + +	+ + + + + + +	+ + + + + + +	+ + + + + + +	- - - - - - -	- - - - - - -	- - - - - - -
Benzoyl chloride	C ₆ H ₅ CHCl ₂		technically pure	20 40 60 80 100 120 140						+ + + + + + +					

(Courtesy George Fischer Engineering Handbook)

Aggressive Media					Chemical Resistance										
Medium	Formula	Boiling point °C	Concentration	Temperature °C	PVC	CPVC	ABS	PE	PP-H	PVC (STYGEN)	EPDM	FRM	NBR	CR	CSM
Benzyl alcohol (SpR8)	C ₆ H ₅ -CH ₂ -OH	206	technically pure	20 40 60 80 100 120 140	O	-	-	O +	O +	O +	-	+	-	++	O
Beryllium chloride				20 40 60 80 100 120 140						+++					
Beryllium sulfate				20 40 60 80 100 120 140						++++		++			
Borax	Na ₂ B ₄ O ₇		aqueous, oil	20 40 60 80 100 120 140	+	+	+	+	+	+	+	+	+	+	O +
Boric acid	H ₃ BO ₃		oil, aqueous	20 40 60 80 100 120 140	+	+	+	+	+	+	+	+	+	+	+
Brine, containing chlorine				20 40 60 80 100 120 140	+	+	-	+	O	O +	O	+	O	O	O
Brombenzene	C ₆ H ₅ Br			20 40 60 80 100 120 140	-	-				+		+			
Bromine, liquid	Br ₂	59	technically pure	20 40 60 80 100 120 140	-	-	-	-	+	O +	-	+	-	-	-

(Courtesy George Fischer Engineering Handbook)

Aggressive Media					Chemical Resistance										
Medium	Formula	Boiling point °C	Concentration	Temperature °C	PVC	CPVC	ABS	PE	PP-H	PVDF (SYGEL)	EPDM	FRM	NBR	CR	CSM
Bromine vapours	Br ₂		high	20 40 60 80 100 120 140	-	-	-	-	-	+	-	+	-	-	-
Bromine water	Br/H ₂ O		saturated, aqueous	20 40 60 80 100 120 140	+	o	-	-	-	+	-	+	-	-	-
Butadiene (Q/EI)	H ₂ C=CH-CH=CH ₂	-4	technically pure	20 40 60 80 100 120 140	+	+	-	+	+	+	-	o	-	+	+
Butane	C ₄ H ₁₀	0	technically pure	20 40 60 80 100 120 140	+	+	+	+	+	+	-	+	+	+	+
Butenediol (SpR8)	HO-ICH ₂ -CH ₂ -OH	230	aqueous, 10%	20 40 60 80 100 120 140	+	+	-	+	+	+	+	+	+	o	+
Butanol (SpR8)	C ₄ H ₉ OH	117	technically pure	20 40 60 80 100 120 140	+	+	-	+	+	+	+	+	+	+	+
Butyl acetate	CH ₃ COOCH ₂ CH ₂ CH ₂ CH ₃	126	technically pure	20 40 60 80 100 120 140	-	-	-	+	o	+	+	o	-	o	o
Butyl phenol, p-tertiary	(CH ₃) ₃ C-C ₆ H ₄ -OH	237	technically pure	20 40 60 80 100 120 140	o	o	-	o	+	+	-	o	-	-	-

(Courtesy George Fischer Engineering Handbook)

Aggressive Media				Chemical Resistance											
Medium	Formula	Boiling point °C	Concentration	Temperature °C	PVC	CPVC	ABS	PE	PPH	PVDF (SUGU)	EPDM	IRM	NBR	CR	CSM
Butylene glycol (SpR)	HO-CH ₂ -CH=CH-CH ₂ -OH	235	technically pure	20 40 60 80 100 120 140	+	+	+	+	+	+	+	+	+	+	+
Butylene liquid	C ₄ H ₈	51	technically pure	20 40 60 80 100 120 140	+					+	+	+	+	+	+
Butyric acid (SpR)	CH ₃ -CH ₂ -CH ₂ -COOH	163	technically pure	20 40 60 80 100 120 140	+	+		+	+	+	+	+		+	+
Cadmium bromide	CdBr ₂			20 40 60 80 100 120 140	+	+	+	+	+		+	+	+	+	+
Cadmium chloride	CdCl ₂			20 40 60 80 100 120 140	+	+	+	+	+		+	+	+	+	+
Cadmium cyanide	Cd(CN) ₂			20 40 60 80 100 120 140	+	+	+	+	+						
Cadmium sulfate	CdSO ₄			20 40 60 80 100 120 140	+	+	+	+	+		+	+	+	+	+
Calcium acetate	[CH ₃ COO] ₂ Ca		saturated	20 40 60 80 100 120 140	+	+	+	+	+	+	+	+			

(Courtesy George Fischer Engineering Handbook)

Aggressive Media				Chemical Resistance											
Medium	Formula	Boiling point °C	Concentration	Temperature °C	PVC	CPVC	ABS	PE	PP-H	PVDF (Kynar)	EPDM	FRM	NBR	CR	CSM
Calcium bisulphite	CaHSO ₃ l		cold saturated, aqueous	20 40 60 80 100 120 140	+	+	+	+		+	+	+			+
Calcium carbonate	CaCO ₃			20 40 60 80 100 120 140	+	+	+	+	+	+	+	+			
Calcium chlorate	Ca(ClO ₃) ₂			20 40 60 80 100 120 140	+	+	+	+	+	+	+	+			
Calcium chloride	CaCl ₂	125	saturated, aqueous, oil	20 40 60 80 100 120 140	+	+	+	+	+	+	+	+	+	+	+
Calcium fluoride	CaF ₂			20 40 60 80 100 120 140	+			+	+			+			
Calcium hydrogencarbonate				20 40 60 80 100 120 140						+	+	+	+		
Calcium hydrosulfide	CaSH ₂			20 40 60 80 100 120 140		+	+			+	+	+			
Calcium hydrosulfite	CaHSO ₃ l		saturated	20 40 60 80 100 120 140						+					

(Courtesy George Fischer Engineering Handbook)

Aggressive Media				Chemical Resistance											
Medium	Formula	Boiling point °C	Concentration	Temperature °C	PVC	CPVC	ABS	PE	PP-H	PVDF (KALOR)	EPDM	FRM	NBR	CR	CSM
Calcium hydroxide	Ca(OH) ₂	100	saturated, aqueous	20 40 60 80 100 120 140	++ ++ ++ ++ ++ ++ ++	++ ++ ++ ++ ++ ++ ++	++ ++ ++ ++ ++ ++ ++	++ ++ ++ ++ ++ ++ ++	++ ++ ++ ++ ++ ++ ++	++ ++ ++ ++ ++ ++ ++	++ ++ ++ ++ ++ ++ ++	++ ++ ++ ++ ++ ++ ++	++ ++ ++ ++ ++ ++ ++	++ ++ ++ ++ ++ ++ ++	++ ++ ++ ++ ++ ++ ++
Calcium nitrate	Ca(NO ₃) ₂	115	50%, aqueous	20 40 60 80 100 120 140	++ ++ ++ ++ ++ ++ ++	++ ++ ++ ++ ++ ++ ++	++ ++ ++ ++ ++ ++ ++	++ ++ ++ ++ ++ ++ ++	++ ++ ++ ++ ++ ++ ++	++ ++ ++ ++ ++ ++ ++	++ ++ ++ ++ ++ ++ ++	++ ++ ++ ++ ++ ++ ++	++ ++ ++ ++ ++ ++ ++	++ ++ ++ ++ ++ ++ ++	++ ++ ++ ++ ++ ++ ++
Calcium phosphate	Ca(H ₂ PO ₄) ₂ CaHPO ₄ Ca ₃ (PO ₄) ₂			20 40 60 80 100 120 140	++ ++ ++ ++ ++ ++ ++	++ ++ ++ ++ ++ ++ ++	++ ++ ++ ++ ++ ++ ++	++ ++ ++ ++ ++ ++ ++	++ ++ ++ ++ ++ ++ ++	++ ++ ++ ++ ++ ++ ++	++ ++ ++ ++ ++ ++ ++	++ ++ ++ ++ ++ ++ ++	++ ++ ++ ++ ++ ++ ++	++ ++ ++ ++ ++ ++ ++	++ ++ ++ ++ ++ ++ ++
Calcium sulfide	CaS			20 40 60 80 100 120 140	++ ++ ++ ++ ++ ++ ++	++ ++ ++ ++ ++ ++ ++	++ ++ ++ ++ ++ ++ ++	++ ++ ++ ++ ++ ++ ++	++ ++ ++ ++ ++ ++ ++	++ ++ ++ ++ ++ ++ ++	++ ++ ++ ++ ++ ++ ++	++ ++ ++ ++ ++ ++ ++	++ ++ ++ ++ ++ ++ ++	++ ++ ++ ++ ++ ++ ++	++ ++ ++ ++ ++ ++ ++
Calcium sulphate	CaSO ₄		suspensions	20 40 60 80 100 120 140	++ ++ ++ ++ ++ ++ ++	++ ++ ++ ++ ++ ++ ++	++ ++ ++ ++ ++ ++ ++	++ ++ ++ ++ ++ ++ ++	++ ++ ++ ++ ++ ++ ++	++ ++ ++ ++ ++ ++ ++	++ ++ ++ ++ ++ ++ ++	++ ++ ++ ++ ++ ++ ++	++ ++ ++ ++ ++ ++ ++	++ ++ ++ ++ ++ ++ ++	++ ++ ++ ++ ++ ++ ++
Calcium sulphite	Ca(HSO ₃) ₂		aqueous, cold saturated	20 40 60 80 100 120 140	++ ++ ++ ++ ++ ++ ++	++ ++ ++ ++ ++ ++ ++	++ ++ ++ ++ ++ ++ ++	++ ++ ++ ++ ++ ++ ++	++ ++ ++ ++ ++ ++ ++	++ ++ ++ ++ ++ ++ ++	++ ++ ++ ++ ++ ++ ++	++ ++ ++ ++ ++ ++ ++	++ ++ ++ ++ ++ ++ ++	++ ++ ++ ++ ++ ++ ++	++ ++ ++ ++ ++ ++ ++
Calcium tungstate				20 40 60 80 100 120 140	++ ++ ++ ++ ++ ++ ++	++ ++ ++ ++ ++ ++ ++	++ ++ ++ ++ ++ ++ ++	++ ++ ++ ++ ++ ++ ++	++ ++ ++ ++ ++ ++ ++	++ ++ ++ ++ ++ ++ ++	++ ++ ++ ++ ++ ++ ++	++ ++ ++ ++ ++ ++ ++	++ ++ ++ ++ ++ ++ ++	++ ++ ++ ++ ++ ++ ++	++ ++ ++ ++ ++ ++ ++
Calcium bromide	CaBr ₂			20 40 60 80 100 120 140	++ ++ ++ ++ ++ ++ ++	++ ++ ++ ++ ++ ++ ++	++ ++ ++ ++ ++ ++ ++	++ ++ ++ ++ ++ ++ ++	++ ++ ++ ++ ++ ++ ++	++ ++ ++ ++ ++ ++ ++	++ ++ ++ ++ ++ ++ ++	++ ++ ++ ++ ++ ++ ++	++ ++ ++ ++ ++ ++ ++	++ ++ ++ ++ ++ ++ ++	++ ++ ++ ++ ++ ++ ++

(Courtesy George Fischer Engineering Handbook)

Aggressive Media				Chemical Resistance											
Medium	Formula	Boiling point °C	Concentration	Temperature °C	PVC	CPVC	ABS	PE	PPH	PVDF (STYGEN)	EPDM	FRM	NBR	CR	CSM
Calcium lactate	$\text{ICH}_2\text{COOCH}_2\text{CO}$		saturated	20 40 60 80 100 120 140				++	++	++	++				
Caprolactam	$\text{C}_6\text{H}_{11}\text{NO}$			20 40 60 80 100 120 140											
Caprolactone	$\text{C}_6\text{H}_{10}\text{O}_2$			20 40 60 80 100 120 140											
Carbon dioxide - carbonic acid	CO_2		technically pure, anhydrous	20 40 60 80 100 120 140	+	+	+	+	+	+	+	+	+	+	+
Carbon disulphide	CS_2	46	technically pure	20 40 60 80 100 120 140	-	-	-	O	O	+		+	-	-	-
Carbon tetrachloride	CCl_4	77	technically pure	20 40 60 80 100 120 140	-	-	-	-	-	+	-	+	-	-	-
Carbonic acid				20 40 60 80 100 120 140	+	+	+	+	+	+	+	+	+	+	+
Caro's acid	see Peroxomonosulfuric acid			20 40 60 80 100 120 140	+	+	+	+	+	+	+	+	+	+	+
Casein				20 40 60 80 100 120 140						+					

(Courtesy George Fischer Engineering Handbook)

Aggressive Media					Chemical Resistance										
Medium	Formula	Boiling point °C	Concentration	Temperature °C	PVC	CPVC	ABS	PE	PP-H	PMMA (50°C)	EPDM	TPE	NBR	CR	CSM
Calcium chloride	CaCl ₂			20						+					
				40											
				60											
				80											
				100											
				120											
				140											
Calcium hydroxide	Ca(OH) ₂			20						+					
				40											
				60											
				80											
				100											
				120											
				140											
Caustic potash solution (potassium hydroxide)	KOH	131	50%, aqueous	20	+	+	+	+	+	-					
				40		+	+	+	+						
				60		+	+	+	+						
				80		+	+	+	+						
				100				+	+	+					
				120											
				140											
Caustic soda solution	NaOH		50%, aqueous	20	+	+	+	+	+		+	+			
				40		+	+	+	+						
				60		+	+	+	+						
				80				+	+	+					
				100											
				120											
				140											
Cerium (III) -chloride	CeCl ₃			20											
				40											
				60											
				80											
				100											
				120											
				140											
Chloral hydrate	CCl ₃ -CH(OH) ₂	98	technically pure	20	-		-	+	0	-	0	0	-	0	+
				40				+							
				60				+							
				80											
				100											
				120											
				140											
Chloric acid (5p88)	HClO ₃		10%, aqueous	20	+	+	-	+	-	+	+	-	-	-	+
				40		+									
				60	0	+									
				80											
				100											
				120											
				140											
Chloric acid (5p88)	HClO ₃		20%, aqueous	20	+	+	-	0	-	+	+	-	-	-	+
				40		+									
				60	0	+									
				80		+									
				100											
				120											
				140											

(Courtesy George Fischer Engineering Handbook)

Aggressive Media				Chemical Resistance											
Medium	Formula	Boiling point °C	Concentration	Temperature °C	PVC	CPVC	ABS	PE	PP-H	PVDF (STGEL)	EPDM	FPM	NBR	CR	CSM
Chlorosulphonic acid	ClSO ₃ H	158	technically pure	20 40 60 80 100 120 140	O	-	-	-	-	O	-	-	-	-	-
Chromic alum (chromium potassium sulphate)	K ₂ (SO ₄) ₂		cold saturated, aqueous	20 40 60 80 100 120 140	+	+	+	+	+	+	+	+	+	+	+
Chronic acid (SpR)	CrO ₃ +H ₂ O		up to 50%, aqueous	20 40 60 80 100 120 140	O	O	-	O	O	+	O	+	-	-	O
Chronic acid (SpR)			oil, aqueous	20 40 60 80 100 120 140	O	O	-	O	O	+	O	+	-	-	O
Chronic acid + sulphuric acid + water (SpR)	CrO ₃ H ₂ SO ₄ H ₂ O		50 g 15 g 35 g	20 40 60 80 100 120 140	+	+	-	-	+	+	O	+	+	-	O
Chromium (III)-chloride				20 40 60 80 100 120 140	+	+	-	-	+	+	+	+	+	+	+
Chromium (III)-fluoride	CrF ₃			20 40 60 80 100 120 140	+	+	-	-	+	+	+	+	+	+	+
Chromium (III)-chloride	CrCl ₃			20 40 60 80 100 120 140	+	+	-	-	+	+	+	+	+	+	+

(Courtesy George Fischer Engineering Handbook)

Aggressive Media					Chemical Resistance										
Medium	Formula	Boiling point °C	Concentration	Temperature °C	PVC	CPVC	ABS	PE	PP-H	PVC (STY/EN)	EPDM	FM	NBR	CR	CSM
Chlorine	Cl ₂		moist, 97%, gaseous	20 40 60 80 100 120 140	-	-	-	-	-	-	-	+	-	-	0
Chlorine	Cl ₂		anhydrous, technically pure	20 40 60 80 100 120 140	-	-	-	0 0 0	-	0 ++ +	0	+	-	-	0
Chlorine	Cl ₂		liquid, technically pure	20 40 60 80 100 120 140	-	-	-	-	+	-	-	0	-	-	-
Chlorine water (SpR)	Cl ₂ H ₂ O		saturated	20 40 60 80 100 120 140	+	+	0	0 0	0	0	0	0	-	0	-
Chloroacetic acid, mono (SpR)	ClCH ₂ COOH		50%, aqueous	20 40 60 80 100 120 140	+	-	-	+	+	+	0	-	-	-	0
Chloroacetic acid, mono (SpR)	ClCH ₂ COOH	188	technically pure	20 40 60 80 100 120 140	+	-	-	+	+	-	0	-	-	-	0
Chlorobenzene	C ₆ H ₅ Cl	132	technically pure	20 40 60 80 100 120 140	-	-	-	0	+	+	-	-	-	-	0
Chloroethanol	ClCH ₂ -CH ₂ OH	129	technically pure	20 40 60 80 100 120 140	-	-	-	+	+	+	0	-	+	-	0

(Courtesy George Fischer Engineering Handbook)

Aggressive Media				Chemical Resistance											
Medium	Formula	Boiling point °C	Concentration	Temperature °C	PVC	CPVC	ABS	PE	PP-H	PVDF (S/GF)	EPDM	FRM	NBR	CR	CSM
Chromium (III) -nitrate	$\text{Cr}(\text{NO}_3)_3$			20 40 60 80 100 120 140	++ ++ ++ ++ ++ ++ ++					++ ++ ++ ++ ++ ++ ++					
Chromium (III) -sulfate	$\text{Cr}_2(\text{SO}_4)_3$			20 40 60 80 100 120 140	++ ++ ++ ++ ++ ++ ++					++ ++ ++ ++ ++ ++ ++					
Cider				20 40 60 80 100 120 140	+	+	+	+	+	+	+	+	+	+	+
Citric acid		fp. •153	10% aqueous	20 40 60 80 100 120 140	++ ++ ++ ++ ++ ++ ++	++ ++ ++ ++ ++ ++ ++	++ ++ ++ ++ ++ ++ ++	++ ++ ++ ++ ++ ++ ++	++ ++ ++ ++ ++ ++ ++	++ ++ ++ ++ ++ ++ ++	++ ++ ++ ++ ++ ++ ++	++ ++ ++ ++ ++ ++ ++	++ ++ ++ ++ ++ ++ ++	++ ++ ++ ++ ++ ++ ++	++ ++ ++ ++ ++ ++ ++
Citric acid				20 40 60 80 100 120 140	+	+	+	+	+	+	+	+	+	+	+
Citric acid up to 10%				20 40 60 80 100 120 140	+	+	+	+	+	+	+	+	+	+	+
Cool gas, benzene free				20 40 60 80 100 120 140	+	+	+	+	+	+	+	+	+	+	+
Coconut fat alcohol (Sp88)			technically pure	20 40 60 80 100 120 140	++ ++ ++ ++ ++ ++ ++	++ ++ ++ ++ ++ ++ ++	++ ++ ++ ++ ++ ++ ++	++ ++ ++ ++ ++ ++ ++	++ ++ ++ ++ ++ ++ ++	++ ++ ++ ++ ++ ++ ++	++ ++ ++ ++ ++ ++ ++	++ ++ ++ ++ ++ ++ ++	++ ++ ++ ++ ++ ++ ++	++ ++ ++ ++ ++ ++ ++	++ ++ ++ ++ ++ ++ ++

(Courtesy George Fischer Engineering Handbook)

Aggressive Media				Chemical Resistance											
Medium	Formula	Boiling point °C	Concentration	Temperature °C	PVC	CPVC	ABS	PE	PPH	PVDF (KALOF)	EPDM	FRM	NBR	CR	CSM
Compressed air, containing oil (Sp88)				20 40 60 80 100 120 140	- - - - - - -	- - - - - - -	- - - - - - -	+ + + + + + +	O O O O O O O	+ + + + + + +	- - - - - - -	+ + + + + + +	+ + + + + + +	+ + + + + + +	+ + + + + + +
Copper salts	CuCl , CuCl_2 , CuF_2 , CuNO_3 , CuSO_4 , CuCNH_2		oil, aqueous	20 40 60 80 100 120 140	+ + + + + + +	+ + + + + + +	+ + + + + + +	+ + + + + + +	+ + + + + + +	+ + + + + + +	+ + + + + + +	+ + + + + + +	+ + + + + + +	+ + + + + + +	+ + + + + + +
Corn oil (Sp88)			technically pure	20 40 60 80 100 120 140	O O O O O O O	O O O O O O O	O O O O O O O	+ + + + + + +	+ + + + + + +	+ + + + + + +	+ + + + + + +	+ + + + + + +	+ + + + + + +	+ + + + + + +	+ + + + + + +
Cresol	$\text{HO}-\text{C}_6\text{H}_4-\text{CH}_3$		cold saturated, aqueous	20 40 60 80 100 120 140	O O O O O O O	- - - - - - -	+ + + + + + +	+ + + + + + +	+ + + + + + +	+ + + + + + +	+ + + + + + +	+ + + + + + +	+ + + + + + +	+ + + + + + +	+ + + + + + +
Crotonic aldehyde	$\text{CH}_3-\text{CH}=\text{CH}-\text{CHO}$	102	technically pure	20 40 60 80 100 120 140	- - - - - - -	- - - - - - -	+ + + + + + +	+ + + + + + +	+ + + + + + +	+ + + + + + +	+ + + + + + +	+ + + + + + +	+ + + + + + +	+ + + + + + +	+ + + + + + +
Cyclohexane (Q/E)	C_6H_{12}	81	technically pure	20 40 60 80 100 120 140	- - - - - - -	- - - - - - -	+ + + + + + +	+ + + + + + +	+ + + + + + +	+ + + + + + +	- - - - - - -	+ + + + + + +	+ + + + + + +	- - - - - - -	- - - - - - -
Cyclohexanol (Sp88)	$\text{C}_6\text{H}_{12}\text{O}$	161	technically pure	20 40 60 80 100 120 140	+ + + + + + +	+ + + + + + +	- - - - - - -	+ + + + + + +	+ + + + + + +	+ + + + + + +	- - - - - - -	+ + + + + + +	O O O O O O O	+ + + + + + +	+ + + + + + +
Cyclohexanone	$\text{C}_6\text{H}_{10}\text{O}$	155	technically pure	20 40 60 80 100 120 140	- - - - - - -	- - - - - - -	+ + + + + + +	+ + + + + + +	+ + + + + + +	+ + + + + + +	O O O O O O O	- - - - - - -	- - - - - - -	- - - - - - -	- - - - - - -

(Courtesy George Fischer Engineering Handbook)

Aggressive Media				Chemical Resistance											
Medium	Formula	Boiling point °C	Concentration	Temperature °C	PVC	CPVC	ABS	PE	PPH	PVDF (STYGEH)	EPDM	FM	NBR	CR	CSM
Densodrine W				20 40 60 80 100 120 140	++ ++ ++ ++ - - -	++ ++ ++ ++ - - -	○ - - - - - -	- - - - - - -	- - - - - - -	++ - - - - - -	- - - - - - -	++ - - - - - -	++ - - - - - -	++ - - - - - -	++ - - - - - -
Detergents (Sp88)	see washing powder		for usual washing laundry												
Dextrose	$C_6H_{12}O_6$		usual commercial	20 40 60 80 100 120 140	++ ++ ++ ++ ++ ++ ++	++ ++ ++ ++ ++ ++ ++	++ ++ ++ ++ ++ ++ ++	++ ++ ++ ++ ++ ++ ++	++ ++ ++ ++ ++ ++ ++	++ ++ ++ ++ ++ ++ ++	++ ++ ++ ++ ++ ++ ++	++ ++ ++ ++ ++ ++ ++	++ ++ ++ ++ ++ ++ ++	++ ++ ++ ++ ++ ++ ++	++ ++ ++ ++ ++ ++ ++
Dextrose	siehe Glucose			20 40 60 80 100 120 140	++ ++ ++ ++ ++ ++ ++	++ ++ ++ ++ ++ ++ ++	++ ++ ++ ++ ++ ++ ++	++ ++ ++ ++ ++ ++ ++	++ ++ ++ ++ ++ ++ ++	++ ++ ++ ++ ++ ++ ++	++ ++ ++ ++ ++ ++ ++	++ ++ ++ ++ ++ ++ ++	++ ++ ++ ++ ++ ++ ++	++ ++ ++ ++ ++ ++ ++	++ ++ ++ ++ ++ ++ ++
Dibutyl ether	$C_4H_9OC_4H_9$	142	technically pure	20 40 60 80 100 120 140	- - - - - - -	- - - - - - -	○ - - - - - -	○ - - - - - -	- - - - - - -	- - - - - - -	++ ○ ○ ○ ○ ○ ○	○ ○ ○ ○ ○ ○ ○	○ ○ ○ ○ ○ ○ ○	- - - - - - -	○ ○ ○ ○ ○ ○ ○
Dibutyl phthalate	$C_4H_9COOC_4H_9$	340	technically pure	20 40 60 80 100 120 140	- - - - - - -	- - - - - - -	○ ○ ○ ○ ○ ○ ○	○ ○ ○ ○ ○ ○ ○	○ ○ ○ ○ ○ ○ ○	○ ○ ○ ○ ○ ○ ○	○ ○ ○ ○ ○ ○ ○	○ ○ ○ ○ ○ ○ ○	- - - - - - -	- - - - - - -	- - - - - - -
Dibutyl sebacate	$C_4H_9COOC_4H_9$	344	technically pure	20 40 60 80 100 120 140	- - - - - - -	- - - - - - -	++ ++ ++ ++ ++ ++ ++	++ ++ ++ ++ ++ ++ ++	++ ++ ++ ++ ++ ++ ++	++ ++ ++ ++ ++ ++ ++	++ ++ ++ ++ ++ ++ ++	++ ++ ++ ++ ++ ++ ++	- - - - - - -	- - - - - - -	- - - - - - -
Dichlorobenzol	$C_6H_4Cl_2$	180	technically pure	20 40 60 80 100 120 140	- - - - - - -	- - - - - - -	- - - - - - -	- - - - - - -	- - - - - - -	- - - - - - -	- - - - - - -	- - - - - - -	- - - - - - -	- - - - - - -	- - - - - - -
Dichloroacetic acid	$Cl_2CHCOOH$	194	technically pure	20 40 60 80 100 120 140	++ ++ ++ ++ ++ ++ ++	- - - - - - -	- ++ ++ ++ ++ ++ ++	- ++ ++ ++ ++ ++ ++	++ ++ ++ ++ ++ ++ ++	++ ++ ++ ++ ++ ++ ++	○ ○ ○ ○ ○ ○ ○	- - - - - - -	○ ○ ○ ○ ○ ○ ○	- - - - - - -	○ ○ ○ ○ ○ ○ ○

(Courtesy George Fischer Engineering Handbook)

Aggressive Media				Chemical Resistance											
Medium	Formula	Boiling point °C	Concentration	Temperature °C	PVC	CPVC	ABS	PE	PP-H	PVDF (STGEE)	EPDM	FRM	NBR	CR	CSM
Dichloroacetic acid (SpRB)	Cl ₂ CHCOOH		50% aqueous	20 40 60 80 100 120 140	+	+	-	++	++	+	++	++	-	-	++
Dichloroacetic acid methyl ester	Cl ₂ CHCOOCH ₃	143	technically pure	20 40 60 80 100 120 140	-	-	-	++	++	+	++	++	-	-	++
Dichloroethan	Ethylene chloride														
Dichloroethylene	ClCH=CHCl	60	technically pure	20 40 60 80 100 120 140	-	-	-	-	+	+	-	+	-	-	-
Dichloromethane				20 40 60 80 100 120 140	-	-	-								
Diesel oil (SpRB, Q/EI)				20 40 60 80 100 120 140	+	+	+	+	+	+	-	+	+	+	+
Diethyl ether				20 40 60 80 100 120 140	-	-	-								
Diethylamine	(C ₂ H ₅) ₂ NH	56	technically pure	20 40 60 80 100 120 140	+	-	-	+	+	+	+	+	+	+	+
Diethylene glycol butyl ether				20 40 60 80 100 120 140	-	-	-								

(Courtesy George Fischer Engineering Handbook)

[illegible]

(Courtesy George Fischer Engineering Handbook)

Aggressive Media					Chemical Resistance										
Medium	Formula	Boiling point °C	Concentration	Temperature °C	PVC	CPVC	ABS	PE	PP-H	PVDF (S/GLEF)	EFDM	PMMA	NBR	CR	CSMA
Ethanolamine	see Ammono ethanol														
Ethyl acetate	CH ₃ COOCH ₂ -CH ₃	77	technically pure	20 40 60 80 100 120 140	-	-	-	O O +	O O +	O	+	-	-	-	-
Ethyl alcohol + acetic acid (fermentation mixture)			technically pure	20 40 60 80 100 120 140	+	O	-	+	+	+	O O	O O O	O O	+	+
Ethyl alcohol (Ethnoc) (5pH)	CH ₃ -CH ₂ -OH	78	technically pure, 99%	20 40 60 80 100 120 140	+	O	-	+	+	+	+	O O O	O	+	+
Ethyl benzene	C ₆ H ₅ -CH ₂ -CH ₃	136	technically pure	20 40 60 80 100 120 140	-	-	-	O	O	O	-	+	-	-	-
Ethyl chloride	CH ₃ -CH ₂ Cl	12	technically pure	20 40 60 80 100 120 140	-	-	-	O	O	O	-	O	-	-	-
Ethyl ether	CH ₃ CH ₂ -O-CH ₂ CH ₃	35	technically pure	20 40 60 80 100 120 140	-	-	-	+	O	+	-	-	-	-	-
Ethylenechloride (1,2-Dichloroethane)				20 40 60 80 100 120 140	-	-	-	-	-	-	-	-	-	-	-
Ethylene chloride	ClCH ₂ -CH ₂ Cl	83	technically pure	20 40 60 80 100 120 140	-	-	-	O	O	+	-	+	O	-	-

(Courtesy George Fischer Engineering Handbook)

Aggressive Media				Chemical Resistance											
Medium	Formula	Boiling point °C	Concentration	Temperature °C	PVC	CPVC	ABS	PE	PPH	PVDF (Kynar)	EPDM	FPM	NBR	CR	CSM
Ethylene diamine	$H_2N-CH_2-CH_2-NH_2$	117	technically pure	20 40 60 80 100 120 140	O	-	-	++	++	-	+	O	O	O	O
Ethylene glycol (SpR2)	$HO-CH_2-CH_2-OH$	198	technically pure	20 40 60 80 100 120 140	++	O	-	++	++	++	+++	O	++	O	++
Ethylene glycol	CH_2OHCH_2OH	198	technically pure	20 40 60 80 100 120 140	++	-	-	++	++	++	++	O	++	O	++
Ethylene oxide	CH_2-CH_2	10	technically pure, moist	20 40 60 80 100 120 140	-	-	-	-	O	+	O	-	-	-	-
Ethylenediaminetetraacetic acid (EDTA)				20 40 60 80 100 120 140				+	+	+	+				
Fatty acids $>C_4$ (SpR2)	$R-COOH$		technically pure	20 40 60 80 100 120 140	+	+	-	+	+	+	+	+	O	O	-
Fatty alcohol sulphonates (SpR2)			aqueous	20 40 60 80 100 120 140	+	+	+	+	+	+	+	+	+	+	+
Fertilizers			aqueous	20 40 60 80 100 120 140	+	+	O	+	+	+	+	+	+	+	+

(Courtesy George Fischer Engineering Handbook)

Aggressive Media					Chemical Resistance										
Medium	Formula	Boiling point °C	Concentration	Temperature °C	PVC	CPVC	ABS	PE	PPH	PVDF (SNGE)	EPDM	PM	NBR	CR	CSM
Fluorine	F ₂		technically pure	20 40 60 80 100 120 140	-	-	-	-	-	-	-	-	-	-	-
Fluorosilicic acid (IQ/E)	H ₂ SiF ₆		32%, aqueous	20 40 60 80 100 120 140	+	+	+	+	+	+	+	○	○	○	+
Formaldehyde (SpR)	HCHO		40%, aqueous	20 40 60 80 100 120 140	+	+	+	+	+	+	+	+	+	+	+
Formamide	HCONH ₂	210	technically pure	20 40 60 80 100 120 140	-	-	-	+	+	+	+	○	+	+	+
Formic acid (SpR)	HCOOH		up to 50%, aqueous	20 40 60 80 100 120 140	+	+	○	+	+	+	+	+	+	+	+
Formic acid (SpR)	HCOOH	101	technically pure	20 40 60 80 100 120 140	+	○	-	+	+	+	+	+	-	+	+
Formic acid (SpR)			25%	20 40 60 80 100 120 140	+	+	+	+	+	+	+	+	+	+	+
Freon 113	see trifluoro, trichloroethane	48		20 40 60 80 100 120 140	+	+	+	+	+	+	+	+	+	+	+
Freon 12 (D/P)	see Freon 12	-30	technically pure	20 40 60 80 100 120 140	+	+	+	+	+	+	+	+	+	+	+

(Courtesy George Fischer Engineering Handbook)

Aggressive Media					Chemical Resistance										
Medium	Formula	Boiling point °C	Concentration	Temperature °C	PVC	CPVC	ABS	PE	PP-H	PVDF (CYGEL)	EPDM	FFM	NBR	CR	CSM
Fruit juices (SpR8)				20	+	+	+	+	+	+	+	+	+	+	+
				40	+	+	+	+	+	+	+	+	+	+	+
				60	+	+	+	+	+	+	+	+	+	+	+
				80	+	+	+	+	+	+	+	+	+	+	+
				100	+	+	+	+	+	+	+	+	+	+	+
				120	+	+	+	+	+	+	+	+	+	+	+
				140	+	+	+	+	+	+	+	+	+	+	+
Fruit pulp				20	+	+	+	+	+	+	+	+	+	+	+
				40	+	+	+	+	+	+	+	+	+	+	+
				60	+	+	+	+	+	+	+	+	+	+	+
				80	+	+	+	+	+	+	+	+	+	+	+
				100	+	+	+	+	+	+	+	+	+	+	+
				120	+	+	+	+	+	+	+	+	+	+	+
				140	+	+	+	+	+	+	+	+	+	+	+
Fuel oil				20	+	+	+	+	+	+	+	+	+	+	+
				40	+	+	+	+	+	+	+	+	+	+	+
				60	+	+	+	+	+	+	+	+	+	+	+
				80	+	+	+	+	+	+	+	+	+	+	+
				100	+	+	+	+	+	+	+	+	+	+	+
				120	+	+	+	+	+	+	+	+	+	+	+
				140	+	+	+	+	+	+	+	+	+	+	+
Furfuryl alcohol (SpR8)	$C_5H_6O_2$	171	technically pure	20	-	-	-	+	+	+	+	+	+	+	+
				40	-	-	-	+	+	+	+	+	+	+	+
				60	-	-	-	+	+	+	+	+	+	+	+
				80	-	-	-	+	+	+	+	+	+	+	+
				100	-	-	-	+	+	+	+	+	+	+	+
				120	-	-	-	+	+	+	+	+	+	+	+
				140	-	-	-	+	+	+	+	+	+	+	+
Gasoline (SpR8)	C_5H_{12} to $C_{12}H_{26}$	80-130	free of lead and aromatic compounds	20	+	+	+	+	+	+	+	+	+	+	+
				40	+	+	+	+	+	+	+	+	+	+	+
				60	+	+	+	+	+	+	+	+	+	+	+
				80	+	+	+	+	+	+	+	+	+	+	+
				100	+	+	+	+	+	+	+	+	+	+	+
				120	+	+	+	+	+	+	+	+	+	+	+
				140	+	+	+	+	+	+	+	+	+	+	+
Gelatin			all, aqueous	20	+	+	+	+	+	+	+	+	+	+	+
				40	+	+	+	+	+	+	+	+	+	+	+
				60	+	+	+	+	+	+	+	+	+	+	+
				80	+	+	+	+	+	+	+	+	+	+	+
				100	+	+	+	+	+	+	+	+	+	+	+
				120	+	+	+	+	+	+	+	+	+	+	+
				140	+	+	+	+	+	+	+	+	+	+	+
Glucose	$C_6H_{12}O_6$	Fp*, 148	all, aqueous	20	+	+	+	+	+	+	+	+	+	+	+
				40	+	+	+	+	+	+	+	+	+	+	+
				60	+	+	+	+	+	+	+	+	+	+	+
				80	+	+	+	+	+	+	+	+	+	+	+
				100	+	+	+	+	+	+	+	+	+	+	+
				120	+	+	+	+	+	+	+	+	+	+	+
				140	+	+	+	+	+	+	+	+	+	+	+
Glycerol	$HO-CH_2-CHOH-CH_2OH$	290	technically pure	20	+	+	+	+	+	+	+	+	+	+	+
				40	+	+	+	+	+	+	+	+	+	+	+
				60	+	+	+	+	+	+	+	+	+	+	+
				80	+	+	+	+	+	+	+	+	+	+	+
				100	+	+	+	+	+	+	+	+	+	+	+
				120	+	+	+	+	+	+	+	+	+	+	+
				140	+	+	+	+	+	+	+	+	+	+	+

(Courtesy George Fischer Engineering Handbook)

Aggressive Media					Chemical Resistance										
Medium	Formula	Boiling point °C	Concentration	Temperature °C	PVC	CPVC	ABS	PE	PP-H	PVDF (STOR®)	EPDM	FRM	NBR	CR	CSM
Glycolic (SpR)	NH ₂ -CH ₂ -COOH	bp. * 233	10%, aqueous	20 40 60 80 100 120 140	+	+	+	+	+	+		+	+	+	+
Glycol	see Ethylene glycol														
Glycolic acid	HO-CH ₂ -COOH	bp. * 80	37%, aqueous	20 40 60 80 100 120 140	+	-	+	+	+	+		+	+	+	+
Heptane (SpR)	C ₇ H ₁₆	98	technically pure	20 40 60 80 100 120 140	+	○	-	+	+	+	-	+	+	+	+
Hexane (SpR)	C ₆ H ₁₄	69	technically pure	20 40 60 80 100 120 140	+	○	-	+	+	+	-	+	+	+	+
Hydrazine hydrate (SpR)	H ₂ N-NH ₂ · H ₂ O	113	aqueous	20 40 60 80 100 120 140	+	-	+	+	+	+	+	○	-	-	+
Hydrobromic acid (SpR)	HBr	124	aqueous, 50%	20 40 60 80 100 120 140	+	+	+	+	+	+	+	+	○	+	+
Hydrochloric acid (Q/E, D/P)	HCl		up to 38%	20 40 60 80 100 120 140	+	+	-	+	○	+	+	+	-	○	+
Hydrochloric acid (Q/E, D/P)	HCl		5%, aqueous	20 40 60 80 100 120 140	+	+	+	+	+	+	+	+	○	○	+

(Courtesy George Fischer Engineering Handbook)

Aggressive Media				Chemical Resistance											
Medium	Formula	Boiling point °C	Concentration	Temperature °C	PVC	CPVC	ABS	PE	PPH	PVDF (GIGEL)	EPDM	FKM	NBR	CR	CSM
Hydrochloric acid (Q/E, D/P)	HCl		10%, aqueous	20 40 60 80 100 120 140	++ O++ +++ +++ +++ +++ +++	+++ +++ +++ +++ +++ +++ +++	++ ++ ++ ++ ++ ++ ++	++ ++ ++ ++ ++ ++ ++	++ ++ ++ ++ ++ ++ ++	++ ++ ++ ++ ++ ++ ++	+++ +++ +++ +++ +++ +++ +++	+++ +++ +++ +++ +++ +++ +++	++ ++ ++ ++ ++ ++ ++	++ ++ ++ ++ ++ ++ ++	++ ++ ++ ++ ++ ++ ++
Hydrochloric acid (Q/E, D/P)	HCl		up to 30%, aqueous	20 40 60 80 100 120 140	++ O++ +++ +++ +++ +++ +++	+++ +++ +++ +++ +++ +++ +++	++ ++ ++ ++ ++ ++ ++	++ ++ ++ ++ ++ ++ ++	++ ++ ++ ++ ++ ++ ++	++ ++ ++ ++ ++ ++ ++	+++ +++ +++ +++ +++ +++ +++	+++ +++ +++ +++ +++ +++ +++	++ ++ ++ ++ ++ ++ ++	++ ++ ++ ++ ++ ++ ++	++ ++ ++ ++ ++ ++ ++
Hydrochloric acid (Q/E, D/P)	HCl		36%, aqueous	20 40 60 80 100 120 140	++ O++ +++ +++ +++ +++ +++	+++ +++ +++ +++ +++ +++ +++	++ ++ ++ ++ ++ ++ ++	++ ++ ++ ++ ++ ++ ++	++ ++ ++ ++ ++ ++ ++	++ ++ ++ ++ ++ ++ ++	+++ +++ +++ +++ +++ +++ +++	+++ +++ +++ +++ +++ +++ +++	++ ++ ++ ++ ++ ++ ++	++ ++ ++ ++ ++ ++ ++	++ ++ ++ ++ ++ ++ ++
Hydrocyanic acid	HCN	26	technically pure	20 40 60 80 100 120 140	++ O++ +++ +++ +++ +++ +++	+++ +++ +++ +++ +++ +++ +++	++ ++ ++ ++ ++ ++ ++	++ ++ ++ ++ ++ ++ ++	++ ++ ++ ++ ++ ++ ++	++ ++ ++ ++ ++ ++ ++	+++ +++ +++ +++ +++ +++ +++	+++ +++ +++ +++ +++ +++ +++	++ ++ ++ ++ ++ ++ ++	++ ++ ++ ++ ++ ++ ++	++ ++ ++ ++ ++ ++ ++
Hydrofluoric acid	HF			20 40 60 80 100 120 140	++ O++ +++ +++ +++ +++ +++	+++ +++ +++ +++ +++ +++ +++	++ ++ ++ ++ ++ ++ ++	++ ++ ++ ++ ++ ++ ++	++ ++ ++ ++ ++ ++ ++	++ ++ ++ ++ ++ ++ ++	++ ++ ++ ++ ++ ++ ++	+++ +++ +++ +++ +++ +++ +++	++ ++ ++ ++ ++ ++ ++	++ ++ ++ ++ ++ ++ ++	++ ++ ++ ++ ++ ++ ++
Hydrogen	H ₂	-253	technically pure	20 40 60 80 100 120 140	++ ++ ++ ++ ++ ++ ++	+++ +++ +++ +++ +++ +++ +++	++ ++ ++ ++ ++ ++ ++	++ ++ ++ ++ ++ ++ ++	++ ++ ++ ++ ++ ++ ++	++ ++ ++ ++ ++ ++ ++	+++ +++ +++ +++ +++ +++ +++	+++ +++ +++ +++ +++ +++ +++	++ ++ ++ ++ ++ ++ ++	++ ++ ++ ++ ++ ++ ++	++ ++ ++ ++ ++ ++ ++
Hydrogen chloride (Q/E)	HCl	-85	technically pure, gaseous	20 40 60 80 100 120 140	++ O++ +++ +++ +++ +++ +++	+++ +++ +++ +++ +++ +++ +++	++ ++ ++ ++ ++ ++ ++	++ ++ ++ ++ ++ ++ ++	++ ++ ++ ++ ++ ++ ++	++ ++ ++ ++ ++ ++ ++	+++ +++ +++ +++ +++ +++ +++	+++ +++ +++ +++ +++ +++ +++	++ ++ ++ ++ ++ ++ ++	++ ++ ++ ++ ++ ++ ++	++ ++ ++ ++ ++ ++ ++
Hydrogen peroxide			70%	20 40 60 80 100 120 140	++ ++ ++ ++ ++ ++ ++	++ ++ ++ ++ ++ ++ ++	++ ++ ++ ++ ++ ++ ++	++ ++ ++ ++ ++ ++ ++	++ ++ ++ ++ ++ ++ ++	++ ++ ++ ++ ++ ++ ++	++ ++ ++ ++ ++ ++ ++	++ ++ ++ ++ ++ ++ ++	++ ++ ++ ++ ++ ++ ++	++ ++ ++ ++ ++ ++ ++	++ ++ ++ ++ ++ ++ ++

(Courtesy George Fischer Engineering Handbook)

Aggressive Media				Chemical Resistance											
Medium	Formula	Boiling point °C	Concentration	Temperature °C	PVC	CPVC	ABS	PE	PP-H	PVDF (S'G'ET)	EPDM	FRM	NBR	CR	CSM
Hydrogen peroxide (SpR8)	H ₂ O ₂		50%, aqueous	20 40 60 80 100 120 140	+	+	-	+	+	O	O	+			
Hydrogen peroxide (SpR8)	H ₂ O ₂		10%, aqueous	20 40 60 80 100 120 140	+	+	-	+	+	O	O	+	O	-	+
Hydrogen peroxide (SpR8)	H ₂ O ₂	139	90%, aqueous	20 40 60 80 100 120 140	+	-	+	-	O		O	-	-	-	O
Hydrogen peroxide (SpR8)	H ₂ O ₂	105	30%, aqueous	20 40 60 80 100 120 140	+	+	-	+	O		O	+	-	-	+
Hydrogen sulphide	H ₂ S		technically pure	20 40 60 80 100 120 140	+	+	+	+	+	+	+	+	+	+	+
Hydrogen sulphide	H ₂ S		saturated, aqueous	20 40 60 80 100 120 140	+	+	+	+	+	+	+	+	+	+	+
Hydroquinone	C ₆ H ₄ /OH ₂		saturated	20 40 60 80 100 120 140	+	+	+	+	+	+	+	+	+	+	+
Hydroxylamine sulfate	see Sodium dithionite			20 40 60 80 100 120 140	+	+	+	+	+	+	+	+	+	+	+

(Courtesy George Fischer Engineering Handbook)

Aggressive Media				Chemical Resistance											
Medium	Formula	Boiling point °C	Concentration	Temperature °C	PVC	CPVC	ABS	PE	PP-H	PVDF (KALGEL)	EPDM	FKM	NBR	CR	CSM
Hydroxylamine sulphate	$(\text{NH}_2\text{OH})_2\text{SO}_4$		oil, aqueous	20 40 60 80 100 120 140	+	+	-	+	+		+	+	+	+	+
Iodine-potassium iodide solution (Lugol's solution)				20 40 60 80 100 120 140	+	-	-			+		+			
Iodine	I_2	185	100%	20 40 60 80 100 120 140	-	-	-			+		+			
Iron (II) -chloride			saturated	20 40 60 80 100 120 140	+	+	+	+	+	+	+	+	+	+	+
Iron (II) -chloride	FeCl_2		saturated	20 40 60 80 100 120 140	+	+	+	+	+	+	+	+	+	+	+
Iron (II) -nitrate	$\text{Fe}(\text{NO}_3)_2$		saturated	20 40 60 80 100 120 140	+	+	+	+	+	+	+	+	+	+	+
Iron (III) -chloride	FeCl_3		saturated	20 40 60 80 100 120 140	+	+	+	+	+	+	+	+	+	+	+
Iron (III) -chloride			saturated	20 40 60 80 100 120 140	+	+	+	+	+	+	+	+	+	+	+

(Courtesy George Fischer Engineering Handbook)

Aggressive Media				Chemical Resistance										
Medium	Formula	Boiling point °C	Concentration	Temperature °C	PVC	CPVC	ABS	PE	PPH	PPH (SYGFI)	EPDM	FPM	NBR	CR
Iron (III) -chloride/sulfate			saturated	20 40 60 80 100 120 140	++ ++ ++ ++ ++ ++ ++	++ ++ ++ ++ ++ ++ ++	++ ++ ++ ++ ++ ++ ++	++ ++ ++ ++ ++ ++ ++	++ ++ ++ ++ ++ ++ ++	++ ++ ++ ++ ++ ++ ++	++ ++ ++ ++ ++ ++ ++	++ ++ ++ ++ ++ ++ ++	++ ++ ++ ++ ++ ++ ++	++ ++ ++ ++ ++ ++ ++
Iron (III) -nitrate			saturated	20 40 60 80 100 120 140	++ ++ ++ ++ ++ ++ ++	++ ++ ++ ++ ++ ++ ++	++ ++ ++ ++ ++ ++ ++	++ ++ ++ ++ ++ ++ ++	++ ++ ++ ++ ++ ++ ++	++ ++ ++ ++ ++ ++ ++	++ ++ ++ ++ ++ ++ ++	++ ++ ++ ++ ++ ++ ++	++ ++ ++ ++ ++ ++ ++	++ ++ ++ ++ ++ ++ ++
Iron (III) -nitrate	$Fe(NO_3)_3$		saturated	20 40 60 80 100 120 140	++ ++ ++ ++ ++ ++ ++	++ ++ ++ ++ ++ ++ ++	++ ++ ++ ++ ++ ++ ++	++ ++ ++ ++ ++ ++ ++	++ ++ ++ ++ ++ ++ ++	++ ++ ++ ++ ++ ++ ++	++ ++ ++ ++ ++ ++ ++	++ ++ ++ ++ ++ ++ ++	++ ++ ++ ++ ++ ++ ++	++ ++ ++ ++ ++ ++ ++
Iron (III) -sulfate	$Fe_2(SO_4)_3$		saturated	20 40 60 80 100 120 140	++ ++ ++ ++ ++ ++ ++	++ ++ ++ ++ ++ ++ ++	++ ++ ++ ++ ++ ++ ++	++ ++ ++ ++ ++ ++ ++	++ ++ ++ ++ ++ ++ ++	++ ++ ++ ++ ++ ++ ++	++ ++ ++ ++ ++ ++ ++	++ ++ ++ ++ ++ ++ ++	++ ++ ++ ++ ++ ++ ++	++ ++ ++ ++ ++ ++ ++
Iron (III) -sulfate			saturated	20 40 60 80 100 120 140	++ ++ ++ ++ ++ ++ ++	++ ++ ++ ++ ++ ++ ++	++ ++ ++ ++ ++ ++ ++	++ ++ ++ ++ ++ ++ ++	++ ++ ++ ++ ++ ++ ++	++ ++ ++ ++ ++ ++ ++	++ ++ ++ ++ ++ ++ ++	++ ++ ++ ++ ++ ++ ++	++ ++ ++ ++ ++ ++ ++	++ ++ ++ ++ ++ ++ ++
Iron (III) -nitrate	$Fe(NO_3)_3$		saturated	20 40 60 80 100 120 140	++ ++ ++ ++ ++ ++ ++	++ ++ ++ ++ ++ ++ ++	++ ++ ++ ++ ++ ++ ++	++ ++ ++ ++ ++ ++ ++	++ ++ ++ ++ ++ ++ ++	++ ++ ++ ++ ++ ++ ++	++ ++ ++ ++ ++ ++ ++	++ ++ ++ ++ ++ ++ ++	++ ++ ++ ++ ++ ++ ++	++ ++ ++ ++ ++ ++ ++
Iron (III) -sulfate	$FeSO_4$		saturated	20 40 60 80 100 120 140	++ ++ ++ ++ ++ ++ ++	++ ++ ++ ++ ++ ++ ++	++ ++ ++ ++ ++ ++ ++	++ ++ ++ ++ ++ ++ ++	++ ++ ++ ++ ++ ++ ++	++ ++ ++ ++ ++ ++ ++	++ ++ ++ ++ ++ ++ ++	++ ++ ++ ++ ++ ++ ++	++ ++ ++ ++ ++ ++ ++	++ ++ ++ ++ ++ ++ ++
Iron (III) -sulfate			saturated	20 40 60 80 100 120 140	++ ++ ++ ++ ++ ++ ++	++ ++ ++ ++ ++ ++ ++	++ ++ ++ ++ ++ ++ ++	++ ++ ++ ++ ++ ++ ++	++ ++ ++ ++ ++ ++ ++	++ ++ ++ ++ ++ ++ ++	++ ++ ++ ++ ++ ++ ++	++ ++ ++ ++ ++ ++ ++	++ ++ ++ ++ ++ ++ ++	++ ++ ++ ++ ++ ++ ++

(Courtesy George Fischer Engineering Handbook)

Aggressive Media				Chemical Resistance											
Medium	Formula	Boiling point °C	Concentration	Temperature °C	PVC	CPVC	ABS	PE	PP-H	PVDF (SUS316)	EPDM	FPM	NBR	CR	CSM
Iron salts			oil, aqueous	20	+	+	+	+	+	+	+	+	+	+	+
				40	+	+	+	+	+	+	+	+	+	+	+
				60	+	+	+	+	+	+	+	+	+	+	+
				80	+	+	+	+	+	+	+	+	+	+	+
				100	+	+	+	+	+	+	+	+	+	+	+
				120	+	+	+	+	+	+	+	+	+	+	+
				140	+	+	+	+	+	+	+	+	+	+	+
Isobutene (SpRt)	$(CH_3)_2C=CH-CH_2CH_3$	99	technically pure	20	+	-	+	+	+	+	+	+	+	+	+
				40	+	-	+	+	+	+	+	+	+	+	+
				60	+	+	+	+	+	+	+	+	+	+	+
				80	+	+	+	+	+	+	+	+	+	+	+
				100	+	+	+	+	+	+	+	+	+	+	+
				120	+	+	+	+	+	+	+	+	+	+	+
				140	+	+	+	+	+	+	+	+	+	+	+
Isophorone (SpRt)	$C_{14}H_{28}O$		technically pure	20	+	-	+	+	+	+	+	+	+	+	+
				40	+	-	+	+	+	+	+	+	+	+	+
				60	+	+	+	+	+	+	+	+	+	+	+
				80	+	+	+	+	+	+	+	+	+	+	+
				100	+	+	+	+	+	+	+	+	+	+	+
				120	+	+	+	+	+	+	+	+	+	+	+
				140	+	+	+	+	+	+	+	+	+	+	+
Isopropyl alcohol (SpRt)	$(CH_3)_2CH-OH$	82	technically pure	20	+	-	+	+	+	+	+	+	+	+	+
				40	+	-	+	+	+	+	+	+	+	+	+
				60	+	+	+	+	+	+	+	+	+	+	+
				80	+	+	+	+	+	+	+	+	+	+	+
				100	+	+	+	+	+	+	+	+	+	+	+
				120	+	+	+	+	+	+	+	+	+	+	+
				140	+	+	+	+	+	+	+	+	+	+	+
Isopropyl ether	$(CH_3)_2CH-O-CH_2CH_3$	68	technically pure	20	-	-	+	+	+	+	+	+	+	+	+
				40	-	-	+	+	+	+	+	+	+	+	+
				60	-	-	+	+	+	+	+	+	+	+	+
				80	-	-	+	+	+	+	+	+	+	+	+
				100	-	-	+	+	+	+	+	+	+	+	+
				120	-	-	+	+	+	+	+	+	+	+	+
				140	-	-	+	+	+	+	+	+	+	+	+
Isopropylbenzene				20	-	-	+	+	+	+	+	+	+	+	+
				40	-	-	+	+	+	+	+	+	+	+	+
				60	-	-	+	+	+	+	+	+	+	+	+
				80	-	-	+	+	+	+	+	+	+	+	+
				100	-	-	+	+	+	+	+	+	+	+	+
				120	-	-	+	+	+	+	+	+	+	+	+
				140	-	-	+	+	+	+	+	+	+	+	+
Isopropylaldehyde				20	+	+	+	+	+	+	+	+	+	+	+
				40	+	+	+	+	+	+	+	+	+	+	+
				60	+	+	+	+	+	+	+	+	+	+	+
				80	+	+	+	+	+	+	+	+	+	+	+
				100	+	+	+	+	+	+	+	+	+	+	+
				120	+	+	+	+	+	+	+	+	+	+	+
				140	+	+	+	+	+	+	+	+	+	+	+
Lactic acid (SpRt)	$CH_3CH(OH)COOH$		10%, aqueous	20	+	+	+	+	+	+	+	+	+	+	+
				40	+	+	+	+	+	+	+	+	+	+	+
				60	+	+	+	+	+	+	+	+	+	+	+
				80	+	+	+	+	+	+	+	+	+	+	+
				100	+	+	+	+	+	+	+	+	+	+	+
				120	+	+	+	+	+	+	+	+	+	+	+
				140	+	+	+	+	+	+	+	+	+	+	+

(Courtesy George Fischer Engineering Handbook)

Aggressive Media					Chemical Resistance										
Medium	Formula	Boiling point °C	Concentration	Temperature °C	PVC	CPVC	ABS	PE	PPH	PVDF (STGEM)	EPDM	FRM	NBR	CR	CSM
lanolin (Sp88)			technically pure	20 40 60 80 100 120 140	O +	+	++	++	++	++		++	++	++	O
lead acetate	Pb(CH ₃ COO) ₂		aqueous, saturated	20 40 60 80 100 120 140	++	++	++	++	++	++	++	++	++	++	++
lead salts	PbCl ₂ , Pb(NO ₃) ₂ , PbSO ₄		saturated	20 40 60 80 100 120 140		+	++								
lead carbonate				20 40 60 80 100 120 140	+	+		+	+	+	+				
lead nitrate	Pb(NO ₃) ₂			20 40 60 80 100 120 140		++	++								
lead nitrate				20 40 60 80 100 120 140	++	++				++					
lead tetrafluoroborate				20 40 60 80 100 120 140						++					
linoleic acid				20 40 60 80 100 120 140						++					

(Courtesy George Fischer Engineering Handbook)

Aggressive Media				Chemical Resistance											
Medium	Formula	Boiling point °C	Concentration	Temperature °C	PVC	CPVC	ABS	PE	PP-H	PVDF (KIGEL)	EPDM	FKM	NBR	CR	CSM
Unseed oil (SpRB)			technically pure	20	+	+	+	+	+	+					
				40	+	+	+	+	+	+					
				60	+	+	+	+	+	+					
				80	+	+	+	+	+	+					
				100	+	+	+	+	+	+					
				120	+	+	+	+	+	+					
				140	+	+	+	+	+	+					
Liquors				20	+	+	+	+	+	+	+	+	+	+	+
				40	+	+	+	+	+	+	+	+	+	+	+
				60	+	+	+	+	+	+	+	+	+	+	+
				80	+	+	+	+	+	+	+	+	+	+	+
				100	+	+	+	+	+	+	+	+	+	+	+
				120	+	+	+	+	+	+	+	+	+	+	+
				140	+	+	+	+	+	+	+	+	+	+	+
Liquid fertilizers				20	+	+	+	+	+	+	+	+	+	+	+
				40	+	+	+	+	+	+	+	+	+	+	+
				60	+	+	+	+	+	+	+	+	+	+	+
				80	+	+	+	+	+	+	+	+	+	+	+
				100	+	+	+	+	+	+	+	+	+	+	+
				120	+	+	+	+	+	+	+	+	+	+	+
				140	+	+	+	+	+	+	+	+	+	+	+
Lithiumbromide	LiBr			20	+	+	+	+	+	+	+	+	+	+	+
				40	+	+	+	+	+	+	+	+	+	+	+
				60	+	+	+	+	+	+	+	+	+	+	+
				80	+	+	+	+	+	+	+	+	+	+	+
				100	+	+	+	+	+	+	+	+	+	+	+
				120	+	+	+	+	+	+	+	+	+	+	+
				140	+	+	+	+	+	+	+	+	+	+	+
Lithiumsulfate				20	+	+	+	+	+	+	+	+	+	+	+
				40	+	+	+	+	+	+	+	+	+	+	+
				60	+	+	+	+	+	+	+	+	+	+	+
				80	+	+	+	+	+	+	+	+	+	+	+
				100	+	+	+	+	+	+	+	+	+	+	+
				120	+	+	+	+	+	+	+	+	+	+	+
				140	+	+	+	+	+	+	+	+	+	+	+
Lubricating oils				20	+	+	+	+	+	+	+	+	+	+	+
				40	+	+	+	+	+	+	+	+	+	+	+
				60	+	+	+	+	+	+	+	+	+	+	+
				80	+	+	+	+	+	+	+	+	+	+	+
				100	+	+	+	+	+	+	+	+	+	+	+
				120	+	+	+	+	+	+	+	+	+	+	+
				140	+	+	+	+	+	+	+	+	+	+	+
Magnesium salts	MgCl ₂ , MgCO ₃ , Mg(NO ₃) ₂ , Mg(OH) ₂ , MgSO ₄		all, aqueous, saturated	20	+	+	+	+	+	+	+	+	+	+	+
				40	+	+	+	+	+	+	+	+	+	+	+
				60	+	+	+	+	+	+	+	+	+	+	+
				80	+	+	+	+	+	+	+	+	+	+	+
				100	+	+	+	+	+	+	+	+	+	+	+
				120	+	+	+	+	+	+	+	+	+	+	+
				140	+	+	+	+	+	+	+	+	+	+	+
Magnesiumhydrogen- carbonate				20	+	+	+	+	+	+	+	+	+	+	+
				40	+	+	+	+	+	+	+	+	+	+	+
				60	+	+	+	+	+	+	+	+	+	+	+
				80	+	+	+	+	+	+	+	+	+	+	+
				100	+	+	+	+	+	+	+	+	+	+	+
				120	+	+	+	+	+	+	+	+	+	+	+
				140	+	+	+	+	+	+	+	+	+	+	+

(Courtesy George Fischer Engineering Handbook)

Aggressive Media				Chemical Resistance											
Medium	Formula	Boiling point °C	Concentration	Temperature °C	PVC	CPVC	ABS	PE	PAH	PVDF (STGEI)	EPDM	FRM	NBR	CR	CSM
Maleic acid (5pRBI)	ICH-COOH ₂	Fp. +131	cold saturated, aqueous	20 40 60 80 100 120 140	+	+	+	+	+	+					
Media water or similar media				20 40 60 80 100 120 140	+	+	+	+	+	+					
Mercury	Hg	357	pure	20 40 60 80 100 120 140	+	+	+	+	+	+	+	+	+	+	+
Mercury III -chloride	HgCl ₂			20 40 60 80 100 120 140	+	+	+	+	+	+	+	+	+	+	+
Mercury III -cyanide	Hg(CNI) ₂			20 40 60 80 100 120 140	+	+	+	+	+	+	+	+	+	+	+
Mercury III -cyanide	Hg(INO) ₃			20 40 60 80 100 120 140	+	+	+	+	+	+	+	+	+	+	+
Mercury III -sulfate				20 40 60 80 100 120 140	+	+	+	+	+	+	+	+	+	+	+
Mercury salts	HgNO ₃ , Hg Cl ₂ , Hg(CNI) ₂		cold saturated, aqueous	20 40 60 80 100 120 140	+	+	+	+	+	+	+	+	+	+	+
Methane	see natural gas	-161	technically pure												

(Courtesy George Fischer Engineering Handbook)

Aggressive Media					Chemical Resistance										
Medium	Formula	Boiling point °C	Concentration	Temperature °C	PVC	CPVC	ABS	PE	PP-H	PVCB (SYGEB)	EPDM	FFM	NBR	CR	CSMA
Methanol (SPBI)	CH ₃ OH	65	all	20 40 60 80 100 120 140	O + +	-	-	+ + +	+ + +	- O +	+ + +	O O O	+ + +	O + +	+ + +
Methyl acetate	CH ₃ COOCH ₃	56	technically pure	20 40 60 80 100 120 140	-	-	-	+	O + +	O +	-	-	-	-	-
Methyl amine	CH ₃ NH ₂	-6	32%, aqueous	20 40 60 80 100 120 140	O	-	-	+	+	O	-	+	-	+	+
Methyl bromide	CH ₃ Br	4	technically pure	20 40 60 80 100 120 140	-	-	-	O	-	+ + +	-	O	-	-	O
Methyl chloride	CH ₃ Cl	-24	technically pure	20 40 60 80 100 120 140	-	-	-	O	-	+ + +	-	-	-	-	-
Methyl ethyl ketone	CH ₃ COC ₂ H ₅	80	technically pure	20 40 60 80 100 120 140	-	-	-	O + +	O O +	-	-	-	-	-	-
Methylene chloride	CH ₂ Cl ₂	40	technically pure	20 40 60 80 100 120 140	-	-	-	O	O	O O +	-	O	-	-	-
Methylisobutylketone	C ₆ H ₁₂ O			20 40 60 80 100 120 140	-	-	-	-	-	-	-	-	-	-	-

(Courtesy George Fischer Engineering Handbook)

Aggressive Media				Chemical Resistance											
Medium	Formula	Boiling point °C	Concentration	Temperature °C	PVC	CPVC	ABS	PE	PP-H	PVDF (SAGEF)	EPDM	FKM	NBR	CR	CSM
Methylmethacrylate	C ₅ H ₈ O ₂			20	+	+	+								
				40											
				60											
				80											
				100											
				120											
				140											
Methylphenylketone (Acetophenone)	C ₉ H ₁₀ O			20	-	-	-								
				40											
				60											
				80											
				100											
				120											
				140											
Milk (5p8)				20	+	+	+	+	+	+		+	+	+	+
				40	+	+	+	+	+	+					
				60	+	+	+	+	+	+					
				80	+	+	+	+	+	+					
				100	+	+	+	+	+	+					
				120	+	+	+	+	+	+					
				140	+	+	+	+	+	+					
Mineral oils, free of aromatics				20	+	+	-	+	+	+		+	+	○	○
				40	+	+	-	+	+	+		+	+	+	+
				60	+	+	-	○	○	+		+	+	+	+
				80	+	+	-	○	+	+		+	+	+	+
				100	+	+	-	+	+	+		+	+	+	+
				120	+	+	-	+	+	+		+	+	+	+
				140	+	+	-	+	+	+		+	+	+	+
Mineral water				20	+	+	+	+	+	+	+	+	+	+	+
				40	+	+	+	+	+	+	+	+	+	+	+
				60	+	+	+	+	+	+	+	+	+	+	+
				80	+	+	+	+	+	+	+	+	+	+	+
				100	+	+	+	+	+	+	+	+	+	+	+
				120	+	+	+	+	+	+	+	+	+	+	+
				140	+	+	+	+	+	+	+	+	+	+	+
Mixed acids - nitric - hydrofluoric - sulphuric	15% HNO ₃ 15% HF 18% H ₂ SO ₄		3 parts 1 part 2 parts	20	○	○	-	○	-	+		+	-	+	+
				40						+		+			+
				60						+		○			○
				80											
				100											
				120											
				140											
Mixed acids - sulphuric - nitric - water	H ₂ SO ₄ HNO ₃ H ₂ O		48% 49% 43%	20	+	+	-	-	-	+		-	-	-	-
				40	○	○									
				60	-	-									
				80											
				100											
				120											
				140											
Mixed acids - sulphuric - nitric - water	H ₂ SO ₄ HNO ₃ H ₂ O		50% 50% 40%	20	○	○	-	-	-	+		-	-	-	-
				40	-	-									
				60											
				80											
				100											
				120											
				140											

(Courtesy George Fischer Engineering Handbook)

Aggressive Media				Chemical Resistance											
Medium	Formula	Boiling point °C	Concentration	Temperature °C	PVC	CHC	ABS	PE	PPH	PMDI (STYREN)	EPDM	FRM	NBR	CR	CSM
Mixed acids - sulphuric - nitric - water	H_2SO_4 HNO_3 H_2O		10% 87% 43%	20	O	O	-	-	-	O		-	-	-	-
				40											
				60											
				80											
				100											
				120											
				140											
Mixed acids - sulphuric - nitric - water	H_2SO_4 HNO_3 H_2O		50% 33% 17%	20	+	+	-	-	-	+		+	-	-	O
				40	O	+									
				60											
				80											
				100											
				120											
				140											
Mixed acids - sulphuric - nitric - water	H_2SO_4 HNO_3 H_2O		10% 20% 70%	20	+	+	-	O	-	+		+	-	O	+
				40	+					+		+			
				60						+					
				80						+					
				100											
				120											
				140											
Mixed acids - sulphuric - nitric - water	H_2SO_4 HNO_3 H_2O		50% 31% 19%	20	+	-	-	-	+			+	-	O	O
				40											
				60											
				80											
				100											
				120											
				140											
Mixed acids - sulphuric - phosphoric - phosphoric	H_2SO_4 H_3PO_4 H_2O		30% 60% 10%	20	+	+	-	+	+	+		+	-	+	+
				40	+	+		O	O	+		+		O	O
				60	+										
				80											
				100											
				120											
				140											
Molasses				20	+	+	+	+	+	+		+	+	+	+
				40	+	+	+	+	+	+		+	+	+	+
				60	O	+	+	+	+	+		+	+	+	+
				80	+							+	+	+	+
				100								+	+	+	+
				120											
				140											
Molasses wort				20	+	+	+	+	+	+		+	+	+	+
				40	+	+	+	+	+	+		+	+	+	+
				60	+	+	+	+	+	+		+	+	+	+
				80								+	+	+	+
				100											
				120											
				140											
Monochloroacetic acid ethyl ester	$ClCH_2COOC_2H_5$	144	technically pure	20	-	-	-	+	+	O		O	-	-	-
				40				+	+						
				60				+	+						
				80				+	+						
				100											
				120											
				140											

(Courtesy George Fischer Engineering Handbook)

Aggressive Media				Chemical Resistance											
Medium	Formula	Boiling point °C	Concentration	Temperature °C	PVC	CPVC	ABS	PE	PP-H	PVDF (STGEEI)	EPDM	FFM	NBR	CR	CSM
Morpholine	C ₄ H ₉ NO	129	technically pure	20 40 60 80 100 120 140	-	-	-	+	+	+		+	-	O	O
Mowlin D			usual commercial	20 40 60 80 100 120 140	+	+		+	+	+		+	+	+	+
Naphthalene		218	technically pure	20 40 60 80 100 120 140	-	-	-	+	+	+	-	+	+	-	O
Sodiumhydrogensulfite	NaHSO ₃			20 40 60 80 100 120 140	+	+		+	+	+	+	+			
Sodiumsulfate				20 40 60 80 100 120 140	+	+	+	+	+	+	+	+			
Sodiumtetraborate (Borax)				20 40 60 80 100 120 140	+	+	+	+	+	+	+	+			
Nickel salts	10CH ₃ COO(2)Ni, NiCl ₂ , Ni(NO ₃) ₂ , Ni SO ₄		cold saturated, aqueous	20 40 60 80 100 120 140	+	+	+	+	+	+	+	+	+	+	+
Nitrolic acid	H ₂ SO ₄ HNO ₃ H ₂ O	65% 15%	20%	20 40 60 80 100 120 140	O	+	+	+	+	+		+	+	+	+

(Courtesy George Fischer Engineering Handbook)

Aggressive Media				Chemical Resistance											
Medium	Formula	Boiling point °C	Concentration	Temperature °C	PVC	CPVC	ABS	PE	PP-H	PVDF (KRYL)	EPDM	FM	NBR	CR	CSM
Nitric acid (SpR)	HNO ₃			20 40 60 80 100 120 140	++ ++ ++ ++ ++ ++ ++	++ ++ ++ ++ ++ ++ ++	++ ++ ++ ++ ++ ++ ++	++ ++ ++ ++ ++ ++ ++	++ ++ ++ ++ ++ ++ ++	++ ++ ++ ++ ++ ++ ++	++ ++ ++ ++ ++ ++ ++	++ ++ ++ ++ ++ ++ ++	++ ++ ++ ++ ++ ++ ++	++ ++ ++ ++ ++ ++ ++	++ ++ ++ ++ ++ ++ ++
Nitric acid (SpR)	HNO ₃			20 40 60 80 100 120 140	++ ++ ++ ++ ++ ++ ++	++ ++ ++ ++ ++ ++ ++	++ ++ ++ ++ ++ ++ ++	++ ++ ++ ++ ++ ++ ++	++ ++ ++ ++ ++ ++ ++	++ ++ ++ ++ ++ ++ ++	++ ++ ++ ++ ++ ++ ++	++ ++ ++ ++ ++ ++ ++	++ ++ ++ ++ ++ ++ ++	++ ++ ++ ++ ++ ++ ++	++ ++ ++ ++ ++ ++ ++
Nitric acid up to 55% (SpR)				20 40 60 80 100 120 140	++ ++ ++ ++ ++ ++ ++	++ ++ ++ ++ ++ ++ ++	++ ++ ++ ++ ++ ++ ++	++ ++ ++ ++ ++ ++ ++	++ ++ ++ ++ ++ ++ ++	++ ++ ++ ++ ++ ++ ++	++ ++ ++ ++ ++ ++ ++	++ ++ ++ ++ ++ ++ ++	++ ++ ++ ++ ++ ++ ++	++ ++ ++ ++ ++ ++ ++	++ ++ ++ ++ ++ ++ ++
Nitric acid (see note 2.3.1 on joining) (SpR)	see Salpêtre		6.3%, aqueous												
Nitric acid (see note 2.3.1 on joining) (SpR)	see Salpêtre		up to 40%, aqueous												
Nitric acid (see note 2.3.1 on joining) (SpR)	see Salpêtre		65%, aqueous												
Nitric acid (see note 2.3.1 on joining) (SpR)	see Salpêtre		100%												
Nitric acid (see note 2.3.1 on joining) (SpR)	see Salpêtre		85%												
Nitric oxide	see Nitrous gases														
Nitroacetic acid	NC(=O)COOH			20 40 60 80 100 120 140				++ ++ ++ ++ ++ ++ ++	++ ++ ++ ++ ++ ++ ++		++ ++ ++ ++ ++ ++ ++				
Nitrobenzene	C ₆ H ₅ -NO ₂	209	technically pure	20 40 60 80 100 120 140	- - - - - - -	- - - - - - -	- - - - - - -	++ ++ ++ ++ ++ ++ ++	++ ++ ++ ++ ++ ++ ++	++ ++ ++ ++ ++ ++ ++	- - - - - - -	++ ++ ++ ++ ++ ++ ++	- - - - - - -	- - - - - - -	- - - - - - -

(Courtesy George Fischer Engineering Handbook)

Aggressive Media					Chemical Resistance										
Medium	Formula	Boiling point °C	Concentration	Temperature °C	PVC	CPVC	ABS	PE	PP-H	PVDF (STYGE)	EPDM	FRM	NBR	CR	CSM
Nitrotoluene (o-, m-, p-)		222-238	technically pure	20 40 60 80 100 120 140	-	-	-	O +	O +	O + + + +	-	O	O	-	-
Nitrous acid	HNO ₂			20 40 60 80 100 120 140	+	+	-	+	-	+	+	+	-	-	-
Nitrous gases	see Nitric oxide		diluted, moist, anhydrous	20 40 60 80 100 120 140	-	-	-	-	-	-	-	-	-	-	-
N-Methylpyrrolidone				20 40 60 80 100 120 140	-	-	-	-	-	-	-	-	-	-	-
N,N-Dimethylaniline	C ₆ H ₅ N(CH ₃) ₂		technically pure	20 40 60 80 100 120 140	-	-	-	+	+	-	+	-	-	-	-
n-Pentylacetate				20 40 60 80 100 120 140	-	-	-	-	-	-	-	-	-	-	-
Oleic acid (SpRl)	C ₁₇ H ₃₃ COOH		technically pure	20 40 60 80 100 120 140	+	O	-	+	+	+	-	O	O	-	-
Oleum (SpRl)	H ₂ SO ₄ +SO ₃		10% SO ₃	20 40 60 80 100 120 140	-	-	-	-	-	-	-	-	-	-	-
Oleum vapours (SpRl)			traces	20 40 60 80 100 120 140	+	-	-	-	-	-	-	+	-	-	O

(Courtesy George Fischer Engineering Handbook)

Aggressive Media					Chemical Resistance										
Medium	Formula	Boiling point °C	Concentration	Temperature °C	PVC	CPVC	ABS	PE	PP-H	PVC (STYGEN)	EPDM	FRM	NBR	CR	CSM
Olive oil (SpR)				20	+	-	-				-				
				40	+										
				60	+			O	+	+		+	+	+	
				80	+				+	+		+	+	+	
				100	+				+	+					
				120											
				140											
Oxalic acid (SpR)	$\text{H}_2\text{C}_2\text{O}_4$		cold saturated, aqueous	20	+	+	+	+	+	+	+				
				40	+	+	+	+	+	+					
				60	+	+	+	+	+	+					
				80		O	+	+	+	+					
				100											
				120											
				140											
Oxygen	O_2		technically pure	20	+	+	+	+	+	+					
				40	+	+	+	+	+	+					
				60	+		+	O	+	+					
				80											
				100											
				120											
				140											
Ozone (SpR)	O_3		up to 2%, in air	20	+	+	-	O	+	O					
				40											
				60											
				80											
				100											
				120											
				140											
Ozone (SpR)	O_3		cold saturated, aqueous	20	+	+	-	O	+	O					
				40	+										
				60											
				80											
				100											
				120											
				140											
Palm oil, palm nut oil (SpR)				20	+	O	+	+	+	+					
				40	-			+	+	+					
				60				O	+	+					
				80					+	+					
				100											
				120											
				140											
Palmitic acid (SpR)	$\text{C}_{15}\text{H}_{31}\text{COOH}$	390	technically pure	20	+	-	+	O	+	+					
				40											
				60											
				80											
				100											
				120											
				140											
Paraffin emulsions			usual commercial, aqueous	20	+	+	O	+	+	+					
				40	+	+		+	+	+					
				60			O	O	+	+					
				80					+	+					
				100											
				120											
				140											

(Courtesy George Fischer Engineering Handbook)

Aggressive Media				Chemical Resistance												
Medium	Formula	Boiling point °C	Concentration	Temperature °C	PVC	CPVC	ABS	PE	PPH	PVDF (STGEM)	EPDM	FRM	NBR	CR	CSM	
Paraffin oil				20 40 60 80 100 120 140	++ ++ ++ ++ ++ ++ ++	+	+	+	+	+	-	++ ++ ++ ++ ++ ++ ++	++ ++ ++ ++ ++ ++ ++	++ ++ ++ ++ ++ ++ ++	++ ++ ++ ++ ++ ++ ++	
p-Dibromo benzene	C ₆ H ₃ Br ₂		technically pure	20 40 60 80 100 120 140	-	-	-	+	+	+	-	+	-	-	-	
Perchloroethylene (tetrachloroethylene)	Cl ₂ C=CCl ₂	121	technically pure	20 40 60 80 100 120 140	-	-	-	+	+	+	-	+	+	-	-	
Perchloric acid (SpR)	HClO ₄		10% aqueous	20 40 60 80 100 120 140	++ ++ ++ ++ ++ ++ ++	+	+	+	+	+	+	+	-	+		
Perchloric acid (SpR)			70% aqueous	20 40 60 80 100 120 140	+	+	-	+	+	+	-	+	+	-	+	
Petroleum			technically pure	20 40 60 80 100 120 140	+	-	-	+	+	+	-	+	+	+	-	
Petroleum ether (SpR)		40-70	technically pure	20 40 60 80 100 120 140	++ ++ ++ ++ ++ ++ ++	-	-	++ ++ ++ ++ ++ ++ ++	++ ++ ++ ++ ++ ++ ++	++ ++ ++ ++ ++ ++ ++	-	++ ++ ++ ++ ++ ++ ++	++ ++ ++ ++ ++ ++ ++	++ ++ ++ ++ ++ ++ ++	++ ++ ++ ++ ++ ++ ++	++ ++ ++ ++ ++ ++ ++
Phenol (SpR)	C ₆ H ₅ -OH	182	up to 10%, aqueous	20 40 60 80 100 120 140	++ ++ ++ ++ ++ ++ ++	+	+	++ ++ ++ ++ ++ ++ ++	++ ++ ++ ++ ++ ++ ++	++ ++ ++ ++ ++ ++ ++	++ ++ ++ ++ ++ ++ ++	++ ++ ++ ++ ++ ++ ++	++ ++ ++ ++ ++ ++ ++	++ ++ ++ ++ ++ ++ ++	++ ++ ++ ++ ++ ++ ++	

(Courtesy George Fischer Engineering Handbook)

Aggressive Media					Chemical Resistance										
Medium	Formula	Boiling point °C	Concentration	Temperature °C	PVC	CPVC	ABS	PE	PPH	PVDF (STYGEN)	EPDM	PPM	NBR	CR	CSM
Phenol (SpRl)			up to 5%	20 40 60 80 100 120 140	+	+	-	+	+	+	O	+	+	-	-
Phenol (SpRl)	C_6H_5OH		up to 90%, aqueous	20 40 60 80 100 120 140	O	-	-	O	+	O	-	O	-	O	-
Phenylhydrazine	$C_6H_5NH-NH_2$	243	technically pure	20 40 60 80 100 120 140	-	-	-	O	O	O	-	+	-	-	-
Phenylhydrazine hydrochloride	$C_6H_5NH-NH_2HCl$		aqueous	20 40 60 80 100 120 140	O	O	-	O	+	+	O	+	O	O	+
Phosgene (SpRl)	$COCl_2$	8	liquid, technically pure	20 40 60 80 100 120 140	-	-	-	-	-	-	-	+	O	+	+
Phosgene (SpRl)			gaseous, technically pure	20 40 60 80 100 120 140	+	O	-	O	O	+	+	+	+	+	O
Phosphate disodium	see disodiumphosphate		saturated												
Phosphoric acid	H_3PO_4		up to 30%, aqueous	20 40 60 80 100 120 140	+	+	+	+	+	+	+	+	O	+	+
Phosphoric acid			50%, aqueous	20 40 60 80 100 120 140	+	+	+	+	+	+	O	+	O	+	+

(Courtesy George Fischer Engineering Handbook)

Aggressive Media				Chemical Resistance											
Medium	Formula	Boiling point °C	Concentration	Temperature °C	PVC	CPVC	ABS	PE	PP-H	PVDF (GYGEH)	EPDM	FPM	NBR	CR	CSM
Phosphoric acid			85%, aqueous	20 40 60 80 100 120 140	++ ++ ++ ++ ++ ++ ++	++ ++ ++ ++ ++ ++ ++	++ ++ ++ ++ ++ ++ ++	++ ++ ++ ++ ++ ++ ++	++ ++ ++ ++ ++ ++ ++	++ ++ ++ ++ ++ ++ ++	++ ++ ++ ++ ++ ++ ++	++ ++ ++ ++ ++ ++ ++	++ ++ ++ ++ ++ ++ ++	++ ++ ++ ++ ++ ++ ++	++ ++ ++ ++ ++ ++ ++
Phosphoric acid	H ₃ PO ₄			20 40 60 80 100 120 140	++ ++ ++ ++ ++ ++ ++	++ ++ ++ ++ ++ ++ ++	++ ++ ++ ++ ++ ++ ++	++ ++ ++ ++ ++ ++ ++	++ ++ ++ ++ ++ ++ ++	++ ++ ++ ++ ++ ++ ++	++ ++ ++ ++ ++ ++ ++	++ ++ ++ ++ ++ ++ ++	++ ++ ++ ++ ++ ++ ++	++ ++ ++ ++ ++ ++ ++	++ ++ ++ ++ ++ ++ ++
Phosphoric acid	H ₃ PO ₄			20 40 60 80 100 120 140	++ ++ ++ ++ ++ ++ ++	++ ++ ++ ++ ++ ++ ++	++ ++ ++ ++ ++ ++ ++	++ ++ ++ ++ ++ ++ ++	++ ++ ++ ++ ++ ++ ++	++ ++ ++ ++ ++ ++ ++	++ ++ ++ ++ ++ ++ ++	++ ++ ++ ++ ++ ++ ++	++ ++ ++ ++ ++ ++ ++	++ ++ ++ ++ ++ ++ ++	++ ++ ++ ++ ++ ++ ++
Phosphoric acid tributyl ester	(H ₂ C ₄ O) ₃ P=O			20 40 60 80 100 120 140	- - - - - - -	- - - - - - -	- - - - - - -	++ ++ ++ ++ ++ ++ ++	++ ++ ++ ++ ++ ++ ++	++ ++ ++ ++ ++ ++ ++	++ ++ ++ ++ ++ ++ ++	++ ++ ++ ++ ++ ++ ++	++ ++ ++ ++ ++ ++ ++	++ ++ ++ ++ ++ ++ ++	++ ++ ++ ++ ++ ++ ++
Phosphorus chlorides: - Phosphorus trichloride - Phosphorus pentachloride - Phosphorus oxychloride (SpRBI)	PCl ₃ PCl ₅ POCl ₃	175 162 105	technically pure	20 40 60 80 100 120 140	- - - - - - -	- - - - - - -	++ ++ ++ ++ ++ ++ ++	++ ++ ++ ++ ++ ++ ++	++ ++ ++ ++ ++ ++ ++	++ ++ ++ ++ ++ ++ ++	++ ++ ++ ++ ++ ++ ++	++ ++ ++ ++ ++ ++ ++	++ ++ ++ ++ ++ ++ ++	++ ++ ++ ++ ++ ++ ++	++ ++ ++ ++ ++ ++ ++
Photographic developer (SpRBI)			usual commercial	20 40 60 80 100 120 140	++ ++ ++ ++ ++ ++ ++	++ ++ ++ ++ ++ ++ ++	++ ++ ++ ++ ++ ++ ++	++ ++ ++ ++ ++ ++ ++	++ ++ ++ ++ ++ ++ ++	++ ++ ++ ++ ++ ++ ++	++ ++ ++ ++ ++ ++ ++	++ ++ ++ ++ ++ ++ ++	++ ++ ++ ++ ++ ++ ++	++ ++ ++ ++ ++ ++ ++	++ ++ ++ ++ ++ ++ ++
Photographic emulsions (SpRBI)				20 40 60 80 100 120 140	++ ++ ++ ++ ++ ++ ++	++ ++ ++ ++ ++ ++ ++	++ ++ ++ ++ ++ ++ ++	++ ++ ++ ++ ++ ++ ++	++ ++ ++ ++ ++ ++ ++	++ ++ ++ ++ ++ ++ ++	++ ++ ++ ++ ++ ++ ++	++ ++ ++ ++ ++ ++ ++	++ ++ ++ ++ ++ ++ ++	++ ++ ++ ++ ++ ++ ++	++ ++ ++ ++ ++ ++ ++
Photographic fixer (SpRBI)			usual commercial	20 40 60 80 100 120 140	++ ++ ++ ++ ++ ++ ++	++ ++ ++ ++ ++ ++ ++	++ ++ ++ ++ ++ ++ ++	++ ++ ++ ++ ++ ++ ++	++ ++ ++ ++ ++ ++ ++	++ ++ ++ ++ ++ ++ ++	++ ++ ++ ++ ++ ++ ++	++ ++ ++ ++ ++ ++ ++	++ ++ ++ ++ ++ ++ ++	++ ++ ++ ++ ++ ++ ++	++ ++ ++ ++ ++ ++ ++

(Courtesy George Fischer Engineering Handbook)

Aggressive Media				Chemical Resistance											
Medium	Formula	Boiling point °C	Concentration	Temperature °C	PVC	CHVC	ABS	PE	PPH	PVDF (STGGEI)	EPDM	TFM	NBR	CR	CSM
Phthalic acid (SpRBI)	C ₆ H ₄ (COOH) ₂	Fp. 208	saturated, aqueous	20 40 60 80 100 120 140	+	+	-	+	+	+	+	+	-	-	+
Phthalic acid dioctyl ester	C ₂₄ H ₃₈ O ₄			20 40 60 80 100 120 140	-	-	-	+	+	-	+	-	-	-	-
Picric acid (SpRBI)	C ₆ H ₃ N ₃ O ₇	Fp. 122	1%, aqueous	20 40 60 80 100 120 140	+	-	-	+	+	+	+	+	+	+	+
Potash	see potassium carbonate		cold saturated, aqueous												
Potash lye	KOH		50%	20 40 60 80 100 120 140	+	+	+	+	+	-	+	+	+	+	+
Potassium (SpRBI)	KMnO ₄		cold saturated, aqueous	20 40 60 80 100 120 140	+	+	+	+	+	+	+	+	+	+	+
Potassium acetate (SpRBI)	CH ₃ COOK		saturated	20 40 60 80 100 120 140	+	+	+	+	+	+	+	-	+	+	+
Potassium bichromate (SpRBI)	K ₂ Cr ₂ O ₇	107	saturated, aqueous	20 40 60 80 100 120 140	+	+	+	+	+	+	+	+	+	+	+
Potassium borate	K ₂ B ₄ O ₇		10%, aqueous	20 40 60 80 100 120 140	+	+	+	+	+	+	+	+	+	+	+

(Courtesy George Fischer Engineering Handbook)

Aggressive Media				Chemical Resistance												
Medium	Formula	Boiling point °C	Concentration	Temperature °C	PVC	CVC	ABS	PE	PP-H	PPG (S/GF)	EPDM	FRM	NBR	CR	CSM	
Potassium bromate	KBrO ₃		cold saturated, aqueous	20 40 60 80 100 120 140	++ ++ O++ ++ ++ ++ ++	++ ++ ++ ++ ++ ++ ++	++ ++ ++ ++ ++ ++ ++	++ ++ O++ ++ ++ ++ ++	++ ++ ++ ++ ++ ++ ++	++ ++ ++ ++ ++ ++ ++	++ ++ ++ ++ ++ ++ ++	++ ++ ++ ++ ++ ++ ++	++ ++ ++ ++ ++ ++ ++	++ ++ ++ ++ ++ ++ ++	++ ++ ++ ++ ++ ++ ++	++ ++ ++ ++ ++ ++ ++
Potassium bromide	KBr		oil, aqueous	20 40 60 80 100 120 140	++ ++ O++ ++ ++ ++ ++	++ ++ ++ ++ ++ ++ ++	++ ++ ++ ++ ++ ++ ++	++ ++ ++ ++ ++ ++ ++	++ ++ ++ ++ ++ ++ ++	++ ++ ++ ++ ++ ++ ++	++ ++ ++ ++ ++ ++ ++	++ ++ ++ ++ ++ ++ ++	++ ++ ++ ++ ++ ++ ++	++ ++ ++ ++ ++ ++ ++	++ ++ ++ ++ ++ ++ ++	++ ++ ++ ++ ++ ++ ++
Potassium carbonate (potash)				20 40 60 80 100 120 140	++ ++ ++ ++ ++ ++ ++	++ ++ ++ ++ ++ ++ ++	++ ++ ++ ++ ++ ++ ++	++ ++ ++ ++ ++ ++ ++	++ ++ ++ ++ ++ ++ ++	++ ++ ++ ++ ++ ++ ++	++ ++ ++ ++ ++ ++ ++	++ ++ ++ ++ ++ ++ ++	++ ++ ++ ++ ++ ++ ++	++ ++ ++ ++ ++ ++ ++	++ ++ ++ ++ ++ ++ ++	++ ++ ++ ++ ++ ++ ++
Potassium chlorate (SpR)	KClO ₃		cold saturated, aqueous	20 40 60 80 100 120 140	++ ++ ++ ++ ++ ++ ++	++ ++ ++ ++ ++ ++ ++	++ ++ ++ ++ ++ ++ ++	++ ++ ++ ++ ++ ++ ++	++ ++ ++ ++ ++ ++ ++	++ ++ ++ ++ ++ ++ ++	++ ++ ++ ++ ++ ++ ++	++ ++ ++ ++ ++ ++ ++	++ ++ ++ ++ ++ ++ ++	++ ++ ++ ++ ++ ++ ++	++ ++ ++ ++ ++ ++ ++	++ ++ ++ ++ ++ ++ ++
Potassium chloride	KCl		oil, aqueous	20 40 60 80 100 120 140	++ ++ ++ ++ ++ ++ ++	++ ++ ++ ++ ++ ++ ++	++ ++ ++ ++ ++ ++ ++	++ ++ ++ ++ ++ ++ ++	++ ++ ++ ++ ++ ++ ++	++ ++ ++ ++ ++ ++ ++	++ ++ ++ ++ ++ ++ ++	++ ++ ++ ++ ++ ++ ++	++ ++ ++ ++ ++ ++ ++	++ ++ ++ ++ ++ ++ ++	++ ++ ++ ++ ++ ++ ++	++ ++ ++ ++ ++ ++ ++
Potassium chromate (SpR)	K ₂ CrO ₄		cold saturated, aqueous	20 40 60 80 100 120 140	++ ++ ++ ++ ++ ++ ++	++ ++ ++ ++ ++ ++ ++	++ ++ ++ ++ ++ ++ ++	++ ++ ++ ++ ++ ++ ++	++ ++ ++ ++ ++ ++ ++	++ ++ ++ ++ ++ ++ ++	++ ++ ++ ++ ++ ++ ++	++ ++ ++ ++ ++ ++ ++	++ ++ ++ ++ ++ ++ ++	++ ++ ++ ++ ++ ++ ++	++ ++ ++ ++ ++ ++ ++	++ ++ ++ ++ ++ ++ ++
Potassium cyanide	KCN		cold saturated, aqueous	20 40 60 80 100 120 140	++ ++ ++ ++ ++ ++ ++	++ ++ ++ ++ ++ ++ ++	++ ++ ++ ++ ++ ++ ++	++ ++ ++ ++ ++ ++ ++	++ ++ ++ ++ ++ ++ ++	++ ++ ++ ++ ++ ++ ++	++ ++ ++ ++ ++ ++ ++	++ ++ ++ ++ ++ ++ ++	++ ++ ++ ++ ++ ++ ++	++ ++ ++ ++ ++ ++ ++	++ ++ ++ ++ ++ ++ ++	++ ++ ++ ++ ++ ++ ++
Potassium dichromate	K ₂ Cr ₂ O ₇		saturated	20 40 60 80 100 120 140	++ ++ ++ ++ ++ ++ ++	++ ++ ++ ++ ++ ++ ++	++ ++ ++ ++ ++ ++ ++	++ ++ ++ ++ ++ ++ ++	++ ++ ++ ++ ++ ++ ++	++ ++ ++ ++ ++ ++ ++	++ ++ ++ ++ ++ ++ ++	++ ++ ++ ++ ++ ++ ++	++ ++ ++ ++ ++ ++ ++	++ ++ ++ ++ ++ ++ ++	++ ++ ++ ++ ++ ++ ++	++ ++ ++ ++ ++ ++ ++

(Courtesy George Fischer Engineering Handbook)

Aggressive Media				Chemical Resistance											
Medium	Formula	Boiling point °C	Concentration	Temperature °C	PVC	CPVC	ABS	PE	PPH	PVDF (STOFF)	EPDM	FPM	NBR	CR	CSM
Potassium fluoride	KF		saturated	20 40 60 80 100 120 140	++ ++ ++ ++ ++ ++ ++	++ ++ ++ ++ ++ ++ ++		++ ++ ++ ++ ++ ++ ++	++ ++ ++ ++ ++ ++ ++				+		
Potassium Hexafluoroantimonate -III	K ₂ SbF ₆ ·2H ₂ O			20 40 60 80 100 120 140	++ ++ ++ ++ ++ ++ ++	++ ++ ++ ++ ++ ++ ++		++ ++ ++ ++ ++ ++ ++	++ ++ ++ ++ ++ ++ ++		+	+			
Potassium hydrogen carbonate	KHCO ₃		saturated	20 40 60 80 100 120 140	++ ++ ++ ++ ++ ++ ++	++ ++ ++ ++ ++ ++ ++		++ ++ ++ ++ ++ ++ ++	++ ++ ++ ++ ++ ++ ++		++ ++ ++ ++ ++ ++ ++	++ ++ ++ ++ ++ ++ ++			
Potassium hydrogen sulphate	KHSO ₄		saturated	20 40 60 80 100 120 140	++ ++ ++ ++ ++ ++ ++	++ ++ ++ ++ ++ ++ ++		++ ++ ++ ++ ++ ++ ++	++ ++ ++ ++ ++ ++ ++		++ ++ ++ ++ ++ ++ ++	++ ++ ++ ++ ++ ++ ++			
Potassium iodide	KI		cold saturated, aqueous	20 40 60 80 100 120 140	++ ++ ++ ++ ++ ++ ++	++ ++ ++ ++ ++ ++ ++	++ ++ ++ ++ ++ ++ ++	++ ++ ++ ++ ++ ++ ++	++ ++ ++ ++ ++ ++ ++		++ ++ ++ ++ ++ ++ ++	++ ++ ++ ++ ++ ++ ++	++ ++ ++ ++ ++ ++ ++	++ ++ ++ ++ ++ ++ ++	++ ++ ++ ++ ++ ++ ++
Potassium nitrate	KNO ₃		50%, aqueous	20 40 60 80 100 120 140	++ ++ ++ ++ ++ ++ ++	++ ++ ++ ++ ++ ++ ++	++ ++ ++ ++ ++ ++ ++	++ ++ ++ ++ ++ ++ ++	++ ++ ++ ++ ++ ++ ++		++ ++ ++ ++ ++ ++ ++	++ ++ ++ ++ ++ ++ ++	++ ++ ++ ++ ++ ++ ++	++ ++ ++ ++ ++ ++ ++	++ ++ ++ ++ ++ ++ ++
Potassium perchlorate (Sp8B)	KClO ₄		cold saturated, aqueous	20 40 60 80 100 120 140	++ ++ ++ ++ ++ ++ ++	++ ++ ++ ++ ++ ++ ++	++ ++ ++ ++ ++ ++ ++	++ ++ ++ ++ ++ ++ ++	++ ++ ++ ++ ++ ++ ++		++ ++ ++ ++ ++ ++ ++	++ ++ ++ ++ ++ ++ ++	++ ++ ++ ++ ++ ++ ++	++ ++ ++ ++ ++ ++ ++	++ ++ ++ ++ ++ ++ ++
Potassium persulphate (Sp8B)	K ₂ S ₂ O ₈		oil, aqueous	20 40 60 80 100 120 140	++ ++ ++ ++ ++ ++ ++	++ ++ ++ ++ ++ ++ ++	++ ++ ++ ++ ++ ++ ++	++ ++ ++ ++ ++ ++ ++	++ ++ ++ ++ ++ ++ ++		++ ++ ++ ++ ++ ++ ++	++ ++ ++ ++ ++ ++ ++	++ ++ ++ ++ ++ ++ ++	++ ++ ++ ++ ++ ++ ++	++ ++ ++ ++ ++ ++ ++

(Courtesy George Fischer Engineering Handbook)

Aggressive Media					Chemical Resistance										
Medium	Formula	Boiling point °C	Concentration	Temperature °C	PVC	CPVC	ABS	PE	PP-H	PVC (ISGEM)	EPDM	FPM	NBR	CR	CSM
Potassium sulphate	K ₂ SO ₄		all, aqueous	20 40 60 80 100 120 140	++ O ++ ++ ++ ++ ++	++ ++ ++ ++ ++ ++ ++	++ ++ ++ ++ ++ ++ ++	++ ++ ++ ++ ++ ++ ++	++ ++ ++ ++ ++ ++ ++	++ ++ ++ ++ ++ ++ ++	++ ++ ++ ++ ++ ++ ++	++ ++ ++ ++ ++ ++ ++	++ ++ ++ ++ ++ ++ ++	++ ++ ++ ++ ++ ++ ++	++ ++ ++ ++ ++ ++ ++
Potassium sulphide	K ₂ S		saturated	20 40 60 80 100 120 140	++ ++ ++ ++ ++ ++ ++	++ ++ ++ ++ ++ ++ ++	++ ++ ++ ++ ++ ++ ++	++ ++ ++ ++ ++ ++ ++	++ ++ ++ ++ ++ ++ ++	++ ++ ++ ++ ++ ++ ++	++ ++ ++ ++ ++ ++ ++	++ ++ ++ ++ ++ ++ ++	++ ++ ++ ++ ++ ++ ++	++ ++ ++ ++ ++ ++ ++	++ ++ ++ ++ ++ ++ ++
Potassium sulphite	K ₂ SO ₃		saturated	20 40 60 80 100 120 140	++ ++ ++ ++ ++ ++ ++	++ ++ ++ ++ ++ ++ ++	++ ++ ++ ++ ++ ++ ++	++ ++ ++ ++ ++ ++ ++	++ ++ ++ ++ ++ ++ ++	++ ++ ++ ++ ++ ++ ++	++ ++ ++ ++ ++ ++ ++	++ ++ ++ ++ ++ ++ ++	++ ++ ++ ++ ++ ++ ++	++ ++ ++ ++ ++ ++ ++	++ ++ ++ ++ ++ ++ ++
Potassium-aluminiumsulfate (alum)			50%	20 40 60 80 100 120 140	++ ++ ++ ++ ++ ++ ++	++ ++ ++ ++ ++ ++ ++	++ ++ ++ ++ ++ ++ ++	++ ++ ++ ++ ++ ++ ++	++ ++ ++ ++ ++ ++ ++	++ ++ ++ ++ ++ ++ ++	++ ++ ++ ++ ++ ++ ++	++ ++ ++ ++ ++ ++ ++	++ ++ ++ ++ ++ ++ ++	++ ++ ++ ++ ++ ++ ++	++ ++ ++ ++ ++ ++ ++
Potassium hexacyanoferrate -(III)	K ₃ [Fe(CN) ₆]			20 40 60 80 100 120 140	++ ++ ++ ++ ++ ++ ++	++ ++ ++ ++ ++ ++ ++	++ ++ ++ ++ ++ ++ ++	++ ++ ++ ++ ++ ++ ++	++ ++ ++ ++ ++ ++ ++	++ ++ ++ ++ ++ ++ ++	++ ++ ++ ++ ++ ++ ++	++ ++ ++ ++ ++ ++ ++	++ ++ ++ ++ ++ ++ ++	++ ++ ++ ++ ++ ++ ++	++ ++ ++ ++ ++ ++ ++
Potassium tartrat				20 40 60 80 100 120 140	++ ++ ++ ++ ++ ++ ++	++ ++ ++ ++ ++ ++ ++	++ ++ ++ ++ ++ ++ ++	++ ++ ++ ++ ++ ++ ++	++ ++ ++ ++ ++ ++ ++	++ ++ ++ ++ ++ ++ ++	++ ++ ++ ++ ++ ++ ++	++ ++ ++ ++ ++ ++ ++	++ ++ ++ ++ ++ ++ ++	++ ++ ++ ++ ++ ++ ++	++ ++ ++ ++ ++ ++ ++
Potassiumhydrogensulfite				20 40 60 80 100 120 140	++ ++ ++ ++ ++ ++ ++	++ ++ ++ ++ ++ ++ ++	++ ++ ++ ++ ++ ++ ++	++ ++ ++ ++ ++ ++ ++	++ ++ ++ ++ ++ ++ ++	++ ++ ++ ++ ++ ++ ++	++ ++ ++ ++ ++ ++ ++	++ ++ ++ ++ ++ ++ ++	++ ++ ++ ++ ++ ++ ++	++ ++ ++ ++ ++ ++ ++	++ ++ ++ ++ ++ ++ ++
Potassiumhypochlorite	KOCl			20 40 60 80 100 120 140	++ ++ ++ ++ ++ ++ ++	++ ++ ++ ++ ++ ++ ++	++ ++ ++ ++ ++ ++ ++	++ ++ ++ ++ ++ ++ ++	++ ++ ++ ++ ++ ++ ++	++ ++ ++ ++ ++ ++ ++	++ ++ ++ ++ ++ ++ ++	++ ++ ++ ++ ++ ++ ++	++ ++ ++ ++ ++ ++ ++	++ ++ ++ ++ ++ ++ ++	++ ++ ++ ++ ++ ++ ++

(Courtesy George Fischer Engineering Handbook)

Aggressive Media				Chemical Resistance											
Medium	Formula	Boiling point °C	Concentration	Temperature °C	PVC	CPVC	ABS	PE	PP-H	PVDF (STYGER)	EPDM	FKM	NBR	CR	CSM
Potassiumperoxodisulfate	K ₂ S ₂ O ₈		saturated	20 40 60 80 100 120 140	+	+	+								
Potassiumphosphate	KH ₂ PO ₄ und K ₂ H PO ₄		all, aqueous	20 40 60 80 100 120 140	+	+	O	+	+	+	+	+	+	+	+
Potassiumphosphate				20 40 60 80 100 120 140	+	+		+	+	+		+	+	+	+
Propane	C ₃ H ₈	-42	technically pure, liquid	20 40 60 80 100 120 140	+	-	-	+	+	+	-	+	+	-	-
Propane			technically pure, gaseous	20 40 60 80 100 120 140	+	+	-	+	+	+	-	+	+	+	O
Propanol, n- and iso- (Sp88)	C ₃ H ₇ OH	97 bzw. 82	technically pure	20 40 60 80 100 120 140	+	O	-	+	+	+	+	+	+	+	+
Propargyl alcohol (Sp88)	CH ₃ C≡CH ₂ OH	114	7%, aqueous	20 40 60 80 100 120 140	+	+	-	+	+	+	+	+	+	+	+
Propionic acid (Sp88)	CH ₃ CH ₂ COOH	141	50%, aqueous	20 40 60 80 100 120 140	+	O	-	+	+	+	+	+	+	O	O

(Courtesy George Fischer Engineering Handbook)

Aggressive Media				Chemical Resistance											
Medium	Formula	Boiling point °C	Concentration	Temperature °C	PVC	CPVC	ABS	PE	PP-H	PNB (STYGF)	EPDM	FPM	NBR	CR	CSM
Propionic acid (SpRBI)		141	technically pure	20 40 60 80 100 120 140	+	○	-	+	+	+	+	+	+	-	-
Propylene glycol (SpRBI)	C ₃ H ₈ O ₂	188	technically pure	20 40 60 80 100 120 140	+	-	○	+	+	+	+	+	+	○	+
Propylene oxide	C ₃ H ₆ O	35	technically pure	20 40 60 80 100 120 140	○	-	-	+	+	+	○	-	-	-	-
Pyridine	C ₅ H ₅ N	115	technically pure	20 40 60 80 100 120 140	-	-	-	+	+	+	○	-	-	-	-
Pyrogallol	C ₃ H ₃ (OH) ₃	100%		20 40 60 80 100 120 140						+		+			
Ramsit fabric waterproofing agents			usual commercial	20 40 60 80 100 120 140	+	+		+	+	+	+	+	+	+	+
Salicylic acid	C ₇ H ₆ (OH)COOH		saturated	20 40 60 80 100 120 140	+	+	○	+	+	+	+	+	+	+	+
Sea water	see Brine			20 40 60 80 100 120 140	+	+	+	+	+	+	+	+	+	+	+
Silicic acid	Si(OH) ₄			20 40 60 80 100 120 140	+	+	+	+	+	+	+	+	+	+	+

(Courtesy George Fischer Engineering Handbook)

Aggressive Media				Chemical Resistance											
Medium	Formula	Boiling point °C	Concentration	Temperature °C	PVC	CPVC	ABS	PE	PPH	PVDF (SG#1)	EPDM	FPM	NBR	CR	CSM
Silicone oil				20	O	+	+	+	+	+	+	+	+	O	+
				40	+	+	+	+	+	+	+	+	+	+	+
				60	+	+	+	+	+	+	+	+	+	+	+
				80	+	+	+	+	+	+	+	+	+	+	+
				100	+	+	+	+	+	+	+	+	+	+	+
				120	+	+	+	+	+	+	+	+	+	+	+
				140	+	+	+	+	+	+	+	+	+	+	+
Silver	AgCN		saturated	20	+	+	+	+	+	+	+	+	+	+	+
				40	+	+	+	+	+	+	+	+	+	+	+
				60	+	+	+	+	+	+	+	+	+	+	+
				80	+	+	+	+	+	+	+	+	+	+	+
				100	+	+	+	+	+	+	+	+	+	+	+
				120	+	+	+	+	+	+	+	+	+	+	+
				140	+	+	+	+	+	+	+	+	+	+	+
Silver salts	AgNO ₃ , AgCN, AgCl		cold saturated, aqueous	20	+	+	+	+	+	+	+	+	+	+	+
				40	+	+	+	+	+	+	+	+	+	+	+
				60	O	+	+	+	+	+	+	+	+	+	+
				80	+	+	+	+	+	+	+	+	+	+	+
				100	+	+	+	+	+	+	+	+	+	+	+
				120	+	+	+	+	+	+	+	+	+	+	+
				140	+	+	+	+	+	+	+	+	+	+	+
Silver cyanide				20	+	+	+	+	+	+	+	+	+	+	+
				40	+	+	+	+	+	+	+	+	+	+	+
				60	+	+	+	+	+	+	+	+	+	+	+
				80	+	+	+	+	+	+	+	+	+	+	+
				100	+	+	+	+	+	+	+	+	+	+	+
				120	+	+	+	+	+	+	+	+	+	+	+
				140	+	+	+	+	+	+	+	+	+	+	+
Soap solution (5pH)			oil, aqueous	20	+	+	+	+	+	+	+	+	+	+	+
				40	+	+	+	+	+	+	+	+	+	+	+
				60	O	+	+	+	+	+	+	+	+	+	+
				80	+	+	+	+	+	+	+	+	+	+	+
				100	+	+	+	+	+	+	+	+	+	+	+
				120	+	+	+	+	+	+	+	+	+	+	+
				140	+	+	+	+	+	+	+	+	+	+	+
Soda	see Sodium carbonate														
Sodium acetate	CH ₃ COONa		oil, aqueous	20	+	+	+	+	+	+	+	+	+	+	O
				40	+	+	+	+	+	+	+	+	+	+	+
				60	+	+	+	+	+	+	+	+	+	+	+
				80	+	+	+	+	+	+	+	+	+	+	+
				100	+	+	+	+	+	+	+	+	+	+	+
				120	+	+	+	+	+	+	+	+	+	+	+
				140	+	+	+	+	+	O	+	+	+	+	+
Sodium aluminium sulfate				20	+	+	+	+	+	+	+	+	+	+	+
				40	+	+	+	+	+	+	+	+	+	+	+
				60	+	+	+	+	+	+	+	+	+	+	+
				80	+	+	+	+	+	+	+	+	+	+	+
				100	+	+	+	+	+	+	+	+	+	+	+
				120	+	+	+	+	+	+	+	+	+	+	+
				140	+	+	+	+	+	+	+	+	+	+	+
Sodium arsenite	Na ₃ AsO ₃		saturated	20	+	+	+	+	+	+	+	+	+	+	+
				40	+	+	+	+	+	+	+	+	+	+	+
				60	+	+	+	+	+	+	+	+	+	+	+
				80	+	+	+	+	+	+	+	+	+	+	+
				100	+	+	+	+	+	+	+	+	+	+	+
				120	+	+	+	+	+	+	+	+	+	+	+
				140	+	+	+	+	+	+	+	+	+	+	+

(Courtesy George Fischer Engineering Handbook)

Aggressive Media				Chemical Resistance											
Medium	Formula	Boiling point °C	Concentration	Temperature °C	PVC	CPVC	ABS	PE	PP-H	PVDF (SUGEN)	EPDM	FPM	NBR	CR	CSM
Sodium benzoate	C ₆ H ₅ -COONa		cold saturated, aqueous	20 40 60 80 100 120 140	++ O++ ++ ++ ++ ++ ++	++ ++ ++ ++ ++ ++ ++	- ++ ++ ++ ++ ++ ++	++ ++ ++ ++ ++ ++ ++	++ ++ ++ ++ O++ ++ ++	++ ++ ++ ++ ++ ++ ++	O+ ++ ++ ++ ++ ++ ++	++ ++ ++ ++ ++ ++ ++	++ ++ ++ ++ ++ ++ ++	++ ++ ++ ++ ++ ++ ++	++ ++ ++ ++ ++ ++ ++
Sodium bicarbonate	NaHCO ₃		cold saturated, aqueous	20 40 60 80 100 120 140	++ ++ ++ ++ ++ ++ ++	++ ++ ++ ++ ++ ++ ++	++ ++ ++ ++ ++ ++ ++	++ ++ ++ ++ ++ ++ ++	++ ++ ++ ++ ++ ++ ++	++ ++ ++ ++ ++ ++ ++	++ ++ ++ ++ ++ ++ ++	++ ++ ++ ++ ++ ++ ++	++ ++ ++ ++ ++ ++ ++	++ ++ ++ ++ ++ ++ ++	++ ++ ++ ++ ++ ++ ++
Sodium bisulphate	NaHSO ₄		10%, aqueous	20 40 60 80 100 120 140	++ ++ O ++ ++ ++ ++	++ ++ ++ ++ ++ ++ ++	++ ++ ++ ++ ++ ++ ++	++ ++ ++ ++ ++ ++ ++	++ ++ ++ ++ ++ ++ ++	++ ++ ++ ++ ++ ++ ++	O+ ++ ++ ++ ++ ++ ++	++ ++ ++ ++ ++ ++ ++	++ ++ ++ ++ ++ ++ ++	++ ++ ++ ++ ++ ++ ++	++ ++ ++ ++ ++ ++ ++
Sodium bisulphite	NaHSO ₃		oil, aqueous	20 40 60 80 100 120 140	++ O - ++ ++ ++ ++	++ ++ ++ ++ ++ ++ ++	++ ++ ++ ++ ++ ++ ++	++ ++ ++ ++ ++ ++ ++	++ ++ ++ ++ ++ ++ ++	++ ++ ++ ++ ++ ++ ++	O+ O- O- O- O- O- O-	++ ++ ++ ++ ++ ++ ++	++ ++ ++ ++ ++ ++ ++	++ ++ ++ ++ ++ ++ ++	++ ++ ++ ++ ++ ++ ++
Sodium borate	Na ₂ BO ₃		saturated	20 40 60 80 100 120 140	++ ++ ++ ++ ++ ++ ++	++ ++ ++ ++ ++ ++ ++	++ ++ ++ ++ ++ ++ ++	++ ++ ++ ++ ++ ++ ++	++ ++ ++ ++ ++ ++ ++	++ ++ ++ ++ ++ ++ ++	++ ++ ++ ++ ++ ++ ++	++ ++ ++ ++ ++ ++ ++	++ ++ ++ ++ ++ ++ ++	++ ++ ++ ++ ++ ++ ++	++ ++ ++ ++ ++ ++ ++
Sodium bromate	NaBrO ₃		oil, aqueous	20 40 60 80 100 120 140	++ O ++ ++ ++ ++ ++	++ ++ ++ ++ ++ ++ ++	++ ++ ++ ++ ++ ++ ++	++ ++ ++ ++ ++ ++ ++	++ ++ ++ ++ ++ ++ ++	++ ++ ++ ++ ++ ++ ++	++ ++ ++ ++ ++ ++ ++	++ ++ ++ ++ ++ ++ ++	++ ++ ++ ++ ++ ++ ++	++ ++ ++ ++ ++ ++ ++	++ ++ ++ ++ ++ ++ ++
Sodium bromide	NaBr		oil, aqueous	20 40 60 80 100 120 140	++ ++ O ++ ++ ++ ++	++ ++ ++ ++ ++ ++ ++	++ ++ ++ ++ ++ ++ ++	++ ++ ++ ++ ++ ++ ++	++ ++ ++ ++ ++ ++ ++	++ ++ ++ ++ ++ ++ ++	++ ++ ++ ++ ++ ++ ++	++ ++ ++ ++ ++ ++ ++	++ ++ ++ ++ ++ ++ ++	++ ++ ++ ++ ++ ++ ++	++ ++ ++ ++ ++ ++ ++
Sodium carbonate	see soda		cold saturated, aqueous												
Sodium chlorate (SpRBI)	NaClO ₃		oil, aqueous	20 40 60 80 100 120 140	++ ++ O ++ ++ ++ ++	++ ++ ++ ++ ++ ++ ++	++ ++ ++ ++ ++ ++ ++	++ ++ ++ ++ ++ ++ ++	++ ++ ++ ++ ++ ++ O	++ ++ ++ ++ ++ ++ ++	++ ++ ++ ++ ++ ++ ++	++ ++ ++ ++ ++ ++ ++	++ ++ ++ ++ ++ ++ ++	++ ++ ++ ++ ++ ++ ++	++ ++ ++ ++ ++ ++ ++

(Courtesy George Fischer Engineering Handbook)

Aggressive Media				Chemical Resistance											
Medium	Formula	Boiling point °C	Concentration	Temperature °C	PVC	CPVC	ABS	PE	PP-H	PVDF (SYGEL)	EPDM	FRM	NBR	CR	CSM
Sodium chlorite (SpRt)	NaClO ₂		diluted, aqueous	20 40 60 80 100 120 140	○	+		○	○	○	++	++	+	○	++
Sodium chromate (SpRt)	Na ₂ CrO ₄		diluted, aqueous	20 40 60 80 100 120 140	+	+	+	+	+	+	+	+	○	+	+
Sodium disulphite	Na ₂ S ₂ O ₅		oil, aqueous	20 40 60 80 100 120 140	+	+		+	+	+	+	+	○	+	+
Sodium dithionite	see hyposulphite		up to 10%, aqueous												
Sodium fluoride	NaF		cold saturated, aqueous	20 40 60 80 100 120 140	+	+	+	+	+	+	+	+	○	+	+
Sodium hydroxide free Caustic soda															
Sodium hypochlorite (SpRt)	NaOCl		12.5% active chlorine, aqueous	20 40 60 80 100 120 140	+	+		○	○	○	+	+	○	○	+
Sodium iodide	NaI		oil, aqueous	20 40 60 80 100 120 140	+	+	+	+	+	+	+	+	○	+	○
Sodium nitrate	NaNO ₃		cold saturated, aqueous	20 40 60 80 100 120 140	+	+	+	+	+	+	+	+	+	+	+
Sodium nitrite	NaNO ₂		cold saturated, aqueous	20 40 60 80 100 120 140	+	+	+	+	+	+	+	+	○	+	+

(Courtesy George Fischer Engineering Handbook)

Aggressive Media				Chemical Resistance											
Medium	Formula	Boiling point °C	Concentration	Temperature °C	PVC	CPVC	ABS	PE	PP-H	PVDF (SUNGEN)	EPDM	TFM	NBR	CR	CSM
Sodium oxalate	Na ₂ C ₂ O ₄		cold saturated, aqueous	20 40 60 80 100 120 140	++ ++ ++ ++ ++ ++ ++	++ ++ ++ ++ ++ ++ ++	++ ++ ++ ++ ++ ++ ++	++ ++ ++ ++ ++ ++ ++	++ ++ ++ ++ ++ ++ ++	++ ++ ++ ++ ++ ++ ++		++ ++ ++ ++ ++ ++ ++	++ ++ ++ ++ ++ ++ ++	++ ++ ++ ++ ++ ++ ++	++ ++ ++ ++ ++ ++ ++
Sodium perborate	NaBO ₃ ·4H ₂ O		saturated	20 40 60 80 100 120 140	++ ++ ++ ++ ++ ++ ++	++ ++ ++ ++ ++ ++ ++	++ ++ ++ ++ ++ ++ ++	++ ++ ++ ++ ++ ++ ++	++ ++ ++ ++ ++ ++ ++	++ ++ ++ ++ ++ ++ ++	++ ++ ++ ++ ++ ++ ++	++ ++ ++ ++ ++ ++ ++	++ ++ ++ ++ ++ ++ ++	++ ++ ++ ++ ++ ++ ++	++ ++ ++ ++ ++ ++ ++
Sodium perchlorate	NaClO ₄		saturated	20 40 60 80 100 120 140	++ ++ ++ ++ ++ ++ ++	++ ++ ++ ++ ++ ++ ++	++ ++ ++ ++ ++ ++ ++	++ ++ ++ ++ ++ ++ ++	++ ++ ++ ++ ++ ++ ++	++ ++ ++ ++ ++ ++ ++	++ ++ ++ ++ ++ ++ ++	++ ++ ++ ++ ++ ++ ++	++ ++ ++ ++ ++ ++ ++	++ ++ ++ ++ ++ ++ ++	++ ++ ++ ++ ++ ++ ++
Sodium persulphate (3p88)	Na ₂ S ₂ O ₈		cold saturated, aqueous	20 40 60 80 100 120 140	++ ++ ++ ++ ++ ++ ++	++ ++ ++ ++ ++ ++ ++	++ ++ ++ ++ ++ ++ ++	++ ++ ++ ++ ++ ++ ++	++ ++ ++ ++ ++ ++ ++	++ ++ ++ ++ ++ ++ ++	++ ++ ++ ++ ++ ++ ++	++ ++ ++ ++ ++ ++ ++	++ ++ ++ ++ ++ ++ ++	++ ++ ++ ++ ++ ++ ++	++ ++ ++ ++ ++ ++ ++
Sodium phosphate	Na ₃ PO ₄		cold saturated, aqueous	20 40 60 80 100 120 140	++ ++ ++ ++ ++ ++ ++	++ ++ ++ ++ ++ ++ ++	++ ++ ++ ++ ++ ++ ++	++ ++ ++ ++ ++ ++ ++	++ ++ ++ ++ ++ ++ ++	++ ++ ++ ++ ++ ++ ++	++ ++ ++ ++ ++ ++ ++	++ ++ ++ ++ ++ ++ ++	++ ++ ++ ++ ++ ++ ++	++ ++ ++ ++ ++ ++ ++	++ ++ ++ ++ ++ ++ ++
Sodium silicate	Na ₂ SiO ₃		oil, aqueous	20 40 60 80 100 120 140	++ ++ ++ ++ ++ ++ ++	++ ++ ++ ++ ++ ++ ++	++ ++ ++ ++ ++ ++ ++	++ ++ ++ ++ ++ ++ ++	++ ++ ++ ++ ++ ++ ++	++ ++ ++ ++ ++ ++ ++	++ ++ ++ ++ ++ ++ ++	++ ++ ++ ++ ++ ++ ++	++ ++ ++ ++ ++ ++ ++	++ ++ ++ ++ ++ ++ ++	++ ++ ++ ++ ++ ++ ++
Sodium Sulfide	Natriumsulfid														
Sodium sulphate	Na ₂ SO ₄ , NaHSO ₄		cold saturated, aqueous	20 40 60 80 100 120 140	++ ++ ++ ++ ++ ++ ++	++ ++ ++ ++ ++ ++ ++	++ ++ ++ ++ ++ ++ ++	++ ++ ++ ++ ++ ++ ++	++ ++ ++ ++ ++ ++ ++	++ ++ ++ ++ ++ ++ ++	++ ++ ++ ++ ++ ++ ++	++ ++ ++ ++ ++ ++ ++	++ ++ ++ ++ ++ ++ ++	++ ++ ++ ++ ++ ++ ++	++ ++ ++ ++ ++ ++ ++
Sodium sulphide	Na ₂ S		cold saturated, aqueous	20 40 60 80 100 120 140	++ ++ ++ ++ ++ ++ ++	++ ++ ++ ++ ++ ++ ++	++ ++ ++ ++ ++ ++ ++	++ ++ ++ ++ ++ ++ ++	++ ++ ++ ++ ++ ++ ++	++ ++ ++ ++ ++ ++ ++	++ ++ ++ ++ ++ ++ ++	++ ++ ++ ++ ++ ++ ++	++ ++ ++ ++ ++ ++ ++	++ ++ ++ ++ ++ ++ ++	++ ++ ++ ++ ++ ++ ++

(Courtesy George Fischer Engineering Handbook)

Aggressive Media				Chemical Resistance											
Medium	Formula	Boiling point °C	Concentration	Temperature °C	PVC	CVC	ABS	PE	PPH	PVDF (KSTGEL)	EPDM	FPM	NBR	CR	CSM
Sodium sulphite	Na ₂ SO ₃		cold saturated, aqueous	20 40 60 80 100 120 140	+	+	+	+	+	+	+	+	+	+	+
Sodium thiosulphate	Na ₂ S ₂ O ₃		cold saturated, aqueous	20 40 60 80 100 120 140	+	+	+	+	+	+	+	+	+	+	+
Sodiumchloride	NaCl		each, aqueous	20 40 60 80 100 120 140	+	+	+	+	+	+	+	+	+	+	+
Sodiumcyanide	NaCN			20 40 60 80 100 120 140	+	+	+	+	+	+	+	+	+	+	+
Sodiumdichromate	Na ₂ Cr ₂ O ₇			20 40 60 80 100 120 140	+	+	+	+	+	+	+	+	+	+	+
Sodiumhydrogen-carbonate	NaHCO ₃			20 40 60 80 100 120 140	+	+	+	+	+	+	+	+	+	+	+
Sodiumhydrogensulfate	NaHSO ₄			20 40 60 80 100 120 140	+	+	+	+	+	+	+	+	+	+	+
Spindle oil				20 40 60 80 100 120 140	+	+	+	+	+	+	+	+	+	+	+

(Courtesy George Fischer Engineering Handbook)

Aggressive Media				Chemical Resistance											
Medium	Formula	Boiling point °C	Concentration	Temperature °C	PVC	CPVC	ABS	PE	PP-H	PVDF (STOR)	EPDM	FPM	NBR	CR	CSM
Spinning bath acids containing carbon disulphide (SpRBI)			100 mg CS ₂ /l	20 40 60 80 100 120 140	+	+		+	+	+		+	-		O
Spinning bath acids containing carbon disulphide (SpRBI)			200 mg CS ₂ /l	20 40 60 80 100 120 140	O			+	+	+		+	-		-
Spinning bath acids containing carbon disulphide (SpRBI)			700 mg CS ₂ /l	20 40 60 80 100 120 140	-			+	+	+		+	-		-
Stannous chloride	see Tin II chloride		cold saturated, aqueous												
Stannous chloride Tin IV chloride	SnCl ₄		cold saturated, aqueous	20 40 60 80 100 120 140				+	+	+					
Starch solution	IC ₆ H ₁₀ O ₅ n		oil, aqueous	20 40 60 80 100 120 140	+	+	+	+	+	+	+	+	+	+	+
Starch syrup			usual commercial	20 40 60 80 100 120 140	+	+	+	+	+	+	+	+	+	+	+
Stearic acid (SpRBI)	C ₁₇ H ₃₅ COOH	Fp. 69	technically pure	20 40 60 80 100 120 140	+	O	+	+	+	+	+	+	+	+	O
Synol				20 40 60 80 100 120 140	-	-	-		+			+			

(Courtesy George Fischer Engineering Handbook)

Aggressive Media				Chemical Resistance											
Medium	Formula	Boiling point °C	Concentration	Temperature °C	PVC	CPVC	ABS	PE	PP-H	PVDF (KRYDUR)	EPDM	IRM	NBR	CR	CSM
Succinic acid	HOOC-CH ₂ -CH ₂ -COOH	bp*, 185	aqueous, all	20 40 60 80 100 120 140	+	+	+	+	+	+	+	+	+	+	+
Sugar syrup			usual commercial	20 40 60 80 100 120 140	+	+	+	+	+	+	+	+	+	+	+
Sulfur	S	bp*, 119	technically pure	20 40 60 80 100 120 140	0	0	-	+	+	+	+	+	+	+	+
Sulfur dioxide	SO ₂	-10	technically pure, anhydrous	20 40 60 80 100 120 140	+	+	-	+	+	0	+	+	-	-	0
Sulfur dioxide	SO ₂		technically pure, moist	20 40 60 80 100 120 140	-	-	-	-	-	-	0	0	-	-	0
Sulfur dioxide	SO ₂		oil, moist	20 40 60 80 100 120 140	+	+	-	+	+	+	+	+	-	-	0
Sulfur trioxide	SO ₃			20 40 60 80 100 120 140	-	-	-	-	-	-	-	-	-	-	-
Sulfuric acid saturated by Chlorine	H ₂ SO ₄ +Cl ₂		60%	20 40 60 80 100 120 140						+					

(Courtesy George Fischer Engineering Handbook)

Aggressive Media				Chemical Resistance											
Medium	Formula	Boiling point °C	Concentration	Temperature °C	PVC	CPVC	ABS	PE	PP-H	PVDF (SUGER)	EPDM	FM	NBR	CR	CSM
Sulfuric acid (see note 2.3.1 on jointing)	H ₂ SO ₄	120	up to 40%, aqueous	20 40 60 80 100 120 140	++ O++ ++ ++ ++ ++ ++	++ ++ ++ ++ ++ ++ ++	O+ ++ ++ ++ ++ ++ ++	++ ++ ++ ++ ++ ++ ++	++ ++ ++ ++ ++ ++ ++	++ ++ ++ ++ ++ ++ ++	++ O++ ++ ++ ++ ++ ++	++ O++ ++ ++ ++ ++ ++	++ O++ ++ ++ ++ ++ ++	++ O++ ++ ++ ++ ++ ++	++ O++ ++ ++ ++ ++ ++
Sulfuric acid (see note 2.3.1 on jointing) (SpR8)	H ₂ SO ₄	140	up to 60%, aqueous	20 40 60 80 100 120 140	++ ++ ++ ++ ++ ++ ++	++ ++ ++ ++ ++ ++ ++	++ ++ ++ ++ ++ ++ ++	++ ++ O++ ++ ++ ++ ++	++ ++ ++ ++ ++ ++ ++	++ ++ ++ ++ ++ ++ ++	++ O++ ++ ++ ++ ++ ++	++ O++ ++ ++ ++ ++ ++	++ O++ ++ ++ ++ ++ ++	++ O++ ++ ++ ++ ++ ++	++ O++ ++ ++ ++ ++ ++
Sulfuric acid (see note 2.3.1 on jointing) (SpR8)	H ₂ SO ₄	195	up to 80%, aqueous	20 40 60 80 100 120 140	++ ++ ++ ++ ++ ++ ++	++ ++ ++ ++ ++ ++ ++	++ ++ O++ ++ ++ ++ ++	++ ++ O++ ++ ++ ++ ++	++ ++ ++ ++ ++ ++ ++	++ O++ ++ ++ ++ ++ ++	++ O++ ++ ++ ++ ++ ++	++ O++ ++ ++ ++ ++ ++	++ O++ ++ ++ ++ ++ ++	++ O++ ++ ++ ++ ++ ++	++ O++ ++ ++ ++ ++ ++
Sulfuric acid (see note 2.3.1 on jointing) (SpR8)	H ₂ SO ₄	250	90%, aqueous	20 40 60 80 100 120 140	++ ++ ++ ++ ++ ++ ++	++ ++ ++ ++ ++ ++ ++	++ ++ O++ ++ ++ ++ ++	++ ++ O++ ++ ++ ++ ++	++ ++ ++ ++ ++ ++ ++	++ ++ ++ ++ ++ ++ ++	++ ++ ++ ++ ++ ++ ++	++ ++ ++ ++ ++ ++ ++	++ ++ ++ ++ ++ ++ ++	++ ++ ++ ++ ++ ++ ++	++ ++ ++ ++ ++ ++ ++
Sulfuric acid (see note 2.3.1 on jointing) (SpR8)	H ₂ SO ₄		96%, aqueous	20 40 60 80 100 120 140	++ ++ O++ ++ ++ ++ ++	++ ++ ++ ++ ++ ++ ++	++ ++ ++ ++ ++ ++ ++	++ ++ ++ ++ ++ ++ ++	++ ++ ++ ++ ++ ++ ++	++ ++ ++ ++ ++ ++ ++	++ ++ ++ ++ ++ ++ ++	++ ++ ++ ++ ++ ++ ++	++ ++ ++ ++ ++ ++ ++	++ ++ ++ ++ ++ ++ ++	++ ++ ++ ++ ++ ++ ++
Sulfuric acid (see note 2.3.1 on jointing) (SpR8)	H ₂ SO ₄		97%	20 40 60 80 100 120 140	++ ++ ++ ++ ++ ++ ++	++ ++ ++ ++ ++ ++ ++	++ ++ ++ ++ ++ ++ ++	++ ++ ++ ++ ++ ++ ++	++ ++ ++ ++ ++ ++ ++	++ ++ ++ ++ ++ ++ ++	++ ++ ++ ++ ++ ++ ++	++ ++ ++ ++ ++ ++ ++	++ ++ ++ ++ ++ ++ ++	++ ++ ++ ++ ++ ++ ++	++ ++ ++ ++ ++ ++ ++
Sulfuric acid (see note 2.3.1 on jointing) (SpR8)	H ₂ SO ₄	340	98%	20 40 60 80 100 120 140	++ O++ ++ O++ ++ ++ ++	++ ++ ++ ++ ++ ++ ++	++ ++ ++ ++ ++ ++ ++	++ ++ ++ ++ ++ ++ ++	++ ++ ++ ++ ++ ++ ++	++ ++ ++ ++ ++ ++ ++	++ O++ ++ ++ ++ ++ ++	++ ++ ++ ++ ++ ++ ++	++ ++ ++ ++ ++ ++ ++	++ ++ ++ ++ ++ ++ ++	++ ++ ++ ++ ++ ++ ++
Sulfurous acid	H ₂ SO ₃		saturated, aqueous	20 40 60 80 100 120 140	++ ++ O++ ++ ++ ++ ++	++ ++ ++ ++ ++ ++ ++	++ ++ ++ ++ ++ ++ ++	++ ++ ++ ++ ++ ++ ++	++ ++ ++ ++ ++ ++ ++	++ ++ ++ ++ ++ ++ ++	++ ++ ++ ++ ++ ++ ++	++ ++ O++ ++ ++ ++ ++	++ ++ ++ ++ ++ ++ ++	++ ++ ++ ++ ++ ++ ++	++ ++ ++ ++ ++ ++ ++

(Courtesy George Fischer Engineering Handbook)

Aggressive Media				Chemical Resistance											
Medium	Formula	Boiling point °C	Concentration	Temperature °C	PVC	CPVC	ABS	PE	PP-H	PVDF (SIGEF)	EPDM	FRM	NBR	CR	CSM
Suluryl chloride	SO ₂ Cl ₂	69	technically pure	20 40 60 80 100 120 140	-	-	-	-	-	○					+
Surfactants (SpRB)			up to 5%, aqueous	20 40 60 80 100 120 140	○	○	-	+	○	+	+	+	+	+	+
Surfactants (ESCI)				20 40 60 80 100 120 140	○	○	○	○	○	○	○	○	○	○	○
Tallow (SpRB)			technically pure	20 40 60 80 100 120 140	+	+	-	+	+	+	+	+	+	+	+
Tannic acid (SpRB)			oil, aqueous	20 40 60 80 100 120 140	+	+	+	+	+			+	+	+	+
Tanning extracts from plants (SpRB)			usual commercial	20 40 60 80 100 120 140	+	+	+	+	+	+	+	+	+	+	+
Tartaric acid				20 40 60 80 100 120 140						+					
Tartaric acid	HO ₂ C-CH(OH)-CH(OH)-CO ₂ H		oil, aqueous	20 40 60 80 100 120 140	+	+	+	+	+	+	+	+	+	+	+

(Courtesy George Fischer Engineering Handbook)

Aggressive Media					Chemical Resistance										
Medium	Formula	Boiling point °C	Concentration	Temperature °C	PVC	CPVC	ABS	PE	PPH	PVDF (STG/ET)	EPDM	FRM	NBR	CR	CSM
Tartaric acid up to 10%				20 40 60 80 100 120 140						++					
Tetrachlorethylene				20 40 60 80 100 120 140	-	-	-	-	-	+	-	+			
Tetrachloroethane	C_2HCl_3	146	technically pure	20 40 60 80 100 120 140	-	-	-	O	O	+	-	O	-	-	-
Tetrachloroethylene	see Perchloroethylene	121													
Tetraethylene lead (SpRBI)	$\text{IC}_2\text{H}_3\text{LPb}$		technically pure	20 40 60 80 100 120 140	+	+	-	+	+	+	O	+	+	O	+
Tetrahydrofurane	$\text{C}_4\text{H}_8\text{O}$	66	technically pure	20 40 60 80 100 120 140	-	-	-	O	O	-	O	-	-	-	-
Tetrahydronaphthalene	Tetralin	207	technically pure												
Thionyl chloride	SOCl_2	79	technically pure	20 40 60 80 100 120 140	-	-	-	-	-	-	O	+	-	-	-
Tin (IV) -chloride				20 40 60 80 100 120 140	+	+				+	+	+	+		

(Courtesy George Fischer Engineering Handbook)

Aggressive Media					Chemical Resistance										
Medium	Formula	Boiling point °C	Concentration	Temperature °C	PVC	CPVC	ABS	PE	PP-H	PVDF (STYGEN)	EPDM	FRM	NBR	CR	CSM
Tin(II) chloride	SnCl ₂			20 40 60 80 100 120 140				++ ++ ++ ++							
Toluene	C ₆ H ₅ -CH ₃	111	technically pure	20 40 60 80 100 120 140	-	-	-	O O O O O O	+		-	+	-	-	-
Triacetin (Glycerintriacetate)	C ₉ H ₁₄ O ₈			20 40 60 80 100 120 140	-	-	-	+	+	+	+				
Tributylphosphate	(C ₄ H ₉) ₃ PO ₄	289	technically pure	20 40 60 80 100 120 140	-	-	-	+	+	+	+	-	-	-	-
Trichloroacetic acid	Cl ₃ C-COOH	196	technically pure	20 40 60 80 100 120 140	O	-	-	+	+	O	O	-	-	-	-
Trichloroacetic acid	Cl ₃ C-COOH		50% aqueous	20 40 60 80 100 120 140	+	O	-	+	+	+	O	-	-	-	-
Trichloroethane	Methylchloroform	74	technically pure					+	+	+	O	-	-	-	-
Trichloroethylene	Cl ₂ C=CHCl	87	technically pure	20 40 60 80 100 120 140	-	-	-	-	O	+	-	+	-	-	-
Trichloromethane	Chloroform	61													

(Courtesy George Fischer Engineering Handbook)

Aggressive Media					Chemical Resistance										
Medium	Formula	Boiling point °C	Concentration	Temperature °C	PVC	CPVC	ABS	PE	PP-H	PVDF (Kynar)	EPDM	FRP	NBR	CR	CSM
Triethyl phosphate (SpRBI)	$H_3C-C_2H_5-O-P(=O)_3$		technically pure	20 40 60 80 100 120 140	-	-	-	+	+		+		-	-	-
Triethanolamine (SpRBI)	$NIH_2CH_2CH_2-OH_3$	Fp. 21	technically pure	20 40 60 80 100 120 140	O	-	-	+	+	+	O	-	O	-	-
Triethylamine (SpRBI)	$NIH_2CH_2CH_3$	89	technically pure	20 40 60 80 100 120 140	-	-	-	+	+	O	-	-	-	-	-
Trifluoroacetic acid (SpRBI)	$F_3C-COOH$		up to 50%	20 40 60 80 100 120 140	-	-	-	+	+	O	O	-	-	-	-
Triacetyl phosphate (SpRBI)	$IC_6H_5PO_4$		technically pure	20 40 60 80 100 120 140	-	-	-	+	+	O	+	-	O	-	-
Turpentine oil (SpRBI)			technically pure	20 40 60 80 100 120 140	+	-	-	O	-	+	-	+	O	-	-
Urea (SpRBI)	$H_2N-CO-NH_2$	Fp. 133	up to 30% aqueous	20 40 60 80 100 120 140	+	+	+	+	+	+	+	+	+	+	+
Urine				20 40 60 80 100 120 140	+	+	+	+	+	+	+	+	+	+	+

(Courtesy George Fischer Engineering Handbook)

Aggressive Media				Chemical Resistance											
Medium	Formula	Boiling point °C	Concentration	Temperature °C	PVC	CPVC	ABS	PE	PPH	PMMA (Styren)	EPDM	FRM	NBR	CR	CSM
Vaseline			technically pure	20 40 60 80 100 120 140	+	+	-	+	+	+	-	+	+	+	-
Vegetable oils				20 40 60 80 100 120 140	+	-	-	+	+	+	-	+	+	+	+
Vegetable oils and fats (SpR3)				20 40 60 80 100 120 140	+	+	-	+	+	+	-	+	+	+	+
Vinegar	see wine vinegar			20 40 60 80 100 120 140	+	+	-	+	+	+	-	+	+	+	+
Vinyl acetate	$\text{CH}_3\text{-CH(OOCCH}_3\text{)}$	73	technically pure	20 40 60 80 100 120 140	-	-	-	+	+	+	+	-	-	-	-
Vinyl chloride	$\text{CH}_2\text{=CHCl}$	-14	technically pure	20 40 60 80 100 120 140	-	-	-	-	+	+	-	+	-	-	-
Viscose spinning solution				20 40 60 80 100 120 140	+	-	-	+	+	+	+	+	-	+	+
Waste gases containing - Alkalies				20 40 60 80 100 120 140	+	+	+	+	+	+	+	+	+	+	+
Waste gases containing - Carbon oxides			oil	20 40 60 80 100 120 140	+	+	+	+	+	+	+	+	+	+	+

(Courtesy George Fischer Engineering Handbook)

Aggressive Media					Chemical Resistance											
Medium	Formula	Boiling point °C	Concentration	Temperature °C	PVC	CPVC	ABS	PE	PP-H	PVDF (50/60/70)	EPDM	FPM	NBR	CR	CSM	
Waste gases containing - Hydrochloric acid			all	20	+	+	+	+	+	+	+	+	+	+	+	
				40	+	+	+	+	+	+	+	+	+	+	+	
				60	+	+	+	+	+	+	+	+	+	+	+	
				80	+	+	+	+	+	+	+	+	+	+	+	
				100	+	+	+	+	+	+	+	+	+	+	+	
				120	+	+	+	+	+	+	+	+	+	+	+	
140	+	+	+	+	+	+	+	+	+	+	+	+	+			
Waste gases containing - Hydrogen fluoride (5pR3)			traces	20	+	+	+	+	+	+	+	+	+	+	+	+
				40	+	+	+	+	+	+	+	+	+	+	+	+
				60	+	+	+	+	+	+	+	+	+	+	+	+
				80	+	+	+	+	+	+	+	+	+	+	+	+
				100	+	+	+	+	+	+	+	+	+	+	+	+
				120	+	+	+	+	+	+	+	+	+	+	+	+
140	+	+	+	+	+	+	+	+	+	+	+	+	+			
Waste gases containing - Nitrous gases			traces	20	+	+	+	+	+	+	+	+	+	+	+	+
				40	+	+	+	+	+	+	+	+	+	+	+	+
				60	+	+	+	+	+	+	+	+	+	+	+	+
				80	+	+	+	+	+	+	+	+	+	+	+	+
				100	+	+	+	+	+	+	+	+	+	+	+	+
				120	+	+	+	+	+	+	+	+	+	+	+	+
140	+	+	+	+	+	+	+	+	+	+	+	+	+			
Waste gases containing - Sulphur dioxide			traces	20	+	+	+	+	+	+	+	+	+	+	+	+
				40	+	+	+	+	+	+	+	+	+	+	+	+
				60	+	+	+	+	+	+	+	+	+	+	+	+
				80	+	+	+	+	+	+	+	+	+	+	+	+
				100	+	+	+	+	+	+	+	+	+	+	+	+
				120	+	+	+	+	+	+	+	+	+	+	+	+
140	+	+	+	+	+	+	+	+	+	+	+	+	+			
Waste gases containing - Sulphur trioxide (5pR3)			traces	20	+	+	+	+	+	+	+	+	+	+	+	+
				40	+	+	+	+	+	+	+	+	+	+	+	+
				60	+	+	+	+	+	+	+	+	+	+	+	+
				80	+	+	+	+	+	+	+	+	+	+	+	+
				100	+	+	+	+	+	+	+	+	+	+	+	+
				120	+	+	+	+	+	+	+	+	+	+	+	+
140	+	+	+	+	+	+	+	+	+	+	+	+	+			
Waste gases containing - Sulphuric acid			all	20	+	+	+	+	+	+	+	+	+	+	+	+
				40	+	+	+	+	+	+	+	+	+	+	+	+
				60	+	+	+	+	+	+	+	+	+	+	+	+
				80	+	+	+	+	+	+	+	+	+	+	+	+
				100	+	+	+	+	+	+	+	+	+	+	+	+
				120	+	+	+	+	+	+	+	+	+	+	+	+
140	+	+	+	+	+	+	+	+	+	+	+	+	+			
Water - distilled - deionised	H ₂ O	100		20	+	+	+	+	+	+	+	+	+	+	+	
				40	+	+	+	+	+	+	+	+	+	+	+	
				60	+	+	+	+	+	+	+	+	+	+	+	
				80	+	+	+	+	+	+	+	+	+	+	+	
				100	+	+	+	+	+	+	+	+	+	+	+	
				120	+	+	+	+	+	+	+	+	+	+	+	
				140	+	+	+	+	+	+	+	+	+	+	+	
Water, condensed				20	+	+	+	+	+	+	+	+	+	+	+	+
				40	+	+	+	+	+	+	+	+	+	+	+	+
				60	+	+	+	+	+	+	+	+	+	+	+	+
				80	+	+	+	+	+	+	+	+	+	+	+	+
				100	+	+	+	+	+	+	+	+	+	+	+	+
				120	+	+	+	+	+	+	+	+	+	+	+	+
140	+	+	+	+	+	+	+	+	+	+	+	+	+			

(Courtesy George Fischer Engineering Handbook)

Aggressive Media					Chemical Resistance										
Medium	Formula	Boiling point °C	Concentration	Temperature °C	PVC	CPVC	ABS	PE	PPH	PVDF (SYGEE)	EPDM	FRM	NBR	CR	CSM
Water, drinking, chlorinated				20 40 60 80 100 120 140	++ ++ ++ ++ ++ ++ ++	++ ++ ++ ++ ++ ++ ++	++ ++ ++ ++ ++ ++ ++	++ ++ ++ ++ ++ ++ ++	++ ++ ++ ++ ++ ++ ++	++ ++ ++ ++ ++ ++ ++	++ ++ ++ ++ ++ ++ ++	++ ++ ++ ++ ++ ++ ++	++ ++ ++ ++ ++ ++ ++	++ ++ ++ ++ ++ ++ ++	++ ++ ++ ++ ++ ++ ++
Water, waste water without organic solvent and surfactants				20 40 60 80 100 120 140	++ ++ ++ ++ ++ ++ ++	++ ++ ++ ++ ++ ++ ++	++ ++ ++ ++ ++ ++ ++	++ ++ ++ ++ ++ ++ ++	++ ++ ++ ++ ++ ++ ++	++ ++ ++ ++ ++ ++ ++	++ ++ ++ ++ ++ ++ ++	++ ++ ++ ++ ++ ++ ++	++ ++ ++ ++ ++ ++ ++	++ ++ ++ ++ ++ ++ ++	++ ++ ++ ++ ++ ++ ++
Wax alcohol (Sp88)	C ₁₁ H ₂₃ OH		technically pure	20 40 60 80 100 120 140	++ ++ ++ ++ ++ ++ ++	++ ++ ++ ++ ++ ++ ++	++ ++ ++ ++ ++ ++ ++	++ ++ ++ ++ ++ ++ ++	++ ++ ++ ++ ++ ++ ++	++ ++ ++ ++ ++ ++ ++	++ ++ ++ ++ ++ ++ ++	++ ++ ++ ++ ++ ++ ++	++ ++ ++ ++ ++ ++ ++	++ ++ ++ ++ ++ ++ ++	++ ++ ++ ++ ++ ++ ++
Wine vinegar (Sp88)			usual commercial	20 40 60 80 100 120 140	++ ++ ++ ++ ++ ++ ++	++ ++ ++ ++ ++ ++ ++	++ ++ ++ ++ ++ ++ ++	++ ++ ++ ++ ++ ++ ++	++ ++ ++ ++ ++ ++ ++	++ ++ ++ ++ ++ ++ ++	++ ++ ++ ++ ++ ++ ++	++ ++ ++ ++ ++ ++ ++	++ ++ ++ ++ ++ ++ ++	++ ++ ++ ++ ++ ++ ++	++ ++ ++ ++ ++ ++ ++
Wines, red and white			usual commercial	20 40 60 80 100 120 140	++ ++ ++ ++ ++ ++ ++	++ ++ ++ ++ ++ ++ ++	++ ++ ++ ++ ++ ++ ++	++ ++ ++ ++ ++ ++ ++	++ ++ ++ ++ ++ ++ ++	++ ++ ++ ++ ++ ++ ++	++ ++ ++ ++ ++ ++ ++	++ ++ ++ ++ ++ ++ ++	++ ++ ++ ++ ++ ++ ++	++ ++ ++ ++ ++ ++ ++	++ ++ ++ ++ ++ ++ ++
Xylene	C ₆ H ₄ (CH ₃) ₂	138.7 144	technically pure	20 40 60 80 100 120 140	++ ++ ++ ++ ++ ++ ++	++ ++ ++ ++ ++ ++ ++	++ ++ ++ ++ ++ ++ ++	++ ++ ++ ++ ++ ++ ++	++ ++ ++ ++ ++ ++ ++	++ ++ ++ ++ ++ ++ ++	++ ++ ++ ++ ++ ++ ++	++ ++ ++ ++ ++ ++ ++	++ ++ ++ ++ ++ ++ ++	++ ++ ++ ++ ++ ++ ++	++ ++ ++ ++ ++ ++ ++
yeasts			oil, aqueous	20 40 60 80 100 120 140	++ ++ ++ ++ ++ ++ ++	++ ++ ++ ++ ++ ++ ++	++ ++ ++ ++ ++ ++ ++	++ ++ ++ ++ ++ ++ ++	++ ++ ++ ++ ++ ++ ++	++ ++ ++ ++ ++ ++ ++	++ ++ ++ ++ ++ ++ ++	++ ++ ++ ++ ++ ++ ++	++ ++ ++ ++ ++ ++ ++	++ ++ ++ ++ ++ ++ ++	++ ++ ++ ++ ++ ++ ++
Zinc salts	ZnCl ₂ , ZnCO ₃ , Zn(NO ₃) ₂ , ZnSO ₄		oil, aqueous	20 40 60 80 100 120 140	++ ++ ++ ++ ++ ++ ++	++ ++ ++ ++ ++ ++ ++	++ ++ ++ ++ ++ ++ ++	++ ++ ++ ++ ++ ++ ++	++ ++ ++ ++ ++ ++ ++	++ ++ ++ ++ ++ ++ ++	++ ++ ++ ++ ++ ++ ++	++ ++ ++ ++ ++ ++ ++	++ ++ ++ ++ ++ ++ ++	++ ++ ++ ++ ++ ++ ++	++ ++ ++ ++ ++ ++ ++

(Courtesy George Fischer Engineering Handbook)

Aggressive Media				Chemical Resistance											
Medium	formula	Boiling point °C	Concentration	Temperature °C	PVC	CPVC	ABS	PE	PP-H	PVDF (CYOTE)	EPDM	FKM	NBR	CR	CSM
Zinc carbonate				20	+	+	+	+	+	+	+	+	+		
				40	+	+	+	+	+	+	+	+	+		
				60	+	+	+	+	+	+	+	+	+		
				80	+	+	+	+	+	+	+	+	+		
				100	+	+	+	+	+	+	+	+	+		
				120	+	+	+	+	+	+	+	+	+		
				140	+	+	+	+	+	+	+	+	+		
Zinc chloride			saturated	20	+	+	+	+	+	+	+	+	+		
				40	+	+	+	+	+	+	+	+	+		
				60	+	+	+	+	+	+	+	+	+		
				80	+	+	+	+	+	+	+	+	+		
				100	+	+	+	+	+	+	+	+	+		
				120	+	+	+	+	+	+	+	+	+		
				140	+	+	+	+	+	+	+	+	+		
Zinc nitrate	$Zn(NO_3)_2$		saturated	20	+	+	+	+	+	+	+	+	+		
				40	+	+	+	+	+	+	+	+	+		
				60	+	+	+	+	+	+	+	+	+		
				80	+	+	+	+	+	+	+	+	+		
				100	+	+	+	+	+	+	+	+	+		
				120	+	+	+	+	+	+	+	+	+		
				140	+	+	+	+	+	+	+	+	+		
Zinc oxide			Suspension	20						+					
				40						+					
				60						+					
				80						+					
				100						+					
				120						+					
				140						+					
Zinc phosphate			saturated	20	+	+	O	+	+	+	+	+	+		
				40	+	+		+	+	+	+	+	+		
				60	+	+		+	+	+	+	+	+		
				80	+	+		+	+	+	+	+	+		
				100	+	+		+	+	+	+	+	+		
				120	+	+		+	+	+	+	+	+		
				140	+	+		+	+	+	+	+	+		
Zinc stearate			Suspension	20	-	-	-	+	+	+	+	O			
				40				+	+	+	+				
				60				+	+	+	+	+			
				80				+	+	+	+	+			
				100				+	+	+	+	+			
				120				+	+	+	+	+			
				140				+	+	+	+	+			
Zinc sulfate	$ZnSO_4$			20	+	+		+	+	+	+	+	+		
				40	+	+		+	+	+	+	+	+		
				60	+	+		+	+	+	+	+	+		
				80	+	+		+	+	+	+	+	+		
				100	+	+		+	+	+	+	+	+		
				120	+	+		+	+	+	+	+	+		
				140	+	+		+	+	+	+	+	+		
1-Chloropentane	$C_5H_{11}Cl$			20	-	-	-	-	-	-	-	-	-		
				40	-	-	-	-	-	-	-	-	-		
				60	-	-	-	-	-	-	-	-	-		
				80	-	-	-	-	-	-	-	-	-		
				100	-	-	-	-	-	-	-	-	-		
				120	-	-	-	-	-	-	-	-	-		
				140	-	-	-	-	-	-	-	-	-		

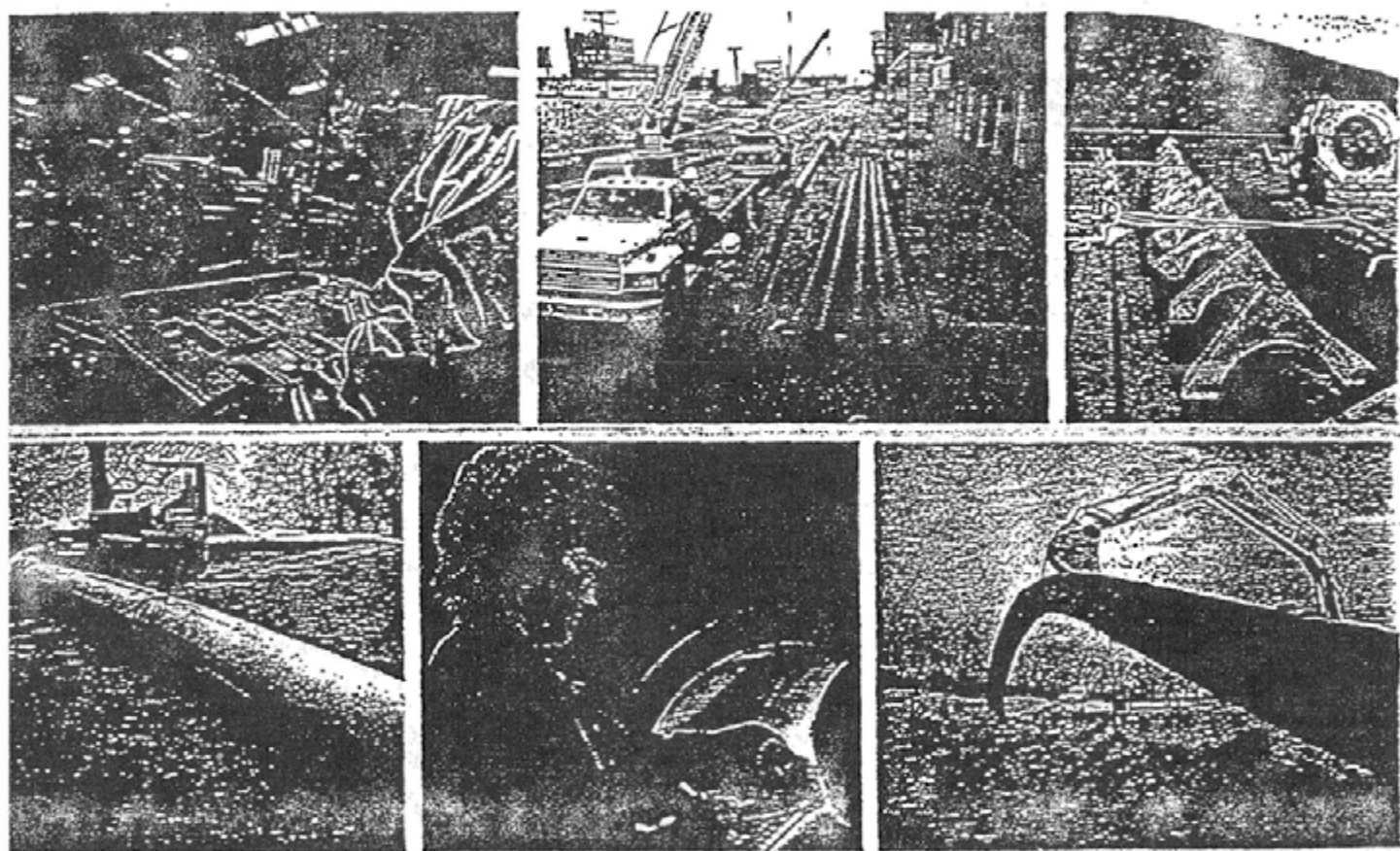
(Courtesy George Fischer Engineering Handbook)

Aggressive Media					Chemical Resistance										
Medium	Formula	Boiling point °C	Concentration	Temperature °C	PVC	CPVC	ABS	PE	PPH	PVDF (KRYDEX)	EPDM	PPM	NBR	CR	CSM
1,1,2-Trifluoro, 1,2,2-Tetrachloroethane (Freon 113) (SpR)	$\text{CF}_3\text{C}-\text{CCl}_2$	47	technically pure	20 40 60 80 100 120 140	+	+	-			+		+	+	+	+

(Courtesy George Fischer Engineering Handbook)

DRISCOPIPE

Engineering Characteristics



STOCKING DISTRIBUTORS OF FINE UTILITY PRODUCTS

IRRIGATION SUPPLY CO., INC.

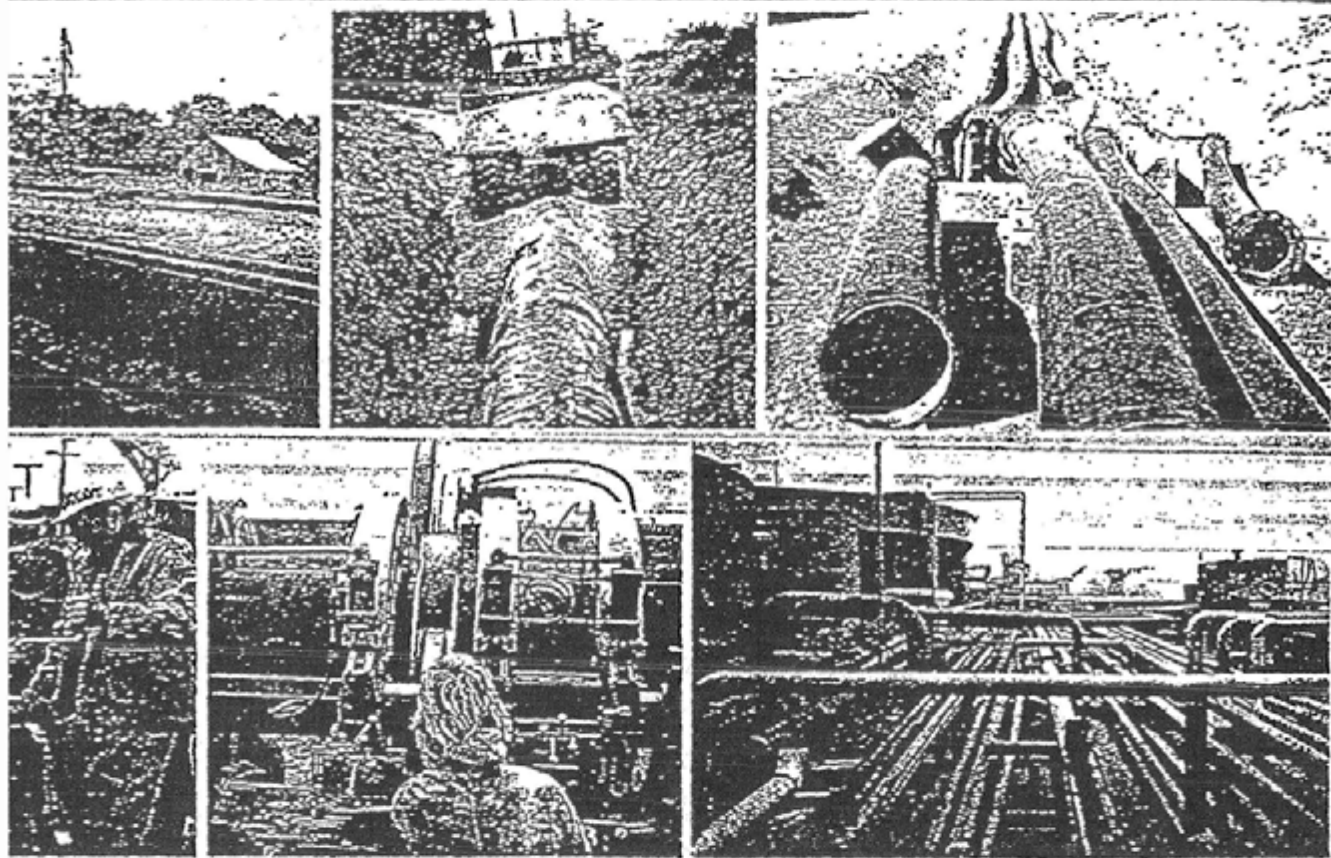
926 BAXTER AVE. P. O. BOX 4545
LOUISVILLE, KY. 40204

502 — 583-6591



Contents

Introduction	1	Chemical Corrosion Resistance	8
Physical Properties	1	Temperature Characteristics	11
Long Term Strength	1	Weatherability	14
Design Pressure Ratings	3	Permeability	14
Flow Characteristics	4	Abrasion Resistance	15
Lightweight—Flexible	4	Heat Fusion Joining Method	16
Toughness—"Ductile PE Pipe"	5	Fatigue Resistance	17
Environmental Stress Crack Resistance	7	Photographs shown are typical Dinscope installations.	



Driscopipe® Engineering Characteristics

Introduction

Driscopipe high density polyethylene piping systems offer the modern engineer the opportunity to take advantage of the unusual characteristics of these materials and use them to solve many old problems and to design systems for applications where traditional materials are either unsuitable or too expensive. When compared to the older traditional piping materials, Driscopipe polyethylene piping systems offer a new freedom in environmental design, extended service life, significant savings for installation labor and equipment costs, and reduced maintenance for pipeline systems where operating conditions are within the pressure and temperature capabilities of the material.

This brochure outlines the Engineering Characteristics of Driscopipe high density polyethylene pipe and fittings and points out many of the advantages and benefits to be realized through the use of these systems. The discussion is directed primarily toward the large diameter (3" through 54") Driscopipe 8600 and Driscopipe 1000 Industrial and Municipal product lines. However, these engineering characteristics are also typical of other Driscopipe polyethylene product lines.

Physical Properties

Driscopipe 8600 is manufactured from Marlex M-8000 very high molecular weight high density PE 3408 resin. Pipe and fittings made from Marlex M-8000 are extremely tough and durable, and possess exceptional long term strength. Marlex M-8000 is a proprietary product and is extruded only by Phillips Driscopipe, Inc.

Driscopipe 1000 is manufactured from Marlex TR-480, a PE 3408 polyethylene pipe resin in a molecular weight range which permits the pipe to be extruded by conventional methods. In this respect, Driscopipe 1000 is comparable to other extra high molecular weight, high density, PE 3408 polyethylene pipes commercially available in North America.

Sheets detailing typical physical properties for Driscopipe 1000 and Driscopipe 8600 are available upon request.

Long Term Hydrostatic Strength

One of the outstanding engineering characteristics of Driscopipe high density polyethylene pipe is its long term hydrostatic strength under various thermal and environmental conditions. Life expectancy is conservatively estimated to be in excess of 50 years using the standard design basis. This strength is determined by standardized methods and procedures which the plastic pipe industry has used for many years to evaluate the long term strength of all types of plastic pipe.

Pipe hoop stress versus time to failure plots of long term hydrostatic pressure data for thermoplastic pipe have been studied and analyzed for many years. The mathematical equations used to evaluate the test data and extrapolate values to longer periods of time were chosen after careful evaluation of more than 1,000 sets of long term test data representing more than 400 plastic pipe compounds. Continued testing on new compounds and extended testing of older compounds have proven the validity of these test methods. Actual data from more than 11½ years (100,000 hours) of continuous testing shows the industry methods to be slightly conservative in that actual values are slightly higher than those calculated by the industry-accepted ASTM method.

The reduction in strength which occurs with time, as indicated by the stress-life curves, does not represent a strength degradation of the material but is more in the nature of a relaxation effect. Plastic pipe samples which have been on test for periods up to 70,000 hours have been de-pressurized and checked for permanent reduction of strength by using the quick-burst test. No loss has been found when compared to samples previously quick-burst from the same test lot.

All evidence confirms that the methods used to predict the long term strength of plastic pipe are sound methods. Through the years, these policies and procedures, used to develop recommended hydrostatic design strengths, have influenced manufacturers to research and develop improved piping products such as Driscopipe 8600 and Driscopipe 1000.

Typical calculated long term strengths are shown below:

Long Term Strength @ 73.4°F(23°C)

Time	Hoop Stress, psi
100,000 hrs. (11.43 yrs.)	1635
438,000 hrs. (50 yrs.)	1604
500,000 hrs. (57 yrs.)	1601
1,000,000 hrs. (114 yrs.)	1586

The 114-year long term strength has been included to show more about the nature of the method used by the industry to evaluate the long term strength of plastic pipe and to illustrate the very slow reduction in strength as time progresses.

Long term hoop stresses for design purposes are normally selected at a level which is much lower than the long term strength of the materials. This ensures that the pipe is operating in a hoop stress range where creep (relaxation) of the materials is nil and assures service life in excess of 50 years. Design stress levels are discussed further in the next section.

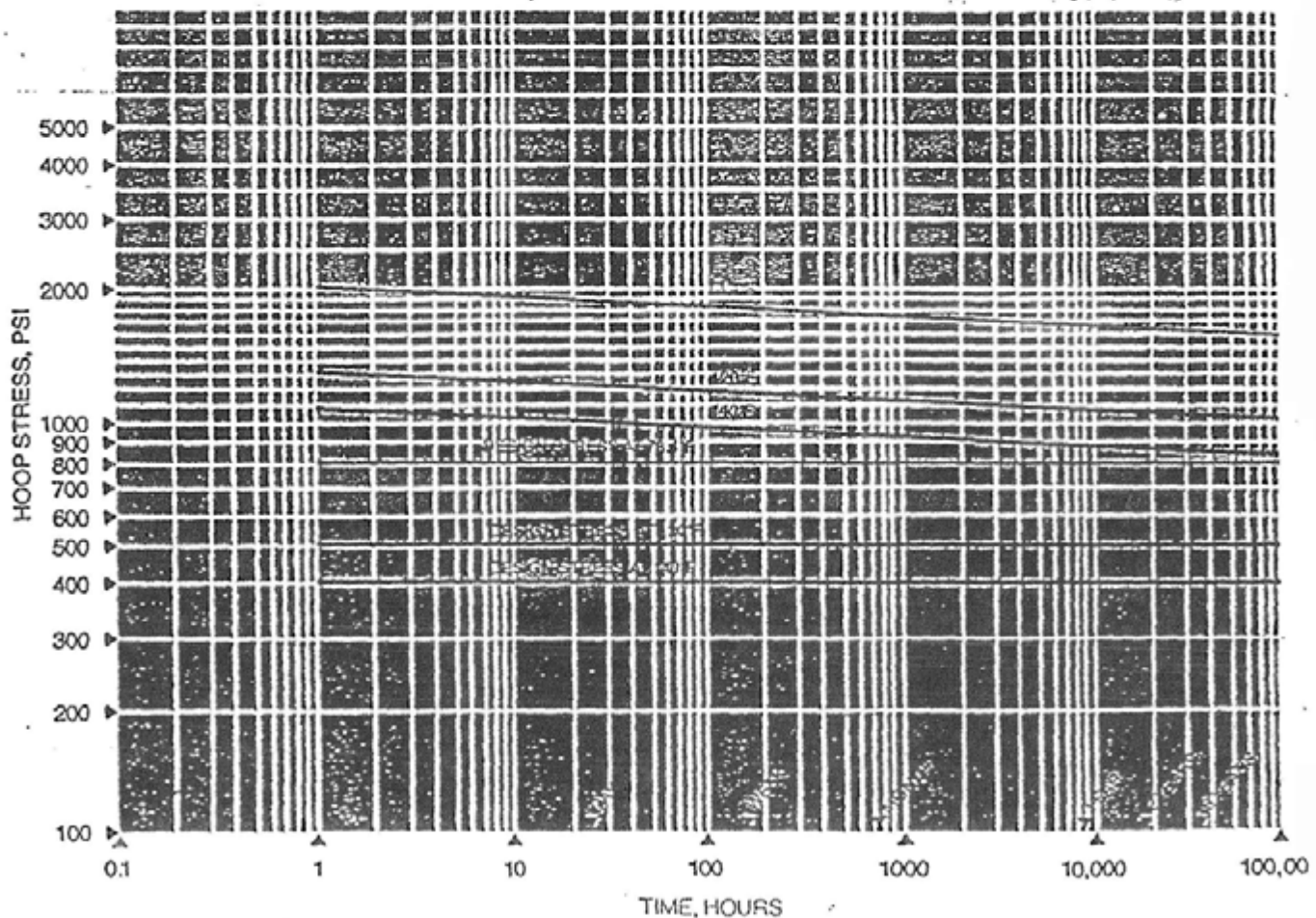
The long term hydrostatic tests are conducted by using ASTM standard test procedures which may be applied to all types of plastic pipe (ASTM D 1598 Test for Time-to-Failure of Plastic Pipe Under Constant Internal Pressure). Stress-life tests are conducted by using numerous pipe samples which are filled with water (or other environmental fluids) and subjected to a controlled pressure at a controlled temperature.

Samples are held on test until they fail. The pressure, temperature and time-to-failure data from all samples are used to calculate and plot stress-life curves for the particular type pipe being tested (ASTM D 2837 Obtaining Hydrostatic Design Basis for Thermoplastic Pipe Materials). This data is then used to predict the probable safe life of the pipe at various stress levels (working pressures) and various temperatures. Because it is not practical to test at all temperature levels, these tests are generally conducted at temperatures of 73.4°F and one or more higher temperatures such as 100°F, 120°F and 140°F.

These stress-life curves give a relationship of the expected life span of the pipe when subjected to various internal stress levels (working pressures) at various temperatures. By comparing stress-life curves, one can compare relative long term performance ability of different plastic pipes. Stress-life curves for Driscopipe 8600 and Driscopipe 1000 are shown in Figure 1.

Figure 1

Stress-Life of Driscopipe® 8600 and Driscopipe® 1000



These stress-life curves were obtained using water as the test medium. However, years of laboratory testing and field experience have shown that these same curves may be used to design Driscopipe systems for natural gas, salt water, sewage and hundreds of other industrial and municipal fluids, mixtures and effluents. The long term strength of Driscopipe indicated by these curves must be de-rated in some environmental circumstances, such as in the presence of liquid hydrocarbons or abrasive fluids, although the pipe is very suitable for use in these environments. An outstanding engineering advantage of Driscopipe is its exceptionally long term service life in the presence of internal and external corrosive service conditions.

Design Pressure Ratings

Since plastic pipe was introduced in the late 50s, the safety factor for design of water systems at standard temperature has been 2 to 1. The 2:1 design factor which was officially adopted by the plastic pipe industry in 1963, was based on allowances for many sources of variation. The guiding principle has always been to make the selection on a conservative basis but not to be unreasonably conservative.

The sources of variation for which allowances are made include ... variation in test methods and procedures among laboratories ... variation among lots of the same compound ... variation of lots of pipe from the compound in different plants and from different extruders ... variation in compounds of the same general class ... variations in handling and installation techniques ... variation in operating pressures (water hammer and surge) ... a strength-time allowance to give service life well beyond 50 years ... and, finally, the great unknown. Each of the

factors was judged to reduce the 100,000 hour design strength by 5%-10% or 20% ... for a total of 100% ... or a design factor of 2:1. This is why polyethylene pipe, with a designated 100,000 hour strength of 1600 psi at 73.4°F, has a hydrostatic design strength of 800 psi hoop stress.

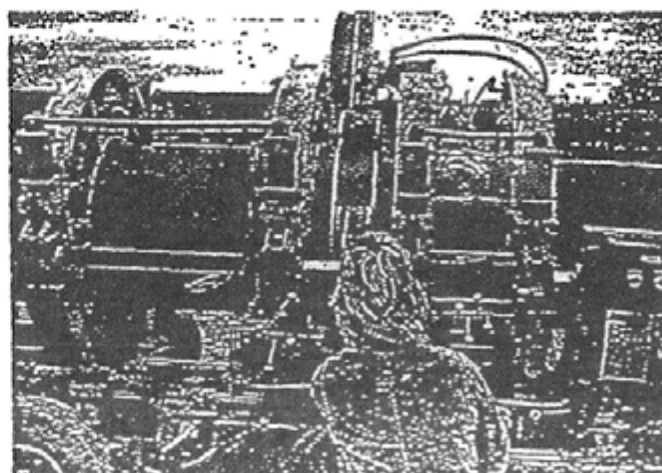
The design pressures for Driscopipe are determined by the following equation, adopted internationally by the industry for this purpose:

$$P = \frac{2S}{SDR-1} \times F \quad \text{or} \quad P = 2S \frac{t}{D-t} \times F$$

Where: D = Specified Outside Diameter, Inches
P = Design Pressure, psi
S = Long Term Hydrostatic Strength, psi, at the design temperature
t = Minimum Wall Thickness, Inches
F = Service Design Factor
SDR = Standard Dimension Ratio of D/t

The traditional Service Design Factor for water at standard temperature (73.4°F) is one-half (.5). The Service Design Factor for oil or liquid hydrocarbons is 0.25 @ 73°F. The service design factor may be adjusted by the design engineer to reflect the particular conditions anticipated for the application. The temperature selected for design should consider both internal and external conditions. The design temperature should be based on the temperature of the pipe itself. For practical purposes, it is safer to design to the highest temperature.

The design service factor for water may also be used for solutions of inorganic salts, alkaline fluids, non-oxidizing acids, low concentrations of oxidizing acids and many other solutions. See the discussion on chemical resistance for more information.



All standard design pressure ratings shown in Driscopipe literature are based on water at 73.4°F temperature; ie, a safety factor of 2:1 based on the long term hydrostatic strength of the material. Driscopipe is applicable at pressures from 0 to 265 psi and temperatures from below 32°F up to 180°F. Standard Dimension Ratios (SDR) are available from SDR 32.5 to SDR 7.0

Flow Characteristics

Driscopipe polyethylene has excellent flow characteristics as compared to traditional materials. An extremely smooth interior surface offers low resistance to flow. It maintains these excellent flow properties throughout its service life in most applications due to the inherent chemical and abrasion resistance of the material. Because of smooth walls and the non-wetting characteristic of polyethylene, higher flow capacity and less friction loss is possible with Driscopipe. In many cases this higher flow capacity may permit the use of smaller pipe at a lower cost.

A "C" factor of 155 is commonly used in the Hazen-Williams formula for calculating flow in pressure applications. For gravity flow, an "n" factor of .009 is used in Manning's formula.

Experimental test data regarding pumping and pressure drop through Driscopipe is available upon request. This study compares the flow through 8" Driscopipe with and without internal fusion beads using clear water. It also includes flow data for some clay-water slurries and clay-water-sand slurries. Velocities up to 20 fps are studied. Data includes determination of Hazen-Williams "C" factor, Reynolds number, boundary drag, relative roughness, sand grain roughness and friction loss at various velocities.

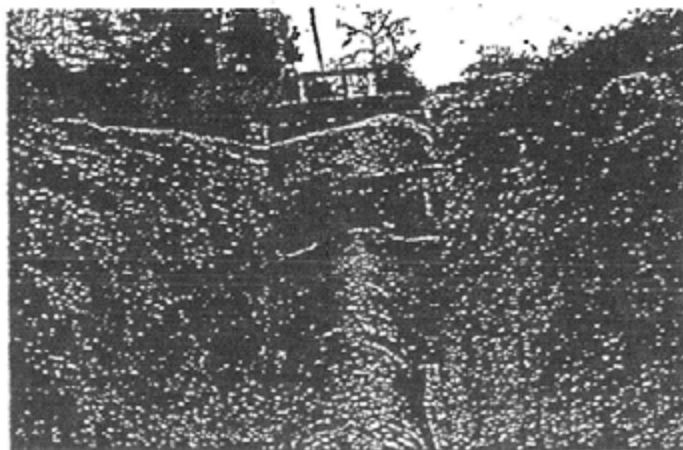
Lightweight - Flexible

The inherent light weight and flexibility of Driscopipe provides many cost saving benefits related to handling, storage, hauling, unloading, stringing, joining and installation. Because of its light weight, Driscopipe can be moved, handled and placed in the ditch with smaller and less expensive construction equipment. Usually, manpower requirements are also reduced.

Driscopipe weighs less than water; it has a specific gravity of .955-.957. Because it will float, it can be joined in long strings and easily towed into position on job sites where water is encountered. The combination of light weight and flexibility provides opportunity to fusion join the pipe in a convenient work area and pull it into position in difficult work areas where terrain or other obstacles present installation problems. The pipe can be joined above ground and rolled or lowered into the trench thus allowing the use of smaller trench widths and eliminating the necessity of placing men and equipment inside the trench. Such installation methods can dramatically reduce the time required for installation in many instances.

The flexibility of Driscopipe allows it to be curved over, under and around obstacles and to make elevation and directional changes, thus eliminating fittings and reducing installation costs. The pipe can be cold bent as it is installed to a radius of 20-40 times the pipe diameter. This flexibility and the butt fusion joining method make Driscopipe ideally suited for inserting it inside older piping systems to renew and renovate such systems at a much lower cost than would be possible otherwise.

Pipe flexibility and toughness also allow small diameter Driscopipe to be plowed-in or pulled-in with suitable equipment.



Toughness — "Ductile PE Pipe"

Overall "toughness" of Driscopipe is an important characteristic of the pipe which is derived from many of the chemical and physical properties of the material as well as the extrusion method. The pipe is ductile. It flexes, bends and absorbs impact loads over a wide temperature range of -180°F up to $+180^{\circ}\text{F}$. This inherent resiliency and flexibility allow the pipe to absorb surge pressures, vibration and stresses caused by soil movement. Driscopipe can be deformed without permanent damage and with no adverse effect on long term service life. It is flexible for contouring to installation conditions. The toughness of Driscopipe is one of its outstanding engineering characteristics leading to innovative piping design.

Even though "toughness" has become generally recognized by the industry as a highly desirable characteristic ... there is no standard test which can be used to directly compare the "toughness" among polyethylenes ... as well as among the different plastic materials which are considered suitable for piping.

A "toughness" test has not been devised simply because it is influenced by so many of the physical and chemical properties of the material. The extreme toughness of Driscopipe has been noted as one of its outstanding features since its introduction to the industry ... yet to explain "toughness", many properties are discussed and demonstrated. To obtain a complete evaluation of the toughness of a plastic material, it is necessary to see demonstrations

of tests and to conduct some tests in person in order to compare it with materials which are more familiar, such as cast iron, steel, cement, copper, etc.

Toughness is related to ... Environmental Stress Crack Resistance (ESCR) ... Notch sensitivity ... Resistance to secondary stresses from external loading ... Impact strength ... Tear strength ... Flexibility ... Kink resistance ... Abrasion and scratch resistance ... Flexural strength ... Elongation ... Chemical resistance ... Tensile strength ... Ductility ... Creep resistance ... Temperature resistance ... Density ... Molecular weight ... and the thermoplastic nature of the material. Part of the toughness of any polyethylene material can be attributed to its flexibility, flexural strength and impact resistance as compared to the more rigid thermoplastic materials such as PVC. Polyethylene is ductile and will elongate many times more than PVC. Consequently, it will absorb more impact without damage or failure. PE will flex or elongate and stress relieve itself rather than rupture. Generally, impact strength is greater for the higher molecular weight PE resins. Impact resistance is also important from the standpoint of a piping system being able to absorb energy imposed on it by external forces.

The expansive force of water freezing inside Driscopipe will not damage it.

ESCR is one of the properties closely related to "toughness" and has been studied as a possible means to define and measure toughness. The exceptional resistance of Driscopipe 8600 to environmental stress cracking as compared to other PE materials is discussed further in the next section.



Driscopipe 8600 is unique and differs from Driscopipe 1000 and from all other polyethylene pipes. Driscopipe 8600 exhibits a superior toughness which gives the pipe the highest impact strength, highest tear strength and lowest notch sensitivity of any polyethylene pipe currently available. Driscopipe 8600 offers the highest resistance to cuts, scratches and abrasions which occur when handling and installing the pipe.

These properties are maintained throughout its temperature range without a loss of ductility or reduced resistance to notch sensitivity. Driscopipe has been successfully installed in numerous arctic applications. Some of these applications have included direct burial in the unstable arctic permafrost.

To learn more of the relative toughness of Driscopipe 8600, we encourage you to take a piece of pipe with a butt fusion joint and try to tear it up without using sharp tools. Pound it flat with a sledge hammer ... slam it against a corner of angle iron ... run over it with a truck ... then do the same with steel, copper, PVC, cast iron and the less rugged PEs. It's not very scientific ... but we believe you'll be convinced that Driscopipe 8600 has extremely high toughness. We have evaluated Driscopipe many times in laboratory and field test experiments to demonstrate and prove this toughness.

- One excellent indicator of the relative toughness of Driscopipe 8600, as compared to other polyethylene pipe materials, can be observed in the ASTM Standard Test for determination of flow rate of the thermoplastic materials.

When Driscopipe 8600 is heated to 190°C (374°F) to measure the flow rate, it requires 432.5 pounds/sq. in. force, applied for 10 minutes, to flow 1½ grams of 8600 material through the orifice of the test unit! Other commercially available polyethylene pipe materials will flow 10 to 20 times this amount under the same conditions.

- When Driscopipe 8600 is heated to 475-500°F to melt it for fusion joining, it requires 150 pounds pressure per square inch of material to make the melted surfaces flow together. This is another indicator of toughness. Other commercially available polyethylene pipe materials require about one-half that amount of pressure and some competitive pipes require less than 25 psi!
- Driscopipe 8600 has been pressure tested for long periods at temperatures up to 140°F and performance requirements at these high temperatures can be used in purchase specifications to assure that the user is getting the highest performing polyethylene pipe.



Environmental Stress Crack Resistance

The most recent ASTM specification written to identify polyethylene plastic pipe and fittings materials is ASTM D 3350, "Polyethylene Plastics Pipe and Fittings Materials", adopted in 1974. This specification uses six (6) properties to classify PE material ... one of these is ESCR.

ASTM D 3350 lists three cell limits for ESCR classification which use the ESCR test outlined in ASTM D 1693, Test Method for Environmental Stress Cracking of Ethylene Plastics. The cell limits are:

Cell Classification Limit	Test Condition ASTM D 1693	Test Duration Hours	Percent of Failures Allowed	Test Temp. °C
1	A	48	50	50°
2	B	24	50	50°
3	C	192	20	100°

Minimum Notch for A is .020"; for B and C is .012". Minimum Thickness for A is .120"; for B and C is .070". A and B use a diluted aqueous solution reagent, C uses full strength reagent.

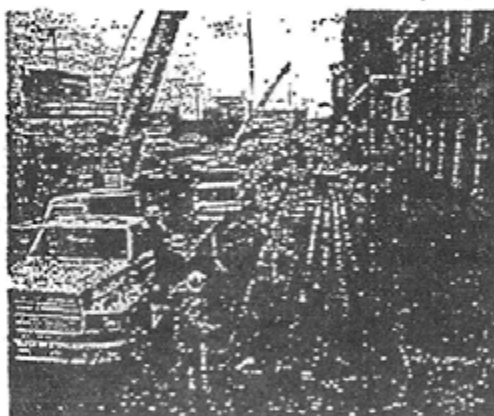
This method of testing for ESCR was first written in 1959 and was developed primarily to evaluate polyethylene as a jacketing material for power and communications cable. Although the method requires the use of laboratory compression molded specimens rather than pipe, it became the generally accepted method for evaluating ESCR of PE materials used for piping. Its wide use was responsible for its inclusion in ASTM D 3550 to describe one of the six primary properties of a PE pipe material.

The test method, ASTM D-1693, is an accelerated test method to determine the resistance of a polyethylene material to environmental stress cracking. It is a measure of the ability of the polyethylene to withstand secondary stress loadings. These loadings are typically thought of as low-level, long-term, external stresses which may act upon the polyethylene pipe in field installations.

Under conditions of the test, high local multiaxial stresses are developed through the introduction of a controlled imperfection (notch). The notched sample is subjected to an elevated temperature bath of a surface active agent. Environmental stress cracking has been found to occur most readily under such conditions.

A note in the test specifications states that, generally, low density (Type I) polyethylenes are tested under Condition A, medium and high density (Type II and Type III) polyethylenes are generally tested under Condition B and high density resins with high melt viscosity, such as pipe grade P34, are tested under Condition C.

As pipe grade polyethylenes have improved, the testing requirements of ASTM D-1693 have become less stringent for P34 pipe grade polyethylenes such as Driscopipe 8600 and Driscopipe 1000. As a result, a more severe stress crack resistance test has been developed to evaluate high density polyethylene pipe. The ASTM F-1248 stress crack resistance test method was developed by a gas distribution company for quality control purposes and is often referred to as Ring ESCR since it tests actual produced pipe ring samples rather than molded specimens.



ASTM F-1248 utilizes rings cut from a pipe sample. The rings are notched on one side and compressed between parallel plates until the distance between the plates is three times the specified pipe minimum wall thickness. The compressed ring samples are subjected to an elevated temperature bath of a surface active agent and visibly inspected for crack formation or propagation.

The Ring ESCR test provides useful information regarding the different polyethylene pipe grade materials. Driscopipe 8600 shows no tendency for sample failures when tested in excess of 10,000 hours. This further reinforces the unique ability of Driscopipe 8600 to provide the highest degree of resistance to the external stresses inherent to a pipeline installation.

Driscopipe 1000, an extra high molecular weight HDPE pipe, will exhibit a ring ESCR of $F_{50} > 1000$ hours. Other lower molecular weight pipes may exhibit lower F_{50} values.

Chemical Corrosion Resistance

The outstanding resistance of Driscopipe to attack by most chemicals makes it suitable to transport these chemicals or to be installed in an environment where these chemicals are present. Factors which determine the suitability and service life of each particular application include the specific chemical and its concentration, pressure, temperature, period of contact and service conditions which may introduce stress concentrations in the pipe or fittings.

Driscopipe is, for all practical purposes, chemically inert within its temperature use range. This advantageous engineering characteristic is one of the primary reasons for the wide use of Driscopipe in industrial applications. It does not rot, rust, pit, corrode or lose wall thickness through chemical or electrical reaction with the surrounding soil, whether acid, alkaline, wet or dry. It neither supports the growth of, nor is affected by, algae, bacteria or fungi and is resistant to marine biological attack. It contains no ingredients which make it attractive to rodents, gophers, etc.

Information relative to the resistance of Driscopipe to a wide range of chemicals is shown in the following tables. This information is based on results of immersion tests (usually 3 months) at various temperatures. Changes in tensile strength and elongation are evaluated at a rapid strain rate to emphasize any strength decay in the material.

Most acids, bases and other chemicals can be transported by Driscopipe using the same design parameters as would apply to water, natural or manufactured gas and water solutions of inorganic salts. Strong oxidizing agents such as fuming sulfuric acid may adversely affect the pipe, depending upon concentration, temperature and period of contact. In many cases, such as gravity flow waste lines, these chemicals can be handled because of dilution and intermittent flow.

Some chemicals, such as all types of liquid hydrocarbons, will mechanically absorb into the wall of the pipe and cause a reduction in hoop stress but this does not degrade the material. This effect is temporary if exposure is intermittent. Where exposure is continuous, it is necessary to derate the pressure capability of the pipe for long term service. This includes such products as gasoline, ethyl alcohol, benzene, carbon tetrachloride, crude and refined oils, etc. Where 5-100% hydrocarbon liquids are continuously present in a pressure system, a service design factor of .25 should be used to calculate design pressures instead of the service design factor of .5 used with water.

$$P = \frac{2S}{SDR-1} \times F \quad \text{or} \quad P = 2S \frac{t}{D-t} \times F$$

Where: D = Outside Diameter, Inches
P = Design Pressure, psi
S = Long Term Hydrostatic Strength, psi, at the design temperature
t = Minimum Wall Thickness, Inches
F = Service Design Factor
SDR = Standard Dimension Ratio of D/t



CHEMICAL RESISTANCE OF DRISCOPE

S – Satisfactory
U – Unsatisfactory
M – Marginal
N – Not known

All concentrations are 100% unless noted otherwise.

On reagents marked marginal, chemical attack will be recognized by a loss of physical properties of the pipe which may require a change in design factors.

Reagent	70°F (21°C)	140°F (60°C)	Reagent	70°F (21°C)	140°F (60°C)
Acetic Acid 1-10%	S	S	Boric Acid Conc.	S	S
Acetic Acid 10-60%	S	M	Bromic Acid 10%	S	S
Acetic Acid 80-100%	S	M	Bromine Liquid 100%	M	U
Acetone	M	U	Butanediol 10%	S	S
Acrylic Emulsions	S	S	Butanediol 60%	S	S
Aluminum Chloride-Dilute	S	S	Butanediol 100%	S	S
Aluminum Chloride Conc.	S	S	Butyl Alcohol 100%	S	S
Aluminum Fluoride Conc.	S	S	Calcium Bisulfide	S	S
Aluminum Sulfate Conc.	S	S	Calcium Carbonate Sattd	S	S
Amms (All Types) Conc.	S	S	Calcium Chlorate Sattd	S	S
Ammonia 100% Dry Gas	S	S	Calcium Chloride Sattd	S	S
Ammonium Carbonate	S	S	Calcium Hydroxide	S	S
Ammonium Chloride Sattd	S	S	Calcium Hypochlorite BLGH Sol.	S	S
Ammonium Fluoride 20%	S	S	Calcium Nitrate 50%	S	S
Ammonium Hydroxide 0.88 S.G.	S	S	Calcium Sulfate	S	S
Ammonium Metaphosphate Sattd	S	S	Camphor Oil	N	U
Ammonium Nitrate Sattd	S	S	Carbon Dioxide 100% Dry	S	S
Ammonium Persulfate Sattd	S	S	Carbon Dioxide 100% Wet	S	S
Ammonium Sulfate Sattd	S	S	Carbon Dioxide Cold Sattd	S	S
Ammonium Thiocyanate Sattd	S	S	Carbon Disulfide	N	U
Amyl Acetate	M	U	Carbon Monoxide	S	S
Amyl Alcohol 100%	S	S	Carbon Tetrachloride	M	U
Amyl Chloride 100%	N	U	Carbonic Acid	S	S
Aniline 100%	S	N	Castor Oil Conc.	S	S
Antimony Chloride	S	S	Chlorine Dry Gas 100%	S	M
Aqua Regia	U	U	Chlorine Moist Gas	M	U
Barium Carbonate Sattd	S	S	Chlorine Liquid	M	U
Barium Chloride	S	S	Chlorobenzene	M	U
Barium Hydroxide	S	S	Chloroform	M	U
Barium Sulfate Sattd	S	S	Chlorosulfonic Acid 100%	M	U
Barium Sulfide Sattd	S	S	Chrome Alum Sattd	S	S
Beer	S	S	Chromic Acid 20%	S	S
Benzene	M	U	Chromic Acid Up to 50%	S	S
Benzene Sulfonic Acid	S	S	Chromic Acid and Sulfuric Acid	S	M
Bismuth Carbonate Sattd	S	S	Cider	S	S
Black Lye 10%	S	S	Citric Acid Sattd	S	S
Black Liquor	S	S	Coconut Oil Alcohols	S	S
Borax Cold Sattd	S	S	Cola Concentrates	S	S
Boric Acid Dilute	S	S	Copper Chloride Sattd	S	S
			Copper Cyanide Sattd	S	S
			Copper Fluoride 2%	S	S
			Copper Nitrate Sattd	S	S
			Copper Sulfate Dilute	S	S
			Copper Sulfate Sattd	S	S
			Cottonseed Oil	S	S
			Crude Oil*	S	M
			Cuprous Chloride Sattd	S	S
			Cyclohexanol	S	S
			Cyclohexanone	M	U
			Detergents Synthetic	S	S
			Developers, Photographic	S	S
			Dextrin Sattd	S	S
			Dextrose Sattd	S	S
			Dibutylphthalate	S	M
			Disodium Phosphate	S	S
			Diazo Salts	S	S
			Diethylene Glycol	S	S
			Diglycolic Acid	S	S
			Dimethylamine	M	U
			Emulsions, Photographic	S	S
			Ethyl Acetate 100%	M	U
			Ethyl Alcohol 100%	S	S
			Ethyl Alcohol 35%	S	S
			Ethyl Butyrate	M	U
			Ethyl Chloride	M	U
			Ethyl Ether	U	U
			Ethylene Chloride	U	U
			Ethylene Chlorohydrin	U	U
			Ethylene Dichloride	M	U
			Ethylene Glycol	S	S
			Ferric Chloride Sattd	S	S
			Ferric Nitrate Sattd	S	S
			Ferrous Chloride Sattd	S	S
			Ferrous Sulfate	S	S
			Fish Solubles	S	S
			Fluoboric Acid	S	S
			Fluorine	S	U
			Fluosilicic Acid 32%	S	S
			Fluosilicic Acid Conc.	S	S
			Formaldehyde 40%	S	N
			Formic Acid 0-20%	S	S
			Formic Acid 20-50%	S	S
			Formic Acid 100%	S	S
			Fructose Sattd	S	S
			Fruit Pulp	S	S
			Fuel Oil	S	U
			Furfural 100%	M	U
			Furfuryl Alcohol	M	U
			Gallic Acid Sattd	S	S
			Gas Liquids*	S	M
			Gasoline*	M	U
			Gin	S	U
			Glucose	S	S
			Glycerine	S	S
			Glycol	S	S
			Glycolic Acid 30%	S	S
			Grape Sugar Sattd Aq.	S	S
			Hexanol, Tert.	S	S
			Hydrobromic Acid 50%	S	S
			Hydrocyanic Acid Sattd	S	S
			Hydrochloric Acid 10%	S	S
			Hydrochloric Acid 30%	S	S
			Hydrochloric Acid 35%	S	S
			Hydrochloric Acid Conc.	S	S
			Hydrofluoric Acid 40%	S	S
			Hydrofluoric Acid 60%	S	S
			Hydrofluoric Acid 75%	S	-S
			Hydrogen 100%	S	S
			Hydrogen Bromide 10%	S	S
			Hydrogen Chloride Gas Dry	S	S

*HDPE Resin Service Design Factor for hydrocarbons per the formula on page 3 and 8 is F = 0.25 to compensate for hydrocarbon saturation effects on long term hydrostatic strength.

continued from page 9

CHEMICAL RESISTANCE OF DRISCOPIPE

Reagent	70°F (21°C)	140°F (60°C)	Reagent	70°F (21°C)	140°F (60°C)	Reagent	70°F (21°C)	140°F (60°C)
Hydrogen Peroxide 30%	S	S	Phosphorous (Yellow) 100%	S	N	Sodium Bicarbonate Sat'd	S	S
Hydrogen Peroxide 90%	S	M	Phosphorus Pentoxide 100%	S	N	Sodium Bisulfate Sat'd	S	S
Hydrogen Phosphide 100%	S	S	Photographic Solutions	S	S	Sodium Bisulfite Sat'd	S	S
Hydroquinone	S	S	Pickling Baths			Sodium Borate	S	S
Hydrogen Sulfide	S	S	Sulfuric Acid	S	S	Sodium Bromide Dilute Sol.	S	S
Hypochlorous Acid Conc.	S	S	Hydrochloric Acid	S	S	Sodium Carbonate Conc.	S	S
Inks	S	S	Sulfuric-Nitric	S	U	Sodium Carbonate	S	S
Iodine (Alc. Sol.) Conc.	S	U	Plating Solutions			Sodium Chlorate Sat'd	S	S
Lactic Acid 10%	S	S	Brass	S	S	Sodium Chloride Sat'd	S	S
Lactic Acid 90%	S	S	Cadmium	S	S	Sodium Cyanide	S	S
Latex	S	S	Chromium	N	N	Sodium Dichromate Sat'd	S	S
Lead Acetate Sat'd	S	S	Copper	S	S	Sodium Ferricyanide	S	S
Lube Oil	S	M	Gold	S	S	Sodium Ferrocyanide Sat'd	S	S
Magnesium Carbonate Sat'd	S	S	Indium	S	S	Sodium Fluoride Sat'd	S	S
Magnesium Chloride Sat'd	S	S	Lead	S	S	Sodium Hydroxide Conc.	S	S
Magnesium Hydroxide Sat'd	S	S	Nickel	S	S	Sodium Hypochlorite	S	S
Magnesium Nitrate Sat'd	S	S	Rhodium	S	S	Sodium Nitrate	S	S
Magnesium Sulfate Sat'd	S	S	Silver	S	S	Sodium Sulfate	S	S
Mercuric Chloride Sat'd	S	S	Tin	S	S	Sodium Sulfide 25%	S	S
Mercuric Cyanide Sat'd	S	S	Zinc	S	S	Sodium Sulfide Sat'd Sol.	S	S
Mercurous Nitrate Sat'd	S	S	Potassium Bicarbonate Sat'd	S	S	Sodium Sulfite Sat'd	S	S
Mercury	S	S	Potassium Borate 1%	S	S	Stannous Chloride Sat'd	S	S
Methyl Alcohol 100%	S	S	Potassium Bromate 10%	S	S	Stannic Chloride Sat'd	S	S
Methyl Bromide	M	U	Potassium Bromide Sat'd	S	S	Starch Solution Sat'd	S	S
Methyl Chloride	M	U	Potassium Carbonate	S	S	Stearic Acid 100%	S	S
Methyl Ethyl Ketone 100%	M	U	Potassium Chlorate Sat'd	S	S	Sulfuric Acid 0-50%	S	S
Methylsulfuric Acid	S	S	Potassium Chloride Sat'd	S	S	Sulfuric Acid 70%	S	M
Methylene Chloride 100%	M	U	Potassium Chromate 40%	S	S	Sulfuric Acid 80%	S	U
Milk	S	S	Potassium Cyanide Sat'd	S	S	Sulfuric Acid 96%	M	U
Mineral Oils	S	U	Potassium Dichromate 40%	S	S	Sulfuric Acid 98%	M	U
Molasses Comm.	S	S	Potassium Ferri/			Sulfuric Acid, Fuming	U	U
Nickel Chloride Sat'd	S	S	Ferro Cyanide Sat'd	S	S	Sulfurous Acid	S	S
Nickel Nitrate Conc.	S	S	Potassium Fluoride	S	S	Tallow	S	M
Nickel Sulfate Sat'd	S	S	Potassium Hydroxide 20%	S	S	Tannic Acid 10%	S	S
Nicotine Dilute	S	S	Potassium Hydroxide Conc.	S	S	Tanning Extracts Comm.	S	S
Nicotinic Acid	S	S	Potassium Nitrate Sat'd	S	S	Tartaric Acid Sat'd	N	N
Nitric Acid 0-30%	S	S	Potassium Perborate Sat'd	S	S	Tetrahydrofurane	N	U
Nitric Acid 30-50%	S	M	Potassium Perchlorate 10%	S	S	Titanium Tetrachloride Sat'd	N	U
Nitric Acid 70%	S	M	Potassium Sulfate Conc.	S	S	Toluene	M	U
Nitric Acid 95-98%	U	U	Potassium Sulfide Conc.	S	S	Transformer Oil	S	M
Nitrobenzene 100%	U	U	Potassium Sulfite Conc.	S	S	Trisodium Phosphate Sat'd	S	S
Octyl Cresol	S	U	Potassium Persulfate Sat'd	S	S	Trichloroethylene	U	U
Oils and Fats	S	M	Propargyl Alcohol	S	S	Urea Up to 30%	S	S
Oleic Acid Conc.	S	U	Propyl Alcohol	S	S	Urine	S	S
Oleum Conc.	U	U	Propylene Dichloride 100%	U	U	Vinegar Comm.	S	S
Orange Extract	S	S	Propylene Glycol	S	S	Vanilla Extract	S	S
Oxalic Acid Dilute	S	S	Rayon Coagulating Bath	S	S	Wetting Agents	S	S
Oxalic Acid Sat'd	S	S	Sea Water	S	S	Whiskey	S	N
Ozone 100%	S	U	Selenic Acid	S	S	Wines	S	S
Perchloric Acid 10%	S	S	Shortening	S	S	Xylene	M	U
Petroleum Ether	U	U	Silicic Acid	S	S	Yeast	S	S
Phenol 90%	U	U	Silver Nitrate Sol.	S	S	Zinc Chloride Sat'd	S	S
Phosphoric Acid Up to 30%	S	S	Soap Solution Any Conc'n	S	S	Zinc Sulfate Sat'd	S	S
Phosphoric Acid Over 30%	S	S	Sodium Acetate Sat'd	S	S			
Phosphoric Acid 90%	S	S	Sodium Benzoate 35%	S	S			

For additional chemical resistance listings, consult the P.P.I. technical report #TR 19/10-84, Table I and the ISO technical report #ISO/Data 8-1979, Tables I, II, III.

Temperature Characteristics

Since polyethylene is a thermoplastic material, many of its physical and chemical properties are dependent on temperature and will change as the temperature of the material is increased or decreased. However, the exposure of Driscopipe to temperature variations within the recommended operating range does not result in degradation of the material. As these temperature changes are reversed, the material properties also reverse to their original values.

You will note from the information on physical properties that Driscopipe has a brittleness temperature below -180°F and a softening temperature of $+257^{\circ}\text{F}$. The recommended operating temperature is limited only on the higher temperature side to a range of $140\text{--}180^{\circ}\text{F}$, dependent upon the pressure of the application and other operating and installation considerations. On the lower temperature side, Driscopipe gains strength without becoming brittle and is ideal for use at sub-zero temperatures.

Driscopipe becomes molten at $400\text{--}500^{\circ}\text{F}$ and temperatures in this range are used to fusion join the piping system. Pipe is extruded at about the same temperature. To protect the material against degradation at the higher temperature, it is chemically stabilized. This stabilizer protects the material against thermal degradation which might otherwise occur during manufacture, outside storage and installation.

Driscopipe has been tested for thousands of hours at elevated temperatures of 140°F and 180°F without thermal degradation. These long term pressure tests at the higher temperatures are used to obtain recommended design strengths for the pipe at these temperatures.

Since all thermoplastic piping materials are affected by temperature, it is a general practice to characterize these materials at ambient temperature of 23°C (73.4°F). Nearly all ASTM tests relating to physical, mechanical and chemical properties of thermoplastic materials are conducted at this temperature. If a test is conducted, or a property defined, at other than 73.4°F , it is always noted.

One example of the effect of temperature on Driscopipe is the change in long term strength of the material as shown on the stress-life curves. This type behavior is true for all thermoplastics but there are large differences between the performance of specific materials at the higher temperatures.

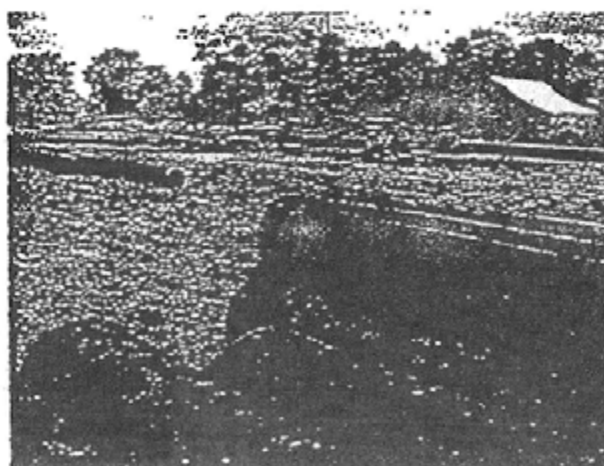
Knowledge of the long term strength of Driscopipe at the various temperatures allows selective design of a system. Accurate interpolations can be made for other temperatures between those which are known when data at three or more temperature levels is available.

Other properties of thermoplastic pipe which change with temperature and can affect system design and installation procedures include the following.

Burst strength — Short term (1 minute) burst tests on Driscopipe at various temperatures show these typical hoop stress values:

Temperature, $^{\circ}\text{F}$	Hoop Stress, psi
73.4°	3250
32°	4300
0°	5290
-20°	5670
-40°	6385

Driscopipe will quick-burst at a pressure approximately four times greater than the rated operating pressure.



Chemical Resistance – The ability of most thermoplastics to resist degradation in the presence of corrosive chemicals is reduced as temperature increases. This is also true for Driscopipe but to a lesser extent because of its high density and high molecular weight. The effect of temperature on Driscopipe in the presence of various chemicals is shown in the chemical resistance tables.

Flexibility – As temperature is decreased, the flexibility of Driscopipe is also decreased. This has very little effect on installation except that at the lower winter temperatures, coiled pipe becomes more difficult, mechanically, to uncoil and stretch out in the ditch. Although Driscopipe becomes stiffer at low temperature, it can be bent, uncoiled or plowed in with sufficient mechanical power and no damage will occur to the pipe because of bending it at cold temperatures.

Other Physical Properties – There is a slight change with temperature of impact strength, notch sensitivity, flexural modulus, hardness and elongation ... but none are of such extent as to affect design parameters or installation procedures over the normal range of temperatures.

Modulus of Elasticity – Typical values for the variance in modulus of elasticity with temperature change is shown below.

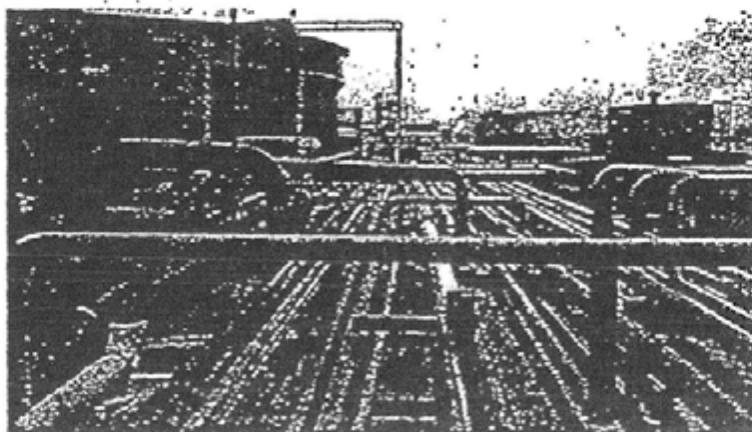
Temperature °F	Modulus of Elasticity, psi
-20°	300,000
0°	260,000
32°	200,000
75°	130,000
100°	105,000
140°	60,000

Thermal Expansion and Contraction – Polyethylene, like other thermoplastics, has a coefficient of expansion higher than metals. This coefficient is usually determined by a standard test method which employs the use of molded specimens. Measurements are made with a quartz dilatometer while the test specimen is held at elevated temperature. Typical coefficient values by this method range from $.75 \times 10^{-4}$ for Driscopipe 8600 to $.83 \times 10^{-4}$ for Driscopipe 1000.

The coefficient of linear expansion may also be determined by measuring the change in length of unrestrained pipe samples at different temperatures. The calculated coefficient is somewhat higher on extruded pipe than on molded test specimens. This appears to be true for all polyethylene pipe. The average coefficient calculated from measurements made on Driscopipe in the temperature range 0°F to 140°F, is 1.2×10^{-4} in/in°F.

The circumferential coefficient of expansion and contraction for Driscopipe is approximately $.6 \times 10^{-4}$ in/in°F in the range of 0° to 140°F ... or about ½ the linear coefficient. This circumferential change with temperature rarely presents any problems in system design. There may be need to consider this factor if compression fittings are used.

The expansion or contraction for Driscopipe can be stated in an easy rule of thumb ... the pipe will expand or contract approximately 1.4" per 100 feet for each 10°F change in temperature. Thus a 1000 foot unrestrained line which undergoes a 20°F increase in temperature change will increase in length 28 inches. The relatively large amount of expansion and contraction of plastic pipe generally presents no real problems in installation. The pipe has a relatively low elastic modulus and consequently there is less stress build-up. These stresses, caused by temperature change, are easily dissipated due to the thermoplastic nature of the material which relaxes and adjusts with time.



Tests have been conducted wherein the temperature of more than 100 feet of unrestrained pipe was changed 130°F in a period of a few minutes. The total force created by contraction was measured and proved to be about (½) one-half the theoretical calculated value. Thermoplastic materials are unique in their ability to stress-relieve themselves. Actual changes in temperature in most applications take place slowly over an extended period of time. The total stresses imposed will vary but are generally much lower than the calculated values.

Direct buried pipe will generally have ample soil friction and interference to restrain movement of the pipe under normal application temperature changes. It is a good idea to make the final tie-ins on a system at a temperature which is as close to operating temperature as possible. This is particularly true for insert liner systems where there is no soil restraint.

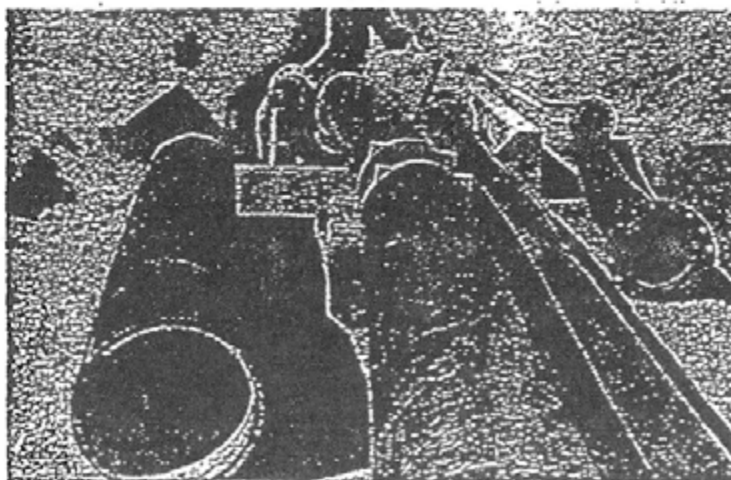
Normal good direct burial installation practices which include snaking the pipe in the ditch, proper backfill and compaction, making the tie-in at the proper temperature, etc. should be used at all times and will substantially reduce the possibility of pull out at tie-in connections on such installations. However, planning the transition tie-in becomes more important when Driscopipe is used for insert renewal inside another pipe because there is no restraint from earth loading.

Contraction of the pipe due to reduction in temperature is freely transmitted to the transition connection and may result in pull-out if proper design

precautions are not taken. In those cases, it may be necessary to provide additional anchoring at the terminations of the insert liner. Concrete anchors poured into undisturbed soil and cast around anchor projections in the Driscopipe line will restrict movement at the end of the line. Anchor projections on the Driscopipe liner can be made by fusing a blind tee into the line or by the use of two reducers, to the next larger size of pipe, fused together in the line.

Thermal Conductivity – This property of Driscopipe is lower than that for metals and can sometimes be exploited in the design of the system. It may eliminate or reduce the need for insulating pipe which carries water or other fluids through freezing temperatures. Thermal Conductivity of Driscopipe is 2.7 BTU per hour per sq. ft. per °F per inch of thickness. The slow heat transfer inhibits freezing and, if normal burial precautions are used, accidental freezing is usually eliminated. If the pipe does freeze, it does not fracture but fluid flow will be stopped. It will resume its function upon thawing. Direct application of intense heat should not be used to thaw a line. Antifreeze compounds such as methanol, isopropanol and ethylene glycol can be used without detrimental effect on the pipe.

Ignition Temperatures – The flash point for high density polyethylene using the Cleveland open cup method (ASTM D92) is 430°F. The flash ignition and self ignition temperatures using ASTM D1929 are 645°F and 660°F.



Weatherability

Two principal factors influence the weathering of plastic pipe in outside above ground applications ... temperature changes caused by seasonal variations and solar heating and solar radiation of ultraviolet rays. Effects of temperature variations on Driscopipe were discussed in the preceding section. Expansion and contraction of a line above ground, due to differential heating, will cause the line to move laterally, particularly if it is empty. This movement can easily be controlled within desired limits through the use of restraints.

Driscopipe is also protected against degradation caused by ultraviolet rays when exposed to direct sunlight. The material contains 2½% of finely divided carbon black which also accounts for the black color of Driscopipe. Carbon black is the most effective single additive capable of enhancing the weathering characteristic of plastic materials. The protection even relatively low levels of carbon black impart to the plastic is so great that it is not necessary to use other light stabilizers or UV absorbers.

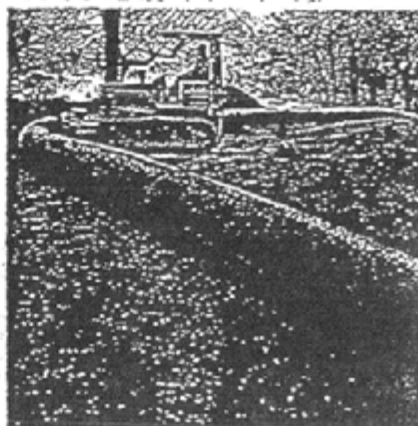
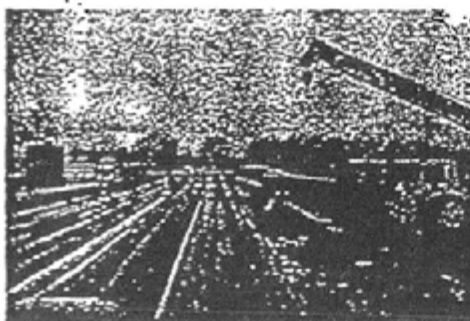
Weatherability tests indicate that Driscopipe can be safely used outside in most climates for periods of many years without danger of loss of physical properties due to UV exposure. Phillips has done extensive testing of polyethylene compounds containing 2 to 3% carbon black and compared these to other UV stabilizers to determine their effectiveness for protection against UV degradation in outdoor exposure. Samples were aged in outdoor exposure in three geographical locations: Phoenix,

Arizona, Bartlesville, Oklahoma (Phillips 66 headquarters) and Akron, Ohio. From these actual tests, it was determined that one year exposure in Arizona was equivalent to at least two years in Bartlesville and greater than three and one-half years in Akron.

Weather-Ometer tests were run under standard conditions as set out in ASTM D 1499-64 and compared with the actual test samples in the three locations described above. From this test work, it was determined, conservatively, that 5000 hours (approximately 7 months) in the Weather-Ometer compares to greater than 42 months exposure in Arizona. Samples containing 2 to 3% carbon black and thermal stabilizers as used in Driscopipe have been tested for greater than 25,000 hours (2.85 years) in the Weather-Ometer without any brittleness or loss of physical properties. This is equivalent to over 17 years in Arizona and over 60 years in Akron, Ohio.

Permeability

The permeability of gases, vapors or liquids through a plastic membrane is generally considered to be an activated diffusion process. That is, the gas, vapor or liquid dissolves in the membrane and then diffuses to a position of lower concentration. The permeation rate is determined by the functional groups of the permeating molecules and by the density of the plastic ... the higher the density, the lower the permeability. Listed below are typical permeability rates for HDPE.



	Permeability Rate*
Carbon Dioxide	345
Hydrogen	321
Oxygen	111
Helium	247
Ethane	236
Natural Gas	113
Freon 12	95
Nitrogen	53

*Cubic centimeters per day per 100 sq. inches per mil thickness at atmospheric pressure differential.

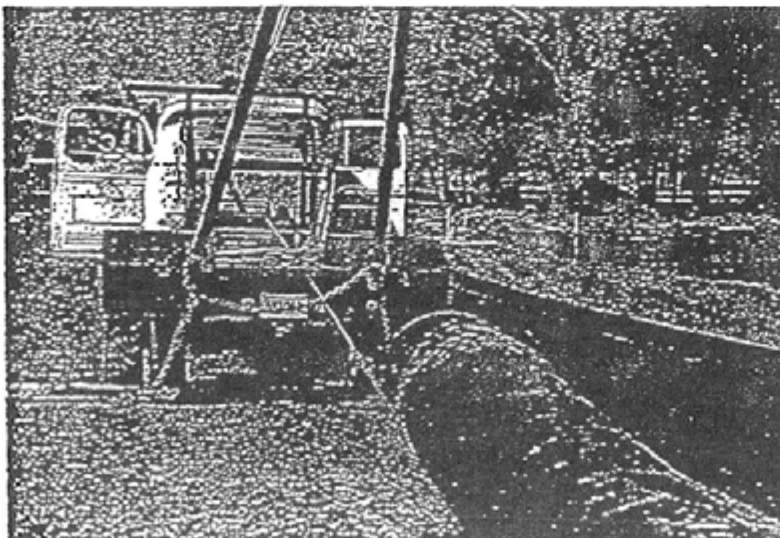
These permeation rates are considered very low. They result in negligible loss of product and create no hazard. For example, polyethylene piping systems are the predominant material used to construct new gas distribution systems and to renew old deteriorated systems. The permeation rate will vary in direct proportion to the differential pressure applied.

If the internal operating pressure is 60 psi, for example, the permeability rate would be approximately 4 times that shown above but volume losses would still be extremely low. Calculated volume loss in one mile of SDR 11 pipe (any size) in one day, for natural gas, would be $\frac{1}{4}$ of one cubic foot. At 120 psi, it would be $\frac{1}{2}$ cubic foot per day.

Abrasion Resistance

One of the many outstanding characteristics of Driscopipe polyethylene is its resistance to abrasion. The inherent resilience and toughness of Driscopipe allows the mining industry to use this pipe in numerous surface applications where more conventional materials would be unsatisfactory, either because of the terrain encountered or the abrasiveness of the slurry to be moved. Quite often, a Driscopipe system offers substantial economic advantage as a means of transport over more conventional transportation methods used in the mining industry. Some of the more common applications include tailings lines and the transport of gypsum, limestone, sand, slimes and coal.

Due to its unique toughness, as indicated by low melt flow values, Driscopipe 8600 provides improved abrasion resistance over all other polyethylene piping materials. Controlled pipe loop pumping tests have demonstrated that Driscopipe can outlast steel pipe by as much as 4 to 1. One such test, performed by Williams Brothers Engineering, Tulsa, Oklahoma, compared Driscopipe to steel in pumping a coarse particle size magnetite iron ore slurry. At 13½ ft/sec velocity, Driscopipe was better by a factor of 4:1 and at 17 ft/sec by a factor of 3:1.



Heat Fusion Joining

The heat fusion joining technique has a long history of use for joining polyethylene pipe materials. The heat fusion method of joining PE pipe began shortly after the first commercial production of high density polyethylene in the early 1950s ... both developed by Phillips 66.

The integrity and superiority of heat fusion are now recognized universally. The modern day heat fusion joint is the same joint made in 1956 ... only the fusion equipment has evolved to gain efficiency, reliability and convenience. The principles learned on early equipment for making a successful joint are still in use today. Phillips designed, developed and built many models of heat fusion equipment from 1956 until the early 1970s. Since that time, Phillips has guided this development by others. The extensive line of high quality, efficient fusion equipment offered by McElroy Manufacturing, Inc., Tulsa, Oklahoma is one of the results of this long history of development. Phillips pioneered the idea and development of heat fusion and has used it exclusively in every high density polyethylene piping system sold by Phillips since 1956. There are millions of these joints in service today. In fact, 92% of all natural gas distribution pipe to homes, farms and factories is installed with polyethylene pipe and fittings. Heat fusion joints are industry accepted and field proven.

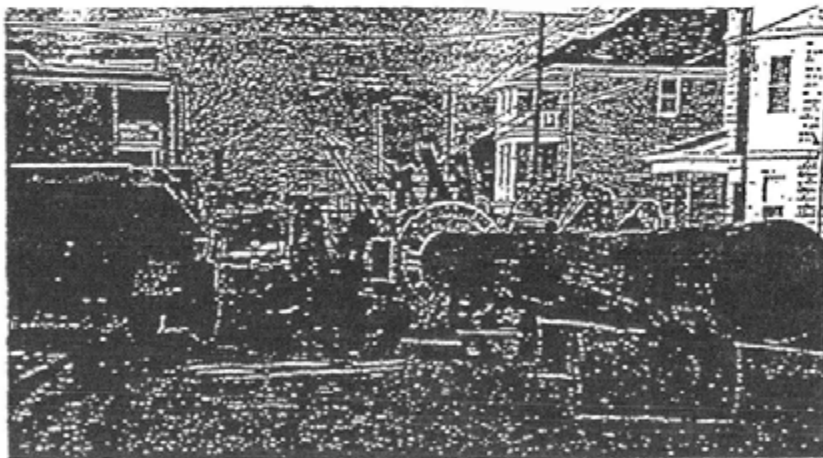
The heat fusion joining system has been so successful that it is the "standard" joining system for polyethylene. There are many reasons ... here are some.

Heat fusion joining ideally meets the requirements for a fast joining method to facilitate all phases of construction work in a safe and reliable manner.

The heat fusion joint is structurally superior to the socket fusion joint by configuration and, therefore, better meets the requirements of service. The heat joint configuration allows it to better disperse stresses initiated by pipe deflection and external loading. Stress concentration is minimized when the joint is placed in a strain and the joint is more "forgiving" when ground settlement occurs. In a socket joint, there is an extremely high ratio of "joint wall" to "pipe wall", resulting in stress intensification from external loading.

The Driscopipe heat fusion joining system is a simple, visual procedure with straight forward instructions. No "timing cycles" are necessary. The visual procedure allows the operator to concentrate on his work rather than a clock. Visually, he knows when the pipe ends have melted to the degree required to fuse them together. Visually, he observes and controls fusion pressure by observing the amount and configuration of the fusion bead as it is formed.

In the course of this work, the fusion operator is faced with a wide variety of job conditions. Changes in air temperature, material temperature, wind velocity, sun exposure, humidity, as well as condition of the terrain and the equipment all influence the joining requirements. Quality work under field conditions is more consistent with a simple, straight-forward, visual procedure.



One heat fusion operator, with equipment, typically runs the whole operation himself, sometimes using a second person as a helper. Pipe tolerances, ovality and curvature are no problem and "melt" is easily controlled by the visual procedure.

Heat fusion joints offer a large advantage over socket coupled joints for plow-in installation and for insert renewal applications. Socket coupled pipe requires larger size plow chutes and bore holes. Heat fused pipe one size larger can usually be handled and installed through bore holes and plow chutes selected for socket coupled pipe. Larger sizes of heat fused pipe can be used inside old mains for insert renewal because it does not require the extra space for the coupling.

Heat fusion joints may easily be cut out and re-done. This fact has a bearing on the quantity and quality of training necessary and favorably affects operator attitude toward quality in the field. These joints can be easily cut out and destructively tested in the field to check joining proficiency and equipment-condition and it's inexpensive. There is no coupling to destroy and throw away.

The heat fusion joining system is especially effective with Driscopipe 8600. The melt of this material is very viscous and tough. The operator can apply ample pressure to form the heat fusion joint with little danger of forcing the molten material from between the two ends of the joint, as can be done with the softer, less viscous, high density materials.



Driscopipe 8600 can be fusion joined to other polyethylene piping materials when necessary. Special joining techniques are required to achieve good joints. Phillips Driscopipe technical personnel are available to instruct and demonstrate the fusion joining procedure for joining Driscopipe to other polyethylene materials.

Fatigue Resistance

Driscopipe 8600 very high molecular weight, high density polyethylene has superior resistance to fatigue failure caused by cyclic loading. Independent laboratory tests were conducted to determine the suitability of Driscopipe 8600 for use as the cold water supply pipe and the barge mooring leg of the Mini-OTEC Project (Hawaii, 1979). In that application, 2150' of 24" 60 psi Driscopipe 8600 was deployed vertically in a deep ocean trench just offshore Keahole Point and was subject to cyclic distortion caused by wave action, current, and barge motion.

Cyclic tests showed that Driscopipe 8600 very high molecular weight PE could endure more than 100,000 cycles at a stress of 1800 psi without failure. Copies of this test report are available upon request.

Driscopipe 1000 offers good fatigue service life also, but not equal to 8600. Neither requires de-rating like PVC AWWA C-900 pipe. In fact, per AWWA C-906 for 4" to 63" HDPE pipe, no water hammer or fatigue de-rating factor need be applied to Driscopipe 8600 or Driscopipe 1000 ductile PE pipe.

The Driscopipe performance team offers you innovative solutions to your piping requirements. Contact your nearest Driscopipe Sales Representative. He'll give you personalized technical service, installation assistance and all the cost-saving advantages of a Driscopipe Piping System. Engineered for Performance!





Phillips Driscopipe, Inc.
A Subsidiary of Phillips 66 Company

To Secure Product Information or Leave a
Message for a Sales Engineer or Technical
Service Representative:

Mail:

Attn: Customer Service Department
P.O. Box 83-3866
2929 North Central Expressway
Suite 100
Richardson, Texas 75083

Phone:

U.S. Domestic Toll Free (800) 527-0662

TWX:

910-867-4818

Fax:

214-783-2689

This document reports accurate and reliable information to the best of our knowledge but our suggestions and recommendations cannot be guaranteed because the conditions of use are beyond our control, the user of such information assumes all risk connected with the use thereof. Phillips 66 Company and its subsidiaries assume no responsibility for the use of information presented herein and hereby expressly disclaims all liability in connection with such use.

**PLASTICS WITH
POWER TO WIN.** 

butane may condense and liquefy in the pipe. Such liquefied fuel gasses are known to permeate polyethylene pipe, and result in unreliable heat fusion or electrofusion joints.

In potable water applications, permeating chemicals could affect the pipe or water in the pipe. ANSI/AWWA standards provide the following guidance for potable water applications:

“The selection of materials is critical for water service and distribution piping where there is likelihood the pipe will be exposed to significant concentrations of pollutants comprised of low molecular weight petroleum products or organic solvents or their vapors. Research has documented that pipe materials such as polyethylene, polybutylene, polyvinyl chloride, and asbestos cement, and elastomers, such as used in jointing gaskets and packing glands, may be subject to permeation by lower molecular weight organic solvents or petroleum products. If water pipe must pass through such a contaminated area or an area subject to contamination, consult with the manufacturer regarding permeation of pipe walls, jointing materials, and so forth, *before* selecting materials for use in that area.”¹

Chemical Attack

A direct chemical attack on the polymer will result in permanent, irreversible polymer damage or chemical change by chain scission, cross-linking, oxidation, or substitution reactions. Such damage

or change cannot be reversed by removing the chemical.

Chemical Resistance Information

The following chemical resistance guide, Table 5-1 (next page), presents immersion test chemical resistance data for a wide variety of chemicals.

- ☐ This data may be applicable to gravity flow and low stress applications.
- ☐ It may not be applicable when there is applied stress such as internal pressure, or applied stress at elevated temperature.

Unless stated otherwise, polyethylene was tested in the relatively pure, or concentrated chemical.

It is generally expected that dilute chemical solutions, lower temperatures, and the absence of stress have less potential to affect the material. At higher temperature, or where there is applied stress, resistance may be reduced, or polyethylene may be unsuitable for the application. Further, combinations of chemicals may have effects where individual chemicals may not.

Testing is recommended where information about suitability for use with chemicals or chemical combinations in a particular environment is not available. PLEXCO cannot provide chemical testing services.

Second Edition
©1998 Chevron
Chemical Company
LLC
Issued 12/98

¹ ANSI/AWWA C906-90, Section 1.2; ANSI/AWWA C901-96, Section 4.1.

Table 5-1 Chemical Resistance

Because the particular conditions of each application may vary, Table 5-1 information should be used only as a preliminary guide for PLEXCO and SPIROLITE polyethylene pipe materials. This information is offered in good faith, and is believed to be accurate at the time of publication, but it is offered without any warranty, expressed or implied. Additional information may be required, particularly in regard to unusual or special applications. Determinations of suitability for use in particular chemical or environmental conditions may require specialized laboratory testing.

Additional information on chemical compatibility may be found in PPI TR-19, *Thermoplastic Piping for the Transport of Chemicals*.

Chemical Resistance Key

Key†	Meaning
X	resistant (swelling <3% or weight loss <0.5%; elongation at break not substantially changed)
/	limited resistance (swelling 3 - 8% or weight loss 0.5 - 5%; elongation at break reduced by <50%)
—	not resistant (swelling > 8% or weight loss >5%; elongation at break reduced by >50%)
D	discoloration
*	aqueous solutions in all concentrations
**	only under low mechanical stress
† Where a key is not printed in the table, data is not available.	

Second Edition
©1998 Chevron
Chemical Company
LLC
Issued 12/98

Medium	73°F	140°F	Medium	73°F	140°F
Acetaldehyde, gaseous	X	/	Ammonia, liquid (100%)	X	X
Acetic acid (10%)	X	X	Ammonium chloride	*X	X
Acetic acid (100%) (Glacial acetic acid)	X	/D	Ammonium fluoride, aqueous (up to 20%)	X	X
Acetic anhydride	X	/D	Ammonium nitrate	*X	X
Acetone	X	X	Ammonium sulphate	*X	X
Acetylene tetrabromide	**/ to —	—	Ammonium sulfide	*X	X
Acids, aromatic	X	X	Amyl acetate	X	X
Acrylonitrile	X	X	Aniline, pure	X	X
Adipic acid	X	X	Anisole	/	—
Allyl alcohol	X	X	Antimony trichloride	X	X
Aluminum chloride, anhydrous	X	X	Aqua regia	—	—
Aluminum sulphate	*X	X	Barium chloride	*X	X
Alums	X	X	Barium hydroxide	*X	X

<i>Medium</i>	<i>73°F</i>	<i>140°F</i>	<i>Medium</i>	<i>73°F</i>	<i>140°F</i>
Beeswax	X	**/ to —	Cyclohexanone	X	X
Benzene	/	/	Decahydronaphthalene	X	/
Benezenesulphonic acid	X	X	Desiccator grease	X	/
Benzoic acid	*X	X	Detergents, synthetic	X	X
Benzyl alcohol	X	X to /	Dextrin, aqueous (18% saturated)	X	X
Borax, all concentrations	X	X	Dibutyl ether	X to /	—
Boric acid	*X	X	Dibutyl phthalate	X	/
Brine, saturated	X	X	Dichloroacetic acid (100%)	X	/D
Bromine	—	—	Dichloroacetic acid (50%)	X	X
Bromine vapor	—	—	Dicloroacetic acid methyl ester	X	X
Butanetriol	X	X	Dichlorobenzene	/	—
Butanol	X	X	Dicloroethane	/	/
Butoxyl	*X	/	Dicloroethylene	—	—
Butyl acetate	X	/	Diesel oil	X	/
Butyl glycol	X	X	Diethyl ether	X to /	/
Butyric acid	X	/	Diisobutyl ketone	X	/ to —
Calcium chloride	*X	X	Dimethyl formamide (100%)	X	X to /
Calcium hypochlorite	*X	X	Dioxane	X	X
Camphor	X	/	Emulsifiers	X	X
Carbon dioxide	X	X	Esters, aliphatic	X	X to /
Carbon disulphide	/	—	Ether	X to /	/
Carbon tetrachloride	**/ to —	—	Ethyl acetate	/	—
Caustic potash	X	X	Ethyl alcohol	X	X
Caustic soda	X	X	Ethyl glycol	X	X
Chlorine, liquid	—	—	Ethyl hexanol	X	X
Chlorine bleaching solution (12% active chlorine)	/	—	Ethylene chloride (dichloroethene)	/	/
Chlorine gas, dry	/	—	Ethylene diamine	X	X
Chlorine gas, moist	/	—	Fatty acids (>C ⁶)	X	/
Chlorine water (disinfection of mains)	X	—	Feric chloride*	X	X
Chloroacetic acid (mono)	X	X	Fluorine	—	—
Chlorobenzene	/	—	Fluorocarbons	/	—
Chloroethanol	X	XD	Fluorosilic acid, aqueous (up to 32%)	X	X
Chloroform	**/ to —	—	Formaldehyde (40%)	X	X
Chlorosulphonic acid	—	—	Formamide	X	X
Chromic acid (80%)	X	—D	Formic acid	X	—
Citric acid	X	X	Fruit juices	X	X
Coconut oil	X	/	Fruit pulp	X	X
Copper salts	*X	X	Furfuryl alcohol	X	XD
Corn oil	X	/	Gelatine	X	X
Creosote	X	XD	Glucose	*X	X
Creosol	X	XD	Glycerol	X	X
Cyclohexane	X	X	Glycerol chlorohydrin	X	X
Cyclohexanol	X	X	Glycol (conc.)	X	X

Second Edition
©1998 Chevron
Chemical Company
LLC
Issued 12/98

<i>Medium</i>	<i>73°F</i>	<i>140°F</i>	<i>Medium</i>	<i>73°F</i>	<i>140°F</i>
Glycolic acid (50%)	X	X	Nitric acid (25%)	X	X
Glycolic acid (70%)	X	X	Nitric acid (50%)	/	—
Halothane	/	/	Nitrobenzene	X	/
Hydrazine hydrate	X	X	o-Nitrotoluene	X	/
Hydrobromic acid (50%)	X	X	Octyl cresol	/	—
Hydrochloric acid (all concentrations)	X	X	Oils, ethereal	/	/
Hydrocyanic acid	X	X	Oils, vegetable & animal	X	X to /
Hydrofluoric acid (40%)	X	/	Oleic acid (conc.)	X	/
Hydrofluoric acid (70%)	X	/	Oxalic acid (50%)	X	X
Hydrogen	X	X	Ozone	/	—
Hydrogen chloride gas, moist and dry	X	X	Ozone, aqueous solution (Drinking water purification)	X	
Hydrogen peroxide (30%)	X	X	Paraffin oil	X	X
Hydrogen peroxide (100%)	X		Perchloric acid (20%)	X	X
Hydrogen sulfide	X	X	Perchloric acid (50%)	X	/
Iodine, tincture of, DAB 7 (German Pharmacopoeia)	X	/D	Perchloric acid (70%)	X	—D
Isooctane	X	/	Petrol	X	X to /
Isopropanol	X	X	Petroleum	X	/
Isopropyl ether	X to /	—	Petroleum ether	X	/
Jam	X	X	Petroleum jelly	**X to /	/
Keotones	X	X to /	Phenol	X	XD
Lactic acid	X	X	Phosphates	*X	X
Lead acetate	*X	X	Phosphoric acid (25%)	X	X
Linseed oil	X	X	Phosphoric acid (50%)	X	X
Magnesium chloride	*X	X	Phosphoric acid (95%)	X	/D
Magnesium sulphate	*X	X	Phosphorus oxychloride	X	/D
Maleic acid	X	X	Phosphorus pentoxide	X	X
Malic acid	X	X			
Menthol	X	/	Phosphorus trichloride	X	/
Mercuric chloride (sublimate)	X	X	Photographic developers, commecial	X	X
Mercury	X	X	Phthalic acid (50%)	X	X
Methanol	X	X	Polyglycols	X	X
Methyl butanol	X	X	Potassium bichromate (40%)	X	X
Methyl ethyl ketone	X	/ to —	Potassium borate, aqueous (1%)	X	X
Methyl glycol	X	X	Potassium bromate, aqueous (up to 10%)	X	X
Methylene chloride	/	/	Potassium bromide	*X	X
Mineral oils	X	X to /	Potassium chloride	*X	X
Molasses	X	X	Potassium chromate, aqueous (40%)	X	
Monochloroacetic acid	X	X	Potassium cyanide	*X	X
Monochloroacetic ethyl ester	X	X	Potassium hydroxide (30% solution)	X	X
Monochloroacetic methyl ester	X	X	Potassium nitrate	*X	X
Morpholine	X	X	Potassium permanganate	X	XD
Naptha	X	/	Propanol	X	X
Naphthalene	X	/	Propionic acid (50%)	X	X
Nickel salts	*X	X	Propionic acid (100%)	X	/

Second Edition
 ©1998 Chevron
 Chemical Company
 LLC
 Issued 12/98

<i>Medium</i>	<i>73°F</i>	<i>140°F</i>	<i>Medium</i>	<i>73°F</i>	<i>140°F</i>
Propylene glycol	X	X	Thiophene	/	/
Pseudocumene	/	/	Toluene	/	—
Pyridine	X	/	Transformer oil	X	/
Seawater	X	X	Tributyl phosphate	X	X
Silicic acid	X	X	Trichloroacetic acid (50%)	X	X
Silicone oil	X	X	Trichloroacetic acid (100%)	X	/ to —
Silver nitrate	X	X	Trichloroethylene	**X to /	—
Sodium benzoate	X	X	Triethanolamine	X	X
Sodium bisulphite, weak aqueous solutions	X	X	Turpentine, oil of	x to /	/
Sodium carbonate	*X	X	Tween 20 and 90 (Atlas Chemicals)	X	X
Sodium chloride	*X	X	Urea	*X	X
Sodium chlorite (50%)	X	/	Vinegar (commercial conc.)	X	X
Sodium hydroxide (30% solution)	X	X	Viscose spinning solutions	X	X
Sodium hypochlorite (12% active chlorine)	/	—	Waste gases containing carbon dioxide	X	X
Sodium nitrate	*X	X	carbon monoxide	X	X
Sodium silicate	*X	X	hydrochloric acid (all conc.)	X	X
Sodium sulfide	*X	X	hydrogen fluoride (traces)	X	X
Sodium thiosulphate	X	X	nitrous vitriol (traces)	X	X
Spermaceti	X	/	sulfur dioxide (low conc.)	X	X
Spindle oil	X to /	/	sulphuric acid, moist (all conc.)	X	X
Starch	X	X	Water gas	X	X
Steric acid	X	/	Xylene	—	—
Succinic acid (50%)	X	X	Yeast, aqueous preparations	X	X
Sugar syrup	X	X	Zinc chloride	*X	X
Sulfates	*X	X			
Sulfur	X	X			
Sulfur dioxide, dry	X	X			
Sulfur dioxide, moist	X	X			
Sulfur trioxide	—	—			
Sulfuric acid (10%)	X	X			
Sulfuric acid (50%)	X	X			
Sulfuric acid (98%)	/	—			
Sulfuric acid, fuming	—	—			
Sulfurous acid	X	X			
Sulfuryl chloride	—				
Tallow	X	X			
Tannic acid (10%)	X	X			
Tartaric acid	X	X			
Tetrachloroethane	**X to /	—			
Tetrahydrofuran	**X to /				
Tetrahydronaphthalene	X	/			
Thionyl chloride	—	—			

Second Edition
©1998 Chevron
Chemical Company
LLC
Issued 12/98

**APPLICATION FOR PERMIT RENEWAL AND MODIFICATION
SANDOVAL COUNTY LANDFILL**

**VOLUME III: LANDFILL ENGINEERING CALCULATIONS
SECTION 4: COMPATIBILITY DEMONSTRATION**

**ATTACHMENT III.4.G
PVC PIPE REFERENCE DOCUMENTATION**

PVC Chemical Resistance

KEY — E = Excellent G = Good L = Limited U = Unsuitable O = No test

Chemical	PVC I		PVC II		Chemical	PVC I		PVC II	
	72°F.	140°F.	72°F.	140°F.		72°F.	140°F.	72°F.	140°F.
Acetaldehyde	U	U	U	U	Beet - Sugar Liquor	E	E	E	E
Acetamide	O	O	U	U	Benzaldehyde	U	U	U	U
Acetate Solvents - Crude	U	U	U	U	Benzene	U	U	U	U
Acetate Solvents - Pure	U	U	U	U	Benzenesulfonic Acid - 10%	E	E	E	E
Acetic Acid 0-10%	E	E	G	L	Benzenesulfonic Acid	U	U	U	U
Acetic Acid 10-20%	E	E	G	L	Benzoic Acid	E	E	E	E
Acetic Acid 20-30%	E	G	G	L	Benzol	U	U	U	U
Acetic Acid 30-60%	E	E	G	L	Bismuth Carbonate	E	E	E	E
Acetic Acid 80%	G	L	L	L	Black Liquor (Paper Industry)	E	E	E	E
Acetic Acid - Glacial	G	U	L	U	Bleach - 12.5% Active Cl ₂	E	G	G	L
Acetic Acid - Vapors	E	E	G	U	Borax	E	E	E	E
Acetic Anhydride	U	U	U	U	Borax Liquors	E	E	E	E
Acetone	U	U	U	U	Boric Acid	E	E	E	E
Acetylene	L	L	E	E	Boron, TriFluoride	E	E	E	E
Adipic Acid	L	E	E	E	Breeder Pellets - Fish Deriv.	E	E	E	E
Alcohol - Allyl - 96%	G	L	U	U	Brine	E	E	E	E
Alcohol - Amyl	E	L	L	U	Bromic Acid	E	E	E	E
Alcohol - Butyl	E	G	L	U	Bromine - Liquid	U	U	U	U
Alcohol - Ethyl	E	E	L	G	Bromine (Gas) - 25%	E	E	U	U
Alcohol - Methyl	E	E	E	E	Bromine - Water	E	E	L	U
Alcohol - Propargyl	E	E	E	E	Butadiene	E	E	E	E
Alcohol - Propyl	E	E	E	G	Butane	E	E	E	E
Allyl - Chloride	U	U	U	U	Butane, Butylene	E	E	E	U
Alum	E	E	E	E	Butane, Diol	E	E	U	U
Alum, Ammonium	E	E	E	E	Butanol	E	U	U	U
Alum, Chrome	E	E	E	E	Butanol - Primary	E	E	U	U
Alum, Potassium	E	E	E	E	Butanol - Secondary	E	L	U	U
Aluminum Chloride	E	E	E	E	Buttermilk	E	E	E	U
Aluminum Fluoride	E	E	E	E	Butyl Acetate	U	U	U	U
Aluminum Hydroxide	E	E	E	E	Butyl Phenol	E	U	L	U
Aluminum Oxychloride	E	E	E	E	Butylene	E	O	U	O
Aluminum Nitrate	E	E	E	E	Butynediol (Erthritol)	E	U	U	U
Aluminum Sulfate	E	E	E	E	Butyric Acid 20%	G	U	U	U
Ammonia - Dry Gas	E	E	E	E	Butyric Acid	E	U	U	U
Ammonia, Aqua (10%)	E	E	E	E					
Ammonia - Liquid	L	U	O	O	Calcium Bisulfide	E	E	E	E
Ammonium Acetate	E	E	E	E	Calcium Bisulfite	E	E	E	E
Ammonium BiFluoride	E	E	E	E	Calcium Carbonate	E	E	E	E
Ammonium Carbonate	E	E	E	E	Calcium Chlorate	E	E	E	E
Ammonium Chloride	E	E	E	E	Calcium Chloride	E	E	E	E
Ammonium Fluoride - 25%	E	L	U	U	Calcium Hydroxide	E	E	E	E
Ammonium Hydroxide - 28%	E	E	E	E	Calcium Hypochlorite	E	E	E	E
Ammonium Metaphosphate	E	E	E	E	Calcium Nitrate	E	E	E	E
Ammonium Monophosphate	E	E	E	E	Calcium Oxide	E	E	E	U
Ammonium Nitrate	E	E	E	E	Calcium Sulfate	E	E	E	E
Ammonium Persulfate	E	E	E	E	Cane Sugar Liquors	E	E	E	E
Ammonium Phosphatel (Ammoniacal)	E	E	O	O	Carbic Acid	E	E	E	E
Ammonium Phosphate - Neutral	E	E	E	E	Carbon Bisulfide	U	U	U	U
Ammonium Sulfate	E	E	E	E	Carbon Dioxide (Aqueous S.L.)	E	E	E	E
Ammonium Sulfide	E	E	E	E	Carbon Dioxide Gas (Wet)	E	E	E	E
Ammonium Thiocyanate	E	E	E	E	Carbon Monoxide	E	E	E	E
Amyl Acetate	U	U	U	U	Carbon Tetrachloride	L	U	U	U
Amyl Chloride	U	U	U	U	Carbonated Water	E	E	E	E
Aniline	U	U	U	U	Carbonic Acid	E	E	E	E
Aniline Chlorohydrate	U	U	U	U	Casein	E	E	E	E
Aniline Dyes	U	U	U	U	Castor Oil	E	E	E	E
Aniline Hydrochloride	U	U	U	U	Caustic Potash	E	E	E	E
Anthraquinone	E	E	E	L	Caustic Soda	E	E	E	E
Anthraquinonesulfonic Acid	E	E	E	E	Cellosolve	G	L	L	U
Anitimony Trichloride	E	E	E	E	Chloracetic Acid	E	L	E	U
Aqua Regia	E	L	U	U	Chloral Hydrate	E	E	E	E
Arsenic Acid - 80%	E	G	E	G	Chloric Acid 20%	E	E	E	E
Arylsulfonic Acid	E	E	L	U	Chlorinated Solvents	U	U	U	U
Asphalt	E	E	E	E	Chlorine (Dry)	E	L	L	L
					Chlorine Gas (Moist)	G	L	L	L
Barium Carbonate	E	E	E	E	Chlorine Water	E	E	E	E
Barium Chloride	E	E	E	E	Chloroacetic Acid	E	E	E	U
Barium Hydroxide	E	E	E	E	Chlorobenzene	U	U	U	U
Barium Sulfate	E	E	E	E	Chlorobenzyl Chloride	U	U	U	U
Barium Sulfide	E	E	E	E	Chloro Form	U	U	U	U
Beer	E	E	E	E	Chlorosulfonic Acid (100%)	E	U	O	O
					Chrome Alum	E	E	E	E

CertainTeed EI

Chemical	PVC I		PVC II		Chemical	PVC I		PVC II	
	72 °F.	140 °F.	72 °F.	140 °F.		72 °F.	140 °F.	72 °F.	140 °F.
Chromic Acid 10%	E	E	E	E	Gas - Natural (Wet)	E	E	E	E
Chromic Acid 25%	E	L	G	L	Gasoline (Leaded)	E	E	E	E
Chromic Acid 30%	E	L	G	U	Gasoline (unleaded)	E	E	E	U
Chromic Acid 40%	E	L	L	U	Gasoline - Refined	E	E	E	E
Chromic Acid 50%	E	L	L	U	Gasoline - Sour	E	E	E	E
Citric Acid	E	E	E	E	Gelatin	E	E	E	E
Coconut Oil	E	E	E	E	Glucose	E	E	E	E
Coke Oven Gas	E	E	E	E	Glycerine (Glycerol)	E	E	E	E
Copper Carbonate	E	E	E	E	Glycol	E	E	E	E
Copper Chloride	E	E	E	E	Glue	E	E	E	E
Copper Cyanide	E	E	E	E	Glycolic Acid 30%	E	E	E	E
Copper Fluoride	E	E	E	E	Green Liquor (Paper Industry)	E	E	E	E
Copper Nitrate	E	E	E	E	Heptane	E	G	L	U
Copper Sulfate	E	E	E	E	Hexane	E	L	U	U
Care Oils	E	E	E	E	Hexanol Tertiary	E	E	E	U
Corn Oil	E	E	E	E	Hydrobromic Acid - 20%	E	E	E	G
Corn Syrup	E	E	E	E	Hydrochloric Acid - 0-25%	E	G	E	G
Cottonseed Oil	E	E	E	E	Hydrochloric Acid - 25-40%	E	E	E	G
Cresol	U	U	U	U	Hydrocyanic Acid or				
Cresylic Acid 50%	U	E	L	U	Hydrogen Cyanide	E	E	E	E
Craton Aldehyde	U	U	U	U	Hydrofluoric Acid 4%	E	L	E	G
Crude Oil - Sour	E	E	E	E	Hydrofluoric Acid 10%	E	L	E	U
Crude Oil - Sweet	E	E	E	E	Hydrofluoric Acid 48%	E	L	G	U
Cuprous Chloride	E	E	E	E	Hydrofluoric Acid 60%	E	L	G	U
Cyclohexane	U	U	U	U	Hydrofluoric Acid 100%	G	L	O	L
Cyclohexanol	U	U	U	U	Hydrogen	E	E	E	G
Cyclohexanon	U	U	U	U	Hydrogen Peroxide - 30%	E	E	E	L
					Hydrogen Peroxide - 50%	E	E	E	U
					Hydrogen Peroxide - 90%	E	E	U	U
Demineralized Water	E	E	E	E	Hydrogen Sulfide - Aqueous				
Dextrin	E	E	E	E	Solution	E	E	E	E
Dextrose	E	E	E	E	Hydrogen Sulfide - Dry	E	E	E	E
Diazo Salts	E	E	E	E	Hydroquinone	E	E	E	E
Diesel Fuels	E	E	E	E	Hydroxylamine Sulfate	E	E	E	E
Diethyle Amine	U	U	U	U	Hypochlorous Acid	E	E	E	E
Diethylphthalate	U	U	U	U	Hypo-(Sodium Thiosulfate)	E	E	E	E
Disodium Phosphate	U	E	E	E					
Diethyl Ether	U	U	U	U	Iodine	U	U	U	U
Diglycolic Acid	E	G	O	O	Iodine (in Alcohol)	U	U	U	U
Dioxane - 1,4	O	O	O	O	Iodine Solution (10%)	U	U	U	U
Divinyl Benzene	O	O	O	O	Iodoform	O	O	O	O
Drying Oil	O	O	O	O	Isopropylalcohol	E	E	E	G
Ethers	U	U	U	U	Jet Fuels, JP4 & JP5	E	E	E	E
Ethyl Acetate	U	U	U	U					
Ethyl Acrylate	U	U	U	U	Kerosene	E	E	E	E
Ethyl Chloride	U	U	U	U	Ketones	U	U	U	U
Ethyl Ether	U	U	U	U	Kraft Liquor (Paper Industry)	E	E	E	E
Ethylene Bromide	U	U	U	U					
Ethylene Chlorohydrin	U	U	U	U	Lacquer Thinners	L	U	L	U
Ethylene Dichloride	U	U	U	U	Lactic Acid 28%	E	E	E	E
Ethylene Glycol	E	E	E	E	Lard Oil	E	E	E	G
Ethylene Oxide	U	U	U	U	Lauryl Acid	E	E	E	E
					Lauryl Chloride	E	E	E	E
Fatty Acids	E	E	E	E	Lauryl Sulfate	E	E	E	E
Ferric Chloride	E	E	E	E	Lead Acetate	E	E	E	E
Ferric Nitrate	E	E	E	E	Lime Sulfur	E	E	E	E
Ferric Sulfate	E	E	E	E	Linoleic Acid	E	E	E	E
Ferrous Nitrate	E	E	E	E	Linseed Oil	E	E	E	E
Fish Solubles	E	E	E	E	Liquers	E	E	E	E
Fluorine Gas - Dry	L	U	U	U	Liquors	E	E	E	E
Fluorine Gas - Wet	L	U	U	U	Lithium Bromide	E	E	E	E
Fluoroboric Acid - 25%	E	E	E	E	Lubricating Oil	E	E	E	E
Fluorosilicic Acid	E	E	E	E					
Formaldehyde	E	G	G	L	Machine Oil	E	E	E	E
Food Products such as Milk,					Magnesium Carbonate	E	E	E	E
Buttermilk, Molasses, Salad					Magnesium Chloride	E	E	E	E
Oils, Fruit	E	E	E	E	Magnesium Citrate	E	E	E	E
Formic Acid	E	U	E	U	Magnesium Hydroxide	E	E	E	E
Freon - 12	E	G	E	G	Magnesium Nitrate	E	E	E	E
Fructose	E	E	E	E	Magnesium Sulfate	E	E	E	E
Fruit Pulp and Juices	E	E	E	E	Maleic Acid	E	E	E	E
Fuel Oil (containing H ₂ SO ₄)	E	E	E	E	Malic Acid	E	E	E	E
Furfural	U	U	U	U	Mercuric Chloride	E	E	G	G
					Mercuric Cyanide	E	E	G	G
Gallic Acid	E	E	E	E	Mercurous Nitrate	E	E	G	G
Gas - Coke Oven	E	E	G	G	Mercury	E	E	G	G
Gas - Manufactured	U	U	U	U					
Gas - Natural (Dry)	E	E	E	E					

Chemical	PVC I		PVC II		Chemical	PVC I		PVC II	
	72 °F.	140 °F.	72 °F.	140 °F.		72 °F.	140 °F.	72 °F.	140 °F.
Methane	E	E	E	E	Photographic Solutions	E	E	E	E
Methyl Bromide	U	U	U	U	Phthalic Acid	O	O	O	O
Methyl Cellosolve	U	U	U	U	Picric Acid	U	U	U	U
Methyl Chloride	U	U	U	U	Plating Solutions:				
Methyl Chloroform	U	U	U	U	Brass	E	E	E	E
Methyl Ethyl Ketone	U	U	U	U	Cadium	E	E	E	E
Methyl Iso-Butyl Ketone	U	U	U	U	Chromium	E	G	E	G
Methyl Salicylate	E	E	E	E	Copper	E	E	E	E
Methyl Sulfate	E	E	E	E	Gold	E	E	E	E
Methyl Sulfonic Acid	E	E	E	E	Iron	E	E	E	E
Methyl Sulfuric Acid	E	E	E	E	Jodium	E	E	O	E
Methylene Chloride	U	U	U	U	Lead	E	E	E	E
Milk	E	E	E	E	Nickel	E	E	E	E
Mineral Oils	E	E	E	E	Rhodium	E	E	E	E
*Mixed Acids (H ₂ SO ₄ & HNO ₃)	E	E	E	E	Silver	E	E	E	E
Molasses	E	E	E	E	Tin	E	E	E	E
Monoethanolamine	U	U	U	U	Zinc	E	E	E	E
Muriatic Acid	E	E	E	E	Potassium Acid Sulfate	E	E	E	E
Naptha	E	E	E	E	Potassium Aluminum Sulfate	E	E	O	E
Napthalene	U	U	U	U	Potassium Alum	E	E	E	E
Natural Gas, Dry & Wet	E	E	E	E	Potassium Antimonate	E	E	E	E
Nickel Acetate	E	E	E	E	Potassium Bicarbonate	E	E	E	E
Nickel Chloride	E	E	E	E	Potassium Bichromate	E	E	E	E
Nickel Nitrate	E	E	E	E	Potassium Bisulfite	E	E	E	E
Nickel Sulfate	E	E	E	E	Potassium Borate 1%	E	E	E	E
Nickel Sulphate	E	E	E	E	Potassium Borate	E	E	E	E
Nicotine	E	E	E	E	Potassium Bromate 10%	E	E	E	E
Nicotine Acid	E	E	E	E	Potassium Bromate	E	E	E	E
Nitric Acid Anhydrous	U	U	U	U	Potassium Bromide	E	E	E	E
Nitric Acid 10%	E	E	E	E	Potassium Carbonate	E	E	E	E
Nitric Acid 20%	E	E	E	E	Potassium Chlorate (ag)	E	E	E	E
Nitric Acid 35%	E	E	E	E	Potassium Chlorate	E	E	E	E
Nitric Acid 40%	E	E	E	E	Potassium Chloride	E	E	E	E
Nitric Acid 60%	E	E	E	E	Potassium Chromate (Aln)	E	E	E	E
Nitric Acid 68%	E	E	E	E	Potassium Chromate (Neut.)	E	E	E	E
Nitric Acid 70%	E	E	E	E	Potassium Chromate 40%	E	E	E	E
Nitric Acid 100%	E	E	E	E	Potassium Cuprocyanide	E	E	E	E
Nitric Acid, Red Fuming	U	U	U	U	Potassium Cyanide	E	E	E	E
Nitrobenzene	U	U	U	U	Potassium Dichromate 40%	E	E	E	E
Nitropropane	U	U	U	U	Potassium Dichromate	E	E	E	E
Nitrous Acid (10%)	E	E	E	E	Potassium Dichrom (Alkaline)	E	E	E	E
Nitrous Oxide	E	E	E	E	Potassium Dichrom (Neutral)	E	E	E	E
Ocenol (Unsaturated Alcohol)	E	E	G	G	Potassium Diphosphate	E	E	E	E
Oil and Fats	E	E	E	E	Potassium Ferricyanide	E	E	E	E
Oleic Acid	E	E	E	E	Potassium Ferrocyanide	E	E	E	E
Oleum	U	U	U	U	Potassium Fluoride	E	E	E	E
Oxalic Acid	E	E	E	E	Potassium Hydroxide	E	E	E	E
Oxygen	E	E	E	E	Potassium Hypochlorite	E	E	E	E
Ozone	G	L	U	U	Potassium Iodide	E	E	E	E
Palmitic Acid 10%	E	E	E	E	Potassium Nitrate	E	E	E	E
Palmitic Acid 70%	E	E	E	E	Potassium Perborate	E	E	E	E
Paraffin	E	E	E	E	Potassium Perchlorate	E	E	E	E
Pentane	O	O	O	O	Potassium Perchlorite	E	E	E	E
Paracetic Acid 40%	E	E	E	E	Potassium Permanganate 10%	E	E	E	E
Perchloric Acid 10%	E	E	E	E	Potassium Permanganate 25 %	G	L	E	E
Perchloric Acid 15%	E	E	E	E	Potassium Persulfate	E	E	E	E
Perchloric Acid 70%	E	E	E	E	Potassium Sulfate	E	E	E	E
Perchloroethylene	O	O	O	O	Potassium Sulfide	E	E	E	E
Petrolatum	E	E	E	E	Potassium Thiosulfate	E	E	E	E
Phenol	E	E	E	E	Propane	E	E	E	E
Phenol (90%)	L	U	U	U	Propylene Dichloride	U	U	U	U
Phenylhydrazine	U	U	U	U	Propylene Glycol	E	E	E	E
Phenylhydrazine Hydrochloride	E	U	L	U	Pyrogalllic Acid	O	O	O	O
Phosgene (Gas)	E	U	E	U	Rayon Coagulating Bath	E	E	E	E
Phosgene (Liquid)	U	G	U	G	Rachelle Salts	E	E	E	E
Phosphoric Acid 0-25%	E	E	E	E	Sea Water	E	E	E	E
Phosphoric Acid 25-50%	E	E	E	E	Salenid Acid (Aqueous)	O	O	O	O
Phosphoric Acid 50-75%	E	E	E	E	Salicylaldehyde	E	E	E	E
Phosphoric Acid - 85%	E	E	E	E	Salt Water	E	E	E	E
Phosphorous (Yellow)	E	E	E	E	Selenic Acid	E	E	E	E
Phosphorous (Red)	E	E	E	E	Sewage	E	E	E	E
Phosphorous Pentoxide	E	E	E	E	Silicic Acid	E	E	E	E
Phosphorous Trichloride	U	U	U	U	Silver Cyanide	E	E	E	E
Photographic Chemicals	E	E	E	E	Silver Nitrate	E	E	E	E
					Silver Sulfate	E	E	E	E
					Soap Solution	E	E	E	E

*Use PVC 1120

CertainTeed

Chemical	PVC I		PVC II		Chemical	PVC I		PVC II	
	72 °F.	140 °F.	72 °F.	140 °F.		72 °F.	140 °F.	72 °F.	140 °F.
Soaps	E	E	E	E	Sulphuric Acid 50-75%	E	E	E	G
Sodium Acetate	E	E	E	E	Sulphuric Acid 75-90%	E	E	L	L
Sodium Alum	E	E	E	E	Sulphuric Acid 95%	E	G	U	U
Sodium Acid Sulfate	E	E	E	E	Sulphurous Acid	G	U	L	U
Sodium Aluminate	E	E	E	E	Tan Oil	E	E	E	E
Sodium Antimonate	E	E	E	E	Tannic Acid	E	E	E	E
Sodium Arsenite	E	E	E	E	Tanning Liquors	E	E	E	E
Sodium Benzoate	E	E	E	E	Tartaric Acid	E	E	E	E
Sodium Bicarbonate	E	E	E	E	Tetrachloroethane	O	O	O	O
Sodium Bisulfate	E	E	E	E	Tetraethyl Lead	E	G	G	L
Sodium Bisulfite	E	E	E	E	Tetrahydro Furane	U	U	U	U
Sodium Borate	E	E	E	E	Thionyl Chloride	U	U	U	U
Sodium Bromide	E	E	E	E	Tepineol	G	L	G	L
Sodium Carbonate (Soda Ash)	E	E	E	E	Tin Chloride	E	E	E	E
Sodium Chlorate	E	G	G	L	Titanium Tetrachloride	E	U	E	U
Sodium Chloride	E	E	E	E	Toluol or Toluene	U	U	U	U
Sodium Chlorite	E	E	O	O	Toxaphene (90%)	O	O	O	O
Sodium Cyanide	E	E	E	E	Tributyl Phosphate	U	U	U	U
Sodium Dichromate	E	E	E	G	Trichloroacetic Acid	E	E	E	E
Sodium Dichromate (Neutral)	E	E	E	E	Trichloroethylene	U	U	U	U
Sodium Ferricyanide	E	E	E	E	Tricresylphosphate	U	U	U	U
Sodium Ferrocyanide	E	E	E	E	Triethanolamine	E	G	G	U
Sodium Fluoride	E	E	E	E	Triethylamine	E	E	G	L
Sodium Hydroxide 10%	E	E	E	E	Trimethyl Propane	E	G	L	U
Sodium Hydroxide 15%	E	E	E	E	Trisodium Phosphate	E	E	E	E
Sodium Hydroxide 35%	E	E	E	E	Turpentine	E	E	L	U
Sodium Hydroxide 70%	E	E	O	O	Urea	E	E	E	E
Sodium Hydroxide (Satr)	E	E	E	E	Urine	E	E	E	E
Sodium Hypochlorite	E	E	E	E	Vegetable Oil	E	E	E	E
Sodium Iodide	E	E	E	E	Vinegar	E	E	E	U
Sodium Nitrate	E	E	E	E	Vinyl Acetate	U	U	U	U
Sodium Nitrite	E	E	E	E	Water - Acid Mine	E	E	E	E
Sodium Perborate	E	E	O	O	Water - Distilled	E	E	E	E
Sodium Peroxide	E	E	E	E	Water - Fresh	E	E	E	E
Sodium Phosphate	E	E	E	E	Water - Salt	E	E	E	E
Sodium Phosphate - Acid	E	E	G	G	Water - Sewage	E	E	E	E
Sodium Silicate	E	E	E	E	Whiskey	E	E	E	E
Sodium Sulfate	E	E	E	E	White Gasoline	E	E	E	E
Sodium Sulfide	E	E	E	E	White Liquor (Paper Industry)	E	E	E	E
Sodium Sulfite	E	E	E	E	Wines	E	E	E	E
Sodium Thiosulfate (Hypo)	E	E	E	E	Xylene or Xylol	U	U	U	U
Sour Crude Oil	E	E	E	E	Zinc Chloride	E	E	E	E
Stannic Chloride	E	E	E	E	Zinc Chromate	E	E	E	E
Stannous Chloride (50%)	E	E	E	E	Zinc Cyanide	E	E	E	E
Stannous Chloride	E	G	E	G	Zinc Nitrate	E	E	E	E
Starch	E	E	E	E	Zinc Sulfate	E	E	E	E
Stearic Acid	E	E	E	E	Mixtures of Acids:				
Stoddards Solvent	E	E	U	U	Nitric 15% -				
Sulfated Detergents	E	E	E	E	Hydrofluoric 4%	E	E	E	G
Sulfur	E	E	E	E	Sodium Dichromate 13% -				
Sulfur Dioxide Gas - Dry	E	E	E	E	Nitric Acid 16				
*Sulfur Dioxide Gas - Wet	E	L	U	U	Water 71%	E	E	E	G
Sulfur Trioxide	E	E	E	G					
Sulphur Dioxide - Liquid	G	U	L	U					
Sulphuric Acid 0-10%	E	E	E	G					
Sulphuric Acid 10-30%	E	E	E	G					
Sulphuric Acid 30-50%	E	E	E	G					

*Use PVC 1120

This information has been obtained from reliable sources and can be used as a guide to assist in the proper application of PVC pipe. CertainTeed, however, cannot warrant its accuracy. It is suggested that you run your own tests for critical applications.

Pipe & Plastics Group

CertainTeed Corporation
P.O. Box 860
Valley Forge, PA 19482
(610) 341-6820
(610) 341-6837 Fax

Code No. 40-10-29

Printed in U.S.A
0398

**APPLICATION FOR PERMIT RENEWAL AND MODIFICATION
SANDOVAL COUNTY LANDFILL**

**VOLUME III: LANDFILL ENGINEERING CALCULATIONS
SECTION 5: PIPE LOADING CALCULATIONS**

TABLE OF CONTENTS

1.0	INTRODUCTION	III.5-1
2.0	PIPE LOADING DESIGN CRITERIA	III.5-1
3.0	PIPE STRENGTH CALCULATIONS.....	III.5-2
3.1	6-Inch SDR 11.0 HDPE Pipe.....	III.5-2
4.0	REFERENCES	III.5-10

LIST OF FIGURES

Figure No.	Title	Page
III.5.1	LANDFILL CROSS SECTIONS	III.5-4

LIST OF TABLES

Table No.	Title	Page
III.5.1	COMPARISON OF PVC AND HDPE PIPE	III.5-2
III.5.2	SDR 11.0 HDPE PIPE RESULTS.....	III.5-9
III.5.3	LEACHATE PIPE STRENGTH REFERENCES	III.5-10

LIST OF ATTACHMENTS

Attachment No.	Title
III.5.A	QIAN, XUEDE; KOERNER, ROBERT M.; AND GRAY, DONALD H. 2002. <i>GEOTECHNICAL ASPECTS OF LANDFILL DESIGN AND CONSTRUCTION</i> . NEW YORK: PRENTICE HALL.
III.5.B	SHARMA, HARI .D. AND SANGEETA P. LEWIS. 1994. <i>WASTE CONTAINMENT SYSTEMS, WASTE STABILIZATION AND LANDFILLS: DESIGN AND EVALUATION</i> . NEW YORK: JOHN WILEY AND SONS.
III.5.C	UNI-BELL PVC PIPE ASSOCIATION. 2001. <i>HANDBOOK OF PVC PIPE DESIGN.</i> , TEXAS: UNI-BELL PVC PIPE ASSOCIATION.
III.5.D	WASHINGTON STATE DEPARTMENT OF ECOLOGY. 1987. <i>SOLID WASTE LANDFILL DESIGN MANUAL</i> . WASHINGTON: WDOE

**APPLICATION FOR PERMIT RENEWAL AND MODIFICATION
SANDOVAL COUNTY LANDFILL**

**VOLUME III: LANDFILL ENGINEERING CALCULATIONS
SECTION 5: PIPE LOADING CALCULATIONS**

- III.5.E POLY PIPE INDUSTRIES, INC. 2008. *DESIGN AND
ENGINEERING GUIDE FOR POLYETHYLENE PIPING.*
WWW.PLASTICPIPE.ORG.
- III.5.F DRISCOPIPE, INC. 2008. *POLYETHYLENE PIPING SYSTEMS
MANUAL.*
- III.5.G CHEVRON PHILLIPS CHEMICAL COMPANY, LP. 2003.
PERFORMANCE PIPE ENGINEERING MANUAL. BULLETIN: PP
900.

**APPLICATION FOR PERMIT RENEWAL AND MODIFICATION
SANDOVAL COUNTY LANDFILL**

**VOLUME III: LANDFILL ENGINEERING CALCULATIONS
SECTION 5: PIPE LOADING CALCULATIONS**

1.0 INTRODUCTION

The Sandoval County Landfill (SCLF) is an existing solid waste facility operating in compliance with its current Permits, SWM-050304 and SWM-050304 (SP), and the New Mexico Environment Department (NMED) Solid Waste Rules (20.9.2-2.9.10 NMAC). SCLF is located at 2708 Iris Road NE in Rio Rancho, New Mexico (NM), and occupies 178.3 acres \pm . SCLF is publicly owned and operated by the County of Sandoval (“the County”), and is currently permitted to accept municipal solid waste (MSW), including construction and demolition debris (C&D) and tires, and two special wastes: petroleum contaminated soils (PCS) and sludge.

2.0 PIPE LOADING DESIGN CRITERIA

The leachate collection system piping for the Sandoval County Landfill (SCLF) is designed to meet the requirements of the regulatory standards identified in the New Mexico Solid Waste Rules 20.9.4 NMAC. More specifically, 20.9.4.15.A.(4) NMAC requires that the leachate collection piping be able to:

“withstand the loads, stresses, and disturbances from overlying waste, waste cover materials, and equipment operation.”

The purpose of these calculations is to confirm that high-density polyethylene (HDPE) standard dimension ratio (SDR 11) solid and perforated piping incorporated into the landfill design will remain intact after placement of waste fill; and retain the required characteristics after exposure to operating equipment and long-term stresses (see **Figure III.5.1**). The basic design approach consists of calculating the deflection on the leachate collection piping, which cannot exceed its allowable value, with a minimum factor of safety against failure of 1.0.

TABLE III.5.1
Comparison of PVC and HDPE Pipe
Sandoval County Landfill

Characteristic	6" Diameter Leachate Collection Pipes	
	Schedule 80 PVC	HDPE
Dimension Ratio	16	11.0
Method of Joining	Gasketed	Welded
Manning's Number (n)	0.009	0.010
Outside Diameter (in)	6.625	6.625
Min. Wall Thickness (in)	0.432	0.602
Nominal Weight/ft (lb/ft)	5.313	4.971
Tensile Strength (psi)	5,000	5,000
Modulus of Elasticity (psi)	400,000	35,000
Flexural Strength (psi)	14,450	135,000

While the Rules allow for either polyvinyl chloride (PVC) or high-density polyethylene (HDPE) piping systems, SDR 11.0 HDPE pipe has been found to be equivalent or better than PVC piping in landfill leachate pipe applications (i.e., greater resistance to buckling and crushing) and therefore was selected for this design. Documentation for the information listed in **Table III.5.1** is provided in **Attachment III.5.C** and **Attachment III.5.F**.

3.0 PIPE STRENGTH CALCULATIONS

3.1 6-Inch SDR 11.0 HDPE Pipe

In order to determine the capability of 6-in HDPE SDR 11.0 perforated collection pipes to withstand maximum stresses from the overlying soil profile, the pipes were analyzed for adequate protection against ring deflection and wall buckling using **Attachment III.5.F**, Driscopipe, Inc., Polyethylene Piping Systems Manual.

Wall buckling occurs if the total external soil pressure exceeds the pipe-soil system's critical buckling pressure; and excessive ring deflection occurs if the vertical strain in the surrounding soil envelope is greater than the allowable ring deflection of the pipe. SDR 11.0 HDPE pipe has been found to be equivalent or better than PVC piping in landfill leachate pipe applications (i.e., greater resistance to buckling and crushing) and therefore was selected for this design. SDR

stands for standard dimension ratio which is the ratio of the outside pipe diameter to the pipe wall thickness $SDR = OD/t$. As opposed to the schedule nomenclature used for PVC piping, as the SDR gets smaller the thickness of the pipe wall is increased. A comparison of the specifications for each of the two pipe types is made in **Table III.5.1**. Section 3.2.1 provides HDPE specifications for the selected diameter.

3.1.1 6-Inch Diameter SDR 11.0 HDPE Pipe Dimensions (Attachment III.5.E)

- Pipe nominal diameter: 6-in
- Pipe Outside Diameter (OD): 6.625-in
- Pipe Wall Thickness (t): 0.602 in
- Pipe Inner Diameter (ID): 5.35 in
- SDR : 11.0
- Perforation /ft: 12 perforation holes
- Perforated Hole Diameter (in): 0.5 in

3.1.2 Loads Acting on the Leachate Collection Pipe

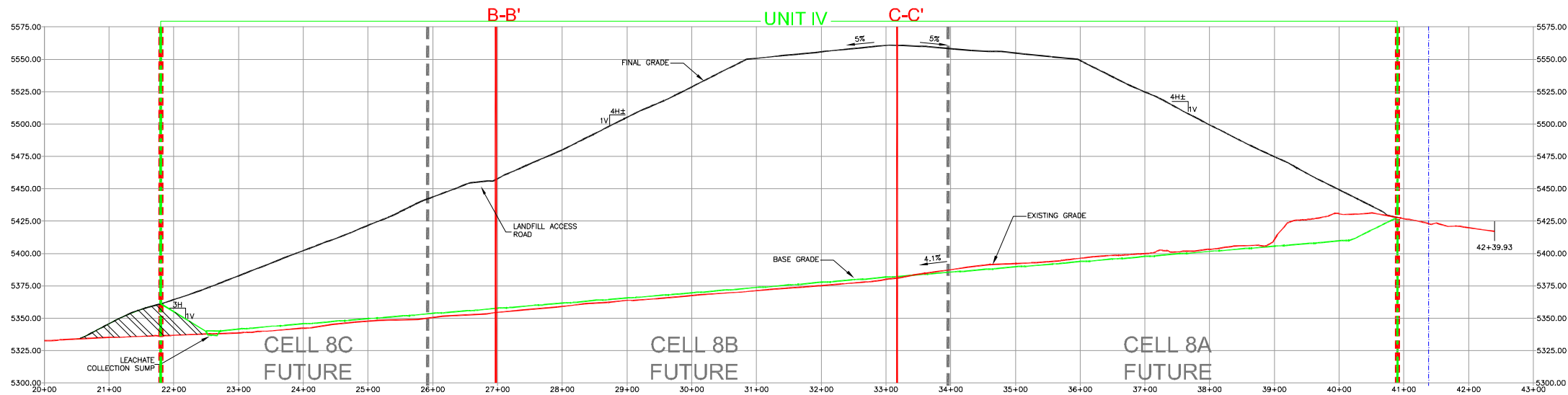
To calculate the total vertical load on the pipes, P_T , the pressure from each overlying layer was calculated and summed. The greatest waste depth occurs above the leachate collection pipe in Cell 8B on cross section C-C' (**Figure III.5.1**). There will be 5 layers:

- 3-ft thick final cover
- 1-ft thick intermediate cover
- 173-ft of total waste
- 2 ft of protective soil layer
- A 1 ft thick leachate collection select aggregate layer
- Total thickness = 180 ft

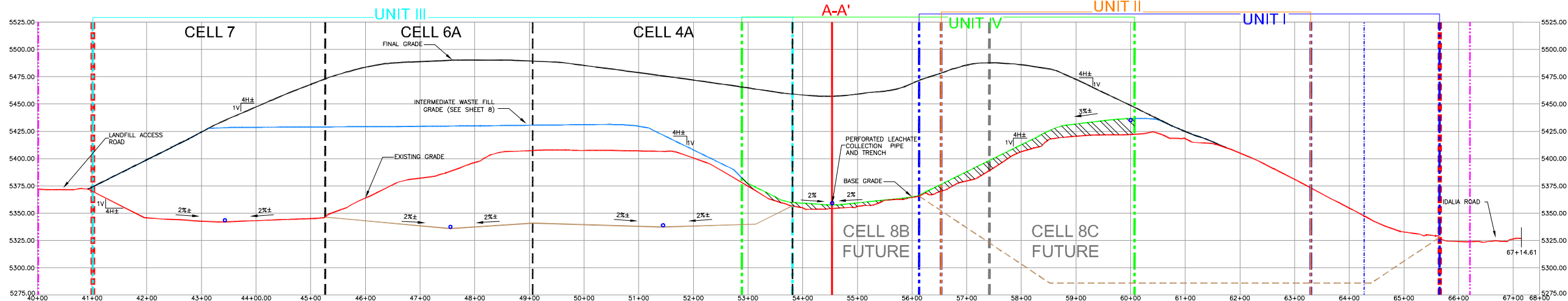
Based on the known thickness of each layer and assigned unit weights, the pressure that will be exerted by each layer was calculated. The results for P_T are presented in **Table III.5.2**.

3.1.3 Correction of Load on Pipe with Perforations (HDPE SDR 11.0)

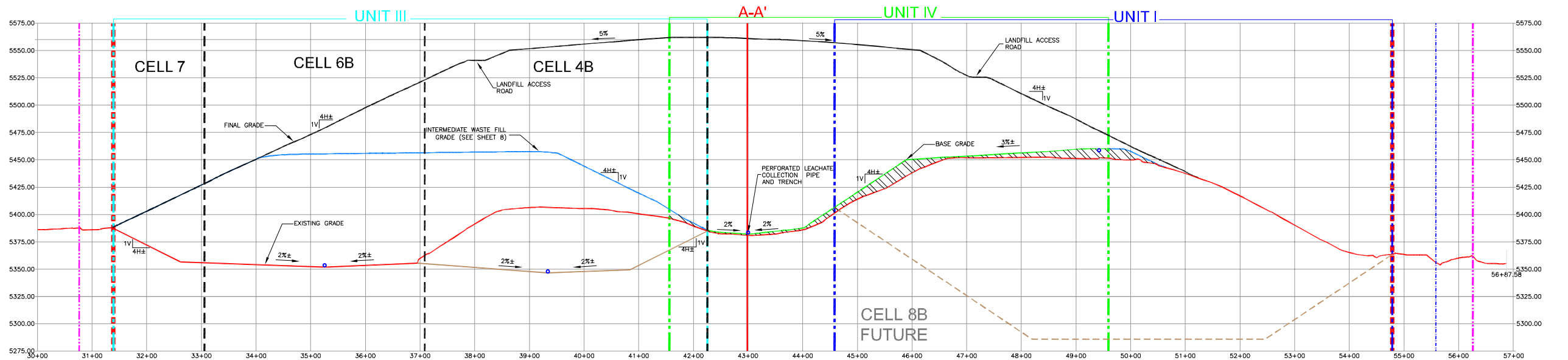
Perforating pipes reduces the effective length of pipe available to carry loads and resist deflection. The effect of perforations can be taken into account by using an increased load per nominal unit length of the pipe. The increased vertical load per unit length of pipe is calculated as follows:



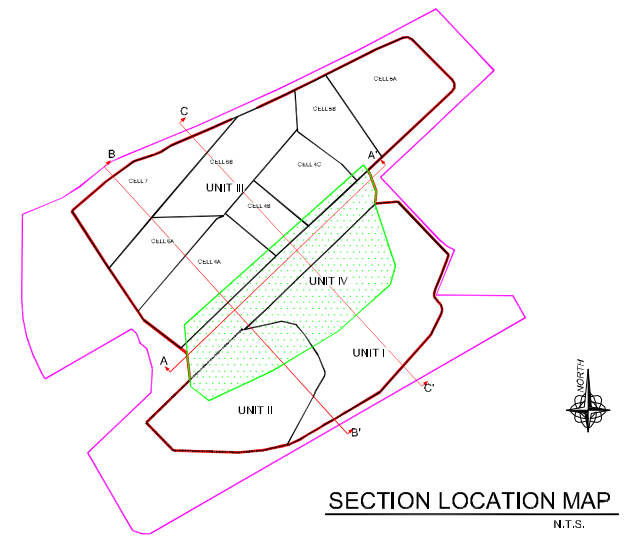
CROSS SECTION A-A'



CROSS SECTION B-B'



CROSS SECTION C-C'



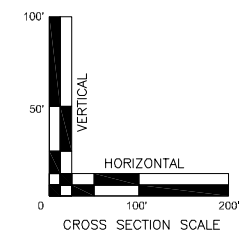
SECTION LOCATION MAP
N.T.S.

LEGEND

- FINAL GRADE
- INTERMEDIATE WASTE FILL GRADE
- EXISTING GRADE
- UNIT IV COMPOSITE LINER GRADE
- STRUCTURAL FILL SOIL COMPACTED TO 90% STANDARD PROCTOR DENSITY
- AS-BUILT BASE GRADE BASED ON COMPLETED CQA REPORTS
- INTERPOLATED UNIT I AND UNIT II BASE GRADES
- UNIT I BOUNDARY
- UNIT II BOUNDARY
- UNIT III BOUNDARY
- UNIT IV BOUNDARY
- CELL BOUNDARY
- LIMIT OF WASTE BOUNDARY
- PROPERTY BOUNDARY

NOT FOR CONSTRUCTION

Drawing/Placed 2003/211,00,01/PERMIT FIGURES/13 X-SEC.dwg
Date/Time: Apr. 16, 2015-16:47:42; LAYOUT: FIGURE 13
Copyright © All Rights Reserved, Gordon Environmental, Inc. 2012



LANDFILL CROSS SECTIONS

SANDOVAL COUNTY LANDFILL
RIO RANCHO, NEW MEXICO

Gordon Environmental, Inc.
Consulting Engineers

213 S. Camino del Pueblo
Bernalillo, New Mexico, USA
Phone: 505-867-6990
Fax: 505-867-6991

DATE: 04/16/2015	CAD: 13 X-SEC.dwg	PROJECT #: 211.00.01
DRAWN BY: DMI	REVIEWED BY: MRH	
APPROVED BY: IKG	g4@gordonenvironmental.com	FIGURE III.5.1

Static Vertical Load per Unit Length of Pipe (W_C):

$$W_C = (P_T)(D_o) / (1 - ((n)(d)/12)) \quad (\text{Attachment III.5.A, p. 306})$$

Where:

- P_T = design load (psi)
- D_o = outside diameter of the pipe (in)
- n = number of perforated holes per ft of pipe
- d = diameter of perforated hole on the pipe (in)

$$W_C = [(83.8 \text{ psi})(6.625)] / [1 - ((12)(0.5 \text{ in}) / 12)]$$

$$W_C = [(83.8 \text{ psi})(6.625)] / 0.5$$

$$W_C = 1,110.4 \text{ lbs/in} = 13,324.8 \text{ lbs/ft}$$

The design value in psi is found by dividing the design load in lbs/in by the diameter of pipe.

$$P_D = 1,110.4 / 6 = 185.1 \text{ psi.}$$

3.1.4 Deflection

The ring deflection of the pipe is calculated from the following Modified Iowa formula:

$$\Delta X = \left(\frac{(D_L)(K)(W_c)(r^3)}{(E)(I) + 0.061(E')(r^3)} \right) \quad (\text{Attachment III.5.A, p. 305})$$

Where:

- ΔX = horizontal and vertical deflection of the pipe (in)
- D_L = a factor, generally taken at a conservative value of 1.5, compensating for the lag or time dependent behavior of the soil/pipe systems (dimensionless) (**Attachment III.5.A, p.307**)
- W_c = vertical load acting on the pipe per unit of pipe length (1,110.4 lbs/in)
- r = mean radius of the pipe ($OD - t = (6.625 \text{ in.} - 0.602 \text{ in})/2 = 3.01 \text{ in}$)
- E = modulus of elasticity of the pipe materials (35,000 psi) (**Attachment III.5.F, p. 43**)
- E' = modulus of passive soil resistance in Crushed Rock (3,000 psi) (**Attachment III.5.A, p. 307**)
- K = bedding constant, reflecting the support the pipe receives from the bottom of the trench (assumes Bedding angle = 180°; therefore $K = 0.083$) (**Attachment III.5.A, p. 306**)
- I = moment of inertia of pipe wall per unit of length (in^4/in); for any round pipe, $I = t^3/12$ where t is the average thickness (in) = $((0.602)^3/12) = 0.018 \text{ in}^4/\text{in}$

Ultimate degree of compaction and E' will increase as waste is placed over the leachate trench resulting in at least 3,000 psi for the modulus of passive soil resistance.

$$\Delta X = \left(\frac{(1.5)(0.083)(1,110.4)(3.01^3)}{(35,000)(0.018) + (0.061)(3,000)(3.01^3)} \right)$$

$$\Delta X = \left(\frac{3,770.1}{630 + 4,990.6} \right) = 0.671 \text{ in}$$

The ring deflection is then used to determine the ring bending strain using the equation:

$$\varepsilon = f_D \left(\frac{\Delta x}{D_M} \right) \left(\frac{2C}{D_M} \right)$$

Where:

- ε = Wall strain
- f_D = deformation shape factor = 6.0 (**Attachment III.5.G, page 112**)
- Δx = Deflection From previous calculation = 0.671 in
- D_M = Mean Diameter, in
- C = Distance from outer fiber to wall centroid, in

$C = 0.5(1.06t)$, where t = wall thickness

$$C = 0.5 \times 1.06 \times 0.602 = 0.319 \text{ in}$$

$$\varepsilon = (6.0) \left(\frac{0.671}{6} \right) \left(\frac{2(0.319)}{6} \right) = 0.0713 = 7.13\%$$

The wall strain of 7.13 % is less than 8 %, which has an acceptable factor of safety of $8\%/7.13\% = 1.12$ (**Attachment III.5.G, page 112**).

3.1.5 Wall Buckling

Wall buckling may govern design of flexible pipes under conditions of loose soil burial, if the external load exceeds the compressive strength of the pipe material. To determine a factor of safety for wall buckling the pipe critical-collapse differential pressure P_c must be calculated using the following formula (**Attachment III.5.F, p. 43**):

$$P_c = \frac{2.32(E)}{SDR^3} \text{ where } E \text{ is the modulus of elasticity, approximately } 35,000 \text{ psi}$$

$$P_c = \frac{2.32(35,000)}{11.0^3} = 61.0 \text{ psi}$$

The critical-collapse pressure can then be used to determine the critical buckling pressure from the following relation (**Attachment III.5.F, p. 43**):

$$P_{cb} = 0.8\sqrt{(E')(P_c)}$$

Where:

$$\begin{aligned} P_{cb} &= \text{Critical buckling pressure} \\ E' &= \text{Long term degree of compaction of bedding} = 3,000 \text{ psi (Attachment III.5.A, p. 307)} \end{aligned}$$

$$P_{cb} = 0.8\sqrt{(3,000)(61.0)} = 342.2 \text{ psi}$$

The factor of safety is then determined:

$$FS = \frac{P_{cb}}{P_D} = \frac{342.2}{185.1} = 1.85$$

3.1.6 Wall Crushing

To determine a factor of safety for wall crushing, the following equations were used (**Attachment III.5.F, p. 42**):

$$S_A = \frac{(SDR-1)}{2} \times P_D$$

Where:

$$\begin{aligned} S_A &= \text{Actual compressive stress, psi} \\ P_D &= \text{Total external pressure on the top of the pipe, psi} \\ P_D &= W_c/D = 1,110.4/6 = 185.1 \text{ psi} \end{aligned}$$

For a SDR of 11.0 the actual compressive stress is:

$$S_A = \frac{(11.0-1)}{2} \times 185.1 = 925.5 \text{ psi}$$

The factor of safety can then be found using the compressive yield strength of HDPE pipe of 1,500 psi (**Attachment III.5.F**):

$$FS = \frac{1,500 \text{ psi}}{925.5 \text{ psi}} = 1.62$$

3.1.7 Equipment Loading (Added at Bureau's Request)

Exceptionally conservative assumptions would include a piece of equipment operating over the leachate collection pipe after 3 ft of protective soil layer has been placed. A loaded CAT 627 Scraper was used conservatively as the piece of equipment operating on top of the leachate collection pipe. The CAT 627 Scraper has the following specifications (Reference Caterpillar Performance Handbook, Edition 29):

- Tractor Weight = 48,061 lbs
- Scraper Weight = 33,399 lbs
- Soil Load (20 cy) = 48,000 lbs
- Total weight = 129,460 lbs
- Max weight per tire = 33,012 lbs (assumes 49% of the total weight acts on the rear tires and 51% of the weight acts on the front tires).
- Tire width = approximately 18 in = 1.5 ft
- Tire contact length = approximately 4 in = 0.33 ft
- Tire contact area = (18 in)(4 in) = 72 in² = 0.50 ft²

Superimposed loads distributed over an area during equipment operations are determined from the following equation (ASCE, 1982):

$$W_{SD} = (C_S)(p)(F)(B_C)$$

Where:

W_{SD}	=	Load on pipe (lbs/ft)
p	=	Intensity of distributed load (lbs/ft ²)
F	=	Impact factor
B_C	=	Outside diameter of pipe (ft)
C_S	=	Load coefficient

The load coefficient is a function of D/2H and M/2H, in which H is the height from the top of the pipe to the ground surface (3 ft); and D and M are the width and length, respectively, or the area over which the distributed load acts. Table 4C.3, **Attachment III.5.D, p. 4C-16**, lists values of the load coefficients for loads centered over the pipe.

Determining the required parameters:

$$\begin{aligned} H &= 3 \text{ ft} \\ D &= 1.5 \text{ ft} \\ M &= 0.33 \text{ ft} \\ F &= 1.0 \text{ (Table 4C.4, Attachment III.5.D, p. 4C-17)} \\ B_C &= 6.625 \text{ in} = 0.55 \text{ ft} \\ D/2H &= 1.5 \text{ ft}/(2(3 \text{ ft})) = 0.250 \\ M/2H &= 0.33 \text{ ft}/(2(3 \text{ ft})) = 0.055 \\ p &= 33,012 \text{ lbs}/(1.5 \text{ ft})(0.33 \text{ ft}) = 66,691 \text{ lbs/ft}^2 \\ C_S &= \sim 0.053 \text{ per Table 4C.3, Attachment III.5.D, p. 4C-16} \end{aligned}$$

Therefore:

$$W_{SD} = (0.053)(66,691 \text{ lbs/ft}^2)(1.0)(0.55 \text{ ft})$$

$$W_{SD} = 1951.40 \text{ lbs/ft} = 162.62 \text{ lbs/in}$$

The superimposed load due to equipment loading is significantly less than static loading conditions (W_C) calculated in Section 3.1.3 as 1,110.4 lbs/in for the ultimate waste/soil surcharge; therefore the static loading conditions govern.

3.1.8 HDPE Pipe Loading Results

Calculations for ring deflection, wall crushing, wall buckling, due to dead and live loading stresses for the proposed 6-in lateral were completed, and the following table summarizes the results.

TABLE III.5.2
SDR 11.0 HDPE Pipe Results
Sandoval County Landfill

Design Criteria	Critical Value	Actual Value	Factor of Safety
Dead Load Only			
Ring Deflection	8.0 %	7.13%	1.12
Wall Buckling	342.2 psi	185.1 psi	1.85
Wall Crushing	1,500 psi	925.5 psi	1.62

As shown, for each limiting design criterion, the factor of safety is greater than established design criteria, thus the performance standard for the HDPE pipes is more than adequate.

4.0 REFERENCES

Leachate pipe strength calculations were completed using establish guidelines provided in the references listed on **Table III.5.3**.

TABLE III.5.3
Leachate Pipe Strength References
Sandoval County Landfill

- A. “Geotechnical Aspects of Landfill Design and Construction”, Xuede Qian, Robert M. Koerner, Donald H. Gray, Prentice Hall, 2002.
- B. “Waste Containment Systems, Waste Stabilization, and Landfills” Hari D. Sharma and Sangeeta P. Lewis. John Wiley & Sons, 1994.
- C. “Handbook of PVC Pipe Design” Uni-Bell PVC Pipe Association, 2001
- D. WDOE Landfill Design Manual, 1987
- E. “Design and Engineering Guide for Polyethylene Piping”, Poly Pipe Industries, Inc, 2008
- F. “Polyethylene Piping Systems Manual”, Driscopipe, Inc., 2008
- G. Chevron Phillips, “Bulletin: PP 900”, Book 2 – Chapter 7, p. 112, 2003

**APPLICATION FOR PERMIT RENEWAL AND MODIFICATION
SANDOVAL COUNTY LANDFILL**

**VOLUME III: LANDFILL ENGINEERING CALCULATIONS
SECTION 5: PIPE LOADING CALCULATIONS**

ATTACHMENT III.5.A

**QIAN, XUEDE; KOERNER, ROBERT M.; AND GRAY, DONALD H. 2002.
GEOTECHNICAL ASPECTS OF LANDFILL DESIGN AND CONSTRUCTION.
NEW YORK: PRENTICE HALL.**

GEOTECHNICAL ASPECTS OF LANDFILL DESIGN AND CONSTRUCTION

Xuede Qian

*Geotechnical Engineering Specialist
Michigan Department of Environmental Quality*

Robert M. Koerner

*H. L. Bowman Professor of Civil Engineering, Drexel University
Director, Geosynthetic Research Institute*

Donald H. Gray

*Professor of Civil and Environmental Engineering
The University of Michigan*



PRENTICE HALL
Upper Saddle River, New Jersey 07458

Number of Perforation Holes:

$$\begin{aligned}
 N &= Q_{in}/Q_b & (9.12) \\
 &= 0.0002184/0.00002114 \\
 &= 10.35 \text{ holes/ft (34 holes/m)}
 \end{aligned}$$

So, use 12 holes/ft (40 holes/m); that is 6 holes per foot (20 holes per meter) each side as shown in Figure 9.3.

9.4 DEFORMATION AND STABILITY OF LEACHATE COLLECTION PIPE

All components of the leachate collection and removal system must have sufficient strength to support the weight of the overlying waste, cover system, and post-closure loadings, as well as the stresses from operating equipment. The component that is perhaps the most vulnerable to compressive strength failure is the drainage layer piping. Leachate collection and removal system piping can fail by excessive deflection, which may lead to buckling or collapsing. Pipe strength calculations should include resistance to pipe deflection and critical buckling pressure. This situation is heightened by the current tendency to create extremely large landfills, sometimes called "megafills."

9.4.1 Pipe Deflection

Leachate collection pipes may excessively deform during construction, during the active life of the landfill or under the post-closure loading. This deformation may lead to buckling and eventual collapse. Thus, leachate pipes should be handled carefully and brought on site only when the trench is ready. Passage of heavy equipment directly over a pipe must be avoided. A pipe can be installed in either a positive or negative projection mode. However, every effort should be made to install it in a negative projection mode (Figure 9.2), although at times it may be necessary to install a pipe in a positive projecting mode (Figure 9.5). The essential difference between these two con-

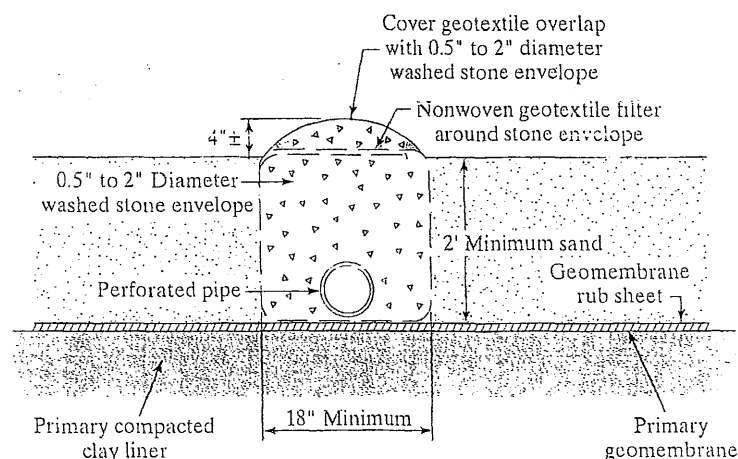


FIGURE 9.5 Leachate Collection Pipe in a Positive Projection Mode

cepts is that a negative projection allows for soil arching which limits the load on the pipe. Conversely, positive projection can actually add load to the pipe. Spangler (1960), among others, explains these concepts for deeply buried pipelines. The design of a pipe must be checked to ascertain whether it will be able to withstand the load during both preconstruction and postconstruction periods. Usually one of two types of pipes are used, HDPE or PVC. These are considered as flexible type pipes. This infers that they do not rupture or break under excessive load, they deform, and if excessively, buckle and/or collapse. The basic design approach consists of calculating the deflection of the pipe, which should not exceed the allowable value. The following formula, commonly known as the Modified Iowa formula, can be used to estimate pipe deflection (Spangler and Handy, 1973; Moser, 1990).

Modified Iowa Formula:

$$\Delta X = \frac{D_L \cdot K \cdot W_c \cdot r^3}{E \cdot I + 0.061 E' \cdot r^3} \quad (9.16)$$

where ΔX = horizontal deflection, in or m (Figure 9.6);

K = bedding constant, its value depending on the bedding angle (see Table 9.1 and Figure 9.7); also, as a general rule, a value of $K = 0.1$ is assumed;

D_L = deflection lag factor (see Table 9.2);

W_c = vertical load per unit length of the pipe, lb/in or kN/m;

r = mean radius of the pipe, $r = (D_o - t)/2$, in or m;

E = elastic modulus of the pipe material, lb/in² or kN/m²;

I = moment of inertia of the pipe wall per unit length,

$I = t^3/12$, in⁴/in = in³ or m⁴/m = m³;

t = thickness of pipe, in or m; and

E' = soil reaction modulus, lb/in² or kN/m², see Table 9.3.

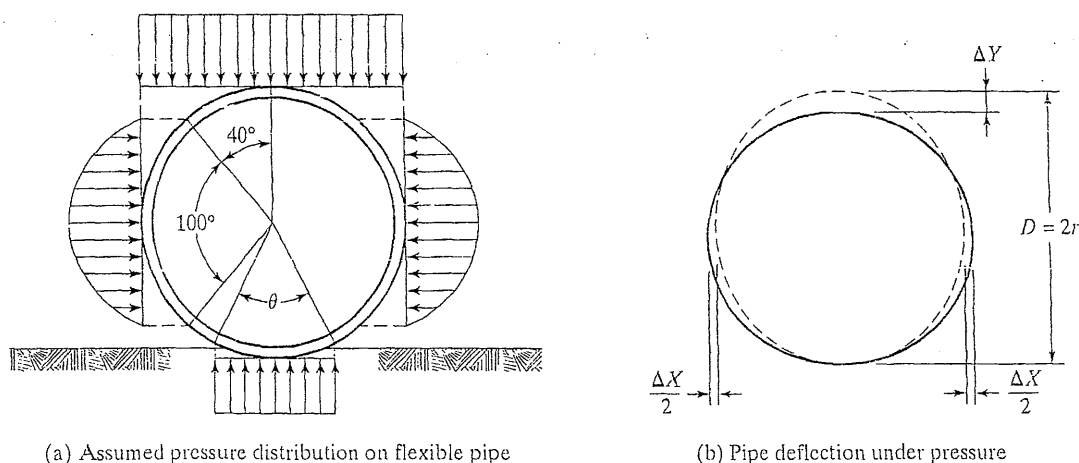


FIGURE 9.6 Buried Flexible Pipe

TABLE 9.1 Values of Bedding Constant, K

Bedding Angle, θ (degree)	Bedding Constant, K
0	0.110
30	0.108
45	0.105
60	0.102
90	0.096
120	0.090
180	0.083

The deflection of the pipe, ΔX , calculated from Equation 9.16 is the deflection in the horizontal direction, as shown in Figure 9.6. When the deflection of pipe is not large (e.g., less than 10%), the vertical deflection of pipe, ΔY , is usually assumed to be approximately equal to the horizontal deflection of pipe, ΔX .

Vertical Load per Unit Length of Pipe:

For Solid Pipe,

$$W_c = (\sum \gamma_i \cdot H_i) \cdot D_o \quad (9.17)$$

where W_c = vertical load per unit length of the pipe, lb/in or kN/m;

γ_i = unit weight of material i on the pipe (sand, clay or solid waste),
lb/in³ or kN/m³;

H_i = thickness of material i , in or m; and

D_o = outside diameter of the pipe, in or m.

For Perforated Pipe,

$$W_c = \frac{(\sum \gamma_i \cdot H_i) \cdot D_o}{(1 - n \cdot d/12)} \quad (9.18)$$

where W_c = vertical load per unit length of the pipe, lb/in or kN/m;

γ_i = unit weight of material i (soils or solid waste), lb/in³ or
kN/m³;

H_i = thickness of material i , in or m;

D_o = outside diameter of the pipe, in or m;

d = diameter of perforated hole or width of perforated slot on the pipe, in
or m; and

n = number of perforated holes or slots per row per foot of pipe.

FIGURE 9.7 Pipe Bedding Angle

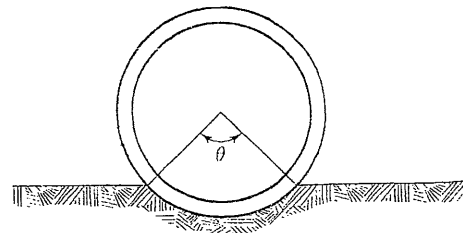


TABLE 9.2 Approximate Range of Values of D_L

Variable	Range	Remarks
D_L	1.5 to 2.5	If the soil in the trench is not compacted, then the higher value of D_L should be used. When deflection calculations are based on prism loads.
	1.0	

TABLE 9.3 Average Values of Soil Reaction Modulus, E' (for Short Term Flexible Pipe Deflection) (Howard, 1977)

Soil type-pipe bedding material (United Classification System) ^a	E' for degree of compaction of bedding			
	Dumped	Slight, < 85 % Proctor, < 40 % relative density	Moderate, 85%–95% Proctor, 40%–70% relative density	High, > 95 % Proctor, > 70 % relative density
Fine-grained soils (LL > 50) ^b Soils with medium to high plasticity CH, MH, CH-MH	No data available; consult a competent soils engineer; Otherwise use $E' = 0$			
Fine-grained soils (LL < 50) Soils with medium to no plasticity CL, ML, ML-CL, with less than 25% coarse-grained particles	50 lb/in ² (345 kN/m ²)	200 lb/in ² (1,380 kN/m ²)	400 lb/in ² (2,760 kN/m ²)	1,000 lb/in ² (6,900 kN/m ²)
Fine-grained soils (LL < 50) Soils with medium to no plasticity CL, ML, ML-CL, with more than 25% coarse-grained particles	100 lb/in ² (690 kN/m ²)	400 lb/in ² (2,760 kN/m ²)	1,000 lb/in ² (6,900 kN/m ²)	2,000 lb/in ² (13,800 kN/m ²)
Coarse-grained soils with fines GM, GC, SM, SC contains more than 12% fines				
Coarse-grained soils with little or no fines GW, GP, SW, SP ^c contains less than 12% fines	200 lb/in ² (1,380 kN/m ²)	1,000 lb/in ² (6,900 kN/m ²)	2,000 lb/in ² (13,800 kN/m ²)	3,000 lb/in ² (20,700 kN/m ²)
Crushed rock	1,000 lb/in ² (6,900 kN/m ²)	3,000 lb/in ² (20,700 kN/m ²)	3,000 lb/in ² (20,700 kN/m ²)	3,000 lb/in ² (20,700 kN/m ²)
Accuracy in term of percentage deflection ^d	± 2	± 2	± 1	± 0.5

^a ASTM Designation D2487, USBR Designation E-3^b LL = Liquid Limit^c or any borderline soil beginning with one of these symbols (i.e., GM-GC, GC-SC)^d for ± 1 % accuracy and predicted deflection of 3 %, actual deflection would be between 2 % and 4 %

Note: Values applicable only for soil fills less than 50 ft (15 m). Table does not include any safety factor. For use in predicting initial deflections only—appropriate deflection lag factor must be applied for long-term deflections. If bedding falls on the borderline between two compaction categories, select lower E' value or average the two values. Percentage Proctor based on laboratory maximum dry density from test standards using about 12,500 ft-lb/ft³ (600 m-kN/m³) (ASTM D698, AASHTO T-99, USBR Designation E-11).

Used with permission of ASCE.

The parameter that controls the pipe deformation is known as the deflection ratio. The deflection ratio of a pipe is defined as the ratio of the vertical deflection of pipe and the mean diameter of the pipe.

Deflection Ratio:

$$\text{Deflection Ratio (\%)} = (\Delta Y/D) \times 100\% \quad (9.19)$$

where ΔY = vertical deflection of pipe, $\Delta Y \approx \Delta X$ when the deflection is less than 10%, in or m; and
 D = mean diameter of pipe, in or m.

Mean Diameter of Pipe:

$$D = (D_o + D_i)/2 = D_o - t = D_i + t \quad (9.20)$$

where D = mean diameter of pipe, in or m;
 D_o = outside diameter of pipe, in or m;
 D_i = inside diameter of pipe, in or m; and
 t = thickness of pipe, in or m.

There is another formula that can be used to estimate the deflection of the pipe. It is essentially an alternative version of the Modified Iowa formula and has been widely used in the engineering field. This formula is

$$\Delta X = \frac{D_L \cdot K \cdot W_c}{0.149 \cdot PS + 0.061 \cdot E'} \quad (9.21)$$

where ΔX = horizontal deflection, in or m (Figure 9.6);
 K = bedding constant, its value depending on the bedding angle (see Table 9.1 and Figure 9.7); as a general rule, a value of $K = 0.1$ is assumed;
 D_L = deflection lag factor, see Table 9.2;
 W_c = vertical load per unit length of the pipe, lb/in or kN/m;
 PS = pipe stiffness, lb/in² or kN/m²; and
 E' = soil reaction modulus, lb/in² or kN/m².

The vertical pressure on solid pipe is given by

$$P_{tp} = \sum \gamma_i \cdot H_i \quad (9.22)$$

The vertical pressure on perforated pipe is given by

$$P_{tp} = \frac{\sum \gamma_i \cdot H_i}{(1 - n \cdot d/12)} \quad (9.23)$$

where P_{tp} = vertical pressure on the pipe, $P_{tp} = W_c/D_o$, lb/in² or kN/m²;
 γ_i = unit weight of material i on the pipe (sand, clay or solid waste), lb/in³ or kN/m³;
 H_i = thickness of material i , in or m;

d = diameter of perforated hole or width of perforated slot on the pipe, in or m; and

n = number of perforated holes or slots per row per foot of pipe.

Pipe stiffness is measured according to ASTM D2412 (Standard Test Method for External Loading Properties of Plastic Pipe by Parallel-Plate Loading). The elastic modulus of the pipe material depends on the type of resin and formulation being used. Three formulas that can be used to calculate pipe stiffness are

$$PS = \frac{E \cdot I}{0.149 \cdot r^3} \quad (9.24)$$

$$PS = 0.559 \cdot E \cdot (t/r)^3 \quad (9.25)$$

and

$$PS = 4.47 \cdot \frac{E}{(SDR - 1)^3} \quad (9.26)$$

where PS = pipe stiffness, lb/in² or kN/m²;

E = elastic modulus of the pipe material, lb/in² or kN/m²;

I = moment of inertia of the pipe wall per unit length,

$I = t^3/12$, in⁴/in = in³ or m⁴/m = m³;

r = mean radius of pipe, in or m;

t = wall thickness of pipe, in or m; and

SDR = standard dimension ratio, the same as the dimension ratio.

The allowable deflection ratios for a typical commercial polyethylene pipe are listed in Table 9.4.

Deflections of buried flexible pipe are commonly calculated using Equation 9.16 or 9.21. These equations use the soil reaction modulus, E' , as a surrogate parameter for soil stiffness. It should be noted that the values of E' in Table 9.3 only apply for soil fills of less than 50 ft (15 m). However, megafills built over leachate collection pipes often exceed 150 ft (46 m) in height. The soil reaction modulus is not a directly measurable soil parameter; instead it must be determined by back-calculation using observed pipe deflections. Research by Selig (1990) showed that E' is a function of the bedding condition and overburden pressure. Selig's studies were carried out to seek a correlation between the soil reaction modulus and soil stiffness parameters such as

TABLE 9.4 Allowable Deflection Ratio of Polyethylene Pipe

SDR	Allowable Deflection Ratio
11	2.7%
13.5	3.4%
15.5	3.9%
17	4.2%
19	4.7%
21	5.2%
26	6.5%
32.5	8.1%

Young's modulus of soil, E_s , and the constrained modulus of soil, M_s , where E_s and D_s are related through Poisson's ratio of soil, ν_s , by

$$M_s = \frac{E_s \cdot (1 - \nu_s)}{(1 + \nu_s)(1 - 2 \cdot \nu_s)} \quad (9.27)$$

where M_s = constrained modulus of soil, lb/ft² or kN/m²;
 E_s = elastic modulus of soil, lb/ft² or kN/m²; and
 ν_s = Poisson's ratio of soil.

The studies and analyses by Neilson (1967), Allgood and Takahashi (1972), and Hartely and Duncan (1987) indicated that for

$$E' = k \cdot M_s \quad (9.28)$$

the value of k may vary from 0.7 to 2.3. Using $k = 1.5$ as a representative value and $\nu_s = 0.3$, in addition to combining Equations 9.27 and 9.28 yields the following relationship between the elastic modulus of the pipe and soil (Selig, 1990):

$$E' = 2 \cdot E_s \quad (9.29)$$

The values of elastic parameters, E_s and ν_s , can be found in Table 9.5 according to different percents of density from a standard Proctor compaction test (ASTM D698).

TABLE 9.5 Elastic Soil Parameters (Selig, 1990)

Soil Type	Stress Level		85% Standard Density			95% Standard Density		
			E_s		ν_s	E_s		ν_s
	psi	kPa	psi	MPa		psi	MPa	
SW, SP, GW, GP	1	7	1,300	9	0.26	1,600	11	0.40
	5	35	2,100	14	0.21	4,100	28	0.29
	10	70	2,600	18	0.19	6,000	41	0.24
	20	140	3,300	23	0.19	8,600	59	0.23
	40	280	4,100	28	0.23	13,000	90	0.25
	60	420	4,700	32	0.28	16,000	110	0.29
GM, SM, ML, and GC, SC with < 20% fines	1	7	600	4	0.25	1,800	12	0.34
	5	35	700	5	0.24	2,500	17	0.29
	10	70	800	6	0.23	2,900	20	0.27
	20	140	850	6	0.30	3,200	22	0.29
	40	280	900	6	0.38	3,700	25	0.32
	60	420	1,000	7	0.41	4,100	28	0.35
CL, MH, GC, SC	1	7	100	1	0.33	400	3	0.42
	5	35	250	2	0.29	800	6	0.35
	10	70	400	3	0.28	1,100	8	0.32
	20	140	600	4	0.25	1,300	9	0.30
	40	280	700	5	0.35	1,400	10	0.35
	60	420	800	6	0.40	1,500	10	0.38

9.4.2 Pipe Wall Buckling

Buckling can occur because of insufficient stiffness. Buckling may govern design of flexible pipes subjected to internal vacuum, external hydrostatic pressure, or high soil pressures in compacted soil (Figure 9.8). As Moser (1990) notes the more flexible the conduit (e.g., high values of SDR), the more unstable the wall structure will be in resisting buckling.

Most conduits are buried in a soil medium that does offer considerable shear resistance. An exact rigorous solution to the problem of buckling of a cylinder in an elastic medium entails some advanced mathematics (Moser, 1990). However, because of uncertainties in the behavior and performance of the surrounding soil, an exact solution is not necessary. Meyerhof and Baize (1963) developed the following empirical formula for computing the critical buckling pressure in a buried circular conduit:

$$P_{cr} = 2 \cdot \{ [E' / (1 - \mu^2)] (E \cdot I / r^3) \}^{1/2} \quad (9.30)$$

Where,

- P_{cr} = critical buckling pressure, lb/in² or kN/m²;
- E' = modulus of soil reaction, lb/in² or kN/m², see Table 9.3;
- μ = Poisson's ratio of pipe material;
- E = modulus of elasticity of the pipe material, lb/in² or kN/m²;
- I = moment of inertia of the pipe wall per unit length,
in⁴/in = in³ or m⁴/m = m³, $I = t^3/12$; and
- r = mean radius of the pipe, in or m.

Because $I = t^3/12$ and $r = D/2$, Equation 9.30 can be rewritten as

$$P_{cr} = 2 \cdot (G_b \cdot E')^{1/2} \quad (9.31)$$

where

$$G_b = \frac{2 \cdot E}{3 \cdot (1 - \mu^2)} \cdot (t/D)^3 \quad (9.32)$$

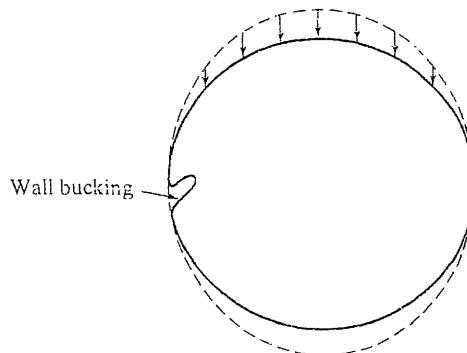


FIGURE 9.8 Localized Wall Buckling

in which

t = thickness of pipe, in or m and
 D = mean diameter of pipe, in or m

The factor of safety for pipe wall buckling can be determined by

$$FS = P_{cr}/P_{ip} \quad (9.33)$$

where P_{ip} = actual vertical pressure at the top of the pipe, obtained from Equation 9.22 or 9.23, lb/in² or kN/m².

In both Equations 9.30 and 9.31 initial out-of-roundness is neglected but the reduction in P_{cr} because of this has been assumed to be no greater than 30% (Moser, 1990). As a result, a factor of safety ≥ 2 is recommended for use with Equation 9.33 in the design of a flexible conduit to resist buckling.

EXAMPLE 9.2

An 8-inch (200-mm) SDR 11 HDPE perforated pipe with 8, 0.25-inch (6-mm) holes per foot (i.e., 4 holes per side per foot) is selected as a primary leachate collection pipe. The maximum load acting on the pipe includes a 2-ft (0.6-m) protective sand layer ($\gamma_{sand} = 115 \text{ lb/ft}^3$ or 18 kN/m^3), 100-ft (30-m) solid waste ($\gamma_{waste} = 60 \text{ lb/ft}^3$ or 9.4 kN/m^3), 12-inch (0.3-m) gas venting layer ($\gamma_{sand} = 115 \text{ lb/ft}^3$ or 18 kN/m^3), 18-inch (0.45-m) compacted clay layer ($\gamma_{clay} = 110 \text{ lb/ft}^3$ or 17.3 kN/m^3), 24-inch (0.6-m) drainage and protective layer ($\gamma_{silt} = 110 \text{ lb/ft}^3$ or 17.3 kN/m^3), and 6-inch (0.15-m) topsoil ($\gamma_{top} = 90 \text{ lb/ft}^3$ or 14 kN/m^3). Assume bedding angle $\theta = 0^\circ$, deflection lag factor $D_L = 1.0$, elastic modulus of the pipe material for 50 years at 73°F (23°C) temperature $E = 28,200 \text{ lb/in}^2$ (194,000 kN/m²), Poisson's ratio of pipe material $\mu = 0.3$. The bedding material of the pipe is poorly graded gravel (GP) with 85% standard density. What will be the deflection ratio (%) and critical buckling pressure of the pipe?

Solution: The maximum load applied on the pipe is given by

$$\begin{aligned} W_c &= \frac{\left(\sum \gamma_i \cdot H_i \right) \cdot D_o}{(1 - n \cdot d/12)} \quad (9.18) \\ &= \frac{[(115)(2) + (60)(100) + (115)(1) + (110)(3.5) + (90)(0.5)] \times 8/12}{(1 - 4 \times 0.25/12)} \\ &= \frac{(230 + 6,000 + 115 + 385 + 45) \times 8/12}{0.917} \\ &= \frac{6,775 \times 8/12}{0.917} \\ &= 4,925 \text{ lb/ft} = 410 \text{ lb/in (72 kN/in)} \end{aligned}$$

The maximum pressure applied on the pipe can be obtained from

$$P_{ip} = W_c/D_o = 410/8 = 51.3 \text{ lb/in}^2 (354 \text{ kN/m}^2)$$

From Table 9.5,

$$P_{ip} = 40 \text{ lb/in}^2, E_s = 4,100 \text{ lb/in}^2$$

and $P_{ip} = 60 \text{ lb/in}^2$, $E_s = 4,700 \text{ lb/in}^2$

For $P_{ip} = 51.3 \text{ lb/in}^2$,

$$E_s = 4,100 + (51.3 - 40)(4,700 - 4,400)/20 = 4,100 + 339 = 4,439 \text{ lb/in}^2$$

The soil reaction modulus is given by

$$E' = 2 \cdot E_s = 2 \times 4,439 = 8,878 \text{ lb/in}^2 (61,200 \text{ kN/m}^2) \quad (9.29)$$

The thickness of pipe is given by

$$\begin{aligned} t &= D_o / SDR \\ &= 8/11 = 0.73 \text{ in (0.0185 m)} \end{aligned} \quad (9.6)$$

The mean diameter of pipe is

$$\begin{aligned} D &= D_o - t \\ &= 8 - 0.73 = 7.27 \text{ in (0.1847 m)} \end{aligned} \quad (9.20)$$

Also,

Deflection lag factor, $D_L = 1.0$;

Bedding angle $\theta = 0^\circ$, $K = 0.11$;

Mean radius of the pipe, $r = 3.635 \text{ in (0.0923 m)}$;

Elastic modulus of the pipe material, $E = 28,200 \text{ lb/in}^2 (194,000 \text{ kN/m}^2)$;

Soil reaction modulus, $E' = 8,878 \text{ lb/in}^2 (61,200 \text{ kN/m}^2)$;

and

Inertia moment of the pipe wall per unit length, $\text{in}^4/\text{in} = \text{in}^3$, given by

$$I = t^3/12 = (0.73)^3/12 = 0.389/12 = 0.0324 \text{ in}^3 (5.276 \times 10^{-7} \text{ m}^3)$$

Modified Iowa Formula:

$$\begin{aligned} \Delta X &= \frac{D_L \cdot K \cdot W_c \cdot r^3}{E \cdot I + 0.061 E' \cdot r^3} \\ &= \frac{(1.0)(0.11)(410)(3.635)^3}{(28,200)(0.0324) + (0.061)(8,878)(3.635)^3} \\ &= \frac{(1.0)(0.11)(410)(48.03)}{(28,200)(0.0324) + (0.061)(8,878)(48.03)} \\ &= \frac{2,166}{914 + 26,011} \\ &= 0.08 \text{ in (2.0 mm)} \end{aligned} \quad (9.16)$$

Deflection Ratio:

$$\begin{aligned} \text{Deflection Ratio} &= (\Delta Y/D) \times 100\% \\ &= (0.08/7.27) \times 100\% \\ &= 1.1\% < 2.7\% \text{ (ok, as shown in Table 9.4)} \end{aligned} \quad (9.19)$$

Wall Buckling of Pipe:

Modulus of soil reaction, $E' = 8,878 \text{ lb/in}^2$, $(61,200 \text{ kN/m}^2)$;

Poisson's ratio of pipe material, $\mu = 0.3$;
 Modulus of elasticity of the pipe material, $E = 28,200 \text{ lb/in}^2$ ($194,000 \text{ kN/m}^2$);
 Moment of inertia of the pipe wall per unit length, $I = 0.0324 \text{ in}^3$ ($5.276 \times 10^{-7} \text{ m}^3$);
 Mean radius of the pipe, $r = 3.635 \text{ in}$ (0.0923 m).
 Thus,

$$\begin{aligned}
 P_{cr} &= 2 \cdot \{ [E' / (1 - \mu^2)] (E \cdot I / r^3) \}^{1/2} & (9.30) \\
 &= 2 \times \{ [8,878 / (1 - 0.3^2)] [(28,200 \times 0.0324) / (3.635)^3] \}^{1/2} \\
 &= 2 \times [9,756 \times (913.68 / 48.03)]^{1/2} \\
 &= 2 \times (185,589)^{1/2} \\
 &= 2 \times 431 \\
 &= 862 \text{ lb/in}^2 \text{ (5,943 kN/m}^2\text{)}
 \end{aligned}$$

The factor of safety for pipe wall buckling is, then,

$$FS = P_{cr} / P_{tp} = 862 / 51.3 = 16.8 > 2 \text{ (OK)} \quad (9.33)$$

9.5 SUMP AND RISER PIPES

Leachate collection sumps are low points in the landfill liner constructed to collect and removal leachate. The sumps are filled with gravel to provide the maximum space (volume) for leachate accumulation, as well as to support the weight of the overlying waste, cover system, and post-closure loadings. Commonly, the composite liner system is slightly depressed or indented to create these sumps (shown in Figures 9.9 and 9.10). The absence of sketches illustrating continued gravity flow of leachate beyond the limits of the cells and/or landfill using liner penetrations is intentional. The authors do not recommend such practice due to the difficulty of making liner seams in this remote of all locations. With double liner systems, the situation is even more difficult. Even with the sketches of Figures 9.9 and 9.10 it is difficult to test the geomembrane seaming in such sumps because of the slope and corners at which the seams occur. Because of the difficulty in seam testing sumps, sump areas often are designed with an additional layer of geomembrane. Sulfates are one of the most common and abundant constituents in landfill leachate. Accordingly, all concrete components in a sump (e.g., riser pipe and foundation pad) must be constructed using low water/cement ratios and sulfate resistant, Class V Portland cement (ACI, 1998). Failure to observe this precaution can lead to sulfate attack and disintegration of the concrete. Sulfate attack occurs when calcium, alumina, and sulfate combine to form the mineral ettringite ($3\text{CaO} \cdot \text{Al}_2\text{O}_3 \cdot 32\text{H}_2\text{O}$) in the cement matrix. The volume of ettringite is over 200% that of the original constituents, which can result in massive swelling and cracking when sufficient ettringite forms by the sulfation of alumina. Alternatively, many sumps now are being constructed using premanufactured units made of HDPE, with large-diameter HDPE pipe or HDPE manholes. Although more costly, the factory manufactured sumps can be thoroughly tested and installed as a unit.

Figure 9.9 shows details of vertical riser (manhole) removal designs for primary and secondary leachate collection systems. The manhole riser extends vertically

**APPLICATION FOR PERMIT RENEWAL AND MODIFICATION
SANDOVAL COUNTY LANDFILL**

**VOLUME III: LANDFILL ENGINEERING CALCULATIONS
SECTION 5: PIPE LOADING CALCULATIONS**

ATTACHMENT III.5.B

**SHARMA, HARI .D. AND SANGEETA P. LEWIS. 1994.
*WASTE CONTAINMENT SYSTEMS, WASTE STABILIZATION
AND LANDFILLS: DESIGN AND EVALUATION.*
NEW YORK: JOHN WILEY AND SONS.**

WASTE CONTAINMENT SYSTEMS, WASTE STABILIZATION, AND LANDFILLS: DESIGN AND EVALUATION

HARI D. SHARMA, PH.D., P.E.

Chief Engineer and Director
EMCON Associates
San Jose, California

SANGEETA P. LEWIS, P.E.

Project Manager
CH₂M Hill
Oakland, California



A Wiley-Interscience Publication

JOHN WILEY & SONS, INC.

New York / Chichester / Toronto / Brisbane / Singapore

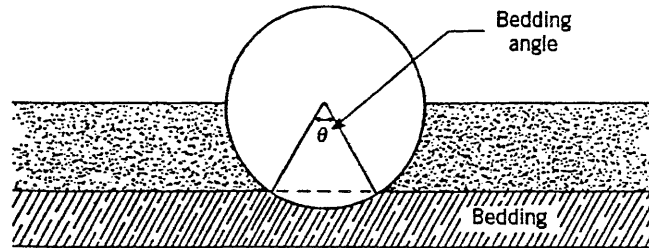


Figure 9.29 Bedding angle. (From Moser, 1990.)

approximately 1.5 times greater than the load determined using Marston's equation. The bedding constant is dependent on the bedding angle, as depicted in Figure 9.29. Values for the bedding constant are given in Table 9.12.

In the preceding paragraphs on soil stiffness we discussed the modulus of passive resistance of the soil, e , and noted that the units for e were not dimensionally correct. The Iowa formula was therefore modified and the following equation is known as the modified Iowa formula:

$$\Delta X \approx \Delta Y = \frac{D_L K W_c r^3}{EI + 0.061 E' r^3} \quad (9.34)$$

where $E' = er$. E' is known as the modulus of soil reaction. Methods for establishing this value were given in the preceding soil stiffness paragraphs. Actual deflections may be estimated using the modified Iowa formula by assuming that horizontal and vertical deflections are equal.

WATKINS' RING STABILITY EQUATION. Deflection may also be calculated using Watkins' (1989) ring stability equation. The ring stability equation is based on assuming incipient collapse of the pipe; however, it is important to note that incipient collapse does not mean imminent collapse. Rather, it refers to a condition of possible col-

TABLE 9.12 Values of Bedding Constant, K

Bedding Angle (deg)	K
0	0.110
30	0.108
45	0.105
60	0.102
90	0.096
120	0.090
180	0.083

Source: Moser (1990).

**APPLICATION FOR PERMIT RENEWAL AND MODIFICATION
SANDOVAL COUNTY LANDFILL**

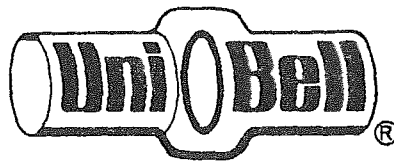
**VOLUME III: LANDFILL ENGINEERING CALCULATIONS
SECTION 5: PIPE LOADING CALCULATIONS**

ATTACHMENT III.5.C

**UNI-BELL PVC PIPE ASSOCIATION. 2001.
HANDBOOK OF PVC PIPE DESIGN., TEXAS:
*UNI-BELL PVC PIPE ASSOCIATION.***

The Uni-Bell PVC Pipe Association

Handbook of PVC Pipe Design and Construction



Uni-Bell PVC Pipe Association
2655 Villa Creek Drive, Suite 155
Dallas, Texas 75234

\$40.00

CHAPTER VII

DESIGN OF BURIED PVC PIPE

Recommendations, Relationships, and Data Essential

to Proper Design of Underground

PVC Pipe Systems

CHAPTER VII

DESIGN OF BURIED PVC PIPE

Historically, a flexible pipe has been defined as a conduit that will deflect at least two percent without any sign of structural distress, such as injurious cracking. However, for a conduit to truly behave as a flexible pipe when buried, it is required that the pipe be more yielding than the embedment soil surrounding it.

A flexible pipe derives its external-load-carrying capacity from its flexibility. Under soil load, the pipe tends to deflect, thereby developing passive soil support at the sides of the pipe. At the same time, the ring deflection relieves the pipe of the major portion of the vertical soil load, which is then carried by the surrounding soil through the mechanism of an arching action over the pipe.

The effective strength of the pipe-soil system is remarkably high. For example, tests at Utah State University indicate that a rigid pipe with a three-edge bearing strength of 3300 lbs/ft (48.15 kN/m), buried in Class C bedding, will fail under a vertical load of 5000 lbs/ft (72.95 kN/m). However, under identical soil conditions and loading, PVC sewer pipe with a minimum pipe stiffness of 46 psi will deflect only 5 percent, far below that which could cause damage to the PVC pipe wall. Thus, in this scenario, the rigid pipe has failed but the flexible pipe has performed successfully.

Of course, in flat-plate or three-edge loading, the rigid pipe will support much more than the flexible pipe. This anomaly tends to mislead, as users often relate low flat-plate supporting strength for flexible pipe to the in-soil load capacity. Flat-plate or three-edge loading is an appropriate measure of load-bearing strength for rigid pipes, but not for flexible pipes.

Pipe Stiffness: The inherent resistance of a flexible pipe to load is called pipe stiffness, which is measured according to ASTM D 2412, "Standard Test Method for External Loading Properties of Plastic Pipe by Parallel-Plate Loading," at an arbitrary datum of 5 percent deflection. Pipe stiffness is defined as:

EQUATION 7.1

$$PS = F/\Delta Y = \frac{EI}{0.149r^3} = \frac{6.71EI}{r^3}$$

For solid-wall pipes Equation 7.1 can be rewritten as:

EQUATION 7.2

$$PS = F/\Delta Y = \frac{6.71Et^3}{12r^3} = 0.559E \left[\frac{t}{r} \right]^3$$

Where: PS = Pipe Stiffness, lbf/in/in or lbs/in²
 F = Force, lbs/in
 ΔY = Vertical deflection, in
 E = Modulus of elasticity, lbs/in²
 I = Moment of inertia of the wall cross-section per unit length of pipe, in⁴/in = in³
 r = Mean radius of pipe, in
 t = wall thickness, in

For solid-wall PVC pipe with outside diameter controlled dimensions (rather than I.D.) Equation 7.2 can be further simplified:

EQUATION 7.3

$$PS = 4.47 \frac{E}{(DR - 1)^3}$$

Where: $DR = \frac{D_o}{t}$

Because pipe stiffness is measured at only one prescribed deflection, it provides little information relative to the overall structural performance of a product. That is, pipe stiffness defines only the flat-plate loading necessary for a particular deflection. The resulting PS values for various dimension ratios and E values of PVC pipe are as shown in Table 7.1.

How a plastic pipe responds to load is very important to an engineer who is involved in the design of an underground pipeline. For a plastic pipe, the question of how pipe stiffness influences the in-ground deflection is important both in terms of performance and economics. A research project was undertaken at Utah State University to address the question.³⁵ Figure 7.1 shows the results of the study. Points in this graph were taken from load-deflection curves of plastic pipe buried in medium dense sand. These curves show that there is a marked increase in pipe deflection for

HANDBOOK OF PVC PIPE

pipe stiffness values less than 35 psi. The curves are nearly flat for pipe stiffness values greater than 39 psi. This indicates that increasing pipe stiffness above 39 psi has little or no effect on in-ground deflections. In fact, a pipe stiffness of approximately 37 psi resulted in the least deflection and could be considered as optimum.

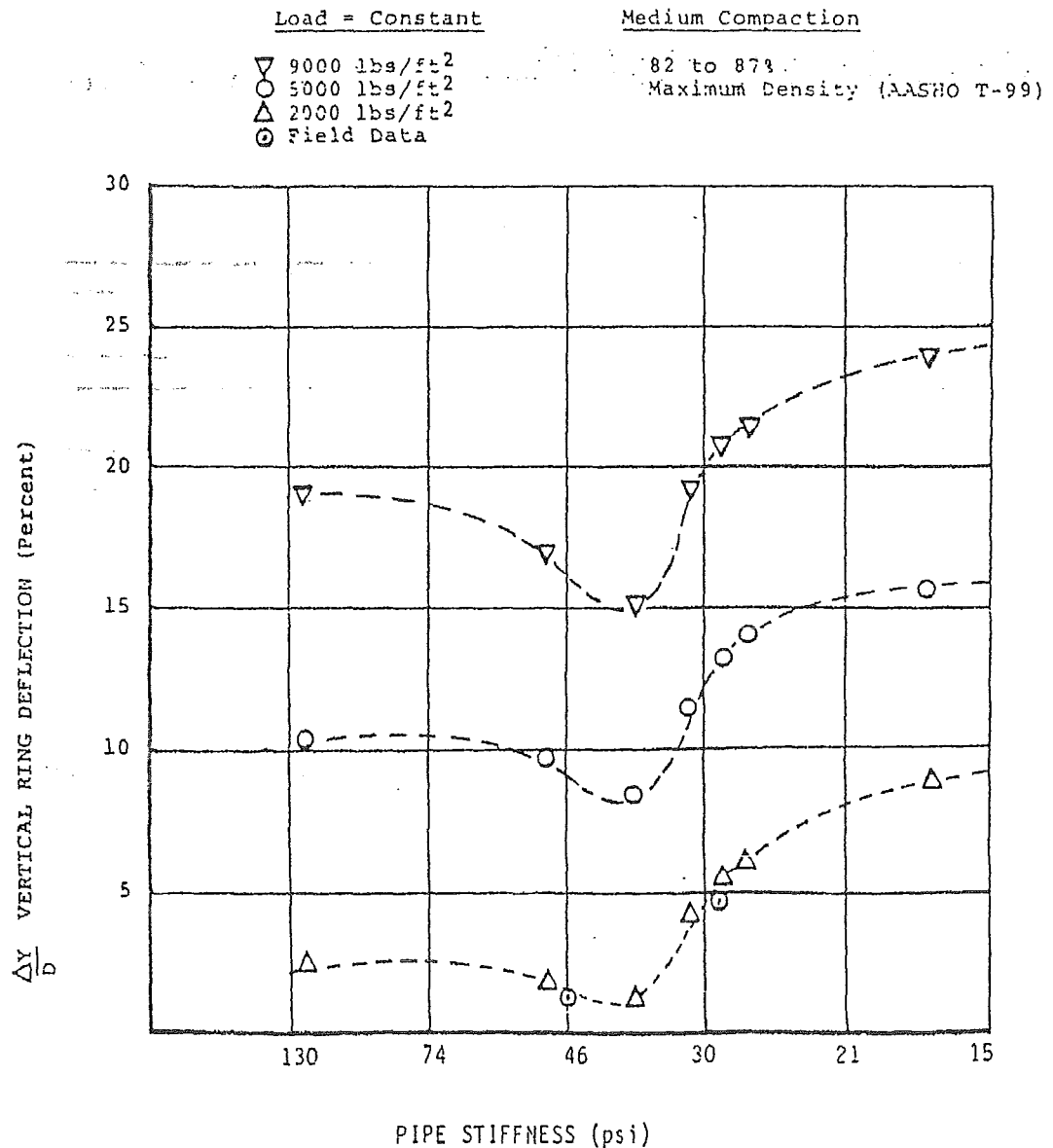
TABLE 7.1
MINIMUM PVC PIPE STIFFNESS (psi)

DR or SDR	Min. E = 400,000 psi	Min. E = 440,000 psi	Min. E = 500,000 psi
64	7	8	9
51	14	16	18
42	26	29	32
41	28	31	35
35	46	50	57
33.5	52	57	65
32.5	57	63	71
28	91	100	114
26	115	126	144
25	129	142	161
23.5	157	173	196
21	224	246	279
18	364	400	455
17	437	480	546
14	815	895	1,019
13.5	916	1,007	1,145

The Utah State University study concluded that the optimum pipe stiffness of approximately 37 psi is independent of both soil compaction and height of cover. Apparently, this optimum pipe stiffness yields a ring flexibility that interacts best with the enveloping soils in limiting ring deflection.

FIGURE 7.1

VERTICAL RING DEFLECTION IN BURIED PLASTIC PIPE



A common pipe stiffness for gravity PVC pipe is 46 psi. At typical summer installation temperatures, this stiffness is very near the optimum. (See Figure 7.7.) Pipes with lower stiffnesses may be used as long as there is proper attention to the selection and placement of the embedment material.

In addition to altering the DR to affect pipe stiffness, alternative shapes can be employed. It is this option of more efficient shapes that has resulted in a variety of profile-wall gravity PVC pipe products for sanitary and drain applications. Users are afforded the economy of a pipe with stiffness comparable to a solid-wall product, that uses less raw material per unit length.

Equation 7.1 shows that the pipe stiffness increases as the moment of inertia of the wall cross section increases. For a solid wall pipe the moment of inertia is equal to $t^3/12$ in⁴/in, with the center of gravity being at the midpoint of the pipe wall.

In the case of a profile-wall pipe, however, the calculation of the moment of inertia is more complex. The center of gravity, or centroid, for the profile must first be computed, and then the parallel axis theorem can be applied to determine the composite moment of inertia. It is the location of the center of gravity in the pipe wall, rather than the overall thickness, that has the greatest effect on the moment of inertia and gives the profile-wall pipes their high stiffness-to-weight ratios.

Because a flexible conduit interacts with the surrounding soil in supporting the vertical load, soil properties are very important. Just as bedding is important in limiting soil-pressure concentrations on rigid pipes, soil compaction or soil density is an important parameter in limiting ring deflection in flexible pipes. Thus, soil selection and soil placement, as well as pipe properties, are important in the design of any buried pipe installation.

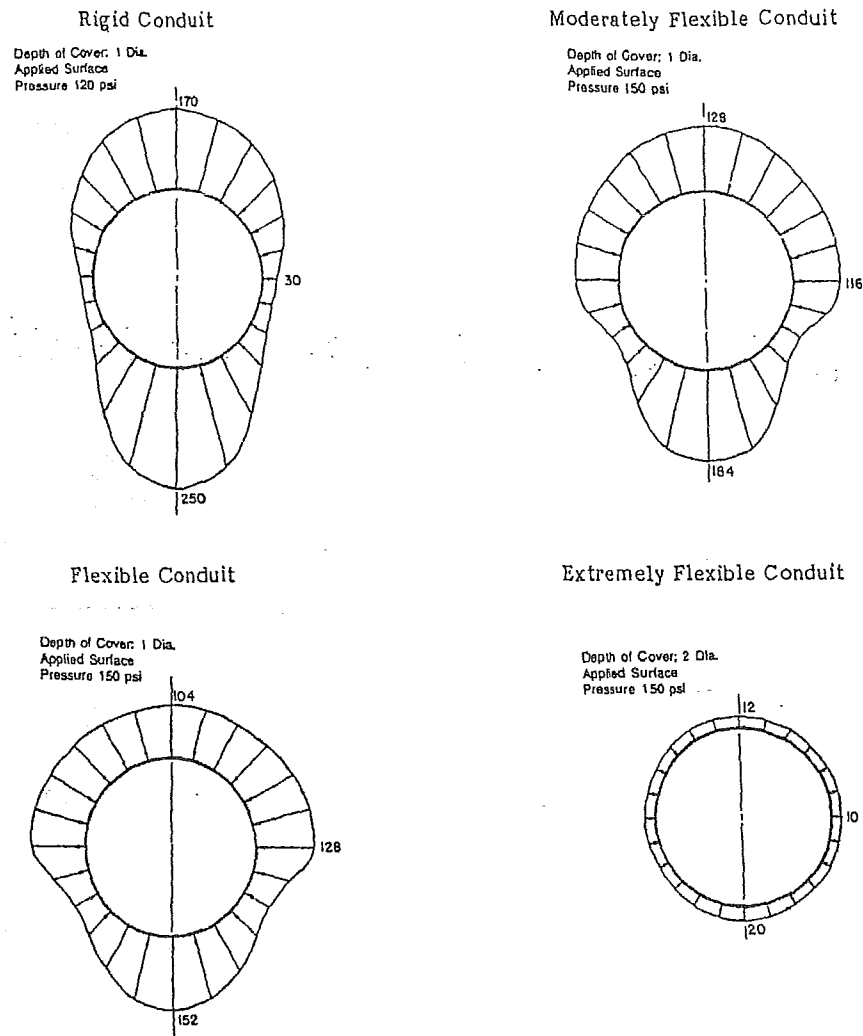
The manner in which flexible pipe performance differs from rigid pipe performance can be understood by visualizing pipe response to applied load. In a rigid-pipe system, the applied vertical load must be carried totally by the inherent strength of the unyielding, rigid pipe since the soil at the sides of the pipe tends to compress and deform away from the load. In a flexible pipe system, the applied earth load is largely carried by the earth at the sides of the pipe, since the flexible pipe deflects away from the load. (See Chapter VI.) That portion of the load carried by the flexible pipe, a vertical vector of force, is transferred principally through the deflection

mechanism into approximately horizontal force vectors assumed by the compressed soil at the sides of the pipe. This ability to redistribute vertical load into near horizontal vectors is a flexible pipe advantage that actually diminishes with increasing pipe stiffness. It is also important to recognize that many thermoset and composite pipe products do not exhibit an ability to resist cracking or breaking over a broad range of deflections. Just as rigid pipes have a definite yield point, some thermoset and composite plastic pipes will experience early structural damage that inhibits their ability to resist loading. Such pipe products, when used, must be designed and limited to very small allowable deflections that are well below levels that can cause structural damage and a decay in load resistance.

In 1968, Dr. Kaare Hoeg reported on his research conducted on buried conduits of different stiffness surrounded by dense Ottawa sand.¹⁷ In the research project, contact-pressure distributions around the circumference of pipes of varying stiffness were measured and reported. His report on a series of four tests demonstrates the relative benefits derived through distribution of load force vectors into the surrounding embedment soils.

In the tests, Dr. Hoeg installed pipe of different stiffness at depths of cover of one or two pipe diameters. He then applied uniformly distributed loads on the ground surface to create the effect of deep burial. Figure 7.2 shows the response of a rigid conduit to an applied ground-surface load of 120 psi. Note that the contact pressure on the external surface of the rigid pipe is not uniformly distributed, but is relatively extreme at top and bottom portions of its circumference. Lateral soil support is negligible. The response of more flexible conduits to the applied loads indicates that pipe flexibility reduces the extreme contact pressures and results in a better distribution of contact pressures around the pipe circumference.

FIGURE 7.2
LOAD DISTRIBUTION AS A FUNCTION OF STIFFNESS



Through the deflection mechanism, the applied vertical load is carried principally by the surrounding soil envelope and to a lesser extent by the flexible pipe. Consequently, the strength provided by most buried flexible pipe is derived through the deflection mechanism from the combined strength provided by the pipe-soil system.

Spangler's Iowa Deflection Formula: M. G. Spangler, a student of Anson Marston, noted that flexible pipes may provide little inherent strength in comparison to rigid pipes, yet when buried, derive a significant ability to support vertical loads from the passive pressures induced as the sides of the pipe move outward against the earth. This fact, coupled with the idea that the ring deflection may also be a basis for flexible-pipe design, prompted Spangler to publish his Iowa Formula in 1941.

CHAPTER VII - DESIGN OF BURIED PVC PIPE

Spangler's first step was to define the ability of a flexible pipe to resist ring deflection when not buried in the soil. Applying the elastic theory of flexure to thin rings for deflections less than 10 percent, he established the following relationships.

EQUATION 7.4

$$\Delta Y = 0.149 \frac{Wr^3}{EI}$$

EQUATION 7.5

$$\Delta X = 0.136 \frac{Wr^3}{EI}$$

EQUATION 7.6

$$\Delta X = 0.913 \Delta Y$$

Where: ΔY and ΔX = the vertical and horizontal deflections or diameter changes, which are derived mathematically for ovalization into the shape of an ellipse, in

W = the load on the pipe per unit length, lbs/in

E = Modulus of elasticity of the pipe material, lbs/in²

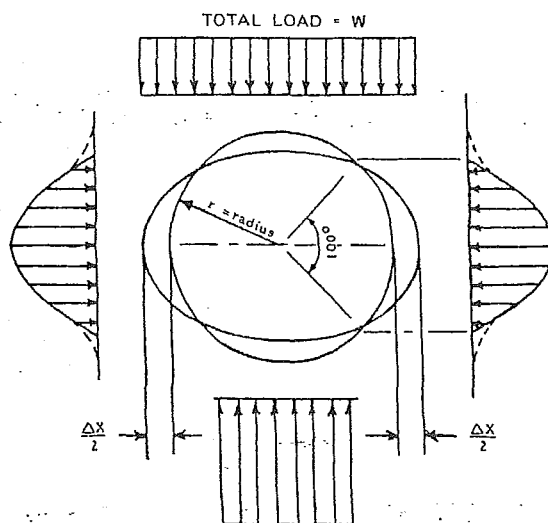
I = Moment of inertia of the wall cross-section per unit length, in⁴/in = in³

r = Mean radius, in

Spangler's next step was to incorporate the effects of the surrounding soil on the pipe's deflection. This was accomplished by assuming that Marston's theory of loads applied, and that this load would be uniformly distributed over a plane at the top of the pipe. He also assumed a uniform pressure over part of the bottom, depending upon the bedding angle. On the sides, he assumed the horizontal pressure on each side would be proportional to the deflection of the pipe in the soil. The constant of proportionality was called the "modulus of passive resistance" of the soil.

The modulus would presumably be a constant for a given soil and could be measured in a simple lab test. Through analysis he derived the Iowa Formula:

FIGURE 7.3
BASIS OF SPANGLER'S DERIVATION OF THE IOWA
FORMULA FOR DEFLECTION OF BURIED PIPES



EQUATION 7.7

$$\Delta X = D_L \frac{KW_c r^3}{EI + 0.061er^4}$$

- Where:
- ΔX = Horizontal deflection or change in diameter, in
 - D_L = Deflection lag factor
 - K = Bedding constant
 - W_c = Marston's load per unit length of pipe, lbs/in
 - r = Mean radius of the pipe, in
 - E = Modulus of elasticity of the pipe material, lbs/in²
 - I = Moment of inertia of the pipe wall per unit length, in⁴/L in = in³
 - e = Modulus of passive resistance of the side fill, lbs/in²/in

CHAPTER VII - DESIGN OF BURIED PVC PIPE

Equation 7.7 can be used to predict deflections of buried pipe if the three empirical constants K , D_L , and e are known. The bedding constant, K , accommodates the response of the buried flexible pipe to the opposite and equal reaction to the load force, derived from the bedding under the pipe. The bedding constant varies with the width and angle of the bedding achieved in the installation. The bedding angle is shown in Figure 7.4. Table 7.2 contains a list of bedding factors, K , dependent upon the bedding angle. These were determined theoretically by Spangler and published in 1941. As a general rule, a value of $K = 0.1$ is assumed.

FIGURE 7.4
BEDDING ANGLE

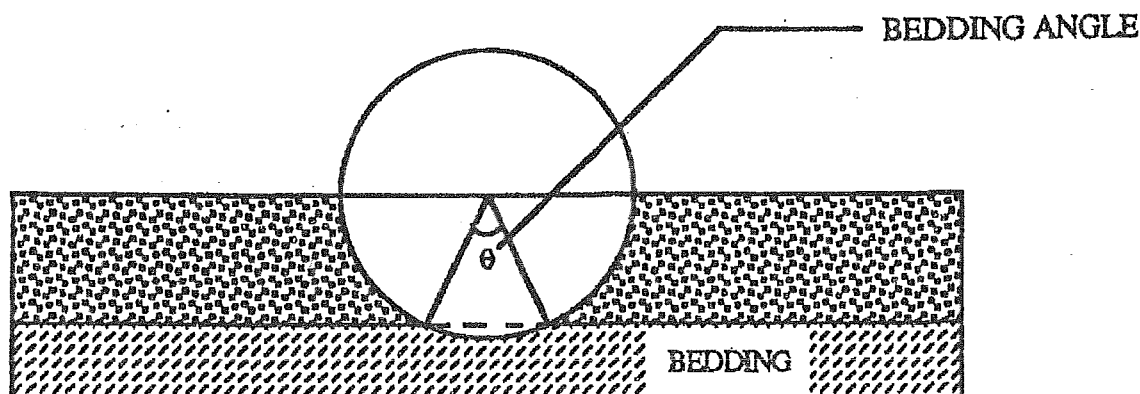


TABLE 7.2
VALUES OF BEDDING CONSTANT, K

<u>BEDDING ANGLE</u>	<u>K</u>
0°	0.110
30°	0.108
45°	0.105
60°	0.102
90°	0.096
120°	0.090
180°	0.083

In 1955, Reynold K. Watkins, a graduate student of Spangler, was investigating the modulus of passive resistance through model studies and

examined the Iowa Formula dimensionally. The analysis determined that e could not possibly be a true property of the soil in that its dimensions are not those of a true modulus. As a result of Watkins' effort, another soil parameter was defined. This was the "modulus of soil reaction," $E' = er$. Consequently, a new formula called the Modified Iowa Formula was written:

EQUATION 7.8

$$\Delta X = D_L \frac{KW_c r^3}{EI + 0.061E'r^3}$$

Two other observations from Watkins' work are of particular note. There is little point in evaluating E' by a model test and then using the modulus to predict ring deflection; the model gives ring deflection directly. Ring deflection may not be the only performance limit.

Many researcher have quantified values of E' by measuring deflections for pipes under which other conditions were known, followed by back-calculation through the Modified Iowa Formula. This requires assumptions regarding the load, bedding factor, and deflection lag factor and has led to a variation in reported values of E' .

The most often cited work to develop appropriate values of E' was conducted by Amster K. Howard of the United States Bureau of Reclamation. Howard reviewed both laboratory and field data from many sources. Using information from over 100 laboratory and field tests, he compiled a table of average E' values for various soil types and densities. (See Table 7.3.) He was able to do this by assuming values of E' , K , and W_c and use the Modified Iowa Formula to calculate a theoretical value of deflection. This theoretical deflection was then compared with actual measurements. By assuming E' values in Table 7.3, a bedding constant $K = 0.1$, and deflection lag factor $D_L = 1.0$, Howard was able to correlate the theoretical and empirical results to within ± 2 percent deflection when he used the prism soil load. For example, if theoretical deflections using Table 7.3 were approximately 5 percent, measured deflection would range between 3 and 7 percent. The data used in this study was taken from tests on PVC, steel, reinforced plastic mortar, and other types of pipe. The study provides guidance to designers of all flexible pipe, including PVC pipe.

TABLE 7.3
AVERAGE VALUES OF MODULUS OF SOIL REACTION, E'
(For Initial Flexible Pipe Deflection)

Soil type-pipe bedding material (Unified Classification System ^a) (1)	E' for Degree of Compaction of Bedding, in pounds per square inch			
	Dumped (2)	Slight, <85% Proctor, <40% relative density (3)	Moderate, 85%-95% Proctor, 40%-70% relative density (4)	High, >95% Proctor, >70% relative density (5)
Fine-grained Soils (LL > 50) ^b Soils with medium to high plasticity CH, MH, CH-MH	No data available; consult a competent soils engineer; Otherwise use $E' = 0$			
Fine-grained Soils (LL < 50) Soils with medium to no plasticity, CL, ML, ML-CL, with less than 25% coarse- grained particles	50	200	400	1,000
Fine-grained Soils (LL < 50) Soils with medium to no plasticity, CL, ML, ML-CL, with more than 25% coarse-grained particles Coarse-grained Soils with Fines GM, GC, SM, SC ^c contains more than 12% Fines	100	400	1,000	2,000
Coarse-grained Soils with Little or no Fines GW, GP, SW, SP ^c contains less than 12% Fines	200	1,000	2,000	3,000
Crushed Rock	1,000	3,000	3,000	3,000
Accuracy in Terms of Percentage Deflection ^d	±2	±2	±1	±0.5

^aASTM Designation D 2487, USBR Designation E-3.

^bLL = Liquid limit.

^cOr any borderline soil beginning with one of these symbols (i.e. GM-GC, GC-SC).

^dFor ±1% accuracy and predicted deflection of 3%, actual deflection would be between 2% and 4%.

Note: Values applicable only for fills less than 50 ft (15 m). Table does not include any safety factor. For use in predicting initial deflections only, appropriate Deflection Lag Factor must be applied for long-term deflections. If bedding falls on the borderline between two compaction categories, select lower E' value or average the two values. Percentage Proctor based on laboratory maximum dry density from test standards using about 12,500 ft-lbs/cu ft (598,000 J/m³) (ASTM D 698, AASHTO T-99, USBR Designation E-11). 1 psi = 6.9 kPa.

SOURCE: "Soil Reaction for Buried Flexible Pipe" by Amster K. Howard, U.S. Bureau of Reclamation, Denver, Colorado. Reprinted with permission from American Society of Civil Engineers.

HANDBOOK OF PVC PIPE

The only parameter remaining in the Iowa Formula now needed to calculate deflections is the deflection lag factor (D_L). Spangler recognized that in pipe-soil systems, as with all engineering systems involving soil, the soil consolidation at the sides of the pipe continues with time after the maximum load reaches the top of the pipe. His experience had shown that deflections could increase by as much as 30 percent over a period of 40 years. For this reason, he recommended the incorporation of a deflection lag factor of 1.5 as a conservative design value.

An alternative to the use of the lag factor with Marston's predicted load, is the use of an ultimate load (prism load) with lag factor equal to unity. Time lag is discussed in much greater detail in a later section of this chapter.

Under most soil conditions, flexible PVC pipe tends to deflect into a nearly elliptical shape and the horizontal and vertical deflections may be considered equal for small deflections (Δ). Since most PVC pipe is described by either pipe stiffness ($F/\Delta Y$) or outside diameter to thickness ratio (DR), the Modified Iowa Equation can be transposed and rewritten as follows:

EQUATION 7.9

$$\% \frac{\Delta Y}{D} = \frac{(D_L KP + KW')(100)}{0.149 \frac{F}{\Delta Y} + 0.061E'}$$

For solid-wall pipes the equations becomes:

EQUATION 7.10

$$\% \frac{\Delta Y}{D} = \frac{(D_L KP + KW')(100)}{[2E/(3(DR - 1)^3)] + 0.061E'}$$

Where:

P	= Prism Load (soil pressure), lbs/in ²
K	= Bedding Constant, 0.1
W'	= Live Load, lbs/in ²
DR	= Dimension Ratio
E	= Modulus of Elasticity, lbs/in ²

CHAPTER VII - DESIGN OF BURIED PVC PIPE

$$\begin{aligned} E' &= \text{Modulus of Soil Reaction, lbs/in}^2 \\ D_L &= 1.0 \end{aligned}$$

The previous equations may be used in conjunction with the values for the empirical constants E' , D_L , and K . The following example illustrates their use.

Example: What will be the deflection of a DR 35 PVC pipe (with modulus of elasticity of 400,000 lbs/in²) buried on a flat bottom trench in a slightly compacted fine grained soil, with unit weight of 120 lbs/ft³ and liquid limit less than 50 percent, if the depth of burial is 10 feet?

From Table 7.3, $E' = 200$ lbs/in², using a bedding constant, $K = 0.1$, assuming a prism load along with a deflection lag factor of $D_L = 1.0$, the following results are derived:

$$\% \frac{\Delta Y}{D} = \frac{(D_L KP + KW')(100)}{[2E / (3(DR - 1)^3)] + 0.061E'}$$

$P = wH$ and $W' = 0$ at a depth of 10 ft

$$P = 120 \frac{\text{lb}}{\text{ft}^3} \times 10 \text{ ft} \times \frac{1 \text{ ft}^2}{144 \text{ in}^2} = 8.33 \text{ lbs/in}^2$$

$$\frac{2E}{3(DR - 1)^3} = \frac{2(400,000)}{3(35 - 1)^3} = 6.78 \text{ lbs/in}^2$$

$$\% \frac{\Delta Y}{D} = \frac{1.0(0.1)(8.33)(100)}{6.78 + 0.061(200)} = 4.4 \text{ percent}$$

Now calculate deflection for an inside-diameter-controlled profile pipe of the same stiffness ($PS = 46$ lbs/in²), given identical installation.

$$\% \frac{\Delta Y}{D} = \frac{D_L KP(100)}{0.149 \frac{F}{\Delta Y} + 0.061E'}$$

$$\% \frac{\Delta Y}{D} = \frac{(1.0)(0.1)(8.33)(100)}{0.149(46) + 0.061(200)} = 4.4 \text{ percent}$$

HANDBOOK OF PVC PIPE

When applicable, live loads should be added to the earth load to determine the total load at the depth being considered, as shown in the formula at the bottom of Table 7.4.

In Table 7.4, results of calculations for deflections of buried AWWA C900 and C905 PVC pipe are presented for cases in which live loads are present.

Deflection Lag and Creep: The length of time that a buried flexible pipe will continue to deflect after the maximum imposed load is realized is limited and is a function of soil density in the pipe zone. As soil density at the sides of the pipe increases, the time during which the pipe will continue to deflect decreases, and the total deflection in response to load decreases.

In fact, after the trench load reaches a maximum, the pipe-soil system continues to deflect only as long as the soil around the pipe is in the process of consolidation. Once the embedment soil has reached the density required to support the load, the pipe will not continue to deflect.

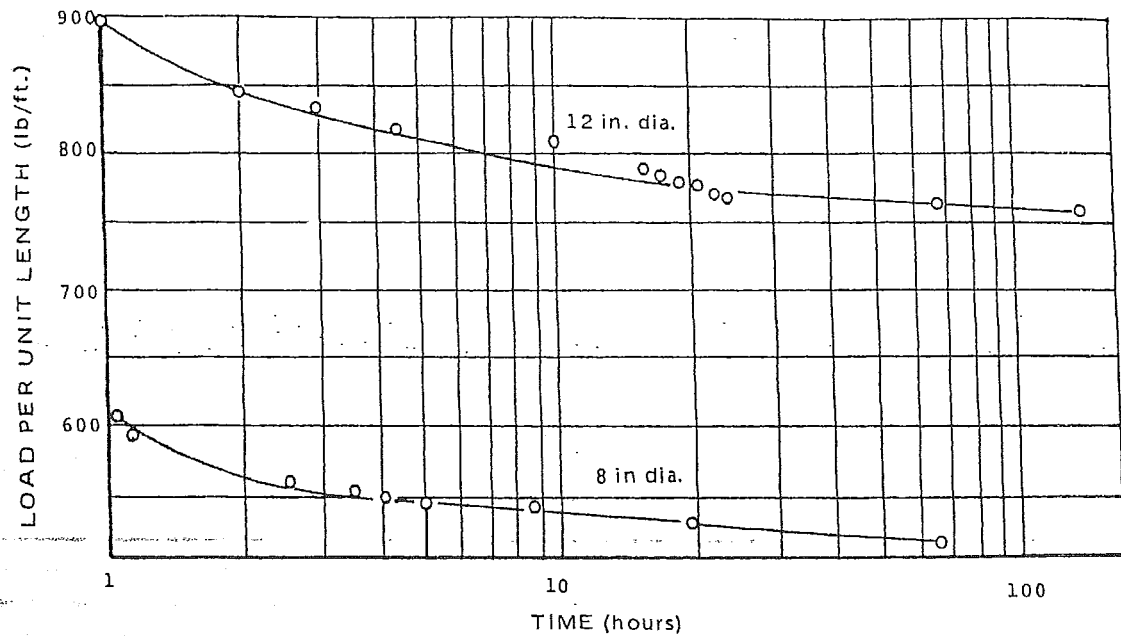
The full load on any buried pipe is not reached immediately after installation unless the final backfill is compacted to a high density. For a pipe with good flexibility, the long-term load will not exceed the prism load. The increase in load with time is the largest contribution to increasing deflection. Therefore, for design, the prism load should be used, thus effectively compensating for the increased trench consolidation load with time and resulting increased deflection. When deflection calculations are based on prism loads, the deflection lag factor, D_L , should be 1.0.

Creep is normally defined as continuing deformation with time when the material is subjected to a constant load. Most plastics exhibit creep. As temperature increases, the creep rate under a given load increases. Also, as stress increases, the creep rate for a given temperature increases. As PVC creeps, it also relaxes with time. Stress relaxation is defined as the decrease in stress, with time, in a material held at a constant deformation.

Figure 7.5 shows stress relaxation curves for PVC pipe samples held in a constant deflection condition, from which it is evident that PVC pipe does relax with time. The highest stress in a buried PVC non-pressure pipe is encountered at the equilibrium deflection condition. The behavior demonstrated in Figure 7.5 results in a decrease in the actual stress in the pipe at that deflection.

Figure 7.6 shows long-term data for PVC pipe buried in a soil box. Long-term deflection tests were run at Utah State University by imposing a given soil load, which was held constant throughout the duration of the test. PVC pipe material creep properties have little influence on deflection lag, but soil properties (such as density) exert great influence.

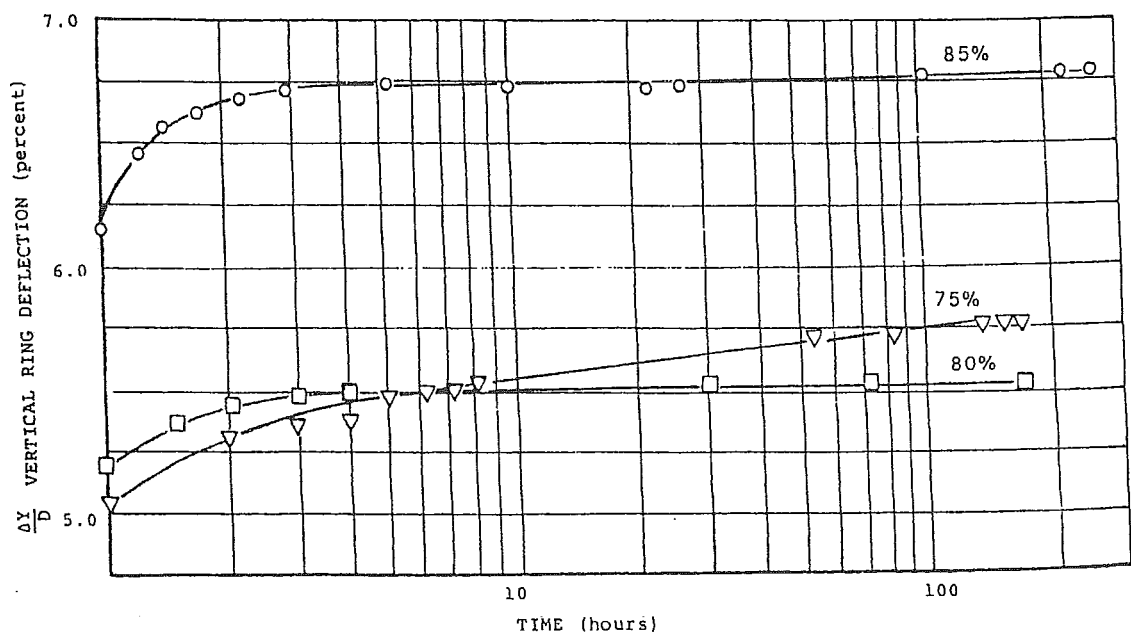
FIGURE 7.5
STRESS RELAXATION CURVES



Load as a function of time for a constant ring deflection of 20 percent

SOURCE: Utah State University

FIGURE 7.6
PVC PIPE CREEP RESPONSE

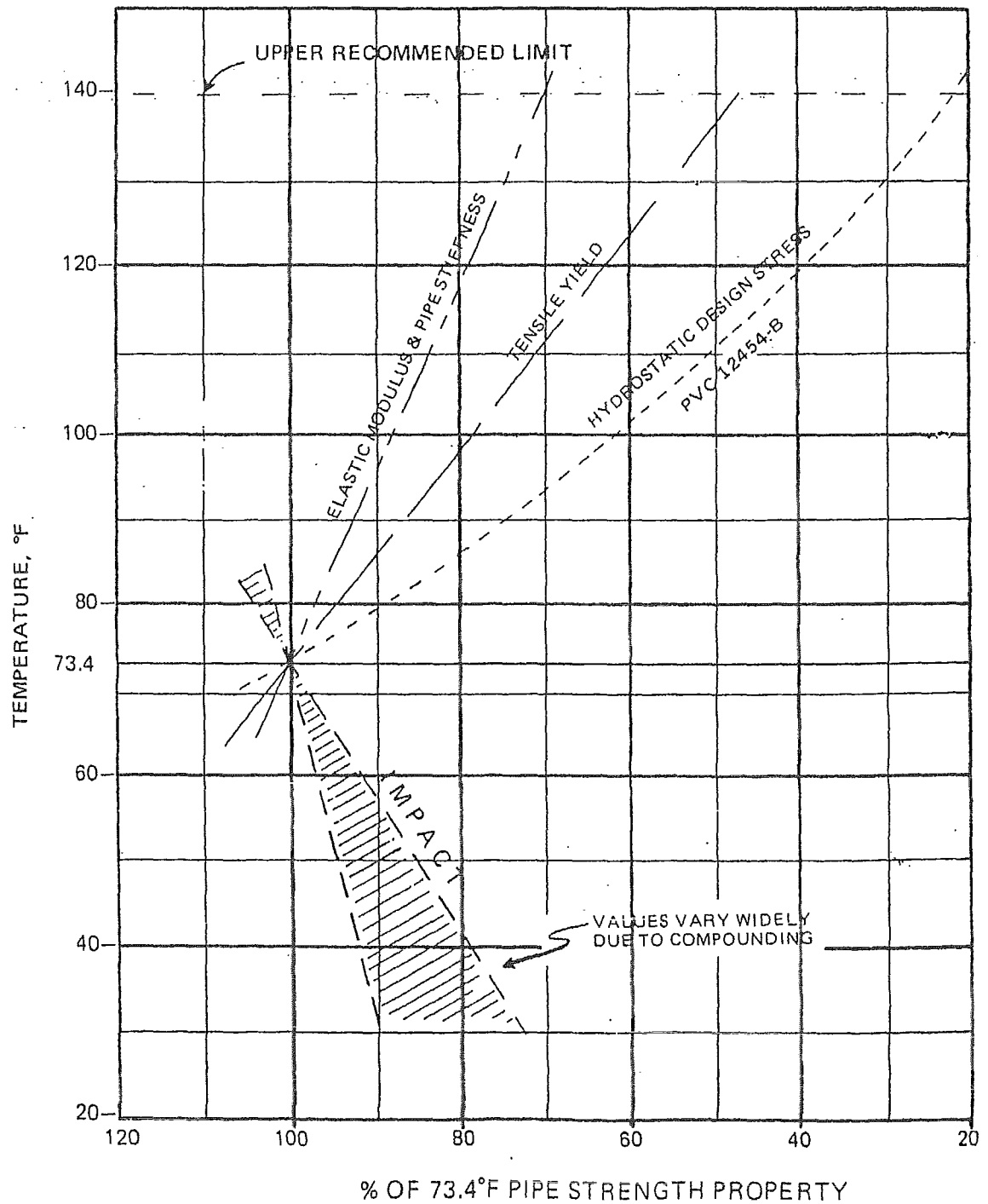


Time vs. vertical ring deflection for three soil densities,
as % of standard proctor density

SOURCE: Utah State University

FIGURE 7.7

APPROXIMATE RELATIONSHIP FOR 12454 PVC
FLEXIBLE PIPE STRENGTH PROPERTIES VS.
TEMPERATURE

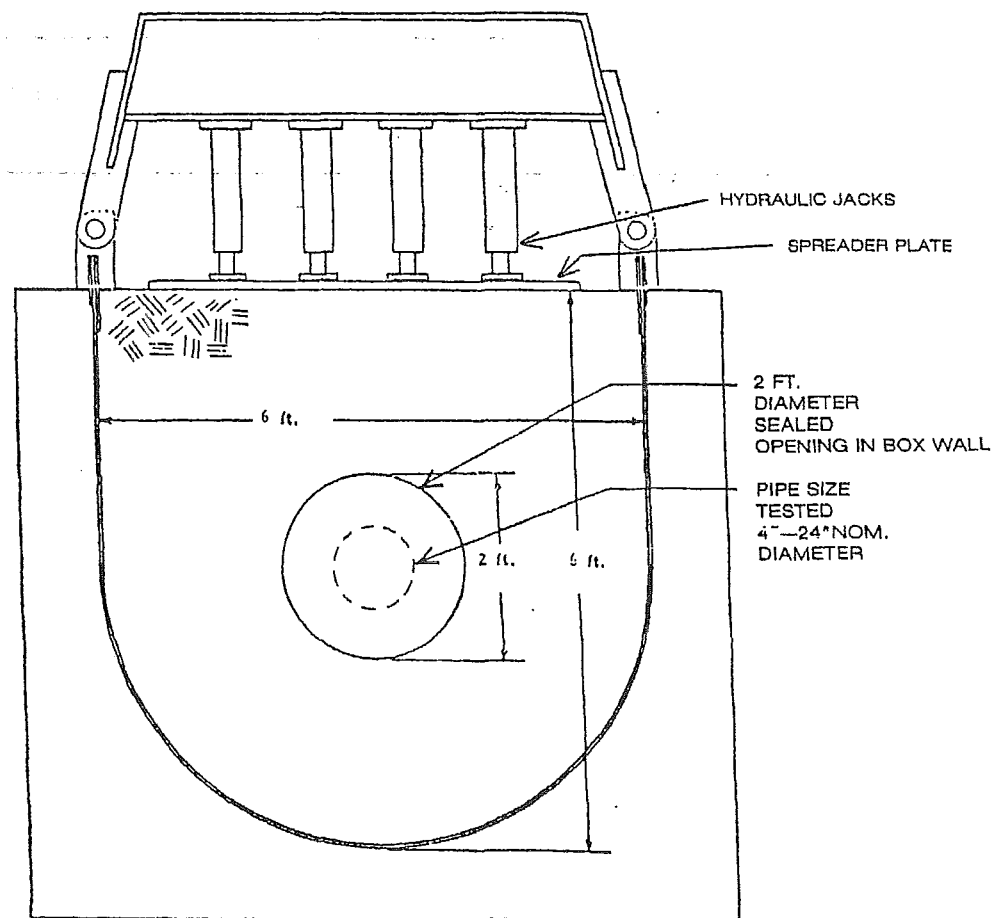


HANDBOOK OF PVC PIPE

The theoretical strength properties of PVC pipe vary with temperature. (See Chapter V - Internal Hydrostatic Pressures.) For flexible pipe considerations, the approximate relationships of pipe strength properties versus temperature are shown by curves in Figure 7.7.

Temperature controlled tests of buried PVC pipe were run to determine the temperature effect on the long-term behavior. Pipe was placed in a load cell (Figure 7.8), was embedded in soil, and compacted to a specified percentage of proctor density. The load on the soil was then increased until the desired starting vertical deflection of the pipe was reached. At this point, the load as well as the temperature was held constant, and the resulting time-dependent deflection was determined.

FIGURE 7.8
CELL CROSS SECTION



SOURCE: UTAH STATE UNIVERSITY

CHAPTER VII - DESIGN OF BURIED PVC PIPE

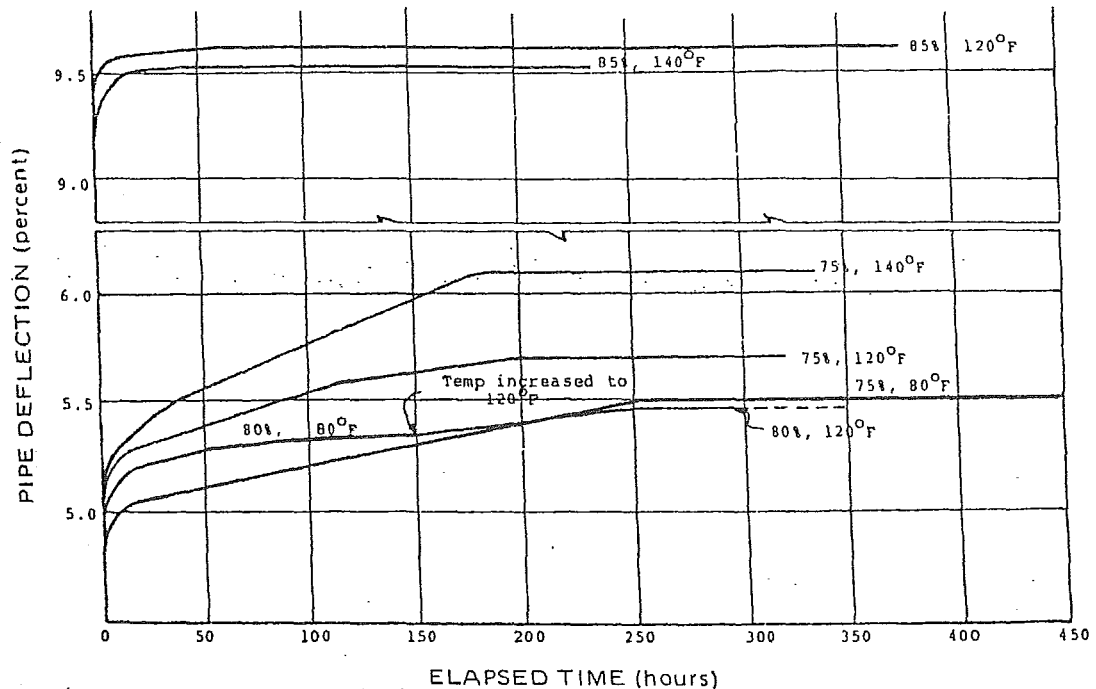
Data from these tests are given in graphical form in Figure 7.9. Arbitrarily, four of these tests were initiated at approximately 5 percent deflection, whereas two were started between 9 and 9.5 percent deflection. The loads required to produce these deflections were different in each case. The limiting deflection and the time required to reach it were largely controlled by the soil density. It is interesting to note for tests at different temperatures with the same soil density:

- The equilibrium deflection is slightly larger for higher temperatures because the effective pipe stiffness is lower.
- The time for equilibrium to be reached is shorter for higher temperatures since the soil-pipe system can interact at a faster rate in achieving equilibrium.
- An equilibrium deflection is reached in all cases. For the temperature range tested, an equilibrium state was reached and the pipe did not deflect beyond that point.

The above described long-term tests were carried out in a soil cell. The imposed load on a pipe in a soil cell is almost instantaneous due to the fact that the loading plane is only about 30 inches (760 mm) above the pipe. This provides a significant advantage over tests in either trench or embankment conditions, in which it takes a substantial amount of time for the full load to reach the pipe -- as much as months or years. When long-term tests are carried out in trenches and embankments, the change in deflection with time is due to increasing loads and soil consolidation. The change in deflection with respect to time in the embankment condition is greater than that measured in soil cell tests, because the soil cell tests are constant load tests. The equilibrium deflections are the same as those obtained with much less time delay, for the same loads in a soil cell.

FIGURE 7.9

TIME-DEFLECTION CURVES TEMPERATURE-CONTROLLED SOIL CELL TEST



Time-deflection curves for buried PVC pipe (temperature-controlled)
for three soil densities, as % of standard proctor density

Other factors, either manmade (such as live loads) or environmental (such as ground water) can result in load increases after initial deflection equilibrium. The result is an incremental deflection increase until side-soil consolidation is sufficient to re-establish equilibrium. Figure 7.10 represents deflection vs. time results over a 15-year period for 10-inch diameter PVC non-pressure pipes. The deflection increase at 150 days (3.6×10^3 hours) after installation was due to the spring groundwater table reaching the pipe zone. Note the incremental increase followed by renewed equilibrium.

FIGURE 7.10

**DEFLECTION VS. TIME FOR 10-INCH
DIAMETER PVC SEWER PIPE
(22-foot deep embankment installed Sept. 1975)**

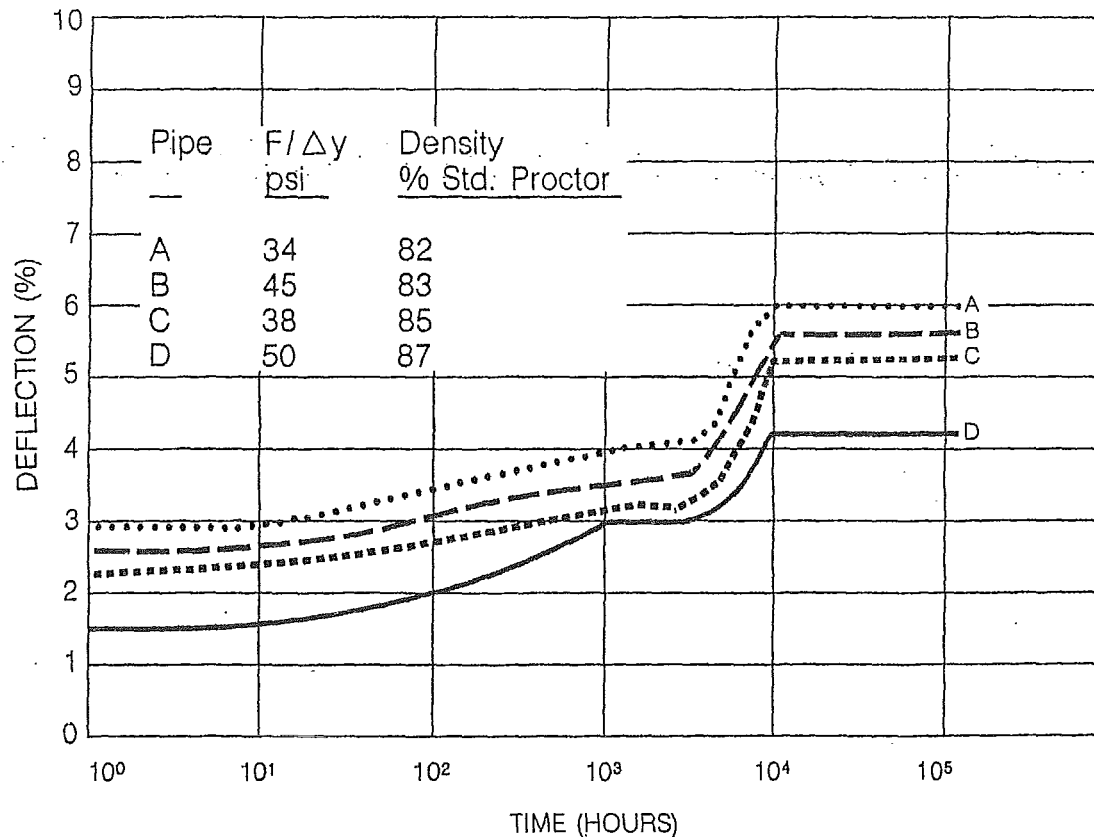
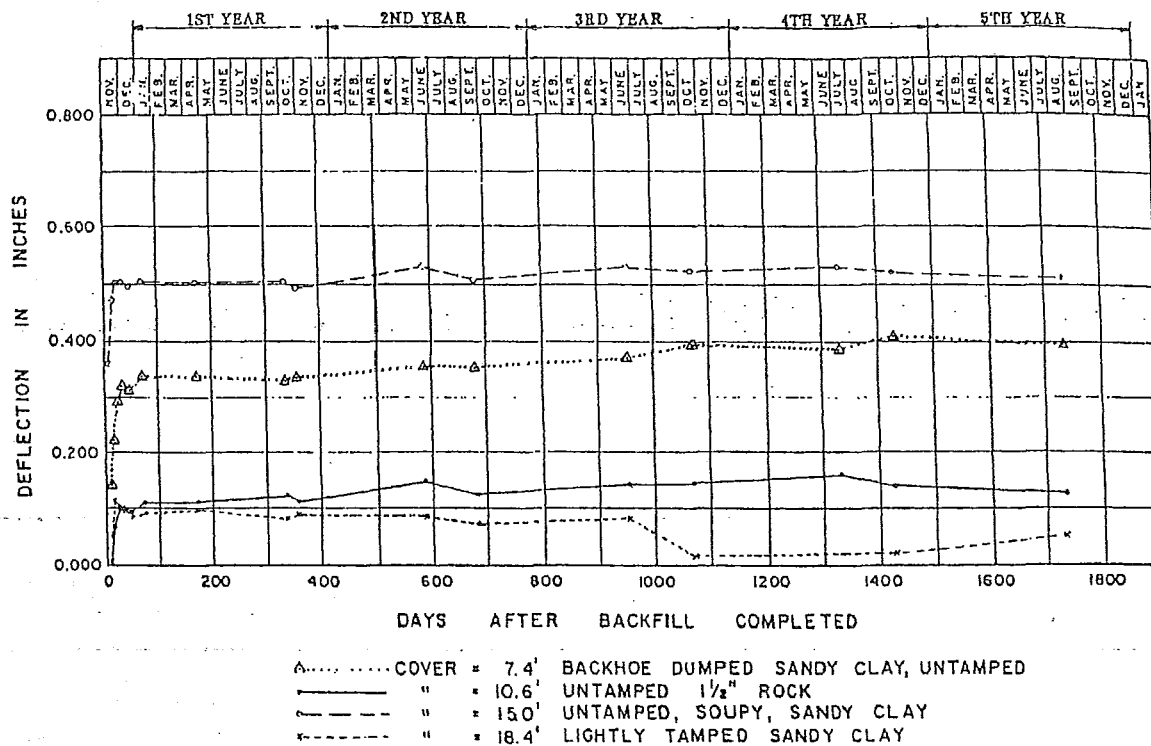


Figure 7.11 depicts long-term deflection data obtained for PVC pipes over a five-year period. All significant deflection occurs in the first few weeks while load and embedment stiffness reach equilibrium.

Extensive research has established that any buried flexible pipe (e.g. steel, fiberglass, plastic) will continue to deflect as long as the surrounding soil consolidates. Thus, as previously stated, the creep properties of pipe materials have little effect on the long-term deflection behavior of flexible pipe when buried in soil. In most cases a deflection lag factor, D_L , of 1.5 conservatively accounts for long-term effects of soil consolidation. Alternatively, design can be based upon the anticipated prism load and a D_L of 1.0.

FIGURE 7.11

DEFLECTION VERSUS TIME FOR BURIED PVC PIPES



Empirical Method: Methods discussed earlier for determining load and deflection have a theoretical basis and, except for the prism-load theory, require experimental investigation to determine the unknown constants. When a pipe having good flexibility is buried, the static pressure will not be greater than the prism-load pressure applied. Trying to calculate the actual pressure loading has frustrated researchers for years. Pipe has been installed and tested in a prism loaded condition (e.g., soil cell), in which resulting deformation can be monitored without the need to calculate actual static pressure.

This procedure has been used with great success at Utah State University under the direction of Reynold K. Watkins and at the United States Bureau of Reclamation under the direction of Amster K. Howard as well as other places. Data obtained in this manner can be used directly in the design of pipe-soil systems and in the prediction of overall performance. Ring buckling and over-deflection are evaluated simultaneously by actual tests. No attempt to explain the pipe-soil interaction phenomenon is necessary in the use of this method and the end results leave nothing to be estimated on the basis of judgment.

For example, if tests show that for a given soil compaction at 25 feet (7.6 m) of cover, a flexible pipe deflects 3 percent, and in every other way performs well, the actual load on the pipe and the soil modulus are academic. Thus a pipe installation can be designed with a known factor of safety provided that enough empirical test data are available.

In collection of this data, pipe was installed in a manner similar to that used in actual practice and the height of cover increased until performance levels were exceeded. The procedure was repeated many times and a reliable empirical curve of pipe performance versus height of fill was plotted. The use of these empirical curves or data eliminates the need to determine the actual soil pressure, since the pipe performance as a function of height of cover is determined directly. Alternate empirical approaches to study the deflection mechanism are:

- the study of actual field installations, or
- the simulation of a large enough earth cover in a soil test box to exceed the performance limits of the pipe.

To avoid the problem of having to establish design data for the infinite variety of installations and bedding conditions that are found in the field, the following design bases have been chosen:

- The embankment condition is selected as critical. (The results are conservative for other than embankment conditions.)
- Time lag or settlement of the embankment is included by analyzing long-term values of deflection.

An added advantage of this approach is that performance limits such as ring crushing, strain, and wall buckling can be analyzed, as well as ring deflection, by means of a single test. Uni-Bell manufacturers have generated such data for their PVC pipe products. The use of such data may be considered the most reliable method of design and is recommended when available. Substantial data is available for PVC sewer pipe made in accordance with ASTM D 3034 with minimum pipe stiffness of 46 psi and has been compiled by researchers at the Buried Structures Laboratory, Utah State University. The results of many measurements are categorized in Table 7.5 according to soil type, soil density and height of cover. Deflections presented in Table 7.5 represent the largest deflections encountered under the conditions specified. Data presented in this manner is intended to provide a variety of choices to engineers, showing that several engineering solutions may be available, of which economic factor may suggest the best solution.

For example, suppose PVC sewer pipe (ASTM D 3034 DR 35) with a minimum pipe stiffness of 46 psi is to be installed where the native soil is a Class IV clay. Ninety percent of the line will be at depths as great as 20 feet. The engineer has selected 7.5 percent deflection as the design limit, consistent with the maximum identified in the appendix of ASTM D 3034. According to Table 7.5 the native Class IV material could be used for that portion of the pipeline with less than 14 feet of cover if compacted to 75 percent of standard proctor, thereby insuring deflections less than 7.5 percent. However, ground water conditions may make compaction difficult, even impossible, or may result in subsequent reduction in soil strength. If this is the case, Class I, II, or III material may be imported and used with appropriate embedment procedures to limit deflection to 7.5 percent. The choice will be based on availability, convenience, and consequently on cost. For the deep portion of the line, Class III material compacted to 85 percent, Class II material compacted to 80 percent, or Class I material without compaction could be used successfully.

Performance Limits: Performance limits are established to prevent those conditions which may jeopardize the effective operation of a pipeline. The following is a list of performance limits which are considered in pipeline design:

- Stress
- Fatigue
- Reverse Curvature
- Longitudinal Bending
- Ring Buckling
- Localized Profile Buckling
- Wall Crushing
- Strain

The *stress* performance limit describes any internal pressure application in which the hoop stresses in the pipe wall due to applied pressure exceed the design strength of the pipe. The stress performance limit for PVC pipe is discussed in Chapter V.

TABLE 7.5
MEASURED LONG-TERM DEFLECTIONS OF SDR 35 PVC
(MINIMUM PIPE STIFFNESS 46 PSI) PIPE (PERCENT)

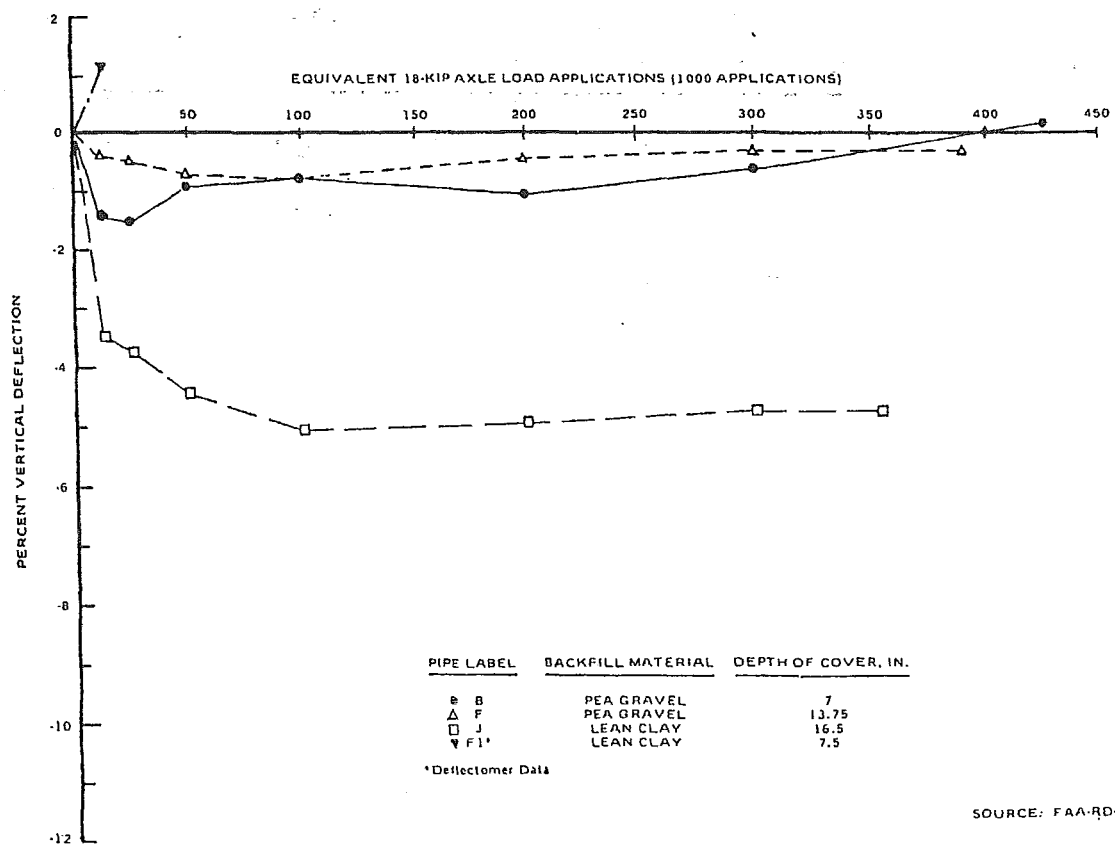
ASTM Embedment Material Classification		Density (Proctor) AASHTO T-99	Height of Cover (feet)													
			3	5	8	10	12	14	16	18	20	22	24	26	28	30
Manufactured Granular Angular	CLASS I		0.2	0.3	0.4	0.5	0.6	0.7	0.9	1.0	1.1	1.2	1.3	1.4	1.5	1.6
Clean Sand & Gravel	CLASS II	90%	0.2	0.3	0.5	0.7	0.8	0.9	1.1	1.2	1.3	1.4	1.6	1.7	1.8	2.0
		80%	0.9	1.4	2.3	3.2	3.6	4.1	5.0	5.5	6.0	6.4	7.3	7.7	8.2	9.1
		90%	0.2	0.4	0.6	0.8	0.9	1.1	1.2	1.4	1.6	1.7	1.9	2.1	2.2	2.3
		85%	0.7	0.9	1.7	2.2	2.6	3.0	3.5	3.9	4.3	4.8	5.2	5.6	6.0	6.5
		75%	1.1	1.8	2.9	3.8	4.5	5.5	6.8	8.5	9.9	11.3	12.7	14.1	15.5	16.8
Sand & Gravel with Fines	CLASS III	65%	1.3	2.4	3.6	4.7	5.5	6.8	8.5	9.6	11.4	13.0	14.5	16.0	17.3	18.0
		85%	0.7	0.9	1.7	2.2	2.6	3.0	3.5	3.9	4.3	4.8	5.2	5.6	6.0	6.5
		75%	1.3	2.3	3.3	4.3	5.0	6.5	7.8	9.5	10.6	12.2	13.5	15.0	16.3	17.0
Silt & Clay	CLASS IV	65%	1.3	2.4	3.6	4.7	5.5	8.0	10.5	12.5	15.0	17.6	20.0	22.0	24.0	26.0

1. Test data indicates no length of pipe installed under conditions specified will deflect more than is indicated; the pipe will deflect less than the amount indicated if specified density is obtained.
2. Embedment material classifications are as per ASTM D 2321, "Underground Installation of Flexible Thermoplastic Sewer Pipe."
3. Listed deflections are those caused by soil loading only and do not include initial out-of-roundness, etc.
4. Data obtained from Utah State University report.

The *fatigue* performance limit may be a consideration in both pressure and gravity flow pipe applications. However, most potable water distribution systems and gravity flow sanitary systems function under conditions which do not warrant consideration of fatigue as a performance limit. PVC is similar to most materials in that it can fail at stresses lower than the strength of the material if a repeating stress application occurs at a sufficiently high frequency and magnitude on a continuous basis over a period of time. Cyclic stress variations can be induced internally by surge pressures and water hammer effects, or the stress cycles can be caused from external loads such as traffic loadings on pipelines at shallow depths of burial.

FIGURE 7.12

PERMANENT DEFLECTION OF 12 IN. PVC PIPE AS A FUNCTION OF TRAFFIC



SOURCE: FAA-RD-79-86

The performance of PVC sewer pipe exposed to dynamic loadings while buried at shallow burial depths has been evaluated at the Geotechnical Laboratory, U. S. Army Engineer Waterways Experiment Station. Figure 7.12 is typical of the results obtained from the evaluation. It was concluded that PVC (DR 35) pipe performed very well under a range of loadings representative of highway and light to medium aircraft traffic. All tests were performed with a flexible bituminous road surface. A minimum cover height of 12 inches is recommended for PVC (DR 35) pipe subjected to highway loads of up to 18 kip axle. Under light to medium aircraft loads of up to 320,000 pounds gross weight, a minimum burial depth of 2 feet is recommended.

It is recommended that special attention be given to the selection, placement, and compaction of backfill material with shallow buried flexible pipe, such as PVC pipe underneath rigid pavement to prevent injurious cracking of the road surface. (See Chapter 10 on Construction and Installation.)

A *reverse curvature* performance limit for flexible steel pipe was established shortly after publication of the Iowa Formula. It was determined that corrugated steel pipe would begin reverse curvature at a deflection of about 20 percent. Design at that time called for a limit of 5 percent deflection, thus providing a structural safety factor of 4.0.

Buried PVC sewer pipe (ASTM D 3034, DR 35), when deflecting in response to external loading, may develop recognizable reversal of curvature at a deflection of 30 percent. This level of deflection has been commonly designated as a conservative performance limit for PVC sewer pipe. Research at Utah State University has demonstrated that the load carrying capacity of PVC sewer pipe continues to increase even when deflections increase substantially beyond the point of reversal of curvature. With consideration of this performance characteristic of PVC sewer pipe, engineers generally consider the 7.5 percent deflection limit, recommended by ASTM D 3034 (Appendix), to provide a very conservative factor of safety against structural failure. Similar to the methodology applied to steel pipe, the resulting structural safety factor for PVC sewer pipe is 4.0.

Longitudinal bending of a pipeline can either be intentional or unintentional and should be controlled. Unlike "rigid pipes," PVC pipe will not break in flexure but will bend. Such bending does not impair a PVC pipeline's performance. Only short radius bends can be considered performance limiting for PVC pipe. (See Chapter VIII - Special Design Applications - Longitudinal Bending.)

The *ring buckling* phenomenon may govern design of flexible pipes under conditions of internal vacuum, sub-aqueous installations, or loose

soil burial. For a circular ring subjected to a uniform external pressure or internal vacuum, the critical buckling pressure (P_{cr}) is defined by Timoshenko as:

EQUATION 7.11

$$P_{cr} = \frac{3EI}{r^3} = 0.447 \text{ PS}$$

Where: r = Mean pipe radius, in
 I = Pipe wall moment of inertia, in⁴/in
 PS = Pipe stiffness, lbs/in²
 E = Modulus of elasticity, lbs/in²

With the moment of inertia (I) defined as $t^3/12$ for solid-wall pipes, Equation 7.11 becomes:

EQUATION 7.12

$$P_{cr} = \frac{2E}{\left[\frac{D_o - t}{t} \right]^3} = \frac{2E}{(DR - 1)^3}$$

Where: E = Modulus of elasticity, lbs/in²
 DR = Dimension ratio
 D_o = Outside pipe diameter, in
 t = Pipe wall thickness, in

For long tubes (pipelines) under combined stress, E is replaced by $E/(1 - \nu^2)$ and the critical buckling pressure is:

EQUATION 7.13

$$P_{cr} = \frac{3EI}{(1 - \nu^2)r^3} = \frac{0.447 \text{ PS}}{(1 - \nu^2)}$$

For solid-wall pipes:

EQUATION 7.14

$$P_{cr} = \frac{2E}{(1 - \nu^2)(DR - 1)^3} = \frac{2E}{(1 - \nu^2)} \left[\frac{t}{D_o - t} \right]^3$$

$$= \frac{2E}{(1 - \nu^2)} \left[\frac{D}{t} \right]^3$$

Where:

ν	= Poisson's Ratio = $\frac{\text{unit lateral contraction}}{\text{unit axial elongation}}$
	= 0.38 for PVC pipe
D_o	= Outside pipe diameter, in
D	= $D_o - t$ = mean pipe diameter, in

Since the mean pipe radius (r) is equal to $D/2$, Equation 7.14 can also be expressed as:

EQUATION 7.15

$$P_{cr} = \frac{E}{4(1 - \nu^2)} \left[\frac{t}{r} \right]^3$$

Pipes that are significantly out-of-round or deflected have less buckling resistance than round pipes. The critical buckling pressure for these elliptical shapes can be determined by using a reduction factor "C", Figure 7.13, to account for the in-service shape such that:

EQUATION 7.16

$$P_{cr} = C \left[\frac{3EI}{(1 - \nu^2)r^3} \right] = C \frac{0.447 \text{ PS}}{(1 - \nu^2)}$$

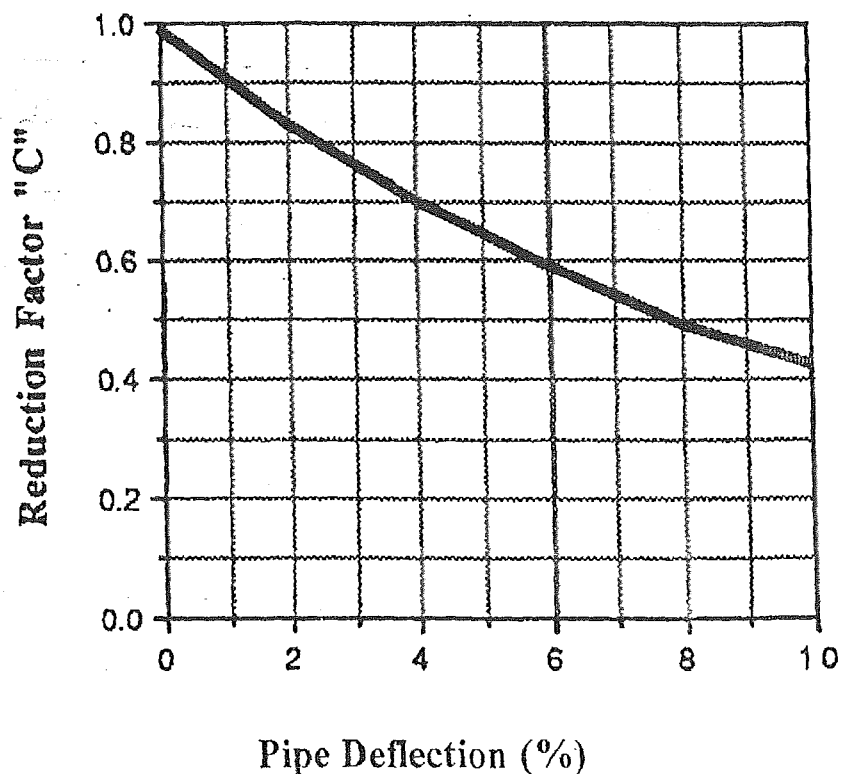
For solid wall pipes:

EQUATION 7.17

$$P_{cr} = \frac{2CE}{(1 - \nu^2) \left[\frac{D}{t} \right]^3} = \frac{CE}{4(1 - \nu^2) \left[\frac{t}{r} \right]^3}$$

FIGURE 7.13

CRITICAL BUCKLING PRESSURE REDUCTION
FACTOR "C" FOR SHAPE



When pipes are buried or are installed in such a manner that the soil surrounding medium provides some resistance against buckling deflection, the buckling pressure (P_b) in the soil has been found to be²³:

EQUATION 7.18

$$P_b = 1.15 \sqrt{P_{cr} E'}$$

Where: P_b = Buckling pressure in a given soil, lbs/in²
 E' = Modulus of soil reaction, lbs/in²

Example:

If a DR 35 PVC sewer pipe with a 400,000 lbs/in² modulus of elasticity was confined in a saturated soil providing $E' = 800$ lbs/in², what height (H) of the saturated soil, which weighs 120 lbs/ft³ (w), would cause buckling? What is the maximum cover height such that deflection does not exceed 7.5 percent? Assume the bedding angle is zero ($K = 0.11$).

$$P_{cr} = \frac{2(400,000)}{[1 - (0.38)^2] (35 - 1)^3} = 23.8 \text{ lbs/in}^2$$

$$P_b = 1.15 \sqrt{23.8 (800)} = 158.7 \text{ lbs/in}^2 = 22,850 \text{ lbs/ft}^2$$

$$H = P/w = 22,850/120 = 190 \text{ ft}$$

To limit deflection (Δ) to 7.5 percent:

$$\Delta = \frac{K P_e}{.149 P S + .061 E'}$$

$$P_e = \frac{\Delta (.149 P S + .061 E')}{K}$$

$$= \frac{0.075 [.149(46) + .061(800)]}{0.11}$$

$$P_e = 37.9 \text{ lbs/in}^2 = 5,464 \text{ lbs/ft}^2$$

$$H \text{ (to limit deflection)} = 5,464/120 = 45.5 \text{ ft}$$

The maximum cover is limited by the allowable deflection, not by buckling. Therefore, the safety factor for the critical failure mode by buckling of DR 35 PVC pipe is ample.

Research has established that flexible steel pipe walls can buckle at deflections considerably less than 20 percent if the load is large and the soil surrounding the pipe is extremely compacted. Based on these

observations, H. L. White and J. P. Layer proposed the "Ring Compression Theory" for the design of buried flexible pipes. This theory assumed that the backfill was highly compacted, that deflection would be negligible, and that the performance limit was *wall crushing*. The design concept is expressed by:

EQUATION 7.19

$$T = P_y \times \frac{D_o}{2}$$

Where: T = Wall Thrust, lbs/in
 P_y = Vertical soil pressure, lbs/in²
 D_o = Outside diameter, in

EQUATION 7.20

$$\sigma_c = \frac{T}{A}$$

Where: σ_c = Compressive stress, lbs/in²
 A = Area of the pipe wall, in²/in

Example: A profile wall PVC pipe ($D_o = 19.15$ in, $A = 2.503$ in²/ft) is concrete-cradled. At what vertical soil pressure or depth of cover could one expect failure by ring compression? ($w = 120$ lbs/ft³)

$$\sigma_c = \frac{T}{A} \quad P_y = wH$$

Conservatively assume σ_c = hydrostatic design basis or hoop tensile = 4000 lbs/in².

$$P_y = \frac{\sigma_c 2A}{D_o} = \frac{4000(2)(2.503/12)}{19.15}$$

$$P_y = 87.1 \text{ lbs/in}^2 = wH$$

$$H = \frac{P_y}{w} = \frac{87.1 \text{ lbs/in}^2}{120 \text{ lbs/ft}^2} \times 144 \text{ in}^2/\text{ft}^2$$

$$H = 104.5 \text{ ft}$$

This example easily illustrates that ring compression is not a governing factor in design of either PVC water or sewer pipe systems.

Strain is generally not a performance-limiting factor for buried PVC pipe. Total strain in a pipe wall can be caused by two actions: (1) flexure of the pipe as it deforms and (2) hoop stress in the pipe wall. Determination of strains due to hoop stress is straightforward. If a homogeneous wall is assumed and pressure concentrations are neglected, the formula follows:

EQUATION 7.21

Hoop Strain

$$\epsilon_h = \frac{PD}{2AE}$$

For solid-wall pipes Equation 7.21 becomes:

EQUATION 7.22

$$\epsilon_h = \frac{PD}{2tE}$$

- Where:
- ϵ_h = Maximum strain in the pipe wall due to hoop stress, in/in
 - P = Pressure on pipe (may be internal and/or external pressure with the appropriate sign), lbs/in²
 - D = Mean pipe diameter, in
 - A = Area of the pipe wall, in²/in
 - E = Modulus of elasticity of the pipe material, lbs/in²
 - t = Pipe wall thickness, in

HANDBOOK OF PVC PIPE

Maximum strains due to ring deflection or flexure may be determined by assuming the pipe remains an ellipse during deflections. The resulting equation is:

EQUATION 7.23

Flexural Strain

$$\epsilon_f = \frac{C_{\max}}{r} \left[\frac{3\Delta Y/D}{1 - 2\Delta Y/D} \right]$$

Again, for solid-wall pipes 7.23 becomes:

EQUATION 7.24

$$\epsilon_f = \frac{t}{D} \left[\frac{3\Delta Y/D}{1 - 2\Delta Y/D} \right] = \frac{1}{DR} \left[\frac{3\Delta Y/D}{1 - 2\Delta Y/D} \right]$$

Where:

- ϵ_f = Maximum strain in pipe wall due to ring deflection or flexure, in/in
- C_{\max} = Distance from the neutral axis to the extreme fiber, in
- r = Mean pipe radius, in
- ΔY = Vertical decrease in diameter, in
- D = Mean pipe diameter, in
- t = Pipe wall thickness, in
- DR = Dimension ratio

Note: See Dimension Tables in the Appendix for specific profile-wall pipe dimensional data.

In a buried pipeline these strain components act simultaneously. The maximum combined strain in the pipe wall can be determined by summing both components.



PVC PIPE DIMENSIONS

Nominal Pipe Size	Wall Thickness		Outside Diameters		
	Minimum	Tolerance	Average OD	Average	Tolerance Out-of-Roundness
ASTM D 1785, PVC PIPE, SCHEDULE 40					
1	0.133	+0.020	1.315	±0.005	±0.010
1¼	0.140	+0.020	1.660	±0.005	±0.012
1½	0.145	+0.020	1.900	±0.006	±0.012
2	0.154	+0.020	2.375	±0.006	±0.012
2½	0.203	+0.024	2.875	±0.007	±0.015
3	0.216	+0.026	3.500	±0.008	±0.015
3½	0.226	+0.027	4.000	±0.008	±0.050
4	0.237	+0.028	4.500	±0.009	±0.050
5	0.258	+0.031	5.563	±0.010	±0.050
6	0.280	+0.034	6.625	±0.011	±0.050
8	0.322	+0.039	8.625	±0.015	±0.075
10	0.365	+0.044	10.750	±0.015	±0.075
12	0.406	+0.049	12.750	±0.015	±0.075

ASTM D 1785, PVC PIPE, SCHEDULE 80

1	0.179	+0.021	1.315	±0.005	±0.010
1¼	0.191	+0.023	1.660	±0.005	±0.012
1½	0.200	+0.024	1.900	±0.006	±0.012
2	0.218	+0.026	2.375	±0.006	±0.012
2½	0.276	+0.033	2.875	±0.007	±0.015
3	0.300	+0.036	3.500	±0.008	±0.015
3½	0.318	+0.038	4.000	±0.008	±0.015
4	0.337	+0.040	4.500	±0.009	±0.015
5	0.375	+0.045	5.563	±0.010	±0.030
6	0.432	+0.052	6.625	±0.011	±0.035
8	0.500	+0.060	8.625	±0.015	±0.075
10	0.593	+0.071	10.750	±0.015	±0.075
12	0.687	+0.082	12.750	±0.015	±0.075

ASTM D 2241, PVC PIPE (SDR-PR), SDR 21 (200)

1	0.063	+0.020	1.315	±0.005	±0.015
1¼	0.079	+0.020	1.660	±0.005	±0.015
1½	0.090	+0.020	1.900	±0.006	±0.030
2	0.113	+0.020	2.375	±0.006	±0.030
2½	0.137	+0.020	2.875	±0.007	±0.030
3	0.167	+0.020	3.500	±0.008	±0.030
3½	0.190	+0.023	4.000	±0.008	±0.050
4	0.214	+0.026	4.500	±0.009	±0.050
5	0.265	+0.032	5.563	±0.010	±0.050

**APPLICATION FOR PERMIT RENEWAL AND MODIFICATION
SANDOVAL COUNTY LANDFILL**

**VOLUME III: LANDFILL ENGINEERING CALCULATIONS
SECTION 5: PIPE LOADING CALCULATIONS**

ATTACHMENT III.5.D

**WASHINGTON STATE DEPARTMENT OF ECOLOGY. 1987.
SOLID WASTE LANDFILL DESIGN MANUAL.
WASHINGTON: WDOE**

TABLE OF CONTENTS

	<u>Page</u>
4C.1 COLLECTION PIPE MATERIALS	4C-1
4C.1.1 Pipe Perforations	4C-3
4C.2 STRUCTURAL REQUIREMENTS	4C-4
4C.2.1 Loading Conditions	4C-4
4C.2.2 Refuse and Earth Loads	4C-6
4C.2.3 Superimposed Loads	4C-13
4C.2.4 Design Safety Factor	4C-18
4C.3 RIGID PIPE DESIGN	4C-19
4C.3.1 Classes of Bedding and Bedding Factors	4C-19
4C.3.2 Selection of Pipe Strength	4C-23
4C.4 FLEXIBLE PIPE DESIGN.....	4C-23
4C.4.1 General Approach.....	4C-23
4C.4.2 Selection of Plastic Pipe.....	4C-25
4C.4.3 Selection of Other Flexible Pipes.....	4C-26
4C.4.4 Bedding Material.....	4C-26

LIST OF FIGURES

	<u>Page</u>
4C.1 Installation Conditions	4C-5
4C.2 Trench Condition-Values of Load Coefficient C_{us} (Trench Uniform Surcharge)	4C-8
4C.3 Trench Condition-Values of Load Coefficient C_d (Backfill).....	4C-10
4C.4 Diagram for Load Coefficient C_c for Positive Projecting Pipes	4C-11
4C.5 Diagrams for Load Coefficient C_n for Negative Projecting and Induced Trench Pipes	4C-14
4C.6 Trench Beddings: Circular Pipe	4C-20
4C.7 Positive Projecting Embankment Beddings: Circular Pipe	4C-21

LIST OF TABLES

	<u>Page</u>
4C.1 Maximum Value of K_u' for Typical Backfill Soils	4C-8
4C.2 Recommended Design Values of r_{sd} (Positive Projecting Embankment <i>Conditions</i>)	4C-12
4C.3 Values of Load Coefficients, C_s , for Concentrated and Distributed Superimposed Loads Vertically Centered over Sever Pipe	4C-16
4C.4 Superimposed Concentrated Load Impact Factors, F	4C-17
4C.5 Equipment Loads	4C-17
4C.6 Values of N for Circular Pipe	4C-22
4C.7 Values of X for Circular Pipe	4C-22
4C.8 Values of Bedding Constant, K_b	4C-25

APPENDIX 4C

COLLECTION PIPE MATERIALS AND STRUCTURAL REQUIREMENTS

4C.1 COLLECTION PIPE MATERIALS

Pipe that may be suitable for leachate collection systems is manufactured -to meet nationally recognized product specifications. Some materials are more appropriate than others for use in a leachate collection system and the various types of pipe should be evaluated carefully. Various factors -to consider are:

- Intended use (type of leachate)
- Flow requirements
- Scour or abrasion conditions
- Corrosion conditions
- Product characteristics
- Physical properties
- Installation requirements
- Handling requirements
- Cost effectiveness

No single pipe product will provide optimum capability in every characteristic for all leachate collection system design conditions. Specific application requirements should be evaluated prior to selecting pipe materials.

Pipe materials for leachate collection applications fall within the two commonly accepted classifications of rigid pipe and flexible pipe. Rigid pipe materials derive a substantial part of their basic earth load carrying capacity from the structural strength inherent in the rigid pipe wall, while flexible pipe materials derive load carrying capacity from the interaction of the flexible pipe and the embedment soils. Products commonly available within these two classes are:

1. Rigid Pipe
 - a. Asbestos-cement pipe (ACP)
 - b. Cast iron pipe (CIP)
 - c. Concrete pipe (CP)
 - d. Vitrified clay pipe (VCP)
2. Flexible Pipe
 - a. Ductile iron pipe (DIP)
 - b. Steel pipe (SP)
 - c. Thermoplastic pipe
 - Acrylonitrile-butadiene-styrene (ABS)
 - ABS composite
 - Polyethylene (PE)
 - Polyvinyl chloride (PVC)
 - d. Thermoset plastic pipe
 - Reinforced plastic mortar (RPM)

- Reinforced thermosetting resin (RTR)

Within the rigid pipe classification, the suitability of cast iron and concrete pipe for leachate collection systems is limited by the difficulty of incorporating perforations in the pipe walls and their susceptibility to corrosion by acidic leachates. The use of asbestos-cement pipe is limited by its low beam strength. It is also susceptible to attack by acidic leachates. Vitrified clay pipe can be perforated and is highly resistant to chemical corrosion, but its relatively low beam strength limits the fill height that can be placed over it. For these reasons, rigid pipes have very limited use potential in leachate collection systems.

As a group, flexible pipes offer good potential for use in leachate collection systems. Within the flexible pipe group, however, only certain products are suitable. Ductile iron and steel pipe have little application for leachate collection systems primarily because of their susceptibility to attack by acidic leachates. Also, although ductile iron pipe has high load bearing capacity, incorporating perforations in the pipe walls is difficult. Thermoplastic and thermoset plastic pipe are more suitable products for leachate collection systems.

Thermoplastic materials are characterized by their ability to be repeatedly softened by heating and hardened by cooling through a temperature range characteristic for each plastic. Materials suitable for use in leachate collection systems include ABS pipe, ABS composite pipe, PE pipe, and PVC pipe. All of these materials are subject to attack by certain organic chemicals, so compatibility with the leachate must be considered in this selection. ABS is generally not as resistant to acids as PVC and neither of these two materials has good resistance to concentrated ketones and esters. Pipes manufactured from any of these materials are subject to excessive deflection when improperly bedded and haunched, so proper design and construction are important. With the exception of PVC pipe, these pipes are also subject to environmental stress cracking. Thermoplastic pipe product design should be based on long-term data.

Thermoset plastic materials, cured by heat or other means, are substantially infusible and insoluble. The two categories of thermoset plastic materials suitable for leachate collection systems include RPM pipe and RTR pipe. RPM pipe is manufactured containing reinforcements, such as fiberglass, and aggregates, such as sand, embedded in or surrounded by cured thermosetting resin. RTR pipe is manufactured using a number of methods including centrifugal casting, pressure laminating, and filament winding. In general, the product contains fibrous reinforcement materials, such as fiberglass, embedded in or surrounded by cured thermosetting resin. Pipes manufactured from both of these materials are subject to strain corrosion in some environments, attack by certain organic chemicals, and excessive deflection when improperly bedded and haunched. Therefore, leachate compatibility and proper design and construction are important when thermoset plastic pipe is used in leachate collection systems.

4C.1.1 Pipe Perforations

By nature of their intended use, leachate collection lines must be perforated. The size and spacing of the openings should be determined based on hydraulic considerations. The effects of the perforations should be considered in the structural design of the leachate collection pipes.

4C.1.1.1 Size and Spacing

A leachate collection line, to function correctly, must be capable of accepting all the leachate flowing to it through the gravel drainage layer. After the pipe is sized to handle the flow, the size and spacing of the perforations should be selected. The rate of flow into the leachate collection pipes through the perforations is dependent on several factors, including the hydraulic conductivity of the gravel material around the pipe and the head loss due to convergence of flow to the perforations in the pipe.

W.T. Moody, as cited in U.S. * Department of the Interior (1978) determined the theoretical relationship among the above factors and concluded that increasing the hydraulic conductivity of the gravel envelope around the pipe was a more effective method for increasing the rate of flow into the pipe than increasing the size of the openings. Therefore, the selection of the size and spacing of the perforations should be based on: consideration of standard perforated pipe commonly available from manufacturer; bedding and backfill requirements for the particular installation; and effects on pipe strength. For a given rate of leachate inflow and a perforated pipe, the minimum required hydraulic conductivity of the gravel envelope around the pipe can be determined using a procedure similar to that presented in U.S. Department of the Interior (1978).

4C.1.1.2 Effects on Load Capacity

The various design procedures for rigid and flexible pipes and the various pipe performance limits are based on solid wall pipe. Pacey, et al., as cited in Dietzler (1984) has suggested that the effect of perforations could be compensated by arbitrarily increasing the earth load on the pipe. Data presented in Dietzler (1984) indicated the inclusion of typical perforations in the lower quarters of 6-inch ABS and PVC pipe has little influence on pipe stiffness and deflection versus load performance. Others have stated there are indications that perforations will reduce the effective length of pipe available to carry loads and resist deflection suggest taking the effect of perforations into account by increasing the load in proportion to the reduction in the effective length. This latter method appears to be an adequately conservative approach. If L_p equals the cumulative length of the perforations per unit length of the pipe, L , then the actual load on the pipe should be increased as follows:

$$\text{Design Load} = \text{Actual Load} \times \frac{L}{L - L_p} \quad (4C-1)$$

Methods to determine the actual load are discussed in the following sections.

4C.2 STRUCTURAL REQUIREMENTS

Leachate collection systems installed underneath a landfill must be designed to withstand the anticipated height and weight of refuse to be placed over them. It is not uncommon to find heights in excess of 100 feet. Appropriately, leachate collection systems must be designed for vertical pressure acting at the base of the landfill, considering the height of the landfill and the weighted average density of the refuse, daily cover, final cover system, and any superimposed loads during the life of the landfill. Perimeter collection systems that generally lie outside the landfill should be designed for the earth loads acting on them along with any superimposed loads.

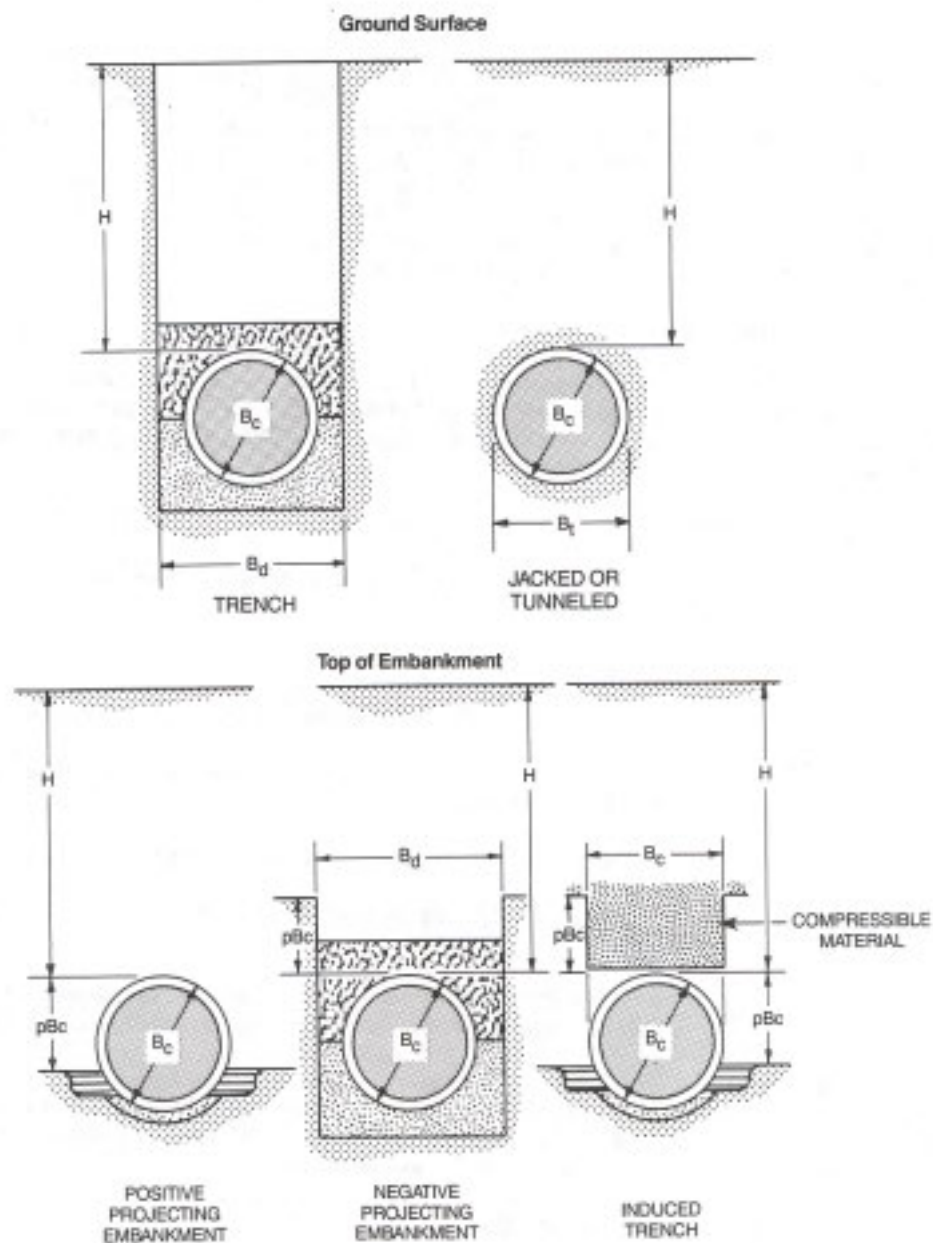
The supporting strength of a leachate collection pipe is a function of installation conditions as well as the strength of the pipe itself. Structural analysis and design of the collection system are problems of soilstructure interaction. This section presents general procedures for determining the structural requirements of the pipes in a leachate collection system. Detailed discussions concerning structural design of pipelines may be found in ASCE and WPCF (1982). The design procedure for the selection of pipe strength consists of the following:

- Determination of loading condition
- Determination of refuse and earth loads
- Determination of superimposed loads
- Selection of bedding and determination of bedding factor
- Application of factor of safety
- Selection of pipe strength

4C.2.1 Loading Conditions

The load transmitted to a pipe is largely dependent on the type of installation. The common types of installation conditions are shown in Figure 4C.1 and include trench, positive projecting embankment, negative projecting embankment, and induced trench. Jacked or tunneled is also an installation condition, but has little application for leachate collection systems. The difficulty in controlling the placement of the embankment material greatly limits the potential use of the induced trench condition for leachate collection systems.

Trench installation* conditions are defined as those in which the pipe is installed in a relatively narrow trench cut in undisturbed ground and covered with backfill to the original ground surface. Embankment conditions are defined as those in which the pipe is covered above the original ground surface or in which a trench in undisturbed soil is so wide that wall friction does not affect the load on the pipe. The embankment classification is further subdivided into positive projecting and negative projecting classification. Pipe is positive projecting when its top is above the adjacent original ground surface. Negative projecting pipe is installed with its top below the adjacent original ground surface in a trench that is narrow with respect to the pipe and depth of cover.



WDOE Solid Waste
Landfill Design Manual

Adapted From: American Concrete Pipe Association, 1980

Figure 4C.1
Installation Conditions

Both the trench condition and either of the embankment conditions may be appropriate in the design of leachate collection systems. A perimeter collection system may be designed for either the trench condition or the negative projecting embankment condition, depending on trench width. Leachate collection systems underneath the landfill would generally be designed for one of the embankment conditions.

4C.2.2 Refuse and Earth Loads

The methods for determining the vertical load on buried conduits caused by soil forces were developed by Marston for all of the most commonly encountered construction conditions (ASCE and WPCF, 1982). The general form of the Marston equation is:

$$W = CWB^2 \quad (4C-2)$$

where: W = Vertical load per unit length acting on the pipe because of gravity soil loads

v = Unit weight of the soil

B = Trench or pipe width, depending on installation conditions

C = Dimensionless coefficient that measures the effects of the following variables:

- The ratio of the height of fill to width of trench or pipe
- The shearing forces between interior and adjacent soil prisms
- The direction and amount of relative settlement between interior and adjacent soil prisms for embankment conditions

While the general form of the Marston equation includes all the factors necessary to analyze all types of installation conditions, it is convenient to write a specialized form of the equation for each of the installation conditions described in the previous subsection.

4C.2.2.1 Loads for Trench Conditions

In the trench condition, the load on the pipe is caused by both the waste fill and the trench backfill (U.S. EPA, 1983). These two components of the total vertical pressure on the pipe are computed separately and then added to obtain the total vertical pressure acting on the top of the pipe.

The waste fill is assumed to develop a uniform surcharge pressure, Of , at the base of the fill. The magnitude of Qf is given by the expression:

where:

$$Q_f = (w_f)(H_f) \quad (4C-3)$$

Q_f = Vertical pressure at the base of the waste fill (lbs/sq ft)

w_f = Weighted average density of the waste fill including refuse, intermediate cover, and final cover system (lbs/cu ft)

H_f = Height of waste fill including cover (ft)

The weighted average density of the waste fill, w_f is computed as follows:

$$w_f = \frac{(w_r)(H_r) + (w_i)(T_i) + (w_c)(T_c)}{H_f} \quad (4C-4)$$

where:

w_r = Average in-place wet density of the refuse (lbs/cu ft)

H_r = Height of refuse excluding cover layers (ft)

w_i = Wet density of intermediate cover (lbs/cu ft)

T_i = Total thickness of intermediate cover layers (ft)

w_c = Wet density of the final cover system (lbs/cu ft)

T_c = Thickness of the final cover system (ft)

$H_f = H_r + T_i + T_c$

The value of the vertical pressure at the top of the pipe due to the waste fill, P_{vf} (in lbs/sq ft), is determined from the following:

$$P_{vf} = (Q_f)(C_{us}) \quad (4C-5)$$

where:

C_{us} = Dimensionless load coefficient that is a function of the ratio of the depth of the trench, H (measured from the original ground surface to the top of the pipe) to the trench width, B_d , and of the friction between the backfill and the sides of the trench.

The load coefficient, C_{us} , may be calculated from the following equation or obtained from Figure 4C.2:

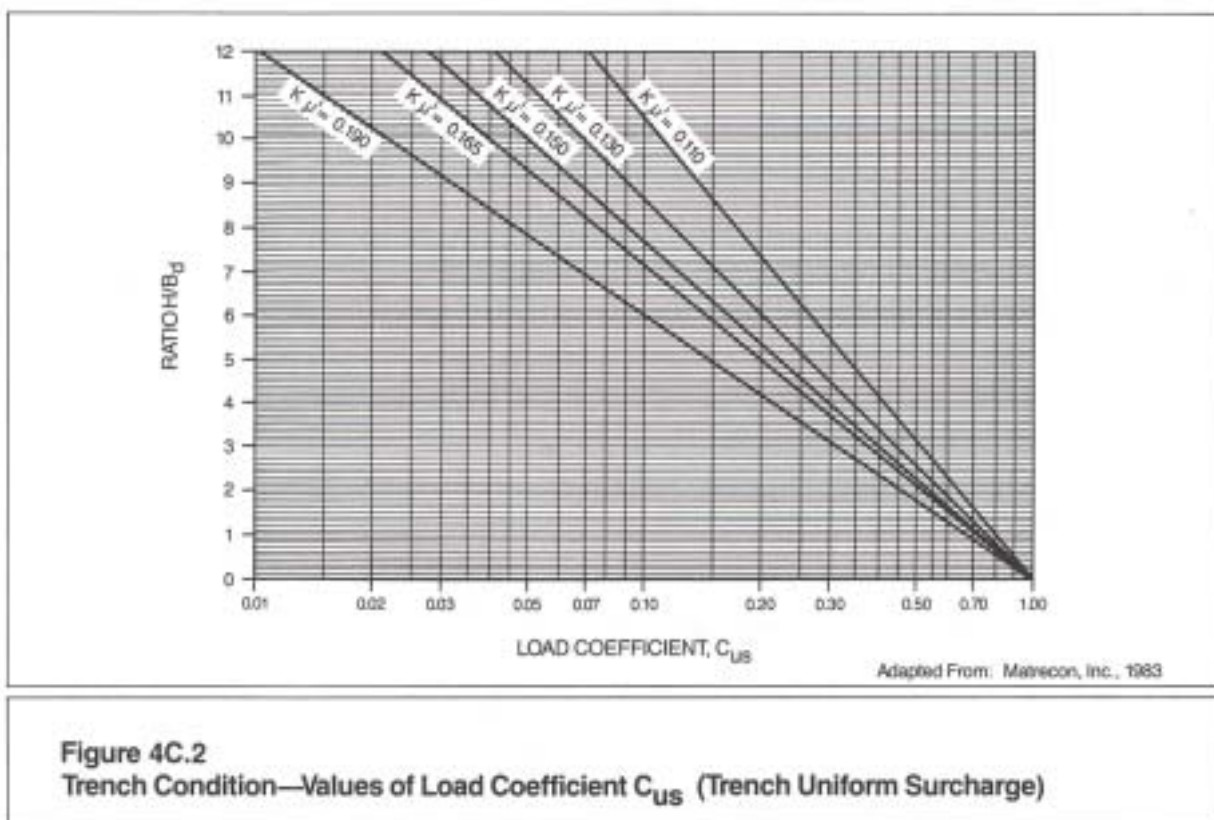
$$C_{us} = e^{-2KU'(H/B_d)} \quad (4C-6)$$

where:

e = Base of natural logarithms

K = Rankine's ratio of lateral pressure to vertical pressure

u' = Coefficient of friction between backfill material and the sides of the trench



H = Depth of trench from original ground surface to top of pipe
(ft)

B_d = Width of trench at top of pipe (ft)

The product of Ku' is characteristic for a given combination of backfills in natural, undisturbed soil. Maximum values of Ku' for typical soils are listed in Table 4C.1.

Table 4C.1. Maximum Value of Ku' for Typical Backfill Soils

Type of Soil	Maximum Value of Ku'
Granular Materials Without Cohesion	0.19
Sand and Gravel	0.165
Saturated Topsoil	0.150
Clay	0.130
Saturated Clay	0.110

Source: U.S. EPA (1983)

The value of the vertical pressure at the top of the pipe due to the trench backfill is determined from the following equation developed by Marston (see U.S. EPA, 1983):

$$P_{vt} = (B_d)(w)(C_d) \quad (4C-7)$$

where:

P_{vt} = Value of the vertical pressure at the top of the pipe (lbs/sq ft)

W = Unit weight of trench backfill (lbs/cu ft)

C_d = Dimensionless load coefficient which is a function of the ratio of the depth of the trench, H , to the trench width, B_d , and of the friction between the backfill and the sides of the trench

The load coefficient, C_d , may be computed from the following equation or obtained from Figure 4C.3:

$$C_d = \frac{1 - e^{-2Ku'(H/B_d)}}{2Ku'} \quad (4C-8)$$

in which the terms are as previously defined.

The total vertical pressure at the top of the pipe, P_v , is equal to:

$$P_v = P_{vf} + P_{vt} \quad (4C-9)$$

$$P_v = (Q_f)(C_{us}) + (B)(w)(C_d) \quad (4C-10)$$

Based on Marston's formula, the load on a rigid pipe in the trench condition would be:

$$w_e = P_v B_d \quad (4C-11)$$

or:

$$w_e = (B_d)(Q_f)(C_{us}) + (B_d)^2 (w)(C_d) \quad (4C-12)$$

where: w_e = Force per unit length of pipe (lb/ft)

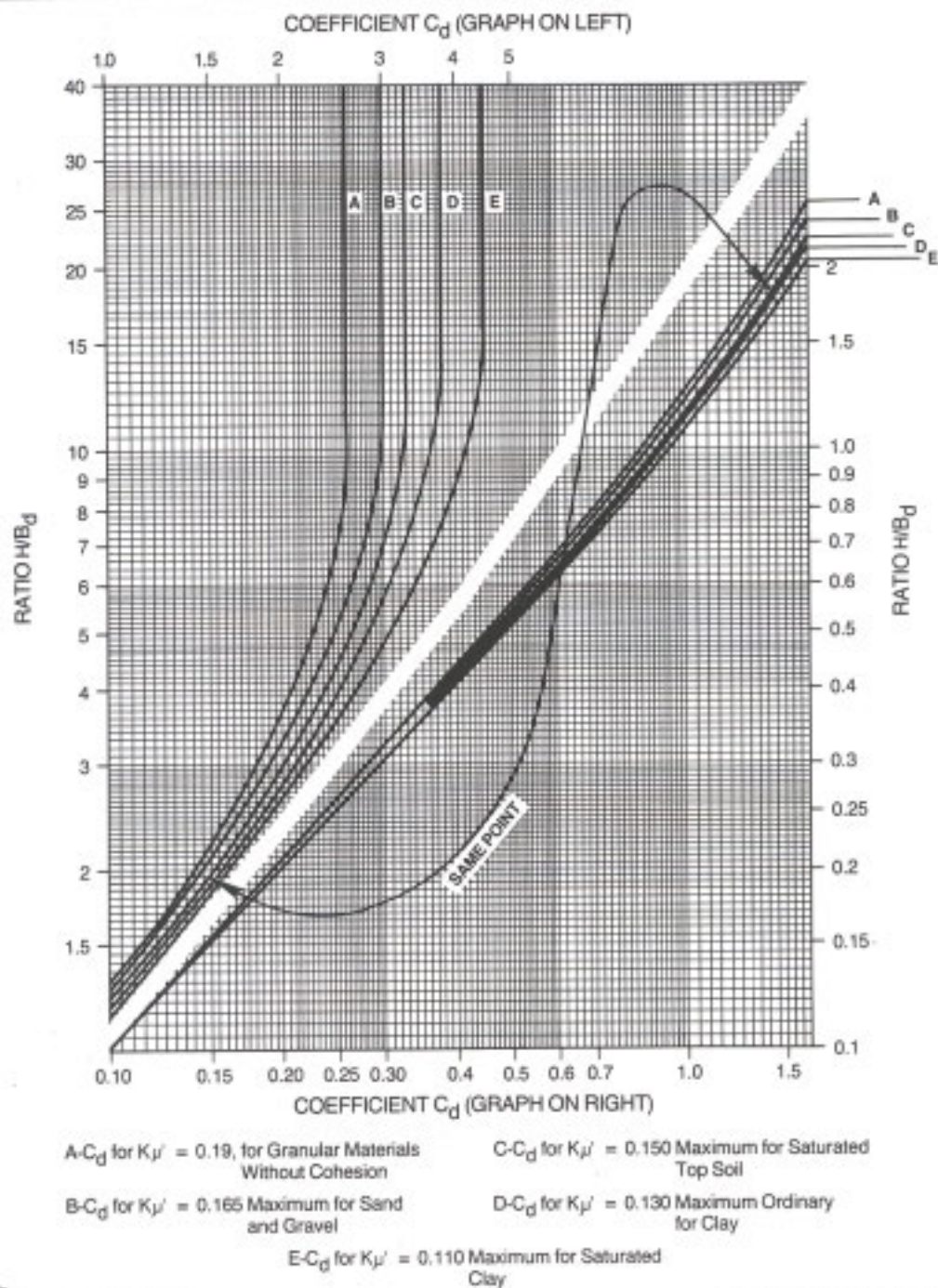
For flexible pipe in the trench condition, the load as given by Marston's formula would be:

$$w_c = P_v B_c \quad (4C-13)$$

or:

$$w_c = (B)(Q_f)(C_{us}) + (B_d)(w)(C_d)(B_c) \quad (4C-14)$$

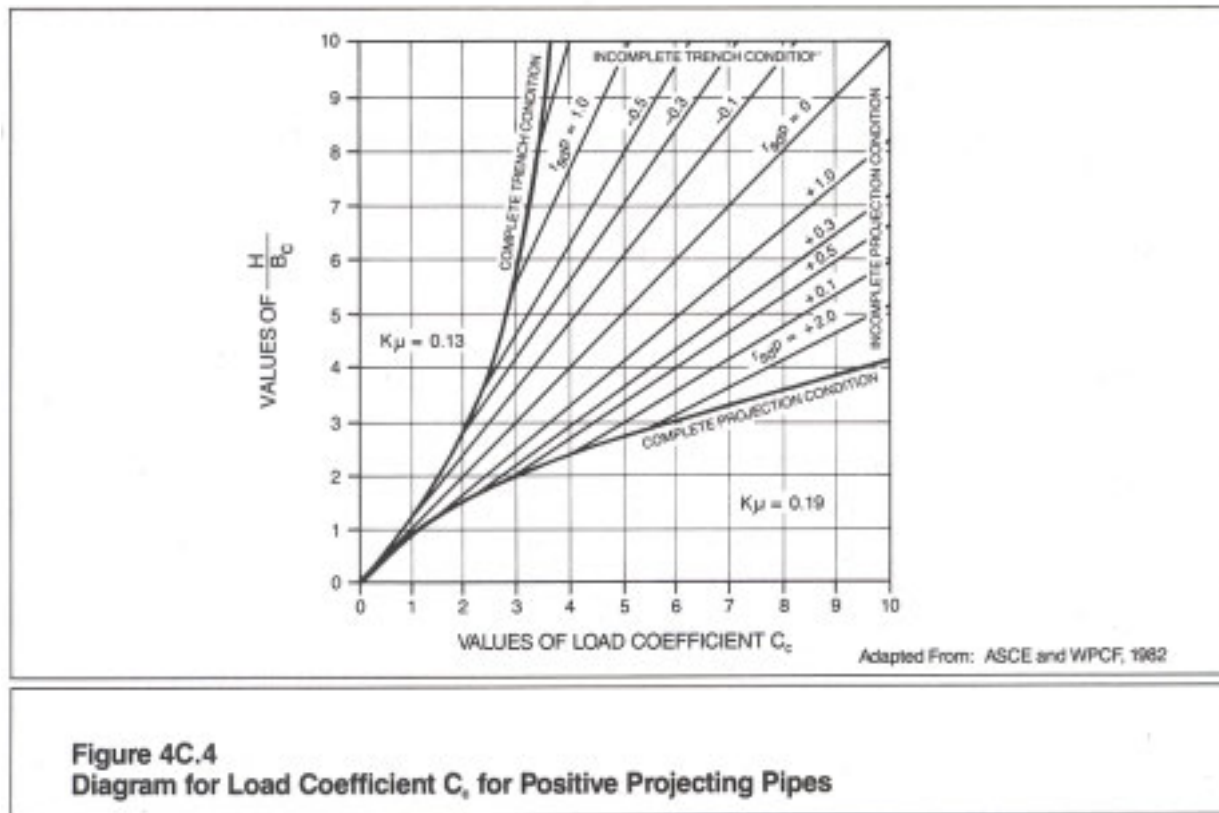
where: B_c = Outside diameter of pipe (ft)



WDOE Solid Waste
Landfill Design Manual

Adapted From: Matrecon, Inc., 1983

Figure 4C.3
Trench Condition—Values of Load Coefficient C_d (Backfill)



This formula is applicable to flexible pipes only if the backfill material at the sides of the pipe is compacted so that it will deform under vertical load less than the pipe itself will deform. In this condition, the side fills between the sides of the pipe and the sides of the trench may be expected to carry their proportional share of the total load. If this condition does not exist, then the loads are determined as described below for the embankment conditions.

4C.2.2.2 Loads for Positive Protecting Embankment Conditions

Marston's formula for the fill load on a pipe in the positive projecting embankment condition is:

$$W_c = C_c w_f B_c^2 \quad (4C-15)$$

where: W_c = Load on the pipe (lbs/ft)

w_f = Weighted average density of the waste fill (lbs/cu ft)

B_c = Outside width of pipe (ft)

C_c = Load coefficient

A complete discussion of this load coefficient may be found in the Concrete Pipe Design Manual developed by the American Concrete Pipe Association (1980)

and Gravity Sanitary Sewer Design and Construction published by the ASCE and WPCF (1982). Values of C_c may be obtained from Figure 4C.4.

Table 4C.2. Recommended Design Values of r_{sd} (Positive , Projecting Embankment Conditions).

Type of Pipe	Soil Conditions	Settlement Ratio, r_{sd}
Rigid	Rock or unyielding foundation	+1.0
Rigid	Ordinary foundation	+0.5 to +0.8
Rigid	Yielding foundation	0 to +0.5
Rigid	Negative projecting installation	-0.3 to -0.5
Flexible	Poorly compacted side fills	-0.4 to 0
Flexible	Well compacted side fills	0

Source: ASCB and WPCF, 1982, p. 178

The fill load on a pipe installed in a positive projecting embankment condition is influenced by the product of the settlement ratio (r_{sd}) and the projecting ratio (p'). The settlement ratio is the relationship between the pipe deflection and the relative settlement between the prism of fill directly above the pipe and the adjacent material. Design values of the settlement ratio is the vertical distance the pipe projects above the original ground divided by the outside vertical height of the pipe, and can be determined when the size and elevation of pipe has been established.

In the last three cases shown in Table 4C.2, the settlement ratio may be conservatively assumed to be zero which results in designing for the weight of the prism of material directly above the pipe. In such cases, C_c is equal to H/B_c and Marston's formula for the prism load becomes:

$$W_c = (H)(w_f)(B_c) \quad (4C-16)$$

where: W_c = Load on pipe (lbs/ft)

H = Height of the fill above the pipe (ft)

w_f = Weighted average density of the waste fill, including gravel backfill above the pipe, refuse, intermediate cover, and final cover system (lbs/cu ft)

B_c = Outside diameter of the pipe (ft)

The load on the pipe is also influenced by the coefficient of internal friction of the embankment material. ASCE and WPCF (1982) recommends the following values of the product Ku for use in Figure 4C.4.

For a positive settlement ratio: $K_u = 0.19$

For a negative settlement ratio: $K_u = 0.13$

4C.2.2.3 Loads for Negative Projecting Embankment and Induced Trench Conditions

The formula for the fill load on a negative projecting pipe is:

$$W_c = C_n w B_d^2 \quad (4C-17)$$

where: W_c = Load on the pipe (lbs/ft)

w = Density of fill above pipe (lbs/cu ft)

B_d = Width of trench (ft)

C_n = Load coefficient

In the case of induced trench pipe, B_c is substituted for B_d in the preceding equation. B_c is the outside diameter of the sewer pipe which is assumed to be the width of the trench.

A complete discussion of the load coefficient, C_n , may be found in American Concrete Pipe Association (1980) and ASCE and WPCF (1982). Values of C_n may be obtained from Figure 4C.5.

As in the case of the positive projecting embankment condition, the fill load is influenced by the product of the settlement ratio (r_{sd}) and the projection ratio (p'). The settlement ratio for the negative projecting embankment condition is the quotient obtained by taking the difference between the settlement of the firm ground surface and the settlement of the plane in the trench backfill which was originally level with the ground surface and dividing this difference by the compression of the column of material in trench. Values for the negative projecting settlement ratio range from -0.1 for $P' = 0.5'$ to -1.0 for $P' = 2.0'$ for rigid pipe (American Concrete Pipe Association, 1980, p. 162). Induced trench settlement ratios range from -0.3 to 0.5 (ASCE and WPCF, 1982). The projection ratio for this condition, p' is equal to the vertical distance from the firm ground surface down to the top of the pipe, divided by the width of the trench, B_d .

4C.2.3 **Superimposed Loads**

Leachate collection pipes in a landfill may be subjected to two types of superimposed loads: concentrated loads and distributed loads. Loads of pipes caused by these loadings can be determined by application of the Boussinesq equations (ASCE and WPCF, 1982).

4C.2.3.1 Concentrated Loads

The formula for load caused by a superimposed concentrated load, such as a

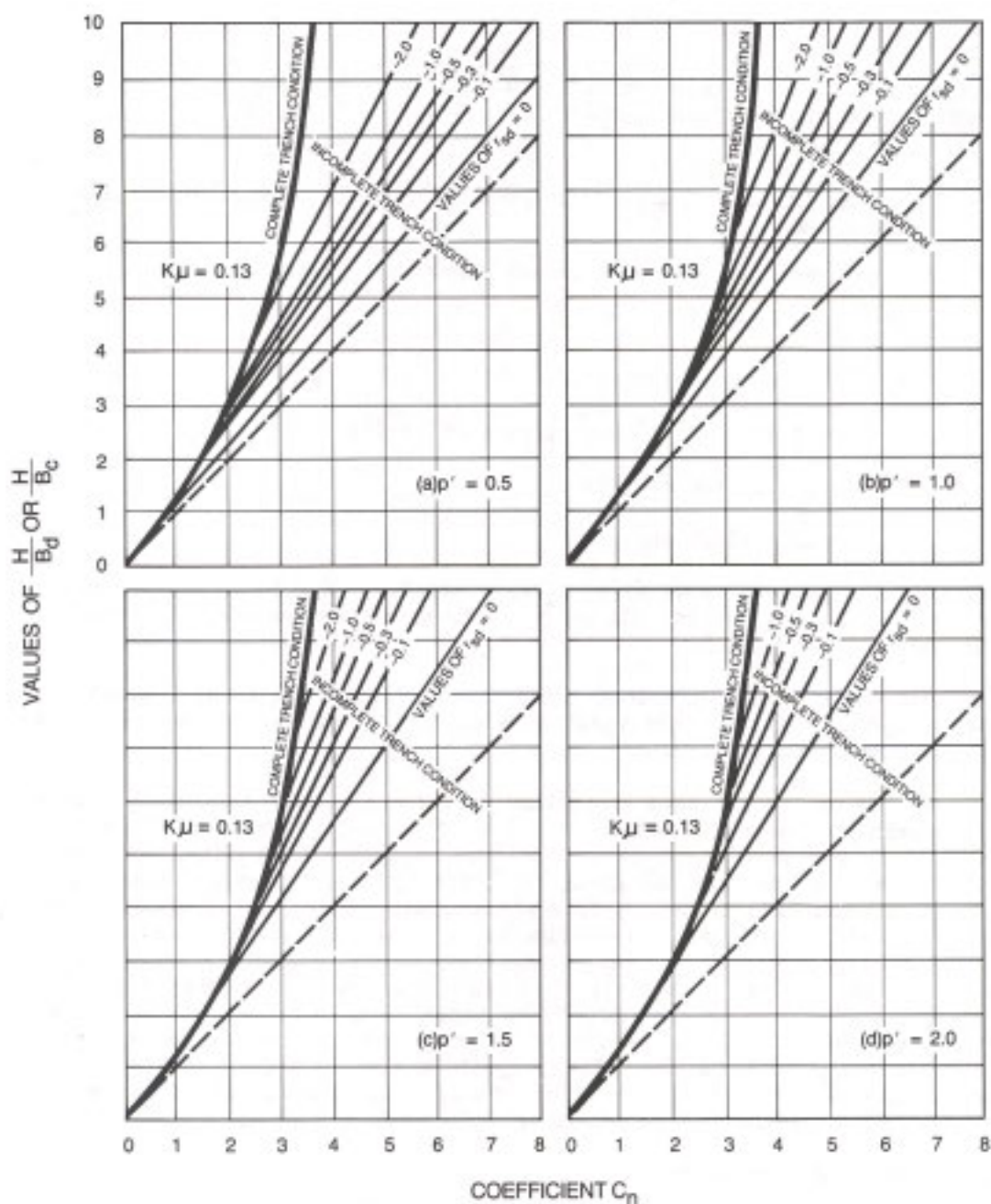


Figure 4C.5
Diagrams for Load Coefficient C_n for Negative
Projecting and Induced Trench Pipes

wheel load during construction, is given the following form (ASCE and WPCF, 1982):

$$W_{sc} = \frac{PF}{C_s L} \quad (4C-18)$$

where: W_{sc} = Load on pipe (lbs/ft)

P = Concentrated load (lbs)

F = Impact factor

L = Effective length of pipe (ft)

C_s = Load coefficient

The load coefficient, C_s , is a function of $B_c/2H$ and $L/2H$, in which B_c is the outside diameter of the pipe and H is the height of fill from the top of the pipe to the ground surface. Table 4C.3 lists values of the load coefficients for concentrated and distributed superimposed loads centered over the pipe.

The effective length, L , is the length over which the average load caused by surface wheels produces nearly the same stress in the pipe wall as does the actual load which varies in intensity from point to point. ASCE and WPCF (1982) recommends using an effective length equal to 3 feet for pipes greater than 3 feet long and using the actual length of pipes shorter than 3 feet.

The impact factor, F , reflects the influence of dynamic loads caused by traffic at ground surface. The impact factors recommended by AASHTO are listed in Table 4C.4 (American Concrete Pipe Association, 1980).

Various equipment loads that may occur during construction are listed in Table 4C.5.

Loads on pipes resulting from concentrated loads during construction may be greater than the loads caused by the refuse placed in the landfill. It is important that both construction loads and long-term loads be considered in determining the maximum load expected on pipes.

4C.2.3.2 Distributed Loads

Superimposed loads distributed over an area of considerable extent such as a truck load during construction may be determined from the following equation (ASCE and WPCF, 1982):

$$W_{sd} = CspFBc \quad (4C-19)$$

where: W_{sd} = Load on pipe (lbs/ft)

p = Intensity of distributed load (lbs/sq ft)

F = Impact factor

Table 4C.3. Values of Load Coefficients, C_g , for Concentrated and Distributed Superimposed Loads Vertically Centered over Sewer Pipe.

$\frac{D}{2H}$ or	$\frac{M}{2H}$ or $\frac{L}{2H}$													
	0.1	0.2	0.3	0.4	0.5	0.6	0.7	0.8	0.9	1.0	1.2	1.5	2.0	5.0
$\frac{R_C}{2H}$														
0.1	0.019	0.037	0.053	0.065	0.079	0.089	0.097	0.103	0.108	0.112	0.117	0.121	0.124	0.128
0.2	0.037	0.072	0.103	0.131	0.155	0.174	0.189	0.202	0.211	0.219	0.229	0.238	0.244	0.248
0.3	0.053	0.103	0.149	0.190	0.224	0.252	0.274	0.292	0.306	0.318	0.333	0.345	0.355	0.360
0.4	0.067	0.131	0.190	0.241	0.284	0.320	0.349	0.373	0.391	0.405	0.425	0.440	0.454	0.460
0.5	0.079	0.155	0.224	0.284	0.336	0.379	0.414	0.441	0.463	0.481	0.505	0.525	0.540	0.548
0.6	0.089	0.174	0.252	0.320	0.379	0.428	0.467	0.499	0.524	0.544	0.572	0.596	0.613	0.624
0.7	0.097	0.189	0.274	0.349	0.414	0.467	0.511	0.546	0.584	0.597	0.628	0.650	0.674	0.688
0.8	0.103	0.202	0.292	0.373	0.441	0.499	0.546	0.584	0.615	0.639	0.674	0.703	0.725	0.740
0.9	0.108	0.211	0.306	0.391	0.463	0.524	0.574	0.615	0.647	0.673	0.711	0.742	0.766	0.784
1.0	0.112	0.219	0.318	0.405	0.481	0.544	0.597	0.639	0.673	0.701	0.740	0.774	0.800	0.816
1.2	0.117	0.229	0.333	0.425	0.505	0.572	0.628	0.674	0.711	0.740	0.783	0.820	0.849	0.868
1.5	0.121	0.238	0.345	0.440	0.525	0.596	0.650	0.703	0.742	0.774	0.820	0.861	0.894	0.916
2.0	0.124	0.244	0.355	0.454	0.540	0.613	0.674	0.725	0.766	0.800	0.849	0.894	0.930	0.956

Bc = Outside diameter of pipe (ft)

Cs = Load coefficient

Table 4C.4 Superimposed Concentrated Load Impact Factors, F.

Height of Cover	Impact Factor
0 - 1.0 ft.	1.3
1.1 - 2.0 ft.	1.2
2.1 - 2.9 ft.	1.1
3.0 ft. and greater	1.0

Table 4C.5 Equipment Loads

<u>Equipment</u>	<u>Operating Weight (lbs)</u>	<u>Ground Contact</u>	<u>Track or Wheel Load (lbs)</u>
Caterpillar D-6	32,850	181101 9.011	16,425 Track Load
Caterpillar D-8	81,950	2211x 1016.5	40,975 Track Load
Scrapers, loaded 21/31 cu yd capacity (631 D)	168,410	Wheel load	45,470 Drive Wheel Load
Compactor Caterpillar 825-C	71,429	81 Width Coverage	35,715 Roller Load

Adapted From: Caterpillar Performance Handbook, 1984

The load coefficient, Cs, is a function of D/2H and M/2H, in which H is the height from the top of the pipe to the ground surface and D and M are the width and length, respectively, or the area over which the distributed load acts. Table 4C.3 lists the values of the load coefficients for loads centered over the pipe. A method for determining the loads on the pipe from offset uniform loads may be found in ASCE and WPCF, 1982. A typical offset uniform load would be the waste fill placed inside and adjacent to a perimeter leachate collection system.

4C.2.4 Design Safety Factor

The factor of safety for a pipe is defined as the ratio of the maximum performance limit to the design or service performance limit. The selection of a suitable safety factor is an essential part of the structural design of leachate collection pipes. The factor of safety should be related either to an allowable working stress or to a pre-established ultimate failure condition. Factors of safety compensate for poor construction practice or for inadequate inspection. Properly established design performance values and adequate factors of safety must be realized in installation and operation to provide reasonable assurance of long-term leachate collection system performance.

The relationship between safety factors and design performance values is similar for rigid and flexible pipes. However, there are differences in the design requirements for each type of pipe and these affect the form of the safety factor associated with each.

4C.2.4.1 Rigid Pipe

Design performance limits for rigid pipes are expressed in terms of strength under load. Testing is generally used to determine the service strength for rigid pipe. Strengths of rigid pipe are measured in terms of 1) the ultimate three-edge bearing strength, and 2) the ultimate and 0.01-inch crack, three-edge bearing strengths for reinforced concrete pipe. A safety factor of 1.0 should be applied to the specified minimum ultimate three-edge bearing strength to determine the working strength for other rigid pipes (ASCE and WPCF, 1982). Common practice is to use a factor of safety of 1.25 for the ultimate load of reinforced concrete pipe, and up to 1.50 for vitrified clay.

4C.2.4.2 Flexible Pipe

Design performance limits for flexible pipes are most commonly expressed in terms of deflection. The design limit varies with different pipe materials and the pipe manufacturing process. Flexible pipes must be able to deflect without experiencing cracking, liner failure, or other distress; and they should be designed with a reasonable factor of safety.

Manufacturers should be consulted on the value of the deflection limits for various types of flexible pipes. The PVC pipe manufacturers suggest limiting the deflection of buried PVC pipe to 7-1/2 percent. This strain is one-fourth the minimum strain level at which cracking and reverse curvature reportedly occurs when subjecting PVC pipe to testing in accordance with ASTM D 2412. To maintain this same factor of safety (FS-4.0) with ABS pipe, the allowable strain for ABS pipe should be limited to 5-1/2 percent. The high safety factor of 4.0 is intended to compensate for the long-term effects of creep of the plastic. Dietzler (1984) suggests that deflections of ABS and PVC pipe should be limited to one-third the deflection at which reverse curvature of splitting occurs in ASTM D 2412, including a deflection lag factor.

4C.3 RIGID PIPE DESIGN

For reasons previously indicated rigid pipes have limited use potential in leachate collection systems. In situations where they are used, their structural design should follow the recognized procedures for the various rigid pipe products available. The design of rigid pipe systems relates to the product's performance limit, expressed in terms of strength of the installed pipe. When determining field strength of rigid pipes, it is convenient to classify the *installation conditions* as either trench or embankment. For each of these conditions, bedding classes and corresponding bedding factors have been developed for use in determining the required pipe strength.

4C-3-1 Classes of Bedding and Bedding Factors

4C.3-1.1 Trench Beddings

Four general classes of bedding for installation of rigid pipes in a trench condition are illustrated in Figure 4C.6. The bedding factor for each of the classes of pipe bedding are also listed in Figure 4C.6. Because leachate collection pipes are normally installed with granular material *surrounding* the pipe, the appropriate bedding class is usually Class B with a bedding factor of 1.9.

4C.3.1.2 Embankment Beddings

Four general classes of bedding for the installation of rigid pipes in a positive projecting embankment condition are illustrated in Figure 4C.7. Most leachate collection lines installed in a positive projecting embankment condition would have Class B or C bedding, depending on the projection ratio, p , of the actual installation. For pipe installed in a positive projecting embankment condition, active lateral pressure is exerted against the sides of the pipe. The bedding factor, L_f , for this type of installation is computed by the equation:

$$L_f = \frac{A}{N-xq} \quad (4C-20)$$

where:	A	Pipe shape factor
	N	A parameter that is a function of the bedding class
	x	A parameter dependent on the area over which lateral pressure effectively acts
	q	Ratio of total lateral pressure to total vertical load on the pipe

For circular pipe, A has a value of 1.431. Values of N for various classes of bedding are given in Table 4C.6. Values of x are listed in Table 4C.7.

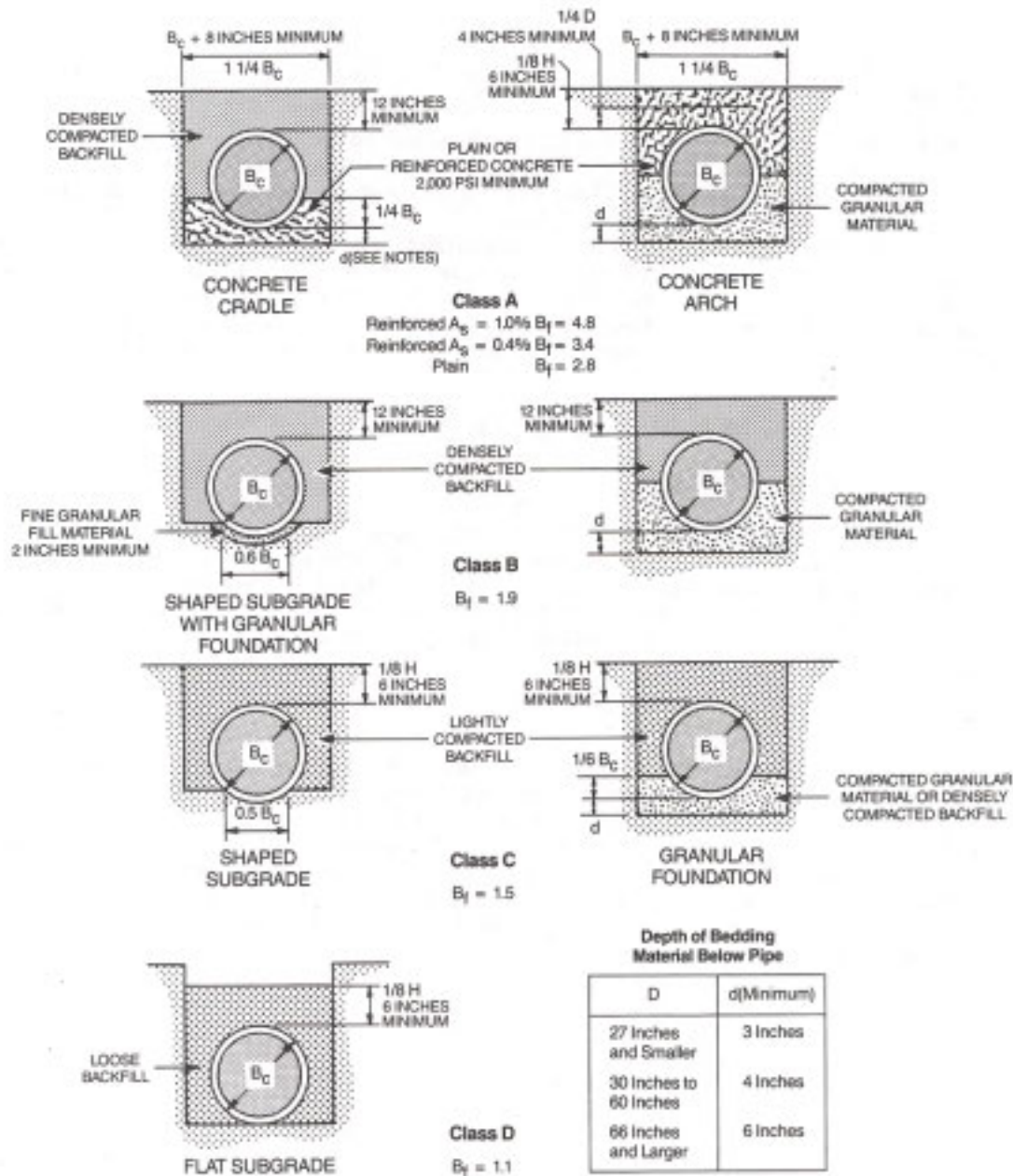


Figure 4C.6
Trench Beddings:
Circular Pipe

B_c = Outside Diameter D = Inside Diameter
 H = Backfill Cover Above Top of Pipe A_s = Area of Transverse Steel in the Cradle or Arch Expressed as a Percentage of Area of Concrete at Invert or Crown
 d = Depth of Bedding Material Below Pipe

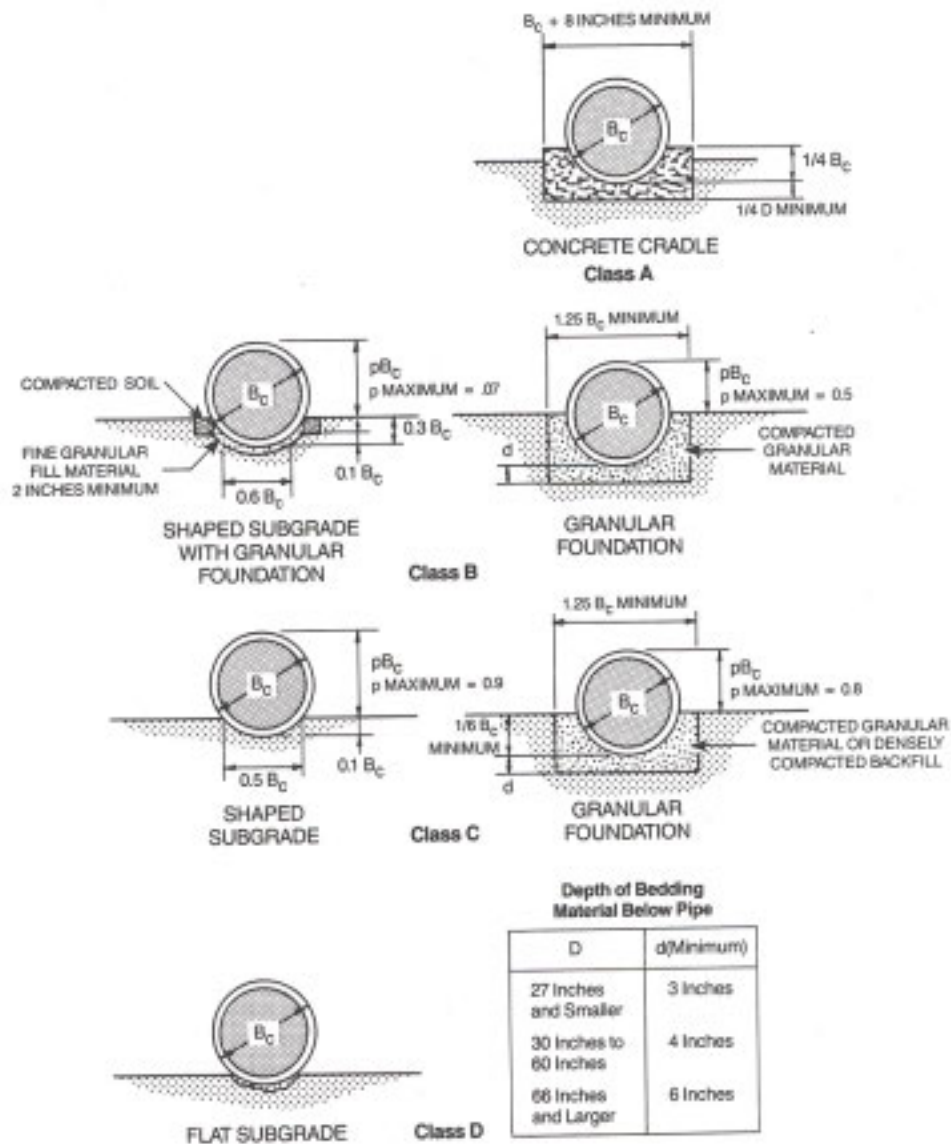


Figure 4C.7
Positive Projecting Embankment Beddings:
Circular Pipe

B_c = Outside Diameter
H = Backfill Cover
Above Top of Pipe
D = Inside Diameter
d = Depth of Bedding
Material Below Pipe

Table 4C.6 Values of N for Circular Pipe

<u>Class of Bedding</u>	<u>N</u>
A (reinforced cradle)	0.421 to 0.505
Aa (unreinforced cradle)	0.505 to 0.636
B	0.707
C	0.840
D	1.310

Adapted from: ASCE and WPCF (1982)

The projection ratio, m , in Table 4C.7 refers to the fraction of the vertical pipe diameter over which lateral pressure is effective. For pressure acting on the top half of the pipe above the horizontal diameter, m equals 0.5. Values for q may be estimated by the formula:

$$q = \frac{mk}{C_c} \left[\frac{H}{B_c} + \frac{m}{2} \right] \quad (4C-21)$$

where: k Ratio of unit lateral pressure to unit vertical pressure (Rankine's ratio)

A value of k equal to 0.33 usually be sufficiently accurate. Values of C_c may be found in Figure 4C.4.

Table 4C.7 Values of x for Circular Pipe

<u>Fraction of Pipe Subjected to Lateral Pressure, m</u>	<u>Class A Bedding</u>	<u>Other Than Class A Bedding</u>
0	0.150	0
0.3	0.743	0.217
0.5	0.856	0.423
0.7	0.811	0.594
0.9	0.678	0.655
1.0	0.638	0.638

Adapted from: ASCE and WPCF (1982)

The classes of bedding for rigid pipes installed in a negative projecting embankment condition are the same as those for the trench condition. The trench condition bedding factors listed in Figure 4C.6 should be used for

negative projecting embankment installations. For leachate collection lines, this would generally be Class B bedding and a bedding factor of 1.9.

4C.3.2 Selection of Pipe Strength

The design strength of rigid pipes is commonly related to a three-edge bearing strength measured at the manufacturing plant in accordance with recognized national testing standards. For pipes installed under specified conditions of bedding and backfilling, the required three-edge bearing strength for a given class of bedding and design load can be determined from the following:

$$\text{Required Three Edge Bearing Strength (lb/ft)} = \frac{\text{Design Load (lb/ft)} \times \text{Factor of Safety}}{\text{Bedding Factor}}$$

The strength of reinforced concrete pipe at either the 0.01-inch crack or ultimate load divided by the internal diameter of the pipe is defined as the D-load strength. The D-load concept provides strength classification of pipe independent of pipe diameter. The required three-edge bearing strength of reinforced concrete pipe expressed as D-load is determined by the following equation:

$$\text{D-Load (lbs)} = \frac{\text{Design Load (lbs/ft)} \times \text{Safety Factor}}{\text{Bedding Factor} \times \text{Diameter (ft)}}$$

The above equations are applicable to rigid pipes installed in both trench conditions and embankment conditions. After determining the design load, the selection of the pipe strength involves applying the appropriate safety factor and bedding factor for the installation conditions in either of the above equations.

4C.4 FT BLE PIPE DESIGN

4C.4.1 General Approach

Flexible pipes derive the majority of their load supporting ability from the passive resistance of the soil in side fills as the pipe deflects under load. Because of this resistance, it is important to examine the interaction between the bedding or fill material and the pipe, rather than simply studying pipe characteristics. The extent to which flexible pipe deflects as installed is most commonly used as a basis for design since it reflects this interaction. The approximate long-term deflection of flexible pipe in place can be calculated using the Modified Iowa Formula developed by Spangler and Watkins (ASCE and WPCF, 1982):

$$Y = \frac{D_i K_b W_c r^3}{EI + 0.061 E' r^3} \quad (4C-22)$$

where: Y = Vertical deflection (inches), assumed to approximately equal horizontal deflection

D_1	=	Deflection lag factor
K_b	=	Bedding constant
W_c	=	Load (lbs/inch)
r	=	Mean radius of pipe (inches)
E	=	Modulus of tensile elasticity (lbs/sq in)
I	=	Moment of inertia per length (in ⁴ /in)
E'	=	Modulus of soil reaction (lbs/sq in)

The above equation can be rewritten to express pipe deflection as a decimal fraction of the pipe outside diameter, B_c , and relate it to the vertical stress on the pipe, P_v , as follows:

$$\frac{W_c}{B_c} = P_v = \frac{Y(EI + 0.061 E'n^3)}{B_c(D_1 K_b r^3)} \quad (4C-23)$$

Pipe manufacturers may establish limits for pipe deflection or vertical stress on the pipe (P_v). Maximum vertical stress is often referred to as critical buckling pressure.

The deflection lag factor, D_1 , compensates for time consolidation of the bedding, which may permit flexible pipes to continue to deform after installation. Long-term deflection will be greater with low degrees of compaction of the bedding in the side fills compared to higher degrees of compaction. Values recommended for this factor range from 1.25 to 1.50 (ASCE and WPCF, 1982), although values over 2.5 have been recorded in dry soil. A deflection lag factor of 2.0 may be realistic for design of leachate collection pipes if weathering and/or softening of the bedding material is likely to occur over the life of the landfill or if the bedding material is rounded or may be placed with minimal compaction (Dietzler, 1984).

Values for the bedding constant, K_b , are listed in Table 4C.8. Spangler's data suggested a K_b value of 0.10 for pipe embedded in native soil with no bedding and a K_b value of 0.083 for pipe embedded in gravel up to the spring line. The installation of leachate collection pipes is more closely represented by the latter case, and a K_b value of 0.083 should therefore be used in lieu of actual field data.

Table 4C.8. Values of Bedding Constant, K_b -

Bedding Angle (Degrees)	K_b
0	0.110
30	0.108
45	0.105
60	0.102
90	0.096
120	0.090
180	0.083

Source: ASCE and WPCF (1982)

Values for the soil reaction modulus, E_1 , range from 0 to 3,000, depending on the soil type of the bedding material and relative degree of compaction (ASCE and WPCF, 1982). The use of a high value for E_1 is not realistic for leachate collection pipes in many localities (Dietzler, 1984). In a situation where a rounded river gravel will be used for the bedding material and a high degree of compaction may be unobtainable in the bedding around the leachate collection pipe, a realistic value for E_1 of 400 may be appropriate (Dietzler, 1984).

The first term in the denominator (EI) of the Modified Iowa Formula is the stiffness factor and reflects the influence of the inherent stiffness of the pipe on deflection. The second term, $0.061 E_1 d$, reflects the influence of the passive pressure on the side of the pipe. With flexible pipes, the second term is normally predominant.

After the allowable strain level in the pipe has been determined, the design procedure for flexible pipes is to perform a trial and adjustment analysis to find a class of pipe that will result in deflections less than the established limit. There are slight variations in the procedure for the various types of flexible pipe.

4C.4.2 Selection of Plastic Pipe

The standard test to determine pipe stiffness or the load deflection characteristic of plastic pipe is the parallel-plate loading test conducted in accordance with ASTM D 2412. The test determines the pipe stiffness, PS , at a prescribed deflection, Y , which for convenience in testing is arbitrarily set at 5 percent. The pipe stiffness is defined as the value obtained by dividing the load per unit length, F , by the resulting deflection at the prescribed percentage deflection:

$$PS = \frac{F}{Y} \quad (4C-24)$$

The stiffness factor, SF, in the Modified Iowa Formula is related to the pipe stiffness by the following expression:

$$SF = EI = 0.149r^3(PS) \quad (4C-25)$$

in which the terms are as previously defined.

For circular plastic pipes, the approximate deflection based on pipe stiffness can be determined by using the following simplified version of the Modified Iowa Formula:

$$Y = \frac{D_1 K_b W_c}{0.149(PS) + 0.061 E'} \quad (4C-26)$$

The pipe stiffness for the various plastic pipe materials and diameters of pipe may be obtained from the manufacturer or may be determined by tests performed in accordance with ASTM D 2412.

4C.4.3 Selection of Other Flexible Pipes

Flexible pipes of material other than plastic, such as ductile iron and corrugated metal, have little potential for general use in leachate collection systems for reasons previously discussed. However, if they are found suitable for a specific installation, their structural design should follow recognized procedures for the particular flexible pipe being considered. Procedures for designing ductile iron and corrugated metal pipes are described in ASCE and WPCF (1982). Manufacturers of the specific products should also be consulted.

4C.4.4 Bedding Material

Bedding provides a: contact between a pipe and the foundation on which it rests. The total load that a pipe will support depends on the width of the contact area and the quality of the contact between the pipe and the bedding material. The influence of the bedding on the supporting strength of the pipe is a factor that must be considered in the design of a leachate collection pipe. This section discusses bedding material considerations. More detailed requirements are given in previous sections of this Appendix.

An important consideration in selecting a material for bedding is positive contact between the bed and the pipe. A well-graded crush stone or a well-graded gravel are suitable bedding materials based on supporting strength considerations, and both are more suitable than a uniformly graded pea gravel (ASCE and WPCF, 1982). Larger particle sizes give greater stability; however, the maximum size and shape of the bedding material should be related to the pipe material and the recommendations of the manufacturer. For small pipes, the maximum size of the bedding material should be limited to about 10 percent of the pipe diameter and, in general, well-graded crush stone or gravel ranging in size from 3/4 inch to the No. 4 sieve will provide the most satisfactory pipe bedding (ASCE and WPCF, 1982).

In addition to providing support, bedding for leachate collection pipes must allow unrestricted flow of leachate through the bedding into the perforated leachate collection pipes. The bedding material must also be resistant to attack from the leachate. Redundancy in the design of leachate collection systems is important to minimize the effects of failures when they occur. One of the primary ways to provide redundancy is to design the bedding to meet drainage requirements through the gravel layer alone if flow through the pipe is restricted (Bass, 1984).

A well-graded material with 100 percent passing the 1-1/2 inch clear, square screen openings and not more than 5 percent passing the No. 50 U.S. Standard Series sieve is recommended for drainage purposes (U.S. Department of the Interior, 1978). To determine whether the material is well-graded, the coefficient of uniformity which describes the slope of the gradation curve must be greater than 4 for gravels and greater than 6 for sands. In addition, the coefficient of curvature that describes the shape of the curve must be between 1 and 3 for both gravels and sands. These coefficients are defined as follows:

$$\text{Coefficient of uniformity, } C_u, = \frac{D_{60}}{D_{10}} \quad (4C-27)$$

and

$$\text{Coefficient of curvature, } C_c, = \frac{(D_{30})^2}{(D_{10})(D_{60})} \quad (4C-28)$$

where: D_{10} , D_{30} , and D_{60} Diameter of particles in millimeters passing the 10, 30, and 60 percent points, respectively, on the base material gradation curve.

Based on the above criteria for supporting strength and drainage, a bedding material for leachate collection pipes should be well-graded gravel with the following properties:

Gradation:	100% passing 1-1/2" sieve 5% maximum passing No. 50 sieve
C_u :	4.0 or greater
C_c :	1.0 to 3.0

The actual bedding material should be selected within these limits after consideration of the pipe material, availability of bedding material, and its resistance to leachate attack.

**APPLICATION FOR PERMIT RENEWAL AND MODIFICATION
SANDOVAL COUNTY LANDFILL**

**VOLUME III: LANDFILL ENGINEERING CALCULATIONS
SECTION 5: PIPE LOADING CALCULATIONS**

ATTACHMENT III.5.E

POLY PIPE INDUSTRIES, INC. 2008.

DESIGN AND ENGINEERING GUIDE FOR POLYETHYLENE PIPING.

WWW.PLASTICPIPE.ORG.

PolyPipe®

Direct Burial



Flexibility



Sliplining

Marine Applications



*Design and Engineering Guide
for Polyethylene Piping*

Table A-2 (cont'd)
PIPE WEIGHTS AND DIMENSIONS (IPS)
PE3608 (BLACK)

OD			SDR	Nominal ID		Minimum Wall		Weight	
Nominal in.	Actual			in.	mm.	in.	mm.	lb. per foot	kg. per meter
	in.	mm.							
			7	2.44	61.98	0.500	12.70	2.047	3.047
			7.3	2.48	63.08	0.479	12.18	1.978	2.943
			9	2.68	67.96	0.389	9.88	1.656	2.464
			9.3	2.70	68.63	0.376	9.56	1.609	2.395
			11	2.83	71.77	0.318	8.08	1.387	2.065
3	3.500	88.90	11.5	2.85	72.51	0.304	7.73	1.333	1.984
			13.5	2.95	74.94	0.259	6.59	1.153	1.716
			15.5	3.02	76.74	0.226	5.74	1.015	1.511
			17	3.06	77.81	0.206	5.23	0.932	1.386
			21	3.15	79.93	0.167	4.23	0.764	1.136
			26	3.21	81.65	0.135	3.42	0.623	0.927
			7	3.14	79.68	0.643	16.33	3.384	5.037
			7.3	3.19	81.11	0.616	15.66	3.269	4.865
			9	3.44	87.38	0.500	12.70	2.737	4.073
			9.3	3.47	88.24	0.484	12.29	2.660	3.958
			11	3.63	92.27	0.409	10.39	2.294	3.413
4	4.500	114.30	11.5	3.67	93.23	0.391	9.94	2.204	3.280
			13.5	3.79	96.35	0.333	8.47	1.906	2.836
			15.5	3.88	98.67	0.290	7.37	1.678	2.497
			17	3.94	100.05	0.265	6.72	1.540	2.292
			21	4.05	102.76	0.214	5.44	1.262	1.879
			26	4.13	104.98	0.173	4.40	1.030	1.533
			32.5	4.21	106.84	0.138	3.52	0.831	1.237
			7	3.88	98.51	0.795	20.19	5.172	7.697
			7.3	3.95	100.27	0.762	19.36	4.996	7.435
			9	4.25	108.02	0.618	15.70	4.182	6.224
			9.3	4.29	109.09	0.598	15.19	4.065	6.049
			11	4.49	114.07	0.506	12.85	3.505	5.216
5	5.563	141.30	11.5	4.54	115.25	0.484	12.29	3.368	5.012
			13.5	4.69	119.11	0.412	10.47	2.912	4.334
			15.5	4.80	121.97	0.359	9.12	2.564	3.816
			17	4.87	123.68	0.327	8.31	2.353	3.502
			21	5.00	127.04	0.265	6.73	1.929	2.871
			26	5.11	129.78	0.214	5.43	1.574	2.343
			32.5	5.20	132.08	0.171	4.35	1.270	1.890
			7	4.62	117.31	0.946	24.04	7.336	10.917
			7.3	4.70	119.41	0.908	23.05	7.086	10.545
			9	5.06	128.64	0.736	18.70	5.932	8.827
			9.3	5.11	129.92	0.712	18.09	5.765	8.579
			11	5.35	135.84	0.602	15.30	4.971	7.398
6	6.625	168.28	11.5	5.40	137.25	0.576	14.63	4.777	7.109
			13.5	5.58	141.85	0.491	12.46	4.130	6.147
			15.5	5.72	145.26	0.427	10.86	3.637	5.413
			17	5.80	147.29	0.390	9.90	3.338	4.967
			21	5.96	151.29	0.315	8.01	2.736	4.072
			26	6.08	154.55	0.255	6.47	2.233	3.322
			32.5	6.19	157.30	0.204	5.18	1.801	2.680

See ASTM D3035, F714 and AWWA C-901/906 for OD and wall thickness tolerances.
Weights are calculated in accordance with PPI TR-7.

EARTHLOADING

PolyPipe®, due to its flexibility, will deflect when it is buried. The degree of deflection will depend upon the soil conditions, burial conditions, trench width, and the depth of burial. The degree of deflection of the pipe is limited by the soil around its periphery, especially in the lateral direction. When the soil compacts around the pipe, there is a supportive effect from the soil itself, and as compaction occurs, there is soil friction and cohesion over the pipe that reduces the direct load on the pipe.

PolyPipe®, as do other flexible conduits, depends on the surrounding soil for support, and has to be considered as one component in a pipe/soil system. The presence of the soil arch and the support derived from the lateral movement limitations are highly beneficial to the efficiency of the system. Therefore, the flexibility of **PolyPipe®** is the major reason for these advantages. As has been stated, the durability of polyethylene is the reason for its resistance to high levels of mechanical abuse, and this is no less true for buried systems where forced deflections may occur due to subsidence, washout and settlement.

External loading analysis must be conducted to determine the application's feasibility. There are two loading calculations necessary when designing or engineering below ground applications of **PolyPipe®**. These calculations are ring deflection and wall buckling. Wall crushing, calculated using the allowable compressive strength of the PE material, is usually not critical when using solid wall **PolyPipe®**, as ring deflection and wall buckling are predominant parameters.

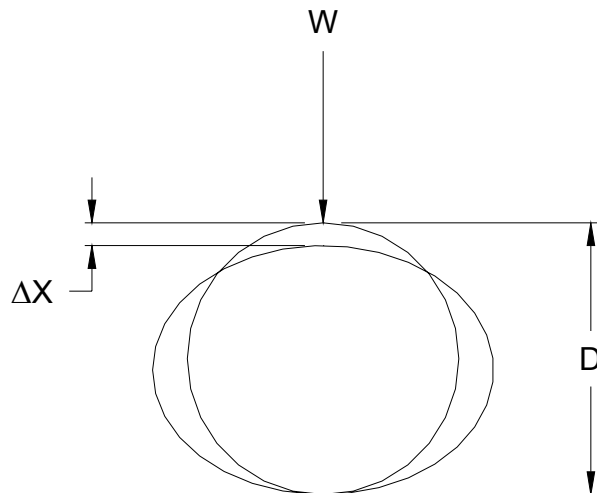
RING DEFLECTION

PolyPipe®, when buried in loose soil conditions, will exhibit the tendency to deflect, called ring deflection. Listed below are the recommended maximum allowable design limits for ring deflection of **PolyPipe®** for the different available Dimension Ratios (DR).

Table C-1
Design Limits for Ring Deflection

DR	Safe Deflection, % of Diameter
32.5	8.0
26	7.0
21	6.0
17	5.0

Figure C-1



PolyPipe®, due to its inherent physical properties of flexibility, resilience and toughness can withstand significant deflection without failure. It can be flattened without causing a fracture of the pipe wall. However, this condition is unacceptable as far as service is concerned. A deflection of 15% would be acceptable for a butt fused polyethylene system, although a reduction in flow would be noted. It would also be difficult to utilize conventional cleaning equipment with this severity of deflection. Ring deflection resulting in hydraulic flow area reductions should be taken into account when engineering the flow characteristics. Refer to Table C-2 for the percentage of area reduction based on percent of ring deflection.

Table C-2
AREA REDUCTION DUE TO RING DEFLECTION

Ring Deflection, %	Area Reduction, %
2	0.04
4	0.16
5	0.25
6	0.36
8	0.64
10	1.00
12	1.44
14	1.96
15	2.25
16	2.56

In calculating the soil load placed on a buried pipe, the designer must be able to calculate to some degree of accuracy the type and condition of the backfill material. Saturated clay would be more difficult to place and adequately compact than would coarse granular material that would not stick together. It is important in the pipe/soil system that the backfill material utilized for haunching and initial backfill (see Installation, Section F, for explanation of terminology) be granular and non-cohesive, free of debris, organic matter, frozen earth and rocks larger than 1½ inch in diameter. This material can be described as Class I or II of ASTM D2321 "Angular ¼ to 1½ inch Graded Stone, Slag, Cinders, Crushed Shells and Stone or Sands and Gravel Containing Small Percentages of Fines, Generally Granular and Non-Cohesive, Wet or Dry." This material can easily be worked into the pipe haunch, and compacted in approximately 4-6 inch lifts.

To determine the ring deflection of externally loaded **PolyPipe®**, you must first determine the earthload in pounds per linear inch of pipe by use of the following modified Marston formula⁵:

$$W = \frac{C_d \cdot \rho \cdot B_d \cdot D}{144} \quad (17)$$

Where

W	=	Earthload per unit length of pipe, lbs/in
C_d	=	Trench Coefficient, (dimensionless) (See Figure C-2)
ρ	=	Soil density, lbs/ft ³
D	=	Outside diameter, inches
B_d	=	Trench width at top of pipe, feet

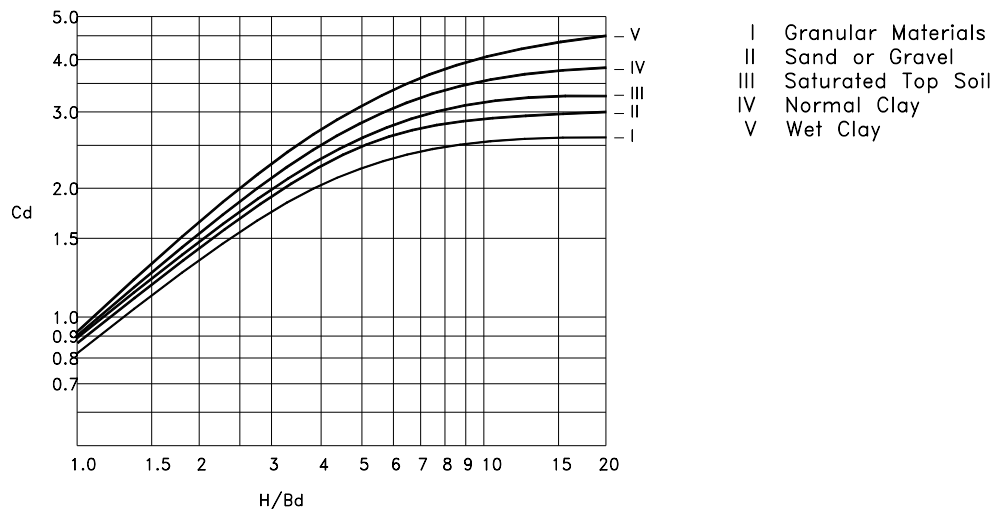
⁵ Moser, A.P. Buried Pipe Design. 2nd Edition. New York: McGraw-Hill, 2001.

Table C-3
CLASSIFICATION OF BACKFILL MATERIAL
PER ASTM D2321*

Class	Comments
<u>Class I</u> - Angular graded stone, $\frac{1}{4}$ " to $1\frac{1}{2}$ ", including a number of fill materials that have regional significance such as coral, slag, cinders, crushed stone, crushed gravel and crushed shells.	100 - 200 pounds per cubic foot. Pipe sizes less than 10" should limit maximum particle size to $\frac{1}{2}$ " to $\frac{3}{4}$ " for ease of placement.
<u>Class II</u> - Coarse sands and gravel with maximum particle size of $1\frac{1}{2}$ ", including variously graded sands and gravel containing small percentages of fines, generally granular and non-cohesive, wet or dry.	110 - 130 pounds per cubic foot. Pipe sizes less than 10" should limit maximum particle size to $\frac{1}{2}$ " to $\frac{3}{4}$ " inch for ease of placement.
<u>Class III</u> - Fine sand and clay gravel, including fine sands, sand-clay mixtures, and gravel-clay mixtures.	140 - 150 pounds per cubic foot.
<u>Class IV</u> - Silt, silty clays, and clays, including inorganic clays and silts of medium to high plasticity and liquid limits.	150 - 180 pounds per cubic foot.
<u>Class V</u> - Includes organic soils as well as soils containing frozen earth, debris, rocks larger than $1\frac{1}{2}$ " in diameter, and other foreign materials.	Not recommended for backfill except in the final backfill zone.

* For further classification of soils the designer may want to review ASTM D2487, "Standard Test Method for Classification of Soil for Engineering Purposes."

Figure C-2
TRENCH COEFFICIENT, C_d
DEPENDENT ON SOIL TYPE AND DITCH CONFIGURATION



In general practice, the trench width can be kept to a minimum of six inches per side greater than the pipe diameter itself. Although this may seem narrow in comparison to trenching of conventional materials, it must be noted that **PolyPipe®** can be pre-assembled above ground and later placed into the trench. The trench width should be maintained as narrow as possible as the soil loading on the pipe is a relationship of the trench width.

The linear deflection of the pipe can be calculated from the following modified Spangler equation⁶:

$$\Delta x = \frac{D_l \cdot K \cdot W}{\left(\frac{2E}{3(DR-1)^3} \right) + 0.061E'} \quad (18)$$

Where

- Δx = Horizontal deflection or change in diameter, inches
- D_l = Deflection lag factor, **PolyPipe**® recommends 1.0 (dimensionless)
- K = Bedding constant, **PolyPipe**® recommends 0.1 (dimensionless)
- W = Earthload, lbs/inch (See Equation (17))
- E = Modulus of elasticity of pipe, 30,000 psi
- E' = Soil modulus, psi
- DR = Dimension ratio, (dimensionless)

* For further values of K see reference.

The percent deflection can be calculated by use of the following formula⁶:

$$d = \frac{\Delta x}{D} \cdot 100 \quad (19)$$

Where

- d = Percent deflection, %
- Δx = Horizontal deflection, inches (See Equation (18))
- D = Outside diameter, inches

Table C-4
TYPICAL SOIL MODULUS VALUES (PSI)

Type of Soil	Depth of Cover		Standard AASHTO relative compaction			
	ft	m	85%	90%	95%	100%
Fine-grained soils with less than 25% sand content (CL, ML, CL-ML)	0-5	0-1.5	500	700	1000	1500
	5-10	1.5-3.1	600	1000	1400	2000
	10-15	3.0-4.6	700	1200	1600	2300
	15-20	4.6-6.1	800	1300	1800	2600
Coarse-grained soils with fines (SM., SC)	0-5	0-1.5	600	1000	1200	1900
	5-10	1.5-3.0	900	1400	1800	2700
	10-15	3.0-4.6	1000	1500	2100	3200
	15-20	4.6-6.1	1100	1600	2400	3700
Coarse-grained soils with little or no fines (SP, SW, GP, GW)	0-5	0-1.5	700	1000	1600	2500
	5-10	1.5-3.0	1000	1500	2200	3300
	10-15	3.0-4.6	1050	1600	2400	3600
	15-20	4.6-6.1	1100	1700	2500	3800

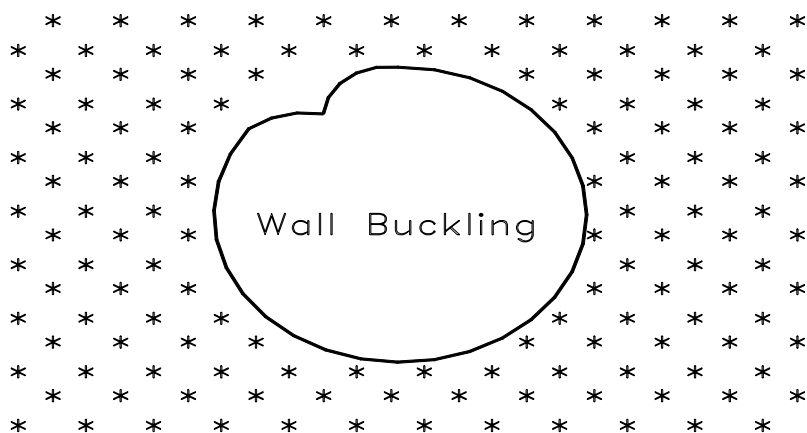
⁶ Plastics Pipe Institute. Underground Installation of Polyethylene Pipe, 1996.

Values of modulus of soil reaction, E' (psi) based on depth of cover, type of soil, and relative compaction. Soil type symbols are from the United Classifications System. Source: Hartley, James D. and Duncan, James M., "E' and its Variation with Depth," Journal of Transportation, Division of ASCE, Sept. 1987.

WALL BUCKLING

PolyPipe®, when buried in dense soil conditions and subjected to excessive external loading, will exhibit the tendency of wall buckling. As seen in Figure C-3, wall buckling is a longitudinal wrinkle that usually occurs between the 10:00 and 2:00 positions. Wall buckling should become a design consideration when the total vertical load exceeds the critical buckling stress of **PolyPipe®**.

Figure C-3



Vertical loading can be determined by the summation of the calculated dead load (load resulting from backfill overburden and static surface loads) and live load (loads resulting from cars, trucks, trains, etc.).

BACKFILL LOAD¹

$$P_b = \frac{\rho_{soil} \cdot H}{144} \quad (20)$$

Where P_b = Backfill load, psi
 ρ_{soil} = Backfill density, lbs/ft³
 H = Height of backfill above pipe, feet

SURFACE LOAD

Surface loads are those forces exerted by permanent structures in close proximity to buried **PolyPipe®**. These loads can be buildings, storage tanks, or other structures of significant weight that could add to the backfill loading. The force exerted on **PolyPipe®** by structural surface loads can be approximated by use of the following Boussinesq¹⁷ formulation:

$$P_s = \frac{3Lz^3}{144 \cdot 2\pi R^5} \quad (21)$$

Where P_s = Surface load on pipe, psi
 L = Static surface load, lbs.
 z = Vertical distance from top of pipe to surface load level, feet
 R = Straight line distance from the top of pipe to surface load, feet

Where,

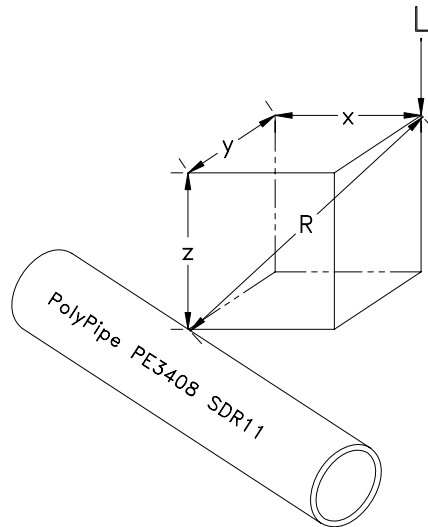
¹ Nayyar, Mohinder L. Ed. Piping Handbook. 6th Edition. New York: McGraw-Hill, Inc., 1992.

¹⁷ Chen, W. F., Liew, Richard L. Y. The Civil Engineering Handbook. New York: CRC Press, 2003. 2nd Edition.

$$R = \sqrt{x^2 + y^2 + z^2} \quad (22)$$

Where x = Horizontal distance from surface load, feet (Refer to Figure C-4)
 y = Horizontal distance from surface load, feet (Refer to Figure C-4)
 z = Vertical distance from top of pipe to surface load level, feet (Refer to Figure C-4)

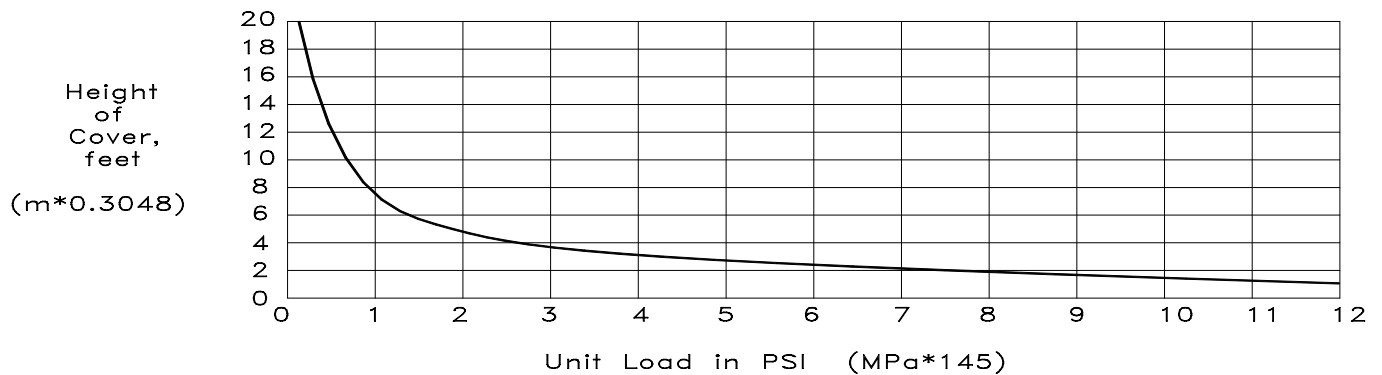
Figure C-4
RESULTANT SURFACE LOAD



LIVE LOAD

Live loading can be determined by extracting the load from Figure C-5 for H20 highway loading or from Figure C-6 for Cooper E-80 loading or by estimating, using available analytical techniques.

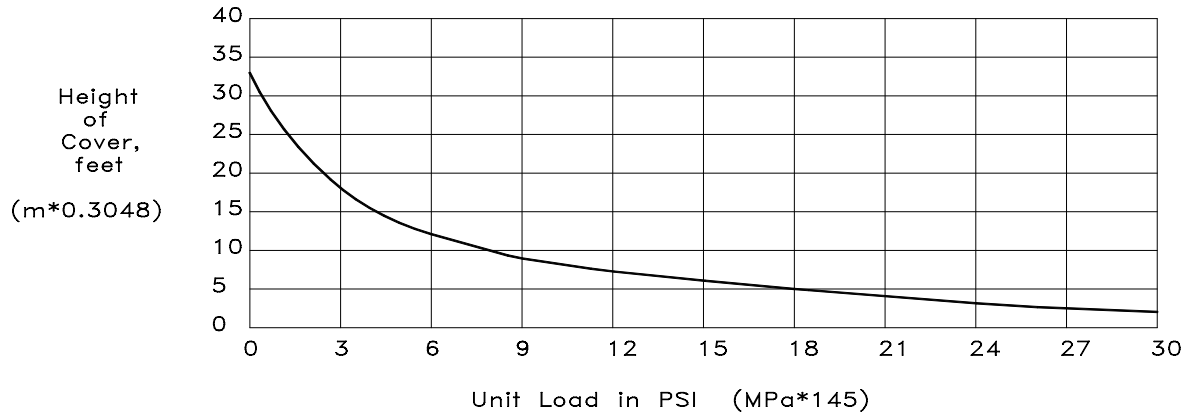
Figure C-5
H20 HIGHWAY LOADING



Note: The H20 live load assumes two 16,000 lb. loads applied to two 18" x 20" areas, one located over the point in question, and the other located at a distance of 72" away. In this manner, a truckload of 20 tons is simulated.

Source: American Iron and Steel Institute, Washington, DC

**Figure C-6
COOPER E-80**



Note: The Cooper E-80 live load assumes 80,000 pounds applied to three 2' x 6' areas on 5' centers, such as might be encountered through live loading from a locomotive with three 80,000 pounds axle loads.

Source: American Iron and Steel Institute, Washington, DC

TOTAL EXTERNAL LOADING

Total Load = Live Load + Backfill Load + Surface Load

$$P_t = P_l + P_b + P_s \quad (23)$$

Once the external loading on buried **PolyPipe**® has been determined, it will be necessary to calculate the critical buckling stress for contained **PolyPipe**® to determine if the pipe can withstand the external loading. The external loading capacity, or critical buckling stress, can be determined by the use of the following Von Mises formula:

$$P_{cb} = \frac{1}{SF} \cdot \left(\frac{2.67 \cdot R_w \cdot B \cdot E_s \cdot E}{DR^3} \right)^{1/2} \quad (24)$$

Where

- P_{cb} = Critical buckling stress, psi
- SF = Safety factor, **PolyPipe**® recommends SF=2
- R_w = Water buoyancy factor, (dimensionless)
- B = Empirical Coefficient of Elastic Support, (dimensionless)
- E_s = Soil modulus, (See Table C-4)
- E = Pipe modulus of elasticity, psi
- DR = Dimension Ratio

Where,

$$R_w = 1 - \left(0.33 \cdot \frac{H_w}{H} \right) \quad (25)$$

- H_w = Height of water table above pipe, feet
- H = Height of soil cover above pipe, feet

Note: H_w must be less than H

and,

$$B = \frac{1}{1 + 4 \cdot e^{-0.065 \cdot H}} \quad (26)$$

Where $e = 2.718$
 $H =$ Height of soil cover above pipe, feet

If the total external loading, Equation (23), is less than the critical buckling stress ($P_t < P_{cb}$), then the application should be considered safe. However, if this is not the case ($P_t > P_{cb}$), then the required parameters can be determined for a safe application from the following variations of the above equation:

$$DR = \left(\frac{2.67 \cdot R_w \cdot B \cdot E_s \cdot E}{SF^2 \cdot P_{cb}^2} \right) \quad (27)$$

or

$$E_s = \frac{P_{cb}^2 \cdot SF^2 \cdot DR^3}{2.67 \cdot R_w \cdot B \cdot E} \quad (28)$$

NOTICE:

The data contained herein is a guide to the use of **PolyPipe®** polyethylene pipe and fittings and is believed to be accurate and reliable. However, general data does not adequately cover specific applications, and its suitability in particular applications should be independently verified. In all cases, the user should assume that additional safety measures might be required in the safe installation or operation of the project. Due to the wide variation in service conditions, quality of installation, etc., no warranty or guarantee, expressed or implied, is given in conjunction with the use of this material.

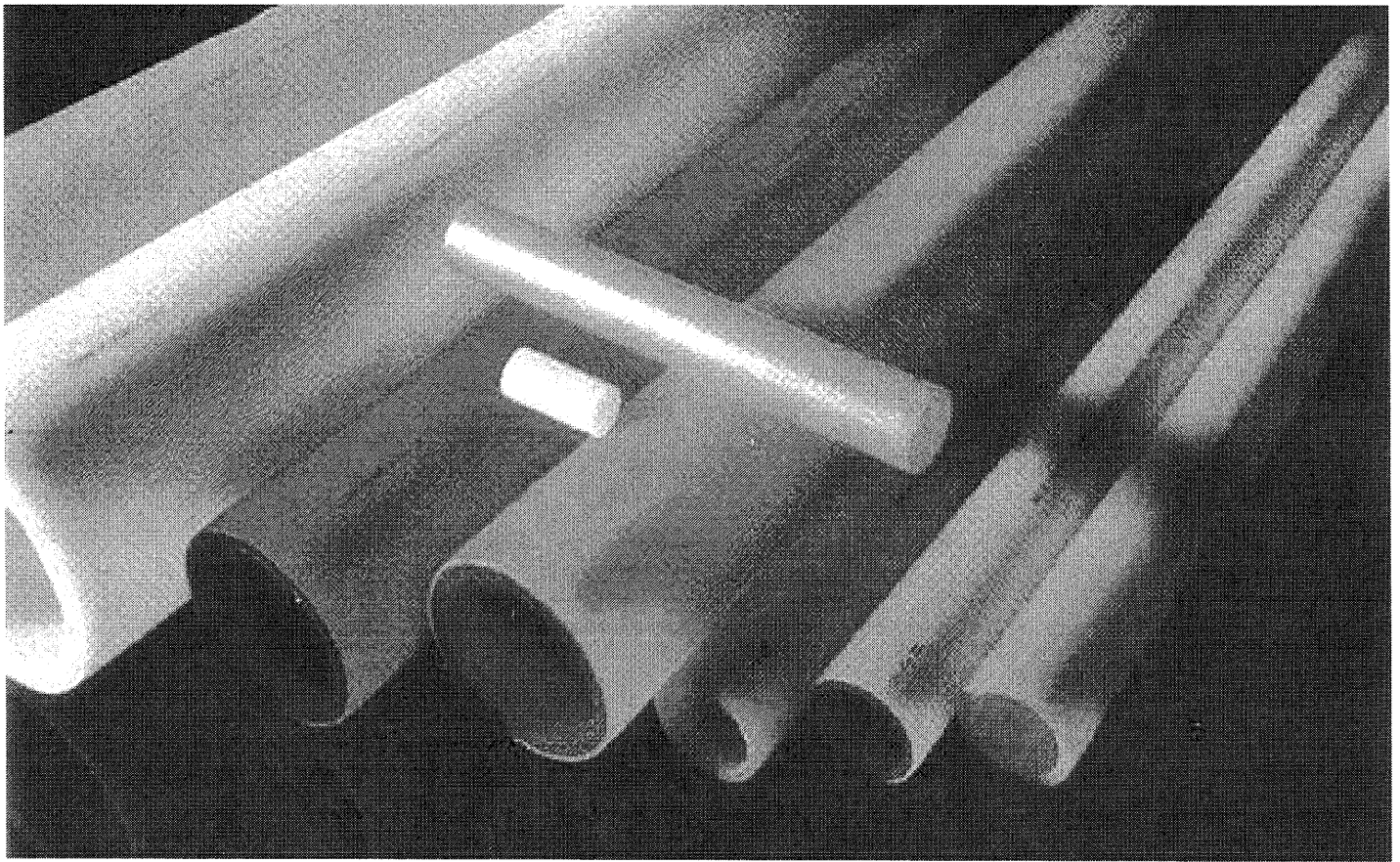
**APPLICATION FOR PERMIT RENEWAL AND MODIFICATION
SANDOVAL COUNTY LANDFILL**

**VOLUME III: LANDFILL ENGINEERING CALCULATIONS
SECTION 5: PIPE LOADING CALCULATIONS**

**ATTACHMENT III.5.F
DRISCOPIPE, INC. 2008.
*POLYETHYLENE PIPING SYSTEMS MANUAL.***



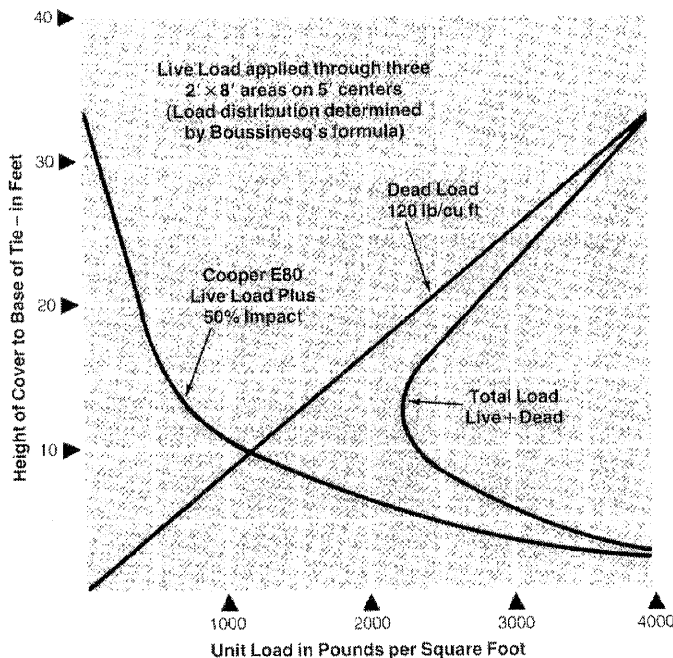
Polyethylene Piping Systems Manual



*Innovative Supplier of
Quality Piping Systems.*



FIGURE 6: COOPER E-80 LIVE LOADING



Note: Cooper E-80 live load assumes 80,000 pounds applied to three 2' x 8' areas on 5' centers such as might be encountered through live loading from a locomotive with three 80,000 pound axle loads.

Source: American Iron and Steel Institute, Washington, DC

APPARENT EXTERNAL PRESSURE DUE TO INTERNAL VACUUM, P_i Vacuum generates a compressive hoop stress in the wall of a pipe and acts to collapse the pipeline. Under vacuum conditions, the value of P_i is positive. P_i is added to the other two external pressure components, P_s and P_L , to obtain the total external pressure, P_T , acting on the pipe. An internal vacuum generates pressure equal to the absolute value of the vacuum. The maximum apparent external pressure due to a vacuum inside the pipe is 14.7 psi (2,117 psf).

BURIAL DESIGN GUIDELINES The design engineer must select the proper pipe DR and specify the backfill conditions to obtain the desired performance of the “pipe-soil” system.

DESIGN BY WALL CRUSHING Wall crushing occurs when external vertical pressure causes the compressive stress in the pipe wall to exceed the long-term compressive strength of the pipe material. To design for wall crushing, the following check should be made:

$$S_A = \frac{(SDR - 1)}{2} P_T$$

Where:

- S_A = Actual compressive stress, psi
- SDR = Standard Dimension Ratio
- P_T = Total external pressure on the top of the pipe, psi

Safety Factor = 1500 psi / S_A (where 1500 psi is the compressive yield strength of Driscopipe HDPE pipe)

DESIGN BY WALL BUCKLING Local wall buckling is a longitudinal wrinkling of the pipe wall. Buckling can occur over the long term in non-pressurized pipe if the total external soil pressure, P_T , exceeds the pipe-soil system's critical buckling pressure, P_{cb} . Although wall buckling is seldom the limiting factor in the design of a Driscopipe system, a check of non-pressurized pipelines can be made according to the following steps to insure $P_T < P_{cb}$. All pipe diameters with the same DR in the same burial situation have the same critical collapse and critical buckling endurance.

1. Calculate or estimate the total soil pressure, P_T , at the top of the pipe.
2. Calculate the stress, S_a , in the pipe wall:

$$S_a = \frac{(SDR - 1)P_T}{2}$$

3. Based upon the stress S_a and the estimated time duration of non-pressurization, find the value of the pipe's modulus of elasticity, E , in psi (approximate value for E is 35,000 psi).
4. Calculate the pipes hydrostatic, critical-collapse differential pressure, P_c

$$P_c = \frac{2E(t/D)^3(D_{MIN}/D_{MAX})^3}{(1-\mu^2)} \quad \text{or} \quad P_c = \frac{2.32(E)}{SDR^3}$$

Where: $(D_{MIN}/D_{MAX}) = 0.95$
 μ = Poission's Ratio = 0.45 for polyethylene pipe
 E = stress and time dependent tensile modulus of elasticity, psi
 E = 35,000 psi (approximate)
 D = Outside Diameter, in.
 t = thickness, in.

5. Calculate the soil modulus, E' , by plotting the total external soil pressure, P_T , against a specified soil density to derive the soil strain as shown in the example problem below Figure 7.
6. Calculate the critical buckling pressure at the top of the pipe by the formula:

$$P_{cb} = 0.8\sqrt{(E')(P_c)}$$

Where: P_{cb} = Critical buckling soil pressure at the top of the pipe, psi
 E' = Soil Modulus, psi
 P_c = Hydrostatic critical-collapse differential pressure, psi

7. Calculate the Safety Factor: $SF = P_{cb} / P_T$.
8. The above procedures can be reversed to calculate the minimum pipe DR required for a given soil pressure and an estimated soil density.

In a direct burial pressurized pipeline, the internal pressure is usually great enough to exceed the external critical-buckling soil pressure. When a pressurized line is to be shut down for a period, wall buckling should be examined.

**APPLICATION FOR PERMIT RENEWAL AND MODIFICATION
SANDOVAL COUNTY LANDFILL**

**VOLUME III: LANDFILL ENGINEERING CALCULATIONS
SECTION 5: PIPE LOADING CALCULATIONS**

ATTACHMENT III.5.G

CHEVRON PHILLIPS CHEMICAL COMPANY, LP. 2003.

PERFORMANCE PIPE ENGINEERING MANUAL.

BULLETIN: PP 900.

DriscoPlex™ 2000 SPIROLITE® pipe is manufactured to ASTM F 894, which states that profile pipe designed for 7.5% deflection will perform satisfactorily when installed in accordance with ASTM D 2321. Deflection is measured at least 30 days after installation.

Manufacturing processes for DriscoPlex™ 2000 SPIROLITE® and DriscoPlex™ OD controlled pipe differ. Deflection limitations for OD controlled pipe are controlled by long-term material strain.

Ring Bending Strain

As pipe deflects, bending strains occur in the pipe wall. For an elliptically deformed pipe, the pipe wall ring bending strain, ε , can be related to deflection:

$$\varepsilon = f_D \frac{\Delta X}{D_M} \frac{2C}{D_M} \quad (7-39) \quad \leftarrow$$

Where

ε	=	wall strain
f_D	=	deformation shape factor
ΔX	=	deflection, in
D_M	=	mean diameter, in
C	=	distance from outer fiber to wall centroid, in

For DriscoPlex™ 2000 SPIROLITE® pipe

$$C = h - z \quad (7-40)$$

For DriscoPlex™ OD Controlled pipe

$$C = 0.5(1.06t) \quad (7-41) \quad \leftarrow$$

Where

h	=	pipe wall height, in
z	=	pipe wall centroid, in
t	=	pipe minimum wall thickness, in

For elliptical deformation, $f_D = 4.28$. However, buried pipe rarely has a perfectly elliptical shape. Irregular deformation can occur from installation forces such as compaction variation alongside the pipe. To account for the non-elliptical shape many designers use $f_D = 6.0$.

Lytton and Chua report that for high performance polyethylene materials such as those used by Performance Pipe, 4.2% ring bending strain is a conservative value for non-pressure pipe. Jansen reports that high performance polyethylene material at an 8% strain level has a life expectancy of at least 50 years.

When designing non-pressure heavy wall OD controlled pipe (DR less than 17), and high RSC (above 200) DriscoPlex™ 2000 SPIROLITE® pipe, the ring bending strain at the predicted deflection should be calculated and compared to the allowable strain.

In pressure pipe, the combined stress from deflection and internal pressure should not exceed the material's long-term design stress rating. Combined stresses are incorporated into Table 7-9 values, which presumes deflected pipe at full pressure. At reduced pressure, greater deflection is allowable.

**APPLICATION FOR PERMIT RENEWAL AND MODIFICATION
SANDOVAL COUNTY LANDFILL**

**VOLUME III: LANDFILL ENGINEERING CALCULATIONS
SECTION 6: EROSION CALCULATIONS**

TABLE OF CONTENTS

1.0	INTRODUCTION	III.6-1
1.1	Project Description.....	III.6-1
2.0	PURPOSE.....	III.6-4
3.0	DESIGN CRITERIA	III.6-4
4.0	RAINFALL EROSION LOSS CALCULATIONS	III.6-4
5.0	WIND EROSION LOSS CALCULATIONS.....	III.6-6
6.0	SUMMARY	III.6-9

LIST OF FIGURES

Figure No.	Title	Page
III.6.1	SITE LOCATION MAP	III.6-2
III.6.2	LANDFILL COMPLETION DRAINAGE PLAN.....	III.6-3
III.6.3	WIND ROSE	III.6-8

LIST OF TABLES

Table No.	Title	Page
III.6.1	RAINFALL EROSION LOSSES	III.6-6

LIST OF ATTACHMENTS

Attachment	Title
III.6.A	NATURAL RESOURCES CONSERVATION SERVICE. T-FACTOR TABLE, WEB SOIL SURVEY. FROM HTTP://WEBSOILSURVEY.NRCS.USDA.GOV ; ACCESSED OCT. 2014. UNITED STATES DEPARTMENT OF AGRICULTURE.
III.6.B	YODER, DANIEL, ET, AL, 2006. RUSLE2, VERSION 1.26.6.4: MODEL CONSTANTS AND OUTPUT. USDA-ARS, USDA-NRCS AND UNIVERSITY OF TENNESSEE, HTTP://WWW.RUSLE2.ORG
III.6.C	UNITED STATES ENVIRONMENTAL PROTECTION AGENCY, LEW RESULTS, US EPA RAINFALL EROSIVITY FACTOR CALCULATOR. HTTP://WATER.EPA.GOV/POLWASTE/NPDES/STORMWATER/RAINFALL-EROSIVITY-FACTOR-CALCULATOR.CFM . ACCESSED SEPT. 2014.

**APPLICATION FOR PERMIT RENEWAL AND MODIFICATION
SANDOVAL COUNTY LANDFILL**

**VOLUME III: LANDFILL ENGINEERING CALCULATIONS
SECTION 6: EROSION CALCULATIONS**

- III.6.D UNITED STATES DEPARTMENT OF AGRICULTURE, 1997. PREDICTING SOIL EROSION BY WATER: A GUIDE TO CONSERVATION PLANNING WITH THE REVISED UNIVERSAL SOIL LOSS EQUATION. FIGURE 3-1: SOIL ERODIBILITY NOMOGRAPH.
- III.6.E GORDON ENVIRONMENTAL, INC. GEOTECHNICAL CLASSIFICATION SUMMARY, 2004. FOR MOST LIKELY FINAL COVER MATERIEL
- III.6.F NATURAL RESOURCES CONSERVATION SERVICE, 2010. NATIONAL ENGINEERING HANDBOOK; COVER FACTOR C VALUES FOR ESTABLISHED PLANTS. UNITED STATES DEPARTMENT OF AGRICULTURE.
- III.6.G NATURAL RESOURCES CONSERVATION SERVICE, 2002, SECTION 501.35; SUPPORT PRACTICE FACTOR, P; FROM NATIONAL AGRONOMY MANUAL, 190-V-NAM, THIRD EDITION, WASHINGTON, D.C.: UNITED STATES DEPARTMENT OF AGRICULTURE
- III.6.H NATURAL RESOURCES CONSERVATION SERVICE, 2002, EXHIBIT 502-2 – WIND EROSION IN NATIONAL AGRONOMY MANUAL, 190-V-NAM, THIRD EDITION, OCTOBER 2002, PART 502, WIND ERODIBILITY GROUPS & WIND ERODIBILITY INDEX. WASHINGTON, D.C.: UNITED STATES DEPARTMENT OF AGRICULTURE.
- III.6.I NATURAL RESOURCES CONSERVATION SERVICE. K-FACTOR TABLE, WEB SOIL SURVEY. FROM [HTTP://WEBSOILSURVEY.NRCS.USDA.GOV](http://websoilsurvey.nrcs.usda.gov); ACCESSED OCT. 2014. UNITED STATES DEPARTMENT OF AGRICULTURE.
- III.6.J NATURAL RESOURCES CONSERVATION SERVICE, 1992, FIGURE 14 - ANNUAL “C” VALUE ISOLINE MAP OF THE WIND EROSION EQUATION NEW MEXICO IN AGRONOMY TECH NOTE 27, JUNE 22, 1992. WASHINGTON, D.C.: UNITED STATES DEPARTMENT OF AGRICULTURE.
- III.6.K NATURAL RESOURCES CONSERVATION SERVICE, 2002, EXHIBIT 502.34 – UNSHELTERED DISTANCE IN NATIONAL AGRONOMY MANUAL, 190-V-NAM, THIRD EDITION, OCTOBER 2002, PART 502, WIND EROSION. WASHINGTON, D.C.: UNITED STATES DEPARTMENT OF AGRICULTURE.
- III.6.L NATURAL RESOURCES CONSERVATION SERVICE, 2002, FIGURE 7 - FLAT SMALL GRAIN EQUIVALENTS OF UNGRAZED MIXTURE OF GRASS IN NATIONAL AGRONOMY MANUAL, 190-V-NAM, THIRD EDITION, OCTOBER 2002, PART 502, WIND EROSION.

**APPLICATION FOR PERMIT RENEWAL AND MODIFICATION
SANDOVAL COUNTY LANDFILL**

**VOLUME III: LANDFILL ENGINEERING CALCULATIONS
SECTION 6: EROSION CALCULATIONS**

WASHINGTON, D.C.: UNITED STATES DEPARTMENT OF
AGRICULTURE.

III.6.M

NATURAL RESOURCES CONSERVATION SERVICE, 1998, SUBPART
G – EXHIBITS (C=120, I=134, K=0.20 & K=0.30) IN NATIONAL
AGRONOMY MANUAL, 190-V-NAM, THIRD EDITION, JANUARY
1998. WASHINGTON, D.C.: UNITED STATES DEPARTMENT OF
AGRICULTURE.

**APPLICATION FOR PERMIT RENEWAL AND MODIFICATION
SANDOVAL COUNTY LANDFILL**

**VOLUME III: LANDFILL ENGINEERING CALCULATIONS
SECTION 6: EROSION**

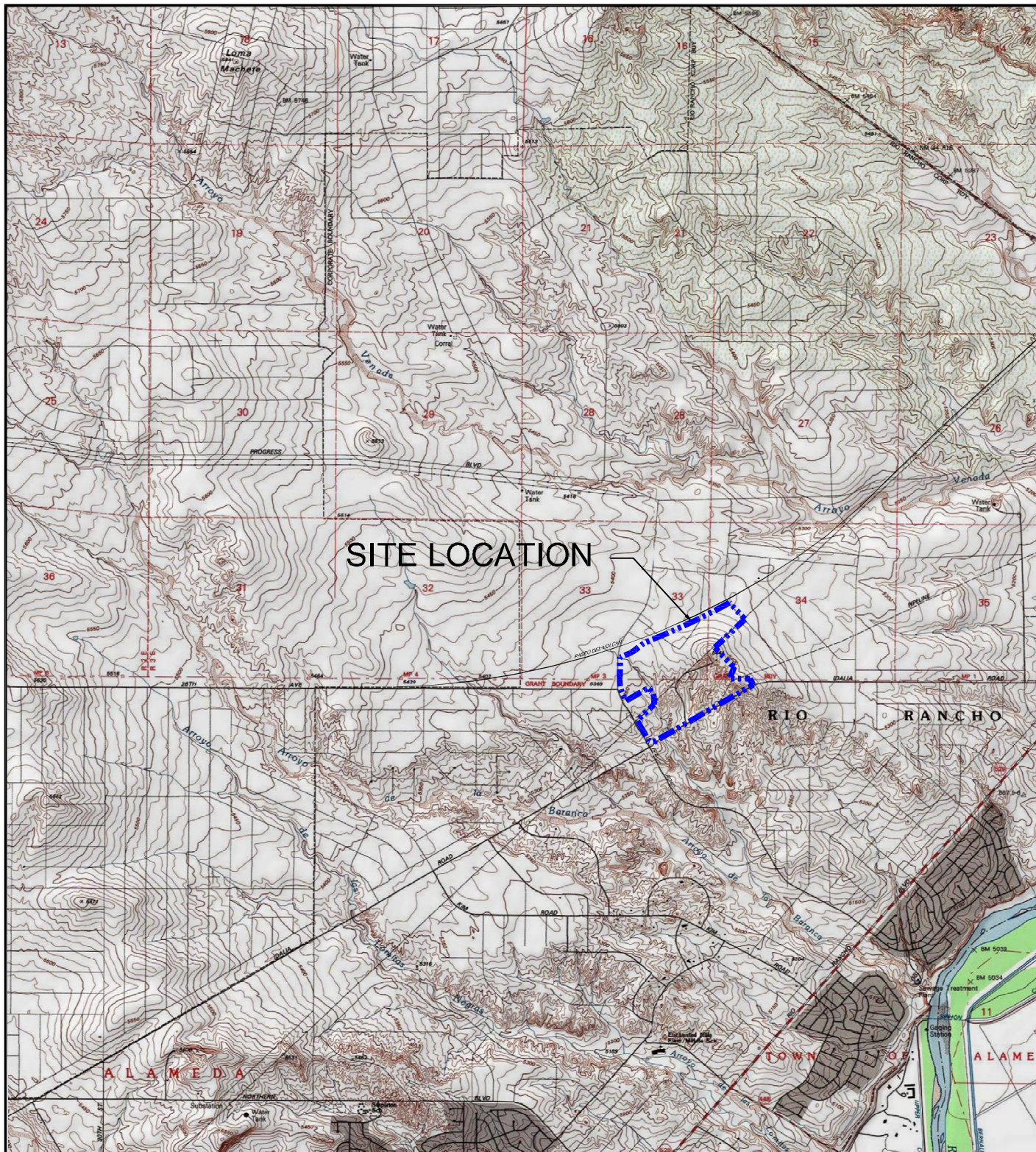
1.0 INTRODUCTION

The Sandoval County Landfill (SCLF) is an existing solid waste facility operating in compliance with its current Permits, SWM-050304 and SWM-050304 (SP), and the New Mexico Environment Department (NMED) Solid Waste Rules (20.9.2-2.9.10 NMAC). SCLF is located at 2708 Iris Road NE in Rio Rancho, New Mexico (NM), and occupies 178.3 acres \pm . SCLF is publicly owned and operated by the County of Sandoval (“the County”), and is currently permitted to accept municipal solid waste (MSW), including construction and demolition debris (C&D) and tires, and two special wastes: petroleum contaminated soils (PCS) and sludge.

1.1 Project Description

SCLF site is comprised of 178.3 \pm acres, with a solid waste footprint of 122.9 \pm acres. The site is located in portions of Sections 33 and 34, Township 13 North, Range 3 East of the New Mexico Prime Meridian, Sandoval County, New Mexico, and is accessed via an entrance off Iris Avenue, adjacent to the Rio Rancho Highway Department (**Figure III.6.1**). The approximate geographic coordinates for the center of the landfill site are **Latitude 35.307° North** and **Longitude 106.622° West**.

Design topography at SCLF ranges from about 5270 feet \pm above mean sea level (AMSL) to 5560 feet \pm AMSL, and generally drains toward the site boundaries at slopes between 5% \pm and 25% \pm . The majority of the site boundaries are roadways, on the northwest, southwest, and southeast property boundaries. The northeast corner of the site is bounded by a PNM easement and transformer station site. Run-on stormwater is managed by existing stormwater management structures. On-site runoff will be managed by three existing stormwater basins (Basins A, B, and C) located at the northeast corner of the site, the south corner of the site, and along the southwest edge of Unit III, respectively; shown in **Figure III.6.2**. Site run-off will be conveyed by three perimeter channels, and two stormwater drainage berms to Stormwater Basins A, B and C, as shown in **Figure III.6.2**.



LEGEND

--- SITE BOUNDARY

NOTES:

1. GEOGRAPHIC COORDINATES FOR THE CENTER OF THE SITE:
35.3092°N, 106.6198°W.
2. MAP REFERENCES:
MAP BASE FROM USA TOPO MAPS, 1:24000
USA TOPOGRAPHIC SERVICES, TOPOI MAP
3. SITE BOUNDARY FROM THE 2014 VACATION PLAT 093013
RRE BOOK 25 PAGE 65 SANDOVAL COUNTY LANDFILL

Drawing: P:\acad 2003\211.00.01\PERMIT FIGURES\SITE LOC MAP.dwg
Date/Time: Apr. 10, 2015-13:28:12; LAYOUT: A (P)
Copyright © All Rights Reserved, Gordon Environmental, Inc. 2015



SITE LOCATION MAP

SANDOVAL COUNTY LANDFILL
RIO RANCHO, NEW MEXICO



Gordon Environmental, Inc.
Consulting Engineers

213 S. Camino del Pueblo
Bernalillo, New Mexico, USA
Phone: 505-867-6990
Fax: 505-867-6991

DATE: 03/24/2015	CAD: SITE LOC MAP.dwg	PROJECT #: 211.00.01
DRAWN BY: DMI	REVIEWED BY: DRT	FIGURE III.6.1
APPROVED BY: IKG	gel@gordonenvironmental.com	



LEGEND

- PROPERTY BOUNDARY (178.3 ACRES)
- EXISTING UNIT LIMIT OF WASTE
- CELL BOUNDARY
- PERMIT MODIFICATION AND RENEWAL LIMIT OF WASTE (122.5 ACRES±)
- UNIT IV EDGE OF LINER
- UNIT IV AREA
- 10' EXISTING GRADE CONTOUR
- 2' EXISTING GRADE CONTOUR
- 10' FINAL GRADE CONTOUR
- 2' FINAL GRADE CONTOUR
- EXISTING CULVERT
- EXISTING FENCE
- PAVED ROAD
- UNPAVED ROAD
- UTILITY EASEMENT BOUNDARY
- UNIT IV LEACHATE COLLECTION PIPE & TRENCH
- UNIT IV LEACHATE COLLECTION SYSTEM RISER PIPE
- STORMWATER FLOW
- STORMWATER WATERSHED BOUNDARY
- STORMWATER BASIN
- EXISTING POWER POLE
- FIRE HYDRANT (3)
- EXISTING GROUNDWATER MONITORING WELL
- GROUNDWATER MONITORING WELL (DECOMMISSIONED)
- EXISTING LFG GAS PROBE (ACTIVE)
- EXISTING LFG GAS PROBE (INACTIVE)
- LFG GAS PROBE (DECOMMISSIONED)
- SURVEY CONTROL POINT
- SITE GRID
- CROSS SECTION LOCATIONS

- NOTES:
- AERIAL TOPOGRAPHIC SURVEY BY AEROTECH MAPPING INC., 6565 AMERICAN PARKWAY N.E., ALBUQUERQUE, NM 87111. PHONE: (505-561-8537) FAX (505-266-3328). EMAIL: TimBurrows@atmlv.com. DATE OF PHOTOGRAPHY: 01-13-2014.
 - SURVEY CONTROL POINTS BY : SURVEYING CONTROL, INC., 131 MADISON ST. N.E., ALBUQUERQUE, NM 87108. PHONE: (505-266-0935) FAX (505-266-9985). DATE OF SURVEY: 01-13-2014.
 - THE COUNTY MAY ELECT TO RETAIN THE EXISTING OVERHEAD STRUCTURE AT THE EAST END OF UNIT IV AS A COMMUNICATIONS TOWER. IN THAT EVENT, FUTURE CONSTRUCTION PLANS WILL ADDRESS THE EXISTENCE OF THIS FEATURE.

TABLE 1 UNIT ACRES	
UNIT I	29.4 ACRES±
UNIT II	19.5 ACRES±
UNIT III	63.6 ACRES±
UNIT IV	10.0 ACRES±
(FORMER PNM EASEMENT)	
TOTAL	122.5 ACRES±

NOTE:
1. TOTAL AREA OF UNIT IV, INCLUDING OVERFILL AREAS IS 30.7 ACRES±

CONTROL POINT DATA				
POINT	NORTHING	EASTING	PANEL ELEVATION	DESCRIPTION
501	1567982.35	1527461.08	5370.34	PP-501
502	1570293.88	1531074.96	5354.66	PP-502
503	1567798.82	1529894.61	5369.53	PP-503
504	1565822.71	1528883.42	5316.47	PP-504
505	1567834.53	1532385.04	5371.17	PP-505

NOTES:
1. ALL POINTS ARE FLUSH WITH THE GROUND.
2. THE COORDINATES AND ELEVATIONS FOR THE PHOTO CONTROL POINTS ON THE ABOVE REFERENCED PROJECT, THE COORDINATES ARE MODIFIED (SURFACE) NEW MEXICO STATE PLANE COORDINATES - CENTRAL ZONE, NAD 83 (NAD83/2007), AND HAVE BEEN ADJUSTED TO NOS MONUMENTS "EAGLE" TO OBTAIN TRUE STATE PLANE GRID COORDINATES. MULTIPLY THE COORDINATES BELOW BY THE PROJECT AVERAGE COMBINED FACTOR CF = 0.999961430. THE ELEVATIONS ARE NAVD 88, AND HAVE BEEN ADJUSTED TO THE NOS 1ST ORDER BENCHMARK "5424". THE COORDINATES AND ELEVATIONS ARE EXPRESSED IN U. S. SURVEY FEET.

GROUNDWATER MONITORING WELL LOCATIONS				
POINT	NORTHING	EASTING	ELEVATION	DESCRIPTION
MW-1	1566727.43	1530025.09	5322.45	MONITORING WELL
MW-2	1568159.63	1531290.50	5414.11	MONITORING WELL
MW-3	1567315.31	1531064.87	5374.32	MONITORING WELL
MW-5	1567869.24	1528110.28	5362.38	MONITORING WELL
MW-6	1568758.30	1530695.17	5421.90	MONITORING WELL
MW-7	1568394.69	1531377.96	5363.30	MONITORING WELL

NOTES:
1. THE COORDINATES AND ELEVATIONS FOR THE GROUNDWATER MONITORING WELL LOCATIONS ON THE ABOVE TABLE ARE MODIFIED (SURFACE) NEW MEXICO STATE PLANE COORDINATES - CENTRAL ZONE, NAD 83. SURVEY DATA OBTAINED BY TIM MARTINEZ SURVEYING ON 3-26-2015. THE COORDINATES AND ELEVATIONS ARE EXPRESSED IN U. S. SURVEY FEET.

TABLE 2 RUNOFF SUMMARY				
WATERSHED (ID)	DRAINAGE AREA (ACRES)	PEAK DISCHARGE (CFS)	ELEVATION	VOLUME (ACRE-FT)
A	71.91	43.5	3.74	
A1	7.05	8.48	0.37	
A1	9.07	10.19	0.47	
B	49.29	52.73	2.79	
B1	4.35	5.61	0.23	
C	49.91	26.07	2.60	
C, RUN-ON	23	20	1.20	
TOTAL	214.58	167	11.17	

TABLE 3 CHANNEL DESIGN SUMMARY							
CHANNEL (ID)	Q25 (CFS)	SLOPE (%)	WIDTH (FT)	DEPTH (FT)	VELOCITY (FT/S)	WATER DEPTH (FT)	FREEBOARD (FT)
A	48.40	3.5	3	2	10.82	0.938	1.06
A1	8.40	9.0	3	2	8.79	0.272	1.73
A2	10.20	4.4	4	2	3.77	0.32	1.68
A3	18.60	7.0	3	2	4.5	0.45	1.55
B	59.70	4.1	4	2	5.77	0.879	1.12
B1	5.80	1.6	0	2	3.74	0.76	1.24
C	46.70	2.4	4	2	4.77	0.681	1.32

TABLE 4 STORMWATER BASIN DESIGN SUMMARY					
STORMWATER DETENTION/RETENTION BASIN	CONTRIBUTING DRAINAGE AREAS	VOLUME	BASIN MAX. CAPACITY WITHOUT USING 1 FT. FREEBOARD	SAFETY FACTOR OF SAFETY WITHOUT USING 1 FT. FREEBOARD	SAFETY FACTOR OF SAFETY WITH 1 FT. FREEBOARD
(ID)	(ID)	(ACRE-FT)	(ACRE-FT)	(ACRE-FT)	
A	A+A1+A2	4.58	5.12	6.83	1.12
B	B+B1	2.82	3.00	3.75	1.06
C	C+C, RUN-ON	3.82	5.49	6.87	1.44

I. KEITH GORDON, P.E.
N.M. PROFESSIONAL ENGINEER NO. 10984

All reports, drawings, specifications, computer files, field data, notes and other documents and instruments prepared by the Engineer as instruments of service shall remain the property of the Engineer. The Engineer shall retain all common law, statutory and other reserved rights, including the copyright thereto.

LANDFILL COMPLETION
DRAINAGE PLAN
SANDOVAL COUNTY LANDFILL
RIO RANCHO, NEW MEXICO

Gordon Environmental, Inc.
Consulting Engineers
213 S. Camino del Pueblo
Bernalillo, New Mexico, USA
Phone: 505-867-6990
Fax: 505-867-6991

DATE: 04/14/2015
DRAWN BY: DMI
APPROVED BY: IKG
CAD: FINAL GRADING.dwg
REVIEWED BY: MRH
PROJECT #: 211.00.01
FIGURE III.6.2

2.0 PURPOSE

The purpose of these calculations is to determine potential soil losses due to rainfall and wind erosion for the SCLF following final cover installation. Erosion calculations project that the average soil loss from rainfall is approximately 1.60 tons/acre/year, and the average soil loss from wind action to be approximately 1.65 tons/acre/year. Combined, the 3.25 tons/acre/year of projected soil loss is below the 5 tons/acre/year soil loss tolerance recommended by the Natural Resource Conservation Service (NRCS) (**Attachment III.6.A**).

3.0 DESIGN CRITERIA

The attached calculations were used to assess the potential for wind and rainfall erosion at the SCLF. These calculations were also used to determine if additional erosion control measures are required. Evaluation of erosion of the final cover surface was based on the following design criteria:

1. The New Mexico Solid Waste Rules 20.9.6 NMAC, Solid Waste Facility and Composting Facility Closure and Post-Closure Requirements. More specifically, 20.9.6.9.A.(2)(d) NMAC states, *“for landfills accepting waste after the effective date of this part and lateral expansions permitted after the effective date of this part, finished grades different than those specified in Subparagraph (e) of Paragraph (1) of this subsection, provided no grade is greater than 33 percent and a demonstration is made in the closure plan or permit or modification application that the alternate grades will prevent erosion...”*
2. The longevity of any temporary erosion protection devices is a minimum of 12 months for the crown, and 24 months for 4H:1V (i.e., 25%) side slopes.
3. The design erosion rate shall not exceed the 6-inch soil thickness of the vegetative soil layer of the landfill cover.
4. The final cover has been conservatively assumed to have poor vegetation ($\leq 50\%$ coverage) established.
5. A maximum erosion rate is established at 5.0 tons/acre/year for soil erosion (**Attachment III.6.A**).

4.0 RAINFALL EROSION LOSS CALCULATIONS

RUSLE2 modeling software (Attachment III.6.B) was used to model the soil erosion rate from the landfill final cover due to rainfall. This program was developed by the Agriculture Research Service (ARS) of the United States Department of Agriculture (USDA), and uses the Revised Universal Soil Loss Equation 2 (RUSLE2) model. The equation is as follows:

$$A = R \times K \times LS \times C \times P$$

Where:

- A** is the soil loss per unit area per year, reported as tons/acre/year
- R** is the rainfall-runoff erosivity factor which varies with location and climate. R was obtained using the Environmental Protection Agency's (EPA's) Erosivity Calculator (**Attachment III.6.C**), which bases the value of R on intensity and duration of rainfall modeled at the latitude and longitude of the site:
R=45.41
- K** is the soil erodibility factor, which varies based on soil type. Final cover soils can be assumed with a common breakdown of 24% Silts, 74% Sand, 2% Organic (since there is not, as yet, a source for final cover soil). The soil erodibility nomograph provided in **Attachment III.6.D** is then employed, thus:
K=0.53
- LS** is the topographic factor which accounts for the site slope gradient and slope length. This factor is calculated based on the Drainage Areas shown on **Figure III.6.2**.
- C** is the cover factor that accounts for quality and quantity of vegetative or artificial ground cover. For SCLF, for $\leq 50\%$ poor grass cover, the cover factor was extrapolated from **Attachment III.6.F**, the factor is taken as:
C=0.093
- P** is the support practice factor, which reduces the erosion if countermeasures are employed, such as terracing or cross-slope berms (**Attachment III.6.G**). No long-term erosion control practices are planned. Therefore, P is not a contributing factor, and is set as:
P=1

Note: The RULSE2 program uses United States Department of Agriculture (USDA) maintained databases as the basis for the majority of its equation values and calculations. The dataset used for SCLF erosion calculations is based upon the latitude and longitude, soil type, anticipated vegetation, and the USEPA-calculated erosivity factor, R. Some of the constants above are superseded by these datasets, and are only used for verification and approximation purposes.

The results of the RULSE2 modeling for soil loss (i.e., erosion in tons/acre/year) due to rainfall-runoff from each drainage area (**Figure III.6.2**) of the final cover are provided on **Table III.6.1**:

TABLE III.6.1
Rainfall Erosion Losses – RULSE2 Model Output
Sandoval County Landfill

Section	Description	Drainage Area	Drainage Slope Length	Average Slope	Slope Gradient	Loss with ≤50% vegetative cover
		(acres)	(ft)	(ft/ft)	(H:1)	(Tons/Yr)
A	Crown & N/NE Slopes	72.0	665.0	0.24	4.17	122.1
A1	N Crown & Corner	7.1	756.0	0.18	5.56	8.5
A2	NE portion of Unit I	9.1	650.0	0.20	5.00	11.9
B	SE Slopes, Unit I & II	49.6	700.0	0.23	4.35	81.4
B1	Low NE Unit I	4.6	191.0	0.21	4.76	4.0
C	SW Slopes	50.5	559.0	0.24	4.17	80.1
Total:		192.9				308.0

$$\text{Average Loss: } (308.0 \text{ tons/yr}) \div 192.9 \text{ acres} = 1.60 \text{ tons/acre/yr}$$

When a ≤50% vegetative cover is considered, the soil loss due to rainfall averages approximately 2.9 tons/acre/year, which, combined with the wind erosion, is well below the established criteria of the maximum 5.0 tons/acre/year (**Attachment III.6.A**).

5.0 WIND EROSION LOSS CALCULATIONS

To estimate the quantity of soil lost as a result of wind using the Wind Erosion Equation (WEQ).

Wind Erosion Equation:

$$E = f(I, K, C, L, V)$$

Where:

- E = The potential average annual soil loss (tons/acre/year).
- I = The soil erodibility index (tons per acre per year).
- K = The ridge roughness factor (0.5-1.0).
- C = The Climactic Factor.
- L = The unsheltered distance along the prevailing wind erosion direction across the area to be evaluated.
- V = Equivalent Vegetative Cover.

Find I:

The on-site soil will consist primarily of a sandy loam with few organics (**Attachment III.6.E**).

The I value for a sandy loam is listed in **Attachment III.6.H** as 134 tons/acre/year:

$$I = 134$$

Find K:

The Roughness Factor (K) is a combination of the random roughness of the soil (K_{rr}), and the roughness effect of ridges (K_r). No artificial ridges or furrows are planned. Therefore, K_r is not evaluated, and $K_{rr}=K$. The roughness of the soil is determined as $K_{rr}=0.244$, in a weighted average. (**Attachment III.6.H**). Therefore, conservatively:

$$K=K_r \times K_{rr}=1 \times 0.244 \approx 0.25$$

Find C:

The Climactic Factor (C) is based on the average wind velocity and the precipitation – evaporation index (PE Index). An isolinear map of New Mexico (**Attachment III.6.J**) was used to find the value of C for the site:

$$C = 120$$

Find L:

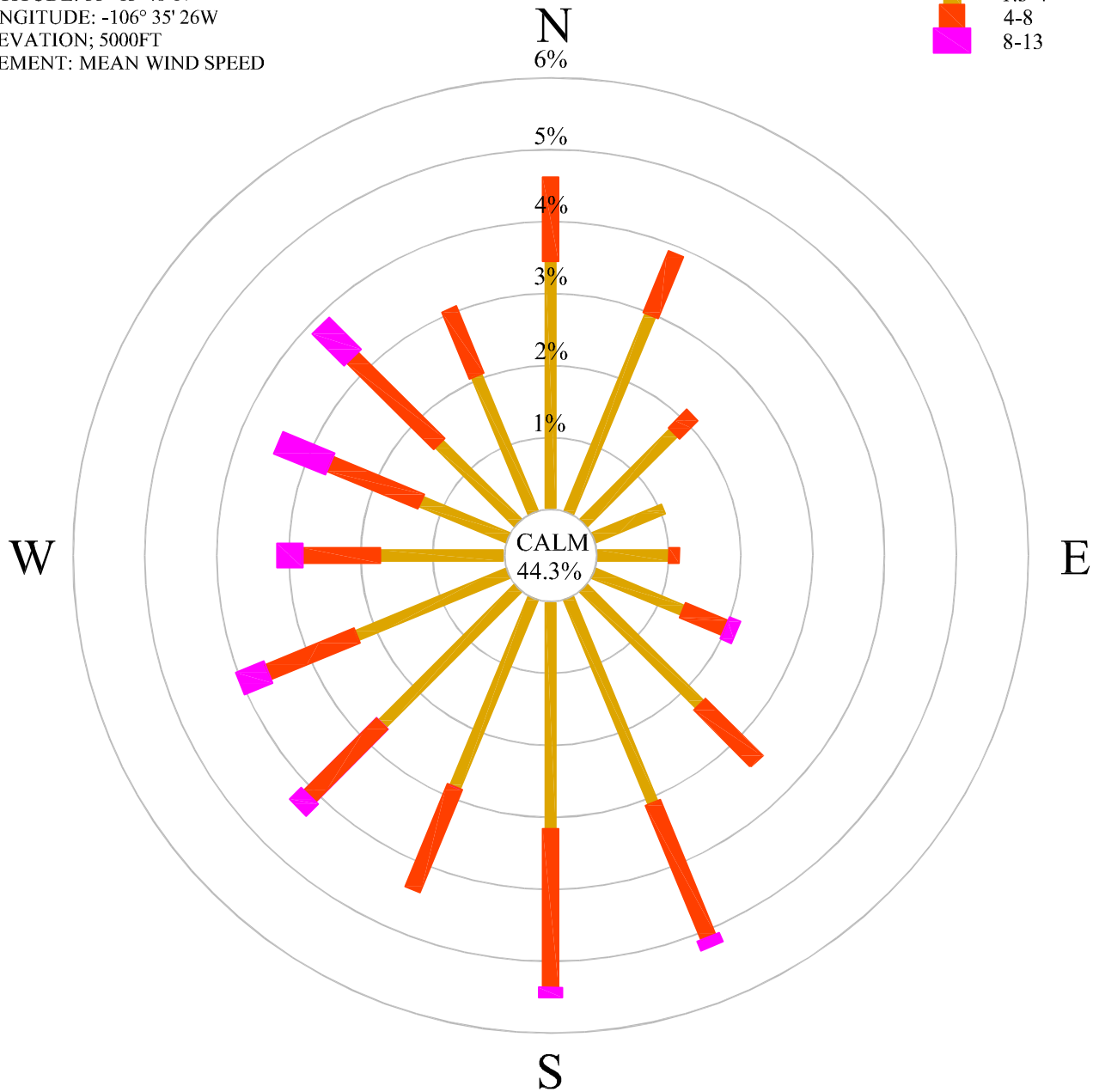
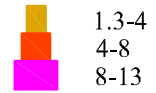
L represents the longest unsheltered distance along the prevailing wind direction for the area to be evaluated. The prevailing wind direction was determined using data obtained from the Western Regional Climate Center in Sandia Lakes, NM. As shown in the Wind Rose chart for the Sandia Lakes provided as **Figure III.6.3**, the prevailing winds are from the southwest quadrant. The maximum unsheltered distance across the site is from the south corner northward to the boundary of the landfill, a distance of approximately 2,900 feet. However, looking beyond the site (**Attachment III.6.K**), the nearest stable areas are the paved roadways to the south and north of the site. Therefore, L must extend beyond the site, extending 3,100 feet from the roundabout to the south of the site, due North to Paseo del Volcan.

$$L = 3,100 \text{ ft}$$

SANDIA LAKES NEW MEXICO

STATION: SANDIA LAKES NEW MEXICO
 LATITUDE: 33° 13' 48"N
 LONGITUDE: -106° 35' 26W
 ELEVATION: 5000FT
 ELEMENT: MEAN WIND SPEED

MPH



START DATE: MAR. 1, 2004
 END DATE: MAR. 1, 2015
 # OF DAYS: 4048 OF 4048
 # OBS: POSS: 05939 OF 97152
 WESTERN REGIONAL CLIMATE CENTER

WIND ROSE

SANDOVAL COUNTY LANDFILL
 RIO RANCHO, NEW MEXICO TEXT



Gordon Environmental, Inc.
 Consulting Engineers

213 S. Camino del Pueblo
 Bernalillo, New Mexico, USA
 Phone: 505-867-6990
 Fax: 505-867-6991

DATE: 04/10/2015	CAD: WIND ROSE.dwg	PROJECT #: 211.00.01
DRAWN BY: DMI	REVIEWED BY: DRT	FIGURE III.6.3
APPROVED BY: IKG	gel@gordonenvironmental.com	

Find V:

The equivalent vegetative cover (V) is a value that relates the kind, amount, and orientation of vegetative material to its equivalent in pounds per acre of a small grain residue reference condition. This Flat Small Grain reference condition is defined as 10-inch-long stalks of small grain lying flat in rows spaced 10 inches apart, perpendicular to the direction of the wind.

The vegetation plan for the SCLF prescribes a final cover seed mix consisting of Western Wheatgrass, Buffalograss, and Blue Grama. This mix should be planted into the soil, and irrigated at least twice, and assuming a poor stand of growth, should produce at least 300 lbs/acre. When this value is converted to the Flat Small Grain equivalent (**Attachment III.6.L**), it conservatively yields an equivalent vegetative factor (V) of approximately 1,500 pounds per acre:

$$V = 1,500 \text{ pounds per acre}$$

Solve for E:

Using the table in **Attachment III.6.M** (where $C=120$, $I=134$, and $K=0.2$ and $K=0.3$), a conservative average wind erosion value of 1.65 tons/acre/year for an unsheltered distance of 3,000 ft is obtained.

6.0 SUMMARY

The erosion from rainfall effects is evaluated to be approximately 1.60 tons/acre/year, and erosion from wind effects is evaluated to be approximately 1.65 tons/acre/year. Combined, the total erosion loss is found to be approximately 3.25 tons/acre/year for wind and rainfall erosion, which is below the recommended soil loss tolerance quantity of 5.0 tons/acre/year (**Attachment III.6.A**).

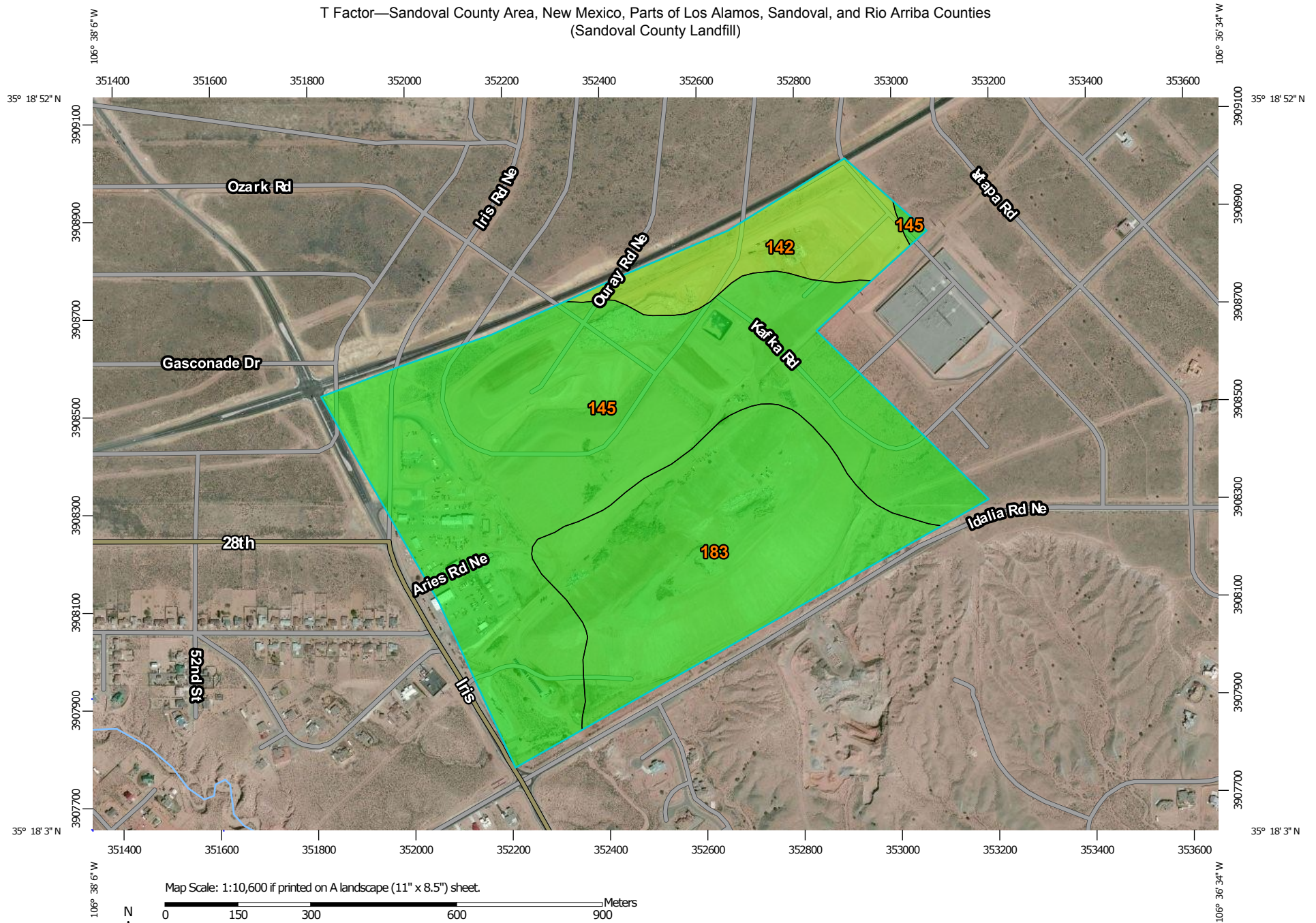
**APPLICATION FOR PERMIT RENEWAL AND MODIFICATION
SANDOVAL COUNTY LANDFILL**

**VOLUME III: LANDFILL ENGINEERING CALCULATIONS
SECTION 6: EROSION CALCULATIONS**

ATTACHMENT III.6.A


**NATURAL RESOURCES CONSERVATION SERVICE. T-FACTOR TABLE, WEB
SOIL SURVEY. FROM [HTTP://WEBSOILSURVEY.NRCS.USDA.GOV](http://websoilsurvey.nrcs.usda.gov); ACCESSED
OCT. 2014. UNITED STATES DEPARTMENT OF AGRICULTURE.**

T Factor—Sandoval County Area, New Mexico, Parts of Los Alamos, Sandoval, and Rio Arriba Counties
(Sandoval County Landfill)







MAP LEGEND

Area of Interest (AOI)


 Area of Interest (AOI)

Soils







Soil Rating Polygons

-  1
-  2
-  3
-  4
-  5
-  Not rated or not available


Soil Rating Lines

-  1
-  2
-  3
-  4
-  5
-  Not rated or not available

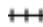




Soil Rating Points

-  1
-  2
-  3
-  4
-  5
-  Not rated or not available

Water Features

 Streams and Canals

Transportation

-  Rails
-  Interstate Highways
-  US Routes
-  Major Roads
-  Local Roads

Background

 Aerial Photography

MAP INFORMATION

The soil surveys that comprise your AOI were mapped at 1:24,000.

Warning: Soil Map may not be valid at this scale.

Enlargement of maps beyond the scale of mapping can cause misunderstanding of the detail of mapping and accuracy of soil line placement. The maps do not show the small areas of contrasting soils that could have been shown at a more detailed scale.

Please rely on the bar scale on each map sheet for map measurements.

Source of Map: Natural Resources Conservation Service
Web Soil Survey URL: <http://websoilsurvey.nrcs.usda.gov>
Coordinate System: Web Mercator (EPSG:3857)

Maps from the Web Soil Survey are based on the Web Mercator projection, which preserves direction and shape but distorts distance and area. A projection that preserves area, such as the Albers equal-area conic projection, should be used if more accurate calculations of distance or area are required.

This product is generated from the USDA-NRCS certified data as of the version date(s) listed below.

Soil Survey Area: Sandoval County Area, New Mexico, Parts of Los Alamos, Sandoval, and Rio Arriba Counties
Survey Area Data: Version 9, Sep 25, 2014

Soil map units are labeled (as space allows) for map scales 1:50,000 or larger.

Date(s) aerial images were photographed: Mar 23, 2011—Mar 24, 2011

The orthophoto or other base map on which the soil lines were compiled and digitized probably differs from the background imagery displayed on these maps. As a result, some minor shifting of map unit boundaries may be evident.

T Factor

T Factor— Summary by Map Unit — Sandoval County Area, New Mexico, Parts of Los Alamos, Sandoval, and Rio Arriba Counties (NM656)				
Map unit symbol	Map unit name	Rating (tons per acre per year)	Acres in AOI	Percent of AOI
142	Grieta fine sandy loam, 1 to 4 percent slopes	4	22.3	10.5%
145	Grieta-Sheppard loamy fine sands, 2 to 9 percent slopes	5	125.6	59.2%
183	Sheppard loamy fine sand, 8 to 15 percent slopes	5	64.1	30.2%
Totals for Area of Interest			211.9	100.0%

Description

The T factor is an estimate of the maximum average annual rate of soil erosion by wind and/or water that can occur without affecting crop productivity over a sustained period. The rate is in tons per acre per year.

Rating Options

Units of Measure: tons per acre per year

Aggregation Method: Dominant Condition

Component Percent Cutoff: None Specified

Tie-break Rule: Lower

Interpret Nulls as Zero: No

**APPLICATION FOR PERMIT RENEWAL AND MODIFICATION
SANDOVAL COUNTY LANDFILL**

**VOLUME III: LANDFILL ENGINEERING CALCULATIONS
SECTION 6: EROSION CALCULATIONS**

ATTACHMENT III.6.B

**YODER, DANIEL, ET, AL, 2006. RUSLE2, VERSION 1.26.6.4: MODEL CONSTANTS
AND OUTPUT. USDA-ARS, USDA-NRCS AND UNIVERSITY OF TENNESSEE,
[HTTP://WWW.RUSLE2.ORG](http://www.rusle2.org)**

About RUSLE2



Rusle2 version: 1.26.6.4

Build date: Nov 13 2006, 15:57:14

Science date: 10/20/06

OK

Credits

License

Versions

RUSLE2 CREDITS

Financial support for RUSLE2 was provided by the USDA-ARS and USDA-NRCS cooperative agreement with the University of Tennessee.

== DEVELOPERS ==

Science: George Foster, Daniel Yoder

Interface: Jim Lyon, Joel Lown, Daniel Yoder

Architecture: Joel Lown, Jim Lyon, Daniel Yoder

10 year EI, US

15

10-yr 24-hr rainfall, in.

1.7

100-yr 24-hr rainfall, in.

0

Annual precip, in.

9.7

Avg. temp., deg C

-0.99 2.1 5.8 10 15 21 23 22 18 12 5.0 -0.089

EI dist. for Req conditions

req

Eros. density, US eros. / in. ppt

0.25 0.22 0.42 1.0 1.8 3.1 4.5 3.6 2.2 1.4 0.75 0.37

How determine runoff?

based on 10-yr 24-hr ppt

How get erosivity distribution?

From monthly eros. density & precip.

In Req area?

No

Month precip., mm

12 12 13 12 15 15 39 46 30 25 14 13

R Equiv, US

27

R Factor, US

22

R values, US

0.12 0.10 0.22 0.49 1.1 1.8 6.9 6.5 2.6 1.4 0.41 0.19

Standard EI distribution

default

Use frozen/thawing soil routines?

No

What Req area?

Normal Req (Pullman)

Add to this management to make new one

No

Base energy use , BTU/ac

18000

Base equiv. diesel use, gal/ac

0.13

Base fuel cost, US\$/ac

0.3250

Cover from addition, %

-

Cover matl add/remove, lb/ac

-

Date, m/d/y

1/1/0

Duration, yr

1

Fuel for all operations

Local\Diesel

Fuel used this operation

Local\Diesel

Graphic

32768

Irrig end date, m/d/y

1/0/0

Irrig. start date, m/d/y

1/0/0

Irrigation system

no irrigation

Long-term natural rough., mm

6.0

Max. canopy, %

50

Normally used as a rotation?

Yes

Op. depth, in.

-

Op. speed, mph

-

Operation

Planting, broadcast seeder

Operation builder

Operation builder

Perm. barrier

-

Rel. row grade, %

100

Standing res. added by op. desc., lb/ac

-

Standing res. added by veg. change, lb/ac

-

Type of cover material

-

Veg. retardance class

no retardance (wide spacing in row)

Vegetation

Range Southern desert shrub

View/edit rotation builder used to make this management

Rotation builder

Yield (# harv. units)

Calc. consolidation from precip?

No

Carib. soil group

none

Clay (<0.002 mm), %

20

Erodibility, US

0.43

Graphic

0

How calc. time-varying erodibility?

daily K values vary about reference location K

How get soil erodibility?

set by user

Hydrologic class

D - highest runoff

Hydrologic class with subsurface drainage

D - highest runoff

Info

NASIS 1:1 H2O ph for top horiz., pH

7.0

NASIS map unit symbol

-

NASIS rep. OM for top horiz., %

1.0

NASIS survey area symbol

-

Nominal consolidation time, yr

7.0

Rock cover, %

0

Sand (0.05-2 mm), %

20

Silt (0.002-0.05 mm), %

60

Soil fuel use ratio (relative to silt loam = 1.0)

1.0

T value, t/ac/yr

3.0

Texture

Silt loam

Adjust res. burial level
Normal res. burial
Adjust runoff by
adjust precip. by daily precip. as portion of max.
Avg. annual slope storm runoff depth, in.
59
Avg. slope steepness, %
24
Consolidation time, yr
7
Crit. slope length, ft
-
Detachment on slope, t/ac/yr
3.1
Location
USA\New Mexico\Sandoval County\NM_Sandoval R 9
Max. storm return period, yr
1.25
Net C factor
0.12
Net K factor
0.14
Net LS factor
8.3
Net contour factor
1.0
Net ponding factor
1.0
Net ridge factor
1.0
Rainfall depth for max. storm, in.
1.7
Rock cover, %
0
Sed. del., t/ac/yr
3.1
Sediment delivery, t/ac/yr
3.1
Seg length (horiz), ft
670
Segment
1
Slope length (horiz), ft
670
Slope segments, ft
49945760
Soil
Generic Soils\sandy loam (l-m OM, slo perm)
Soil loss, t/ac/yr
3.1
Soil loss erod. portion, t/ac/yr
3.1
Soil loss for cons. plan, t/ac/yr
3.1
Surf. cover after planting, %
2.9
Surf. res. cov. values
Surf. cover
T value, t/ac/yr

3.0
Tillage translocation per width, lb/ft width
0
Tillage translocation rate, t/ac/yr
0

Adjust res. burial level
Normal res. burial
Adjust runoff by
adjust precip. by daily precip. as portion of max.
Avg. annual slope storm runoff depth, in.
59
Avg. slope steepness, %
18
Consolidation time, yr
7
Crit. slope length, ft
-
Detachment on slope, t/ac/yr
2.2
Location
USA\New Mexico\Sandoval County\NM_Sandoval R 9
Max. storm return period, yr
1.25
Net C factor
0.12
Net K factor
0.14
Net LS factor
5.7
Net contour factor
1.0
Net ponding factor
1.0
Net ridge factor
1.0
Rainfall depth for max. storm, in.
1.7
Rock cover, %
0
Sed. del., t/ac/yr
2.2
Sediment delivery, t/ac/yr
2.2
Seg length (horiz), ft
760
Segment
1
Slope length (horiz), ft
760
Slope segments, ft
0
Soil
Generic Soils\sandy loam (l-m OM, slo perm)
Soil loss, t/ac/yr
2.2
Soil loss erod. portion, t/ac/yr
2.2
Soil loss for cons. plan, t/ac/yr
2.2
Surf. cover after planting, %
2.9
Surf. res. cov. values
Surf. cover
T value, t/ac/yr

3.0
Tillage translocation per width, lb/ft width
0
Tillage translocation rate, t/ac/yr
0

Adjust res. burial level
Normal res. burial
Adjust runoff by
adjust precip. by daily precip. as portion of max.
Avg. annual slope storm runoff depth, in.
59
Avg. slope steepness, %
20
Consolidation time, yr
7
Crit. slope length, ft
-
Detachment on slope, t/ac/yr
2.4
Location
USA\New Mexico\Sandoval County\NM_Sandoval R 9
Max. storm return period, yr
1.25
Net C factor
0.12
Net K factor
0.14
Net LS factor
6.3
Net contour factor
1.0
Net ponding factor
1.0
Net ridge factor
1.0
Rainfall depth for max. storm, in.
1.7
Rock cover, %
0
Sed. del., t/ac/yr
2.4
Sediment delivery, t/ac/yr
2.4
Seg length (horiz), ft
650
Segment
1
Slope length (horiz), ft
650
Slope segments, ft
0
Soil
Generic Soils\sandy loam (l-m OM, slo perm)
Soil loss, t/ac/yr
2.4
Soil loss erod. portion, t/ac/yr
2.4
Soil loss for cons. plan, t/ac/yr
2.4
Surf. cover after planting, %
2.9
Surf. res. cov. values
Surf. cover
T value, t/ac/yr

3.0
Tillage translocation per width, lb/ft width
0
Tillage translocation rate, t/ac/yr
0

Adjust res. burial level
Normal res. burial
Adjust runoff by
adjust precip. by daily precip. as portion of max.
Avg. annual slope storm runoff depth, in.
59
Avg. slope steepness, %
23
Consolidation time, yr
7
Crit. slope length, ft
-
Detachment on slope, t/ac/yr
3.0
Location
USA\New Mexico\Sandoval County\NM_Sandoval R 9
Max. storm return period, yr
1.25
Net C factor
0.12
Net K factor
0.14
Net LS factor
7.8
Net contour factor
1.0
Net ponding factor
1.0
Net ridge factor
1.0
Rainfall depth for max. storm, in.
1.7
Rock cover, %
0
Sed. del., t/ac/yr
3.0
Sediment delivery, t/ac/yr
3.0
Seg length (horiz), ft
700
Segment
1
Slope length (horiz), ft
700
Slope segments, ft
0
Soil
Generic Soils\sandy loam (l-m OM, slo perm)
Soil loss, t/ac/yr
3.0
Soil loss erod. portion, t/ac/yr
3.0
Soil loss for cons. plan, t/ac/yr
3.0
Surf. cover after planting, %
2.9
Surf. res. cov. values
Surf. cover
T value, t/ac/yr

3.0
Tillage translocation per width, lb/ft width
0
Tillage translocation rate, t/ac/yr
0

Adjust res. burial level
Normal res. burial
Adjust runoff by
adjust precip. by daily precip. as portion of max.
Avg. annual slope storm runoff depth, in.
59
Avg. slope steepness, %
21
Consolidation time, yr
7
Crit. slope length, ft
-
Detachment on slope, t/ac/yr
1.6
Location
USA\New Mexico\Sandoval County\NM_Sandoval R 9
Max. storm return period, yr
1.25
Net C factor
0.12
Net K factor
0.14
Net LS factor
4.2
Net contour factor
1.0
Net ponding factor
1.0
Net ridge factor
1.0
Rainfall depth for max. storm, in.
1.7
Rock cover, %
0
Sed. del., t/ac/yr
1.6
Sediment delivery, t/ac/yr
1.6
Seg length (horiz), ft
190
Segment
1
Slope length (horiz), ft
190
Slope segments, ft
0
Soil
Generic Soils\sandy loam (l-m OM, slo perm)
Soil loss, t/ac/yr
1.6
Soil loss erod. portion, t/ac/yr
1.6
Soil loss for cons. plan, t/ac/yr
1.6
Surf. cover after planting, %
2.9
Surf. res. cov. values
Surf. cover
T value, t/ac/yr

3.0
Tillage translocation per width, lb/ft width
0
Tillage translocation rate, t/ac/yr
0

Accounting period
Accounting period
Adjust res. burial level
Normal res. burial
Adjust runoff by
adjust precip. by daily precip. as portion of max.
Avg. annual slope storm runoff depth, in.
59
Avg. slope steepness, %
24
Caribbean phosphorus index
Caribbean phosphorus index
Crit. slope length, ft
-
Detachment on slope, t/ac/yr
2.9
Energy use for entire simulation, BTU/ac
16200
Equiv. diesel use for entire simulation, gal/ac
0.117
Fuel cost for entire simulation, US\$/ac
0.2925
Fuel type for entire run
(none)
Kentucky phosphorus index
Kentucky phosphorus index
Limits set
(none)
Location
USA\New Mexico\Sandoval County\NM_Sandoval R 9
Man. strip builder
Man. strip builder
Max. storm return period, yr
1.25
Minnesota phosphorus index
Minnesota phosphorus index
Net C factor
0.12
Net K factor
0.14
Net LS factor
7.6
Net contour factor
1.0
Net ponding factor
1.0
Net ridge factor
1.0
Nitrogen leaching index
Nitrogen leaching index
Pennsylvania phosphorus index
Pennsylvania phosphorus index
Perm. barrier set
Perm. barrier set
Rainfall depth for max. storm, in.
1.7
Rock cover, %
0
Rotation builder

Rotation builder
Sediment delivery, t/ac/yr
2.9
Single-storm erosivity
Single-storm erosivity
Slope length (horiz), ft
560
Slope segments, ft
0
Soil conditioning index
Soil conditioning index
Soil loss erod. portion, t/ac/yr
2.9
Soil loss for cons. plan, t/ac/yr
2.9
Surf. cover after planting, %
2.9
Surf. res. cov. values
Surf. cover
T value, t/ac/yr
3.0
Tennessee phosphorus index
Tennessee phosphorus index
Tillage translocation per width, lb/ft width
0
Tillage translocation rate, t/ac/yr
0
WI SNAP parameters
WI SNAP parameters
WI channel delivery calc
WI channel delivery

**APPLICATION FOR PERMIT RENEWAL AND MODIFICATION
SANDOVAL COUNTY LANDFILL**

**VOLUME III: LANDFILL ENGINEERING CALCULATIONS
SECTION 6: EROSION CALCULATIONS**

ATTACHMENT III.6.C

**UNITED STATES ENVIRONMENTAL PROTECTION AGENCY, LEW RESULTS, US
EPA RAINFALL EROSIVITY FACTOR CALCULATOR.
[HTTP://WATER.EPA.GOV/POLWASTE/NPDES/STORMWATER/RAINFALL-
EROSIVITY-FACTOR-CALCULATOR.CFM](http://water.epa.gov/polwaste/npdes/stormwater/rainfall-erosivity-factor-calculator.cfm). ACCESSED SEPT. 2014.**

**Water: Stormwater**

You are here: [Water](#) » [Pollution Prevention & Control](#) » [Permitting \(NPDES\)](#) » [Stormwater](#) » LEW Results

LEW Results**Rainfall Erosivity Factor Calculator for Small Construction Sites****Facility Information**

Start Date:	03/01/2017
End Date:	03/01/2018
Latitude:	35.307
Longitude:	-106.622

Erosivity Index Calculator Results

AN EROSIVITY INDEX VALUE OF **21.86** HAS BEEN DETERMINED FOR THE CONSTRUCTION PERIOD OF **03/01/2017 - 03/01/2018**.

A rainfall erosivity factor of 5.0 or greater has been calculated for your site and period of construction. **You do NOT qualify for a waiver from NPDES permitting requirements.**

Start Over

Last updated on Monday, July 28, 2014

**APPLICATION FOR PERMIT RENEWAL AND MODIFICATION
SANDOVAL COUNTY LANDFILL**

**VOLUME III: LANDFILL ENGINEERING CALCULATIONS
SECTION 6: EROSION CALCULATIONS**

ATTACHMENT III.6.D

**UNITED STATES DEPARTMENT OF AGRICULTURE, 1997. PREDICTING SOIL
EROSION BY WATER: A GUIDE TO CONSERVATION PLANNING WITH THE
REVISED UNIVERSAL SOIL LOSS EQUATION. FIGURE 3-1: SOIL ERODIBILITY
NOMOGRAPH.**

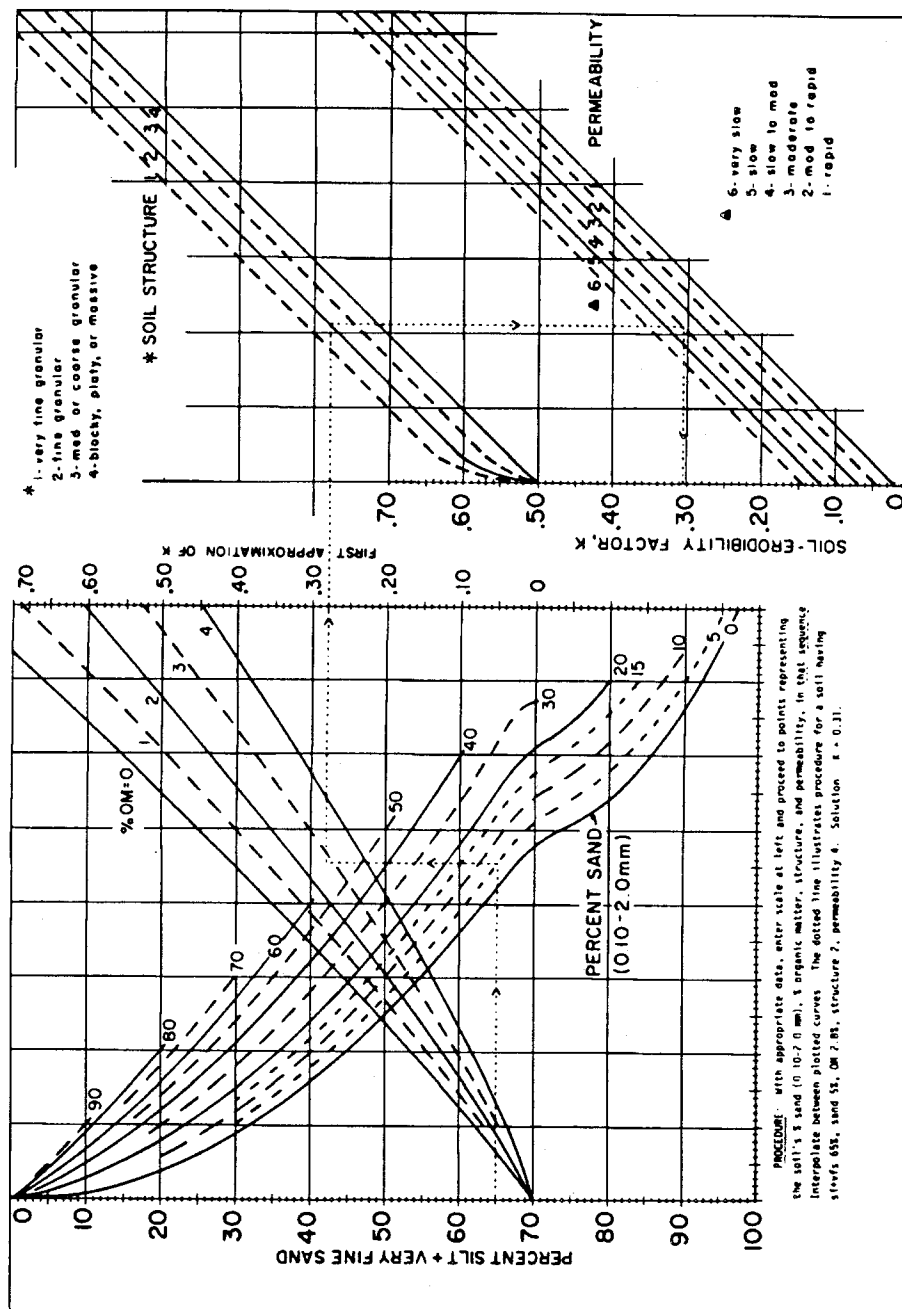


Figure 3-1. Soil-erodibility nomograph (after Wischmeier and Smith 1978). For conversion to SI divide K values of this nomograph by 7.59. K is in U.S. customary units.

**APPLICATION FOR PERMIT RENEWAL AND MODIFICATION
SANDOVAL COUNTY LANDFILL**

**VOLUME III: LANDFILL ENGINEERING CALCULATIONS
SECTION 6: EROSION CALCULATIONS**

ATTACHMENT III.6.E

**GORDON ENVIRONMENTAL, INC. GEOTECHNICAL CLASSIFICATION
SUMMARY, 2004. FOR MOST LIKELY FINAL COVER MATERIEL**

SUMMARY OF GEOTECHNICAL TEST RESULTS
SANDOVAL COUNTY LANDFILL
GORDON ENVIRONMENTAL, Inc.

Sample Number	Sample Depth (fbgs)	USCS Class	Grain Size Distribution			Uniformity Coefficient	Natural Moisture (%)	Standard Proctor		Permeability (cm/sec)
			Pass #10 (%)	Pass #40 (%)	Pass #200 (%)			Max. Dry Density (PCF)	Optimum Moisture (%)	
BH-1	10	SP	88.5	77.6	4.7	3.05	2.5			
BH-1	20	SP-SM	95.5	80.9	7.4	3.04	3.9			
BH-1	35	SP-SM	99.3	91.3	5.4	2.61	4.0			
BH-1	40	SP	98.8	92.2	3.7	2.38	2.6			
BH-2	10	SP-SM	99.9	94.0	9.4	3.17	2.8			
BH-2	20	SP								9.88 E-06
BH-2	25	SP	99.6	95.6	2.6	1.90	3.7			
BH-2	30	SP	99.7	92.4	1.5	1.87	3.5			
BH-2	40	SP	99.7	92.1	1.9	1.85	3.4			
BH-2	40-45	SP						126.3	12.5	
BH-3	10	SP	97.5	89.4	1.6	1.84	2.5			
BH-3	15	SP								2.48 E-06
BH-3	20	SP	91.9	81.9	1.4	1.90	6.8			
BH-3	30	SP	99.1	90.6	1.0	1.80	3.5			
BH-3	35	SP	97.0	72.4	0.6	1.96	3.0			
BH-3	40-45	SP						129.7	10.5	
BH-4	10	SP	96.8	91.9	2.0	1.82	3.4			
BH-4	15	SP	99.8	95.8	1.4	1.79	3.7			
BH-4	20	SP	99.7	93.8	1.5	1.80	4.9			
BH-4	40	SP	99.2	95.2	1.0	1.77	2.8			
BH-5	10	SP	95.6	87.4	0.9	1.83	3.1			
BH-5	20	SP	99.0	95.3	2.0	1.79	2.7			
BH-5	30	SP	98.5	84.8	0.4	1.82	3.0			
BH-5	35	SP	99.9	92.5	0.4	1.77	3.9			
BH-5	40-45	SP						130.6	12.8	
Stockpile		SP	76.9	45.6	0.2	3.34				2.45 E-07

**APPLICATION FOR PERMIT RENEWAL AND MODIFICATION
SANDOVAL COUNTY LANDFILL**

**VOLUME III: LANDFILL ENGINEERING CALCULATIONS
SECTION 6: EROSION CALCULATIONS**

ATTACHMENT III.6.F

**NATURAL RESOURCES CONSERVATION SERVICE, 2010. NATIONAL
ENGINEERING HANDBOOK; COVER FACTOR C VALUES FOR ESTABLISHED
PLANTS. UNITED STATES DEPARTMENT OF AGRICULTURE.**

Cover Factor C Values for Established Plants

(data from NEH chapter 3 and Wischmeier and Smith 1978)

	Percent cover ¹	Plant type	Percentage of surface covered by residue in contact with the soil:					
			0 %	20	40	60	80	95+
C factor for grass, grasslike plants, or decaying compacted plant litter.	0	Grass	0.45	0.20	0.10	0.042	0.013	0.003
C factor for broadleaf herbaceous plants (including most weeds with little lateral root networks), or undecayed residues.	0	Weeds	0.45	0.24	0.15	0.091	0.043	0.011
Tall weeds or short brush with average drop height ² of ≥20 inches	25	Grass	0.36	0.17	0.09	0.038	0.013	0.003
		Weeds	0.36	0.20	0.13	0.083	0.041	0.011
	50	Grass	0.26	0.13	0.07	0.035	0.012	0.003
		Weeds	0.26	0.16	0.11	0.076	0.039	0.011
	75	Grass	0.17	0.10	0.06	0.032	0.011	0.003
		Weeds	0.17	0.12	0.09	0.068	0.038	0.011
Mechanically prepared sites, with no live vegetation and no topsoil, and no litter mixed in.	0	None	0.94	0.44	0.30	0.20	0.10	Not given

¹ percent cover is the portion of the total area surface that would be hidden from view by canopy if looking straight downward.

² drop height is the average fall height of water drops falling from the canopy to the ground.

(from the NRCS's National Engineering Handbook) lists cover management C factors for land covers, with no trees. This table can be applied to construction sites having temporary or permanent vegetative covers, or mulches. It indicates the improved erosion control as the ground coverage increases. With good coverage (more than 80% ground cover), the erosion control could be 95%, or greater. These values assume that the vegetation or mulch is randomly distributed over the entire area. In areas with canopies where the rain drops have much less effective drop heights, and correspondingly less energy, the C factors are further decreased. A mechanically prepared site with no topsoil and no forest residue mixed in would have a C close to 1.0, if no cover was applied. With an 80% cover of mulch, this type of site (indicative of most construction sites) would have about 90% erosion control. In comparison, the C factor for a woodland with 100 percent duff cover (partly decayed organic matter on the forest floor) would be a low 0.0001 (99.99% erosion control), the lowest reported value.

$$C_{50} = \frac{C_{40} + C_{60}}{2} = \frac{0.11 + 0.076}{2} = \frac{0.186}{2} = 0.093$$

**APPLICATION FOR PERMIT RENEWAL AND MODIFICATION
SANDOVAL COUNTY LANDFILL**

**VOLUME III: LANDFILL ENGINEERING CALCULATIONS
SECTION 6: EROSION CALCULATIONS**

ATTACHMENT III.6.G

**NATURAL RESOURCES CONSERVATION SERVICE, 2002, SECTION 501.35;
SUPPORT PRACTICE FACTOR, P; FROM NATIONAL AGRONOMY MANUAL, 190-
V-NAM, THIRD EDITION, WASHINGTON, D.C.: UNITED STATES DEPARTMENT
OF AGRICULTURE**

meability and organic matter content. Values for K should be selected from those given in the NRCS soil survey database in NASIS or in published reports the RUSLE soil erodibility nomograph can also be used to estimate K values for most soils. Soil erodibility K varies by season. It tends to be high in early spring during and immediately following thawing, and other periods when the soil is wet. NRCS further modifies the seasonally adjusted K by rounding the value to the nearest K factor class or half-class (exhibit 501-1).

Rock fragments in the soil profile affect the soil erodibility factor ^{1/}. The K value is adjusted upwards to account for rock fragments in the soil profile of sandy soils that reduce infiltration. No adjustment to the K value is recommended by NRCS for rocks in the profile of medium and heavy textured soils.

501.33 The slope length and steepness factors, L and S

The slope length factor, L, is the ratio of soil loss from the field slope length to soil loss from a 72.6-foot length under identical conditions.

The slope steepness factor, S, is the ratio of soil loss from the field slope gradient to soil loss from a 9 percent slope under otherwise identical conditions.

In erosion prediction as used by NRCS, the factors L and S are evaluated together, and LS values for uniform slopes can be selected from tables 4-1, 4-2, 4-3, and 4-4 in Agriculture Handbook 703.

The slope length is defined as the horizontal distance from the origin of overland flow to the location of either concentrated flow or deposition. Slope lengths normally do not exceed 400 feet because sheet and rill flows will almost always coalesce into concentrated flow paths within that distance. Lengths longer than 1,000 feet should not be used in RUSLE.

Slope length and steepness determinations are best made in the field. In conservation planning, the hillslope profile representing a significant portion of the field having the most severe erosion is often chosen. Slope lengths are best determined by pacing out flow paths and making measurements

directly on the ground. Steep slopes should be converted to horizontal distances. Slope steepness determinations are best made in the field using a clinometer, Abney level or similar device. Chapter 4, Agriculture Handbook 703 contains additional guides for choosing and measuring slopes.

Most naturally occurring hillslope profiles are irregular in shape. When the slope profile is significantly curved (convex or concave, or sigmoid), convex at the shoulder and concave at the toe, the conservationist should represent it as a series of slope segments, using the irregular slope procedure in the RUSLE computer program.

501.34 The cover-management factor, C

The cover-management factor, C, is the ratio of soil loss from an area with specified cover and management to soil loss from an identical area in tilled continuous fallow. The C factor is used most often to compare the relative impacts of management options on conservation plans.

The impacts of cover and management on soil losses are divided into a series of subfactors in RUSLE. These include the impacts of previous vegetative cover and management, canopy cover, surface roughness, and in some cases the impact of soil moisture.

In RUSLE, these subfactors are assigned values, and when multiplied together yield a soil loss ratio (SLR). Individual SLR values are calculated for each period over which the important parameters are assumed to remain constant. Each SLR value is then weighted by the fraction of rainfall and runoff erosivity, EI, associated with the corresponding period, and these weighted values are combined (summed) into an overall C factor value.

501.35 The support practice factor, P

The support practice factor, P, is the ratio of soil loss with a support practice like contouring, stripcropping, or terracing to soil loss with straight-row farming up and down the slope.

The contour P subfactor accounts for the beneficial effects of redirected runoff that modifies the flow pattern because of ridges or oriented roughness that are partially or completely oriented along the contour.

^{1/} Rock fragments on the soil surface are accounted for in the C factor.

The contour P subfactor includes the effects of storm severity, ridge height, off-grade contouring, slope length and steepness, infiltration, and soil cover and roughness.

The stripcropping P subfactor is a support practice where strips of clean-tilled or nearly clean-tilled crops are alternated with strips of close growing vegetation, or strips with relatively smooth tilled soil surfaces are alternated with strips with rough tilled surfaces.

The stripcropping P subfactor evaluates what are variously described as contour stripcropping, cross-slope stripcropping, field stripcropping, buffer strips and vegetated filter strips.

Terraces in RUSLE are support practices where high and large ridges of soil are constructed across the slope at intervals. These ridges and their accompanying channels intercept runoff and divert it around the slope or into a closed outlet. Terraces can affect sheet and rill erosion by reducing slope length and cause deposition in the terrace channel.

Tile drainage, under optimum conditions, can reduce erosion by reducing runoff. Because of a lack of support data, NRCS does not use the tile drainage subfactor in RUSLE, except in the Willamette Valley in the Oregon and Puget Sound basin in Washington.

In addition to the support practice factor, P, used in conservation planning, RUSLE estimates sediment yield for contour strips and terraces. The sediment yield, or delivery ratio, used in RUSLE is the ratio to the amount of sediment leaving the end of the slope length to the amount of sediment produced on the slope length.

Subpart 501E Principles of water erosion control

501.40 Overview of principles

The principle factors that influence soil erosion by water are climate, soil properties, topography, vegetative cover, and conservation practices. Climate and soil properties are conditions of the site and are not modified by ordinary management measures. Conservation treatment primarily involves manipulation of vegetative cover, modification of topography, and manipulation of soil conditions in the tillage zone.

The greatest deterrent to soil erosion by water is vegetative cover, living or dead, on the soil surface. Cover and cultural practices influence both the detachment of soil particles and their transport. Growing plants and plant residue absorb the energy of raindrops, decrease the velocity of runoff water, and help create soil conditions that resist erosion. Cultural practices that affect vegetative cover include crop rotations, cover crops, management of crop residue, and tillage practices.

501.41 Relation of control to RUSLE factors

In conservation planning, the cover and management factor, C, and the support practices factor, P, can be manipulated in RUSLE to develop alternatives for erosion reduction. In addition, where slope length is reduced with some terrace and diversion systems, the slope length and steepness factor, LS, will be reduced.

Using RUSLE technology, estimates of erosion reduction are illustrated in the subfactors of factor C.

Benefits to erosion control are achieved in the:

- prior land use subfactor by increasing the mass of roots and buried residue and increasing periods since soil disturbance,
- canopy cover subfactor by increasing the canopy cover of the field area and low raindrop fall height from the canopy,
- surface cover subfactor by increasing the ground cover of plant residue, and by permanent cover such as rock fragments,
- surface roughness subfactor by increasing the random surface roughness that ponds water, and thereby reduces the erosive effect of raindrops and traps sediment, and

**APPLICATION FOR PERMIT RENEWAL AND MODIFICATION
SANDOVAL COUNTY LANDFILL**

**VOLUME III: LANDFILL ENGINEERING CALCULATIONS
SECTION 6: EROSION CALCULATIONS**

ATTACHMENT III.6.H

**NATURAL RESOURCES CONSERVATION SERVICE, 2002, EXHIBIT 502-2 – WIND
EROSION IN NATIONAL AGRONOMY MANUAL, 190-V-NAM, THIRD EDITION,
OCTOBER 2002, PART 502, WIND ERODIBILITY GROUPS & WIND ERODIBILITY
INDEX. WASHINGTON, D.C.: UNITED STATES DEPARTMENT OF
AGRICULTURE.**

Exhibit 502–2

Wind erodibility groups and wind erodibility index

Soil texture ¹	EWE texture wetness factor ²	Predominant soil texture class of surface layer	Wind Erodibility Group ³ (WEG) ³	Soil Erodibility Index (I) ^{4, 5} (ton/ac/yr)	Soil Erodibility Index (I) for irrigated soils (ton/ac/yr) ⁴
C	1	Very fine sand, fine sand, sand, or coarse sand	1	310 ⁴	310
				250	250
				220	220
				180	160
				160	134
C	1	Loamy very fine sand, loamy fine sand, loamy sand, loamy coarse sand, sapric organic soil materials, and all horizons that meet andic ⁶ soil properties as per Criteria 2 in Soil Taxonomy, regardless of the fine earth texture	2	134	104
C	1	Very fine sandy loam, fine sandy loam, sandy loam, coarse sandy loam, and noncalcareous silt loam with 35 to 50% very fine sand and <10% clay	3	86	56
F	3	Clay, silty clay, non-calcareous clay loam, or silty clay loam with more than 35% clay	4	86	56
M	2	Calcareous ⁷ loam and silt loam or calcareous clay loam and silty clay loam	4L	86	56
M	2	Non-calcareous loam and silt loam with more than 20% clay (but does not meet WEG 3 criteria), or sandy clay loam, sandy clay, and hemic organic soil materials	5	56	38
M	2	Non-calcareous loam and silt loam with more than 20% clay, or non-calcareous clay loam with less than 35% clay or silty clay loam with less than 35% clay	6	48	21
M	2	Silt and fibric organic soil material	7	38	21
—	—	Soils not susceptible to wind erosion because of surface rock and pararock fragments or wetness	8	—	—

1/ Soil texture, C = Coarse; M = Medium; F = Fine

2/ Texture wetness factor for adjustment of Erosive Wind Energy (EWE) for the period (Irrigated fields only).

3/ For all WEGs except sand and loamy sand textures, if percent rock and pararock fragments (>2mm) by volume is 15-35, reduce **I** value by one group with more favorable rating. If percent rock and pararock fragments by volume is 35-60, reduce **I** value by two favorable groups except for sands and loamy sand textures which are reduced by one group with more favorable rating. If percent rock and pararock fragments by volume is more than 60, use **I** value of zero for all textures except sands and loamy sand textures which are reduced by three groups with more favorable rating.

4/ The wind erodibility index is based on the relationship of dry soil aggregates greater than 0.84 millimeters to potential soil erosion. Value for irrigated soils is applicable throughout the year. Values for irrigated soils determined by Dr. E.L. Skidmore, USDA, ARS, Wind Erosion Research Unit, Manhattan, Kansas.

5/ The **I** factor for WEG 1 vary from 160 for coarse sands to 310 for very fine sands. Use an **I** value of 220 as an average figure.

6/ Vitrandic, Vitritrandic, and Vitixerandic Subgroups with ashy textural modifiers move one group with less favorable rating.

7/ Calcareous is a strongly or violently effervescent reaction of the fine-earth fraction to cold dilute (IN) HCL.

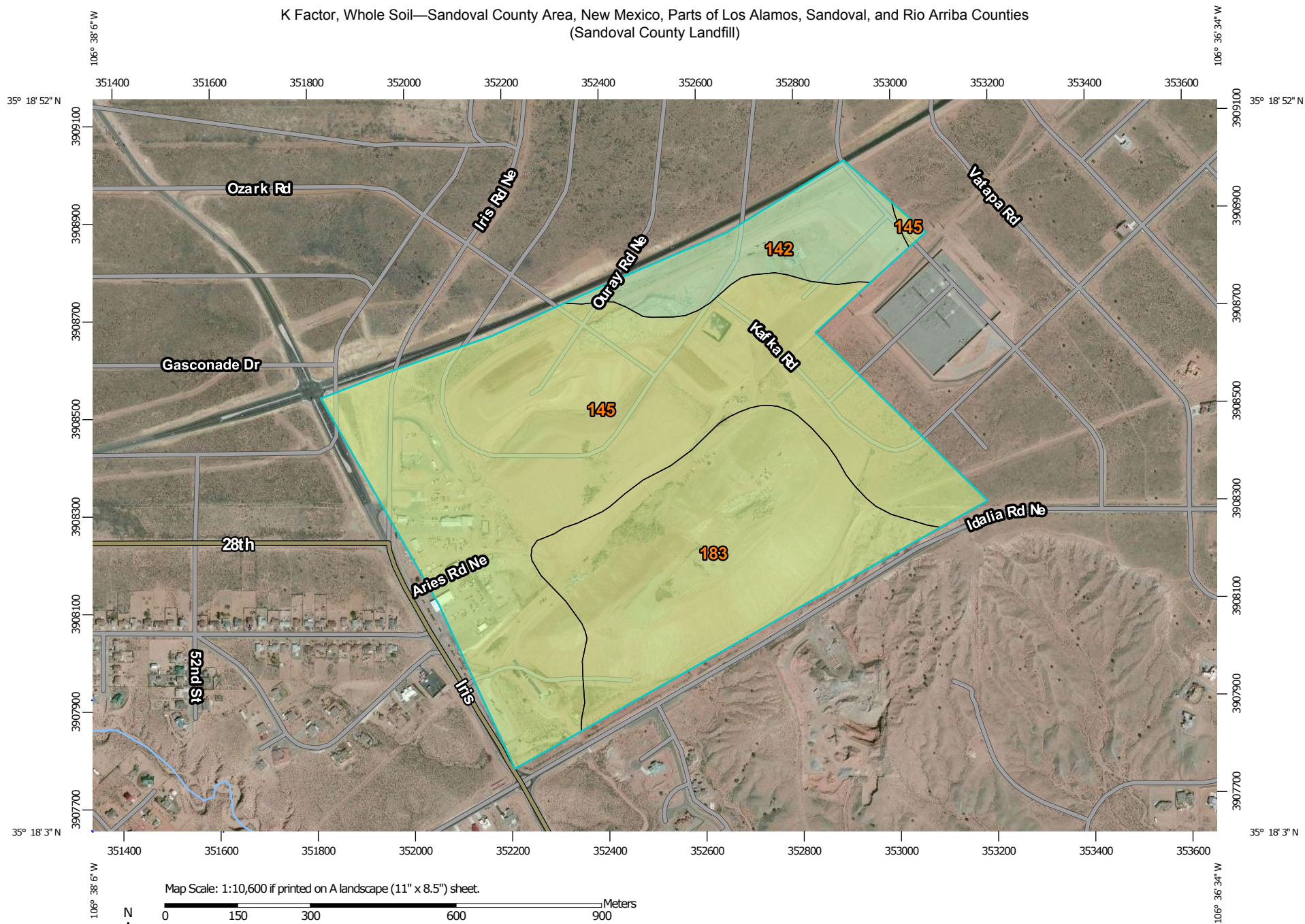
**APPLICATION FOR PERMIT RENEWAL AND MODIFICATION
SANDOVAL COUNTY LANDFILL**

**VOLUME III: LANDFILL ENGINEERING CALCULATIONS
SECTION 6: EROSION CALCULATIONS**

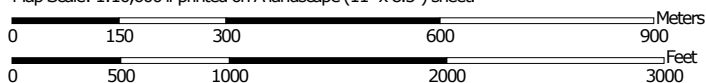
ATTACHMENT III.6.I

**NATURAL RESOURCES CONSERVATION SERVICE. K-FACTOR TABLE, WEB
SOIL SURVEY. FROM [HTTP://WEBSOILSURVEY.NRCS.USDA.GOV](http://websoilsurvey.nrcs.usda.gov); ACCESSED
OCT. 2014. UNITED STATES DEPARTMENT OF AGRICULTURE.**

K Factor, Whole Soil—Sandoval County Area, New Mexico, Parts of Los Alamos, Sandoval, and Rio Arriba Counties
(Sandoval County Landfill)



Map Scale: 1:10,600 if printed on A landscape (11" x 8.5") sheet.



Map projection: Web Mercator Corner coordinates: WGS84 Edge tics: UTM Zone 13N WGS84




**Natural Resources
Conservation Service**

Web Soil Survey
National Cooperative Soil Survey

4/7/2015
Page 1 of 3







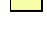


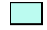





MAP LEGEND

Area of Interest (AOI)







 Area of Interest (AOI)










Soils

Soil Rating Polygons





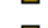










	.02
	.05
	.10
	.15
	.17
	.20
	.24
	.28
	.32
	.37
	.43
	.49
	.55
	.64
	Not rated or not available

Soil Rating Lines



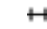




	.02
	.05
	.10
	.15
	.17
	.20

	.24
	.28
	.32
	.37
	.43
	.49
	.55
	.64
	Not rated or not available

Soil Rating Points

	.02
	.05
	.10
	.15
	.17
	.20
	.24
	.28
	.32
	.37
	.43
	.49
	.55
	.64
	Not rated or not available

Water Features

	Streams and Canals
	Rails
	Interstate Highways
	US Routes
	Major Roads
	Local Roads
	Aerial Photography

MAP INFORMATION

The soil surveys that comprise your AOI were mapped at 1:24,000.

Warning: Soil Map may not be valid at this scale.

Enlargement of maps beyond the scale of mapping can cause misunderstanding of the detail of mapping and accuracy of soil line placement. The maps do not show the small areas of contrasting soils that could have been shown at a more detailed scale.

Please rely on the bar scale on each map sheet for map measurements.

Source of Map: Natural Resources Conservation Service
Web Soil Survey URL: <http://websoilsurvey.nrcs.usda.gov>
Coordinate System: Web Mercator (EPSG:3857)

Maps from the Web Soil Survey are based on the Web Mercator projection, which preserves direction and shape but distorts distance and area. A projection that preserves area, such as the Albers equal-area conic projection, should be used if more accurate calculations of distance or area are required.

This product is generated from the USDA-NRCS certified data as of the version date(s) listed below.

Soil Survey Area: Sandoval County Area, New Mexico, Parts of Los Alamos, Sandoval, and Rio Arriba Counties
Survey Area Data: Version 9, Sep 25, 2014

Soil map units are labeled (as space allows) for map scales 1:50,000 or larger.

Date(s) aerial images were photographed: Mar 23, 2011—Mar 24, 2011

The orthophoto or other base map on which the soil lines were compiled and digitized probably differs from the background imagery displayed on these maps. As a result, some minor shifting of map unit boundaries may be evident.

K Factor, Whole Soil

K Factor, Whole Soil— Summary by Map Unit — Sandoval County Area, New Mexico, Parts of Los Alamos, Sandoval, and Rio Arriba Counties (NM656)				
Map unit symbol	Map unit name	Rating	Acres in AOI	Percent of AOI
142	Grieta fine sandy loam, 1 to 4 percent slopes	.28	22.3	10.5%
145	Grieta-Sheppard loamy fine sands, 2 to 9 percent slopes	.24	125.6	59.2%
183	Sheppard loamy fine sand, 8 to 15 percent slopes	.24	64.1	30.2%
Totals for Area of Interest			211.9	100.0%

Description

Erosion factor K indicates the susceptibility of a soil to sheet and rill erosion by water. Factor K is one of six factors used in the Universal Soil Loss Equation (USLE) and the Revised Universal Soil Loss Equation (RUSLE) to predict the average annual rate of soil loss by sheet and rill erosion in tons per acre per year. The estimates are based primarily on percentage of silt, sand, and organic matter and on soil structure and saturated hydraulic conductivity (Ksat). Values of K range from 0.02 to 0.69. Other factors being equal, the higher the value, the more susceptible the soil is to sheet and rill erosion by water.

"Erosion factor Kw (whole soil)" indicates the erodibility of the whole soil. The estimates are modified by the presence of rock fragments.

Rating Options

Aggregation Method: Dominant Condition

Component Percent Cutoff: None Specified

Tie-break Rule: Higher

Layer Options (Horizon Aggregation Method): All Layers (Weighted Average)

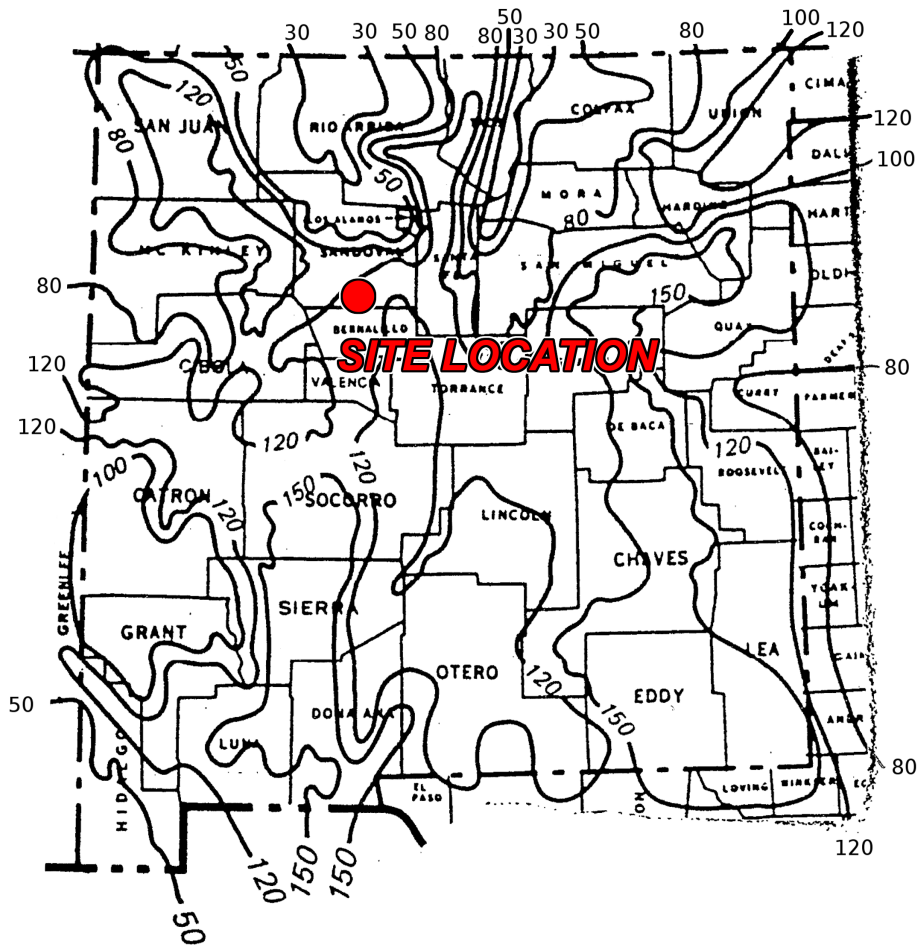
**APPLICATION FOR PERMIT RENEWAL AND MODIFICATION
SANDOVAL COUNTY LANDFILL**

**VOLUME III: LANDFILL ENGINEERING CALCULATIONS
SECTION 6: EROSION CALCULATIONS**

ATTACHMENT III.6.J

**NATURAL RESOURCES CONSERVATION SERVICE, 1992, FIGURE 14 - ANNUAL
“C” VALUE ISOLINE MAP OF THE WIND EROSION EQUATION NEW MEXICO IN
AGRONOMY TECH NOTE 27, JUNE 22, 1992. WASHINGTON, D.C.: UNITED
STATES DEPARTMENT OF AGRICULTURE.**

Annual "C" Values
of the Wind Erosion Equation
New Mexico



**APPLICATION FOR PERMIT RENEWAL AND MODIFICATION
SANDOVAL COUNTY LANDFILL**

**VOLUME III: LANDFILL ENGINEERING CALCULATIONS
SECTION 6: EROSION CALCULATIONS**

ATTACHMENT III.6.K

**NATURAL RESOURCES CONSERVATION SERVICE, 2002, EXHIBIT 502.34 –
UNSHELTERED DISTANCE IN NATIONAL AGRONOMY MANUAL, 190-V-NAM,
THIRD EDITION, OCTOBER 2002, PART 502, WIND EROSION. WASHINGTON,
D.C.: UNITED STATES DEPARTMENT OF AGRICULTURE.**

502.34 Unsheltered distance, L

The L factor represents the unsheltered distance along the prevailing wind erosion direction for the field or area to be evaluated. Its place in the equation is to relate the *isolated, unsheltered, and wide* field condition of **I** to the size and shape of the field for which the erosion estimate is being prepared. Because **V** is considered after **L** in the 5-step solution of the equation (502.22), the unsheltered distance is always considered as if the field were bare except for vegetative barriers.

1. L begins at a point upwind where no saltation or surface creep occurs and ends at the downwind edge of the area being evaluated (figure 502-5). The point may be at a field border or stable area where vegetation is sufficient to eliminate the erosion process. An area should be considered stable only if it is able to trap or hold virtually all expected saltation and surface creep from upwind. If vegetative barriers, grassed waterways, or other stable areas divide an agricultural field being evaluated, each subdivision will be *isolated* and shall be evaluated as a separate

field. Refer to the appropriate NRCS Conservation Practice Standards to determine when practices are of adequate width, height, spacing, and density to create a stable area.

2. When erosion estimates are being calculated for cropland or other relatively unstable conditions, upwind pasture or rangeland should be considered a stable border. However, if the estimate is being made for a pasture or range area, L should be determined by measuring from the nearest stable point upwind of the area or field in question (figure 502-6). The only case where L is equal to zero is where the area is fully sheltered by a barrier.
3. When a barrier is present on the upwind side of a field, measure L across the field along the prevailing wind erosion direction and subtract the distance sheltered by the barrier. Use 10 times the barrier height for the sheltered distance (figure 502-7).

Figure 502-5 Unsheltered distance L

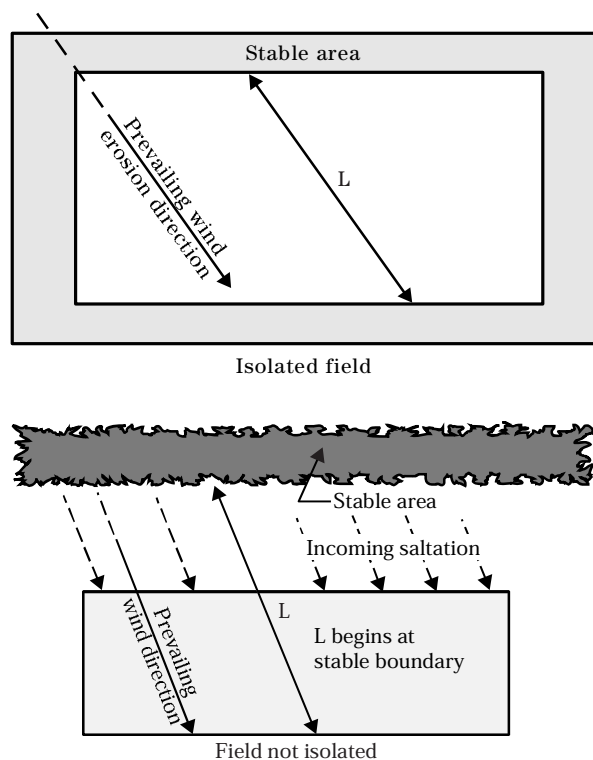


Figure 502-6 Unsheltered distance L, perennial vegetation (pasture or range)

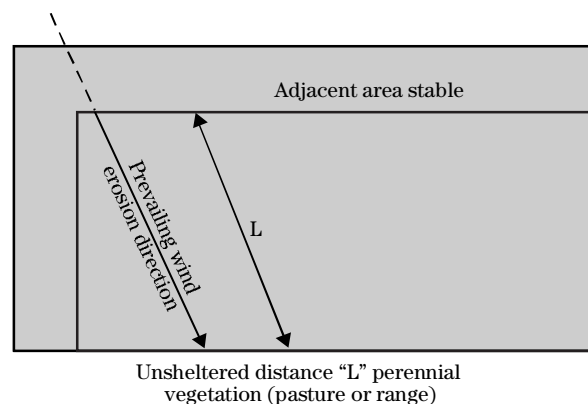
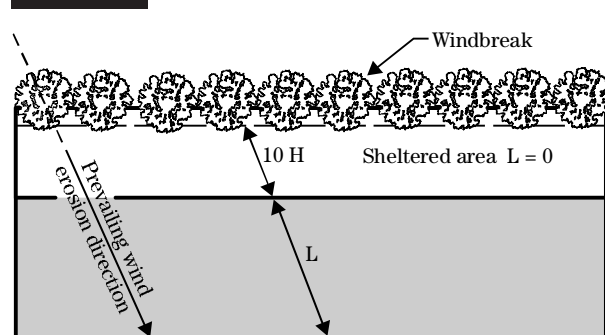


Figure 502-7 Unsheltered distance L – windbreak or barrier



4. When a properly designed wind stripcropping system is applied, alternate strips are protected during critical wind erosion periods by a growing crop or by crop residue. These strips are considered stable. L is measured across each erosion-susceptible strip, along the prevailing wind erosion direction (figure 502–8).

The prevailing wind erosion direction is the direction from which the greatest amount of erosion occurs during the critical wind erosion period. The direction is usually expressed as one of the 16 compass points. When predicting erosion by management periods, the prevailing wind erosion direction may be different for each period (exhibit 502–7a).

Preponderance is a ratio between wind erosion forces parallel and perpendicular to the prevailing wind erosion direction. Wind forces parallel to the prevailing wind erosion direction include those coming from the exact opposite direction (180°). A preponderance of 1.0 indicates that as much wind erosion force is exerted perpendicular to the prevailing direction as along that direction. A higher preponderance indicates that more of the force is along the prevailing wind erosion direction. Wind patterns are complex; low preponderance indicates high complexity and as a result, less wind will be from the prevailing erosive wind direction than locations that have a high preponderance.

L can be measured directly on a map or calculated using a wind erosion direction factor:

- For uses of the Wind Erosion Equation involving a single annual calculation, L should be the measured distance across the area in the prevailing wind erosion direction from the stable upwind edge of the field to the downwind edge of the field. When the prevailing

wind erosion direction is at an angle that is not perpendicular to the long side of the field, L can be determined by multiplying the width of the field by the appropriate conversion factor obtained from table 502-3.

- For management period calculations, wind erosion direction factors based on preponderance are to be used instead of a measured distance to determine L except
 - Where irregular fields cannot be adequately represented by a circle, square, or rectangle.
 - Where preponderance data are not available.

Steps to determine L for management period estimates:

1. Obtain local values for prevailing the wind erosion direction and preponderance (exhibit 502–7a).
2. Measure actual length and width of the field and determine the ratio of length to width.
3. Determine angle of deviation between prevailing wind erosion direction and an imaginary line perpendicular to the long side of the field.

Using data from steps 1 through 3, determine the wind erosion direction factor from wind erosion direction factor tables, tables 502–81 a-e. These are adjustment factors that account for prevailing wind erosion direction, preponderance of wind erosion forces, and size and shape of the field.

Multiply the width of the field by the wind erosion direction factor. This is the L for the field.

If a barrier is on the upwind side of the field, reduce L by a distance equal to 10 times the height of the barrier.

For circular fields, $L = 0.915$ times the diameter, regardless of the prevailing wind erosion direction or preponderance.

Figure 502–8 Unsheltered distance L, stripcropping system

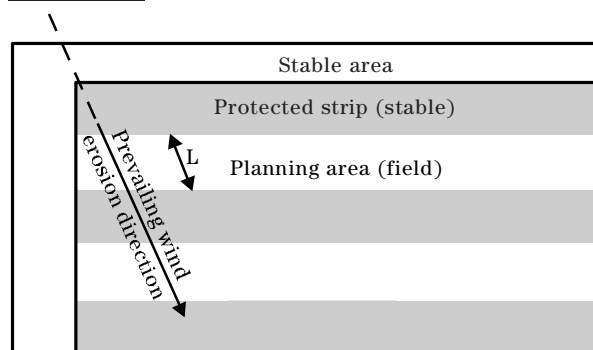


Table 502-3 Wind erosion direction factors ^{1/}

Angle of deviation ^{2/}	Adjustment factor
0	1.00
22.5°	1.08
45°	1.41
67.5°	2.61
90°	L = Length of field

^{1/} These adjustment factors are applicable when preponderance is not considered. L cannot exceed the longest possible measured distance across the field.

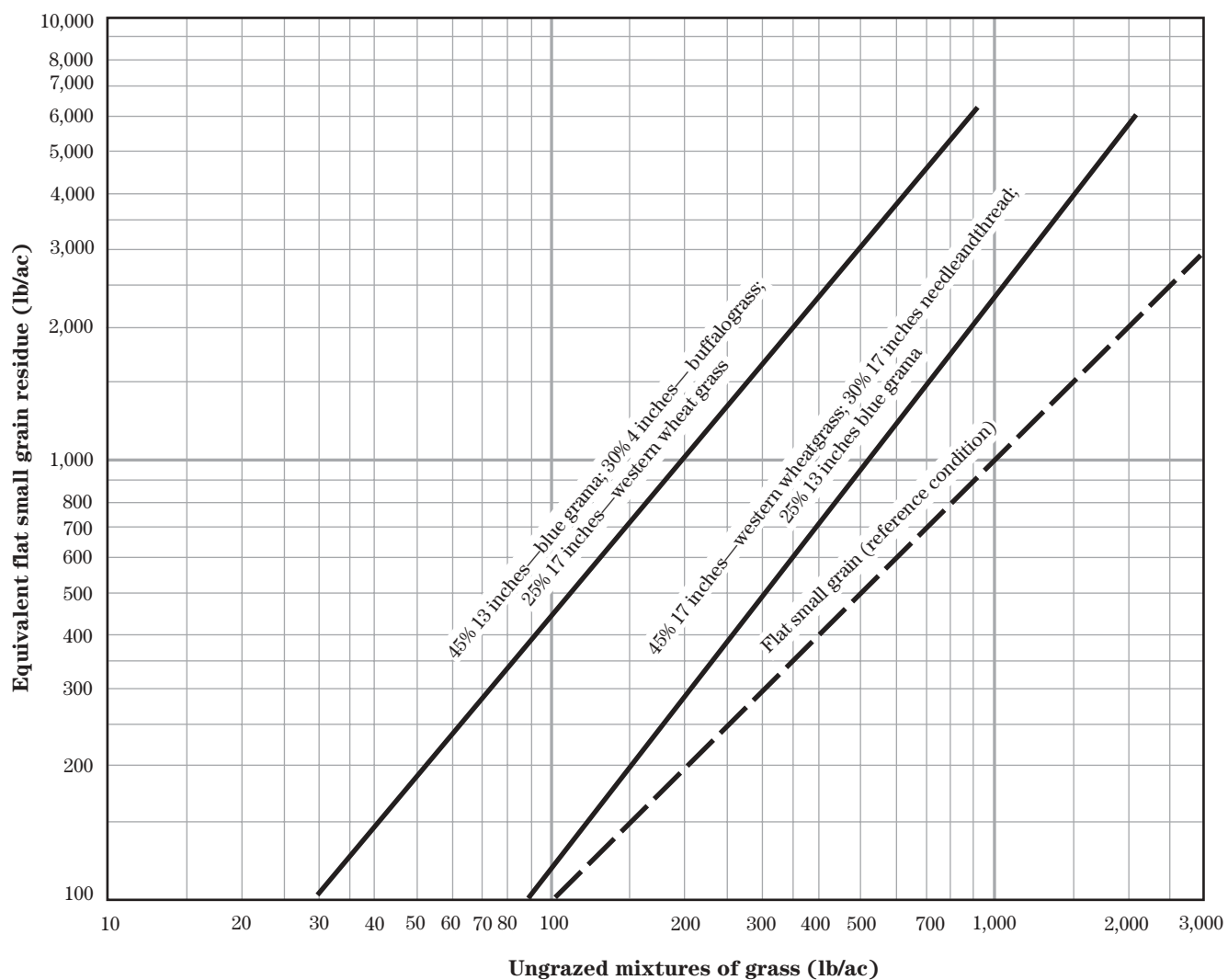
^{2/} Angle of deviation of the prevailing erosive wind from a direction perpendicular to the long side of the field.

**APPLICATION FOR PERMIT RENEWAL AND MODIFICATION
SANDOVAL COUNTY LANDFILL**

**VOLUME III: LANDFILL ENGINEERING CALCULATIONS
SECTION 6: EROSION CALCULATIONS**

ATTACHMENT III.6.L

**NATURAL RESOURCES CONSERVATION SERVICE, 2002, FIGURE 7 - FLAT
SMALL GRAIN EQUIVALENTS OF UNGRAZED MIXTURE OF GRASS IN
NATIONAL AGRONOMY MANUAL, 190-V-NAM, THIRD EDITION, OCTOBER 2002,
PART 502, WIND EROSION. WASHINGTON, D.C.: UNITED STATES DEPARTMENT
OF AGRICULTURE.**

Figured-8 Flat small grain equivalents of ungrazed western wheatgrass, needleandthread, blue grama, and buffalograss mixtures

Reference condition: Dry small grain stalks 10 inches long, lying flat on the soils surface in 10 inch rows perpendicular to wind direction, stalks oriented to wind direction.

Source: Lyles and Allison, 1980, Journal Range Management, 33(2), pages 143-146.

**APPLICATION FOR PERMIT RENEWAL AND MODIFICATION
SANDOVAL COUNTY LANDFILL**

**VOLUME III: LANDFILL ENGINEERING CALCULATIONS
SECTION 6: EROSION CALCULATIONS**

ATTACHMENT III.6.M

**NATURAL RESOURCES CONSERVATION SERVICE, 1998, SUBPART G – EXHIBITS
(C=120, I=134, K=0.20 & K=0.30) IN NATIONAL AGRONOMY MANUAL, 190-V-NAM,
THIRD EDITION, JANUARY 1998. WASHINGTON, D.C.: UNITED STATES
DEPARTMENT OF AGRICULTURE.**

SUBPART G - EXHIBITS

502.60(a)

(E)* SOIL LOSS FROM WIND EROSION IN TONS PER ACRE PER YEAR JANUARY, 1998

C = 120

I = 134

SURFACE - K =0.40

(V)** - FLAT SMALL GRAIN RESIDUE IN POUNDS PER ACRE

(L) UNSHelterED													
DISTANCE IN FEET	0	250	500	750	1000	1250	1500	1750	2000	2250	2500	2750	3000
10000	64.3	55.7	43.8	32.3	18.7	10.2	4.9	2.4	1.2				
8000	64.3	55.7	43.8	32.3	18.7	10.2	4.9	2.4	1.2				
6000	64.3	55.7	43.8	32.3	18.7	10.2	4.9	2.4	1.2				
4000	62.3	53.8	42.3	31.0	17.9	9.6	4.6	2.2	1.1				
3000	60.4	52.1	40.8	29.8	17.1	9.1	4.4	2.1	1.1				
2000	58.0	50.0	39.1	28.4	16.2	8.5	4.0	1.9	1.0				
1000	52.2	44.8	34.7	24.9	13.9	7.1	3.3	1.5	0.7				
800	49.9	42.8	33.0	23.5	13.0	6.6	3.0	1.3	0.4				
600	45.8	39.1	29.9	21.1	11.5	5.7	2.5	1.1	0.3				
400	41.0	34.9	26.5	18.4	9.8	4.7	2.0	0.9	0.3				
300	37.4	31.7	23.9	16.4	8.6	4.0	1.7	0.6					
200	32.2	27.1	20.2	13.6	7.0	3.1	1.3	0.4					
150	27.3	22.9	16.8	11.1	5.5	2.3	0.9						
100	23.1	19.2	13.9	9.0	4.3	1.8	0.7						
80	20.7	17.1	12.3	7.8	3.7	1.5	0.5						
60	16.2	13.3	9.4	5.8	2.6	1.0							
50	14.1	11.5	8.0	4.9	2.1	0.8							
40	12.3	10.0	6.9	4.1	1.8	0.4							
30	9.2	7.4	5.0	2.9	1.2	0.3							
20	5.0	4.0	2.5	1.4	0.4								
10	1.9	1.5	0.8										

(E)* SOIL LOSS FROM WIND EROSION IN TONS PER ACRE PER YEAR JANUARY, 1998

C = 120

I = 134

SURFACE - K =0.30

(V)** - FLAT SMALL GRAIN RESIDUE IN POUNDS PER ACRE

(L) UNSHelterED													
DISTANCE IN FEET	0	250	500	750	1000	1250	1500	1750	2000	2250	2500	2750	3000
10000	48.2	41.3	31.7	22.5	12.4	6.2	2.8	1.2	0.4				
8000	48.2	41.3	31.7	22.5	12.4	6.2	2.8	1.2	0.4				
6000	48.2	41.3	31.7	22.5	12.4	6.2	2.8	1.2	0.4				
4000	45.9	39.2	30.1	21.2	11.6	5.7	2.5	1.1	0.3				
3000	44.4	37.9	28.9	20.3	11.0	5.4	2.4	1.0	0.3				
2000	41.0	34.8	26.4	18.4	9.8	4.7	2.0	0.9	0.3				
1000	35.8	30.3	22.7	15.5	8.1	3.7	1.6	0.5					
800	33.8	28.5	21.3	14.5	7.5	3.4	1.4	0.5					
600	31.1	26.1	19.4	13.0	6.6	2.9	1.2	0.4					
400	26.2	21.9	16.0	10.5	5.2	2.2	0.8						
300	23.5	19.5	14.1	9.2	4.4	1.8	0.7						
200	19.5	16.1	11.5	7.3	3.4	1.3							
150	15.9	13.0	9.1	5.6	2.5	0.9							
100	13.1	10.7	7.4	4.4	1.9	0.4							
80	11.0	8.9	6.1	3.6	1.5	0.3							
60	8.0	6.4	4.3	2.4	0.8								
50	6.0	4.8	3.1	1.7	0.6								
40	4.6	3.6	2.3	1.2	0.4								
30	3.4	2.7	1.7	0.8									
20	1.7	1.3	0.7										
10													

* NOTE: SOIL LOSS FOR VALUES WHERE 'E' IS LESS THAN 0.1 OR GREATER THAN 440.0 ARE NOT SHOWN; OTHER VALUES NOT SHOWN ARE INVALID

** NOTE: VALUES SHOWN ARE FLAT SMALL GRAIN EQUIVALENT, NOT 'V'

SUBPART G - EXHIBITS

502.60(a)

(E)* SOIL LOSS FROM WIND EROSION IN TONS PER ACRE PER YEAR JANUARY, 1998

C = 120

I = 134

SURFACE - K =0.20

(V)** - FLAT SMALL GRAIN RESIDUE IN POUNDS PER ACRE

(L) UNSHelterED													
DISTANCE IN FEET	0	250	500	750	1000	1250	1500	1750	2000	2250	2500	2750	3000
10000	32.2	27.1	20.1	13.6	6.9	3.1	1.3	0.4					
8000	32.2	27.1	20.1	13.6	6.9	3.1	1.3	0.4					
6000	31.2	26.3	19.5	13.1	6.7	2.9	1.2	0.4					
4000	29.5	24.7	18.3	12.2	6.1	2.7	1.0						
3000	27.4	22.9	16.8	11.1	5.5	2.3	0.9						
2000	24.9	20.8	15.1	9.9	4.8	2.0	0.8						
1000	20.9	17.3	12.4	7.9	3.8	1.5	0.5						
800	19.2	15.8	11.3	7.1	3.3	1.3							
600	16.2	13.3	9.4	5.8	2.6	1.0							
400	13.6	11.1	7.7	4.6	2.0	0.7							
300	11.2	9.1	6.2	3.7	1.6	0.3							
200	8.1	6.5	4.3	2.4	0.8								
150	5.2	4.1	2.6	1.4	0.5								
100	3.8	3.0	1.8	0.9									
80	2.7	2.0	1.2	0.6									
60	1.6	1.2	0.6										
50	1.2	0.9	0.5										
40	0.9	0.5											
30	0.5	0.3											
20													
10													

(E)* SOIL LOSS FROM WIND EROSION IN TONS PER ACRE PER YEAR JANUARY, 1998

C = 120

I = 134

SURFACE - K =0.10

(V)** - FLAT SMALL GRAIN RESIDUE IN POUNDS PER ACRE

(L) UNSHelterED													
DISTANCE IN FEET	0	250	500	750	1000	1250	1500	1750	2000	2250	2500	2750	3000
10000	16.1	13.2	9.3	5.7	2.6	0.9							
8000	15.5	12.7	8.9	5.5	2.5	0.9							
6000	14.7	12.1	8.4	5.1	2.3	0.8							
4000	13.6	11.1	7.7	4.7	2.0	0.7							
3000	12.7	10.3	7.1	4.3	1.9	0.4							
2000	10.9	8.8	6.0	3.5	1.5	0.3							
1000	7.4	5.9	3.9	2.2	0.7								
800	5.9	4.7	3.0	1.6	0.5								
600	4.4	3.4	2.2	1.1	0.4								
400	3.1	2.4	1.5	0.7									
300	2.0	1.5	0.8										
200	1.2	0.9	0.5										
150	0.8	0.4											
100													
80													
60													
50													
40													
30													
20													
10													

* NOTE: SOIL LOSS FOR VALUES WHERE 'E' IS LESS THAN 0.1 OR GREATER THAN 440.0 ARE NOT SHOWN; OTHER VALUES NOT SHOWN ARE INVALID

** NOTE: VALUES SHOWN ARE FLAT SMALL GRAIN EQUIVALENT, NOT 'V'

**APPLICATION FOR PERMIT RENEWAL AND MODIFICATION
SANDOVAL COUNTY LANDFILL**

**VOLUME III: LANDFILL ENGINEERING CALCULATIONS
SECTION 7: GEOSYNTHETICS TENSILE STRESS AND STABILITY ANALYSIS**

TABLE OF CONTENTS

1.0	INTRODUCTION	III.7-1
2.0	DESIGN CRITERIA	III.7-1
3.0	CALCULATION OF TENSILE STRESSES IN UNIT 4 GEOSYNTHETICS DUE TO UNIT I, UNIT II AND UNIT III WASTE OVERFILL	III.7-3
3.1	Method of Analysis.....	III.7-3
3.2	Total and Differential Settlement.....	III.7-3
3.3	Localized Differential Settlement	III.7-13
3.4	Determination of Structural Geogrid Properties	III.7-23
3.5	Conclusions.....	III.7-25
4.0	CALCULATION OF TENSILE STRESSES AND STABILITY OF SIDESLOPE LINER GEOSYNTHETICS DUE TO WASTE PLACEMENT	III.7-26
5.0	CALCULATION OF TENSILE STRESSES IN GEOSYNTHETICS DUE TO EQUIPMENT LOADING	III.7-35
6.0	ANCHOR TRENCH PULLOUT ANALYSIS.....	III.7-37
6.1	Geocomposite HDPE Geogrid Interface.....	III.7-38
7.0	GEOSYNTHETIC SLIPPAGE ANALYSIS.....	III.7-39

LIST OF FIGURES

Figure No.	Title	Page
III.7.1	SIDESLOPE AND FLOOR LINER DETAIL	III.7-42
III.7.2	BASE GRADING PLAN	III.7-43
III.7.3	UNIT IV GEOSYNTHETIC STRAIN ANALYSIS, SECTION A-A'	III.7-44
III.7.4	UNIT IV GEOSYNTHETIC STRAIN ANALYSIS, SECTION B-B'	III.7-45
III.7.5	GEOSYNTHETIC FRICTION FORCES.....	III.7-46
III.7.6	GEOSYNTHETIC SLIPPAGE ANALYSIS.....	III.7-47
III.7.7	GEOSYNTHETIC SLIPPAGE ANALYSIS LOCATION	III.7-48

**APPLICATION FOR PERMIT RENEWAL AND MODIFICATION
SANDOVAL COUNTY LANDFILL**

**VOLUME III: LANDFILL ENGINEERING CALCULATIONS
SECTION 7: GEOSYNTHETICS TENSILE STRESS AND STABILITY ANALYSIS**

LIST OF TABLES

Table No.	Title	Page
III.7.1	SETTLEMENT AND ANGULAR DISTORTION OF FOUNDATION SOILS BETWEEN POINTS, CROSS SECTION A-A', SANDOVAL COUNTY LANDFILL-UNIT 4 OVERFILL ONTO UNIT I.....	III.7-15
III.7.2	SETTLEMENT AND ANGULAR DISTORTION OF WASTE SETTLEMENT BETWEEN POINTS, CROSS SECTION A-A', SANDOVAL COUNTY LANDFILL-UNIT 4 OVERFILL ONTO UNIT I.....	III.7-16
III.7.3	SETTLEMENT AND ANGULAR DISTORTION OF SOILS BETWEEN POINTS, CROSS SECTION A-A', SANDOVAL COUNTY LANDFILL-UNIT 4 OVERFILL ONTO UNIT I.....	III.7-17
III.7.4	TOTAL SETTLEMENT AND ANGULAR DISTORTION BETWEEN POINTS, CROSS SECTION A-A', SANDOVAL COUNTY LANDFILL-UNIT 4 OVERFILL ONTO UNIT I.....	III.7-18
III.7.5	SETTLEMENT AND ANGULAR DISTORTION OF FOUNDATION SOILS BETWEEN POINTS, CROSS SECTION B-B', SANDOVAL COUNTY LANDFILL-UNIT 4 OVERFILL ONTO UNIT II	III.7-19
III.7.6	SETTLEMENT AND ANGULAR DISTORTION OF WASTE SETTLEMENT BETWEEN POINTS, CROSS SECTION B-B', SANDOVAL COUNTY LANDFILL-UNIT 4 OVERFILL ONTO UNIT II.....	III.7-20
III.7.7	SETTLEMENT AND ANGULAR DISTORTION OF SOILS BETWEEN POINTS, CROSS SECTION B-B', SANDOVAL COUNTY LANDFILL-UNIT 4 OVERFILL ONTO UNIT II	III.7-21
III.7.8	TOTAL SETTLEMENT AND ANGULAR DISTORTION BETWEEN POINTS, CROSS SECTION B-B', SANDOVAL COUNTY LANDFILL-UNIT 4 OVERFILL ONTO UNIT II	III.7-22
III.7.9	GEOSYNTHETIC INTERFACE FRICTION ANGLES AND ADHESION – SIDESLOPE, SIDESLOPE NORMAL LOAD.....	III.7-29
III.7.10	GEOSYNTHETIC INTERFACE FRICTION ANGLES AND ADHESION – SIDESLOPE, FLOOR NORMAL LOAD.....	III.7-30
III.7.11	GEOSYNTHETIC INTERFACE FRICTION ANGLES AND ADHESION – SIDESLOPE LINER SYSTEM.....	III.7-31
III.7.12	GEOSYNTHETIC INTERFACE FRICTION ANGLES AND ADHESION – FLOOR LINER SYSTEM.....	III.7-32
III.7.13	SOIL INTERNAL FRICTION ANGLE AND COHESION.....	III.7-33
III.7.14	TRANSLATIONAL FAILURE ANALYSIS.....	III.7-42

**APPLICATION FOR PERMIT RENEWAL AND MODIFICATION
SANDOVAL COUNTY LANDFILL**

**VOLUME III: LANDFILL ENGINEERING CALCULATIONS
SECTION 7: GEOSYNTHETICS TENSILE STRESS AND STABILITY ANALYSIS**

LIST OF ATTACHMENTS

Attachment No.	Title
III.7.A	SHARMA, HARI D. AND LEWIS, SANGEETA, P. 1994. <i>WASTE CONTAINMENT SYSTEMS, WASTE STABILIZATION, AND LANDFILLS: DESIGN AND EVALUATION</i> . NEW YORK: JOHN WILEY AND SONS.
III.7.B	QIAN, XUEDE; KOERNER, ROBERT M.; AND GRAY, DONALD H. 2002. <i>GEOTECHNICAL ASPECTS OF LANDFILL DESIGN AND CONSTRUCTION</i> . NEW YORK: PRETENCE HALL.
III.7.C	CARTER, M. AND BENTLEY, S.P., <i>CORRELATIONS OF SOIL PROPERTIES</i> , 1991.
III.7.D	CHEN, Y., GAU, D. AND ZHU, B., <i>CONTROLLING STRAIN IN GEOSYNTHETIC LINER SYSTEMS USED IN VERTICALLY EXPANDED LANDFILLS</i> , JOURNAL OF ROCK MECHANICS AND GEOTECHNICAL ENGINEERING (2009), PPS 48-55.
III.7.E	GIROUD, J.P., BONAPARTE, R., BEECH, J.F. AND GROSS, B.A., <i>DESIGN OF SOIL LAYER-GEOSYNTHETIC SYSTEMS OVERLYING VOIDS</i> , GEOTEXTILES AND GEOMEMBRANES 9 (1990), PPS 11-50.
III.7.F	<i>TENSAR UNIAXIAL GEOGRIDS FOR SOIL REINFORCEMENT</i> , TENSAR INTERNATIONAL, 2007.
III.7.G	<i>DETERMINATION OF THE LONG-TERM DESIGN STRENGTH OF FLEXIBLE GEOGRIDS</i> , GRI STANDARD PRACTICE GG4(B), GEOSYNTHETIC INSTITUTE (2013).
III.7.H	THIEL, RICHARD. <i>A TECHNICAL NOTE REGARDING INTERPRETATION OF COHESION (OR ADHESION) AND FRICTION ANGLE IN DIRECT SHEAR TESTS</i> . GEOSYNTHETICS, APRIL MAY 2009 VOLUME 27: PPS 10-19.
III.7.I	THIEL, RICHARD. <i>PEAK VS RESIDUAL SHEAR STRENGTH FOR LANDFILL BOTTOM LINER STABILITY ANALYSIS</i> . THIEL ENGINEERING, OREGON HOUSE, CA.
III.7.J	KOERNER, ROBERT M. ANA KOERNER, GEORGE R. 2007. INTERPETATION(S) OF LABORATORY GENERATED INTERFACE SHEAR STRENGTH DATA FOR GEOSYNTHETIC MATERIALS WITH EMPHISIS ON THE ADHESION VALUE. GRI WHITE PAPER #11. GEOSYNTHETICS INSTITUTE.
III.7.K	“BENTOMAT® GCL DIRECT SHEAR DATABASE (TR-114BM), CETCO® LINING TECHNOLOGIES, 2009
III.7.L	RICHARDSON, CLINTON P., PHD, P.E. 2009. <i>MUNICIPAL LANDFILL DESIGN CALCULATIONS, AN ENTRY LEVEL MANUAL OF PRACTICE</i> ,

**APPLICATION FOR PERMIT RENEWAL AND MODIFICATION
SANDOVAL COUNTY LANDFILL**

**VOLUME III: LANDFILL ENGINEERING CALCULATIONS
SECTION 7: GEOSYNTHETICS TENSILE STRESS AND STABILITY ANALYSIS**

	RICHARDSON ENVIRONMENTAL SOLUTIONS & DESIGN, LLC. UBUILDABOOK, LLC., CAMARILLO, CA.
III.7.M	US FABRICS, INC., <i>WOVEN GEOTEXTILE CATALOG SHEET</i>
III.7.N	GSE LINING TECHNOLOGY, INC., <i>GSE HD TEXTURED PRODUCT DATA SHEET</i>
III.7.O	GSE LINING TECHNOLOGY, INC., GSE 6 OZ FABRINET GEOCOMPOSITE WIDE-WIDTH TENSILE TEST RESULTS.

APPLICATION FOR PERMIT RENEWAL AND MODIFICATION SANDOVAL COUNTY LANDFILL

VOLUME III: LANDFILL ENGINEERING CALCULATIONS SECTION 7: GEOSYNTHETICS TENSILE STRESS AND STABILITY ANALYSIS

1.0 INTRODUCTION

The Sandoval County Landfill (SCLF) is an existing solid waste facility operating in compliance with its current Permits, SWM-050304 and SWM-050304 (SP), and the New Mexico Environment Department (NMED) Solid Waste Rules (20.9.2-2.9.10 NMAC). SCLF is located at 2708 Iris Road NE in Rio Rancho, New Mexico (NM), and occupies 178.3 acres \pm . SCLF is publicly owned and operated by the County of Sandoval (“the County”), and is currently permitted to accept municipal solid waste (MSW), including construction and demolition debris (C&D) and tires, and two special wastes: petroleum contaminated soils (PCS) and sludge.

2.0 DESIGN CRITERIA

The liner system for the Sandoval County Landfill (SCLF) is designed to meet the requirements of the New Mexico Solid Waste Rules 20.9.4 NMAC. More specifically, 20.9.4.13.E.(1)(a) NMAC requires:

“all liners must be able to withstand the projected loading stresses and disturbances from overlying waste, waste cover materials, and equipment operation;”

and further 20.9.4.13.E.(2)(b) NMAC requires:

“any geosynthetic materials installed on slopes greater than 25 percent, or on any slope where waste is projected to be more than 100 feet deep, must be designed to withstand the calculated tensile forces acting upon the geosynthetic materials; the design must consider the maximum friction angle of the geosynthetic with regard to any soil-geosynthetic or geosynthetic-geosynthetic interface and must ensure that overall slope stability is maintained;”

Although the overfill geosynthetic lined sideslopes of the SCLF are designed at a maximum 4H \pm :1V, the maximum depth of waste is greater than 100 feet (ft) in some locations. Tensile stresses in liner components were evaluated using guidelines provided in the following documents:

1. Sharma, Hari D. and Lewis, Sangeeta, P. 1994. *Waste Containment Systems, Waste Stabilization and Landfills: Design and Evaluation*. New York: John Wiley and Sons. (**Attachment III.7.A**).
2. Qian, Xuede; Koerner, Robert M.; and Gray, Donald H. *Geotechnical Aspects of Landfill Design and Construction*. New York: Pretence Hall. (**Attachment III.7.B**).

3. Carter, M. and Bentley, S.P. *Correlations of Soil Properties*, 1991. (**Attachment III.7.C**).
4. Chen, Y., Gau, D. and Zhu, B. *Controlling strain in Geosynthetic Liner Systems used in Vertically Expanded Landfills*. Journal of Rock Mechanics and Geotechnical Engineering, 2009, Pages 48-55. (**Attachment III.7.D**).
5. Giroud, J.P., Bonaparte, R., Beech, J.F., and Gross, B.A. 1990. *Design of Soil Layer-Geosynthetic Systems Overlying Voids*, Geotextiles and Geomembranes (1990) 11-50. (**Attachment III.7.E**).
6. Tensar International, Inc., *Tensar Uniaxial Geogrids for Soil Reinforcement*. 2007. (**Attachment III.7.F**).
7. Geosynthetic Institute. *Determination of the Long-Term Design Strength of Flexible Geogrids*, GRI Standard Practice GG4(b). 2013. (**Attachment III.7.G**).
8. Thiel, Richard. *A Technical Note Regarding Interpretation of Cohesion (or Adhesion) and Friction Angle in Direct Shear Tests*. Geosynthetics, April May 2009 Volume 27: Pages 10-19. (**Attachment III.7.H**).
9. Thiel, Richard. *Peak vs Residual Shear Strength for Landfill Bottom Liner Stability Analysis*. Thiel Engineering, Oregon, CA. (**Attachment III.7.I**).
10. Koerner, Robert M. and Koerner, George R. 2007. *Interpretation(s) of Laboratory Generated Interface Shear Strength Data for Geosynthetic Materials with Emphasis on the Adhesion Value*. GRI White Paper #11. Geosynthetic Institute. (**Attachment III.7.J**).
11. *Bentomat® GCL Direct Shear Database (TR-114BM)*, CETCO® Lining Technologies, 2009. (**Attachment III.7.K**).
12. Richardson, Clinton P., PhD, P.E. 2009. *Municipal Landfill Design Calculations, An Entry Level Manual of Practice*. Richardson Environmental Solutions & Design, LLC., UBUILDABOOK, LLC, Camarillo, CA. (**Attachment III.7.L**).
13. US Fabrics, Inc. *Woven Geotextile Catalog Sheet*. (**Attachment III.7.M**).
14. GSE Lining Technology, Inc. *GSE HD Textured Project Data Sheet*. (**Attachment III.7.N**).
15. GSE Lining Technology, Inc. *GSE 6 oz Fabrinet Geocomposite Wide-Width Tensile Test Results* (**Attachment III.7.O**).

The liner design for the landfill sideslopes and floor (**Figure III.7.1**), from top to bottom, consists of the following components below the new waste being placed in Unit IV; and “overfill” above over Unit I, Unit II and Unit III (**Figures III.7.2, III.7.3 and III.7.4**):

- 24-inches (in.) protective soil layer (on-site typically “SP-SM” soils)
- 60-mil double-sided textured HDPE liner
- Geosynthetic clay liner
- 10 oz/yd²/Geonet Geocomposite (Gas Collection – Units I and II overfill only)
- Structural Geogrid
- Compacted structural fill (common soils); varying depth

3.0 CALCULATION OF TENSILE STRESSES IN UNIT 4 GEOSYNTHETICS DUE TO UNIT I, UNIT II AND UNIT III WASTE OVERFILL

The incorporation of the geosynthetic liner system on the slopes overlying existing waste in Units I, II and III (**Figures III.7.2, III.7.3 and III.7.4**) make it necessary to consider “overfill” design aspects for the system that are not commonly required when designing geosynthetic liners systems on stable compacted subgrade soils. The analysis and design for the SCLF geosynthetic liner system over Units I, II and III address the following critical issues regarding the SCLF vertical landfill expansion:

- Limited overall settlement of the existing in-place waste in Units I, II and III could occur during and after overfill waste placement, and could introduce stresses in the sideslope geosynthetic liner system components. A determination of the effect of settlement on the integrity and stability of the components is required.
- Localized areas of excessive waste settlement represent the worst-case scenario, and the design of the geosynthetic liner system components is required to address this scenario.
- The number of geosynthetic components proposed for the liner system results in a number of interfaces along the frictional resistance surfaces require the determination of the location and magnitude of critical friction angles for each.

3.1 Method of Analysis

The methods used to evaluate the tensile stresses in the geosynthetic liner system over the existing waste in Units I, II and III include the following:

1. Estimate the overall total settlement of the existing waste and foundation soils using the procedure established by Sowers (1993) to determine liner system component deformations due to the weight and decomposition of the existing waste due to the superimposed weight of the additional overfill waste.
2. Estimate the tensile stresses in the geosynthetic liner system components assuming localized differential settlement using reinforced earth and soil arching theory by Terzaghi and presented by Quain, et al, Chen, et al and Giroud, et al (**Attachments III.7.B and III.7.D and III.7.E**, respectively)

3.2 Total and Differential Settlement

The total waste settlement comprises an initial, reasonably rapid, primary consolidation followed by a secondary compression that can continue for decades, which can be a significant portion of the total or ultimate settlement. Settlement characteristics of the existing waste are sensitive to the age of the waste fill and generally become more complex and non-uniform with age. For the purposes in these calculations, the existing waste is conservatively assumed to have the same settlement characteristics as the newly placed overlying waste. This is extremely conservative, as

some of the waste (i.e., Unit I) is over 40 years old, and significant additional settlement is unlikely. “Differential settlement” associated with the underlying waste may impact the structural fill soils; and these calculations as used to determine the degree of settlement and the resulting strain in the geosynthetic liner system components.

Load-related compressibility of waste (primary consolidation) is expressed as:

$$\Delta H_c = C_c \frac{H_o}{1 + e_o} \log \frac{\sigma_i}{\sigma_o} \quad \text{Equation 12.4, Attachment III.2.B, p. 449}$$

Where:

- ΔH_c = Primary settlement
- C_c = Primary compression index
- H_o = Initial thickness of the waste layer before settlement
- e_o = Waste void ratio before settlement
- σ_o = Previously applied pressure in waste layer
- σ_i = Total overburden pressure applied at the mid-level of the waste layer

Long-term secondary consolidation is a function of void ratio and can be expressed by:

$$\Delta H_s = C_a \left[\frac{H_o}{1 + e_o} \right] \log \frac{t_2}{t_1} \quad \text{Equation 12.6, Attachment III.2.B, p.450}$$

Where:

- ΔH_s = Secondary settlement
- C_a = Secondary compression index
- H_o = Waste thickness at start of secondary settlement
- e_o = Waste void ratio
- t_1 = Starting time of secondary settlement
- t_2 = Ending time of secondary settlement

3.2.1 *Foundation Soils Settlement*

The methodology for estimating the potential foundation settlement involves selecting pertinent points on the surface of the landfill (**Figures III.7.3 and III.7.4**), computing the settlement at each point, and evaluating the resultant change in foundation soil elevations. Points were selected from Cross Sections A – A’ and B – B’ (**Figures III.7.3 and III.7.4**, respectively) where the existing waste, newly vertical expansion waste and soil material profile is shown. Qian et al. (2002), presents a method to determine landfill foundation settlement that evaluates elastic, primary, and secondary settlement. Geotechnical analyses of on-site soils indicate that the soils available at the SCLF site consist primarily of a mixture of silts and sands (i.e., SP-SM, sandy silt). **Attachment III.7.A** provides a summary of the laboratory testing results compiled from samples collected at

the SCLF site. Since the foundation soils consist primarily of silty sands, elastic settlement is conservatively assumed for this calculation. The elastic settlement is estimated using the equation:

$$Z_e = \left(\frac{\Delta\sigma}{M_s} \right) H_o \quad \text{Equation 12.20, Attachment III.2.B, p. 469}$$

Where:

- Z_e = elastic settlement of soil layer (ft)
- H_o = initial thickness of soil layer (ft)
- $\Delta\sigma$ = increment of vertical effective stress, lbs/ft²
- M_s = constrained modulus of soil, lbs/ft²

The constrained modulus in Equation 12.20 above is provided by:

$$M_s = \frac{E_s(1 - \nu_s)}{(1 + \nu_s)(1 - 2\nu_s)} \quad \text{Equation 12.21. Attachment III.2.B, p. 470}$$

Where:

- M_s = constrained modulus of soil, lbs/ft²
- E_s = elastic modulus of soil (lbs/ft²) **Attachment III.7.B, p. 310**
 E_s was interpolated from the data from Table 9.5, p. 310 (**Attachment III.7.B**) for GM, SM, ML, and GC, SC with < 20% fines soils between 85% and 95% standard Proctor dry density to determine E_s for 90% as specified in the subgrade soils. $E_s = (1,000 \text{ psi} + 4,100 \text{ psi})/2 = 2,550 \text{ psi}$
 $\times 144 \text{ in}^2/\text{ft}^2 = 367,200 \text{ lbs/ft}^2$
- ν_s = Poisson's ratio for soil = 0.38, which was found using the same method to estimate the elastic modulus of soil

Settlement is estimated at the select locations (Points 0+00 through 7+60, Section A – A' (**Figure III.7.3**), and Points 0+00 through 7+75, Section B – B' (**Figure III.7.4**). An example calculation is demonstrated at point 5+05 on Cross Section A-A', with a total overburden depth of 178.0 ft. (existing waste, structural fill soil + new overfill waste + final cover + intermediate cover + protective soil layer).

Point 5+05, Section A – A' (Figure III.7.3)

Elastic Foundation Soil Settlement:

Unit Weight of Soil = 115 lbs/ft³ standard Proctor dry density

Unit Weight of Waste = 65 lbs/ft³ (industry standard unit weight)

$\Delta\sigma$ = (waste effective stress) + (protective soil layer effective stress) + (intermediate cover effective stress) + (final cover effective stress) + (structural fill effective stress)

Depth of waste (existing and new overlying) = 164.0 ft

Depth of protective soil layer = 4.0 ft

Depth of structural fill layer = 6.0 ft

Depth of final cover layer = 3.0 ft

Depth of intermediate cover soil layer = 1.0 ft

$$\Delta\sigma = (164.0 \text{ ft})(65 \text{ lb/ft}^3) + (4 \text{ ft})(115 \text{ lb/ft}^3) + (1 \text{ ft})(115 \text{ lb/ft}^3) + (3.0 \text{ ft})(115 \text{ lb/ft}^3) + (6.0 \text{ ft})(115 \text{ lb/ft}^3)$$

$$\Delta\sigma = 12,270.0 \text{ lbs/ft}^2$$

$$M_S = \frac{367,200 \frac{\text{lbs}}{\text{ft}^2} (1-0.38)}{(1+0.38)(1-(2)(0.38))} = 687,391.3 \frac{\text{lbs}}{\text{ft}}$$

H_o = 50 ft; the thickness of the compressible soils < 20% (the soil is considered incompressible at the depths below 50 ft).

$$Z_S = \left(\frac{12,270 \frac{\text{lbs}}{\text{ft}^2}}{687,391.3 \frac{\text{lbs}}{\text{ft}}} \right) 50 \text{ ft} = 0.893 \text{ ft} = \text{foundation soil settlement at point 5+05 on}$$

Cross Section A – A' (**Figure III.7.3**).

3.2.2 Waste Settlement Calculations

The methodology to estimate waste settlement involves selecting pertinent points on the final cover surface, computing the settlement at each point, and evaluating the resultant change in surface elevation. Points were selected from Cross Sections A-A' and B-B' (**Figures III.7.3 and III.7.4**, respectively). Qian et al. (2002; **Attachment III.7.B**) refines a method developed by Sowers (1973) for determining settlement in landfills. This method is based on developed soils consolidation theory, which relates settlement to layer thickness and changes in void ratio.

The primary settlement is estimated using the following equation:

$$\Delta H_c = C_c \frac{H_o}{1+e_0} \log \frac{\sigma_i}{\sigma_o} \quad \text{Equation 12.4, Attachment III.7.B, p. 449}$$

Where:

ΔH_c = Primary settlement

C_c = Primary compression index = 0.05 (**Attachment III.2.B, Figure 6.10, p. 202**)

- H_o = Initial thickness of the waste layer before settlement (assume entire thickness of waste from intermediate cover to the top of protective soil layer; this provides a conservative analysis) [**Figure III.7.3**] = 164.0 ft
 e_o = Waste void ratio before settlement = 2.03 (**Attachment III.7.B, p. 188**)
 σ_o = Previously applied pressure in waste layer [assumed to equal the compaction pressure (i.e., waste density) = 1,000 lbs/ft²]
 σ_i = Total overburden pressure applied at the mid-level of the waste layer (lbs/ft²)

Long-term secondary settlement is estimated by the following equation:

$$\Delta H_s = C_\alpha \left[\frac{H_o}{1 + e_o} \right] \log \frac{t_2}{t_1} \quad \text{Equation 12.7, Attachment III.7.B, page 450}$$

Where:

- ΔH_s = Secondary settlement
 C_α = Secondary compression index (Arid Climate, conditions are unfavorable for decomposition) = 0.03(e_o) if $e_o = 2.03$ then (0.03)(2.03) = 0.0609 (**Attachment III.7.B, Figure 6.11, p. 203**)
 H_o = Waste thickness at start of secondary settlement = H-H_c (**Figure III.7.3**)
 e_o = Waste void ratio = 2.03 (**Attachment III.2.B, p. 188**)
 t_1 = Starting time of secondary settlement (1 month = 0.0833 years)
 t_2 = Ending time of secondary settlement = Assume 30 years (conservative as the site must maintain the final cover and landfill for a minimum of 30 years)

Waste settlement calculations for the points (Points 0+00 through 7+60 and Points 0+00 through 7+75) shown on the landfill Cross Sections A - A' and B - B' (**Figures III.7.3 and III.7.4, respectively**).; and presented in **Tables III.7.2 and III.7.6**, respectively.

Point 5+05, Cross Section A – A', Figure III.7.3

Primary Waste Settlement

Maximum Thickness of Waste = 164.0 ft.

$$\Delta H_c = C_c \frac{H_o}{1 + e_o} \log \frac{\sigma_i}{\sigma_o}$$

Where:

- C_c = Primary compression index = 0.05 (**Attachment III.7.B, Figure 6.10, p. 202**)
 H_o = 164.0 ft
 e_o = 2.03 (**Attachment III.2.B, p. 188**)

$$\begin{aligned}\sigma_o &= 1,000 \text{ lbs/ft}^2 \text{ (typical waste density)} \\ \sigma_i &= 0.5[(164.0 \text{ ft})(65 \text{ lbs/ft}^3) + (14.0 \text{ ft})(115 \text{ lbs/ft}^2)] = 6,135 \text{ lbs/ft}^2\end{aligned}$$

$$\Delta H_C = 0.05 \frac{164.0 \text{ ft}}{1 + 2.03} \log \frac{6,135 \frac{\text{lbs}}{\text{ft}^2}}{1,000 \frac{\text{lbs}}{\text{ft}^2}}$$

$$\Delta H_C = 0.05 (54.13 \text{ ft})(\log 6.14 \frac{\text{lbs}}{\text{ft}^2})$$

$$\Delta H_C = 2.13 \text{ ft}$$

Secondary Waste Settlement

$$H_o = 164.0 \text{ ft} - 2.13 \text{ ft} = 161.87 \text{ ft}$$

$$\Delta H_S = 0.0609 \left[\frac{161.87 \text{ ft}}{1 + 2.03} \right] \log \frac{30 \text{ years}}{0.0833 \text{ years}}$$

$$\Delta H_S = 0.0609 [53.42 \text{ ft}] \log (360.14 \text{ years})$$

$$\Delta H_S = 8.32 \text{ ft}$$

$$\text{Total waste settlement} = 2.13 \text{ ft.} + 8.32 \text{ ft.} = 10.45 \text{ ft.}$$

The maximum final settlement of waste is the sum of primary and secondary settlement at point 5+05 on Cross Sections A – A' (**Figure III.7.3**). The waste settlement is conservatively estimated at 2.13 ft. + 8.32 ft. = 10.45 ft. A summary of waste settlement calculations for the points on Cross Sections A – A' and B – B' is provided in **Tables III.7.2** and **III.7.6**, respectively.

3.2.3 Soil Cover and Structural Fill Settlement Calculations

The final cover soil layer consisting of vegetative, barrier, intermediate cover and structural soil fill will also experience nominal consolidation due to its own weight and overburden, as applicable. The method for evaluating settlement of the soil cover and cushion layers is based on following equation:

Primary Soil Settlement

$$\Delta H_P = C_C \left[\frac{H_o}{1 + e_s} \right] \log \frac{P_o + \Delta P}{P_o} \quad \text{Equation B.2, Attachment III.7.A, page 569}$$

e_s = Soil void ratio = 0.83 based on a porosity of 0.453:

$$e_s = \frac{n}{1 - n}$$

Where:

n = Soil Porosity
 e_s = Soil Void Ratio

$$e_s = \frac{0.453}{1-0.453} = 0.83$$

Thickness of Soil = H_o = 3.0 feet of final cover + 1 foot of intermediate cover soil + 4 feet of protective soil layer + 6 feet of structural fill soils = 14.0 ft

Unit Weight of Soil = 115 lb/ft³ Dry Density

$$H_p = 14.0 \text{ ft}$$

$C_c = 0.30 (e_o - 0.27) = 0.16$ (for inorganic, cohesive soil; silt, some clay; silty clay; clay)
[Attachment III.7.C]

$$\Delta P = (3.0 \text{ ft}) (115 \text{ lbs/ft}^3) + (1 \text{ ft}) (115 \text{ lbs/ft}^3) + (4.0 \text{ ft.}) (115 \text{ lbs/ft}^3) + (6.0 \text{ ft.}) (115 \text{ lbs/ft}^3)$$

$$\Delta P = 1,610.0 \text{ lbs/ft}^2$$

$$P_o = \frac{H_o}{2} \left(115 \frac{\text{lbs}}{\text{ft}^3} \right) = \frac{14 \text{ ft}}{2} \left(115 \frac{\text{lbs}}{\text{ft}^3} \right) = 805 \frac{\text{lbs}}{\text{ft}^3}$$

$$\Delta H_p = C_c \left[\frac{H_o}{1 + e_s} \right] \log \frac{P_o + \Delta P}{P_o}$$

$$\Delta H_p = 0.16 \left[\frac{14 \text{ ft}}{1 + 0.83} \right] \log \left[\frac{805 \frac{\text{lbs}}{\text{ft}^3} + 1,610 \frac{\text{lbs}}{\text{ft}^3}}{805 \frac{\text{lbs}}{\text{ft}^3}} \right]$$

$$\Delta H_p = 0.16 (7.65 \text{ ft}) \log(3.0)$$

$$\Delta H_p = 0.584 \text{ ft}$$

Secondary Soil Cover Settlement

$$\Delta H_s = C_s \left[\frac{H_o}{1 + e_o} \right] \log \frac{t_2}{t_1} \quad \text{Equation 12.7, Attachment III.7.B, page 450}$$

C_s = Secondary compression index = 5-10% (C_c) **[Attachment III.7.C]**

Assume $C_s = 0.10 (C_c)$

$$C_s = 0.10 (0.16) = 0.016$$

$$H_o = 14.0 \text{ ft.} - 0.584 \text{ ft.} = 13.42 \text{ ft}$$

$$e_s = 0.83$$

$$t_2 = 30 \text{ years}$$

$$t_1 = 0.0833 \text{ years (1 month)}$$

$$\Delta H_s = 0.016 \left[\frac{13.42 \text{ ft}}{1 + 0.83} \right] \log \frac{30 \text{ years}}{0.0833 \text{ years}}$$

$$\Delta H_s = 0.016 [7.33] \log 360.14$$

$$\Delta H_s = 0.30 \text{ ft}$$

The maximum settlement of the soils is the sum of primary and secondary settlement at point 5+05 on Section A – A' (**Figure III.7.3**). The soils layer settlement is equal to 0.584 ft. + 0.30 ft. = 0.884 ft. Soil settlement calculations for all points shown on Cross Sections A – A' and B – B' are presented in **Tables III.7.3** and **III.7.7**, respectively.

Total settlement for point 5 + 05 on Section A – A' (**Figure III.7.3**):

Total settlement = foundation settlement + waste settlement + soils settlement

Total settlement = 0.893 ft + 10.45 ft + 0.884 ft

Total settlement = 12.23 ft

Total settlement for points shown on Cross Section A – A' and B – B' is presented in **Tables III.7.4** and **III.7.8**, respectively.

3.2.4 Tensile Strain in Geosynthetic Liner System Between Points

The differential settlement between adjacent points is calculated using the equation:

$$\Delta Z_{i,i+1} = Z_{i+1} - Z_i \quad \text{Equation 14.4, Attachment III.7.B, page 550}$$

Where:

$\Delta Z_{i,i+1}$ = differential settlement between points i and $i + 1$

Z_{i+1} = total settlement of point $i + 1$

Z_i = total settlement of point i

$$\Delta Z_{5+05,5+55} = Z_{5+55} - Z_{5+05}$$

$$\Delta Z_{5+05,5+55} = 12.76 \text{ ft} - 12.23 \text{ ft}$$

$$\Delta Z_{5+05,5+55} = 0.53 \text{ ft}$$

The distance between points i and $i + 1$ in their initial positions is calculated using the equation:

$$((L_{i,i+1})_{Initial}) = \left[((X_{i,i+1})^2) + \left\{ ((X_{i,i+1})(\tan B_{Initial}))^2 \right\} \right]^{1/2}$$

Equation 14.7, Attachment III.7.B, page 550

Where:

$$\begin{aligned} X_{i,i+1} &= \text{horizontal distance between points } i \text{ and } i + 1 \\ B_{Initial} &= \text{initial slope angle between points } i \text{ and } i + 1 \\ (L_{i,i+1})_{Initial} &= \text{distance between points } i \text{ and } i + 1 \text{ in their initial position} \end{aligned}$$

The distance between points i and $i + 1$ in their post-settlement positions is calculated using the equation:

$$((L_{i,i+1})_{Final}) = \left[((X_{i,i+1})^2) + \left\{ ((X_{i,i+1})(\tan B_{Initial}) - \Delta Z_{i,i+1}) \right\}^2 \right]^{1/2}$$

Equation 14.8, Attachment III.7.B, page 550

Where:

$$\begin{aligned} X_{i,i+1} &= \text{horizontal distance between points } i \text{ and } i + 1 \\ B_{Initial} &= \text{initial slope angle between points } i \text{ and } i + 1 \\ (L_{i,i+1})_{Final} &= \text{distance between points } i \text{ and } i + 1 \text{ in their post-settlement position} \end{aligned}$$

The tensile strain of the geosynthetic liner system resulting from the settlements is estimated using the following equation:

$$\varepsilon_{i,i+1} = \frac{(L_{i,i+1})_{Final} - (L_{i,i+1})_{Initial}}{(L_{i,i+1})_{Initial}} \times 100\% \quad \text{Equation 14.6, Attachment III.7.B, page 550}$$

Where:

$$\begin{aligned} \varepsilon_{i,i+1} &= \text{tensile strain in liner system between points } i \text{ and } i + 1 \\ (L_{i,i+1})_{Initial} &= \text{distance between points } i \text{ and } i + 1 \text{ in their initial position} \\ (L_{i,i+1})_{Final} &= \text{distance between points } i \text{ and } i + 1 \text{ in their post-settlement position} \end{aligned}$$

For points 5+05 and 5+50 on Section A – A' (**Figure III.7.3**), the tensile strain in the geosynthetic liner system components is as follows:

$$\Delta Z_{5+05,5+55} = 0.53 \text{ ft}$$

The distance between points 5+05 and 5+55 in their initial positions is calculated using the equation:

$$((L_{5+05,5+55})_{Initial}) = \left[((X_{5+05,5+55})^2) + \left\{ ((X_{5+05,5+55})(\tan B_{Initial})) \right\}^2 \right]^{1/2}$$

Where:

$$X_{5+05,5+55} = 50 \text{ ft}$$

$$\tan \beta_{initial} = 0.04$$

$$((L_{5+05,5+55})_{Initial}) = \left[((50 \text{ ft})^2) + \left\{ ((50 \text{ ft})(0.04))^2 \right\} \right]^{1/2}$$

$$((L_{5+05,5+55})_{Initial}) = [2,500 \text{ ft}^2 + \{4.0 \text{ ft}^2\}]^{1/2}$$

$$((L_{5+05,5+55})_{Initial}) = [2,504 \text{ ft}^2]^{1/2}$$

$$((L_{5+05,5+55})_{Initial}) = 50.040 \text{ ft}$$

The distance between points 5+05 and 5 + 55 in their “post-settlement” positions is calculated using the equation:

$$((L_{5+05,5+55})_{Final}) = \left[((X_{5+05,5+55})^2) + \left\{ ((X_{5+05,5+55})(\tan B_{Initial}) - \Delta Z_{i,i+1})^2 \right\} \right]^{1/2}$$

$$((L_{5+05,5+55})_{Final}) = [(2,500 \text{ ft}^2) + \{(2.0 \text{ ft} - 0.53)^2\}]^{1/2}$$

$$((L_{5+05,5+55})_{Final}) = [(2,500 \text{ ft}^2) + \{2.161\}]^{1/2}$$

$$((L_{5+05,5+55})_{Final}) = 50.022 \text{ ft}$$

The tensile strain of the geosynthetic liner system between points 5+05 and 5+55 resulting from the settlements is estimated using the following equation:

$$\varepsilon_{5+05,5+55} = \frac{(L_{5+05,5+55})_{Final} - (L_{5+05,5+55})_{Initial}}{(L_{5+05,5+55})_{Initial}} \times 100\%$$

$$\varepsilon_{5+05,5+55} = \frac{50.022 \text{ ft} - 50.040 \text{ ft}}{50.040 \text{ ft}} \times 100\%$$

$$\varepsilon_{5+05,5+55} = -0.036 \%$$

3.2.5 Summary

The maximum allowable tensile strains for the geosynthetic liner system components are obtained from the project specific laboratory testing or manufacturer’s literature. The maximum allowable tensile strains (i.e., elongation at yield) for the various geosynthetic liner system components that are to utilized in the Unit 4 sideslope and floor systems are based on manufacture’s literature:

1. 60-mil HDPE double-sided textured liner = 12% (typically the value is limited to 10%, which was used in these calculations) [Reference 5, **Attachment III.7.E**]
2. Geosynthetic clay liner = 5 - 16%; average = 10.5% (Reference 2, **Attachment III.7.B**)

3. 10 oz/yd²/200-mil geonet/gas collection geocomposite = based on HDPE manufactured geonet = 10%; geotextiles have an elongation at yield on the order of 15% (woven geotextile elongation at yield, **Attachment III.7.M**)

Based on the vertical expansion settlement calculation results presented in **Tables III.7.4** and **III.7.8**, the maximum strain in the liner system components is 2.09%. The factor of safety (FOS) against tensile strain failure occurs in the HDPE components and is 10%/2.09% = 4.78.

3.3 Localized Differential Settlement

Aside from the overall settlement that could occur along the geosynthetic liner system interface, localized pockets of subsidence in the existing waste fill could also occur. Localized depressions would most likely be temporary and short-term, and represent a “worst-case scenario” since it is more probable that surrounding waste would fill the void. However, this conservative scenario was investigated as part of these calculations to evaluate excessive elongation of the geosynthetic liner system components due to localized settlement. To prevent the excessive elongation of the geosynthetic liner components placed over Units I, II and III, a geosynthetic reinforcement geogrid is incorporated into the liner system design at the interface of the liner system and the top of structural fill (see **Figure III.7.1**); and the structural geogrid’s sole purpose is to limit the potential deflection of the overlying geosynthetic liner system.

The design for localized settlement conservatively assumes that the subsidence would take the form of a six-foot diameter, approximately circular void (i.e., the “collapsing refrigerator effect”), creating a void of infinite depth (**Attachment III.7.D**). Additionally, the maximum strain in the geosynthetic liner system components due to localized settlement was limited to 10%; i.e., 2% less than the yield strength for the HDPE manufactured components of the geosynthetic liner system. The following methodology used in the analysis is based on Terzaghi’s equation for soil arching for a near circular void to determine the pressure exerted on the geosynthetic liner system due to the future waste overlying the liner and void:

$$p = \frac{(\gamma_{avg})(r)}{(2)(K)(\tan \phi)} \left(1 - e^{-2(K)(\tan \phi)\left(\frac{H}{r}\right)} \right) \quad \text{Equation 3, Attachment III.7.D, page 51}$$

TABLE III.7.1
Settlement and Angular Distortion of Foundation Soils Between Points
Cross Section A-A'
Sandoval County Landfill - Unit IV Overfill Onto Unit I

Point Location	Total Depth	$\Delta\sigma$	Total Settlement (feet)	Distance Between Points (feet)	Angular Distortion (%)	Design Base Grade Elevation (feet)	Updated Base Grade Elevation (feet)
0+00	191.0	13,205.00	0.96			5,418.00	5,417.04
0+50	172.0	11,645.00	0.85	50	0.227	5,406.00	5,405.15
0+75	154.0	10,355.00	0.75	25	0.375	5,395.00	5,394.25
1+10	150.0	10,287.90	0.75	35	0.014	5,393.00	5,392.25
1+95	137.0	9,270.00	0.67	85	0.087	5,398.00	5,397.33
2+90	112.0	7,485.00	0.54	95	0.137	5,428.00	5,427.46
3+55	132.0	9,945.00	0.72	65	-0.275	5,450.00	5,449.28
4+05	145.0	10,650.00	0.77	50	-0.103	5,452.00	5,451.23
4+55	163.0	11,310.00	0.82	50	-0.096	5,455.00	5,454.18
5+05	178.0	12,270.00	0.89	50	-0.140	5,456.00	5,455.11
5+55	185.0	12,840.00	0.93	50	-0.083	5,457.00	5,456.07
6+05	202.0	14,060.00	1.02	50	-0.177	5,458.00	5,456.98
6+55	209.0	14,550.00	1.06	50	-0.071	5,460.00	5,458.94
7+05	201.0	14,080.00	1.02	50	0.068	5,461.00	5,459.98
7+40	191.0	13,480.00	0.98	35	0.125	5,462.00	5,461.02
7+60	189.0	13,350.00	0.97	20	0.047	5,462.00	5,461.03

Notes:

Points Correspond to **Figure III.7.3**

Elevations based on NM State Plan Coordinate System

Variables and values used in equations listed in the test:

E_s 367200

ν_s 0.38

H_o 50

M_s 687391.3

TABLE III.7.2
Settlement and Angular Distortion of Waste Settlement Between Points
Cross Section A-A'
Sandoval County Landfill - Unit IV Overfill Onto Unit I

Point Location	Total depth (feet)	Waste Depth (feet)	σ_1	Primary Settlement (feet)	New Waste depth (feet)	Secondary Settlement (feet)	Total Settlement (feet)	Distance Between Points (feet)	Angular Distortion (%)
0+00	191.0	183.00	6,407.50	2.44	180.56	9.28	11.71	50	0.66
0+50	172.0	164.00	5,790.00	2.06	161.94	8.32	10.38	25	0.28
0+75	154.0	148.00	5,155.00	1.74	146.26	7.52	9.25	35	0.10
1+10	150.0	144.00	5,025.00	1.67	142.33	7.31	8.98	85	0.76
1+95	137.0	131.00	4,602.50	1.43	129.57	6.66	8.09	95	2.30
2+90	112.0	93.00	4,115.00	0.94	92.06	4.73	5.67	65	-0.60
3+55	132.0	106.00	4,940.00	1.21	104.79	5.38	6.60	50	-0.67
4+05	145.0	127.00	5,162.50	1.49	125.51	6.45	7.94	50	-0.76
4+55	163.0	150.00	5,622.50	1.86	148.14	7.61	9.47	50	-0.49
5+05	178.0	164.00	6,135.00	2.13	161.87	8.32	10.45	50	-0.21
5+55	185.0	170.00	6,387.50	2.26	167.74	8.62	10.88	50	-0.57
6+05	202.0	186.00	6,965.00	2.59	183.41	9.42	12.01	50	-0.19
6+55	209.0	191.00	7,242.50	2.71	188.29	9.67	12.39	50	0.31
7+05	201.0	182.00	7,007.50	2.54	179.46	9.22	11.76	35	0.27
7+40	191.0	171.00	6,707.50	2.33	168.67	8.67	11.00	20	0.03
7+60	189.0	169.00	6,642.50	2.29	166.71	8.57	10.86		

Notes:

Points Correspond to **Figure III.7.3**

Elevations based on NM State Plane Coordinate System

Variables and values used in equations listed in the text:

C_c 0.05

e_o 2.03

σ_o 1030

C_a 0.0609

TABLE III.7.3
Settlement and Angular Distortion of Soils Between Points
Cross Section A-A'
Sandoval County Landfill - Unit IV Overfill Onto Unit I

Point Location	Total Soil Depth (feet)	AP	P _o	Primary Settlement (feet)	New Soil Depth (feet)	Secondary Settlement (feet)	Total Settlement (feet)	Distance Between Points (feet)	Angular Distortion (%)
0+00	8.0	920.00	460.00	0.33	7.67	0.17	0.51	50	0.00
0+50	8.0	920.00	460.00	0.33	7.67	0.17	0.51	25	0.03
0+75	6.0	690.00	345.00	0.25	5.75	0.13	0.38	35	0.00
1+10	6.0	690.00	345.00	0.25	5.75	0.13	0.38	85	0.00
1+95	6.0	690.00	345.00	0.25	5.75	0.13	0.38	95	-0.78
2+90	19.0	2,185.00	1,092.50	0.79	18.21	0.41	1.20	65	-0.29
3+55	26.0	2,990.00	1,495.00	1.08	24.92	0.56	1.64	50	0.25
4+05	18.0	2,070.00	1,035.00	0.75	17.25	0.39	1.14	50	0.16
4+55	13.0	1,495.00	747.50	0.54	12.46	0.28	0.82	50	-0.03
5+05	14.0	1,610.00	805.00	0.58	13.42	0.30	0.88	50	-0.03
5+55	15.0	1,725.00	862.50	0.63	14.37	0.32	0.95	50	-0.03
6+05	16.0	1,840.00	920.00	0.67	15.33	0.34	1.01	50	-0.06
6+55	18.0	2,070.00	1,035.00	0.75	17.25	0.39	1.14	50	-0.03
7+05	19.0	2,185.00	1,092.50	0.79	18.21	0.41	1.20	35	-0.02
7+40	20.0	2,300.00	1,150.00	0.83	19.17	0.43	1.26	20	0.00
7+60	20.0	2,300.00	1,150.00	0.83	19.17	0.43	1.26		

Notes:

Points Correspond to **Figure III.7.3**

Elevations based on NM State Plan Coordinate System

Variables and Values used in Equations in text:

C_c 0.16

e_s 0.83

C_s 0.016

TABLE III.7.4
Total Settlement and Angular Distortion Between Points
Cross Section A-A'
Sandoval County Landfill - Unit IV Overfill onto Unit I

Point Location	Total Settlement (Z _t) (feet)	ΔZ	Horizontal Distance Between Points (feet)	Original Liner System Elevation (feet)	Slope Between Points Prior to Settlement (foot/foot)	L _{Initial} = Initial Liner Distance Between Points (feet)	Liner System Elevation following Settlement (feet)	L _{Final} = Final Distance Between Points (feet)	Tensile Strain in Liner System (%)
0+00	13.18	1.44	50.00	5418.00	-0.240	51.42	5404.82	51.78	0.692
0+50	11.74	1.35	25.00	5406.00	-0.440	27.31	5394.26	27.88	2.091
0+75	10.39	0.28	35.00	5395.00	-0.057	35.06	5384.61	35.07	0.049
1+10	10.11	-0.96	85.00	5393.00	0.059	85.15	5382.89	85.21	0.073
1+95	9.14	-1.73	95.00	5398.00	0.368	101.24	5388.86	101.85	0.602
2+90	7.42	1.55	65.00	5428.00	0.338	68.62	5420.58	68.14	-0.699
3+55	8.96	0.89	50.00	5450.00	0.040	50.04	5441.04	50.01	-0.055
4+05	9.85	1.26	50.00	5452.00	0.060	50.09	5442.15	50.03	-0.119
4+55	11.11	1.11	50.00	5455.00	0.020	50.01	5443.89	50.00	-0.020
5+05	12.23	0.53	50.00	5456.00	0.040	50.04	5443.77	50.02	-0.037
5+55	12.76	1.29	50.00	5457.00	0.020	50.01	5444.24	50.00	-0.018
6+05	14.04	0.54	50.00	5458.00	0.040	50.04	5443.96	50.02	-0.037
6+55	14.58	-0.60	50.00	5460.00	0.020	50.01	5445.42	50.03	0.031
7+05	13.98	-0.74	35.00	5461.00	0.029	35.01	5447.02	35.04	0.083
7+40	13.24	-0.15	20.00	5462.00	0.000	20.00	5448.76	20.00	0.003
7+60	13.09			5462.00			5448.91		

Notes:
Points Correspond to **Figure III.7.3**
Elevations based on NM State Plan Coordinate System

TABLE III.7.5
Settlement and Angular Distortion of Foundation Soils Between Points
Cross Section B-B'
Sandoval County Landfill - Unit IV Overfill Onto Unit II

Point Location	Total Depth	$\Delta\sigma$	Total Settlement (feet)	Distance Between Points (feet)	Angular Distortion (%)	Design Base Grade Elevation (feet)	Updated Base Grade Elevation (feet)
0+00	154.0	10,410.00	0.76	50	0.170	5,390.00	5,389.24
0+50	136.0	9,240.00	0.67		0.145	5,379.00	5,378.33
1+05	121.0	8,145.00	0.59	75	-0.021	5,365.00	5,364.41
1+80	124.0	8,360.00	0.61	50	-0.019	5,362.00	5,361.39
2+30	126.0	8,490.00	0.62	85	-0.017	5,365.00	5,364.38
3+15	129.0	8,685.00	0.63	50	-0.297	5,372.00	5,371.37
3+65	155.0	10,725.00	0.78	50	-0.132	5,387.00	5,386.22
4+15	162.0	11,630.00	0.85	50	-0.207	5,404.00	5,403.15
4+65	180.0	13,050.00	0.95	35	0.083	5,419.00	5,418.05
5+00	170.0	12,650.00	0.92	50	-0.037	5,430.00	5,429.08
5+50	177.0	12,905.00	0.94	65	-0.007	5,435.00	5,434.06
6+15	181.0	12,965.00	0.94	50	-0.007	5,440.00	5,439.06
6+65	181.0	13,015.00	0.95	50	-0.012	5,441.00	5,440.05
7+15	180.0	13,100.00	0.95	60	0.072	5,444.00	5,443.05
7+75	169.0	12,510.00	0.91			5,446.50	5,445.59

Notes:

Points Correspond to **Figure III.7.4**

Elevations based on NM State Plan Coordinate System

Variables and values used in equations listed in the test:

E_s 367200

v_s 0.38

H_o 50

M_s 687391.3

TABLE III.7.6
Settlement and Angular Distortion of Waste Settlement Between Points
Cross Section B-B'
Sandoval County Landfill - Unit IV Overfill Onto Unit II

Point Location	Total depth (feet)	Waste Depth (feet)	σ_1	Primary Settlement (feet)	New Waste depth (feet)	Secondary Settlement (feet)	Total Settlement (feet)	Distance Between Points (feet)	Angular Distortion (%)
0+00	154.0	146.00	5,205.00	1.73	144.27	7.41	9.14	50	0.62
0+50	136.0	128.00	4,620.00	1.40	126.60	6.50	7.91	55	0.49
1+05	121.0	115.00	4,082.50	1.16	113.84	5.85	7.01	75	-0.15
1+80	124.0	118.00	4,180.00	1.21	116.79	6.00	7.21	50	-0.07
2+30	126.0	120.00	4,245.00	1.24	118.76	6.10	7.35	85	-0.17
3+15	129.0	123.00	4,342.50	1.29	121.71	6.25	7.55	50	-0.68
3+65	155.0	142.00	5,362.50	1.71	140.29	7.21	8.92	50	0.02
4+15	162.0	140.00	5,815.00	1.77	138.23	7.10	8.87	50	-0.47
4+65	180.0	153.00	6,525.00	2.06	150.94	7.76	9.81	35	0.35
5+00	170.0	138.00	6,325.00	1.82	136.18	7.00	8.82	50	-0.36
5+50	177.0	149.00	6,452.50	1.99	147.01	7.55	9.54	65	-0.34
6+15	181.0	157.00	6,482.50	2.10	154.90	7.96	10.06	50	0.03
6+65	181.0	156.00	6,507.50	2.09	153.91	7.91	10.00	50	0.12
7+15	180.0	152.00	6,550.00	2.05	149.95	7.70	9.75	60	0.55
7+75	169.0	138.50	6,255.00	1.82	136.68	7.02	8.84		

Notes:

Points Correspond to **Figure III.7.4**

Elevations based on NM State Plane Coordinate System

Variables and values used in equations listed in the text:

C_c 0.05

e_0 2.03

σ'_o 1030

C_a 0.0609

TABLE III.7.7
Settlement and Angular Distortion of Soils Between Points
Cross Section B-B'
Sandoval County Landfill - Unit IV Overfill Onto Unit II

Point Location	Total Soil Depth (feet)	ΔP	P_o	Primary Settlement (feet)	New Soil Depth (feet)	Secondary Settlement (feet)	Total Settlement (feet)	Distance Between Points (feet)	Angular Distortion (%)
0+00	8.0	920.00	460.00	0.33	7.67	0.17	0.51	50	0.00
0+50	8.0	920.00	460.00	0.33	7.67	0.17	0.51	55	0.07
1+05	6.0	690.00	345.00	0.25	5.75	0.13	0.38	75	0.00
1+80	6.0	690.00	345.00	0.25	5.75	0.13	0.38	50	0.00
2+30	6.0	690.00	345.00	0.25	5.75	0.13	0.38	85	0.00
3+15	6.0	690.00	345.00	0.25	5.75	0.13	0.38	50	-0.22
3+65	13.0	1,495.00	747.50	0.54	12.46	0.28	0.82	50	-0.16
4+15	18.0	2,070.00	1,035.00	0.75	17.25	0.39	1.14	50	-0.28
4+65	27.0	3,105.00	1,552.50	1.13	25.87	0.58	1.70	35	-0.11
5+00	32.0	3,680.00	1,840.00	1.33	30.67	0.69	2.02	50	0.13
5+50	28.0	3,220.00	1,610.00	1.17	26.83	0.60	1.77	65	0.16
6+15	24.0	2,760.00	1,380.00	1.00	23.00	0.51	1.52	50	-0.03
6+65	25.0	2,875.00	1,437.50	1.04	23.96	0.54	1.58	50	-0.09
7+15	28.0	3,220.00	1,610.00	1.17	26.83	0.60	1.77	60	-0.09
7+75	30.5	3,507.50	1,753.75	1.27	29.23	0.65	1.93		

Notes:

Points Correspond to **Figure III.7.4**

Elevations based on NM State Plane Coordinate System

Variables and Values used in Equations in text:

C_c 0.16

e_s 0.83

C_s 0.016

TABLE III.7.8
Total Settlement and Angular Distortion Between Points
Cross Section B-B'
Sandoval County Landfill - Unit IV Overfill onto Unit II

Point Location	Total Settlement (Z _t) (feet)	ΔZ	Horizontal Distance Between Points (feet)	Original Liner System Elevation (feet)	Slope Between Points Prior to Settlement (foot/foot)	L _{Initial} = Initial Liner Distance Between Points (feet)	Liner System Elevation following Settlement (feet)	L _{Final} = Final Distance Between Points (feet)	Tensile Strain in Liner System (%)
0+00	10.40	1.32	50.0	5,390.00	-0.220	51.20	5,379.60	51.49	0.583
0+50	9.09	1.11	55.0	5,379.00	-0.255	56.75	5,369.91	57.04	0.498
1+05	7.98	-0.22	75.0	5,365.00	-0.040	75.06	5,357.02	75.05	-0.011
1+80	8.20	0.14	50.0	5,362.00	0.060	50.09	5,353.80	50.08	-0.017
2+30	8.34	0.22	85.0	5,365.00	0.118	85.59	5,356.66	85.56	-0.029
3+15	8.56	1.96	50.0	5,372.00	0.300	52.20	5,363.44	51.67	-1.014
3+65	10.52	0.33	50.0	5,387.00	0.340	52.81	5,376.48	52.70	-0.201
4+15	10.85	1.61	50.0	5,404.00	0.300	52.20	5,393.15	51.76	-0.845
4+65	12.47	-0.70	35.0	5,419.00	0.314	36.69	5,406.53	36.91	0.593
5+00	11.76	0.49	50.0	5,430.00	0.200	50.99	5,418.24	50.90	-0.184
5+50	12.25	0.27	65.0	5,435.00	0.077	65.19	5,422.75	65.17	-0.031
6+15	12.52	0.01	50.0	5,440.00	0.020	50.01	5,427.48	50.01	0.000
6+65	12.53	-0.05	50.0	5,441.00	0.060	50.09	5,428.47	50.09	0.007
7+15	12.47	-0.79	60.0	5,444.00	0.042	60.05	5,431.53	60.09	0.064
7+75	11.68			5,446.50			5,434.82		

Notes:

Points Correspond to **Figure III.7.4**

Elevations based on NM State Plan Coordinate System

Where: p = pressure exerted on the liner system (lbs/ft²)
 γ_{avg} = average unit weight of additional waste above the void (lbs/ft³)
 r = radius of the void (ft)
 K = lateral earth pressure coefficient

$$K = 1.06 (\cos^2 \theta + K_a \sin^2 \theta) \quad \text{Equation 6, Attachment III.7.E, page 24}$$

$$\text{Where: } \theta = 45^\circ + \frac{\phi}{2} \quad \text{Equation 7, Attachment III.7.E, page 24}$$

$$K_a = \tan^2 \left(45^\circ - \frac{\phi}{2} \right) \quad \text{Equation 8, Attachment III.7.E, page 24}$$

H = height of new waste above the void (ft)

ϕ = internal friction angle of waste

Assuming a nearly circular void six feet in diameter, and using a depth of 72 feet of waste and final cover for point number 3+55 on Section A – A' and point number 5+00 on Section B – B' (Figures III.7.3 and III.7.4, respectively), the variables identified above have the following values:

γ_{avg} = Average unit weight of additional waste and soils above the void (unit weight of waste = 65 lbs/ft³ and unit weight of cover soils = 115 lbs/ft³)

$$\gamma_{avg} = \frac{(68 \text{ ft}) \left(65 \frac{\text{lbs}}{\text{ft}^3} \right) + (3 \text{ ft}) \left(115 \frac{\text{lbs}}{\text{ft}^3} \right)}{72 \text{ ft}} = 66.2 \text{ lbs/ft}^3$$

r = radius of the void = 3.0 ft

H = height of new waste and soil above the void = 72 ft

$$K = 1.06 \left(\cos^2 \left(45^\circ + \frac{\phi}{2} \right) + \left[\left(\tan^2 \left(45^\circ - \frac{\phi}{2} \right) \right) \sin^2 \left(45^\circ + \frac{\phi}{2} \right) \right] \right)$$

$$K = 1.06 \left(\cos^2 \left(45^\circ + \frac{33^\circ}{2} \right) + \left[\left(\tan^2 \left(45^\circ - \frac{33^\circ}{2} \right) \right) \sin^2 \left(45^\circ + \frac{33^\circ}{2} \right) \right] \right)$$

$$K = 1.06 \left(\cos^2 (61.5^\circ) + \left[\left(\tan^2 (28.5^\circ) \right) \sin^2 (61.5^\circ) \right] \right)$$

$$K = 1.06 (0.2277) + [(0.2948)(0.7723)]$$

$$K = 0.2414 + 0.2277$$

$$K = 0.4691$$

Based on these values for the variables, the pressure exerted on the geosynthetic liner system equals:

$$p = \frac{(\gamma_{avg})(r)}{(2)(K)(\tan \phi)} \left(1 - e^{-2(K)(\tan \phi)\left(\frac{H}{r}\right)} \right)$$

$$p = \frac{\left(66.2 \frac{lbs}{ft^3}\right)(3ft)}{(2)(0.4691)(\tan 33^\circ)} \left(1 - e^{-2(0.4691)(\tan 33^\circ)\left(\frac{72ft}{3ft}\right)} \right)$$

$$p = \left(326.0 \frac{lbs}{ft^2}\right) (1 - e^{-14.6})$$

$$p = \left(326.0 \frac{lbs}{ft^2}\right) (1 - 4.56 \times 10^{-7})$$

$$p = \left(326.0 \frac{lbs}{ft^2}\right) (1)$$

$$p = \left(326.0 \frac{lbs}{ft^2}\right)$$

3.4 Determination of Structural Geogrid Properties

The vertical pressure of $326 \frac{lbs}{ft^2}$ is transferred to the proposed geosynthetic reinforcement geogrid in the form of tensile stresses. The design of the geosynthetic reinforcement geogrid is based on this worst-case scenario in which it is assumed that the void is located directly underneath the geosynthetic liner system; and the load the geosynthetic reinforcement geogrid must carry is given by:

$$T_r = (p)(r)(\Omega) \quad \text{Equation 4, Attachment III.7.D, page 51}$$

Where: T_r = Tensile load of geosynthetic reinforcement geogrid
 r = Radius of circular void = 3 ft
 Ω = dimensionless factor related to geosynthetic reinforcement geogrid deflection y or strain \mathcal{E} :

Ω can be determined using **Table 2, Attachment III.7.E, page 27** where Ω is based on an assumed maximum allowable strain, \mathcal{E} , in the geosynthetic reinforcement geogrid. A Tensar UX1400MSE Structural Geogrid is being proposed as the structural support in the SCLF geosynthetic liner system (**Figure III.7.1**). Based on the technical specifications for a Tensar UX1400MSE Structural Geogrid (**Attachment III.7.F**), the ultimate tensile is 4,800 lbs/ft. For the purposes of these calculations, assume a maximum strain of 10% as previously discussed. Based on **Table 2, Attachment III.7.E**, for yield point elongation of 10%, $\Omega = 0.73$.

$$T_r = (326.0 \frac{lbs}{ft^2})(3 ft)(0.73)$$

$$T_r = 684.6 \frac{lbs}{ft}; \text{ Minimum}$$

The ultimate tensile strength of the proposed Tensar UX1400MSE Structural Geogrid is 4,800 lbs/ft (**Attachment III.7.E**). The ultimate tensile strength for the Tensar UX1400MSE Structural Geogrid needs to be adjusted using Reduction Factors as recommended in the “Geosynthetics Institute, GRI Standard Practice GG4(b), *“Determination of the Long-Term Design Strength of Flexible Geogrids”* (**Attachment III.7.F**):

$$T_{allowable} = T_{ultimate} \left[\frac{1}{RF_{ID} \times RF_{CR} \times RF_{CRD} \times RF_{SM}} \right]$$

Where: $T_{allowable}$ = allowable (or design) strength $\left(\frac{lbs}{ft}\right)$

$T_{ultimate}$ = ultimate (or as-manufactured) strength $\left(\frac{lbs}{ft}\right)$

Reduction Factors (RF) are based on **Table 1, Attachment III.7.G** and engineering judgement:

RF_{ID} = reduction factor for installation damage = 1.10 (based on a good CQA program)

RF_{CR} = reduction factor for creep = 2.60

RF_{CRD} = reduction factor for chemical and biological degradation = 1.20
(A HDPE geogrid is resistant to chemical and biological degradation)

RF_{SM} = reduction factor for seams = 1.10 (based on a good CQA program)

$$T_{allowable} = 4,800 \frac{lbs}{ft} \left[\frac{1}{1.10 \times 2.60 \times 1.20 \times 1.10} \right]$$

$$T_{allowable} = 4,800 \frac{lbs}{ft} \left[\frac{1}{3.8} \right]$$

$$T_{allowable} = 4,800 \frac{lbs}{ft} [0.2632]$$

$$T_{allowable} = 1,263.2 \frac{lbs}{ft}$$

$$\text{Factor of Safety} = \frac{T_{allowable}}{T_r} = \frac{1,263.2 \frac{lbs}{ft}}{684.6 \frac{lbs}{ft}}$$

Factor of Safety for the structural geogrid = 1.84 against failure in tension due to localized settlement

3.5 Conclusions

Settlement projections were calculated for the landfill foundation, for the waste mass and for the landfill soils based on the proposed vertical expansion at the SCLF. Settlement estimates include elastic deformation for both primary and secondary consolidation in the:

- Foundations soils
- Existing and new overfill waste
- Compacted structural fill soils
- Liner protective soils
- Final cover soils.

Settlement values for the vertical expansion were calculated to determine the tensile strain in the geosynthetic liner system components; and consisted of two analyses:

- overall settlement of the landfill due to the vertical expansion
- a conservative localized differential settlement beneath the geosynthetic liner system

The geosynthetic liner system components consist of a structural geogrid at the base of the liner system (**Figure III.7.1**); and the tensile strain calculated within the system will be carried by the structural geogrid. The resulting factors of safety against failure due to tensile strains in the geosynthetic liner system components were conservatively computed as:

- Over settlement of the landfill waste and soil components: 4.78
- Localized differential settlement beneath the geosynthetic liner components: 1.84

4.0 CALCULATION OF TENSILE STRESSES AND STABILITY OF SIDESLOPE LINER GEOSYNTHETICS DUE TO WASTE PLACEMENT

External shear forces will develop on the 4H±:1V sideslopes assuming the placement of an initial 2-ft lift of protective soil, and 10-ft lift of waste; assuming the lifts are unsupported and no adhesion (**Attachment III.7.A**, **Attachment III.7.B** and **Attachment III.7.C**). The unbalanced forces, must be supported by the liner components above the interface with the least amount of frictional resistance. **Table III.7.9**, **Table III.7.10**, **Table III.7.11**, **Table III.7.12** and **Table III.7.13** present the interface friction angles and soil internal friction angles to be used to determine the tensile stresses in the geosynthetics that will be installed as part of the vertical expansion geosynthetic liner at SCLF based on the review of the eight (8) references listed in **Section 2.0** above.

Based on the liner design, the geosynthetic interface with the least amount of frictional resistance occurs at the geotextile of the geocomposite to HDPE structural geogrid ($\Phi = 15.30^\circ$) for the sideslopes and ($\Phi = 18.1^\circ$) for the floor. The unbalanced forces, due to the assumed unsupported waste and protective soil layer, are based on the sideslope liner stability calculations presented in Reference 12; *Municipal Landfill Design Calculations: An Entry Level Manual of Practice* (Richardson, 2009) [**Attachment III.7.L**]:

Where given the following:

β	=	slope angle for 4H:1V sideslope = 14.04°
F_x	=	Shear forces that are equal to the product of the normal force ($W_w \cos \beta$) and the tangent of the friction angle between the two neighboring materials.
W_w	=	Weight of Waste.
T_w	=	Friction force on edge of waste.
W_{net}	=	Net weight of waste acting upon the liner system ($W_w - T_w$)
h_{waste}	=	Height of waste layer = 10 ft
h_{soil}	=	Height of protective soil layer = 2 ft
Φ_{waste}	=	Waste internal angle of friction = 33°
Φ_{soil}	=	Soil Internal angle of friction = 33°
Density of waste	=	65 lbs/ft ³
Density of protective soil	=	115 lbs/ft ³ dry density

TABLE III.7.9
Geosynthetic Interface Friction Angles and Adhesion – Sideslope Normal Load
Sandoval County Landfill

Normal Load	Thickness (ft)	Unit Weight (lbs/ft ³)	Total Weight (lbs/ft ²)	Range of Shear Testing Loads ¹ per ASTM D 5321 (lbs/in ²)
1. Final Cover Soil	3	115	345	0.25 (48.0) = 12.0 0.50 (48.0) = 24.0 1.0 (48.0) = 48.0
2. Intermediate Cover Soils	1	115	115	
3. New Overfill Waste	99	65	6,435	
4. Protective Soil Layer	2	115	230	
Design Vertical Load:		Total:	7,125 (49.5 lbs/in ²)	12.0 24.0 48.0
Design Normal Load: [(49.5 lbs/in ²) (cos 14.04°)] = 48.0 lbs/in ²		Total:	48.0 lbs/in ²	

Notes:

1. Liner system components values reported for Φ and Adhesion/Cohesion are based on review of available literature. Interface friction angles for geosynthetics represent peak shear strength values. For the purposes of these calculations, no adhesion/cohesion was assumed providing an additional factor of safety.
2. Geotechnical laboratory testing of on-site soils show predominately silty sands (i.e., SP-SM) soils. For the purposes of these calculations, no cohesion was assumed providing an additional factor of safety.

TABLE III.7.10
Geosynthetic Interface Friction Angles and Adhesion – Floor Normal Load
Sandoval County Landfill

Normal Load	Thickness (ft)	Unit Wt (lbs/ft ³)	Total Wt (lbs/ft ²)	Range of Shear Testing Loads ¹ per ASTM D 5321 (lbs/in ²)
1. Final Cover Soil	3	115	345	0.25 (70.5) = 17.6 0.50 (70.5) = 35.3 1.0 (70.5) = 70.5
2. Intermediate Cover Soils	1	115	115	
3. Waste	144	65	9,360	
4. Protective Soil Layer	2	115	230	
5. Select Aggregate above Pipe	0.75	130	98	
Design Vertical Load:		Total:	10,148 (70.5 lbs/in ²)	17.6 35.3 70.5

Notes:

1. Liner system components values reported for Φ and Adhesion/Cohesion are based on review of available literature. Interface friction angles for geosynthetics represent peak shear strength values. For the purposes of these calculations, no adhesion/cohesion was assumed providing an additional factor of safety.
2. Geotechnical laboratory testing of on-site soils show predominately silty sands (i.e., SP-SM) soils. For the purposes of these calculations, no cohesion was assumed providing an additional factor of safety.

TABLE III.7.11
Geosynthetic Interface Friction Angles and Adhesion¹ – Sideslope Liner System
Sandoval County Landfill

Geosynthetic to Geosynthetic Interface	Normal Stresses lbs/in ²	Mohr-Coulomb Failure Envelope ³	
		Φ	Adhesion
HDPE Geogrid to Structural Fill Soils (SM) [undrained]	Reference 3	30°	0 lbs/ft ²
Nonwoven Geotextile of Geocomposite to HDPE Geogrid	20.0 45.0 90.0	15.3°	243 lbs/ft ²
Nonwoven Geotextile of Geocomposite to Woven Geotextile of GCL	27.7 55.6 104.2	19°	50 lbs/ft ²
Nonwoven Geotextile of GCL to 60-mil Double-Sided Textured HDPE FML	27.7 55.6 104.2	19°	20 lbs/ft ²
Protective Soil Layer (SP-SM) to 60-mil Double-Sided Textured HDPE FML	55.6	21°	0 lbs/ft ²

Notes:

1. Values reported for Φ and Adhesion are based on review of available literature and are used to predict the performance of the liner system.
2. Geotechnical laboratory testing of on-site soils show predominately silty sands (i.e., SP-SM) soils. For the purposes of these calculations, it was assumed these soils would behave similar to SM soils that have no cohesion; providing an additional factor of safety.
3. As recommended in Reference 9, the values for Φ and Adhesion (when available in the literature) represent “Residual Shear Strength” values.

TABLE III.7.12
Geosynthetic Interface Friction Angles and Adhesion¹ – Floor Liner System
Sandoval County Landfill

Geosynthetic to Geosynthetic Interface	Normal Stresses lbs/in ²	Mohr-Coulomb Failure Envelope ³	
		Φ	Adhesion
HDPE Geogrid to Structural Fill Soils (SM) [undrained]	Reference 3	35°	0 lbs/ft ²
Nonwoven Geotextile of Geocomposite to HDPE Geogrid	14.1 28.3 56.5	21.4°	279 lbs/ft ²
Nonwoven Geotextile of Geocomposite to Woven Geotextile of GCL	13.9 55.6 83.3	19.7°	0 lbs/ft ²
Nonwoven Geotextile of GCL to 60-mil Double-Sided Textured HDPE FML	13.9 27.8 55.6	18.1°	70.5 lbs/ft ²
Protective Soil Layer (SM) to 60-mil Double-Sided Textured HDPE FML	56	24°	0 lbs/ft ²

Notes:

1. Values reported for Φ and Adhesion are based on review of available literature and are used to predict the performance of the liner system. Site specific shear strength testing should be conducted using actual liner system components and soils as specified by the Engineer for the facility prior to construction.
2. Geotechnical laboratory testing of on-site soils show predominately silty sands (i.e., SP-SM) soils. For the purposes of these calculations, it was assumed these soils would behave similar to SM soils that have no cohesion; providing an additional factor of safety.
3. As recommended in Reference 9, the values for Φ and Adhesion (when available in the literature) represent “Peak Shear Strength” values.

TABLE III.7.13
Soils Internal Friction Angle and Cohesion¹
Sandoval County Landfill

Material	Density	Mohr-Col Mohr-Coulomb Failure Envelope ¹	
		Φ	Cohesion [Assumed]
Protective Soil Layer	115 lbs/ft ³	33°	0 lbs/ft ²
Waste	65 lbs/ft ³	33°	0 lbs/ft ²
Compacted Subgrade (SP-SM soils)	115 lbs/ft ³	33°	0 lbs/ft ²
Natural Foundation Soils (SP-SM soils)	115 lbs/ft ³	33°	0 lbs/ft ²

Notes:

1. Soil components of the liner system (i.e., SP-SM soils), values reported for Φ and Cohesion are based on review of available literature. Site-specific shear strength testing should be conducted and internal friction angle and cohesion of soils specified by the Engineer for the facility prior to construction. For the purposes of these calculations, no cohesion was assumed providing an additional factor of safety.

A. Determine weight of waste and protective soil layer on sideslope:

Weight of waste and protective soil layer = [$\frac{1}{2}$ (base)(height)] x (density of material)]

$$\begin{aligned}
 W_{\text{waste/soil}} &= 0.5 (h_{\text{waste}}) [(h_{\text{waste}})(\text{slope})] (\text{density of waste}) \\
 &\quad + 0.5 (h_{\text{soil}}) [(h_{\text{soil}})(\text{slope})] (\text{density of protective soil layer}) \\
 W_{\text{waste/soil}} &= 0.5 (10 \text{ ft}) [(10 \text{ ft})(4)] (65 \text{ lbs/ft}^3) + 0.5 (2 \text{ ft}) [(2 \text{ ft})(4)] (115 \text{ lbs/ft}^3) \\
 W_{\text{waste/soil}} &= 13,000 \text{ lbs/ft} + 920 \text{ lbs/ft} = 13,920 \text{ lbs/ft}
 \end{aligned}$$

B. Determine friction force on edge of waste and protective soil layer:

$$T_W = (K_o) (\sigma_v) (\tan (\Phi_{\text{waste}}) (h_{\text{lift}}) + (K_o) (\sigma_v) (\tan (\Phi_{\text{soil}}) (h_{\text{lift}}))$$

Where:

$$\begin{aligned}
 K_o &= 1 - \sin (\Phi_{\text{waste}}) = 0.455 \\
 K_o &= 1 - \sin (\Phi_{\text{soil}}) = 0.455 \\
 \sigma_v &= (0.5) (h_{\text{waste}}) (\text{density of waste}) = 325 \text{ lbs/ft}^2 \\
 \sigma_v &= (0.5) (h_{\text{soil}}) (\text{density of soil}) = 115 \text{ lbs/ft}^2 \\
 \Phi_{\text{waste}} &= \text{Internal friction angle of waste} = 33^\circ \\
 \Phi_{\text{soil}} &= \text{Internal friction angle of protective soil} = 33^\circ \\
 h_{\text{waste}} &= \text{height of lift of waste} = 10 \text{ ft} \\
 h_{\text{soil}} &= \text{height of lift of soil} = 2 \text{ ft}
 \end{aligned}$$

$$T_W = (0.455)(325 \text{ lbs/ft}^2)(\tan (33^\circ)) (10 \text{ ft}) + (0.455)(115 \text{ lbs/ft}^2)(\tan (33^\circ)) (2 \text{ ft})$$

$$T_W = 960.3 \text{ lbs/ft} + 67.9 \text{ lbs/ft}$$

$$T_W = 1,028.2 \text{ lbs/ft}$$

C. Net weight of waste and protective soil layer

$$W_{\text{net}} = W_{\text{waste/soil}} - T_W$$

$$W_{\text{net}} = 13,920 \text{ lbs/ft} - 1,028.2 \text{ lbs/ft}$$

$$W_{\text{net}} = 12,891.8 \text{ lbs/ft}$$

D. Determine weight force component

$$N_A = (W_{\text{net}}) (\cos (\text{slope angle}))$$

Where N_A is the normal force perpendicular to the sideslope (**Figure III.7.5**)

$$N_A = 12,891.8 \text{ lbs/ft} (\cos 14.04^\circ)$$

$$N_A = 12,506.7 \text{ lbs/ft}$$

E. Calculate shear forces on geosynthetics (Figure III.7.5)

Determine friction forces:

1. Interface friction angle between double-sided textured FML and protective soil layer, $\Phi = 21^\circ$.

$$F_1 = N_A (\tan 21^\circ)$$

$$F_1 = 12,506.7 \text{ lbs/ft} (0.384)$$

$$F_1 = 4,802.6 \text{ lbs/ft}$$

2. Interface friction angle between double-sided textured HDPE FML and nonwoven geotextile of GCL, $\Phi = 19^\circ$

$$F_2 = N_A (\tan 19^\circ)$$

$$F_2 = 12,506.7 \text{ lbs/ft} (0.344)$$

$$F_2 = 4,147.5 \text{ lbs/ft}$$

$F_1 > F_2$, therefore the HDPE FML is in tension.

$$\text{Geocomposite tension} = 4,802.6 \text{ lbs/ft} - 4,147.5 \text{ lbs/ft.}$$

$$\text{Geocomposite tension} = 655.1 \text{ lbs/ft} = 54.6 \text{ lbs/in.}$$

The force difference must be carried by the 60-mil double-sided textured HDPE FML. The actual stress in the HDPE FML is given by:

$$\sigma_{\text{actual}} = (F_1 - F_2)/t_{\text{geomembrane}}$$

σ_{actual} = actual stress in HDPE FML

$t_{\text{geomembrane}}$ = geomembrane thickness = 60 mil = 0.06 in.

$$\sigma_{\text{actual}} = 54.6 \text{ lbs/in} / 0.06 \text{ in}$$

$$\sigma_{\text{actual}} = 910.0 \text{ lbs/in}^2$$

The factor of safety for the geocomposite against failure in tension is:

$$FS_{\text{geomembrane}} = \sigma_{\text{yield}} / \sigma_{\text{actual}}$$

The “wide-width” tensile strength for the specified 60-mil HDPE FML is provided by the manufacturer (**Attachment III.7.N**); and is computed to be 2,100 lbs/in². Therefore a HDPE FML with a wide-width tensile strength of 54.6 lbs/in or greater will not be adversely affected if a 10-ft lift of waste and 2-ft lift of PSL is placed on the sideslope as calculated below:

$$FS_{\text{geomembrane}} = 2,100 \text{ lbs/in}^2 / 910.0 \text{ lbs/in}^2$$

$$FS_{\text{geomembrane}} = 2.3$$

3. $F_3 = F_2 = 4,147.5 \text{ lbs/ft}$ for static no-slip condition.
4. Interface friction angle between woven geotextile of GCL and nonwoven geotextile of the geocomposite, $\Phi = 19^\circ$

$$F_4 = N_A (\tan 19^\circ)$$

$$F_4 = 12,506.7 \text{ lbs/ft} (0.344)$$

$$F_4 = 4,147.5 \text{ lbs/ft}$$

$F_4 = F_3$, therefore the GCL is not in tension.

5. $F_5 = F_4 = 4,147.5 \text{ lbs/ft}$ for static no-slip condition.
6. Interface friction angle between nonwoven geotextile of geocomposite and HDPE structural geogrid, $\Phi = 15.3^\circ$

$$F_6 = N_A (\tan 15.3^\circ)$$

$$F_6 = 12,506.7 \text{ lbs/ft} (0.274)$$

$$F_6 = 3,426.8 \text{ lbs/ft}$$

$F_5 > F_6$, therefore the geocomposite is in tension.

Geocomposite tension = 4,147.5 lbs/ft – 3,426.8 lbs/ft.

Geocomposite tension = 720.7 lbs/ft = 60.1 lbs/in.

The force difference must be carried by the geocomposite. The actual stress in the geocomposite is given by:

$$\sigma_{\text{actual}} = (F_6 - F_5)/t_{\text{geocomposite}}$$

σ_{actual} = actual stress in geocomposite

$t_{\text{geocomposite}}$ = geocomposite thickness = 200 mil = 0.2 in.

$$\sigma_{\text{actual}} = 60.1 \text{ lbs/in} / 0.2 \text{ in}$$

$$\sigma_{\text{actual}} = 300.5 \text{ lbs/in}^2$$

The factor of safety for the geocomposite against failure in tension is:

$$FS_{\text{geocomposite}} = \sigma_{\text{yield}} / \sigma_{\text{actual}}$$

GSE Lining Technology, Inc. (GSE) has conducted wide-width tensile testing for a 200-mil/6 oz/yd² geocomposite which typically has an allowable wide tensile rating of 210 lbs/in (1,050 lbs/in²; **Attachment III.7.O**). Per GSE, the 200-mil/10 oz/yd² geocomposite should perform equal to or better than the 200-mil/6 oz/yd² geocomposite. Therefore a geocomposite with a wide-width tensile strength of 210 lbs/in or greater will not be adversely affected if a 10-ft lift of waste and 2-ft lift of PSL is placed on the sideslope as calculated below:

$$FS_{\text{geocomposite}} = 1,050 \text{ lbs/in}^2 / 300.5 \text{ lbs/in}^2$$

$$FS_{\text{geocomposite}} = 3.5$$

7. $F_7 = F_6 = 3,426.8 \text{ lbs/ft}$ for static no-slip condition.

8. Interface friction angle between HDPE geogrid and structural fill soils, $\Phi = 30^\circ$

$$F_8 = N_A (\tan 30^\circ)$$

$$F_8 = 12,506.7 \text{ lbs/ft} (0.577)$$

$$F_8 = 7,216.4 \text{ lbs/ft}$$

$F_8 < F_7$, therefore the geogrid is not in tension.

F. Conclusion

The tensile stress in the double-side textured HDPE FML and geocomposite is 54.6 lbs/in and 60.1 lbs/in, respectively. This positive value indicates that both of the geosynthetics are in wide-width tension. It should be noted that the calculation of the tensile stress in each of the geosynthetics within the liner system is conservatively based on a pure friction based scenario, as no adhesion is incorporated into the calculations. In addition to the conservative choice of interface friction angles, it is more than likely that the geosynthetics in the liner system will not be in wide-width tension; especially considering the relatively low tensile stress calculated for the HDPE FML and geocomposite. The factor of safety for tensile stress for the HDPE FML and geocomposite are 2.3 and 3.5, respectively. Therefore, the HDPE FML with a wide-width tensile strength of 126 lbs/in; and the geocomposite with a wide-width tensile strength of 210 lbs/in., or greater, will not be adversely affected if a 10-ft lift of waste and 2-ft lift of PSL is placed on the sideslope. The zero and negative values for tensile stress in the GCL and HDPE geogrid indicates that they are not in tension. Therefore, the proposed liner system design is compatible with calculated external forces.

5.0 CALCULATION OF TENSILE STRESSES IN GEOSYNTHETICS DUE TO EQUIPMENT LOADING

It is assumed that a Caterpillar D6E dozer or equivalent will be used to place the protective soil layer up the sideslope a sufficient distance to accommodate an approximate 10 ft lift of waste placed on the floor of the landfill. The maximum unsupported length of protective soil to accommodate this lift will be approximately 50 ft for a 4H:1V sideslope. Parameters to be used in the analysis include:

- Unit weight of protective soil = 115 lbs/ft³ Dry Density.
- Internal friction angle of protective soil = 33 degrees.
- Sideslope @ 4H±:1V; Slope angle = 14.04 degrees.
- Critical liner interface friction angle occurs between the geocomposite and HDPE geogrid = 15.3° (Table III.7.2).
- Equipment loading assuming a D6E dozer: (CAT Performance Handbook, Edition 29)
 - Weight = 32,000 lbs.
 - Track width = 22 in. = 1.83 ft.
 - Pressure distribution: Assume a 2H:1V distribution, therefore width acting on geomembrane = 9.83 ft.
- Tensile forces acting on Geocomposite:

- Protective soil layer, F_{soil}
- D6E dozer, F_{dozer}
- Total resisting forces:
 - Geocomposite interface friction, $F_{\text{geocomposite}}$
 - Soil buttress friction at toe of slope, F_{buttress}

The minimum interface friction angle for the liner system is 15.3° and occurs between the geocomposite and the HDPE geogrid (**Table III.7.11**).

Tensile forces acting on geocomposite:

$$F_{\text{soil}} = h_{\text{lift}} (\text{unsupported slope length}) (\text{unit weight of protective soil}) (\sin (\text{slope angle}))$$

$$F_{\text{soil}} = (2 \text{ ft}) (50 \text{ ft}) (115 \text{ lbs/ft}^3) (\sin (14.04^\circ))$$

$$F_{\text{soil}} = 2,789.9 \text{ lbs/ft}$$

$$F_{\text{dozer}} = [0.5 (\text{dozer weight}) / (\text{width acting on geocomposite})] (\sin (14.04^\circ))$$

$$F_{\text{dozer}} = [0.5 (32,000 \text{ lbs}) / 9.83 \text{ ft}] (\sin (14.04^\circ))$$

$$F_{\text{dozer}} = [16,000 \text{ lbs} / 9.83 \text{ ft}] (0.243)$$

$$F_{\text{dozer}} = 395.5 \text{ lbs/ft}$$

$$\text{Total tensile force acting on geocomposite} = 2,789.9 \text{ lbs/ft} + 395.5 \text{ lbs/ft} = 3,185.4 \text{ lbs/ft}$$

Total Resisting Forces acting on geocomposite:

$$F_{\text{geocomposite}} = (\text{Weight of protective soil} + \text{Weight of Dozer}) (\cos (\text{slope angle})) (\tan (\text{interface friction angle}))$$

$$F_{\text{geocomposite}} = [(2 \text{ ft}) (50 \text{ ft}) (115 \text{ lbs/ft}^3) + (16,000 \text{ lbs} / 9.83 \text{ ft})] (\cos 14.04^\circ) (\tan 15.3^\circ)$$

$$F_{\text{geocomposite}} = (11,500.0 \text{ lbs/ft} + 1,627.7 \text{ lbs/ft}) (0.970) (0.274)$$

$$F_{\text{geocomposite}} = 3,489.1 \text{ lbs/ft}$$

$$F_{\text{buttress}} = [[\cos (\text{internal friction angle of soil})] / [\cos (\text{internal friction angle of soil} + \text{slope angle})]] [[(\text{Unit weight of soil}) (\text{thickness of soil})^2 / \sin 2 (\text{slope angle})] \tan (\text{internal friction angle of soil})]$$

$$F_{\text{buttress}} = [[\cos (33^\circ) / \cos (33^\circ + 14.04^\circ)] [(115 \text{ lbs/ft}^3 (2 \text{ ft})^2) / \sin (2 (14.04^\circ))] [\tan (33^\circ)]$$

$$F_{\text{buttress}} = [0.839 / 0.682] [460 \text{ lbs/ft} / 0.471] [0.649]$$

$$F_{\text{buttress}} = [1.23] [976.6] [0.649]$$

$$F_{\text{buttress}} = 779.6 \text{ lbs/ft}$$

Total resisting force acting on geocomposite = 3,489.1 lbs/ft + 779.6 lbs/ft = 4,268.7 lbs/ft

Tensile forces (3,185.4 lbs/ft) < Resisting forces (4,268.7 lbs/ft); therefore geocomposite is not in tension.

Summary:

Tensile stress in geocomposite = 3,185.4 lbs/ft – 4,548.8 lbs/ft = -1,363.4 lbs/ft = -113.6 lbs/in.

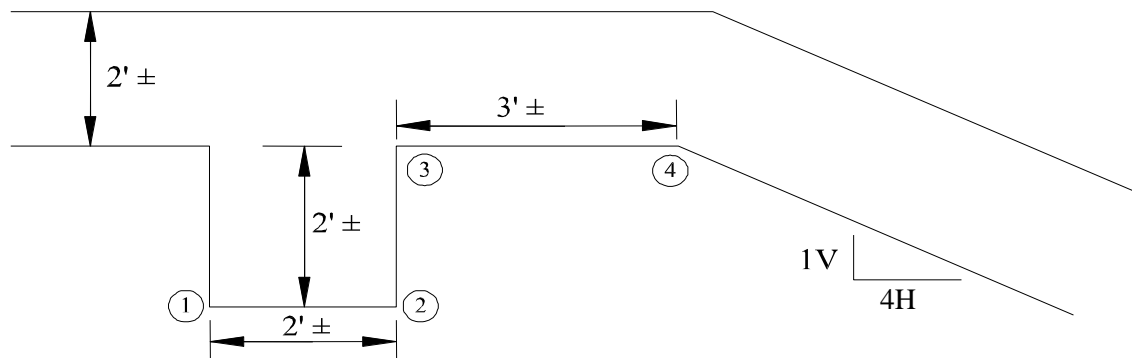
The negative tensile stress indicates that the geocomposite is not in tension. Therefore, placing the protective soil layer 12 ft up the sideslope will not adversely impact the geocomposite.

Conclusion:

The tensile stress upon the geocomposite due to equipment loading is -113.6 lbs/in. This value is less than the tensile (yield) strength for the geocomposite of 270 lbs/in, as previously referenced.

6.0 ANCHOR TRENCH PULLOUT ANALYSIS

Anchor trench configuration:



The anchor trench consists of extending the geosynthetics along the trench bottom to increase resistive force. In order to establish the static equilibrium equation, two imaginary and frictionless pulleys are assumed at the top edge and the bottom corner of the anchor trench (**Attachment III.7.B, page 111, Equation 4-28** and verified by Reference 12). The friction force above a runout geosynthetic is always neglected in the anchor trench. Based on the calculation in **Section 4.0**, the geocomposite is in tension and, the interface friction angle between the geocomposite and the

HDPE geogrid is the minimum interface friction angle of the liner system; therefore theoretically, any pullout will occur at this interface.

6.1 Geocomposite HDPE Geogrid Interface

$\Sigma F_H = 0$ yields the following equation for the calculation of T (where T = geocomposite tensile force per unit width lbs/ft:

$$T = \frac{(\gamma_s)(d_{cs})(L_{ro})(\tan \delta_c) + [(1 - \sin \theta)((\gamma_s)(d_{cs} + 0.5d_{AT}))d_{AT} + \gamma_s(d_{cs} + d_{AT})L_{AT}](\tan \delta_c + \tan \delta_F)}{\cos \beta - (\sin \beta)(\tan \delta_c)}$$

Where:

- γ_s = unit weight of cover and backfill soil = 115 lbs/cf dry density
- d_{cs} = depth of cover soil = 2 ft
- L_{ro} = runout length = 3 ft
- δ_c = friction angle between the geocomposite and underlying HDPE geogrid = 15.3°
- θ = internal friction angle of backfill soil in anchor trench = 33°
- d_{AT} = depth of anchor trench = 2 ft
- L_{AT} = width of anchor trench = 2 ft
- δ_F = interface friction angle between the double-sided textured HDPE FML and the backfill soil = 21°
- β = sideslope angle, measured from horizontal = 14.04°

$$T = \frac{(115 \text{ lbs/cf})(2')(3')(\tan 15.3^\circ) + [(1 - \sin 33^\circ)((115 \text{ lbs/cf})(2' + 0.5(2'))(2') + 115 \text{ lbs/cf}(2' + 2')2'](\tan 15.3^\circ + \tan 21^\circ)}{\cos 14.04^\circ - (\sin 14.04^\circ)(\tan 15.3^\circ)}$$

$$T = \frac{(188.8 \text{ lbs/ft}) + [(0.455)(115 \text{ lbs/cf})(3.0 \text{ ft})(2 \text{ ft}) + 115 \text{ lb/cf}(8 \text{ sf})](0.657)}{0.904}$$

$$T = \frac{188.8 \text{ lbs/ft} + [313.95 \text{ lbs/ft} + 920 \text{ lbs/ft}](0.657)}{0.904}$$

$$T = \frac{188.8 \text{ lbs/ft} + 810.7 \text{ lbs/ft}}{0.904}$$

$$T = \frac{999.5 \text{ lbs/ft}}{0.904}$$

$$T = 1,105.6 \text{ lbs/ft} = 92.1 \text{ lbs/in}/0.20 \text{ in (Geocomposite Thickness)} = 460.5 \text{ lbs/in}^2$$

Ultimate Strength > Anchor Trench Resistance > Allowable Strength

Assume Allowable Strength = Ultimate Strength/Assumed Factor of Safety

Assumed Factor of Safety = 3

Ultimate Strength = 1,050 lbs/in² (**Attachment III.7.O**)

$$1,050 \text{ lbs/in}^2 > 460.5 \text{ lbs/in}^2 > 350.0 \text{ lbs/in}^2$$

The results indicate that the anchor trench, as designed, provides more than sufficient capacity such that the anchor trench capacity is correctly positioned between the geocomposite yield stress and allowable stress.

7.0 GEOSYNTHETIC SLIPPAGE ANALYSIS

In order to determine the factor of safety for slippage and subsequent tension in the liner geosynthetics, the method of active and passive wedges developed by Qian et al. (2002) was used (**Attachment III.7.B, pg. 521**). This calculation utilizes the passive wedge that supports the active wedge on the sideslope, consistent with actual conditions in the field. These calculations were performed along the geomembrane covered slope shown on the cross section (**Figure III.7.6**). The lowest friction angle values taken from **Tables III.7.11** and **III.7.12** are $\delta_A = 15.3^\circ$, for the interface friction angle between the geocomposite and HDPE geogrid on the sideslope; and $\delta_P = 18.1^\circ$ for the interface friction angle between the geosynthetic clay liner nonwoven geotextile and double-sided textured HDPE geomembrane on the floor. The total height of the active wedge is the maximum height of waste over the sloped portion of liner system.

For the purposes of this calculation, the following assumptions and nomenclature (**Table III.7.14**) were used from the literature (**Attachment III.7.B, pg. 521**):

TABLE III.7.14
Translational Failure Analysis
Sandoval County Landfill

$W_P =$	total weight of the passive wedge
$N_P =$	normal force acting on the bottom of the passive wedge
$F_P =$	Frictional force acting on the bottom of the passive wedge (parallel to the bottom of the passive wedge)
$E_{HP} =$	normal force from the active wedge acting on the passive wedge
$E_{VP} =$	frictional force acting on the side of the passive wedge
$FS_P =$	Factor of safety for the passive wedge
$\delta_P =$	Minimum interface friction angle of multi-layer liner components beneath the passive wedge = 18.1° (interface friction angle between the geocomposite and the HDPE geogrid, from Table III.7.11)
$\Phi_S =$	friction angle of the solid waste = 33°
$\alpha =$	angle of the solid waste slope, measured from horizontal
$\theta =$	angle of the landfill cell subgrade, measured from horizontal = 1.15°
$W_A =$	weight of the active wedge
$W_T =$	total weight of active and passive wedges
$N_A =$	normal force acting on the bottom of the active wedge
$F_A =$	Frictional force acting on the bottom of the active wedge (parallel to the bottom of the active wedge)
$E_{HA} =$	normal force from the active wedge acting on the active wedge, $E_{HA} = E_{HP}$
$E_{VA} =$	frictional force acting on the side of the active wedge, $E_{VA} = E_{VP}$
$FS_A =$	factor of safety for the active wedge
$b =$	Horizontal length of the Active Wedge (cell sideslope at its maximum depth) = 75 ft
$b_p =$	Horizontal length of the Passive Wedge = 108 ft
$h_t =$	Total Height of the Wedges = 36 ft
$\delta_A =$	minimum interface friction angle of multi-layer liner components beneath the active wedge = 15.3° (Table III.7.12)
$\beta =$	angle of sideslope, measured from the horizontal = 14.04°
$FS =$	factor of safety for the entire solid waste mass

Figure III.7.6 also shows measured values for b , b_p , and h_t and **Figure III.7.7** identifies the location of the slippage analysis of the geosynthetic liner system at SCLF.

The active wedge is considered first:

$$W_A = \frac{1}{2}((b_a * h_a * \gamma) + (b_b * h_b * \gamma))$$

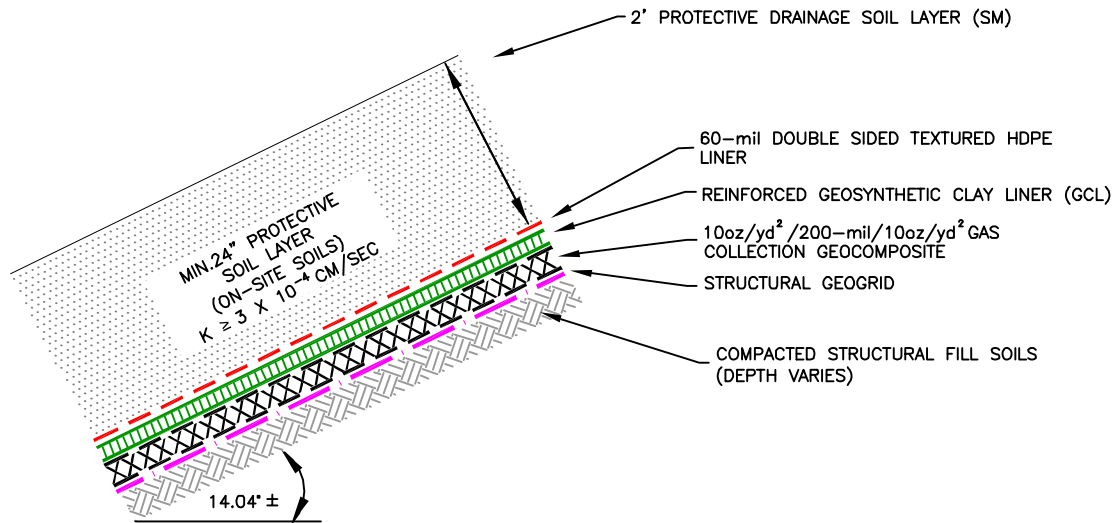
$$W_A = \frac{1}{2} \left(54 \text{ ft} * 18 \text{ ft} * 65 \left(\frac{\text{lbs}}{\text{ft}^3} \right) + 72 \text{ ft} * 18 \text{ ft} * 65 \left(\frac{\text{lbs}}{\text{ft}^3} \right) \right) = 73,710 \frac{\text{lbs}}{\text{ft}}$$

The passive wedge is then considered by multiplying the cross sectional area by the unit weight of waste.

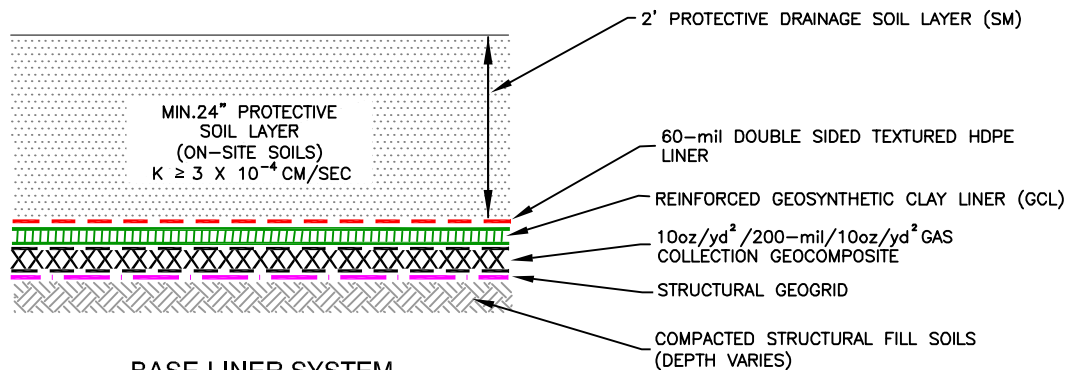
$$W_P = \frac{1}{2}(b_P * h_t * \gamma) = W_P = \frac{1}{2} \left(108 \text{ ft} * 36 \text{ ft} * 65 \left(\frac{\text{lbs}}{\text{ft}^3} \right) \right) = 126,360 \frac{\text{lbs}}{\text{ft}}$$

$$W_T = 73,710 \frac{\text{lbs}}{\text{ft}} + 126,360 \frac{\text{lbs}}{\text{ft}} = 200,010 \frac{\text{lbs}}{\text{ft}}$$

Based on the above calculations, the active wedge weighs 73,710 lbs/ft, and the minimum interface friction angle of the geosynthetics is 15.3°; the passive wedge weighs 126,360 lbs/ft and the minimum interface friction angle of the geosynthetics on the floor is 18.1°. Therefore, the passive wedge is more than capable of supporting the active without slippage; and the proposed liner system design is compatible with calculated external forces.



SIDEWALL LINER SYSTEM



BASE LINER SYSTEM

SIDESLOPE AND FLOOR LINER SYSTEM DETAIL

SANDOVAL COUNTY LANDFILL
RIO RANCHO, NEW MEXICO



Gordon Environmental, Inc.

Consulting Engineers

213 S. Camino del Pueblo
Bernalillo, New Mexico, USA
Phone: 505-867-6990
Fax: 505-867-6991

Drawing: P:\acad 2003\211.00.01\PERMIT FIGURES\LINER SCHEM.dwg
Date/Time: Apr. 10, 2015-07:31:29
Copyright © All Rights Reserved, Gordon Environmental, Inc. 2015

DATE: 04/10/2015

CAD: LINER SCHEM.dwg

PROJECT #: 211.00.01

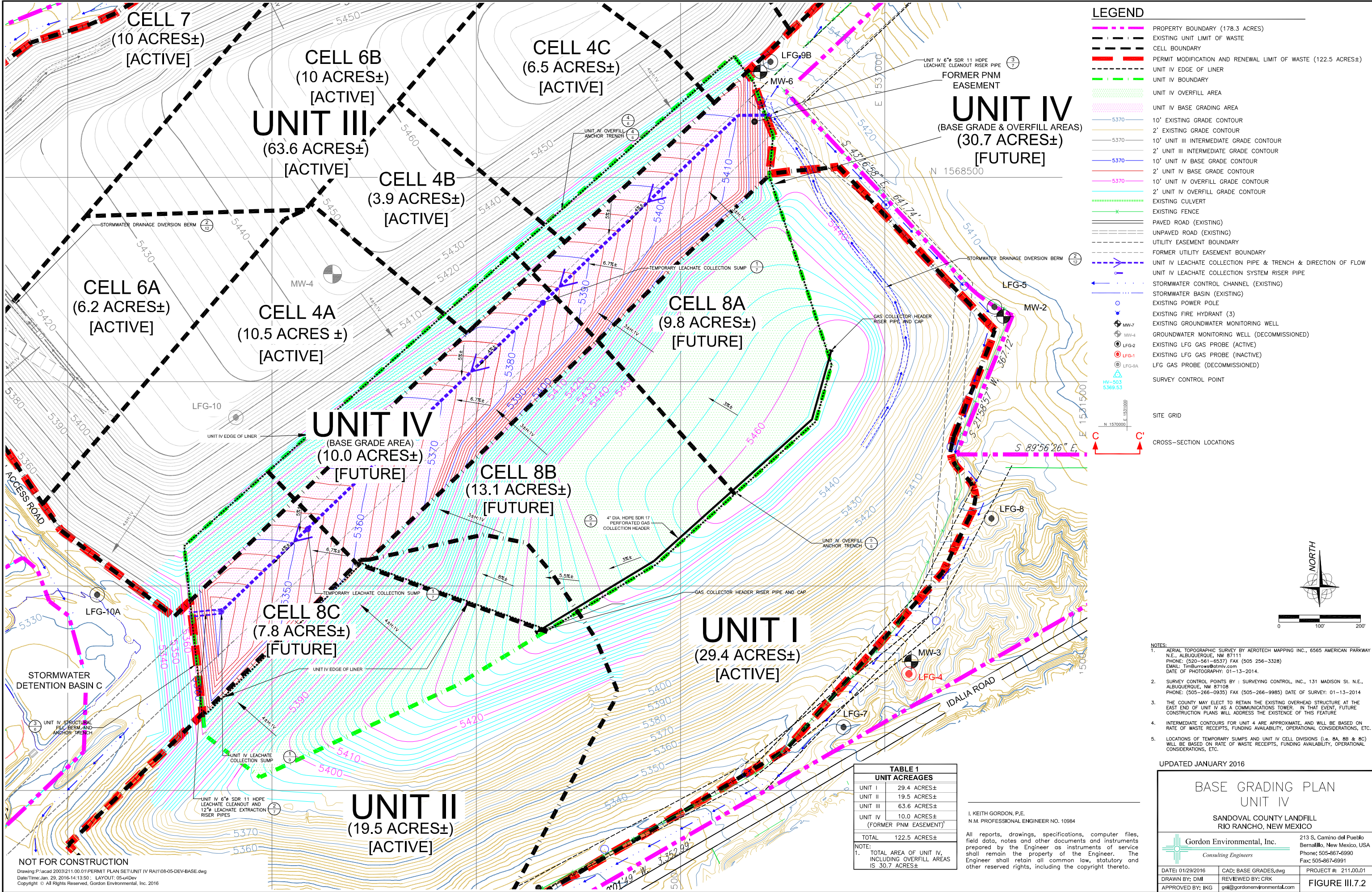
DRAWN BY: DMI

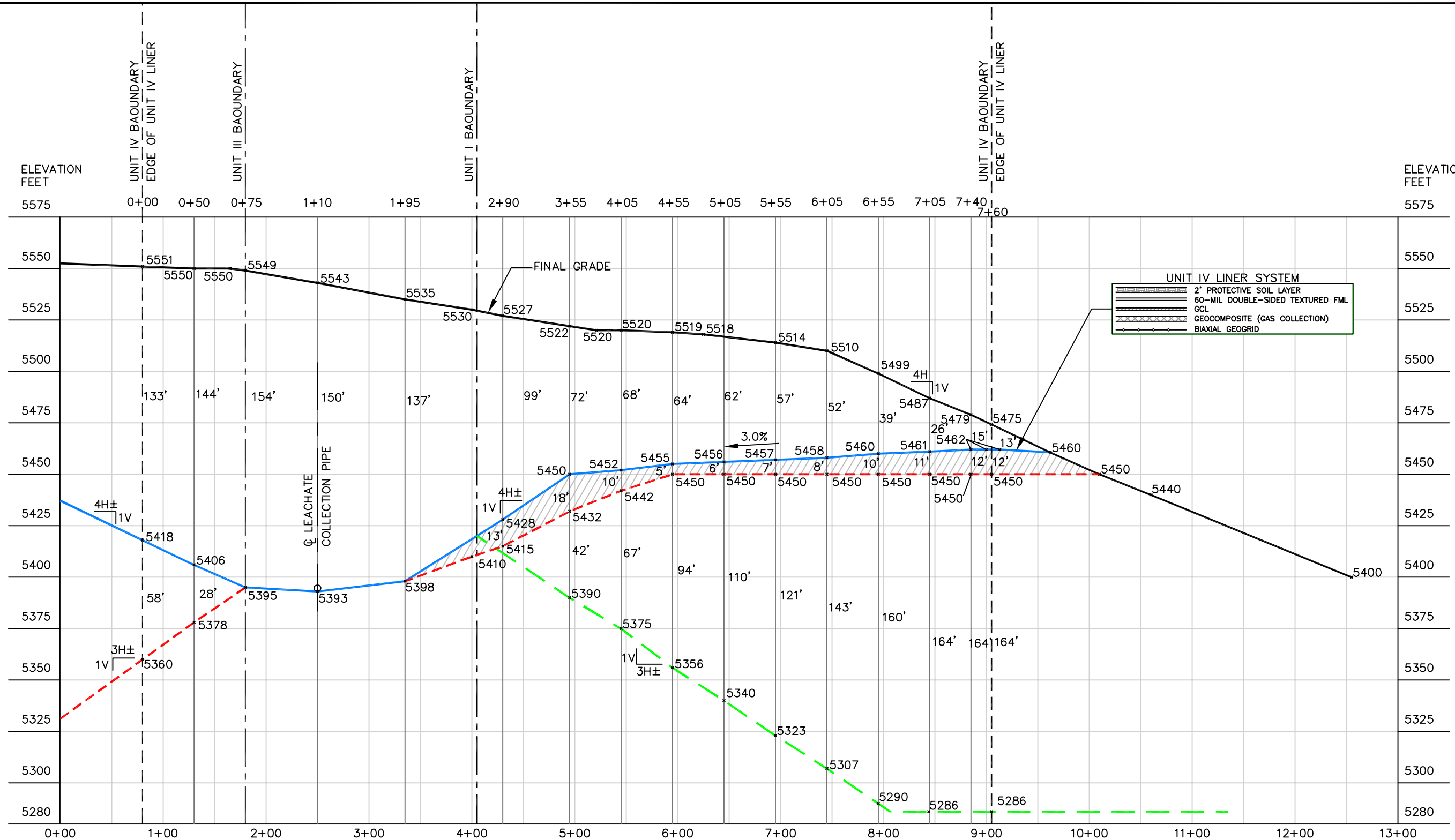
REVIEWED BY: MRH

APPROVED BY: JKG

gei@gordonenvironmental.com

FIGURE III.7.1





CROSS SECTION A-A'

LEGEND

- EDGE OF LINER
- UNIT BOUNDARY
- - - - - APPROXIMATE UNIT III BASE GRADE
- LINER
- FINAL GRADE
- APPROXIMATE UNIT I BASE GRADE

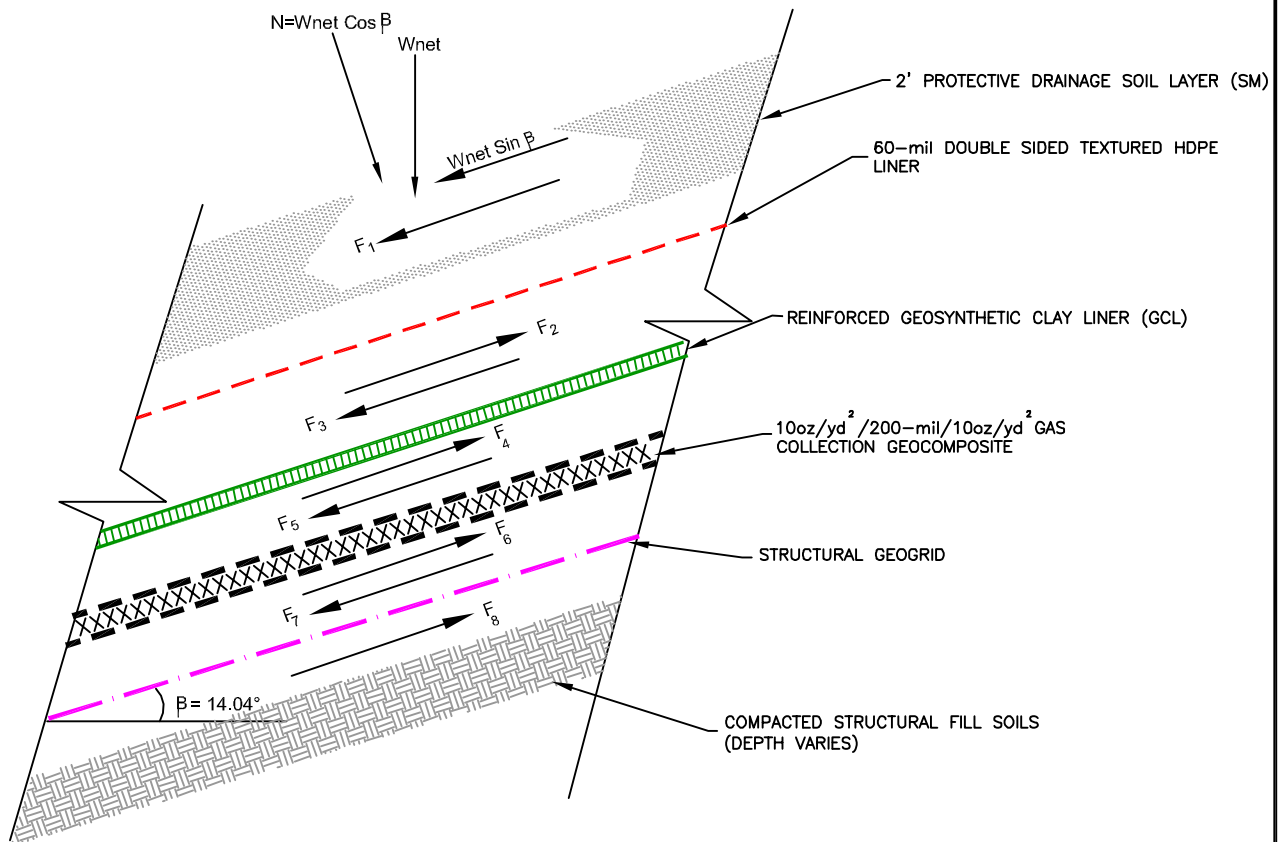
UNIT IV GEOSYTHETIC STRAIN
ANALYSIS SECTION A-A'

SANDOVAL COUNTY LANDFILL
SANDOVAL COUNTY, NEW MEXICO



213 S. Camino del Pueblo
Bernalillo, New Mexico, USA
Phone: 505-867-6990
Fax: 505-867-6991

DATE: 04/08/2015	CAD: Unit IV Geosynthetic CS	PROJECT #: 211.00.01
DRAWN BY: CM	REVIEWED BY: MRH	
APPROVED BY: IKG	gel@gordonenvironmental.com	FIGURE III.7.3



FREE BODY DIAGRAM

NOT TO SCALE

GEOSYNTHETIC FRICTION FORCES

SANDOVAL COUNTY LANDFILL
RIO RANCHO, NEW MEXICO



Gordon Environmental, Inc.

Consulting Engineers

213 S. Camino del Pueblo
Bernalillo, New Mexico, USA
Phone: 505-867-6990
Fax: 505-867-6991

DATE: 04/10/2015

CAD: FRICTION FORCES.dwg

PROJECT #: 211.00.01

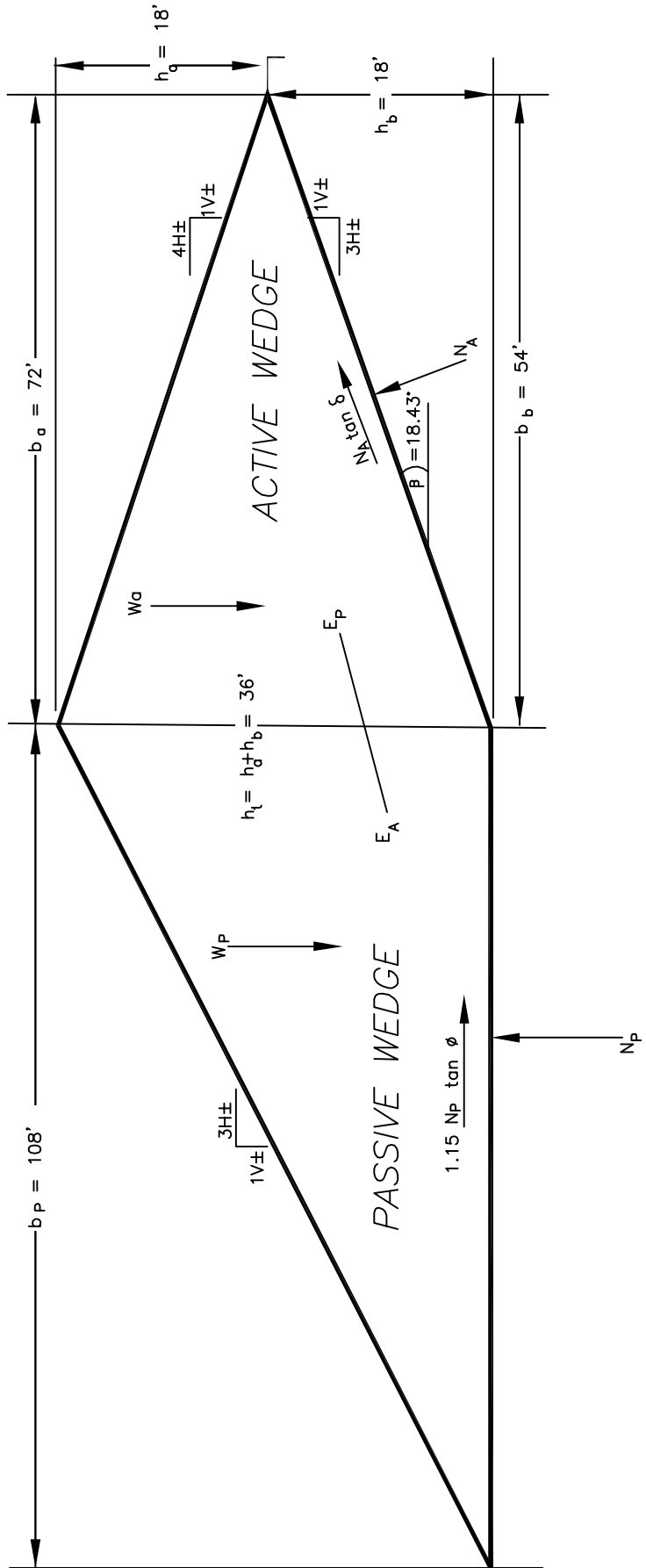
DRAWN BY: DMI

REVIEWED BY: MRH

APPROVED BY: IKG

gel@gordonenvironmental.com

FIGURE III.7.5



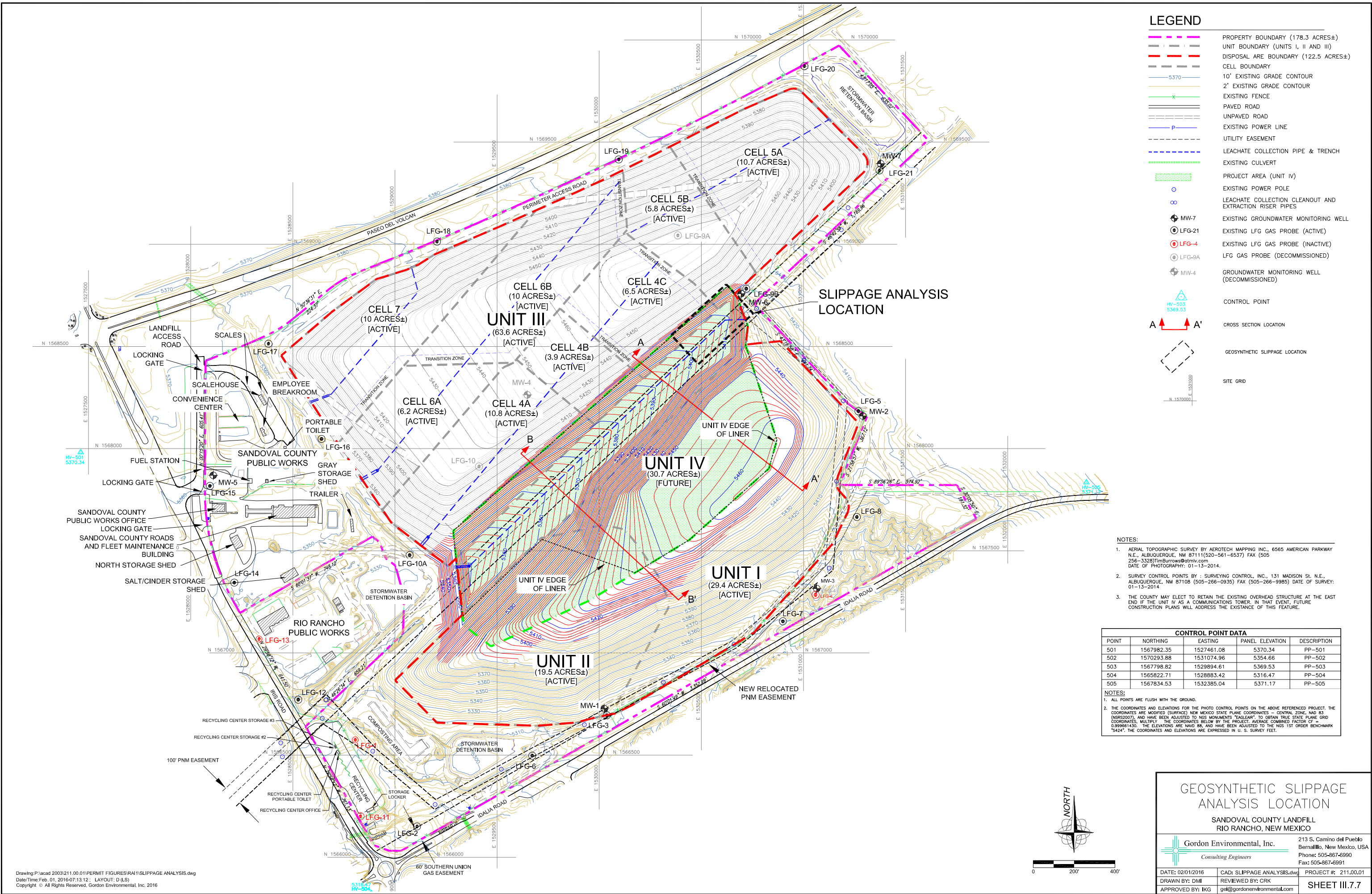
GEOSYNTHETIC SLIPPAGE ANALYSIS

SANDOVAL COUNTY LANDFILL
RIO RANCHO, NEW MEXICO

Gordon Environmental, Inc.
Consulting Engineers

213 S. Camino del Pueblo
Bernalillo, New Mexico, USA
Phone: 505-867-6990
Fax: 505-867-6991

DATE: 03/31/2015	CAD: GEO ANALYSIS.dwg	PROJECT #: 211.00.01
DRAWN BY: DMI	REVIEWED BY: MRH	FIGURE III.7.6
APPROVED BY: IKG	9a@gordonenvironmental.com	



**APPLICATION FOR PERMIT RENEWAL AND MODIFICATION
SANDOVAL COUNTY LANDFILL**

**VOLUME III: LANDFILL ENGINEERING CALCULATIONS
SECTION 7: GEOSYNTHETICS TENSILE STRESS AND STABILITY ANALYSIS**

ATTACHMENT III.7.A

**SHARMA, HARI D. AND LEWIS, SANGEETA, P. 1994.
*WASTE CONTAINMENT SYSTEMS, WASTE STABILIZATION,
AND LANDFILLS: DESIGN AND EVALUATION.*
NEW YORK: JOHN WILEY AND SONS.**

WASTE CONTAINMENT SYSTEMS, WASTE STABILIZATION, AND LANDFILLS: DESIGN AND EVALUATION

HARI D. SHARMA, Ph.D, P.E.

Chief Engineer and Director
EMCON Associates
San Jose, California

SANGETTA P. LEWIS, P.E.

Project Manager
CH₂M Hill
Oakland, California



A Wiley-Interscience Publication

JOHN WILEY & SONS, INC.

New York / Chichester / Toronto / Brisbane / Singapore

stress cracking may occur. The recommended elongation for shear test acceptance is greater than 50 percent (Rollin et al., 1991; Giroud and Peggs, 1990; Carlson et al., 1993).

Destructive testing procedures other than shear and peel tests are available to evaluate geomembrane seams, although their use has not yet been widely accepted. Several researchers (Peggs and Charron, 1989; Rollin et al., 1989, 1991; Halse et al., 1991b; Carlson et al., 1993) have suggested the use of microtomes (microscopic evaluation of thin geomembrane sections) to evaluate possible initiation of stress cracking in seams. Another reported method is impact testing (Rollin et al., 1993).

Geomembrane seams may also be tested using nondestructive test methods. These test methods do not measure the seam strength, but rather, detect whether holes exist in the seams. The most commonly used methods are the vacuum test, pressure test, and copper wire spark test. The vacuum test procedure involves placing a soapy solution over a seam approximately 1 to 2 feet in length. A vacuum box with a clear viewing window is placed over the seam length and a vacuum pressure of approximately 5 psi is applied. If a stream of soap bubbles is detected through the viewing window, a leak exists and must be repaired.

Pressure tests can be performed only on double-wedge weld seams. These tests are performed by sealing both ends of an unobstructed double-wedge weld length and then applying approximately 30 psi of air pressure in the channel between the welds through a fine needle. A pressure gage is attached to the needle, and the pressure is monitored for approximately 5 minutes. A reduction in pressure greater than 2 psi during the 5-minute period usually indicates that air is escaping through a leak in the seam. This leak must be located and repaired. In the copper wire spark test, a copper wire is welded into the seam. A current is passed through the copper wire, and any sparks indicate that a hole is present.

3.2 GEOTEXTILES

3.2.1 Types and Functions

Geotextiles are synthetic fabrics used in geotechnical engineering for various applications. The majority of geotextiles are composed of polypropylene or polyester fibers; a small percentage are composed of polyamide or polyethylene. Among the geosynthetics, geotextiles appear to have the most associated terminology and the widest ranging properties. This is due in part to the numerous types of fibers and geotextile manufacturing processes.

The types of fibers used in the manufacture of geotextiles include monofilament, staple, and slit²⁰ film. If fibers are twisted or spun together, they are known as a yarn. Monofilament fibers are created by extruding molten polymer through an apparatus containing several small-diameter holes, known as a spinnaret. The extruded polymer strings are then cooled and stretched to align the polymers and give

²⁰Slit-film fibers are also known as split-film fibers.

the fiber increased strength. Staple fibers are also manufactured by extruding polymer through a spinnaret; however, the extruded strings are twisted together and cut into 1- to 4-inch lengths. The staple fibers are then spun into longer fibers known as staple yarns. Finally, slit-film fibers are manufactured by extruding a continuous sheet of polymer and cutting it into fibers by knives or lanced air jets. Slit-film fibers are rectangular in cross section rather than the circular cross sections of the monofilament and staple fibers.

The fibers or yarns are formed into geotextiles using either woven or nonwoven (spunbonded) methods. Woven geotextiles are formed using traditional weaving methods and a variety of weave types. Common terminology associated with woven geotextiles include machine direction, cross machine direction, selvage, warp, and weft. The machine direction refers to the direction in the plane of fabric parallel to the direction of manufacture, and conversely, the cross machine direction refers to the direction in the plane of fabric perpendicular to the direction of manufacture. The machine direction is also known as the warp, since warp yarns are those yarns placed lengthwise on the weaving loom; and the cross machine direction is known as the weft, since weft yarns are woven between and perpendicular to the warp yarns. The selvage is the finished area on both sides of the geotextile width that prevents the yarns from unraveling.

To create nonwoven geotextiles, the manufactured fibers are placed and oriented on a moving conveyor belt. The fibers are bonded by needle punching, melt bonding, or resin bonding. The needle-punching process consists of pushing numerous barbed needles through the fiber web. The fibers are thus mechanically interlocked into a stable configuration. As the name implies, the melt bonding process consists of melting and pressurizing fibers together at their crossover points. In resin bonding, an acrylic resin is applied to the fiber web to form the geotextile.

In waste containment facilities, geotextiles are most commonly used for filtration, separation, reinforcement, cushioning, and drainage. A relatively new application for geotextiles is an alternative daily cover over refuse. Typically, nonwoven geotextiles are used in waste containment facilities for filtration, separation, cushioning, and drainage. Woven geotextiles are usually used for reinforcement. Both woven and nonwoven geotextiles may be used for alternative daily cover.

3.2.2 Material Properties

As with geomembranes, there are numerous tests that may be performed on geotextiles. However, geotextiles have numerous different applications where geomembranes are used almost exclusively as a barrier material. In developing geotextile specifications, it is important that the designer understand the material tests and specify material properties important for the geotextiles' intended use. The following sections therefore indicate the geotextile application for which the material test is significant. Index or quality control tests are also discussed.

The material properties generally specified for waste containment system applications are thickness, mass per unit area, uniaxial tensile strength, multiaxial tensile strength, puncture resistance, trapezoid tear strength, apparent opening size, per-

mittivity, transmissivity, and ultraviolet resistance. In specifying geotextile material properties, the designer should be aware that many reported material properties and test methods were borrowed from the textile industry. Many tests are therefore more applicable to evaluating fabric for clothing rather than for engineering fabrics. Most geotextile properties reported by manufacturers are index or quality control tests and are not intended for engineering design. Hopefully, as further research on geotextiles is performed, material tests to evaluate engineering properties will be developed.

Thickness (ASTM D 177,²¹ D 5199). The average thickness of a geotextile is measured using a thickness gage under a gradually applied, specified pressure. The pressure to be applied depends on the material type. For geotextiles, a pressure of approximately 0.3 psi is typically used. The thickness of a geotextile alone is generally not critical for design. It is, however, related to other material properties, such as mass per unit area, tensile strength, puncture resistance, and tear resistance. Thickness is also important if the geotextile is used for cushioning and in calculating permeability coefficients.

Mass per Unit Area (ASTM D 5261²²). The mass per unit area of a geotextile is determined by weighing several test specimens of known area, taken from various locations of the fabric sample. The calculated values are averaged to obtain the mean mass per unit area of the sample. Geotextiles, especially nonwoven geotextiles, are commonly referred to by an abbreviated form of their mass per unit area. For example, a nonwoven geotextile that is 8 ounces per square yard is commonly referred to as an 8-ounce geotextile. Although this is obviously incorrect, the problem is not as much in the terminology as it is in specifying the mass per unit area as a design value. Many specifiers attribute a certain mass per unit area to a certain set of mechanical and hydraulic properties, such as puncture resistance, tear resistance, apparent opening size, and tensile strength. While the mass per unit area is related to these properties, there is not a direct correlation. Therefore, geotextiles with a mass per unit area of 8 oz/yd² can have widely varying mechanical and hydraulic properties. A certain mass per unit area may be required, however, if the geotextile is to be used as a cushion.

Uniaxial Tensile Strength (ASTM D 4632,²³ D 4595²⁴). The uniaxial tensile strength of geotextiles is measured in a tensile testing machine by applying a continually increasing load along the longitudinal length of a specimen. The specimen is grasped within clamps, specially designed to prevent slippage (Figure 3.33). The distance between clamps (called the gage dimension) and the specimen dimensions

²¹ ASTM D 1777: Standard Method for Measuring Thickness of Textile Materials.

²² ASTM D 5261: Standard Test Method for Measuring Mass per Unit Area of Geotextiles.

²³ ASTM D 4632: Standard Test Method for Breaking Load and Elongation of Geotextiles (Grab Method).

²⁴ ASTM D 4595: Standard Test Method for Tensile Properties by the Wide-Width Strip Method.

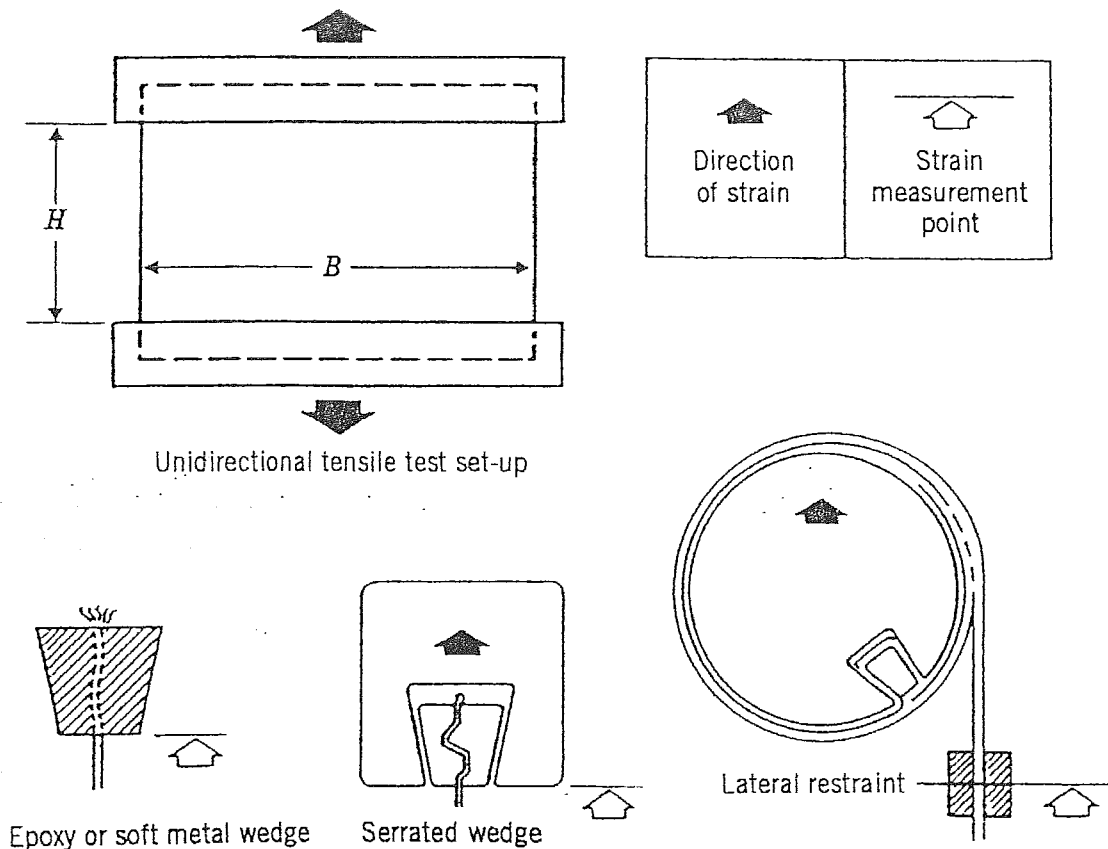


Figure 3.33 Clamping systems for uniaxial tension test. (From Myles, 1987.)

are standardized. While the test values typically reported are the breaking load (reported in pounds) and apparent elongation (reported as a percentage increase in length), a load elongation curve or a stress-strain curve can also be produced (Figure 3.34). The stress-strain curve is generated by dividing the load by the width and thickness of the geotextile specimen. Since the thickness of the geotextile typically decreases as tensile load is applied and is also variable throughout the specimen, the "stress" is often reported as the load divided by the specimen width (in lb/in.). This curve is important in assessing geotextile strength, particularly for strain compatibility in soil reinforcement applications.

Researchers throughout the world have studied the factors affecting the uniaxial tensile strength of geotextiles (Shrestha and Bell, 1982; Moritz and Murray, 1982; Richards and Scott, 1986; Rowe and Ho, 1986; Cazzuffi et al., 1986; Myles, 1987; deGroot et al., 1990; Anjiang et al., 1990; Wayne et al., 1993). These factors include specimen size, aspect ratio (width-to-length ratio), stain rates, gage length, clamping conditions, fabric type and construction, and anisotropic conditions. This research has led to the standardization of uniaxial tension testing procedures and the following general trends:

- The breaking force per unit width measured in a uniaxial tensile test is not affected significantly by the sample width (Moritz and Murray, 1982; Shrestha and Bell, 1982; Richards and Scott, 1986; Rowe and Ho, 1986; Cazzuffi et

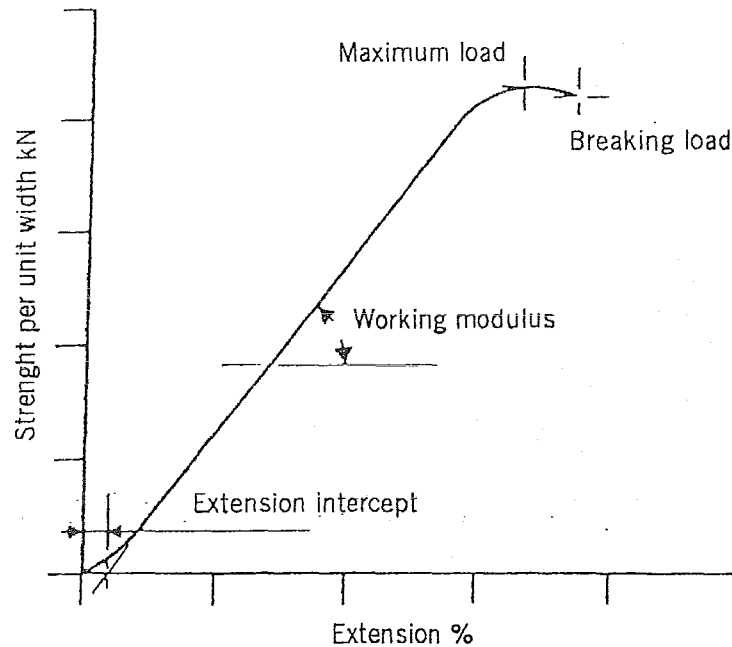


Figure 3.34 Strength per unit width versus extension curve for uniaxial tension test. (From Myles, 1987.)

al., 1986; Wayne et al., 1993) but may be influenced by the gage length²⁵ (Shrestha and Bell, 1982; Richards and Scott, 1986; Montalvo and Sickler, 1993).

- Depending on the type of geotextile, the modulus and elongation properties may vary with specimen width and gage length (Shrestha and Bell, 1982; Rowe and Ho, 1986; Richards and Scott, 1986; Wayne et al., 1993).
- Both woven and nonwoven geotextiles show anisotropic behavior. The anisotropic behavior in woven geotextile is expected due to the machine and cross directions. For nonwoven geotextiles, anisotropy is due to potential fluctuations and irregularity in the manufacturing process (Novais-Ferreira and Quarasma, 1982; Richards and Scott, 1986; Cazzuffi et al., 1986).
- Fabric structure has a significant influence on the stress-strain behavior. Woven and heat-bonded geotextiles show high strength and modulus and low elongation; needle-punched geotextiles have low strength and modulus and high elongation (Moritz and Murray, 1982; Shrestha and Bell, 1982; Richards and Scott, 1986).

Standard test methods have been developed for uniaxial geotextile tensile testing. The two commonly used standards include the grab (ASTM D 4632) and wide-width (ASTM D 4595) methods. The strip test is also often used and reported in the literature. Figure 3.35 shows various tensile test specimen sizes.

The strip and grab tensile tests utilize procedures originally established for the

²⁵The gage length is defined as the length of the specimen between clamps.

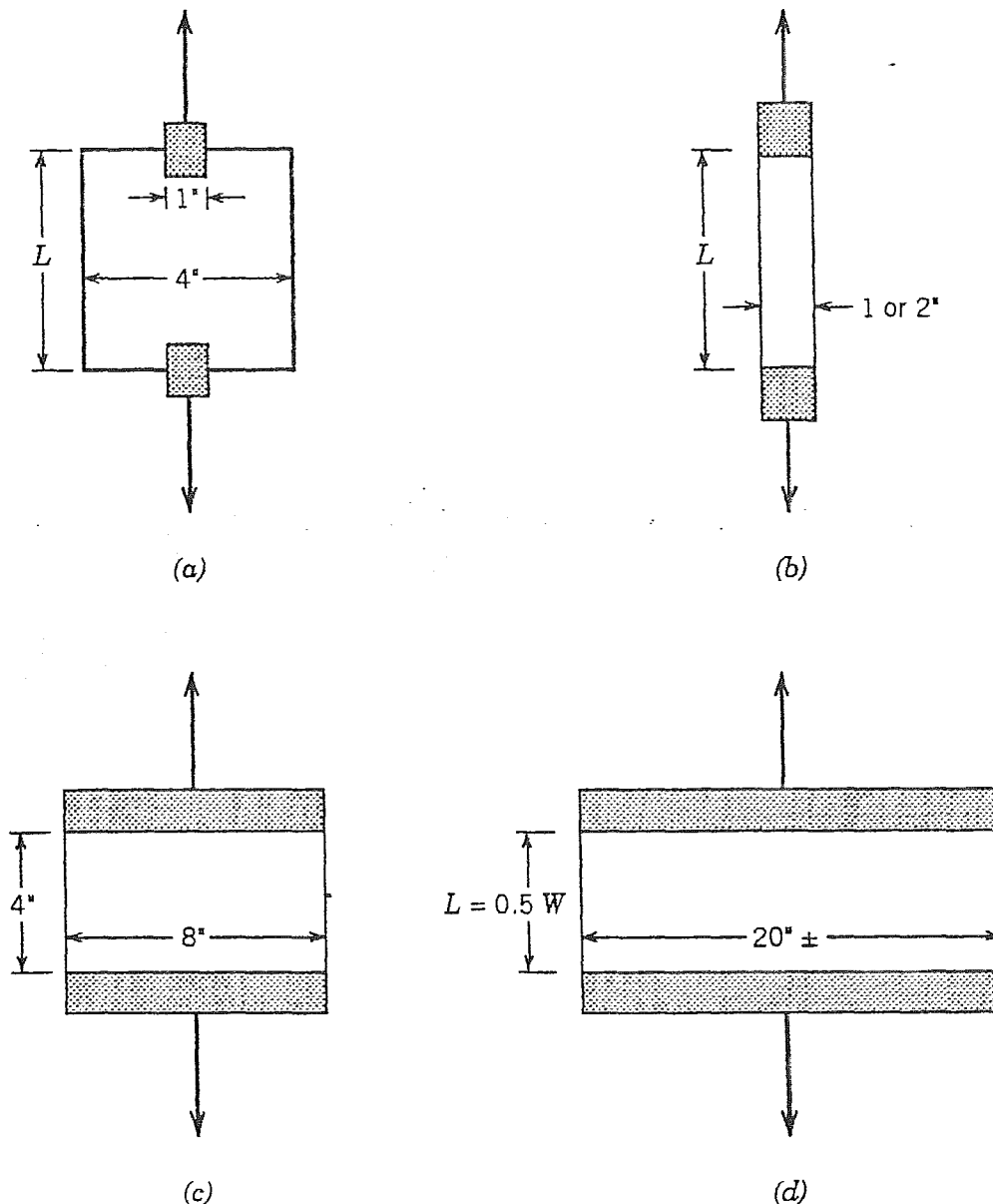


Figure 3.35 Various tensile test specimen sizes: (a) ASTM D4632 grab; (b) "narrow" strip; (c) ASTM D4595 wide width; (d) very wide width. (From Koerner, 1990.)

textile industry. The *strip tensile test* is typically performed on a 1- to 2-inch-wide specimen. As the tensile load is applied to this specimen, the specimen necks in its central region. These edge effects have significant influence on the tensile strength. In the *grab tensile test*, as shown in Figure 3.35, the clamps holding the specimen do not hold the entire width of the specimen. The grab method measures the "effective strength" of the geotextile, that is, the strength of the material in a specific width, together with the additional strength contributed by adjacent material. Both the grab and strip tests are useful as quality control or acceptance tests but have limited usefulness for design. Table 3.9 presents a range of typical grab tensile strength values for some nonwoven geotextiles.

The recommended tensile test for design is the *wide-width tensile test*, ASTM D 4595. This test was developed specifically for geotextiles and uses an 8-inch-wide

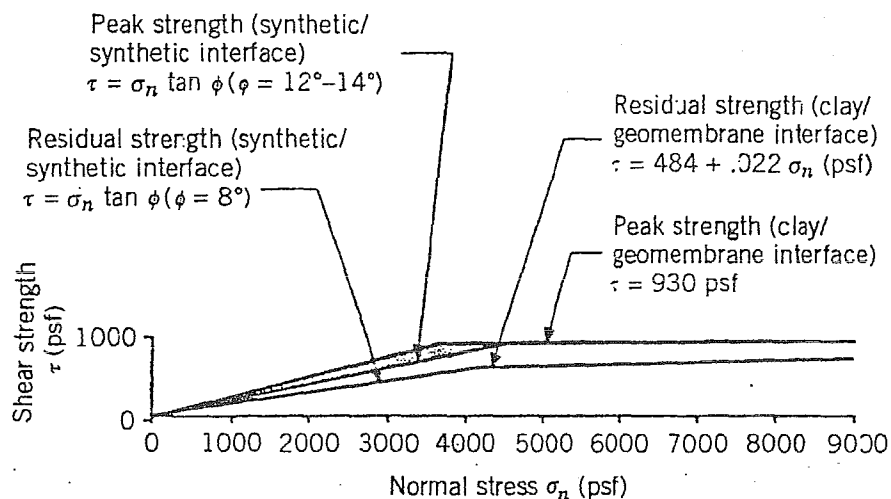


Figure 3.61 Liner strength relations. (From Byrne et al., 1992. Reproduced by permission of ASCE.)

1987; Soil and Material Engineers, 1987; Leach et al., 1987; Koutsourais et al., 1990; Swan et al., 1990; O'Rourke et al., 1990; Mitchell et al., 1990; Ojeshina, 1990; Druschel and O'Rourke, 1991; Somasundaram and Khilnani, 1991; Sharma and Hullings, 1993). The results are highly variable due to the large range of soil types and testing conditions. Both peak and residual values are included within the reported range. Table 3.14 also includes recommended soil geomembrane interface strengths.

As shown in Figure 3.61, the interface strength of clay-geomembrane exhibits a linear shear strength (τ) and normal stress (σ_n) relationship at lower normal stresses. The interface friction angles (δ) reported in Table 3.14 represent this behavior. At higher normal loads, the interface friction angle becomes very low and for all practical purposes τ tends to become independent of σ_n . The authors' experience on various low-plasticity (CL) and high-plasticity (CH) clays tested against both smooth and textured HDPE geomembrane confirms this τ - σ_n behavior. Recommended values presented in Table 3.14 should be used only as a guide in feasibility studies. Tests on site-specific materials and selected geomembranes should be conducted for final design purposes.

3.6.3 Geosynthetic-to-Geosynthetic Shear Strength

Several researchers have tested various geosynthetic-to-geosynthetic interfaces (Martin et al., 1984; Williams and Houlihan, 1986; Koutsourais et al., 1990; Mitchell et al., 1990; Lydick and Zagorski, 1990; Ojeshina, 1990; Somasundaram and Khilnani, 1991). The results of these studies are summarized in Table 3.15. The primary components of interface friction between multiple layers of geosynthetics are sliding between layers and dilation at the geosynthetic surface (Williams and Houlihan, 1986).

TABLE 3.15 Typical Range of Reported Geosynthetic to Geosynthetic Friction Angles (Degrees)

	PVC	HDPE Smooth	HDPE Textured	Geonet
Woven Geotextile	10–28	7–11	9–17	9–18
Nonwoven, needle-punched Geotextile	16–26	8–12	15–33	10–27
Nonwoven, resin/heat-bonded Geotextile	18–21	9–11	15–16	17–21
Geonet	11–24	5–19	7–25	—

The testing conditions may also have a significant effect on results. Mitchell et al. (1990) noted that polishing of geomembrane surfaces by geotextiles reduced interface friction. Also, the orientation of geonet strands can affect the interface strength between geonets and geomembranes (Geotek, 1987; Mitchell et al., 1990). Site-specific tests should therefore be performed using the actual materials and anticipated shear conditions.

3.6.4 Geosynthetic Clay Liner Shear Strength

Limited information is currently available on the internal shear strength of GCLs, due primarily to their relatively short history. The tests that have been performed are also difficult to compare, due to the numerous variations in test conditions. Many of these variations, such as strain rate, normal load, sample size, and consolidation conditions, are similar to the variations experienced when comparing shear strength testing of other geosynthetics. An additional variation of GCLs, however, is the hydrating conditions, including the hydrating liquid. Hydration can occur under free swell, constrained swell, or partially constrained swell, or the sample may be tested unhydrated. Even if hydrated under free-swell conditions, it may be difficult to assess whether full hydration has occurred since the bentonite may be restricted from free swell by the bonded geotextiles. Also, due to the large water absorption of bentonite, most shear strength test results will incorporate some immeasurable pore pressure effects unless the test is performed at extremely low displacement rates.

Table 3.16 presents the results of direct shear testing performed under various hydration conditions. The tests were performed at a strain rate of 9 mm/min and at normal stresses up to 60 kPa. Although these test results provide some information on the internal shear strength of GCLs, it is highly recommended that project specific testing be performed.

since creases in the geomembrane caused by sharp corners may lead to environmental stress cracking.

8.3.3.6 Placement of Soils over Geomembranes. As discussed in Section 8.3.3.2, soil should be “floated” over geomembranes such that a minimum 12 inches of this material exists between the construction equipment and the geomembrane at all times. This minimizes the possibility of geomembrane puncture and impact damage since the effective stress exerted by the construction equipment is reduced and the soil is not dumped on top of the geomembrane.

Soil placement over polyethylene geomembranes should occur in the early morning when there is adequate lighting and the geomembrane is contracted. By midday, wrinkles often develop in polyethylene geomembranes, making soil placement difficult. On days where the temperature exceeds 100°F, the wrinkles can be as large as 1 to 2 feet high. Even in the morning, 6-inch-high wrinkles can easily develop. If it cannot be avoided, soils may be placed over geomembrane wrinkles by placing the soil directly on top of the wrinkle such that it forms two smaller wrinkles. By continuously placing soil directly above the wrinkle, the wrinkle will eventually work itself out. Therefore, if possible, the geomembrane should not be permanently anchored until the soil overlying the geomembrane has been placed. In no situation should the geomembrane wrinkle be allowed to fold over under the weight of the overlying soil. These folds will crease the geomembrane and provide a preferential location for stress cracking and eventual leakage.

Placement of soils over geomembranes on slopes should occur from the bottom of slope upward. This will minimize the stresses on the geomembrane from construction equipment. Soils should be placed over geomembranes as soon as possible following geomembrane installation. This prevents UV degradation of the geomembrane and damage from ongoing construction activities, and also provides for good contact between the geomembrane and underlying material.

8.3.4 Structural Details

8.3.4.1 Anchorage. Anchor trenches are used at the top of side-slope liners to hold installed geosynthetics in place against applied loads and to prevent potential tears caused by wind intrusion beneath the geosynthetics. As shown in Figure 8.19, anchor trenches can generally be classified as flat, rectangular, or V-shaped. Selection of the appropriate anchor trench configuration for any particular site depends on the required holding capacity, access considerations, dimensional constraints, and available construction equipment. Often, a contractor may request that the anchor trench configuration be modified based on the equipment available. All such modifications should be checked and approved by the designer.

The holding capacity of anchor trenches is developed by the applied normal load of the soil placed above the geosynthetics, which creates frictional resistance between the geosynthetics and the underlying soil; there is minimal friction resistance developed between the upper soil and the geosynthetic since the soil above the

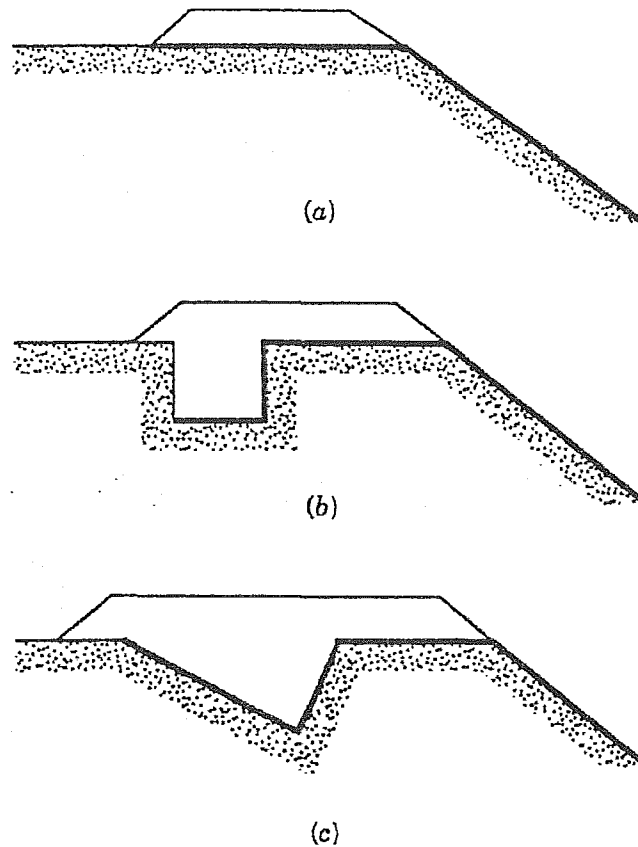


Figure 8.19 Typical anchor trench configurations: (a) flat anchor; and (b) rectangular anchor; and (c) V-shaped anchor.

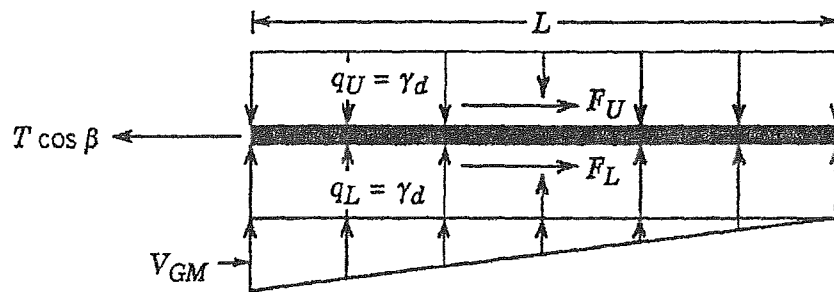
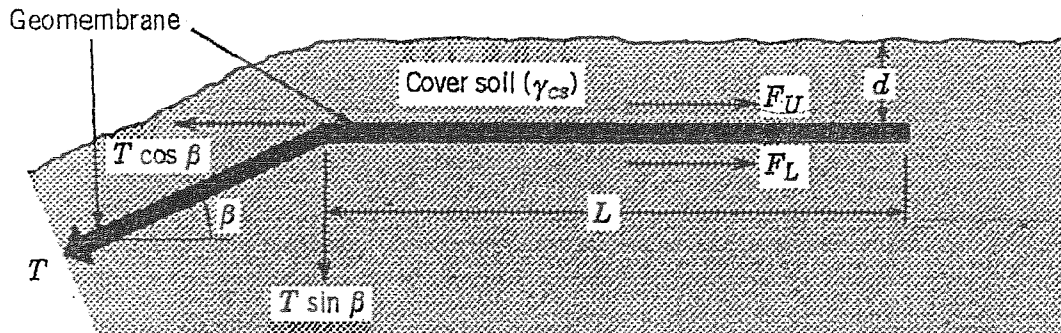
geosynthetic is likely to move with the geosynthetic. The soil depth, type of soil or other material underlying the geosynthetics, and geosynthetic anchorage length are therefore the key factors in developing the required anchor trench holding capacity.

The easiest anchor trench configuration to analyze is the flat anchor. The free-body diagram for the flat anchor and the development of equation (8.14) for anchorage length is shown in Figure 8.20.

$$L = \frac{T \cos \beta - T \sin \beta \tan \delta_L}{\gamma d \tan \delta_L} \quad (8.14)$$

There is no ideal solution for rectangular or V trenches. Koerner (1990) recommends that the problem be solved using imaginary, frictionless pulleys, as shown in Figure 8.21.

The anchor trench should be designed to resist pullout loads (T) caused by the self-weight of the geosynthetics. For geomembranes that may be exposed to severe temperature and wind loading conditions, stresses caused by these forces should also be evaluated. Ideally, the anchor trench should be designed to allow the geosynthetics to pull out slightly rather than cause tearing of the geosynthetics. The reasoning for this is that even if complete pullout occurred, it would usually be easier to replace pulled-out materials than to repair torn geosynthetics. The maxi-



$$F_U = q_U \tan \delta_U(L) \text{ (neglected since cover soil moves with geomembrane)}$$

$$F_L = q_L + 0.5 v_{GM} \tan \delta_L(L)$$

$$= \left[q_U + 0.5 \left(\frac{2 T \sin \beta}{L} \right) \right] \tan \delta_L(L)$$

$$T \cos \beta = q_L \tan \delta_L(L) + T \sin \beta \tan \delta_L$$

$$L = \frac{T \cos \beta - T \sin \beta \tan \delta_L}{\gamma_d \tan \delta_L}$$

Where: V_{GM} = vertical force due to geomembrane

F_U = friction force above geomembrane

F_L = friction force below geomembrane

q_U = stress above geomembrane due to cover soil weight

q_L = stress below geomembrane due to cover soil weight

T = tensile force in geomembrane

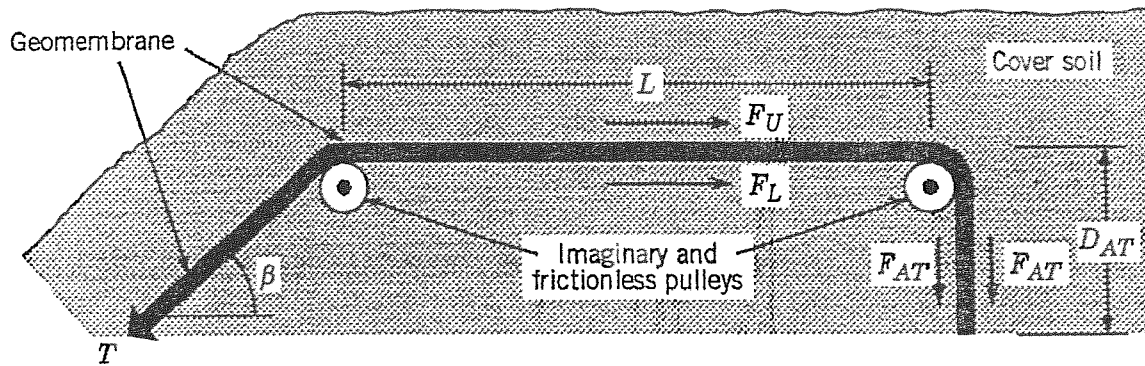
β = slope angle

d =

= unit weight of cover soil

δ = interface friction angle

Figure 8.20 Design of a flat anchor. (From Koerner, 1990.)



$$T = F_U + F_L + 2F_{AT}$$

Where: T = tensile stress in geomembrane

F_U = friction force above geomembrane
(assumed to be negligible since cover soil likely moves with geomembrane)

$$F_L = q \tan \delta (L)$$

q = surcharge pressure = γd

d = depth of cover soil

γ = unit weight of cover soil

δ = interface friction angle

L = runout length

$$F_{AT} = (\sigma_h \text{ ave}) \tan \delta (d_{AT})$$

σ_h = average horizontal stress in anchor trench

$$= k_o \sigma_v$$

$$\sigma_v = \gamma H_{ave}$$

H_{ave} = average depth of anchor trench (requires an estimate)

$$k_o = 1 - \sin \phi$$

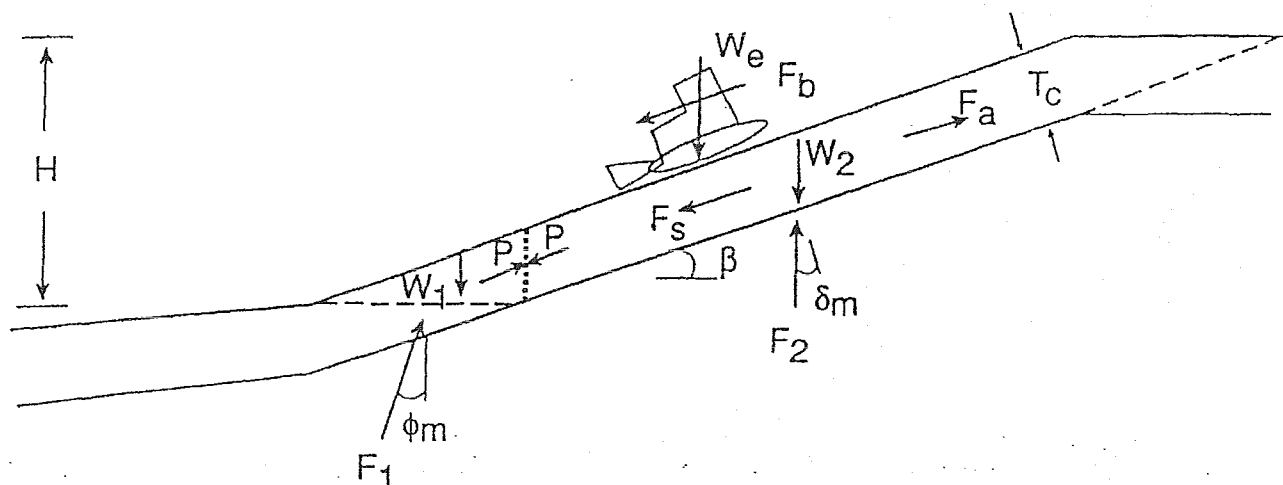
ϕ = angle of shearing resistance of backfill soil

d_{AT} = depth of anchor trench (unknown)

Figure 8.21 Design of a rectangular and V anchor trenches. (From Koerner, 1990.)

imum holding capacity of the anchor trench should therefore be slightly less than the ultimate tensile strength of the geosynthetic to be anchored, irrespective of the applied loads. If the applied loads are greater than the tensile strength of the geosynthetics, measures should be taken to reduce the applied loads or higher-strength geosynthetics should be used.

If soil materials are placed above side-slope geosynthetics, the load caused by soil, seepage forces, and construction equipment should be assessed. Often, a high-strength reinforcing geotextile or geogrid is required to hold the soil on the slopes. Druschel and Underwood (1993) used a force equilibrium method to assess the required anchorage force for these high-strength materials. The free-body and force vector diagram for this method are illustrated in Figures 8.22 and 8.23, respectively. As shown, the items⁴ to be evaluated include the toe buttress resistance, soil



Note: P , F_s , F_a , and F_b , are assumed to be parallel to β

Figure 8.22 Free-body diagram of side-slope forces. (From Druschel and Underwood, 1993.)

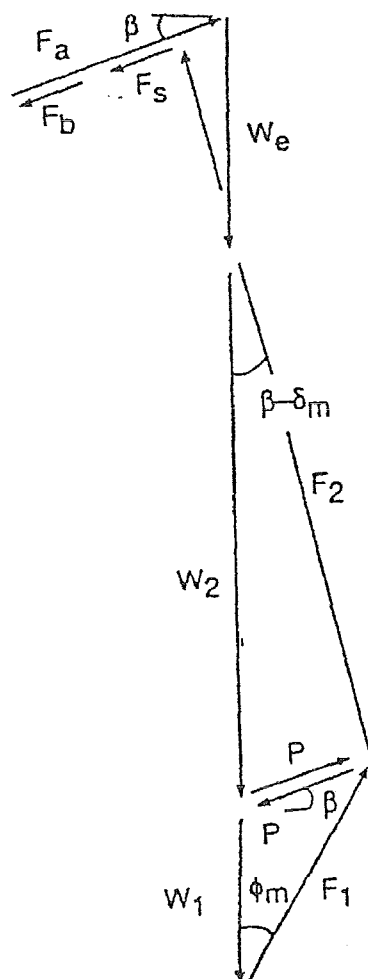


Figure 8.23 Force vector diagram. (From Druschel and Underwood, 1993.)

cover, equipment load, and seepage forces. The equation for the required anchorage force is

$$F_a = \frac{\gamma_w T_w^2}{2 \tan \beta} \left(\frac{\tan \phi_m}{\cos^2 \beta} + \frac{2H \tan \delta_m}{\cos \beta} - \frac{\tan \delta_m}{\cos \beta} \right) + W_e \left[0.3 + \frac{\sin(\beta - \delta_m)}{\cos \delta_m} \right] \quad (8.15)$$

$$- \frac{\gamma_c T_c^2 \sin(\beta - \delta_m)}{2 \sin \beta \cos \beta \cos \delta_m} \left[\frac{\sin \phi_m \cos \delta_m}{\cos(\beta + \phi_m) \sin(\beta - \delta_m)} + 1 - \frac{2H \cos \beta}{T_c} \right]$$

where H = side-slope height

T_c = cover soil thickness

β = side-slope angle

γ_w = unit weight of water

γ_c = unit weight of cover soil

δ = interface friction angle

δ_m = interface friction angle (mobilized)

ϕ = soil shear strength angle

ϕ_m = soil shear strength angle (mobilized)

W_2 = weight of side slope soil

W_1 = weight of toe buttress soil

W_e = weight of equipment on the sideslope (equipment weight divided by equipment width)

F_b = equipment braking force (approximately 30 percent of equipment's weight acting downslope and parallel to interface)

T_w = thickness of seepage

W_{w1} = weight of seepage water in toe buttress

W_{w2} = weight of seepage water in side-slope soil

F_a = geosynthetic anchorage force

F_s = seepage force

F_1 = toe buttress reaction force

F_2 = side-slope reaction force

P = side slope/toe buttress reaction force

Although this equation may seem complex, it is relatively straightforward and easily adaptable to a computer spreadsheet. Figures 8.24 and 8.25 present the variation in anchorage force with slope height assuming an interface friction angle of 9 and 12°, respectively. The reinforcing geotextile or geogrid selected should have a yield strength greater than the required anchorage force and should be able to attain the required anchorage force at a strain level of approximately 2 percent.

⁴Further discussion of these forces is provided in Chapter 10.

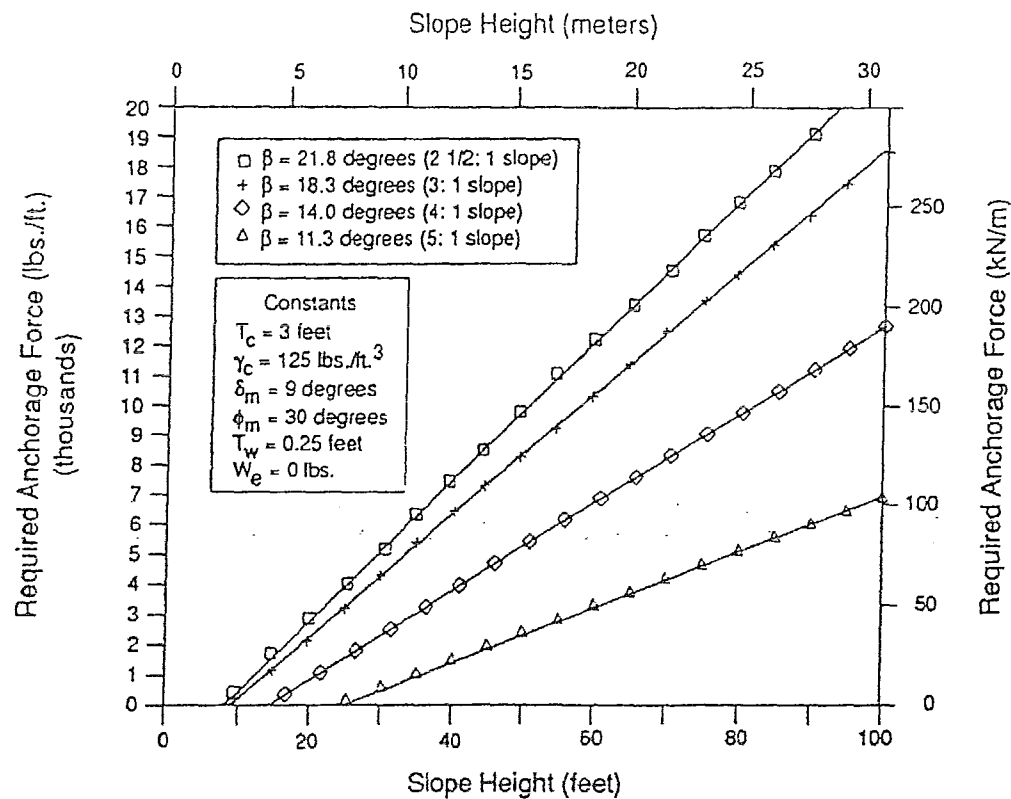


Figure 8.24 Anchorage force required for slope with 9° interface friction angle. (From Druschel and Underwood, 1993.)

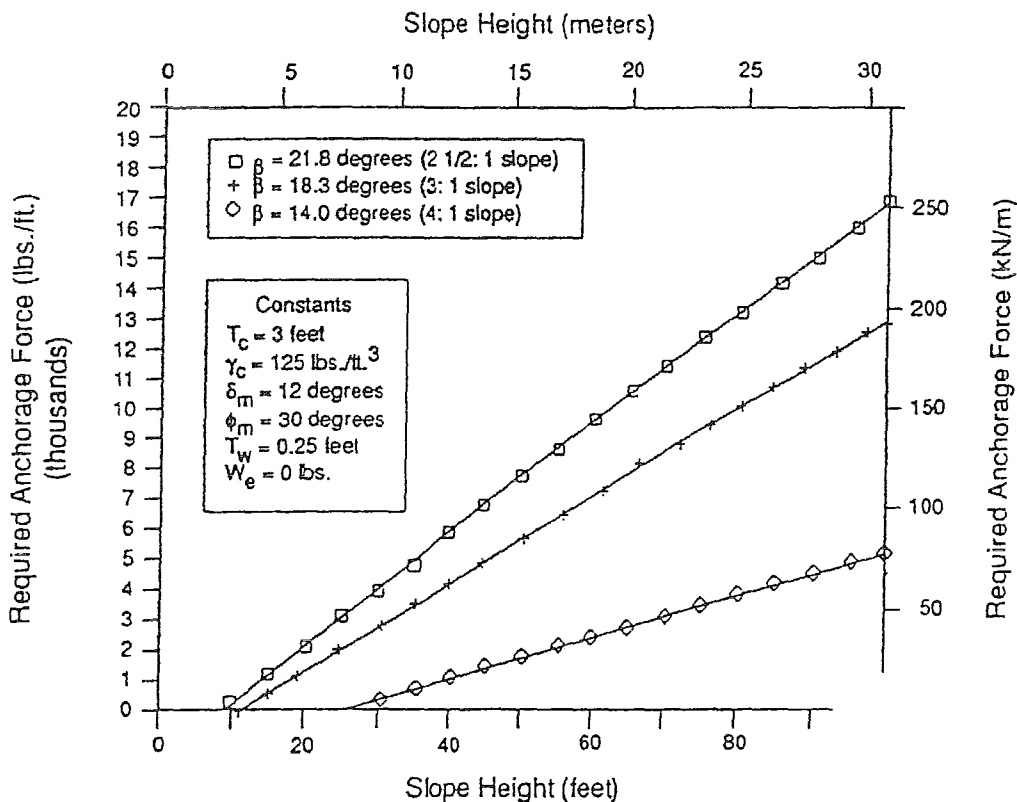


Figure 8.25 Anchorage force required for slope with 12° interface friction angle. (From Druschel and Underwood, 1993.)

Example 8.4. A 50-foot-high 3H:1V side slope is lined with 60-mil single sided textured HDPE (textured side down against underlying clay and smooth side facing up). Calculate various stresses in the liner and determine the anchor trench capacity assuming that it is 3 feet deep and 2 feet wide. At the base, a 3-foot thickness of soil, consisting of a 1-foot drainage layer and a 2-foot-thick operations layer, is already in place.

SOLUTION

A. *Forces on Geomembrane.* The forces on the geomembrane include those due to self-weight, temperature, and wind.

1. *Force (F_w) per foot width due to self-weight (W).*

$$F_w = W \sin \beta - F$$

where

$$W = L t \gamma = \frac{H}{\sin \beta} t \gamma$$

and where

$$F = W \cos \beta \tan \beta$$

$$H = \text{exposed height of geomembrane} = 50 - 3 = 47 \text{ ft}$$

$$\sin \beta = \sin [\tan^{-1}(1/3)] = \sin 18.3^\circ = 0.314$$

$$\cos \beta = 18.3^\circ = 0.95$$

$$t = \text{geomembrane thickness} = \frac{60}{1000 \times 12} = 0.005 \text{ ft}$$

$$\gamma = \text{unit weight of geomembrane} = SG \cdot \gamma_w = (0.94)(62.4 \text{ lb/ft}^3) = 59 \text{ lb/ft}^3$$

Therefore,

$$W = \frac{47}{0.314} (0.005)(59) = 44.1 \text{ lb/ft width}$$

and assuming that $\delta = 15^\circ$ yields

$$F = (44.1)(0.95)(\tan 15^\circ) = 11.23 \text{ lb/ft width}$$

and

$$\begin{aligned} F_w &= 44.1(0.314) - 11.23 \\ &= 2.62 \text{ lb/ft width} \end{aligned}$$

2. *Thermal forces (F_t) per foot width due to temperature change (ΔT).* Assume that the coefficient of thermal expansion $\mu = 1 \times 10^{-4}/^\circ\text{F}$ and the temperature fluctuations of the geomembrane during the day and the night are 120°F and 60°F , respectively. From equation (8.12),

$$\Delta L = \mu L \Delta T$$

which in terms of thermal strain may be written as

$$\epsilon_t = \mu \Delta T$$

Therefore,

$$\epsilon_t = 1 \times 10^{-4} \times (120 - 60) = 6 \times 10^{-3}$$

From the geomembrane stress-strain curve (test data sheet), σ corresponding to $\epsilon_t = 6 \times 10^{-3}$ is ~ 300 psi.

$$F_t = \sigma A = 300 \times 144 \times \frac{0.06}{12} = 216 \text{ lb/ft}$$

3. *Forces (F_{wind}) per foot width due to wind loading.* From equation (8.13)

$$q = 0.002556 V^2$$

Assuming that $V = 50$ miles/h, we have

$$q = 0.002556(50)^2 = 6.39 \text{ lb/ft}^2$$

Assuming that half of this force is supported by the drainage and operations layer and the other half is supported by the anchor trench gives us

$$F_{\text{wind}} = \frac{1}{2} q L = (6.39)(\frac{1}{2})(149.7) = 478 \text{ lb/ft width}$$

4. *Total design forces (F_d)*

$$\begin{aligned} F_d &= F_w + F_t + F_{\text{wind}} \\ &= 3 + 216 + 478 = 697 \text{ lb/ft width} \end{aligned}$$

B. *Anchor Trench Capacity.* From Figure 8.21.

$$\begin{aligned} T &= F_U + F_L + 2F_{\text{AT}} \\ &= 0 + \gamma d \tan \delta L + 2\sigma_{\text{have}} \tan \delta(d_{\text{AT}}) \end{aligned}$$

Assuming that $d = 3$ ft, $\delta = 15^\circ$, $L = 3$ ft, $\phi = 30^\circ$, $d_{\text{AT}} = 3$ ft yields

$$\sigma_{\text{have}} = k_0 \left(\frac{\gamma h}{2} \right) = (1 - \sin \phi) \left(\frac{125 \times 3}{2} \right) = 94$$

$$T = 125(2) \tan 15(3) + 2(94) \tan 15(3) = 352 \text{ lb/ft width}$$

$$\text{additional resistance due to backfill soil} = (3 + 3) \times 2 \times 125 (\tan 20^\circ + \tan 15^\circ) = 948 \text{ lb/ft}$$

$$\text{total } T = 352 + 948 = 1300 \text{ lb/ft}$$

C. Allowable Stress

Minimum allowable stress at yield = 2000 psi:

$$\begin{aligned} F_{\text{all}} &= \sigma t \\ &= 2000(0.06) = 120 \text{ lb/in.} = 1440 \text{ lb/ft} \end{aligned}$$

D. Comparison of Various Forces

$$\begin{aligned} F_d &= \text{design force} = 697 \text{ lb/ft width} \\ T &= \text{anchor trench capacity} = 1300 \text{ lb/ft width} \\ F_{\text{all}} &= \text{allowable force} = 1440 \text{ lb/ft width} \end{aligned}$$

The anchor trench should be designed to:

- Resist the design force = 697 lb/ft
- Allow the geomembrane to slip out before the allowable stress is reached

Therefore,

$$\begin{aligned} F_d &< T < F_{\text{all}} \\ 697 &< 1300 < 1440 \text{ lb/ft width} \quad \text{OK} \end{aligned}$$

$$\text{FS against pullout} = \frac{T}{F_d} = \frac{1300}{697} = 1.87$$

$$\text{FS against geomembrane failure} = \frac{F_{\text{all}}}{F_d} = \frac{1440}{697} = 2.07$$

8.3.4.2 Connection/Termination. As discussed in Section 8.3.1, most landfill liners are constructed in phases. Adequate liner connection and termination details are therefore critical in maintaining liner continuity between phases. To provide satisfactory connection/termination details, the designer must first envision how the connection will be constructed, the required construction equipment access, and how much overlap is necessary between the lining systems. Typically a 4- to 5-foot overlap is sufficient for the clay liner and 2 to 3 feet for the geosynthetics. To avoid a preferential leachate flow path, the connection between clay liners should not be vertical but rather, stair-stepped at an angle (Figure 8.26). This requires some reworking of the existing clay liners but will lead to a continuous bond between the existing and future clay liners. For future connection of geomembrane liners, the edge of the existing geomembrane liner should be kept as clean as possible for proper seaming. This is often achieved by wrapping the final leading edge of the geomembrane with a nonwoven geotextile prior to placing any cover materials over the geomembrane.

Connection/termination details parallel to landfill sideslopes should also be considered, especially for geomembranes. Often the edge of a geomembrane is left

**APPLICATION FOR PERMIT RENEWAL AND MODIFICATION
SANDOVAL COUNTY LANDFILL**

**VOLUME III: LANDFILL ENGINEERING CALCULATIONS
SECTION 7: GEOSYNTHETICS TENSILE STRESS AND STABILITY ANALYSIS**

ATTACHMENT III.7.B

**QIAN, XUEDE; KOERNER, ROBERT M.; AND GRAY, DONALD H. 2002.
GEOTECHNICAL ASPECTS OF LANDFILL DESIGN AND CONSTRUCTION.
NEW YORK: PRETENCE HALL.**

GEOTECHNICAL ASPECTS *of* LANDFILL DESIGN *and* CONSTRUCTION



Xuede Qian • Robert M. Koerner • Donald H. Gray

Solution:

Assume the runout resistance force is equal to the geomembrane allowable tensile force. From the design equations just presented,

$$\begin{aligned} T \cdot (\cos \beta) &= 350(144)(0.030/12) \cos 18.4^\circ \\ &= 120 \text{ lb/ft (1.75 kN/m)} \end{aligned}$$

$$T \cdot (\sin \beta) = 39.8 \text{ lb/ft (0.58 kN/m)}$$

$$q_B = \gamma_s \cdot d_{CS} = (100)(1.0) = 100 \text{ lb/ft (1.46 kN/m)}$$

which, when substituted into Equation 4.11, gives

$$\begin{aligned} T \cdot (\cos \beta) &= q_B \cdot \tan \delta_C (L_{RO}) + T \cdot \sin \beta \cdot \tan \delta_C \\ 120 &= 100(\tan 20^\circ)(L_{RO}) + 39.8(\tan 20^\circ) \end{aligned} \quad (4.11)$$

$$120 = 36.4 \cdot L_{RO} + 14.5$$

from which it follows that

$$L_{RO} = 2.9 \text{ ft (0.88 m); use 3.0 ft (use 1 m)}$$

Note that the runout length is strongly dependent on the value of allowable stress used in the analysis. To mobilize the full strength of the geomembrane would require a longer runout length or an anchor trench. However, this might not be desirable. Pullout, without geomembrane failure, might be preferable to tensile rupture and separation of the geomembrane. Thus, the design runout or anchor resistance capacity should fall between the ultimate strength and allowable strength of a geosynthetic liner (Qian, 1995). That is,

Ultimate Strength > Runout and/or Anchor Resistance Capacity > Allowable Strength

Runout and/or Anchor Resistance Capacity = T/t

$$\sigma_{\text{allow}} = \sigma_{\text{ult}}/FS, \text{ and } T_{\text{allow}} = \sigma_{\text{allow}} \cdot t,$$

where T = geomembrane tensile force (i.e., runout or anchor resistance force) per unit width;
 t = geomembrane thickness;
 σ_{ult} = ultimate geomembrane stress (e.g., yield or break);
 FS = factor of safety based on geomembrane strength;
 σ_{allow} = allowable geomembrane stress; and
 T_{allow} = allowable geomembrane force per unit width.

4.7.2 Design of Rectangular Anchor Trench

The situation with a rectangular anchor trench in place at the end of the runout section is illustrated in Figure 4.9. The configuration requires some important assumptions regarding the state of stress within the anchor trench and its resistance mechanism. In order to establish static equilibrium, an imaginary and frictionless pulley is assumed at

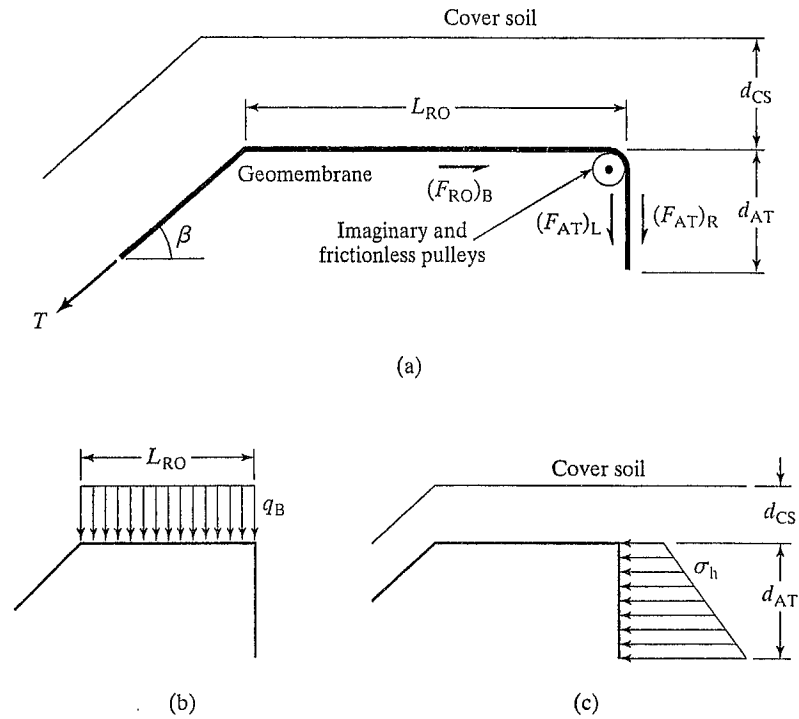


FIGURE 4.9 Cross Section of Geomembrane Runout Section with a Rectangular Anchor Trench and Related Stresses and Forces Involved

the top edge of the anchor trench, as shown in Figure 4.9 (Qian, 1995), which allows the geomembrane to be considered as a continuous member along its entire length.

From Figure 4.9, the following force summations lead to the appropriate design equations:

From $\sum F_v = 0$,

$$T \cdot (\sin \beta) = 0.5 \cdot V_{GM} L_{RO}$$

The cover soil pressure on the runout length is

$$q_B = \gamma_s \cdot d_{CS}$$

The lateral earth force acting on both sides of the geomembrane buried in the anchor trench is

$$P_L = P_R = K_o \cdot \gamma_s \cdot (d_{CS} + 0.5 \cdot d_{AT}) \cdot d_{AT}$$

The vertical force due to the geomembrane force is

$$V_{GM} = \frac{2 \cdot T \cdot \sin \beta}{L_{RO}}$$

The friction force above the runout geomembrane is always neglected in the anchor trench design, since the cover soil probably moves along with the geomembrane as it deforms.

From $\sum F_H = 0$,

$$T \cdot (\cos \beta) = (F_{RO})_B + (F_{AT})_L + (F_{AT})_R \quad (4.13)$$

$$\begin{aligned} \text{and } (F_{RO})_B &= q_B \cdot L_{RO} \cdot \tan \delta_C + 0.5 \cdot V_{GM} \cdot L_{RO} \cdot \tan \delta_C \\ &= q_B \cdot L_{RO} \cdot \tan \delta_C + 0.5 \cdot (2 \cdot T \cdot \sin \beta / L_{RO}) \cdot L_{RO} \cdot \tan \delta_C \end{aligned}$$

$$\text{or } (F_{RO})_B = q_B \cdot L_{RO} \cdot \tan \delta_C + T \cdot \sin \beta \cdot \tan \delta_C \quad (4.14)$$

Because $q_B = \gamma_s \cdot d_{CS}$, the friction force beneath the runout geomembrane is

$$(F_{RO})_B = \gamma_s \cdot d_{CS} \cdot L_{RO} \cdot \tan \delta_C + T \cdot \sin \beta \cdot \tan \delta_C \quad (4.15)$$

The friction force between the left side of the geomembrane and the side wall of the anchor trench is

$$(F_{AT})_L = (\sigma_h)_{ave} \cdot d_{AT} \cdot \tan \delta_C$$

The friction force between the right side of the geomembrane and the side wall of the anchor trench is

$$(F_{AT})_R = (\sigma_h)_{ave} \cdot d_{AT} \cdot \tan \delta_F$$

where $(\sigma_h)_{ave} = K_o \cdot (\sigma_v)_{ave}$

Because $K_o = 1 - \sin \phi$ and $(\sigma_v)_{ave} = \gamma_s \cdot (d_{CS} + 0.5 \cdot d_{AT})$

$$(\sigma_h)_{ave} = (1 - \sin \phi) \cdot \gamma_s \cdot (d_{CS} + 0.5 d_{AT}) \quad (4.16)$$

$$\text{So } (F_{AT})_L = (1 - \sin \phi) \cdot \gamma_s \cdot (d_{CS} + 0.5 \cdot d_{AT}) \cdot d_{AT} \cdot \tan \delta_C \quad (4.17)$$

$$\text{and } (F_{AT})_R = (1 - \sin \phi) \cdot \gamma_s \cdot (d_{CS} + 0.5 \cdot d_{AT}) \cdot d_{AT} \cdot \tan \delta_F \quad (4.18)$$

Substituting Equations 4.15, 4.17, and 4.18 into Equation 4.13 gives

$$\begin{aligned} T \cdot (\cos \beta - \sin \beta \cdot \tan \delta_L) &= \gamma_s \cdot d_{CS} \cdot L_{RO} \cdot \tan \delta_C + \\ &\quad (1 - \sin \phi) \cdot \gamma_s \cdot (d_{CS} + 0.5 \cdot d_{AT}) \cdot d_{AT} \cdot (\tan \delta_C + \tan \delta_F) \end{aligned}$$

which leads to

$$T = \frac{\gamma_s \cdot d_{CS} \cdot L_{RO} \cdot \tan \delta_C + (1 - \sin \phi) \cdot \gamma_s \cdot (d_{CS} + 0.5 \cdot d_{AT}) \cdot d_{AT} \cdot (\tan \delta_C + \tan \delta_F)}{\cos \beta - \sin \beta \cdot \tan \delta_C} \quad (4.19)$$

or

$$T = \frac{q_B \cdot L_{RO} \cdot \tan \delta_C + K_o \cdot (\sigma_v)_{ave} \cdot d_{AT} \cdot (\tan \delta_C + \tan \delta_F)}{\cos \beta - \sin \beta \cdot \tan \delta_C} \quad (4.20)$$

When $\delta_C = \delta_F = \delta$, Equation 4.19 becomes

$$T = \frac{\gamma_s \cdot d_{CS} \cdot L_{RO} \cdot \tan \delta + 2 \cdot (1 - \sin \phi) \cdot \gamma_s \cdot 0.5 \cdot d_{AT} \cdot \tan \delta}{\cos \beta - \sin \beta \cdot \tan \delta} \quad (4.21)$$

and Equation 4.20 becomes

$$T = \frac{q_B \cdot L_{RO} \cdot \tan \delta + 2 \cdot K_o \cdot (\sigma_v)_{ave} \cdot d_{AT} \cdot \tan \delta}{\cos \beta - \sin \beta \cdot \tan \delta} \quad (4.22)$$

where T = geomembrane tensile force (i.e., anchor trench resistance force) per unit width;

$(F_{RO})_B$ = friction force beneath runout geomembrane;

$(F_{AT})_L$ = friction force between the left side of the geomembrane and the side wall of the anchor trench;

$(F_{AT})_R$ = friction force between the right side of the geomembrane and the side wall of the anchor trench;

$(\sigma_h)_{ave}$ = average horizontal stress in anchor trench;

$(\sigma_v)_{ave}$ = average vertical stress in anchor trench;

H_{ave} = average depth of anchor trench;

K_o = coefficient of at-rest earth pressure;

L_{RO} = runout length;

d_{CS} = depth of cover soil;

d_{AT} = anchor trench depth;

γ_s = unit weight of cover and backfill soil;

ϕ = friction angle of backfill soil in anchor trench;

δ_C = friction angle between geomembrane and underlying soil;

δ_F = friction angle between geomembrane and backfill soil;

δ = friction angle between geomembrane and soil; and

β = sideslope angle, measured from horizontal.

Note that because this situation results in one equation with two unknowns, thus a choice of L_{RO} or d_{AT} is necessary to calculate the other.

EXAMPLE 4.4

A 60-mil (1.5-mm) HDPE geomembrane of allowable stress 840 lb/in² (5,800 kN/m²) is placed on a 3(H) to 1(V) sideslope. There is a cover soil of 12 inches (0.3 m) placed over the geomembrane. The unit weight of cover soil and backfill soil in the anchor trench is 110 lb/ft³ (17.3 kN/m³). The friction angle between the geomembrane and the underlying soil is 18 degrees, and the friction angle between the geomembrane and the backfill soil in the anchor trench is 22 degrees. The friction of the backfill soil is 30 degrees. Determine the required runout length for a 24-inch-deep (0.6-meter-deep) anchor trench.

Solution:

Assume the anchor resistance force is equal to the geomembrane allowable tensile force.

Using the previously developed design equation from Figure 4.9,

$$T \cdot (\cos \beta) = (F_{RO})_B + (F_{AT})_L + (F_{AT})_R \quad (4.13)$$

where $T = T_{allow} = \sigma_{allow} \cdot t$

From Equation 4.19, we have

$$T = \frac{\gamma_s \cdot d_{CS} \cdot L_{RO} \cdot \tan \delta_C + (1 - \sin \phi) \cdot \gamma_s \cdot (d_{CS} + 0.5 \cdot d_{AT}) \cdot d_{AT} \cdot (\tan \delta_C + \tan \delta_F)}{\cos \beta - \sin \beta \cdot \tan \delta_C} \quad (4.19)$$

and

$$\sigma_{\text{allow}} \cdot t \cdot (\cos \beta - \sin \beta \cdot \tan \delta_C) = \gamma_s \cdot d_{CS} \cdot L_{RO} \cdot \tan \delta_C + (1 - \sin \phi) \cdot \gamma_s \cdot (d_{CS} + 0.5 \cdot d_{AT}) \cdot d_{AT} \cdot (\tan \delta_C + \tan \delta_F)$$

so that

$$\sigma_{\text{allow}} \cdot t = (840)(144)(0.060)/12 = 605 \text{ lb/ft (8.83 kN/m)} \text{ and } (605)[(\cos 18.4^\circ) - (\sin 18.4^\circ)(\tan 18^\circ)] = (110)(1)(\tan 18^\circ)(L_{RO}) + (0.5)(110)(2)(2)(\tan 18^\circ + \tan 22^\circ)$$

or

$$(605)(0.846) = (35.74) \cdot L_{RO} + (220)(0.729) \text{ which yields } 512.83 = (35.74) \cdot L_{RO} + 160.38 \text{ or } L_{RO} = 9.86 \text{ ft (2.96 m)}$$

Thus, use the runout length $L_{RO} = 10 \text{ ft (3 m)}$.

The geomembrane can also be extended along the trench bottom to increase resistance force, which is called an L-shaped rectangular anchor trench. A typical layout in an L-shaped rectangular anchor trench, which is widely used in landfill projects, is shown in Figure 4.10. In order to establish the static equilibrium equation, two imaginary and frictionless pulleys are assumed at the top edge and the bottom corner of the anchor trench, as shown in Figure 4.10 (Qian, 1995). This assumption again allows the geomembrane to be considered as a continuous member.

The friction force above a runout geomembrane is always neglected in the anchor trench design, since the cover soil probably moves together with the geomembrane as it deforms.

From $\Sigma F_H = 0$

$$T \cdot (\cos \beta) = (F_{RO})_B + (F_{AT})_L + (F_{AT})_R + (F_{AB})_B + (F_{AB})_U \quad (4.23)$$

The friction force between the geomembrane and the underlying soil at the bottom of the anchor trench is

$$(F_{AB})_B = \sigma_{vB} \cdot L_{AT} \cdot \tan \delta_C \quad (4.24)$$

The friction force between the geomembrane and the overlying soil at the bottom of the anchor trench is

$$(F_{AB})_U = \sigma_{vB} \cdot L_{AT} \cdot \tan \delta_F \quad (4.25)$$

Because $\sigma_{vB} = \gamma_s \cdot (d_{CS} + d_{AT})$,

$$(F_{AB})_B = \gamma_s \cdot (d_{CS} + d_{AT}) \cdot L_{AT} \cdot \tan \delta_C \quad (4.26)$$

and

$$(F_{AB})_U = \gamma_s \cdot (d_{CS} + d_{AT}) \cdot L_{AT} \cdot \tan \delta_F \quad (4.27)$$

Substituting Equations 4.15, 4.17, 4.18, 4.26, and 4.27 into Equation 4.23 gives

$$T \cdot (\cos \beta - \sin \beta \cdot \tan \delta_L) = \gamma_s \cdot d_{CS} \cdot L_{RO} \cdot \tan \delta_C + \gamma_s \cdot (\tan \delta_C + \tan \delta_F) [(1 - \sin \phi) \cdot \gamma_s \cdot (d_{CS} + 0.5 \cdot d_{AT}) \cdot d_{AT} + (d_{CS} + d_{AT}) \cdot L_{AT}]$$

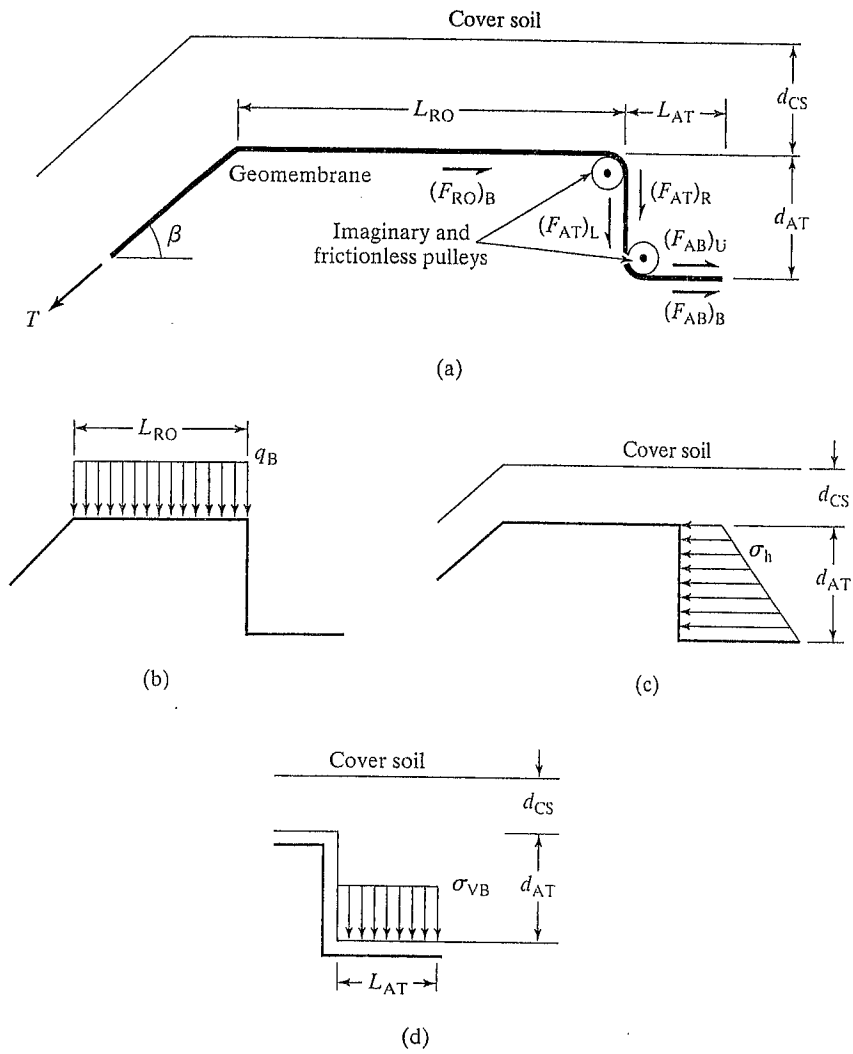


FIGURE 4.10 Cross Section of Geomembrane Runout Section with an L-Shaped Rectangular Anchor Trench and Related Stresses and Forces Involved

which leads to

$$T = \frac{\gamma_s \cdot d_{CS} \cdot L_{RO} \cdot \tan \delta_C + \gamma_s \cdot [(1 - \sin \phi) \cdot \gamma_s \cdot (d_{CS} + 0.5 \cdot d_{AT}) \cdot d_{AT} + (d_{CS} + d_{AT}) \cdot L_{AT}] (\tan \delta_C + \tan \delta_F)}{\cos \beta + \sin \beta \cdot \tan \delta_C} \quad (4.28)$$

or

$$T = \frac{q_B \cdot L_{RO} \cdot \tan \delta_C + [K_o \cdot (\sigma_v)_{ave} \cdot d_{AT} + \sigma_{vB} \cdot L_{AT}] (\tan \delta_C + \tan \delta_F)}{\cos \beta - \sin \beta \cdot \tan \delta_C} \quad (4.29)$$

When $\delta_C = \delta_F = \delta$, Equation 4.28 becomes

$$T = \frac{\gamma_s \cdot d_{CS} \cdot L_{RO} \cdot \tan \delta + 2 \cdot \gamma_s \cdot [(1 - \sin \phi) \cdot \gamma_s \cdot (d_{CS} + 0.5 \cdot d_{AT}) \cdot d_{AT} + (d_{CS} + d_{AT}) \cdot L_{AT}] \cdot \tan \delta}{\cos \beta - \sin \beta \cdot \tan \delta} \quad (4.30)$$

and Equation 4.29 becomes

$$T = \frac{q_B \cdot L_{RO} \cdot \tan \delta + 2 \cdot [K_o \cdot (\sigma_v)_{ave} \cdot d_{AT} + \sigma_{vB} \cdot L_{AT}] \cdot \tan \delta}{\cos \beta - \sin \beta \cdot \tan \delta} \quad (4.31)$$

where T = geomembrane tensile force (i.e., anchor trench resistance force) per unit width;

$(F_{RO})_B$ = friction force beneath runout geomembrane;

$(F_{AT})_L$ = friction force between the left side of the geomembrane and the side wall of the anchor trench;

$(F_{AT})_R$ = friction force between the right side of the geomembrane and the side wall of the anchor trench;

$(F_{AB})_B$ = friction force between the geomembrane and the underlying soil at the bottom of the anchor trench;

$(F_{AB})_U$ = friction force between the geomembrane and the overlying soil at the bottom of the anchor trench;

$(\sigma_v)_{ave}$ = average vertical stress in anchor trench;

K_o = coefficient of at-rest earth pressure;

L_{RO} = runout length;

d_{CS} = depth of cover soil;

d_{AT} = anchor trench depth;

γ_s = unit weight of cover and backfill soil;

ϕ = friction angle of backfill soil in anchor trench;

δ_C = friction angle between the geomembrane and the underlying soil;

δ_F = friction angle between the geomembrane and the backfill soil;

δ = friction angle between the geomembrane and the soil; and

β = sideslope angle, measured from horizontal.

The design of an anchor trench is considered to be adequate if mobilized stress lies between the yield stress and allowable stress of the geosynthetic components. It should be mentioned that many manufacturers specify 1.5-foot- (0.45-m)-deep anchor trenches and a 3.0-foot- (0.90-m)-long runout section.

EXAMPLE 4.5

Calculate the resistant capacity of a given geomembrane in a L-shaped rectangular anchor trench of known dimensions. The geomembrane is 60-mil (1.5-mm) HDPE with an ultimate strength (at yield) 2,100 lb/in² (14,500 kN/m²) and an allowable strength 840 lb/in² (5,800 kN/m²).

The runout length is 3 feet (0.9 m). The cover soil is 1 foot (0.3 m). The anchor trench is 2 feet (0.6 m) wide and 2 feet (0.6 m) deep. The side slope angle is 18.4 degrees [3(H):1(V)]. The unit weight of soil is 110 lb/ft³ (17.3 kN/m³). The soil friction angle is 30 degrees. The friction angle between the soil and the geomembrane is 20 degrees.

Solution:

The resistance capacity of the geomembrane in the anchor can be calculated from Equation 4.31 as

$$T = \frac{q_B \cdot L_{RO} \cdot \tan \delta + 2 \cdot [K_o \cdot (\sigma_v)_{ave} \cdot d_{AT} + \sigma_{vB} \cdot L_{AT}] \cdot \tan \delta}{\cos \beta - \sin \beta \cdot \tan \delta}$$

where

$$q_B = \gamma_s \cdot d_{CS} = 110 \times 1 = 110 \text{ lb/ft}^2 \text{ (5.27 kN/m}^2\text{)}$$

$$K_o = 1 - \sin \phi = 1 - 0.5 = 0.5$$

$$(\sigma_v)_{ave} = \gamma_s \cdot (d_{CS} + 0.5 \cdot d_{AT})$$

$$= 110 \times (1 + 0.5 \times 2) = 110 \times 2 = 220 \text{ lb/ft}^2 \text{ (10.53 kN/m}^2\text{)}$$

$$\sigma_{vB} = \gamma_s \cdot (d_{CS} + d_{AT}) = 110 \times (1 + 2) = 330 \text{ lb/ft}^2 \text{ (15.80 kN/m}^2\text{)}$$

Substituting these calculated values into Equation 4.31 yields

$$\begin{aligned} T &= \frac{q_B \cdot L_{RO} \cdot \tan \delta + 2 \cdot [K_o \cdot (\sigma_v)_{ave} \cdot d_{AT} + \sigma_{vB} \cdot L_{AT}] \cdot \tan \delta}{\cos \beta - \sin \beta \cdot \tan \delta} \\ &= \frac{(110)(2)(\tan 20^\circ) + 2[(0.5)(220)(2) + (330)(2)](\tan 20^\circ)}{\cos 18.4^\circ - (\sin 18.4^\circ)(\tan 20^\circ)} \\ &= \frac{(110)(2)(0.364) + 2(220 + 660)(0.364)}{0.949 - (0.316)(0.364)} \\ &= \frac{80.08 + 640.64}{0.834} \\ &= \frac{720.72}{0.834} \\ &= 864 \text{ lb/ft (12.61 kN/m)} \end{aligned}$$

So,

Anchor Resistance Capacity = 864 lb/ft = 72 lb/in \div 0.06 in = 1,200 lb/in² (8,270 kN/m²), which leads to the following inequalities:

$$\begin{aligned} \text{Ultimate Strength} &> \text{Anchor Resistance Capacity} > \text{Allowable Strength} \\ 2,100 \text{ lb/in}^2 &> 1,200 \text{ lb/in}^2 &> 840 \text{ lb/in}^2 \\ (14,500 \text{ kN/m}^2) &> 8,270 \text{ kN/m}^2 &> 5,800 \text{ kN/m}^2 \end{aligned}$$

The results of the calculation indicate the design anchor resistance capacity falls between the yield stress and allowable stress of a geosynthetic membrane liner. Therefore, the anchor trench dimensions are acceptable.

By using a model as presented here, any set of conditions can be used to analyze and arrive at an acceptable design solution. Even situations in which geotextiles and geonets or geocomposites are used in conjunction with a geomembrane can be analyzed in a similar manner.

TABLE 6.5 Index Properties of Solid Waste

Source	Unit Weight		Volumetric Moisture Content	Porosity	Void Ratio
	lb/ft ³	kN/m ³			
Rovers and Farquhar (1973)	59	9.3	0.16	—	—
Fungaroli (1979)	63	9.9	0.05	—	—
Wigh (1979)	73	11.5	0.08	—	—
Walsh and Kinman (1979)	90	14.1	0.17	—	—
Walsh and Kinman (1981)	89	14.0	0.17	—	—
Schroeder et al. (1984a, b)	—	—	0.28	0.52	1.08
Oweis et al. (1990)	40 to 90	6.3 to 14.1	0.10 to 0.20	0.40 to 0.50	0.67 to 1.0
Schroeder et al. (1994a, b)	—	—	0.29	0.67	2.03
Zornberg et al. (1999)	64 to 95	10 to 15	0.30	0.49 to 0.62	1.02 to 1.65

Based on its constituent composition the average moisture content of the solid waste shown in Table 6.4 can be calculated as follows:

$$\begin{aligned}
 w_d &= [(60.0)(10.4) + (50.0)(19.1) + (20.0)(34.6) + (10.0)(6.0) + (15.0)(5.0) \\
 &\quad + (15.0)(9.5) + (2.0)(4.0) + (2.0)(7.2) + (8.0)(2.8) + (3.0)(1.4)]/100 \\
 &= (624 + 955 + 692 + 60 + 75 + 142.5 + 8 + 14.4 + 22.4 + 4.2)/100 \\
 &= 2597.5/100 \\
 &= \underline{26.0\%}
 \end{aligned}$$

Thus, the average dry gravimetric moisture content of the solid waste shown in Table 6.4 is 26.0%.

More information about the moisture content of solid waste can be found in Table 6.5. It should be noted that the values of moisture content listed in Table 6.5 are calculated on a volume basis and differ from those calculated on a weight basis, which is more common to geotechnical analyses.

6.4 POROSITY OF MUNICIPAL SOLID WASTE

Porosity is defined as the ratio of the volume of voids to the total volume occupied by a solid waste or soil. Void ratio is defined as the ratio of the volume of voids to the volume of solids. Porosity can be related to the void ratio by using the relationships

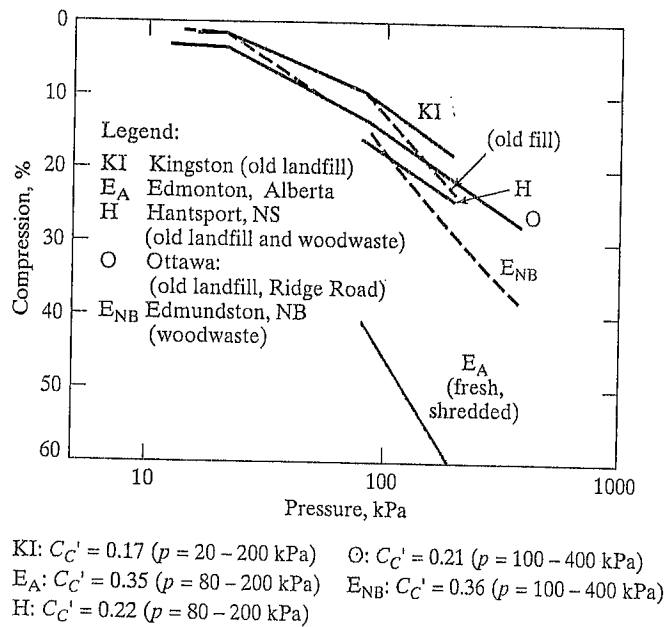
$$n = \frac{e}{1 + e} \quad (6.7)$$

and

$$e = \frac{n}{1 - n} \quad (6.8)$$

where n = porosity of solid waste; and
 e = void ratio of solid waste.

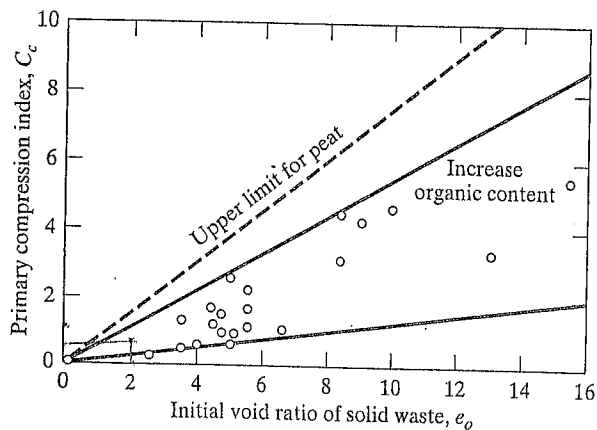
FIGURE 6.9 Compressive Strain versus Log Pressure for Various Landfills in Canada (Landva and Clark, 1990)



cans; the lower values are for the less resilient materials. The maximum C_c for peat is about one-third greater than the maximum observed for waste fills.

Landva and Clark (1990) found that the coefficient of secondary consolidation, C_{α} , (the gradient of the compression versus log time relationship) was in the range 0.2 to 3.0 percent per log cycle time, depending on the type of waste involved. Field testing results using a settlement platform (Keene, 1977) showed that the coefficient of secondary consolidation, C_{α} , varies between 0.014 and 0.034. Too few tests have been carried out for any firm relationship to be established between the value of C_{α} and the type of waste, but it does appear that C_{α} increases with increasing organic content. Sowers (1973) pointed that the coefficient of secondary consolidation, C_{α} , is also a

FIGURE 6.10 Compressibility of MSW Landfills (Sowers, 1973)



Young's modulus of soil, E_s , and the constrained modulus of soil, M_s , where E_s and D_s are related through Poisson's ratio of soil, ν_s , by

$$M_s = \frac{E_s \cdot (1 - \nu_s)}{(1 + \nu_s)(1 - 2\nu_s)} \quad (9.27)$$

where M_s = constrained modulus of soil, lb/ft² or kN/m²;
 E_s = elastic modulus of soil, lb/ft² or kN/m²; and
 ν_s = Poisson's ratio of soil.

The studies and analyses by Neilson (1967), Allgood and Takahashi (1972), and Hartely and Duncan (1987) indicated that for

$$E' = k \cdot M_s \quad (9.28)$$

the value of k may vary from 0.7 to 2.3. Using $k = 1.5$ as a representative value and $\nu_s = 0.3$, in addition to combining Equations 9.27 and 9.28 yields the following relationship between the elastic modulus of the pipe and soil (Selig, 1990):

$$E' = 2 \cdot E_s \quad (9.29)$$

The values of elastic parameters, E_s and ν_s , can be found in Table 9.5 according to different percents of density from a standard Proctor compaction test (ASTM D698).

TABLE 9.5 Elastic Soil Parameters (Selig, 1990)

Soil Type	Stress Level		85% Standard Density			95% Standard Density		
			E_s			E_s		
	psi	kPa	psi	MPa	ν_s	psi	MPa	ν_s
SW, SP, GW, GP	1	7	1,300	9	0.26	1,600	11	0.40
	5	35	2,100	14	0.21	4,100	28	0.29
	10	70	2,600	18	0.19	6,000	41	0.24
	20	140	3,300	23	0.19	8,600	59	0.23
	40	280	4,100	28	0.23	13,000	90	0.25
	60	420	4,700	32	0.28	16,000	110	0.29
GM, SM, ML, and GC, SC with < 20% fines	1	7	600	4	0.25	1,800	12	0.34
	5	35	700	5	0.24	2,500	17	0.29
	10	70	800	6	0.23	2,900	20	0.27
	20	140	850	6	0.30	3,200	22	0.29
	40	280	900	6	0.38	3,700	25	0.32
	60	420	1,000	7	0.41	4,100	28	0.35
CL, MH, GC, SC	1	7	100	1	0.33	400	3	0.42
	5	35	250	2	0.29	800	6	0.35
	10	70	400	3	0.28	1,100	8	0.32
	20	140	600	4	0.25	1,300	9	0.30
	40	280	700	5	0.35	1,400	10	0.35
	60	420	800	6	0.40	1,500	10	0.38

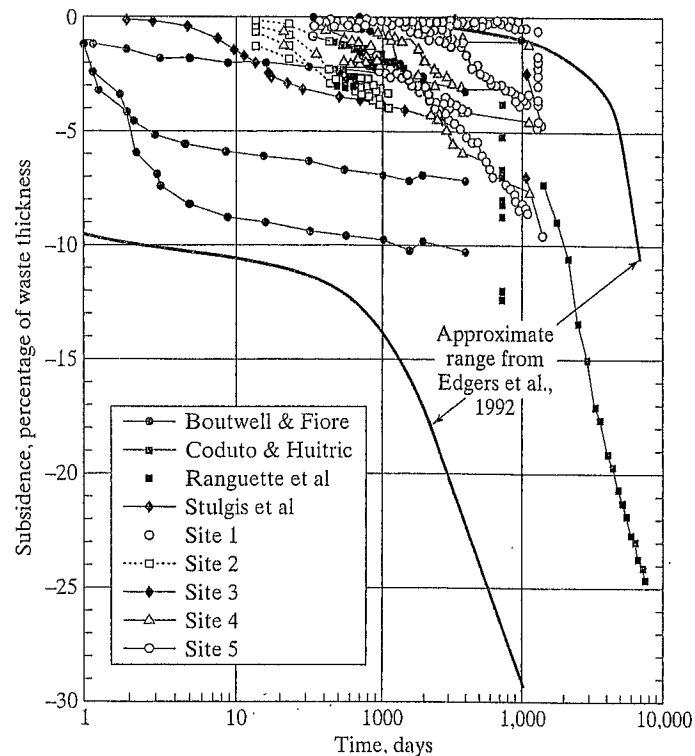


FIGURE 12.1 Landfill Subsidence, New and Previously Published Data (after Spikula, 1997)

drains. The latter outcome may increase the amount of moisture entering the landfill, which, in turn, will produce more leachate.

Settlement of municipal solid waste often begins rapidly as load is placed and continues to occur for long periods thereafter. The mechanisms of refuse settlement are complex, even more so than for soil, because of the extreme heterogeneity of waste fill and the presence of large voids. The main mechanisms involved in waste settlement are the following (Sowers, 1973; Murphy and Gilbert, 1985; Edil et al., 1990; Edgers et al., 1992):

- (i) *Mechanical Compression*: Densification, distortion, bending, crushing, and reorientation; similar to consolidation of organic soils. Compression caused by the self-weight of the landfill and imposed loads, occurs in the form of initial, and/or primary consolidation, and/or secondary (delayed) compression.
- (ii) *Raveling*: The movement of finer particles into larger voids or cavities within the fill. It is usually difficult to distinguish this mechanism from others.
- (iii) *Physical-Chemical Change*: The deterioration and volume loss of waste products by corrosion, oxidation, and combustion.
- (iv) *Bio-Chemical Decomposition*: The reduction of waste mass by fermentation and decay, both aerobic and anaerobic processes. This mechanism will be discussed at length in Chapter 15 on bioreactor landfills.

Many factors affect the magnitude of the settlement, and several of them are interrelated: (i) initial density or void ratio of the solid waste, including the types and amount of daily cover used; (ii) waste compaction effort and placement sequence; (iii) content of the decomposable materials in the waste; (iv) overburden pressure and stress history, such as conducting vertical expansion to overfill over an old landfill; (v) leachate level and fluctuations in landfills; (vi) landfill operation methods, such as leachate recirculation can accelerate waste biodegradation; and (vii) environmental factors, such as moisture content, oxygen which reaches the waste, temperature within the landfill, and gases present or generated within the landfill (Edil et al., 1990).

Settlement can occur jointly with evolution and release of large quantities of landfill gas. A detailed geotechnical mechanism or explanation for settlement caused by or associated with gas generation is not available at present. Similarly, the role of moisture equilibration (Noble et al, 1989) and hydrodynamic effects in the compression of partially saturated materials also is not well understood.

It should be noted that waste settles substantially both under its own weight and under the weight of a new load (for example, the placement of new waste over existing waste as in vertical expansions, which will be covered in Chapter 14). The introduction of cover soil to or on top of the waste fill complicates the computation of stresses due to these weights. As a result, two types of waste unit weight can be defined: (i) Actual waste unit weight (weight of refuse per unit volume of refuse); and (ii) Effective waste unit weight (weight of waste plus cover per unit volume of landfill) (Ham, et al., 1978). Waste unit weights are highly erratic, typically varying within a landfill from 32 to 70 lb/ft³ (5 to 11 kN/m³). Moisture contents typically range from 10 to 50% on a dry-weight basis (Sowers, 1968, 1973; Ham et al., 1978).

Settlement of waste fill is characteristically irregular. Initially, there is a large settlement within one or two months after completing construction, followed by a substantial amount of secondary compression over an extended period of time (recall Figure 12.1). The magnitude of settlement decreases over time and with increasing depth below the surface of the landfill. Waste settlement under its own weight typically ranges from 5 to 30% of the original thickness, with most of the settlement occurring in the first year or first two years (Edil et al., 1990).

12.2 EFFECT OF DAILY COVER

Complications arising from the settlement behavior of the daily cover itself are normally ignored when estimating landfill settlement. Placement of a daily cover of inorganic soil over waste fill is standard practice at most landfill sites; it is done to keep waste from blowing away, to restrict access to rodents, birds, and insects, and to provide additional overburden pressure. Typical procedures consist of placing 2 feet (0.60 m) of compacted waste and 6 inches (0.15 m) of soil cover. A simple settlement analysis assumes that this intermediate zone of soil material would settle as an independent layer between the much thicker layers of waste, while remaining largely intact and undergoing some consolidation settlement of its own.

This conceptual model of cover soil behavior does not accurately simulate actual behavior. Although the inert soil component initially occupies approximately 20% of

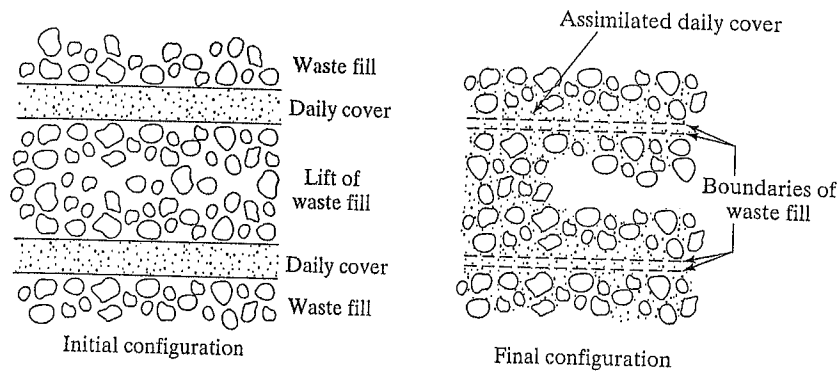


FIGURE 12.2 Absorption of Daily Cover into Waste Fill (Morris and Woods, 1990)

the total fill volume, observations at operating landfills indicate that the proportion becomes significantly reduced as settlement proceeds. This reduction is caused to some extent by compression of the soil under self-weight, but more importantly, it is caused by migration of the soil into the voids in the adjacent solid waste (Morris and Woods, 1990), as shown in Figure 12.2. The net result is that this soil layer can compress over time to less than one-quarter of the original volume. The resultant density of the fill is therefore considerably more than would be expected if this effect was ignored.

The soil particle migration effect has implications also for daily operation and design. One suggested way of increasing the storage efficiency of a landfill is to increase waste lift thickness relative to daily cover thickness. The suggestion is superficially appealing as it appears to minimize dilution of valuable storage volume with natural soil. Furthermore, the decreased overall density achieved by eliminating some or all of the denser cover soil (which is typically much denser than solid waste by a factor of 2 to 4) should reduce overall settlement of the final landfill and make design of final closure and abandonment easier. As pointed out by Morris and Woods (1990), these arguments are flawed for the following reasons:

Effect on Storage Volume: The net loss of storage due to the presence of the extra daily cover of soil is not large in practice for the reasons described next. A soil layer that may initially have occupied 20% of the overall disposal volume will occupy only 5% of the overall fill volume at depth after assimilation into adjacent fill. This minor loss of waste storage volume no longer represents a serious economic penalty for the operator. Indeed, the corresponding increase in overall fill density will assist in self-weight compression of the landfill as a whole.

Effect on Settlement: The second argument that reduction of daily cover will decrease post-construction settlement by reducing self-weight densities is true, but its applicability is debatable. Overall fill settlement may be less as a result of lower self-weight stresses, but not by as much as might be supposed, because the absence of soil "infilling" of the voids in the solid waste will cause the overall compressibility to be increased. Furthermore, the time taken for settlement will generally be increased such that a large proportion of the settlement is likely to take place after closure. If this is the case, then it is possible that postclosure set-

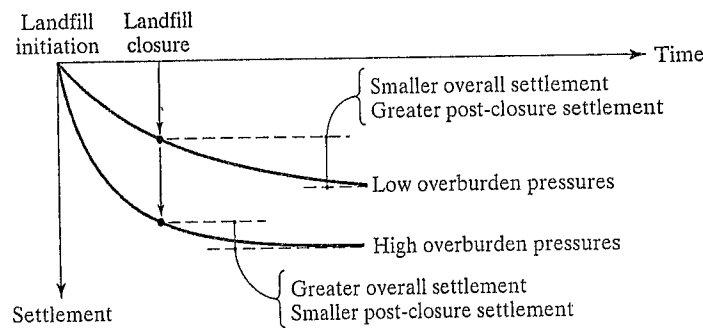


FIGURE 12.3 Possible Settlement Curves for Dense and Light Fills (Morris and Woods, 1990)

tlement of the landfill may actually be more than before, although preclosure settlement may have been reduced somewhat, as illustrated in Figure 12.3.

Morris and Woods (1990) conclude from the results of these conflicting tendencies or outcomes that recommended practice should specify fairly generous layers of daily cover soil. This reduces fire hazard, blowing, vermin problems, etc., and greatly improves landfill management at the expense of relatively minor (at worst) reductions in storage capacity. However, another strategy is to use alternative daily cover materials (ADCMs), as described by Pohland and Graven (1993).

12.3 LANDFILL SETTLEMENT RATE

Yen and Scanlon (1975) studied field settlement records extending up to nine years for three completed sanitary landfills located in Los Angeles County, California, to establish a general trend of landfill settlement rates. The areas of the three filled sites are 19 acres (7.6 ha), 80 acres (32 ha), and 22 acres (8.8 ha); the maximum height of fill was approximately 125 feet (38 m).

A sketch illustrating the parameters/variables used in the settlement rate analyses is shown in Figure 12.4. The settlement rate is defined as

$$m = \frac{(\text{Change in elevation of survey monument, in feet or meter})}{(\text{Elapsed time between surveys, in months})} \quad (12.1)$$

The time variable used here is the estimated "median age of a fill column" as defined by Yen and Scanlon (1975). This is measured as the elapsed time between the date of the settlement survey and that time when the fill column is half completed. The term "fill column" is defined (Yen and Scanlon, 1975) as the column of earth and waste fill lying directly below a survey monument, and extending to the natural soil. Other variables used were the completed fill column depth, H_f , and the total fill construction time t_c , in months. These parameters are chosen because the construction or filling period of a sanitary landfill is usually long and should be taken into consideration for settlement rate analyses. From Figure 12.4 and the data available, the median age of the fill column is estimated as

$$t_1 = t - t_c/2 \quad (12.2)$$

where t = the total elapsed time since the beginning of construction.

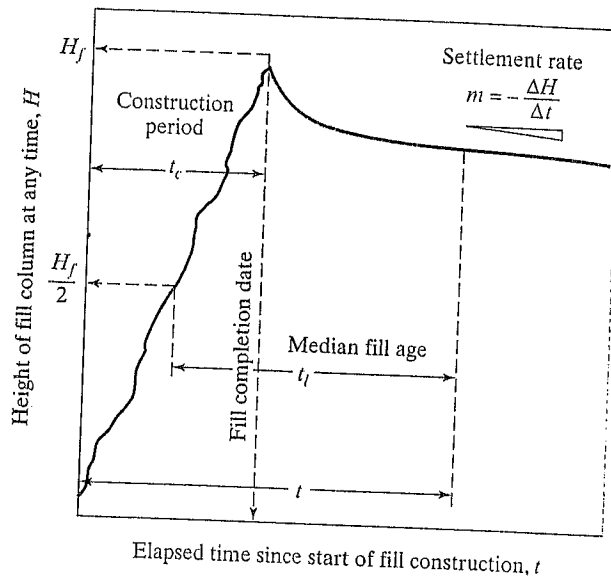


FIGURE 12.4 Diagram Showing Notations Used in Analysis (Yen and Scanlon, 1975). Used with permission of ASCE.

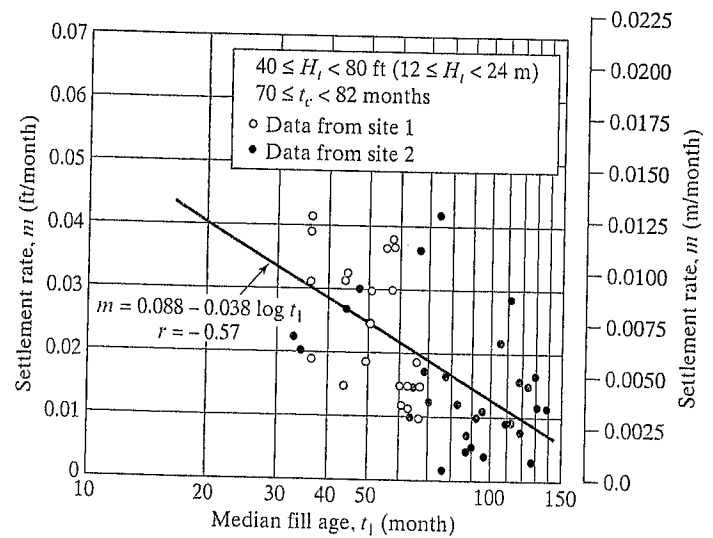
Yen and Scanlon (1975) then analyze the data to identify the relationships between median fill age (t_f), rate of settlement m , depth of fill H_f , and construction time t_c . Since the fill column, H_f , is a measure of average stress acting upon and within the waste, the fill columns were divided into subgroups based on ranges of H_f and construction time t_c . Thus, within each subgroup, the variation in H_f and t_c is restricted, and the relationship between elapsed time t_f and settlement rate m can be seen more clearly.

Plots of m versus $\log(t_f)$ for fills between 40 feet and 80 feet (12 m and 24 m), between 80 feet and 100 feet (24 m and 30 m), and greater than 100 feet (30 m) are shown in Figures 12.5, 12.6 and 12.7. The linear relationship between m and t_f is obtained by least-squares fitting with the regression coefficient shown. These three plots are only for the fill column subgroups with t_c between 70 months and 82 months. Table 12.1 summarizes results of other subgroups in which the construction period, t_c , ranges from less than one year to nearly seven years. The mean values of settlement rate, m , for the fill column of different depth ranges are shown in Table 12.1. Values of mean m were computed only in those intervals that contained at least three field survey measurements.

Effect of Median Fill Age on Settlement Rates as Function of Fill Depth

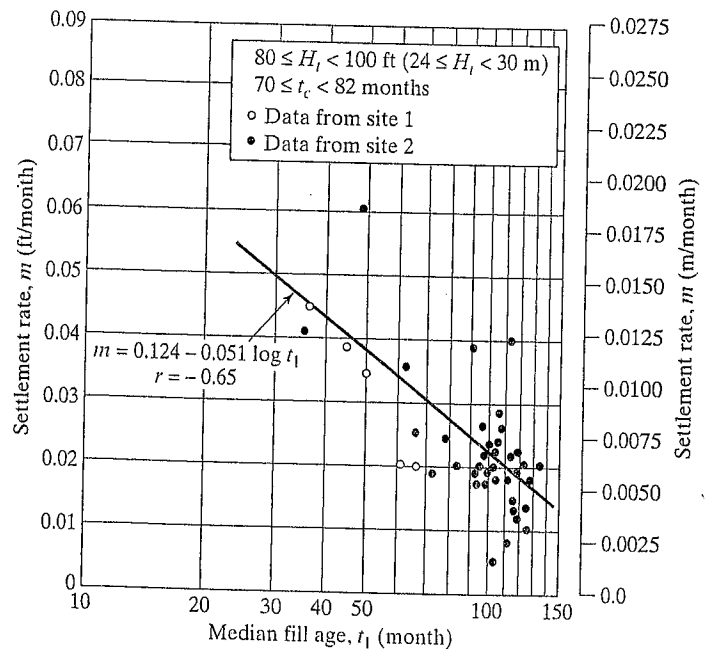
The decreasing trend of m with respect to t_f can be seen in each of the referenced figures and in Table 12.1. However, after a period of 6 years from the completion of a fill (70 months to 120 months of median fill age), settlement rates on the order of 0.02 ft/month (6 mm/month) may still be expected. It is also interesting to note the range of post-construction settlement for the sites investigated. An estimate of the average total post-construction settlement was computed (Yen and Scanlon, 1975) by integrating the m and $\log(t_f)$ functions of Figures 12.5, 12.6, and 12.7 between the fill completion date and the extrapolated value of t_f for which $m = 0$. The results show

FIGURE 12.5 Settlement Rates versus Time Elapsed for Fill Depths between 40 ft and 80 ft (12 m and 24 m) (Yen and Scanlon, 1975). Used with permission of ASCE.



that post-construction settlement ranges between 4.5% and 6% of total fill depth, i.e., about 4.5 feet to 6 feet (1.4 m to 1.8 m) of past construction settlement would be expected for a 100 feet (30 m) of fill without subjecting the fill to any external load other than its own weight and biodegradation.

FIGURE 12.6 Settlement Rates versus Time Elapsed for Fill Depths between 80 ft and 100 ft (24 m and 31 m) (Yen and Scanlon, 1975). Used with permission of ASCE.



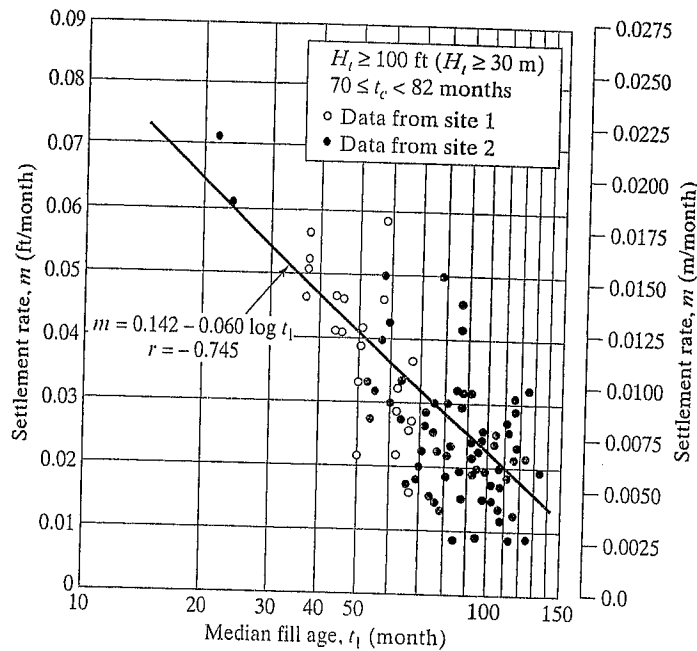


FIGURE 12.7 Settlement Rates versus Time Elapsed for Fill Depths Greater than 100 ft (31 m) (Yen and Scanlon, 1975). Used with permission of ASCE.

Effect of Depth on Rate of Settlement

As can be seen from Figures 12.5 to 12.7 and from Table 12.1, deeper fill depth generally shows a faster rate of settlement regardless of construction period, t_c , and median fill age t_1 . However, the differences are not linearly proportional to the depth of fill, H_f . The results from the three sites studied indicate that although the rate of settlement increases with depth, this effect levels off for depths greater than 90 feet (27 m). The settlement rates for fill depth of more than 100 feet (30 m) are substantially the same after five years as those with H_f between 80 feet to 100 feet (24 m to 30 m). This finding is not surprising when considering that waste at greater depth has been subjected to a higher number of compaction cycles and prior densification.

Effect of Construction Period on Settlement Rate

The length of the construction period, t_c , also affects settlement rate. In Table 12.2, the time required for the completion of settlement (i.e., when $m = 0$) was computed by Yen and Scanlon (1975) using least-squares fitted $m - \log(t_1)$ functions (Figures 12.5, 12.6, and 12.7). The data in Table 12.2 indicate that a faster rate of the construction (smaller t_c values) will result in a much shorter time for the fill to complete its settlement. This effect is more pronounced for the shallower fills. This finding suggests it may be advantageous to construct a sanitary landfill as fast as possible in order to accelerate settlement.

Length of Post-Construction Settlement

The fill column subgroups with $70 \leq t_c \leq 82$ months had the largest data populations with the widest coverage in terms of t_1 . For some of the fill columns in this group,

Table 12.1 Mean Values of Settlement Rate, m , in feet/month (millimeter/month) (Yen and Scanlon, 1975)

Completed Fill Height H_f , feet (meter)	Construction Period $t_c \leq 12$ months	Construction Period $24 \leq t_c \leq 50$ months	Construction Period $70 \leq t_c \leq 82$ months
(a) For Median Fill Age, $t_1 \leq 40$ months			
40 (12)	×	×	×
41 to 80 (12.3 to 24)	0.030 (9.14)	×	0.030 (9.14)
81 to 100 (24.3 to 30)	0.050 (15.24)	×	×
> 100 (> 30)	×	×	0.057 (17.37)
(b) For Median Fill Age, $40 \leq t_1 \leq 60$ months			
40 (12)	0.016 (4.88)	0.016 (4.88)	0.015 (4.57)
41 to 80 (12.3 to 24)	0.010 (3.05)	0.026 (7.92)	0.029 (8.84)
81 to 100 (24.3 to 30)	0.030 (9.14)	×	0.040 (12.19)
> 100 (> 30)	×	×	0.041 (12.50)
(c) For Median Fill Age, $60 \leq t_1 \leq 80$ months			
40 (12)	0.016 (4.88)	0.010 (3.05)	0.009 (2.74)
41 to 80 (12.3 to 24)	0.009 (2.74)	0.012 (3.66)	0.016 (4.88)
81 to 100 (24.3 to 30)	0.036 (10.97)	×	0.025 (7.62)
> 100 (> 30)	×	×	0.025 (7.62)
(d) For Median Fill Age, $80 \leq t_1 \leq 100$ months			
40 (12)	0.008 (2.44)	0.012 (3.66)	×
41 to 80 (12.3 to 24)	×	0.012 (3.66)	0.008 (2.44)
81 to 100 (24.3 to 30)	×	×	0.022 (6.71)
> 100 (> 30)	×	×	0.025 (7.62)
(e) For Median Fill Age, $100 \leq t_1 \leq 120$ months			
40 (12)	×	×	×
41 to 80 (12.3 to 24)	×	×	0.015 (4.57)
81 to 100 (24.3 to 30)	×	×	0.020 (6.19)
> 100 (> 30)	×	×	0.020 (6.19)

"×" indicates that less than three field settlement survey data were available in that particular H_f , t_1 , t_c interval, and therefore, no mean value of settlement rate m was computed.

Data in Column 2 from Site 2; data in Column 3 from Sites 2 and 3; data in Column 4 from Site 1 and 2.

Used with permission of ASCE.

the settlement observations extended over a nine-year period. Figures 12.5, 12.6, and 12.7 show the scatter diagrams for these subgroups along with their regression coefficient r . Extrapolation of these functions suggests that, even without the addition of surface loads, the settlement process may last over 250 months before $m = 0$. This represents a very long time for completion of settlement from a geotechnical engineering viewpoint, and appears to be one of the major limitations of using deep landfill sites as load-bearing fills.

Table 12.2 Comparison of Settlement and Construction Period (Yen and Scanlon, 1975)

Range of Fill Depth H_f , feet, (meter)	Average Construction Period, t_c (month)	Total Time Required for Construction and Settlement (months)	Approximate Time Required for Settlement to Complete (month)
40 to 80 (12 to 24)	12	113	101
40 to 80 (12 to 24)	72	324	252
80 to 100 (24 to 30)	12	245	233
80 to 100 (24 to 30)	72	310	238

Used with permission of ASCE.

12.4 ESTIMATION OF LANDFILL SETTLEMENT

The usual laboratory tests for soil consolidation testing are not well suited for obtaining accurate consolidation parameters for solid waste that has a heterogeneous composition and extremely large particle sizes. By analyzing the field settlement data from some large-scale pilot landfill cells, Sowers (1973) proposed an alternative method to estimate the amount of the landfill settlement. In recent years, this method has been revised and refined several times by other investigators.

The settlement of solid waste includes primary settlement and long-term secondary compression. The total amount of settlement is given by the expression

$$\Delta H = \Delta H_c + \Delta H_\alpha \quad (12.3)$$

where ΔH = total settlement of solid waste;

ΔH_c = primary settlement of solid waste;

ΔH_α = long-term secondary settlement of solid waste.

12.4.1 Settlement of New Solid Waste

Based on the procedure proposed by Sowers (1973), the equations that follow can be used to calculate the settlement for new landfilled solid waste. The *Initial primary settlement* is given by

$$\Delta H_c = C_c \cdot \frac{H_o}{1 + e_o} \cdot \log \frac{\sigma_i}{\sigma_o} \quad (12.4)$$

or

$$\Delta H_c = C'_c \cdot H_o \cdot \log \frac{\sigma_i}{\sigma_o} \quad (12.5)$$

where ΔH_c = primary settlement;

e_o = initial void ratio of the waste layer before settlement;

H_o = initial thickness of the waste layer before settlement;

C_c = primary compression index (recall Figure 6.10);

C'_c = modified primary compression index, $C'_c = 0.17 \sim 0.36$;

σ_o = previously applied pressure in the waste layer (assumed equal to the compaction pressure, $\sigma_o = 1,000 \text{ lb/ft}^2$ or 48 kN/m^2);

σ_i = total overburden pressure applied at the mid level of the waste layer.

The previous compaction pressure applied on the solid waste layer during placement with compaction equipment is assumed to be 1,000 lb/ft² (48 kN/m²) based on 1973 compaction efforts for municipal solid waste landfills. In other words, the waste that has been placed in the landfill is essentially incompressible at normal pressure below 1,000 lb/ft² (48 kN/m²) due to the preconsolidation effect caused by previous compaction of the material. The value of the previously applied pressure, σ_o , should be changed during estimation of settlement if the compaction effort is much lower or higher than 1,000 lb/ft² (48 kN/m²) for a specific landfill project. Indeed, current practices of using waste compactors in the 100 to 150 U.S. tons (900 to 1,300 kN) range will significantly increase the value of σ_o .

The long-term secondary settlement can be obtained from

$$\Delta H_\alpha = C_\alpha \cdot \frac{H_o}{1 + e_o} \cdot \log \frac{t_2}{t_1} \quad (12.6)$$

or

$$\Delta H_\alpha = C'_\alpha \cdot H_o \cdot \log \frac{t_2}{t_1} \quad (12.7)$$

where ΔH_α = long-term secondary settlement;
 e_o = initial void ratio of the waste layer before settlement;
 H_o = initial thickness of the waste layer before settlement;
 C_α = secondary compression index (recall Figure 6.11);
 C'_α = modified secondary compression index, $C'_\alpha = 0.03 \sim 0.1$;
 t_1 = starting time of the time period for which long-term settlement of the layer is desired, $t_1 = 1$ month;
 t_2 = ending time of the time period for which long-term settlement of the layer is desired.

Because a standard consolidation test method for solid waste has not yet been developed, the selection of waste compression indices are mainly based on experience and limited field data. The value of the primary compression index C_c can be selected from Figure 6.10 based on the initial void ratio and organic content of the solid waste. The value of the secondary compression index C_α can be selected from Figure 6.11 based on the initial void ratio of the waste and the decomposition conditions.

Generally, the initial void ratio of municipal solid waste placed in a landfill after compaction is quite difficult to determine, and hence the values of the primary compression index C_c and the secondary compression index C_α cannot be estimated readily for settlement analysis. Accordingly, an alternative approach has been used in engineering practice—namely, the use of a “modified” primary compression index C'_c and a “modified” secondary compression index C'_α . Based on experience, the value of the modified primary compression index C'_c varies from 0.17 to 0.36, and the value of the modified secondary compression index C'_α varies from 0.03 to 0.1 for municipal solid waste (depending on the initial compaction effort and composition of the solid waste). The value of the modified secondary compression index C'_α for common clay ranges from 0.005 to 0.02. Therefore, the secondary settlement for municipal solid waste is approximately five to six times that of common clay.

12.4.2 Settlement of Existing Solid Waste

The following equations can be used to calculate the settlement of an existing solid waste landfill caused by vertical expansion (Chapter 14) or other additional extra loading, such as a light structure on a raft foundation.

The *primary settlement* is obtained by

$$\Delta H_c = C_c \cdot \frac{H_o}{1 + e_o} \cdot \log \frac{\sigma_o + \Delta\sigma}{\sigma_o} \quad (12.8)$$

or

$$\Delta H_c = C'_c \cdot H_o \cdot \log \frac{\sigma_o + \Delta\sigma}{\sigma_o} \quad (12.9)$$

where ΔH_c = primary settlement;
 e_o = initial void ratio of the waste layer before settlement;
 H_o = initial thickness of the waste layer of the existing landfill;
 C_c = primary compression index;
 C'_c = modified primary compression index, $C'_c = 0.17 \sim 0.36$;
 σ_o = existing overburden pressure acting at the mid level of the waste layer;
 $\Delta\sigma$ = increment of overburden pressure due to vertical expansion or other extra load.

The *long-term secondary settlement* is given by

$$\Delta H_\alpha = C_\alpha \cdot \frac{H_o}{1 + e_o} \cdot \log \frac{t_2}{t_1} \quad (12.10)$$

or

$$\Delta H_\alpha = C'_\alpha \cdot H_o \cdot \log \frac{t_2}{t_1} \quad (12.11)$$

where ΔH_α = secondary settlement;
 e_o = initial void ratio of the waste layer before starting secondary settlement;
 H_o = initial thickness of the waste layer before starting secondary settlement;
 C_α = secondary compression index;
 C'_α = modified secondary compression index, $C'_\alpha = 0.03 \sim 0.1$;
 t_1 = starting time of the secondary settlement. It is assumed to be equal to the age of the existing landfill for vertical expansion project;
 t_2 = ending time of the secondary settlement.

FIGURE 12.14 Variation of Parameters with Water Content of Waste Materials for Power Function (Ling et al., 1998). Used with permission of ASCE.

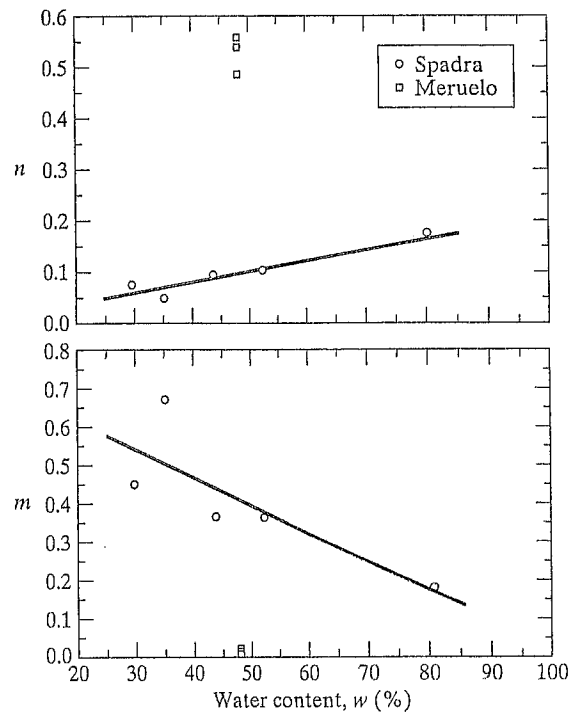
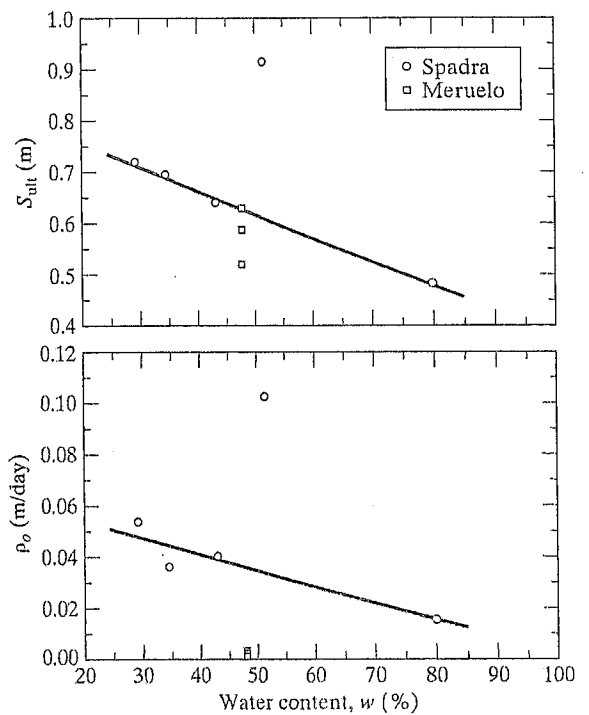


FIGURE 12.15 Variation of Parameters with Water Content of Waste Materials for Hyperbolic Function (Ling et al., 1998). Used with permission of ASCE.



(e.g., temperature within landfill and oxygen reaching the waste) still is not entirely clear. These functions should be used with caution in engineering practice and should be supported by additional testing data and research.

12.7 ESTIMATION OF LANDFILL FOUNDATION SETTLEMENT

If the landfill is underlain by a soil layer, particularly a thick layer of soft, fine-grained soil, consolidation settlements may be large. In these cases, design analyses should consider settlement of the foundation clay layer. Both primary consolidation and long-term secondary settlement should be considered. Calculations are performed using conventional equations from soil mechanics theory and a time frame at least equal to the active life and postclosure care period of the landfill.

Excessive settlement of an underlying foundation clay layer will affect the performance of a landfill liner and leachate collection system. The purposes of analyzing the settlement of a foundation clay layer and overlying landfill liner and leachate collection/removal system are as follows:

- (i) Tensile strain induced in the liner system and leachate collection and removal system must be limited to a minimum allowable tensile strain for the components of these two systems. The compacted clay liner usually has the smallest allowable tensile strain value between 0.1% and 1.0% and an average allowable tensile strain of 0.5%.
- (ii) Post-settlement grades of the landfill cell subbase and the leachate collection pipes must be sufficient to maintain leachate performance to prevent grade reversal and leachate ponding in accordance with the rule requirements.

12.7.1 Total Settlement of Landfill Foundation

The total settlement of landfill foundation soil can be divided into three portions: elastic settlement, primary consolidation settlement, and secondary consolidation settlement. The settlement of sandy soils includes only elastic settlement. The settlement of clayey soils includes all three types of settlements. The total settlement of clayey soil is equal to the sum of the elastic settlement and the primary and secondary settlements. Because the permeability of clay is quite low, it takes a long time to complete the whole process of consolidation settlement. The settlement of clayey soil is usually much larger than the settlement of sandy soils.

Because the settlement of sandy soils includes only elastic settlement, the settlement of sand layer can be calculated from the Elastic Settlement equation, which is

$$Z_e = (\Delta\sigma/M_s)H_o \quad (12.20)$$

where Z_e = elastic settlement of soil layer, ft or m;
 H_o = initial thickness of soil layer, ft or m;
 $\Delta\sigma$ = increment of vertical effective stress, lb/ft² or kN/m²;
 M_s = constrained modulus of soil, lb/ft² or kN/m².

The constrained modulus is given by

$$M_s = \frac{E_s \cdot (1 - v_s)}{(1 + v_s)(1 - 2 \cdot v_s)} \quad (12.21)$$

where M_s = constrained modulus of soil, lb/ft² or kN/m²;
 E_s = elastic modulus of soil, see Table 9.5, lb/ft² or kN/m²;
 v_s = Poisson's ratio of soil, see Table 9.5.

The *primary consolidation settlement* is given by

$$Z_c = C_r \cdot \frac{H_{oi}}{1 + e_{oi}} \cdot \log \frac{p_c}{\sigma_o} + C_c \cdot \frac{H_o}{1 + e_{oi}} \cdot \log \frac{\sigma_o + \Delta\sigma}{p_c} \quad (12.22)$$

where Z_c = primary consolidation settlement of clay layer, ft or m;
 H_o = initial thickness of clay layer, ft or m;
 e_{oi} = initial void ratio of clay layer;
 C_r = recompression index;
 C_c = primary compression index.
 σ_o = initial vertical effective stress, lb/ft² or kN/m²;
 p_c = preconsolidation pressure, lb/ft² or kN/m²;
 $\Delta\sigma$ = increment of vertical effective stress, lb/ft² or kN/m².

The *secondary compression settlement* is given by

$$Z_\alpha = C_\alpha \cdot \frac{H_{os}}{1 + e_{os}} \cdot \log \frac{t_2}{t_1} \quad (12.23)$$

where Z_α = long-term secondary compression settlement, ft or m;
 e_{os} = initial void ratio of clay layer before starting secondary consolidation settlement;
 C_α = secondary consolidation compression index;
 H_{os} = initial thickness of clay layer before starting secondary consolidation settlement, ft or m;
 t_1 = starting time of the time period for which long-term settlement of the layer is desired;
 t_2 = ending time of the time period for which long-term settlement of the layer is desired.

The total settlement of clay layer includes three portions: elastic settlement, primary consolidation settlement, and secondary consolidation settlement. These three types of settlement for clayey soil layers can be calculated from Equations 12.20, 12.22, and 12.23, respectively. The total settlement of clayey soil at point i can be determined from the equation

$$Z_i = (Z_e)_i + (Z_c)_i + (Z_\alpha)_i \quad (12.24)$$

where Z_i = total settlement of points i ;
 $(Z_e)_i$ = elastic settlement of point i ;
 $(Z_c)_i$ = primary consolidation settlement of point i ;
 $(Z_\alpha)_i$ = secondary consolidation settlement of point i .

The preceding settlement equations (Equations 12.20 through 12.24) provide a framework and means to account for different types of settlement. Not all foundations on soil settle exactly in the manner previously described. In addition to soil type, the amount of settlement in each category also depends on the degree of saturation, load duration, and load distribution.

The settlement calculations should be performed at discrete points along several selected settlement lines, such as Lines 1, 2, 3, and 4 for a municipal solid waste landfill as shown in Figure 12.16. The following principles should guide the arrangement of the settlement lines for landfill foundation settlement calculations:

- (i) Some settlement lines should be set along the leachate collection pipelines (usually 1% slope) to check the grade changes and tensile strains of the leachate collection pipes due to settlement.

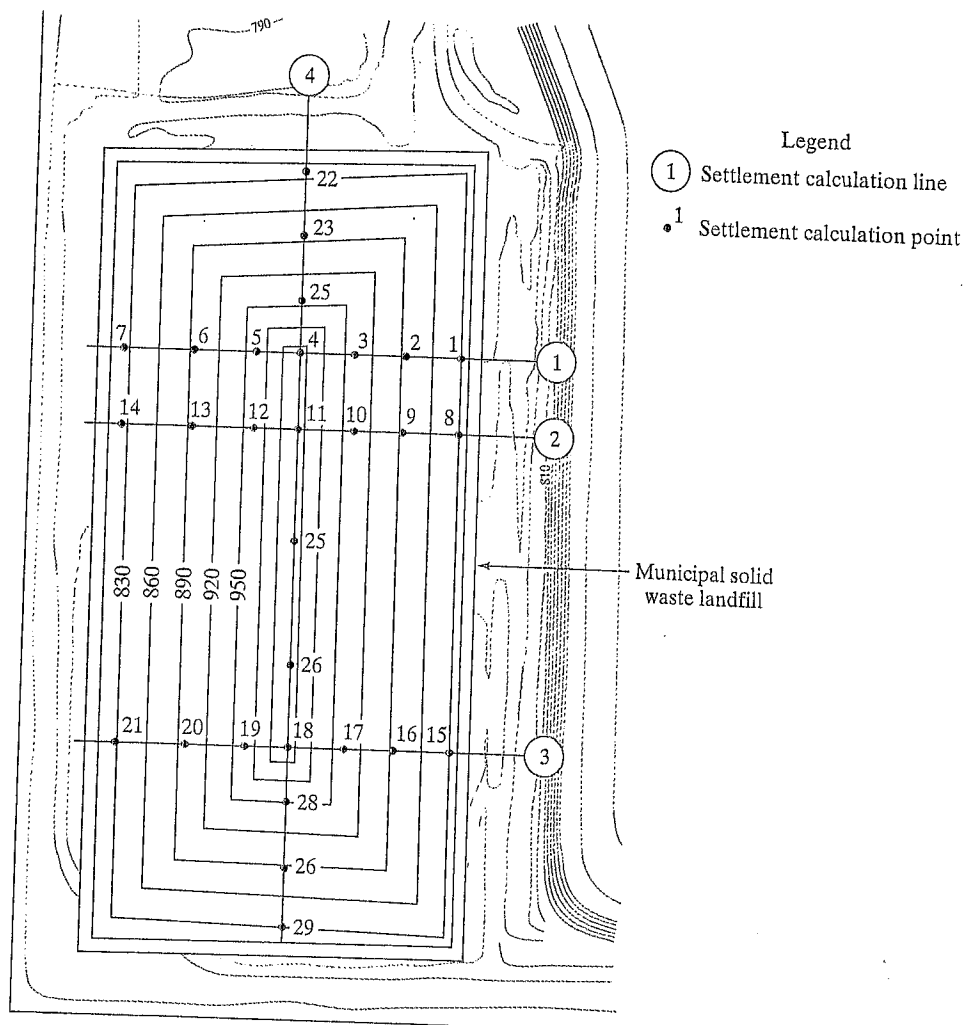


FIGURE 12.16 Settlement Calculation Locations for Landfill Liner System Foundation

- (ii) Some settlement lines should be set perpendicular to the leachate collection pipes (i.e., along the direction of leachate flow in the leachate drainage layer—usually 2% slope), to check the slope change of leachate drainage layer.
- (iii) Settlement lines are usually set locations where there are the large changes of overburden pressures, which may cause large differential settlements of the subgrade.

At each settlement point shown in Figure 12.16 (i.e., Point 1 to Point 29), the thickness of the various soil units at each point and the thickness of the waste to be placed (i.e., overburden pressure) can be estimated from the engineering plans or cross-sections for the specific projects. The value of the total settlement at each point depends on both the engineering properties of soils and the load due to the waste fill.

12.7.2 Differential Settlement of Landfill Foundation

The differential settlements, tensile strains of liner system materials and leachate collection pipes, and changes of final grades between adjacent settlement points after settlement can be evaluated from the calculated values of the total settlements at various settlement points along each settlement line ranged on the landfill subgrade.

The differential settlement between adjacent points can be calculated using the equation

$$\Delta Z_{i,i+1} = Z_{i+1} - Z_i \quad (12.25)$$

where $\Delta Z_{i,i+1}$ = differential settlement between points i and $i + 1$;

Z_i = total settlement of point i ;

Z_{i+1} = total settlement of point $i + 1$.

The final slope angle between adjacent points after settlement can be calculated using the equation

$$\tan \beta_{\text{Fnl}} = \frac{X_{i,i+1} \cdot \tan \beta_{\text{Int}} - \Delta Z_{i,i+1}}{X_{i,i+1}} \quad (12.26)$$

where $X_{i,i+1}$ = horizontal distance between points i and $i + 1$;

$\Delta Z_{i,i+1}$ = differential settlement between points i and $i + 1$;

β_{Int} = initial slope angle between points i and $i + 1$;

β_{Fnl} = final slope angle between points i and $i + 1$ after settlement.

The landfill subgrade changes along each settlement line due to different settlement can be calculated from the Equation 12.26. Figure 12.17 presents the slope changes due to differential settlement along a settlement line. The differential settlement will result in grade reversal between points 3 and 4 as shown in Figure 12.17. As a result, leachate will pond on the liner at this area.

The tensile strains of a liner system and a leachate collection system resulting from the settlements can be estimated using the equation

$$\varepsilon_{i,i+1} = \frac{(L_{i,i+1})_{\text{Fnl}} - (L_{i,i+1})_{\text{Int}}}{(L_{i,i+1})_{\text{Int}}} \times 100\% \quad (12.27)$$

where $\varepsilon_{i,i+1}$ = tensile strain in liner system between points i and $i + 1$;

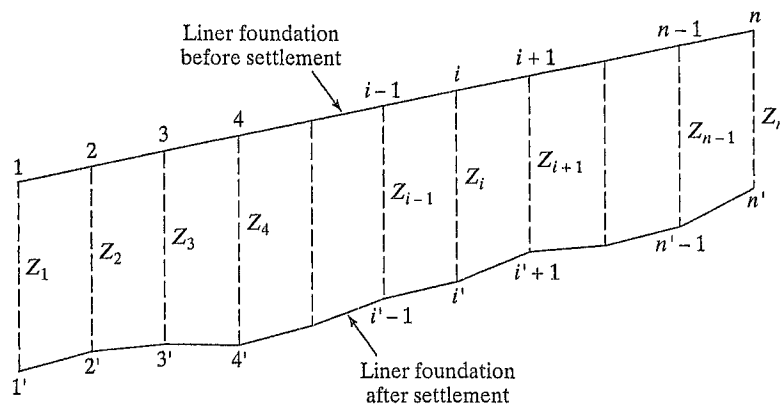


FIGURE 12.17 Subgrade Changes along a Settlement Line due to Differential Settlement

$(L_{i,i+1})_{\text{Int}}$ = distance between points i and $i+1$ in their initial positions;
 $(L_{i,i+1})_{\text{Fnl}}$ = distance between points i and $i+1$ in their post-settlement positions.

The distance between points i and $i+1$ in their initial positions can be calculated using the equation

$$(L_{i,i+1})_{\text{Int}} = [(X_{i,i+1})^2 + (X_{i,i+1} \cdot \tan \beta_{\text{Int}})^2]^{1/2} \quad (12.28)$$

The distance between points i and $i+1$ in their post-settlement positions can be calculated using the equation

$$(L_{i,i+1})_{\text{Fnl}} = [(X_{i,i+1})^2 + (X_{i,i+1} \cdot \tan \beta_{\text{Int}} - \Delta Z_{i,i+1})^2]^{1/2} \quad (12.29)$$

The maximum acceptable tensile strains (i.e., the elongations at yield) of various liner system and leachate collection system components must be obtained from material specific laboratory testing.

PROBLEMS

- 12.1 What benefit does a landfill operation gain from some settlement in the landfill waste?
- 12.2 Describe the impact of landfill settlement on landfill design and performance.
- 12.3 What are the main mechanisms of solid waste settlement?
- 12.4 List the main factors that influence the amount of landfill settlement.
- 12.5 What are the main differences of the settlement of solid waste compared with the settlement of clay?
- 12.6 What are the main advantages and disadvantages of the calculation method for landfill settlement described in Section 12.4?

be normally consolidated under the surcharge of about 4 m of fill. The soft clay layer, however, was underconsolidated below the fill layer. The excess pore pressures caused by the placement of the fill in the 1970s and 1980s had experienced very little dissipation—particularly between elevations of -10 and -20 m—at the time waste placement started. In the middle zone of the soft clay layer, the difference between the actual undrained strength and the one used in the stability analyses was of the order of 10 kN/m^2 . The original short-term stability analysis did not consider the possibility of failure surfaces extending to the river (like the one that actually happened), where there was no fill layer over the soft clay, and, hence, the soft clay did not have the undrained strength assumed in the stability calculations.

As noted, this case history had a geosynthetic lining system that failed along with the rotational movement. However, the lining system could not (and was not) a contributing issue to the failure. The little reinforcement benefit that may have been provided by the geosynthetic layer is negligible in the context of this large of a waste mass. This, as with the previous two case histories, was completely a geotechnical-related failure of the classical rotational failure mode except now a portion of the failure surface passes through waste materials.

13.5.3 General Remarks

It should be obvious from these three case histories that proper site characterization during the design stage and well before waste placement is critical. Irrespective of the high shear strength of waste materials, if the soil foundation fails, it will eventually propagate through the waste mass and cause the entire system to fail. Once a crack is observed on the surface of the waste mass, the entire failure surface beneath it has been mobilized. Failure of the mass is then imminent.

The situation is obviously important when dealing with soft, fine-grained soils. Typically, but certainly not always, such soils are near rivers, harbors, and estuaries. Best available geotechnical practice must be followed (recall Section 13.3.3). Even beyond site investigation, laboratory testing, and design which lead to site-specific plans and specifications, one should consider field instrumentation. Piezometers placed in the subsoil and inclinometers placed at the toe of the waste slope (and beyond) could be most valuable in providing an instantaneous assessment of the landfill as waste is being placed. Unfortunately, such instrumentation is rarely provided, even for sensitive site situations.

13.6 WASTE MASS FAILURES

The relatively low interface shear strengths of components within liner systems can lead to translational failures of the type shown in Figure 13.1(f). However, failure can only occur if the toe of the waste mass is unsupported by an opposing slope or large soil berm. Unfortunately, unsupported toe conditions are often the case. Canyon landfills are very common in areas of mountainous or rolling topography. Even when an excavation is dug for a landfill, the waste mass during filling is generally left unsupported at its toe. This section deals with the instability of such situations.

13.6.1 Translational Failure Analysis

While the approach to translational failures is generally similar to that described in Section 13.5.1, the failure surface is not circular, but usually piecewise linear. Thus, the simplified Bishop method is not applicable. A translational (or two-wedge) failure analysis is used to calculate the factor of safety for the landfill against possible mass movement of the type of "translational (or wedge) failure along liner" [Figure 13.1(f)] in the interim filling condition.

The waste mass shown in Figure 13.24(a) can be divided into two discrete parts, one active wedge lying on the side slope and tending to cause failure, and another passive wedge lying on the cell bottom floor and tending to resist failure. The forces acting on the active and passive wedges are shown in Figure 13.24(a). The individual forces, friction angles, and slope angles involved in the analysis are listed as follows:

- W_p = weight of the passive wedge;
- N_p = normal force acting on the bottom of the passive wedge;
- F_p = frictional force acting on the bottom of the passive wedge (parallel to the bottom of the passive wedge);
- E_{HP} = normal force from the active wedge acting on the passive wedge (unknown in magnitude, but with the direction perpendicular to the interface of the active and passive wedges);

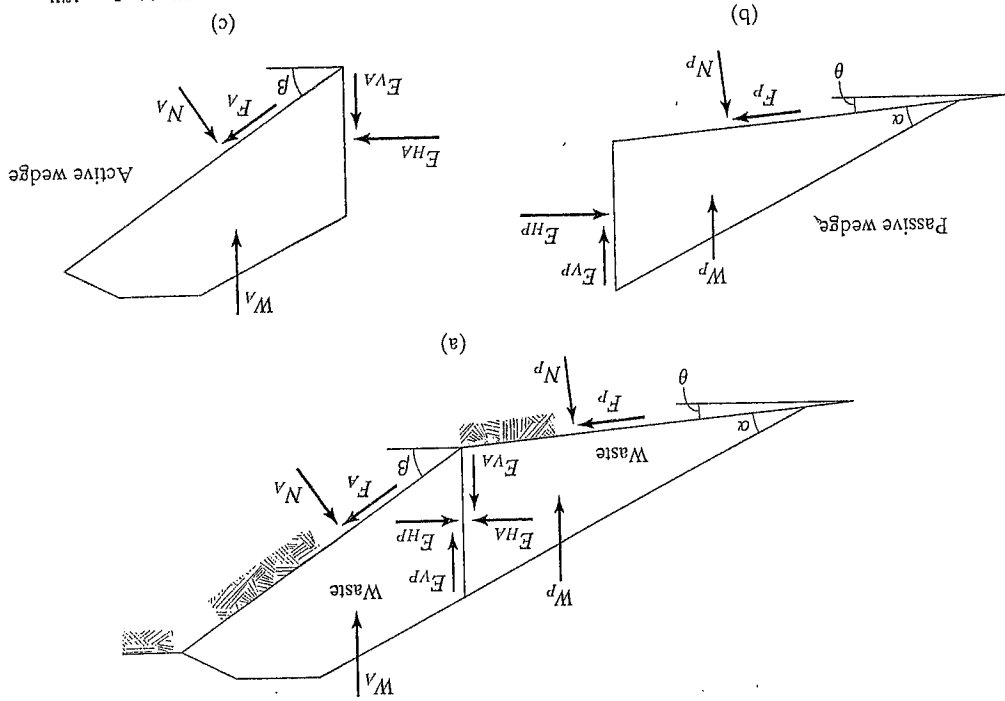


FIGURE 13.24 Forces Acting on Two adjacent Wedges for Solid Waste Filled in Landfill

E_{VP} = frictional force acting on the side of the passive wedge (unknown in magnitude, but with the direction parallel to the interface of the active and passive wedges);

FS_P = factor of safety for the passive wedge;

δ_P = minimum interface friction angle of multi-layer liner components beneath the passive wedge;

ϕ_s = friction angle of the solid waste;

α = angle of the solid waste slope, measured from horizontal, degrees;

θ = angle of the landfill cell subgrade, measured from horizontal, degrees;

W_A = weight of the active wedge;

W_T = total weight of the active and passive wedges;

N_A = normal force acting on the bottom of the active wedge;

F_A = frictional force acting on the bottom of the active wedge (parallel to the bottom of the active wedge);

E_{HA} = normal force from passive wedge acting on the active wedge (unknown in magnitude, but with the direction perpendicular to the interface of the active and passive wedges), $E_{HA} = E_{HP}$;

E_{VA} = frictional force acting on the side of the active wedge (unknown in magnitude, but with the direction parallel to the interface of the active and passive wedges), $E_{VA} = E_{VP}$;

FS_A = factor of safety for the active wedge;

δ_A = minimum interface friction angle of multi-layer liner components beneath the active wedge;

β = angle of the side slope, measured from horizontal, degrees;

FS = factor of safety for the entire solid waste mass.

Considering the force equilibrium of the passive wedge [Figure 13.24(b)], the forces acting on it are

$$\Sigma F_Y = 0:$$

$$W_P + E_{VP} = N_P \cdot \cos \theta + F_P \cdot \sin \theta \quad (13.47)$$

$$F_P = N_P \cdot \tan \delta_P / FS_P \quad (13.48)$$

$$E_{VP} = E_{HP} \cdot \tan \phi_s / FS_P \quad (13.49)$$

Substituting Equations 13.48 and 13.49 into Equation 13.47 gives

$$W_P + E_{HP} \cdot \tan \phi_s / FS_P = N_P \cdot (\cos \theta + \sin \theta \cdot \tan \delta_P / FS_P), \text{ and} \quad (13.50)$$

when $\Sigma F_X = 0$,

$$F_P \cdot \cos \theta = E_{HP} + N_P \cdot \sin \theta \quad (13.51)$$

Substituting Equation (13.48) into Equation (13.51) gives

$$N_P \cdot \cos \theta \cdot \tan \delta_P / FS_P = E_{HP} + N_P \cdot \sin \theta$$

$$N_P \cdot (\cos \theta \cdot \tan \delta_P / FS_P - \sin \theta) = E_{HP}$$

$$N_p = \frac{E_{HP}}{\cos \theta \cdot \tan \delta_p / FS_p - \sin \theta} \quad (13.52)$$

Substituting Equation 13.52 into Equation 13.50 gives

$$\begin{aligned} W_p + E_{HP} \cdot \tan \phi_s / FS_p &= \frac{E_{HP} \cdot (\cos \theta + \sin \theta \cdot \tan \delta_p / FS_p)}{\cos \theta \cdot \tan \delta_p / FS_p - \sin \theta} \\ E_{HP} \cdot (\cos \theta + \sin \theta \cdot \tan \delta_p / FS_p) &= W_p \cdot (\cos \theta \cdot \tan \delta_p / FS_p - \sin \theta) \\ &\quad + E_{HP} \cdot (\cos \theta \cdot \tan \delta_p / FS_p - \sin \theta) \cdot \tan \phi_s / FS_p \\ E_{HP} \cdot (\cos \theta + \sin \theta \cdot \tan \delta_p / FS_p - \cos \theta \cdot \tan \delta_p \cdot \tan \phi_s / FS_p^2 + \sin \theta \cdot \tan \phi_s / FS_p) &= W_p \cdot (\cos \theta \cdot \tan \delta_p / FS_p - \sin \theta) \\ E_{HP} &= \frac{W_p \cdot (\cos \theta \cdot \tan \delta_p / FS_p - \sin \theta)}{\cos \theta + (\tan \delta_p + \tan \phi_s) \cdot \sin \theta / FS_p - \cos \theta \cdot \tan \delta_p \cdot \tan \phi_s / FS_p^2} \quad (13.53) \end{aligned}$$

Considering the force equilibrium of the active wedge [Figure 13.12(c)] yields

$$\Sigma F_Y = 0:$$

$$W_A = F_A \cdot \sin \beta + N_A \cdot \cos \beta + E_{VA} \quad (13.54)$$

$$F_A = N_A \cdot \tan \delta_A / FS_A \quad (13.55)$$

$$E_{VA} = E_{HA} \cdot \tan \phi_s / FS_A \quad (13.56)$$

Substituting Equations 13.55 and 13.56 into Equation 13.54 gives

$$W_A = N_A \cdot (\cos \beta + \sin \beta \cdot \tan \delta_A / FS_A) + E_{HA} \cdot \tan \phi_s / FS_A \quad (13.57)$$

$$\Sigma F_X = 0:$$

$$F_A \cdot \cos \beta + E_{HA} = N_A \cdot \sin \beta \quad (13.58)$$

Substituting Equation 13.55 into Equation 13.58 gives

$$\begin{aligned} E_{HA} &= N_A \cdot (\sin \beta - \cos \beta \cdot \tan \delta_A / FS_A) \\ N_A &= \frac{E_{HA}}{\sin \beta - \cos \beta \cdot \tan \delta_A / FS_A} \quad (13.59) \end{aligned}$$

Substituting Equation 13.59 into Equation 13.57 gives

$$\begin{aligned} W_A &= E_{HA} \cdot \frac{\cos \beta + \sin \beta \cdot \tan \delta_A / FS_A}{\sin \beta - \cos \beta \cdot \tan \delta_A / FS_A} + E_{HA} \cdot \tan \phi_s / FS_A \\ E_{HA} \cdot \frac{\cos \beta + \sin \beta \cdot \tan \delta_A / FS_A + \sin \beta \cdot \tan \phi_s / FS_A - \cos \beta \cdot \tan \delta_A \cdot \tan \phi_s / FS_A^2}{\sin \beta - \cos \beta \cdot \tan \delta_A / FS_A} &= W_A \\ E_{HA} &= \frac{W_A \cdot (\sin \beta - \cos \beta \cdot \tan \delta_A / FS_A)}{\cos \beta + (\tan \delta_A + \tan \phi_s) \cdot \sin \beta / FS_A - \cos \beta \cdot \tan \delta_A \cdot \tan \phi_s / FS_A^2} \quad (13.60) \end{aligned}$$

Because $E_{HA} = E_{HP}$ and $FS_A = FS_P = FS$, Equation 13.60 must equal Equation 13.53, giving

$$\begin{aligned}
 & \frac{W_A \cdot (\sin \beta - \cos \beta \cdot \tan \delta_A / FS)}{\cos \beta + (\tan \delta_A + \tan \phi_s) \cdot \sin \beta / FS - \cos \beta \cdot \tan \delta_A \cdot \tan \phi_s / FS^2} \\
 &= \frac{W_P \cdot (\cos \theta \cdot \tan \delta_P / FS - \sin \theta)}{\cos \theta + (\tan \delta_P + \tan \phi_s) \cdot \sin \theta / FS - \cos \theta \cdot \tan \delta_P \cdot \tan \phi_s / FS^2} \\
 & W_A \cdot (\sin \beta - \cos \beta \cdot \tan \delta_A / FS) [\cos \theta + (\tan \delta_P + \tan \phi_s) \cdot \sin \theta / FS - \cos \theta \cdot \tan \delta_P \cdot \tan \phi_s / FS^2] \\
 &= W_P \cdot (\cos \theta \cdot \tan \delta_P / FS - \sin \theta) [\cos \beta + (\tan \delta_A + \tan \phi_s) \cdot \sin \beta / FS - \cos \beta \cdot \tan \delta_A \cdot \tan \phi_s / FS^2] \\
 & (W_A \cdot \sin \beta - W_A \cdot \cos \beta \cdot \tan \delta_A / FS) [\cos \theta + (\tan \delta_P + \tan \phi_s) \cdot \sin \theta / FS - \cos \theta \cdot \tan \delta_P \cdot \tan \phi_s / FS^2] \\
 &= (W_P \cdot \cos \theta \cdot \tan \delta_P / FS - W_P \cdot \sin \theta) [\cos \beta + (\tan \delta_A + \tan \phi_s) \cdot \sin \beta / FS - \cos \beta \cdot \tan \delta_A \cdot \tan \phi_s / FS^2] \\
 & W_A \cdot \sin \beta \cdot \cos \theta + W_A \cdot (\tan \delta_P + \tan \phi_s) \cdot \sin \beta \cdot \sin \theta / FS - W_A \cdot \sin \beta \cdot \cos \theta \cdot \tan \delta_P \cdot \tan \phi_s / FS^2 \\
 &- W_A \cdot \cos \beta \cdot \cos \theta \cdot \tan \delta_A / FS - W_A \cdot (\tan \delta_P + \tan \phi_s) \cdot \cos \beta \cdot \sin \theta \cdot \tan \delta_A / FS^2 \\
 &+ W_A \cdot \cos \beta \cdot \cos \theta \cdot \tan \delta_A \cdot \tan \delta_P \cdot \tan \phi_s / FS^3 = W_P \cdot \cos \beta \cdot \cos \theta \cdot \tan \delta_P / FS \\
 &+ W_P \cdot (\tan \delta_A + \tan \phi_s) \cdot \sin \beta \cdot \cos \theta \cdot \tan \delta_P / FS^2 - W_P \cdot \cos \beta \cdot \cos \theta \cdot \tan \delta_A \cdot \tan \delta_P \cdot \tan \phi_s / FS^3 \\
 &- W_P \cdot \cos \beta \cdot \sin \theta - W_P \cdot (\tan \delta_A + \tan \phi_s) \cdot \sin \beta \cdot \sin \theta / FS + W_P \cdot \cos \beta \cdot \sin \theta \cdot \tan \delta_A \cdot \tan \phi_s / FS^2 \\
 & (W_A \cdot \sin \beta \cdot \cos \theta + W_P \cdot \cos \beta \cdot \sin \theta) \cdot FS^3 + [W_A \cdot (\tan \delta_P + \tan \phi_s) \cdot \sin \beta \cdot \sin \theta \\
 &+ W_P \cdot (\tan \delta_P + \tan \phi_s) \cdot \sin \beta \cdot \sin \theta - W_A \cdot \cos \beta \cdot \cos \theta \cdot \tan \delta_A - W_P \cdot \cos \beta \cdot \cos \theta \cdot \tan \delta_P] \cdot FS^2 \\
 &- [W_A \cdot (\tan \delta_P + \tan \phi_s) \cdot \cos \beta \cdot \sin \theta \cdot \tan \delta_A + W_P \cdot (\tan \delta_A + \tan \phi_s) \cdot \sin \beta \cdot \cos \theta \cdot \tan \delta_P \\
 &+ W_A \cdot \sin \beta \cdot \cos \theta \cdot \tan \delta_P \cdot \tan \phi_s + W_P \cdot \cos \beta \cdot \sin \theta \cdot \tan \delta_A \cdot \tan \phi_s] \cdot FS \\
 &+ (W_A \cdot \cos \beta \cdot \cos \theta \cdot \tan \delta_A \cdot \tan \delta_P \cdot \tan \phi_s + W_P \cdot \cos \beta \cdot \cos \theta \cdot \tan \delta_A \cdot \tan \delta_P \cdot \tan \phi_s) = 0 \\
 & (W_A \cdot \sin \beta \cdot \cos \theta + W_P \cdot \cos \beta \cdot \sin \theta) \cdot FS^3 + [(W_A \cdot \tan \delta_P + W_P \cdot \tan \delta_A + W_T \cdot \tan \phi_s) \cdot \sin \beta \cdot \sin \theta \\
 &- (W_A \cdot \tan \delta_A + W_P \cdot \tan \delta_P) \cdot \cos \beta \cdot \cos \theta] \cdot FS^2 - [W_T \cdot \tan \phi_s \cdot (\sin \beta \cdot \cos \theta \cdot \tan \delta_P \\
 &+ \cos \beta \cdot \sin \theta \cdot \tan \delta_A) + (W_A \cdot \cos \beta \cdot \sin \theta + W_P \cdot \sin \beta \cdot \cos \theta) \cdot \tan \delta_A \cdot \tan \delta_P] \cdot FS \\
 &+ W_T \cdot \cos \beta \cdot \cos \theta \cdot \tan \delta_A \cdot \tan \delta_P \cdot \tan \phi_s = 0 \tag{13.61}
 \end{aligned}$$

Equation 13.61 is now solved as follows:

$$a \cdot FS^3 + b \cdot FS^2 + c \cdot FS + d = 0 \tag{13.62}$$

$$a = W_A \cdot \sin \beta \cdot \cos \theta + W_P \cdot \cos \beta \cdot \sin \theta$$

$$b = (W_A \cdot \tan \delta_P + W_P \cdot \tan \delta_A + W_T \cdot \tan \phi_s) \cdot \sin \beta \cdot \sin \theta - (W_A \cdot \tan \delta_A + W_P \cdot \tan \delta_P) \cdot \cos \beta \cdot \cos \theta$$

$$c = -[W_T \cdot \tan \phi_s \cdot (\sin \beta \cdot \cos \theta \cdot \tan \delta_P + \cos \beta \cdot \sin \theta \cdot \tan \delta_A) + (W_A \cdot \cos \beta \cdot \sin \theta + W_P \cdot \sin \beta \cdot \cos \theta) \cdot \tan \delta_A \cdot \tan \delta_P]$$

$$d = W_T \cdot \cos \beta \cdot \cos \theta \cdot \tan \delta_A \cdot \tan \delta_P \cdot \tan \phi_s$$

When the cell subgrade is very small (i.e., $\theta \approx 0$), $\sin \theta \approx 0$, and $\cos \theta \approx 1$, Equation 13.62 then becomes

$$a \cdot FS^3 + b \cdot FS^2 + c \cdot FS + d = 0 \tag{13.63}$$

$$\text{where } a = W_A \cdot \sin \beta$$

$$b = -(W_A \cdot \tan \delta_A + W_P \cdot \tan \delta_P) \cdot \cos \beta$$

$$c = -(W_T \cdot \tan \phi_s + W_P \cdot \tan \delta_A) \cdot \sin \beta \cdot \tan \delta_P$$

$$d = W_T \cdot \cos \beta \cdot \tan \delta_A \cdot \tan \delta_P \cdot \tan \phi_s$$

In the conventional translational (or two-wedge) failure analysis method, the direction of the resultant force E_P of E_{HP} and E_{VP} (or the resultant force E_A of E_{HA} and E_{VA}), which acts on the interface between the passive wedge and active wedge, is usually assumed to be parallel to waste filling slope. The effect of the waste property of the interface between the active and passive wedges (i.e., shear strength of the waste) on the stability is not considered for this assumption. Actually, the real direction of the resultant force E_A of E_{HA} and E_{VA} (or the direction of the interwedge force) should be calculated as

$$\begin{aligned} \tan \omega &= E_{VP}/E_{HP} \\ &= (E_{HP} \cdot \tan \phi_s / FS) / E_{HP} \\ &= \tan \phi_s / FS \\ \omega &= \tan^{-1}(\tan \phi_s / FS) \end{aligned} \quad (13.64)$$

where ω = inclination angle of the interwedge force (i.e., the resultant force of E_{HP} and E_{VP}), measured from horizontal, degrees;
 ϕ_s = friction angle of solid waste;
 FS = factor of safety for the entire solid waste mass.

Municipal solid waste usually settles a considerable amount during the filling operation. Review of field settlements from several landfills indicates that municipal solid waste landfills usually settle approximately 15 to 30% of the initial height because of placement and decomposition. The large settlement of the waste fill induces shear stresses in the liner system on the side slope, all of which tends to displace the liner downslope. The large settlement of the waste fill also causes the large deformation of the landfill cover to induce shear stresses in the final cover system. These shear stresses induce shear displacements along specific interfaces in the liner and cover systems that may lead to the mobilization of a residual interface strength. In addition, thermal expansion and contraction of the side slope liner and cover systems during construction and filling may also contribute to the accumulation of shear displacements and the mobilization of a residual interface shear strength in the liner system (Qian, 1994; Stark and Poeppel, 1994).

Earthquake loading can provide permanent displacements along landfill liner interfaces, resulting in a permanent reduction in their available shear resistance following the completion of the dynamic loading. Post-earthquake static stability must therefore be evaluated using shear strengths that are compatible with the shear displacements predicted to be experienced during the earthquake. In areas of high seismicity, this probably implies that the static stability of the final configuration of the landfill should be assured assuming the mobilization of full residual strength conditions (Byrne, 1994).

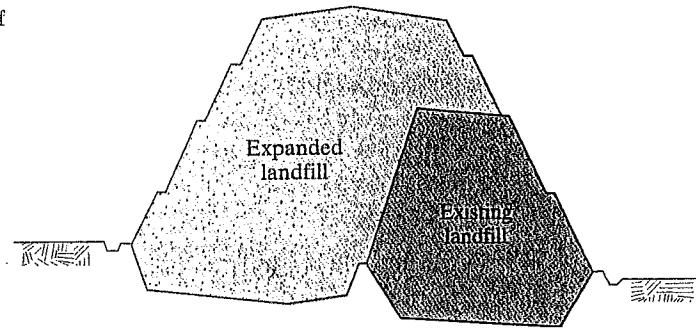
CHAPTER 14

Vertical Landfill Expansions

-
- 14.1 CONSIDERATIONS INVOLVED IN VERTICAL EXPANSIONS
 - 14.2 LINER SYSTEMS FOR VERTICAL EXPANSION
 - 14.3 SETTLEMENT OF EXISTING LANDFILL
 - 14.4 ESTIMATION OF DIFFERENTIAL SETTLEMENT DUE TO WASTE HETEROGENEITY
 - 14.4.1 CURRENT METHODS FOR ESTIMATING LOCALIZED SUBSIDENCE
 - 14.4.2 ELASTIC SOLUTION METHOD APPLIED TO A VERTICAL EXPANSION
 - 14.5 VERTICAL EXPANSION OVER UNLINED LANDFILLS
 - 14.6 DESIGN CONSIDERATIONS FOR LANDFILL STRUCTURES
 - 14.7 GEOSYNTHETIC REINFORCEMENT DESIGN FOR VERTICAL EXPANSIONS
 - 14.7.1 THEORETICAL BACKGROUND FOR GEOSYNTHETIC REINFORCEMENT
 - 14.7.2 ASSUMPTIONS FOR GEOSYNTHETIC REINFORCEMENT DESIGN
 - 14.7.3 SELECTION OF MATERIAL PROPERTIES
 - 14.7.4 DETERMINATION OF GEOMETRIC AND LOADING PARAMETERS
 - 14.7.5 DESIGN CRITERIA
 - 14.7.6 SELECTION OF ALLOWABLE REINFORCEMENT STRAIN
 - 14.7.7 SELECTION OF LONG TERM ALLOWABLE DESIGN TENSILE LOAD
 - 14.7.8 DESIGN STEPS
 - 14.7.9 SPECIAL DESIGN CASES
 - 14.7.10 DESIGN EXAMPLE
 - 14.8 STABILITY ANALYSIS FOR VERTICAL EXPANSIONS
 - PROBLEMS
 - REFERENCES
-

The acquisition and permitting of new landfill sites poses several difficulties. An attractive alternative to landfill owners is to consider expansions to existing landfills. This option may entail the design and permitting of a vertical expansion over old landfill areas. The advantages of vertical landfill expansion include (1) optimal use of landfill area, (2) high waste volume filled per unit area, (3) low construction cost, (4) less public opposition, and (5) easier permitting. Expansion can occur by vertical and/or lateral expansion in which the old landfill is encapsulated by the new (vertical and lateral expansion), or by placement of new landfill atop the old (piggyback expansion). Figure 14.1 shows a cross-section of a vertical and lateral expansion landfill; Figure 14.2 shows a cross section of a piggyback vertical expansion landfill.

FIGURE 14.1 Cross Section of a Vertical and Lateral Expansion Landfill



14.1 CONSIDERATIONS INVOLVED IN VERTICAL EXPANSIONS

The additional waste fill from a vertical landfill expansion will cause settlement of the existing landfill and result in liner system and slope stability problems for both existing and expanded landfills. A gas collection system in the existing landfill may also be of concern due to the large deformation of the solid waste surrounding gas collection pipes. A liner and leachate collection system constructed on an existing landfill may experience large differential settlements. The long-term performance of these systems is thus a major design consideration.

Large differential settlements within existing refuse may occur because of the collapse or degradation of large objects, which have been deposited in old landfills. These settlements could result in tensile strains in a liner system placed on the top of an old landfill. If the tensile strain within the liner exceeds the tensile capacity of the material, whether it is a soil or a geosynthetic, tension cracks or tensile failure will develop. The tension cracks will reduce the effectiveness of the liner as a hydraulic barrier by providing a direct flow path through the liner system (Jang and Montero, 1993). Under extreme conditions, large differential settlements could result in the reversal of leachate flow gradients and directions. If grade reversal takes place at the surface of a liner and leachate collection system, leachate will pond on the liner, and increase the potential for infiltration of the leachate into the old landfill.

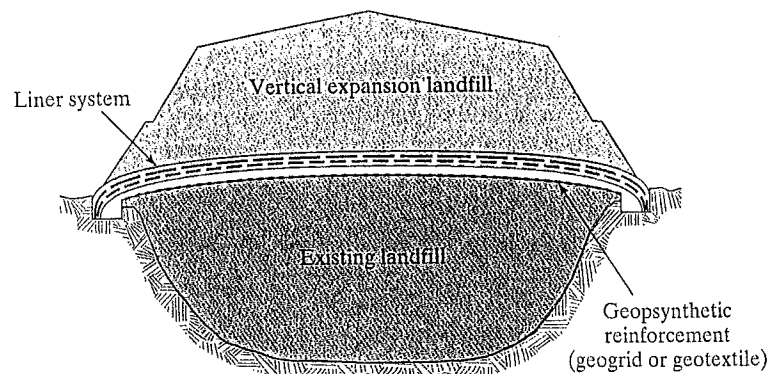


FIGURE 14.2 Cross Section of a Piggyback Vertical Expansion Landfill

The additional waste fill due to the vertical expansion may also affect the bottom topography or subgrade elevations beneath the existing landfill and cause ponding problems on the bottom liner. Almost certainly, this extra load will increase the deflection and wall stress of the leachate and gas collection pipes buried in the existing landfill (if any are present) and may also cause pipe failure or pipe wall stability problems.

Major design steps and considerations for vertical landfill expansion include (Qian, 1996)

- (i) Selecting a suitable composite liner system for placement over the existing landfill.
- (ii) Estimating the overall total settlement and differential settlement of the existing landfill caused by new waste fill.
- (iii) Estimating the differential settlement due to the degradation of large objects in the old landfill, or reinforcing the liner system to minimize this differential settlement.
- (iv) Calculating subgrade elevation changes beneath the existing landfill caused by the differential settlements due to both existing and extra waste filling.
- (v) Evaluating the deformation and stability conditions of the leachate and gas collection pipes in the existing landfill due to the extra waste fill.
- (vi) Evaluating the stability of the soil mass, liner system, waste mass, and final cover system in various conditions (e.g., excavation, construction, operation, and closure conditions).

14.2 LINER SYSTEMS FOR VERTICAL EXPANSION

The existing solid waste mass, which is relatively compressible, must provide the foundation of the liner system for the vertical expansion landfill. Tensile strains and stresses can develop within the various bottom liner components as a result of differential settlements due to the compression of the underlying solid waste landfill. These tensile strains and stresses can adversely affect the integrity of the liner components. If a compacted clay liner is proposed, it must be recognized that it possesses very little tensile strength (allowable tensile strain is less than 1.0 percent) and is susceptible to cracking as a result of differential settlement. Thus, it is likely that the effectiveness of a compacted clay liner as a hydraulic barrier would be seriously compromised in a vertical expansion landfill. As such, compacted clay liners are generally not recommended for vertical or lateral expansions. A geosynthetic clay liner (GCL) can be used as an alternative to a compacted clay liner. Geosynthetic clay liners are considerably more effective as impervious barriers. They can withstand relatively high in-plane tensile strains and stresses induced by differential settlement (recall Section 5.3). The allowable tensile strain of geosynthetic clay liners range from 6 to 20 percent, contrasted to less than 1 percent for a compacted clay liner.

With respect to the geomembrane components of a composite liner system placed over an existing landfill, several different geomembranes can be selected. These include linear low density polyethylene (LLDPE), flexible polypropylene (fPP), and polyvinyl chloride (PVC) geomembranes. It should be noted that

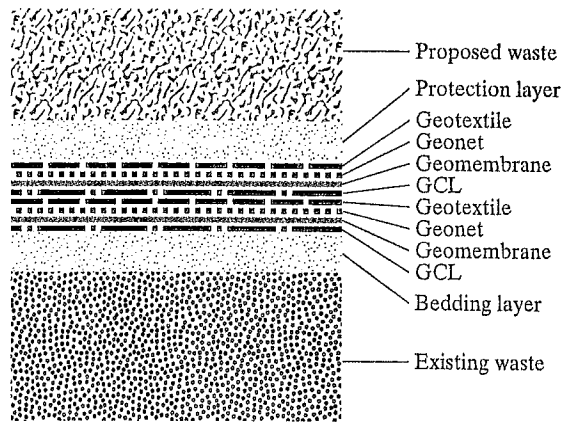


FIGURE 14.3 Double Composite Liner System over Existing Waste

high density polyethylene (HDPE) can also be considered if the tensile strain is mobilized slowly. The reason HDPE is often not used in these situations is that the test method used to simulate differential subsidence (ASTM D5617) applies load very fast in comparison to actual conditions in a landfill. The default pressure rate is 1.0 lb/in²/min; thus, stress relaxation does not occur and the HDPE fails at relatively low strains of approximately 25%. The other geomembranes cited fail at strains from 75 to 100%. A textured geomembrane should generally be selected to provide a relatively greater interface strength between geomembrane and geosynthetic clay liner or geosynthetic composite drainage layer. Because of the magnitude of the settlements that the liner system will experience and the possibility of "local" liner deformations due to localized subsidence effects, it is important to select a geomembrane with superior extension properties. For a number of reasons (differential settlement, substandard liner under existing waste, etc.) a double liner system is desirable under a vertical expansion.

Cross sections of typical double-composite liner systems used in vertical expansions of landfills are shown in Figures 14.3 and 14.4. A geogrid or high strength geotextile is placed beneath the bottom of the liner system to reinforce the liner system in

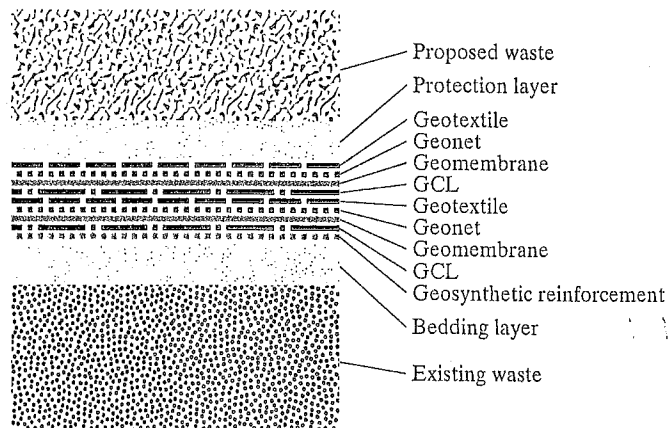


FIGURE 14.4 Double Composite Liner System Reinforced with Geosynthetic Reinforcement over Existing Waste



FIGURE 14.5 A Liner System Placed over an Existing Landfill for a Vertical Expansion Project

Figure 14.4. The geosynthetic reinforcement can prevent excessive tensile strain in the liner system over the existing landfill. Figure 14.5 shows a double composite liner system placed over an existing landfill for a vertical expansion project.

14.3 SETTLEMENT OF EXISTING LANDFILL

The area-wide (also the “total”) settlement of waste when subjected to an increase in overburden pressure due to the vertical expansion is characterized by two components, a rapid primary settlement and a long-term, time-dependent secondary settlement. The primary and secondary settlements of the existing landfill due to the vertical expansion can be calculated by using the following equations from Chapter 12:

Primary Settlement of Existing Landfill

$$\Delta Z_c = C'_c \cdot H_o \cdot \log \frac{\sigma_o + \Delta \sigma}{\sigma_o} \quad (14.1)$$

where ΔZ_c = primary settlement of existing landfill;
 H_o = initial thickness of the waste layer of the existing landfill;
 C'_c = modified primary compression index. $C'_c = 0.17 \sim 0.36$;
 σ_o = existing overburden pressure acting at the mid level of the waste layer;
 $\Delta \sigma$ = increment of overburden pressure due to vertical expansion.

Secondary Settlement of Existing Landfill

$$\Delta Z_{\alpha} = C'_{\alpha} \cdot H_0 \cdot \log \frac{t_2}{t_1} \quad (14.2)$$

where ΔZ_c = secondary settlement of existing landfill;
 H_0 = initial thickness of the waste layer before starting secondary settlement;
 C'_{α} = modified secondary compression index. $C'_{\alpha} = 0.03 \sim 0.1$;
 t_1 = starting time of the secondary settlement. It is assumed to be equal to the age of existing landfill for vertical expansion project;
 t_2 = ending time of the secondary settlement.

Total Settlement of Existing Landfill

$$\Delta Z = \Delta Z_c + \Delta Z_{\alpha} \quad (14.3)$$

where ΔZ = total settlement of existing landfill;
 ΔZ_c = primary settlement of existing landfill;
 ΔZ_{α} = long-term secondary settlement of existing landfill.

The calculations should be performed at discrete points along several selected settlement lines over the existing landfill. At each point, the thickness of the existing waste in the existing landfill and the thickness of the proposed waste to be placed in the vertical expansion (i.e., the overburden pressure) can be estimated. As an example, see the cross-section, shown in Figure 14.6. The value of the total settlement at each point depends on both the thickness of the existing waste and the load due to the proposed waste fill.

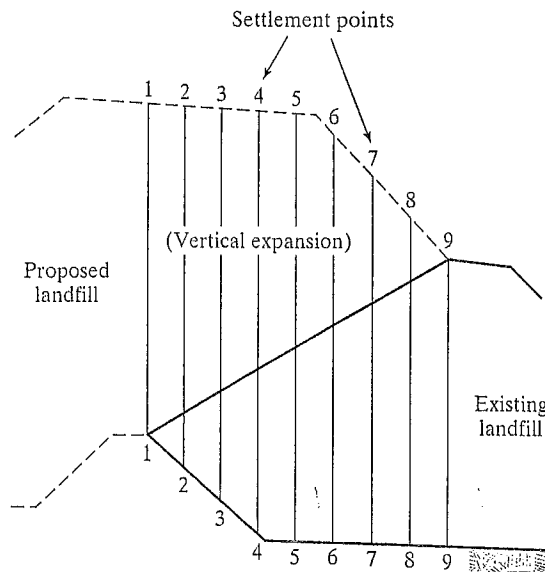


FIGURE 14.6 Cross Section of Existing and Proposed Landfills along Settlement Lines

The differential settlements resulting in tensile strains of liner system materials and leachate collection pipes over the existing landfill, and final grades between adjacent settlement points after settlement can be evaluated from the calculated values of the total settlements at various settlement points along each settlement line on the landfill subgrade.

The differential settlement between adjacent points can be calculated using the equation

$$\Delta Z_{i,i+1} = Z_{i+1} - Z_i \quad (14.4)$$

where $\Delta Z_{i,i+1}$ = differential settlement between points i and $i + 1$,

Z_i = total settlement of point i ,

Z_{i+1} = total settlement of point $i + 1$.

The final slope angle between adjacent points after settlement can be calculated using the equation

$$\tan \beta_{Fnl} = \frac{X_{i,i+1} \cdot \tan \beta_{Int} - \Delta Z_{i,i+1}}{X_{i,i+1}} \quad (14.5)$$

where $X_{i,i+1}$ = horizontal distance between points i and $i + 1$,

$\Delta Z_{i,i+1}$ = differential settlement between points i and $i + 1$,

β_{Int} = initial slope angle between points i and $i + 1$,

β_{Fnl} = final slope angle between points i and $i + 1$ after settlement.

The landfill subgrade changes along each settlement line due to different settlements can be calculated from the preceding equation.

The tensile strains of the liner system and leachate collection system resulting from the settlements can be estimated using the equation

$$\epsilon_{i,i+1} = \frac{(L_{i,i+1})_{Fnl} - (L_{i,i+1})_{Int}}{(L_{i,i+1})_{Int}} \times 100\% \quad (14.6)$$

where $\epsilon_{i,i+1}$ = tensile strain in liner system between points i and $i + 1$,

$(L_{i,i+1})_{Int}$ = distance between points i and $i + 1$ in their initial positions,

$(L_{i,i+1})_{Fnl}$ = distance between points i and $i + 1$ in their post-settlement positions.

The distance between points i and $i + 1$ in their initial positions can be calculated using the equation

$$(L_{i,i+1})_{Int} = [(X_{i,i+1})^2 + (X_{i,i+1} \cdot \tan \beta_{Int})^2]^{1/2} \quad (14.7)$$

The distance between points i and $i + 1$ in their post-settlement positions can be calculated using the equation

$$(L_{i,i+1})_{Fnl} = [(X_{i,i+1})^2 + (X_{i,i+1} \cdot \tan \beta_{Int} - \Delta Z_{i,i+1})^2]^{1/2} \quad (14.8)$$

The maximum acceptable tensile strains (i.e., the elongations at yield) of various liner system and leachate collection system components can be obtained from the product specific laboratory testing.

**APPLICATION FOR PERMIT RENEWAL AND MODIFICATION
SANDOVAL COUNTY LANDFILL**

**VOLUME III: LANDFILL ENGINEERING CALCULATIONS
SECTION 7: GEOSYNTHETICS TENSILE STRESS AND STABILITY ANALYSIS**

**ATTACHMENT III.7.C
CARTER, M. AND BENTLEY, S.P.,
CORRELATIONS OF SOIL PROPERTIES, 1991.**

Table 5.3 SOME PUBLISHED CORRELATIONS FOR COMPRESSION INDICES (AFTER AZZOUZ ET AL. 1976)

Equation	Regions of applicability
$C_c = 0.007 (LL - 7)$	Remoulded clays
$C_{cr} = 0.208e_0 + 0.0083$	Chicago clays
$C_c = 17.66 \times 10^{-3} w_n^2 + 5.93 \times 10^{-3} w_n - 1.35 \times 10^{-1}$	Chicago clays
$C_c = 1.15(e_0 - 0.35)$	All clays
$C_c = 0.30(e_0 - 0.27)$	Inorganic, cohesive soil; silt, some clay; silty clay; clay
$C_c = 1.15 \times 10^{-2} w_n$	Organic soils-meadow mats, peats, and organic silt and clay
$C_c = 0.75(e_0 - 0.50)$	Soils of very low plasticity
$C_{cr} = 0.156e_0 + 0.0107$	All clays
$C_u = 0.01 w_n$	Chicago clays

As summarized by Azzouz, Krizek, and Corotis (1976).
Note: w_n = natural water content.

clays:

$$C_c = 0.007(LL - 10).$$

Terzaghi and Peck (1967) proposed a similar relationship, based on research with clays of low and medium sensitivity:

$$C_c = 0.009(LL - 10).$$

This relationship has a reliability range of $\pm 30\%$ and is valid for inorganic clays of sensitivity up to 4 (see Chapter 6) and liquid limit up to 100. Based on the work of Skempton and Northey (1952) and Roscoe *et al.* (1958), Wroth and Wood (1978) used critical state soil mechanics considerations to deduce a relationship between compression index and plasticity index (PI) for remoulded clays:

$$C_c = \frac{1}{2} PI \cdot G_s$$

where G_s is the specific gravity of the soil solids. Table 5.3 produced by Azzouz *et al.* (1976) gives a summary of a number of published correlations.

The recompression index, C_{cr} , is defined in the same way as C_c except that it applies to the unloading phase of the consolidation test. Typical values of C_{cr} range from 0.015 to 0.35 (Roscoe *et al.* 1958) and are often assumed to be 5-10% of C_c .

5.1.5 Settlement corrections

If the results of oedometer tests are used directly to calculate settlements, the values obtained tend to over-estimate the settlements

**APPLICATION FOR PERMIT RENEWAL AND MODIFICATION
SANDOVAL COUNTY LANDFILL**

**VOLUME III: LANDFILL ENGINEERING CALCULATIONS
SECTION 7: GEOSYNTHETICS TENSILE STRESS AND STABILITY ANALYSIS**

ATTACHMENT III.7.D

**CHEN, Y., GAU, D. AND ZHU, B., *CONTROLLING STRAIN IN GEOSYNTHETIC LINER
SYSTEMS USED IN VERTICALLY EXPANDED LANDFILLS*, JOURNAL OF ROCK
MECHANICS AND GEOTECHNICAL ENGINEERING (2009), PPS 48-55.**



Controlling strain in geosynthetic liner systems used in vertically expanded landfills

Yunmin Chen*, Deng Gao, Bin Zhu

MOE Key Laboratory of Soft Soils and Geoenvironmental Engineering, Institute of Geotechnical Engineering, Zhejiang University, Hangzhou, 310027, China

Received 12 February 2009; received in revised form 10 August 2009; accepted 28 August 2009

Abstract: According to relevant new regulations in China, a composite liner system involving geosynthetic materials must be installed at the bottom of an expanded landfill. The deformation and integrity of the composite liner under a variety of factors are important issue to be considered in the design of a landfill expansion. In this paper, we investigate the strain distribution in geosynthetic materials within the composite liner system of expanded landfills, including strains in geosynthetic materials resulting from overall settlement and lateral movement of landfills, localized subsidence in landfills, and differential settlement around gas venting wells. The allowable strains of geosynthetic materials are discussed based on the results of tensile tests, and the corresponding design criteria for composite liner systems are proposed. Meanwhile, practical measures allowing strain control in geosynthetic materials used in landfill engineering are proposed.

Key words: landfill; composite liner system; geosynthetics; strain

1 Introduction

Significant growth in the population and economy of most urban areas of China since the 1990s has resulted in a rapid increase in the generation of municipal solid waste (MSW). About 90% of these highly compressible materials are disposed of in landfills. However, most of the landfills in major cities were built in the early 1990s and have now reached their designed service lifespan [1]. Expansion of these landfills is hampered because many of the earlier-constructed landfills were not appropriately lined with clay liners or geomembranes (GMs). According to new Chinese regulations [2], expanded landfills must incorporate a composite liner system using geosynthetic materials.

The expansion of existing landfills is currently underway in many cities of China due to difficulties in obtaining new landfill sites. However, the addition of waste through vertical landfill expansions will cause overall settlement and lateral movement in the underlying older landfill, which could strain geosynthetic materials in a composite liner system and alter the inclination of the leachate drainage layer. Voids (holes or cavings) or local subsidence are often caused by

progressive degradation and collapse of large-sized objects buried in existing landfills. Such voids can cause “localized” deformations and strains in geosynthetic materials in the composite liner systems. In addition, GMs in composite liner systems are often connected to rigid circular structures (e.g. gas venting wells in the existing landfills). GMs can exhibit excessive tensions and strains in the areas connected to such rigid structures due to differential settlement [3]. Thus, the serviceability and structural integrity of geosynthetic materials in composite liner systems subjected to differential settlements are important design consideration for landfill expansion. If the induced tensile strain in the geosynthetic material exceeds the tensile strength of the sealing material, tensile failure (e.g. cracking) will occur and the effectiveness of the liner as a hydraulic barrier will be compromised because such cracks may provide direct flow pathways through the composite liner system [4].

This paper investigates strain within geosynthetic materials in the composite liner systems of expanded landfills, including strain resulting from the overall settlement and lateral movement of existing landfills, local subsidence and differential settlement around gas venting wells. The allowable strains of the geosynthetic materials are discussed based on the results of tensile tests, and a design criterion is proposed. Finally, practical recommendations are proposed for controlling

tensile strains in geosynthetic materials for landfill engineering.

2 Analysis of strain in geosynthetic materials

The Suzhou landfill near Shanghai was commissioned in 1993. It is located in a valley surrounded by hills, about 13 km from Suzhou City. The landfill has reached its maximum design level by the end of 2008. Designs for vertical and lateral expansions of the existing landfill are underway. The preliminary design involves the vertical expansion of the existing landfill from 80 to 120 m, and an outward expansion of 400 m from the present landfill boundaries, as illustrated in Fig.1.

The bottom of the existing landfill was not lined with any form of engineering barrier when it was constructed. An injected grouted curtain was installed under the retaining wall of the leachate pond to limit downstream leachate movements. The grouted curtain extended to the underlying fresh rock which had a high structural integrity and a permeability less than 1×10^{-9} m/s. The grouted curtain and the fresh rock were expected to constitute a closed barrier system against leachate movement in the existing landfill. However, monitoring of the downstream flow of groundwater in the grouted curtain indicated that the barrier system did not perform as expected. In accordance with the new regulation, the bottom of the expanded waste body will be lined with a composite liner system.

2.1 Overall settlement and lateral movement in existing landfill

The assessment of strain in potential geosynthetic materials requires not only a reliable estimate of the overall deformation in an existing landfill but also an understanding of the interactions between a new

liner system and the old underlying landfill material. This is a challenging problem. Qian et al. [5] presented a simple equation for the rough estimation of strain in geosynthetic materials subjected to overall settlement. The equation is based on the assumptions that the landfill has negligible lateral movement and that no slippage occurs at the interface between the liner system and the waste body. The strain in the geosynthetic material of the composite liner system can be evaluated by observing progressive changes in selected cross-sections through the existing landfill and comparing the pre- and post-settlement liner configurations (Fig.2). It should be noted that the magnitudes of strain for the geosynthetic materials may be significantly underestimated by this method. An existing landfill sitting on sloping ground usually undergoes some lateral movement during vertical expansion (Fig.3). Thus, the composite liner system will also be subjected to lateral movement, leading to deformation and strain accumulation.

To predict the settlement behavior of the Suzhou landfill, samples were taken at boreholes with a range of depths [6]. The samples were tested in the laboratory with primary compressions.

For the purpose of illustration, a cross-section with a horizontal length of 200 m was chosen for the settlement analyses (Fig.1). Due to the absence of reliable parameters for describing the time-dependent compression behavior of the waste layers, only the primary settlement due to the incremental load of the expanded fill was calculated using the experimental values of the primary compression index (C_c). Figure 4 shows the calculated primary settlement of the existing landfill and induced tensile strain in the geosynthetic materials. The incremental load of the expanded landfill can result in a maximum settlement of about 3.9 m. The maximum tensile strain ε_{\max} in the geosynthetic materials estimated by the equation presented by Qian et al. [5] is only 0.8%.

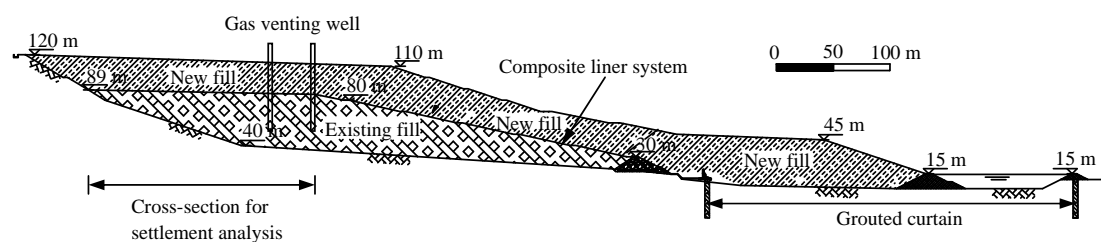


Fig.1 A preliminary design of expansion in Suzhou landfill.

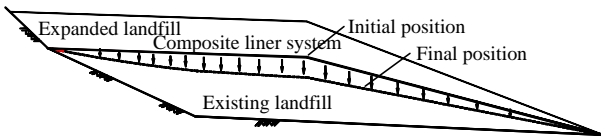


Fig.2 Overall settlement of existing landfill.

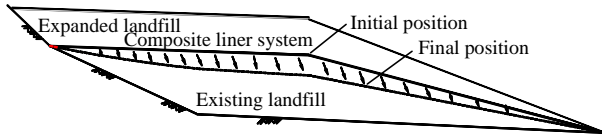


Fig.3 Overall settlement and lateral movement of existing landfill.

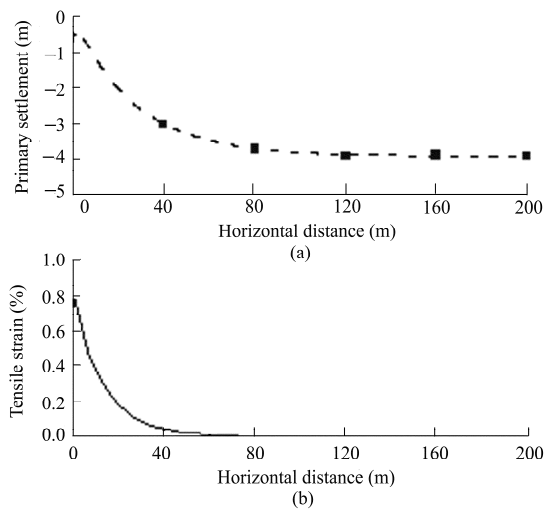


Fig.4 Primary settlement of the existing landfill and induced tensile strain in the geosynthetic material.

At present, no analytical or empirical method has been established for evaluating the lateral movement of a landfill. However, numerical modeling can be adopted to solve this two-dimensional (2D) problem, in which the constitutive model for MSW is important.

A composite exponential model for MSW was proposed based on large-scale triaxial shearing test results by Chen et al. [7]. The expressions of the model are

$$\sigma_1 - \sigma_3 = \left[k_1 P_a \left(\frac{\sigma_3}{P_a} \right)^{n_1} \varepsilon_a + k_c \sigma_3 \right] \left\{ 1 - e^{-\left[\frac{k_2}{k_c} \left(\frac{\sigma_3}{P_a} \right)^{n_2-1} \right] \varepsilon_a} \right\} \quad (1)$$

$$\nu = \min\{0.3 + k_v (\sigma_3 / P_a), 0.45\} \quad (2)$$

where $\sigma_1 - \sigma_3$ is the deviatoric stress, ν is the Poisson's ratio, P_a is the atmospheric air pressure ($P_a = 101.3$ kPa), and k_1 , n_1 , k_2 , n_2 , k_c , k_v are all experimental constants. This constitutive model for MSW has been incorporated into a computer code FLAC, which is capable of numerically modeling deformation due to gravitational forces. In this model,

the time-dependent degradation of MSW is not taken into account.

The code FLAC with the composite exponential model was adopted to analyze the potential strains of the geosynthetic materials in the composite liner systems that were induced by the overall settlement and lateral movement of the existing landfill. The parameters for the composite exponential model of MSW are shown in Table 1. The composite liner system was modeled by beam elements without bending resistance. The main part of the Suzhou landfill was taken into consideration in the analysis. Figure 5 shows the calculated results. It can be seen that the maximum lateral movement of the existing landfill is 2.44 m, which happens at the front of the slope, and the maximum settlement is 4.55 m.

Table 1 Parameters for composite exponential model.

k_1	n_1	k_c	k_2	n_2	k_v
15.022	0.404	0.368	76.033	0.428	0.0314

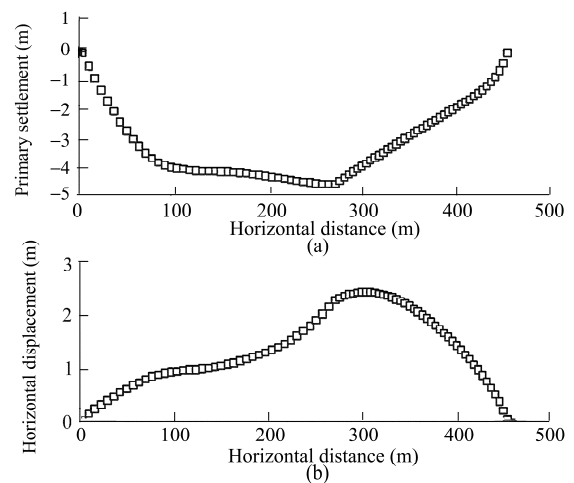


Fig.5 Settlement and horizontal displacement of the surface of the existing landfill.

Figures 6 and 7 show the displacement vectors of the composite liner system and the horizontal distribution of strains in the geosynthetic materials, respectively. The maximum tensile strain ε_{\max} in the geosynthetics is 2.06%, which appears near the anchor trench on the back slope of the existing landfill. It is interesting that compressive strains (negative values) occur on the front slope of the existing landfill, which means that the liner system in this location will relax. The lateral movement of the existing landfill will have an apparent effect on the magnitudes and distribution of strains in the geosynthetic materials at local positions. Further theoretical and experimental studies involving

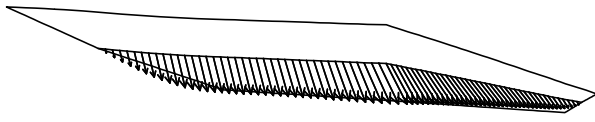


Fig.6 Displacement vectors of composite liner system.

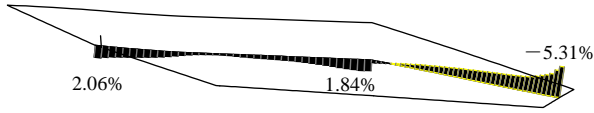


Fig.7 Strain horizontal distribution of geosynthetic material.

time-dependent degradation of MSW are required for an improved understanding on this problem.

2.2 Local subsidence in an existing landfill

As stated before, voids or local subsidence within the existing landfill may occur because of the collapse or degradation of large-size objects in the MSW. At present, it is common engineering practice to reinforce composite liner system with geogrids or high strength geotextiles to accommodate subsidence effects. The current state-of-the-practice is to design for a void of 1.8–2.4 m in diameter (the so-called “refrigerator effect”). The design of the geosynthetic reinforcement is based on a worst-case scenario with the assumption that a void is located immediately underneath the liner. The liner is then treated as a plate bridging the void and carrying the load of the proposed overlying waste (Fig.8).

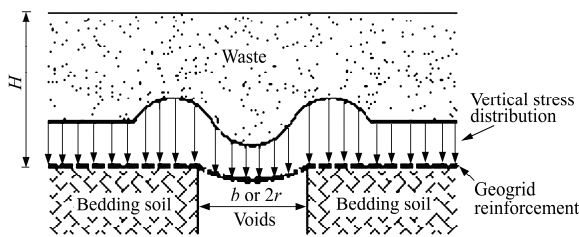


Fig.8 Geosynthetic reinforcement landfill voids.

The design method has been developed using arching theory and tensioned membrane theory [8]. The calculation formulas are expressed as

$$p = \frac{\gamma r}{2K \tan \phi} [1 - e^{-2K \tan \phi (H/r)}] \quad (3)$$

$$T_r = pr\Omega \quad (4)$$

$$\Omega = 0.25 \left(\frac{y}{r} + \frac{r}{y} \right) \quad (5)$$

where p is the normal pressure acting on the reinforcement over the void, T_r is the tensile load of reinforcement, γ is the unit weight of waste

contained above the lining system, K is the coefficient lateral earth pressure coefficient, ϕ is the friction angle of waste, H is the thickness of waste contained above the lining system, r is the radius of the void, and Ω is the dimensionless factor related to reinforcement deflection y or strain ε .

Equations (3) and (4) are also valid for long voids where r is replaced by a width of void b , while r is replaced by $b/2$ in Eq.(5). Since the stress state of the soil in the arching zone is not fully understood at present, various values of the lateral earth pressure coefficient K have been adopted. Terzaghi [9] referred to K as “an empirical coefficient”, while Giroud et al. [8] and McKelvey [10] preferred the use of Handy coefficient [11] in the expression of Terzaghi loosen earth pressure (Eq.(3)), which is defined as

$$K = 1.06(\cos^2 \theta + K_a \sin^2 \theta) \quad (6)$$

where $\theta = 45^\circ + \phi/2$. Recently, the authors proposed a modified lateral earth pressure coefficient K' considering rotations of principal stress axes of soil in the arching zone, and its expression is

$$K' = \frac{\cos^2 \theta + K_p \sin^2 \theta}{\sin^2 \theta + K_p \cos^2 \theta} \quad (7)$$

where K_p is the Rankine passive earth pressure coefficient. Calculated values of K' vary between 1.43 and 2.41 for a range of friction angle from 25° to 40° . Figure 9 shows the normal pressures on the trapdoor, calculated by the present lateral earth pressure coefficient and some other available ones. It can be found that the present result is in the best agreement with the tested result of Adachi et al. [12] compared with other coefficients.

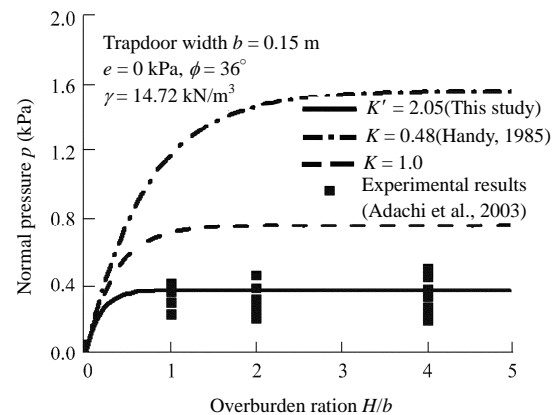


Fig.9 Comparison of calculated normal pressures.

A default assumption in the method of Giroud et al. [9] is that the soil deformation required for arch generation is compatible with the tensile strain required to mobilize tension in the geosynthetic materials. However, it is

possible that the degree of the soil arching depends on the deflection of the geosynthetic liner. In an idealized case in which the geosynthetic reinforcement is perfectly rigid, there is no deflection that leads to stretching of the reinforcement. As such, there will be no soil arching or tensioned membrane effects. In this paper, the vertical earth pressure acting on the geosynthetic liner, which is related to the vertical displacement of the geosynthetic liner, is given as

$$p(y) = (\gamma H - p_0) e^{\frac{\gamma E \lambda}{r \gamma H}} + p_0 \quad (8)$$

where the normal pressure p_0 is calculated by Eq.(3) using the modified lateral earth pressure coefficient K' , λ is a dimensionless factor and is suggested to be 1.76, E is the elastic modulus of the waste. For long voids, r can be replaced by the width b in Eq.(8). Figure 10 shows the effect of the normalized geosynthetic liner deflection ($y/(2r)$) on the load ratio ($p/(\gamma H)$). Clearly, $p(y)$ is equal to γH when y is zero, which means that there is no soil arching effect. The value of $p(y)$ will approach p_0 when the geosynthetic liner deflection y is large enough. Parametric studies also show that with an increase of the waste thickness (H), a larger geosynthetic liner deflection is needed to reach the full degree of soil arching (see Fig.11).

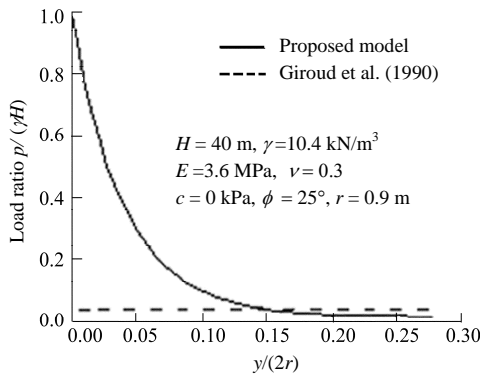


Fig.10 Effect of geosynthetic liner deflection on load ratio.

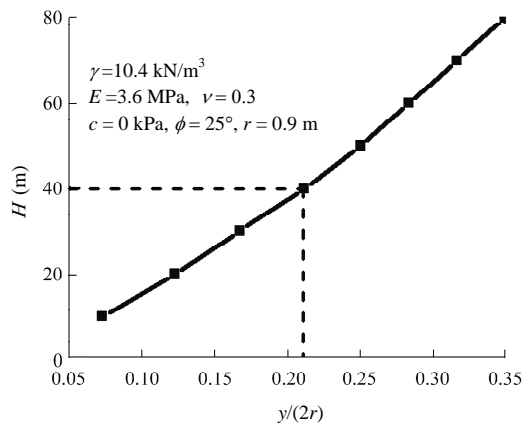


Fig.11 Relationship between waste thickness H and geosynthetic liner deflection needed to reach full degree of soil arching.

Figure 12 shows the calculated tensile load of the geosynthetic reinforcement using the present method and that presented by Giroud et al. [8]. The radius of the void is selected to be 0.9 m. The allowable design strain ε is considered to be 7%. For $\varepsilon = 7\%$, $\Omega = 0.84$ and $y/(2r) = 0.164$ according to Giroud et al. [8]. Thus, the normal pressure $p(y)$ in Eq.(8) and tensile load T_r in Eq.(4) can be determined. The method presented by Giroud et al. [8] is conservative when the overlying waste thickness is less than about 42 m. However, it will significantly underestimate the value of T_r when the overlying waste thickness is larger than 42 m. This is because that the method in Giroud et al. [8] cannot consider the displacement-related vertical earth pressure, and it underestimates this value when a large overlying waste thickness is needed. For the Suzhou expanded landfill ($H = 40$ m), the calculated tensile load in the geosynthetic liner is 12.2 kN/m by the method of Giroud et al. [8]. Considering the reduction factor RF_{CR} accounting for creep of geosynthetic liner ($RF_{CR} = 2.5$), RF_{ID} accounting for installation damage ($RF_{ID} = 1.5$), and RF_{CBD} accounting for chemical and biological degradation ($RF_{CBD} = 1.2$), the long-term allowable design tensile load is 54.9 kN/m. If the considered void radius is 1.2 m, the value will be about 100 kN/m. Therefore, two layers of the geogrids with high strength would be needed to satisfy the design requirement.

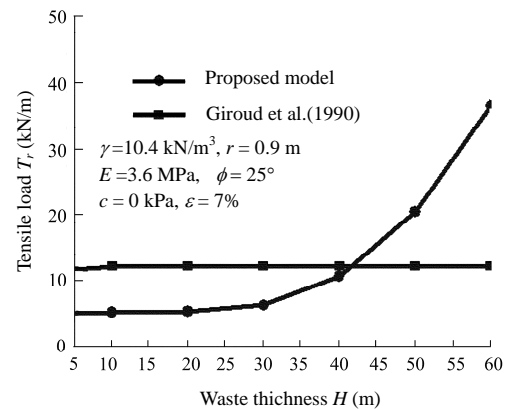


Fig.12 Comparison of tensile load of geosynthetic liner calculated by different methods.

2.3 Differential settlement around gas venting wells

When vertical gas venting wells are constructed in a landfill expansion, the integrity of the GM in the composite liner system connected with the rigid well structures should be of concern due to differential settlement. Giroud and Soderman [3] analyzed the tension and strain in a large-scale GM connected to long rigid structures. This work provides critical information to guide the construction of rigid structures

connected to GMs. However, the problems presented by Giroud and Soderman [3] were posed as 2D plane strain problems. A solution to the three-dimensional (3D) problem is still needed.

To analyze tension and strain in a GM around a circular structure subjected to differential settlement, a simplified model based on conventional membrane theory is considered [13]. As shown in Fig.13, the surface of the medium supporting the GM is assumed to be horizontal with the GM uniformly loaded by a vertical pressure p . The GM deforms sufficiently to remain completely in contact with the circular rigid structure. Thus, the total elongation of the GM in the radial direction is equal to the differential settlement s . The tension-strain curve for the GM is assumed to be linear. The radial strain ε_r in the geomembrane can be calculated by the following equations:

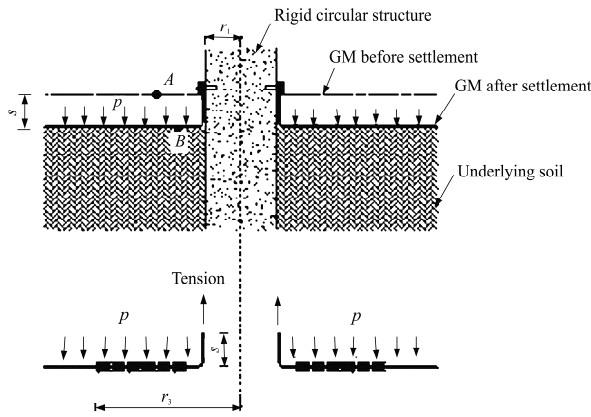


Fig.13 GM subjected to differential settlement around a circular structure.

$$\varepsilon_r = \frac{a}{6r^2} (r_3'^3 + 3r^2 r_3' - 4r'^3) \quad (9)$$

$$r_3 = \sqrt[3]{A + \sqrt{B}} + \sqrt[3]{A - \sqrt{B}} \quad (10)$$

$$a = \frac{p(\tan \phi_1 + \tan \phi_2)(1 - \nu^2)}{E_t} \quad (11)$$

$$A = \frac{3sr_1}{a} - r_1^3 \quad (12)$$

$$B = \frac{9s^2 r_1^2}{a^2} - \frac{6sr_1^4}{a} \quad (13)$$

where r' is the radial distance from the center of the GM, r_3 is the outer radius of the deformed region in the GM, r_1 is the radius of the gas venting well, ϕ_1 is the interface friction angle between the GM and the overlying medium, ϕ_2 is the interface friction angle between the GM and the underlying medium, and E_t is the tensile stiffness of the GM.

Three kinds of GMs (0.75 mm polyvinylchloride (PVC), 1 mm linear low density polyethylene (LLDPE) and 0.75 mm high density polyethylene (HDPE)) were selected for the analysis. Their tensile stiffnesses E_t are 76, 170, and 540 kN/m, respectively. The other properties used in the calculation are: $\nu = 0.45$, $r_1 = 0.5$ m, $p = 100$ kPa, $\phi_1 = \phi_2 = 10^\circ$. As shown in Fig.14, the stiffness of the GM can greatly influence the maximum tensile strain ε_{\max} in GMs that happens at the edges of gas venting wells. The stiffer the GM is, the smaller the ε_{\max} is. The calculated ε_{\max} is much larger than those calculated by the equations presented by Giroud and Soderman [3], in which a GM was connected to a rigid structure. The value of ε_{\max} increases rapidly with an increase in differential settlement.

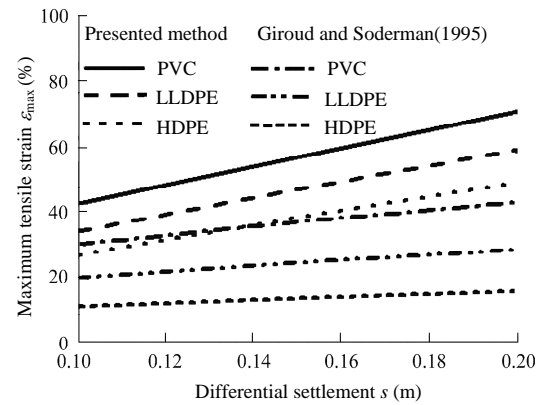


Fig.14 Effects of differential settlement on the maximum strain in GM.

3 Tensile tests and design criteria for geosynthetic liner systems

The allowable strain in geosynthetic materials $\varepsilon_{\text{allow}}$ can be evaluated by wide-width tension tests (e.g. yield strain divided by a factor of safety). Figure 15 shows the behavior of axial tensile strength versus axial strain for some geosynthetic materials from our tests. It can be seen that the curves for the HDPE and LLDPE GMs show a pronounced yield point. According to Koerner [14], the initial response of a geosynthetic clay layer (GCL) is greatly influenced by the woven slit film geotextiles (GTs) that take the load until this component fails, and thereafter, the curve shows a distinct reduction in strength. The curve then rises gradually because the non-woven geotextile again takes the load until its ultimate failure. The tensile strength curve for the geogrid is steepest initially; however, brittle rupture happens when the axial strain is only 12%.

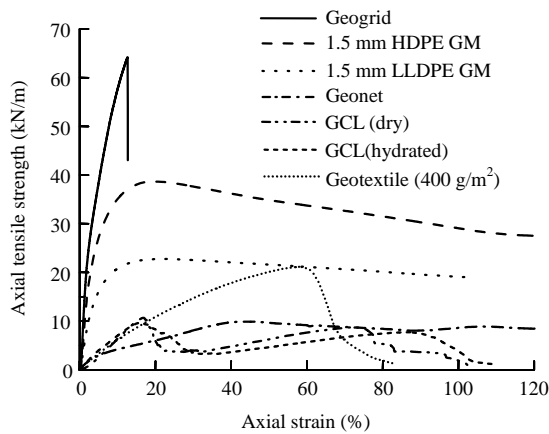


Fig.15 Tensile strength-strain behavior of geosynthetic materials.

The safe design of a landfill liner system requires that the maximum tensile strain be lower than the allowable tensile strain of the geosynthetic materials used, especially for the sealing materials such as GMs and GCLs:

$$\varepsilon_{\max} \leq \varepsilon_{\text{allow}} \quad (14)$$

According to Qian et al. [5], the allowable tensile strain of a compacted clay layer (CCL) is usually less than 1%, and that of a GCL is 6%–20%. Thus, it is likely that the effectiveness of a CCL as a hydraulic barrier would not be appropriate for a vertically expanded landfill, and the GCL should be considered as an alternative. With respect to the GM component of the composite liner systems, two GMs (HDPE and LLDPE) were considered. However, HDPE has a much larger potential for stress cracking (brittle fracture under a constant stress less than the yield stress or break stress of the material) and lower allowable strain than LLDPE [15, 16]. Peggs et al. [16] presented some general guidance for the maximum allowable strains of GMs, with values ranging from 4% to 8% for HDPE and 8% to 12% for LLDPE. Thus, a textured LLDPE combined with GCL is recommended to serve as the sealing materials for the composite liner system in the Suzhou landfill.

4 Practical measures

As shown in Fig.7, the maximum tensile strain resulting from the overall settlement and lateral deformation of the existing landfill is lower than the allowable tensile strain of LLDPE and GCL. Thus, it will not cause tensile damage to the LLDPE and GCL in the proposed composite liner system. However, the inclination of the leachate drainage layer above the composite liner will be altered due to the overall settlement of the existing landfill. If the slope direction

of the leachate drainage layer was reversed, a large amount of leachate would stay in the composite liner system. The potential for infiltration of the leachate into the existing landfill would increase. Thus, practical measures need to be taken, which may involve adjusting the thickness of the base backfill under the composite liner system (e.g. increasing the backfill thickness at locations where settlement is anticipated to be greater). The inclination of the leachate drainage layer should be set to at least 2% after the settlement of the existing landfill is completed.

As shown in Fig.8, geogrid reinforcement is a commonly used technique for mitigating local subsidence in an existing landfill. Measures for stabilizing existing refuse before the construction of a composite liner system can include: preloading with excess mass, deep dynamic compaction, and lime/fly ash slurry injection. Jang et al. [4] stated that placing controlled fill (soil or waste) above an existing landfill is a feasible and economical method to protect a non-reinforced liner system from the impact of local subsidence. It can provide a thick buffer or a strain-transition zone. As shown in Fig.16, the proposed composite liner system for the Suzhou landfill includes a thick bedding layer (acting as a buffer) and two layers of geogrid reinforcement, which are expected to effectively reduce the strain in the geosynthetic liners resulting from local subsidence.

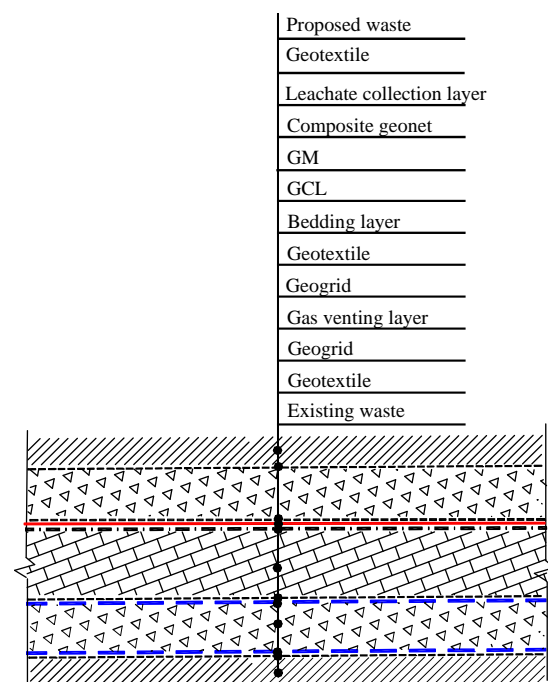


Fig.16 Illustration of the composite liner system in the Suzhou landfill expansion.

As shown in Fig.14, the calculated strain has exceeded the allowable strain of LLDPE, even when the differential settlement is only 0.1 m. Therefore, special attention needs to be paid to the behavior of the GM around the gas venting wells where differential settlements are the most significant. According to Giroud and Soderman [3], battering the walls of rigid structures was an effective solution to the problem, which created a progressive transition of settlement between the compressed medium (waste) and the structure. However, constructing a battered gas venting well may be difficult or expensive. A battered wall may also cause a load transfer from the compressed medium and conflict with the strategy to lubricate the walls of a structure to minimize load transfer as the waste settles. For these reasons, Flex connectors are recommended to connect the GM to the gas venting wells. These connections may consist of a flexible corrugated tube that can compensate for anticipated differential settlement [13].

5 Conclusions

The deformation and integrity of a composite liner under a variety of factors are important issues to be considered in landfill expansion design. Based on a case study, this paper has investigated strain in exemplary geosynthetic materials used in composite liner systems for expanded landfills, with strain resulting from both overall settlement and lateral movement of the existing landfill, local subsidence and differential settlement around gas venting wells. The following conclusions are drawn.

(1) The lateral movement of the existing landfill has a greater effect on the strain in liners than that caused by overall settlement. Significant tensile strain (about 2%) occurs near the anchor trench on the back slope and the shoulder of the front slope of the existing landfill. The tensile strain resulting from lateral movement and overall settlement of the existing landfill is not expected to induce tensile damage in the geosynthetic materials proposed for the composite liner system of the Suzhou landfill.

(2) The vertical earth pressure acting on the geosynthetic liner that is subjected to local subsidence may be larger than the Terzaghi loose earth pressure if the overlying waste is sufficiently thick. The displacement-related earth pressure is recommended for the design of a reinforced composite liner system. The use of a geogrid can reduce the tensile strain due to the local subsidence. A two-layer high-strength geogrid can usually satisfy

the design requirement for the expanded landfills when the thickness of expanded masses is less than 40 m.

(3) Special attention must be paid to the behavior of the GM around gas venting wells where differential settlement can be induced with landfill expansions. Flex connectors are recommended to be used to connect the GM and the gas venting well, which can compensate the effects caused by likely differential settlement in such areas.

References

- [1] Zhan Liangtong, Chen Yunmin, Lin Weian. Shear strength characterization of municipal solid waste at the Suzhou landfill, China. *Engineering Geology*, 2008, 97 (1): 97–111 (in Chinese).
- [2] Technical code for municipal solid waste sanitary landfill (CJJ 17–2004). Beijing: China Architecture and Building Press, 2004 (in Chinese).
- [3] Giroud J P, Soderman K L. Design of structure connected to geomembranes. *Geosynthetic International*, 1995, 2 (3): 379–428.
- [4] Jang D J, Montero C. Design of liner systems under vertical expansions: an alternative a geogrids. In: *Proceeding of Geosynthetics*. Vancouver: Industrial Assoc Int., 1993: 1 487–1 510.
- [5] Qian X D, Koerner R M, Grey D H. *Geotechnical aspects of landfill design and construction*. New Jersey: Prentice Hall Inc., 2001.
- [6] Chen Yunmin, Zhan Liangtong, Wei Haiyun. Aging and compressibility of municipal solid wastes. *Waste Management*, 2009, 29 (1): 86–95.
- [7] Chen Yunmin, Gao Deng, Zhu Bin. Composite exponential stress-strain model of municipal solid waste and its application. *Chinese Journal of Geotechnical Engineering*, 2009, 31 (7): 120–129 (in Chinese).
- [8] Giroud J P, Bonaparte R, Beech J F, et al. Design of soil layer-geosynthetic systems overlying voids. *Geotextiles and Geomembranes*, 1990, 9 (1): 11–50.
- [9] Terzaghi K. *Theoretical soil mechanics*. New York: John Wiley and Son Inc., 1943.
- [10] Mckelvey III J A. The anatomy of soil arching. *Geotextiles and Geomembranes*, 1994, 13 (5): 317–329.
- [11] Handy R L. The arch in soil arching. *Journal of Geotechnical Engineering*, 1985, 113 (3): 302–318.
- [12] Adachi T, Kimura M, Kishida K. Experimental study on the distribution of earth pressure and surface settlement through three-dimensional trapdoor tests. *Tunneling and Underground Space Technology*, 2003, 18 (2): 171–183.
- [13] Zhu Bin, Gao Deng, Chen Yunmin. Geomembrane tensions and strains resulting from differential settlement around rigid circular structures. *Geotextiles and Geomembranes*, 2009, 27 (1): 53–62.
- [14] Koerner R M. *Designing with geosynthetics*. New Jersey: Prentice Hall Inc., 1997.
- [15] Stulgis R P, Soydemir C, Telgener R J, et al. Use of geosynthetic in “piggyback landfills”: a case study. *Geotextiles and Geomembranes*, 1996, 14 (7): 341–364.
- [16] Peggs I D, Schmucker B, Carey P. Assessment of maximum allowable strains in polyethylene and polypropylene geomembranes. In: *Proceedings of the Geo-frontiers 2005 Congress*. Austin: [s.n.], 2005: 24–26.

**APPLICATION FOR PERMIT RENEWAL AND MODIFICATION
SANDOVAL COUNTY LANDFILL**

**VOLUME III: LANDFILL ENGINEERING CALCULATIONS
SECTION 7: GEOSYNTHETICS TENSILE STRESS AND STABILITY ANALYSIS**

ATTACHMENT III.7.E

**GIROUD, J.P., BONAPARTE, R., BEECH, J.F. AND GROSS, B.A.,
DESIGN OF SOIL LAYER-GEOSYNTHETIC SYSTEMS OVERLYING VOIDS,
GEOTEXTILES AND GEOMEMBRANES 9 (1990), PPS 11-50.**

Design of Soil Layer-Geosynthetic Systems Overlying Voids

J. P. Giroud, R. Bonaparte, J. F. Beech & B. A. Gross

GeoServices Inc. Consulting Engineers,
1200 South Federal Highway, Suite 204
Boynton Beach, Florida 33435, USA

ABSTRACT

This paper presents equations, tables, and charts to design soil layer-geosynthetic systems to span voids such as tension cracks, sinkholes, dissolution cavities, and depressions in foundation soils due to differential settlements or localized subsidence. These equations, tables, and charts were developed by combining tensioned membrane theory (for the geosynthetic) with arching theory (for the soil layer), thereby providing a more complete design approach than one that considers tensioned membrane theory only.

Design examples are presented to illustrate the solution of typical problems such as: selection of the required geosynthetic properties, determination of the maximum void size that can be bridged by a given system, and evaluation of the load-bearing capacity of a given system.

NOTATION

b	Width of the infinitely long void (m)
c	Cohesion of the soil (N/m^2)
D	Depth of the void (m)
H	Thickness of the soil layer (m)
K	Coefficient of lateral earth pressure (dimensionless)
K_a	Coefficient of active earth pressure (dimensionless)
p	Pressure on the geosynthetic (i.e. vertical stress at the bottom of the soil layer) over the void area (N/m^2)

p_{lim}	Limit value for the pressure on the geosynthetic, over the void area (N/m^2)
p_b	Pressure transmitted to the bottom of the void (N/m^2)
p_0	Pressure on the geosynthetic over the void area neglecting soil arching (N/m^2)
q	Uniformly distributed normal stress applied on top of the soil layer (N/m^2)
r	Radius of the circular void (m)
r_{max}	Maximum radius of a circular void which can be bridged by a given geosynthetic (m)
s	Soil shear strength (N/m^2)
y	Geosynthetic deflection (m)
z	Depth measured from the top of the soil layer (m)
α	Geosynthetic tension (force per unit width) corresponding to the geosynthetic strain ε (N/m)
α_{lim}	Limit value for the required geosynthetic tension (N/m)
ε	Geosynthetic strain (dimensionless)
γ	Unit weight of soil (N/m^3)
Ω	Factor related to y and ε (dimensionless)
ϕ	Friction angle of the soil (degrees and dimensionless)
σ_H	Horizontal stress at depth z (N/m^2)
σ_V	Vertical stress at depth z (N/m^2)

INTRODUCTION

Description of the Problem

In many practical situations, a load is applied on a soil layer-geosynthetic system that will eventually overlie a void. (In this paper, the term 'void' is used generically for cracks, cavities, depressions, etc.) Two typical examples are a road embankment or a lining system for a reservoir constructed on a foundation where localized subsidence may develop.

The design engineer has to verify that, should subsidence develop, the geosynthetic layer can support the loads applied by the overlying soil and any other source (such as traffic on the road or the liquid in the reservoir) without failing or undergoing excessive deflection. The soil-geosynthetic system deflects over the void, and, from a design standpoint, three possibilities must be considered:

- The geosynthetic fails (Fig. 1(a)).

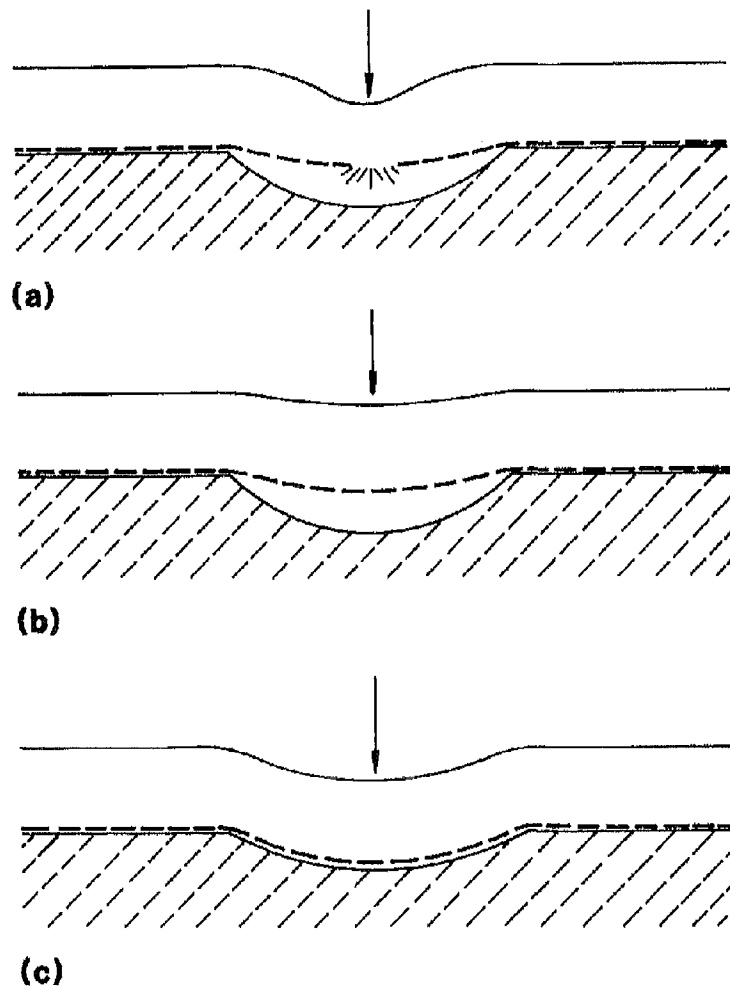


Fig. 1. Three design situations: (a) the geosynthetic fails; (b) the geosynthetic undergoes limited deflection and bridges the void; and (c) the geosynthetic deflects until it comes in contact with the bottom of the void.

- The geosynthetic undergoes limited deflection and bridges the void (Fig. 1(b)).
- The geosynthetic deflects until it comes in contact with the bottom of the void (Fig. 1(c)).

The Nature of Voids

Examples of voids that can develop under a geosynthetic are discussed below:

Tension Cracks

Such cracks can occur in non-saturated cohesive soils subjected to tensile stresses and/or differential movements caused by settlement or other



Fig. 2. Large tension crack formed under a geomembrane liner.

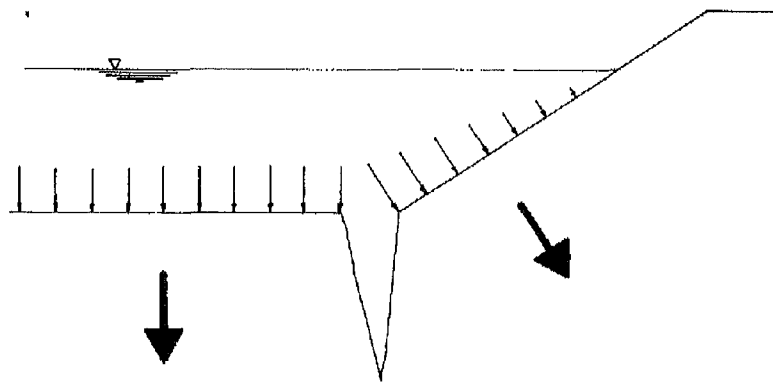


Fig. 3. Mechanism of tension crack formation at the toe of the side slope of a reservoir (not to scale). (After Loudière and Perrin.¹)

mechanisms. A case has been reported¹ where very large cracks (0.1–0.3 m wide) developed in the cohesive soil located under the geomembrane liner of a reservoir (Fig. 2). The cracks occurred near the toe of the side slopes of the reservoir. In this area, tensile stresses and differential movements resulted from the different water pressure orientations on the bottom and on the slopes, as shown in Fig. 3.

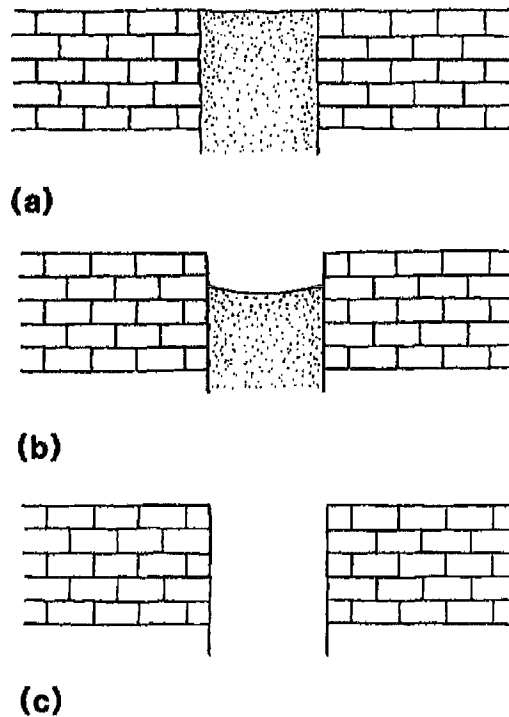


Fig. 4. Sinkhole in a karstic limestone mass: (a) before collapse; (b) after partial collapse; and (c) after complete collapse.

Fissures and Cracks in Bedrock

Soil layers or masses are sometimes constructed on a bedrock with fissures or cracks. A rare but important case is the construction of the clay core of a dam on a bedrock where cracks may develop. Some dam failures have resulted from this situation.

Sinkholes due to Karstic Collapse

Karstic limestone masses contain pockets or chimneys filled with soil. Water or other liquids seeping through a karstic limestone mass may remove soil from these pockets or chimneys, thereby creating a void which can be on the order of one to several meters in diameter (Fig. 4). These voids are usually referred to as sinkholes. The bursting of a geomembrane liner installed on a mass of karstic limestone which subsequently collapsed has been described by Giroud and Goldstein² and Giroud.³ Karstic collapses can occur under other types of structures, such as road embankments, as discussed by Bonaparte and Berg.⁴

Soil Dissolution

Dissolution cavities can be caused by water in soils containing gypsum or by acid in soils containing calcium carbonate. The senior author has

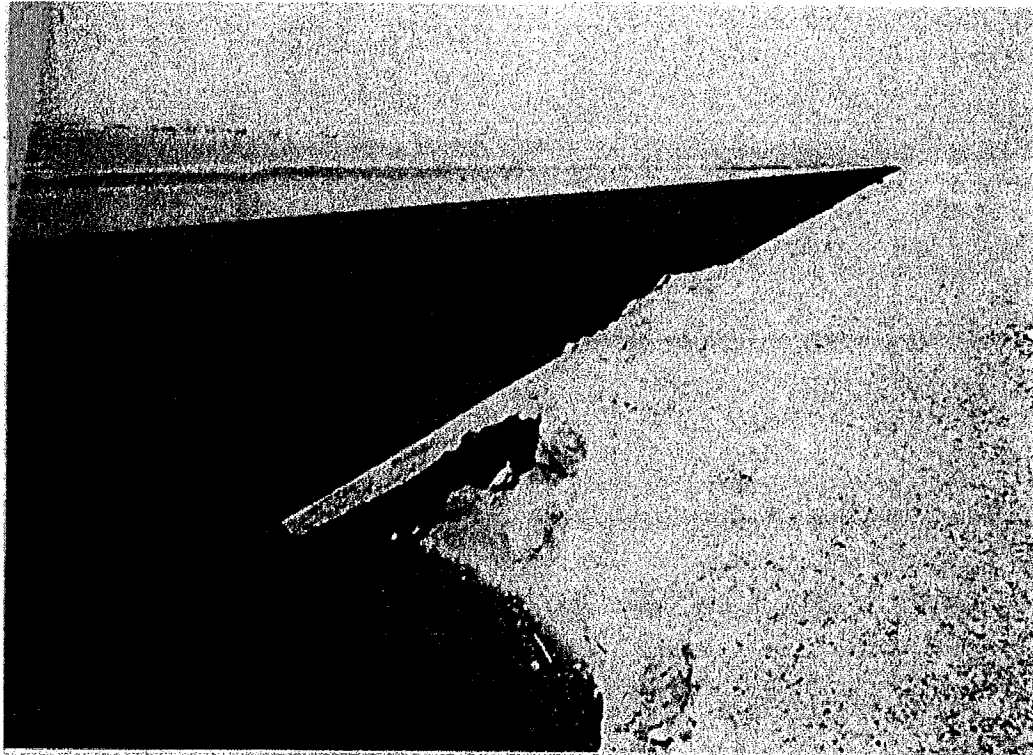


Fig. 5. Dissolution Cavity. This cavity in high gypsum content soil was caused by water leaking through a concrete canal liner.

observed cavities about one meter deep and one meter wide caused by: (i) water leaking through the concrete liner of canals constructed in soils with a high gypsum content (Fig. 5); and (ii) phosphoric acid leaking through a faulty seam of the geomembrane liner of a reservoir constructed on a high calcium-carbonate content soil (Fig. 6).⁵

Differential Settlement

Depressions in the ground surface may be formed when a localized area settles more than the rest ('differential settlement'). There are many situations where depressions result from differential settlement. These include depressions resulting from: (i) differential settlement of municipal solid waste (resulting from the heterogeneity of the waste) affecting a geosynthetic-soil cover system placed on the waste; (ii) settlement of a

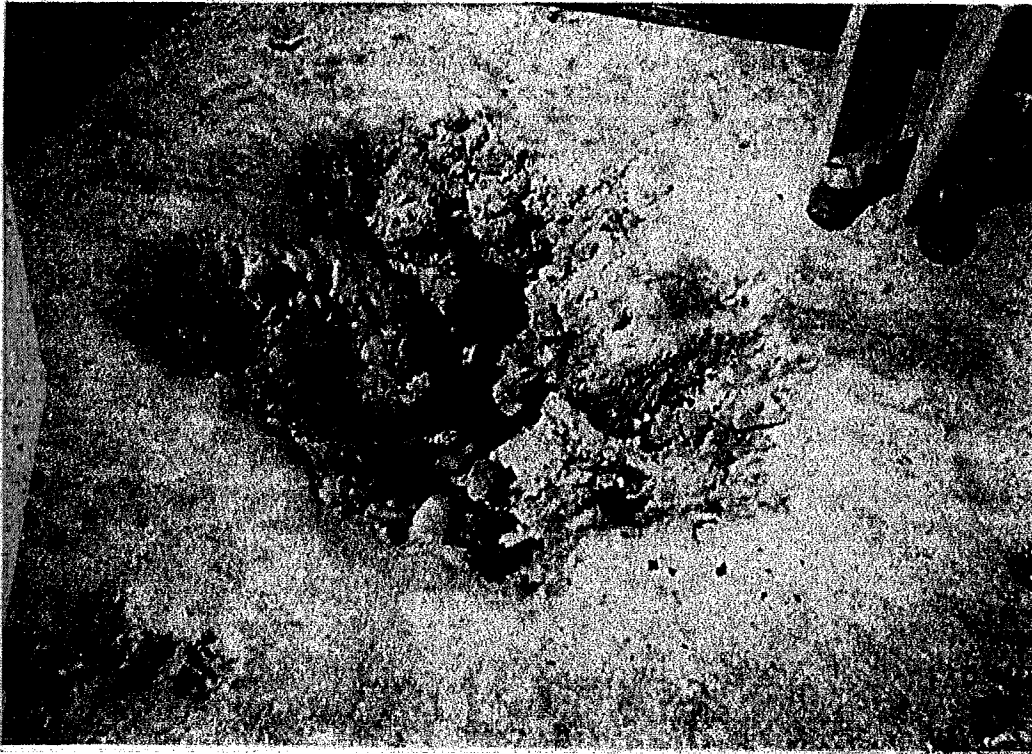


Fig. 6. Dissolution Cavity. This cavity in high calcium-carbonate content soil was caused by phosphoric acid leaking through a geomembrane liner.

localized lens of compressible soil; (iii) thawing of subsurface ice lenses; and (iv) settlement of a poorly compacted trench backfill. Tisserand⁶ has reported a case of geomembrane failure over the depression resulting from trench backfill settlement. Differential settlement due to lenses of compressible soils frequently occur under road embankments.

Localized Subsidence

The surface of the ground may be locally depressed as a result of the collapse of underground cavities such as: natural caves, tunnels, mine workings, pipes, and tanks. Localized subsidence may also occur at the surface of municipal solid waste as a result of the collapse of deteriorating structures such as refrigerators.

Classification of Voids

Two shapes of voids are considered in the study presented in this paper: infinitely long voids with a width b and circular voids with a diameter $2r$. The voids presented above can therefore be put into two categories:

- Cracks and depressions resulting from trench backfill settlement may be modeled approximately as an infinitely long void.
- Karstic sinkholes, dissolution cavities, municipal solid waste settlement, lens settlement, soil surface depressions and ground subsidence may be modeled approximately as a circular void.

In the case of cracks and complete karstic collapse (Fig. 4(c)), the geosynthetic deflects without reaching the bottom of the void. With the other types of voids, the geosynthetic may or may not reach the bottom of the void, depending on the geometry of the void, the modulus of the geosynthetic and the applied loads.

Load-Carrying Mechanism

The soil layer and underlying geosynthetic are assumed initially to be resting on a firm foundation. At some point in time, a void of a certain size opens below the geosynthetic. Under the weight of the soil layer and any applied loads, the geosynthetic deflects. The deflection has two effects; *bending* of the soil layer and *stretching* of the geosynthetic.

The *bending* of the soil layer generates arching inside the soil, which transfers part of the applied load away from the void area, as shown in Fig. 7. As a result, the vertical stress, σ_v , over the void area is smaller than the average vertical stress, $\gamma H + q$, due to the weight of a soil layer of thickness H and an applied uniform normal stress of magnitude q .

The *stretching* of the geosynthetic mobilizes a portion of the geosynthetic's strength. Consequently, the geosynthetic acts as a 'tensioned membrane' and can carry a load applied normally to its surface. As a result of geosynthetic stretching, two cases can be considered:

- In the first case, the stretched geosynthetic comes in contact with the bottom of the void. The mobilized portion of the geosynthetic strength carries a portion of the load applied normal to the surface of the geosynthetic. The rest of the load is transmitted to the bottom of the void.
- In the second case, the geosynthetic does not deflect enough to come in contact with the bottom of the void. In this case, either the geosynthetic is strong enough to support the entire load applied normal to its surface or it fails.

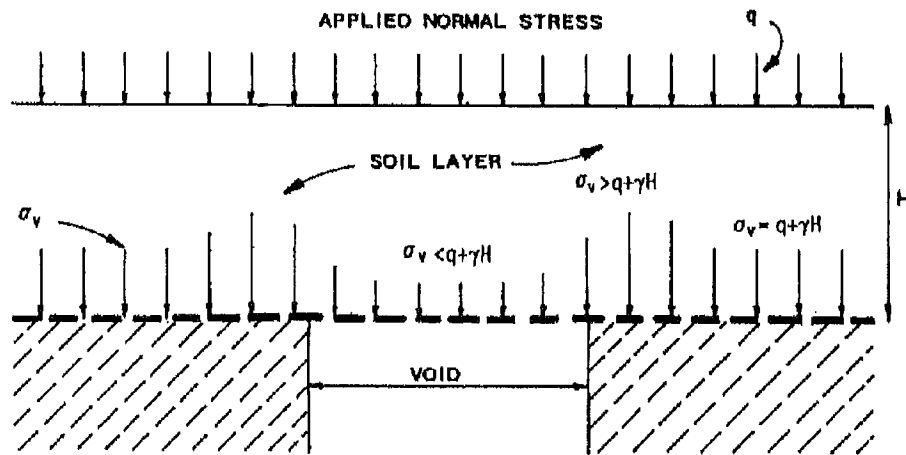


Fig. 7. Effect of soil arching on load distribution.

In summary, the soil-geosynthetic system deflects and the geosynthetic stretches until it fails (Fig. 1(a)) or until an equilibrium condition is reached (Fig. 1(b) or 1(c)).

Scope of this Paper

This paper presents the development and use of equations, tables, and charts for the case of a soil layer subjected to a uniformly distributed normal load and resting on a geosynthetic overlying a rigid foundation containing a single infinitely long void (plane-strain problem) or circular void (axisymmetric problem). The parameters considered in this paper are:

- **Geometric Parameters:** These include the thickness of the soil layer and the geometry of the void (width of an infinitely long void or diameter of a circular void, and depth of void) (Fig. 8).
- **Mechanical Parameters:** These include the soil mechanical properties and the geosynthetic tensile behavior (expressed by its tension-strain curve).
- **Loading Conditions:** These include the unit weight of the soil layer and the load exerted on the top of the soil layer, which is assumed to be normal and uniformly distributed.

The equations, tables, and charts make it possible to solve design problems such as:

- select the required geosynthetic mechanical properties when the geometric parameters and the loading conditions are known;

- determine the required thickness of the soil layer associated with a given geosynthetic over a given void and subjected to given loading conditions;
- determine the void size that a given geosynthetic may bridge when it is associated with a given soil layer subjected to given loading conditions; and
- determine the maximum load which can be carried by a given soil-geosynthetic system over a given void.

The solution of any of the above design problems depends on the allowable geosynthetic strain.

Originality of this Paper

The use of tensioned membrane theory to evaluate the load-carrying capacity of a geosynthetic bridging a void was presented by Giroud.⁷ Subsequently, Giroud⁸ developed a design chart based on tensioned membrane theory. This chart has often been used to evaluate the load-carrying capacity of a soil layer associated with a geosynthetic. By doing so, the internal shear strength of the soil layer is neglected, and this can be very conservative. Therefore, Bonaparte and Berg⁴ combined arching theory (for the soil layer) with tensioned membrane theory (for the geosynthetic) to formulate a more complete design approach.

This paper significantly extends the earlier work of Giroud^{7,8} and Bonaparte and Berg⁴ and provides an extensive analysis of soil-geosynthetic system bridging a void.

ANALYSIS

Assumptions

The void can be either circular (diameter $2r$) or infinitely long (width b). Regarding the bottom of the void, two cases can be considered: (i) a bottomless void (Fig. 8(a)); and (ii) a bottom with a maximum depth D and a spherical shape (for the circular void) or a cylindrical shape with a circular cross section (for the infinite void) (Fig. 8(b)). From a design standpoint, both cases are identical if the deflection y of the geosynthetic is less than the depth of D of the void.

The soil layer is assumed to be horizontal and to have a uniform thickness H . The stress q applied on the soil layer is assumed to be normal and uniformly distributed.

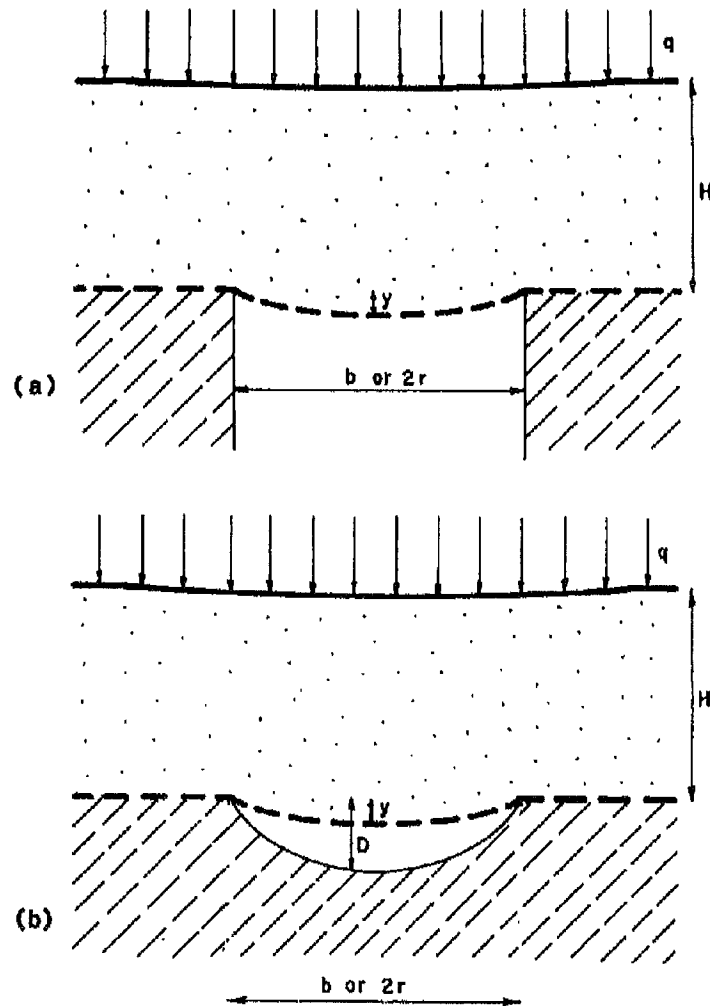


Fig. 8. Schematic cross section for theoretical analysis. Two cases can be considered: (a) the void is bottomless; and (b) the bottom of the void is assumed to have a circular cross section and the depth of the void is D . The void located under the geosynthetic is either infinitely long (with a width b), or circular (with a diameter $2r$); y is the geosynthetic deflection.

Relevant geosynthetic properties are the tension-strain curve or, at least, the tension α corresponding to the design strain ϵ .

Relevant soil properties are the friction angle ϕ and the cohesion c . For the analysis presented in this paper, the cohesion is neglected. In other words, the charts are established for $c = 0$ and can be conservatively used for $c > 0$. Also, it will be shown that the friction angle ϕ does not have a significant influence on the analysis results if it is equal to or greater than 20° .

Approach

The problem under consideration involves a complex soil-geosynthetic interaction. The problem can be greatly simplified, however, if the soil response (arching) is uncoupled from the geosynthetic response (tensioned membrane). Therefore, a two-step approach is used. First, the behavior of the soil layer is analyzed using classical *arching theory*. This step gives the pressure at the base of the soil layer on the portion of the geosynthetic located above the void. Second, *tensioned membrane theory* is used to establish a relationship between the pressure on the geosynthetic, the tension and strain in the geosynthetic, and the deflection of the geosynthetic. Accordingly, the following sections deal with arching theory, tensioned membrane theory, and the combination of both.

An inherent assumption in this uncoupled two-step approach is that the soil deformation required to generate the soil arch is compatible with the tensile strain required to mobilize the geosynthetic tension. This assumption has not been verified.

Arching Theory (see Fig. 9)

When the geosynthetic deflects, arching develops in the soil layer. As a result, a portion of the applied stress is transmitted laterally and, consequently, the normal stress transmitted to the portion of the geosynthetic located above the void is smaller than the average vertical stress due to the weight of the soil layer and the uniformly distributed normal stress applied on top of the soil layer (Fig. 7). The procedures for calculating the reduced

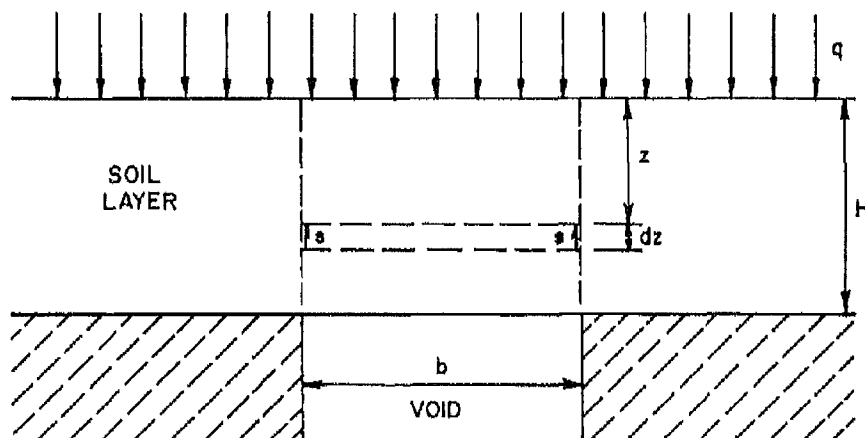


Fig. 9. Derivation of arching equation.

stress transmitted to the portion of the geosynthetic located above the void are presented below for an infinitely long void and a circular void.

Infinitely Long Void

Terzaghi⁹ has established equations for soil arching over an infinitely long void assuming that the lateral load transfer is achieved through shear stresses along vertical planes located at the edges of the void (Fig. 9). As a result of this assumption, the incremental change in vertical stress, $d\sigma_v$, due to an incremental change in depth, dz , is given by

$$d\sigma_v = [\gamma - 2(s/b)]dz \quad (1)$$

where: b = width of the infinitely long void; σ_v = vertical stress at depth z ; γ = unit weight of soil; z = depth measured from the top of the soil layer; and s = soil shear strength. Basic SI units are: b (m), σ_v (N/m²), γ (N/m³), z (m), and s (N/m²).

The soil shear strength along a vertical plane is expressed by

$$s = c + \sigma_H \tan \phi \quad (2)$$

where: c = cohesion of the soil; σ_H = horizontal stress at depth z ; and ϕ = friction angle of the soil. Basic SI units are: s (N/m²), c (N/m²), σ_H (N/m²), and ϕ (degrees); ϕ is dimensionless.

The relationship between the horizontal stress and the vertical stress is given by the following classical relationship

$$\sigma_H = K\sigma_v \quad (3)$$

where: K = coefficient of lateral earth pressure (dimensionless).

It should be noted that many of the relationships presented in this paper are valid for both effective and total stress conditions; however, eqn (3) is valid only for effective stress conditions.

Combining eqns (1), (2) and (3) and solving the differential equation for the boundary condition $\sigma_v = q$ for $z = 0$ gives

$$\sigma_v = \frac{b(\gamma - 2c/b)}{2K \tan \phi} [1 - e^{-K \tan \phi (2z/b)}] + q e^{-K \tan \phi (2z/b)} \quad (4)$$

where: q = uniformly distributed normal stress applied on the top of the soil layer (basic SI unit: N/m²); all other notations as defined above and in the Notations section.

The pressure on top of the geosynthetic, over the void area, p , is the

value of σ_v for $z = H$ in eqn (4). If the soil cohesion, c , is assumed to equal zero, the value of p is

$$p = \frac{\gamma b}{2K \tan \phi} [1 - e^{-2K \tan \phi H/b}] + q e^{-2K \tan \phi H/b} \quad (5)$$

where: p = pressure on top of the geosynthetic (i.e. vertical stress at the bottom of the soil layer), over the void area (basic SI unit: N/m²); and other notations as defined above and in the Notations section.

Circular Void

Using the same approach, Kezdi¹⁰ has established that eqn (5) can be used for a circular void if b is replaced by r (and not by $2r$), which shows that arching is twice as significant for a circular void compared to an infinitely long void.

Practical Approximate Equations

Selection of the value of the coefficient of lateral earth pressure is not easy since the state of stress of the soil in the zone where arching develops is not fully understood. Handy¹¹ has made a thorough analysis of soil arching and proposed the following value

$$K = 1.06(\cos^2 \theta + K_a \sin^2 \theta) \quad (6)$$

with

$$\theta = 45^\circ + \phi/2 \quad (7)$$

and

$$K_a = \tan^2(45^\circ - \phi/2) \quad (8)$$

where: K_a = coefficient of active earth pressure (dimensionless); and other notations as defined above and in the Notations section.

Another approach would consist of using the coefficient of earth pressure at rest, expressed as follows, according to Jaky¹²

$$K = 1 - \sin \phi \quad (9)$$

In eqn (5), K is multiplied by $\tan \phi$. Values of $K \tan \phi$, calculated using eqns (6) and (9), are given in Table 1. It appears that $K \tan \phi$ does not vary significantly with ϕ , if ϕ is equal to or greater than 20° , which is the case for virtually all granular soils and for many fine-grained soils under drained conditions. Therefore, a constant value of 0.25 can be used for $K \tan \phi$ when ϕ is equal to or greater than 20° . As a result, eqn (5) becomes

$$p = 2\gamma b(1 - e^{-0.5H/b}) + q e^{-0.5H/b} \quad (10)$$

TABLE 1
Values of $K \tan \phi$

Soil friction angle (ϕ , degrees)	Values of $K \tan \phi$	
	Using K from Handy (eqn (6))	Using K from Jaky (eqn (9))
0	0	0
5	0.08	0.08
10	0.15	0.15
15	0.21	0.20
20	0.25	0.24
25	0.29	0.27
30	0.31	0.29
35	0.32	0.30
40	0.32	0.30
45	0.31	0.29
50	0.30	0.28
55	0.27	0.26

Two values of K , the coefficient of lateral earth pressure, are considered: the value proposed by Handy¹¹ for arching and the value proposed by Jaky¹² for the 'at rest' state of stress.

Like eqn (5), eqn (10) is also valid for the circular void if b is replaced by r .

Equation 10 was used to establish Tables 3 and 4, and the charts given in Figs 11 and 14.

Comment on the Validity of Arching Theory

The analysis presented above is the classical analysis by Terzaghi.⁹ This analysis does not consider soil dilatancy, which can increase the horizontal stress in the soil, thereby increasing the ability of the soil to arch. Therefore, the analysis presented in this paper can be considered conservative from this viewpoint. On the other hand, the analysis may not be conservative for loose soils that tend to contract when sheared.

Tensioned Membrane Theory

The tensioned membrane theory has been used by Giroud^{3,7} to deal with the case of a geosynthetic overlying a void and subjected to a uniformly distributed stress normal to its surface.

The equations given below have been established with the following assumptions: (i) the strain in the portion of the geosynthetic overlying the

void (i.e. the deflected portion of the geosynthetic) is uniformly distributed; and (ii) the strain in the portion of the geosynthetic outside the void area is zero and, therefore, that portion of the geosynthetic does not move (i.e. the geosynthetic does not slide toward the void). These two assumptions greatly simplify the analysis, but no attempt has been made to evaluate their range of validity.

Infinitely Long Void

In the case of an infinitely long void, the deflected shape of the geosynthetic across the width of the void is cylindrical with a circular cross section, the strain is uniform, and the following relationships exist

$$1 + \varepsilon = 2\Omega \sin^{-1}[1/(2\Omega)] \quad (\text{valid if } y/b \leq 0.5) \quad (11)$$

$$1 + \varepsilon = 2\Omega\{\pi - \sin^{-1}[1/(2\Omega)]\} \quad (\text{valid if } y/b \geq 0.5) \quad (12)$$

where: ε = geosynthetic strain; y = geosynthetic deflection; b = width of the infinitely long void; and Ω = dimensionless factor. Basic SI units are: $y(\text{m})$ and $b(\text{m})$; ε and Ω are dimensionless.

The dimensionless factor Ω is defined by

$$\Omega = (1/4)[2y/b + b/(2y)] \quad (13)$$

As a result of eqns (11), (12) and (13), there is a unique relationship between y/b , ε and Ω , which is given in Table 2 and shown in Fig. 10.

It is interesting to note that as ε tends towards zero eqn (11) tends toward

$$\Omega = 1/\sqrt{24\varepsilon} \quad (14)$$

This equation gives a good approximation of Ω when ε is less than 1% (see Fig. 10).

Giroud^{3,7} has also shown that the tension in the geosynthetic, in the case of an infinitely long void, is given by

$$\alpha = pb\Omega \quad (15)$$

where: α = geosynthetic tension; p = pressure on the geosynthetic over the void area (i.e. vertical stress at the bottom of the soil layer over the void area); b = width of the infinitely long void; Ω = dimensionless factor

this paper should use appropriate factors of safety. The factor of safety can be applied to the geosynthetic tension or the applied loads, with application to the geosynthetic tension being more common. The factor of safety should not be applied to the soil shear strength (as is commonly the case in geotechnical problems) due to the insensitivity of the arching theory results (eqn (5)) to the soil shear strength.

Determination of Required Geosynthetic Properties

The relevant equation for an infinitely long void is

$$\alpha/\Omega = pb = 2\gamma b^2(1 - e^{-0.5H/b}) + qb e^{-0.5H/b} \quad (16)$$

Equation (16) can be rewritten in a dimensionless form as follows:

$$\frac{\alpha}{\gamma b^2 \Omega} = \frac{p}{\gamma b} = 2(1 - e^{-0.5H/b}) + \frac{q}{\gamma b} e^{-0.5H/b} \quad (17)$$

Equations (16) and (17) can be used for a circular void if b is replaced by r . Equation (17) was used to establish the chart in Fig. 11.

The above equations can be used to solve problems that consist of determining the required geosynthetic tension, α , for a given strain, ϵ , when all other parameters are given (b or r , q , H , and γ). Alternatively, the chart given in Fig. 11 and the corresponding Table 3 can be used.

Example 1. The bedding soil supporting a geomembrane liner is placed on a geosynthetic reinforcement resting on a soil where karstic sinkholes may develop (Fig. 12). The function of the geosynthetic reinforcement is to support the bedding soil and the geomembrane liner should a sinkhole develop. The thickness of the bedding soil layer is 0.45 m and the depth of water on the geomembrane when the reservoir is full is 9 m. The unit weight of the bedding soil is 19,600 N/m³. A deep sinkhole with a radius of 0.75 m is assumed for design purposes. Since the function of the geosynthetic reinforcement is only to act as a 'safety net', a rather large geosynthetic reinforcement strain is acceptable: $\epsilon = 10\%$. What is the required geosynthetic reinforcement tensile strength?

First, the applied stress, q , is calculated

$$q = 1000 \times 9.81 \times 9 = 88\,290 \text{ N/m}^2$$

Then, eqn (16) is used as follows, with $H/r = 0.45/0.75 = 0.6$

$$\alpha/\Omega = 2 \times 19\,600 \times (0.75)^2 (1 - e^{-0.3}) + 88\,290 \times 0.75 e^{-0.3}$$

$$\alpha/\Omega = 54\,395 \text{ N/m}$$

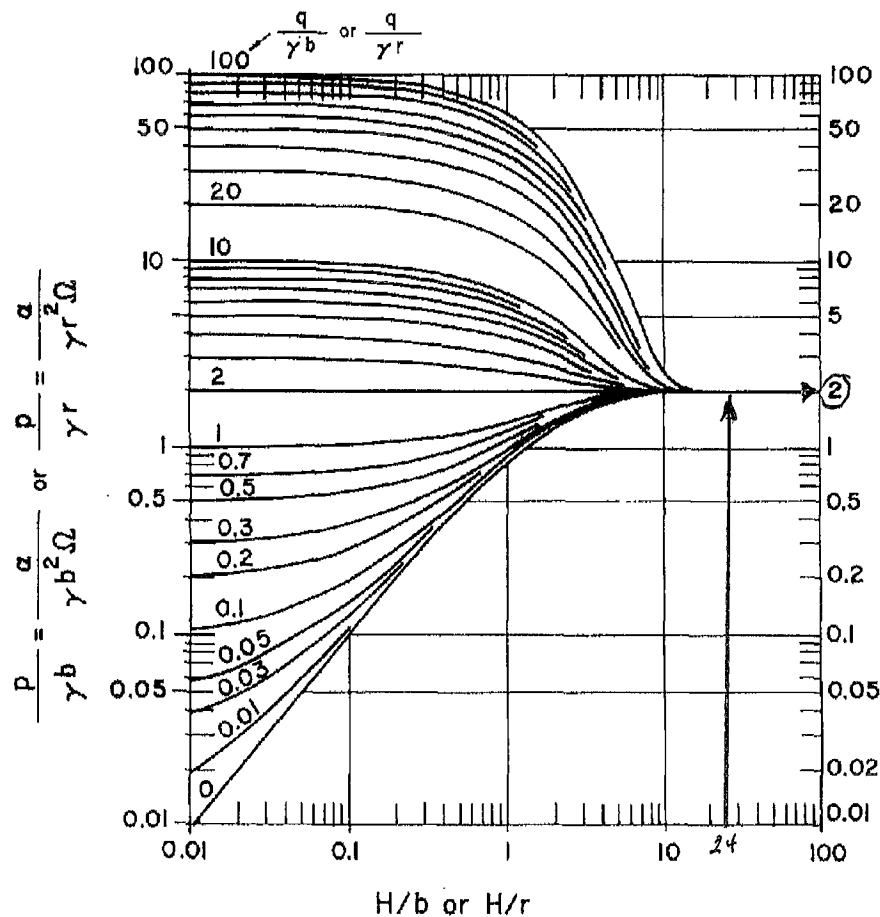


Fig. 11. Pressure on and tension in the geosynthetic. An example of use of this chart is given in Fig. 13. Notations: p = pressure on the geosynthetic over the void area; q = uniformly distributed normal stress applied on the top of the soil layer; H = thickness of the soil layer; γ = unit weight of soil; b = width of the infinitely long void; r = radius of the circular void; α = geosynthetic tension; and Ω = dimensionless factor given in Table 2 and Fig. 10. (Values of $p/(\gamma b)$ or $p/(\gamma r)$ used to draw the curves in this figure can be found in Table 3.)

Finally, according to Table 2 or Fig. 10, $\Omega = 0.73$ for $\varepsilon = 10\%$. Therefore, the required value of the geosynthetic tension at a 10% strain is:

$$\alpha = 0.73 \times 54\,395 = 39\,708 \text{ N/m} = 40 \text{ kN/m}$$

The same problem can be solved using the tables and charts with

$$H/r = 0.45/0.75 = 0.6 \text{ and}$$

$$q/(\gamma r) = 88\,290/(19\,600 \times 0.75) = 6.0$$

Table 3 or the chart given in Fig. 11 (see also Fig. 13) gives:

$$\alpha/(\gamma r^2 \Omega) = 4.963 \text{ hence}$$

$$\alpha = (4.963) \times 19\,600 \times (0.75)^2 \times 0.73 = 39\,943 \text{ N/m} = 40 \text{ kN/m}$$

It is interesting to compare the required geosynthetic reinforcement tension calculated above to that required if the bedding soil is a layer of compacted clay associated with the geomembrane to form a composite liner. In this case, it is important that the integrity of the clay layer be maintained. Therefore, the geosynthetic reinforcement strain must be small enough to prevent the development of tension cracks in the clay layer. Calculations similar to the above, with $\varepsilon = 1\%$ instead of 10% , give a required geosynthetic reinforcement tension of 113 kN/m , which is about three times greater than 40 kN/m . Therefore, the geosynthetic reinforcement required in the case of a 1% allowable strain has a tension about three times greater, and consequently a modulus about 30 times greater, than in the case of a 10% allowable strain. (Several layers of a very high-modulus geotextile would probably be needed.)

Determination of Required Soil Layer Thickness

The relevant equation for an infinitely long void is

$$H = 2b \ln \frac{[q/(\gamma b)] - 2}{[\alpha/(\gamma b^2 \Omega)] - 2} \quad (18)$$

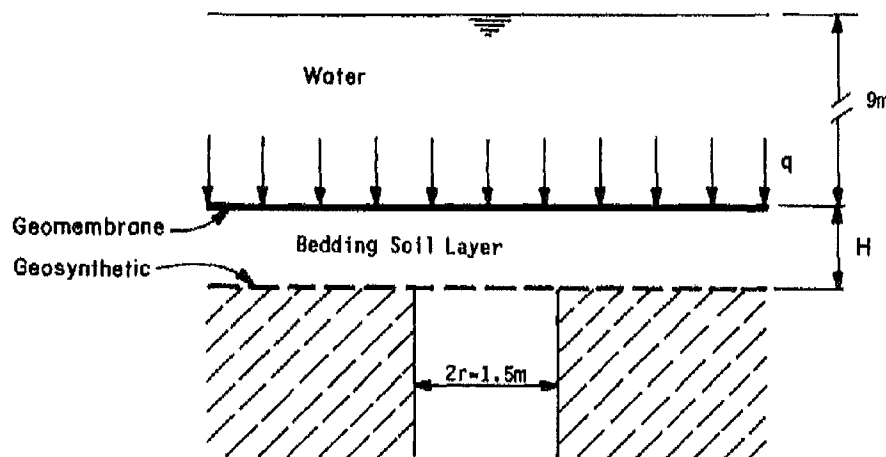


Fig. 12. Cross section for design examples.

TABLE 3
Pressure on the Geosynthetic

$q/(\gamma b)$ or $q/(\gamma r)$	H/b or H/r													
	0	0.01	0.03	0.1	0.3	0.5	0.6	1.0	3.0	5.0	7.0	10.0	20.0	∞
	$(\text{Values of } p/(\gamma b) = \alpha/(\gamma b^2 \Omega) \text{ or } p/(\gamma r) = \alpha/(\gamma r^2 \Omega))$													
0.0	0	0.010	0.030	0.098	0.279	0.442	0.518	0.787	1.554	1.836	1.940	1.987	2.000	2.000
0.01	0.010	0.020	0.040	0.107	0.287	0.450	0.526	0.793	1.556	1.837	1.940	1.987	2.000	2.000
0.03	0.030	0.040	0.059	0.126	0.304	0.466	0.541	0.805	1.560	1.838	1.941	1.987	2.000	2.000
0.05	0.050	0.060	0.079	0.145	0.322	0.481	0.555	0.817	1.565	1.840	1.941	1.987	2.000	2.000
0.1	0.100	0.109	0.128	0.193	0.365	0.520	0.592	0.848	1.576	1.844	1.943	1.987	2.000	2.000
0.2	0.200	0.209	0.227	0.288	0.451	0.598	0.667	0.908	1.598	1.852	1.946	1.988	2.000	2.000
0.3	0.300	0.308	0.325	0.383	0.537	0.676	0.741	0.969	1.621	1.860	1.949	1.989	2.000	2.000
0.5	0.500	0.507	0.522	0.573	0.709	0.832	0.889	1.090	1.665	1.877	1.955	1.990	2.000	2.000
0.7	0.700	0.706	0.719	0.763	0.881	0.988	1.037	1.212	1.710	1.893	1.961	1.991	2.000	2.000
1.0	1.000	1.005	1.015	1.049	1.139	1.221	1.259	1.393	1.777	1.918	1.970	1.993	2.000	2.000
1.5	1.500	1.502	1.507	1.524	1.570	1.611	1.630	1.697	1.888	1.959	1.985	1.997	2.000	2.000
2.0	2.000	2.000	2.000	2.000	2.000	2.000	2.000	2.000	2.000	2.000	2.000	2.000	2.000	2.000
2.5	2.500	2.498	2.493	2.476	2.430	2.389	2.370	2.303	2.112	2.041	2.015	2.003	2.000	2.000
3.0	3.000	2.995	2.985	2.951	2.861	2.779	2.741	2.607	2.223	2.082	2.030	2.007	2.000	2.000
4.0	4.000	3.990	3.970	3.902	3.721	3.558	3.482	3.213	2.446	2.164	2.060	2.013	2.000	2.000
5.0	5.000	4.985	4.955	4.854	4.582	4.336	4.222	3.820	2.669	2.246	2.091	2.020	2.000	2.000

6.0	6.000	5.980	5.940	5.805	5.443	5.115	4.963	4.426	2.893	2.328	2.121	2.027	2.000	2.000
7.0	7.000	6.975	6.926	6.756	6.304	5.894	5.704	5.033	3.116	2.410	2.151	2.034	2.000	2.000
8.0	8.000	7.970	7.911	7.707	7.164	6.673	6.445	5.639	3.339	2.493	2.181	2.040	2.000	2.000
9.0	9.000	8.965	8.896	8.659	8.025	7.452	7.186	6.246	3.562	2.575	2.211	2.047	2.000	2.000
10	10.000	9.960	9.881	9.610	8.886	8.230	7.927	6.852	3.785	2.657	2.242	2.054	2.000	2.000
15	15.000	14.935	14.806	14.366	13.189	12.124	11.631	9.885	4.901	3.067	2.393	2.088	2.000	2.000
20	20.000	19.910	19.732	19.122	17.493	16.018	15.335	12.918	6.016	3.478	2.544	2.121	2.000	2.000
25	25.000	24.885	24.658	23.878	21.796	19.912	19.039	15.950	7.132	3.888	2.695	2.155	2.000	2.000
30	30.000	29.860	29.583	28.634	26.100	23.806	22.743	18.983	8.248	4.298	2.846	2.189	2.000	2.000
40	40.000	39.810	38.434	38.147	34.707	31.594	30.151	25.048	10.479	5.119	3.148	2.256	2.000	2.000
50	50.000	49.761	49.285	47.659	43.314	39.382	37.559	31.113	12.710	5.940	3.449	2.323	2.000	2.000
60	60.000	59.711	59.136	57.171	51.921	47.170	44.967	37.179	14.942	6.761	3.751	2.391	2.000	2.000
70	70.000	69.661	68.988	66.684	60.528	54.958	52.376	43.244	17.173	7.582	4.053	2.458	2.000	2.000
80	80.000	79.611	78.839	76.196	69.135	62.746	59.784	49.309	19.404	8.403	4.355	2.526	2.000	2.000
90	90.000	89.561	88.690	85.708	77.742	70.534	67.192	55.375	21.635	9.223	4.657	2.593	2.000	2.000
100	100.000	99.511	98.541	95.220	86.349	78.322	74.600	61.440	23.867	10.044	4.959	2.660	2.000	2.000

This table gives $p/(\gamma b)$ or $p/(\gamma r)$ and the geosynthetic tension as a function of the other parameters involved. Notation: p = pressure on the geosynthetic over the void area; q = uniformly distributed normal stress applied on the top of the soil layer; H = thickness of the soil layer; γ = unit weight of the soil in the soil layer; b = width of the infinitely long void; r = radius of the circular void; α = geosynthetic tension; and Ω = dimensionless factor given in Table 2 as a function of the geosynthetic strain, ϵ . Note that: values of $p/(\gamma b)$ or $p/(\gamma r)$ for $H/b = 0$ are identical to values of $q/(\gamma b)$ or $q/(\gamma r)$; and $p = 2\gamma b$ if H is greater than approximately $20b$ and $p = 2\gamma r$ if H is greater than approximately $20r$. (See the chart given in Fig. 11.)

The same equation can be used for a circular void by substituting r for b .

The above equations can be used to solve problems that consist of determining the required soil layer thickness, H , when all other parameters are given (b or r , q , γ , α , and ε). Alternatively, the charts given in Fig. 11, and the corresponding Table 3, can be used.

Example 2. This example is identical to Example 1, except that the soil layer thickness, H , is unknown, and the geosynthetic tension at a strain $\varepsilon = 10\%$ is known and is equal to 40 kN/m. What is the required soil layer thickness?

From Example 1, the relevant parameters are: $q = 88\,290\text{ N/m}^2$; $\gamma = 19\,600\text{ N/m}^3$; and $r = 0.75\text{ m}$.

In order to use eqn (18), the following values must be calculated

$$q/(\gamma r) = 6.0 \text{ (from Example 1)}$$

$$\alpha/(\gamma r^2 \Omega) = 40\,000/(19\,600 \times (0.75)^2 \times 0.73) = 4.97$$

Hence, using eqn 18

$$H = 2 \times 0.75 \times \ln \frac{6.0 - 2}{4.97 - 2} = 0.44\text{ m}$$

It is also possible to solve this problem using Table 3 or Fig. 11 which gives $H/r = 0.6$ for $q/(\gamma r) = 6.0$ and $\alpha/(\gamma r^2 \Omega) = 4.97$ (see Fig. 13). Hence, $H = 0.6 \times 0.75 = 0.45\text{ m}$.

Determination of Maximum Void Size

There is no simple equation giving the void size (b or r) as a function of the other parameters. In order to determine the maximum void size that a given soil layer-geosynthetic system can bridge, it is necessary to solve eqn (16) by trial and error. To facilitate the process, a chart has been established (Fig. 14) by rewriting the two parts of eqn (17) in a dimensionless form as follows:

$$\frac{p}{\gamma H} = \frac{2(1 - e^{-0.5H/b})}{H/b} + \frac{q}{\gamma H} e^{-0.5H/b} \quad (19)$$

$$\frac{p}{\gamma H} = \frac{\alpha}{\gamma H^2 \Omega} \frac{H}{b} \quad (20)$$

In Fig. 14, eqn (19) is represented by a family of curves and eqn (20) is represented by a family of straight lines at 45° . For a given set of parameters, the abscissa of the intersection between the relevant curve

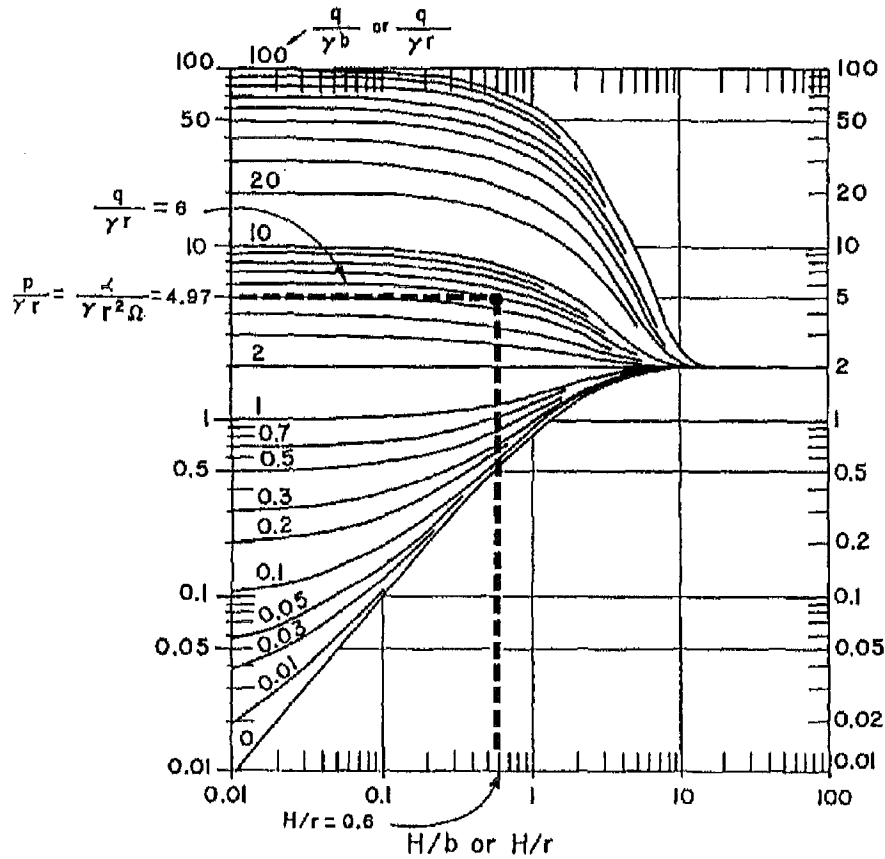


Fig. 13. Example of use of the chart given in Fig. 11.

and the relevant straight line gives the maximum value of the width, b , of an infinitely long void or the radius, r , of a circular void.

Example 3. This example is identical to Example 1, except that the radius of the void, r , is unknown, and the geosynthetic tension at a strain $\varepsilon = 10\%$ is known and is equal to 40 kN/m . What maximum void radius can be bridged by the considered soil-geosynthetic system?

From Example 1, the relevant parameters are: $q = 88\,290 \text{ N/m}^2$; $\gamma = 19\,600 \text{ N/m}^3$; and $H = 0.45 \text{ m}$.

In order to use the chart given in Fig. 14, the following must be calculated

$$q/(\gamma H) = 88\,290 / (19\,600 \times 0.45) = 10.0$$

$$\alpha/(\gamma H^2 \Omega) = 40\,000 / (19\,600 \times (0.45)^2 \times 0.73) = 13.8$$

(Note: $\Omega = 0.73$ is obtained from Table 2 with $\varepsilon = 10\%$)

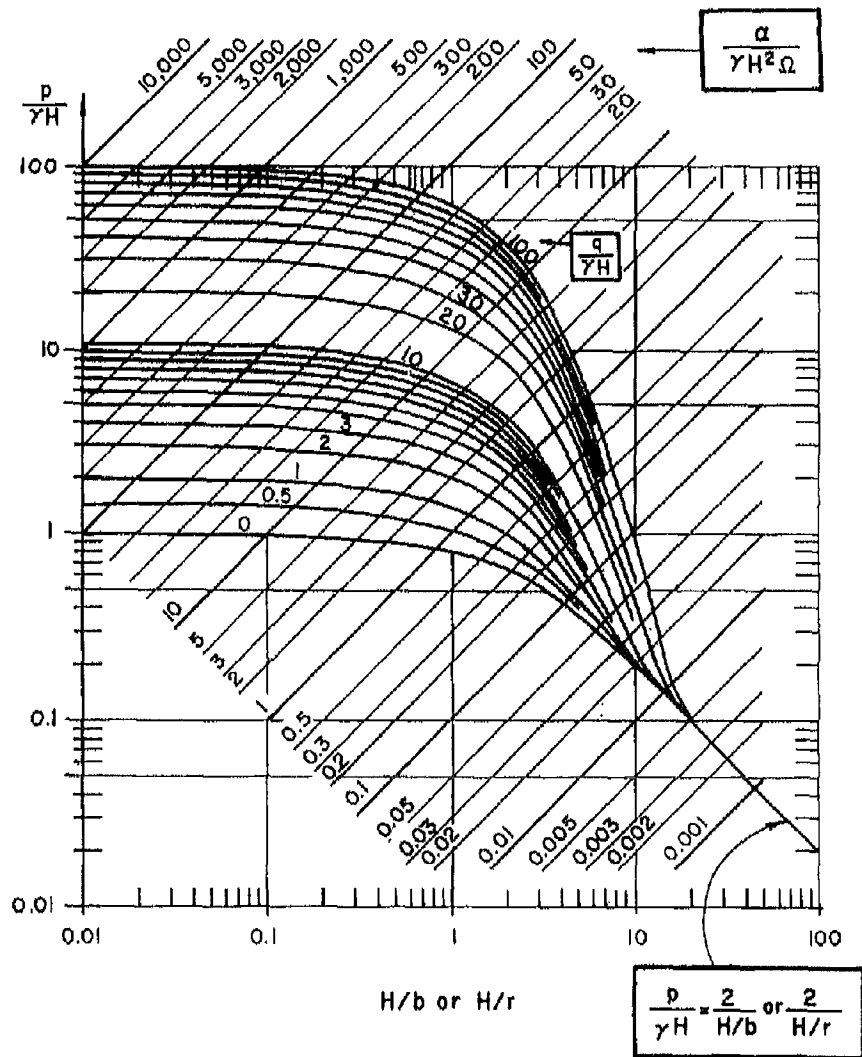


Fig. 14. Pressure on and tension in the geosynthetic. An example of use of this chart is given in Fig. 15. Notations: p = pressure on the geosynthetic over the void area; q = uniformly distributed normal stress applied on the top of the soil layer; H = thickness of the soil layer; γ = unit weight of soil; b = width of the infinitely long void; r = radius of the circular void; α = geosynthetic tension; and Ω = dimensionless factor given in Table 2 and Fig. 10. (Values of $p/(\gamma H)$ which were used to draw the curves in this figure can be found in Table 4.)

In Fig. 14, the curve related to $q/(\gamma H) = 10$ and the straight line at 45° related to $\alpha/(\gamma H^2 \Omega) = 13.8$ intersect at a point the abscissa of which is $H/r = 0.6$ (see Fig. 15). Hence

$$r_{\max} = 0.45/0.6 = 0.75 \text{ m}$$

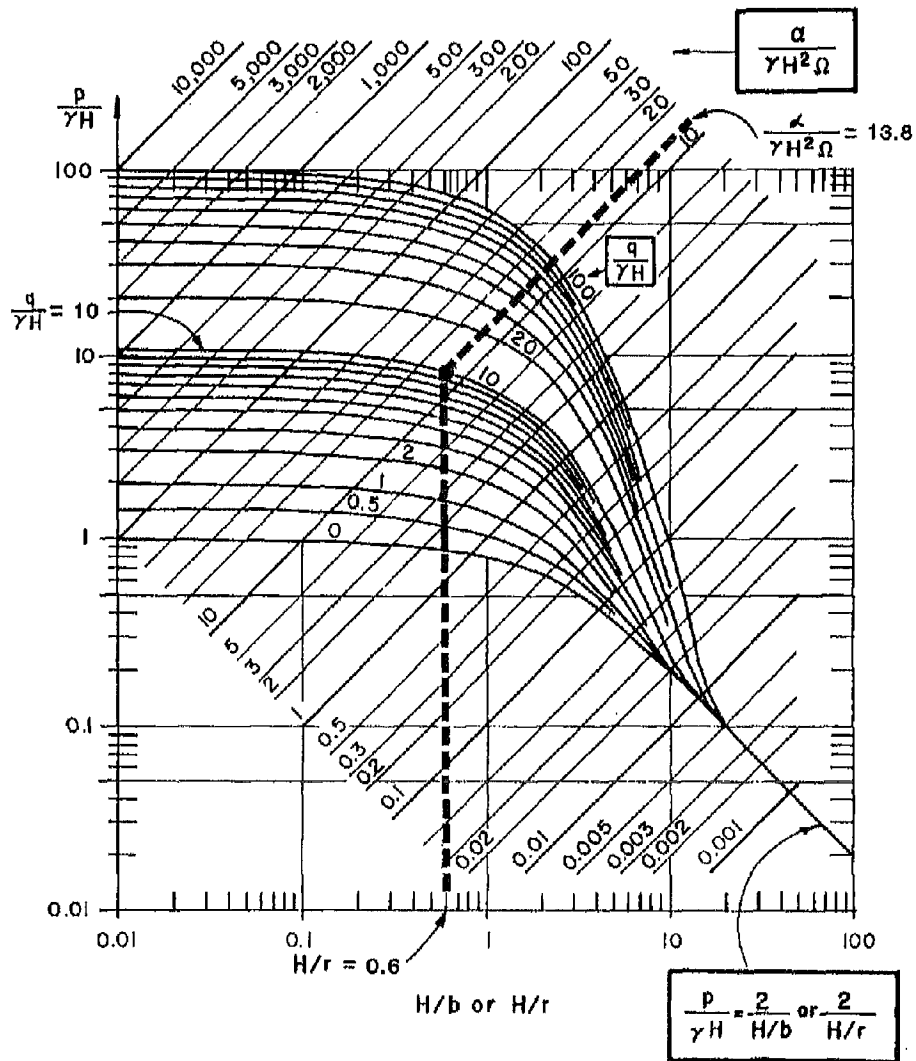


Fig. 15. Example of use of the chart given in Fig. 14.

Determination of the Maximum Load

The relevant equation for an infinitely long void is

$$q = 2\gamma b + \left\{ \frac{[\alpha/(\gamma b^2 \Omega)] - 2}{e^{-0.5H/b}} \right\} \gamma b \quad (21)$$

The same equation can be used for a circular void by substituting r for b .

The above equation can be used to solve problems that consist of determining the maximum uniform normal stress, q , which can be applied on the top of the soil layer, when all other parameters are given (b or r , γ , H , α , and ε). Alternatively, the charts given in Fig. 11 or 14 can be used, as well as Table 3 or 4.

TABLE 4
Pressure on the Geosynthetic

H/b or H/r													
$q/(\gamma H)$	0	0.01	0.1	0.3	0.5	0.7	1.0	3.0	5.0	7.0	10.0	20.0	∞
	(Values of $p/(\gamma H)$)												
0.0	∞	0.998	0.975	0.929	0.885	0.844	0.787	0.518	0.367	0.277	0.199	0.100	0
0.5	∞	1.495	1.451	1.359	1.274	1.196	1.090	0.629	0.408	0.292	0.202	0.100	0
1.0	∞	1.993	1.927	1.789	1.664	1.548	1.393	0.741	0.449	0.307	0.205	0.100	0
2.0	∞	2.988	2.878	2.650	2.442	2.253	2.000	0.964	0.531	0.337	0.212	0.100	0
3.0	∞	3.983	3.829	3.511	3.221	2.958	2.607	1.187	0.613	0.368	0.219	0.100	0
4.0	∞	4.978	4.780	4.371	4.000	3.663	3.213	1.410	0.696	0.398	0.226	0.100	0
5.0	∞	5.973	5.732	5.232	4.779	4.367	3.820	1.634	0.778	0.428	0.232	0.100	0
6.0	∞	6.968	6.683	6.093	5.558	5.072	4.426	1.857	0.860	0.458	0.239	0.100	0
7.0	∞	7.963	7.634	6.954	6.336	5.777	5.033	2.080	0.942	0.488	0.246	0.100	0
8.0	∞	8.958	8.585	7.814	7.115	6.481	5.639	2.303	1.024	0.519	0.253	0.100	0
9.0	∞	9.953	9.536	8.675	7.894	7.186	6.246	2.526	1.106	0.549	0.259	0.100	0
10	∞	10.948	10.488	9.536	8.673	7.891	6.852	2.749	1.188	0.579	0.266	0.100	0
15	∞	15.923	15.244	13.839	12.567	11.414	9.885	3.865	1.598	0.730	0.300	0.101	0
20	∞	20.898	20.000	18.143	16.461	14.938	12.918	4.981	2.009	0.881	0.333	0.101	0
25	∞	25.873	24.756	22.446	20.355	18.461	15.950	6.096	2.419	1.032	0.367	0.101	0
30	∞	30.848	29.512	26.750	24.249	21.984	18.983	7.212	2.830	1.183	0.401	0.101	0
40	∞	40.798	39.025	35.357	32.037	29.031	15.048	9.443	3.651	1.485	0.468	0.102	0
50	∞	50.748	48.537	43.964	39.825	36.078	31.113	11.674	4.471	1.787	0.536	0.102	0
60	∞	60.698	58.049	52.571	47.613	43.125	37.179	13.906	5.292	2.089	0.603	0.103	0
70	∞	70.648	67.561	61.178	55.401	50.172	43.244	16.137	6.113	2.391	0.670	0.103	0
80	∞	80.599	77.074	69.786	63.189	57.219	49.309	18.368	6.934	2.693	0.738	0.104	0
90	∞	90.549	86.586	78.392	70.977	64.266	55.375	20.600	7.755	2.995	0.805	0.104	0
100	∞	100.499	96.098	86.999	78.765	71.313	61.440	22.831	8.576	3.297	0.872	0.105	0

This table gives $p/(\gamma H)$. Notation: p = pressure on the geosynthetic over the void area; q = uniformly distributed normal stress applied on the top of the soil layer; H = thickness of the soil layer; γ = unit weight of the soil in the soil layer; b = width of the infinitely long void; and r = radius of the circular void. Note that: values of $p/(\gamma H)$ are equal to: $1 + q/(\gamma H)$ if $H/b = 0$ or $H/r = 0$; and $2b/H$ or $2r/H$ if $H/b > 20$ or $H/r > 20$. (See the chart given in Fig. 14.)

Example 4. This example is identical to Example 1, except that the stress on top of the soil layer, q , is unknown, and the geosynthetic tension at strain $\varepsilon = 10\%$ is known and is equal to 40 kN/m. What maximum stress on top of the soil layer can be supported by the soil-geosynthetic system? From Example 1, the relevant parameters are: $H = 0.45$ m; $r = 0.75$ m; and $\gamma = 19\,600$ N/m³.

In order to use eqn (21), the value of Ω must be obtained first from Table 2

$$\Omega = 0.73 \quad \text{for } \varepsilon = 10\%.$$

Then, eqn (21) is used as follows

$$\begin{aligned} q &= 2 \times 19\,600 \times 0.75 \\ &\quad + \left\{ \frac{[40\,000 / (19\,600 \times (0.75)^2 \times 0.73)] - 2}{e^{-0.5 \times 0.45 / 0.75}} \right\} 19\,600 \times 0.75 \\ &= 88\,334 \text{ N/m}^2 \end{aligned}$$

The problem can also be solved using charts and tables. To use Table 3 or the chart given in Fig. 11, the following must be calculated:

$$H/r = 0.45/0.75 = 0.6$$

$$\alpha/(\gamma r^2 \Omega) = 40\,000 / (19\,600 \times (0.75)^2 \times 0.73) = 4.97$$

With $H/r = 0.6$ and $\alpha/(\gamma r^2 \Omega) = 4.97$, Table 3 or the chart given in Fig. 11 show that $q/(\gamma r) = 6$ (see Fig. 13). Therefore

$$q = 6 \times 19\,600 \times 0.75 = 88\,200 \text{ N/m}^2 = 88 \text{ kN/m}^2$$

To use the chart given in Fig. 14, the following must be calculated

$$\alpha/(\gamma H^2 \Omega) = 40\,000 / (19\,600 \times (0.45)^2 \times 0.73) = 13.8$$

With $H/r = 0.6$ and $\alpha/(\gamma H^2 \Omega) = 13.8$, the chart given in Fig. 14 shows that $q/(\gamma H) = 10$ (see Fig. 15). Therefore

$$q = 10 \times 19\,600 \times 0.45 = 88\,200 \text{ N/m}^2 = 88 \text{ kN/m}^2$$

DISCUSSION OF SPECIAL PROBLEMS

Anisotropic Geosynthetic

A geosynthetic is isotropic regarding a given characteristic when this characteristic has the same value in all directions. In this paper, a geosynthetic will be considered isotropic when it has the same tension-strain

curve in all directions. This requirement is fulfilled by some nonwoven geotextiles. Woven geotextiles and biaxial geogrids are stronger in two directions ('principal directions') than in the others and, therefore, they are anisotropic. However, we assume that the design method presented in this paper can be used with woven geotextiles and biaxial geogrids that have the same tensile characteristics in the two principal directions (i.e. in the design, these materials are considered isotropic).

Special precautions must be taken when using the design method presented in this paper for geosynthetics that cannot be considered isotropic, as discussed below.

Infinitely Long Void

In the case of an infinitely long void, no geosynthetic tension is required in the direction of the length of the void (according to the plane-strain model which corresponds to an infinitely long void). Therefore, the value of α to be used in the equations, tables, and charts related to the infinitely long void is the geosynthetic tension in the direction of the width of the void for the considered design strain. However, some strength is required lengthwise in places where the actual situation departs from a pure plane-strain situation (for instance near the end of the void).

Circular Void

In the case of a circular void, the tensioned membrane equation (eqn (15)) is valid only if the geosynthetic has isotropic tensile characteristics. For practical purposes, eqn (15), and other equations as well as tables and charts related to circular voids, can be used for woven geotextiles and biaxial geogrids that have the same tension-strain curve *in the two principal directions* (instead of *in all directions* for a truly isotropic material). For woven geotextiles and biaxial geogrids that have different tensile characteristics in the two principal directions, two cases can be considered, depending on the ratio between the geosynthetic tensions at the design strain in the weak and the strong directions: (i) if the ratio is more than 0.5, α should be taken equal to the tension in the weak direction; and (ii) if the ratio is less than 0.5, α should be taken equal to half the tension in the strong direction.

The rationale for the above recommendation is as follows. There are two conservative approaches and the less conservative, which is closer to reality, should be selected.

The first conservative approach consists of designing with an isotropic geosynthetic weaker than the considered anisotropic geosynthetic. This is achieved by taking the geosynthetic strength in all directions equal to the

strength in the weak direction, α_{weak} . Equation (15) thus gives for the pressure which can be carried by the geosynthetic

$$p_1 = \frac{\alpha_{\text{weak}}}{r\Omega} \quad (22)$$

The second conservative approach consists of designing with: (i) a void larger than the circular void by replacing the circular void by an infinitely long void with a width, b , equal to the diameter, $2r$, of the circular void; and (ii) a geosynthetic weaker than the considered anisotropic geosynthetic by neglecting the tensile strength in the weak direction ($\alpha_{\text{weak}} = 0$). Equation (15) thus gives for the pressure which can be carried by the geosynthetic

$$p_2 = \frac{\alpha_{\text{strong}}}{b\Omega} = \frac{\alpha_{\text{strong}}}{2r\Omega} \quad (23)$$

To compare p_1 and p_2 , it is important to note that the values of Ω in eqns (22) and (23) are identical because they are both determined for $y/(2r)$, according to Table 2. Therefore, the comparison between p_1 and p_2 boils down to a comparison between α_{weak} and $0.5 \alpha_{\text{strong}}$.

It appears that

$$p_1 > p_2 \quad \text{if} \quad \alpha_{\text{weak}} > 0.5 \alpha_{\text{strong}}$$

$$p_1 < p_2 \quad \text{if} \quad \alpha_{\text{weak}} < 0.5 \alpha_{\text{strong}}$$

hence the above recommendation.

There is another consideration when an anisotropic geosynthetic is used over a circular void. The complex pattern of strains in the geosynthetic resulting from different tensions in different directions may have a detrimental effect on the behavior of the geosynthetic. Therefore, it is recommended that for holes which can be modeled as circular, one of the following solutions be adopted: (i) an isotropic geosynthetic (only some nonwoven geotextiles are isotropic but usually they do not have adequate tensile characteristics for this application); or (ii) a 'practically isotropic' geosynthetic (such as a woven geotextile or a biaxial geogrid having similar tension-strain curves in the two principal directions); or (iii) two perpendicularly orientated layers of the same anisotropic geosynthetic.

Geosynthetic in Contact with Void Bottom

In some cases, the geosynthetic elongates to the point that it comes in contact with the bottom of the void (Fig. 1(c)); the geosynthetic deflection

is then equal to the void depth ($y = D$). In design, these cases correspond to a calculated geosynthetic deflection greater than or equal to the void depth ($y \geq D$). Usually, the design is complete when it is found that $y \geq D$. However, it may be of interest to *determine the pressure actually transmitted to the bottom of the void*. This pressure is obtained by subtracting the pressure inducing geosynthetic tension (which results from the tensioned membrane effect) from the pressure exerted by the soil layer on the geosynthetic.

In the case of an infinitely long void, the following equation can be obtained by subtracting the pressure given by eqn (15) from the pressure given by eqn (10)

$$p_b = 2\gamma b(1 - e^{-0.5H/b}) + q e^{-0.5H/b} - \frac{\alpha}{b\Omega} \quad (24)$$

where: p_b = pressure transmitted to the bottom of the void; γ = unit weight of the soil (in the soil layer above the geosynthetic); b = width of the infinitely long void; H = soil layer thickness; q = uniformly distributed normal stress applied on the top of the soil layer; α = geosynthetic tension corresponding to the geosynthetic strain, ε , when the geosynthetic is in contact with the bottom of the void (i.e., ε corresponding to a deflection $y = D$ in Table 2); Ω = dimensionless factor given in Table 2 as a function of ε or y ; and y = geosynthetic deflection, which, in this case, is equal to D ; and D = depth of the void. Basic SI units are: p_b (N/m²), γ (N/m³), b (m), H (m), q (N/m²), α (N/m), y (m), and D (m); Ω is dimensionless. Note that eqn (24) assumes that the shape of the bottom of the void is approximately cylindrical with a circular cross section, so the geosynthetic will come in contact with all points on the surface of the void at the same time. If this were not the case, portions of the geosynthetic which come in contact with the bottom of the void last would elongate more than the others.

The same equation can be used for a circular void by substituting r for b , with r = radius of the circular void.

If a negative value were obtained for p_b when using the above equation, it would mean that the load on the geosynthetic is not large enough to force the geosynthetic to come in contact with the bottom of the void.

Example 5. This example is identical to Example 1 except that: (i) the void is not bottomless but has a depth $D = 0.2$ m; and (ii) the geosynthetic tension-strain curve is assumed to be a straight line between the origin and a tension $\alpha = 40$ kN/m for a strain $\varepsilon = 10\%$. What is the stress transmitted to the bottom of the hole?

From Example 1, the relevant parameters are: $r = 0.75$ m; $H = 0.45$ m; $\gamma = 19\,600$ N/m³; and $q = 88\,290$ N/m².

First, the approximate value of the average strain of the geosynthetic when it is in contact with the bottom of the void (assumed spherical) must be determined using Table 2 with y (geosynthetic deflection) = D (void depth)

$$y/2r = D/2r = 0.2/(2 \times 0.75) = 0.133$$

Hence, interpolating in Table 2, $\varepsilon = 4.65\%$ and $\Omega = 1.01$.

Then, the geosynthetic tension corresponding to a 4.65% geosynthetic strain can be calculated as follows:

$$\alpha = 40\,000 \times 4.65/10 = 18\,600 \text{ N/m}$$

Finally, eqn (24) can be used with the values $H/r = 0.6$ and $q = 88\,290$ N/m² determined in Example 1. This equation gives the stress transmitted to the bottom of the void as follows

$$\begin{aligned} p_b &= 2 \times 19\,600 \times 0.75(1 - e^{-0.3}) + 88\,290 e^{-0.3} - \frac{18\,600}{0.75 \times 1.01} \\ &= 73\,029 - 24\,554 = 48\,475 \text{ N/m}^2 = 48.5 \text{ kN/m}^2 \end{aligned}$$

Therefore, this design example can be summarized as follows:

- A stress of 88.3 kN/m² is applied on top of the soil layer.
- As a result of soil arching, the soil layer transmits only a stress of 73 kN/m² to the top of the geosynthetic.
- As a result of the tensioned membrane effect, the geosynthetic supports 24.5 kN/m².
- The remainder, 48.5 kN/m², is transmitted to the bottom of the void.

It should be noted that, if the depth of the void had been $D = 0.3$ m, the strain of the geosynthetic would have been 10% and the last term of the above equation would have been

$$\frac{\alpha}{r\Omega} = \frac{40\,000}{0.75 \times 0.73} = 73\,059 \text{ N/m}^2$$

Hence, $p_b = 0$. In this case, Example 5 becomes identical to Example 1.

Influence of Soil Layer Thickness

The influence of the thickness of the soil layer is illustrated in Fig. 11. Three cases can be considered:

- (1) *Large Applied Stress.* If the applied stress, q , is large (i.e. $q > 2\gamma b$ or $2\gamma r$), the pressure, p , on the geosynthetic and consequently the required geosynthetic tension, α , decrease towards a limit when the soil layer thickness increases. In this case, *it is beneficial to increase the thickness of the soil layer.* For each particular situation, the amount by which the thickness should be increased can be determined using the chart given in Fig. 11 or Table 3. The chart and table show that it would be useless to increase the soil layer thickness beyond a limiting value of $H = 20b$ or $20r$.
- (2) *Small Applied Stress.* If the applied stress, q , is small (i.e. $q < 2\gamma b$ or $2\gamma r$), the pressure, p , on the geosynthetic and consequently the required geosynthetic tension, α , increase toward a limit when the soil thickness increases. In this case, from the perspective of the design of the geosynthetic, *it is detrimental to increase the thickness of the soil layer.* (This is because the added load due to soil weight is not fully compensated by the effect of soil arching.)
- (3) *Limit Applied Stress.* If the applied stress, q , equals the limit (i.e. $q = 2\gamma b$ or $2\gamma r$), the pressure, p , on the geosynthetic remains constant and equal to q , regardless of the soil layer thickness.

The limit values for p and α are independent of the applied stress, q . The limit value for the pressure on the geosynthetic is

$$p_{\text{lim}} = 2\gamma b \quad \text{for an infinitely long void} \quad (25)$$

The limit value for the required geosynthetic tension is

$$\alpha_{\text{lim}} = 2\gamma b^2 \Omega \quad \text{for an infinitely long void} \quad (26)$$

Equations (25) and (26) can be used for a circular void by substituting r for b .

Comparison with Tensioned Membrane Theory

In the past, the tensioned membrane theory has been used alone to evaluate the required tensile characteristics of a geosynthetic located beneath a soil layer and bridging a void. This method neglects arching in

the soil layer and is, therefore, conservative. This conservativeness can be evaluated by comparing the pressure on the geosynthetic over the void area, p , calculated taking soil arching into account to the following value obtained by neglecting soil arching

$$p_0 = \gamma H + q \quad (27)$$

where: p_0 = pressure on the geosynthetic over the void area neglecting soil arching; γ = unit weight of the soil in the soil layer; H = thickness of the soil layer; and q = uniformly distributed normal stress applied on the top of the soil layer. Basic SI units are: p_0 (N/m²), γ (N/m³), H (m), and q (N/m²).

The pressure, p , obtained taking soil arching into account is given by eqn (10).

Values of p/p_0 are given in Table 5 and Fig. 16. It appears that neglecting soil arching is conservative. However, when the soil thickness, H , is large

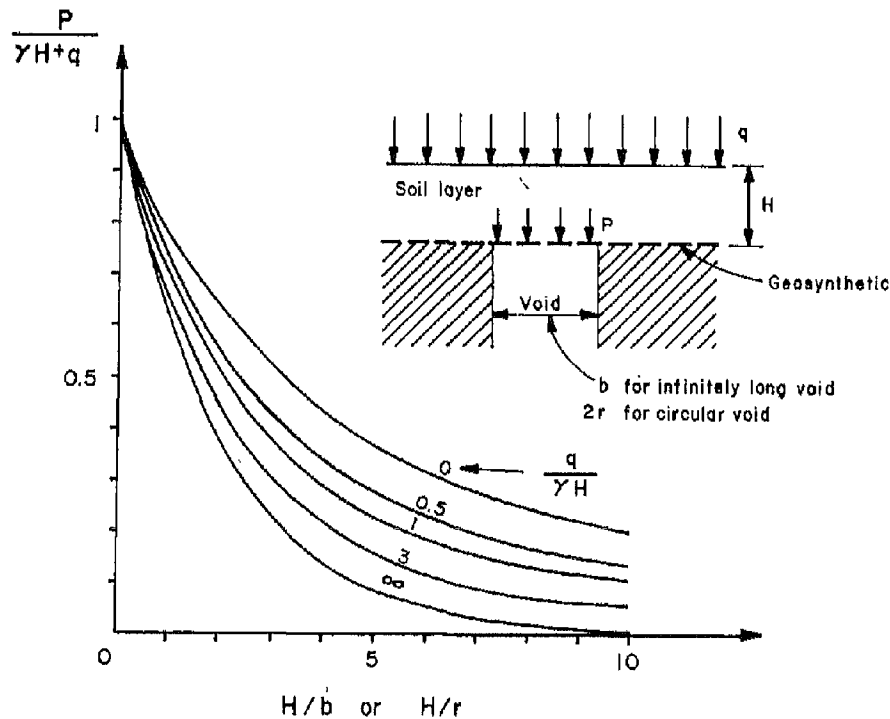


Fig. 16. Effectiveness of soil arching. The curves give the ratio between the pressure, p , on the geosynthetic over the void area, calculated taking soil arching into account, and the pressure $p_0 = \gamma H + q$ obtained by neglecting soil arching. The values of p/p_0 used to plot the curve can be found in Table 5.

TABLE 5
Effectiveness of Soil Arching

$q/(\gamma H)$	H/b or H/r										
	0	0.3	0.6	1	1.5	2	2.3	3	4	5	∞
							<i>(Values of p/p_0)</i>				
0	1	0.929	0.864	0.787	0.704	0.632	0.571	0.518	0.432	0.367	0.199
0.5	1	0.906	0.823	0.727	0.626	0.544	0.476	0.420	0.333	0.272	0.135
1	1	0.895	0.802	0.697	0.588	0.500	0.429	0.371	0.284	0.225	0.103
2	1	0.883	0.782	0.667	0.549	0.456	0.381	0.321	0.234	0.177	0.071
3	1	0.878	0.772	0.652	0.530	0.434	0.358	0.297	0.210	0.153	0.055
5	1	0.872	0.761	0.637	0.511	0.412	0.334	0.272	0.185	0.130	0.039
10	1	0.867	0.752	0.623	0.493	0.392	0.312	0.250	0.162	0.108	0.024
20	1	0.864	0.747	0.615	0.483	0.380	0.300	0.237	0.149	0.096	0.016
∞	1	0.861	0.741	0.607	0.472	0.368	0.287	0.223	0.135	0.082	0.007

This table gives the ratio of the pressure on the geosynthetic over the void area calculated taking arching into account (p) or neglecting arching (p_0). The value of p is given by eqn (10). The value of p_0 is given by eqn (27). Notation: q = uniformly distributed stress applied on the top of the soil layer; γ = unit weight of the soil in the soil layer; H = soil layer thickness; b = width of an infinitely long void; and r = radius of circular void. (See also Fig. 16.)

compared to the width or radius of the void, neglecting soil arching is over-conservative.

CONCLUSION

This paper has presented an approach to the design of soil layer-geosynthetic systems overlying voids. The design approach superimposes arching theory for the soil layer with tensioned membrane theory for the geosynthetic. The analysis presented in this paper shows that neglecting soil arching would be over-conservative in many instances. The paper presents equations, tables, and charts that make it easy to perform design analyses for a range of possible field situations.

The analysis shows that the thickness of the soil layer associated with the geosynthetic plays a significant role. In contrast, the soil mechanical properties do not. It should not be inferred, however, that any soil will provide the same degree of arching. The equations used to prepare the tables and charts assume that the friction angle of the soil is at least 20° . Granular soils virtually always meet this condition. However, they should be well compacted to ensure arching because loose granular soils tend to contract when they are sheared or vibrated, which may destroy the arch.

Further refinements of the method presented herein can be considered. For instance, it is possible that the degree of soil arching (i.e. the amount of soil shear strength mobilized) depends on the geosynthetic strain, whereas the method presented in this paper does not consider the concept of degree of soil arching. Also, the method could be expanded to include cohesive soils, and could be refined to take into account elongation of the geosynthetic in the anchorage zone. Lastly, the method could be expanded to consider a system of regularly spaced voids.

In spite of its limitations, the method presented in this paper is believed to be a useful tool for engineers designing soil-geosynthetic systems resting on subgrades where voids may develop.

ACKNOWLEDGMENTS

This paper is an expanded version of the paper presented at the Kyushu International Geotechnical Symposium on Theory and Practice of Earth Reinforcement.¹³ The authors are grateful to Professors Yamanouchi and Miura, organizers of the Kyushu Symposium, for authorizing the publication of this expanded version.

The authors are indebted to G. Saunders, A. Mozzar, G. Kent, S. Berdy, and A. H. Perry for assistance during the preparation of this paper.

REFERENCES

1. Loudière, D. & Perrin, J., Désordres dans les revêtements minces de bassin. In *Colloque sur l'étanchéité superficielle des bassins, barrages, et canaux*, Vol. 1, Paris, Feb. 1983. CEMAGREF, Antony, France, pp. 147–52.
2. Giroud, J. P., & Goldstein, J. S., Geomembrane liner design. *Waste Age* (Sept. 1982) 27–30.
3. Giroud, J. P., *Geotextiles and Geomembranes, Definitions, Properties and Design*. I.F.A.I. Publisher, St Paul, MN, 1984, 325 pp.
4. Bonaparte, R. & Berg, R. R., The use of geosynthetics to support roadways over sinkhole prone areas. In *Proceedings of the Second Multidisciplinary Conference on Sinkholes and the Environmental Impacts of Karst*, Orlando, FL, Feb. 1987. Balkema, Rotterdam, pp. 437–45.
5. Giroud, J. P. & Fluet, J. E., Jr, Quality assurance of geosynthetic lining systems. *Geotextiles and Geomembranes*, 3 (1986) 249–87.
6. Tisserand, C., Le réservoir de Guazza: un grand bassin à membrane non protégée. *Colloque sur l'étanchéité superficielle des bassins, barrages et canaux*, Vol. 1, Paris, Feb. 1983. CEMAGREF, Antony, France, pp. 87–9.
7. Giroud, J. P., Designing with geotextiles. *Matériaux et Constructions*, 14 (1981), 257–72.
8. Giroud, J. P., Design of geotextiles associated with geomembranes. In *Proceedings of the Second International Conference on Geotextiles*, Vol. 1, Las Vegas, USA, Aug. 1982, pp. 37–42.
9. Terzaghi, K., *Theoretical Soil Mechanics*. John Wiley and Sons, Inc., New York, 1943, 510 pp.
10. Kezdi, A., Lateral earth pressure. In *Foundation Engineering Handbook*, ed. H. F. Winterkorn & H. Y. Fang. Van Nostrand Reinhold, New York, 1975, pp. 197–220.
11. Handy, R. L., The arch in soil arching. *Journal of Geotechnical Engineering*, ASCE, 111 (1985) 302–18.
12. Jaky, J., The coefficient of earth pressure at rest. *Journal for Society of Hungarian Architects and Engineers*, Budapest, Oct. 1944, pp. 355–8 (in Hungarian).
13. Giroud, J. P., Bonaparte, R., Beech, J. F. & Gross, B. A., Load carrying capacity of a soil layer supported by a geosynthetic located on a void. In *Proceedings of the International Geotechnical Symposium on Theory and Practice of Earth Reinforcement*, Fukuoka/Kyushu, Japan, Oct. 1988. Balkema, Rotterdam, pp. 185–90.

TABLE 2
Values of Ω as a Function of Deflection or Strain

y/b or $y/(2r)$	$\varepsilon(\%)$	Ω	y/b or $y/(2r)$	$\varepsilon(\%)$	Ω
0.000	0.000	∞	0.242	15.00	0.64
0.010	0.027	12.51	0.250	15.91	0.62
0.020	0.107	6.26	0.260	17.15	0.61
0.030	0.240	4.18	0.270	18.43	0.60
0.040	0.425	3.15	0.280	19.75	0.59
0.050	0.663	2.53	0.282	20.00	0.58
0.060	0.960	2.11	0.290	21.10	0.58
0.061	1.000	2.07	0.300	22.50	0.57
0.070	1.30	1.82	0.310	23.93	0.56
0.080	1.70	1.60	0.317	25.00	0.55
0.087	2.00	1.47	0.320	25.39	0.55
0.090	2.15	1.43	0.330	26.89	0.54
0.100	2.65	1.30	0.340	28.43	0.54
0.107	3.00	1.23	0.350	30.00	0.53
0.110	3.20	1.19	0.360	31.60	0.53
0.120	3.80	1.10	0.370	33.23	0.52
0.123	4.00	1.08	0.380	34.90	0.52
0.130	4.45	1.03	0.381	35.00	0.52
0.138	5.00	0.97	0.390	36.60	0.52
0.140	5.15	0.96	0.400	38.32	0.51
0.150	5.90	0.91	0.410	40.00	0.52
0.151	6.00	0.90	0.420	41.86	0.51
0.160	6.69	0.86	0.430	43.67	0.51
0.164	7.00	0.84	0.437	45.00	0.50
0.170	7.54	0.82	0.440	45.51	0.50
0.175	8.00	0.80	0.450	47.38	0.50
0.180	8.43	0.78	0.460	49.27	0.50
0.186	9.00	0.76	0.464	50.00	0.50
0.190	9.36	0.75	0.470	51.18	0.50
0.197	10.00	0.73	0.480	53.13	0.50
0.200	10.35	0.72	0.490	55.00	0.50
0.210	11.37	0.70	0.500	57.08	0.50
0.216	12.00	0.69	0.562	70.00	0.50
0.220	12.44	0.68	0.631	85.00	0.51
0.230	13.56	0.66	0.696	100.00	0.53
0.240	14.71	0.64	0.819	130.00	0.56

This table also gives values of the strain as a function of the deflection, and vice versa. (See also Fig. 10.) Notations: Ω = dimensionless factor used for the calculation of the tension in the geosynthetic; y = geosynthetic deflection; b = width of the infinitely long void; $2r$ = diameter of the circular void; and ε = geosynthetic strain. (Note: in the case of a circular void, the values of ε and Ω given in this table are approximate.)

noted that, for a circular void, r is substituted for b in eqn (15) whereas $2r$ is used to determine Ω , as indicated in Table 2 and Fig. 10.

Equation (15) can be used for a circular void only if the geosynthetic has isotropic tensile characteristics, i.e. the same tensile characteristics in all directions. If this is not the case, recommendations given in the section 'Discussion of Special Problems' should be followed.

Applications of Tensioned Membrane Theory

Tensioned membrane theory can be used alone (i.e. not combined with arching theory) to solve design problems relating to the case of a geosynthetic acting alone and subjected to a uniformly distributed pressure. This typically occurs in the case of geomembranes directly overlying a void and subjected to pressure from a liquid. Typical design problems are as follows:

- Determine the maximum pressure that a geomembrane can withstand over a void of a given size.
- Select the required geomembrane properties for a geomembrane to bridge a given void when it is subjected to a given pressure.
- Determine the void size that a given geomembrane may bridge when it is subjected to a given pressure.
- Determine the deflection of a geomembrane subjected to a given pressure on a given void, and determine if the deflected geomembrane will come in contact with the bottom of the void.

A chart has been published² to help solve these problems. It is also possible to use Table 3 with $H = 0$.

Combination of Arching and Tensioned Membrane Theories

The problem of a bottomless void is entirely solved by using eqns (10) and (15). The case when the geosynthetic comes in contact with the bottom of the void is more complex and will be discussed later in this paper, in the section 'Discussion of Special Problems'.

Equation (10) gives a relationship between the applied stress, the soil layer thickness, the void size, and the pressure on the geosynthetic. This equation was established using *arching theory*.

Equation (15) gives a relationship between the pressure on the geosynthetic, the void size, and the geosynthetic tensile characteristics (tension and strain). This equation was established using *tensioned membrane theory*.

The solution of typical design problems using the equations mentioned above is discussed in the next section.

SOLUTION OF TYPICAL DESIGN PROBLEMS

Overview of the Methods Used

In the presentation of the scope of this paper, a list of typical design problems was given. Solutions to these problems are presented below for the case when the geosynthetic does not come in contact with the bottom of the void. Solutions for the case where the geosynthetic comes in contact with the bottom of the void are presented in the section 'Discussion of Special Problems'.

Allowable Strain and Deflection

In all of the design cases considered below, the solution depends on the value of Ω , which depends either on the allowable geosynthetic strain, ϵ , or the allowable geosynthetic deflection, y . The *allowable geosynthetic strain* is the lesser of the maximum design strain for the considered geosynthetic and the strain beyond which the soil layer would be unacceptably deformed or cracked. The *allowable geosynthetic deflection* is considered when excessive deflection of the soil surface impairs the serviceability of the system. No method is proposed in this paper to evaluate the deflection of the soil surface; however, in the case of relatively thin soil layers, the soil surface deflection can be assumed to be on the same order as the geosynthetic deflection. In some instances, both the allowable geosynthetic strain and the allowable geosynthetic deflection may need to be considered.

Equations and Notations

All equations presented below were obtained by combining eqns (10) and (15). Notations for all subsequent equations are: b = width of the infinitely long void; r = radius of the circular void; Ω = dimensionless factor given in Table 2 as a function of ϵ or y ; H = soil layer thickness; p = normal stress applied on the portion of the geosynthetic located over the void ('pressure on the geosynthetic'); q = uniformly distributed normal stress applied on the top of the soil layer; y = geosynthetic deflection; α = geosynthetic tension; γ = unit weight of soil; and ϵ = geosynthetic strain. Basis SI units are: b (m), r (m), H (m), p (N/m²), q (N/m²), y (m), α (N/m), and γ (N/m³); Ω and ϵ are dimensionless.

Factor of Safety

In the following sections, each design problem is illustrated by an example. For the sake of simplicity, no factor of safety is used in the design examples. Engineers using the equations, tables, and charts presented in

**APPLICATION FOR PERMIT RENEWAL AND MODIFICATION
SANDOVAL COUNTY LANDFILL**

**VOLUME III: LANDFILL ENGINEERING CALCULATIONS
SECTION 7: GEOSYNTHETICS TENSILE STRESS AND STABILITY ANALYSIS**

**ATTACHMENT III.7.F
TENSAR UNIAXIAL GEOGRIDS FOR SOIL REINFORCEMENT,
TENSAR INTERNATIONAL, 2007.**



Tensar® Uniaxial Geogrids for Soil Reinforcement

The Engineered Advantage®

Tensar® Uniaxial (UX) Geogrids are manufactured using select grades of high-density polyethylene (HDPE) resins that are highly oriented and resist elongation (creep) when subjected to high tensile loads for long periods of time. Geogrids manufactured from HDPE provide high resistance to installation damage and chemical or biological long-term degradation. In fact, Tensar UX Geogrids have shown no degradation in pH situations as high as 12 and can be used in both dry and wet-cast environments.



A high-density polyethylene, homogeneous product that does not require weaving, coating or welding to maintain the product's integrity.

Tensile Strength

Tensar UX Geogrids can carry high tensile loads applied in one direction (along the roll). Their open aperture structure interlocks with fill material to provide superior load transfer from the soil to the geogrid. Tensar UX Geogrids achieve their strength by punching and drawing a homogenous polymer sheet to provide a uniform, consistent product that does not require weaving, coating or welding to maintain the product's integrity. This unique process provides superior junction strength allowing high strength connections to other rolls of geogrid or facing components.



Tensar Geogrids are used for high strength soil reinforcement in wall and slope applications. Over 100-million square feet of retaining structures in service today are reinforced with Tensar UX Geogrid.

Experience You Can Rely On

Tensar International Corporation, the leader in geosynthetic soil reinforcement, offers a variety of solutions for foundation, retaining wall and roadway projects. Our products and technologies, backed by the most thorough quality assurance practices, are at the forefront of the industry. Highly adaptable, cost-effective and installation friendly, they provide exceptional, long-term performance under the most demanding conditions. Our support services include site evaluation, design consulting and site construction assistance. For innovative solutions to your engineering challenges, rely on the experience, resources and expertise that have set the industry standard for more than two decades.

For more information on Uniaxial Geogrid or other Tensar Systems, visit www.tensar-international.com, call 800-TENSAR-1, or e-mail info@tensarcorp.com.



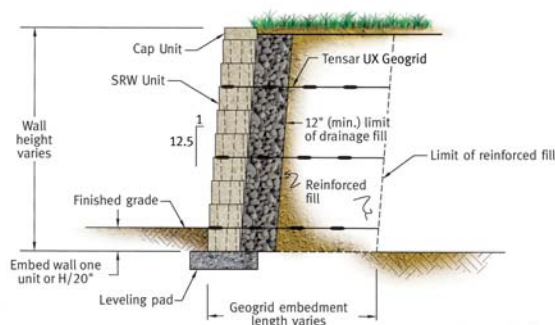
Tensar UX Geogrids install easily in stand alone applications as well as in conjunction with one of our proprietary soil stabilization systems.

PROPERTY SPECIFICATIONS FOR TENSAR® UNIAXIAL GEOGRIDS*

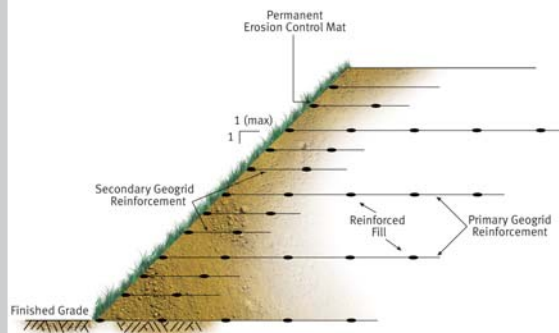
Index Properties							
GEOGRID PROPERTIES	LH800	UX1000	UX1100	UX1400	UX1500	UX1600	UX1700
Tensile Strength @ 5% Strain (kN/m (lb/ft))	14 (960)	23 (1,570)	27 (1,850)	31 (2,130)	52 (3,560)	58 (3,980)	75 (5,140)
Ultimate Tensile Strength (kN/m (lb/ft))	38 (2,600)	46 (3,150)	58 (3,970)	70 (4,800)	114 (7,810)	144 (9,870)	175 (11,990)
Junction Strength (kN/m (lb/ft))	32.5 (2,230)	43 (2,950)	54 (3,690)	66 (4,520)	105 (7,200)	135 (9,250)	160 (10,970)
Flexural Stiffness (mg-cm)	350,000	400,000	500,000	730,000	5,100,000	6,000,000	9,075,000
Load Capacity							
GEOGRID PROPERTIES	LH800	UX1000	UX1100	UX1400	UX1500	UX1600	UX1700
Maximum Allowable (Design) Strength (kN/m (lb/ft))	12.2 (835)	16.8 (1,150)	21.2 (1,450)	25.6 (1,760)	41.8 (2,860)	52.7 (3,620)	64.1 (4,390)
Recommended Allowable Strength Reduction Factors							
GEOGRID PROPERTIES	LH800	UX1000	UX1100	UX1400	UX1500	UX1600	UX1700
Minimum Reduction Factor for Installation Damage (RF _{ID})	1.05	1.05	1.05	1.05	1.05	1.05	1.05
Reduction Factor for Creep for 120 yr design life (RF _{CR})	2.96	2.60	2.60	2.60	2.60	2.60	2.60
Minimum Reduction Factor for Durability (RF _D)	1.00	1.00	1.00	1.00	1.00	1.00	1.00

* Tensar International Corporation (Tensar) reserves the right to change its product specifications at any time. It is the responsibility of the specifier and purchaser to ensure that product specifications used for design and procurement purposes are current and consistent with the products used in each instance. Tensar warrants that at the time of delivery the geogrid furnished hereunder shall meet its published specifications as of the date of manufacture of the product. NO OTHER WARRANTY, EXPRESSED OR IMPLIED, INCLUDING MERCHANTABILITY OF FITNESS FOR A PARTICULAR PURPOSE, IF PROVIDED AND ANY AND ALL SUCH OTHER WARRANTIES ARE SPECIFICALLY EXCLUDED. The sole remedy to the purchaser or user of our products for breach of the above-mentioned warranty is the replacement of the geogrid material. Notification of any such breach shall be made within three (3) months of product delivery and prior to installation. The applicable product specification supersedes all prior specifications for the product. Unless indicated otherwise, values shown are minimum average roll values determined in accordance with ASTM D4759. Brief descriptions of test procedures are given in the notes found online at www.tensar-international.com. Call 800-TENSAR-1 for a complete list of property specifications and notes associated with these Tensar® UX Geogrid properties.

SRW Typical Cross-Section



RSS Typical Cross-Section



THE COMPANY YOU CAN BUILD ON®

Tensar International Corporation
 5883 Glenridge Drive, Suite 200
 Atlanta, Georgia 30328
800-TENSAR-1
www.tensar-international.com

**APPLICATION FOR PERMIT RENEWAL AND MODIFICATION
SANDOVAL COUNTY LANDFILL**

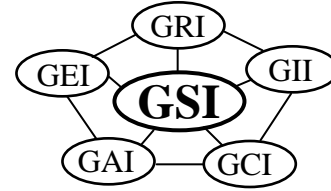
**VOLUME III: LANDFILL ENGINEERING CALCULATIONS
SECTION 7: GEOSYNTHETICS TENSILE STRESS AND STABILITY ANALYSIS**

ATTACHMENT III.7.G

***DETERMINATION OF THE LONG-TERM DESIGN STRENGTH OF FLEXIBLE
GEOGRIDS, GRI STANDARD PRACTICE GG4(B),
GEOSYNTHETIC INSTITUTE (2013).***

Geosynthetic Institute

475 Kedron Avenue
Folsom, PA 19033-1208 USA
TEL (610) 522-8440
FAX (610) 522-8441



adopted - 1991
revised 2005, 2012
current revision 12/21/12

GRI Standard Practice GG4(b)*

Standard Practice for

"Determination of the Long-Term Design Strength of Flexible Geogrids"

This specification was developed by the Geosynthetic Research Institute (GRI) with the cooperation of the member organizations for general use by the public. It is completely optional in this regard and can be superseded by other existing or new specifications on the subject matter in whole or in part. Neither GRI, the Geosynthetic Institute, nor any of its related institutes, warrant or indemnifies any materials produced according to this specification either at this time or in the future.

1. Scope

- 1.1 This standard practice is to be used to determine the long-term design strength of flexible geogrids for use in the reinforcement of such structures as embankments, slopes, retaining walls, improved bearing capacity, and other permanent geotechnical and transportation engineering systems. By "flexible" the Standard Practice is meant to be applicable to those geogrids exhibiting less than 1000 g-cm flexural rigidity in the ASTM D1388 stiffness test.
- 1.2 The method is based on the concept of identifying and quantifying reduction factors for those phenomena which can impact the long-term performance of flexible geogrid reinforced systems and are not taken into account in traditional laboratory testing procedures.
- 1.3 The reduction factors to be considered are for installation damage, creep deformation, long term degradation, and joints (seams and connections).

*This GRI standard is developed by the Geosynthetic Research Institute through consultation and review by the member organizations. This practice will be reviewed at least every 2-years, or on an as-required basis. In this regard it is subject to change at any time. The most recent revision date is the effective version.

Note 1: Previous versions of this practice included a reduction factor for biological degradation. Since this has not been a factor for the polymers used in geogrid manufacturing it has been removed in this revision.

- 1.4 These reduction factors values can be obtained by direct experimentation and measurement, or by using default values which are given for the various applications which use geogrids.

2. Reference Documents

2.1 ASTM Standards

D123 Terminology Relating to Textiles
D1388 Test Methods for Stiffness of Fabrics
D4354 Practice for Sampling Geotextiles
D4439 Terminology for Geotextiles
D4595 Tensile Properties of Geotextiles by the Wide Width Strip Method
D5262 Tension Creep Testing of Geosynthetics
D5322 Practice for Laboratory Immersion Procedures for Evaluating the Chemical Resistance of Geosynthetics to Liquids
D5818 Practice for Exposure and Retrieval of Samples to Evaluate Installation Damage of Geosynthetics
D6213 Practice for Tests to Evaluate the Chemical Resistance of Geogrids to Liquids
D6637 Standard Test Method for Determining Tensile Properties of Geogrids by the Single or Multi Rib Tensile Method
D6992 Test Method for Accelerated Tensile Creep and Creep Rupture of Geosynthetic Materials Based on Time-Temperature Superposition Using the Stepped Isothermal Method
D7737 Test Method for Individual Geogrid Junction Strength

3. Terminology

- 3.1 General - Many of the terms used in this standard are relatively new and undefined by standards groups such as ASTM, ISO, etc. Therefore a section devoted to definitions follows.

3.2 Definitions

3.2.1 Geogrids - A synthetic planar structure formed by a regular network of tensile strength elements with apertures of sufficiently large size to allow for interlocking with the surrounding soil so as to perform the primary function of reinforcement.

3.2.2 Flexible Geogrids - Those geogrids exhibiting a stiffness, or flexural rigidity, of less than 1000 g-cm as tested via ASTM D1388. These geogrids are generally made by a textile weaving process and generally involve polyester, polyvinyl alcohol or fiberglass yarns.

3.2.3 Apertures - The open spaces formed between the interconnected network of longitudinal and transverse ribs of a geogrid.

3.2.4 Strike-Through - The ability of the soil backfill to be continuous through the apertures of the geogrid allowing for bearing capacity against the transverse ribs.

3.2.5 Longitudinal Ribs - The continuous elements of a geogrid which are in the machine direction as manufactured, or in the major principal stress direction as placed in the field.

3.2.6 Transverse Ribs - The continuous elements of a geogrid which are in the cross machine direction as manufactured, or in the minor principal stress direction as placed in the field.

3.2.7 Junctions (or Nodes) - The interconnections between the longitudinal and transverse ribs of a geogrid which hold the grid structure together providing dimensional stability and load transfer mechanisms.

3.2.8 Joints (or Connections) - The connections made between separate geogrid rolls or between geogrids and wall panels or other parts of the structural system.

3.2.9 Design Strength (T_{design}) - The design, or required, strength of a geogrid needed for successful functioning of the system. It is often arrived at by an appropriate geotechnical design model.

3.2.10 Ultimate Geogrid Strength (T_{ult}) - The ultimate or maximum geogrid strength, T_{ult} , as determined by a short-term strength test in accordance with an accepted ASTM D6637.

3.2.11 Allowable Geogrid Strength (T_{allow}) - The long-term, allowable strength, T_{allow} , to be used in design taking into account all of the phenomena which could influence the geogrid during its service lifetime.

3.2.12 Factor-of-Safety - A numeric comparison of the geogrid's allowable tensile strength to the design or required tensile strength. The minimum acceptable value reflects the accuracy in defining load conditions, uncertainties in design methods, definition of soil strength and other design parameters.

3.2.13 Reduction Factors - A set of numeric values each of which is focused on a particular phenomenon which may adversely impact the geogrid's performance.

3.2.14 Atmosphere for Testing Geogrids - Ambient air conditions maintained at a temperature of $21 \pm 2^{\circ}\text{C}$ ($70 \pm 4^{\circ}\text{F}$) and a relative humidity of $65 \pm 5\%$.

4. Summary

- 4.1 This standard practice is meant to adjust a laboratory generated short term ultimate geogrid tensile strength value to a site-specific allowable long-term tensile strength value by using reduction factors for selected phenomena. It is then to be used with a factor-of-safety for the site-specific situation under consideration.
- 4.2 The focus of the standard is toward flexible geogrids with a flexural rigidity of less than 1000 g-cm.
- 4.3 Specific procedures for quantifying each of the reduction factors are provided. If these procedures are not followed default values are provided.

5. Significance and Use

- 5.1 Rather than use an unusually high overall factor-of-safety for geogrid reinforced structures (in comparison to those factors-of-safety used in a conventional design involving soil, concrete or steel), this standard of practice uses reduction factors for those particular phenomena which may diminish the performance of the as-received geogrid material.
- 5.2 The reduction factors to be discussed are those of installation damage, creep deformation, chemical degradation, and joints (seams and connections). The result of compensating for these phenomena is an allowable geogrid strength which can be used directly in design.

Note 2: Some applications such as walls and slopes require holes for guard posts, lights, signage, etc. to penetrate through the geogrid reinforcement. If this is the case, an additional reduction factor should be included, e.g., “RF_{Holes}”. Its value has been shown to be a linear reduction of its diameter to the width of the geogrid product: See Reference 11.3.

- 5.3 Procedures are given as to how one obtains each of the above reduction factors for the various phenomenon to be discussed, e.g., installation damage, creep, chemical degradation and joint strength.
- 5.4 As an option to conducting the above procedures, default values are given for each of the different phenomena depending on the particular geogrid reinforcement application.
- 5.5 The standard practice is site specific, application specific, and geogrid product specific, the latter being for flexible geogrids of flexural rigidity of less than 1000 g-cm.
- 5.6 This standard practice is not meant to be a test method, but does require various test protocols to obtain the necessary values for the different reduction factors.

6. Reduction Factor Concept

- 6.1 Required Strength ($T_{\text{reqd.}}$) - The required (or design) strength of a geogrid is that numeric value needed for successful functioning of the geogrid under consideration. For geogrid applications it is often calculated by a geotechnical engineer using an applicable design model, adapted for the geogrid's inclusion. It might also be defined in a formal specification or recommended by an owner. The units of T_{reqd} are in kN/m or lb/ft.
- 6.2 Ultimate Strength (T_{ult}) - The ultimate strength of a geogrid is obtained by one of the following tests. Note that some of them are short term tests which are often used for quality control, while others are long term tests used as performance indicators.
- 6.2.1 ASTM 6637 - This test is a single or multiple rib tensile strength test measuring the short term strength of the longitudinal ribs (or transverse ribs) resulting in a value in units of kN or lbs. By calculation using the number of repeating ribs it is extended to units of kN/m or lb/ft.
- 6.2.2 ASTM D5262 - This test is a sustained load (or creep) test for geosynthetics. It is of the wide width variety in that multiple ribs are evaluated simultaneously. The test is conducted for a minimum time of 10,000 hours. It has been traditionally used to obtain a RF_{CR} -value.
- 6.2.3 ASTM D6992 - This is also an accelerated sustained load (creep) test using stepped temperature increments under the concept of time-temperature-superposition. It greatly shortens the time to arrive at a long term strength value. It is presently generally used to obtain a RF_{CR} -value.
- 6.3 Allowable Strength (T_{allow}) - The allowable long-term strength of a flexible geogrid is to be used in a traditional factor-of-safety formulation and compared directly to the required, or design strength. Note that the allowable strength must always be greater than or equal to the required, or design.

$$T_{\text{allow}} \geq T_{\text{reqd}} \quad (1)$$

Furthermore, both T_{allow} and T_{reqd} are less than T_{ult} since they are used to determine the global factor-of-safety value.

$$FS = T_{\text{ult}} / T_{\text{allow}} \quad (2)$$

where

FS = factor-of-safety for unanticipated loading, construction and material uncertainties and other unknowns (typically a value from 1.25 to 1.5)
 T_{ult} = ultimate strength (kN/m or lb/ft)

T_{allow} = allowable strength (kN/m or lb/ft)
 T_{reqd} = required (or design) strength (kN/m or lb/ft)

- 6.4 Reduction factors - A mechanism by which an ultimate strength of a particular geogrid can be adapted to an allowable strength using values tuned to site specific conditions is affording by using reduction factors. For example, using geogrids in reinforcement applications the following should be used.

$$T_{\text{allow}} = T_{\text{ult}} \left[\frac{1}{\text{RF}_{\text{ID}} \times \text{RF}_{\text{CR}} \times \text{RF}_{\text{CD}} \times \text{RF}_{\text{JNT}}} \right] \quad (3)$$

where

RF_{ID} = reduction factor for installation damage
 RF_{CR} = reduction factor for creep deformation
 RF_{CD} = reduction factor for chemical degradation
 RF_{JNT} = reduction factor for joints (seams and connections)

Note 3: Temperature, per se, is not included as a reduction factor. If site-specific temperatures are of concern the various tests should be suitably accommodated with the mutual agreement of the parties involved.

7. Default Values for Reduction Factors

In the absence of test information and documentation as to the site specific values for the above listed values of reduction factors in Equation 3, the following default values should be used.

Table 1 - Default Values for Flexible Geogrids for Various Reduction Factors
(Terms are Defined in Equation 3)

Application	RF_{ID}	RF_{CR}	RF_{CD}	RF_{JNT}
embankments	1.4	3.0	1.4	2.0
slopes	1.4	3.0	1.4	2.0
retaining walls	1.4	3.0	1.4	2.0
bearing capacity	1.5	3.0	1.6	2.0

It should be mentioned that the values given in Table 1 are considered to be upper-bound values. Since the impact of multiplying these numbers together for a particular application is very significant in decreasing the ultimate strength, it is usually worthwhile to consider the specific procedures for evaluating the individual reduction factors. They follow in the order presented in Equation 3.

8. Procedures for Evaluating Individual Reduction Factor Values

- 8.1 Installation Damage, RF_{ID} - Installation damage of a specific type of geogrid is determined by installing a field test strip on the actual site's subgrade, or on a closely simulated version thereof. The geogrid is positioned in place, tensioned as per the intended final installation, and then backfilled using the site specific backfill material, lift height, placement equipment and compaction equipment. If these details are not known at the time of the test, worst case conditions should be assumed. The minimum size of the geogrid test strip is to be 9 m^2 (100 ft^2). If possible, the full roll width should be used. Upon completion of the backfilling the geogrid should be carefully exhumed so as not to create damage. The exhuming should be done immediately, i.e., it is a survivability test and not a long-term aging type of test.

Note 4: Past exhuming of geogrids has shown the removal of backfill to be an important consideration in that a significant amount of hand excavation is necessary. If the backfill layer is 30 cm (12 in.) or more, some of it can be removed by a front end loader or backhoe but the lower 15 cm (6 in.) should be removed by hand. Never use a bulldozer or road grader since the scraping action will likely damage the geogrid.

The exhumed geogrid is now tested for its residual strength using single or multiple ribs per ASTM D6637 and compared to test values of the comparable geogrid material which was not installed. The non-installed geogrid should be taken from the same roll as was the installed and exhumed geogrid.

The resulting reduction factor is formulated in a traditional matter, i.e.

$$RF_{ID} = T_{\text{orig.}}/T_{\text{exh.}} \quad (4)$$

where

RF_{ID} = reduction factor for installation damage

$T_{\text{orig.}}$ = original strength as per D6637

$T_{\text{exh.}}$ = exhumed strength as per D6637

A minimum number of thirty single rib tests in the machine direction for unidirectional geogrids, and twenty single rib tests in both the machine and cross machine directions for bidirectional geogrids, is necessary. The average value of these tests is to be used in the above formulation for the value of reduction factor for installation damage. The same type of test must be used for both original and exhumed samples, e.g., if multiple rib tests are being used for the original strength they must also be used to evaluate the exhumed strength.

Note 5: The above protocol for determining the installation damage of geogrids can alternatively use the ASTM D5818 Standard Practice. The procedures are approximately equivalent to one another.

- 8.2 Sustained Load Creep, RF_{CR} - The long-term deformation of geogrids under constant tensile stress can be avoided by using a suitable reduction factor. Called a creep reduction factor, FS_{CR} , it is obtained by hanging a dead weight on a suitably supported geogrid test specimen and monitoring its deformation versus time. The recommended test procedure for geogrids is contained in ASTM D5262 entitled, "Tension Creep Testing of Geosynthetics". Typical creep response curves are shown in Figure 1 for 10,000 hour duration tests. These are the minimum test times using this method.

This data can be extrapolated out one order of magnitude, to approximately 10 years, as a standard polymeric rule of thumb (ASCE Manual of Practice No. 66). RF_{CR} for calculating the T_{allow} for design lives in excess of 10 years may be determined as outlined in 8.2.2 or 8.2.3.

8.2.1 RF_{CR} for 10 Year Design Life - The reduction factor for creep is determined from the 10,000 hour curves as being the load at which the creep curve becomes asymptotic to a constant strain line, of 10 percent or less. This value of strength is then compared to the short term strength of the geogrid in D6637 evaluation as follows:

$$RF_{CR} = T_{ST}/T_{LT}$$

where

- RF_{CR} = reduction factor against creep
- T_{LT} = 10 year design life strength of the geogrid in sustained D6637 or ASTM D5262 testing at which curve becomes asymptotic to a constant strain line (see "limit" on following curves)
- T_{ST} = short term strength of the geogrid in D6637 testing whichever is comparable to the long term creep test, i.e., wide width or single rib test

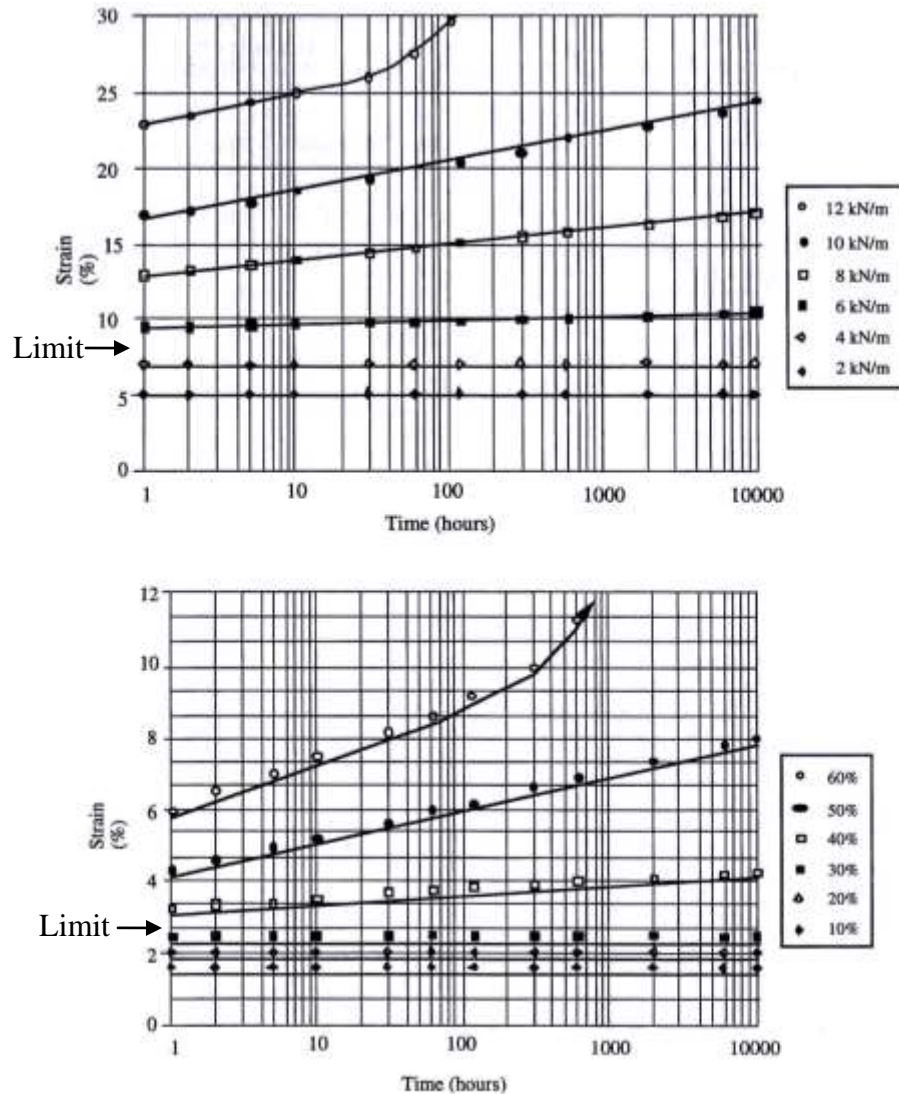


Fig. 1 - Typical Geogrid Curves Taken to 10,000 Hour Duration

8.2.2 RF_{CR} -values for Design Times Greater Than 10 Years - Creep performance data of a polymer product at a desired temperature is limited to one order of magnitude in extrapolation with time (as per ASCE). However, creep performance data at an elevated temperature permits an additional order of magnitude in extrapolation with time via time-temperature superposition principles. Creep curves from elevated temperature testing may be overlaid upon the creep curves at the desired temperature by shifting the abscissa time scale. The magnitude of the shift in time for overlay is the magnitude of the extrapolation of creep data beyond 10 years. Thus elevated temperature testing can predict creep performance of a polymer geogrid at the desired temperature level in excess of 10 years. See the Appendix to ASTM D5262 for the procedure.

8.2.3 The stepped isothermal method (SIM), per ASTM D6992, takes temperature shifting with discrete specimens a step further. SIM increments both temperature and time (appropriately called time-temperature-superposition) on the same test specimen so as to project long term creep in extremely short testing durations. The advantage in addition to greatly shortened testing duration is that there is no test specimen variation between different temperature increments.

- 8.3 Chemical Degradation - The reduction factor for potential chemical degradation of a geogrid is determined by testing before and after immersion in the specific liquid environment under consideration. Resistivity data is a good indication if a problem may arise. Such resistivity charts should be based on immersion tests. The immersion procedure to be used follows the ASTM D5322 Test Methods. Note that the EPA 9090 test method is presently depreciated. In these procedures samples are immersed in a closed container made from stainless steel which is filled with the agreed upon liquid and generally with zero head space. Four (4) geogrid samples measuring approximately 30 by 30 cm (12 by 12 in.) are to be used in each of two identical immersion tanks. One tank is kept at a constant temperature of 23°C, the second tank is kept at 50°C. The selection of the incubation liquid should model site specific conditions as closely as possible and be mutually agreed upon by the parties involved in the testing and acceptance. The precise procedure to be followed is set forth in the referenced standards.

Note 6: The selection of the liquid to be used for immersion is a critical decision and must be well planned and agreed upon by all parties concerned. If it is an aggressive and/or hazardous liquid, proper laboratory procedures and cautions must be followed. The standard operating procedures used for geomembrane evaluation must be followed.

At time periods of 30, 60, 90, and 120 days one sample from each tank is removed, blotted dry of liquid and cut for test specimens to be used in ASTM D6213. As many replicate test specimens as possible from each sample should be obtained for statistical averaging.

Note 7: This is a geogrid specific decision since the geometric patterns of different geogrids vary widely. Discussion among the parties involved should agree upon the specimen cutting pattern before incubation of the samples begins.

For uniaxial applications, the longitudinal ribs are to be tested, for biaxial applications, both the longitudinal and the transverse ribs are to be tested. The results of the average values of the incubated test specimens are to be compared to nonincubated test specimens (in the same type of test) and plotted as per Figure 2.

If the data appears well behaved in that no erratic trends are observed and if the 50°C change is greater or equal to the 23°C change and in the same direction (i.e., increasing or decreasing), the reduction factor is obtained as follows.

$$RF_{CD} = \frac{1}{1 - R_{50-120}}$$

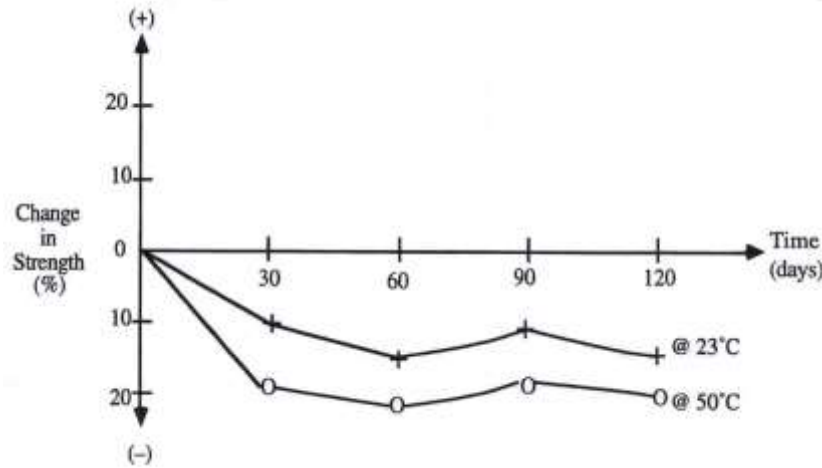


Figure 2. - Example Trend Curves from Chemical Incubation

where

RF_{CD} = reduction factor for chemical degradation

R_{50-120} = strength reduction ratio of the 50°C incubation test at 120 days exposure (absolute value)

If the data is not well-behaved the entire immersion and subsequent strength tests must be repeated.

Note 8: Previous versions of this standard practice had a separate reduction factor for “biological degradation”. Presently it is the institute’s opinion that degradation from bacteria and fungi is so unlikely as to not warrant this remote form of degradation to geosynthetic polymer products. This is clearly not the case for natural biologic products, e.g., jute, coir, etc.

8.4 Joint Strength - Whenever seams are required to join geogrid panels together or connections are to be made with wall panels or other structural systems, a reduction factor for joint strength must be included. The test procedure to be followed is a sustained ASTM D5262 test. Note that this test is to be conducted for 1,000 hours at a minimum. The comparative tests include one with the joint in the center of the test specimen and the second with no joint included. In both cases, the stress at which a horizontal asymptote is reached is to be used in calculating the value of RF_{JNT} . Its formulation is as follows:

$$RF_{JNT} = T_{\text{as-received geogrid}} / T_{\text{joined geogrid}}$$

Note 9: This section on joint strength has been written around a mechanical joint such as a bodkin, pin or clamp. For those cases where the joint strength is mobilized by overlapping two sheets of geogrid, or a geogrid placed within a structural system (e.g., a block wall), a friction test is necessary. ASTM D5321 should be used in this regard.

9. Report

- 9.1 A complete description of the geogrid product tested including the product name, manufacturer and style; longitudinal rib dimensions, repeat pattern and other relevant characteristics; transverse rib dimensions, repeat pattern and other relevant characteristics; junction (node) construction, fabrication including coating type and approximate thickness, and other relevant characteristics; mass per unit area of the product and stiffness as per ASTM D1388.
- 9.2 Details as to determination of RF_{ID} and the resulting average value. This must describe the entire process in a step-by-step procedure. If the value obtained is less than the default value given in Table 1, it should be clearly stated as being such.
- 9.3 Details as to determination of RF_{CR} and the resulting average value. This must describe the entire process in a step-by-step procedure. If the value obtained is less than the default value given in Table 1, it should be clearly stated as being such.
- 9.4 Details as to determination of RF_{CD} and the resulting average value. This must describe the entire process in a step-by-step procedure. If the geogrid changes in color, texture, appearance or other surface feature it must be described. If the value obtained is less than the default value given in Table 1, it should be clearly stated as being such.
- 9.5 Details as to determination of RF_{JNT} and the resulting value. This must describe the entire process in a step-by-step procedure. If the value obtained is less than the default value given in Table 1, it should be clearly stated as such. If no seams or connections are involved, this item is to be omitted.
- 9.6 Details as to determination of the ultimate strength of the geogrid (T_{ult}) which is to be used in Equation 3.
- 9.7 Calculation of the allowable strength of the geogrid (T_{allow}), as per Equation 3, for use in long-term design of geogrids.

10. Example

The use of the method of modifying a short term index-type test value of strength into a site specific long term allowable (or performance) value of strength using reduction factors is illustrated in the following example.

Example: What is the allowable tensile strength of a flexible geogrid to be used in the construction of a permanent embankment if the ultimate short-term strength is 4200 lb/ft and the reduction factors have the following values? (Note that this problem does not require a RF_{JNT} since full rolls will be involved and no facing panels are present)

$$RF_{ID} = 1.25 (< 1.4 \text{ default value})$$

$$RF_{CR} = 2.5 (< 3.0 \text{ default value})$$

$$RF_{CD} = 1.2 (< 1.4 \text{ default value})$$

Solution: Since the measured values were all less than (or equal to) the default values, the measured values are used in the calculations.

$$\begin{aligned} T_{\text{allow}} &= T_{\text{ult}} \left[\frac{1}{RF_{ID} \times RF_{CR} \times RF_{CD}} \right] \\ &= 4000 \left[\frac{1}{1.25 \times 2.5 \times 1.2} \right] \\ &= 4200 \left[\frac{1}{3.75} \right] \\ &= 1120 \text{ lb/ft} \end{aligned}$$

11. References

- 11.1 American Society of Civil Engineers, "Structural Plastics Selection Manual," ASCE Manuals and Reports on Engineering Practice No. 66, prepared by Task Committee on Properties of Selected Plastics Systems of the Structural Plastics Research Council of the Technical Council on Research of ASCE, New York, 1985, pp. 584.
- 11.2 See White Paper #25 (2012) on GSI's website www.geosynthetic-institute.org which in turn is based on Koerner, R. M., Hwu, B.-L. and Wayne, M. H. (1986), "Soft Soil Stabilization Designs Using Geosynthetics," Proc. GRI-1 on Soft Soil Stabilization Using Geosynthetics Conference, GSI, Folsom, PA, pp. 33-51 and Jour. Geotextiles and Geomembranes, Vol. 6 (1987), pp. 33-51.

**APPLICATION FOR PERMIT RENEWAL AND MODIFICATION
SANDOVAL COUNTY LANDFILL**

**VOLUME III: LANDFILL ENGINEERING CALCULATIONS
SECTION 7: GEOSYNTHETICS TENSILE STRESS AND STABILITY ANALYSIS**

ATTACHMENT III.7.H

**THIEL, RICHARD. A *TECHNICAL NOTE REGARDING INTERPRETATION OF
COHESION (OR ADHESION) AND FRICTION ANGLE IN DIRECT SHEAR TESTS.*
GEOSYNTHETICS, APRIL MAY 2009 VOLUME 27: PPS 10-19.**

A TECHNICAL NOTE REGARDING INTERPRETATION OF COHESION AND FRICTION ANGLE IN DIRECT SHEAR TESTS

There is often confusion expressed in the geosynthetics industry over how laboratory direct shear results should be interpreted, specifically whether one should use both the friction angle and cohesion (or adhesion) parameters. The attached technical note from the April/May 2009 issue of *Geosynthetics* provides some guidance regarding this question, as well as several other issues related to direct shear results.

Please note that this article is not intended to replace education or experience and should only be used in conjunction with professional judgment. In the end, all data should be evaluated by an experienced practitioner qualified to use the test results properly.

A technical note regarding interpretation of cohesion (or adhesion) and friction angle in direct shear tests

By Richard Thiel

Introduction

Direct shear testing with geosynthetics is generally performed in accordance with ASTM D5321, *Standard Test Method for Determining the Coefficient of Soil to Geosynthetic or Geosynthetic to Geosynthetic Friction by the Direct Shear Method*. There is also a related standard, D6243, *Standard Test Method for Determining the Internal and Interface Shear Resistance of Geosynthetic Clay Liner by the Direct Shear Method*. This technical note applies to both equally.

Interpreting lab results

There is often confusion expressed in the industry regarding how laboratory results should be interpreted, specifically: whether one should use both the friction angle and cohesion (or adhesion) parameters; whether cohesion should be ignored; whether secant friction angles are more appropriate; what to do if the data are nonlinear; and how the data should be interpolated or extrapolated.

The goal of this technical note is to provide some guidance to take the mystery out of these questions. In the end, all data should be evaluated by an experienced practitioner qualified to use the test results properly.

What this note will not do is go into the subtleties of requesting, setting up, calibrating, and performing a direct shear test. That would be the subject of additional articles.

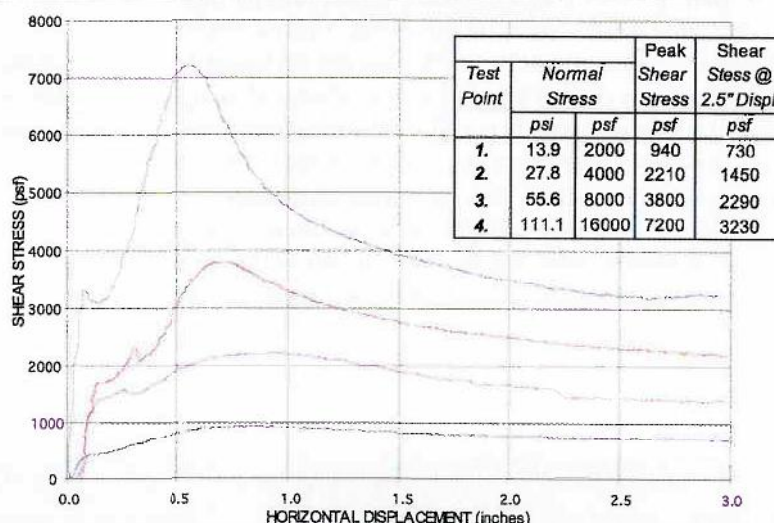
This article will also not definitively describe how direct shear test data should be interpreted. That is the responsibility of a professional with specific expertise, and one article could never presume to cover all of the considerations that might apply to any unique design problem that might arise. That is why professionals are trained and mentored in basic geotechnical principles: so they can appropriately account for

the various factors affecting a design and make appropriate decisions regarding test data interpretations.

The typical sequence of events related to direct shear testing includes the following:

1. An engineer requests a direct shear test series to obtain data to help solve a problem. The request should be very specific with regard to all the necessary details regarding

Material 1:	GSE 40 mil HDPE Tex / Tex (White side towards GCL)
Material 2:	Bentomat DN GCL (black side up) Roll # 00000481
Substrate:	GSE 60 mil HDPE Tex-white / Tex-black (Black side toward GCL)



The "gap" between shear boxes was set at 80 mil (2.0 mm)
The test specimens were flooded during testing.
High Normal Stresses, >5psi (35 kPa) was applied using air pressure.
Low Normal Stresses, <5psi (35 kPa) was applied using dead weights.
The tests were terminated after 3.0" (75 mm) of displacement unless otherwise noted.
Tests were performed in general accordance with ASTM procedure D-5321 using a Brainard-Killman LG-112 direct shear machine with an effective area of 12" x 12" (300 x300 mm).
Each specimen of 60 mil geomembrane was cut to 14" x 20" and clamped to the lower shear box. Avg. Asperity =0.025"
Each specimen of 40 mil geomembrane was cut to 14" x 16" and clamped to the upper shear box. Avg. Asperity =0.016"
Each GCL specimen was Hydrated for 48 hrs at the 250 psf, then placed, unclamped between upper & lower HDPEs
The grouped specimens were consolidated 16 hrs. under the specified normal stress, then sheared
Shearing occurred at the interface of the GCL's and 40 mil geomembrane specimens.
Extrusion of bentonite was noted on the surface of the 40 mil & white side of the GCL contact area for points 2,3 & 4
The Friction Angle and Adhesion (or Cohesion) results given here are based on a mathematically determined best fit line.
Further interpretation should be conducted by a qualified professional experienced in geosynthetic and geotechnical engineering.

| Richard Thiel is a senior project manager at Vector Engineering Inc. in Grass Valley, Calif.

The Designer's Forum column is refereed by Greg Richardson, Ph.D., P.E., a principal at RSG & Associates, Raleigh, N.C., www.rsgengineers.com

sampling, specimen preparation and setup in the testing device, and test execution in accordance with both project-specific conditions and industry standards.

2. A competent and certified laboratory performs the test series in accordance with the request and the industry standard test method (e.g., ASTM D5321 or D6243). The laboratory reports results to the engineer.

3. The engineer interprets and applies the results to the project design.

What we are measuring in the direct shear test is shear strength as a function of normal load. The test does not measure "friction" or "cohesion," as these are simply mathematical parameters derived from the laboratory test results.

Ideally the engineer who originally specified and required the shear test would be the same one who reviews and interprets the results. Sometimes, such as in a third-party construction quality assurance (CQA) project, an engineer other than the original designer will commission and review the testing. Interactions with test laboratories and other engineers over time have shown that there are often misconceptions and misunderstandings related to the interpretation of direct shear test data. Thus, this article is intended to serve the purpose of helping project participants avoid confusion. The key point of this article is that what we are measuring in the direct shear test is shear strength as a function of normal load. The test does not measure "friction" or "cohesion," as these are simply mathematical parameters derived from the laboratory test results.

Figure 1 presents shear test results of a 4-point test for an interface between a textured geomembrane and a reinforced GCL. Three shear points, each at a different normal stress, are the most common number of points used to run a test series, but the number of points could

vary from as few as one, to perhaps as many as six points, depending on many factors beyond the scope of this article. The figure shows: (a) a table of the normal stresses vs. peak and large-displacement shear strengths measured at 2.5in. of displacement, (b) graphs of the shear stress vs. displacement measurements, and (c) notes describing test conditions and observations.

There is adequate information in this figure for a trained practitioner to evaluate and use the data. The laboratory has performed its duty, which is to measure and report the shear strength under specified normal stresses (we are simplifying the dis-



cussion here by not elaborating on other factors such as hydration, consolidation, etc.), showing how the shear strength changed with displacement of the two surfaces, and providing descriptive and observational notes.

Figure 2 shows additional information that can be provided by a laboratory in the form of a graph of the peak and large-displacement strengths plotted as a function of normal stress. Best-fit straight lines, called Mohr-Coulomb strength envelopes, named after the gentlemen who first publicized the relationship between shear strength and normal stress, have been drawn through the two sets (peak and large-displacement) of data points.

Equations can be written for these lines, as we learned in first-year algebra class, in the form of $y = mx + b$. In this case we define y as the shear strength (S); m as the slope of the line that we call the "coefficient of friction" and whose angle is ϕ (ϕ), which we call the "friction angle" (and thus $\tan[\phi]$ is the slope of the line); x is the normal stress (N); and b is the y-intercept of the line that we call either "adhesion" (a , usually used for geosynthetics-only tests) or "cohesion" (c , usually used for tests involving soils, which will be used for the remainder of this article).

Mohr-Coulomb

In geotechnical engineering, we write the Mohr-Coulomb equation for these lines as:

$$S = N \cdot \tan(\phi) + c$$

This equation is written for peak, large-displacement, or residual shear strength conditions. The fundamental points in this article regarding the presentation of the data in Figure 2 include the following:

1. **The Mohr-Coulomb envelope should not be extrapolated beyond the limits of the normal stresses under which the testing was conducted.** To do so would never be conservative and, in fact, may be significantly nonconservative. The reason that simple extension-extrapolations of the Mohr-Coulomb

envelope are nonconservative is presented in Figure 3. Most shear strength envelopes are truly curved (nonlinear). This tendency for a curved failure envelope is exaggerated in Figure 3, but can clearly be identified for the real-life strength envelopes presented in Figure 2, in particular for large-displacement conditions.

The Mohr-Coulomb model is merely a linear simplification of a portion of the entire envelope over a limited range of normal stresses. If testing were performed over a large enough range of normal stresses the curvature would become

more apparent. True shear strength envelopes are found to be most accurately described by hyperbolic functions. Giroud et al. (1993) provides a good method to describe hyperbolic strength envelopes.

2. **The values of ϕ and c should be considered nothing more than mathematical parameters to describe the shear strength vs. normal stress over the normal-load range the test was conducted.** It is perhaps better not to think of "friction" and "cohesion" as real material properties, but simply as mathematical parameters to describe the failure envelope.

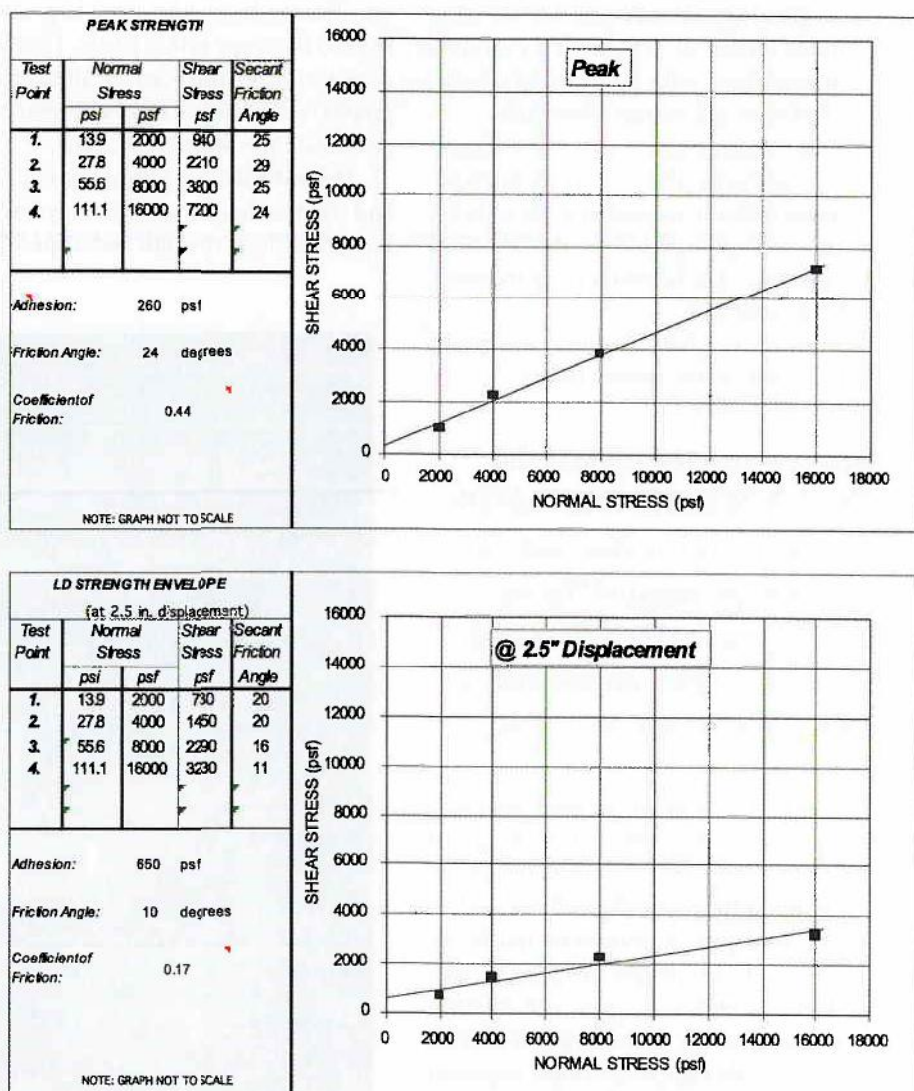


Figure 2 | Example of supplemental data interpretation provided by the laboratory.

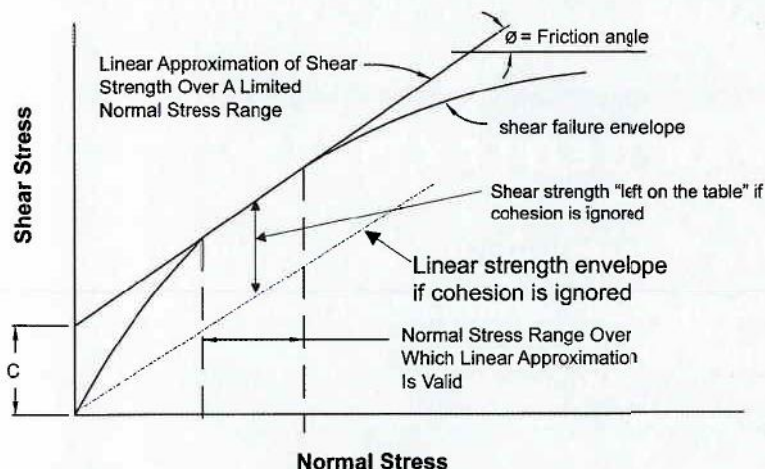


Figure 3 | Exaggerated schematic of true curvilinear shear strength envelope, linear interpretation over a selected normal stress range, and the penalty for ignoring cohesion.

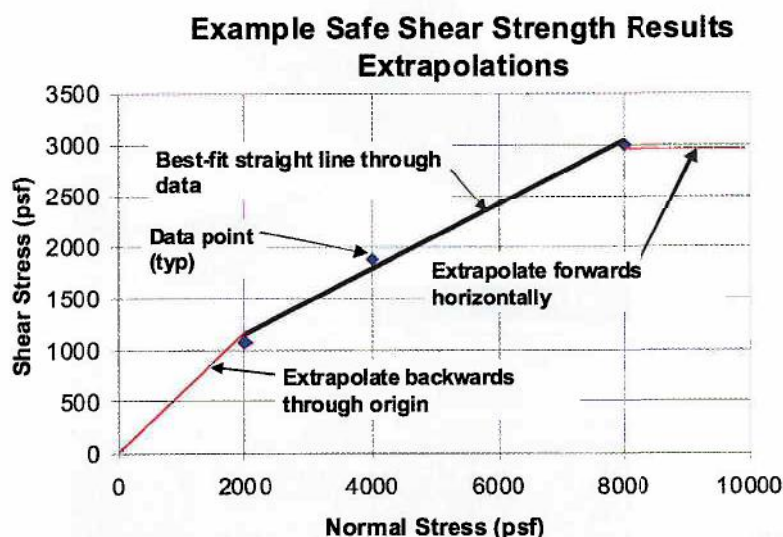


Figure 4 | Example of safe shear strength extrapolation.

In geotechnical practice with soils, there are situations and examples where the cohesion parameter is evaluated separately from the friction parameter, but these are sophisticated considerations that involve very project-specific materials and conditions and should only be done by experienced professionals.

For many geosynthetic interfaces and in the context of many types of projects, there is absolutely no reason to dissociate the slope of the line from its y-intercept, and the shear strength should be taken as

a whole in those cases. Other situations may occur, however, where it is appropriate, but those considerations are beyond the scope of this article.

3. In many, if not most, cases with geosynthetics where there is no reason to ignore the cohesion value, it is important to re-emphasize that shear strength should only be defined within the range of normal stresses for which the Mohr-Coulomb envelope was derived. Ignoring the cohesion may be unjustifiably penalizing the shear strength values that

were measured in the test, as illustrated in **Figure 3**.

Using the cohesion value at normal stresses extrapolated below the range of testing, however, could have dire consequences on the safety of a design project. This problem may occur when designers consider only the operational or final build-out of a facility and they ignore the construction condition. Several failures have occurred during construction because of this. For example, an embossed geomembrane against a geotextile may perform well under high normal loads by providing a good friction angle and a modest y-intercept for operating and final build-out conditions. However, under the low normal loads experienced during construction of a thin soil veneer on a steep sideslope, testing might reveal that the adhesion extrapolated from the high-normal load results do not exist at low normal loads. In this case, a more aggressive texturing that exhibits a "Velcro®-effect" type of adhesion, or a very high friction angle, at low normal loads may be needed and should be verified at the proper normal loads.

4. **Figures 1 and 2** also report *secant* friction angles for each point. These are the angles of the straight lines from each point drawn back to the origin. A key concept regarding secant friction angles is that you should never extrapolate a secant angle line beyond the normal load for which it is measured. Secant values are conservative as long as the secant values are derived from a test whose normal stress was greater than the normal stresses of the design. They can quickly become nonconservative if the same friction angle is used for higher normal loads.

5. If users wish to extrapolate shear strength data, **Figure 4** illustrates the only "safe" way to accomplish this. Going from the low end of the Mohr-Coulomb envelope and extrapolating backward, the data can be extrapolated by drawing a straight line back to the origin. Going from the high end of the Mohr-Coulomb envelope and extrapolating forward, the data can be extrapolated by drawing a straight line

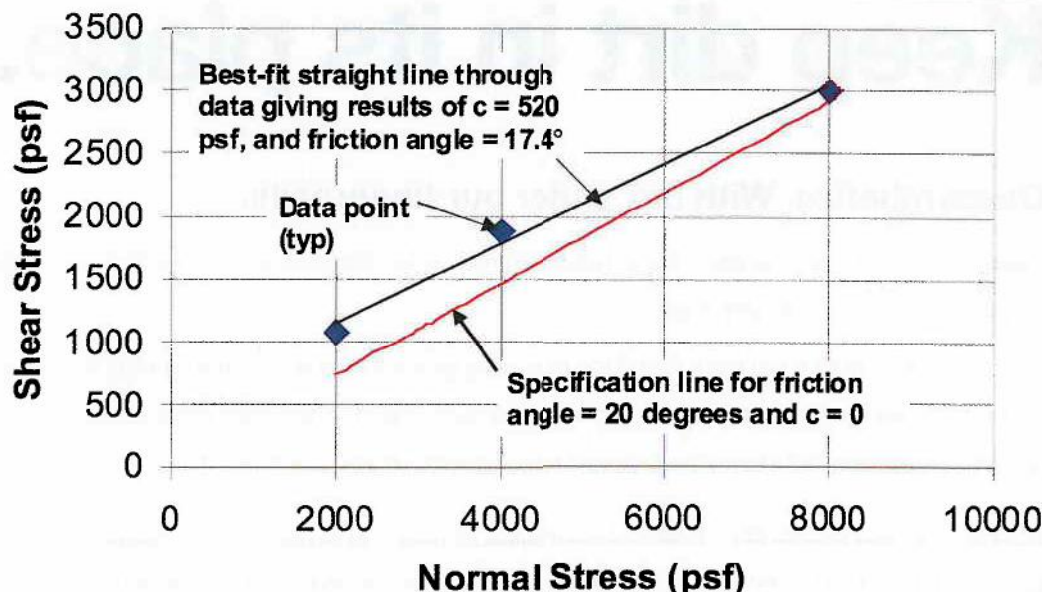


Figure 5 | Example project results where interpretation of test data results in lower friction angle than specified value, even though shear strength results are higher than the failure envelope implied by the specifications.

horizontally forward. This extrapolation rule is safe only when considering a single interface. When multiple interfaces are involved, it is not safe to extrapolate a multi-layered system on the high side of the Mohr-Coulomb envelope.

From the discussion above, we can now look at the ASTM standard D5321 with more understanding and critical thought. The first thing to note is that the title of that standard is poorly worded. The title is “*Determining the Coefficient of...Friction...*” This is somewhat misleading because it implies that the designer is simply after a coefficient of friction. In fact, what designers need is a relationship between shear strength and normal stress. Therefore, a more appropriate title for this method would be “*Determining the Relationship between Shear Strength and Normal Stress for Soil-to-Geosynthetic or Geosynthetic-to-Geosynthetic Interfaces Using the Direct Shear Method.*” Note that ASTM D6243 has already rectified this problem in its title.

Another misleading element in ASTM D5321 is the definition of *adhesion* (which applies equally to cohesion), which it states as: “The shearing resistance between two adjacent materi-

als *under zero normal stress* (emphasis added). Practically, this is determined as the y-intercept to a straight line relating the limiting value of shear stress that resists slippage between two materials and the normal stress across the contact surface of the two materials.”

This is actually *two separate definitions*, which are most likely not the intent of the standard. The first part of this definition, which defines the adhesion as the shear strength at zero normal stress, is not applicable relative to the test method. It *could be true* if we proposed to test the interface at zero normal load, but that is rarely done and generally of no use. The industry would be better served by deleting the first part of the definition. In reality, the second part of the definition is the controlling aspect of the definition, and the “y-intercept” concept is the true nature of the adhesion value which, as stated above, is simply a mathematical parameter.

Note that ASTM D6243 has a different set of definitions, and it is not clear if those definitions are unique to that standard, or are intended to be industry norms. ASTM D6243 suggests that adhesion is the true shear strength when

there is truly zero normal load, and that cohesion is the mathematical parameter of the y-intercept obtained from the Mohr-Coulomb envelope. In the author’s opinion these definitions are acceptable as stated, but the audience should know that the definition of *adhesion* may conflict with other definitions put forward in the industry. Also, other authors have introduced other terms for the measurable shear strength under zero normal load, such as Lambe and Whitman’s (1969) “*true cohesion*.” Interested readers can research ASTM D6243 and the literature and judge for themselves.

Example problem 1

The following situation illustrates a common example of a problem that occurs with shear test data interpretation:

- A specification is written that requires a certain minimum interface friction angle to be achieved between a textured geomembrane and a GCL. For purposes of this example, the requirement is 20° peak shear strength for normal loads tested between 2,000 and 8,000 pounds per square foot (psf).
- The laboratory results, shown as an

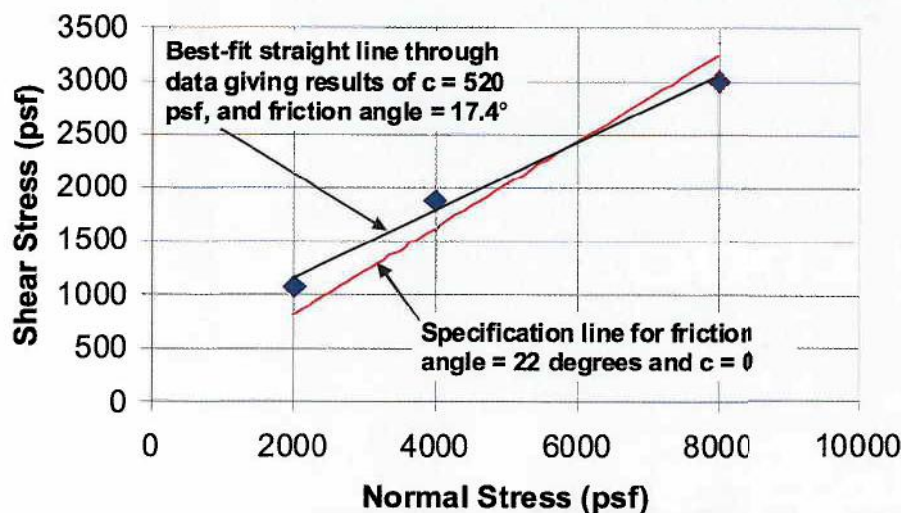


Figure 6 | Example project results where the two lower points are above the specification and the upper point is below the specification.

example in Figure 5, report a best-fit Mohr-Coulomb peak strength envelope with shear strength parameters of 500 psf cohesion and 15° friction. Figure 5 also shows the line representing the minimum project specification.

Inspection of Figure 5 shows that the shear strengths achieved in the direct shear test plot above the shear strength envelope required by the specification. Even though the plot appears to clearly indicate that the minimum required shear strength is achieved by the products tested, the author has experienced several projects where one of the project parties (e.g., the design engineer or perhaps a regulator) have declared the test a failure because the reported Mohr-Coulomb friction angle was less than the specified friction angle.

In the author's opinion, in many cases involving this particular interface, there is no reason to consider this a failing test.

This example illustrates the confusion that might arise when specification is written in terms of a shear-strength parameter, when the real objective is to achieve a certain value of absolute shear strength. Even though the materials provided the shear strength required by the specification, there is some confusion because one of the strength parameters did not meet the specified value for that parameter.

It is possible that the original specifier had taken into account the potential for cohesion, and had wished to discount cohesion, and really wanted a true minimum friction angle of 20°. If the specifier were truly that sophisticated and had such complex reasoning, then more than likely the specification would have also been more sophisticated in explaining these constraints on the test results.

In the author's experience it is rare that other designers and specifiers are discounting cohesion with geosynthetic interfaces, and usually it is simply a matter of proper interpretation and communication of the design intent compared to the actual test results. Nevertheless, as stated at the beginning of this article, it is not the intent of this article to provide guidance and suggestions on interpreting test results. Rather, the intent is to shed light on some common misunderstandings.

Example problem 2

The following problem has the same laboratory shear strength results as Problem 1, but the specification requirement is increased to 22° peak shear strength.

The relationship between the test results and the specification is shown in Figure 6. In this example, the two lower-normal load shear strength test results plot above the specification line, while the up-

per-normal load shear strength test result plots below the specification line. Based on the failing result of the upper-normal load test, most reviewers would initially say that this is a noncompliant test result and fails to meet the specification.

In the author's experience, curved failure envelopes are common, and the tendency for the highest normal-load result to fall beneath a straight-line friction-based specification is not unusual.

In this case, a more detailed review by the design engineer might reveal that the shear strength results provide an acceptable factor of safety for the intended purpose. It may be that the additional strength capacity provided in the lower normal load range that is above the specification more than offsets the reduced strength capacity in the upper normal load range that is below the specification. Clearly, the only person who can evaluate this issue, and who carries the requisite authority and responsibility, is the design engineer.

The following lessons can be gleaned from this example:

- Design engineers often attempt to specify a unique set of shear strength parameters as a minimum requirement for a given design. In reality, there may be an infinite combination of shear strength variations over the applicable range of normal loads that may satisfy the stability and shear resistance requirements, and many of these combinations may have a portion of their failure envelopes that fall below the specification.
- The tendency for natural and geosynthetic interfaces to yield curved failure envelopes can present a challenge to engineers, owners, and manufacturers who wish to optimize a design using simple straight-line shear strength specifications.
- A learned interpretation of direct shear testing data by an experienced practitioner may allow acceptance of apparently failing test results. This can occur because overly simplistic specification parameters may not ac-

count for other combinations of shear strength results that could provide acceptable overall shear resistance.

Summary

The direct shear test measures shear strengths as a function of normal stress. Period.

The test does not measure "friction angle" or "cohesion," as these values are parameters that are derived from the test results. Consideration of "friction angle" and "cohesion" simply as mathematical parameters used to describe shear strength data is of great benefit to practitioners for the following four reasons:

1. Interpretation of laboratory shear strength data should not be confused with the mathematical parameters used to describe it.

2. Proper data interpretation may avoid unnecessary penalization of the results by arbitrarily reducing the measured values.

3. This understanding can improve a designer's sensitivity to how important it is that shear strength is measured within the range of normal stresses that represent the design. Thus, the only defensible extrapolation of data should be: (a) back through the origin from the lowest normal stress, and (b) horizontally from the highest normal stress.

4. Laboratory shear strength data should be interpreted by a qualified practitioner experienced in the use and application of the results.

Often of much more importance than deciding whether to include or omit the cohesion (or adhesion) parameter is the

decision of whether to use peak, post-peak, or residual shear strength. This discussion is beyond the scope of this technical note, and anyone commissioning and interpreting shear strength testing should be well versed in the issues surrounding this topic, as well.

Acknowledgements

The author would like to thank Richard Erickson and Chris Athanassopoulos for their review of this article.

References

- Giroud, J.P., Darrasse, J., and Bachus, R.C., (1993). "Hyperbolic Expression for Soil-Geosynthetic or Geosynthetic-Geosynthetic Interface Shear Strength", *Geotextiles and Geomembranes*, Vol. 12, No.3, pp. 275-286.
- Lambe, T.W. and Whitman, R.V., (1969). *Soil Mechanics*. John Wiley & Sons, New York, NY.

**APPLICATION FOR PERMIT RENEWAL AND MODIFICATION
SANDOVAL COUNTY LANDFILL**

**VOLUME III: LANDFILL ENGINEERING CALCULATIONS
SECTION 7: GEOSYNTHETICS TENSILE STRESS AND STABILITY ANALYSIS**

ATTACHMENT III.7.I

**THIEL, RICHARD. *PEAK VS RESIDUAL SHEAR STRENGTH FOR LANDFILL BOTTOM
LINER STABILITY ANALYSIS*. THIEL ENGINEERING, OREGON HOUSE, CA.**

PEAK VS RESIDUAL SHEAR STRENGTH FOR LANDFILL BOTTOM LINER STABILITY ANALYSES

Richard Thiel

Thiel Engineering, Oregon House, CA, USA

ABSTRACT

The decision whether to use peak or residual shear strengths for a stability analysis must be made in the context of a specific design situation. Yet even when the specific situation is defined, the decision of whether to use peak or residual shear strength is often unclear. In general, if there are potential construction, operation, or design conditions that might cause relative displacement between layers, then a post-peak or residual shear strength for the layer having the lowest peak strength is appropriate. If seismic analyses predict deformation on a given interface, then the design should use the post-peak or residual shear strength for that interface. For bottom liner systems, where stress distribution along the liner system is very complex, it is advisable to verify that the slope stability has a factor of safety greater than unity for residual shear strength conditions along the critical interface.

INTRODUCTION

This paper is concerned with the forces that support a landfill on its liner system, and the shear strength of geosynthetic interfaces that keep the mass from sliding. Figure 1 schematically portrays the shear forces that work to keep the waste mass from sliding. If sliding occurs, the surface along which sliding would occur is called the critical surface, or potential slip plane. Bottom liner systems that use geosynthetics often have their critical surface along one of the geosynthetic interfaces. The shear strength of these interfaces can usually be measured by means of laboratory testing. These interfaces often realize their peak shear strength within a small amount of relative displacement (on the order of 25 mm), after which their shear strength decreases. Typically, after 50 to 300 mm of relative displacement, the shear strength is reduced to a steady minimum value, which is called the residual shear strength of that interface. Figure 2 shows a typical shear stress-displacement curve for a geosynthetic interface.

Over the life of a landfill the following activities occur: the liner system is built; waste is placed; settlement occurs; a final cover system is installed; and settlement and degradation of the waste continues. Each of these phases of the landfill's life produces different combinations of normal and shear stresses on the liner system. Landfill leachate and gas, which can create destabilizing pore pressures, are by-products of the landfill, and are removed with varying degrees of efficiency. The primary questions addressed in this paper are:

- Should a designer use peak or residual shear strengths, something in between, or a combination of peak and residual strengths, when evaluating a landfill design?
- What does the profession really know about the mobilized shear stresses? (This paper will focus on bottom liner systems.)
- Should the same choice whether to use peak or residual shear strengths be applied along the entire lining system, or should slopes and base liners be treated differently?
- Is there a preferred design approach?
- What factors of safety are appropriate for design?

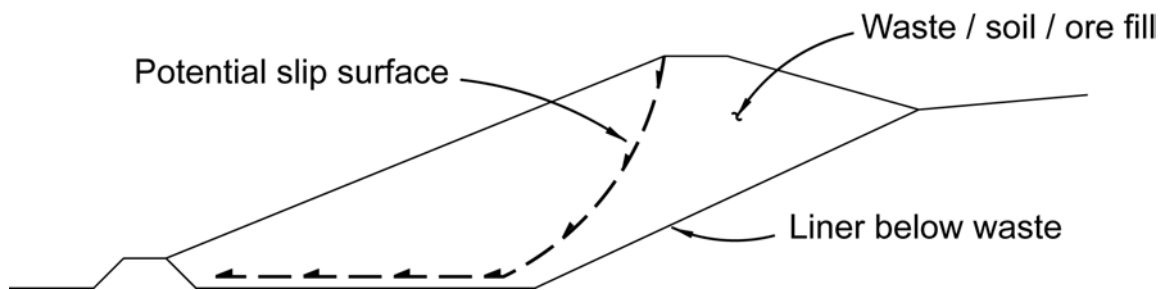


Figure 1 – Schematic of Shear Forces Along Critical Slip Plane

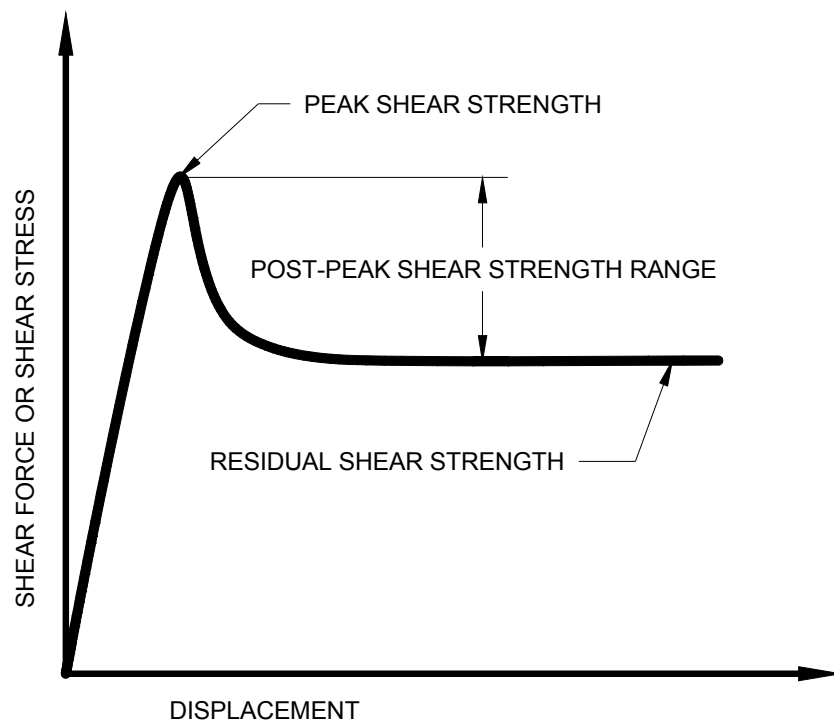


Figure 2 – Example Graph of Shear Force vs. Deformation for Geosynthetic Interface

ORGANIZATION OF THIS PAPER

Part 1 of the paper describes general considerations in performing slope stability analyses. It begins with a discussion of different types of slope stability analyses, including limit equilibrium, finite element, and 2-dimensional (2-D) vs. 3-dimensional (3-D) analyses. Understanding how the state-of-the-practice has developed, and the limitations of the analytical approach, both contribute strongly to making the right selection of appropriate shear strengths and factors of safety.

2-D limit-equilibrium analyses are by far the most common approach for evaluating slope stability. Part 1 discusses practical guidelines and common pitfalls that affect the results of these analyses, especially the selection of the critical shear plane on which the peak or residual shear strength will be modeled. Part 1 also discusses how pore pressures might cause a surface to exceed its peak shear strength and induce progressive failure. Selecting the appropriate shear strength requires an understanding of the effective normal stress range. Also, commissioning direct shear testing from a laboratory requires that one understand the proper testing parameters needed to obtain appropriate peak and/or residual shear strength values.

Part 2 of the paper directly addresses the question of peak vs. residual shear strength, and begins by discussing ductile vs. brittle behavior. Progressive failure, which occurs with brittle materials, then emerges as the chief concern of this paper. The discussion that follows considers conditions that could cause a brittle material to exceed its peak strength in the context of a landfill bottom liner, followed by a brief summary of field observations in this regard.

Part 3 discusses possible design approaches in terms of the selection of peak strength, residual strength, and hybrid approaches, and then considers the appropriate factors of safety for these different approaches.

Part 4 then presents conclusions reached from the preceding discussions. It also provides recommendations for practical design approaches based on the author's experience, as well as recommendations for further research.

This paper surveys the key considerations one employs when deciding whether to use peak or residual shear strength for bottom liner systems in landfills. It does not presume to make that decision, but rather seeks to outline and discuss all considerations that are necessary and pertinent to that process. Although many of the considerations this paper presents may be general enough to apply to cover (veneer) systems, it has been written solely with bottom liner systems in mind, and does not consider the long-term issues related to cover systems.

PART 1 – GENERAL CONSIDERATIONS

LIMIT-EQUILIBRIUM VS FINITE-ELEMENT ANALYSES

Limit-equilibrium analyses, whether 2-D or 3-D, are the most common methods of assessing slope stability. These methods can be performed by hand or, more commonly, by using a computer program. Such analyses evaluate the force and moment equilibrium of a slope on an assumed slip plane given assumed shear strength, unit weight, and pore pressure parameters. The result of these analyses is then presented as a factor of safety (*FS*) defined as:

$$FS = \frac{\text{Shear strength along the slip surface}}{\text{Shear stress along the slip surface}}$$

One defining characteristic of the limit-equilibrium approach is that it presumes that the factor of safety is the same everywhere along the slip plane. Therefore, the mobilized shear stress distribution along the slip plane is simplistically assumed to be a constant ratio of the shear strength along that plane. Such analyses also do not take into account elastic or plastic deformation. These are both significant considerations when deciding whether to use peak or residual shear strength.

Finite-element analyses attempt to calculate the stress distribution and deformations in a soil mass. In addition to considering force and moment equilibrium, these analyses also typically consider the materials' elastic modulus and Poisson's ratio, and some models can also calculate the change in shear strength with displacement for various materials. The result of these analyses is usually presented as a distribution of mobilized shear stress and displacements.

At first glance it would seem that finite-element analyses offer more of what we wish from a slope stability analysis as opposed to limit-equilibrium analyses. So much so, that we might even ask ourselves why we continue to bother with limit-equilibrium analyses. The fact remains, however, that the limit-equilibrium approach has been and will continue to be the basis of standard practice in the industry. The reasons for this, some of which also appear in the next section that considers 2-D vs. 3-D, are:

- Limit-equilibrium approaches have been performed and “calibrated” through industry experience for the past 80 years. Properly performed limit-equilibrium analyses have been proven to be adequate.
- Finite-element analyses are sophisticated and complicated to perform. The average design practitioner often is not adequately trained to perform such analyses, and the low frequency of projects that require their use do not justify the

resources needed to keep an engineer qualified to perform them on every landfill-design firm's staff.

- In the past few years the author has peer-reviewed a number of slope stability analyses. On four major landfill projects for which calculations had been prepared by separate reputable nationwide and local design firms, the author found fundamental errors in 2-D limit-equilibrium analyses. Some of these projects had already been built and were, in the author's opinion, at serious risk of large-scale failure. If such fundamental errors continue to be made with analyses as simple as 2-D limit-equilibrium, the prospects of universalizing a finite-element approach for the solid waste industry is not very promising. Finite-element analyses epitomize the expression "garbage-in garbage-out", so strict quality control and quality assurance is in order whenever they are employed.

2-D vs. 3-D ANALSYES

One issue that is periodically debated in the literature and at professional gatherings is the use of 2-D as opposed to 3-D analyses. Soong et al. (1998) question whether 2-D analyses are appropriate for landfills, and suggest it would be more appropriate to use 3-D analyses with residual strengths. From a pragmatic point of view, the everyday stability analysis has been, and will continue to be, 2-D in actual practice. There are three main reasons for this, clearly laid out by Duncan (1996):

- **Inherent Conservatism.** Properly performed 2-D analyses always give a factor of safety that is equal to or less than those given by 3-D analyses. 2-D analyses, therefore, are more conservative.
- **Ease of Application.** The average professional consulting engineer is interested in the amount of time it will take to arrive at an answer, the frequency of projects that will require special attention, and the effort it will take to organize the results in a final report. 3-D applications are simply not as easy to use as 2-D.
- **Avoidance of Errors.** As illustrated above, analyses are prone to errors, and 3-D analyses are more complicated than 2-D analyses. The author believes that the emphasis in the profession needs to be on performing solid, fundamental engineering, rather than on increased sophistication that invites more errors.

3-D analyses have mostly been used for forensic studies, and for those few complex situations that involve a very unusual geometry and/or distribution of shear strengths in the potential sliding mass. Examples of these can be found in Stark and Eid (1998). In the author's 16 years of experience performing stability analyses on dams, embankments, cut slopes, and landfills, there were only three situations where a 3-D analysis was warranted during design, and all three were satisfactorily accomplished using multiple 2-D sections. One of these projects was given as an example in the Stark

and Eid (1998) paper. In that case Stark and Eid (1998) felt that a 2-D slope stability analysis could not anticipate the combined effects of the project's complicated geometry and shear strength zones. After discussion of the project's complexity, they reported a minimum 3-D factor of safety of 1.65 using a 3-D analysis program. In fact, the original design team, of which the author was a part, had two years earlier calculated a factor of safety of 1.60 using weighted averages of several 2-D cross-sections. Thus, even in this circumstance that had unusually complicated geometry and shear strength conditions, a modified-2-D approach gave results one would expect relative to the 3-D analysis results.

Notwithstanding the reservations given above, 3-D analyses will well serve those who have the time and budget to perform them.

To summarize, the refinements in accuracy offered by 3-D analyses are rarely matched by the average practitioner's understanding of basic slope stability mechanics, much less the level of confidence ordinarily offered by assumed shear-strength and pore-pressure parameters. Most often, the differences in shear strength and pore-pressure assumptions made by different engineers will substantially outweigh the refinements obtained by favoring 3-D over 2-D analyses. Compare, for example, the different conclusions reached by Schmucker and Hendron (1998) versus Stark et al. (2000) regarding the cause of a major landfill failure; or the difference in 2-D vs. 3-D comparisons for a landfill failure described by Soong et al. (1998), from those made by Stark et al. (1998). These case histories, recently published by experienced professionals, do not provide a compelling argument that 3-D analyses should be preferred. They do, however, reinforce the notion that the major factors contributing to uncertainty in a slope's performance are shear strengths and fluid pressures, and that this is where our attention should be focused. The purpose of this paper is to focus specifically on one of these issues, namely, when it is appropriate to use residual vs. peak shear strength for geosynthetic interfaces at the base of a waste containment facility.

GENERAL DISCUSSION OF 2-D ANALYSIS APPROACH

Method of Analysis

Slope stability analyses are most commonly assessed using computer programs that evaluate the limit equilibrium of a 2-D cross-section. Less sophisticated limit equilibrium analyses can be performed using hand-calculation methods or charts. Hand calculations are an effective analysis tool because they often provide a clearer understanding of the critical aspects of the problem, and mistakes in geometry and assumed failure planes are less likely. A common approach is to perform a hand check on the most critical surface that has been analyzed by a computer program. A good summary of slope stability approaches using hand calculations is provided by Abramson et al. (1996).

Limit-equilibrium analyses of varying complexity that have been developed are available to design practitioners. One of the first approaches was the Ordinary Method of Slices developed by Fellenius. Later refinements were presented by Bishop, Janbu, Morgenstern and Price, Spencer, and others. A review of these methods is beyond the scope of this paper, and the reader is referred to Abramson et al. (1996) and Duncan (1996) as a starting place for a comparison of the various limit-equilibrium methods. The author would, however, offer three points from his own practice as to which method to use for performing stability analyses of bottom liner systems:

- The Bishop method is generally not applicable when analyzing bottom liner system geometries because it was developed for circular failure surfaces. The critical slip plane for liner systems is often a translational block that is non-circular.
- Spencer's method, which is now commonly available in computer codes, is considered more rigorous and complete in its analysis than the simplified Janbu method, which is commonly used for block analyses. Spencer's method is computationally more intensive, however, and may be difficult to use for random searches for a critical failure surface, even with modern computers. It is also less stable and can yield incorrect results unless the line of thrust results are checked by the user. Therefore, a good practice is to search for the critical surface using Janbu's simplified approach, and then perform a final check on the stability using Spencer's method. Usually, but not always, Janbu's method will result in a slightly higher factor of safety.
- The approach developed by NAVFAC (1982) for translational block analyses is often a good and appropriate method for performing a hand-check on the computer results for a 2-D translational block failure along a bottom liner system.

Identification of Critical Slip Plane

The most typical requirement for static stability is to meet a specified factor of safety. Just what constitutes an appropriate factor of safety will be discussed later in this paper. The idea is that if the stability analysis is performed correctly with the proper input variables, the factor of safety should provide a level of confidence that the slope will in fact be stable.

The essential operative words in the above paragraph relating to stability analyses is that they are "*performed correctly*". The safety margin in a factor of safety exists to account for unknown or unpredicted deviations from the original design assumptions. It is not, however, supposed to account for errors in the analysis, or incorrect geometric and material property assumptions.

When performing a correct analysis the critical slip plane for analysis must be identified correctly. An experienced geotechnical engineer is usually required in order to

select the critical cross-sections for analysis of a slope. Even for experienced practitioners, though, it is not always obvious which section is the most critical, and several trials generally need to be performed. For very complicated geometries, as described in the previous section, multiple 2-D sections may need to be weighted in order to simulate a 3-D analysis, or the more complex 3-D analysis can actually be performed.

In addition to selecting the proper cross-section, it is also important to search for and select the correct critical slip plane within that cross-section. In peer-reviewing slope stability analyses performed by others, the author has found errors in which the designer had correctly identified the critical cross-section, but incorrectly identified the critical slip plane within that cross-section. He found others, too, in which the designer had conceptually identified the correct slip plane, but failed to code the computer program to correctly place the slip plane at the correct interface within the liner system. The effects of such errors was to drop from an ignorantly-blissful factor of safety of 2 to 3, to an uncomfortable factor of safety of less than 1.1.

When the critical slip plane is along the liner system, the critical surface is always the one that has the lowest peak strength. If residual strengths are used in the analysis, they should reflect the surface that has the lowest peak shear strength, because that is the one that will govern deformations.

Pore Pressures

Next to gravity, pore pressures (most pervasively those caused by liquid as opposed to gas) are the single most prevalent factor contributing to slope stability failures. They are also among the most overlooked elements in slope stability analyses. Schmucker and Hendron (1998) illuminate this problem when they state that “Very little is known at this time regarding the generation and distribution of pore pressures in MSW landfills.”

The one area where evaluating the influence of pore pressures on slope stability has been well focused has been in the design of dams. For this reason there have been few dam failures due to the neglect of pore pressures, with dam failures in the past century generally being caused by other factors (e.g. liquefaction or piping). Pore pressures are not commonly included in landfill analyses. Yet most (or at least many) of the dramatic landfill failures reported in the industry can be attributed to pore pressures that built up either in the foundation, due to waste loading, or in the waste itself, due to leachate buildup or leachate injection. Examples are the Rumpke landfill failure (see Schmucker and Hendron, 1998, who attributed the failure in part to leachate buildup caused by an ice dam at the toe), and the Dona Juana landfill failure (see Hendron et al., 1999, who attributed the failure to high-pressure leachate injection).

When performing slope stability analyses, designers should consider the potential for unanticipated pore pressures. Unanticipated conditions may occur in landfills due to clogging of the leachate collection systems, or aggressive leachate recirculation in the waste mass. Additional discussion of this issue is provided by Koerner and Soong (2000). Further discussion later in this paper describes how pore pressures could lead to a localized exceedence of peak strength, leading ultimately to a progressive failure.

Selecting and Measuring Material Shear Strengths

Shear Strength Definition. Figure 3 illustrates a non-linear shear strength envelope, which is typical for many soil and geosynthetic interfaces. Sometimes the non-linearity is slight, and a straight-line approximation over the entire load range under consideration can be valid. This is often true for very narrow load ranges such as those considered for cover veneer systems. At other times this non-linearity is quite significant, especially when shear strength characteristics are evaluated over the broad range of normal loads indicative of bottom lining systems.

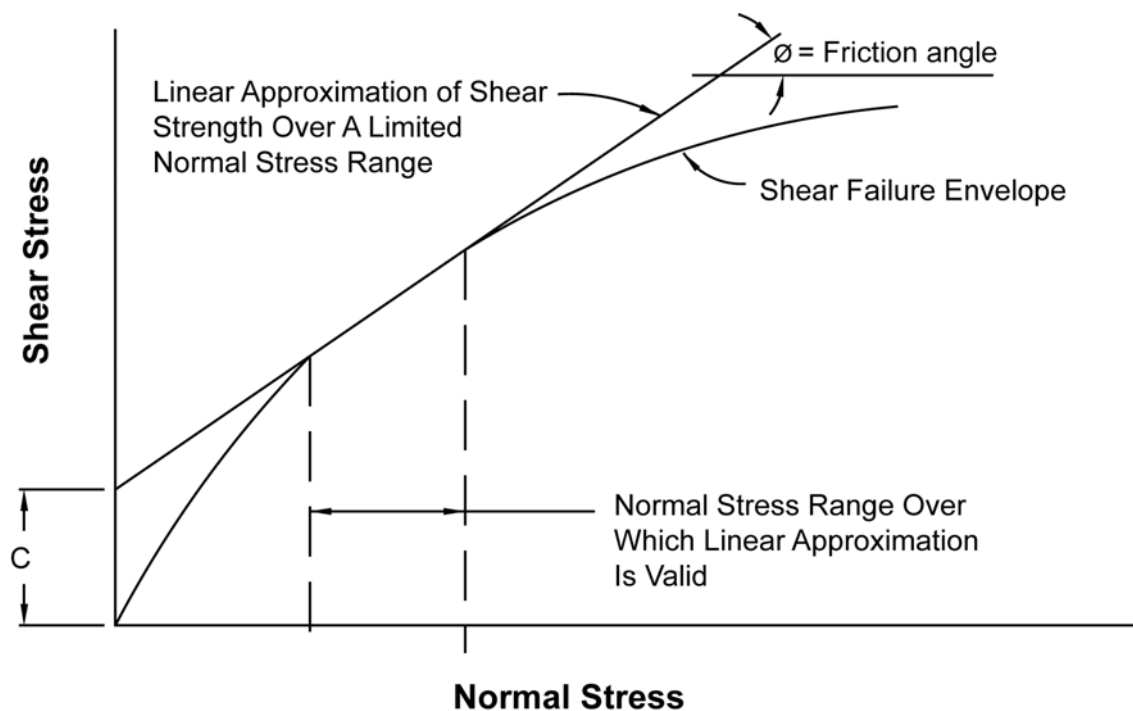


Figure 3 - Typical Shear Failure Envelope for Soil and Geosynthetic Materials.

If the shear strength curve of the evaluated materials is non-linear with respect to normal load, then special consideration should be given to defining the shear strength parameters within a specific normal load range. Many computer programs only allow the input of linear shear strength parameters. These parameters are normally identified as a friction parameter (ϕ) and a cohesion (or adhesion) parameter (c). It is useful to

recognize that these are often only mathematical parameters that describe the shear strength of a material or interface over a specific normal load range. The shear strength parameters are demonstrated in Figure 3.

Draft European Standards, and other publications (e.g. Koerner and Daniel, 1997) suggest that the apparent cohesion of a shear strength envelope can be ignored. As stated by Jones and Dixon (1998): “This assumption can have a significant effect in that the shear strength for any particular normal stress will be quoted as being lower than measured... It is possible that the failure envelope may curve to the origin at very low normal stresses, in which case ignoring the apparent cohesion will result in over conservative results.” If we recognize that the values of the parameters ϕ and c are only mathematical tools used to describe the measured or estimated shear strength over a given normal load range, we can discount statements that advocate that cohesion can be ignored.

The friction parameter (ϕ) is related to the slope of the line (slope = $\tan\phi$), the cohesion parameter (c) is the y-intercept, and the normal load range is the abscissa range over which the straight-line approximation of the shear strength envelope is valid. Use of the shear strength parameters outside of the normal load range for which they were defined is generally non-conservative, as illustrated in Figure 3.

If the computer program only allows the consideration of linear shear strength envelopes, the shear strength envelope for non-linear materials should be discretized into a series of straight-line approximations for different normal load ranges. Furthermore, where the critical slip surface runs through a material or interface that exhibits a non-linear strength envelope, the designer should either use a computer code that allows input of a non-linear shear strength envelope, or assign different strength parameters to different zones of the material or interface according to the normal loading it theoretically experiences. For computer codes that do not allow non-linear shear strength envelopes, the delineation of different normal-load zones for non-linear materials is usually calculated by hand. This procedure is outlined in detail by Thiel et al. (2001).

Shear Strength Measurement. For geosynthetic lining systems, the internal and interface shear strength is normally determined by using the direct shear test in accordance with ASTM D 5321. For GCL internal and interface shear strength evaluation, direct shear testing is conducted in accordance with ASTM D 6243. In these direct shear tests, the geosynthetic material and one or more contact surfaces, such as soil or other geosynthetics, are placed within a direct shear box. The specimens are hydrated, consolidated, and placed under a constant normal load in accordance with the ASTM procedures, along with any project-specific testing clarifications/instructions from the design engineer. A tangential (shear) force is applied to the materials, causing one section of the box to move in relation to the other section. The shear force needed to cause movement is recorded as a function of horizontal displacement.

The test is normally performed for several different normal loads. Typically a series of at least three individual tests are performed at specified normal load conditions. The normal load and shear forces are converted to stresses by the given area over which shear occurred, typically a 12 in x 12 in (300 mm x 300 mm) sample. The peak and post-peak (or residual, if deformation is taken far enough) shear strengths are plotted on a graph, and a best-fit straight line or curve is fit through the data to represent the shear strength envelope. Several factors can influence the interface shear strength of geosynthetics. The most important of these are discussed below.

Valid Testing Technique. While not offering any endorsements, the author can state that he trusts very few laboratories in the nation to provide high quality direct shear test data. Initial ASTM round-robin testing of even the most simple interface (nonwoven geotextile against a smooth HDPE geomembrane) produced a shot-gun scatter of results with very poor correlation. Unless the initial test data has integrity, most of the further considerations offered in this paper become meaningless. It is imperative that the designer screen the testing laboratory in order to obtain test data of assured accuracy.

Rate of Shear Displacement. The typical default shear rate for direct shear testing with geosynthetics as presented in ASTM D 5321 is 0.04 in/min (1.0 mm/min). For testing hydrated GCLs, ASTM D 6243 provides guidance on attaining consolidated drained conditions that should preclude the build-up of excess pore pressures.

In general the rate of shear displacement affects peak strength more than residual strength. Depending on the interface being tested, the strain rate of the test should be slow enough to give results representative of long-term (slow) shear conditions.

Hydration. The moisture content, degree of saturation, and degree of consolidation of adjacent soils and geosynthetics can all exert an influence on the shear strength results. It is important to direct the testing laboratory as to the sequence of hydration and consolidation. With clay soils adjacent to geosynthetics, it is generally more conservative to hydrate under low normal loads before consolidating. Thus far, the type of hydrating fluid has not been reported in the literature as affecting shear strength results, especially in regard to typical landfill leachates.

Normal Stress. The most common strength-related errors in computer slope stability analyses stem from using strength parameters that do not correspond to the normal load conditions at the surface being analyzed (Lambe et al., 1989). It is generally unconservative to extrapolate linear strength envelopes beyond the limits for which they were defined. It is, therefore, important that shear test data be acquired under normal loading conditions that are representative of the conditions being analyzed. For base liners this is zero to full height of the waste mass.

Utilization of Representative Materials. Designers often tend to use either published literature values or previously obtained test results for shear strengths. In such cases, their experience and judgment may assist them in selecting shear strength parameters for the purposes of preliminary design. It is highly recommended, however, that material-specific testing be performed to assist in preparing the final construction specifications, and/or to verify the actual materials delivered as part of a CQA program. The reason for this is that the variation in geosynthetic manufacturing parameters from job to job can have a significant effect on shear strength. The most significant of these is the degree of texturing on coextruded geomembranes. Figure 4 presents a graph showing the difference in peak and post-peak shear strengths obtained with two different degrees of texturing. Designers can use this concept to their advantage, as will be discussed later. Designers unaware of this issue may test a manufacturer's sample and obtain passing results, and then use GRI-GM 13 as a texturing specification. This would provide an extremely low-level requirement for texturing that may not achieve the same interface shear strength as the nice sample provided for initial testing by the manufacturer. The same principle may hold for geotextile-based products, whose fiber denier size, fiber type, degree of needling, etc. can influence its interface shear strength properties. The only way to be sure is to test the actual materials provided for construction.

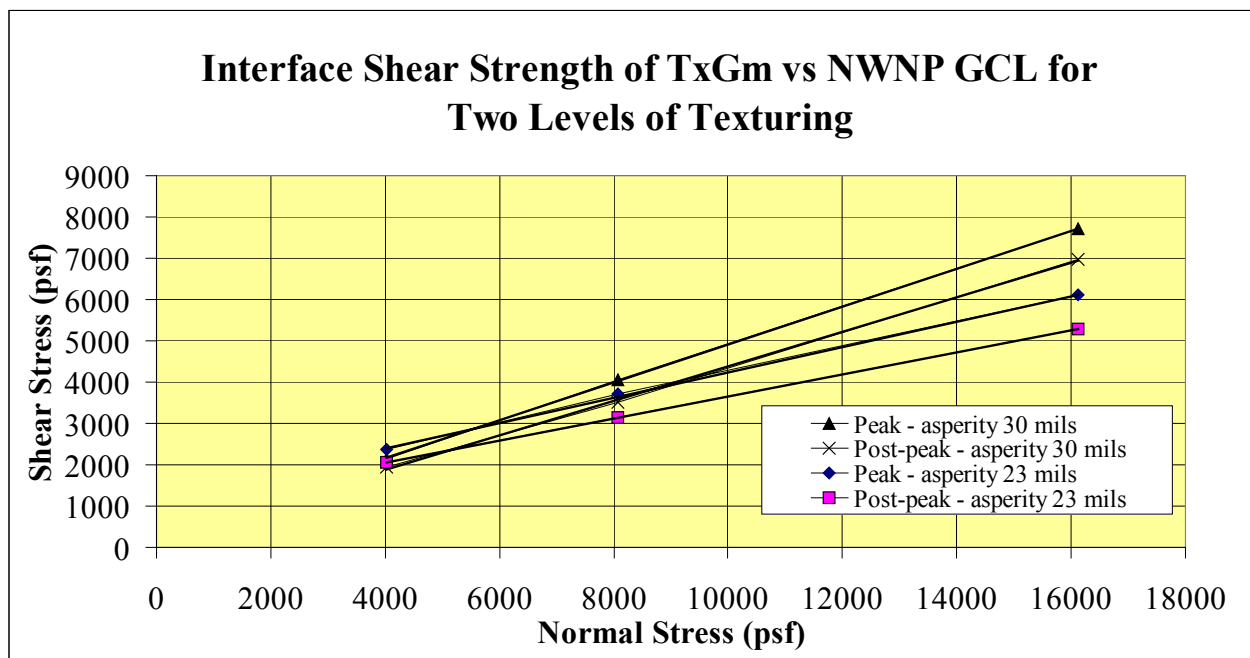


Figure 4 – Variation of Interface Shear Strength with Different Degrees of Geomembrane Texturing

Adjacent Materials and Consolidation Time. Using representative materials for direct shear testing refers not just to the materials for the interface being tested, but also to the adjacent materials. The use of realistic adjacent soil materials will typically provide slightly higher interface shear strengths than will, for example, the use of steel plates. In

the same vein, Breitenbach and Swan (1999) show that longer load consolidation times result in a significant increase in interface shear strengths, apparently due to micro-scale load-induced deformation of the interface materials. Jones and Dixon (1998) question the use of the ring-shear apparatus for testing, because the narrow specimen of limited surface area on hard, smooth boundaries may not be representative of field conditions. These factors can affect both the peak and post-peak shear strength results.

Peak vs. Post-Peak vs. Residual Shear Strength. The highest level of shear strength measured in a direct shear test under a given normal load is defined as the peak strength. With continued shear displacement there is typically a loss of strength. The shear strength at any given displacement past the point of peak strength is referred to as “post-peak strength”. The strength at which there is no further strength loss with continued displacement is called the “residual strength”. Many of the most common direct shear devices do not allow enough displacement to occur that would enable true residual strength to be measured (e.g., see Stark et al., 1996). Therefore, in some cases it is not technically correct to refer to end-of-test conditions as representing the “residual” strength, but rather, to refer to “post-peak” strength while also specifying the amount of displacement. For the purposes of this paper, the lowest expected shear strength after significant deformation (typically more than 3-6 inches [70-150 mm]) is described as the residual shear strength. Shear strengths between the peak and residual shear strength are referred to as post-peak. This brings us then, to the main focus of this paper, which is whether it is appropriate to use peak or residual shear strengths (or something in between).

PART 2 – PEAK vs. RESIDUAL: THEORETICAL AND PRACTICAL CONSIDERATIONS

BACKGROUND DISCUSSION ON BRITTLE MATERIALS AND PROGRESSIVE FAILURE

Many, but not all, geosynthetic interfaces are strain softening. This highlights the essence of the peak vs. residual question. With a relatively short amount of deformation (typically less than 25 mm), the materials pass beyond peak strength into a lower post-peak shear strength, ultimately becoming what we call residual. In geotechnical engineering these shear strength characteristics are also sometimes called ‘brittle’ – brittle meaning that the material substantially decreases in strength after it is “broken”, that is, has gone past peak strength. (Note that this has nothing to do with the tensile behavior of the material.) This behavior is in contrast to a ductile shear interface, which continues to deform after reaching its peak strength, but retains its strength close to the peak. An example of a brittle geosynthetic interface is an HDPE textured geomembrane against a geotextile, which produces a dramatic drop in strength after the peak strength is

exceeded. An example of a ductile geosynthetic interface is a smooth PVC geomembrane against a geotextile (see data published by Hillman and Stark, 2001). Also, MSW waste is generally considered a ductile material in terms of shear strength (Kavazanjian, 2001).

As a progressive failure develops, the shear stresses are redistributed within the slope. This often involves the slow deformation of the failing mass over time, followed by an abrupt slide. If the critical plane supporting a slope is brittle, and for some reason part of it is stressed past its peak strength, then that part quickly becomes significantly weaker, which means it can carry less of the load. That in turn puts more of the load on other parts of the critical plane, which may in turn cause another part of that plane to become overstressed and exceed its peak strength. The continuation of this process is called progressive failure. At some point the entire system becomes overstressed and an abrupt failure occurs. This is the concern when there is a brittle interface.

Progressive failures have been characteristically noted for stiff clays, as described by LaRochelle (1989): “We have come to realize that we cannot count on the peak strength in this strain-softening material either for short- or long-term stability.” Past landfill failures have been attributed to this same phenomenon (Schmucker and Hendron, 1998; Mazzucato et al., 1999; Stark et al., 2000), which holds significant potential for future failures (Gilbert and Byrne, 1996).

POTENTIAL CONDITIONS THAT MAY LEAD TO PROGRESSIVE FAILURE

Several reasons are provided below which explain why the peak strength of a bottom liner interface might unexpectedly be exceeded.

Non-Uniform Stress Distribution and Strain Incompatibility

Perhaps one of the most compelling reasons to be concerned about progressive failure in liner systems is that the stress distribution along the liner interface is not known. “It is impossible to obtain all of the necessary information in most cases” to perform a rigorous analysis of a progressive failure process (Tiande et al. 1999). “It is difficult to determine the available shear resistance along an interface exhibiting strain-softening behavior. It may be unsafe to assume that peak strength is available, while it may be excessively conservative and costly to assume that only the residual strength is available” (Gilbert and Byrne, 1996).

The complexities of stress distribution are affected by the type of loading and by pore pressures. According to Li and Lam (2001) “.. the development of progressive failure will also be different depending on whether failure is triggered by a rise in water table [*insert by author: namely, leachate*] or an increase in external loading [*insert by author: namely, continued waste stacking*]”.

Reddy et al. (1996) present a most interesting finite-element modeling study that evaluates the stress distribution and deformations along a landfill liner system for an assumed landfill geometry. Their study compares smooth and textured interfaces for different stiffnesses of waste. Although their analysis did not model strain-softening behavior of the interfaces, the results provide valuable insight into stress and strain distribution. Some of the conclusions from their study are:

- The stiffness of the waste influences the distribution of interface stress and shear displacements. Stiffer waste puts more stress and strain on side slopes (especially the lower part of the slope). Softer (more compressible) waste puts more stress on the base liner below the highest part of the waste, and more strain accumulation towards the toe. The overall factor of safety, however, is not affected by the waste stiffness, assuming that no strain-softening of the interface shear strength occurs.
- The smooth interface with 11° friction reached its peak strength in a number of places along the interface in their example, even though the global factor of safety was 1.5. The textured interface did not approach its peak strength anywhere along the interface in their example, but had a factor of safety of over 4. This means that a typical stability evaluation that results in a factor of safety of 1.5 may actually result in areas of the critical interface achieving their peak strength and possibly going into a reduced post-peak strength.

A finite element study was performed by Filz et al. (2001) who reached conclusions similar to those obtained by Reddy et al. (1996). Filz et al. (2001) provided a compelling demonstration that a smooth clay-geomembrane interface exhibiting strain-softening characteristics might be inappropriate to analyze based on peak shear strengths. They showed that the distribution of mobilized shear stresses was not uniform along the base and side slope, and would result in progressive exceedence of peak strength. Their comparative analyses demonstrated that whereas a limit-equilibrium analysis based on peak strengths might result in $FS = 1.6$, the finite-element analysis would suggest impending failure (i.e. $FS = 1.0$). The same problems analyzed using residual shear strengths in limit-equilibrium analyses resulted in an average $FS = 0.94$. Furthermore, for a finite-element analysis to show $FS = 1.5$, the limit-equilibrium analysis based on peak strengths needed to show a FS of about 2.2, and the limit-equilibrium analyses using residual shear strength resulted in $FS = 1.3$.

Differences in the relative stiffnesses of the overlying waste as compared to that of the liner interface are also cited by Gilbert and Byrne (1996) as a significant potential cause of deformations along the liner interface that could lead to residual shear strengths.

Similar suppositions are made by Stark et al. (2000), who postulate that strain incompatibility between MSW and underlying interfaces can lead to progressive failure, as they believe was the underlying cause of the Rumpke landfill failure. The weaker lower interfaces may achieve post-peak strengths before the MSW ever achieves peak

strength. After peak strength of the interfaces is achieved, the peak strength of the MSW may be mobilized at a time when the strength of the interfaces is reduced to the residual value. They state: “The greater the difference between the stress-strain characteristics of the MSW and the foundation soil or geosynthetic interfaces, the smaller the percentage of [peak] strength mobilized in the MSW and underlying materials.”¹

Unexpected Increases in Pore Pressure

The typical effect of pore pressures is to decrease the effective normal stress, which in turn decreases the effective shear strength, even as the shear stress that is driving instability remains unchanged. When pore pressures are introduced, the effective shear strength may be reduced to the point that the peak shear strength at that location is exceeded, at which point progressive failure can begin. This was what Schmucker and Hendron (1998) concluded was the triggering mechanism for the Rumpke landfill failure.

Seismic Loading

With seismic loading there is certainly the potential for deformation to occur along the critical failure plane, which can reduce the strength of the critical interface below its peak strength. In this regard the design practitioner needs to assess the potential for this type of deformation and, if the design earthquake is expected to produce deformation greater than about 20 mm, then the residual strength of that interface must be considered.

Construction Deformation

Construction conditions frequently result in temporary stability conditions with lower factors of safety than the completed fill scenario. To the author’s knowledge, the effect of preliminary interface deformation at low normal loads on the subsequent shear strength at higher normal loads has only been documented in one recent study by Esterhuizen et al. (2001). They showed that for a smooth clay-geomembrane interface, deformations at low normal loads would partially, but not fully, reduce the peak strength of the interface at higher normal loads. They provide a very interesting “work-softening” model to describe this behavior in a manner that can be used in a finite-element analysis. Although their model fits the data very well, it is only applicable to the specific clay and geomembrane used for their study, and it is not known at this time how well their approach would work for other interfaces. This is an area for further research.

¹ For years now the author has heard the statement that the strain incompatibility between waste and liner systems could be a major consideration in selecting appropriate shear strengths. It is interesting, however, that some of the literature reports surprisingly low amounts of deformation required to reach the peak strength of the waste; on the order of only 40 mm for rigid-body deformation. See, for example, Eid et al. (2000), Stark et al. (1998), Mazzucato et al. (1999). Also Kavazanjian (2001) states his belief that strain compatibility with MSW is not nearly as significant an issue as has generally been supposed, based on direct- and simple-shear test results that show that the strains and deformations required to reach peak strength are comparable to those required for most soils.

Waste and Foundation Settlement

Over time there is substantial deformation and settlement of the waste that may cause unknown redistribution of stresses. The settlement of waste adjacent to a sideslope has often been noted as a source of downdrag forces, which may become great enough to exceed the peak strength of one of the slope liner interfaces. This phenomenon was cited by Stark and Poeppel (1994) as a mechanism contributing to the Kettleman Hills landfill failure, and is echoed in Gilbert and Byrne's (1996) theoretical study: "...it is more likely that the residual strength will be mobilized along the side slope rather than the buttress [bottom liner]", and they even go so far as to say "...it is unlikely that an average stress greater than the residual value could be mobilized along a typical side slope in a containment system." Likewise, foundation settlement has the potential to cause differential movements of the liner system.

Aging and Creep

Geosynthetic durability has been the subject of many papers and studies which address the ability of geosynthetics to maintain their physical properties as containment barriers, and to some extent as tensile reinforcement. Little has been published, however, regarding the long-term durability of shear interfaces such as, for example, the long-term dependence on the strength of geotextile fibers at interfaces with textured geomembranes, or within reinforced GCLs. Quantitative predictions regarding the long-term aging and creep potential of geosynthetic interfaces are certainly beyond the author's capacity, but are noted as an additional potential mechanism whereby the assumed peak strength of an interface might be reduced.

FIELD OBSERVATIONS

From the author's experience and his informal polling of industry representatives, two general field observations that have been made regarding deformations along geosynthetic interfaces on slopes:

- Slopes that were designed with robust interfaces using textured geomembrane or granular materials against geosynthetics, have not been observed to undergo tension or deformation.
- Slopes that had less brittle, but also less strong interfaces, such as a geotextile over a smooth geomembrane, have been observed to result in tension in the upper geosynthetic, presumably due to slippage along the interface which occurred as a result of downdrag forces.

It is worthwhile to note in the Gilbert and Byrne (1996) model that strain softening on the slope would generally only occur if the slope angle was greater than the peak friction angle of the lining material. Although unverified by the author, this may be a

general guideline for estimating whether or not peak or residual shear strength would occur on a slope (excluding seismic forces). For example, on a 3(H):1(V) slope, perhaps a peak interface strength of 18° or more would maintain its peak strength, and an interface strength of less than that would have a higher potential for going into residual.

Given the large number of landfills constructed with geosynthetic bottom liner systems, it is quite surprising how few failures have actually been reported. Furthermore, none of the reported failures, to the author's knowledge, involved the progressive failure of a substantially brittle geosynthetic interface. Most of those failures have involved soil (including bentonite failures associated with unreinforced GCLs, which are ductile relative to shear strength). The best example of a pure geosynthetic failure that involved some degree of strain softening is the notorious Kettleman Hills failure, but the interfaces in that failure were fairly weak to begin with (all against smooth HDPE), and the initial factor of safety, even assuming peak strengths of the interfaces as they existed, was low, and below standard industry guidelines.

The conclusion of industry observations is that actual industry experience has not shown degradation of peak strength (i.e. progressive failure) to be a pervasive problem. Nonetheless, it definitely presents a potential problem that has on occasion bloomed into an unfortunate reality. It is, therefore, worth taking it into account by means of design and analysis considerations, which are discussed in the next section.

PART 3 - DESIGN APPROACHES

THE PEAK vs. RESIDUAL ISSUE IN THE CONTEXT OF THE DESIGN PROCESS

Many elements of a landfill are not designed, per se, but are largely dictated either by the owner's desires or by regulatory constraints. For example, the geometry of a landfill (boundaries, slopes, height, etc.) is often governed by an attempt to maximize the resource (i.e. volume) while meeting the constraints presented by conditional use permits, property line setbacks, maximum slope regulations and the like. Furthermore, the liner system is usually prescribed by regulation, at least in its fundamental requirements, and oftentimes by a default regulatory configuration.

In many cases then, the two major elements that influence a stability analysis are largely predetermined. That is, both the preferred landfill geometry and the liner system are more or less given to the "designer", who is charged with producing the "final design". From the point of view of slope stability, what is there left to do? Obviously the slope stability should be checked and verified. What does this mean and how is it done?

The first step in performing a slope stability analysis is to define the basis of the analysis. This is often documented in the project files as a Design Basis Memorandum (DBM), in which the following kinds of determinations are made:

- Will the analysis look at only the final configuration, or at interim operational configurations as well? (The latter option is highly recommended for risk management.)
- What unit weight will be assumed for the waste?
- What material strength values will be assumed for the different materials, and how will they be determined?
- Which pore-pressure scenarios will be evaluated?
- What will be the minimum acceptable factors of safety?
- Are seismic analyses required? If so, what approach will be used? How is the design earthquake defined? If a deformation approach is used, what is the maximum allowable deformation?

The results of the slope stability analyses will be:

- A static factor of safety (for each configuration analyzed).
- If a seismic analysis is required, the results will present either a potential magnitude of deformation along the critical slip plane, or a factor of safety for a simplified pseudo-static analysis.
- A description of the minimum required interface shear strength properties for the liner system construction.

It is this last point that makes slope stability analyses a design function rather than a mere geotechnical engineering exercise. It is essential that a clear linkage be made between the slope stability calculations and the ultimate project specifications, to ensure that the proper materials are provided during construction to meet the slope stability requirements. If the analysis results do not meet expectations, iterations of laboratory testing and/or alterations in slope geometry and/or liner materials may be required in order to achieve an acceptable design that can be adequately specified.

The design aspect of slope stability analyses becomes even more interesting when an additional constraint is put on the design criteria, namely to position the critical slip surface above the primary geomembrane. This is a common practice in Germany that is also employed by several design practitioners in the United States (and likely in other places as well, given the author's limited knowledge of practices worldwide). This design approach helps to ensure that, if for any reason slippage does occur, the barrier liner system will remain intact. Ensuring that the slip plane is above the primary geomembrane is not necessarily a simple matter; laboratory shear testing programs and

iterations of slope stability analyses are often required in order to achieve acceptable results.

Implicit in the slope stability design and analysis process is the need to decide whether peak or residual shear strengths should be used. Though this is not generally an issue for waste materials, which are usually considered ductile, it is often a significant issue for liner system interfaces. This decision will significantly influence the calculated factor of safety. For seismic analyses, the influence is often less significant, because if the seismic analysis indicates deformation will occur, a prudent designer will use a post-peak shear strength (even as the question remains whether to use a deformation-based post-peak strength, or a true residual strength).

WHAT IS AN APPROPRIATE FACTOR OF SAFETY?

The author previously co-authored a paper whose title posed this same question concerning cover systems (Liu et al., 1997). That paper discussed assessing the degree of confidence in each of the variables that went into assessing the factor of safety, and assessing the potential risk and cost of a failure. This approach is espoused by Gilbert (pers. comm.) who believes that the factor of safety should be based on “uncertainties, assumptions, and the consequences of failure.”

It is common in the literature to see geotechnical references that reiterate the idea that the greatest degree of uncertainty in performing slope stability analyses is the shear strength of the materials (e.g. Liu et al, 1997; Stark and Poeppel, 1994; Duncan, 1996). Given that the factor of safety is a reflection of uncertainty, it should logically reflect the degree of uncertainty in the shear strength properties. This was clearly noted by Terzaghi and Peck (1948, pg. 106):

“The practical consequences of the observed differences between real soils and their ideal substitutes must be compensated by adequate factors of safety.”

A commonly accepted value for the factor of safety in geotechnical engineering slope stability analyses is $FS \geq 1.5$. Many engineers blindly accept this value while remaining ignorant of its basis. The origin of this value was the empirical result of analyzing the relative success and failure of dams that have been constructed over the past century. Experience proved that when an analysis was performed correctly, assuming reasonable and prudent material properties, an earthen structure with a factor of safety of 1.5 can be expected to remain stable even when some of its structural geometry and material properties have varied from those assumed in the analysis. Similarly, other values for an acceptable factor of safety have been established as general industry practice for other types of problems, such as bearing capacity (required FS generally between 2 and 5) or drainage applications (FS generally ranging from 1 to 20 depending on the problem).

It is also fundamental to the establishment of generally accepted factors of safety that analyses are performed correctly, and are based on prudent assumptions regarding material properties, geometry, unit weights, and pore pressures. Factors of safety are not intended to compensate for engineering errors or omissions. Indeed, the author has evaluated failures where the design factor of safety exceeded 1.5, which means that the original design neglected to take into account one or more critical factors.

With containment lining systems we meet a unique opportunity. We have a greater ability to know where the potential critical slip plane is, and can measure its shear strength characteristics more accurately than we can in a number of traditional geotechnical problems. We have far more knowledge of the geometry and shear strengths than when we are confronted with a natural slope, for example. Knowing where slippage is most likely to occur, we have to assess the implications for deformation. As described previously in this paper, we often don't really know if some deformation will occur, but experience from many analogous failures, along with the process of deduction, tells us that it *could* occur. Knowing this, we should at least be prepared to use the post-peak shear strength of the surface having the lowest peak strength.

SPECIFIC APPROACHES

Some specific design approaches, which the author has himself employed, are summarized below. This does not imply that others approaches do not exist, but simply that this paper is based on the author's experience.

1. The Most Conservative Approach – Force the Slip Plane Above the Geomembrane and Use Residual Shear Strengths Everywhere the Slip Plane Occurs in the Liner System. A simple and common way of achieving this objective is to use single-side textured geomembrane for the primary liner, and then cover it with a geotextile or geonet product. In nearly every case the author has been involved with (save a few inevitable exceptions), single-sided textured geomembrane (textured side down, of course) always caused whatever slippage occurred to take place on the top surface of the geomembrane, if it was covered with another geosynthetic. Even when directly covered by a granular material, it was often possible to make the bottom (textured) interface stronger than the smooth geomembrane/granular soil interface. In our experience there is often not a large difference between the peak and residual shear strength on smooth geomembrane interfaces with either other geosynthetics or granular soils, and these interfaces would not be considered very brittle. There may be some exceptions, such as a smooth HDPE geomembrane against a wet clay as described by Filz et al. (2001) for the Kettleman Hills failure analysis.

Some designs may need greater shear strength for interim construction and operational conditions than can be provided by a smooth geomembrane surface, so a double-sided textured geomembrane may be required. In this case the design condition of having the weak interface above the primary geomembrane may still be achieved by specifying a more aggressive texturing on the lower side of the geomembrane (see shear data presented in Figure 4).

If a designer is able to use the residual shear strength of the upper geomembrane interface and achieve acceptable factors of safety, this design can be very safe from the point of view of both stability and environmental containment. This approach is favored by Hullings and Sansome (1997), who recommend: “If possible, provide a slip plane and a stress-free geomembrane.”

If true residual shear strengths are used for the analysis, and those strengths are measured with a degree of confidence that they represent worst case for the liner system interfaces, it follows that a lower-than-typical factor of safety can be allowed. Gilbert and Byrne (1996) suggest that a factor of safety simply greater than unity may be an adequate design criterion for analyses that assume residual shear strengths are the only strengths mobilized along the entire slip surface. Part of Gilbert’s rationale (personal communication, 2001) is that even if a failure were induced for a slope analyzed with this criterion, things could not degenerate quickly, presuming the analysis were properly performed. The slope could subsequently be monitored and measures taken to reduce the deformation rate, if deemed necessary.

A similar recommendation is given by Stark et al. (1998): “...strain incompatibility can facilitate the development of slope instability because the geosynthetic interface may mobilize a post-peak or residual strength while the waste is mobilizing a strength that is significantly below the peak strength. This can be incorporated into a design by assigning a residual strength to the critical interface or slip surface and requiring a factor of safety, $FS > 1$...Because field interface displacements and *effect(s) of progressive failure are not known [emphasis by author]*, a factor of safety, $FS > 1$ with a ring shear residual interface strength assigned to all potential slip surfaces should be satisfied in addition to meeting regulatory requirements.”

Filz et al. (2001) suggest that if true residual shear strengths are used for the analysis, then whatever factor of safety would normally be deemed appropriate for a given project could be reduced by the following reduction factor (RF):

$$RF = \tau_r / [\tau_r + 0.1(\tau_p - \tau_r)]$$

Where τ_r = residual shear strength, and τ_p = peak shear strength. They imply that the normally appropriate factor of safety would be determined based on considerations of uncertainty and consequences as described by Duncan (2000). Also, it should be noted that their discussion and recommendations were restricted to smooth-geomembrane/clay interfaces.

2. Safe Approach – Use Residual Shear Strength of the Interface with the Lowest Peak Strength. This approach could be the same as the above approach if the interface having the lowest shear strength happens to be above the primary geomembrane. If, due to overall slope stability constraints, the interface with the lowest peak strength is below the primary geomembrane (e.g. weak subgrade interface), this approach will still result in a very safe design relative to slope stability. It could, however, be less conservative in terms of environmental containment should deformation occur, causing a tear in the primary geomembrane. This approach is recommended by Gilbert and Byrne (1996) who “strongly recommended that the potential for instability be explored in a limit equilibrium analysis using residual strengths along all interfaces....It is strongly recommended that a factor of safety greater than one be achieved in all containment system slope designs, assuming residual strengths are mobilized along the entire slip surface.”

The same degree of factor of safety for this approach would apply as for Approach # 1 above. Holley et al. (1997) reported using residual shear strengths for a critical surface below the primary geomembrane in a steep canyon landfill, and obtaining operating factors of safety of 1.2 and an ultimate factor of safety of 1.4 for the final build-out. It is not clear if these were their minimum design criteria, or simply the results that they accepted.

3. Brute Strength Approach – This approach would employ very aggressive texturing to achieve high interface strengths, although the assumed strengths may be prorated by some factor to account for variability. The need to occasionally use this approach is suggested by Hullings and Sansome (1997): “Overall slope stability conditions often do not allow low interface strengths, so the interface strengths above the geomembrane cannot be much lower than the interface strength on the underside of the geomembrane.”

If the approach of high interface strength is used everywhere, and seismic analysis shows no deformation, an acceptable design basis may be to use peak shear strength with an adequately high factor of safety. How high is adequate is difficult to say, because the theoretical possibility of progressive failure still exists. The finite-element study performed by Filz et al. (2001) indicates that $FS > 2$ should be required for analyses based on peak strength of smooth-geomembrane/clay interfaces.

We have only the record of successful designs that were constructed based on peak strength to testify that the brute strength approach may be valid, but this does not demonstrate that it is conservative. The analysis should account for potential leachate build-up under worst case assumptions, for example after a post-closure maintenance period with substantial leachate still being generated, and the operations or leachate-collection layer completely clogged. Check that a submerged condition at the toe does not result in a reduction in shear strength (due to reduction in effective normal stresses) to the point that it fails the peak strength at the toe, which could lead to progressive failure through the rest of the fill (such as that discussed by Schmucker and Hendron, 1998).

4. Hybrid Approaches

- a) *Use Residual on the Side Slope and Peak on the Base.* To the author's knowledge, this approach was first documented in the literature by Stark and Poeppel (1994) in their review of the notorious Kettleman Hills failure. As they so aptly stated: "...it appears that peak and residual interface strengths should be assigned to the base and sideslopes, respectively, for design purposes." This was later echoed by Jones and Dixon (1998) from the U.K., who stated: "In some instances residual values may be appropriate on the side slope where large displacements are anticipated, used together with peak values on the base." In the author's opinion, this approach is a strong qualifier for accepting a traditional factor of safety in the range of 1.5 for ultimate build-out conditions (assuming unexpected pore-pressure scenarios are included in the evaluation), and 1.3 for operations.
- b) *Use Post-Peak Strength Values that Anticipate a Limited Amount of Deformation.* Shear strength reductions may occur due to relative deformations during construction, landfill operations, and waste settlement, but these deformations may be less than those which would lead to the minimum residual shear strength conditions. Also, based on their observation of numerous apparently successful facilities, design practitioners may consider peak shear strengths with an adequate factor of safety to be valid designs, while still wishing to incorporate an additional degree of conservatism by reducing the measured peak strength of the geosynthetic interfaces. These strength reductions would be applied to the side slope as well as the base. Use of this approach is suggested by Filz et al. (2001), who suggest using a mobilized strength that is higher than the residual by about 10% of the increment from residual to peak strength, and applying an appropriate factor of safety to this based on reliability concepts as described by Duncan (2000).

- c) *Use Lower Waste Shear Strengths.* From the observation of trends published in the literature, shear strengths of 30° or more are commonly used for municipal solid waste. This level of shear strength has been documented as being generally conservative (e.g. Kavazanjian, 2001), but may require some amount of strain to become fully mobilized. As an approach to stability analyses designers may wish to reduce the mobilized strength of the waste material to more closely match the strain compatibility of the liner system.

The author has used all the above approaches in his own practice, which over the years has been based on improved levels of understanding. Currently (subject to change!) the author employs a combination of Approach #1 and #4 as his standard practice. That is, he usually defines a “design condition” which he believes will be the actual long-term conditions that interface shear strengths will experience. The decision as to what long-term shear strengths he selects is project-specific (there are many variations), and a complete discussion of this is beyond the scope of this paper. Suffice it to say that the decision is usually related to the criteria described for Approach #4. Next, the author follows the advice of Gilbert and Byrne (1996) and checks that the stability under the worst-case shear strength conditions (e.g. hydrated residual shear strength) results in $FS > 1.0$. This latter test is often the more significant.

A good example of the above approach is for bottom liner designs that involve the encapsulation of unreinforced bentonite between two geomembranes. The design scenario argues that most of the bentonite will remain dry for at least several centuries, and the basic slope stability analysis is performed on this basis. A second analysis is performed, however, to verify that the stability factor of safety is greater than unity even when all of the bentonite is under fully hydrated residual shear strength conditions. This example is more fully described in Thiel et al. (2001).

PART 4 – CONCLUSIONS AND RECOMMENDATIONS

CONCLUSIONS

- Many geosynthetic interfaces are highly strain-softening (i.e. “brittle”). The most common example is a textured geomembrane against some form of geotextile (whether it be a cushion, part of a geonet composite, or a GCL).
- There are mechanisms that can lead to exceedence of peak strength even though a correctly-performed slope stability analysis predicts a factor of safety greater than one. Examples of these mechanisms include:
 - Non-uniform mobilized stress distribution.

- Relative differences in stiffness between waste and liner materials.
 - Unexpected pore pressures.
 - Seismic loading.
 - Deformation during construction.
 - Waste settlement.
 - Foundation settlement.
 - Aging and creep of the geosynthetics.
- Exceedence of peak strength in a brittle interface can result in progressive failure.
 - Based on field observation, most facilities designed with aggressive interface shear strengths are not experiencing post-peak shear strength, which means that the working shear stress is probably less than or equal to the peak strength. Only a few examples of progressive failure along geosynthetic interfaces have occurred in the industry, and these have not been along highly brittle interfaces, which means that the projects did not have high factors of safety to begin with, even assuming peak interface strengths.
 - Several design approaches have been used over the years and the standard-of-practice is evolving. In the United States a preferred approach has not yet clearly emerged.

RECOMMENDATIONS FOR PRACTICE

- Designers and CQA firms should conduct material-specific testing of interfaces to verify that the materials specified and/or supplied for a project are realistic and meet the design requirements. Whoever commissions the testing should possess a skilled familiarity with the design objectives as well as the testing technique.
- Designers should attempt to position the critical slip plane above the primary geomembrane to the extent feasible for a given project. If a double-sided textured geomembrane is required for construction or operational stability, attempt to specify more aggressive texturing on the under side of the geomembrane.
- Using peak shear strengths on the landfill base, and residual shear strengths on the side slopes appears to be a successful state-of-the-practice in many situations.
- Designers should consider evaluating all facilities for stability using the residual shear strength along the geosynthetic interface that has the lowest peak strength. This would be an advisable risk-management practice for designers, even if the FS under these conditions is simply greater than unity.

- Regardless of the design assumptions, specify soil spreading by pushing up-slope only, and require close monitoring of LCRS and operations soil placement on slopes during construction to verify that relative shear displacement does not occur during construction. Exceptions to this practice should be allowed only with field tests and CQA verification.
- If LCRS or operations soils are placed as part of landfill operations, designers should assume the worst and automatically assume residual side-slope shear strength conditions will occur (and extra leakage rates as well). The reason for this is that construction by landfill operators is usually not controlled and monitored closely.
- Check stability for a potential leachate buildup, especially near the toe of the landfill.

RECOMMENDATIONS FOR FURTHER RESEARCH

- More finite element analyses at an academic level, such as those performed by Reddy et al. (1996) and Filz et al. (2001) would be warranted, to gain a better understanding of the threshold beyond which localized stress distributions might cause exceedence of peak shear resistance. Refinements in the analyses would include modeling the strain-softening behavior of the geosynthetic interfaces, and checking different types of interfaces and geometries. The results of these analyses might prove useful for establishing guidelines as to when peak strengths might be exceeded and when they might be maintained. Ultimately, the author envisions correlations between the FS determined by limit equilibrium analyses, ratios of peak interface strengths to waste fill strengths, and relative stiffnesses (somewhat as proposed by Gilbert and Byrne (1996), but more specific and less general), being used to estimate when and where peak vs. post-peak strengths would be reached at the interfaces.
- The monitoring of slope deformation on geosynthetic interfaces that are being buried by waste is recommended. One fairly easy way to do this would be to use the simple tell-tale technique employed for the Cincinnati cover demonstration project (Koerner et al., 1996), though this would require participation by landfill owners and operators. This avenue of research echoes that suggested by Gilbert and Byrne (1996), who state: “Future research should focus on measuring deformations and mobilized shear resistances in existing waste containment facilities.”
- The monitoring of pore pressures in the LCRS above liner systems, with the reporting of the worst-case conditions, would provide valuable information regarding long term conditions in landfills. Unfortunately, any high pressures would likely result in a permit violation at many facilities, so it is improbable that

an existing owner will voluntarily monitor high pressures, much less report them. We are therefore left with only orphan or Superfund sites as a possible basis for monitoring. Because of this limitation, participation in international waste conferences is increasingly valuable.

- Additional laboratory testing, conducted on various types of interfaces, would be useful to assess the impact of interface deformations at low normal loads on the peak strength reductions at higher normal loads.

REFERENCES

Abramson, L.W., Lee, T.S., Sharma, S., and Boyce, G.M. (1996). Slope Stability and Stabilization Methods. John Wiley & Sons, Inc. New York.

Breitenbach, A.J. (1997) "Overview Study of Several Geomembrane Liner Failures Under High Fill Load Conditions." Proc. of Geosynthetics '97, IFAI, Vol. 2, pp. 1045-1061.

Breitenbach, A.J. and Swan, R.H. (1999) "Influence of High Load Deformations on Geomembrane Liner Interface Strengths." Proc. of Geosynthetics '99, IFAI, Vol. 1, pp. 517-529.

Brink, D., Day, P.W. and DuPreez, L. (1999) "Failure and Remediation of Bulbul Drive Landfill: Kwazulu-Natal, South Africa." Proc. Sardinia '99 Seventh International Waste Management and Landfill Symposium, CISA, Vol. III, pp. 555-562.

Duncan, J.M. (1996) "State of the Art: Limit Equilibrium and Finite-Element Analyses of Slopes." J. of Geotechnical Engineering, ASCE, Vol. 122, No. 7, May, pp. 577-596.

Duncan, J.M. (2000) "Factors of Safety and Reliability in Geotechnical Engineering" J. of Geotechnical and Geoenvironmental Engineering, ASCE, Vol. 126, No. 4, Apr., pp. 307-316.

Eid, H.T., Stark, T.D., Evans, W.D. and Sherry, P.E. (2000) "Municipal Solid Waste Slope Failure. I: Waste and Foundation Soil Properties." J. of Geotechnical and Geoenvironmental Engineering, ASCE, Vol. 126, No. 5, May, pp. 397-407.

Esterhuizen, J.B., Filz, G.M., and Duncan, J.M. (2001) "Constitutive Behavior of Geosynthetic Interfaces" J. of Geotechnical and Geoenvironmental Engineering, ASCE, Vol. 127, No. 10, Oct., pp. 834-840.

Filz, G.M., Esterhuizen, J.B., and Duncan, J.M. (2001) "Progressive Failure of Lined Waste Impoundments" J. of Geotechnical and Geoenvironmental Engineering, ASCE, Vol. 127, No. 10, Oct., pp. 841-848.

Gilbert, R.B. and Byrne, R.J. (1996) "Strain-Softening Behavior of Waste Containment System Interfaces." *Geosynthetics International, IFAI*, Vol. 3, No. 2, pp. 181-203.

Gilbert, R.B. (2001) Personal communication with the author.

Hendron, D.M., Fernandez, G., Prommer, P.J., Giroud, J.P., and Orozco, L.F. (1999) "Investigation of the Cause of the 27 September 1997 Slope Failure at the Dona Juana Landfill" *Proc. Sardinia '99 Seventh International Waste Management and Landfill Symposium, CISA*, Vol. III, pp. 545-554.

Hillman, R.P. and Stark, T.D. (2001) "Shear Strength Characteristics of PVC Geomembrance-Geosynthetic Interfaces." *Geosynthetics International, IFAI*, Vol. 8, No. 2, pp. 135-162.

Holley, K., Richardson, J., and Sadlier, M. (1997) "Design and Construction to Optimise Landfill Stability at the Nent Landfill, Hong Kong." *Proc. Sardinia '99 Seventh International Waste Management and Landfill Symposium, CISA*, Vol. III, pp. 565-574.

Hullings, D.E. and Sanome, L.J. (1997) "Geomembrane Anchor Trenches." *J. of Geotextiles and Geomembranes, Elsevier*, Vol. 15, Nos. 4-6, pp. 403-417.

Jones, D.R.V. and Dixon, N. (1998) "Shear Strength Properties of Geomembrane/Geotextile Interfaces." *J. of Geotextiles and Geomembranes, Elsevier*, Vol. 16, Nos. 1, pp. 45-71.

Kavazanjian, E. (2001) "Mechanical Properties of Solid Waste." *Proc. Sardinia '01 Eighth International Waste Management and Landfill Symposium, CISA*, Vol. III, pp. .

Koerner, R.M., Carson, D.A., Daniel, D.E., and Bonaparte, R. (1996) "Current Status of the Cincinnati GCL Test Plots" *Proceedings of the 10th GRI Conference, Field Performance of Geosynthetics and Geosynthetic Related Systems*. Geosynthetic Research Institute, Drexel University, Philadelphia, PA, pp. 147-175.

Koerner, R.M. and Daniel, D.E. (1997) Final Covers for Solid Waste Landfill and Abandoned Dumps. ASCE Press, Reston, VA.

Koerner, R.M. and Soong, T.Y. (2000) "Leachate in Landfills: The Stability Question." *Geotextiles and Geomembranes, Elsevier*, Vol. 18, pp. 293-309.

LaRochelle, P. (1989) "Problems of Stability: Progress and Hopes." The Art and Science of Geotechnical Engineering. Ed. by Corning et al., Prentice Hall, N.J., pp. 269-290.

Li, K.S. and Lam, J. (2001) Discussion of “Evolution of Progressive Failure of Landslides.” J. of Geotechnical and Geoenvironmental Engineering, ASCE, Vol. 127, No. 1, Jan., pg. 98.

Liu, C.N., Gilbert, R.B., Thiel, R.S., and Wright, S.G. (1997). “What is an Appropriate Factor of Safety for Landfill Cover Slopes?” Conference Proceedings from Geosynthetics '97. IFAI, Roseville, MN, pp. 481-496.

Mazzucato, A., Somonini, P. and Colombo, S. (1999) “Analysis of Block Slide in a MSW Landfill.” Proc. Sardinia '99 Seventh International Waste Management and Landfill Symposium, CISA, Vol. III, pp. 537-544.

NAVFAC (1982) Soil Mechanics. Design Manual 7.1, Department of the Navy, Naval Facilities Engineering Command, Alexandria, VA.

Reddy, K.R., Kosgi, S. and Motan, S. (1996) “Interface Shear Behavior of Landfill Composite Liner Systems: A Finite Element Analysis.” Geosynthetics International, IFAI, Vol. 3, No. 2, pp. 247-275.

Schmucker, B.O. and Hendron, D.M. (1998) “Forensic Analysis of the 9 March 1996 Landslide at the Rumpke Sanitary Landfill, Hamilton County, Ohio.” Proc. of the 12th GRI Conference, Lessons Learned from Geosynthetic Case Histories, Geosynthetic Institute, Folsom, PA, pp. 269-295.

Soong, T.Y., Hungr, O., and Koerner, R.M. (1998) “Stability Analyses of Selected Landfill Failures by 2-D and 3-D Methods” Proc. of the 12th GRI Conference, Lessons Learned from Geosynthetic Case Histories, Geosynthetic Institute, Folsom, PA, pp. 296-329.

Stark, T.D. and Eid, H.T. (1998) “Performance of Three-Dimensional Slope Stability Methods in Practice” J. of Geotechnical and Geoenvironmental Engineering, ASCE, Vol. 124, No.11, Nov., pp. 1049-1060.

Stark, T.D., Arellano, D., Evans, W.D., Wilson, V.L., and Gonda, J.M. (1998) “Unreinforced Geosynthetic Clay Liner Case History.” Geosynthetics International, IFAI, Vol. 5, No. 5, pp. 521-544.

Stark, T.D., Eid, H.T., Evans, W.D. and Sherry, P.E. (2000) “Municipal Solid Waste Slope Failure. II: Stability Analyses.” J. of Geotechnical and Geoenvironmental Engineering, ASCE, Vol. 126, No. 5, May, pp. 408-419.

Stark, T.D., and Poeppel, A.R. (1994) “Landfill Liner Interface Strengths from Torsional Ring Shear Tests.” J. of Geotechnical Engineering, ASCE, Vol. 120, No. 3, March, pp. 597-615.

Terzaghi, K. and Peck, R. (1948) Soil Mechanics in Engineering Practice. John Wiley & Sons, New York, NY.

Thiel, R., Daniel, D.E., Erickson, R., Kavazanjian, E., and Giroud, J.P. (2001) *GundSeal GCL Design Manual*. Published by GSE, Houston, TX.

Tiande, M., Chongwu, M, and Shengzhi, W. (1999) “Evolution Model of Progressive Failure of Landslides.” J. of Geotechnical and Geoenvironmental Engineering, ASCE, Vol. 125, No. 10, Oct., pp. 827-831.

**APPLICATION FOR PERMIT RENEWAL AND MODIFICATION
SANDOVAL COUNTY LANDFILL**

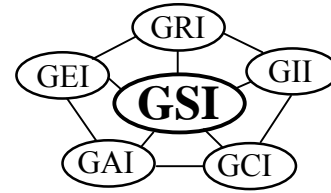
**VOLUME III: LANDFILL ENGINEERING CALCULATIONS
SECTION 7: GEOSYNTHETICS TENSILE STRESS AND STABILITY ANALYSIS**

ATTACHMENT III.7.J

**KOERNER, ROBERT M. AND KOERNER, GEORGE R. 2007.
INTERPRETATION(S) OF LABORATORY GENERATED INTERFACE SHEAR
STRENGTH DATA FOR GEOSYNTHETIC MATERIALS WITH EMPHASIS ON THE
ADHESION VALUE. GRI WHITE PAPER #11. GEOSYNTHETICS INSTITUTE.**

Geosynthetic Institute

475 Kedron Avenue
Folsom, PA 19033-1208 USA
TEL (610) 522-8440
FAX (610) 522-8441



GRI White Paper #11

**Interpretation(s) of Laboratory Generated Interface Shear Strength
Data for Geosynthetic Materials With Emphasis on the Adhesion Value**

by

**Robert M. Koerner and George R. Koerner
Geosynthetic Institute
475 Kedron Avenue
Folsom, PA 19033 USA**

**Phone (610) 522-8440
Fax (610) 522-8441**

**E-mail:
robert.koerner@coe.drexel.edu
gkoerner@dca.net**

September 11, 2007

Interpretation(s) of Laboratory Generated Interface Shear Strength Data for Geosynthetic Materials With Emphasis on the Adhesion Value

The beginning point of this White Paper is based on the assumption that a designer has a credible set of laboratory generated shear stress versus shear displacement curves on the desired geosynthetic-to-geosynthetic or geosynthetic-to-soil interface tested per ISO 12957 or ASTM D5321, or ASTM D6243 if geosynthetic clay liners are involved. In this regard we are considering having such data as shown in Figure 1. It is clearly seen that many behavioral trends are possible.

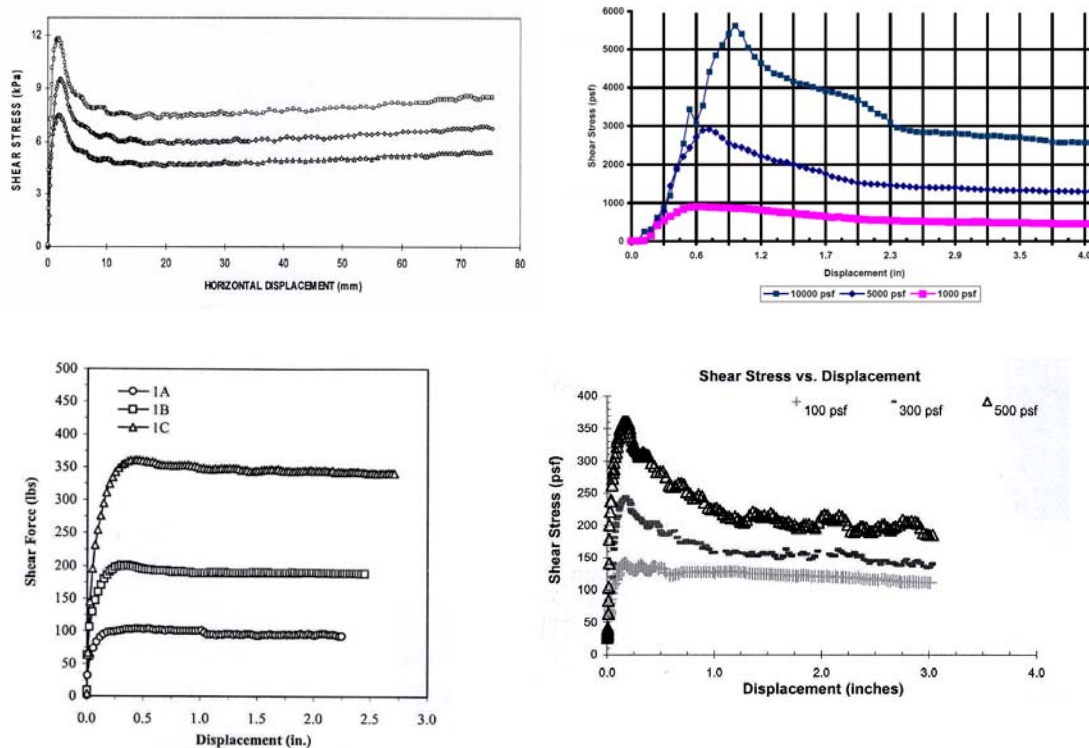


Figure 1 – Various stress versus displacement curves for different geosynthetic materials. (Data compliments of TRI, Golder, Precision and SGI Laboratories)

Either the designer or the testing laboratory will have to generate the Mohr-Coulomb failure envelope from these curves by selecting one point on each normal stress curve and plotting the results on a normal stress versus shear stress curve as shown in Figure 2a. A least squares fit of the data point produces the failure envelope. Even further, one might have more than one such failure envelopes; peak, large displacement and/or residual. Please note, however, that this White Paper is not about the selection of peak, large displacement or residual values and the technical literature is abundant on that subject.

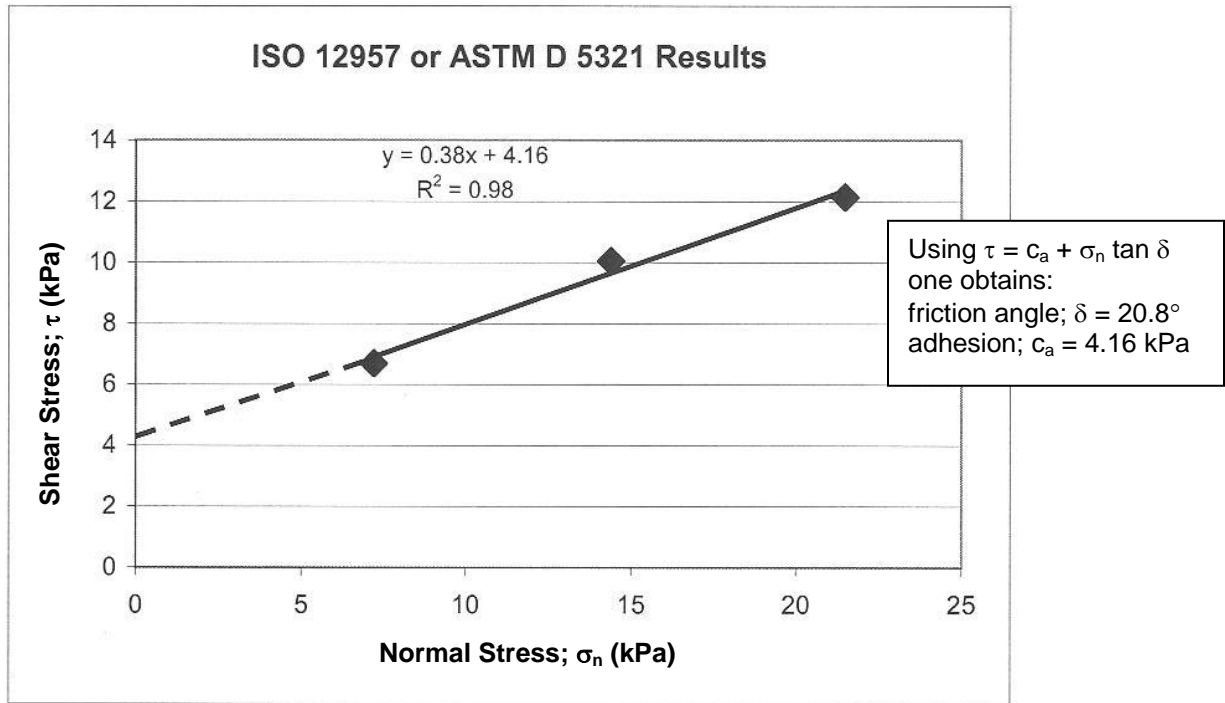


Figure 2a – Three point laboratory data leading to the drawing of a failure envelope and subsequent measurement of friction angle and shear strength intercept (or adhesion) values.

At any rate, to begin the present discussion on the interpretation of the selected failure envelope, the designer is confronted with something like that shown Figure 2a. Here the data points are clearly identified and the failure envelope is usually generated by a least squares fitting procedure. The dashed extension to the y-axis is often the general assumption particularly for low normal stresses as indicated. Note that there are indeed exceptions to this situation such as curved failure envelopes within the normal stress range tested, or zero normal stress tests. They are special cases and will be discussed later.

Interpretation #1 – Use of full “ c_a ” and full “ δ ” values

Assuming that the previous failure envelope is based on credible laboratory procedures, properly simulated insofar as representative samples, normal stress selection, moisture conditions, strain rate, etc., our recommended approach is to use the shear strength parameters directly in your slope stability analysis and, if found to be adequate, for your materials specification criteria as well. For landfill cover veneer stability problems all GSI Members and Associate Members should have our spreadsheet calculation program which is extremely easy to use. For others, there are many computer codes available. For a hypothetical veneer slope stability example using the two shear strength parameters (c_a and δ) from Figure 2a, the input information is as follows:

- cover soil thickness $h = 0.3$ m
- slope angle $\beta = 18.4^\circ$ (3-to-1)
- length of slope $L = 30.0$ m
- unit weight of cover soil $\gamma = 18.0$ kN/m³
- friction angle of cover soil $\phi = 30.0$ deg
- cohesion of cover soil $c = 0.0$ kN/m²
- friction angle of interface $\delta = 20.8$ deg
- adhesion of interface $c_a = 4.16$ kPa (= 87 psf)

By using the program just mentioned or similar procedure, the resulting slope factor-of-safety value is; $FS = 3.62$. This is a relatively high value and would generally be considered quite conservative. One point worth mentioning, however, is the strong influence of the adhesion value on factor-of-safety. To illustrate this, we now vary the c_a -value between zero and ten while holding everything else the same. This procedure results in the following table; clearly illustrating the sensitivity of the FS-value to this particular parameter.

Adhesion; " c_a "		Resulting FS-value
kPa	lb/ft ²	
0	0	1.18
2	42	2.35
4	84	3.53
6	125	4.70
8	167	5.80
10	209	7.05

Presented now is the heart of this White Paper concerning the *issue of how reliable is this laboratory generated c_a -value?* The ultimate decision is yours as the designer, but our opinions on different geosynthetic materials and related interfaces are as follows:

- For textured geomembranes against geotextiles or soil, the asperities (be they manufactured as structured, blown film, or impinged) are on the material giving rise to the high adhesion values, so we recommend using the adhesion value accordingly. Only by continuously rubbing the surfaces against one another can asperity reorientation occur and we feel this is an artifact of aggressive laboratory testing as has been done (and reported) using the ring shear testing device in particular. Alternatively, concern has been expressed when testing at very high normal stresses. The thought in both instances is that if you eliminate adhesion from textured geomembranes you are essentially assuming smooth geomembrane sheet. This is a designer's prerogative, but be prepared to have very gentle slopes in so doing.
- For smooth geomembranes against other geosynthetics or soil, a small adhesion is often observed. This is particularly the case for LLDPE, fPP, EPDM, and PVC. Each of these geomembranes are less hard than HDPE, and thus an indentation can be visualized (particularly dealing with soil) which is clearly a function of the

- applied normal stress. Assuming that the appropriate normal stresses were used in the direct shear test, we feel that one is generally justified in its use.
- (c) For geotextiles thermally bonded to geonets or other types of drainage cores, we feel that the full value of adhesion should be used. Most of these geocomposites can barely be “delaminated” in the conducting of the test and we have never heard of a field delamination problem from a properly manufactured geocomposite interface in this regard.
 - (d) For the internal shear strength of reinforced GCLs, the fibers would have to pull-out or break (or both) for a loss of adhesion. While you can force this to happen in the lab, we have no evidence of this occurring in the field. Test results invariably show high adhesion values. Furthermore, longevity (durability) of the fibers in a hydrated bentonite atmosphere promises 100-year lifetime, or longer. We have a creep-related paper in this regard. Thus, we see no reason not to use the laboratory generated value of adhesion for reinforced GCLs manufactured by either needlepunching or stitching. Of course, the upper and lower interfaces of the GCLs must be independently evaluated.
 - (e) For certain geosynthetic-to-soil interfaces, the interface shear behavior may force the failure plane into the soil. This results in the identification of the soil’s shear strength and if there is a shear strength intercept it is a cohesion value and can be used accordingly.

Thus, if adhesion from short-term testing is indicated by the failure envelope and the long-term permanence of the physical or mechanical mechanism giving rise to this adhesion is logical to anticipate, its use in a stability analysis and subsequent material’s specification is felt to be generally justified.

Interpretation #2 – Use of zero “ c_a ” and full “ δ ” value

For the situation where an adhesion is indicated by the failure envelope and you as the designer feel that its long-term existence is not justified, the most conservative approach you can take is to simply translate the entire failure envelope in a parallel manner down by the amount of adhesion indicated on the original data-generated graph; see Figure 2b.

The effect of this very conservative approach on the FS-value of the slope is substantial. The shear strength is now represented by a friction angle alone and the site-specific result will be very flat slopes. For example, the 3-to-1 slope in the hypothetical example given previously with an adhesion of zero, now has a FS = 1.18 using this approach. For the interfaces mentioned previously, we do not recommend this approach.

Alternatively, one could also decrease the adhesion slightly, but not entirely. That said, we really don’t know how to comment on this type of “compromise” situation?

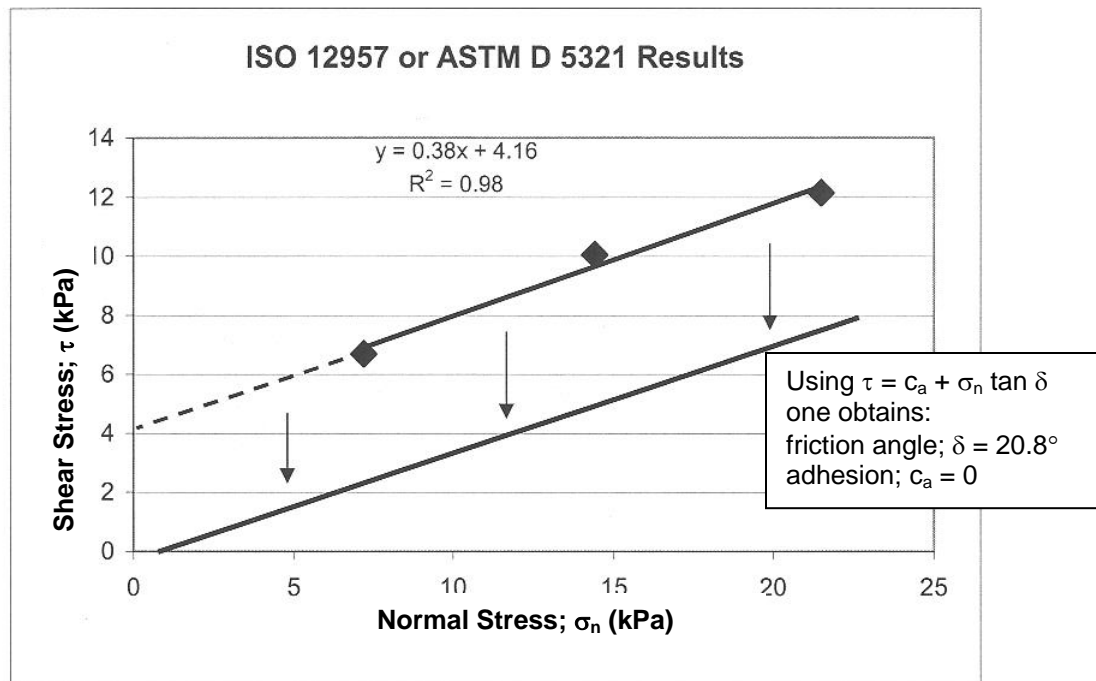


Figure 2b – Parallel translation downward of the entire laboratory generated failure envelope by an amount equal to the y-axis intercept, i.e., the adhesion.

Interpretation #3 – Use of zero “ c_a ” at zero normal stress only

A hybrid interpretation somewhere between the interpretations just presented is sometimes suggested, but its logic is somewhat difficult to fathom. In essence, the adhesion is lost only at zero normal stress but not at higher normal stresses. Thus, the failure envelope is forced through the origin but thereafter it is based on a least squares fit of the laboratory tested points as they were generated. Figure 3 illustrates the situation where the resulting friction angle is seen to be 32.2° . For our hypothetical example, this results in $FS = 1.93$. Alternatively, and equally difficult to fathom, is when only one laboratory point is generated and the failure envelope is forced through it and the origin. Both approaches are the least conservative of those mentioned in this White Paper giving rise to a rotation of the failure envelope and the highest friction angle possible. The angle resulting from this practice has been variously called “secant friction angle”, “secant angle”, or “modulus angle”. Of the group, secant angle is probably the best description for this interpretation since it shouldn’t be confused with the Mohr-Coulomb friction angle, and modulus brings with it completely other test procedures like tension testing.

We generally do not recommend such approaches for the reason that adhesion should be an intrinsic property of the interface involved and not be arbitrarily eliminated or used on the basis of a particular normal stress, or stresses. (That stated, if the interface is tested at

zero normal stress and found to have zero adhesion, the origin is a valid point and should then be used accordingly).

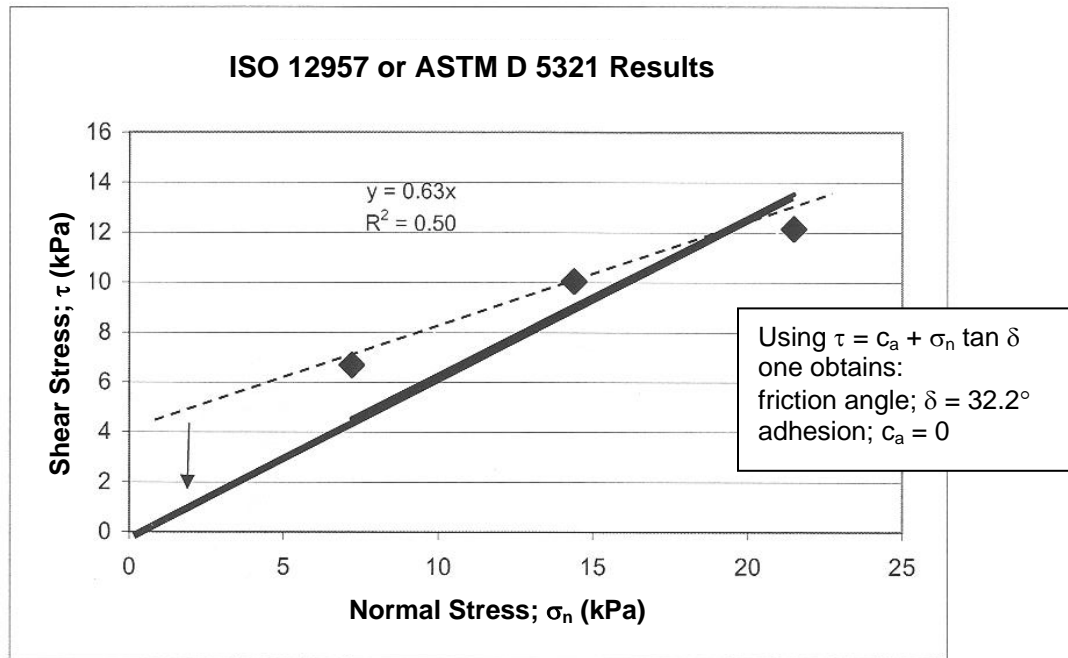


Figure 3 – Elimination of adhesion at zero normal stress but not at any of the three laboratory measured data points.

Interpretation #4 – Use of the total shear strength at a particular normal stress

A very straightforward approach to a specification value is to require a certain shear strength value at a particular normal stress. This is particularly the case if the failure envelope is curved as mentioned previously. In so doing, a specifier is requiring a single point to be taken from the failure envelope which is targeted at the expected field normal stress. Figure 4 suggests that if the field normal stress is 17.2 kPa it results in a required shear strength of 10.7 kPa, or greater. The shear strength value is thereby reflective of both a frictional component and adhesion, neither of which are specifically identified.

In so doing one avoids specifying individual “ c_a ” and “ δ ” values and much of the previous discussion is altogether avoided. The method can be extended to give two, or more, values of shear strength (or even the equation of the failure envelope) at different normal stresses in the form of a “required” table.

This approach has been used by a select few designers but is far from common practice. There is nothing of a fundamental nature which says it cannot be done and it would avoid some of the other complications inherent with different approaches.

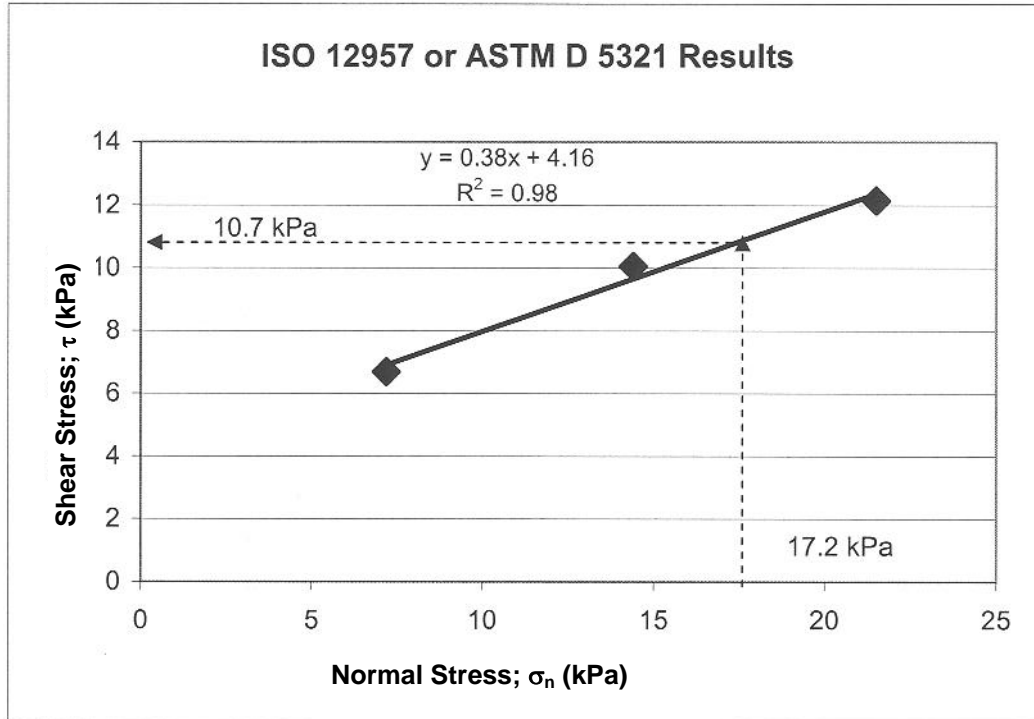


Figure 4 – Use of a laboratory generated failure envelope by specifying a site-specific normal stress and requiring a minimum value of shear strength taken directly off of the y-axis.

In summary, there are probably other or intermediate interpretations of an interface shear strength failure envelope for use in design and then a subsequent specification, but those presented here are felt to be the most common.

**APPLICATION FOR PERMIT RENEWAL AND MODIFICATION
SANDOVAL COUNTY LANDFILL**

**VOLUME III: LANDFILL ENGINEERING CALCULATIONS
SECTION 7: GEOSYNTHETICS TENSILE STRESS AND STABILITY ANALYSIS**

**ATTACHMENT III.7.K
BENTOMAT® GCL DIRECT SHEAR DATABASE (TR-114BM),
CETCO® LINING TECHNOLOGIES, 2009**

BENTOMAT[®] DIRECT SHEAR TESTING SUMMARY

The following table summarizes the direct shear testing on Bentomat that has been performed by CETCO and other laboratories on a project-specific basis for the past several years. This data will give the designer some general information about the shear strength of commonly used GCL interfaces and should be the first step in evaluating a proposed liner system where slope stability is a concern.

The variables in any direct shear test are numerous, including specimen preparation; hydration pressures, liquids, and sequencing, and rate of shear, and others. Test results will vary accordingly, which is partially accountable for the wide range of data reported even for similar interfaces.

This data is for informational purposes only and is not intended to replace project-specific interface testing, which CETCO emphatically recommends. CETCO makes no warranty as to the usefulness of the data. Individual test reports for most of the summarized data can be provided upon request.

BENTOMAT GCL DIRECT SHEAR DATABASE

TR-114BM

Lab ¹	Report Date	GCL Tested	Interface Tested ²		Testing Conditions					Mohr-Coulomb Failure Envelopes ⁶				Comments ⁸	
										Peak		Large Displacement ⁷			
			GCL	Other	Normal Stresses (psi)	Hydration. ³		Consol. ⁴	SDR ⁵ (in/min)	Angle (deg)	adhesion (psf)	Angle (deg)	adhesion (psf)		
psf	hrs														
Internal Shear Results															
SGL	Oct-08	200R	Internal		75		200	24	48 hrs @ load	0.04	23 °	0	7 °	0	
SGL	Apr-09	ST	Internal		1.4		200	24	48 hrs @ load	0.004	73 °	0	--	--	sliding at gripping surface
PGL	Feb-08	ST	Internal		1.4		48 hrs @ load			0.004	77 °	0	--	--	sliding at gripping surface
SGL	Jun-06	ST	Internal		34.7		200	24	24 hrs	0.04	27 °	0	7 °	0	
SGL	Jun-06	ST	Internal		34.7		200	24	24 hrs	0.04	31 °	0	8 °	0	
SGL	Jun-06	ST	Internal		34.7		200	24	24 hrs	0.04	38 °	0	9 °	0	
SGL	Jun-06	ST	Internal		34.7		200	24	24 hrs	0.04	31 °	0	7 °	0	
SGL	Jun-06	ST	Internal		34.7		200	24	24 hrs	0.04	42 °	0	9 °	0	
SGL	Jun-06	ST	Internal		34.7		200	24	24 hrs	0.04	34 °	0	7 °	0	
SGL	Jun-06	ST	Internal		34.7		200	24	24 hrs	0.04	26 °	0	7 °	0	
SGL	Oct-06	ST	Internal		34.7		200	24	24 hrs	0.04	37 °	0	8 °	0	
PGL	Feb-03	ST	Internal		5 20 45	432	7 days	48 hrs @ load	0.004	22.7 °	1146	19.3 °	676		
SGL	Aug-01	ST	Internal		10 30 50	24 hrs @ load			0.001	32 °	1645	13 °	160		
SGL	Aug-01	ST	Internal		10 30 50	24 hrs @ load			0.001	39 °	1050	15 °	220		
SGL	Aug-01	ST	Internal		10 30 50	24 hrs @ load			0.001	38 °	1105	17 °	190		
SGL	Apr-09	ST	Internal		75		200	24	48 hrs @ load	0.004	32 °	0	8 °	0	

BENTOMAT GCL DIRECT SHEAR DATABASE

TR-114BM

Lab ¹	Report Date	GCL Tested	Interface Tested ²		Testing Conditions					Mohr-Coulomb Failure Envelopes ⁶				Comments ⁸
										Peak		Large Displacement ⁷		
			GCL	Other	Normal Stresses (psi)	Hydration: ³ psf hrs		Consol. ⁴	SDR ⁵ (in/min)	Angle (deg)	adhesion (psf)	Angle (deg)	adhesion (psf)	
SGI	Jan-09	ST	Internal		75	200	24	48 hrs @ load	0.04	32 °	0	7 °	0	
SGI	Feb-08	ST	Internal		75	200	24	48 hrs @ load	0.04	38 °	0	8 °	0	
SGI	Jan-07	ST	Internal		75	200	24	48 hrs @ load	0.004	33 °	0	11 °	0	
SGI	Oct-98	ST	Internal		36 75 145	167	6 days	step-load	0.00006	22 °	1545	6 °	731	
SGI	Jan-09	ST	Internal		150	200	24	48 hrs @ load	0.04	24 °	0	6 °	0	
SGI	Feb-01	ST	Internal		50 100 150	48 hrs @ load			0.04	15 °	1195	8 °	-310	
SGI	Feb-01	ST	Internal		150 250 400	48 hrs @ load			0.04	11 °	2875	5 °	1080	
SGI	Feb-01	ST	Internal		50 to 400 psi	48 hrs @ load			0.04	12 °	2095	6 °	275	
SGI	Apr-09	DN	Internal		1.4	200	24	48 hrs @ load	0.004	75 °	0	--	--	sliding at gripping surface
SGI	Feb-08	DN	Internal		1.4	24 hrs @ load			0.004	77 °	0	--	--	sliding at gripping surface
TRI	Apr-03	DN	Internal		0.7 1.7 3.5	24 hrs @ load			0.04	47.3 °	2813	26.6 °	392	
SGI	Jun-01	DN	Internal		1.0 2.6 6.5	72	120	step-load	0.004	46 °	215	42 °	120	
PGL	Jul-06	DN	Internal		7 21	200	48	24 hrs @ load	0.04	14.5 °	2326	0.5 °	1436	
SGI	Sep-08	DN	Internal		5 25 50	200	24	24 hrs	0.04	34 °	1155	7 °	425	
SGI	Sep-08	DN	Internal		5 25 50	200	24	24 hrs	0.04	33 °	1260	8 °	425	
SGI	Sep-08	DN	Internal		5 25 50	200	24	24 hrs	0.04	35 °	990	8 °	430	

BENTOMAT GCL DIRECT SHEAR DATABASE

TR-114BM

Lab ¹	Report Date	GCL Tested	Interface Tested ²		Testing Conditions						Mohr-Coulomb Failure Envelopes ⁶				Comments ⁸	
											Peak		Large Displacement ⁷			
			GCL	Other	Normal Stresses (psi)			Hydration. ³ psf hrs		Consol. ⁴	SDR ⁵ (in/min)	Angle (deg)	adhesion (psf)	Angle (deg)		adhesion (psf)
SGI	Sep-08	DN	Internal		5	25	50	200	24	24 hrs	0.04	32 °	1185	8 °	380	
SGI	Sep-08	DN	Internal		5	25	50	200	24	24 hrs	0.04	35 °	1120	7 °	385	
SGI	Sep-08	DN	Internal		5	25	50	200	24	24 hrs	0.04	33 °	1190	8 °	380	
SGI	Sep-08	DN	Internal		5	25	50	200	24	24 hrs	0.04	34 °	1150	7 °	410	
SGI	Sep-00	DN	Internal		10	25	50	24 hrs @ load			0.001	31 °	1000	12 °	770	GCL peel = 45 lbs
SGI	Sep-00	DN	Internal		10	25	50	24 hrs @ load			0.001	30 °	1155	10 °	170	GCL peel = 27 lbs
SGI	Mar-01	DN	Internal		15	30	60	48 hrs @ load			0.04	24 °	1655	7 °	180	
SGI	Apr-09	DN	Internal		75			200	24	48 hrs @ load	0.004	33 °	0	8 °	0	
SGI	Feb-08	DN	Internal		75			200	24	48 hrs @ load	0.04	40 °	0	8 °	0	
SGI	Jan-07	DN	Internal		75			200	24	48 hrs @ load	0.004	36 °	0	12 °	0	
SGI	Jun-08	DN	Internal		150			200	24	48 hrs @ load	0.04	28 °	0	7 °	0	
SGI	Sep-02	DN	Internal		34.7	150		As-received (21.6%)			0.04	23 °	1715	13 °	1100	
SGI	Apr-09	SDN	Internal		1.4			200	24	48 hrs @ load	0.004	76 °	0	--	--	sliding at gripping surface
GT	Nov-08	SDN	Internal		1.4			200	24	48 hrs @ load	0.004	74 °	0	--	--	
SGI	Aug-09	SDN	Internal		10	30	70	144	48	24 hrs @ load	0.004	34 °	1248	6 °	1020	
SGI	Apr-09	SDN	Internal		75			200	24	48 hrs @ load	0.004	37 °	0	8 °	0	

BENTOMAT GCL DIRECT SHEAR DATABASE

TR-114BM

Lab ¹	Report Date	GCL Tested	Interface Tested ²		Testing Conditions					Mohr-Coulomb Failure Envelopes ⁶				Comments ⁸
										Peak		Large Displacement ⁷		
			GCL	Other	Normal Stresses (psi)	Hydration. ³ psf hrs		Consol. ⁴	SDR ⁵ (in/min)	Angle (deg)	adhesion (psf)	Angle (deg)	adhesion (psf)	
SGI	Feb-08	SDN	Internal		75	200	24	48 hrs @ load	0.04	34 °	0	7 °	0	
SGI	Jan-07	SDN	Internal		75	200	24	48 hrs @ load	0.004	36 °	0	12 °	0	
TRI	Apr-08	SDN	Internal		90	24 hrs @ load			0.04	39.1 °	0	15.5 °	0	
SGI	Oct-06	SDN	Internal		5 20 90	115	24	step-load	0.004	22 °	755	5 °	435	
TRI	Oct-07	SDN	Internal		41.7 83.3 125	200	24	step-load	0.04	27.2 °	680	17.1 °	0	
SGI	Jun-03	SDN	Internal		150 250 400	48 hrs @ load			0.04	12 °	1390	5 °	1715	
SGI	Aug-08	STM	Internal		1.4	48 hrs @ load			0.004	73 °	0	--	--	sliding at gripping surface
SGI	Feb-01	CL	Internal		139	144	21 days	168 hrs @ load	0.04	25 °	0	7 °	0	
Interface Shear Results (with geomembranes)														
TRI	May-09	200R		40-mil smooth LLDPE	1 2 4	24 hrs @ load			0.04	11.2 °	4	10 °	4	
SGI	Mar-05	ST	W	60-mil text. HDPE	0.7	48 hrs @ load			0.04	34 °	0	25 °	0	co-extruded textured geomembrane
PGL	Feb-01	ST	white NW	40-mil text. LLDPE	0.35 0.69 1.39	50	24	24 hrs @ load	0.04	29 °	196	16 °	176	co-extruded textured geomembrane
SGI	Dec-08	ST	W	60-mil text. HDPE	2.8	200	24	48 hrs @ load	0.04	40 °	0	26 °	0	co-extruded textured geomembrane
SGI	Apr-07	ST	W	30-mil PVC	1 2 3	100	24	24 hrs @ load	0.04	16 °	5	15 °	5	smooth side
SGI	Apr-07	ST	NW	30-mil PVC	1 2 3	100	24	24 hrs @ load	0.04	14 °	0	14 °	0	smooth side
SGI	Jan-06	ST	W	30-mil PVC	1 2 3	200	48	--	0.04	15 °	5	15 °	0	faillie side
SGI	Jan-96	ST	W	30-mil PVC	2 4 6	24 hrs @ load			0.04	17 °	24	17 °	24	

BENTOMAT GCL DIRECT SHEAR DATABASE

TR-114BM

Lab ¹	Report Date	GCL Tested	Interface Tested ²		Testing Conditions							Mohr-Coulomb Failure Envelopes ⁶				Comments ⁸
												Peak		Large Displacement ⁷		
			GCL	Other	Normal Stresses (psi)			Hydration. ³		Consol. ⁴	SDR ⁵ (in/min)	Angle (deg)	adhesion (psf)	Angle (deg)	adhesion (psf)	
psf	hrs															
PGL	Jun-01	ST	NW	40-mil text. LLDPE	1.3	2.6	6.3	72	72	step-load	0.001	24.8 °	230	18.9 °	203	embossed textured geomembrane
TRI	Apr-08	ST		60-mil text. HDPE	0.7	3.5	6.9	100	24	step-load	0.04	23.9 °	107	16.4 °	62	co-extruded textured geomembrane
TRI	Feb-06	ST	NW	60-mil text. HDPE	1.7	3.5	6.9	200	48	24 hrs @ load	0.04	26.7 °	0	23.9 °	0	co-extruded textured geomembrane
TRI	Sep-05	ST	NW	60-mil text. HDPE	2	5	10	24 hrs @ load			0.04	33.8 °	223	20.2 °	181	embossed textured geomembrane
TRI	Aug-06	ST	W	60-mil text. HDPE	3.5	6.9	13.9	48 hrs @ load			0.04	28 °	50	23.6 °	9	embossed textured geomembrane
TRI	Aug-09	ST	W	60-mil text. HDPE	6.9	13.9	20.8	24 hrs @ load			0.04	21.5 °	291	15.1 °	129	embossed textured geomembrane
PGL	Feb-03	ST	W	80-mil text. HDPE	5	20	45	432	7 days	48 hrs @ load	0.004	22.5 °	83	13.6 °	130	embossed textured geomembrane
PGL	Mar-06	ST	W	80-mil text. HDPE	5	20	45	432	7 days	48 hrs @ load	0.004	20 °	379	13.3 °	413	embossed textured geomembrane
PGL	Mar-07	ST	NW	60-mil text. HDPE	13.9	27.8	55.6	500	6 days	24 hrs @ load	0.04	18.1 °	70.5	12.2 °	222.5	
EMCON	Jun-05	ST	NW	60-mil text. HDPE	13.9	34.7	69.4	300	48	24 hrs @ load	0.04	20.6 °	426	8.1 °	738	embossed textured geomembrane
SGI	Jun-09	ST	W	60-mil text. HDPE	75			200	24	48 hrs @ load	0.04	24 °	0	10 °	0	co-extruded textured geomembrane
SGI	Jun-09	ST	W	60-mil text. HDPE	75			200	24	48 hrs @ load	0.04	23 °	0	11 °	0	co-extruded textured geomembrane
SGI	Dec-08	ST	W	60-mil text. HDPE	75			200	24	48 hrs @ load	0.04	22 °	0	11 °	0	co-extruded textured geomembrane
EMCON	Jul-05	ST	NW	60-mil text. HDPE	13.9	55.6	83.3	300	48	24 hrs @ load	0.04	17.8 °	404.9	6.4 °	463.6	
JLT	Oct-04	ST		60-mil text. HDPE	20	45	90	108	3 days	step-load	0.001	24.3 °	323	15.3 °	243	co-extruded textured geomembrane
TRI	Apr-08	ST		60-mil text. HDPE	6.9	69.4	139	100	24	step-load	0.04	18.9 °	0	7.6 °	192	co-extruded textured geomembrane

BENTOMAT GCL DIRECT SHEAR DATABASE

TR-114BM

Lab ¹	Report Date	GCL Tested	Interface Tested ²		Testing Conditions						Mohr-Coulomb Failure Envelopes ⁶				Comments ⁸	
											Peak		Large Displacement ⁷			
			GCL	Other	Normal Stresses (psi)		Hydration. ³		Consol. ⁴	SDR ⁵ (in/min)	Angle (deg)	adhesion (psf)	Angle (deg)	adhesion (psf)		
psf	hrs															
SGI	2003	ST	W	60-mil text. HDPE	139		Hydrated			0.04	14.5 °	0	10.1 °	0	Encapsulated design	
SGI	Sep-09	ST	NW	60-mil text. HDPE	13.9	139	200	24	step-load	0.04	21 °	550	8 °	590	co-extruded textured geomembrane	
SGI	Sep-09	ST	W	60-mil text. HDPE	13.9	139	200	24	step-load	0.04	18 °	575	8 °	385	co-extruded textured geomembrane	
VE	Jun-09	ST		60-mil text. LLDPE	39	78	156	96 hrs @ load		0.04	18 °	990	4 °	1600	embossed textured geomembrane	
SGI	2003	ST	W	60-mil text. HDPE	208		Hydrated			0.04	13.7 °	0	9.8 °	0	Encapsulated design	
GA	Oct-08	ST		60-mil smooth LLDPE	75	150	300	24 hrs @ load		0.04	15 °	662	4.2 °	3355	GCL internal failure @ 300 psi	
SGI	Mar-09	DN	white NW	60-mil text. HDPE	1	2	3	240	48	24 hrs @ load	0.04	33 °	65	27 °	30	embossed textured geomembrane
SGI	Mar-09	DN	white NW	60-mil text. HDPE	1	2	3	240	48	24 hrs @ load	0.04	36 °	50	26 °	45	embossed textured geomembrane
SGI	Mar-09	DN	white NW	60-mil text. HDPE	1	2	3	240	48	24 hrs @ load	0.04	35 °	60	27 °	40	embossed textured geomembrane
SGI	Jan-06	DN	black NW	30-mil PVC	1	2	3	200	48	--	0.04	15 °	0	15 °	0	faillie side
PGL	Jun-01	DN	black NW	Textured HDPE	1.3	2.6	6.3	216	72	step-load	0.001	21.4 °	225	18.5 °	184	2-inch displacement
PGL	Jun-01	DN	black NW	Textured HDPE	1.3	2.6	6.3	72	72	step-load	0.001	24.8 °	230	18.9 °	203	2-inch displacement
SGI	May-01	DN	black NW	40-mil text. LLDPE	1	2.6	6.5	72	120	step-load	0.004	32 °	5	28 °	5	embossed textured geomembrane
PGL	Mar-08	DN	white NW	60-mil text. HDPE	5	7	9	24 hrs @ load		0.04	22.5 °	309	22.5 °	305		
EMCON	May-03	DN		Textured HDPE	13.9		Partially hydrated b/w 2 GMs with 0.3" holes			0.04	18.8 °	0	14.3 °	0	Encapsulated b/w GMs with 0.3" holes	
GT	Aug-07	DN	black NW	60-mil text. HDPE	18		Hydrated			0.04	26.6 °	0	18.5 °	0	embossed textured geomembrane	

BENTOMAT GCL DIRECT SHEAR DATABASE

TR-114BM

Lab ¹	Report Date	GCL Tested	Interface Tested ²		Testing Conditions							Mohr-Coulomb Failure Envelopes ⁶				Comments ⁸
												Peak		Large Displacement ⁷		
			Normal Stresses			Hydration. ³		Consol. ⁴	SDR ⁵ (in/min)	Angle (deg)	adhesion (psf)	Angle (deg)	adhesion (psf)			
GCL	Other	(psi)	psf	hrs	(deg)	(psf)	(deg)			(psf)						
SGI	Feb-00	DN	black NW	60-mil text. HDPE	7	14	35	72	72	step-load	0.0016	29 °	370	18 °	375	
PGL	Jul-05	DN		60-mil text. HDPE	13.9	27.8	41.7	48 hrs @ load			0.04	17.2 °	359	15.4 °	275	
SGI	Jul-03	DN	black NW	60-mil text. HDPE	10.4	20.8	41.7	48 hrs @ load			0.04	27 °	60	18 °	25	co-extruded textured geomembrane
SGI	Feb-08	DN	black NW	60-mil text. HDPE	15	30	50	1440	48	24 hrs @ load	0.04	27 °	530	16 °	390	co-extruded textured geomembrane
PGL	Jan-05	DN	white NW	80-mil text. HDPE	15	30	50	1440	48	24 hrs @ load	1	17.2 °	151	8.5 °	303	
PGL	Feb-07	DN		60-mil text. HDPE	10	30	60	24 hrs @ load			0.02	24 °	254	22.6 °	65	
PGL	Dec-06	DN		60-mil text. HDPE	10	30	60	24 hrs @ load			0.02	19.2 °	155	15.5 °	147	
PGL	Dec-06	DN		60-mil text. HDPE	10	30	60	24 hrs @ load			0.02	18.5 °	342	18.6 °	108	
SGI	Jul-02	DN	white NW	60-mil text. HDPE	6.9	34.7	69.4	125	24	48 hrs @ load	0.04	23 °	520	12 °	380	co-extruded textured geomembrane
SGI	Jun-03	DN		40- and 60-mil textured HDPE	69.4			Partially hydrated b/w 2 GMS with 0.25" holes			0.04	29 °	0	21 °	0	Encapsulated b/w GMS with 0.25" holes
EMCON	Jun-03	DN		Textured HDPE	69.4			Partially hydrated b/w 2 GMS with 0.3" holes			0.04	19.6 °	0	6.5 °	0	Encapsulated b/w GMS with 0.3" holes
SGI	Feb-08	DN	white NW	60-mil text. HDPE	25	50	75	1440	48	24 hrs @ load	0.04	23 °	570	10 °	420	co-extruded textured geomembrane
SGI	Feb-08	DN	white NW	60-mil text. HDPE	25	50	75	1440	48	24 hrs @ load	0.04	28 °	345	13 °	415	co-extruded textured geomembrane
PGL	Mar-08	DN	black NW	60-mil text. HDPE	25	50	75	24 hrs @ load			0.04	23.6 °	0	22.2 °	0	
SGI	Apr-09	DN	black NW	60-mil text. HDPE	75			200	24	step-load	0.04	30 °	0	14 °	0	embossed textured geomembrane
TRI	Oct-07	DN	black NW	60-mil textured HDPE	25	50	75	24 hrs @ load			0.04	22.7 °	52	11.9 °	409	co-extruded textured geomembrane

BENTOMAT GCL DIRECT SHEAR DATABASE

TR-114BM

Lab ¹	Report Date	GCL Tested	Interface Tested ²		Testing Conditions							Mohr-Coulomb Failure Envelopes ⁶				Comments ⁸	
												Peak		Large Displacement ⁷			
			GCL	Other	Normal Stresses (psi)			Hydration. ³ psf hrs		Consol. ⁴	SDR ⁵ (in/min)	Angle (deg)	adhesion (psf)	Angle (deg)	adhesion (psf)		
TRI	Oct-07	DN	black NW	60-mil textured HDPE	25	50	75	24 hrs @ load			0.04	10.8 °	1516	5.4 °	1194	co-extruded textured geomembrane	
TRI	Oct-07	DN	black NW	60-mil textured HDPE	25	50	75	24 hrs @ load			0.04	20.4 °	455	9.6 °	644	co-extruded textured geomembrane	
PGL	Mar-07	DN	white NW	60-mil text. LLDPE	25	50	75	24 hrs @ load			0.04	23 °	0	22 °	0	embossed textured geomembrane	
PGL	Mar-06	DN	white NW	60-mil text. LLDPE	25	50	75	24 hrs @ load			0.04	20 °	334	8.6 °	1216	embossed textured geomembrane	
GA	Mar-02	DN	black NW	80-mil text. LLDPE	20.8	41.7	83.3	288	24	10 minutes	0.04	21.7 °	789	11.7 °	559	co-extruded textured geomembrane	
GA	Mar-02	DN	black NW	60-mil text. LLDPE	20.8	41.7	83.3	288	24	10 minutes	0.04	21.5 °	361	6.7 °	880.5	embossed textured geomembrane	
PGL	Apr-07	DN		60-mil text. HDPE	20.8	41.7	83.3	48 hrs @ load			0.04	20.9 °	0	12.3 °	545		
JLT	May-07	DN	black NW	60-mil text. HDPE	20	45	90	115	4 days	step-load	0.005	22.1 °	77	13 °	239	co-extruded textured geomembrane	
SGI	May-08	DN	black NW	60-mil text. HDPE	1.4 100			200	24	48 hrs @ load	0.04	24 °	130	12 °	80	co-extruded textured geomembrane	
TRI	Jul-08	DN		60-mil text. HDPE	139			144	24	step-load	0.04	22 °	0	10.2 °	0	co-extruded textured geomembrane	
VE	May-03	DN		40- and 60-mil text. HDPE	13.9	27.8	55.6	111	250	48	16 hrs @ load	0.04	24 °	260	10 °	650	Encapsulated design
SGI	Jul-09	DN	black NW	60-mil text. HDPE	13.9	27.8	55.6	111	144	24	24 hrs @ load	0.04	22 °	560	11 °	585	co-extruded textured geomembrane
VE	May-03	DN		40- and 60-mil text. HDPE	27.8 111			As-received (25% moisture)			0.04	26 °	0	16 °	140	Encapsulated design	
EMCON	Nov-02	DN		60-mil text. HDPE	27.8	55.6	111	48 hrs @ load			0.04	26 °	0	16.8 °	0	co-extruded textured geomembrane	
SGI	2003	DN		40- and 80-mil HDPE	5	20	80	120	wetted conditions (not fully hydrated)			0.04	27 °	150	19 °	95	Encapsulated design (slip b/w 80-mil + GCL)
SGI	2003	DN		40- and 80-mil HDPE	5	20	80	120	wetted conditions (not fully hydrated)			0.04	29 °	270	19 °	120	Encapsulated design (slip b/w 80-mil + GCL)

BENTOMAT GCL DIRECT SHEAR DATABASE

TR-114BM

Lab ¹	Report Date	GCL Tested	Interface Tested ²		Testing Conditions							Mohr-Coulomb Failure Envelopes ⁶				Comments ⁸	
												Peak		Large Displacement ⁷			
			Normal Stresses				Hydration. ³		Consol. ⁴	SDR ⁵ (in/min)	Angle (deg)	adhesion (psf)	Angle (deg)	adhesion (psf)			
GCL	Other	(psi)				psf	hrs										
SGI	2003	DN		40- and 80-mil HDPE	5	20	80	120	wetted conditions (not fully hydrated)		0.04	28 °	140	20 °	20	Encapsulated design (slip b/w 80-mil + GCL)	
SGI	2003	DN		40- and 80-mil HDPE	5	20	80	120	wetted conditions (not fully hydrated)		0.04	29 °	145	19 °	50	Encapsulated design (slip b/w 80-mil + GCL)	
SGI	2003	DN		40- and 80-mil HDPE	5	20	80	120	wetted conditions (not fully hydrated)		0.04	27 °	580	20 °	70	Encapsulated design (slip b/w 80-mil + GCL)	
SGI	2003	DN		40- and 80-mil HDPE	5	20	80	120	wetted conditions (not fully hydrated)		0.04	27 °	235	19 °	95	Encapsulated design (slip b/w 80-mil + GCL)	
SGI	Jun-08	DN	black NW	60-mil text. HDPE	41.7	83.3	125		24 hrs @ load		0.04	26 °	105	15 °	620	2-inch displacement	
SGI	Jun-08	DN	black NW	60-mil text. HDPE	41.7	83.3	125		24 hrs @ load		0.04	25 °	165	13 °	870	2-inch displacement	
SGI	Jun-08	DN	black NW	60-mil text. HDPE	41.7	83.3	125		24 hrs @ load		0.04	26 °	110	16 °	485	2-inch displacement	
SGI	Jun-08	DN	black NW	60-mil text. HDPE	41.7	83.3	125		24 hrs @ load		24 hrs @ load	0.04	26 °	20	16 °	350	2-inch displacement
SGI	Jun-08	DN	black NW	60-mil text. HDPE	41.7	83.3	125		24 hrs @ load		0.04	26 °	50	15 °	165	2-inch displacement	
SGI	Jul-08	DN	black NW	60-mil text. HDPE	125				24 hrs @ load		24 hrs @ load	0.04	25.1 °	0	16.4 °	0	2-inch displacement
SGI	Aug-03	DN	white NW	60-mil text. HDPE	41.7	83.3	125		0	24	48 hrs @ load	0.04	22 °	835	15 °	40	2-inch displacement
SGI	Aug-03	DN	white NW	60-mil text. HDPE	41.7	83.3	125		0	24	48 hrs @ load	0.04	25 °	315	16 °	255	2-inch displacement
TRI	Jun-09	DN		60-mil text. HDPE	20.8	55.6	104	139	125	20	24 hrs @ load	0.04	24.9 °	0	8.7 °	617	embossed textured geomembrane
GTX	Apr-07	DN		HDPE	34.7	69.4	104	139	48 hrs @ load			0.04	26 °	588	12 °	398	
SGI	Feb-00	DN	black NW	60-mil text. HDPE	7 to 150 psi				72	72	step-load	0.0016	22 °	760	11 °	710	
SGI	Oct-02	DN		80-mil text. HDPE	15	25	100	150	1440	48	24 hrs @ load	0.04	23 °	120	14 °	330	co-extruded textured geomembrane

BENTOMAT GCL DIRECT SHEAR DATABASE

TR-114BM

Lab ¹	Report Date	GCL Tested	Interface Tested ²		Testing Conditions							Mohr-Coulomb Failure Envelopes ⁶				Comments ⁸	
												Peak		Large Displacement ⁷			
			GCL	Other	Normal Stresses (psi)			Hydration. ³		Consol. ⁴	SDR ⁵ (in/min)	Angle (deg)	adhesion (psf)	Angle (deg)	adhesion (psf)		
psf	hrs																
SGI	Nov-02	DN		80-mil text. HDPE	25	100	150	As-received (25% moisture)			0.04	24 °	335	18 °	120	co-extruded textured geomembrane	
SGI	Feb-00	DN	black NW	60-mil text. HDPE	35	100	150	72	72	step-load	0.0016	21 °	1305	9 °	1105		
GTX	Jul-05	DN	white NW	60-mil text. HDPE	69.4	111	167	24 hrs @ load			0.04	16 °	102	5 °	707		
SGI	Apr-09	DN	black NW	60-mil text. HDPE	75	150	250	400	200	24	step-load	0.04	18 °	2450	5 °	2220	embossed textured geomembrane
SGI	Jul-09	DN	black NW	60-mil text. HDPE	150	250	400	200	24	step-load	0.04	17 °	3705	4 °	3435	GCL internal failure @ 400 psi	
TRI	Mar-07	SDN	black NW	40-mil text. LLDPE	0.7	2.8	4.9	100	24	24 hrs @ load	0.04	32.6 °	148	22.5 °	83	embossed textured geomembrane	
TRI	Mar-07	SDN	black NW	60-mil text. HDPE	0.7	2.8	4.9	24 hrs @ load			0.04	39.3 °	31	26.7 °	44	embossed textured geomembrane	
TRI	Mar-07	SDN	black NW	50-mil text. LLDPE	0.7	2.8	4.9	24 hrs @ load			0.04	44.3 °	97	44.5 °	0	structured GM/Drainage Liner	
TRI	Mar-07	SDN	black NW	40-mil text. LLDPE	0.7	2.8	4.9	100	24	24 hrs @ load	0.04	32.6 °	148	22.5 °	83	embossed textured geomembrane	
SGI	May-03	SDN	black NW	40-mil text. HDPE	0.7	3.5	6.9	100	24	24 hrs @ load	0.04	30 °	25	19 °	20	co-extruded textured geomembrane	
TRI	Jul-08	SDN	Black NW	60-mil text. HDPE	3.5	13.9	31.3	62.5	200	24	step-load	0.04	15.8 °	243	6.5 °	303	co-extruded textured geomembrane
TRI	May-07	SDN		60-mil text. HDPE	6.9	41.7	83.3	250	24	step-load	0.04	23.8 °	467	10.6 °	365	embossed textured geomembrane	
SGI	Oct-06	SDN	white NW	60-mil text. HDPE	5	20	90	115	24	step-load	0.04	23 °	695	8 °	425	co-extruded textured geomembrane	
PGL	Apr-04	SDN		60-mil text. HDPE	25	60	100	24 hrs @ load			0.04	24.7 °	308	14.1 °	155		
PGL	Sep-04	SDN		60-mil text. HDPE	25	60	100	24 hrs @ load			0.04	22.6 °	0	14.5 °	203		
PGL	Sep-04	SDN		60-mil text. HDPE	25	60	100	24 hrs @ load			0.04	18.9 °	387	15.2 °	333		

BENTOMAT GCL DIRECT SHEAR DATABASE

TR-114BM

Lab ¹	Report Date	GCL Tested	Interface Tested ²		Testing Conditions						Mohr-Coulomb Failure Envelopes ⁶				Comments ⁸	
											Peak		Large Displacement ⁷			
			Normal Stresses (psi)	Hydration. ³ psf hrs		Consol. ⁴	SDR ⁵ (in/min)	Angle (deg)	adhesion (psf)	Angle (deg)	adhesion (psf)					
PGL	Sep-04	SDN		60-mil text. HDPE	25 60 100			24 hrs @ load			0.04	26.4 °	0	24.1 °	0	
PGL	Sep-04	SDN		60-mil text. HDPE	25 60 100	24 hrs @ load			0.04	22.6 °	0	14.5 °	203			
PGL	Sep-04	SDN		60-mil text. HDPE	25 60 100	24 hrs @ load			0.04	18.9 °	387	15.2 °	333			
PGL	Sep-04	SDN		60-mil text. HDPE	25 60 100	24 hrs @ load			0.04	26.4 °	0	24.1 °	0			
EMCON	Dec-02	SDN	white NW	60-mil text. HDPE	27.8 55.6 111	220	24	24 hrs @ load	0.04	21.2 °	0	11.4 °	0	co-extruded textured geomembrane		
TRI	Oct-07	SDN	black NW	60-mil text. HDPE	41.7 83.3 125	200	24	step-load	0.04	22.7 °	0	10.5 °	0	embossed textured geomembrane		
GA	Oct-08	SDN		60-mil smooth LLDPE	75 150 300	24 hrs @ load			0.04	18.3 °	662	12.4 °	2246			
SGI	Jun-03	SDN		80-mil text. LLDPE	150 250 400	48 hrs @ load			0.04	11 °	540	7 °	325	co-extruded textured geomembrane		
TRI	Jun-07	STM	white NW	60-mil text. LLDPE	100			200	24	step-load	0.04	20.1 °	0	11.5 °	0	co-extruded textured geomembrane
SGI	May-07	STM	white NW	40-mil text. LLDPE	100			200	24	48 hrs @ load	0.04	24 °	0	10 °	0	co-extruded textured geomembrane
SGI	Aug-09	STM	white NW	60-mil text. LLDPE	39 78 156	96 hrs @ load			0.04	21 °	720	9 °	1185	embossed textured geomembrane		
Interface Shear Results (with soil)																
ARD	Aug-01	ST	W	SOIL	2.3 3 3.75	24 hrs @ load			0.04	38.7 °	0	38.7 °	0	CIDCO Pit sand		
ARD	Aug-01	ST	NW	SOIL	2.3 3 3.75	24 hrs @ load			0.04	36.5 °	0	36.5 °	0	CIDCO Pit sand		
ARD	Aug-01	ST	W	SOIL	2.3 3 3.75	24 hrs @ load			0.04	38.1 °	0	38.1 °	0	Michigan Pit sand		
ARD	Aug-01	ST	NW	SOIL	2.3 3 3.75	24 hrs @ load			0.04	36.7 °	0	35.6 °	0	Michigan Pit sand		
STS	Jan-00	ST	W	SOIL	1 2 4	48 hrs @ load			0.04	28.6 °	293	28 °	241	Topsoil: 62 pcf, 15%		

BENTOMAT GCL DIRECT SHEAR DATABASE

TR-114BM

Lab ¹	Report Date	GCL Tested	Interface Tested ²		Testing Conditions							Mohr-Coulomb Failure Envelopes ⁶				Comments ⁸	
												Peak		Large Displacement ⁷			
			GCL	Other	Normal Stresses (psi)			Hydration. ³		Consol. ⁴	SDR ⁵ (in/min)	Angle (deg)	adhesion (psf)	Angle (deg)	adhesion (psf)		
psf	hrs																
TRI	Nov-03	ST	NW	SOIL	1.4	3.6	7.1	24 hrs @ load			0.04	17.7 °	139	18.2 °	135	Soil: 99 pcf, 17%	
TRI	Oct-05	ST	W	SOIL	2	5	10	24 hrs @ load			0.04	23.2 °	134	19.9 °	117	Soil: 114 pcf, 14%	
TRI	Aug-09	ST	NW	SOIL	7.4	15.4	23.5	24 hrs @ load			0.04	28.1 °	5	25.9 °	0		
PGL	Mar-07	ST	W	SOIL	13.9	27.8	55.6	500	6 days	24 hrs @ load	0.04	21.4 °	279	8.7 °	926	Soil: 110 pcf, 15.2%	
TRI	Jul-08	ST	NW	SOIL	3.5	13.9	55.6	24 hrs @ load			0.04	28.7 °	176	16.1 °	474	Soil: 94 pcf, 14.2%	
TRI	Nov-06	ST	NW	SOIL	8.1	27.8	55.7	24 hrs @ load			0.04	21.6 °	0	21.6 °	0	Soil: 110 pcf, 12.4%	
SGI	Jul-04	ST	W	SOIL	1	20	40	60	24 hrs @ load			0.04	23 °	145	22 °	120	
SGI	Aug-08	ST	NW	SOIL	10	35	60	100	24	24 hrs @ load	0.04	7 °	475	7 °	360		
SGI	Feb-04	ST	W	SOIL	20.8	52.1	79.9	72	7 days	step-load	0.0016	9.9 °	930	6.7 °	500	Clay	
SGI	Feb-04	ST	W	SOIL	20.8	52.1	79.9	72	7 days	step-load	0.0016	10 °	1025	7 °	590	Clay	
EMCON	Jul-05	ST	W	SOIL	13.9	55.6	83.3	300	48	24 hrs @ load	0.04	15.6 °	561.1	15.6 °	435.8		
NTH	2005	ST	NW	SOIL	25	50	100	144	24	--	0.04	11.9 °	0	7.9 °	0	Clay: 95 pcf, 8%	
SGI	Apr-06	ST	W	SOIL	20.8	79.9	139	72	7 days	step-load	0.004	12 °	905	--	--	Clay: GCL internal failure at 139 psi load	
JLT	Jan-03	DN		SOIL	0.3	0.7	1.4	24 hrs @ load			0.04	36.3 °	2	29 °	1	Angular gravel	
CETCO	Mar-00	DN	black NW	SOIL	0.7	1.4	2.1	24 hrs @ load			0.04	25.2 °	315	--	--	SP, 108 pcf, 11%	
GTX	Jul-05	DN	black NW	SOIL	0.7	1.4	2.8	24 hrs @ load		24 hrs @ load	0.04	31 °	60	18 °	27		

BENTOMAT GCL DIRECT SHEAR DATABASE

TR-114BM

Lab ¹	Report Date	GCL Tested	Interface Tested ²		Testing Conditions							Mohr-Coulomb Failure Envelopes ⁶				Comments ⁸
												Peak		Large Displacement ⁷		
			Normal Stresses			Hydration. ³		Consol. ⁴	SDR ⁵ (in/min)	Angle (deg)	adhesion (psf)	Angle (deg)	adhesion (psf)			
(psi)			psf	hrs	(deg)	(psf)	(deg)			(psf)						
TRI	Nov-08	DN	white NW	SOIL	0.8	1.6	2.9	24 hrs @ load			0.04	41.1 °	0	28.4 °	29	Soil: 105 pcf, 13.5%
SGI	Nov-08	DN	black NW	SOIL	1	2	3	240	48	24 hrs @ load	0.04	32 °	25	31 °	5	
SGI	Nov-08	DN	black NW	SOIL	1	2	3	240	48	24 hrs @ load	0.04	31 °	25	31 °	5	
TRI	Nov-08	DN	black NW	SOIL	0.7	1.5	3	24 hrs @ load			0.04	18.9 °	70	10.9 °	82	Soil: 105 pcf, 14.1%
PGL	Jun-01	DN	white NW	SOIL	1.3	2.6	6.3	72	72	step-load	0.001	21.2 °	207	21.6 °	184	2-inch displacement; soil: 103 pcf, 17%
PGL	Jun-01	DN	white NW	SOIL	1.3	2.6	6.3	216	72	step-load	0.001	23.2 °	206	20.8 °	194	2-inch displacement; soil: 103 pcf, 17%
SGI	Jun-01	DN	white NW	SOIL	1.0	2.6	6.5	72	120	step-load	0.004	35 °	65	34 °	40	
PGL	Mar-08	DN	black NW	SOIL	5	7	9	24 hrs @ load			0.04	33.6 °	342	33.6 °	337	Soil: 107 pcf, 13.4%
ARD	Oct-05	DN	white NW	SOIL	2	5	9.9	48 hrs @ load			0.04	28.2 °	64	28.4 °	47	Medium to fine silty sand: 117 pcf, 9.5%
ARD	Oct-05	DN	black NW	SOIL	2	5	9.9	48 hrs @ load			0.04	29.3 °	42	29.4 °	38	Medium to fine silty sand: 117 pcf, 9.5%
SGI	Apr-01	DN	black NW	SOIL	1	5	10	48 hrs @ load			0.04	36 °	35	35 °	10	Soil: 124 pcf, 9 %
GT	Aug-07	DN	white NW	SOIL	3	5	10	18	Hydrated		0.04	25.8 °	81	24.3 °	92	Soil: 100 pcf, 19.4%
GT	Aug-07	DN	white NW	SOIL	3	5	10	18	Hydrated		0.04	25.1 °	96	16.1 °	135	Soil: 93 pcf, 20.9%
SGI	Jul-03	DN	white NW	SOIL	10.4	20.8	41.7	48 hrs @ load			0.04	28 °	40	26 °	10	
SGI	Mar-01	DN	white NW	SOIL	55.6			1000	24	24 hrs @ load	0.04	26 °	0	23 °	0	
PGL	Dec-06	DN		SOIL	10	30	60	24 hrs @ load			0.02	32.5 °	491	7.5 °	1319	Soil: 92 pcf, 17.5%

BENTOMAT GCL DIRECT SHEAR DATABASE

TR-114BM

Lab ¹	Report Date	GCL Tested	Interface Tested ²		Testing Conditions							Mohr-Coulomb Failure Envelopes ⁶				Comments ⁸	
												Peak		Large Displacement ⁷			
			Normal Stresses (psi)			Hydration. ³ psf hrs		Consol. ⁴	SDR ⁵ (in/min)	Angle (deg)	adhesion (psf)	Angle (deg)	adhesion (psf)				
PGL	Dec-06	DN		SOIL	10	30	60			24 hrs @ load		0.02	36.9 °	305	23.2 °	751	
PGL	Aug-04	DN	white NW	SOIL	6.9	41.7	69.4	125	20	16 hrs @ load	0.04	28.6 °	312	15.6 °	854	Soil: 120 pcf, 12%	
PGL	Aug-04	DN	white NW	SOIL	6.9	34.7	69.4	125	20	16 hrs @ load	0.04	20.8 °	177	17.3 °	190	Soil: 114 pcf, 14.9%	
PGL	Aug-04	DN	white NW	SOIL	6.9	41.7	69.4	125	20	16 hrs @ load	0.04	28.6 °	312	15.6 °	854	Soil: 120 pcf, 12%	
PGL	Aug-04	DN	white NW	SOIL	6.9	34.7	69.4	125	20	16 hrs @ load	0.04	20.8 °	177	17.3 °	190	Soil: 114 pcf, 14.9%	
PGL	Mar-06	DN	black NW	SOIL	25	50	75	24 hrs @ load			0.04	32 °	61	32 °	0	Soil: 109 pcf, 14.9%	
PGL	Apr-07	DN		SOIL	20.8	41.7	83.3	48 hrs @ load			0.04	32.2 °	0	31.9 °	0		
PGL	Jul-03	DN		SOIL	3.5	20.8	41.7	83.3	125	24	16 hrs @ load	0.04	22.3 °	320	19 °	322	Soil: 91 pcf, 22%; GCL internal failure at 83 psi
GTX	Apr-07	DN		SOIL	34.7	69.4	104	139	48 hrs @ load			0.04	20 °	1940	-3 °	3247	Brown silty gravel
GTX	Jul-05	DN	black NW	SOIL	69.4	111	167	24 hrs @ load			0.04	11 °	1833	4 °	975	Brown clay with silt: 69 pcf, 45%	
OSU	Jan-05	SDN	white NW	SOIL	0.8			Dry			0.04	40.5 °	0	33.2 °	0	Topsoil: 93 pcf, 18%	
OSU	Jan-05	SDN	white NW	SOIL	0.8			2 days @ load			0.04	36.1 °	0	25.5 °	0	Topsoil: 93 pcf, 37.8%	
OSU	Jan-05	SDN	black NW	FGD	0.8			Dry			0.04	44.8 °	0	41.5 °	0	FGD: 93 pcf, 68.4%	
OSU	Jan-05	SDN	black NW	FGD	0.8			2 days @ load			0.04	38.3 °	0	35.3 °	0	FGD: 93 pcf, 68.4%	
OSU	Jan-05	SDN	white NW	SOIL	0.8			2 days @ load			0.04	36.3 °	0	14.3 °	0	Topsoil: 93 pcf, 38.2%	
JLT	Feb-07	SDN		SOIL	0.7	2.1	12 hrs @ load			0.04	27 °	44	17 °	41	Soil: 116 pcf, 16.4%		

BENTOMAT GCL DIRECT SHEAR DATABASE

TR-114BM

Lab ¹	Report Date	GCL Tested	Interface Tested ²		Testing Conditions							Mohr-Coulomb Failure Envelopes ⁶				Comments ⁸	
												Peak		Large Displacement ⁷			
			Normal Stresses (psi)			Hydration. ³		Consol. ⁴	SDR ⁵ (in/min)	Angle (deg)	adhesion (psf)	Angle (deg)	adhesion (psf)				
						psf	hrs										
SGI	2/205	SDN	black NW	COAL REFUSE	0.7	2.8	144	24	24 hrs @ load	0.04	32 °	40	31 °	40	Coal Refuse		
SGI	Jul-06	SDN	black NW	SOIL	0.7	1.4	2.8	24 hrs @ load			0.04	34 °	5	33 °	0	Gravel (34R)	
SGI	Jul-06	SDN	white NW	SOIL	0.7	1.4	2.8	24 hrs @ load			0.04	32 °	30	31 °	10	Fine brown sand	
TRI	Apr-07	SDN	white NW	SOIL	0.9	3.0	5.2	100	24	24 hrs @ load	0.04	25.3 °	108	23.6 °	117	Soil: 103 pcf, 19.6%	
ARD	Jul-03	SDN	white NW	SOIL	2	3.8	5.9	24 hrs @ load			0.04	28.5 °	72	27.7 °	79	Fine brown sand with silt	
ARD	Jul-03	SDN	black NW	SOIL	2	3.8	5.9	24 hrs @ load			0.04	33.5 °	43	33.5 °	43	Fine brown sand with silt	
TRI	Jul-08	SDN	Black NW	SOIL	3.5	13.9	31.3	62.5	100	24	step-load	0.04	19.3 °	587	19.1 °	561	Soil: 112 pcf, 17%
SGI	2/205	SDN	white NW	SOIL	83			144	24	24 hrs @ load	0.04	27 °	0	22 °	0	Compacted Subgrade	
SGI	2/205	SDN	white NW	SOIL	13.9	34.7	55.6	83.3	144	24	24 hrs @ load	0.04	23 °	365	18 °	485	Compacted Subgrade
SGI	Oct-06	SDN	black NW	SOIL	5	20	90	115	24	step-load	0.04	17 °	245	9 °	140	Compacted clay	
TRI	May-07	SDN		SOIL	9.3	52.3	91.6	250	24	step-load	0.04	21.6 °	317	6.6 °	1270	Soil: 102 pcf, 12.9%	
EMCON	Dec-02	SDN	white NW	SOIL	27.8	55.6	111	220	24	24 hrs @ load	0.04	26.8 °	1320	2.7 °	3140	Sand	
TRI	Oct-07	SDN	white NW	SOIL	41.7	83.3	125	200	24	step-load	0.04	28.8 °	0	5.8 °	2935	Soil: 100 pcf, 12.9%	
SGI	Feb-02	CL	smooth plastic	SOIL	0.7	1.4	2.8	24 hrs @ load			0.04	20 °	50	20 °	40	Graded Aggregate Base	
SGI	Feb-02	CL	smooth plastic	SOIL	0.7	1.4	2.8	24 hrs @ load			0.04	18 °	40	16 °	40	Silty sand	
SGI	Feb-02	CL	smooth plastic	SOIL	0.7	1.4	2.8	24 hrs @ load			0.04	19 °	70	18 °	70	Clay	

BENTOMAT GCL DIRECT SHEAR DATABASE

TR-114BM

Lab ¹	Report Date	GCL Tested	Interface Tested ²		Testing Conditions							Mohr-Coulomb Failure Envelopes ⁶				Comments ⁸
												Peak		Large Displacement ⁷		
			Normal Stresses (psi)			Hydration. ³ psf hrs		Consol. ⁴	SDR ⁵ (in/min)	Angle (deg)	adhesion (psf)	Angle (deg)	adhesion (psf)			
PGL	Dec-05	CL	smooth plastic	SOIL	0.7	1.4	2.8	Interface sprayed with water			0.04	29.6 °	67	24.4 °	54	Clayey sand: 113 pcf, 14%
PGL	Dec-05	CL	smooth plastic	SOIL	0.7	1.4	2.8	Interface sprayed with water			0.04	37 °	14	33 °	8	Silty sand: 115 pcf, 11.5%
PGL	Dec-05	CL	smooth plastic	SOIL	0.7	1.4	2.8	Interface sprayed with water			0.04	25 °	66	18.5 °	71	CL: 102 pcf, 17.5%
PGL	Dec-05	CL	smooth plastic	SOIL	0.7	1.4	2.8	Interface sprayed with water			0.04	22.9 °	78	21.8 °	49	CH: 92.8 pcf, 22.6%
PGL	Dec-05	CL	smooth plastic	SOIL	0.7	1.4	2.8	Interface sprayed with water			0.04	22.9 °	57	22.5 °	58	SP: 106.5 pcf, 5%
SGI	May-00	CL	W	SOIL	0.5	1.0	2.1	24 hrs @ load			0.04	36 °	10	36 °	10	
CETCO	Mar-00	CLT	W	SOIL	0.7	1.4	2.1	24 hrs @ load			0.04	24.9 °	278	--	--	SP, 108 pcf, 11%
CETCO	Feb-00	CLT	20-mil text. HDPE	SOIL	0.7	1.4	2.1	24 hrs @ load			0.04	41.7 °	108	--	--	SP, 108 pcf, 11%
SGI	Mar-01	CLT	20-mil text. HDPE	SOIL	55.6			1000	24	24 hrs @ load	0.04	24 °	0	21 °	0	
Interface Shear Results (with drainage geocomposites, geonets, and geotextiles)																
GT	Dec-00	ST	W	drainage geocomposite	1.4	2.8	4.2	100	24	--	0.04	25 °	0	20.7 °	1	
EMCON	Jul-05	ST	W	drainage geocomposite	13.9	55.6	83.3	300	48	24 hrs @ load	0.04	19.7 °	0	8.3 °	331	
PGL	Sep-03	ST	NW	drainage geocomposite	5	19.4	60 83.3	144	48	24 hrs @ load	0.04	19.8 °	129	13.6 °	164	
PGL	Jul-06	ST	W	geonet	1.5	3	6	24 hrs @ load			0.04	23.5 °	33.5	23.6 °	29	
GT	Dec-00	DN	black NW	drainage geocomposite	1.4	2.8	4.2	100	24	--	0.04	28 °	0	21.9 °	0	
TRI	Sep-06	DN		drainage geocomposite	1.4	2.8	5.6	24 hrs @ load			0.04	30.1 °	14	27.2 °	0	
PGL	Sep-09	DN	white NW	drainage geocomposite	0.35	2.78	6.94	24 hrs @ load			0.04	21.7 °	96	13.8 °	68	

BENTOMAT GCL DIRECT SHEAR DATABASE

TR-114BM

Lab ¹	Report Date	GCL Tested	Interface Tested ²		Testing Conditions							Mohr-Coulomb Failure Envelopes ⁶				Comments ⁸
												Peak		Large Displacement ⁷		
			GCL	Other	Normal Stresses (psi)			Hydration. ³ psf hrs		Consol. ⁴	SDR ⁵ (in/min)	Angle (deg)	adhesion (psf)	Angle (deg)	adhesion (psf)	
GTX	Oct-00	DN	black NW	drainage geocomposite	10	30	70	144	72	24 hrs @ load	0.04	22 °	144	18 °	0	
GT	Aug-08	DN	white NW	drainage geocomposite	20.8	41.7	83.3	200	24	48 hrs @ load	0.04	28.7 °	152	16.5 °	515	
PGL	Dec-06	DN		Nonwoven geotextile	2	3.5	5	24 hrs @ load			0.04	20.7 °	160	6.3 °	167	
GT	Dec-04	SDN	black NW	drainage geocomposite	0.7	1.4	2.8	Hydrated			0.04	21.6 °	9	17.2 °	10	
TRI	Jun-07	SDN		drainage geocomposite	6.9	41.7	83.3	250	24	step-load	0.04	21.4 °	0	9.5 °	278	
TRI	Oct-07	SDN	white NW	drainage geocomposite	41.7	83.3	125	200	24	step-load	0.04	27.5 °	0	21.6 °	0	
SGI	Jul-06	SDN	white NW	Nonwoven geotextile	0.7	1.4	2.8	24 hrs @ load			0.04	27 °	35	20 °	20	
TRI	Jun-07	CL	smooth plastic	drainage geocomposite	0.7	1.4	2.8	200	24	24 hrs @ load	0.04	19.2 °	33	10.8 °	46	
ATT	Dec-98	CL	smooth plastic	drainage geocomposite	1	2	3	72	48	--	0.04	14 °	72	11.6 °	72	
SGI	Mar-01	CLT	20-mil text. HDPE	drainage geocomposite	55.6			1000	48	24 hrs @ load	0.04	23 °	0	19 °	0	

BENTOMAT GCL DIRECT SHEAR DATABASE

TR-114BM

Notes:

(1) Laboratories:

ARD = Ardaman and Associates, Orlando FL

ATT = Advanced Terra Testing, inc. Lakewood, CO

CETCO = CETCO, Hoffman Estates, IL

EMCON = Emcon Assoc. (now Shaw Group), Mahwah, NJ

GA = Golder Associates, Atlanta, Georgia

GT = Geotechnics, East Pittsburgh, PA

GTX = Geotesting Express, Boxborough, MA

JLT = J&L Testing, Canonsburg, PA

OSU = Ohio State University, Columbus, OH

PGL = Precision Laboratory, Orange, CA

SGI = SGI Testing Services LLC, Atlanta, GA (formerly GeoSyntec)

STS = STS Consultants, Ltd., Vernon Hills, IL

TRI = TRI Laboratory, Austin, TX

VE = Vector Engineering, Grass Valley, CA

(2) Internal = Failure forced within the GCL (between the geotextiles).

NW = Non-woven geotextile of Bentomat.

W = Woven geotextile of Bentomat.

(3) Hydrated = specimen was soaked under the specified load for the specified duration prior to testing. Hydration methods may vary

Dry = specimen was tested in the as-received moisture (typically 25-30 percent).

Wetted = specimen was partially hydrated.

(4) Consolidation. If the hydration load does not equal the ultimate normal load for shearing, the normal load is increased in steps.

(5) SDR = Shear Displacement Rate.

(6) Mohr-Coulomb failure envelope, $\tau = c_a + \sigma \tan \phi$, determined by a least-squares, "best-fit" straight line through the shear strength-normal stress test results. Two shear strength components are shown: c_a = adhesion and ϕ = friction angle. Caution should be exercised in using these strength parameters for applications involving normal stresses outside the range of the stresses covered. Refer to TR-264 for discussion of cohesion (or adhesion) and friction angle in direct shear tests.

(7) Measured at 3" displacement, unless otherwise noted.

(8) Including information on: geomembrane type; soil type, density, and moisture content; observed GCL internal failure during interface shearing; and any other unique testing conditions.

**APPLICATION FOR PERMIT RENEWAL AND MODIFICATION
SANDOVAL COUNTY LANDFILL**

**VOLUME III: LANDFILL ENGINEERING CALCULATIONS
SECTION 7: GEOSYNTHETICS TENSILE STRESS AND STABILITY ANALYSIS**

ATTACHMENT III.7.L

RICHARDSON, CLINTON P., PHD, P.E. 2009.

***MUNICIPAL LANDFILL DESIGN CALCULATIONS, AN ENTRY
LEVEL MANUAL OF PRACTICE, RICHARDSON ENVIRONMENTAL
SOLUTIONS & DESIGN, LLC., UBUILDABOOK, LLC., CAMARILLO, CA.***

Municipal Landfill Design Calculations

An Entry Level Manual
of Practice

Clinton P. Richardson, PhD. PE.



Chapter 28 Side-slope Liner Stability

Problem Statement

Liner stability or side-slope slippage is complicated for multi-layered liner and collection system. A unit load of waste gravitationally induces shear stress and a portion of stress is transmitted by means of friction to the geosynthetic components beneath. The difference between frictional components must be carried by the particular component in the form of tensile stress and then compared to the component's yield stress for the resulting factor of safety. The portion transmitted to upper component is then propagated to the next component in the multilayered sequence. An unbalanced portion is eventually transmitted to the subgrade soil beneath the lower geosynthetic. If mass failure is going to occur, it will seek the interface with the lowest friction angle. The liner stability method is simply a resolution of shear stresses Koerner, 1994).

Design Objective

Calculate the tensile stresses and shear stresses carried by the upper and lower geosynthetic components and estimate the factor of safety.

Design Equations

Figure 1 shows a schematic of a multi-layered liner and resolution of forces assuming a single waste lift thickness.

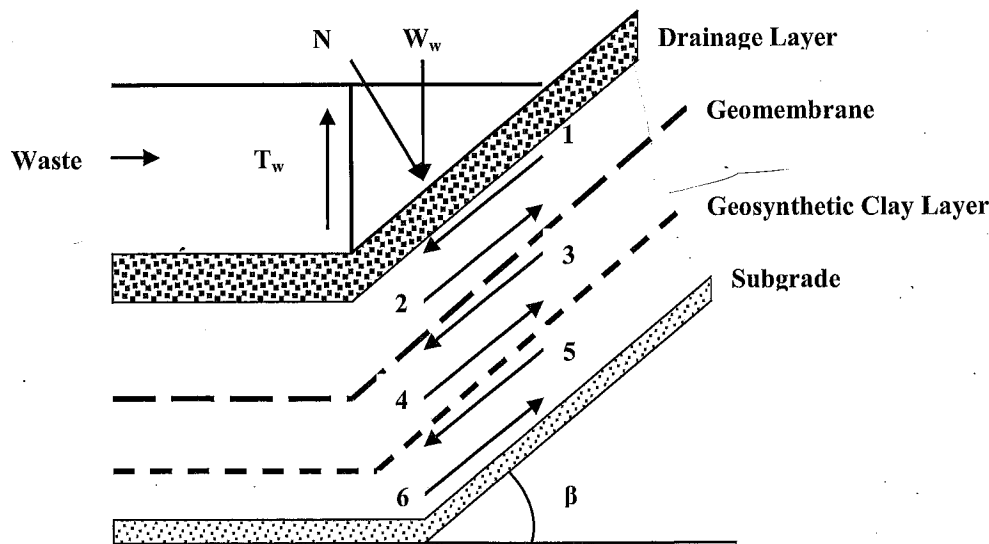


Figure 1: Resolution of Shear Forces in A Multi-layered Landfill Barrier Liner (adapted from Koerner, 1990).

The simple barrier system consists of a geomembrane underlain by a geosynthetic clay liner (GCL). The procedure may be extended to any number of interfaces, such as a geotextile, geomembrane, clay

liner, etc. Time is assumed to be sufficiently long between waste lifts that system readjustment will occur and either equilibrium or failure will exist. A unit width is assumed. The numbers 1 through 6 shown in the figure represent the forces that must be resolved sequentially.

The weight of a unit width of compacted waste is given by

$$W_w = \frac{1}{2} \gamma_w H \frac{H}{\tan \beta} \quad \text{Eq. 1}$$

where

W_w = weight of waste per unit width (lb_f/ft or kN/m)

H = lift height (ft or m)

β = slope angle (°)

γ_w = unit weight of waste (lb_f/ft³ or kN/m³)

The frictional resistance along the waste edge is given by

$$T_w = \sigma_h \tan \phi_w H = K_o \sigma_v \tan \phi_w H \quad \text{Eq. 2}$$

$$K_o = (1 - \sin \phi_w) \quad \text{Eq. 3}$$

$$\sigma_v = \frac{1}{2} \gamma_w H \quad \text{Eq. 4}$$

where

T_w = frictional resistance force per unit width (lb_f/ft or kN/m)

σ_h = horizontal stress of waste lift (lb_f/ft² or kN/m²)

ϕ_w = waste friction angle (°)

K_o = coefficient of earth pressure at rest (unitless)

σ_v = vertical stress of waste lift (lb_f/ft² or kN/m²)

The net weight of the waste is the difference between the downward acting waste weight and the upward acting resistance force, or

$$W_{net} = W_w - T_w \quad \text{Eq. 5}$$

The net weight can now be resolved into its two components: a normal force component acting perpendicular to the slope and a parallel force component acting downslope, or

$$N = W_{net} \cos \beta \quad \text{Eq. 6}$$

$$P = W_{net} \sin \beta \quad \text{Eq. 7}$$

where

N = normal force component of net weight (lb_f/ft or kN/m)

P = parallel force component of net weight (lb_f/ft or kN/m)

This latter force component is assumed to be dissipated through the drainage layer (Koerner, 1990). The forces that must be determined are a function of the normal force and the frictional resistance provided by the respective interface; for example, in the first force couple, the following relationships hold:

$$F_1 = N \tan \delta_1 = (W_{net} \cos \beta) \tan \delta_1 \quad \text{Eq. 8}$$

$$F_2 = N \tan \delta_2 = (W_{net} \cos \beta) \tan \delta_2 \quad \text{Eq. 9}$$

where

δ_1 = drainage layer friction angle with respect to the upper geomembrane surface (°)

δ_2 = lower geomembrane surface friction angle with respect to the upper GCL surface (°)

If F_1 exceeds F_2 , then the geomembrane is in tension. The force difference must be carried by the geomembrane. The actual stress in the geomembrane is given by

$$\sigma_{\text{actual geomembrane}} = \left(\frac{F_1 - F_2}{t_{geo}} \right) \quad \text{Eq. 10}$$

where

$\sigma_{\text{actual geomembrane}}$ = actual stress in geomembrane (lb_f/ft² or kN/m²)

t_{geo} = geomembrane thickness (ft or m)

The factor of safety for the geomembrane against failure in tension is

$$FS_{\text{geomembrane}} = \frac{\sigma_{\text{yield}}}{\sigma_{\text{actual geomembrane}}} \quad \text{Eq. 11}$$

where

σ_{yield} = allowable geomembrane stress at yield (lb_f/ft² or kN/m²)

The allowable geomembrane stress at yield is usually given in terms of lb_f/in^2 or kN/m^2 or kPa based on a wide-width tensile test (ASTM D 4885-01 Determining Performance Strength of Geomembranes by the Wide Width Strip Tensile Method).

The frictional shear force acting on the lower geomembrane surface, or F_2 , is equal and opposite to the frictional shear force above the GCL surface, or F_3 ; thus,

$$F_2 = N \tan \delta_2 = F_3 \quad \text{Eq. 12}$$

The frictional shear force acting on the lower GCL is given by

$$F_4 = N \tan \delta_4 \quad \text{Eq. 13}$$

where

δ_4 = friction angle between the lower GCL surface and the subgrade soil

The difference between F_3 and F_4 determines the tensile force carried by the GCL. If negative, the GCL is not in tension. If positive, then the GCL is in tension and a factor of safety must be evaluated based on the wide width strength test (ASTM D 6768-04 Standard Test Method for Tensile Strength of Geosynthetic Clay Liners). The force difference must be carried by the geomembrane. The actual stress in the GCL is given by

$$\sigma_{\text{actual GCL}} = \left(\frac{F_3 - F_4}{t_{\text{GCL}}} \right) \quad \text{Eq. 14}$$

where

$\sigma_{\text{actual GCL}}$ = actual stress in GCL (lb_f/ft^2 or kN/m^2)

t_{geo} = GCL thickness (ft or m)

The factor of safety for the GCL against failure is

$$\text{FS}_{\text{GCL}} = \frac{\sigma_{\text{yield}}}{\sigma_{\text{actual GCL}}} \quad \text{Eq. 15}$$

where

σ_{yield} = allowable GCL stress at yield (lb_f/ft^2 or kN/m^2)

If $\delta_2 = \delta_4$, then $F_4 = F_2 = F_3$. If the lower frictional shear force exceeds the upper frictional shear force for a given interface, then the factor of safety is infinite and only a value of the upper frictional shear force will be mobilized at the upper surface of the next interface below. This procedure is repeated for multiple interfaces until the lower most interface is encountered, i.e. a

compacted subgrade or compacted clay. For compacted clay, special attention must be paid to its short-term friction angle *versus* its long-term friction angle with respect to the interface above. Compacted clay can consolidate with overburden stress and expel moisture, which can reduce the friction between it and the contact surface above, potentially placing the upper geosynthetic in tension.

Design Example #1

Evaluate the maximum stresses, if any, in the landfill liner system described in Figure 1 consisting of a textured 60 mil HDPE/non-woven, needle-punched Bentomat® GCL/USCS SP compacted subgrade sequence. The following data may be assumed:

$$H = 10 \text{ ft (3.0 m)}$$

$$\beta = 18.43^\circ \text{ (3H:1V)}$$

$$\gamma_w = 60 \text{ lb}_f/\text{ft}^3 \text{ or (9.4 kN/m}^3\text{)}$$

$$\phi_w = 20^\circ$$

$$\delta_1 = 18^\circ$$

$$\delta_2 = 16^\circ$$

$$\delta_4 = 30^\circ$$

$$\sigma_{\text{allow geomembrane}} = 2100 \text{ lb}_f/\text{in}^2 \text{ (14,478 kN/m}^2\text{)}$$

$$T_{\text{GCL}} = 100 \text{ lb}_f/\text{in (17.5 kN/m)}$$

$$t_{\text{GCL}} = 0.25 \text{ in (6.4 mm)}$$

Solution:

The critical interface lies between the HDPE geomembrane and the GCL based on the magnitude of the respective friction angles. The following parameters are calculated:

$$W_w = 9.0 \times 10^3 \text{ lb}_f/\text{ft (131 kN/m)} \quad \text{Eq. 1}$$

$$K_o = 0.658 \quad \text{Eq. 3}$$

$$\sigma_v = 300 \text{ lb}_f/\text{ft}^2 \text{ (14.4 kN/m}^2\text{)} \quad \text{Eq. 4}$$

$$\sigma_h = 197 \text{ lb}_f/\text{ft}^2 \text{ (9.4 kN/m}^2\text{)} \quad \text{Eq. 2}$$

$$T_w = 718 \text{ lb}_f/\text{ft (10.5 kN/m)} \quad \text{Eq. 2}$$

$$W_{\text{net}} = 8282 \text{ lb}_f/\text{ft (120.9 kN/m)} \quad \text{Eq. 5}$$

$$N = 7857 \text{ lb}_f/\text{ft (114.7 kN/m}^2\text{)} \quad \text{Eq. 6}$$

$$F_1 = 2553 \text{ lb}_f/\text{ft (37.3 kN/m)} \quad \text{Eq. 8}$$

**APPLICATION FOR PERMIT RENEWAL AND MODIFICATION
SANDOVAL COUNTY LANDFILL**

**VOLUME III: LANDFILL ENGINEERING CALCULATIONS
SECTION 7: GEOSYNTHETICS TENSILE STRESS AND STABILITY ANALYSIS**

ATTACHMENT III.7.M

US FABRICS, INC., *WOVEN GEOTEXTILE CATALOG SHEET*

800-518-2290

- ✓ Spec Interpretation
- ✓ Product Application
- ✓ Pricing & Availability
- ✓ Product Comparison

[Contact Us](#)

Our Products By Category

All US Fabrics' products listed by category.

[-Find US Fabric's Product](#)

Equivalent Products

Find a US Fabrics' equivalent to the specified product.

[-Find USF Equivalent](#)

Geotextile Applications

Find which products work for your application.

[-Choose An Application](#)

Helpful References

Design and Installation help, packaging info, support literature

[- Select a Reference](#)

[Home](#) → [Products](#) → [Geotextiles](#) → [Woven Geotextiles](#) → [Woven Geotextile Catalog Sheet](#)

Woven Geotextile Catalog Sheet

Woven Stabilization & Separation

Woven stabilization fabrics give you the strength and separation you need for your paved or unpaved application. High tensile strength at low elongation reduces rutting in both paved and unpaved surfaces. These fabrics separate the base course while reinforcing the adjacent soft soil.

A lightweight fabric where separation is primary function.

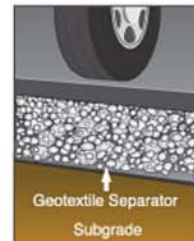
These medium weight fabrics provide separation and stabilization. They meet many DOT and federal specifications for separation and are the most utilized fabrics for this application.

A high strength, high modulus stabilization fabric for use with heavy loads and soft soils.

A heavy stabilization and reinforcement fabric for many applications.



Without Geotextile Separator



With a Geotextile Separator

Standard | Metric

Woven Geotextile Catalog Sheet

PROPERTY	METHOD	US 200	US 250	US 315	US 2700	US 4000	US 4800
Tensile Strength	ASTM D-4632	200 lbs	250 lbs	315 lbs	350 x 350 lbs	400 x 400 lbs	600 x 600 lbs
Elongation @ Break	ASTM D-4632	15%	15%	15%	20 x 15%	20 x 15%	20 x 15%
Mullen Burst*	ASTM D-3786*	400 psi	450 psi	600 psi	NA	NA	NA
Puncture Strength*	ASTM D-4833*	90 lbs	100 lbs	120 lbs	NA	NA	NA
CBR Puncture	ASTM D-6241	700 lbs	900 lbs	1,000 lbs	1,000 lbs	1,200 lbs	1,400 lbs
Trapezoidal Tear	ASTM D-4533	75 lbs	90 lbs	120 lbs	120 x 120 lbs	150 x 150 lbs	200 x 200 lbs
Apparent Opening Size	ASTM D-4751	40 US Sieve	40 US Sieve	40 US Sieve	40 US Sieve	40 US Sieve	80 US Sieve
Permittivity	ASTM D-4491	0.05 Sec-1	0.05 Sec-1	0.05 Sec-1	0.150 Sec-1	0.16 sec-1	0.15 Sec-1
Water Flow Rate	ASTM D-4491	5 g/min/sf	4 g/min/sf	4 g/min/sf	11 g/min/sf	12 g/min/sf	10 g/min/sf
UV Resistance @ 500 Hours	ASTM D-4355	70%	70%	70%	80%	80%	80%
Wide Width Tensile	ASTM D-4595	NA	NA	NA	3,179 x 2,711 lbs/ft (265 x 226 lbs/in)	3,749 x 4,030 lbs/ft (312.42 x 335.83 lbs/in)	4,800 x 4,800 lbs/foot (400 x 400 lbs/in)
Wide Width Elongation	ASTM D-4595	NA	NA	NA	11.4 x 7.9%	9.4 x 6.6%	10.2 x 7.2%
Wide Width Tensile @ 5 %	ASTM D-4595	NA	NA	NA	NA	NA	1,452 x 2,604 lbs/ft

This information is provided for reference only and is not intended as a warranty or guarantee. US Fabrics assumes no liability in connection with the use of this information (1/2015).

**APPLICATION FOR PERMIT RENEWAL AND MODIFICATION
SANDOVAL COUNTY LANDFILL**

**VOLUME III: LANDFILL ENGINEERING CALCULATIONS
SECTION 7: GEOSYNTHETICS TENSILE STRESS AND STABILITY ANALYSIS**

ATTACHMENT III.7.N

GSE LINING TECHNOLOGY, INC., *GSE HD TEXTURED PRODUCT DATA SHEET*



Geomembranes Manufacturing Quality Assurance Manual

Appendix B - Minimum Testing Frequencies and Properties for GSE Geomembranes

MINIMUM PROPERTIES FOR GSE HD TEXTURED

TESTED PROPERTY	TEST METHOD	FREQUENCY	MINIMUM VALUE				
Product Code			HDT 030G000	HDT 040G000	HDT 060G000	HDT 080G000	HDT 100G000
Thickness, (minimum average) mil (mm)	ASTM D 5994	every roll	29 (0.73)	38 (0.96)	57 (1.45)	76 (1.93)	95 (2.41)
Lowest individual for 8 out of 10 values			27 (0.69)	36 (0.91)	54 (1.40)	72 (1.80)	90 (2.30)
Lowest individual for any of the 10 values			26 (0.66)	34 (0.86)	51 (1.30)	68 (1.73)	85 (2.16)
Density, g/cm ³	ASTM D 1505	200,000 lb	0.94	0.94	0.94	0.94	0.94
Tensile Properties (each direction) ⁽¹⁾	ASTM D 6693, Type IV Dumbell, 2 ipm	20,000 lb					
Strength at Break, lb/in-width (N/mm)			45 (8)	60 (11)	90 (16)	120(21)	150 (27)
Strength at Yield, lb/in-width (N/mm)			63 (11)	84 (15)	126 (22)	168 (29)	210 (37)
Elongation at Break, %	G.L. = 2.0 in (51 mm)		100	100	100	100	100
Elongation at Yield, %	G.L. = 1.3 in (33 mm)		12	12	12	12	12
Tear Resistance, lb (N)	ASTM D 1004	45,000 lb	21 (93)	28 (125)	42 (187)	56 (249)	70 (311)
Puncture Resistance, lb (N)	ASTM D 4833	45,000 lb	45 (200)	60 (267)	90 (400)	120 (534)	150 (667)
Carbon Black Content, %	ASTM D 1603*/4218	20,000 lb	2.0	2.0	2.0	2.0	2.0
Carbon Black Dispersion	ASTM D 5596	45,000 lb	+Note 1	+Note 1	+Note 1	+Note 1	+Note 1
Asperity Height	GRI GM 12	second roll	+Note 2	+Note 2	+Note 2	+Note 2	+Note 2
Notched Constant Tensile Load ⁽²⁾ , hr	ASTM D 5397, Appendix	200,000 lb	300	300	300	300	300
REFERENCE PROPERTY	TEST METHOD	FREQUENCY	NOMINAL VALUE				
Oxidative Induction Time, min	ASTM D 3895, 200° C; O ₂ , 1 atm	200,000 lb	>100	>100	>100	>100	>100
Roll Length ⁽³⁾ (approximate), ft (m)	Standard Textured		830 (253)	700 (213)	520 (158)	400 (122)	330 (101)
Roll Width ⁽³⁾ , ft (m)			22.5 (6.9)	22.5 (6.9)	22.5 (6.9)	22.5 (6.9)	22.5 (6.9)
Roll Area, ft ² (m ²)			18,674 (1,735)	15,750 (1,463)	11,700 (1,087)	9,000 (836)	7,425 (690)

NOTES:

- +Note 1: Dispersion only applies to near spherical agglomerates. 9 of 10 views shall be Category 1 or 2. No more than 1 view from Category 3.
- +Note 2: 10 mil average. 8 of 10 readings ≥ 7 mils. Lowest individual ≥ 5 mils.
- GSE HD Standard Textured is available in rolls weighing about 4,000 lb (1,800 kg).
- ⁽¹⁾The combination of stress concentrations due to coextrusion texture geometry and the small specimen size results in large variation of test results. Therefore, these tensile properties are minimum average values.
- ⁽²⁾NCTL for HD Textured is conducted on representative smooth membrane samples.
- All GSE geomembranes have dimensional stability of $\pm 2\%$ when tested with ASTM D 1204 and LTb of $< 77^\circ \text{C}$ when tested with ASTM D 746.
- ⁽³⁾Roll lengths and widths have a tolerance of $\pm 1\%$.
- *Modified.

**APPLICATION FOR PERMIT RENEWAL AND MODIFICATION
SANDOVAL COUNTY LANDFILL**

**VOLUME III: LANDFILL ENGINEERING CALCULATIONS
SECTION 7: GEOSYNTHETICS TENSILE STRESS AND STABILITY ANALYSIS**

**ATTACHMENT III.7.O
GSE LINING TECHNOLOGY, INC., GSE 6 OZ FABRINET GEOCOMPOSITE
WIDE-WIDTH TENSILE TEST RESULTS.**

Mike Heinstein

From: Walter Steinbeck [wsteinbeck@gseworld.com]
Sent: Tuesday, January 05, 2010 4:03 PM
To: Mike Heinstein
Subject: RE: Question concerning wide width tensile strength of GSE FabriNet Geocomposite
Attachments: T5019-F4206-WW.XLS

Mike,

Unfortunately, we do not have the 10oz FabriNet geocomposite wide-width tensile information. However, we do have information for 6oz FabriNet geocomposite - which has the break strength of 270 lbs/inch and the break elongation of 80%. Again, while we do not have the 10oz FabriNet values available – this product should perform a little better than 6 oz. FabriNet. I hope these values help you.

The material price for the product is approximately \$0.40/sf + scrap/lap of 8% + mark up of 15% = \$0.50/sf + installation (\$0.25/sf) ~ \$0.75/sf - \$0.80/sf should cover you.

I appreciate you contacting us and let me know if I can help you out any further.

Thanks,

Walt Steinbeck
GSE Lining Technology, Inc.
Phone: (951) 273-3474
Cell: (310) 617-2966

From: Mike Heinstein [mailto:MHeinstein@gordonenvironmental.com]
Sent: Tuesday, January 05, 2010 10:51 AM
To: Walter Steinbeck
Subject: Question concerning wide width tensile strength of GSE FabriNet Geocomposite

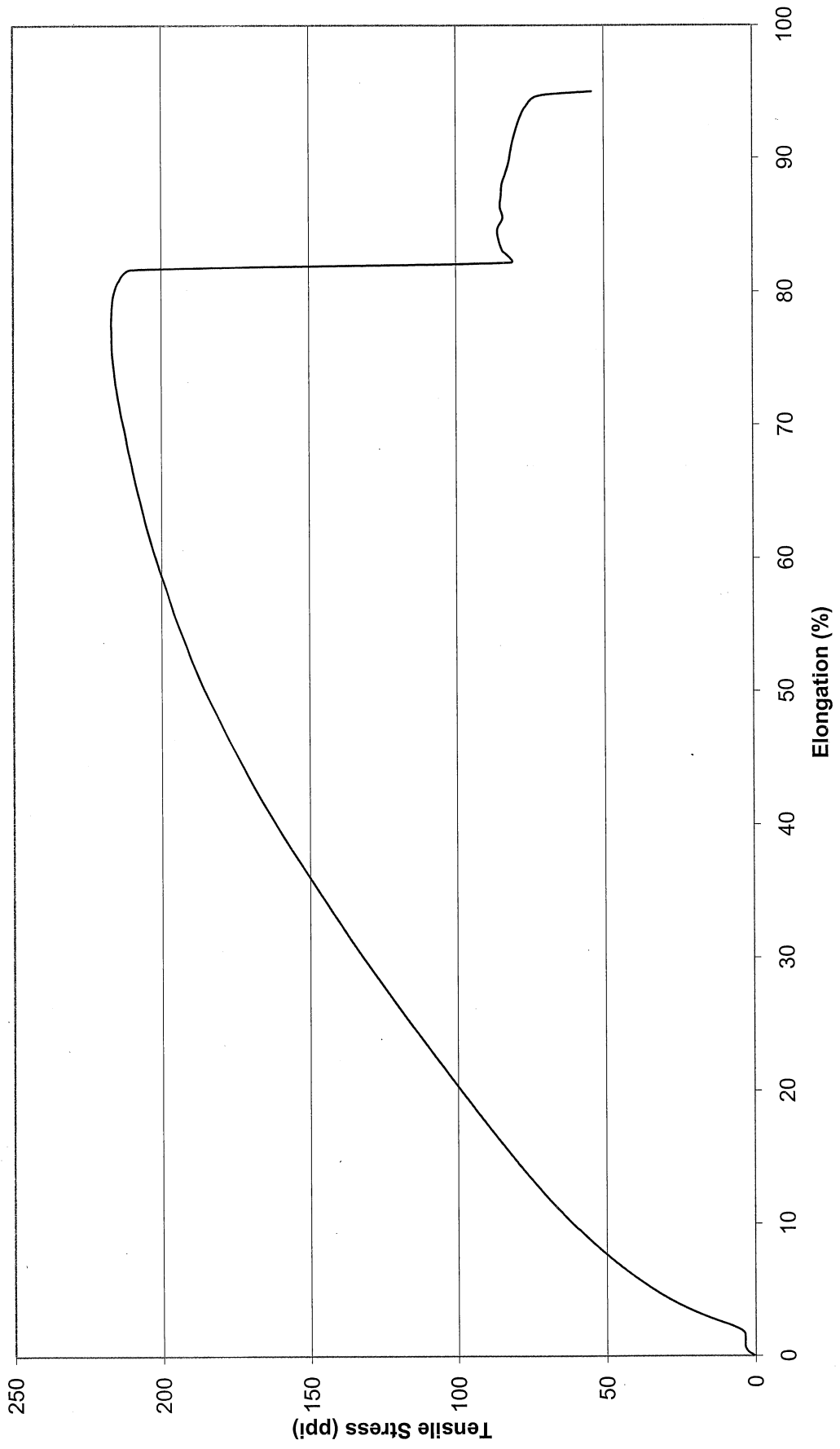
Walt

Can you please provide some information concerning the wide width tensile strength of GSE FabriNet Geocomposite with a 10 oz/sy non-woven geotextile bonded to it.

Thanks, Mike

Michael R. Heinstein, P.E.
Senior Project Engineer
Gordon Environmental, Inc.
213 S. Camino del Pueblo
Bernalillo, NM 87004
(505) 867-6990 (Office)
(505) 867-6991 (Fax)
mheinstein@gordonenvironmental.com

Wide Width Tensile Test of F42060060S Geocomposite
8" x8" Specimen, 4" gage Length, 0.4 in/min Test Speed, Tested in Machine Direction



**APPLICATION FOR PERMIT RENEWAL AND MODIFICATION
SANDOVAL COUNTY LANDFILL**

**VOLUME III: LANDFILL ENGINEERING CALCULATIONS
SECTION 8: DRAINAGE CALCULATIONS**

TABLE OF CONTENTS

1.0	INTRODUCTION	III.8-1
1.1	Project Description	III.8-1
2.0	DESIGN CRITERIA	III.8-3
3.0	METHODOLOGY	III.8-3
4.0	SURFACE WATER RUNOFF CALCULATIONS	III.8-3
5.0	STORMWATER BASIN DESIGN	III.8-12
6.0	CHANNEL DESIGN AND CAPACITY	III.8-13
7.0	LOW WATER CROSSING DESIGN AND CAPACITY	III.8-14

LIST OF FIGURES

Figure No.	Title	Page
III.8.1	SITE DEVELOPMENT PLAN	III.8-2
III.8.2	LANDFILL COMPLETION DRAINAGE PLAN	III.8-4

LIST OF TABLES

Table No.	Title	Page
III.8.1	RUNOFF DRAINAGE AREAS	III.8-5
III.8.2	WATERSHED “A” CALCULATIONS	III.8-7
III.8.3	WATERSHED “A1” CALCULATIONS	III.8-8
III.8.4	WATERSHED “A2” CALCULATIONS	III.8-9
III.8.5	WATERSHED “B” CALCULATIONS	III.8-10
III.8.6	WATERSHED “B1” CALCULATIONS	III.8-11
III.8.7	WATERSHED “C” CALCULATIONS	III.8-12
III.8.8	RUNOFF SUMMARY	III.8-13
III.8.9	STORMWATER BASIN DESIGN SUMMARY	III.8-13
III.8.10	CHANNEL DESIGN SUMMARY	III.8-15
III.8.11	LOW WATER CROSSING DESIGN SUMMARY	III.8-16

**APPLICATION FOR PERMIT RENEWAL AND MODIFICATION
SANDOVAL COUNTY LANDFILL**

**VOLUME III: LANDFILL ENGINEERING CALCULATIONS
SECTION 8: DRAINAGE CALCULATIONS**

LIST OF ATTACHMENTS

Attachment No.	Title
III.8.A	PHILIPS, CHRISTOPER S.; EASTERLING, CHARLES M.; HEGGEN, RICHARD J.; AND SCHALL, JAMES D. 1995. <i>DRAINAGE MANUAL, VOLUME I: HYDROLOGY</i> . NEW MEXICO STATE HIGHWAY AND TRANSPORTATION DEPARTMENT.
III.8.B	U.S. DEPT. OF COMMERCE NATIONAL OCEANIC AND ATMOSPHERIC ADMINISTRATION NATIONAL WEATHER SERVICE OFFICE OF HYDROLOGIC DEVELOPMENT HYDROMETEOROLOGICAL DESIGN STUDIES CENTER, JUNE 2006, NOAA ATLAS 14, VOLUME 1, VERSION 4 SEMIARID SOUTHWESTERN UNITED STATES, NEW MEXICO, ISOPLUVIALS OF 24 HOUR PRECIPITATION (INCHES) WITH AVERAGE RECURRENCE INTERVAL OF 25 YEARS.

**APPLICATION FOR PERMIT RENEWAL AND MODIFICATION
SANDOVAL COUNTY LANDFILL**

**VOLUME III: LANDFILL ENGINEERING CALCULATIONS
SECTION 8: DRAINAGE CALCULATIONS**

1.0 INTRODUCTION

The Sandoval County Landfill (SCLF) is an existing solid waste facility operating in compliance with its current Permits, SWM-050304 and SWM-050304 (SP), and the New Mexico Environment Department (NMED) Solid Waste Rules (20.9.2-2.9.10 NMAC). SCLF is located at 2708 Iris Road NE in Rio Rancho, New Mexico (NM), and occupies 178.3 acres \pm . SCLF is publicly owned and operated by the County of Sandoval (“the County”), and is currently permitted to accept municipal solid waste (MSW), including construction and demolition debris (C&D) and tires, and two special wastes: petroleum contaminated soils (PCS) and sludge.

1.1 Project Description

SCLF site is comprised of 178.3 \pm acres, with a solid waste footprint of 122.9 \pm acres. The site is located in portions of Sections 33 and 34, Township 13 North, Range 3 East of the New Mexico Prime Meridian, Sandoval County, New Mexico, and is accessed via an entrance off Iris Avenue, adjacent to the Rio Rancho Highway Department. The approximate geographic coordinates for the center of the landfill site are **Latitude 35.307° North** and **Longitude 106.622° West**.

Design topography at SCLF ranges from about 5270 feet \pm above mean sea level (AMSL) to 5560 feet \pm AMSL, and generally drains toward the site boundaries at slopes between 5% \pm and 25% \pm . The majority of the site boundaries are roadways, on the northwest, southwest, and southeast property boundaries. The northeast corner of the site is bounded by a PNM easement and transformer station site. Run-on stormwater is managed by existing stormwater management structures. On-site runoff will be managed by three existing stormwater basins (Basins A, B, and C) located at the northeast corner of the site, the south corner of the site, and along the southwest edge of Unit III, respectively, as shown in **Figure III.8.1**. Site run-off will be conveyed by three perimeter channels, and two stormwater drainage berms to Stormwater Basins A, B and C, as shown in **Figure III.8.2**.



LEGEND

- PROPERTY BOUNDARY (178.3 ACRES)
- EXISTING UNIT LIMIT OF WASTE
- CELL BOUNDARY
- PERMIT MODIFICATION AND RENEWAL LIMIT OF WASTE (122.5 ACRES±)
- UNIT IV EDGE OF LINER
- UNIT IV BOUNDARY
- UNIT IV OVERFILL AREA
- UNIT IV BASE GRADING AREA
- EXISTING UNITS I, II & III
- 10' EXISTING GRADE CONTOUR
- 2' EXISTING GRADE CONTOUR
- EXISTING CULVERT
- EXISTING FENCE
- PAVED ROAD
- UNPAVED ROAD
- UTILITY EASEMENT BOUNDARY
- FORMER UTILITY EASEMENT BOUNDARY
- EXISTING LEACHATE COLLECTION PIPE & TRENCH
- EXISTING LEACHATE COLLECTION SYSTEM RISER PIPE
- PROPOSED LEACHATE COLLECTION PIPE & TRENCH
- PROPOSED LEACHATE COLLECTION SYSTEM RISER PIPE
- STORMWATER FLOW
- STORMWATER BASIN
- EXISTING POWER POLE
- FIRE HYDRANT (3)
- EXISTING GROUNDWATER MONITORING WELL
- GROUNDWATER MONITORING WELL (DECOMMISSIONED)
- EXISTING LFG GAS PROBE (ACTIVE)
- EXISTING LFG GAS PROBE (INACTIVE)
- LFG GAS PROBE (DECOMMISSIONED)
- SURVEY CONTROL POINT

SITE GRID

CROSS-SECTION LOCATIONS

NOTES:

- AERIAL TOPOGRAPHIC SURVEY BY AEROTECH MAPPING INC., 6565 AMERICAN PARKWAY N.E., ALBUQUERQUE, NM 87111
PHONE: (520-561-6537) FAX (505 256-3328)
EMAIL: TimBurrows@aerotech.com
DATE OF PHOTOGRAPHY: 01-13-2014.
- SURVEY CONTROL POINTS BY: SURVEYING CONTROL, INC., 131 MADISON ST. N.E., ALBUQUERQUE, NM 87108
PHONE: (505-266-0935) FAX (505-266-9985) DATE OF SURVEY: 01-13-2014
- THE COUNTY MAY ELECT TO RETAIN THE EXISTING OVERHEAD STRUCTURE AT THE EAST END OF UNIT IV AS A COMMUNICATIONS TOWER. IN THAT EVENT, FUTURE CONSTRUCTION PLANS WILL ADDRESS THE EXISTENCE OF THIS FEATURE.

CONTROL POINT DATA

POINT	NORTHING	EASTING	PANEL ELEVATION	DESCRIPTION
501	1567982.35	1527461.08	5370.34	PP-501
502	1570293.88	1531074.96	5354.66	PP-502
503	1567798.82	1529894.61	5369.53	PP-503
504	1565822.71	1528883.42	5316.47	PP-504
505	1567834.53	1532385.04	5371.17	PP-505

NOTES:

- ALL POINTS ARE FLUSH WITH THE GROUND.
- THE COORDINATES AND ELEVATIONS FOR THE PHOTO CONTROL POINTS ON THE ABOVE REFERENCED PROJECT. THE COORDINATES ARE MODIFIED (SURFACE) NEW MEXICO STATE PLANE COORDINATES - CENTRAL ZONE, NAD 83 (NAD83/2007), AND HAVE BEEN ADJUSTED TO NGS MONUMENTS "EAGLEART" TO OBTAIN TRUE STATE PLANE GRID COORDINATES. MULTIPLY THE COORDINATES BELOW BY THE PROJECT AVERAGE COMBINED FACTOR OF 0.999661430. THE ELEVATIONS ARE NAVD 88, AND HAVE BEEN ADJUSTED TO THE NGS 1ST ORDER BENCHMARK "S424". THE COORDINATES AND ELEVATIONS ARE EXPRESSED IN U. S. SURVEY FEET.

GROUNDWATER MONITORING WELL LOCATIONS

POINT	NORTHING	EASTING	ELEVATION	DESCRIPTION
MW-1	1566727.43	1530025.09	5322.45	MONITORING WELL
MW-2	1568159.63	1531290.50	5414.11	MONITORING WELL
MW-3	1567315.31	1531064.87	5374.32	MONITORING WELL
MW-5	1567869.24	1528110.28	5362.38	MONITORING WELL
MW-6	1568758.30	1530695.17	5421.90	MONITORING WELL
MW-7	1569394.69	1531377.96	5363.30	MONITORING WELL

NOTES:

- THE COORDINATES AND ELEVATIONS FOR THE GROUNDWATER MONITORING WELL LOCATIONS ON THE ABOVE TABLE. ARE MODIFIED (SURFACE) NEW MEXICO STATE PLANE COORDINATES - CENTRAL ZONE, NAD 83. SURVEY DATA OBTAINED BY TM MARTINEZ SURVEYING ON 3-26-2015. THE COORDINATES AND ELEVATIONS ARE EXPRESSED IN U. S. SURVEY FEET.

UPDATED JANUARY 2016

SITE DEVELOPMENT PLAN

SANDOVAL COUNTY LANDFILL
RIO RANCHO, NEW MEXICO



Gordon Environmental, Inc.
Consulting Engineers

213 S. Camino del Pueblo
Bernalillo, New Mexico, USA
Phone: 505-867-6990
Fax: 505-867-6991

DATE: 01/18/2016	CAD: 03 Site Plan Unit IV.dwg	PROJECT #: 211.00.01
DRAWN BY: DMJ	REVIEWED BY: CRK	
APPROVED BY: IKG	get@gordonenvironmental.com	FIGURE III.8.1

I. KEITH GORDON, P.E.
N.M. PROFESSIONAL ENGINEER NO. 10984

All reports, drawings, specifications, computer files, field data, notes and other documents and instruments prepared by the Engineer as instruments of service shall remain the property of the Engineer. The Engineer shall retain all common law, statutory and other reserved rights, including the copyright thereto.

NOT FOR CONSTRUCTION

Drawing: P:\acad 2003\211.00.01\PERMIT PLAN SET\UNIT IV\RAI1103 SITE PLAN UNIT IV.dwg
Date/Time: Jan. 29, 2016 14:23:09 LAYOUT: 3-SiteDev
Copyright © All Rights Reserved, Gordon Environmental, Inc. 2016

2.0 DESIGN CRITERIA

The stormwater management systems for the SCLF are designed to meet the requirements of the regulatory standards identified in the New Mexico Solid Waste Rules 20.9.5 NMAC. More specifically, 20.9.5.9.E NMAC requires:

a plan to control run-on water onto the site and runoff water from the site, such that:

- (1) the run-on control system shall prevent flow onto the active portion of the land fill during the peak discharge from a 24-hour, 25-year storm;*
- (2) the runoff control system from the active portion of the landfill collects and controls at least the water volume resulting from a 24-hour, 25-year storm;*

and further, 20.9.6.9.A.(1) NMAC specifies that:

Each operator shall have a plan to control run-on water onto the site and runoff water from the site, such that:

- (f) runoff controls designed for a peak discharge of a 24-hour, 25-year storm.*

3.0 METHODOLOGY

The methodology for the calculation of runoff stormwater flows is based on the New Mexico State Highway and Transportation Department (NMSHTD) Drainage Manual, Volume 1: Hydrology (Philips et al., 1995; **Attachment III.8.A**). The NMSHTD Drainage Manual specifies that the Simplified Peak Flow Method be used on drainage areas that are no larger than 5 square miles (i.e., 3,200 acres); and where land use is consistent throughout the watershed. This method was used to calculate the runoff volume from the landfill due to a 25-year, 24-hour storm event. The total enclosed drainage basin acreage for the project area is determined to be approximately 214 acres (**Figure III.8.2**).

Off-site run-on enters the site through a culvert under Paseo del Volcan from the northwest, and is collected in Stormwater Basin C, representing a contributing area of 23 acres± (**Figure III.8.2**).

4.0 SURFACE WATER RUNOFF CALCULATIONS

The Simplified Peak Flow method is used to determine runoff surface water flow from the landfill. The Simplified Peak Flow method estimates the peak rate of runoff rates from small to medium size watersheds. This method was developed by the Soil Conservation Service (SCS) and revised by the SCS for use in New Mexico. Infiltration and other losses are estimated using the SCS Curve Number (CN) methodology. Input parameters are consistent with those used in the SCS Unit



LEGEND

- PROPERTY BOUNDARY (178.3 ACRES)
- EXISTING UNIT LIMIT OF WASTE
- CELL BOUNDARY
- PERMIT MODIFICATION AND RENEWAL LIMIT OF WASTE (122.5 ACRES±)
- UNIT IV EDGE OF LINER
- UNIT IV AREA
- 10' EXISTING GRADE CONTOUR
- 2' EXISTING GRADE CONTOUR
- 10' FINAL GRADE CONTOUR
- 2' FINAL GRADE CONTOUR
- EXISTING CULVERT
- EXISTING FENCE
- PAVED ROAD
- UNPAVED ROAD
- UTILITY EASEMENT BOUNDARY
- UNIT IV LEACHATE COLLECTION PIPE & TRENCH
- UNIT IV LEACHATE COLLECTION SYSTEM RISER PIPE
- STORMWATER FLOW
- STORMWATER WATERSHED BOUNDARY
- STORMWATER BASIN
- EXISTING POWER POLE
- FIRE HYDRANT (3)
- EXISTING GROUNDWATER MONITORING WELL
- GROUNDWATER MONITORING WELL (DECOMMISSIONED)
- EXISTING LFG GAS PROBE (ACTIVE)
- EXISTING LFG GAS PROBE (INACTIVE)
- LFG GAS PROBE (DECOMMISSIONED)
- SURVEY CONTROL POINT
- SITE GRID
- CROSS SECTION LOCATIONS

- NOTES:
1. AERIAL TOPOGRAPHIC SURVEY BY AEROTECH MAPPING INC., 6565 AMERICAN PARKWAY N.E., ALBUQUERQUE, NM 87111
PHONE: (520-561-6537) FAX (505-256-3328)
EMAIL: TimBurrows@bomlv.com
DATE OF PHOTOGRAPHY: 01-13-2014.
 2. SURVEY CONTROL POINTS BY : SURVEYING CONTROL, INC., 131 MADISON ST. N.E., ALBUQUERQUE, NM 87108
PHONE: (505-266-0935) FAX (505-266-9985)
DATE OF SURVEY: 01-13-2014
 3. THE COUNTY MAY ELECT TO RETAIN THE EXISTING OVERHEAD STRUCTURE AT THE EAST END OF UNIT IV AS A COMMUNICATIONS TOWER. IN THAT EVENT, FUTURE CONSTRUCTION PLANS WILL ADDRESS THE EXISTENCE OF THIS FEATURE.

TABLE 1
UNIT ACREAGES

UNIT I	29.4 ACRES±
UNIT II	19.5 ACRES±
UNIT III	63.6 ACRES±
UNIT IV	10.0 ACRES±
(FORMER PNM EASEMENT) ¹	
TOTAL	122.5 ACRES±

NOTE:
1. TOTAL AREA OF UNIT IV, INCLUDING OVERFILL AREAS IS 30.7 ACRES±

CONTROL POINT DATA

POINT	NORTHING	EASTING	PANEL ELEVATION	DESCRIPTION
501	1567982.35	1527461.08	5370.34	PP-501
502	1570293.88	1531074.96	5354.66	PP-502
503	1567798.82	1529894.61	5369.53	PP-503
504	1565822.71	1528883.42	5316.47	PP-504
505	1567834.53	1532385.04	5371.17	PP-505

NOTES:
1. ALL POINTS ARE FLUSH WITH THE GROUND.
2. THE COORDINATES AND ELEVATIONS FOR THE PHOTO CONTROL POINTS ON THE ABOVE REFERENCED PROJECT. THE COORDINATES ARE MODIFIED (SURFACE) NEW MEXICO STATE PLANE COORDINATES - CENTRAL ZONE, NAD 83 (NAD83/2011), AND HAVE BEEN ADJUSTED TO NGS MONUMENTS "EAGLE". TO OBTAIN TRUE STATE PLANE GRID COORDINATES BELOW BY THE PROJECT AVERAGE CORRECTION FACTOR OF 0.999661430. THE ELEVATIONS ARE NAVD 83, AND HAVE BEEN ADJUSTED TO THE NGS 1ST ORDER BENCHMARK "5424". THE COORDINATES AND ELEVATIONS ARE EXPRESSED IN U. S. SURVEY FEET.

GROUNDWATER MONITORING WELL LOCATIONS

POINT	NORTHING	EASTING	ELEVATION	DESCRIPTION
MW-1	1566727.43	1530025.09	5322.45	MONITORING WELL
MW-2	1568159.63	1531290.50	5414.11	MONITORING WELL
MW-3	1567315.31	1531064.87	5374.32	MONITORING WELL
MW-5	1567869.24	1528110.28	5362.38	MONITORING WELL
MW-6	1568758.30	1530695.17	5421.90	MONITORING WELL
MW-7	1569394.69	1531377.96	5363.30	MONITORING WELL

NOTES:
1. THE COORDINATES AND ELEVATIONS FOR THE GROUNDWATER MONITORING WELL LOCATIONS ON THE ABOVE TABLE ARE MODIFIED (SURFACE) NEW MEXICO STATE PLANE COORDINATES - CENTRAL ZONE, NAD 83. SURVEY DATA OBTAINED BY TIM MARTINEZ SURVEYING ON 3-26-2015. THE COORDINATES AND ELEVATIONS ARE EXPRESSED IN U. S. SURVEY FEET.

TABLE 2
RUNOFF SUMMARY

WATERSHED (ID)	DRAINAGE AREA (ACRES)	PEAK DISCHARGE (CFS)	VOLUME (ACRE-FT)
A	71.91	49.5	3.74
A1	7.05	8.48	0.37
A2	9.07	10.19	0.47
B	49.29	52.73	2.79
B1	4.35	5.61	0.23
C	49.91	26.07	2.60
C RUN-ON	20	1.20	
TOTAL	214.58	167	11.17

TABLE 3
CHANNEL DESIGN SUMMARY

CHANNEL (ID)	Q25 (CFS)	SLOPE (%)	WIDTH (FT)	DEPTH (FT)	VELOCITY (FT/S)	WATER DEPTH (FT)	FREEBOARD (FT)
A	49.40	3.5	3	2	10.82	0.938	1.06
A1	8.40	9.0	3	2	8.79	0.272	1.73
A2	10.20	4.4	4	2	3.77	0.32	1.68
A3	18.60	7.0	3	2	4.5	0.45	1.55
B	59.70	4.1	4	2	5.77	0.879	1.12
B1	5.80	1.6	0	2	3.74	0.76	1.24
C	46.70	2.4	4	2	4.77	0.681	1.32

TABLE 4
STORMWATER BASIN DESIGN SUMMARY

STORMWATER DETENTION / RETENTION BASIN	CONTRIBUTING DRAINAGE AREAS	RUNOFF VOLUME	BASIN CAPACITY WITHOUT FREEBOARD	BASIN MAX. CAPACITY USING 1 FT. FREEBOARD	FACTOR OF SAFETY USING 1 FT. FREEBOARD
A	A+A1+A2	4.58	5.12	6.83	1.12
B	B+B1	2.82	3.00	3.75	1.06
C	C+C RUN-ON	3.62	5.49	6.87	1.44

I. KEITH GORDON, P.E.
N.M. PROFESSIONAL ENGINEER NO. 10984

All reports, drawings, specifications, computer files, field data, notes and other documents and instruments prepared by the Engineer as instruments of service shall remain the property of the Engineer. The Engineer shall retain all common law, statutory and other reserved rights, including the copyright thereto.

UPDATED JANUARY 2016

FINAL COMPLETION DRAINAGE PLAN

SANDOVAL COUNTY LANDFILL
RIO RANCHO, NEW MEXICO

Gordon Environmental, Inc.
Consulting Engineers

213 S. Camino del Pueblo
Bernalillo, New Mexico, USA
Phone: 505-867-6990
Fax: 505-867-6991

DATE: 02/01/2016
DRAWN BY: DMI
APPROVED BY: IKG

CAD: FINAL GRADING.dwg
REVIEWED BY: CRK
gk@gordonenvironmental.com

PROJECT #: 211,00,01
FIGURE III.8.2

Hydrograph Method. The Simplified Peak Flow method is limited for use in New Mexico to single basins less than 5 square miles in area (i.e., 3,200 acres), and is to be used when the Time of Concentration (T_c) is expected not to exceed 8.0 hours; and where channels will be used to convey runoff. The Simplified Peak Flow method calculations used to determine stormwater runoff flows at SCLF site are presented in **Tables III.8.2 – III.8.7**. **Figure III.8.2** provides landfill runoff drainage areas for the finished landform (i.e. final contours). The methodology used to estimate stormwater runoff includes the following tasks:

- Obtain the 24-hour rainfall depth directly from *Figure E-8* (see **Attachment III.3.B**); $P_{24} = 2.1$ inches.
- Estimate the area, A, for each watershed identified on **Figure III.8.2**:

TABLE III.8.1
Runoff Drainage areas
Sandoval County Landfill

WATERSHED	DRAINAGE AREA (ACRES)±
A	71.96
A1	7.05
A2	9.07
B	49.62
B1	4.55
C	50.48
Site Total	192.73

- Determine curve number “CN”: From Table 3-1 “Runoff Curve Numbers for Arid and Semiarid Rangelands” in **Attachment III.8.A pg. 3-23**; for a herbaceous mixture of grass, weeds, and low growing brush, with brush the minor element, Soil Group **B** (consisting of silty sands, the predominate soils on-site) and <30% Vegetation Cover; Hydrologic Condition “poor”; **Run-on CN = 80**;
- Determine drainage length, L_n , of the longest path runoff may travel within the drainage area. The slopes are averaged in this path to determine velocity of flow.
- Determine Flow Velocities, V, in foot per second (ft/s): From *Figure 3-10* “Flow Velocities for Overland and Shallow Concentrated Flows” in **Attachment III.8.A pg. 3-33**; for Nearly Bare and Untilled (Overland Flow), Alluvial Fans in Western Mountain Regions (Shallow Concentrated Flow).
- Calculate the Time of Concentration, T_c , in hours.
 - A. Upland method was used for areas where there were no defined gullies and the Kirpich Formula was used where a defined channel is used to convey stormwater (see **Attachment III.8.A pg. 3-31**).
 - B. The overland flow Time of Concentration is calculated in minutes using this equation:

$$T_c = \left(\frac{L_1}{V_1} + \frac{L_2}{V_2} + \frac{L_3}{V_3} + \dots \frac{L_n}{V_n} \right) \frac{1}{60} \text{ EQ (3-17) (see Attachment III.8.A pg. 3-30).}$$

C. The Kirpich Formula is calculated using the equation

$$T_c = 0.0078L^{0.77}S^{-0.385}, \text{ in minutes; EQ (3-18) (see Attachment III.8.A pg. 3-34).}$$

The above methodology was used to determine the stormwater runoff from the four drainage areas at SCLF and are presented in **Tables III.8.2 – III.8.7** and are summarized in **Table III.8.8**.

TABLE III.8.2
Watershed “A” Calculations
Sandoval County Landfill

Watershed “A”: Discharge point to northwest end of Basin A (25-year, 24-hour storm event; estimated at 2.1 inches, **Attachment III.8.B**).

1. Area (A)= 71.96 acres
2. Longest travel distance (L_1) = 450' (overland flow)
3. Average slope = 4.7 % (overland flow)
4. Velocity (V_1) = 1.9 ft/s (*Figure 3-10, Attachment III.8.A pg. 3-33*; overland flow)
5. $T_{c1} = \left[\frac{L}{V} \right] \left(\frac{1}{60} \right) = \left[\frac{450 \text{ ft}}{2.1 \frac{\text{ft}}{\text{s}}} \right] \left(\frac{1}{60} \right) = 3.57 \text{ min}$ **Equation 3-17, Attachment III.8.A pg. 3-30**;
overland flow)
6. Longest travel distance (L_3) = 5312' (channel flow)
7. Average slope (S) = 0.035 ft/ft (channel flow)
8. $T_{c2} = 0.0078 \times (L)^{0.77} \times (S)^{-0.385} = 0.0078 \times (5312)^{0.77} \times (0.035)^{-0.385} =$
20.98 min (Equation 3-18, Attachment III.8.A pg. 3-34; channel flow)
9. $T_c = T_{c1} + T_{c2} = 3.57 \text{ min} + 20.98 \text{ min} = 24.55 \text{ min} = 0.41 \text{ hrs}$
10. Curve Number = 80 (**Table 3-1, Attachment III.8.A pg. 3-23**) for Desert shrub, Soil Group B (consisting of silty sand, the predominate soils on-site).
11. Unit peak discharge (**Equation 3-22, Attachment III.8.A pg. 3-50**)
$$q_u = 0.543(T_c^{-0.812})10^{\frac{(|\log(T_c)+0.3|-\log(T_c)-0.3)^{1.5}}{10}} = 1.10 \text{ cfs/ac-in.}$$
12. Average Run-off Depth (**Equation 3-23, Attachment III.8.A pg. 3-50**).
$$Q_d = \frac{[P_{24} - (200/CN) + 2]^2}{P_{24} + (800/CN) - 8} = \frac{[2.1 - (200/80) + 2]^2}{2.1 + (800/80) - 8} = 0.62439 \text{ inches} \approx 0.624 \text{ inches}$$
13. Design Frequency Peak Flow (**Equation 3-24, Attachment III.8.A pg. 3-50**);
$$Q_P = A \times Q_d \times q_u = 71.96 \text{ ac} \times .624 \text{ in} \times 1.10 \frac{\text{cfs}}{\text{ac} - \text{in}} = 49.4 \text{ cfs}$$
14. Stormwater volume (**Equation 3-25, Attachment III.8.A pg. 3-50**)
$$Q_v = \frac{A \times Q_d}{12} = \frac{71.96 \text{ ac} \times .624 \text{ in}}{12} = 3.74 \text{ ac} - \text{ft}$$

TABLE III.8.3
Watershed “A1” Calculations
Sandoval County Landfill

Watershed A1: Discharge point at southeast side of Stormwater Basin #A (25-year, 24-hour storm event; estimated at 2.1 inches, **Attachment III.8.B**).

1. Area (A) = 7.05 acres
2. Longest travel distance (L_1) = 220' (overland flow)
3. Average slope = 2.7 % (overland flow)
4. Velocity (V_1) = 1.7 ft/s (*Figure 3-10, Attachment III.8.A pg. 3-33*; overland flow)
5. $T_{C1} = \left[\frac{L}{V} \right] \left(\frac{1}{60} \right) = \left[\frac{220 \text{ ft}}{1.7 \frac{\text{ft}}{\text{s}}} \right] \left(\frac{1}{60} \right) = 2.16 \text{ min}$ **Equation 3-17, Attachment III.8.A pg. 3-30**;
overland flow)
6. Longest travel distance (L_2) = 2183' (channel flow)
7. Average slope (S) = 0.090 ft/ft (channel flow)
8. $T_{C2} = 0.0078 \times (L)^{0.77} \times (S)^{-0.385} = 0.0078 \times (5312)^{0.77} \times (0.090)^{-0.385} =$
 7.35 min (**Equation 3-18, Attachment III.8.A pg. 3-34**; channel flow)
9. $T_C = T_{C1} + T_{C2} = 2.16 \text{ min} + 7.35 \text{ min} = 9.51 \text{ min} = 0.16 \text{ hrs}$
10. Curve Number = 80 (**Table 3-1, Attachment III.8.A pg. 3-23**) for Desert shrub, Soil Group B (consisting of silty sand, the predominate soils on-site).
11. Unit peak discharge (**Equation 3-22, Attachment III.8.A pg. 3-50**)
$$q_u = 0.543(T_c^{-0.812})^{10} \frac{(|\log(T_c)+0.3| - |\log(T_c)-0.3|)^{1.5}}{10} = 1.92 \text{ cfs/ac-in.}$$
12. Average Run-off Depth (**Equation 3-23, Attachment III.8.A pg. 3-50**).
$$Q_d = \frac{[P_{24} - (200/CN) + 2]^2}{P_{24} + (800/CN) - 8} = \frac{[2.1 - (200/80) + 2]^2}{2.1 + (800/80) - 8} = 0.62439 \text{ inches} \approx 0.624 \text{ inches}$$
13. Design Frequency Peak Flow (**Equation 3-24, Attachment III.8.A pg. 3-50**);
$$Q_P = A \times Q_d \times q_u = 7.05 \text{ ac} \times .624 \text{ in} \times 1.92 \frac{\text{cfs}}{\text{ac} - \text{in}} = 8.4 \text{ cfs}$$
14. Stormwater volume (**Equation 3-25, Attachment III.8.A pg. 3-50**)

$$Q_v = \frac{A \times Q_d}{12} = \frac{7.05 \text{ ac} \times .624 \text{ in}}{12} = 0.37 \text{ ac-ft}$$

TABLE III.8.4
Watershed “A2” Calculations
Sandoval County Landfill

Watershed A2: Discharge point at southeast side of Stormwater Basin #A (25-year, 24-hour storm event; estimated at 2.1 inches, **Attachment III.8.B**).

1. Area (A)= 9.07 acres
2. Longest travel distance (L_1) = 420' (overland flow)
3. Average slope = 21.9 % (overland flow)
4. Velocity (V_1) = 5.2 ft/s (*Figure 3-10, Attachment III.8.A pg. 3-33*; overland flow)
5. $T_{C1} = \left[\frac{L}{V} \right] \left(\frac{1}{60} \right) = \left[\frac{420 \text{ ft}}{5.2 \frac{\text{ft}}{\text{s}}} \right] \left(\frac{1}{60} \right) = 1.35 \text{ min}$ **Equation 3-17, Attachment III.8.A pg. 3-30**;
overland flow)
6. Longest travel distance (L_2) = 2113' (channel flow)
7. Average slope (S) = 0.044 ft/ft (channel flow)
8. $T_{C2} = 0.0078 \times (L)^{0.77} \times (S)^{-0.385} = 0.0078 \times (2113)^{0.77} \times (0.044)^{-0.385} =$
 9.47 min (**Equation 3-18, Attachment III.8.A pg. 3-34**; channel flow)
9. $T_c = T_{C1} + T_{C2} = 1.35 \text{ min} + 9.47 \text{ min} = 10.82 \text{ min} = 0.18 \text{ hrs}$
10. Curve Number = 80 (**Table 3-1, Attachment III.8.A pg. 3-23**) for Desert shrub, Soil Group B (consisting of silty sand, the predominate soils on-site).
11. Unit peak discharge (**Equation 3-22, Attachment III.8.A pg. 3-50**)

$$q_u = 0.543(T_c^{-0.812})10^{\frac{(|\log(T_c)+0.3|-\log(T_c)-0.3)^{1.5}}{10}} = 1.80 \text{ cfs/ac-in}$$
12. Average Run-off Depth (**Equation 3-23, Attachment III.8.A pg. 3-50**).

$$Q_d = \frac{[P_{24} - \frac{(200/CN)+2}{P_{24} + \frac{(800/CN)-8}{2.1}}]^2}{P_{24} + \frac{(800/CN)-8}{2.1}} = \frac{[2.1 - \frac{(200/80)+2}{2.1 + \frac{(800/80)-8}{2.1}}]^2}{2.1 + \frac{(800/80)-8}{2.1}} = 0.62439 \text{ inches} \approx 0.624 \text{ inches}$$
13. Design Frequency Peak Flow (**Equation 3-24, Attachment III.8.A pg. 3-50**);

$$Q_P = A \times Q_d \times q_u = 9.07 \text{ ac} \times .624 \text{ in} \times 1.10 \frac{\text{cfs}}{\text{ac} - \text{in}} = 10.2 \text{ cfs}$$
14. Stormwater volume (**Equation 3-25, Attachment III.8.A pg. 3-50**)

$$Q_v = \frac{A \times Q_d}{12} = \frac{9.07 \text{ ac} \times .624 \text{ in}}{12} = 0.47 \text{ ac} - \text{ft}$$

TABLE III.8.5
Watershed “B” Calculations
Sandoval County Landfill

Watershed B: Discharge point at northeast side of Stormwater Basin #B (25-year, 24-hour storm event; estimated at 2.1 inches, **Attachment III.8.B**).

1. Area (A)= 49.29 acres
2. Longest travel distance (L_1) = 730' (overland flow)
3. Average slope = 10.5 % (overland flow)
4. Velocity (V_1) = 4ft/s (*Figure 3-10, Attachment III.8.A pg. 3-33*; overland flow)
5. $T_{C1} = \left[\frac{L}{V} \right] \left(\frac{1}{60} \right) = \left[\frac{730 \text{ ft}}{4 \frac{\text{ft}}{\text{s}}} \right] \left(\frac{1}{60} \right) = 3.04 \text{ min}$ **Equation 3-17, Attachment III.8.A pg. 3-30**;
overland flow)
6. Longest travel distance (L_2) = 1775' (channel flow)
7. Average slope (S) = 0.041 ft/ft (channel flow)
8. $T_{C2} = 0.0078 \times (L)^{0.77} \times (S)^{-0.385} = 0.0078 \times (1775)^{0.77} \times (0.041)^{-0.385} =$
8.46 min (**Equation 3-18, Attachment III.8.A pg. 3-34**; channel flow)
9. $T_c = T_{C1} + T_{C2} = 3.04 \text{ min} + 8.46 \text{ min} = 11.50 \text{ min} = 0.19 \text{ hrs}$
10. Curve Number = 80 (**Table 3-1, Attachment III.8.A pg. 3-23**) for Desert shrub, Soil Group B (consisting of silty sand, the predominate soils on-site).
11. Unit peak discharge (**Equation 3-22, Attachment III.8.A pg. 3-50**)

$$q_u = 0.543(T_c^{-0.812})10^{\frac{(|\log(T_c)+0.3|-\log(T_c)-0.3)^{1.5}}{10}} = 1.742 \text{ cfs/ac-in} \approx 1.74 \text{ cfs/ac-in.}$$
12. Average Run-off Depth (**Equation 3-23, Attachment III.8.A pg. 3-50**).

$$Q_d = \frac{[P_{24} - \frac{(200/CN)+2}{24}]^2}{P_{24} + \frac{(800/CN)-8}{24}} = \frac{[2.1 - \frac{(200/80)+2}{24}]^2}{2.1 + \frac{(800/80)-8}{24}} = 0.62439 \text{ inches} \approx 0.624 \text{ inches}$$
13. Design Frequency Peak Flow (**Equation 3-24, Attachment III.8.A pg. 3-50**);

$$Q_P = A \times Q_d \times q_u = 49.29 \text{ acres} \times 0.624 \text{ in} \times 1.74 \frac{\text{cfs}}{\text{ac-in}} = 53.6 \text{ cfs}$$
14. Stormwater volume (**Equation 3-25, Attachment III.8.A pg. 3-50**)

$$Q_v = \frac{A \times Q_d}{12} = \frac{49.3 \text{ ac} \times 0.624 \text{ in}}{12} = 2.57 \text{ ac-ft}$$

TABLE III.8.6
Watershed “B1” Calculations
Sandoval County Landfill

Watershed B1: Discharge point at northeast side of Stormwater Basin B (25-year, 24-hour storm event; estimated at 2.1 inches, **Attachment III.8.B**).

1. Area (A)= 4.35 acres
2. Longest travel distance (L_1) = 76' (overland flow)
3. Average slope = 10.5 % (overland flow)
4. Velocity (V_1) = 4 ft/s (*Figure 3-10, Attachment III.8.A pg. 3-33*; overland flow)
5. $T_{C1} = \left[\frac{L}{V} \right] \left(\frac{1}{60} \right) = \left[\frac{76 \text{ ft}}{4 \frac{\text{ft}}{\text{s}}} \right] \left(\frac{1}{60} \right) = 0.32 \text{ min}$ **Equation 3-17, Attachment III.8.A pg. 3-30**;
overland flow)
6. Longest travel distance (L_2) = 1035' (channel flow)
7. Average slope (S) = 0.016 ft/ft (channel flow)
8. $T_{C2} = 0.0078 \times (L)^{0.77} \times (S)^{-0.385} = 0.0078 \times (1035)^{0.77} \times (0.016)^{-0.385} =$
 7.95 min (**Equation 3-18, Attachment III.8.A pg. 3-34**; channel flow)
9. $T_c = T_{C1} + T_{C2} = 0.32 \text{ min} + 7.95 \text{ min} = 8.27 \text{ min} = 0.14 \text{ hrs}$
10. Curve Number = 80 (**Table 3-1, Attachment III.8.A pg. 3-23**) for Desert shrub, Soil Group B (consisting of silty sand, the predominate soils on-site).
11. Unit peak discharge (**Equation 3-22, Attachment III.8.A pg. 3-50**)

$$q_u = 0.543(T_c^{-0.812})10^{\frac{(|\log(T_c)+0.3|-\log(T_c)-0.3)^{1.5}}{10}} = 2.06 \text{ cfs/ac-in.}$$
12. Average Run-off Depth (**Equation 3-23, Attachment III.8.A pg. 3-50**).

$$Q_d = \frac{[P_{24} - \frac{(200}{CN}) + 2]^2}{P_{24} + \frac{(800}{CN}) - 8} = \frac{[2.1 - \frac{(200}{80}) + 2]^2}{2.1 + \frac{(800}{80}) - 8} = 0.62439 \text{ inches} \approx 0.624 \text{ inches}$$
13. Design Frequency Peak Flow (**Equation 3-24, Attachment III.8.A pg. 3-50**);

$$Q_P = A \times Q_d \times q_u = 4.35 \text{ ac} \times .624 \text{ in} \times 2.06 \frac{\text{cfs}}{\text{ac} - \text{in}} = 5.8 \text{ cfs}$$
14. Stormwater volume (**Equation 3-25, Attachment III.8.A pg. 3-50**)

$$Q_v = \frac{A \times Q_d}{12} = \frac{4.35 \text{ ac} \times .624 \text{ in}}{12} = 0.24 \text{ ac} - \text{ft}$$

TABLE III.8.7
Watershed “C” Calculations
Sandoval County Landfill

Watershed C: Discharge point at northwest side of Stormwater Basin #C (25-year, 24-hour storm event; estimated at 2.1 inches, **Attachment III.8.B**).

1. Area (A)= 50.48 acres
2. Longest travel distance (L_1) = 1300' (overland flow)
3. Average slope = 0.7 % (overland flow)
4. Velocity (V_1) = 0.82 ft/s (*Figure 3-10, Attachment III.8.A pg. 3-33*; overland flow)
5. $T_{C1} = \left[\frac{L}{V} \right] \left(\frac{1}{60} \right) = \left[\frac{1300 \text{ ft}}{0.82 \frac{\text{ft}}{\text{s}}} \right] \left(\frac{1}{60} \right) = 26.42 \text{ min}$ **Equation 3-17, Attachment III.8.A pg. 3-30**; overland flow)
6. Longest travel distance (L_2) = 1542' (channel flow)
7. Average slope (S) = 0.028 ft/ft (channel flow)
8. $T_{C2} = 0.0078 \times (L)^{0.77} \times (S)^{-0.385} = 0.0078 \times (1542)^{0.77} \times (0.028)^{-0.385} = 8.82 \text{ min}$ (**Equation 3-18, Attachment III.8.A pg. 3-34**; channel flow)
9. $T_c = T_{C1} + T_{C2} = 27.42 \text{ min} + 8.82 \text{ min} = 35.24 \text{ min} = 0.59 \text{ hrs}$
10. Curve Number = 80 (**Table 3-1, Attachment III.8.A pg. 3-23**) for Desert shrub, Soil Group B (consisting of silty sand, the predominate soils on-site).
11. Unit peak discharge (**Equation 3-22, Attachment III.8.A pg. 3-50**)

$$q_u = 0.543(T_c^{-0.812})10^{\frac{(|\log(T_c)+0.3|-\log(T_c)-0.3)^{1.5}}{10}} = 0.84 \text{ cfs/ac-in.}$$
12. Average Run-off Depth (**Equation 3-23, Attachment III.8.A pg. 3-50**).

$$Q_d = \frac{[P_{24} - (200/CN) + 2]^2}{P_{24} + (800/CN) - 8} = \frac{[2.1 - (200/80) + 2]^2}{2.1 + (800/80) - 8} = 0.62439 \text{ inches} \approx 0.624 \text{ inches}$$
13. Design Frequency Peak Flow (**Equation 3-24, Attachment III.8.A pg. 3-50**);

$$Q_P = A \times Q_d \times q_u = 50.48 \text{ ac} \times .624 \text{ in} \times 0.84 \frac{\text{cfs}}{\text{ac} - \text{in}} = 26.5 \text{ cfs}$$
14. Stormwater volume (**Equation 3-25, Attachment III.8.A pg. 3-50**)

$$Q_v = \frac{A \times Q_d}{12} = \frac{71.91 \text{ ac} \times .624 \text{ in}}{12} = 2.62 \text{ ac} - \text{ft}$$

Watershed C, Off-Site Run-On

1. Area (A)= 23 acres
2. Storm water volume (**Equation 3-25, Attachment III.8.A pg. 3-50**)

$$Q_v = \frac{A \times Q_d}{12} = \frac{23 \text{ ac} \times .624 \text{ in}}{12} = 1.20 \text{ ac} - \text{ft}$$

TABLE III.8.8
Runoff Summary
Sandoval County Landfill

RUNOFF DRAINAGE AREAS			
WATERSHED	DRAINAGE AREA (ACRES)	PEAK DISCHARGE (CFS)	VOLUME (ACRE-FT)
A	71.91	49.5	3.74
A1	7.05	8.48	0.37
A1	9.07	10.19	0.47
B	49.29	52.73	2.79
B1	4.35	5.61	0.23
C	49.91	26.07	2.60
C, Run-On	23	20	1.20
Total	214.58	167	11.17

5.0 STORMWATER BASIN DESIGN

The stormwater retention basins are designed to store the design volume of runoff flow. To determine the volume required of the basin, the Simplified Peak Flow Method was used as identified in the NMSHTD Drainage Manual. The Simplified Peak Flow Method calculates volume in acre-ft, as summarized in **Table III.8.8**.

TABLE III.8.9
Stormwater Basin Design Summary
Sandoval County Landfill

STORMWATER DETENTION/ RETENTION BASIN	CONTRIBUTING DRAINAGE AREAS	RUNOFF VOLUME (ACRE-FT)	BASIN CAPACITY WITHOUT USING 1FT. FREEBOARD (ACRE-FT)	BASIN MAX. CAPACITY USING 1FT. FREEBOARD (ACRE-FT)	FACTOR OF SAFETY WITHOUT USING FREEBOARD
A	A+A1+A2	4.58	5.12	6.83	1.12
B	B+B1	2.82	3.00	3.75	1.06
C	C+C,Run-on	3.82	5.49	6.87	1.44

Based on the available volume in Stormwater Basin A compared to incoming flow, storage in Stormwater Basin A peaks at 5,356 ft AMSL. At one foot below this elevation, there is 5.12 acre-ft of available storage volume, and the total inflow from the 25-year, 24-hour storm event is 4.58 acre-ft. Therefore, even without the additional volume of the 1' freeboard, there is sufficient storage in Stormwater Basin A to handle the runoff from a 25-year, 24-hour storm event with a factor of safety of 1.12.

Based on the available volume in Stormwater Basin B compared to incoming flow, storage in Stormwater Basin B peaks at 5,305 ft AMSL. At one foot below this elevation, there is 3.00 acre-ft of available storage volume, and the total inflow from the 25-year, 24-hour storm event is 2.79 acre-ft. Therefore, even without the additional volume of the 1' freeboard, there is sufficient storage in Stormwater Basin B to handle the runoff from a 25-year, 24-hour storm event with a factor of safety of 1.08. Only in an extreme situation will there be any flow out of the overflow structure.

Based on the available volume in Stormwater Basin C compared to incoming flow, storage in Stormwater Basin C peaks at 5,333 ft AMSL. At one foot below this elevation, there is 5.49 acre-ft of available storage volume, and the total inflow from the 25-year, 24-hour storm event is 3.79 acre-ft. Therefore, even without the additional volume of the 1' freeboard, there is sufficient storage in Stormwater Basin C to handle the run-on and runoff from a 25-year, 24-hour storm event with a factor of safety of 1.45. Only in an extreme situation will there be any flow out of the overflow structure.

The Factor of Safety for each retention basin does not include freeboard designed into each basin. Considerable additional volume is available when the freeboard is considered (**Table III.8.9**).

6.0 CHANNEL DESIGN AND CAPACITY

The design frequency peak flow (Q_p) from the Simplified Peak Flow Method was used to size the landfill perimeter drainage channels. Drainage channels are sized to convey the volume of runoff based on Federal Highway Administration (FHWA) Hydraulic Toolbox 2.1 software. Hydraulic Toolbox computes the velocity and depth based on the input values of flow rate, slope, and channel dimensions. Channel design parameters are summarized in **Table III.8.10**, which demonstrates that each of the channels has more than adequate carrying capacity with a minimum freeboard of >1.0 ft (see **Permit Plans**).

TABLE III.8.10
Channel Design Summary
Sandoval County Landfill

CHANNEL	Q ₂₅ (CFS)	SLOPE (%)	WIDTH	DEPTH	VELOCITY (FT/S)	WATER DEPTH (FT)	FREEBOARD (FT)
A	49.40	3.5	3	2	10.82	0.938	1.06
A1	8.40	9.0	3	2	8.79	0.272	1.73
A2	10.20	4.4	4	2	3.77	0.320	1.68
A3	18.60	7.0	3	2	4.50	0.450	1.55
B	59.70	4.1	4	2	5.77	0.879	1.12
B1	5.80	1.6	0	2	3.74	0.760	1.24
C	46.70	2.4	4	2	4.77	0.681	1.32

Notes:

1. Q₂₅ represents 25-year, 24-hour storm event flow.
2. Refer to Figure III.8.2 for channel locations.
3. Channel B1 is a V-shaped channel, hence the 0-width

7.0 LOW WATER CROSSING DESIGN AND CAPACITY

The design frequency peak flow (Q_p) from the Simplified Peak Flow Method was used to size the Low Water Crossing. The Low Water Crossing is sized to convey the volume of runoff across roads, and sizing is based on Federal Highway Administration (FHWA) Hydraulic Toolbox 2.1 software computes the velocity, depth based on the input values of flowrate, slope, and low water crossing dimensions. The Low Water Crossing design parameters are summarized in **Table III.8.11**, which demonstrates that the channel has more than adequate carrying capacity with freeboard remaining.

TABLE III.8.11
Low Water Crossing Design Summary
Sandoval County Landfill

LOW WATER CROSSING	Q ₂₅ (CFS)	SLOPE (%)	VELOCITY (FT/S)	WATER DEPTH (FT)	FREEBOARD (FT)
#1	26.1	2.0	3.026	0.271	0.729

Notes:

1. Q₂₅ represents 25-year, 24-hour storm event flow.

**APPLICATION FOR PERMIT RENEWAL AND MODIFICATION
SANDOVAL COUNTY LANDFILL**

**VOLUME III: LANDFILL ENGINEERING CALCULATIONS
SECTION 8: DRAINAGE CALCULATIONS**

ATTACHMENT III.8.A

**PHILIPS, CHRISTOPER S.; EASTERLING, CHARLES M.;
HEGGEN, RICHARD J.; AND SCHALL, JAMES D. 1995.**

DRAINAGE MANUAL, VOLUME I: HYDROLOGY.

NEW MEXICO STATE HIGHWAY AND TRANSPORTATION DEPARTMENT.

DRAINAGE MANUAL
VOLUME 1, HYDROLOGY
DECEMBER, 1995

*NEW MEXICO STATE HIGHWAY
AND TRANSPORTATION DEPARTMENT
PRELIMINARY DESIGN BUREAU/DRAINAGE SECTION
P. O. BOX 1149
SANTA FE, NEW MEXICO 87504-1149*

FOREWORD

The New Mexico State Highway and Transportation Department Drainage Section is pleased to present a comprehensive update to its Drainage Manual. Volume 1 focuses on Hydrology and the prediction of flood flows at highway crossings. A companion document is presently under development which will address drainage structure hydraulics as well as sediment and erosion at highway structures. Together these documents will summarize and standardize methods by which drainage structures are designed for NMSHTD Projects. Comments regarding the content of this document are welcomed, and should be addressed to: Section Head, Drainage Section, NMSHTD, P.O. Box 1149, Santa Fe, NM 87504-1149.



Pete K. Rahn, Secretary
New Mexico State Highway and Transportation Department

7-18-96

Date

***NEW MEXICO STATE HIGHWAY AND
TRANSPORTATION DEPARTMENT***

DRAINAGE MANUAL

VOLUME 1, HYDROLOGY

PREPARED BY:

***CHRISTOPHER S. PHILIPS, P.E.
CHARLES M. EASTERLING, P.E.
EASTERLING & ASSOCIATES, INC.
10131 COORS ROAD, N.W.
SUITE H-7
ALBUQUERQUE, NM 87114-4048***

IN COOPERATION WITH

***RICHARD J. HEGGEN, P.E., P.H., PH.D.
UNIVERSITY OF NEW MEXICO
DEPARTMENT OF CIVIL ENGINEERING
ALBUQUERQUE, NM 87131***

AND

***JAMES D. SCHALL, P.E., PH.D.
OWEN AYRES & ASSOCIATES, INC.
3665 JOHN F. KENNEDY PARKWAY
BUILDING II, SUITE 300
FORT COLLINS, CO 80525***

DECEMBER 1995

NMSHTD DRAINAGE MANUAL

VOLUME 1, HYDROLOGY

TABLE OF CONTENTS

	PAGE NUMBER
1 INTRODUCTION	1-1
1.1 DRAINAGE MANUAL PURPOSE AND USE	1-1
1.2 DRAINAGE DESIGN CRITERIA GUIDELINES	1-1
1.3 USE OF METRIC STANDARDS IN THE DESIGN OF NMSHTD PROJECTS	1-2
2 BASIC REQUIREMENTS FOR DRAINAGE STUDIES	2-1
2.1 DRAINAGE FIELD INSPECTION	2-1
2.2 PRELIMINARY DRAINAGE REPORT	2-5
2.3 FINAL DRAINAGE REPORT	2-5
2.4 TEMPORARY EROSION AND SEDIMENT CONTROL PLAN	2-5
3 HYDROLOGY	3-1
3.1 NMSHTD APPROACH TO HYDROLOGIC ANALYSIS	3-1
3.2 SELECTION OF A HYDROLOGIC METHOD	3-1
3.3 DRAINAGE BASINS WITHOUT GAGE DATA	3-4
3.3.1 GENERAL DATA FOR HYDROLOGIC ANALYSIS	3-4
3.3.1.1 DRAINAGE BASIN DELINEATION	3-5
3.3.1.2 RAINFALL	3-7
3.3.1.2.1 RAINFALL IN THE RATIONAL FORMULA	3-7
3.3.1.2.2 RAINFALL IN THE SIMPLIFIED PEAK FLOW METHOD	3-16
3.3.1.2.3 RAINFALL IN THE SCS UNIT HYDROGRAPH METHOD	3-16
3.3.1.3 RAINFALL LOSSES AND RUNOFF CURVE NUMBERS	3-19
3.3.1.3.1 CURVE NUMBER SELECTION	3-19
3.3.1.3.2 CURVE NUMBER WEIGHTING	3-29
3.3.1.4 TIME OF CONCENTRATION	3-30
3.3.1.4.1 THE UPLAND METHOD	3-32
3.3.1.4.2 TIME OF CONCENTRATION BY THE KIRPICH FORMULA	3-34
3.3.1.4.3 THE STREAM HYDRAULIC METHOD	3-34

TABLE OF CONTENTS (CONTINUED)

	PAGE NUMBER
3.3.2 <i>RATIONAL FORMULA METHOD</i>	3-36
3.3.2.1 <i>APPLICATION OF THE RATIONAL FORMULA</i>	3-37
3.3.2.1.1 <i>RATIONAL FORMULA METHOD EXAMPLE PROBLEMS</i>	3-44
3.3.3 <i>SIMPLIFIED PEAK FLOW METHOD</i>	3-49
3.3.3.1 <i>APPLICATION</i>	3-49
3.3.3.2 <i>SIMPLIFIED PEAK FLOW METHOD EXAMPLE PROBLEMS</i> ..	3-55
3.3.4 <i>USGS REGRESSION EQUATIONS FOR NEW MEXICO</i>	3-62
3.3.4.1 <i>RURAL PEAK DISCHARGE METHOD</i>	3-64
3.3.4.2 <i>URBAN USE OF USGS REGRESSION EQUATIONS</i>	3-72
3.3.4.3 <i>BASIN DEVELOPMENT FACTOR</i>	3-72
3.3.4.4 <i>THREE PARAMETER ESTIMATING EQUATIONS</i>	3-74
3.3.4.4.1 <i>USGS REGRESSION EQUATION EXAMPLE PROBLEMS</i>	3-76
3.3.5 <i>SCS UNIT HYDROGRAPH METHOD</i>	3-79
3.3.5.1 <i>UNIT HYDROGRAPH PREPARATION</i>	3-79
3.3.5.2 <i>APPLICATION OF THE SCS UNIT HYDROGRAPH METHOD</i> ..	3-85
3.4 <i>WATERSHEDS WITH STREAM GAGE DATA</i>	3-86
3.5 <i>RISK AND UNCERTAINTY IN HYDROLOGIC ANALYSIS</i>	3-87

TABLE OF CONTENTS (CONTINUED)

PAGE NUMBER

FIGURES

Figure 1-1	NMSHTD Facilities Map	1-3
Figure 2-1	Drainage Structure Field Inspection Form	2-4
Figure 3-1	Methodology Selection Flow Chart, Rural Conditions	3-2
Figure 3-2	Methodology Selection Flow Chart, Urban Conditions	3-3
Figure 3-3	Effect of Drainage Basin Shape on Hydrograph Shape	3-6
Figure 3-4	DDF/IDF Worksheet	3-14
Figure 3-5	Precipitation Intensity Duration Frequency (IDF) Graph	3-15
Figure 3-6	The Modified NOAA-SCS Rainfall Distribution Worksheet	3-18
Figure 3-7	Estimating Ground Cover Density	3-21
Figure 3-8	Hydrologic Soil – Cover Complexes and Associated Curve Numbers . . .	3-22
Figure 3-9	Composite CN for Urban Areas with Connected and Unconnected Impervious Areas	3-28
Figure 3-10	Flow Velocities for Overland and Shallow Concentrated Flows	3-33
Figure 3-11	Rational “C” Coefficient Upland Rangeland (Grass & Brush)	3-38
Figure 3-12	Rational “C” Coefficient Desert (Cactus, Grass & Brush)	3-39
Figure 3-13	Rational “C” Coefficient Mountain (Juniper & Grass)	3-40
Figure 3-14	Rational “C” Coefficient Mountain (Grass & Brush)	3-41
Figure 3-15	Rational “C” Coefficient Mountain (Ponderosa Pine)	3-42
Figure 3-16	Rational “C” Coefficient Developed Watersheds	3-43
Figure 3-17	Estimating Direct Runoff	3-51
Figure 3-18	Unit Peak Discharge for the Simplified Peak Flow Method	3-52
Figure 3-19	Simplified Peak Flow Worksheet	3-54
Figure 3-20	USGS Physiographic Regions	3-63
Figure 3-21	Dividing Urban Drainage Basins Into Thirds	3-73
Figure 3-22	Dimensionless Unit Hydrograph and Mass Curve for SCS Synthetic Hydrograph	3-82
Figure 3-23	Dimensionless Curvilinear Unit Hydrograph and Equivalent Triangular Hydrograph	3-83
Figure 3-24	Regression Line and Average Standard Error of Prediction Range	3-91

TABLE OF CONTENTS (CONTINUED)

PAGE NUMBER

TABLES

Table 3-1	— Runoff Curve Numbers for Arid and Semiarid Rangelands	3-23
Table 3-2	— Runoff Curve Numbers for Cultivated Agricultural Lands	3-24
Table 3-3	— Runoff Curve Numbers for Other Agricultural Lands	3-25
Table 3-4	— Runoff Curve Numbers Urban Areas	3-26
Table 3-5	— Conversion from Average Antecedent Moisture Conditions to Dry and Wet Conditions	3-27
Table 3-6	— Time of Concentration Method Selection Chart	3-31
Table 3-7	— USGS Rural Flood Frequency Equations for New Mexico	3-65
Table 3-8	— USGS Small Rural Basin Flood Frequency Equations for New Mexico . .	3-71
Table 3-9	— USGS Urban Peak Discharge Three Parameter Estimating Equations . . .	3-75
Table 3-10	— Ratios for Dimensionless Unit Hydrograph and Mass Curve, SCS Synthetic Hydrograph	3-84
Table 3-11	— Tabulation of Risk of at Least One Exceedance During the Design Life .	3-92

APPENDICES

APPENDIX A	— Photographic Guide to Hydrologic Conditions	A-1
APPENDIX B	— Glossary of Terms	B-1
APPENDIX C	— Metric Equations and Conversion Factors	C-1
APPENDIX D	— Text References and Other Selected References	D-1
APPENDIX E	— NOAA Isopluvial Maps for New Mexico	E-1

Table 3-1 — Runoff Curve Numbers for Arid and Semiarid Rangelands¹

Source: USDA SCS, TR-55, 1986

Cover Description		Curve Numbers for Hydrologic Soil Group --			
Cover Type	Hydrologic Condition ²	A ³	B	C	D
Herbaceous—mixture of grass, weeds, and low growing brush, with brush the minor element.	Poor		80	87	93
	Fair		71	81	89
	Good		62	74	85
Oak—aspens—mountain brush mixture of oak brush, aspens, mountain mahogany, bitter brush, maple, and other brush.	Poor				
	Fair		66	74	79
	Good		48	57	63
Piñon, juniper, or both; grass understory.	Poor		75	85	89
	Fair		58	73	80
	Good		41	61	71
Sagebrush with grass understory.	Poor		67	80	85
	Fair		51	63	70
	Good		35	47	55
Desert shrub—major plants include saltbush, greasewood, creosotebush, blackbrush, bursage, palo verde, mesquite, and cactus.	Poor	63	77	85	88
	Fair	55	72	81	86
	Good	49	68	79	84

¹ Average runoff condition.

² Poor: <30% ground cover (litter, grass, and brush overstory).
Fair: 30 to 70% ground cover.
Good: >70% ground cover.

³ Curve numbers for group A have been developed only for desert shrub.

3.3.1.4 TIME OF CONCENTRATION

Time of Concentration is defined as the time required for runoff to travel from the hydraulically most distant part of the watershed to the point of interest. Time of concentration is one of the most important drainage basin characteristics needed to calculate the peak rate of runoff. An accurate estimate of a watershed's time of concentration is crucial to every type of hydrologic modeling.

The method used to calculate time of concentration must be consistent with the method of hydrologic analysis selected for design. Designers working on NMSHTD projects must use the time of concentration methods specified in this section for each hydrologic method. Mixing of methods is not allowed on NMSHTD projects. **Table 3-6** defines the correct time of concentration method to be used for each hydrologic method.

Within each watershed the designer must locate the primary watercourse. This is the watercourse that extends from the bottom of the watershed or drainage structure to the most hydraulically remote point in the watershed. Most designers begin at the bottom of the watershed and work their way upstream until the longest watercourse has been found. At the top of the watershed a defined watercourse may not exist. In these areas overland flow will be the dominant flow type. As the runoff proceeds downstream, overland flows will naturally begin to coalesce, gradually concentrating together. Shallow concentrated flow often has enough force to shape small gullies in erosive soils. Gullies eventually gather together until a defined stream channel is formed. The water course is now large enough to be identified on a quadrangle topographic map.

Sections along the primary watercourse should be identified which are hydraulically similar. Time of concentration is estimated for each section of the watercourse. Time of concentration in any given watershed is simply the sum of flow travel times within hydraulically similar reaches along the longest watercourse. Time of concentration is determined from measured reach lengths and estimated average reach velocities. The basic equation for time of concentration is:

$$T_c = \left(\frac{L_1}{V_1} + \frac{L_2}{V_2} + \frac{L_3}{V_3} + \dots + \frac{L_n}{V_n} \right) \frac{1}{60} \quad (3-17)$$

where

- T_c = Time of concentration, minutes
- V_1 = Average flow velocity in the uppermost reach of the watercourse, ft./sec.
- L_1 = Length of the uppermost reach of the watercourse, ft.
- V_2, V_3, \dots = Average flow velocities in subsequent reaches progressing downstream, ft./sec.
- L_2, L_3, \dots = Lengths of subsequent reaches progressing downstream, ft.

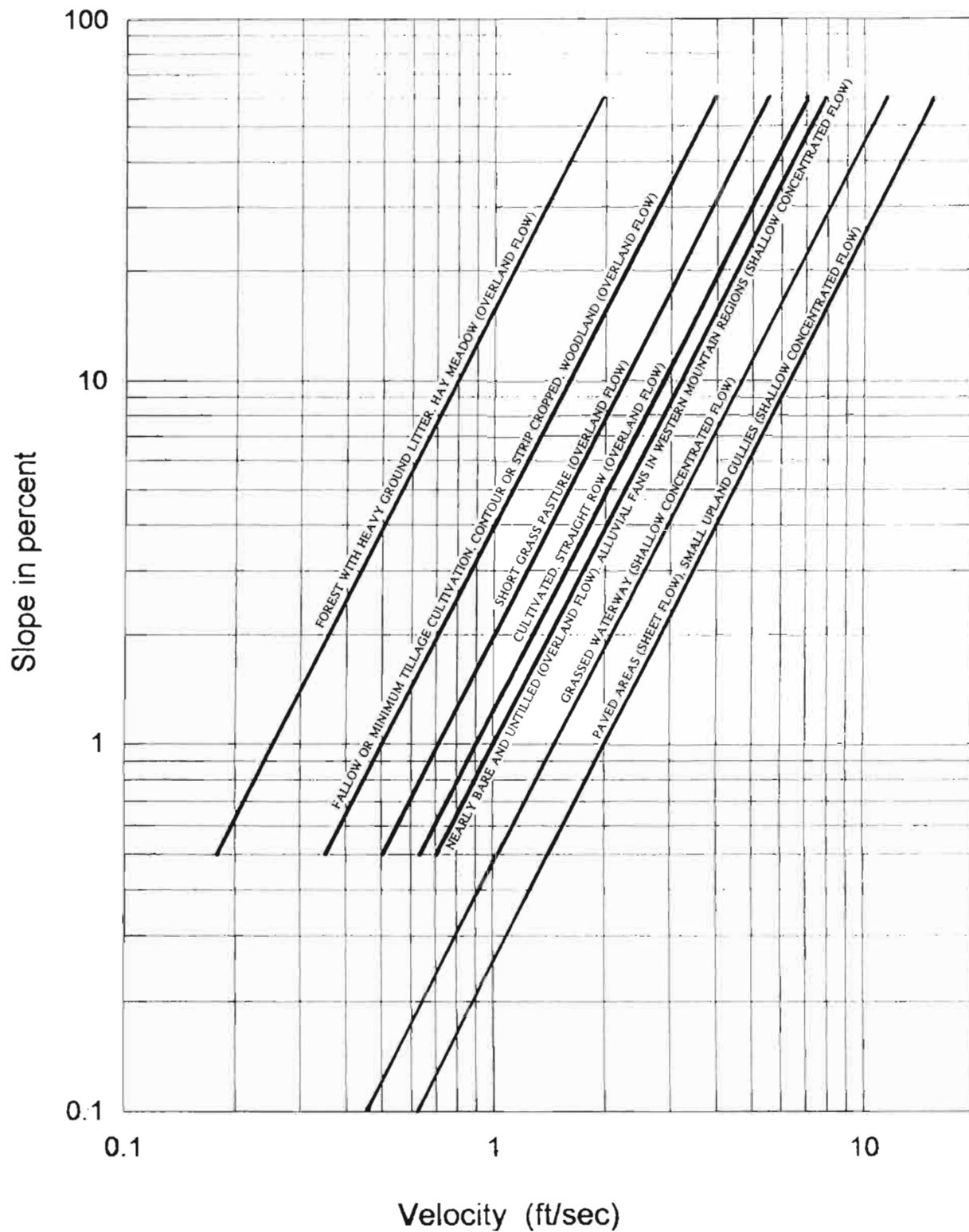
Hydrologic Method	Watershed Condition	Time of Concentration Method
Rational Method	Un-gullied Watershed*	Upland Method
	Gullied Watershed*	Kirpich Formula
Simplified Peak Flow Method	Un-gullied Watershed*	Upland Method
	Gullied Watershed*	Kirpich Formula
	Watershed Partially Gullied	Upland Method for the Un-gullied Portion, then Kirpich Formula for the Gullied Portion**
USGS Regression Equations	—	NOT REQUIRED
Unit Hydrograph Method	No Defined Stream Channel	Upland Method
	Defined Stream Channel	Stream Hydraulic Method
Approved Urban Method	All Conditions	Use T_c Method Specified for the Approved Urban Method***

*A watershed is considered un-gullied if 10% or less of the primary watercourse exhibits gullying.

**Mixing T_c Methods in a watershed is only allowed with the Simplified Peak Flow Method.

***When using AHYMO with the COMPUTE NM HYD routine, compute the time of concentration in accordance with the City of Albuquerque Design Process Manual. See **SECTIONS 3.2 AND 3.3.5** of this manual for limitations on the use of AHYMO.

Table 3-6
Time of Concentration Method Selection Chart



Note: For watercourses with slopes less than 0.5 percent, use the overland flow velocity given for 0.5 percent, except for shallow concentrated flow where a flatter slope may be considered.

Figure 3-10
Flow Velocities for
Overland and Shallow
Concentrated Flows

Modified from SCS, NEH-4, 1972

3.3.1.4.2 TIME OF CONCENTRATION BY THE KIRPICH FORMULA

This method is used to calculate time of concentration in gullied watersheds when using the Rational Method or the Simplified Peak Flow Method. The Kirpich Formula should be used when gullying is evident in more than 10% of the primary watercourse. Gullying can be assumed if a blue line appears on the watercourse shown on the USGS quadrangle topographic map. The Kirpich Formula is given as:

$$T_c = 0.0078 L^{0.77} S^{-0.385} \quad (3-18)$$

where

T_c = time of concentration, in minutes

L = length from drainage to outlet along the primary drainage path, in feet

S = average slope of the primary drainage path, in ft./ft.

The Kirpich Formula should generally be used for the entire drainage basin. The exception to this rule occurs when the Simplified Peak Flow Method is being used on NMSHTD projects and the watercourse has a mixture of gullied and un-gullied sections. In these situations, mixing of time of concentration methods is allowed. The Upland Method is used for the ungullied portion of the primary watercourse, and the Kirpich Formula is used for the gullied portion of the watercourse. The two times of concentration are added together to obtain the total time of concentration of the watershed. Typically the Kirpich Formula is only used for that portion of the watercourse shown in blue on the quadrangle topo map. **Mixing of time of concentration methods is only allowed with the Simplified Peak Flow Method for NMSHTD projects.**

3.3.1.4.3 THE STREAM HYDRAULIC METHOD

The stream hydraulic method is used when calculating peak flows by the Unit Hydrograph Method in a watercourse where a defined stream channel is evident (blue line, solid or broken, on a quadrangle topo map). The designer must measure or estimate the hydraulic properties of the stream channel, and must divide the total watercourse into channel reaches which are hydraulically similar. Field reconnaissance measurements of the stream channel are best, however sometimes direct measurements are not possible. The designer must determine the slope, channel cross section and an appropriate hydraulic roughness coefficient for each channel reach. Average slope is often determined from the topographic mapping of the watershed. Channel cross section should be measured in the field whenever possible. Roughness coefficients of the waterway should be based on actual observations of the watercourse or of nearby watercourses which are believed to be similar and which are more accessible.

Time of Concentration by the stream hydraulic method is simply the travel time in the stream channel. Channel flow velocities can be estimated from normal depth calculations for the watercourse. In addition to the average flow velocity, designers should compute the Froude Number of the flow. If the Froude number of the flow exceeds a value of 1.3, then the designer should verify that supercritical flow conditions can actually be sustained. For most earth lined channels the velocity calculation should be recomputed using a larger effective

Step 2 Determine the unit peak discharge, q_u , for the watershed. The unit peak discharge can be read from **Figure 3-18**, given the time of concentration, or calculated directly by the following equation:

$$q_u = 0.543 T_c^{-0.812} 10^{-\frac{[|\log(T_c) + 0.3| - \log(T_c) - 0.3]^{1.5}}{10}} \quad (3-22)$$

where

q_u = unit peak discharge from the watershed, in cfs/ac-in

T_c = time of concentration, in hours

Note: for $T_c > 0.5$ hours, the last term of the equation, $10^{-\frac{[|\log(T_c) + 0.3| - \log(T_c) - 0.3]^{1.5}}{10}}$, is equal to 1.0

Step 3

Calculate the direct runoff from the watershed. The direct runoff is expressed as an average depth of water over the entire watershed, in inches. The direct runoff may be read from **Figure 3-17** using the 24-hour rainfall depth P_{24} in inches, and the runoff curve number, CN. The runoff depth may also be calculated from the following equation:

$$Q_d = \frac{[P_{24} - (200/CN) + 2]^2}{P_{24} + (800/CN) - 8} \quad (3-23)$$

where

Q_d = average runoff depth for the entire watershed, in inches

Step 4

Compute the peak discharge from the watershed by the following equation:

$$Q_p = A \cdot Q_d \cdot q_u \quad (3-24)$$

where

Q_p = peak discharge, in cfs

A = drainage area, in acres

Step 5

Compute the runoff volume, if required. The runoff volume is obtained by the equation:

$$Q_v = \frac{Q_d \cdot A}{12} \quad (3-25)$$

where

Q_v = runoff volume from the watershed, in ac-ft

**APPLICATION FOR PERMIT RENEWAL AND MODIFICATION
SANDOVAL COUNTY LANDFILL**

**VOLUME III: LANDFILL ENGINEERING CALCULATIONS
SECTION 8: DRAINAGE CALCULATIONS**

ATTACHMENT III.8.B

**U.S. DEPT. OF COMMERCE NATIONAL OCEANIC AND ATMOSPHERIC
ADMINISTRATION NATIONAL WEATHER SERVICE OFFICE OF HYDROLOGIC
DEVELOPMENT HYDROMETEOROLOGICAL DESIGN STUDIES CENTER, JUNE
2006, NOAA ATLAS 14, VOLUME 1, VERSION 4 SEMIARID SOUTHWESTERN
UNITED STATES, NEW MEXICO, ISOPLUVIALS OF 24 HOUR PRECIPITATION
(INCHES) WITH AVERAGE RECURRENCE INTERVAL OF 25 YEARS.**

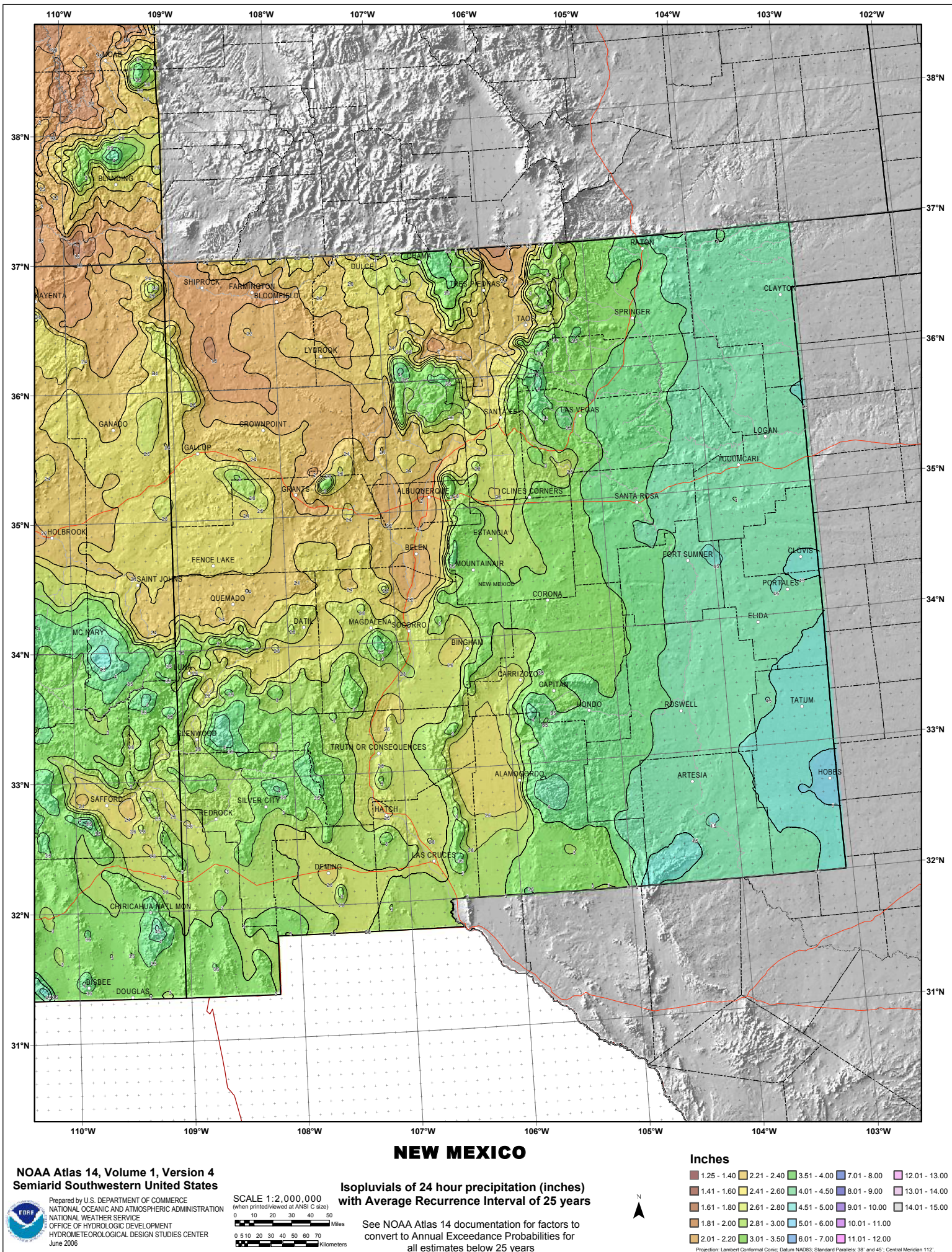


Figure E-8

**APPLICATION FOR PERMIT RENEWAL AND MODIFICATION
SANDOVAL COUNTY LANDFILL**

**VOLUME III: LANDFILL ENGINEERING CALCULATIONS
SECTION 9: GEOTEXTILE FILTER FABRIC ANALYSIS**

TABLE OF CONTENTS

1.0	INTRODUCTION	III.9-1
2.0	DESIGN CRITERIA	III.9-1
3.0	REFERENCES	III.9-2
4.0	FACTOR OF SAFETY AGAINST PUNCTURE OF THE 10 OZ/YD ² NONWOVEN GEOTEXTILE	III.9-2
5.0	10 OZ/YD ² NONWOVEN GEOTEXTILE RETENTION, PERMEABILITY, PERMITTIVITY AND POROSITY	III.9-4
5.1	Protective Soil Layer Properties	III.9-4
5.2	AASHTO Requirements	III.9-5
5.3	Landfilldesign.com Geotextile Filter – Design Calculator Requirements	III.9-5
6.0	PROPOSED NONWOVEN GEOTEXTILE PROJECT SPECIFICATIONS	III.9-7

LIST OF TABLES

Table No.	Title	Page
III.9.1	LANDFILL STATIC LOAD PARAMETERS	III.9-3
III.9.2	RECOMMENDED GEOTEXTILE FILTER CRITERIA (AASHTO M288-96)	III.9-5
III.9.3	PROPOSED NONWOVEN GEOTEXTILE SPECIFICATIONS	III.9.7

**APPLICATION FOR PERMIT RENEWAL AND MODIFICATION
SANDOVAL COUNTY LANDFILL**

**VOLUME III: LANDFILL ENGINEERING CALCULATIONS
SECTION 9: GEOTEXTILE FILTER FABRIC ANALYSIS**

LIST OF ATTACHMENTS

Attachment No.	Title
III.9.A	KOERNER, ROBERT M. 2005. CHAPTER 2.5.4, “PUNCTURE RESISTANCE” IN <i>DESIGNING WITH GEOSYNTHETICS, FIFTH EDITION</i> , PAGES 171-173. NEW JERSEY: PEARSON PRENTICE HALL.
III.9.B	“GSE LINING TECHNOLOGY, INC.”, NONWOVEN GEOTEXTILE PRODUCT DATA SHEET 2007
III.9.C	SUMMARY OF GEOTECHNICAL LABORATORY TESTING RESULTS
III.9.D	ADVANCED GEOTECH SYSTEMS. GEOTEXTILE FILTER CALCULATOR.LANDFILLDESIGN.COM. HTTP://WWW.LANDFILL DESIGN.COM/DESIGN/CALCULATORS/GEOFIL.ASPX (2013).
III.9.E	KOERNER, ROBERT M. 2005. “POROSITY” IN CHAPTER 2.3.4, “HYDRAULIC PROPERTIES” IN <i>DESIGNING WITH GEOSYNTHETICS, FIFTH EDITION</i> , PAGE 128. NEW JERSEY: PEARSON PRENTICE HALL.

**APPLICATION FOR PERMIT RENEWAL AND MODIFICATION
SANDOVAL COUNTY LANDFILL**

**VOLUME III: LANDFILL ENGINEERING CALCULATIONS
SECTION 9: GEOTEXTILE FILTER FABRIC ANALYSIS**

1.0 INTRODUCTION

The Sandoval County Landfill (SCLF) is an existing solid waste facility operating in compliance with its current Permits, SWM-050304 and SWM-050304 (SP), and the New Mexico Environment Department (NMED) Solid Waste Rules (20.9.2-2.9.10 NMAC). SCLF is located at 2708 Iris Road NE in Rio Rancho, New Mexico (NM), and occupies 178.3 acres \pm . SCLF is publicly owned and operated by the County of Sandoval (“the County”), and is currently permitted to accept municipal solid waste (MSW), including construction and demolition debris (C&D) and tires, and two special wastes: petroleum contaminated soils (PCS) and sludge.

2.0 DESIGN CRITERIA

The liner system for the Southwest New Mexico Regional Landfill (SWRL) is designed to meet the requirements of the New Mexico Solid Waste Rules 20.9.4 NMAC. More specifically, 20.9.4.13.E.(1)(a) NMAC requires:

“all liners must be able to withstand the projected loading stresses and disturbances from overlying waste, waste cover materials, and equipment operation;”

The purpose of these calculations is to evaluate that:

- The proposed 10 oz/yd² nonwoven cushion geotextile provides adequate puncture resistance as to prevent damage the underlying 60-mil high-density polyethylene (HDPE) flexible membrane liner (FML) from the ¾ to 2-inch select aggregate in the leachate collection system.
- The proposed 10 ounces per square yard (oz/yd²) nonwoven geotextile meets certain retention, permeability, permittivity and porosity criteria based on the geotechnical characteristics of the proposed protective soil layer material to be used in the SWRL.

3.0 REFERENCES

The following references were used to determine the adequacy of a 10 oz/yd² nonwoven geotextile for use in the select aggregate leachate collection system and protective drainage layer system:

1. Koerner, Robert M. 2005. Chapter 2.5.4, "Puncture Resistance" In *Designing With Geosynthetics, Fifth Edition*, Pages 171-173. New Jersey: Pearson Prentice Hall.
2. Advanced Geotech Systems. Geotextile Filter Calculator. Landfilldesign.com. <http://www.landfilldesign.com/design/calculators/geofil.aspx> (2013).
3. Geotextile Criteria for Subsurface Drainage", AASHTO M288-96

4.0 FACTOR OF SAFETY AGAINST PUNCTURE OF THE 10 OZ/YD² NONWOVEN GEOTEXTILE

A 10 oz/yd² nonwoven geotextile is to be installed to provide a cushion between the ¾ to 2-inch select aggregate in the leachate collection system and the underlying 60-mil HDPE FML. The purpose of the nonwoven geotextile is to provide adequate puncture resistance so that the underlying HDPE FML is not damaged by the select aggregate; and to act as a filter to prevent soil fines from infiltrating into the system.

The load on the 10 oz/yd² nonwoven geotextile is based on the maximum depth of the landfill components. For the SCLF, this occurs at point in Cell 8B cross section C-C' as identified in the Pipe Loading Calculations (**Volume III.5**). In the same Section, it was shown that dynamic equipment loading was significantly less than the static load due to the landfill components. The static load is calculated using the thickness of each layer and assigned unit weights. This static load will be used to determine the puncture resistance of the 10 oz/yd² nonwoven geotextile to protect the underlying 60-mil HDPE FML. The required vertical puncturing force is summarized in **Table III.9.1**.

TABLE III.9.1
Landfill Static Load Parameters
Sandoval County Landfill

Layer	Thickness (feet)	Unit Weight (pcf)	Actual Load (psf)
Final Cover Soil	3.0	115	345.0
Intermediate Cover Soils	1.0	115	115.0
Waste	173.0	65	11,245.0
Protective Soil Layer	2.0	115	230.0
Select Aggregate above the 10 oz/yd ² nonwoven geotextile in the leachate collection trench	1.33	130	172.90
Design Load (P')		TOTAL:	12,107.9 psf (84.1 psi)

The vertical puncturing force of the 10 oz/yd² nonwoven geotextile to protect the underlying 60-mil HDPE FML is calculated using the following equation (**Attachment III.9.A, Pages 171, 172, and 173**):

$$F_{\text{required}} = (p')(d_a)^2(S_1)(S_2)(S_3)$$

Where:

- F_{required} = required vertical puncturing force to be resisted
- p' = pressure exerted on the 10 oz/yd² geotextile = 84.1 psi
- d_a = average diameter of puncturing aggregate = 1.375 inches
- S_1 = protrusion factor of puncturing aggregate = 0.7
- S_2 = scale factor to adjust the ASTM D4833 puncture test value that uses a 8.0 mm diameter puncture probe to the actual puncturing object= 0.6
- S_3 = shape factor to adjust the ASTM D4833 flat puncture probe to the actual shape of the puncturing object=0.6

Note: Values used for S_1 , S_2 and S_3 assumes the puncturing object is subrounded and relatively large.

$$F_{\text{required}} = (84.1 \text{ psi})(1.375 \text{ inches})^2(0.7)(0.6)(0.6)$$

$$F_{\text{required}} = 40.1 \text{ lbs}$$

Assuming a Factor of Safety of 2.0, $F_{\text{required}} = 2.0 (40.1 \text{ lbs}) = 80.2 \text{ lbs}$. The puncture strength for a 10 oz/yd² nonwoven geotextile is established at 165 lbs (**Attachment III.9.B**); providing a factor of safety of 2.1. Therefore, the 10 oz/yd² nonwoven geotextile will provide adequate puncture

resistance to a ¾ to 2-inch aggregate; and the underlying 60-mil HDPE FML will not be damaged by the select aggregate in the leachate collection system.

5.0 10 OZ/YD² NONWOVEN GEOTEXTILE RETENTION, PERMEABILITY, PERMITTIVITY AND POROSITY

One function of the 10 oz/yd² nonwoven geotextile filter within the leachate collection system is the retain soils fines while allowing leachate to flow freely. In order to achieve this objective, the 10 oz/yd² nonwoven geotextile filter must meet certain retention, permeability, permittivity, maximum AOS size, and porosity criteria. These criteria were evaluated using the “Geotextile Filter – Design Calculator” listed on the landfilldesign.com website; and the requirements of AASHTO M288-96 (**Attachment III.9.D**).

5.1 Protective Soil Layer Properties

Attachment III.9.C provides laboratory geotechnical data for SCLF protective soils. Based upon the geotechnical data, New Mexico Solid Waste Rules, and standard landfill practices; the SCLF is proposing a protective drainage layer (i.e., protective soil layer, PSL) that meets the following properties:

- $\leq 15\%$ passing the No. 200 sieve by weight
- Uniformity coefficient ≤ 7.5
- Hydraulic conductivity $\geq 5.0 \times 10^{-5}$ cm/sec

The on-site soils encountered within the excavation of Cells 4C, 6B and 7 consist primarily of silty sand that generally meet these criteria (i.e., SM) and any imported materials will be pre-qualified. As waste placement operations proceeds, SCLF will use the stockpiled soils as the protective drainage layer. Proposed PSL materials will be pre-qualified as described in the SCLF CQA Plan (**Volume II.4**).

For the purposes of the 10 oz/yd² nonwoven geotextile filter design, the soil samples tested for PSL in Cells 4C, 6B and 7 are used. The typical particle size distributions are provided in **Attachment III.9.C**.

5.2 AASHTO Requirements

The American Association of State Highway and Transportation Officials (AASHTO) recommends that the minimum hydraulic requirements shown in **Table III.9.2** be used for a nonwoven geotextile subsurface filter.

TABLE III.9.2
Recommended Geotextile Filter Criteria (AASHTO M288-96)
Sandoval County Landfill

Nonwoven Geotextile Filter Criteria	Percent of Soil Passing the No. 200 Sieve By Weight		
	<15%	15% to 50%	>50%
Minimum Permittivity (ASTM D4491)	0.5 sec ⁻¹	0.2 sec ⁻¹	0.1 sec ⁻¹
Maximum AOS (ASTM D4751)	0.43 mm	0.25 mm	0.22 mm

Based on the criteria in **Table III.9.2**, the nonwoven geotextile filter should have a minimum permittivity of 0.5 sec⁻¹ and a maximum AOS size of 0.43 millimeters (mm).

5.3 Landfilldesign.com Geotextile Filter – Design Calculator Requirements

5.3.1 Retention Requirement (Maximum AOS) Under Steady State Flow

The particle size distribution of the soils was inputted into the Geotextile Filter – Design Calculator (**Attachment III.9.D**) and the resulting maximum AOS size was computed to be 1.06 mm, which is greater than the maximum AOS size recommended by AASHTO; therefore an AOS size of 0.43 mm was used.

5.3.2 Permeability

The principle of the permeability (k) criteria is that, as long as the permittivity (Ψ) of the nonwoven geotextile is greater than the permeability of the soil, leachate will flow freely at the soil/geotextile interface. Given the importance of long-term function of the protective soil layer and geotextile, industry standards recommend a minimum Factor of Safety of 10 for the nonwoven geotextile permittivity:

$k_{\text{geotextile}} > 10 k_{\text{soil}}$ where the permeability of the protective soil layer is $\geq 5.0 \times 10^{-5}$ cm/sec

$\Psi_{\text{geotextile}} > 10 (5.0 \times 10^{-5} \text{ cm/sec})$

$\Psi_{\text{geotextile}} > 5.0 \times 10^{-4} \text{ cm/sec}$

A typical 10 oz/yd² nonwoven geotextile product has a minimum permeability of 0.3 cm/sec (**Attachment III.9.B**); therefore the selected nonwoven geotextile meets the permeability criterion.

5.3.3 Clogging (Porosity Criteria)

The nonwoven geotextile must remain at a high porosity to prevent clogging of the leachate collection system. Per Landfilldesign.com (**Attachment III.9.D.**), the porosity of the nonwoven geotextile is sufficient if it is greater than 30%. A GSE 10 oz/yd² nonwoven geotextile is selected as the example for use in the leachate collection system for the SWRL. Porosity is calculated using the following equation (**Attachment III.9.E, Page 128**):

$$n_{\text{geotextile}} = 1 - [\mu / ((\rho)(t))]$$

Where:

- $n_{\text{geotextile}}$ = porosity of the GSE 10 oz/yd² nonwoven geotextile filter (dimensionless)
- μ = mass per unit area of the GSE 10 oz/yd² nonwoven geotextile filter (0.0335 g/cm²)
- ρ = density of polymeric compound = 0.94 g/cm³ for Polypropylene
- t = thickness of the GSE 10 oz/yd² nonwoven geotextile filter = 100 mil (0.254 cm)

The design nonwoven geotextile filter has a weight of 10 oz/yd². Properties of the proposed 10 oz/yd² nonwoven geotextile filter are listed in **Attachment III.9.B**.

Therefore:

$$n_{\text{geotextile}} = 1 - [\mu / ((\rho)(t))]$$

$$n_{\text{geotextile}} = 1 - [0.0335 \text{ g/cm}^2 / ((0.94 \text{ g/cm}^3) (0.254 \text{ cm}))]$$

$$n_{\text{geotextile}} = 1 - [0.0335 \text{ g/cm}^2 / 0.2388 \text{ g/cm}^2]$$

$$n_{\text{geotextile}} = 1 - [0.1403]$$

$$n_{\text{geotextile}} = 0.8597$$

Since the porosity of the GSE 10 oz/yd² nonwoven geotextile is greater than 0.3, the selected nonwoven geotextile meets the required porosity criteria.

6.0 PROPOSED NONWOVEN GEOTEXTILE PROJECT SPECIFICATIONS

The proposed 10 oz/yd² nonwoven geotextile for the use in the SCLF leachate collection system must meet the product properties calculated above. The 10 oz/yd² nonwoven geotextile product properties are specified on the data sheet published by GSE Lining Technology, Inc. as an example (**Attachment III.9.B**). The product properties specified for the 10 oz/yd² nonwoven geotextile are summarized in **Table III.9.3**.

TABLE III.9.3
Proposed Nonwoven Geotextile Specifications
Sandoval County Landfill

Property	Calculated/Recommended Value	Product Specification
Puncture	80.2 lbs	165 lbs
Minimum Permittivity	0.5 sec ⁻¹	1.20 sec ⁻¹
Maximum AOS	0.43 mm	0.15 mm
Permeability	> 5 x 10 ⁻⁴ cm/sec	0.30 cm/sec
Porosity	> 0.30	0.86

**APPLICATION FOR PERMIT RENEWAL AND MODIFICATION
SANDOVAL COUNTY LANDFILL**

**VOLUME III: LANDFILL ENGINEERING CALCULATIONS
SECTION 9: GEOTEXTILE FILTER FABRIC ANALYSIS**

ATTACHMENT III.9.A

**KOERNER, ROBERT M. 2005. CHAPTER 2.5.4, “PUNCTURE RESISTANCE” IN
DESIGNING WITH GEOSYNTHETICS, FIFTH EDITION, PAGES 171-173.
NEW JERSEY: PEARSON PRENTICE HALL.**

DESIGNING WITH GEOSYNTHETICS

FIFTH EDITION



ROBERT M. KOERNER

- b = width of stone void, and
 y = deformation into stone void.

Example 2.9

Given a truck with 700 kPa tire inflation pressure on a stone base course consisting of 50 mm maximum-sized stone with a geotextile beneath it, calculate (a) the required grab tensile stress on the geotextile, and (b) the factor of safety for a geotextile whose maximum grab strength is 500 N with cumulative reduction factors of 2.5. Use a value of $f(\epsilon) = 0.52$.

Solution: (a) Using an empirical relationship that $d_v = 0.33 d_a$ and the value of $f(\epsilon) = 0.52$, the required grab tensile strength is as follows:

$$\begin{aligned} T_{\text{reqd}} &= p'(d_v)^2(0.52) \\ &= p'(0.33 d_a)^2(0.52) \\ &= 0.057 p' d_a^2 \\ &= 0.057(700)(1000)(0.050)^2 \\ T_{\text{reqd}} &= 100 \text{ N} \end{aligned}$$

- (b) The factor of safety on a 500 N maximum grab tensile geotextile with reduction factors of 2.5, is as follows:

$$\begin{aligned} \text{FS} &= \frac{T_{\text{allow}}}{T_{\text{reqd}}} \\ &= \frac{500/2.5}{100} \\ \text{FS} &= 2.0, \text{ which is acceptable.} \end{aligned}$$

2.5.4 Puncture Resistance

The geotextile must always survive the installation process. This is not just related to the roadway separation function; indeed, fabric survivability is critical in all types of applications; without it the best of designs are futile (recall Figure 2.20). In this regard, sharp stones, tree stumps, roots, miscellaneous debris, and other items, either on the ground surface beneath the geotextile or placed above it, could puncture through the geotextile during backfilling and when traffic loads are imposed. The design method suggested for this situation is shown schematically in Figure 2.32. For these conditions, the vertical force exerted on the geotextile (which is gradually tightening around the protruding object) is as follows:

$$F_{\text{reqd}} = p' d_a^2 S_1 S_2 S_3 \quad (2.30)$$

where

- F_{reqd} = required vertical puncturing force to be resisted,
 d_a = average diameter of the puncturing aggregate or sharp object,

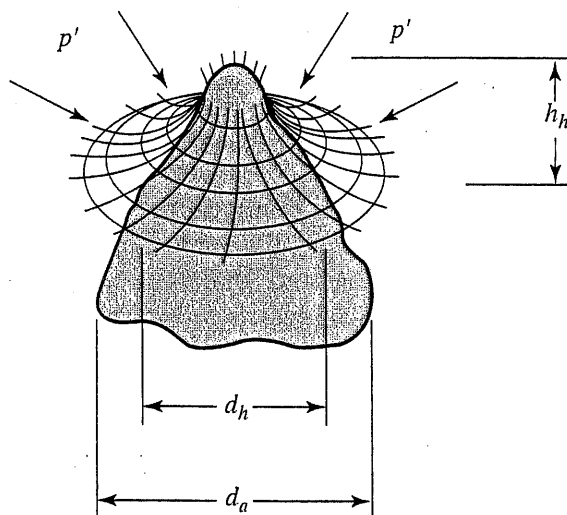


Figure 2.32 Visualization of a stone puncturing a geotextile as pressure is applied from above.

- p' = pressure exerted on the geotextile (approximately 100% of tire inflation pressure at the ground surface for thin covering thicknesses),
 S_1 = protrusion factor of the puncturing object (see Table 2.13),
 S_2 = scale factor to adjust the ASTM D4833 puncture test value that uses a 8.0 mm diameter puncture probe to the actual puncturing object (see Table 2.13), and
 S_3 = shape factor to adjust the ASTM D4833 flat puncture probe to the actual shape of the puncturing object (see Table 2.13).

Example 2.10

What is the factor of safety against puncture of a geotextile from a subrounded 25 mm diameter stone on the ground surface mobilized by a loaded truck with tire inflation pressure of 550 kPa traveling on the surface of the base course? The geotextile has an ultimate puncture strength of 300 N according to ASTM D4833.

TABLE 2.13 RECOMMENDED VALUES FOR FACTORS USED IN PUNCTURE ANALYSIS (DIMENSIONLESS)

Puncturing Object	S_1	S_2	S_3
Angular and relatively large	0.9	0.8	0.9
Angular and relatively small	0.6	0.6	0.7
Subrounded and relatively large	0.7	0.6	0.6
Subrounded and relatively small	0.4	0.4	0.5
Rounded and relatively large	0.5	0.4	0.4
Rounded and relatively small	0.2	0.2	0.3

S_1 = protrusion factor
 S_2 = scale factor
 S_3 = shape factor

} see equation (2.30)

Solution: Using the full stress on the geotextile of 550 kPa and factors from Table 2.13 of 0.55, 0.50, and 0.55 for S_1 , S_2 , and S_3 respectively, we see that

$$\begin{aligned} F_{\text{reqd}} &= p' d_a^2 S_1 S_2 S_3 \\ &= (550)(1000)(25 \times 0.001)^2 (0.55)(0.50)(0.55) \\ F_{\text{reqd}} &= 52 \text{ N} \end{aligned}$$

Assuming that the cumulative reduction factors are 2.0, the factor of safety is as follows:

$$\begin{aligned} \text{FS} &= \frac{F_{\text{allow}}}{F_{\text{reqd}}} \\ &= \frac{300/2.0}{52} \\ \text{FS} &= 2.9, \text{ which is acceptable} \end{aligned}$$

2.5.5 Impact (Tear) Resistance

As with the puncture requirement just described, the resistance of a geotextile to impact is as much a survivability criterion as it is a separation function. Yet in many instances of separation the geotextile must resist the impact of various objects. The most obvious one is that of a rock falling on it, but there are also situations in which construction equipment and materials can cause or contribute to impact damage on geotextiles.

The problem addresses the energy mobilized by a free-falling object of known weight and height of drop. Rarely will an object be intentionally impelled onto an exposed geotextile with additional force, so only gravitational energy will be assumed.

To develop a design procedure, we assume a free-falling rock of specific gravity of 2.60, varying in diameter from 25 to 600 mm and falling from heights of 0.5 to 5 m. Using this data, the design curves in Figure 2.33 are developed. The relationship used is as follows:

$$\begin{aligned} E &= mgh \\ &= (V \times \rho)gh \\ &= [V \times (\rho_w G_s)]gh \\ &= \left(\frac{\pi(d_a/1000)^3}{6} \right) \left(\frac{1000 \text{ kg}}{\text{m}^3} \right) (2.6)(9.81)h \\ E &= 13.35 \times 10^{-6} d_a^3 h \end{aligned} \tag{2.31}$$

where

- E = energy developed (Joules),
- m = mass of the falling object (kg),
- g = acceleration due to gravity (m/sec^2),

**APPLICATION FOR PERMIT RENEWAL AND MODIFICATION
SANDOVAL COUNTY LANDFILL**

**VOLUME III: LANDFILL ENGINEERING CALCULATIONS
SECTION 9: GEOTEXTILE FILTER FABRIC ANALYSIS**

ATTACHMENT III.9.B

**“GSE LINING TECHNOLOGY, INC.”, NONWOVEN GEOTEXTILE
PRODUCT DATA SHEET *2007***



GSE Nonwoven Geotextiles is a family of polypropylene, staple fiber, nonwoven, needlepunched geotextiles. Manufactured using an advanced manufacturing and quality system, these products are the most uniform and consistent nonwoven, needlepunched geotextile currently available in the industry. GSE combines a fiber selection and approval system with in-line quality control and a state-of-the-art laboratory to ensure that every roll shipped meets customer specifications. The company has performed extensive performance testing to evaluate suitability of its nonwovens for various applications. GSE Nonwoven Geotextiles are available in a range of weights to meet your specific project needs. *These product specifications meet or exceed GRI GT12, GRI GT13 and AASHTO M288.*

Product Specifications

TESTED PROPERTY	TEST METHOD	FREQUENCY	NW4	NW6	NW8	NW10	NW12	NW16
Product Code			GEO 0408002	GEO 0608002	GEO 0808002	GEO 1008002	GEO 1208002	GEO 1608002
AASHTO M288 Class			3	2	1	>1	>>1	>>>1
Mass per Unit Area, oz/yd ² (g/m ²)	ASTM D 5261	90,000 ft ²	4 (135)	6 (200)	8 (270)	10 (335)	12 (405)	16 (540)
Grab Tensile Strength, lb (N)	ASTM D 4632	90,000 ft ²	120 (530)	170 (755)	220 (975)	260 (1,155)	320 (1,420)	390 (1,735)
Grab Elongation, %	ASTM D 4632	90,000 ft ²	50	50	50	50	50	50
Puncture Strength, lb (N)	ASTM D 4833	90,000 ft ²	60 (265)	90 (395)	120 (525)	165 (725)	190 (835)	240 (1,055)
Trapezoidal Tear Strength, lb (N)	ASTM D 4533	90,000 ft ²	50 (220)	70 (310)	95 (420)	100 (445)	125 (555)	150 (665)
Apparent Opening Size, Sieve No. (mm)	ASTM D 4751	540,000 ft ²	70 (0.212)	70 (0.212)	80 (0.180)	100 (0.150)	100 (0.150)	100 (0.150)
Permittivity, sec ⁻¹	ASTM D 4491	540,000 ft ²	1.50	1.50	1.50	1.20	0.80	0.70
Permeability, cm/sec.	ASTM D 4491	540,000 ft ²	0.22	0.30	0.30	0.30	0.29	0.27
Water Flow Rate, gpm/ft ² (l/min/m ²)	ASTM D 4491	540,000 ft ²	120 (4,885)	110 (4,480)	110 (4,480)	85 (3,460)	60 (2,440)	50 (2,035)
UV Resistance (% retained after 500 hours)	ASTM D 4355	per formulation	70	70	70	70	70	70
Roll Length ⁽¹⁾ , ft (m)			600 (182)	600 (182)	600 (182)	300 (91)	300 (91)	300 (91)
Roll Width ⁽¹⁾ , ft (m)			15 (4.6)	15 (4.6)	15 (4.6)	15 (4.6)	15 (4.6)	15 (4.6)
Roll Area, ft ² (m ²)			9,000 (836)	9,000 (836)	9,000 (836)	4,500 (418)	4,500 (418)	4,500 (418)

NOTES:

- The property values listed are in weaker principal direction. All values listed are Minimum Average Roll Values (MARV) except apparent opening size in mm and UV resistance. Apparent opening size (mm) is a Maximum Average Roll Value. UV is a typical value.
- ⁽¹⁾Roll lengths and widths have a tolerance of ±1%.

DS037 NW R08/30/07

This information is provided for reference purposes only and is not intended as a warranty or guarantee. GSE assumes no liability in connection with the use of this information. Please check with GSE for current, standard minimum quality assurance procedures and specifications.

GSE and other trademarks in this document are registered trademarks of GSE Lining Technology, Inc. in the United States and certain foreign countries.

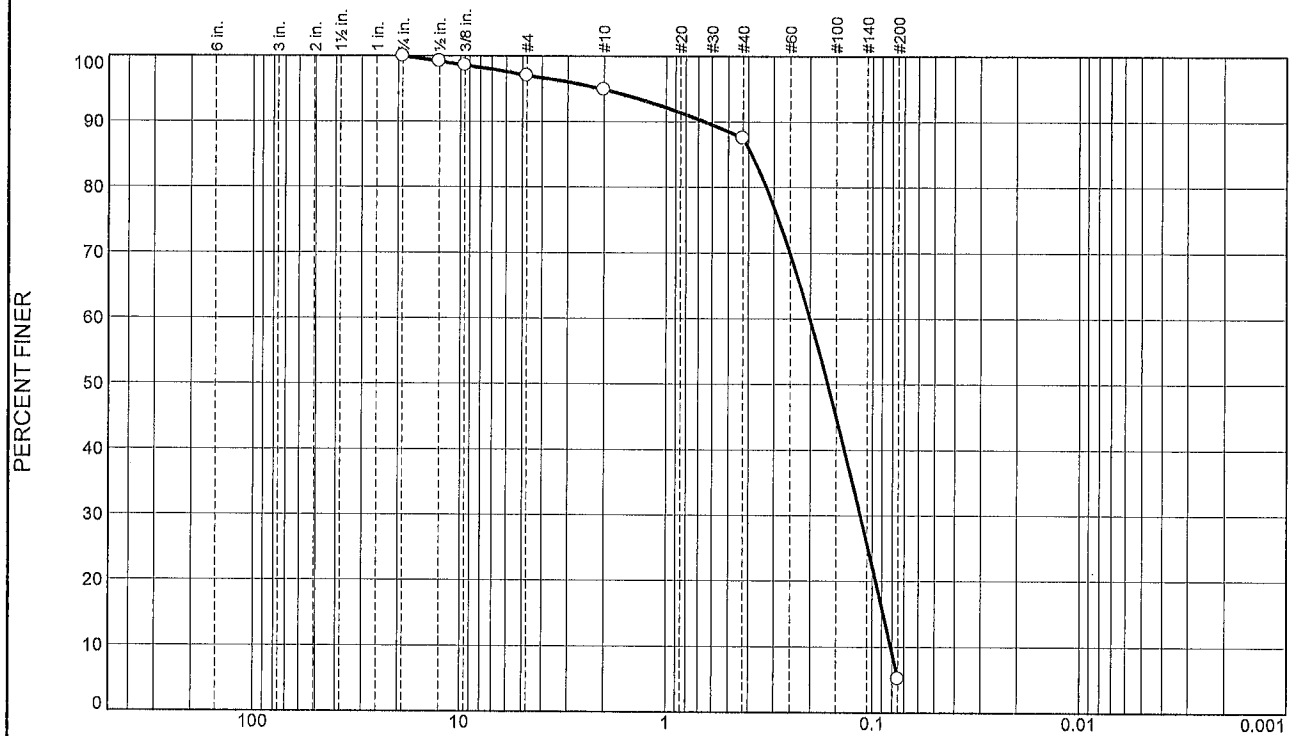
North America	GSE Lining Technology, Inc.	Houston, Texas	800.435.2008	281.443.8564	Fax: 281.230.6739
South America	GSE Lining Technology Chile S.A.	Santiago, Chile		56.2.595.4200	Fax: 56.2.595.4290
Asia Pacific	GSE Lining Technology Company Limited	Bangkok, Thailand		66.2.937.0091	Fax: 66.2.937.0097
Europe & Africa	GSE Lining Technology GmbH	Hamburg, Germany		49.40.767420	Fax: 49.40.7674234
Middle East	GSE Lining Technology-Egypt	The 6th of October City, Egypt		20.2.828.8888	Fax: 20.2.828.8889

**APPLICATION FOR PERMIT RENEWAL AND MODIFICATION
SANDOVAL COUNTY LANDFILL**

**VOLUME III: LANDFILL ENGINEERING CALCULATIONS
SECTION 9: GEOTEXTILE FILTER FABRIC ANALYSIS**

**ATTACHMENT III.9.C
SUMMARY OF LABORATORY GEOTECHNICAL TESTING RESULTS**

Particle Size Distribution Report



% +3"	% Gravel		% Sand			% Fines	
	Coarse	Fine	Coarse	Medium	Fine	Silt	Clay
0.0	0.0	3.0	2.1	7.4	82.3	5.2	

SIEVE SIZE	PERCENT FINER	SPEC.* PERCENT	PASS? (X=NO)
3/4"	100.0		
1/2"	99.2		
3/8"	98.6		
#4	97.0		
#10	94.9		
#40	87.5		
#200	5.2		

* (no specification provided)

Soil Description
 Sandoval County Landfill Cells 4C, 5B, 6B, and 7 PSL soil evaluation.

Atterberg Limits
 PL= NP LL= NV PI=

Coefficients
 D₉₀= 0.6506 D₈₅= 0.3852 D₆₀= 0.2010
 D₅₀= 0.1646 D₃₀= 0.1144 D₁₅= 0.0885
 D₁₀= 0.0813 C_u= 2.47 C_c= 0.80

Classification
 USCS= SP-SM AASHTO= A-3

Remarks

Source of Sample: Sandoval County Landfill
Sample Number: 1

Depth: Excavated Soils

Date: 03/24/15



Client: Sandoval County Landfill
Project: Application for Permit Modification

Project No: 211.00.01

Figure 1

GRAIN SIZE DISTRIBUTION TEST DATA

3/24/2015

Client: Sandoval County Landfill

Project: Application for Permit Modification

Project Number: 211.00.01

Location: Sandoval County Landfill

Depth: Excavated Soils

Sample Number: 1

Material Description: Sandoval County Landfill Cells 4C, 5B, 6B, and 7 PSL soil evaluation.

Date: 03/24/15

PL: NP

LL: NV

USCS Classification: SP-SM

AASHTO Classification: A-3

Sieve Test Data

Dry Sample and Tare (grams)	Tare (grams)	Cumulative Pan Tare Weight (grams)	Sieve Opening Size	Cumulative Weight Retained (grams)	Percent Finer
530.00	30.00	0.00	3/4"	0.00	100.0
			1/2"	4.00	99.2
			3/8"	7.00	98.6
			#4	15.00	97.0
			#10	25.50	94.9
			#40	62.50	87.5
			#200	474.00	5.2

Fractional Components

Cobbles	Gravel			Sand				Fines		
	Coarse	Fine	Total	Coarse	Medium	Fine	Total	Silt	Clay	Total
0.0	0.0	3.0	3.0	2.1	7.4	82.3	91.8			5.2

D ₁₀	D ₁₅	D ₂₀	D ₃₀	D ₅₀	D ₆₀	D ₈₀	D ₈₅	D ₉₀	D ₉₅
0.0813	0.0885	0.0963	0.1144	0.1646	0.2010	0.3269	0.3852	0.6506	2.0627

Fineness Modulus	C _u	C _c
1.04	2.47	0.80

GORDON ENVIRONMENTAL, INC.

PSL LABORATORY ANALYSIS RESULTS SUMMARY

PROJECT INFORMATION			
PROJECT NAME:	Cell 4C Construction	PROJECT NO:	211,14.03
OWNER:	Sandoval County	CONTACTOR:	H R Construction, Inc.
PROJECT LOCATION:	Sandoval County Landfill		

SAMPLE ID	PERCENT FINER THAN BY WEIGHT - U.S. STANDARD SIEVE NUMBER							C.U. (d_{60}/d_{10})
	3/4"	1/2"	3/8"	4	10	40	200	
	19 mm	12.5 mm	9.5 mm	4.75 mm	2.0 mm	0.425 mm	0.075 mm	
1434024	100	100.0	99.0	97.0	94.0	84.0	5.1	2.61
1432025	100	99.0	99.0	97.0	95.0	86.0	4.8	2.53
1434026	97	97.0	96.0	95.0	92.0	83.0	5.1	2.64
1434027	100	99.0	98.0	96.0	94.0	84.0	5.1	2.62
1434028	100	98.0	98.0	96.0	93.0	84.0	4.7	2.59
1434029	100	99.0	97.0	95.0	92.0	81.0	3.5	2.70
1434030	100	96.0	94.0	93.0	90.0	81.0	5.3	2.73
1434031	100	99.0	97.0	95.0	92.0	82.0	4.2	2.67
1434032	100	97.0	97.0	96.0	93.0	84.0	5.1	2.60
1434033	97	96.0	94.0	92.0	90.0	80.0	3.4	2.74
1434034	100	100.0	100.0	98.0	95.0	85.0	5.4	2.58
1434035	100	99.0	99.0	96.0	93.0	83.0	5.0	2.65
1434036	100	99.0	99.0	97.0	93.0	83.0	4.4	2.63
1434037	100	97.0	96.0	93.0	90.0	76.0	3.2	2.97
1434038	100	100.0	99.0	97.0	94.0	84.0	4.6	2.60
1434039	100	98.0	97.0	95.0	92.0	83.0	4.7	2.63
1434040	100	99.0	98.0	96.0	93.0	83.0	5.0	2.65
1434041	100	100.0	99.0	98.0	95.0	85.0	4.7	2.56
1434042	100	99.0	98.0	96.0	94.0	84.0	5.0	2.61
1434043	100	99.0	99.0	97.0	94.0	83.0	4.2	2.64
AVERAGE:	100	98.5	97.7	95.8	92.9	82.9	4.6	2.65

REVIEWED BY:

[Signature]



(505) 867-6990

GORDON ENVIRONMENTAL, INC.

213 S. Camino del Pueblo

(505) 867-6991 Fax

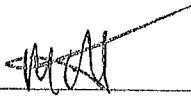
Consulting Engineers

Bernalillo, New Mexico 87004

PSL LABORATORY ANALYSIS RESULTS SUMMARY

PROJECT INFORMATION			
PROJECT NAME:	Cell 6B Construction	PROJECT NO:	211.14.03
OWNER:	Sandoval County Public Works	CONTACTOR:	H R Construction, Inc.
PROJECT LOCATION:	Sandoval County Landfill		

SAMPLE ID	PERCENT FINER THAN BY WEIGHT - U.S. STANDARD SIEVE NUMBER							C.U. (d_{60}/d_{10})
	3/4"	1/2"	3/8"	4	10	40	200	
	19 mm	12.5 mm	9.5 mm	4.75 mm	2.0 mm	0.425 mm	0.075 mm	
1434044	100	100.0	99.0	96.0	93.0	86.0	6.2	2.54
1434045	100	100.0	99.0	96.0	94.0	86.0	6.2	2.55
1434046	100	100.0	99.0	98.0	96.0	89.0	7.1	2.46
1434047	100	96.0	96.0	93.0	90.0	84.0	6.7	2.62
1434048	100	99.0	98.0	95.0	92.0	86.0	6.3	2.54
1434049	100	99.0	97.0	95.0	92.0	89.0	6.6	2.42
1434050	100	100.0	99.0	96.0	94.0	88.0	6.8	2.48
1434051	100	100.0	100.0	97.0	95.0	88.0	6.5	2.49
1434052	97	96.0	96.0	93.0	90.0	84.0	4.3	2.56
1434053	100	99.0	97.0	95.0	92.0	85.0	5.7	2.56
1434054	100	99.0	98.0	96.0	94.0	88.0	6.8	2.48
1434055	100	100.0	98.0	96.0	94.0	88.0	6.7	2.48
1434056	100	99.0	97.0	95.0	92.0	85.0	4.9	2.54
1434057	100	99.0	97.0	95.0	92.0	85.0	4.9	2.54
1434058	100	99.0	98.0	94.0	89.0	82.0	5.5	2.67
1434059	100	100.0	100.0	96.0	93.0	86.0	5.5	2.53
1434060	100	100.0	99.0	97.0	95.0	88.0	5.1	2.45
1434061	100	99.0	99.0	97.0	94.0	87.0	6.4	2.51
1434062	100	98.0	97.0	95.0	92.0	86.0	5.8	2.52
1434063	100	100.0	100.0	99.0	96.0	89.0	4.9	2.41
1434064	100	100.0	99.0	97.0	94.0	88.0	5.9	2.46
1434065	100	100.0	100.0	98.0	96.0	90.0	5.9	2.40
1434066	100	100.0	99.0	97.0	95.0	88.0	5.5	2.46
1434067	100	100.0	100.0	98.0	95.0	88.0	6.3	2.48
1434068	100	100.0	100.0	98.0	97.0	90.0	5.8	2.41
1434069	100	98.0	97.0	96.0	94.0	87.0	4.9	2.48
1434070	100	97.0	96.0	95.0	92.0	86.0	5.3	2.51
1434071	100	100.0	99.0	97.0	95.0	88.0	5.4	2.46
1434072	100	100.0	100.0	98.0	96.0	89.0	6.7	2.46
1434073	100	100.0	100.0	99.0	97.0	90.0	5.3	2.39
AVERAGE:	100	99.2	98.4	96.2	93.7	87.1	5.9	2.50

REVIEWED BY: 

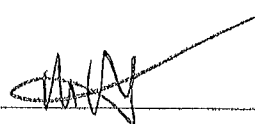
SHEET 1 OF 1

PSL LABORATORY ANALYSIS RESULTS SUMMARY

PROJECT INFORMATION			
PROJECT NAME:	Cell 7 Construction	PROJECT NO:	211.14.03
OWNER:	Sandoval County Public Works	CONTACTOR:	H R Construction, Inc.
PROJECT LOCATION:	Sandoval County Landfill		

SAMPLE ID	PERCENT FINER THAN BY WEIGHT - U.S. STANDARD SIEVE NUMBER							C.U. (d_{60}/d_{10})
	3/4"	1/2"	3/8"	4	10	40	200	
	19 mm	12.5 mm	9.5 mm	4.75 mm	2.0 mm	0.425 mm	0.075 mm	
1434076	100	99.0	99.0	99.0	98.0	94.0	4.3	2.25
1434077	100	100.0	100.0	99.0	99.0	96.0	5.7	2.23
1434078	100	100.0	100.0	100.0	99.0	96.0	5.9	2.23
1434079	100	99.0	99.0	98.0	97.0	94.0	5.5	2.27
1434080	100	99.0	99.0	99.0	98.0	95.0	6.7	2.26
1434081	100	100.0	100.0	99.0	98.0	95.0	6.4	2.26
1434082	100	100.0	100.0	99.0	98.0	95.0	5.6	2.25
1434083	100	100.0	100.0	99.0	98.0	95.0	4.7	2.23
1434084	100	100.0	100.0	99.0	98.0	85.0	3.7	2.57
1434085	100	100.0	99.0	99.0	97.0	88.0	4.0	2.44
1434086	100	100.0	100.0	99.0	98.0	84.0	4.0	2.63
1434087	100	100.0	100.0	99.0	99.0	95.0	5.3	2.25
1434088	100	100.0	100.0	99.0	98.0	89.0	4.9	2.43
1434089	100	100.0	100.0	99.0	98.0	81.0	3.5	2.76
1434090	100	100.0	100.0	99.0	98.0	95.0	5.3	2.24
1434091	100	100.0	100.0	100.0	99.0	96.0	5.3	2.22
1434092	100	100.0	100.0	100.0	99.0	96.0	6.0	2.23
1434093	100	100.0	100.0	99.0	98.0	88.0	4.1	2.46
1434094	100	100.0	100.0	100.0	99.0	95.0	5.2	2.24
1434095	100	100.0	100.0	99.0	98.0	94.0	4.0	2.25
1434096	100	100.0	100.0	99.0	99.0	95.0	6.1	2.26
1434097	100	100.0	100.0	99.0	98.0	85.0	4.6	2.60
1434098	100	100.0	100.0	99.0	99.0	96.0	5.6	2.21
1434099	100	100.0	100.0	99.0	98.0	95.0	5.5	2.24
1434100	100	100.0	100.0	100.0	98.0	95.0	4.3	2.22
1434101	100	100.0	100.0	99.0	98.0	93.0	4.8	2.29
1434102	100	100.0	99.0	98.0	97.0	94.0	5.7	2.27
1434103	100	100.0	100.0	99.0	98.0	83.0	4.5	2.69
1434104	100	100.0	100.0	100.0	99.0	96.0	6.5	2.24
1434105	100	100.0	100.0	99.0	98.0	95.0	5.8	2.25
AVERAGE:	100	99.9	99.8	99.1	98.2	92.4	5.1	2.33

REVIEWED BY: _____



**APPLICATION FOR PERMIT RENEWAL AND MODIFICATION
SANDOVAL COUNTY LANDFILL**

**VOLUME III: LANDFILL ENGINEERING CALCULATIONS
SECTION 9: GEOTEXTILE FILTER FABRIC ANALYSIS**

ATTACHMENT III.9.D

**ADVANCED GEOTECH SYSTEMS. GEOTEXTILE FILTER CALCULATOR.
LANDFILLDESIGN.COM. [HTTP://WWW.LANDFILL
DESIGN.COM/DESIGN/CALCULATORS/GEOFIL.ASPX](http://www.landfilldesign.com/design/calculators/geofil.aspx) (2013).**

landfilldesign.com
Design Calculator
Geotextile Filter

Problem Statement

The function of a geotextile filter is to retain the soil while allowing the liquid to flow as freely as possible. In order to achieve this objective, a geotextile filter needs to meet: (1) **Retention criterion**: the filter opening size must be sufficiently small to retain soil particles. (2) **Permeability criterion**: the filter must be sufficiently permeable to ensure that the liquid flow is as free as possible, and (3) **Porosity criterion**: the filter should remain a high porosity so the probability for clogging is small.

Giroud's filter criteria is used in the calculation. It is recommended that AASHTO M288-96 minimum hydraulic requirements as shown in the table below be also considered in the selection of a geotextiles filter.

Table 1 - Geotextile Criteria for Subsurface Drainage
(after AASHTO M288-96)

Filter Criteria	Percent Soil Passing No. 200 (0.075mm) Sieve		
	<15	15 - 50	>50
Minimum Permittivity, ASTM D-4491	0.5 sec ⁻¹	0.2 sec ⁻¹	0.1 sec ⁻¹
Maximum AOS, ASTM D-4751	0.43 mm	0.25 mm	0.22 mm

Retention Criterion

Giroud (2000) uses a linearization of the particle distribution curve that, when plotted with the classical log scale horizontal axis, is as close as possible to the actual particle distribution curve (Figure 1). A least variance approach was used to determine the best linearization of the central portion (Equation 1 & 2). It should be noted in Figure 1 that there is greater uncertainty on the two extremities (d_0 and d_{100}) of the actual particle size distribution. This justifies the use of the linear particle size distribution curve. The result obtained using Giroud's retention criterion is not affected by the truncation of the particle size distribution curve. A coefficient of determination (R^2) is calculated to indicate the effectiveness of the linearization (Equation 3).

$m = \frac{n(\sum xy) - (\sum x)(\sum y)}{n(\sum x^2) - (\sum x)^2}$	$b = \frac{(\sum y)(\sum x^2) - (\sum x)(\sum xy)}{(\sum x^2) - (\sum x)^2}$	$R^2 = \frac{n(\sum xy) - (\sum x)(\sum y)}{\sqrt{[n\sum x^2 - (\sum x)^2][n\sum y^2 - (\sum y)^2]}}$
Eq. 1 - Slope determination by the method of the least squares	Eq. 2 - Intercept determination by the method of the least squares	Eq. 3 - The r-squared value can be interpreted as the proportion of the variance in y attributable, to the variance in x

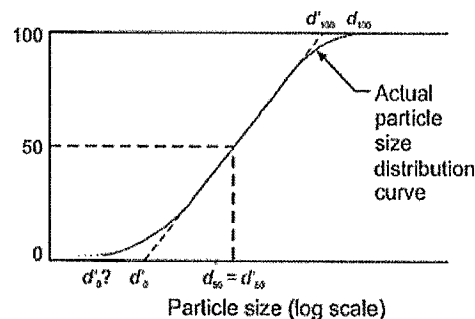


Figure 1 - Linearization of Particle Size Distribution Curve (after Giroud, 2000)

Table 2 - Retention Criterion for the Hyperstable Case
($C'_{ou} = 3$) expressed using d'_{85S}

Soil Density	Density Index (Relative Density) I_D	Relative Compaction (R_C)	Linear coefficient of uniformity of the soil, C'_u	
			$1 \leq C'_u \leq 3$	$C'_u \geq 3$
loose	$I_D \leq 35\%$	$R_C \leq 86\%$	$O_F \leq (C'_u)^{0.3} d'_{85S}$	$O_F \leq (9/C'_u)^{1.7} d'_{85S}$
medium dense	$35\% < I_D \leq 65\%$	$86\% < R_C \leq 92\%$	$O_F \leq 1.5 (C'_u)^{0.3} d'_{85S}$	$O_F \leq (13.5/C'_u)^{1.7} d'_{85S}$
dense	$I_D > 65\%$	$R_C > 92\%$	$O_F \leq 2 (C'_u)^{0.3} d'_{85S}$	$O_F \leq (18/C'_u)^{1.7} d'_{85S}$

Table 3 - Retention Criterion for the Hyperstable Case
($C'_{ou} = 3$) expressed using d'_{50S}

Soil Density	Density Index (Relative Density) I_D	Relative Compaction (R_C)	Linear coefficient of uniformity of the soil, C'_u	
			$1 \leq C'_u \leq 3$	$C'_u \geq 3$
loose	$I_D \leq 35\%$	$R_C \leq 86\%$	$O_F \leq (C'_u) d'_{50S}$	$O_F \leq (9/C'_u) d'_{50S}$
medium dense	$35\% < I_D \leq 65\%$	$86\% < R_C \leq 92\%$	$O_F \leq 1.5 (C'_u) d'_{50S}$	$O_F \leq (13.5/C'_u) d'_{50S}$
dense	$I_D > 65\%$	$R_C > 92\%$	$O_F \leq 2 (C'_u) d'_{50S}$	$O_F \leq (18/C'_u) d'_{50S}$

where:

C'_u	linear coefficient of uniformity of the soil = d'_{60s} / d'_{10s}
I_D	relative density or density index of the soil
d'_{ms}	the particle size such that m% (on the linear particle size distribution curve) of the linear soil particles by mass are smaller than d'_{ms}
R_c	relative compaction
O_F	maximum filter opening size

Permeability Criteria

$K_f \geq K_s \cdot I_s$	-> against excessive pore water pressure
$K_f \geq K_s$	-> against excessive reduction of flow rate

where:

K_f - Hydraulic conductivity of the geotextile filter

K_s - Hydraulic conductivity of the soil

I_s - Hydraulic gradient in the soil (typical values presented in Table 4)

Table 4 - Typical Hydraulic Gradients in the Soil in the Vicinity of the Filter

Application	Typical hydraulic gradient
Ordinary dewatering trench	1
Vertical wall drain	1.5
Pavement edge drain	1
Landfill leachate collection/detection removal system	1
Landfill closure surface water collection removal system	1
Dam toe drains	2
Dam clay cores	3 to 10
Island channel protection	1
Shoreline protection	10
Liquid impoundment with clay liners	>10

Porosity Criteria

$$N_{GTX} > 0.3$$

where N_{GTX} is the porosity of geotextile filter.

There are two mechanisms that are known to cause progressive clogging in a filter: (1) Chemical, biological and biochemical clogging. (2) Accumulation of soil particles on or in the filter.

Input Values

Particle Size Distribution

d_{10}	0.0885	mm
d_{20}	0.0963	mm
d_{50}	0.1646	mm
d_{60}	0.2010	mm
d_{85}	0.3852	mm

w factor

2

w Factor

loose	medium dense	dense
1	1.5	2

Calculate

Solution

Input data

Actual Particle Distribution Curve

d_{10}	0.089 mm
d_{20}	0.096 mm
d_{50}	0.165 mm
d_{60}	0.201 mm
d_{85}	0.385 mm

Output Data

Values of the Linear Particle Distribution Curve

d'_0	0.059 mm
d'_{10}	0.622 mm
d'_{20}	6.551 mm
d'_{60}	7637.824 mm
d'_{80}	80388.517 mm

d' ₈₅	28890490.933 mm
d' ₁₀₀	986487224.702 mm

Coefficient of Determination (R^2)	0.2999
Indicates how accurate the linearization is	

Coefficient of Uniformity	2.2712
If greater than 1 and smaller than 5, it is said to be uniformly graded. If greater than 20, it is said to be broadly graded.	

Linear Coefficient of Uniformity	129158.15
---	------------------

Maximum Filter Opening Size	1.0644 mm
------------------------------------	------------------

Assistance

References

Grourd, J.P., 2000, "Filter Criteria", in Jubilee Volume 75th Anniversary of K. Terzaghi's Erdbaumechanik (Soil Mechanics), Technical University, Vienna, Austria, Vol 5/2000, Brandl, H., editor.

Grourd, J. P., 1994, "Quantification of Geosynthetics Behavior", Special Lecture, Proceedings of the Fifth International Conference on Geotextiles, Geomembranes and Related Products, Singapore, September 1994, Vol. 4, pp. 1249-1273.

Grourd, J. P., 1988, "Review of Geotextile Filter Criteria", Proceedings of the First Indian Geotextiles Conference, Bombay, India, December 1988, pp. 1-6.

Grourd, J. P., 1982, "Filter Criteria for Geotextiles", Proceedings of the Second International Conference of Geotextiles, Vol. 1, Las Vegas, Nevada, USA, August 1982, pp. 103-108.

Copyright 2010 Advanced Geotech Systems. All rights reserved.

**APPLICATION FOR PERMIT RENEWAL AND MODIFICATION
SANDOVAL COUNTY LANDFILL**

**VOLUME III: LANDFILL ENGINEERING CALCULATIONS
SECTION 9: GEOTEXTILE FILTER FABRIC ANALYSIS**

ATTACHMENT III.9.E

**KOERNER, ROBERT M. 2005. “POROSITY” IN CHAPTER 2.3.4, “HYDRAULIC
PROPERTIES” IN *DESIGNING WITH GEOSYNTHETICS, FIFTH EDITION*, PAGE 128.
NEW JERSEY: PEARSON PRENTICE HALL.**

DESIGNING WITH GEOSYNTHETICS

FIFTH EDITION



ROBERT M. KOERNER

Since the test greatly resembles a direct shear test, albeit with stationary soil on both sides of the tensioned geotextile, a possible design strategy is to take direct shear test results (for both sides of the geotextile) and use these values for pullout design purposes. However, this may not be a conservative practice.

Test results by Collios et al. [36] show a relationship of pullout test results to shear test results with some notable exceptions. For pullout testing, if the soil particles are smaller than the geotextile openings, efficiencies are high; if not, they can be low. In all cases, however, pullout test resistances are less than the sum of the direct shear test resistances. This is due to the fact that the geotextile is taut in the pullout test and exhibits large deformations. This in turn causes the soil particles to reorient themselves into a reduced shear strength mode at the soil-to-geotextile interfaces, resulting in lower pullout resistance. The stress state mobilized in this test is both interesting and complex as evidenced by a large number of technical references on this topic.

2.3.4 Hydraulic Properties

Unlike the physical and mechanical properties just discussed, traditional tests on textile materials rarely have hydraulic applications; that is, the garment and industrial fabrics industry obviously does not test for liquid flow. As a result, hydraulic testing of geotextiles has required completely new and original test concepts, methods, devices, interpretation, and databases. Both geotextile tests in-isolation and with soil will be described in this section.

Porosity. As conventionally defined with soils in geotechnical engineering, the porosity of a geotextile is the ratio of void volume to total volume. It is related to the ability of liquid to flow through or within the geotextile but is rarely measured directly. Instead, it is calculated from other properties of the geotextile:

$$n = 1 - \frac{m}{\rho t} \quad (2.15)$$

where

- n = porosity (dimensionless),
- m = mass per unit area, i.e., weight, (g/m^2),
- ρ = density (g/m^3), and
- t = thickness (m).

It is seen in equation (2.15) that for a given geotextile's weight and density, the porosity is directly related to thickness. Thickness in turn is related to the applied normal stress (see again Figure 2.6).

Pore size can be measured by careful sieving with controlled-size glass beads (see the AOS test later in this section), by the use of image analyzers [37], or by the use of

**APPLICATION FOR PERMIT RENEWAL AND MODIFICATION
SANDOVAL COUNTY LANDFILL**

**VOLUME III: LANDFILL ENGINEERING CALCULATIONS
SECTION 10: HELP MODEL**

TABLE OF CONTENTS

1.0	INTRODUCTION	III.10-1
2.0	DESIGN CRITERIA	III.10-1
3.0	PURPOSE.....	III.10-2
4.0	HELP MODEL METHODOLOGY	III.10-3
5.0	OVERVIEW OF DEMONSTRATION MODELING	III.10-3
6.0	HELP MODEL DEMONSTRATION ANALYSES	III.10-4
6.1	Design Parameters	III.10-4
6.2	Tier I Prescriptive Liner Demonstration.....	III.10-7
6.2.1	Prescriptive Liner System Design.....	III.10-7
6.2.2	HELP Model Input Parameters	III.10-7
6.2.3	Tier I Prescriptive Liner Simulation Analysis	III.10-9
6.3	Tier I Alternate Final Cover Demonstration.....	III.10-9
6.3.1	Alternate Final Cover System Design.....	III.10-12
6.3.2	HELP Model Input Parameters	III.10-12
6.3.3	Alternate Final Cover Simulation Analysis	III.10-13
6.3.4	Tier I Alternate Final Cover Demonstration Results	III.10-13
6.4	Tier II Prescriptive liner and Alternate Final Cover Demonstration	III.10-14
6.4.1	Liner and Cover System Design	III.10-15
6.4.2	HELP Model Input Parameters	III.10-15
6.4.3	Tier II Prescriptive liner and Alternate Final Cover Simulation Analyses	III.10-16
6.4.4	Tier II Prescriptive liner and Alternate Final Cover Demonstration Results	III.10-22
7.0	HELP MODEL DEMONSTRATION ANALYSES INTERMEDIATE COVER UNIT III.....	III.10-23
7.1	Unit III Ten Year Waste Mass Demonstration Analysis	III.10-23
8.0	CONCLUSIONS AND REQUEST FOR APPROVAL.....	III.10-27

**APPLICATION FOR PERMIT RENEWAL AND MODIFICATION
SANDOVAL COUNTY LANDFILL**

**VOLUME III: LANDFILL ENGINEERING CALCULATIONS
SECTION 10: HELP MODEL**

LIST OF FIGURES

Figure No.	Title	Page
III.10.1	BASE GRADING PLAN	III.10-5
III.10.2	FINAL GRADING PLAN	III.10-6

LIST OF TABLES

Table No.	Title	Page
III.10.1	TIER I, SIMULATION 5-1: PRESCRIPTIVE LINER SYSTEM.....	III.10-11
III.10.2	TIER I, PERFORMANCE RESULTS FOR PRESCRIPTIVE LINER SYSTEM.....	III.10-11
III.10.3	TIER I, SIMULATION 3-1: ALTERNATE FINAL COVER SYSTEM	III.10-13
III.10.4	TIER I, PERFORMANCE RESULTS FOR PRESCRIPTIVE LINER AND ALTERNATE FINAL COVER SYSTEMS	III.10-14
III.10.5	TIER II, CLIMATE DATA	III.10-16
III.10.6	TIER II, EVAPORATIVE ZONE DEPTH, MAXIMUM LEAF AREA INDEX AND TYPE OF VEGETATION.....	III.10-16
III.10.7	TIER II, METHODS USED TO ESTABLISH INITIAL MOISTURE CONDITIONS	III.10-17
III.10.8	TIER II, SIMULATION 7-1: OPEN LANDFILL, NO WASTE.....	III.10-19
III.10.9	TIER II, SIMULATION 8-1: PARTIALLY FILLED LANDFILL	III.10-19
III.10.10	TIER II, SIMULATION 9-1: CLOSED LANDFILL, NO COVER VEGETATION	III.10-21
III.10.11	TIER II, SIMULATION 10-1: CLOSED LANDFILL, PARTIAL VEGETATION	III.10-21
III.10.12	TIER II, PERFORMANCE RESULTS FOR PRESCRIPTIVE LINER AND ALTERNATE FINAL COVER SYSTEMS	III.10-22
III.10.13	UNIT III TEN-YEAR HELP MODEL SIMULATION – INPUT PARAMETERS	III.10-25
III.10.14	UNIT III TEN-YEAR HELP MODEL SIMULATION SUMMARY – AVERAGE ANNUAL TOTALS	III.10-26
III.10.15	UNIT III TEN-YEAR HELP MODEL SIMULATION SUMMARY – INITIAL AND FINAL MOISTURE CONTENTS	III.10-26

**APPLICATION FOR PERMIT RENEWAL AND MODIFICATION
SANDOVAL COUNTY LANDFILL**

**VOLUME III: LANDFILL ENGINEERING CALCULATIONS
SECTION 10: HELP MODEL**

LIST OF ATTACHMENTS

Attachment No.	Title
III.10.A	HELP MODEL OUTPUT FILES
III.10.A-1	TIER I, SIMULATION 5-1: PRESCRIPTIVE LINER, SOIL TYPE 6
III.10.A-2	TIER I, SIMULATION 3-1A AND 3-1B: ALTERNATE FINAL COVER, SOIL TYPE 6
III.10.A-3	TIER II, SIMULATION 7-1: PRESCRIPTIVE LINER WITH SOIL TYPE 6
III.10.A-4	TIER II, SIMULATION 8-1: PRESCRIPTIVE LINER WITH SOIL TYPE 6, INTERMEDIATE COVER WITH SOIL TYPE 6
III.10.A-5	TIER II, SIMULATION 9-1A AND 9-1B: PRESCRIPTIVE LINER WITH SOIL TYPE 6, ALTERNATE FINAL COVER WITH SOIL TYPES 6
III.10.A-6	TIER II, SIMULATION 10-1A AND 10-1B: PRESCRIPTIVE LINER WITH SOIL TYPE 6, ALTERNATE COVER WITH SOIL TYPE 6
III.10.A-7	UNIT III TEN-YEAR INTERMEDIATE COVER
III.10.A-8	CELLS 1 – 6 TWENTY YEAR INTERMEDIATE COVER
III.10.B	SUMMARY OF GEOTECHNICAL SOIL TEST DATA
III.10.C	HELP MODEL GUIDANCE DOCUMENT (NMED SWB, 1998)
III.10.D	HELP MODEL INPUT AND OUTPUT FILES: CD ROM

**APPLICATION FOR PERMIT RENEWAL AND MODIFICATION
SANDOVAL COUNTY LANDFILL**

**VOLUME III: LANDFILL ENGINEERING CALCULATIONS
SECTION 10: HELP MODEL**

1.0 INTRODUCTION

The Sandoval County Landfill (SCLF) is an existing solid waste facility operating in compliance with its current Permits, SWM-050304 and SWM-050304 (SP), and the New Mexico Environment Department (NMED) Solid Waste Rules (20.9.2-2.9.10 NMAC). SCLF is located at 2708 Iris Road NE in Rio Rancho, New Mexico (NM), and occupies 178.3 acres \pm . SCLF is publicly owned and operated by the County of Sandoval (“the County”), and is currently permitted to accept municipal solid waste (MSW), including construction and demolition debris (C&D) and tires, and two special wastes: petroleum contaminated soils (PCS) and sludge.

2.0 DESIGN CRITERIA

The prescriptive design for SCLF Unit IV liner system includes the use of a compacted subgrade/structural fill; a geosynthetic clay layer (GCL); and a double-sided 60-mil HDPE textured geomembrane is shown on the **Permit Plans**. In addition, an alternate evapotranspiration (ET) cover design using on-site soils is proposed for the final cover system at the SCLF Facility. The prescriptive liner and alternate cover are designed to meet the requirements of the New Mexico Solid Waste Regulations 20.9.4 NMAC. More specifically, 20.9.4.13.A.(1) NMAC requires:

“with a composite liner consisting of two components:

(a) the upper component shall consist of a minimum 30-mil flexible or a 60-mil high density polyethylene (HDPE) geomembrane liner or equivalent material; the geomembrane shall be installed in direct and uniform contact with the lower component; and

(b) the lower component shall consist of a geosynthetic clay liner (GCL) or a minimum 24-inch thick layer of compacted soil having a saturated hydraulic conductivity of no more than 1×10^{-7} centimeters per second (cm/sec) throughout its thickness; the soil must be free of particles greater than one inch in any dimension;”

and further, 20.9.4.13.E.(4) specifies that:

“all liners shall have a top protective cover of at least two feet of granular soil or other material specifically approved by the department; the protective cover shall, in addition to providing physical protection for the liner, facilitate the collection of leachate in the leachate collection system; materials used to construct the protective cover must ensure the hydraulic leachate head on the liner does not exceed one foot;...”

3.0 PURPOSE

This document presents the results of mathematical modeling conducted using the United States Environmental Protection Agency (USEPA) Hydrologic Evaluation of Landfill Performance (HELP) Model. This document presents the results of modeling conducted using HELP to evaluate the performance of the alternate final cover system so as to not create a “bathtub” effect in the landfill in which the percolation through the alternate final cover does not exceed that of the prescriptive liner system. This document also presents a formal request for New Mexico Environment Department (NMED), Solid Waste Bureau (SWB) approval for the SCLF Facility to use the alternate final cover design; and to allow the use of alternate soil gradation specifications when identifying soils for construction of the protective soil layer (PSL) in the liner system. The remainder of this document is organized as follows:

- Section 4 presents the methodology in this demonstration.
- Section 5 presents an overview of the demonstration modeling for the prescriptive liner and alternate final cover designs.
- Section 6 presents a discussion of HELP model simulation analyses for the:
 - Tier I demonstration for the prescriptive liner system
 - Tier I demonstration for the alternate final cover system
 - Tier II demonstration for the prescriptive liner and alternate final cover systems
- Section 7 presents a discussion of HELP model simulation analyses for intermediate cover for Unit III as this Unit is anticipated to remain inactive for approximately 10 years prior to resuming operations.
- Section 8 presents the conclusions drawn from this demonstration modeling and the request for approval for the use of the alternate final cover and PSL layer designs and alternate soil specifications.

The primary objectives of the design approach include sustainability, in which the constructed elements are comprised principally of on-site materials; precluding the use of costly off-site and imported manufactured materials.

4.0 HELP MODEL METHODOLOGY

The methodology used to demonstrate that the performance of the alternate final cover system meets the performance of the prescriptive liner system outlined in 20.9.4 NMAC was based on the procedures developed by the NMED, SWB [the Guidance Document].

The following Guidance Document is provided in **Attachment III.10.C**:

- *Performance Demonstration for an Alternate Cover Design Under Section 502.A.2 of the New Mexico Solid Waste Management Regulations (20 NMAC 9.1) Using HELP Modeling*, April 1, 1998.

NMED Guidance Document provide a subjective means to evaluate liner and cover systems using very conservative assumptions. The demonstrations described below were performed using the USEPA HELP Model, Version 3.07 in accordance with associated NMED guidance.

5.0 OVERVIEW OF DEMONSTRATION MODELING

The prescriptive liner design uses on-site soils and a geocomposite for the leachate collection layer; and a prescriptive flexible membrane liner and geosynthetic clay liner (GCL) are used as the composite liner. In the proposed alternate final cover design, an ET cover system will be used for the 122.9 acres \pm final cover (8.9 acres with 5% \pm sloped area and 114 acres with 4H \pm :1V slope area). Gordon Environmental, Inc. (GEI) has prepared a performance demonstration for an alternate landfill final cover design.

Because the SCLF Facility is planning to use an alternate design for its final cover system, the HELP model simulation analyses were organized to support three demonstrations:

- First, evaluate the performance of the prescriptive liner system. GEI has performed the HELP model simulation analysis for SCLF Facility that meets the requirements of the Guidance Document (**Attachment III.10.C**). This simulation is presented in Section 6.2.
- Second, demonstrate that percolation through the alternate final cover system does not create a “bathtub” effect within the landfill. GEI has performed the HELP model simulation analysis for the SCLF Facility that meets the requirements of the Guidance Document (**Attachment III.10.C**). This simulation is presented in Section 6.3.
- Third, demonstrate that the performance of the prescriptive liner ensures that the uppermost aquifer will be protected. GEI has performed HELP model simulation analyses for the SCLF Facility that meet the requirements of the Guidance Document

(**Attachment III.10.C**) for a Tier II prescriptive liner demonstration. Those simulations are presented in Section 6.4. In addition, the depth to groundwater is at least 100 ft. below basegrade, as document in **Volume IV.2**.

- Fourth, demonstrate the performance of the intermediate cover on Unit III during a 10-year period before the Unit becomes operational and placement of waste from the existing waste mass grades to final grades begin.

6.0 HELP MODEL DEMONSTRATION ANALYSES

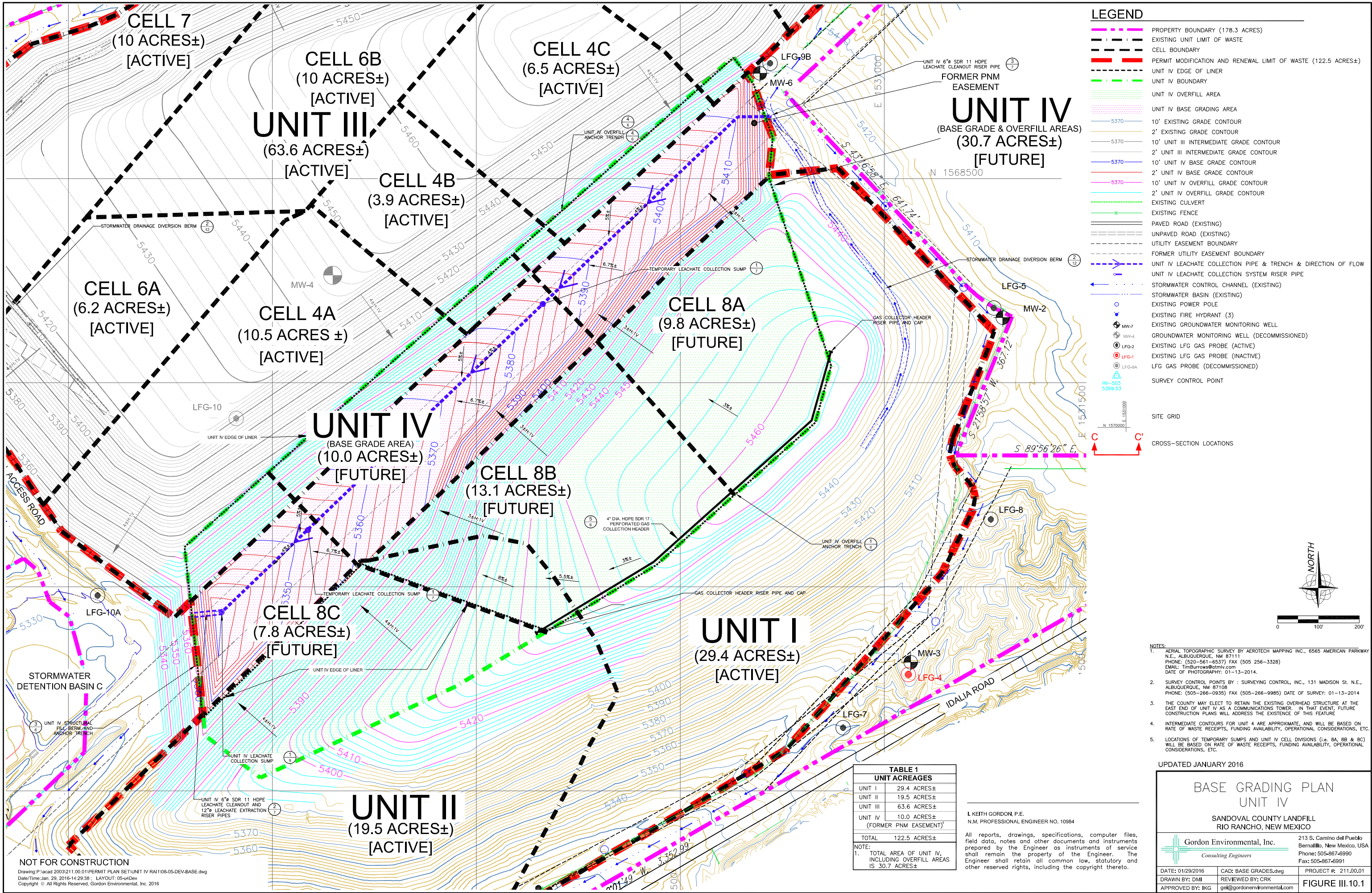
In each of the following three demonstrations, the input parameters for the HELP model have been selected in accordance with the Guidance Document (**Attachment III.10.C**).

6.1 Design Parameters

Slope steepness and lateral drainage distance for the landfill cover were selected using the design parameters for the SCLF Facility. The longest lateral drainage distances and the shallowest slope were used for the purpose of modeling to obtain conservative results. The basegrade for the Unit IV floor has a minimum design slope of 5.0%, and the longest lateral drainage distance is 200 ft. (**Figure III.10.1**). The shallowest design slope for the alternative final cover system is 5%, with a longest lateral drainage distance of 258 ft for an area of 8.9 acres \pm ; and 25%, with a longest lateral drainage distance of 650 ft for an area of 114.0 acres \pm (**Figure III.10.2**). Throughout these analyses, the following design parameters therefore have been used:

- Liner system:
 - lateral drainage distance = 200 ft.
 - slope = 5%
 - area = 30.7 acres \pm
- Final cover system: (5% \pm sloped area)
 - lateral drainage distance = 258 ft.
 - slope = 5%
 - cap area = 8.9 acres \pm
- Final cover system: (4H \pm :1V sloped area)
 - lateral drainage distance = 650 ft.
 - slope = 25%
 - cap area = 114.0 acres \pm

The outputs from the HELP model runs, which include a listing of the input parameters, are provided as attachments to this document in both hard copy (**Attachment III.10.A**) and electronic format (**Attachment III.10.E**).



LEGEND

- PROPERTY BOUNDARY (178.3 ACRES)
- EXISTING UNIT LIMIT OF WASTE
- CELL BOUNDARY
- PERMIT MODIFICATION AND RENEWAL LIMIT OF WASTE (122.5 ACRES±)
- UNIT IV EDGE OF LINER
- UNIT IV BOUNDARY
- UNIT IV OVERFILL AREA
- UNIT IV BASE GRADING AREA
- 10' EXISTING GRADE CONTOUR
- 2' EXISTING GRADE CONTOUR
- 10' UNIT III INTERMEDIATE GRADE CONTOUR
- 2' UNIT III INTERMEDIATE GRADE CONTOUR
- 10' UNIT IV BASE GRADE CONTOUR
- 2' UNIT IV BASE GRADE CONTOUR
- 10' UNIT IV OVERFILL GRADE CONTOUR
- 2' UNIT IV OVERFILL GRADE CONTOUR
- EXISTING CULVERT
- EXISTING FENCE
- PAVED ROAD (EXISTING)
- UNPAVED ROAD (EXISTING)
- UTILITY EASEMENT BOUNDARY
- FORMER UTILITY EASEMENT BOUNDARY
- UNIT IV LEACHATE COLLECTION PIPE & TRENCH & DIRECTION OF FLOW
- UNIT IV LEACHATE COLLECTION SYSTEM RISER PIPE
- STORMWATER CONTROL CHANNEL (EXISTING)
- STORMWATER BASIN (EXISTING)
- EXISTING POWER POLE
- EXISTING FIRE HYDRANT (3)
- EXISTING GROUNDWATER MONITORING WELL
- GROUNDWATER MONITORING WELL (DECOMMISSIONED)
- EXISTING LFG GAS PROBE (ACTIVE)
- EXISTING LFG GAS PROBE (INACTIVE)
- LFG GAS PROBE (DECOMMISSIONED)
- SURVEY CONTROL POINT

SITE GRID

CROSS-SECTION LOCATIONS

- NOTES:
- AERIAL TOPOGRAPHIC SURVEY BY AEROTECH MAPPING INC., 6565 AMERICAN PARKWAY N.E., ALBUQUERQUE, NM 87111
PHONE: (520-561-6537) FAX (505-256-3328)
EMAIL: TimBurrows@aerotech.com
DATE OF PHOTOGRAPHY: 01-13-2014.
 - SURVEY CONTROL POINTS BY : SURVEYING CONTROL, INC., 131 MADISON ST. N.E., ALBUQUERQUE, NM 87108
PHONE: (505-266-0935) FAX (505-266-9985) DATE OF SURVEY: 01-13-2014
 - THE COUNTY MAY ELECT TO RETAIN THE EXISTING OVERHEAD STRUCTURE AT THE EAST END OF UNIT IV AS A COMMUNICATIONS TOWER. IN THAT EVENT, FUTURE CONSTRUCTION PLANS WILL ADDRESS THE EXISTENCE OF THIS FEATURE.
 - INTERMEDIATE CONTOURS FOR UNIT 4 ARE APPROXIMATE, AND WILL BE BASED ON RATE OF WASTE RECEIPTS, FUNDING AVAILABILITY, OPERATIONAL CONSIDERATIONS, ETC.
 - LOCATIONS OF TEMPORARY SUMPS AND UNIT IV CELL DIVISIONS (I.e. 8A, 8B & 8C) WILL BE BASED ON RATE OF WASTE RECEIPTS, FUNDING AVAILABILITY, OPERATIONAL CONSIDERATIONS, ETC.

UPDATED JANUARY 2016

BASE GRADING PLAN
UNIT IV

SANDOVAL COUNTY LANDFILL
RIO RANCHO, NEW MEXICO

Gordon Environmental, Inc.
Consulting Engineers

213 S. Camino del Pueblo
Bernalillo, New Mexico, USA
Phone: 505-867-6990
Fax: 505-867-6991

DATE: 01/29/2016 CAD: BASE GRADES.dwg PROJECT #: 211.00.01
DRAWN BY: DMI REVIEWED BY: CRK
APPROVED BY: IKG gsk@gordonenvironmental.com

FIGURE III.10.1

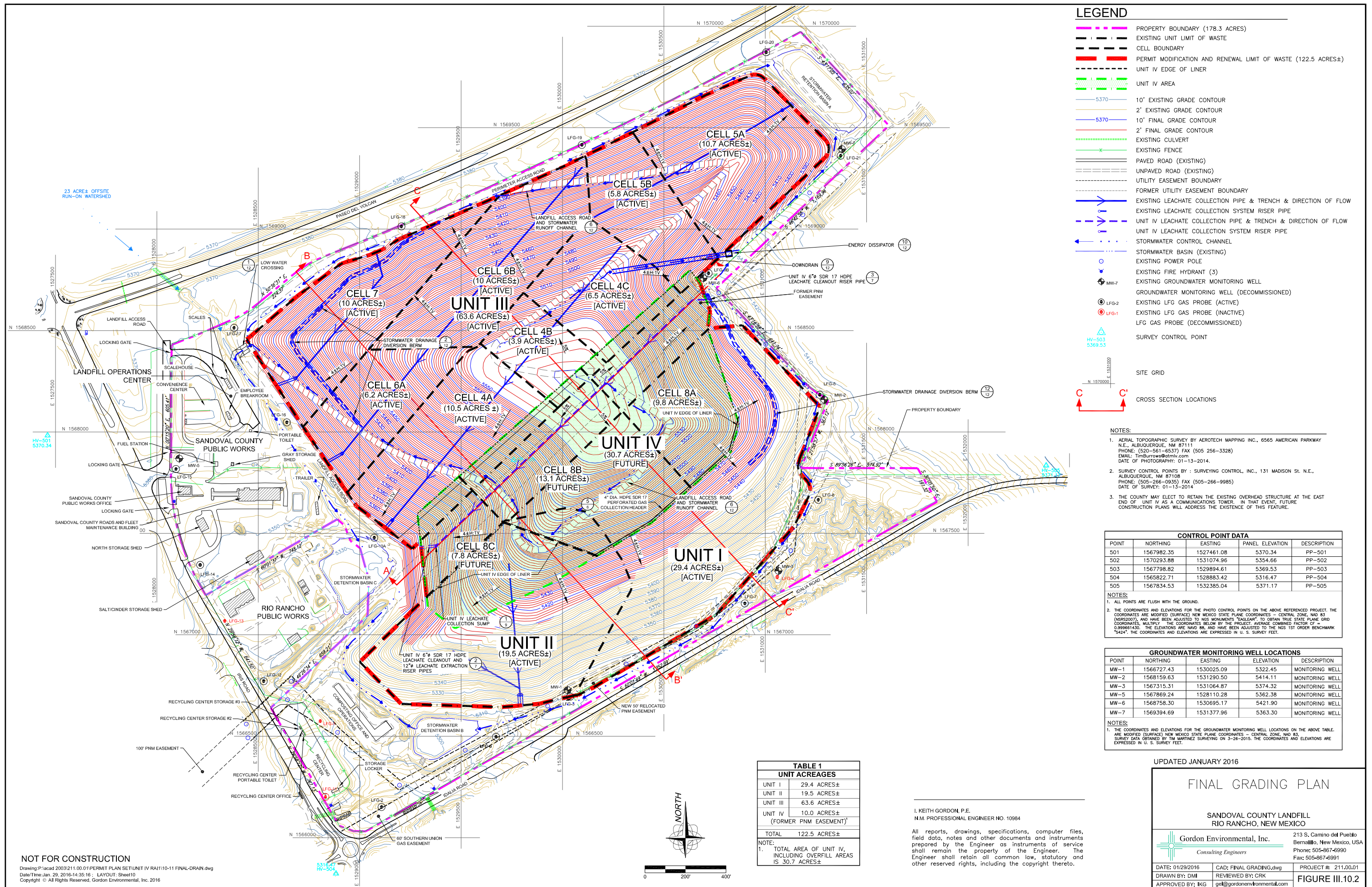
TABLE 1 UNIT ACREAGES	
UNIT I	29.4 ACRES±
UNIT II	19.5 ACRES±
UNIT III	63.6 ACRES±
UNIT IV	10.0 ACRES±
(FORMER PNM EASEMENT)	
TOTAL	122.5 ACRES±

NOTE:
1. TOTAL AREA OF UNIT IV, INCLUDING OVERFILL AREAS IS 30.7 ACRES±

I. KEITH GORDON, P.E.
N.M. PROFESSIONAL ENGINEER NO. 10984

All reports, drawings, specifications, computer files, field data, notes and other documents and instruments prepared by the Engineer as instruments of service shall remain the property of the Engineer. The Engineer shall retain all common law, statutory and other reserved rights, including the copyright thereto.

NOT FOR CONSTRUCTION
Drawing: P:\acad 2003\211.00.01\PERMIT PLAN SET\UNIT IV RAI\108-05-DEV-BASE.dwg
Date/Time: Jan. 29, 2016-14:29:38 LAYOUT: 05-u4Dev
Copyright © All Rights Reserved, Gordon Environmental, Inc. 2016



6.2 Tier I Prescriptive Liner Demonstration

One HELP model simulation analysis has been performed to support the Tier I liner demonstration. In this demonstration, the performance of the prescriptive liner design is evaluated. The simulation analysis has been numbered to correspond to the Guidance Document (**Attachment III.10.C**).

6.2.1 Prescriptive Liner System Design

The design for the prescriptive liner system includes the following layers from the top down:

- 24-in. protective/drainage layer using on-site soils ($k \geq 5.0 \times 10^{-5}$ cm/sec)
- FML (60-mil HDPE)
- Geosynthetic Clay Liner
- Compacted subgrade/structural fill to 90% standard Proctor dry density

In the prescriptive liner design, on-site soils are used for the leachate collection layer; and a flexible membrane liner and geosynthetic clay liner (GCL) are used as the composite liner.

6.2.2 HELP Model Input Parameters

6.2.2.1 Soils

20.9.4.13 NMAC requires that the protective drainage layer be constructed using granular soils that contain no more than 5% fines by weight (e.g., material passing a No. 200 sieve) and that have a uniformity coefficient (C_u) less than 6.0. As part of the design for the prescriptive liner system, SCLF proposes to use on-site soils in the PSL that may have a fines content up to 15%, and a C_u of $\leq 7.5\%$.

Geotechnical analyses of on-site soils indicate that the soils available at the SCLF site consist primarily of a mixture of silts with varying amounts of sand (SP-SM, well-graded silt with sand) and that they meet the proposed criteria for the protective soil layer. **Attachment III.10.B** provides a summary of geotechnical test results for soils excavated from Cells 4C, 6B and 7 during their construction in the summer of 2014. The on-site soil that SCLF proposes to use is within the range of soil types applied in this modeling based on the sieve analyses conducted on on-site soils (**Attachment III.10.B**). The type of soil used to represent the protective soil layer in the simulation for the Tier I liner demonstration is listed below:

Soil Description	HELP Model Soil Type	USCS Soil Type
Silty Sand	6	SM

It is anticipated, that as on-site stockpiled soils are used as PSL, the resulting mixture of soils will be best represented by the USCS classification SM, silty sand. Waste layers were modeled as HELP Model soil type 18 with default HELP Model values used for all parameters.

The primary parameters that differentiate soils from one another are the saturated hydraulic conductivity, K_{sat} , and the moisture-retention characteristics which are related to the field capacity and the wilting point. As the HELP model soil type number increases, the saturated hydraulic conductivity decreases, and the soils tend to retain more water and hold it more strongly. Default values from the HELP model were assigned to the porosity, field capacity, and wilting point for each layer material type.

6.2.2.2 Environmental Factors

Precipitation and temperature data were derived from the National Climatic Data Center's Summary of the Day database. The nearest station location with sufficient data (i.e., minimum of 40 years of data) is Albuquerque, NM (290234).

The Tier I simulations use data from 1984 through 1988, the wettest five consecutive year period from the most recent forty-year period for which complete records existed at the time these simulations were performed. Solar radiation data were synthetically generated by the HELP model based on coefficients for Albuquerque, NM, and on the latitude of the site (e.g., 35.30°). Evapotranspiration data (e.g., average wind speed and seasonal relative humidity) were also obtained from El Paso, Texas. The evaporative zone depth was set to 18 inches for bare soil; and the maximum leaf area index was set to 0.0 for no vegetation.

6.2.2.3 Initial Conditions

In each of the Tier I liner simulation analyses, the initial moisture content for each material in the liner systems was calculated using the equation suggested by the NMED Guidance Document:

$$\theta_i = \theta_{wp} + 0.25(\theta_{fc} - \theta_{wp}) \quad (2)$$

Where:

θ_i	=	the initial water content
θ_{wp}	=	the wilting point
θ_{fc}	=	the field capacity

6.2.3 Tier I Prescriptive Liner Simulation Analysis

In the Tier I liner simulation analysis, the landfill has conservatively been assumed to be in an open condition with no waste present with 100% precipitation retained within the landfill; and there is no runoff. The FML was represented by using the default parameters for soil type 35 from the HELP model. The GCL layer in the prescriptive liner system was represented by using the default parameters for HELP soil type 17 and $K_{sat} = 5.0 \times 10^{-9}$ cm/sec. The compacted subgrade in the 30.7 acres \pm for Unit IV prescriptive liner system was represented by using the default parameters for HELP soil type 6 with a permeability of 4.2×10^{-6} cm/sec to represent compacted on-site soils to 90% standard Proctor dry density (**Attachment III.10.B**).

The first Tier I simulation analysis (Simulation 5-1) is based on Simulation 5 of the Guidance Document (**Attachment III.10.C**). This analysis evaluates the performance of the prescriptive liner system prescribed by the regulations (20.9.4.13.E.(3) NMAC) using on-site soils as the protective/drainage soil layer. The input parameters used to represent the prescriptive liner system are provided in **Table III.10.1**. The landfill was modeled as “active” with 0% of the surface area available for stormwater runoff. The performance of the prescriptive liner system; is the average annual percolation rate calculated by the HELP model as provided in **Table III.10.2**. For the soil type analyzed, the hydraulic head on the FML is 4.961 inches; which is less than the regulatory standard of 12 inches.

6.3 Tier I Alternate Final Cover Demonstration

HELP model simulations have been performed to support the Tier I 122.9 acre \pm (8.9 acres with 5% \pm slopes and 114 acres with 4H \pm :1V slopes) alternate final cover demonstration. In this demonstration, the performance of the alternate final cover system is compared to the performance of the prescriptive liner system analyzed in Simulation 5-1. The alternate final cover must achieve equivalent reduction of infiltration as the bottom liner as to not to create a “bathtub” effect where percolation through the alternate final cover does not exceed that of the prescriptive liner system. The simulation analysis (Simulation 3-1) is based on Simulation 3 in the Guidance Document (**Attachment III.10.C**).

TABLE III.10.1
Tier I, Simulation 5-1: Prescriptive Liner System (30.7 acres ±)
Sandoval County Landfill

Simulation	Protective/Drainage Soil Layer			FML			GCL			Compacted Subgrade/Structural Fill		
	HELP Model Soil Type	Layer Thickness (in)	K _{sat} (cm/s)	HELP Model Soil Typ22 00e	FML	K _{sat} (cm/s)	HELP Model Soil Type	Layer Thickness (in)	K _{sat} (cm/s)	HELP Model Soil Type	Layer Thickness (in)	K _{sat} (cm/s)
5-1	6	24	3.0 x 10 ⁻⁴	35	60-mil HDPE	2.0 x 10 ⁻¹³	17	0.25	5.0 x 10 ⁻⁹	6	6	4.2 x 10 ⁻⁶

TABLE III.10.2
Tier I, Performance Results for Prescriptive Liner System (30.7 acres ±)
Sandoval County Landfill

Liner System	Simulation	Soil Type for Protective Soil Layer	Average Annual Percolation Rate Through Bottom Liner (in/yr)	Average Annual Head on HDPE Liner (in)
Prescriptive	5-1	7	0.00000	4.961

6.3.1 Alternate Final Cover System Design

The alternate final cover system includes the following layers from the top down:

- 6-in. Vegetative (Erosion) Layer
- 30-in. Barrier (Infiltration) Layer
- 12-in. Intermediate Soil Cover layer

6.3.2 HELP Model Input Parameters

6.3.2.1 Soils

The type soil type that was used to represent the vegetative (erosion), barrier (infiltration), and intermediate cover layers in the simulation for the 122.9 acre \pm (8.9 acres with 5% \pm slopes and 114 acres with 4H \pm : 1V slopes) alternate final cover demonstration is listed below.

Soil Description	HELP Model Soil Type	USCS Soil Type
Silty Sand	6	SM

Default values from the HELP model were assigned to the porosity, field capacity, and wilting point for this soil type. Soil analysis conducted on on-site soils indicated at 90% of maximum standard Proctor dry density, $K_{\text{sat}} = 7.2 \times 10^{-4}$; and this value was used for modeling purposes.

The HELP model automatically accounts for the effects of root channels and decay whenever vegetation is assumed to be present on the vegetative (erosion) layer, and this zone is placed uncompacted. The model multiplied the saturated hydraulic conductivity by a factor of 1.6 to account for these potential effects in the vegetative (erosion) layer.

6.3.2.2 Environmental Factors

For the Tier I alternate final cover simulation analysis, the environmental loading conditions listed below were the same as those used in Simulation 5-1:

- precipitation (1984 through 1988)
- temperature (1984 through 1988)
- solar radiation
- evapotranspiration.

The evaporative zone depth for the cover system was set to 28 inches and the maximum leaf area index was set to 0.8. Vegetation on the cover was modeled as “poor stand of grass”.

6.3.2.3 Initial Conditions

The initial moisture contents for the alternate final cover system were calculated using Equation (2).

6.3.3 Alternate Final Cover Simulation Analysis

This simulation analysis (Simulation 3-1) is based on Simulation 3 of the Guidance Document (**Attachment III.10.C**). This analysis evaluates the performance of the 122.9 acre \pm (8.9 acres with 5% \pm slopes and 114 acres with 4H \pm : 1V slopes) alternate final cover system as to not create a “bathtub” effect in the landfill where the percolation through the alternate final cover does not exceed that of the prescriptive liner system. The input parameters used to represent the alternate final cover system are provided in **Table III.10.3**. In the simulation analysis for the alternative final cover, the landfill has been assumed to be in a closed condition with 100% of the surface area available for stormwater runoff.

TABLE III.10.3
Tier I, Simulation 3-1: Alternate Final Cover System
122.9 acre \pm (8.9 acres with 5% \pm slopes and 114 acres with 4H \pm : 1V slopes)
Sandoval County Landfill

Simulation	Vegetative (Erosion) Layer			Barrier (Infiltration) Layer			Intermediate Soil Cover		
	HELP Model Soil Type	Layer Thickness (in)	K _{sat} (cm/s)	HELP Model Soil Type	Layer Thickness (in)	K _{sat} (cm/s)	HELP Model Soil Type	Layer Thickness (in)	K _{sat} (cm/s)
3-1	6	6	7.2 x 10 ⁻⁴	6	30	7.2 x 10 ⁻⁴	6	12	7.2 x 10 ⁻⁴

6.3.4 Tier I Alternate Final Cover Demonstration Results

According to the Guidance Document (**Attachment III.10.C**), an alternate cover system is considered acceptable if its performance has been demonstrated to be equal to or better than the permeability performance of the prescriptive liner system. The performance measure is the average annual rate of percolation through the bottom layer of the liner versus the cover system. Performance is evaluated by comparing the percolation rate calculated for the alternate

cover system to that calculated for the prescriptive liner system. The average annual percolation rates calculated for the two systems are summarized in **Table III.10.4**.

TABLE III.10.4
Tier I, Performance Results for Prescriptive Liner and Alternate Final Cover Systems
Sandoval County Landfill

System	Simulation	HELP Model Soil Type		Average Annual Percolation Rate (in/yr)
		Protective Drainage Layer	Barrier (Infiltration) Layer	
Alternate Final Cover (Average of 5% Percolation and 25% Percolation)¹	3-1	—	6	0.000009
Prescriptive Liner	5-1	6	—	0.000000

Note: 1. Average percolation based on area and percolation as calculated by HELP Model: $[(8.9 \text{ acres})(0.00000 \text{ in.}) + (114 \text{ acres})(0.00001 \text{ in.})]/(122.9 \text{ acres}) = 0.000009 \text{ in.}$

When the alternate cover system barrier (infiltration) layer is modeled using HELP model soil type 6, the rate of percolation calculated for the alternate final cover system is equivalent to the percolation rate calculated for the prescriptive liner system (as referenced in **Attachment III.10.C**; “If the two Average Annual Percolation values are within 0.00001 of each other, then the demonstration is successful since these values are practically equal (the definition of equivalent) and well within modeling uncertainty”). Therefore, the performance of the alternate final cover system design using soil type 6 meets the Tier I demonstration requirements.

6.4 Tier II Prescriptive liner and Alternate Final Cover Demonstration

Four HELP model simulation analyses (Simulations 7-1 through 10-1) based on Simulations 7 through 10 of the Guidance Document (**Attachment III.10.C**) have been performed to support the Tier II liner and cover demonstration. In this demonstration, the performance of the finished liner and cover systems is evaluated to ensure that the uppermost aquifer will be protected. The evaluation is based on the results of a series of simulations that represent hypothetical operating conditions over the life and closure of the landfill.

6.4.1 Liner and Cover System Design

The alternate cover and prescriptive liner systems include the following layers from the top down:

- 6-in. vegetative (erosion) layer
- 30-in. barrier (infiltration) layer
- 12-in. intermediate cover
- Waste (thickness varies)
- 24-in. protective soil layer
- 60-mil HDPE Liner
- Geosynthetic Clay Liner
- Compacted Subgrade/Structural Fill

Note that not all layers are present in every simulation.

6.4.2 HELP Model Input Parameters

6.4.2.1 Soils

The type of soil that was used to represent the vegetative (erosion) layer, barrier (infiltration) layer, intermediate cover layer, and protective soil layer used in the simulations for the Tier II demonstration is listed below.

Soil Description	HELP Model Soil Type	USCS Soil Type
Silty Sand	6	SM

Default values from the HELP model were assigned to the porosity, field capacity, and wilting point for this soil type. Soil analysis conducted on on-site soils indicated at 90% of maximum dry density $K_{sat} = 7.2 \times 10^{-4}$, (except for the uncompacted vegetative (erosion) layer) and this value was used for modeling purposes.

6.4.2.2 Environmental Factors

Precipitation and temperature data were derived from the National Climatic Data Center for 1917 through 2014. The nearest station location with sufficient data is Albuquerque, NM (290234). Various portions of the climate data sets were used in each simulation as described in **Table III.10.5**.

TABLE III.10.5
Tier II, Climate Data
Sandoval County Landfill

Simulation	Description of Climate Data	Period of Synthetically Generated Precipitation Data
7-1	First two of the five wettest years	2 years
8-1	Five wettest years	5 years
9-1	First two of the thirty years	2 years
10-1	Final twenty-eight of the thirty years	28 years

The evaporative zone depth, the maximum leaf area index and the type of vegetation on the surface varied from one simulation to the next due to the type of vegetation being modeled. The parameters used for each HELP model simulation are listed in **Table III.10.6**.

TABLE III.10.6
Tier II, Evaporative Zone Depth, Maximum Leaf Area Index and Type of Vegetation
Sandoval County Landfill

Simulation	Evaporative Zone Depth (in)	Maximum Leaf Area Index	Type of Vegetation
7-1	18	0.0	Bare ground
8-1	18	0.0	Bare ground
9-1	18	0.0	Bare ground
10-1	28	0.8	Poor stand of grass

6.4.2.3 Initial Conditions

The initial moisture contents for Simulations 7-1 through 10-1 were calculated using Equation (2) or derived from the moisture-content output from the previous simulation in the sequence. The methods used to select the initial moisture conditions for each layer for each simulation are listed in **Table III.10.7**.

6.4.3 Tier II Prescriptive liner and Alternate Final Cover Simulation Analyses

Four stages of landfill operations, numbered to correspond with the Guidance Document (**Attachment III.10.C**), were simulated to satisfy the Tier II demonstration requirements:

- Simulation 7-1: open conditions for a two-year start-up period, when the landfill contains no waste.
- Simulation 8-1: partially filled conditions for five years, with intermediate cover.
- Simulation 9-1: closed conditions with bare ground for the initial two-year post-closure care period.
- Simulation 10-1: closed conditions with poor vegetation for the remaining twenty-eight years of the post-closure care period.

TABLE III.10.7
Tier II, Methods Used to Establish Initial Moisture Conditions
Sandoval County Landfill

Simulation	Layers	Method
7-1	24-in. protective drainage layer	Equation (2)
	FML (60-mil HDPE)	
	GCL	
	Compacted Subgrade/Structural Fill	
8-1	12.11.-in. intermediate cover layer	Equation (2)
	20-ft waste layer	Output from Simulation 7
	24-in. protective drainage layer	
	FML (60-mil HDPE)	
	GCL	
	Compacted Subgrade/Structural Fill	
9-1	6-in. vegetative (erosion) layer	Equation (2)
	30-in. barrier (infiltration) layer	Output from Simulation 8
	12-in. intermediate cover	
	173-ft waste layer	
	24-in. protective drainage layer	
	FML (60-mil HDPE)	
	GCL	
	Compacted Subgrade/Structural Fill	
10-1	6-in. vegetative (erosion) layer	Output from Simulation 9
	30-in. barrier (infiltration) layer	
	12-in. intermediate cover	
	173-ft waste layer	
	24-in. protective drainage layer	
	FML (60-mil HDPE)	
	GCL	
	Compacted Subgrade/Structural Fill	

6.4.3.1 Simulation 7-1, Open Landfill, No Waste

Simulation 7-1 models the landfill in an open condition over a two-year start-up period. This condition is based on the assumptions that no waste is present in the landfill and that the Unit IV liner system is fully exposed to the weather. The model included the following layers from the top down:

- 24-in. protective soil layer
- 60-mil HDPE Liner
- GCL
- Compacted subgrade/structural fill

The input parameters used to represent the layer configuration for Simulation 7-1 are listed in **Table III.10.8**. The landfill was conservatively modeled as “active”, with 0% of the surface area available for stormwater runoff.

6.4.3.2 Simulation 8-1, Partially Filled Landfill

Simulation 8-1 models the landfill under partially filled conditions with intermediate cover for a five-year period. The model included the following layers from the top down:

- 12-in. intermediate cover layer
- 20-ft waste layer
- 24-in. protective soil layer
- 60-mil HDPE Liner
- GCL
- Compacted subgrade/structural fill

The input parameters used to represent the layer configuration for Simulation 8-1 are listed in **Table III.10.9**. The landfill was conservatively modeled as “active”, with 0% of the surface area available for stormwater runoff.

TABLE III.10.8
Tier II, Simulation 7-1: Open Landfill, No Waste
Sandoval County Landfill

Simulation	Protective/Drainage Soil Layer			FML			GCL			Compacted Subgrade/Structural Fill		
	HELP Model Soil Type	Layer Thickness (in)	K _{sat} (cm/s)	HELP Model Soil Type	FML	K _{sat} (cm/s)	HELP Model Soil Type	Layer Thickness (in)	K _{sat} (cm/s)	HELP Model Soil Type	Layer Thickness (in)	K _{sat} (cm/s)
7-1	6	24	3.0 x 10 ⁻⁴	35	60-mil HDPE	2.0 x 10 ⁻¹³	17	0.25	5.0 x 10 ⁻⁹	6	6	4.2 x 10 ⁻⁶

TABLE III.10.9
Tier II, Simulation 8-1: Partially Filled Landfill
Sandoval County Landfill Permit

Simulation	Intermediate Cover Layer			Waste Layer			Protective/Drainage Soil Layer			FML			GCL			Compacted Subgrade/Structural Fill		
	HELP Model Soil Type	Layer Thickness (in)	K _{sat} (cm/s)	HELP Model Soil Type	Layer Thickness (ft)	K _{sat} (cm/s)	HELP Model Soil Type	Layer Thickness (in)	K _{sat} (cm/s)	HELP Model Soil Type	FML	K _{sat} (cm/s)	HELP Model Soil Type	Layer Thickness (in)	K _{sat} (cm/s)	HELP Model Soil Type	Layer Thickness (in)	K _{sat} (cm/s)
8-1	6	12	7.2 x 10 ⁻⁴	18	20	1.0 x 10 ⁻³	6	24	3.0 x 10 ⁻⁴	35	60-mil HDPE	2.0 x 10 ⁻¹³	17	0.25	5.0 x 10 ⁻⁹	6	6	4.2 x 10 ⁻⁶

6.4.3.3 Simulation 9-1, Closed Landfill, No Cover Vegetation

Simulation 9-1 conservatively models the landfill in the closed condition with no cover vegetation for the first two years of the thirty-year post-closure care period. The model included the following layers from the top down:

- 6-in. vegetative (erosion) layer
- 30-in. barrier (infiltration) layer
- 12-in. intermediate cover
- 173-ft waste layer
- 24-in. protective soil layer
- 60-mil HDPE Liner
- GCL
- Compacted subgrade/structural fill

The input parameters used to represent the layer configuration for Simulation 9-1 are listed in **Table III.10.10**. The landfill was modeled as “closed” with 100% of the surface area available for stormwater runoff.

6.4.3.4 Simulation 10-1, Closed Landfill, Partial Cover Vegetation

Simulation 10-1 models the landfill in the closed condition with poor cover vegetation for the final 28 years of the 30-year post-closure care period. The layers included in the model were the same as those for Simulation 9-1:

- 6-in. vegetative (erosion) layer
- 30-in. barrier (infiltration) layer
- 12-in. intermediate cover
- 173-ft waste layer
- 24-in. protective soil layer
- 60-mil HDPE Liner
- GCL
- Compacted subgrade/structural fill

The input parameters used to represent the layer configuration for Simulation 10-1 are listed in **Table III.10.11**. The landfill was modeled as “closed” with 100% of the surface area available for stormwater runoff.

TABLE III.10.10
Tier II, Simulation 9: Closed Landfill, No Cover Vegetation
Sandoval County Landfill

Simulation	Vegetative (Erosion) Layer			Barrier (Infiltration) Layer			Waste Layer			Protective/Drainage Soil Layer			FML			GCL			Compacted Subgrade/Structural Fill		
	HELP Model Soil Type	Layer Thick-ness (in)	K _{sat} (cm/s)	HELP Model Soil Type	Layer Thick-ness (in)	K _{sat} (cm/s)	HELP Model Soil Type	Layer Thick-ness (ft)	K _{sat} (cm/s)	HELP Model Soil Type	Layer Thick-ness (in)	K _{sat} (cm/s)	HELP Model Soil Type	FML	K _{sat} (cm/s)	HELP Model Soil Type	Layer Thick-ness (in)	K _{sat} (cm/s)	HELP Model Soil Type	Layer Thick-ness (in)	K _{sat} (cm/s)
9-1	6	6	7.2 x 10 ⁻⁴	7	30	7.2 x 10 ⁻⁴	18	173	1.0 x 10 ⁻³	6	24	3.0 x 10 ⁻⁴	35	60-mil HDPE	2.0 x 10 ⁻¹³	17	0.25	5.0 x 10 ⁻⁹	6	6	4.2 x 10 ⁻⁶

TABLE III.10.11
Tier II, Simulation 10: Closed Landfill, Partial Vegetation
Sandoval County Landfill

Simulation	Vegetative (Erosion) Layer			Barrier (Infiltration) Layer			Waste Layer			Protective/Drainage Soil Layer			FML			GCL			Compacted Subgrade/Structural Fill		
	HELP Model Soil Type	Layer Thick-ness (in)	K _{sat} (cm/s)	HELP Model Soil Type	Layer Thick-ness (in)	K _{sat} (cm/s)	HELP Model Soil Type	Layer Thick-ness (ft)	K _{sat} (cm/s)	HELP Model Soil Type	Layer Thick-ness (in)	K _{sat} (cm/s)	HELP Model Soil Type	FML	K _{sat} (cm/s)	HELP Model Soil Type	Layer Thick-ness (in)	K _{sat} (cm/s)	HELP Model Soil Type	Layer Thick-ness (in)	K _{sat} (cm/s)
10-1	6	6	7.2 x 10 ⁻⁴	6	30	7.2 x 10 ⁻⁴	18	173	1.0 x 10 ⁻³	6	24	3.0 x 10 ⁻⁴	35	60-mil HDPE	2.0 x 10 ⁻¹³	17	0.25	5.0 x 10 ⁻⁹	6	6	4.2 x 10 ⁻⁶

6.4.4 Tier II Prescriptive liner and Alternate Final Cover Demonstration Results

According to the Guidance Document (**Attachment III.10.C**), a combined prescriptive liner system and alternate cover system is considered acceptable if its performance meets the following Tier II criteria:

Simulation	Performance Criterion
7-1	Determine percolation through bottom of the liner system.
8-1	Percolation rate through the bottom of the liner system should be zero at the end of the simulation.
9-1	Average annual percolation rate through the bottom of the liner system must be zero.
10-1	Average annual percolation rate through the bottom of the liner system must be zero.

The percolation rates calculated for the prescriptive liner and alternate final cover systems modeled in these demonstration analyses are summarized in **Table III.10.12**.

TABLE III.10.12
Tier II, Performance Results for Prescriptive Liner and Alternate Final Cover Systems
Sandoval County Landfill

Simulation	HELP Model Soil Type			Percolation Rate for Fifth Year (in/yr)	Average Annual Percolation Rate (in/yr)
	Protective Soil Layer	Vegetative (Erosion) and Intermediate Cover Layers	Barrier (Infiltration) Layer		
7-1	6	6	6	—	0.00000
8-1				0.00000	0.00000
9-1				—	0.00000
10-1				—	0.00000

The finished landfill, including both the prescriptive liner system and the alternate final cover system, has been modeled using on-site soils in the vegetative (erosion), barrier (infiltration), intermediate cover, and protective soil layers. The soil types modeled are representative of the soils that exist on the SCLF site and that will be used to construct these layers.

The percolation rate calculated for the fifth year of Simulation 8–1 is zero; and the annual average percolation rates calculated for Simulations 9-1 and 10-1 are zero. Therefore, the performance of the prescriptive liner and alternate final cover designs meets the Tier II demonstration requirements for the soil types modeled for the vegetative (erosion) layer, protective soil layer, intermediate cover layer, and barrier (infiltration) layer.

7.0 HELP MODEL DEMONSTRATION ANALYSES INTERMEDIATE COVER UNIT III

GEI performed HELP Model Analyses for Unit III to evaluate the performance of intermediate cover installed on the Unit for the longevity of approximately 10 years; the time period for which Unit III is estimated to remain with intermediate cover prior to becoming operational again. Once operational again, Unit III will be filled to reach final design grades.

HELP Model Analyses were performed for Unit III to estimate the moisture content of the waste mass during the period from reaching the intermediate grades shown on **Figure III.10.1** and becoming operational as Unit IV reaches these intermediate grades; and “overfilling” onto Unit III will begin. HELP Modeling was performed based on the following:

- Unit III has an approximate longevity of 21 years to reach the intermediate grades shown on **Figure III.10.1** (i.e., January 2015 to January 2036).
- Unit IV will be constructed after Unit III reaches the intermediate grades; and “overfilling” onto Unit III will begin approximately 10 years (i.e., January 2036 to January 2046) following construction of the Unit IV liner system.

7.1 Unit III Ten Year Waste Mass Demonstration Analysis

The HELP Model input parameters used in the Unit III analysis of the waste mass and liner components that will be in-place for 10 years (i.e., January 2036 – January 2046) were based on the NMED Guidance Document. Specifically, the input data were used in accordance with the Guidance Document:

- Five wettest years of precipitation from Albuquerque, NM (1984 – 1988) averaging 13.92 in. per year. These data were conservatively used to synthetically generate 10 years of precipitation data for use in the modeling.
- The input data for evapotranspiration and solar radiation were synthetically generated by the HELP model for the 10 year period based on coefficients for Albuquerque, NM

and the Latitude of SCLF (e.g. 35.30°), respectively.

- The evaporative zone depth was set to 18 in. for “bare ground”.
- The area available for runoff: To account for the approximately 70 ft of waste mass above existing grade, the entire area (60.4 acres±) was allowed to drain stormwater (i.e, 100% available area for runoff).
- The maximum leaf area index was set to 0.0 for no vegetation.
- Initial moisture content for each material was calculated using Equation 2.

The liner system design for Cells in Unit III and used in the modeling consisted of the following (from top to bottom) [CQA Reports for Cells 4A, 4B, 4C, 5A, 5B, 6B and 7 construction]:

- 24-in. protective soil/leachate drainage layer ($k = 3 \times 10^{-4}$ cm/sec) [minimum PSL hydraulic conductivity reported in the CQA Reports for cells constructed in Unit III]
- 60-mil HDPE geomembrane
- 0.25-in. GCL ($k = 5 \times 10^{-9}$ cm/sec)
- 6 -in. compacted subgrade ($k = 4.2 \times 10^{-6}$ cm/sec) [Average hydraulic conductivity of on-site soils (i.e., SP-SM) compacted to 90% standard Proctor dry density (**Attachment III.10.B**).

The base grade design parameters for Cells in Unit III are based on the as-built base grade surveys completed as part of the CQA Reports; and are as follows:

- Longest lateral drainage distance = 420 ft
- Base grade slope = 2.8%

The input parameters used to represent Unit III soil and liner components are provided in **Table III.10.13**.

TABLE III.10.13
Unit III Ten-Year HELP Model Simulation
Input Parameters
Sandoval County Landfill

Simulation	Intermediate Cover Layer			Waste Layer			Protective/Drainage Soil Layer			FML			GCL			Compacted Subgrade/Structural Fill		
	HELP Model Soil Type	Layer Thickness (in)	K _{sat} (cm/s)	HELP Model Soil Type	Layer Thickness (ft)	K _{sat} (cm/s)	HELP Model Soil Type	Layer Thickness (in)	K _{sat} (cm/s)	HELP Model Soil Type	FML	K _{sat} (cm/s)	HELP Model Soil Type	Layer Thickness (in)	K _{sat} (cm/s)	HELP Model Soil Type	Layer Thickness (in)	K _{sat} (cm/s)
11-1	6	12	7.2 x 10 ⁻⁴	18	90	1.0 x 10 ⁻³	6	24	3 x 10 ⁻⁴	35	60-mil HDPE	2.0 x 10 ⁻¹³	17	0.25	5.0 x 10 ⁻⁹	6	6	4.2 x 10 ⁻⁶

Table III.10.14 presents a summary of the average annual parameters for the 10-year HELP model analysis.

TABLE III.10.14
Unit III Ten-Year HELP Model Simulation Summary
Average Annual Totals
Sandoval County Landfill

Precipitation	12.91 in.
Runoff	0.221 in.
Evapotranspiration	12.224 in.
Percolation through 12-in. Intermediate Cover	0.465 in.
Lateral Drainage from Leachate Collection Layer	0.00000 in.
Average Head on Top of the Liner	0.000 in.
Percolation through Bottom Liner	0.00000 in.

Table III.10.15 presents the conservative initial and final moisture contents for the waste mass and liner system components prior to the 20-year intermediate cover model analysis.

TABLE III.10.15
Unit III Ten-Year HELP Model Simulation Summary
Initial and Final Moisture Contents
Sandoval County Landfill

Layer	Initial Moisture Content	Final Moisture Content
12-in. Intermediate Cover	0.1110	0.0880
Waste Mass	0.1310	0.1355
Protective Soil/Leachate Drainage Layer	0.1111	0.1141
60-mil HDPE Geomembrane	-	-
GCL	0.7500	0.7500
Compacted Subgrade	0.1335	0.1111

8.0 CONCLUSIONS AND REQUEST FOR APPROVAL

SCLF has prepared performance demonstrations for its prescriptive liner system design and alternate final cover system design. These analyses were based on the conservative parameters prescribed in the Guidance Document (**Attachment III.10.C**) and the analyses demonstrate the following:

- In the Tier I alternate final cover simulation analysis, when the barrier (infiltration) layer is modeled using HELP model soil type 6 with a hydraulic conductivity of 3.0×10^{-4} cm/sec, the average annual percolation rate calculated for the alternate final cover system is equivalent to the percolation rate calculated for the prescriptive liner system. Therefore, for this soil type, the performance of the alternate final cover system design meets the Tier I demonstration requirements.
- In the Tier II simulation analyses, the complete landfill, including both prescriptive liner and the alternate cover system designs, has been modeled. The vegetative (erosion), barrier (infiltration), intermediate cover, and protective soil layers were modeled using soil type 7. In this case, the percolation rate calculated for the fifth year of Simulation 8-1 is zero. Also the annual average percolation rate calculated for Simulations 9-1 and 10-1 are zero. Therefore, for the soil types modeled for the vegetative (erosion), barrier (infiltration), intermediate cover, and protective soil layers, the performance of the prescriptive liner and alternate final cover system designs meets the Tier II demonstration requirements.
- For the Unit III intermediate cover analyses, the percolation through the intermediate cover for the 10-year analyses did not generate any leachate as the waste mass in the Unit provided sufficient absorption, resulting in no head on the liner.

The HELP modeling for the analyses presented in this document demonstrates that the performance of the prescriptive liner and alternate final cover system designs meets the requirements of 20.9.4 NMAC. For the purposes of this demonstration, both the prescriptive liner design and the alternate cover design have been shown to be effective using soils available on the SCLF site or importing of off-site materials.

To allow SCLF flexibility in using on-site as well as offsite materials to construct the vegetative (erosion) layer, the barrier (infiltration) layer, intermediate cover layer, and the protective soil layer, this document serves as a request to SWB for approval to use the prescriptive liner and alternate final cover system designs proposed in this Permit Application. SCLF is also requesting approval to use alternative specifications for the PSL (i.e., $\leq 20\%$ fine; $C_u \leq 7.5$); as these on-site materials will accomplish the required performance standards.

**APPLICATION FOR PERMIT RENEWAL AND MODIFICATION
SANDOVAL COUNTY LANDFILL**

**VOLUME III: LANDFILL ENGINEERING CALCULATIONS
SECTION 10: HELP MODEL**

**ATTACHMENT III.10.A
HELP MODEL OUTPUT FILES**

**APPLICATION FOR PERMIT RENEWAL AND MODIFICATION
SANDOVAL COUNTY LANDFILL**

**VOLUME III: LANDFILL ENGINEERING CALCULATIONS
SECTION 10: HELP MODEL**

**ATTACHMENT III.10.A-1
TIER I, SIMULATION 5-1
PRESCRIPTIVE LINER, SOIL TYPE 6**

```

*****
*****
**
**
**
**      HYDROLOGIC EVALUATION OF LANDFILL PERFORMANCE      **
**      HELP MODEL VERSION 3.07  (1 NOVEMBER 1997)          **
**      DEVELOPED BY ENVIRONMENTAL LABORATORY                **
**      USAE WATERWAYS EXPERIMENT STATION                   **
**      FOR USEPA RISK REDUCTION ENGINEERING LABORATORY      **
**
**
*****
*****

```

```

PRECIPITATION DATA FILE:   C:\RAIN1.D4
TEMPERATURE DATA FILE:    C:\TEMP1.D7
SOLAR RADIATION DATA FILE: C:\SOLAR1.D13
EVAPOTRANSPIRATION DATA:  C:\EVAP1.D11
SOIL AND DESIGN DATA FILE: C:\UIVBASE.D10
OUTPUT DATA FILE:         C:\UIVBASE.OUT

```

TIME: 16:18 DATE: 4/ 8/2015

```

*****

```

TITLE: Sandoval County Landfill-Unit IV Base Grading-Prescip Liner
Simulation 5 - Prescription Liner in Unit IV

```

*****

```

NOTE: INITIAL MOISTURE CONTENT OF THE LAYERS AND SNOW WATER
WERE SPECIFIED BY THE USER.

LAYER 1

TYPE 2 - LATERAL DRAINAGE LAYER
MATERIAL TEXTURE NUMBER 0

THICKNESS	=	24.00	INCHES
POROSITY	=	0.4530	VOL/VOL
FIELD CAPACITY	=	0.1900	VOL/VOL
WILTING POINT	=	0.0850	VOL/VOL
INITIAL SOIL WATER CONTENT	=	0.1110	VOL/VOL
EFFECTIVE SAT. HYD. COND.	=	0.300000014000E-03	CM/SEC
SLOPE	=	5.00	PERCENT
DRAINAGE LENGTH	=	200.0	FEET

LAYER 2

TYPE 4 - FLEXIBLE MEMBRANE LINER

MATERIAL TEXTURE NUMBER 35

THICKNESS	=	0.06	INCHES
POROSITY	=	0.0000	VOL/VOL
FIELD CAPACITY	=	0.0000	VOL/VOL
WILTING POINT	=	0.0000	VOL/VOL
INITIAL SOIL WATER CONTENT	=	0.0000	VOL/VOL
EFFECTIVE SAT. HYD. COND.	=	0.199999996000E-12	CM/SEC
FML PINHOLE DENSITY	=	1.00	HOLES/ACRE
FML INSTALLATION DEFECTS	=	4.00	HOLES/ACRE
FML PLACEMENT QUALITY	=	3	- GOOD

LAYER 3

TYPE 3 - BARRIER SOIL LINER

MATERIAL TEXTURE NUMBER 0

THICKNESS	=	0.25	INCHES
POROSITY	=	0.7500	VOL/VOL
FIELD CAPACITY	=	0.7470	VOL/VOL
WILTING POINT	=	0.4000	VOL/VOL
INITIAL SOIL WATER CONTENT	=	0.7500	VOL/VOL
EFFECTIVE SAT. HYD. COND.	=	0.499999997000E-08	CM/SEC

LAYER 4

TYPE 1 - VERTICAL PERCOLATION LAYER

MATERIAL TEXTURE NUMBER 0

THICKNESS	=	6.00	INCHES
POROSITY	=	0.4530	VOL/VOL
FIELD CAPACITY	=	0.1900	VOL/VOL
WILTING POINT	=	0.0850	VOL/VOL
INITIAL SOIL WATER CONTENT	=	0.1110	VOL/VOL
EFFECTIVE SAT. HYD. COND.	=	0.419999997000E-04	CM/SEC

GENERAL DESIGN AND EVAPORATIVE ZONE DATA

NOTE: SCS RUNOFF CURVE NUMBER WAS USER-SPECIFIED.

SCS RUNOFF CURVE NUMBER	=	0.00	
FRACTION OF AREA ALLOWING RUNOFF	=	0.0	PERCENT
AREA PROJECTED ON HORIZONTAL PLANE	=	30.700	ACRES
EVAPORATIVE ZONE DEPTH	=	18.0	INCHES
INITIAL WATER IN EVAPORATIVE ZONE	=	1.998	INCHES
UPPER LIMIT OF EVAPORATIVE STORAGE	=	8.154	INCHES
LOWER LIMIT OF EVAPORATIVE STORAGE	=	1.530	INCHES
INITIAL SNOW WATER	=	0.000	INCHES
INITIAL WATER IN LAYER MATERIALS	=	3.517	INCHES
TOTAL INITIAL WATER	=	3.517	INCHES
TOTAL SUBSURFACE INFLOW	=	0.00	INCHES/YEAR

EVAPOTRANSPIRATION AND WEATHER DATA

NOTE: EVAPOTRANSPIRATION DATA WAS OBTAINED FROM
ALBUQUERQUE NEW MEXICO

STATION LATITUDE	=	35.30	DEGREES
MAXIMUM LEAF AREA INDEX	=	0.00	
START OF GROWING SEASON (JULIAN DATE)	=	98	
END OF GROWING SEASON (JULIAN DATE)	=	299	
EVAPORATIVE ZONE DEPTH	=	18.0	INCHES
AVERAGE ANNUAL WIND SPEED	=	9.00	MPH
AVERAGE 1ST QUARTER RELATIVE HUMIDITY	=	48.00	%
AVERAGE 2ND QUARTER RELATIVE HUMIDITY	=	30.00	%
AVERAGE 3RD QUARTER RELATIVE HUMIDITY	=	45.00	%
AVERAGE 4TH QUARTER RELATIVE HUMIDITY	=	50.00	%

NOTE: PRECIPITATION DATA WAS SYNTHETICALLY GENERATED USING
COEFFICIENTS FOR ALBUQUERQUE NEW MEXICO

NORMAL MEAN MONTHLY PRECIPITATION (INCHES)

JAN/JUL	FEB/AUG	MAR/SEP	APR/OCT	MAY/NOV	JUN/DEC
-----	-----	-----	-----	-----	-----
0.37	0.47	0.48	0.99	0.72	0.99
1.39	2.34	1.20	1.50	0.55	0.47

NOTE: TEMPERATURE DATA WAS SYNTHETICALLY GENERATED USING
COEFFICIENTS FOR ALBUQUERQUE NEW MEXICO

NORMAL MEAN MONTHLY TEMPERATURE (DEGREES FAHRENHEIT)

JAN/JUL	FEB/AUG	MAR/SEP	APR/OCT	MAY/NOV	JUN/DEC
-----	-----	-----	-----	-----	-----
35.20	40.90	47.10	55.30	64.90	73.50
77.30	75.60	67.30	57.20	44.40	35.70

NOTE: SOLAR RADIATION DATA WAS SYNTHETICALLY GENERATED USING
 COEFFICIENTS FOR ALBUQUERQUE NEW MEXICO
 AND STATION LATITUDE = 35.30 DEGREES

MONTHLY TOTALS (IN INCHES) FOR YEAR 1

	JAN/JUL	FEB/AUG	MAR/SEP	APR/OCT	MAY/NOV	JUN/DEC
	-----	-----	-----	-----	-----	-----
PRECIPITATION	0.11	0.01	0.26	0.55	0.86	0.01
	0.99	3.66	1.17	1.12	1.67	0.57
RUNOFF	0.000	0.000	0.000	0.000	0.000	0.000
	0.000	0.000	0.000	0.000	0.000	0.000
EVAPOTRANSPIRATION	0.316	0.218	0.103	0.115	1.062	0.318
	0.295	2.606	2.213	0.482	1.716	0.606
LATERAL DRAINAGE COLLECTED FROM LAYER 1	0.0000	0.0000	0.0000	0.0000	0.0000	0.0000
	0.0000	0.0000	0.0000	0.0000	0.0000	0.0000
PERCOLATION/LEAKAGE THROUGH LAYER 3	0.0000	0.0000	0.0000	0.0000	0.0000	0.0000
	0.0000	0.0000	0.0000	0.0000	0.0000	0.0000
PERCOLATION/LEAKAGE THROUGH LAYER 4	0.0000	0.0000	0.0000	0.0000	0.0000	0.0000
	0.0000	0.0000	0.0000	0.0000	0.0000	0.0000

MONTHLY SUMMARIES FOR DAILY HEADS (INCHES)

AVERAGE DAILY HEAD ON TOP OF LAYER 2	0.000	0.000	0.000	0.000	0.000	0.000
	0.000	0.000	0.000	0.000	0.000	0.000
STD. DEVIATION OF DAILY HEAD ON TOP OF LAYER 2	0.000	0.000	0.000	0.000	0.000	0.000
	0.000	0.000	0.000	0.000	0.000	0.000

ANNUAL TOTALS FOR YEAR 1

	INCHES	CU. FEET	PERCENT
	-----	-----	-----
PRECIPITATION	10.98	1223622.370	100.00
RUNOFF	0.000	0.000	0.00
EVAPOTRANSPIRATION	10.050	1119979.000	91.53
DRAINAGE COLLECTED FROM LAYER 1	0.0000	0.000	0.00
PERC./LEAKAGE THROUGH LAYER 3	0.000000	0.000	0.00
AVG. HEAD ON TOP OF LAYER 2	0.0000		
PERC./LEAKAGE THROUGH LAYER 4	0.000000	0.000	0.00
CHANGE IN WATER STORAGE	0.930	103643.141	8.47
SOIL WATER AT START OF YEAR	3.517	391991.219	
SOIL WATER AT END OF YEAR	4.448	495634.375	
SNOW WATER AT START OF YEAR	0.000	0.000	0.00
SNOW WATER AT END OF YEAR	0.000	0.000	0.00
ANNUAL WATER BUDGET BALANCE	0.0000	0.213	0.00

MONTHLY TOTALS (IN INCHES) FOR YEAR 2

	JAN/JUL	FEB/AUG	MAR/SEP	APR/OCT	MAY/NOV	JUN/DEC
	-----	-----	-----	-----	-----	-----
PRECIPITATION	0.09	1.07	0.00	1.64	1.35	2.03
	1.08	3.29	1.76	5.91	0.03	0.42
RUNOFF	0.000	0.000	0.000	0.000	0.000	0.000

	0.000	0.000	0.000	0.000	0.000	0.000
EVAPOTRANSPIRATION	0.276	0.848	0.389	1.144	1.231	1.927
	0.996	2.566	1.477	3.092	1.295	0.427
LATERAL DRAINAGE COLLECTED FROM LAYER 1	0.0000	0.0000	0.0000	0.0000	0.0000	0.0000
	0.0000	0.0000	0.0000	0.0039	0.1152	0.1227
PERCOLATION/LEAKAGE THROUGH LAYER 3	0.0000	0.0000	0.0000	0.0000	0.0000	0.0000
	0.0000	0.0000	0.0000	0.0000	0.0003	0.0003
PERCOLATION/LEAKAGE THROUGH LAYER 4	0.0000	0.0000	0.0000	0.0000	0.0000	0.0000
	0.0000	0.0000	0.0000	0.0000	0.0000	0.0000

MONTHLY SUMMARIES FOR DAILY HEADS (INCHES)

AVERAGE DAILY HEAD ON TOP OF LAYER 2	0.000	0.000	0.000	0.000	0.000	0.000
	0.000	0.000	0.000	0.299	9.058	9.330
STD. DEVIATION OF DAILY HEAD ON TOP OF LAYER 2	0.000	0.000	0.000	0.000	0.000	0.000
	0.000	0.000	0.000	1.181	0.667	0.190

ANNUAL TOTALS FOR YEAR 2

	INCHES	CU. FEET	PERCENT
	-----	-----	-----
PRECIPITATION	18.67	2080603.750	100.00
RUNOFF	0.000	0.000	0.00
EVAPOTRANSPIRATION	15.668	1746034.000	83.92
DRAINAGE COLLECTED FROM LAYER 1	0.2419	26952.254	1.30
PERC./LEAKAGE THROUGH LAYER 3	0.000595	66.283	0.00
AVG. HEAD ON TOP OF LAYER 2	1.5572		
PERC./LEAKAGE THROUGH LAYER 4	0.000000	0.016	0.00
CHANGE IN WATER STORAGE	2.760	307616.875	14.78
SOIL WATER AT START OF YEAR	4.448	495634.375	

SOIL WATER AT END OF YEAR	7.208	803251.250	
SNOW WATER AT START OF YEAR	0.000	0.000	0.00
SNOW WATER AT END OF YEAR	0.000	0.000	0.00
ANNUAL WATER BUDGET BALANCE	0.0000	0.522	0.00

MONTHLY TOTALS (IN INCHES) FOR YEAR 3

	JAN/JUL	FEB/AUG	MAR/SEP	APR/OCT	MAY/NOV	JUN/DEC
	-----	-----	-----	-----	-----	-----
PRECIPITATION	0.47	0.61	0.91	0.33	1.68	2.49
	0.75	1.16	2.62	1.24	0.77	0.17
RUNOFF	0.000	0.000	0.000	0.000	0.000	0.000
	0.000	0.000	0.000	0.000	0.000	0.000
EVAPOTRANSPIRATION	0.248	0.305	1.156	0.350	1.583	2.207
	0.362	0.579	3.065	0.737	1.322	0.391
LATERAL DRAINAGE COLLECTED FROM LAYER 1	0.1125	0.1001	0.1044	0.0952	0.0931	0.0958
	0.1077	0.1039	0.0994	0.1121	0.1034	0.1027
PERCOLATION/LEAKAGE THROUGH LAYER 3	0.0003	0.0002	0.0002	0.0002	0.0002	0.0002
	0.0003	0.0002	0.0002	0.0003	0.0002	0.0002
PERCOLATION/LEAKAGE THROUGH LAYER 4	0.0000	0.0000	0.0000	0.0000	0.0000	0.0000
	0.0000	0.0000	0.0000	0.0000	0.0000	0.0000

MONTHLY SUMMARIES FOR DAILY HEADS (INCHES)

AVERAGE DAILY HEAD ON TOP OF LAYER 2	8.557	8.427	7.944	7.485	7.077	7.533
	8.194	7.906	7.810	8.524	8.125	7.808
STD. DEVIATION OF DAILY HEAD ON TOP OF LAYER 2	0.797	0.124	0.163	0.119	0.136	0.588
	0.017	0.130	0.380	0.052	0.143	0.775

ANNUAL TOTALS FOR YEAR 3

	INCHES	CU. FEET	PERCENT
	-----	-----	-----
PRECIPITATION	13.20	1471021.370	100.00
RUNOFF	0.000	0.000	0.00
EVAPOTRANSPIRATION	12.307	1371460.000	93.23
DRAINAGE COLLECTED FROM LAYER 1	1.2303	137109.844	9.32
PERC./LEAKAGE THROUGH LAYER 3	0.002820	314.248	0.02
AVG. HEAD ON TOP OF LAYER 2	7.9491		
PERC./LEAKAGE THROUGH LAYER 4	0.000000	0.000	0.00
CHANGE IN WATER STORAGE	-0.337	-37548.539	-2.55
SOIL WATER AT START OF YEAR	7.208	803251.250	
SOIL WATER AT END OF YEAR	6.871	765702.687	
SNOW WATER AT START OF YEAR	0.000	0.000	0.00
SNOW WATER AT END OF YEAR	0.000	0.000	0.00
ANNUAL WATER BUDGET BALANCE	0.0000	0.000	0.00

MONTHLY TOTALS (IN INCHES) FOR YEAR 4

	JAN/JUL	FEB/AUG	MAR/SEP	APR/OCT	MAY/NOV	JUN/DEC
	-----	-----	-----	-----	-----	-----
PRECIPITATION	0.00	0.07	0.17	0.19	0.38	1.20
	3.02	2.72	1.04	3.38	0.35	0.36
RUNOFF	0.000	0.000	0.000	0.000	0.000	0.000
	0.000	0.000	0.000	0.000	0.000	0.000

EVAPOTRANSPIRATION	0.239	0.224	0.203	0.175	0.171	0.493
	2.551	2.235	1.117	2.275	0.899	0.424
LATERAL DRAINAGE COLLECTED FROM LAYER 1	0.1008	0.0928	0.0942	0.0865	0.0848	0.0776
	0.0762	0.0787	0.0950	0.1129	0.1301	0.1313
PERCOLATION/LEAKAGE THROUGH LAYER 3	0.0002	0.0002	0.0002	0.0002	0.0002	0.0002
	0.0001	0.0002	0.0002	0.0003	0.0003	0.0003
PERCOLATION/LEAKAGE THROUGH LAYER 4	0.0000	0.0000	0.0000	0.0000	0.0000	0.0000
	0.0000	0.0000	0.0000	0.0000	0.0000	0.0000

MONTHLY SUMMARIES FOR DAILY HEADS (INCHES)

AVERAGE DAILY HEAD ON TOP OF LAYER 2	7.670	7.545	7.163	6.796	6.450	6.099
	5.797	5.984	7.468	8.586	10.227	9.990
STD. DEVIATION OF DAILY HEAD ON TOP OF LAYER 2	0.593	0.112	0.113	0.103	0.100	0.114
	0.075	0.380	0.136	1.201	0.104	0.158

ANNUAL TOTALS FOR YEAR 4

	INCHES	CU. FEET	PERCENT
	-----	-----	-----
PRECIPITATION	12.88	1435360.120	100.00
RUNOFF	0.000	0.000	0.00
EVAPOTRANSPIRATION	11.005	1226453.750	85.45
DRAINAGE COLLECTED FROM LAYER 1	1.1610	129384.359	9.01
PERC./LEAKAGE THROUGH LAYER 3	0.002621	292.040	0.02
AVG. HEAD ON TOP OF LAYER 2	7.4814		
PERC./LEAKAGE THROUGH LAYER 4	0.000000	0.000	0.00
CHANGE IN WATER STORAGE	0.714	79521.656	5.54
SOIL WATER AT START OF YEAR	6.871	765702.687	
SOIL WATER AT END OF YEAR	7.585	845224.375	

SNOW WATER AT START OF YEAR	0.000	0.000	0.00
SNOW WATER AT END OF YEAR	0.000	0.000	0.00
ANNUAL WATER BUDGET BALANCE	0.0000	0.266	0.00

MONTHLY TOTALS (IN INCHES) FOR YEAR 5

	JAN/JUL	FEB/AUG	MAR/SEP	APR/OCT	MAY/NOV	JUN/DEC
	-----	-----	-----	-----	-----	-----
PRECIPITATION	0.27	0.68	0.78	1.73	0.97	0.20
	1.40	1.86	1.82	3.13	0.00	1.03
RUNOFF	0.000	0.000	0.000	0.000	0.000	0.000
	0.000	0.000	0.000	0.000	0.000	0.000
EVAPOTRANSPIRATION	0.295	0.321	1.034	1.611	0.687	0.268
	1.228	2.129	0.506	3.228	1.183	0.744
LATERAL DRAINAGE COLLECTED FROM LAYER 1	0.1241	0.1057	0.1108	0.1009	0.1064	0.1009
	0.0985	0.0917	0.0821	0.0905	0.0963	0.1017
PERCOLATION/LEAKAGE THROUGH LAYER 3	0.0003	0.0003	0.0003	0.0002	0.0002	0.0002
	0.0002	0.0002	0.0002	0.0002	0.0002	0.0002
PERCOLATION/LEAKAGE THROUGH LAYER 4	0.0000	0.0000	0.0000	0.0000	0.0000	0.0000
	0.0000	0.0000	0.0000	0.0000	0.0000	0.0000

MONTHLY SUMMARIES FOR DAILY HEADS (INCHES)

AVERAGE DAILY HEAD ON TOP OF LAYER 2	9.442	8.900	8.428	7.930	8.089	7.932
	7.494	6.974	6.453	6.886	7.572	7.734
STD. DEVIATION OF DAILY HEAD ON TOP OF LAYER 2	0.163	0.086	0.164	0.143	0.045	0.111
	0.158	0.189	0.108	0.542	0.118	0.060

ANNUAL TOTALS FOR YEAR 5

	INCHES	CU. FEET	PERCENT
	-----	-----	-----
PRECIPITATION	13.87	1545687.000	100.00
RUNOFF	0.000	0.000	0.00
EVAPOTRANSPIRATION	13.234	1474761.620	95.41
DRAINAGE COLLECTED FROM LAYER 1	1.2097	134814.109	8.72
PERC./LEAKAGE THROUGH LAYER 3	0.002757	307.211	0.02
AVG. HEAD ON TOP OF LAYER 2	7.8195		
PERC./LEAKAGE THROUGH LAYER 4	0.000000	0.000	0.00
CHANGE IN WATER STORAGE	-0.573	-63889.430	-4.13
SOIL WATER AT START OF YEAR	7.585	845224.375	
SOIL WATER AT END OF YEAR	7.011	781334.937	
SNOW WATER AT START OF YEAR	0.000	0.000	0.00
SNOW WATER AT END OF YEAR	0.000	0.000	0.00
ANNUAL WATER BUDGET BALANCE	0.0000	0.651	0.00

AVERAGE MONTHLY VALUES IN INCHES FOR YEARS 1 THROUGH 5

	JAN/JUL	FEB/AUG	MAR/SEP	APR/OCT	MAY/NOV	JUN/DEC
	-----	-----	-----	-----	-----	-----
PRECIPITATION						

TOTALS	0.19 1.45	0.49 2.54	0.42 1.68	0.89 2.96	1.05 0.56	1.19 0.51
STD. DEVIATIONS	0.19 0.91	0.45 1.03	0.40 0.63	0.74 1.95	0.49 0.69	1.09 0.32
RUNOFF						

TOTALS	0.000	0.000	0.000	0.000	0.000	0.000

	0.000	0.000	0.000	0.000	0.000	0.000
STD. DEVIATIONS	0.000	0.000	0.000	0.000	0.000	0.000
	0.000	0.000	0.000	0.000	0.000	0.000

EVAPOTRANSPIRATION

TOTALS	0.275	0.384	0.577	0.679	0.947	1.043
	1.086	2.023	1.676	1.963	1.283	0.518
STD. DEVIATIONS	0.032	0.264	0.486	0.665	0.540	0.944
	0.912	0.833	0.993	1.291	0.295	0.152

LATERAL DRAINAGE COLLECTED FROM LAYER 1

TOTALS	0.0675	0.0597	0.0619	0.0565	0.0568	0.0549
	0.0565	0.0549	0.0553	0.0639	0.0890	0.0917
STD. DEVIATIONS	0.0622	0.0547	0.0568	0.0519	0.0525	0.0508
	0.0528	0.0509	0.0509	0.0573	0.0514	0.0528

PERCOLATION/LEAKAGE THROUGH LAYER 3

TOTALS	0.0002	0.0001	0.0001	0.0001	0.0001	0.0001
	0.0001	0.0001	0.0001	0.0001	0.0002	0.0002
STD. DEVIATIONS	0.0002	0.0001	0.0001	0.0001	0.0001	0.0001
	0.0001	0.0001	0.0001	0.0001	0.0001	0.0001

PERCOLATION/LEAKAGE THROUGH LAYER 4

TOTALS	0.0000	0.0000	0.0000	0.0000	0.0000	0.0000
	0.0000	0.0000	0.0000	0.0000	0.0000	0.0000
STD. DEVIATIONS	0.0000	0.0000	0.0000	0.0000	0.0000	0.0000
	0.0000	0.0000	0.0000	0.0000	0.0000	0.0000

AVERAGES OF MONTHLY AVERAGED DAILY HEADS (INCHES)

DAILY AVERAGE HEAD ON TOP OF LAYER 2

AVERAGES	5.1340	4.9744	4.7068	4.4422	4.3233	4.3127
	4.2970	4.1728	4.3462	4.8592	6.9964	6.9725
STD. DEVIATIONS	4.7284	4.5670	4.3203	4.0752	3.9896	3.9955
	4.0183	3.8694	3.9988	4.3544	4.0386	4.0174

AVERAGE ANNUAL TOTALS & (STD. DEVIATIONS) FOR YEARS 1 THROUGH 5

	INCHES		CU. FEET	PERCENT
	-----		-----	-----
PRECIPITATION	13.92	(2.864)	1551258.9	100.00
RUNOFF	0.000	(0.0000)	0.00	0.000
EVAPOTRANSPIRATION	12.453	(2.1700)	1387737.75	89.459
LATERAL DRAINAGE COLLECTED FROM LAYER 1	0.76859	(0.59791)	85652.117	5.52146
PERCOLATION/LEAKAGE THROUGH LAYER 3	0.00176	(0.00135)	195.957	0.01263
AVERAGE HEAD ON TOP OF LAYER 2	4.961	(3.862)		
PERCOLATION/LEAKAGE THROUGH LAYER 4	0.00000	(0.00000)	0.003	0.00000
CHANGE IN WATER STORAGE	0.699	(1.3224)	77868.74	5.020

PEAK DAILY VALUES FOR YEARS	1 THROUGH	5
	(INCHES)	(CU. FT.)
PRECIPITATION	1.97	219538.781
RUNOFF	0.000	0.0000
DRAINAGE COLLECTED FROM LAYER 1	0.00437	487.06210
PERCOLATION/LEAKAGE THROUGH LAYER 3	0.000011	1.27737
AVERAGE HEAD ON TOP OF LAYER 2	10.305	
MAXIMUM HEAD ON TOP OF LAYER 2	16.072	
LOCATION OF MAXIMUM HEAD IN LAYER 1 (DISTANCE FROM DRAIN)	43.6 FEET	
PERCOLATION/LEAKAGE THROUGH LAYER 4	0.000000	0.01604
SNOW WATER	0.58	64670.8828
MAXIMUM VEG. SOIL WATER (VOL/VOL)		0.3458
MINIMUM VEG. SOIL WATER (VOL/VOL)		0.0859

*** Maximum heads are computed using McEnroe's equations. ***

Reference: Maximum Saturated Depth over Landfill Liner
by Bruce M. McEnroe, University of Kansas
ASCE Journal of Environmental Engineering
Vol. 119, No. 2, March 1993, pp. 262-270.

FINAL WATER STORAGE AT END OF YEAR 5

LAYER	(INCHES)	(VOL/VOL)
1	6.1489	0.2562
2	0.0000	0.0000
3	0.1875	0.7500
4	0.6748	0.1125
SNOW WATER	0.000	

**APPLICATION FOR PERMIT RENEWAL AND MODIFICATION
SANDOVAL COUNTY LANDFILL**

**VOLUME III: LANDFILL ENGINEERING CALCULATIONS
SECTION 10: HELP MODEL**

ATTACHMENT III.10.A-2

TIER I, SIMULATION 3-1A AND 3-1B
ALTERNATE FINAL COVER, SOIL TYPE 6

```

*****
*****
**
**
**
HYDROLOGIC EVALUATION OF LANDFILL PERFORMANCE
HELP MODEL VERSION 3.07 (1 NOVEMBER 1997)
DEVELOPED BY ENVIRONMENTAL LABORATORY
USAE WATERWAYS EXPERIMENT STATION
FOR USEPA RISK REDUCTION ENGINEERING LABORATORY
**
**
**
*****
*****

```

```

PRECIPITATION DATA FILE:  C:\RAINFCD4
TEMPERATURE DATA FILE:   C:\TEMPFCD7
SOLAR RADIATION DATA FILE: C:\SOLARFCD13
EVAPOTRANSPIRATION DATA: C:\EVAPFCD11
SOIL AND DESIGN DATA FILE: C:\ALTFC5%.D10
OUTPUT DATA FILE:        C:\ALTFC5%.OUT

```

TIME: 14:30 DATE: 4/ 8/2015

```

*****

```

TITLE: Sandoval County Landfill - Alternative Final Cover 5% Slope

Simulation 3A - Alternative Final Cover; 5% Slope Area: 8.9 Acres

```

*****

```

NOTE: INITIAL MOISTURE CONTENT OF THE LAYERS AND SNOW WATER
WERE SPECIFIED BY THE USER.

LAYER 1

TYPE 1 - VERTICAL PERCOLATION LAYER

MATERIAL TEXTURE NUMBER 6

THICKNESS	=	6.00	INCHES
POROSITY	=	0.4530	VOL/VOL
FIELD CAPACITY	=	0.1900	VOL/VOL
WILTING POINT	=	0.0850	VOL/VOL
INITIAL SOIL WATER CONTENT	=	0.1110	VOL/VOL
EFFECTIVE SAT. HYD. COND.	=	0.720000011000E-03	CM/SEC

NOTE: SATURATED HYDRAULIC CONDUCTIVITY IS MULTIPLIED BY 1.60
FOR ROOT CHANNELS IN TOP HALF OF EVAPORATIVE ZONE.

LAYER 2

TYPE 1 - VERTICAL PERCOLATION LAYER

MATERIAL TEXTURE NUMBER 6

THICKNESS	=	30.00	INCHES
POROSITY	=	0.4530	VOL/VOL
FIELD CAPACITY	=	0.1900	VOL/VOL
WILTING POINT	=	0.0850	VOL/VOL
INITIAL SOIL WATER CONTENT	=	0.1110	VOL/VOL
EFFECTIVE SAT. HYD. COND.	=	0.720000011000E-03	CM/SEC

LAYER 3

TYPE 1 - VERTICAL PERCOLATION LAYER

MATERIAL TEXTURE NUMBER 6

THICKNESS	=	12.00	INCHES
POROSITY	=	0.4530	VOL/VOL
FIELD CAPACITY	=	0.1900	VOL/VOL
WILTING POINT	=	0.0850	VOL/VOL
INITIAL SOIL WATER CONTENT	=	0.1110	VOL/VOL
EFFECTIVE SAT. HYD. COND.	=	0.720000011000E-03	CM/SEC

GENERAL DESIGN AND EVAPORATIVE ZONE DATA

NOTE: SCS RUNOFF CURVE NUMBER WAS COMPUTED FROM A USER-SPECIFIED CURVE NUMBER OF 85.0, A SURFACE SLOPE OF 5.% AND A SLOPE LENGTH OF 258. FEET.

SCS RUNOFF CURVE NUMBER	=	85.60	
FRACTION OF AREA ALLOWING RUNOFF	=	100.0	PERCENT
AREA PROJECTED ON HORIZONTAL PLANE	=	8.900	ACRES
EVAPORATIVE ZONE DEPTH	=	28.0	INCHES
INITIAL WATER IN EVAPORATIVE ZONE	=	3.108	INCHES
UPPER LIMIT OF EVAPORATIVE STORAGE	=	12.684	INCHES
LOWER LIMIT OF EVAPORATIVE STORAGE	=	2.380	INCHES
INITIAL SNOW WATER	=	0.000	INCHES
INITIAL WATER IN LAYER MATERIALS	=	5.328	INCHES
TOTAL INITIAL WATER	=	5.328	INCHES
TOTAL SUBSURFACE INFLOW	=	0.00	INCHES/YEAR

EVAPOTRANSPIRATION AND WEATHER DATA

NOTE: EVAPOTRANSPIRATION DATA WAS OBTAINED FROM
ALBUQUERQUE NEW MEXICO

STATION LATITUDE	=	35.30 DEGREES
MAXIMUM LEAF AREA INDEX	=	0.80
START OF GROWING SEASON (JULIAN DATE)	=	98
END OF GROWING SEASON (JULIAN DATE)	=	299
EVAPORATIVE ZONE DEPTH	=	28.0 INCHES
AVERAGE ANNUAL WIND SPEED	=	9.00 MPH
AVERAGE 1ST QUARTER RELATIVE HUMIDITY	=	48.00 %
AVERAGE 2ND QUARTER RELATIVE HUMIDITY	=	30.00 %
AVERAGE 3RD QUARTER RELATIVE HUMIDITY	=	45.00 %
AVERAGE 4TH QUARTER RELATIVE HUMIDITY	=	50.00 %

NOTE: PRECIPITATION DATA WAS SYNTHETICALLY GENERATED USING
COEFFICIENTS FOR ALBUQUERQUE NEW MEXICO

NORMAL MEAN MONTHLY PRECIPITATION (INCHES)

JAN/JUL	FEB/AUG	MAR/SEP	APR/OCT	MAY/NOV	JUN/DEC
-----	-----	-----	-----	-----	-----
0.37	0.47	0.48	0.99	0.72	0.99
1.39	2.34	1.20	1.50	0.55	0.47

NOTE: TEMPERATURE DATA WAS SYNTHETICALLY GENERATED USING
COEFFICIENTS FOR ALBUQUERQUE NEW MEXICO

NORMAL MEAN MONTHLY TEMPERATURE (DEGREES FAHRENHEIT)

JAN/JUL	FEB/AUG	MAR/SEP	APR/OCT	MAY/NOV	JUN/DEC
-----	-----	-----	-----	-----	-----
35.20	40.90	47.10	55.30	64.90	73.50
77.30	75.60	67.30	57.20	44.40	35.70

NOTE: SOLAR RADIATION DATA WAS SYNTHETICALLY GENERATED USING
COEFFICIENTS FOR ALBUQUERQUE NEW MEXICO
AND STATION LATITUDE = 35.30 DEGREES

MONTHLY TOTALS (IN INCHES) FOR YEAR 1

	JAN/JUL	FEB/AUG	MAR/SEP	APR/OCT	MAY/NOV	JUN/DEC
	-----	-----	-----	-----	-----	-----
PRECIPITATION	0.11	0.01	0.26	0.55	0.86	0.01
	0.99	3.66	1.17	1.12	1.67	0.57
RUNOFF	0.000	0.000	0.000	0.000	0.000	0.000
	0.000	0.000	0.000	0.000	0.000	0.000
EVAPOTRANSPIRATION	0.603	0.116	0.110	0.319	1.352	0.020
	0.837	3.243	1.746	1.087	1.568	0.700
PERCOLATION/LEAKAGE THROUGH LAYER 3	0.0000	0.0000	0.0000	0.0000	0.0000	0.0000
	0.0000	0.0000	0.0000	0.0000	0.0000	0.0000

ANNUAL TOTALS FOR YEAR 1

	INCHES	CU. FEET	PERCENT
	-----	-----	-----
PRECIPITATION	10.98	354730.906	100.00
RUNOFF	0.000	0.000	0.00
EVAPOTRANSPIRATION	11.700	377984.187	106.56
PERC./LEAKAGE THROUGH LAYER 3	0.000008	0.250	0.00
CHANGE IN WATER STORAGE	-0.720	-23253.684	-6.56
SOIL WATER AT START OF YEAR	5.328	172130.984	
SOIL WATER AT END OF YEAR	4.608	148877.297	
SNOW WATER AT START OF YEAR	0.000	0.000	0.00
SNOW WATER AT END OF YEAR	0.000	0.000	0.00
ANNUAL WATER BUDGET BALANCE	0.0000	0.120	0.00

MONTHLY TOTALS (IN INCHES) FOR YEAR 2

	JAN/JUL	FEB/AUG	MAR/SEP	APR/OCT	MAY/NOV	JUN/DEC
PRECIPITATION	0.09 1.08	1.07 3.29	0.00 1.76	1.64 5.91	1.35 0.03	2.03 0.42
RUNOFF	0.000 0.000	0.000 0.019	0.000 0.000	0.000 0.350	0.000 0.000	0.015 0.000
EVAPOTRANSPIRATION	0.064 1.101	1.095 2.795	0.002 1.569	1.627 2.998	1.181 1.887	2.178 0.579
PERCOLATION/LEAKAGE THROUGH LAYER 3	0.0000 0.0000	0.0000 0.0000	0.0000 0.0000	0.0000 0.0000	0.0000 0.0000	0.0000 0.0000

ANNUAL TOTALS FOR YEAR 2

	INCHES	CU. FEET	PERCENT
PRECIPITATION	18.67	603171.750	100.00
RUNOFF	0.384	12406.544	2.06
EVAPOTRANSPIRATION	17.077	551706.250	91.47
PERC./LEAKAGE THROUGH LAYER 3	0.000000	0.003	0.00
CHANGE IN WATER STORAGE	1.209	39058.746	6.48
SOIL WATER AT START OF YEAR	4.608	148877.297	
SOIL WATER AT END OF YEAR	5.817	187936.047	
SNOW WATER AT START OF YEAR	0.000	0.000	0.00
SNOW WATER AT END OF YEAR	0.000	0.000	0.00
ANNUAL WATER BUDGET BALANCE	0.0000	0.136	0.00

MONTHLY TOTALS (IN INCHES) FOR YEAR 3

	JAN/JUL	FEB/AUG	MAR/SEP	APR/OCT	MAY/NOV	JUN/DEC
	-----	-----	-----	-----	-----	-----
PRECIPITATION	0.47	0.61	0.91	0.33	1.68	2.49
	0.75	1.16	2.62	1.24	0.77	0.17
RUNOFF	0.000	0.000	0.000	0.000	0.000	0.015
	0.000	0.000	0.000	0.000	0.000	0.000
EVAPOTRANSPIRATION	0.370	0.312	0.563	0.486	1.942	3.871
	0.747	0.837	2.945	1.023	0.985	0.145
PERCOLATION/LEAKAGE THROUGH LAYER 3	0.0000	0.0000	0.0000	0.0000	0.0000	0.0000
	0.0000	0.0000	0.0000	0.0000	0.0000	0.0000

ANNUAL TOTALS FOR YEAR 3

	INCHES	CU. FEET	PERCENT
	-----	-----	-----
PRECIPITATION	13.20	426452.406	100.00
RUNOFF	0.015	494.403	0.12
EVAPOTRANSPIRATION	14.227	459622.469	107.78
PERC./LEAKAGE THROUGH LAYER 3	0.000000	0.000	0.00
CHANGE IN WATER STORAGE	-1.042	-33664.762	-7.89
SOIL WATER AT START OF YEAR	5.817	187936.047	
SOIL WATER AT END OF YEAR	4.775	154271.281	
SNOW WATER AT START OF YEAR	0.000	0.000	0.00
SNOW WATER AT END OF YEAR	0.000	0.000	0.00

ANNUAL WATER BUDGET BALANCE 0.0000 0.273 0.00

MONTHLY TOTALS (IN INCHES) FOR YEAR 4

	JAN/JUL	FEB/AUG	MAR/SEP	APR/OCT	MAY/NOV	JUN/DEC
	-----	-----	-----	-----	-----	-----
PRECIPITATION	0.00	0.07	0.17	0.19	0.38	1.20
	3.02	2.72	1.04	3.38	0.35	0.36
RUNOFF	0.000	0.000	0.000	0.000	0.000	0.000
	0.074	0.006	0.000	0.072	0.000	0.000
EVAPOTRANSPIRATION	0.026	0.070	0.170	0.190	0.341	1.218
	2.505	2.550	1.632	1.889	1.576	0.449
PERCOLATION/LEAKAGE THROUGH LAYER 3	0.0000	0.0000	0.0000	0.0000	0.0000	0.0000
	0.0000	0.0000	0.0000	0.0000	0.0000	0.0000

ANNUAL TOTALS FOR YEAR 4

	INCHES	CU. FEET	PERCENT
	-----	-----	-----
PRECIPITATION	12.88	416114.156	100.00
RUNOFF	0.152	4900.638	1.18
EVAPOTRANSPIRATION	12.617	407622.250	97.96
PERC./LEAKAGE THROUGH LAYER 3	0.000000	0.000	0.00
CHANGE IN WATER STORAGE	0.111	3591.224	0.86
SOIL WATER AT START OF YEAR	4.775	154271.281	
SOIL WATER AT END OF YEAR	4.886	157862.500	

SNOW WATER AT START OF YEAR	0.000	0.000	0.00
SNOW WATER AT END OF YEAR	0.000	0.000	0.00
ANNUAL WATER BUDGET BALANCE	0.0000	0.026	0.00

MONTHLY TOTALS (IN INCHES) FOR YEAR 5

	JAN/JUL	FEB/AUG	MAR/SEP	APR/OCT	MAY/NOV	JUN/DEC
	-----	-----	-----	-----	-----	-----
PRECIPITATION	0.27 1.40	0.68 1.86	0.78 1.82	1.73 3.13	0.97 0.00	0.20 1.03
RUNOFF	0.000 0.000	0.000 0.000	0.000 0.010	0.003 0.000	0.000 0.000	0.000 0.000
EVAPOTRANSPIRATION	0.343 1.145	0.176 2.115	1.324 0.729	1.692 3.048	1.029 1.152	0.200 0.934
PERCOLATION/LEAKAGE THROUGH LAYER 3	0.0000 0.0000	0.0000 0.0000	0.0000 0.0000	0.0000 0.0000	0.0000 0.0000	0.0000 0.0000

ANNUAL TOTALS FOR YEAR 5

	INCHES	CU. FEET	PERCENT
	-----	-----	-----
PRECIPITATION	13.87	448098.156	100.00
RUNOFF	0.013	414.906	0.09
EVAPOTRANSPIRATION	13.888	448677.281	100.13
PERC./LEAKAGE THROUGH LAYER 3	0.000001	0.021	0.00
CHANGE IN WATER STORAGE	-0.031	-994.111	-0.22
SOIL WATER AT START OF YEAR	4.886	157862.500	

SOIL WATER AT END OF YEAR	4.856	156868.391	
SNOW WATER AT START OF YEAR	0.000	0.000	0.00
SNOW WATER AT END OF YEAR	0.000	0.000	0.00
ANNUAL WATER BUDGET BALANCE	0.0000	0.042	0.00

AVERAGE MONTHLY VALUES IN INCHES FOR YEARS 1 THROUGH 5

	JAN/JUL	FEB/AUG	MAR/SEP	APR/OCT	MAY/NOV	JUN/DEC
	-----	-----	-----	-----	-----	-----
PRECIPITATION						

TOTALS	0.19 1.45	0.49 2.54	0.42 1.68	0.89 2.96	1.05 0.56	1.19 0.51
STD. DEVIATIONS	0.19 0.91	0.45 1.03	0.40 0.63	0.74 1.95	0.49 0.69	1.09 0.32
RUNOFF						

TOTALS	0.000 0.015	0.000 0.005	0.000 0.002	0.001 0.084	0.000 0.000	0.006 0.000
STD. DEVIATIONS	0.000 0.033	0.000 0.008	0.000 0.004	0.001 0.152	0.000 0.000	0.008 0.000
EVAPOTRANSPIRATION						

TOTALS	0.282 1.267	0.354 2.308	0.434 1.724	0.863 2.009	1.169 1.434	1.497 0.561
STD. DEVIATIONS	0.239 0.713	0.424 0.918	0.541 0.793	0.735 0.987	0.578 0.362	1.584 0.294
PERCOLATION/LEAKAGE THROUGH LAYER 3						

TOTALS	0.0000 0.0000	0.0000 0.0000	0.0000 0.0000	0.0000 0.0000	0.0000 0.0000	0.0000 0.0000
STD. DEVIATIONS	0.0000 0.0000	0.0000 0.0000	0.0000 0.0000	0.0000 0.0000	0.0000 0.0000	0.0000 0.0000

AVERAGE ANNUAL TOTALS & (STD. DEVIATIONS) FOR YEARS 1 THROUGH 5

	INCHES		CU. FEET	PERCENT
	-----		-----	-----
PRECIPITATION	13.92	(2.864)	449713.5	100.00
RUNOFF	0.113	(0.1638)	3643.30	0.810
EVAPOTRANSPIRATION	13.902	(2.0425)	449122.47	99.869
PERCOLATION/LEAKAGE THROUGH LAYER 3	0.00000	(0.00000)	0.055	0.00001
CHANGE IN WATER STORAGE	-0.094	(0.8709)	-3052.52	-0.679

PEAK DAILY VALUES FOR YEARS	1 THROUGH	5
	(INCHES)	(CU. FT.)
PRECIPITATION	1.97	63644.789
RUNOFF	0.264	8539.8535
PERCOLATION/LEAKAGE THROUGH LAYER 3	0.000002	0.07191
SNOW WATER	0.58	18748.2344
MAXIMUM VEG. SOIL WATER (VOL/VOL)		0.2003
MINIMUM VEG. SOIL WATER (VOL/VOL)		0.0850

FINAL WATER STORAGE AT END OF YEAR 5

LAYER	(INCHES)	(VOL/VOL)
1	0.5933	0.0989
2	2.9077	0.0969
3	1.3545	0.1129
SNOW WATER	0.000	


```

*****
*****
**
**
**
HYDROLOGIC EVALUATION OF LANDFILL PERFORMANCE
HELP MODEL VERSION 3.07 (1 NOVEMBER 1997)
DEVELOPED BY ENVIRONMENTAL LABORATORY
USAE WATERWAYS EXPERIMENT STATION
FOR USEPA RISK REDUCTION ENGINEERING LABORATORY
**
**
*****
*****

```

```

PRECIPITATION DATA FILE:  C:\RAINFCD4
TEMPERATURE DATA FILE:   C:\TEMPFCD7
SOLAR RADIATION DATA FILE: C:\SOLARFCD13
EVAPOTRANSPIRATION DATA: C:\EVAPFCD11
SOIL AND DESIGN DATA FILE: C:\ALFCD25.D10
OUTPUT DATA FILE:        C:\ALFCD25.OUT

```

TIME: 14:36 DATE: 4/ 8/2015

```

*****

```

TITLE: Sandoval County Landfill - Alternative Final Cover 25% Slope

Simulation 3B - Alternative Final Cover; 25% Sloped Area: 114 Acres

```

*****

```

NOTE: INITIAL MOISTURE CONTENT OF THE LAYERS AND SNOW WATER
WERE SPECIFIED BY THE USER.

LAYER 1

TYPE 1 - VERTICAL PERCOLATION LAYER

MATERIAL TEXTURE NUMBER 6

THICKNESS	=	6.00	INCHES
POROSITY	=	0.4530	VOL/VOL
FIELD CAPACITY	=	0.1900	VOL/VOL
WILTING POINT	=	0.0850	VOL/VOL
INITIAL SOIL WATER CONTENT	=	0.1110	VOL/VOL
EFFECTIVE SAT. HYD. COND.	=	0.720000011000E-03	CM/SEC

NOTE: SATURATED HYDRAULIC CONDUCTIVITY IS MULTIPLIED BY 1.60
FOR ROOT CHANNELS IN TOP HALF OF EVAPORATIVE ZONE.

LAYER 2

TYPE 1 - VERTICAL PERCOLATION LAYER

MATERIAL TEXTURE NUMBER 6

THICKNESS	=	30.00	INCHES
POROSITY	=	0.4530	VOL/VOL
FIELD CAPACITY	=	0.1900	VOL/VOL
WILTING POINT	=	0.0850	VOL/VOL
INITIAL SOIL WATER CONTENT	=	0.1110	VOL/VOL
EFFECTIVE SAT. HYD. COND.	=	0.720000011000E-03	CM/SEC

LAYER 3

TYPE 1 - VERTICAL PERCOLATION LAYER

MATERIAL TEXTURE NUMBER 6

THICKNESS	=	12.00	INCHES
POROSITY	=	0.4530	VOL/VOL
FIELD CAPACITY	=	0.1900	VOL/VOL
WILTING POINT	=	0.0850	VOL/VOL
INITIAL SOIL WATER CONTENT	=	0.1110	VOL/VOL
EFFECTIVE SAT. HYD. COND.	=	0.720000011000E-03	CM/SEC

GENERAL DESIGN AND EVAPORATIVE ZONE DATA

NOTE: SCS RUNOFF CURVE NUMBER WAS COMPUTED FROM A USER-SPECIFIED CURVE NUMBER OF 95.0, A SURFACE SLOPE OF 25.% AND A SLOPE LENGTH OF 650. FEET.

SCS RUNOFF CURVE NUMBER	=	95.20	
FRACTION OF AREA ALLOWING RUNOFF	=	100.0	PERCENT
AREA PROJECTED ON HORIZONTAL PLANE	=	114.000	ACRES
EVAPORATIVE ZONE DEPTH	=	28.0	INCHES
INITIAL WATER IN EVAPORATIVE ZONE	=	3.108	INCHES
UPPER LIMIT OF EVAPORATIVE STORAGE	=	12.684	INCHES
LOWER LIMIT OF EVAPORATIVE STORAGE	=	2.380	INCHES
INITIAL SNOW WATER	=	0.000	INCHES
INITIAL WATER IN LAYER MATERIALS	=	5.328	INCHES
TOTAL INITIAL WATER	=	5.328	INCHES
TOTAL SUBSURFACE INFLOW	=	0.00	INCHES/YEAR

EVAPOTRANSPIRATION AND WEATHER DATA

NOTE: EVAPOTRANSPIRATION DATA WAS OBTAINED FROM
ALBUQUERQUE NEW MEXICO

STATION LATITUDE	=	35.30 DEGREES
MAXIMUM LEAF AREA INDEX	=	0.80
START OF GROWING SEASON (JULIAN DATE)	=	98
END OF GROWING SEASON (JULIAN DATE)	=	299
EVAPORATIVE ZONE DEPTH	=	28.0 INCHES
AVERAGE ANNUAL WIND SPEED	=	9.00 MPH
AVERAGE 1ST QUARTER RELATIVE HUMIDITY	=	48.00 %
AVERAGE 2ND QUARTER RELATIVE HUMIDITY	=	30.00 %
AVERAGE 3RD QUARTER RELATIVE HUMIDITY	=	45.00 %
AVERAGE 4TH QUARTER RELATIVE HUMIDITY	=	50.00 %

NOTE: PRECIPITATION DATA WAS SYNTHETICALLY GENERATED USING
COEFFICIENTS FOR ALBUQUERQUE NEW MEXICO

NORMAL MEAN MONTHLY PRECIPITATION (INCHES)

JAN/JUL	FEB/AUG	MAR/SEP	APR/OCT	MAY/NOV	JUN/DEC
-----	-----	-----	-----	-----	-----
0.37	0.47	0.48	0.99	0.72	0.99
1.39	2.34	1.20	1.50	0.55	0.47

NOTE: TEMPERATURE DATA WAS SYNTHETICALLY GENERATED USING
COEFFICIENTS FOR ALBUQUERQUE NEW MEXICO

NORMAL MEAN MONTHLY TEMPERATURE (DEGREES FAHRENHEIT)

JAN/JUL	FEB/AUG	MAR/SEP	APR/OCT	MAY/NOV	JUN/DEC
-----	-----	-----	-----	-----	-----
35.20	40.90	47.10	55.30	64.90	73.50
77.30	75.60	67.30	57.20	44.40	35.70

NOTE: SOLAR RADIATION DATA WAS SYNTHETICALLY GENERATED USING
COEFFICIENTS FOR ALBUQUERQUE NEW MEXICO
AND STATION LATITUDE = 35.30 DEGREES

MONTHLY TOTALS (IN INCHES) FOR YEAR 1

	JAN/JUL	FEB/AUG	MAR/SEP	APR/OCT	MAY/NOV	JUN/DEC
	-----	-----	-----	-----	-----	-----
PRECIPITATION	0.11 0.99	0.01 3.66	0.26 1.17	0.55 1.12	0.86 1.67	0.01 0.57
RUNOFF	0.000 0.004	0.000 0.321	0.000 0.044	0.057 0.064	0.182 0.005	0.000 0.011
EVAPOTRANSPIRATION	0.576 0.988	0.138 2.705	0.108 1.764	0.228 1.023	1.215 1.595	0.017 0.659
PERCOLATION/LEAKAGE THROUGH LAYER 3	0.0000 0.0000	0.0000 0.0000	0.0000 0.0000	0.0000 0.0000	0.0000 0.0000	0.0000 0.0000

ANNUAL TOTALS FOR YEAR 1

	INCHES	CU. FEET	PERCENT
	-----	-----	-----
PRECIPITATION	10.98	4543744.000	100.00
RUNOFF	0.687	284266.156	6.26
EVAPOTRANSPIRATION	11.014	4557920.500	100.31
PERC./LEAKAGE THROUGH LAYER 3	0.000008	3.189	0.00
CHANGE IN WATER STORAGE	-0.721	-298446.375	-6.57
SOIL WATER AT START OF YEAR	5.328	2204824.000	
SOIL WATER AT END OF YEAR	4.607	1906377.500	
SNOW WATER AT START OF YEAR	0.000	0.000	0.00
SNOW WATER AT END OF YEAR	0.000	0.000	0.00
ANNUAL WATER BUDGET BALANCE	0.0000	0.832	0.00

MONTHLY TOTALS (IN INCHES) FOR YEAR 2

	JAN/JUL	FEB/AUG	MAR/SEP	APR/OCT	MAY/NOV	JUN/DEC
PRECIPITATION	0.09 1.08	1.07 3.29	0.00 1.76	1.64 5.91	1.35 0.03	2.03 0.42
RUNOFF	0.000 0.041	0.067 0.387	0.000 0.124	0.356 1.597	0.000 0.000	0.488 0.000
EVAPOTRANSPIRATION	0.063 1.066	1.028 2.416	0.002 1.567	1.283 2.798	1.169 1.875	1.698 0.536
PERCOLATION/LEAKAGE THROUGH LAYER 3	0.0000 0.0000	0.0000 0.0000	0.0000 0.0000	0.0000 0.0000	0.0000 0.0000	0.0000 0.0000

ANNUAL TOTALS FOR YEAR 2

	INCHES	CU. FEET	PERCENT
PRECIPITATION	18.67	7726020.000	100.00
RUNOFF	3.060	1266413.250	16.39
EVAPOTRANSPIRATION	15.503	6415511.500	83.04
PERC./LEAKAGE THROUGH LAYER 3	0.000000	0.188	0.00
CHANGE IN WATER STORAGE	0.107	44093.992	0.57
SOIL WATER AT START OF YEAR	4.607	1906377.500	
SOIL WATER AT END OF YEAR	4.713	1950471.500	
SNOW WATER AT START OF YEAR	0.000	0.000	0.00
SNOW WATER AT END OF YEAR	0.000	0.000	0.00
ANNUAL WATER BUDGET BALANCE	0.0000	1.193	0.00

MONTHLY TOTALS (IN INCHES) FOR YEAR 3

	JAN/JUL	FEB/AUG	MAR/SEP	APR/OCT	MAY/NOV	JUN/DEC
PRECIPITATION	0.47 0.75	0.61 1.16	0.91 2.62	0.33 1.24	1.68 0.77	2.49 0.17
RUNOFF	0.002 0.000	0.001 0.012	0.003 0.362	0.000 0.011	0.144 0.044	0.592 0.000
EVAPOTRANSPIRATION	0.204 0.750	0.283 0.822	1.169 2.582	0.500 1.030	1.451 0.923	2.250 0.170
PERCOLATION/LEAKAGE THROUGH LAYER 3	0.0000 0.0000	0.0000 0.0000	0.0000 0.0000	0.0000 0.0000	0.0000 0.0000	0.0000 0.0000

ANNUAL TOTALS FOR YEAR 3

	INCHES	CU. FEET	PERCENT
PRECIPITATION	13.20	5462424.500	100.00
RUNOFF	1.171	484590.719	8.87
EVAPOTRANSPIRATION	12.134	5021357.000	91.93
PERC./LEAKAGE THROUGH LAYER 3	0.000001	0.444	0.00
CHANGE IN WATER STORAGE	-0.105	-43523.133	-0.80
SOIL WATER AT START OF YEAR	4.713	1950471.500	
SOIL WATER AT END OF YEAR	4.608	1906948.370	
SNOW WATER AT START OF YEAR	0.000	0.000	0.00
SNOW WATER AT END OF YEAR	0.000	0.000	0.00

ANNUAL WATER BUDGET BALANCE 0.0000 -0.641 0.00

MONTHLY TOTALS (IN INCHES) FOR YEAR 4

	JAN/JUL	FEB/AUG	MAR/SEP	APR/OCT	MAY/NOV	JUN/DEC
PRECIPITATION	0.00 3.02	0.07 2.72	0.17 1.04	0.19 3.38	0.38 0.35	1.20 0.36
RUNOFF	0.000 0.608	0.000 0.432	0.000 0.022	0.000 0.682	0.000 0.000	0.102 0.000
EVAPOTRANSPIRATION	0.001 2.369	0.070 2.064	0.170 1.272	0.190 1.794	0.381 1.060	1.099 0.434
PERCOLATION/LEAKAGE THROUGH LAYER 3	0.0000 0.0000	0.0000 0.0000	0.0000 0.0000	0.0000 0.0000	0.0000 0.0000	0.0000 0.0000

ANNUAL TOTALS FOR YEAR 4

	INCHES	CU. FEET	PERCENT
PRECIPITATION	12.88	5330001.500	100.00
RUNOFF	1.846	764018.187	14.33
EVAPOTRANSPIRATION	10.904	4512305.500	84.66
PERC./LEAKAGE THROUGH LAYER 3	0.000009	3.860	0.00
CHANGE IN WATER STORAGE	0.130	53674.504	1.01
SOIL WATER AT START OF YEAR	4.608	1906948.370	
SOIL WATER AT END OF YEAR	4.738	1960622.870	

SNOW WATER AT START OF YEAR	0.000	0.000	0.00
SNOW WATER AT END OF YEAR	0.000	0.000	0.00
ANNUAL WATER BUDGET BALANCE	0.0000	-0.505	0.00

MONTHLY TOTALS (IN INCHES) FOR YEAR 5

	JAN/JUL	FEB/AUG	MAR/SEP	APR/OCT	MAY/NOV	JUN/DEC
	-----	-----	-----	-----	-----	-----
PRECIPITATION	0.27	0.68	0.78	1.73	0.97	0.20
	1.40	1.86	1.82	3.13	0.00	1.03
RUNOFF	0.000	0.013	0.020	0.332	0.132	0.000
	0.000	0.137	0.332	0.577	0.000	0.000
EVAPOTRANSPIRATION	0.375	0.337	1.107	1.368	0.878	0.199
	1.219	1.905	0.709	2.595	0.731	0.977
PERCOLATION/LEAKAGE THROUGH LAYER 3	0.0000	0.0000	0.0000	0.0000	0.0000	0.0000
	0.0000	0.0000	0.0000	0.0000	0.0000	0.0000

ANNUAL TOTALS FOR YEAR 5

	INCHES	CU. FEET	PERCENT
	-----	-----	-----
PRECIPITATION	13.87	5739684.500	100.00
RUNOFF	1.542	638061.375	11.12
EVAPOTRANSPIRATION	12.401	5131741.000	89.41
PERC./LEAKAGE THROUGH LAYER 3	0.000022	9.074	0.00
CHANGE IN WATER STORAGE	-0.073	-30127.543	-0.52
SOIL WATER AT START OF YEAR	4.738	1960622.870	

SOIL WATER AT END OF YEAR	4.665	1930495.370	
SNOW WATER AT START OF YEAR	0.000	0.000	0.00
SNOW WATER AT END OF YEAR	0.000	0.000	0.00
ANNUAL WATER BUDGET BALANCE	0.0000	0.447	0.00

AVERAGE MONTHLY VALUES IN INCHES FOR YEARS 1 THROUGH 5

JAN/JUL FEB/AUG MAR/SEP APR/OCT MAY/NOV JUN/DEC

TOTALS	0.19	0.49	0.42	0.89	1.05	1.19
	1.45	2.54	1.68	2.96	0.56	0.51

TOTALS	0.000	0.016	0.005	0.149	0.092	0.236
	0.130	0.258	0.177	0.586	0.010	0.002

TOTALS	0.244	0.371	0.511	0.714	1.019	1.052
	1.279	1.983	1.579	1.848	1.237	0.555

TOTALS	0.0000	0.0000	0.0000	0.0000	0.0000	0.0000
	0.0000	0.0000	0.0000	0.0000	0.0000	0.0000

AVERAGE ANNUAL TOTALS & (STD. DEVIATIONS) FOR YEARS 1 THROUGH 5

	INCHES		CU. FEET	PERCENT
	-----		-----	-----
PRECIPITATION	13.92	(2.864)	5760375.0	100.00
RUNOFF	1.661	(0.8938)	687469.94	11.934
EVAPOTRANSPIRATION	12.391	(1.8613)	5127767.00	89.018
PERCOLATION/LEAKAGE THROUGH LAYER 3	0.00001	(0.00001)	3.351	0.00006
CHANGE IN WATER STORAGE	-0.133	(0.3452)	-54865.71	-0.952

PEAK DAILY VALUES FOR YEARS	1 THROUGH	5
	(INCHES)	(CU. FT.)
PRECIPITATION	1.97	815225.437
RUNOFF	1.039	430101.2190
PERCOLATION/LEAKAGE THROUGH LAYER 3	0.000002	0.99577
SNOW WATER	0.58	240145.9530
MAXIMUM VEG. SOIL WATER (VOL/VOL)		0.1589
MINIMUM VEG. SOIL WATER (VOL/VOL)		0.0850

FINAL WATER STORAGE AT END OF YEAR 5

LAYER	(INCHES)	(VOL/VOL)
1	0.5474	0.0912
2	2.7818	0.0927
3	1.3359	0.1113
SNOW WATER	0.000	

**APPLICATION FOR PERMIT RENEWAL AND MODIFICATION
SANDOVAL COUNTY LANDFILL**

**VOLUME III: LANDFILL ENGINEERING CALCULATIONS
SECTION 10: HELP MODEL**

ATTACHMENT III.10.A-3

TIER II, SIMULATION 7-1

PRESCRIPTIVE LINER WITH SOIL TYPE 6

```

*****
*****
**
**
**
**      HYDROLOGIC EVALUATION OF LANDFILL PERFORMANCE      **
**      HELP MODEL VERSION 3.07  (1 NOVEMBER 1997)          **
**      DEVELOPED BY ENVIRONMENTAL LABORATORY                **
**      USAE WATERWAYS EXPERIMENT STATION                    **
**      FOR USEPA RISK REDUCTION ENGINEERING LABORATORY      **
**
**
*****
*****

```

```

PRECIPITATION DATA FILE:  C:\RAIN1.D4
TEMPERATURE DATA FILE:   C:\TEMP1.D7
SOLAR RADIATION DATA FILE: C:\SOLAR1.D13
EVAPOTRANSPIRATION DATA:  C:\EVAP1.D11
SOIL AND DESIGN DATA FILE: C:\UNITIV2Y.D10
OUTPUT DATA FILE:        C:\UNITIV2Y.OUT

```

TIME: 16:25 DATE: 4/ 8/2015

```

*****

```

TITLE: Sandoval County Landfill-Unit IV Base Grading-Simulation 7

Simulation 7 - Open Unit IV for two years.

```

*****

```

NOTE: INITIAL MOISTURE CONTENT OF THE LAYERS AND SNOW WATER
WERE SPECIFIED BY THE USER.

LAYER 1

TYPE 2 - LATERAL DRAINAGE LAYER
MATERIAL TEXTURE NUMBER 0

THICKNESS	=	24.00	INCHES
POROSITY	=	0.4530	VOL/VOL
FIELD CAPACITY	=	0.1900	VOL/VOL
WILTING POINT	=	0.0850	VOL/VOL
INITIAL SOIL WATER CONTENT	=	0.1110	VOL/VOL
EFFECTIVE SAT. HYD. COND.	=	0.300000014000E-03	CM/SEC
SLOPE	=	5.00	PERCENT
DRAINAGE LENGTH	=	200.0	FEET

LAYER 2

TYPE 4 - FLEXIBLE MEMBRANE LINER

MATERIAL TEXTURE NUMBER 35

THICKNESS	=	0.06	INCHES
POROSITY	=	0.0000	VOL/VOL
FIELD CAPACITY	=	0.0000	VOL/VOL
WILTING POINT	=	0.0000	VOL/VOL
INITIAL SOIL WATER CONTENT	=	0.0000	VOL/VOL
EFFECTIVE SAT. HYD. COND.	=	0.199999996000E-12	CM/SEC
FML PINHOLE DENSITY	=	1.00	HOLES/ACRE
FML INSTALLATION DEFECTS	=	4.00	HOLES/ACRE
FML PLACEMENT QUALITY	=	3	- GOOD

LAYER 3

TYPE 3 - BARRIER SOIL LINER

MATERIAL TEXTURE NUMBER 0

THICKNESS	=	0.25	INCHES
POROSITY	=	0.7500	VOL/VOL
FIELD CAPACITY	=	0.7470	VOL/VOL
WILTING POINT	=	0.4000	VOL/VOL
INITIAL SOIL WATER CONTENT	=	0.7500	VOL/VOL
EFFECTIVE SAT. HYD. COND.	=	0.499999997000E-08	CM/SEC

LAYER 4

TYPE 1 - VERTICAL PERCOLATION LAYER

MATERIAL TEXTURE NUMBER 0

THICKNESS	=	6.00	INCHES
POROSITY	=	0.4530	VOL/VOL
FIELD CAPACITY	=	0.1900	VOL/VOL
WILTING POINT	=	0.0850	VOL/VOL
INITIAL SOIL WATER CONTENT	=	0.1110	VOL/VOL
EFFECTIVE SAT. HYD. COND.	=	0.420000015000E-05	CM/SEC

GENERAL DESIGN AND EVAPORATIVE ZONE DATA

NOTE: SCS RUNOFF CURVE NUMBER WAS USER-SPECIFIED.

SCS RUNOFF CURVE NUMBER	=	0.00	
FRACTION OF AREA ALLOWING RUNOFF	=	0.0	PERCENT
AREA PROJECTED ON HORIZONTAL PLANE	=	30.700	ACRES
EVAPORATIVE ZONE DEPTH	=	18.0	INCHES
INITIAL WATER IN EVAPORATIVE ZONE	=	1.998	INCHES
UPPER LIMIT OF EVAPORATIVE STORAGE	=	8.154	INCHES
LOWER LIMIT OF EVAPORATIVE STORAGE	=	1.530	INCHES
INITIAL SNOW WATER	=	0.000	INCHES
INITIAL WATER IN LAYER MATERIALS	=	3.517	INCHES
TOTAL INITIAL WATER	=	3.517	INCHES
TOTAL SUBSURFACE INFLOW	=	0.00	INCHES/YEAR

EVAPOTRANSPIRATION AND WEATHER DATA

NOTE: EVAPOTRANSPIRATION DATA WAS OBTAINED FROM
ALBUQUERQUE NEW MEXICO

STATION LATITUDE	=	35.30	DEGREES
MAXIMUM LEAF AREA INDEX	=	0.00	
START OF GROWING SEASON (JULIAN DATE)	=	98	
END OF GROWING SEASON (JULIAN DATE)	=	299	
EVAPORATIVE ZONE DEPTH	=	18.0	INCHES
AVERAGE ANNUAL WIND SPEED	=	9.00	MPH
AVERAGE 1ST QUARTER RELATIVE HUMIDITY	=	48.00	%
AVERAGE 2ND QUARTER RELATIVE HUMIDITY	=	30.00	%
AVERAGE 3RD QUARTER RELATIVE HUMIDITY	=	45.00	%
AVERAGE 4TH QUARTER RELATIVE HUMIDITY	=	50.00	%

NOTE: PRECIPITATION DATA WAS SYNTHETICALLY GENERATED USING
COEFFICIENTS FOR ALBUQUERQUE NEW MEXICO

NORMAL MEAN MONTHLY PRECIPITATION (INCHES)

JAN/JUL	FEB/AUG	MAR/SEP	APR/OCT	MAY/NOV	JUN/DEC
-----	-----	-----	-----	-----	-----
0.37	0.47	0.48	0.99	0.72	0.99
1.39	2.34	1.20	1.50	0.55	0.47

NOTE: TEMPERATURE DATA WAS SYNTHETICALLY GENERATED USING
COEFFICIENTS FOR ALBUQUERQUE NEW MEXICO

NORMAL MEAN MONTHLY TEMPERATURE (DEGREES FAHRENHEIT)

JAN/JUL	FEB/AUG	MAR/SEP	APR/OCT	MAY/NOV	JUN/DEC
-----	-----	-----	-----	-----	-----
35.20	40.90	47.10	55.30	64.90	73.50
77.30	75.60	67.30	57.20	44.40	35.70

NOTE: SOLAR RADIATION DATA WAS SYNTHETICALLY GENERATED USING
 COEFFICIENTS FOR ALBUQUERQUE NEW MEXICO
 AND STATION LATITUDE = 35.30 DEGREES

MONTHLY TOTALS (IN INCHES) FOR YEAR 1

	JAN/JUL	FEB/AUG	MAR/SEP	APR/OCT	MAY/NOV	JUN/DEC
	-----	-----	-----	-----	-----	-----
PRECIPITATION	0.11	0.01	0.26	0.55	0.86	0.01
	0.99	3.66	1.17	1.12	1.67	0.57
RUNOFF	0.000	0.000	0.000	0.000	0.000	0.000
	0.000	0.000	0.000	0.000	0.000	0.000
EVAPOTRANSPIRATION	0.316	0.218	0.103	0.115	1.062	0.318
	0.295	2.606	2.213	0.482	1.716	0.606
LATERAL DRAINAGE COLLECTED FROM LAYER 1	0.0000	0.0000	0.0000	0.0000	0.0000	0.0000
	0.0000	0.0000	0.0000	0.0000	0.0000	0.0000
PERCOLATION/LEAKAGE THROUGH LAYER 3	0.0000	0.0000	0.0000	0.0000	0.0000	0.0000
	0.0000	0.0000	0.0000	0.0000	0.0000	0.0000
PERCOLATION/LEAKAGE THROUGH LAYER 4	0.0000	0.0000	0.0000	0.0000	0.0000	0.0000
	0.0000	0.0000	0.0000	0.0000	0.0000	0.0000

MONTHLY SUMMARIES FOR DAILY HEADS (INCHES)

AVERAGE DAILY HEAD ON TOP OF LAYER 2	0.000	0.000	0.000	0.000	0.000	0.000
	0.000	0.000	0.000	0.000	0.000	0.000
STD. DEVIATION OF DAILY HEAD ON TOP OF LAYER 2	0.000	0.000	0.000	0.000	0.000	0.000
	0.000	0.000	0.000	0.000	0.000	0.000

ANNUAL TOTALS FOR YEAR 1

	INCHES	CU. FEET	PERCENT
	-----	-----	-----
PRECIPITATION	10.98	1223622.370	100.00
RUNOFF	0.000	0.000	0.00
EVAPOTRANSPIRATION	10.050	1119979.000	91.53
DRAINAGE COLLECTED FROM LAYER 1	0.0000	0.000	0.00
PERC./LEAKAGE THROUGH LAYER 3	0.000000	0.000	0.00
AVG. HEAD ON TOP OF LAYER 2	0.0000		
PERC./LEAKAGE THROUGH LAYER 4	0.000000	0.000	0.00
CHANGE IN WATER STORAGE	0.930	103643.141	8.47
SOIL WATER AT START OF YEAR	3.517	391991.219	
SOIL WATER AT END OF YEAR	4.448	495634.375	
SNOW WATER AT START OF YEAR	0.000	0.000	0.00
SNOW WATER AT END OF YEAR	0.000	0.000	0.00
ANNUAL WATER BUDGET BALANCE	0.0000	0.213	0.00

MONTHLY TOTALS (IN INCHES) FOR YEAR 2

	JAN/JUL	FEB/AUG	MAR/SEP	APR/OCT	MAY/NOV	JUN/DEC
	-----	-----	-----	-----	-----	-----
PRECIPITATION	0.09	1.07	0.00	1.64	1.35	2.03
	1.08	3.29	1.76	5.91	0.03	0.42
RUNOFF	0.000	0.000	0.000	0.000	0.000	0.000
	0.000	0.000	0.000	0.000	0.000	0.000

EVAPOTRANSPIRATION	0.276	0.848	0.389	1.144	1.231	1.927
	0.996	2.566	1.477	3.092	1.295	0.427
LATERAL DRAINAGE COLLECTED FROM LAYER 1	0.0000	0.0000	0.0000	0.0000	0.0000	0.0000
	0.0000	0.0000	0.0000	0.0039	0.1152	0.1227
PERCOLATION/LEAKAGE THROUGH LAYER 3	0.0000	0.0000	0.0000	0.0000	0.0000	0.0000
	0.0000	0.0000	0.0000	0.0000	0.0003	0.0003
PERCOLATION/LEAKAGE THROUGH LAYER 4	0.0000	0.0000	0.0000	0.0000	0.0000	0.0000
	0.0000	0.0000	0.0000	0.0000	0.0000	0.0000

MONTHLY SUMMARIES FOR DAILY HEADS (INCHES)

AVERAGE DAILY HEAD ON TOP OF LAYER 2	0.000	0.000	0.000	0.000	0.000	0.000
	0.000	0.000	0.000	0.299	9.058	9.330
STD. DEVIATION OF DAILY HEAD ON TOP OF LAYER 2	0.000	0.000	0.000	0.000	0.000	0.000
	0.000	0.000	0.000	1.181	0.667	0.190

ANNUAL TOTALS FOR YEAR 2

	INCHES	CU. FEET	PERCENT
	-----	-----	-----
PRECIPITATION	18.67	2080603.750	100.00
RUNOFF	0.000	0.000	0.00
EVAPOTRANSPIRATION	15.668	1746034.000	83.92
DRAINAGE COLLECTED FROM LAYER 1	0.2419	26952.254	1.30
PERC./LEAKAGE THROUGH LAYER 3	0.000595	66.283	0.00
AVG. HEAD ON TOP OF LAYER 2	1.5572		
PERC./LEAKAGE THROUGH LAYER 4	0.000000	0.000	0.00
CHANGE IN WATER STORAGE	2.760	307616.937	14.78
SOIL WATER AT START OF YEAR	4.448	495634.375	
SOIL WATER AT END OF YEAR	7.208	803251.312	

SNOW WATER AT START OF YEAR	0.000	0.000	0.00
SNOW WATER AT END OF YEAR	0.000	0.000	0.00
ANNUAL WATER BUDGET BALANCE	0.0000	0.485	0.00

AVERAGE MONTHLY VALUES IN INCHES FOR YEARS 1 THROUGH 2

	JAN/JUL	FEB/AUG	MAR/SEP	APR/OCT	MAY/NOV	JUN/DEC
	-----	-----	-----	-----	-----	-----
PRECIPITATION						

TOTALS	0.10 1.03	0.54 3.47	0.13 1.47	1.10 3.51	1.11 0.85	1.02 0.50

STD. DEVIATIONS	0.01 0.06	0.75 0.26	0.18 0.42	0.77 3.39	0.35 1.16	1.43 0.11
-----------------	--------------	--------------	--------------	--------------	--------------	--------------

RUNOFF

TOTALS	0.000 0.000	0.000 0.000	0.000 0.000	0.000 0.000	0.000 0.000	0.000 0.000
STD. DEVIATIONS	0.000 0.000	0.000 0.000	0.000 0.000	0.000 0.000	0.000 0.000	0.000 0.000

EVAPOTRANSPIRATION

TOTALS	0.296 0.646	0.533 2.586	0.246 1.845	0.629 1.787	1.146 1.506	1.123 0.516
STD. DEVIATIONS	0.028 0.495	0.445 0.028	0.202 0.520	0.728 1.846	0.119 0.298	1.138 0.126

LATERAL DRAINAGE COLLECTED FROM LAYER 1

TOTALS	0.0000 0.0000	0.0000 0.0000	0.0000 0.0000	0.0000 0.0020	0.0000 0.0576	0.0000 0.0613
STD. DEVIATIONS	0.0000 0.0000	0.0000 0.0000	0.0000 0.0000	0.0000 0.0028	0.0000 0.0815	0.0000 0.0867

PERCOLATION/LEAKAGE THROUGH LAYER 3

TOTALS	0.0000	0.0000	0.0000	0.0000	0.0000	0.0000
	0.0000	0.0000	0.0000	0.0000	0.0001	0.0002

STD. DEVIATIONS	0.0000	0.0000	0.0000	0.0000	0.0000	0.0000
	0.0000	0.0000	0.0000	0.0000	0.0002	0.0002

PERCOLATION/LEAKAGE THROUGH LAYER 4

TOTALS	0.0000	0.0000	0.0000	0.0000	0.0000	0.0000
	0.0000	0.0000	0.0000	0.0000	0.0000	0.0000

STD. DEVIATIONS	0.0000	0.0000	0.0000	0.0000	0.0000	0.0000
	0.0000	0.0000	0.0000	0.0000	0.0000	0.0000

AVERAGES OF MONTHLY AVERAGED DAILY HEADS (INCHES)

DAILY AVERAGE HEAD ON TOP OF LAYER 2

AVERAGES	0.0000	0.0000	0.0000	0.0000	0.0000	0.0000
	0.0000	0.0000	0.0000	0.1494	4.5288	4.6652

STD. DEVIATIONS	0.0000	0.0000	0.0000	0.0000	0.0000	0.0000
	0.0000	0.0000	0.0000	0.2113	6.4047	6.5976

AVERAGE ANNUAL TOTALS & (STD. DEVIATIONS) FOR YEARS 1 THROUGH 2

	INCHES		CU. FEET	PERCENT
	-----		-----	-----
PRECIPITATION	14.83	(5.438)	1652113.0	100.00
RUNOFF	0.000	(0.0000)	0.00	0.000
EVAPOTRANSPIRATION	12.859	(3.9724)	1433006.62	86.738
LATERAL DRAINAGE COLLECTED FROM LAYER 1	0.12093	(0.17102)	13476.127	0.81569
PERCOLATION/LEAKAGE THROUGH LAYER 3	0.00030	(0.00042)	33.142	0.00201
AVERAGE HEAD ON TOP OF LAYER 2	0.779	(1.101)		
PERCOLATION/LEAKAGE THROUGH LAYER 4	0.00000	(0.00000)	0.000	0.00000
CHANGE IN WATER STORAGE	1.845	(1.2942)	205630.05	12.446

PEAK DAILY VALUES FOR YEARS	1 THROUGH	2
	(INCHES)	(CU. FT.)
PRECIPITATION	1.97	219538.781
RUNOFF	0.000	0.0000
DRAINAGE COLLECTED FROM LAYER 1	0.00409	455.40921
PERCOLATION/LEAKAGE THROUGH LAYER 3	0.000010	1.15132
AVERAGE HEAD ON TOP OF LAYER 2	9.635	
MAXIMUM HEAD ON TOP OF LAYER 2	15.170	
LOCATION OF MAXIMUM HEAD IN LAYER 1 (DISTANCE FROM DRAIN)	42.2 FEET	
PERCOLATION/LEAKAGE THROUGH LAYER 4	0.000000	0.00000
SNOW WATER	0.55	61327.6484
MAXIMUM VEG. SOIL WATER (VOL/VOL)		0.3458
MINIMUM VEG. SOIL WATER (VOL/VOL)		0.0859

*** Maximum heads are computed using McEnroe's equations. ***

Reference: Maximum Saturated Depth over Landfill Liner
by Bruce M. McEnroe, University of Kansas
ASCE Journal of Environmental Engineering
Vol. 119, No. 2, March 1993, pp. 262-270.

FINAL WATER STORAGE AT END OF YEAR 2

LAYER	(INCHES)	(VOL/VOL)
1	6.3538	0.2647
2	0.0000	0.0000
3	0.1875	0.7500
4	0.6666	0.1111
SNOW WATER	0.000	

**APPLICATION FOR PERMIT RENEWAL AND MODIFICATION
SANDOVAL COUNTY LANDFILL**

**VOLUME III: LANDFILL ENGINEERING CALCULATIONS
SECTION 10: HELP MODEL**

ATTACHMENT III.10.A-4

TIER II, SIMULATION 8-1

PRESCRIPTIVE LINER WITH SOIL TYPE 6

INTERMEDIATE COVER WITH SOIL TYPE 6

```

*****
*****
**
**
**
HYDROLOGIC EVALUATION OF LANDFILL PERFORMANCE
HELP MODEL VERSION 3.07 (1 NOVEMBER 1997)
DEVELOPED BY ENVIRONMENTAL LABORATORY
USAE WATERWAYS EXPERIMENT STATION
FOR USEPA RISK REDUCTION ENGINEERING LABORATORY
**
**
**
*****
*****

```

```

PRECIPITATION DATA FILE:  C:\RAIN1.D4
TEMPERATURE DATA FILE:   C:\TEMP1.D7
SOLAR RADIATION DATA FILE: C:\SOLAR1.D13
EVAPOTRANSPIRATION DATA:  C:\EVAP1.D11
SOIL AND DESIGN DATA FILE: C:\SIM820FT.D10
OUTPUT DATA FILE:         C:\SIM820FT.OUT

```

TIME: 16:34 DATE: 4/ 8/2015

```

*****

```

TITLE: Sandoval County Landfill - Unit IV Base Grading-20 ft Waste
Simulation 8 - Partially Filled Unit IV; no runoff

```

*****

```

NOTE: INITIAL MOISTURE CONTENT OF THE LAYERS AND SNOW WATER
WERE SPECIFIED BY THE USER.

LAYER 1

TYPE 1 - VERTICAL PERCOLATION LAYER
MATERIAL TEXTURE NUMBER 6

THICKNESS	=	12.00	INCHES
POROSITY	=	0.4530	VOL/VOL
FIELD CAPACITY	=	0.1900	VOL/VOL
WILTING POINT	=	0.0850	VOL/VOL
INITIAL SOIL WATER CONTENT	=	0.1110	VOL/VOL
EFFECTIVE SAT. HYD. COND.	=	0.720000011000E-03	CM/SEC

LAYER 2

TYPE 1 - VERTICAL PERCOLATION LAYER

MATERIAL TEXTURE NUMBER 18

THICKNESS	=	240.00	INCHES
POROSITY	=	0.6710	VOL/VOL
FIELD CAPACITY	=	0.2920	VOL/VOL
WILTING POINT	=	0.0770	VOL/VOL
INITIAL SOIL WATER CONTENT	=	0.1310	VOL/VOL
EFFECTIVE SAT. HYD. COND.	=	0.100000005000E-02	CM/SEC

LAYER 3

TYPE 2 - LATERAL DRAINAGE LAYER

MATERIAL TEXTURE NUMBER 0

THICKNESS	=	24.00	INCHES
POROSITY	=	0.4730	VOL/VOL
FIELD CAPACITY	=	0.2220	VOL/VOL
WILTING POINT	=	0.1040	VOL/VOL
INITIAL SOIL WATER CONTENT	=	0.2647	VOL/VOL
EFFECTIVE SAT. HYD. COND.	=	0.300000014000E-03	CM/SEC
SLOPE	=	5.00	PERCENT
DRAINAGE LENGTH	=	200.0	FEET

LAYER 4

TYPE 4 - FLEXIBLE MEMBRANE LINER

MATERIAL TEXTURE NUMBER 35

THICKNESS	=	0.06	INCHES
POROSITY	=	0.0000	VOL/VOL
FIELD CAPACITY	=	0.0000	VOL/VOL
WILTING POINT	=	0.0000	VOL/VOL
INITIAL SOIL WATER CONTENT	=	0.0000	VOL/VOL
EFFECTIVE SAT. HYD. COND.	=	0.199999996000E-12	CM/SEC
FML PINHOLE DENSITY	=	1.00	HOLES/ACRE
FML INSTALLATION DEFECTS	=	4.00	HOLES/ACRE
FML PLACEMENT QUALITY	=	3 - GOOD	

LAYER 5

TYPE 3 - BARRIER SOIL LINER
MATERIAL TEXTURE NUMBER 0

THICKNESS	=	0.25	INCHES
POROSITY	=	0.7500	VOL/VOL
FIELD CAPACITY	=	0.7470	VOL/VOL
WILTING POINT	=	0.4000	VOL/VOL
INITIAL SOIL WATER CONTENT	=	0.7500	VOL/VOL
EFFECTIVE SAT. HYD. COND.	=	0.499999997000E-08	CM/SEC

LAYER 6

TYPE 1 - VERTICAL PERCOLATION LAYER
MATERIAL TEXTURE NUMBER 0

THICKNESS	=	6.00	INCHES
POROSITY	=	0.4530	VOL/VOL
FIELD CAPACITY	=	0.1900	VOL/VOL
WILTING POINT	=	0.0850	VOL/VOL
INITIAL SOIL WATER CONTENT	=	0.1110	VOL/VOL
EFFECTIVE SAT. HYD. COND.	=	0.420000015000E-05	CM/SEC

GENERAL DESIGN AND EVAPORATIVE ZONE DATA

NOTE: SCS RUNOFF CURVE NUMBER WAS USER-SPECIFIED.

SCS RUNOFF CURVE NUMBER	=	0.00	
FRACTION OF AREA ALLOWING RUNOFF	=	0.0	PERCENT
AREA PROJECTED ON HORIZONTAL PLANE	=	30.700	ACRES
EVAPORATIVE ZONE DEPTH	=	18.0	INCHES
INITIAL WATER IN EVAPORATIVE ZONE	=	2.118	INCHES
UPPER LIMIT OF EVAPORATIVE STORAGE	=	9.462	INCHES
LOWER LIMIT OF EVAPORATIVE STORAGE	=	1.482	INCHES
INITIAL SNOW WATER	=	0.000	INCHES
INITIAL WATER IN LAYER MATERIALS	=	39.978	INCHES
TOTAL INITIAL WATER	=	39.978	INCHES
TOTAL SUBSURFACE INFLOW	=	0.00	INCHES/YEAR

EVAPOTRANSPIRATION AND WEATHER DATA

NOTE: EVAPOTRANSPIRATION DATA WAS OBTAINED FROM
ALBUQUERQUE NEW MEXICO

STATION LATITUDE	=	35.30 DEGREES
MAXIMUM LEAF AREA INDEX	=	0.00
START OF GROWING SEASON (JULIAN DATE)	=	98
END OF GROWING SEASON (JULIAN DATE)	=	299
EVAPORATIVE ZONE DEPTH	=	18.0 INCHES
AVERAGE ANNUAL WIND SPEED	=	9.00 MPH
AVERAGE 1ST QUARTER RELATIVE HUMIDITY	=	48.00 %
AVERAGE 2ND QUARTER RELATIVE HUMIDITY	=	30.00 %
AVERAGE 3RD QUARTER RELATIVE HUMIDITY	=	45.00 %
AVERAGE 4TH QUARTER RELATIVE HUMIDITY	=	50.00 %

NOTE: PRECIPITATION DATA WAS SYNTHETICALLY GENERATED USING
COEFFICIENTS FOR ALBUQUERQUE NEW MEXICO

NORMAL MEAN MONTHLY PRECIPITATION (INCHES)

JAN/JUL	FEB/AUG	MAR/SEP	APR/OCT	MAY/NOV	JUN/DEC
-----	-----	-----	-----	-----	-----
0.37	0.47	0.48	0.99	0.72	0.99
1.39	2.34	1.20	1.50	0.55	0.47

NOTE: TEMPERATURE DATA WAS SYNTHETICALLY GENERATED USING
COEFFICIENTS FOR ALBUQUERQUE NEW MEXICO

NORMAL MEAN MONTHLY TEMPERATURE (DEGREES FAHRENHEIT)

JAN/JUL	FEB/AUG	MAR/SEP	APR/OCT	MAY/NOV	JUN/DEC
-----	-----	-----	-----	-----	-----
35.20	40.90	47.10	55.30	64.90	73.50
77.30	75.60	67.30	57.20	44.40	35.70

NOTE: SOLAR RADIATION DATA WAS SYNTHETICALLY GENERATED USING
COEFFICIENTS FOR ALBUQUERQUE NEW MEXICO
AND STATION LATITUDE = 35.30 DEGREES

MONTHLY TOTALS (IN INCHES) FOR YEAR 1

	JAN/JUL	FEB/AUG	MAR/SEP	APR/OCT	MAY/NOV	JUN/DEC
PRECIPITATION	0.11 0.99	0.01 3.66	0.26 1.17	0.55 1.12	0.86 1.67	0.01 0.57
RUNOFF	0.000 0.000	0.000 0.000	0.000 0.000	0.000 0.000	0.000 0.000	0.000 0.000
EVAPOTRANSPIRATION	0.441 0.574	0.298 3.161	0.085 2.512	0.174 0.528	0.211 1.530	0.198 0.785
LATERAL DRAINAGE COLLECTED FROM LAYER 3	0.0370 0.0393	0.0411 0.0373	0.0478 0.0343	0.0444 0.0336	0.0436 0.0309	0.0401 0.0303
PERCOLATION/LEAKAGE THROUGH LAYER 5	0.0001 0.0001	0.0001 0.0001	0.0001 0.0001	0.0001 0.0000	0.0001 0.0000	0.0001 0.0000
PERCOLATION/LEAKAGE THROUGH LAYER 6	0.0000 0.0000	0.0000 0.0000	0.0000 0.0000	0.0000 0.0000	0.0000 0.0000	0.0000 0.0000

MONTHLY SUMMARIES FOR DAILY HEADS (INCHES)

AVERAGE DAILY HEAD ON TOP OF LAYER 4	2.817 2.990	3.461 2.838	3.639 2.695	3.491 2.559	3.316 2.430	3.149 2.308
STD. DEVIATION OF DAILY HEAD ON TOP OF LAYER 4	0.347 0.046	0.096 0.044	0.029 0.040	0.052 0.039	0.051 0.036	0.047 0.036

ANNUAL TOTALS FOR YEAR 1

	INCHES	CU. FEET	PERCENT
PRECIPITATION	10.98	1223622.370	100.00
RUNOFF	0.000	0.000	0.00
EVAPOTRANSPIRATION	10.499	1170000.000	95.62
DRAINAGE COLLECTED FROM LAYER 3	0.4599	51253.789	4.19
PERC./LEAKAGE THROUGH LAYER 5	0.000708	78.884	0.01

AVG. HEAD ON TOP OF LAYER 4	2.9745		
PERC./LEAKAGE THROUGH LAYER 6	0.000000	0.000	0.00
CHANGE IN WATER STORAGE	0.021	2368.308	0.19
SOIL WATER AT START OF YEAR	39.978	4455218.500	
SOIL WATER AT END OF YEAR	40.000	4457587.000	
SNOW WATER AT START OF YEAR	0.000	0.000	0.00
SNOW WATER AT END OF YEAR	0.000	0.000	0.00
ANNUAL WATER BUDGET BALANCE	0.0000	0.256	0.00

MONTHLY TOTALS (IN INCHES) FOR YEAR 2

	JAN/JUL	FEB/AUG	MAR/SEP	APR/OCT	MAY/NOV	JUN/DEC
PRECIPITATION	0.09 1.08	1.07 3.29	0.00 1.76	1.64 5.91	1.35 0.03	2.03 0.42
RUNOFF	0.000 0.000	0.000 0.000	0.000 0.000	0.000 0.000	0.000 0.000	0.000 0.000
EVAPOTRANSPIRATION	0.386 0.817	0.371 3.044	0.298 1.553	1.468 2.910	1.120 1.915	2.478 0.559
LATERAL DRAINAGE COLLECTED FROM LAYER 3	0.0288 0.0212	0.0247 0.0201	0.0261 0.0185	0.0240 0.0181	0.0235 0.0167	0.0216 0.0164
PERCOLATION/LEAKAGE THROUGH LAYER 5	0.0000 0.0000	0.0000 0.0000	0.0000 0.0000	0.0000 0.0000	0.0000 0.0000	0.0000 0.0000
PERCOLATION/LEAKAGE THROUGH LAYER 6	0.0000 0.0000	0.0000 0.0000	0.0000 0.0000	0.0000 0.0000	0.0000 0.0000	0.0000 0.0000

MONTHLY SUMMARIES FOR DAILY HEADS (INCHES)

AVERAGE DAILY HEAD ON	2.190	2.084	1.982	1.882	1.788	1.698
TOP OF LAYER 4	1.612	1.530	1.453	1.380	1.310	1.245
STD. DEVIATION OF DAILY	0.034	0.029	0.030	0.028	0.028	0.025
HEAD ON TOP OF LAYER 4	0.025	0.024	0.022	0.021	0.020	0.019

ANNUAL TOTALS FOR YEAR 2

	INCHES	CU. FEET	PERCENT
	-----	-----	-----
PRECIPITATION	18.67	2080603.750	100.00
RUNOFF	0.000	0.000	0.00
EVAPOTRANSPIRATION	16.919	1885522.250	90.62
DRAINAGE COLLECTED FROM LAYER 3	0.2596	28934.287	1.39
PERC./LEAKAGE THROUGH LAYER 5	0.000345	38.471	0.00
AVG. HEAD ON TOP OF LAYER 4	1.6795		
PERC./LEAKAGE THROUGH LAYER 6	0.000000	0.000	0.00
CHANGE IN WATER STORAGE	1.491	166146.328	7.99
SOIL WATER AT START OF YEAR	40.000	4457587.000	
SOIL WATER AT END OF YEAR	41.490	4623733.500	
SNOW WATER AT START OF YEAR	0.000	0.000	0.00
SNOW WATER AT END OF YEAR	0.000	0.000	0.00
ANNUAL WATER BUDGET BALANCE	0.0000	0.864	0.00

MONTHLY TOTALS (IN INCHES) FOR YEAR 3

	JAN/JUL	FEB/AUG	MAR/SEP	APR/OCT	MAY/NOV	JUN/DEC
PRECIPITATION	0.47 0.75	0.61 1.16	0.91 2.62	0.33 1.24	1.68 0.77	2.49 0.17
RUNOFF	0.000 0.000	0.000 0.000	0.000 0.000	0.000 0.000	0.000 0.000	0.000 0.000
EVAPOTRANSPIRATION	0.362 0.508	0.300 0.384	0.566 3.455	0.464 0.653	1.706 1.446	2.984 0.493
LATERAL DRAINAGE COLLECTED FROM LAYER 3	0.0155 0.0114	0.0133 0.0108	0.0141 0.0100	0.0129 0.0098	0.0127 0.0090	0.0116 0.0088
PERCOLATION/LEAKAGE THROUGH LAYER 5	0.0000 0.0000	0.0000 0.0000	0.0000 0.0000	0.0000 0.0000	0.0000 0.0000	0.0000 0.0000
PERCOLATION/LEAKAGE THROUGH LAYER 6	0.0000 0.0000	0.0000 0.0000	0.0000 0.0000	0.0000 0.0000	0.0000 0.0000	0.0000 0.0000

MONTHLY SUMMARIES FOR DAILY HEADS (INCHES)

AVERAGE DAILY HEAD ON TOP OF LAYER 4	1.181 0.869	1.123 0.825	1.069 0.783	1.015 0.744	0.964 0.707	0.915 0.671
STD. DEVIATION OF DAILY HEAD ON TOP OF LAYER 4	0.018 0.013	0.016 0.013	0.016 0.012	0.015 0.011	0.015 0.011	0.014 0.010

ANNUAL TOTALS FOR YEAR 3

	INCHES	CU. FEET	PERCENT
PRECIPITATION	13.20	1471021.370	100.00
RUNOFF	0.000	0.000	0.00
EVAPOTRANSPIRATION	13.322	1484593.370	100.92
DRAINAGE COLLECTED FROM LAYER 3	0.1400	15601.349	1.06
PERC./LEAKAGE THROUGH LAYER 5	0.000169	18.796	0.00

AVG. HEAD ON TOP OF LAYER	4	0.9056		
PERC./LEAKAGE THROUGH LAYER	6	0.000000	0.000	0.00
CHANGE IN WATER STORAGE		-0.262	-29173.002	-1.98
SOIL WATER AT START OF YEAR		41.490	4623733.500	
SOIL WATER AT END OF YEAR		41.229	4594560.500	
SNOW WATER AT START OF YEAR		0.000	0.000	0.00
SNOW WATER AT END OF YEAR		0.000	0.000	0.00
ANNUAL WATER BUDGET BALANCE		0.0000	-0.420	0.00

MONTHLY TOTALS (IN INCHES) FOR YEAR 4

	JAN/JUL	FEB/AUG	MAR/SEP	APR/OCT	MAY/NOV	JUN/DEC
PRECIPITATION	0.00 3.02	0.07 2.72	0.17 1.04	0.19 3.38	0.38 0.35	1.20 0.36
RUNOFF	0.000 0.000	0.000 0.000	0.000 0.000	0.000 0.000	0.000 0.000	0.000 0.000
EVAPOTRANSPIRATION	0.335 2.327	0.148 2.871	0.154 0.882	0.154 2.314	0.113 1.566	0.178 0.565
LATERAL DRAINAGE COLLECTED FROM LAYER 3	0.0084 0.0062	0.0074 0.0058	0.0076 0.0054	0.0070 0.0053	0.0068 0.0048	0.0063 0.0047
PERCOLATION/LEAKAGE THROUGH LAYER 5	0.0000 0.0000	0.0000 0.0000	0.0000 0.0000	0.0000 0.0000	0.0000 0.0000	0.0000 0.0000
PERCOLATION/LEAKAGE THROUGH LAYER 6	0.0000 0.0000	0.0000 0.0000	0.0000 0.0000	0.0000 0.0000	0.0000 0.0000	0.0000 0.0000

MONTHLY SUMMARIES FOR DAILY HEADS (INCHES)

AVERAGE DAILY HEAD ON	0.637	0.605	0.575	0.546	0.519	0.493
TOP OF LAYER 4	0.468	0.444	0.422	0.401	0.380	0.361
STD. DEVIATION OF DAILY	0.010	0.009	0.009	0.008	0.008	0.007
HEAD ON TOP OF LAYER 4	0.007	0.007	0.006	0.006	0.006	0.006

ANNUAL TOTALS FOR YEAR 4

	INCHES	CU. FEET	PERCENT
	-----	-----	-----
PRECIPITATION	12.88	1435360.120	100.00
RUNOFF	0.000	0.000	0.00
EVAPOTRANSPIRATION	11.607	1293494.620	90.12
DRAINAGE COLLECTED FROM LAYER 3	0.0756	8429.336	0.59
PERC./LEAKAGE THROUGH LAYER 5	0.000087	9.680	0.00
AVG. HEAD ON TOP OF LAYER 4	0.4876		
PERC./LEAKAGE THROUGH LAYER 6	0.000000	0.000	0.00
CHANGE IN WATER STORAGE	1.197	133436.375	9.30
SOIL WATER AT START OF YEAR	41.229	4594560.500	
SOIL WATER AT END OF YEAR	42.426	4727996.500	
SNOW WATER AT START OF YEAR	0.000	0.000	0.00
SNOW WATER AT END OF YEAR	0.000	0.000	0.00
ANNUAL WATER BUDGET BALANCE	0.0000	-0.288	0.00

MONTHLY TOTALS (IN INCHES) FOR YEAR 5

	JAN/JUL	FEB/AUG	MAR/SEP	APR/OCT	MAY/NOV	JUN/DEC
PRECIPITATION	0.27 1.40	0.68 1.86	0.78 1.82	1.73 3.13	0.97 0.00	0.20 1.03
RUNOFF	0.000 0.000	0.000 0.000	0.000 0.000	0.000 0.000	0.000 0.000	0.000 0.000
EVAPOTRANSPIRATION	0.387 1.019	0.283 2.154	0.483 0.712	2.313 3.350	0.603 1.285	0.383 0.850
LATERAL DRAINAGE COLLECTED FROM LAYER 3	0.0045 0.0033	0.0039 0.0031	0.0041 0.0029	0.0037 0.0028	0.0037 0.0026	0.0034 0.0026
PERCOLATION/LEAKAGE THROUGH LAYER 5	0.0000 0.0000	0.0000 0.0000	0.0000 0.0000	0.0000 0.0000	0.0000 0.0000	0.0000 0.0000
PERCOLATION/LEAKAGE THROUGH LAYER 6	0.0000 0.0000	0.0000 0.0000	0.0000 0.0000	0.0000 0.0000	0.0000 0.0000	0.0000 0.0000

MONTHLY SUMMARIES FOR DAILY HEADS (INCHES)

AVERAGE DAILY HEAD ON TOP OF LAYER 4	0.343 0.252	0.326 0.239	0.310 0.227	0.295 0.216	0.280 0.205	0.266 0.195
STD. DEVIATION OF DAILY HEAD ON TOP OF LAYER 4	0.005 0.004	0.005 0.004	0.005 0.003	0.004 0.003	0.004 0.003	0.004 0.003

ANNUAL TOTALS FOR YEAR 5

	INCHES	CU. FEET	PERCENT
PRECIPITATION	13.87	1545687.000	100.00
RUNOFF	0.000	0.000	0.00
EVAPOTRANSPIRATION	13.822	1540351.120	99.65
DRAINAGE COLLECTED FROM LAYER 3	0.0406	4528.788	0.29
PERC./LEAKAGE THROUGH LAYER 5	0.000046	5.137	0.00

AVG. HEAD ON TOP OF LAYER 4	0.2629		
PERC./LEAKAGE THROUGH LAYER 6	0.000000	0.000	0.00
CHANGE IN WATER STORAGE	0.007	806.866	0.05
SOIL WATER AT START OF YEAR	42.426	4727996.500	
SOIL WATER AT END OF YEAR	42.433	4728803.500	
SNOW WATER AT START OF YEAR	0.000	0.000	0.00
SNOW WATER AT END OF YEAR	0.000	0.000	0.00
ANNUAL WATER BUDGET BALANCE	0.0000	0.161	0.00

AVERAGE MONTHLY VALUES IN INCHES FOR YEARS 1 THROUGH 5

	JAN/JUL	FEB/AUG	MAR/SEP	APR/OCT	MAY/NOV	JUN/DEC
	-----	-----	-----	-----	-----	-----
PRECIPITATION						

TOTALS	0.19 1.45	0.49 2.54	0.42 1.68	0.89 2.96	1.05 0.56	1.19 0.51
STD. DEVIATIONS	0.19 0.91	0.45 1.03	0.40 0.63	0.74 1.95	0.49 0.69	1.09 0.32
RUNOFF						

TOTALS	0.000 0.000	0.000 0.000	0.000 0.000	0.000 0.000	0.000 0.000	0.000 0.000
STD. DEVIATIONS	0.000 0.000	0.000 0.000	0.000 0.000	0.000 0.000	0.000 0.000	0.000 0.000
EVAPOTRANSPIRATION						

TOTALS	0.382 1.049	0.280 2.323	0.317 1.823	0.915 1.951	0.751 1.548	1.245 0.650
STD. DEVIATIONS	0.039 0.743	0.081 1.152	0.206 1.155	0.948 1.296	0.665 0.232	1.371 0.157

LATERAL DRAINAGE COLLECTED FROM LAYER 3

TOTALS	0.0188	0.0181	0.0199	0.0184	0.0181	0.0166
	0.0163	0.0155	0.0142	0.0139	0.0128	0.0126
STD. DEVIATIONS	0.0138	0.0151	0.0177	0.0165	0.0162	0.0148
	0.0146	0.0138	0.0127	0.0125	0.0115	0.0112

PERCOLATION/LEAKAGE THROUGH LAYER 5

TOTALS	0.0000	0.0000	0.0000	0.0000	0.0000	0.0000
	0.0000	0.0000	0.0000	0.0000	0.0000	0.0000
STD. DEVIATIONS	0.0000	0.0000	0.0000	0.0000	0.0000	0.0000
	0.0000	0.0000	0.0000	0.0000	0.0000	0.0000

PERCOLATION/LEAKAGE THROUGH LAYER 6

TOTALS	0.0000	0.0000	0.0000	0.0000	0.0000	0.0000
	0.0000	0.0000	0.0000	0.0000	0.0000	0.0000
STD. DEVIATIONS	0.0000	0.0000	0.0000	0.0000	0.0000	0.0000
	0.0000	0.0000	0.0000	0.0000	0.0000	0.0000

AVERAGES OF MONTHLY AVERAGED DAILY HEADS (INCHES)

DAILY AVERAGE HEAD ON TOP OF LAYER 4

AVERAGES	1.4336	1.5199	1.5151	1.4459	1.3732	1.3041
	1.2385	1.1752	1.1161	1.0599	1.0066	0.9560
STD. DEVIATIONS	1.0458	1.2753	1.3476	1.2937	1.2287	1.1668
	1.1081	1.0515	0.9985	0.9483	0.9006	0.8553

AVERAGE ANNUAL TOTALS & (STD. DEVIATIONS) FOR YEARS 1 THROUGH 5

	INCHES		CU. FEET	PERCENT
PRECIPITATION	13.92	(2.864)	1551258.9	100.00
RUNOFF	0.000	(0.0000)	0.00	0.000
EVAPOTRANSPIRATION	13.234	(2.4528)	1474792.25	95.071
LATERAL DRAINAGE COLLECTED FROM LAYER 3	0.19517	(0.16990)	21749.510	1.40206
PERCOLATION/LEAKAGE THROUGH LAYER 5	0.00027	(0.00027)	30.193	0.00195
AVERAGE HEAD ON TOP OF LAYER 4	1.262	(1.099)		
PERCOLATION/LEAKAGE THROUGH LAYER 6	0.00000	(0.00000)	0.000	0.00000
CHANGE IN WATER STORAGE	0.491	(0.7937)	54716.98	3.527

PEAK DAILY VALUES FOR YEARS	1 THROUGH	5
	(INCHES)	(CU. FT.)
PRECIPITATION	1.97	219538.781
RUNOFF	0.000	0.0000
DRAINAGE COLLECTED FROM LAYER 3	0.00156	174.10240
PERCOLATION/LEAKAGE THROUGH LAYER 5	0.000003	0.28592
AVERAGE HEAD ON TOP OF LAYER 4	3.684	
MAXIMUM HEAD ON TOP OF LAYER 4	6.451	
LOCATION OF MAXIMUM HEAD IN LAYER 3 (DISTANCE FROM DRAIN)	24.4 FEET	
PERCOLATION/LEAKAGE THROUGH LAYER 6	0.000000	0.00000
SNOW WATER	0.58	64670.8828
MAXIMUM VEG. SOIL WATER (VOL/VOL)		0.3207
MINIMUM VEG. SOIL WATER (VOL/VOL)		0.0823

*** Maximum heads are computed using McEnroe's equations. ***

Reference: Maximum Saturated Depth over Landfill Liner
by Bruce M. McEnroe, University of Kansas
ASCE Journal of Environmental Engineering
Vol. 119, No. 2, March 1993, pp. 262-270.

FINAL WATER STORAGE AT END OF YEAR 5

LAYER	(INCHES)	(VOL/VOL)
1	1.4645	0.1220
2	34.7383	0.1447
3	5.3756	0.2240
4	0.0000	0.0000
5	0.1875	0.7500
6	0.6674	0.1112
SNOW WATER	0.000	

**APPLICATION FOR PERMIT RENEWAL AND MODIFICATION
SANDOVAL COUNTY LANDFILL**

**VOLUME III: LANDFILL ENGINEERING CALCULATIONS
SECTION 10: HELP MODEL**

ATTACHMENT III.10.A-5

**TIER II, SIMULATION 9-1A AND 9-1B
PRESCRIPTIVE LINER WITH SOIL TYPE 6
ALTERNATE COVER WITH SOIL TYPE 6**

```

*****
*****
**
**
**
**      HYDROLOGIC EVALUATION OF LANDFILL PERFORMANCE      **
**      HELP MODEL VERSION 3.07  (1 NOVEMBER 1997)          **
**      DEVELOPED BY ENVIRONMENTAL LABORATORY                **
**      USAE WATERWAYS EXPERIMENT STATION                   **
**      FOR USEPA RISK REDUCTION ENGINEERING LABORATORY      **
**
**
*****
*****

```

```

PRECIPITATION DATA FILE:  C:\RAIN1.D4
TEMPERATURE DATA FILE:   C:\TEMP1.D7
SOLAR RADIATION DATA FILE: C:\SOLAR1.D13
EVAPOTRANSPIRATION DATA: C:\EVAP1.D11
SOIL AND DESIGN DATA FILE: C:\SIM95%2.D10
OUTPUT DATA FILE:        C:\SIM95%2.OUT

```

TIME: 17: 0 DATE: 4/ 8/2015

```

*****

```

TITLE: Sandoval County Landfill - 2 Years Closed - Bare Soil - 5%

Simulation 9A - Alternate Final Cover - 5% Sloped Area: 8.9 Acres

```

*****

```

NOTE: INITIAL MOISTURE CONTENT OF THE LAYERS AND SNOW WATER
WERE SPECIFIED BY THE USER.

LAYER 1

TYPE 1 - VERTICAL PERCOLATION LAYER

MATERIAL TEXTURE NUMBER 6

THICKNESS	=	6.00	INCHES
POROSITY	=	0.4530	VOL/VOL
FIELD CAPACITY	=	0.1900	VOL/VOL
WILTING POINT	=	0.0850	VOL/VOL
INITIAL SOIL WATER CONTENT	=	0.1110	VOL/VOL
EFFECTIVE SAT. HYD. COND.	=	0.720000011000E-03	CM/SEC

LAYER 2

TYPE 1 - VERTICAL PERCOLATION LAYER

MATERIAL TEXTURE NUMBER 6

THICKNESS	=	30.00	INCHES
POROSITY	=	0.4530	VOL/VOL
FIELD CAPACITY	=	0.1900	VOL/VOL
WILTING POINT	=	0.0850	VOL/VOL
INITIAL SOIL WATER CONTENT	=	0.1110	VOL/VOL
EFFECTIVE SAT. HYD. COND.	=	0.720000011000E-03	CM/SEC

LAYER 3

TYPE 1 - VERTICAL PERCOLATION LAYER

MATERIAL TEXTURE NUMBER 6

THICKNESS	=	12.00	INCHES
POROSITY	=	0.4530	VOL/VOL
FIELD CAPACITY	=	0.1900	VOL/VOL
WILTING POINT	=	0.0850	VOL/VOL
INITIAL SOIL WATER CONTENT	=	0.1110	VOL/VOL
EFFECTIVE SAT. HYD. COND.	=	0.720000011000E-03	CM/SEC

LAYER 4

TYPE 1 - VERTICAL PERCOLATION LAYER

MATERIAL TEXTURE NUMBER 18

THICKNESS	=	2076.00	INCHES
POROSITY	=	0.6710	VOL/VOL
FIELD CAPACITY	=	0.2920	VOL/VOL
WILTING POINT	=	0.0770	VOL/VOL
INITIAL SOIL WATER CONTENT	=	0.1447	VOL/VOL
EFFECTIVE SAT. HYD. COND.	=	0.100000005000E-02	CM/SEC

LAYER 5

TYPE 2 - LATERAL DRAINAGE LAYER

MATERIAL TEXTURE NUMBER 0

THICKNESS	=	24.00	INCHES
POROSITY	=	0.4730	VOL/VOL
FIELD CAPACITY	=	0.2220	VOL/VOL
WILTING POINT	=	0.1040	VOL/VOL
INITIAL SOIL WATER CONTENT	=	0.2240	VOL/VOL
EFFECTIVE SAT. HYD. COND.	=	0.300000014000E-03	CM/SEC
SLOPE	=	5.00	PERCENT
DRAINAGE LENGTH	=	200.0	FEET

LAYER 6

TYPE 4 - FLEXIBLE MEMBRANE LINER

MATERIAL TEXTURE NUMBER 35

THICKNESS	=	0.06	INCHES
POROSITY	=	0.0000	VOL/VOL
FIELD CAPACITY	=	0.0000	VOL/VOL
WILTING POINT	=	0.0000	VOL/VOL
INITIAL SOIL WATER CONTENT	=	0.0000	VOL/VOL
EFFECTIVE SAT. HYD. COND.	=	0.199999996000E-12	CM/SEC
FML PINHOLE DENSITY	=	1.00	HOLES/ACRE
FML INSTALLATION DEFECTS	=	4.00	HOLES/ACRE
FML PLACEMENT QUALITY	=	3 - GOOD	

LAYER 7

TYPE 3 - BARRIER SOIL LINER

MATERIAL TEXTURE NUMBER 0

THICKNESS	=	0.25	INCHES
POROSITY	=	0.7500	VOL/VOL
FIELD CAPACITY	=	0.7470	VOL/VOL
WILTING POINT	=	0.4000	VOL/VOL
INITIAL SOIL WATER CONTENT	=	0.7500	VOL/VOL
EFFECTIVE SAT. HYD. COND.	=	0.499999997000E-08	CM/SEC

LAYER 8

TYPE 1 - VERTICAL PERCOLATION LAYER

MATERIAL TEXTURE NUMBER 0

THICKNESS	=	6.00	INCHES
POROSITY	=	0.4530	VOL/VOL
FIELD CAPACITY	=	0.1900	VOL/VOL
WILTING POINT	=	0.0850	VOL/VOL

INITIAL SOIL WATER CONTENT = 0.1112 VOL/VOL
EFFECTIVE SAT. HYD. COND. = 0.420000015000E-05 CM/SEC

GENERAL DESIGN AND EVAPORATIVE ZONE DATA

NOTE: SCS RUNOFF CURVE NUMBER WAS COMPUTED FROM DEFAULT
SOIL DATA BASE USING SOIL TEXTURE # 6 WITH BARE
GROUND CONDITIONS, A SURFACE SLOPE OF 5.% AND
A SLOPE LENGTH OF 258. FEET.

SCS RUNOFF CURVE NUMBER	=	86.20	
FRACTION OF AREA ALLOWING RUNOFF	=	100.0	PERCENT
AREA PROJECTED ON HORIZONTAL PLANE	=	8.900	ACRES
EVAPORATIVE ZONE DEPTH	=	18.0	INCHES
INITIAL WATER IN EVAPORATIVE ZONE	=	1.998	INCHES
UPPER LIMIT OF EVAPORATIVE STORAGE	=	8.154	INCHES
LOWER LIMIT OF EVAPORATIVE STORAGE	=	1.530	INCHES
INITIAL SNOW WATER	=	0.000	INCHES
INITIAL WATER IN LAYER MATERIALS	=	311.956	INCHES
TOTAL INITIAL WATER	=	311.956	INCHES
TOTAL SUBSURFACE INFLOW	=	0.00	INCHES/YEAR

EVAPOTRANSPIRATION AND WEATHER DATA

NOTE: EVAPOTRANSPIRATION DATA WAS OBTAINED FROM
ALBUQUERQUE NEW MEXICO

STATION LATITUDE	=	35.30	DEGREES
MAXIMUM LEAF AREA INDEX	=	0.00	
START OF GROWING SEASON (JULIAN DATE)	=	98	
END OF GROWING SEASON (JULIAN DATE)	=	299	
EVAPORATIVE ZONE DEPTH	=	18.0	INCHES
AVERAGE ANNUAL WIND SPEED	=	9.00	MPH
AVERAGE 1ST QUARTER RELATIVE HUMIDITY	=	48.00	%
AVERAGE 2ND QUARTER RELATIVE HUMIDITY	=	30.00	%
AVERAGE 3RD QUARTER RELATIVE HUMIDITY	=	45.00	%
AVERAGE 4TH QUARTER RELATIVE HUMIDITY	=	50.00	%

NOTE: PRECIPITATION DATA WAS SYNTHETICALLY GENERATED USING
COEFFICIENTS FOR ALBUQUERQUE NEW MEXICO

NORMAL MEAN MONTHLY PRECIPITATION (INCHES)

JAN/JUL	FEB/AUG	MAR/SEP	APR/OCT	MAY/NOV	JUN/DEC
-----	-----	-----	-----	-----	-----
0.37	0.47	0.48	0.99	0.72	0.99
1.39	2.34	1.20	1.50	0.55	0.47

NOTE: TEMPERATURE DATA WAS SYNTHETICALLY GENERATED USING
COEFFICIENTS FOR ALBUQUERQUE NEW MEXICO

NORMAL MEAN MONTHLY TEMPERATURE (DEGREES FAHRENHEIT)

JAN/JUL	FEB/AUG	MAR/SEP	APR/OCT	MAY/NOV	JUN/DEC
-----	-----	-----	-----	-----	-----
35.20	40.90	47.10	55.30	64.90	73.50
77.30	75.60	67.30	57.20	44.40	35.70

NOTE: SOLAR RADIATION DATA WAS SYNTHETICALLY GENERATED USING
COEFFICIENTS FOR ALBUQUERQUE NEW MEXICO
AND STATION LATITUDE = 35.30 DEGREES

MONTHLY TOTALS (IN INCHES) FOR YEAR 1

	JAN/JUL	FEB/AUG	MAR/SEP	APR/OCT	MAY/NOV	JUN/DEC
	-----	-----	-----	-----	-----	-----
PRECIPITATION	0.11	0.01	0.26	0.55	0.86	0.01
	0.99	3.66	1.17	1.12	1.67	0.57
RUNOFF	0.000	0.000	0.000	0.000	0.001	0.000
	0.000	0.001	0.000	0.000	0.000	0.000
EVAPOTRANSPIRATION	0.440	0.145	0.085	0.172	0.209	0.196
	0.572	3.149	2.502	0.527	1.533	0.776
LATERAL DRAINAGE COLLECTED	0.0023	0.0021	0.0022	0.0020	0.0020	0.0018
FROM LAYER 5	0.0018	0.0017	0.0016	0.0015	0.0014	0.0014
PERCOLATION/LEAKAGE THROUGH	0.0000	0.0000	0.0000	0.0000	0.0000	0.0000
LAYER 7	0.0000	0.0000	0.0000	0.0000	0.0000	0.0000
PERCOLATION/LEAKAGE THROUGH	0.0000	0.0000	0.0000	0.0000	0.0000	0.0000
LAYER 8	0.0000	0.0000	0.0000	0.0000	0.0000	0.0000

MONTHLY SUMMARIES FOR DAILY HEADS (INCHES)

AVERAGE DAILY HEAD ON	0.174	0.178	0.169	0.161	0.153	0.145
TOP OF LAYER 6	0.138	0.131	0.124	0.118	0.112	0.106
STD. DEVIATION OF DAILY	0.024	0.002	0.003	0.002	0.002	0.002
HEAD ON TOP OF LAYER 6	0.002	0.002	0.002	0.002	0.002	0.002

ANNUAL TOTALS FOR YEAR 1

	INCHES	CU. FEET	PERCENT
	-----	-----	-----
PRECIPITATION	10.98	354730.906	100.00
RUNOFF	0.001	47.680	0.01
EVAPOTRANSPIRATION	10.306	332944.656	93.86
DRAINAGE COLLECTED FROM LAYER 5	0.0220	710.767	0.20
PERC./LEAKAGE THROUGH LAYER 7	0.000025	0.815	0.00
AVG. HEAD ON TOP OF LAYER 6	0.1423		
PERC./LEAKAGE THROUGH LAYER 8	0.000000	0.000	0.00
CHANGE IN WATER STORAGE	0.651	21027.943	5.93
SOIL WATER AT START OF YEAR	311.956	10078358.000	
SOIL WATER AT END OF YEAR	312.607	10099386.000	
SNOW WATER AT START OF YEAR	0.000	0.000	0.00
SNOW WATER AT END OF YEAR	0.000	0.000	0.00
ANNUAL WATER BUDGET BALANCE	0.0000	-0.174	0.00

MONTHLY TOTALS (IN INCHES) FOR YEAR 2

	JAN/JUL	FEB/AUG	MAR/SEP	APR/OCT	MAY/NOV	JUN/DEC
PRECIPITATION	0.09 1.08	1.07 3.29	0.00 1.76	1.64 5.91	1.35 0.03	2.03 0.42
RUNOFF	0.000 0.000	0.000 0.061	0.000 0.000	0.010 0.596	0.000 0.000	0.053 0.000
EVAPOTRANSPIRATION	0.380 0.834	0.462 2.731	0.295 1.565	1.490 3.048	1.104 1.923	2.503 0.554
LATERAL DRAINAGE COLLECTED FROM LAYER 5	0.0013 0.0010	0.0011 0.0009	0.0012 0.0009	0.0011 0.0008	0.0011 0.0008	0.0010 0.0008
PERCOLATION/LEAKAGE THROUGH LAYER 7	0.0000 0.0000	0.0000 0.0000	0.0000 0.0000	0.0000 0.0000	0.0000 0.0000	0.0000 0.0000
PERCOLATION/LEAKAGE THROUGH LAYER 8	0.0000 0.0000	0.0000 0.0000	0.0000 0.0000	0.0000 0.0000	0.0000 0.0000	0.0000 0.0000

MONTHLY SUMMARIES FOR DAILY HEADS (INCHES)

AVERAGE DAILY HEAD ON TOP OF LAYER 6	0.101 0.074	0.096 0.070	0.091 0.067	0.087 0.064	0.082 0.060	0.078 0.057
STD. DEVIATION OF DAILY HEAD ON TOP OF LAYER 6	0.002 0.001	0.001 0.001	0.001 0.001	0.001 0.001	0.001 0.001	0.001 0.001

ANNUAL TOTALS FOR YEAR 2

	INCHES	CU. FEET	PERCENT
PRECIPITATION	18.67	603171.750	100.00
RUNOFF	0.720	23262.074	3.86
EVAPOTRANSPIRATION	16.888	545601.812	90.46

DRAINAGE COLLECTED FROM LAYER 5	0.0120	386.211	0.06
PERC./LEAKAGE THROUGH LAYER 7	0.000014	0.455	0.00
AVG. HEAD ON TOP OF LAYER 6	0.0773		
PERC./LEAKAGE THROUGH LAYER 8	0.000000	0.000	0.00
CHANGE IN WATER STORAGE	1.050	33920.969	5.62
SOIL WATER AT START OF YEAR	312.607	10099386.000	
SOIL WATER AT END OF YEAR	313.657	10133307.000	
SNOW WATER AT START OF YEAR	0.000	0.000	0.00
SNOW WATER AT END OF YEAR	0.000	0.000	0.00
ANNUAL WATER BUDGET BALANCE	0.0000	0.633	0.00

AVERAGE MONTHLY VALUES IN INCHES FOR YEARS 1 THROUGH 2

	JAN/JUL	FEB/AUG	MAR/SEP	APR/OCT	MAY/NOV	JUN/DEC
	-----	-----	-----	-----	-----	-----
PRECIPITATION						
TOTALS	0.10 1.03	0.54 3.47	0.13 1.47	1.10 3.51	1.11 0.85	1.02 0.50
STD. DEVIATIONS	0.01 0.06	0.75 0.26	0.18 0.42	0.77 3.39	0.35 1.16	1.43 0.11
RUNOFF						
TOTALS	0.000 0.000	0.000 0.031	0.000 0.000	0.005 0.298	0.000 0.000	0.026 0.000
STD. DEVIATIONS	0.000 0.000	0.000 0.042	0.000 0.000	0.007 0.421	0.000 0.000	0.037 0.000
EVAPOTRANSPIRATION						
TOTALS	0.410	0.303	0.190	0.831	0.656	1.349

	0.703	2.940	2.034	1.787	1.728	0.665
STD. DEVIATIONS	0.043	0.224	0.148	0.932	0.633	1.631
	0.185	0.296	0.662	1.783	0.276	0.157

LATERAL DRAINAGE COLLECTED FROM LAYER 5

TOTALS	0.0018	0.0016	0.0017	0.0016	0.0015	0.0014
	0.0014	0.0013	0.0012	0.0012	0.0011	0.0011
STD. DEVIATIONS	0.0007	0.0007	0.0007	0.0007	0.0007	0.0006
	0.0006	0.0006	0.0005	0.0005	0.0005	0.0005

PERCOLATION/LEAKAGE THROUGH LAYER 7

TOTALS	0.0000	0.0000	0.0000	0.0000	0.0000	0.0000
	0.0000	0.0000	0.0000	0.0000	0.0000	0.0000
STD. DEVIATIONS	0.0000	0.0000	0.0000	0.0000	0.0000	0.0000
	0.0000	0.0000	0.0000	0.0000	0.0000	0.0000

PERCOLATION/LEAKAGE THROUGH LAYER 8

TOTALS	0.0000	0.0000	0.0000	0.0000	0.0000	0.0000
	0.0000	0.0000	0.0000	0.0000	0.0000	0.0000
STD. DEVIATIONS	0.0000	0.0000	0.0000	0.0000	0.0000	0.0000
	0.0000	0.0000	0.0000	0.0000	0.0000	0.0000

AVERAGES OF MONTHLY AVERAGED DAILY HEADS (INCHES)

DAILY AVERAGE HEAD ON TOP OF LAYER 6

AVERAGES	0.1375	0.1369	0.1302	0.1237	0.1175	0.1116
	0.1060	0.1005	0.0955	0.0907	0.0861	0.0818
STD. DEVIATIONS	0.0518	0.0580	0.0551	0.0524	0.0497	0.0472
	0.0449	0.0426	0.0404	0.0384	0.0365	0.0346

AVERAGE ANNUAL TOTALS & (STD. DEVIATIONS) FOR YEARS 1 THROUGH 2

	INCHES		CU. FEET	PERCENT
	-----		-----	-----
PRECIPITATION	14.83	(5.438)	478951.3	100.00
RUNOFF	0.361	(0.5081)	11654.88	2.433
EVAPOTRANSPIRATION	13.597	(4.6544)	439273.28	91.716
LATERAL DRAINAGE COLLECTED FROM LAYER 5	0.01698	(0.00710)	548.489	0.11452
PERCOLATION/LEAKAGE THROUGH LAYER 7	0.00002	(0.00001)	0.635	0.00013
AVERAGE HEAD ON TOP OF LAYER 6	0.110	(0.046)		
PERCOLATION/LEAKAGE THROUGH LAYER 8	0.00000	(0.00000)	0.000	0.00000
CHANGE IN WATER STORAGE	0.850	(0.2822)	27474.46	5.736

PEAK DAILY VALUES FOR YEARS	1 THROUGH	2
	(INCHES)	(CU. FT.)
PRECIPITATION	1.97	63644.789
RUNOFF	0.412	13322.4834
DRAINAGE COLLECTED FROM LAYER 5	0.00008	2.58823
PERCOLATION/LEAKAGE THROUGH LAYER 7	0.000000	0.00295
AVERAGE HEAD ON TOP OF LAYER 6	0.189	
MAXIMUM HEAD ON TOP OF LAYER 6	0.372	
LOCATION OF MAXIMUM HEAD IN LAYER 5 (DISTANCE FROM DRAIN)	2.6 FEET	
PERCOLATION/LEAKAGE THROUGH LAYER 8	0.000000	0.00000
SNOW WATER	0.55	17779.0234
MAXIMUM VEG. SOIL WATER (VOL/VOL)		0.2904
MINIMUM VEG. SOIL WATER (VOL/VOL)		0.0850

*** Maximum heads are computed using McEnroe's equations. ***

Reference: Maximum Saturated Depth over Landfill Liner
by Bruce M. McEnroe, University of Kansas
ASCE Journal of Environmental Engineering
Vol. 119, No. 2, March 1993, pp. 262-270.

FINAL WATER STORAGE AT END OF YEAR 2

LAYER	(INCHES)	(VOL/VOL)
1	0.5610	0.0935
2	4.9276	0.1643
3	1.5741	0.1312
4	300.3972	0.1447
5	5.3420	0.2226
6	0.0000	0.0000
7	0.1875	0.7500
8	0.6672	0.1112
SNOW WATER	0.000	


```

*****
*****
**
**
**
HYDROLOGIC EVALUATION OF LANDFILL PERFORMANCE
HELP MODEL VERSION 3.07 (1 NOVEMBER 1997)
DEVELOPED BY ENVIRONMENTAL LABORATORY
USAE WATERWAYS EXPERIMENT STATION
FOR USEPA RISK REDUCTION ENGINEERING LABORATORY
**
**
**
*****
*****

```

```

PRECIPITATION DATA FILE:  C:\RAIN1.D4
TEMPERATURE DATA FILE:   C:\TEMP1.D7
SOLAR RADIATION DATA FILE: C:\SOLAR1.D13
EVAPOTRANSPIRATION DATA: C:\EVAP1.D11
SOIL AND DESIGN DATA FILE: C:\SIM925%2.D10
OUTPUT DATA FILE:        C:\SIM925%2.OUT

```

TIME: 17: 5 DATE: 4/ 8/2015

```

*****

```

TITLE: Sandoval County Landfill - 2 Years Closed - Bare Soil-25%

Simulation 9B - Alternate Final Cover; 25 % Slope Area: 114 Acres

```

*****

```

NOTE: INITIAL MOISTURE CONTENT OF THE LAYERS AND SNOW WATER
WERE SPECIFIED BY THE USER.

LAYER 1

TYPE 1 - VERTICAL PERCOLATION LAYER
MATERIAL TEXTURE NUMBER 6

THICKNESS	=	6.00	INCHES
POROSITY	=	0.4530	VOL/VOL
FIELD CAPACITY	=	0.1900	VOL/VOL
WILTING POINT	=	0.0850	VOL/VOL
INITIAL SOIL WATER CONTENT	=	0.1110	VOL/VOL
EFFECTIVE SAT. HYD. COND.	=	0.720000011000E-03	CM/SEC

LAYER 2

TYPE 1 - VERTICAL PERCOLATION LAYER

MATERIAL TEXTURE NUMBER 6

THICKNESS	=	30.00	INCHES
POROSITY	=	0.4530	VOL/VOL
FIELD CAPACITY	=	0.1900	VOL/VOL
WILTING POINT	=	0.0850	VOL/VOL
INITIAL SOIL WATER CONTENT	=	0.1110	VOL/VOL
EFFECTIVE SAT. HYD. COND.	=	0.720000011000E-03	CM/SEC

LAYER 3

TYPE 1 - VERTICAL PERCOLATION LAYER

MATERIAL TEXTURE NUMBER 6

THICKNESS	=	12.00	INCHES
POROSITY	=	0.4530	VOL/VOL
FIELD CAPACITY	=	0.1900	VOL/VOL
WILTING POINT	=	0.0850	VOL/VOL
INITIAL SOIL WATER CONTENT	=	0.1110	VOL/VOL
EFFECTIVE SAT. HYD. COND.	=	0.720000011000E-03	CM/SEC

LAYER 4

TYPE 1 - VERTICAL PERCOLATION LAYER

MATERIAL TEXTURE NUMBER 18

THICKNESS	=	2076.00	INCHES
POROSITY	=	0.6710	VOL/VOL
FIELD CAPACITY	=	0.2920	VOL/VOL
WILTING POINT	=	0.0770	VOL/VOL
INITIAL SOIL WATER CONTENT	=	0.1447	VOL/VOL
EFFECTIVE SAT. HYD. COND.	=	0.100000005000E-02	CM/SEC

LAYER 5

TYPE 2 - LATERAL DRAINAGE LAYER

MATERIAL TEXTURE NUMBER 0

THICKNESS	=	24.00	INCHES
-----------	---	-------	--------

POROSITY	=	0.4730	VOL/VOL
FIELD CAPACITY	=	0.2220	VOL/VOL
WILTING POINT	=	0.1040	VOL/VOL
INITIAL SOIL WATER CONTENT	=	0.2240	VOL/VOL
EFFECTIVE SAT. HYD. COND.	=	0.300000014000E-03	CM/SEC
SLOPE	=	5.00	PERCENT
DRAINAGE LENGTH	=	200.0	FEET

LAYER 6

TYPE 4 - FLEXIBLE MEMBRANE LINER

MATERIAL TEXTURE NUMBER 35

THICKNESS	=	0.06	INCHES
POROSITY	=	0.0000	VOL/VOL
FIELD CAPACITY	=	0.0000	VOL/VOL
WILTING POINT	=	0.0000	VOL/VOL
INITIAL SOIL WATER CONTENT	=	0.0000	VOL/VOL
EFFECTIVE SAT. HYD. COND.	=	0.199999996000E-12	CM/SEC
FML PINHOLE DENSITY	=	1.00	HOLES/ACRE
FML INSTALLATION DEFECTS	=	4.00	HOLES/ACRE
FML PLACEMENT QUALITY	=	3 - GOOD	

LAYER 7

TYPE 3 - BARRIER SOIL LINER

MATERIAL TEXTURE NUMBER 0

THICKNESS	=	0.25	INCHES
POROSITY	=	0.7500	VOL/VOL
FIELD CAPACITY	=	0.7470	VOL/VOL
WILTING POINT	=	0.4000	VOL/VOL
INITIAL SOIL WATER CONTENT	=	0.7500	VOL/VOL
EFFECTIVE SAT. HYD. COND.	=	0.499999997000E-08	CM/SEC

LAYER 8

TYPE 1 - VERTICAL PERCOLATION LAYER

MATERIAL TEXTURE NUMBER 0

THICKNESS	=	6.00	INCHES
POROSITY	=	0.4530	VOL/VOL
FIELD CAPACITY	=	0.1900	VOL/VOL
WILTING POINT	=	0.0850	VOL/VOL
INITIAL SOIL WATER CONTENT	=	0.1112	VOL/VOL
EFFECTIVE SAT. HYD. COND.	=	0.420000015000E-05	CM/SEC

GENERAL DESIGN AND EVAPORATIVE ZONE DATA

NOTE: SCS RUNOFF CURVE NUMBER WAS COMPUTED FROM A USER-SPECIFIED CURVE NUMBER OF 95.0, A SURFACE SLOPE OF 25.% AND A SLOPE LENGTH OF 650. FEET.

SCS RUNOFF CURVE NUMBER	=	95.20	
FRACTION OF AREA ALLOWING RUNOFF	=	100.0	PERCENT
AREA PROJECTED ON HORIZONTAL PLANE	=	114.000	ACRES
EVAPORATIVE ZONE DEPTH	=	18.0	INCHES
INITIAL WATER IN EVAPORATIVE ZONE	=	1.998	INCHES
UPPER LIMIT OF EVAPORATIVE STORAGE	=	8.154	INCHES
LOWER LIMIT OF EVAPORATIVE STORAGE	=	1.530	INCHES
INITIAL SNOW WATER	=	0.000	INCHES
INITIAL WATER IN LAYER MATERIALS	=	311.956	INCHES
TOTAL INITIAL WATER	=	311.956	INCHES
TOTAL SUBSURFACE INFLOW	=	0.00	INCHES/YEAR

EVAPOTRANSPIRATION AND WEATHER DATA

NOTE: EVAPOTRANSPIRATION DATA WAS OBTAINED FROM ALBUQUERQUE NEW MEXICO

STATION LATITUDE	=	35.30	DEGREES
MAXIMUM LEAF AREA INDEX	=	0.00	
START OF GROWING SEASON (JULIAN DATE)	=	98	
END OF GROWING SEASON (JULIAN DATE)	=	299	
EVAPORATIVE ZONE DEPTH	=	18.0	INCHES
AVERAGE ANNUAL WIND SPEED	=	9.00	MPH
AVERAGE 1ST QUARTER RELATIVE HUMIDITY	=	48.00	%
AVERAGE 2ND QUARTER RELATIVE HUMIDITY	=	30.00	%
AVERAGE 3RD QUARTER RELATIVE HUMIDITY	=	45.00	%
AVERAGE 4TH QUARTER RELATIVE HUMIDITY	=	50.00	%

NOTE: PRECIPITATION DATA WAS SYNTHETICALLY GENERATED USING COEFFICIENTS FOR ALBUQUERQUE NEW MEXICO

NORMAL MEAN MONTHLY PRECIPITATION (INCHES)

JAN/JUL	FEB/AUG	MAR/SEP	APR/OCT	MAY/NOV	JUN/DEC
0.37	0.47	0.48	0.99	0.72	0.99
1.39	2.34	1.20	1.50	0.55	0.47

NOTE: TEMPERATURE DATA WAS SYNTHETICALLY GENERATED USING
COEFFICIENTS FOR ALBUQUERQUE NEW MEXICO

NORMAL MEAN MONTHLY TEMPERATURE (DEGREES FAHRENHEIT)

JAN/JUL	FEB/AUG	MAR/SEP	APR/OCT	MAY/NOV	JUN/DEC
-----	-----	-----	-----	-----	-----
35.20	40.90	47.10	55.30	64.90	73.50
77.30	75.60	67.30	57.20	44.40	35.70

NOTE: SOLAR RADIATION DATA WAS SYNTHETICALLY GENERATED USING
COEFFICIENTS FOR ALBUQUERQUE NEW MEXICO
AND STATION LATITUDE = 35.30 DEGREES

MONTHLY TOTALS (IN INCHES) FOR YEAR 1

	JAN/JUL	FEB/AUG	MAR/SEP	APR/OCT	MAY/NOV	JUN/DEC
	-----	-----	-----	-----	-----	-----
PRECIPITATION	0.11	0.01	0.26	0.55	0.86	0.01
	0.99	3.66	1.17	1.12	1.67	0.57
RUNOFF	0.000	0.000	0.000	0.057	0.193	0.000
	0.010	0.442	0.081	0.067	0.018	0.014
EVAPOTRANSPIRATION	0.435	0.149	0.085	0.165	0.201	0.187
	0.406	2.726	2.134	0.502	1.602	0.742
LATERAL DRAINAGE COLLECTED	0.0023	0.0021	0.0022	0.0020	0.0020	0.0018
FROM LAYER 5	0.0018	0.0017	0.0016	0.0015	0.0014	0.0014
PERCOLATION/LEAKAGE THROUGH	0.0000	0.0000	0.0000	0.0000	0.0000	0.0000
LAYER 7	0.0000	0.0000	0.0000	0.0000	0.0000	0.0000
PERCOLATION/LEAKAGE THROUGH	0.0000	0.0000	0.0000	0.0000	0.0000	0.0000
LAYER 8	0.0000	0.0000	0.0000	0.0000	0.0000	0.0000

MONTHLY SUMMARIES FOR DAILY HEADS (INCHES)

AVERAGE DAILY HEAD ON	0.174	0.178	0.169	0.161	0.153	0.145
TOP OF LAYER 6	0.138	0.131	0.124	0.118	0.112	0.106
STD. DEVIATION OF DAILY	0.024	0.002	0.003	0.002	0.002	0.002
HEAD ON TOP OF LAYER 6	0.002	0.002	0.002	0.002	0.002	0.002

ANNUAL TOTALS FOR YEAR 1

	INCHES	CU. FEET	PERCENT
	-----	-----	-----
PRECIPITATION	10.98	4543744.000	100.00
RUNOFF	0.883	365606.125	8.05
EVAPOTRANSPIRATION	9.334	3862644.250	85.01
DRAINAGE COLLECTED FROM LAYER 5	0.0220	9104.206	0.20
PERC./LEAKAGE THROUGH LAYER 7	0.000025	10.440	0.00
AVG. HEAD ON TOP OF LAYER 6	0.1423		
PERC./LEAKAGE THROUGH LAYER 8	0.000000	0.000	0.00
CHANGE IN WATER STORAGE	0.740	306399.562	6.74
SOIL WATER AT START OF YEAR	311.956	129093576.000	
SOIL WATER AT END OF YEAR	312.696	129399976.000	
SNOW WATER AT START OF YEAR	0.000	0.000	0.00
SNOW WATER AT END OF YEAR	0.000	0.000	0.00
ANNUAL WATER BUDGET BALANCE	0.0000	-9.976	0.00

MONTHLY TOTALS (IN INCHES) FOR YEAR 2

	JAN/JUL	FEB/AUG	MAR/SEP	APR/OCT	MAY/NOV	JUN/DEC
PRECIPITATION	0.09 1.08	1.07 3.29	0.00 1.76	1.64 5.91	1.35 0.03	2.03 0.42
RUNOFF	0.000 0.048	0.070 0.488	0.000 0.160	0.407 1.953	0.001 0.000	0.616 0.000
EVAPOTRANSPIRATION	0.375 0.493	0.360 2.539	0.292 1.564	1.305 2.657	0.790 1.918	2.135 0.554
LATERAL DRAINAGE COLLECTED FROM LAYER 5	0.0013 0.0010	0.0011 0.0009	0.0012 0.0009	0.0011 0.0008	0.0011 0.0008	0.0010 0.0008
PERCOLATION/LEAKAGE THROUGH LAYER 7	0.0000 0.0000	0.0000 0.0000	0.0000 0.0000	0.0000 0.0000	0.0000 0.0000	0.0000 0.0000
PERCOLATION/LEAKAGE THROUGH LAYER 8	0.0000 0.0000	0.0000 0.0000	0.0000 0.0000	0.0000 0.0000	0.0000 0.0000	0.0000 0.0000

MONTHLY SUMMARIES FOR DAILY HEADS (INCHES)

AVERAGE DAILY HEAD ON TOP OF LAYER 6	0.101 0.074	0.096 0.070	0.091 0.067	0.087 0.064	0.082 0.060	0.078 0.057
STD. DEVIATION OF DAILY HEAD ON TOP OF LAYER 6	0.002 0.001	0.001 0.001	0.001 0.001	0.001 0.001	0.001 0.001	0.001 0.001

ANNUAL TOTALS FOR YEAR 2

	INCHES	CU. FEET	PERCENT
PRECIPITATION	18.67	7726020.000	100.00
RUNOFF	3.743	1548904.370	20.05
EVAPOTRANSPIRATION	14.981	6199578.500	80.24

DRAINAGE COLLECTED FROM LAYER 5	0.0120	4946.968	0.06
PERC./LEAKAGE THROUGH LAYER 7	0.000014	5.823	0.00
AVG. HEAD ON TOP OF LAYER 6	0.0773		
PERC./LEAKAGE THROUGH LAYER 8	0.000000	0.000	0.00
CHANGE IN WATER STORAGE	-0.066	-27417.090	-0.35
SOIL WATER AT START OF YEAR	312.696	129399976.000	
SOIL WATER AT END OF YEAR	312.630	129372560.000	
SNOW WATER AT START OF YEAR	0.000	0.000	0.00
SNOW WATER AT END OF YEAR	0.000	0.000	0.00
ANNUAL WATER BUDGET BALANCE	0.0000	7.264	0.00

AVERAGE MONTHLY VALUES IN INCHES FOR YEARS 1 THROUGH 2

	JAN/JUL	FEB/AUG	MAR/SEP	APR/OCT	MAY/NOV	JUN/DEC
	-----	-----	-----	-----	-----	-----
PRECIPITATION						

TOTALS	0.10 1.03	0.54 3.47	0.13 1.47	1.10 3.51	1.11 0.85	1.02 0.50
STD. DEVIATIONS	0.01 0.06	0.75 0.26	0.18 0.42	0.77 3.39	0.35 1.16	1.43 0.11
RUNOFF						

TOTALS	0.000 0.029	0.035 0.465	0.000 0.120	0.232 1.010	0.097 0.009	0.308 0.007
STD. DEVIATIONS	0.000 0.027	0.049 0.032	0.000 0.056	0.247 1.333	0.136 0.013	0.436 0.010
EVAPOTRANSPIRATION						

TOTALS	0.405 0.450	0.255 2.632	0.189 1.849	0.735 1.579	0.495 1.760	1.161 0.648

STD. DEVIATIONS	0.043	0.149	0.146	0.806	0.416	1.378
	0.062	0.132	0.403	1.524	0.224	0.133

LATERAL DRAINAGE COLLECTED FROM LAYER 5

TOTALS	0.0018	0.0016	0.0017	0.0016	0.0015	0.0014
	0.0014	0.0013	0.0012	0.0012	0.0011	0.0011
STD. DEVIATIONS	0.0007	0.0007	0.0007	0.0007	0.0007	0.0006
	0.0006	0.0006	0.0005	0.0005	0.0005	0.0005

PERCOLATION/LEAKAGE THROUGH LAYER 7

TOTALS	0.0000	0.0000	0.0000	0.0000	0.0000	0.0000
	0.0000	0.0000	0.0000	0.0000	0.0000	0.0000
STD. DEVIATIONS	0.0000	0.0000	0.0000	0.0000	0.0000	0.0000
	0.0000	0.0000	0.0000	0.0000	0.0000	0.0000

PERCOLATION/LEAKAGE THROUGH LAYER 8

TOTALS	0.0000	0.0000	0.0000	0.0000	0.0000	0.0000
	0.0000	0.0000	0.0000	0.0000	0.0000	0.0000
STD. DEVIATIONS	0.0000	0.0000	0.0000	0.0000	0.0000	0.0000
	0.0000	0.0000	0.0000	0.0000	0.0000	0.0000

AVERAGES OF MONTHLY AVERAGED DAILY HEADS (INCHES)

DAILY AVERAGE HEAD ON TOP OF LAYER 6

AVERAGES	0.1375	0.1369	0.1302	0.1237	0.1175	0.1116
	0.1060	0.1005	0.0955	0.0907	0.0861	0.0818
STD. DEVIATIONS	0.0518	0.0580	0.0551	0.0524	0.0497	0.0472
	0.0449	0.0426	0.0404	0.0384	0.0365	0.0346

AVERAGE ANNUAL TOTALS & (STD. DEVIATIONS) FOR YEARS 1 THROUGH 2

	INCHES		CU. FEET	PERCENT
	-----		-----	-----
PRECIPITATION	14.83	(5.438)	6134882.0	100.00
RUNOFF	2.313	(2.0219)	957255.25	15.603
EVAPOTRANSPIRATION	12.158	(3.9932)	5031111.50	82.008
LATERAL DRAINAGE COLLECTED FROM LAYER 5	0.01698	(0.00710)	7025.587	0.11452
PERCOLATION/LEAKAGE THROUGH LAYER 7	0.00002	(0.00001)	8.132	0.00013
AVERAGE HEAD ON TOP OF LAYER 6	0.110	(0.046)		
PERCOLATION/LEAKAGE THROUGH LAYER 8	0.00000	(0.00000)	0.000	0.00000
CHANGE IN WATER STORAGE	0.337	(0.5704)	139491.23	2.274

PEAK DAILY VALUES FOR YEARS	1 THROUGH	2
	(INCHES)	(CU. FT.)
PRECIPITATION	1.97	815225.437
RUNOFF	1.187	491039.1560
DRAINAGE COLLECTED FROM LAYER 5	0.00008	33.15267
PERCOLATION/LEAKAGE THROUGH LAYER 7	0.000000	0.03772
AVERAGE HEAD ON TOP OF LAYER 6	0.189	
MAXIMUM HEAD ON TOP OF LAYER 6	0.372	
LOCATION OF MAXIMUM HEAD IN LAYER 5 (DISTANCE FROM DRAIN)	2.6 FEET	
PERCOLATION/LEAKAGE THROUGH LAYER 8	0.000000	0.00000
SNOW WATER	0.55	227731.3440
MAXIMUM VEG. SOIL WATER (VOL/VOL)		0.2611
MINIMUM VEG. SOIL WATER (VOL/VOL)		0.0850

*** Maximum heads are computed using McEnroe's equations. ***

Reference: Maximum Saturated Depth over Landfill Liner
by Bruce M. McEnroe, University of Kansas
ASCE Journal of Environmental Engineering
Vol. 119, No. 2, March 1993, pp. 262-270.

FINAL WATER STORAGE AT END OF YEAR 2

LAYER	(INCHES)	(VOL/VOL)
1	0.5608	0.0935
2	4.1419	0.1381
3	1.3333	0.1111
4	300.3972	0.1447
5	5.3420	0.2226
6	0.0000	0.0000
7	0.1875	0.7500
8	0.6672	0.1112
SNOW WATER	0.000	

**APPLICATION FOR PERMIT RENEWAL AND MODIFICATION
SANDOVAL COUNTY LANDFILL**

**VOLUME III: LANDFILL ENGINEERING CALCULATIONS
SECTION 10: HELP MODEL**

ATTACHMENT III.10.A-6

TIER II, SIMULATION 10-1A AND 10-1B
PRESCRIPTIVE LINER WITH SOIL TYPE 6
ALTERNATE COVER WITH SOIL TYPE 6

```

*****
*****
**
**
**
**      HYDROLOGIC EVALUATION OF LANDFILL PERFORMANCE      **
**      HELP MODEL VERSION 3.07  (1 NOVEMBER 1997)          **
**      DEVELOPED BY ENVIRONMENTAL LABORATORY                **
**      USAE WATERWAYS EXPERIMENT STATION                   **
**      FOR USEPA RISK REDUCTION ENGINEERING LABORATORY      **
**
**
*****
*****

```

```

PRECIPITATION DATA FILE:  c:\RAIN30.D4
TEMPERATURE DATA FILE:   C:\TEMP30.D7
SOLAR RADIATION DATA FILE: C:\SOLAR30.D13
EVAPOTRANSPIRATION DATA:  C:\EVAP30.D11
SOIL AND DESIGN DATA FILE: C:\SIM10A5%.D10
OUTPUT DATA FILE:        C:\sim10a5%.OUT

```

TIME: 17:21 DATE: 4/ 8/2015

```

*****

```

TITLE: Sandoval County Landfill - 28 Years Closed - Poor Veg - 5%

Simulation 10A - Alternate Final Cover; 5% Sloped Area: 8.9 Acres

```

*****

```

NOTE: INITIAL MOISTURE CONTENT OF THE LAYERS AND SNOW WATER
WERE SPECIFIED BY THE USER.

LAYER 1

TYPE 1 - VERTICAL PERCOLATION LAYER

MATERIAL TEXTURE NUMBER 6

THICKNESS	=	6.00	INCHES
POROSITY	=	0.4530	VOL/VOL
FIELD CAPACITY	=	0.1900	VOL/VOL
WILTING POINT	=	0.0850	VOL/VOL
INITIAL SOIL WATER CONTENT	=	0.0935	VOL/VOL
EFFECTIVE SAT. HYD. COND.	=	0.720000011000E-03	CM/SEC

NOTE: SATURATED HYDRAULIC CONDUCTIVITY IS MULTIPLIED BY 1.60
FOR ROOT CHANNELS IN TOP HALF OF EVAPORATIVE ZONE.

LAYER 2

TYPE 1 - VERTICAL PERCOLATION LAYER

MATERIAL TEXTURE NUMBER 6

THICKNESS	=	30.00	INCHES
POROSITY	=	0.4530	VOL/VOL
FIELD CAPACITY	=	0.1900	VOL/VOL
WILTING POINT	=	0.0850	VOL/VOL
INITIAL SOIL WATER CONTENT	=	0.1381	VOL/VOL
EFFECTIVE SAT. HYD. COND.	=	0.720000011000E-03	CM/SEC

LAYER 3

TYPE 1 - VERTICAL PERCOLATION LAYER

MATERIAL TEXTURE NUMBER 6

THICKNESS	=	12.00	INCHES
POROSITY	=	0.4530	VOL/VOL
FIELD CAPACITY	=	0.1900	VOL/VOL
WILTING POINT	=	0.0850	VOL/VOL
INITIAL SOIL WATER CONTENT	=	0.1110	VOL/VOL
EFFECTIVE SAT. HYD. COND.	=	0.720000011000E-03	CM/SEC

LAYER 4

TYPE 1 - VERTICAL PERCOLATION LAYER

MATERIAL TEXTURE NUMBER 18

THICKNESS	=	2076.00	INCHES
POROSITY	=	0.6710	VOL/VOL
FIELD CAPACITY	=	0.2920	VOL/VOL
WILTING POINT	=	0.0770	VOL/VOL
INITIAL SOIL WATER CONTENT	=	0.1447	VOL/VOL
EFFECTIVE SAT. HYD. COND.	=	0.100000005000E-02	CM/SEC

LAYER 5

TYPE 2 - LATERAL DRAINAGE LAYER

MATERIAL TEXTURE NUMBER 0

THICKNESS	=	24.00	INCHES
POROSITY	=	0.4730	VOL/VOL
FIELD CAPACITY	=	0.2220	VOL/VOL

WILTING POINT	=	0.1040	VOL/VOL
INITIAL SOIL WATER CONTENT	=	0.2226	VOL/VOL
EFFECTIVE SAT. HYD. COND.	=	0.300000014000E-03	CM/SEC
SLOPE	=	5.00	PERCENT
DRAINAGE LENGTH	=	200.0	FEET

LAYER 6

TYPE 4 - FLEXIBLE MEMBRANE LINER

MATERIAL TEXTURE NUMBER 35

THICKNESS	=	0.06	INCHES
POROSITY	=	0.0000	VOL/VOL
FIELD CAPACITY	=	0.0000	VOL/VOL
WILTING POINT	=	0.0000	VOL/VOL
INITIAL SOIL WATER CONTENT	=	0.0000	VOL/VOL
EFFECTIVE SAT. HYD. COND.	=	0.199999996000E-12	CM/SEC
FML PINHOLE DENSITY	=	1.00	HOLES/ACRE
FML INSTALLATION DEFECTS	=	4.00	HOLES/ACRE
FML PLACEMENT QUALITY	=	3	- GOOD

LAYER 7

TYPE 3 - BARRIER SOIL LINER

MATERIAL TEXTURE NUMBER 0

THICKNESS	=	0.25	INCHES
POROSITY	=	0.7500	VOL/VOL
FIELD CAPACITY	=	0.7470	VOL/VOL
WILTING POINT	=	0.4000	VOL/VOL
INITIAL SOIL WATER CONTENT	=	0.7500	VOL/VOL
EFFECTIVE SAT. HYD. COND.	=	0.499999997000E-08	CM/SEC

LAYER 8

TYPE 1 - VERTICAL PERCOLATION LAYER

MATERIAL TEXTURE NUMBER 0

THICKNESS	=	6.00	INCHES
POROSITY	=	0.4530	VOL/VOL
FIELD CAPACITY	=	0.1900	VOL/VOL
WILTING POINT	=	0.0850	VOL/VOL
INITIAL SOIL WATER CONTENT	=	0.1112	VOL/VOL
EFFECTIVE SAT. HYD. COND.	=	0.420000015000E-05	CM/SEC

GENERAL DESIGN AND EVAPORATIVE ZONE DATA

NOTE: SCS RUNOFF CURVE NUMBER WAS COMPUTED FROM A USER-SPECIFIED CURVE NUMBER OF 85.0, A SURFACE SLOPE OF 5.% AND A SLOPE LENGTH OF 258. FEET.

SCS RUNOFF CURVE NUMBER	=	85.60	
FRACTION OF AREA ALLOWING RUNOFF	=	100.0	PERCENT
AREA PROJECTED ON HORIZONTAL PLANE	=	8.900	ACRES
EVAPORATIVE ZONE DEPTH	=	28.0	INCHES
INITIAL WATER IN EVAPORATIVE ZONE	=	3.599	INCHES
UPPER LIMIT OF EVAPORATIVE STORAGE	=	12.684	INCHES
LOWER LIMIT OF EVAPORATIVE STORAGE	=	2.380	INCHES
INITIAL SNOW WATER	=	0.000	INCHES
INITIAL WATER IN LAYER MATERIALS	=	312.630	INCHES
TOTAL INITIAL WATER	=	312.630	INCHES
TOTAL SUBSURFACE INFLOW	=	0.00	INCHES/YEAR

EVAPOTRANSPIRATION AND WEATHER DATA

NOTE: EVAPOTRANSPIRATION DATA WAS OBTAINED FROM ALBUQUERQUE NEW MEXICO

STATION LATITUDE	=	35.30	DEGREES
MAXIMUM LEAF AREA INDEX	=	0.80	
START OF GROWING SEASON (JULIAN DATE)	=	98	
END OF GROWING SEASON (JULIAN DATE)	=	299	
EVAPORATIVE ZONE DEPTH	=	28.0	INCHES
AVERAGE ANNUAL WIND SPEED	=	9.00	MPH
AVERAGE 1ST QUARTER RELATIVE HUMIDITY	=	48.00	%
AVERAGE 2ND QUARTER RELATIVE HUMIDITY	=	30.00	%
AVERAGE 3RD QUARTER RELATIVE HUMIDITY	=	45.00	%
AVERAGE 4TH QUARTER RELATIVE HUMIDITY	=	50.00	%

NOTE: PRECIPITATION DATA WAS SYNTHETICALLY GENERATED USING COEFFICIENTS FOR ALBUQUERQUE NEW MEXICO

NORMAL MEAN MONTHLY PRECIPITATION (INCHES)

JAN/JUL	FEB/AUG	MAR/SEP	APR/OCT	MAY/NOV	JUN/DEC
0.37	0.47	0.48	0.99	0.72	0.99
1.39	2.34	1.20	1.50	0.55	0.47

NOTE: TEMPERATURE DATA WAS SYNTHETICALLY GENERATED USING
COEFFICIENTS FOR ALBUQUERQUE NEW MEXICO

NORMAL MEAN MONTHLY TEMPERATURE (DEGREES FAHRENHEIT)

JAN/JUL	FEB/AUG	MAR/SEP	APR/OCT	MAY/NOV	JUN/DEC
-----	-----	-----	-----	-----	-----
35.20	40.90	47.10	55.30	64.90	73.50
77.30	75.60	67.30	57.20	44.40	35.70

NOTE: SOLAR RADIATION DATA WAS SYNTHETICALLY GENERATED USING
COEFFICIENTS FOR ALBUQUERQUE NEW MEXICO
AND STATION LATITUDE = 35.30 DEGREES

MONTHLY TOTALS (IN INCHES) FOR YEAR 1

	JAN/JUL	FEB/AUG	MAR/SEP	APR/OCT	MAY/NOV	JUN/DEC
	-----	-----	-----	-----	-----	-----
PRECIPITATION	0.11	0.01	0.26	0.55	0.86	0.01
	0.99	3.66	1.17	1.12	1.67	0.57
RUNOFF	0.000	0.000	0.000	0.000	0.000	0.000
	0.000	0.000	0.000	0.000	0.000	0.000
EVAPOTRANSPIRATION	0.600	0.355	0.200	0.233	0.683	0.929
	0.986	3.115	1.718	1.097	1.495	0.762
LATERAL DRAINAGE COLLECTED	0.0007	0.0006	0.0007	0.0006	0.0006	0.0006
FROM LAYER 5	0.0005	0.0005	0.0005	0.0005	0.0004	0.0004
PERCOLATION/LEAKAGE THROUGH	0.0000	0.0000	0.0000	0.0000	0.0000	0.0000
LAYER 7	0.0000	0.0000	0.0000	0.0000	0.0000	0.0000
PERCOLATION/LEAKAGE THROUGH	0.0000	0.0000	0.0000	0.0000	0.0000	0.0000
LAYER 8	0.0000	0.0000	0.0000	0.0000	0.0000	0.0000

MONTHLY SUMMARIES FOR DAILY HEADS (INCHES)

AVERAGE DAILY HEAD ON	0.055	0.053	0.051	0.048	0.046	0.043
-----------------------	-------	-------	-------	-------	-------	-------

TOP OF LAYER 6	0.041	0.039	0.037	0.035	0.033	0.032
STD. DEVIATION OF DAILY	0.005	0.001	0.001	0.001	0.001	0.001
HEAD ON TOP OF LAYER 6	0.001	0.001	0.001	0.001	0.000	0.000

ANNUAL TOTALS FOR YEAR 1

	INCHES	CU. FEET	PERCENT
PRECIPITATION	10.98	354730.906	100.00
RUNOFF	0.000	0.000	0.00
EVAPOTRANSPIRATION	12.175	393326.375	110.88
DRAINAGE COLLECTED FROM LAYER 5	0.0066	213.806	0.06
PERC./LEAKAGE THROUGH LAYER 7	0.000009	0.283	0.00
AVG. HEAD ON TOP OF LAYER 6	0.0428		
PERC./LEAKAGE THROUGH LAYER 8	0.000000	0.000	0.00
CHANGE IN WATER STORAGE	-1.201	-38809.215	-10.94
SOIL WATER AT START OF YEAR	312.630	10100146.000	
SOIL WATER AT END OF YEAR	311.429	10061337.000	
SNOW WATER AT START OF YEAR	0.000	0.000	0.00
SNOW WATER AT END OF YEAR	0.000	0.000	0.00
ANNUAL WATER BUDGET BALANCE	0.0000	-0.075	0.00

MONTHLY TOTALS (IN INCHES) FOR YEAR 2

JAN/JUL FEB/AUG MAR/SEP APR/OCT MAY/NOV JUN/DEC

PRECIPITATION	0.09 1.08	1.07 3.29	0.00 1.76	1.64 5.91	1.35 0.03	2.03 0.42
RUNOFF	0.000 0.000	0.000 0.019	0.000 0.000	0.000 0.353	0.000 0.000	0.015 0.000
EVAPOTRANSPIRATION	0.092 1.080	1.068 2.762	0.002 1.602	1.625 2.972	1.182 1.871	2.201 0.588
LATERAL DRAINAGE COLLECTED FROM LAYER 5	0.0004 0.0003	0.0003 0.0003	0.0004 0.0003	0.0003 0.0002	0.0003 0.0002	0.0003 0.0002
PERCOLATION/LEAKAGE THROUGH LAYER 7	0.0000 0.0000	0.0000 0.0000	0.0000 0.0000	0.0000 0.0000	0.0000 0.0000	0.0000 0.0000
PERCOLATION/LEAKAGE THROUGH LAYER 8	0.0000 0.0000	0.0000 0.0000	0.0000 0.0000	0.0000 0.0000	0.0000 0.0000	0.0000 0.0000

MONTHLY SUMMARIES FOR DAILY HEADS (INCHES)

AVERAGE DAILY HEAD ON TOP OF LAYER 6	0.030 0.022	0.029 0.021	0.027 0.020	0.026 0.019	0.025 0.018	0.023 0.017
STD. DEVIATION OF DAILY HEAD ON TOP OF LAYER 6	0.000 0.000	0.000 0.000	0.000 0.000	0.000 0.000	0.000 0.000	0.000 0.000

ANNUAL TOTALS FOR YEAR 2

	INCHES	CU. FEET	PERCENT
PRECIPITATION	18.67	603171.750	100.00
RUNOFF	0.387	12504.579	2.07
EVAPOTRANSPIRATION	17.046	550692.687	91.30
DRAINAGE COLLECTED FROM LAYER 5	0.0036	115.564	0.02
PERC./LEAKAGE THROUGH LAYER 7	0.000006	0.196	0.00
AVG. HEAD ON TOP OF LAYER 6	0.0231		

PERC./LEAKAGE THROUGH LAYER 8	0.000001	0.025	0.00
CHANGE IN WATER STORAGE	1.234	39858.246	6.61
SOIL WATER AT START OF YEAR	311.429	10061337.000	
SOIL WATER AT END OF YEAR	312.663	10101195.000	
SNOW WATER AT START OF YEAR	0.000	0.000	0.00
SNOW WATER AT END OF YEAR	0.000	0.000	0.00
ANNUAL WATER BUDGET BALANCE	0.0000	0.615	0.00

MONTHLY TOTALS (IN INCHES) FOR YEAR 3

	JAN/JUL	FEB/AUG	MAR/SEP	APR/OCT	MAY/NOV	JUN/DEC
PRECIPITATION	0.47 0.75	0.61 1.16	0.91 2.62	0.33 1.24	1.68 0.77	2.49 0.17
RUNOFF	0.000 0.000	0.000 0.000	0.000 0.000	0.000 0.000	0.000 0.000	0.016 0.000
EVAPOTRANSPIRATION	0.376 0.750	0.319 0.835	0.564 2.945	0.485 1.022	1.935 0.986	3.922 0.145
LATERAL DRAINAGE COLLECTED FROM LAYER 5	0.0002 0.0002	0.0002 0.0001	0.0002 0.0001	0.0002 0.0001	0.0002 0.0001	0.0002 0.0001
PERCOLATION/LEAKAGE THROUGH LAYER 7	0.0000 0.0000	0.0000 0.0000	0.0000 0.0000	0.0000 0.0000	0.0000 0.0000	0.0000 0.0000
PERCOLATION/LEAKAGE THROUGH LAYER 8	0.0000 0.0000	0.0000 0.0000	0.0000 0.0000	0.0000 0.0000	0.0000 0.0000	0.0000 0.0000

MONTHLY SUMMARIES FOR DAILY HEADS (INCHES)

AVERAGE DAILY HEAD ON	0.016	0.015	0.015	0.014	0.013	0.013
-----------------------	-------	-------	-------	-------	-------	-------

TOP OF LAYER 6	0.012	0.011	0.011	0.010	0.010	0.009
STD. DEVIATION OF DAILY	0.000	0.000	0.000	0.000	0.000	0.000
HEAD ON TOP OF LAYER 6	0.000	0.000	0.000	0.000	0.000	0.000

ANNUAL TOTALS FOR YEAR 3

	INCHES	CU. FEET	PERCENT
PRECIPITATION	13.20	426452.406	100.00
RUNOFF	0.016	500.822	0.12
EVAPOTRANSPIRATION	14.282	461414.906	108.20
DRAINAGE COLLECTED FROM LAYER 5	0.0019	62.284	0.01
PERC./LEAKAGE THROUGH LAYER 7	0.000005	0.146	0.00
AVG. HEAD ON TOP OF LAYER 6	0.0125		
PERC./LEAKAGE THROUGH LAYER 8	0.000002	0.074	0.00
CHANGE IN WATER STORAGE	-1.100	-35526.062	-8.33
SOIL WATER AT START OF YEAR	312.663	10101195.000	
SOIL WATER AT END OF YEAR	311.563	10065669.000	
SNOW WATER AT START OF YEAR	0.000	0.000	0.00
SNOW WATER AT END OF YEAR	0.000	0.000	0.00
ANNUAL WATER BUDGET BALANCE	0.0000	0.372	0.00

MONTHLY TOTALS (IN INCHES) FOR YEAR 4

JAN/JUL FEB/AUG MAR/SEP APR/OCT MAY/NOV JUN/DEC

	-----	-----	-----	-----	-----	-----
PRECIPITATION	0.00	0.07	0.17	0.19	0.38	1.20
	3.02	2.72	1.04	3.38	0.35	0.36
RUNOFF	0.000	0.000	0.000	0.000	0.000	0.000
	0.074	0.006	0.000	0.072	0.000	0.000
EVAPOTRANSPIRATION	0.026	0.070	0.170	0.190	0.343	1.218
	2.531	2.483	1.674	1.854	1.603	0.452
LATERAL DRAINAGE COLLECTED FROM LAYER 5	0.0001	0.0001	0.0001	0.0001	0.0001	0.0001
	0.0001	0.0001	0.0001	0.0001	0.0001	0.0001
PERCOLATION/LEAKAGE THROUGH LAYER 7	0.0000	0.0000	0.0000	0.0000	0.0000	0.0000
	0.0000	0.0000	0.0000	0.0000	0.0000	0.0000
PERCOLATION/LEAKAGE THROUGH LAYER 8	0.0000	0.0000	0.0000	0.0000	0.0000	0.0000
	0.0000	0.0000	0.0000	0.0000	0.0000	0.0000

MONTHLY SUMMARIES FOR DAILY HEADS (INCHES)

AVERAGE DAILY HEAD ON TOP OF LAYER 6	0.009	0.008	0.008	0.008	0.007	0.007
	0.006	0.006	0.006	0.006	0.005	0.005
STD. DEVIATION OF DAILY HEAD ON TOP OF LAYER 6	0.000	0.000	0.000	0.000	0.000	0.000
	0.000	0.000	0.000	0.000	0.000	0.000

ANNUAL TOTALS FOR YEAR 4

	INCHES	CU. FEET	PERCENT
	-----	-----	-----
PRECIPITATION	12.88	416114.156	100.00
RUNOFF	0.152	4910.562	1.18
EVAPOTRANSPIRATION	12.615	407546.906	97.94
DRAINAGE COLLECTED FROM LAYER 5	0.0010	33.617	0.01
PERC./LEAKAGE THROUGH LAYER 7	0.000004	0.118	0.00
AVG. HEAD ON TOP OF LAYER 6	0.0067		

PERC./LEAKAGE THROUGH LAYER 8	0.000003	0.103	0.00
CHANGE IN WATER STORAGE	0.112	3623.298	0.87
SOIL WATER AT START OF YEAR	311.563	10065669.000	
SOIL WATER AT END OF YEAR	311.675	10069292.000	
SNOW WATER AT START OF YEAR	0.000	0.000	0.00
SNOW WATER AT END OF YEAR	0.000	0.000	0.00
ANNUAL WATER BUDGET BALANCE	0.0000	-0.359	0.00

MONTHLY TOTALS (IN INCHES) FOR YEAR 5

	JAN/JUL	FEB/AUG	MAR/SEP	APR/OCT	MAY/NOV	JUN/DEC
PRECIPITATION	0.27 1.40	0.68 1.86	0.78 1.82	1.73 3.13	0.97 0.00	0.20 1.03
RUNOFF	0.000 0.000	0.000 0.000	0.000 0.010	0.003 0.000	0.000 0.000	0.000 0.000
EVAPOTRANSPIRATION	0.344 1.194	0.121 2.066	1.301 0.751	1.766 3.017	0.893 1.162	0.340 0.930
LATERAL DRAINAGE COLLECTED FROM LAYER 5	0.0001 0.0000	0.0001 0.0000	0.0001 0.0000	0.0001 0.0000	0.0001 0.0000	0.0000 0.0000
PERCOLATION/LEAKAGE THROUGH LAYER 7	0.0000 0.0000	0.0000 0.0000	0.0000 0.0000	0.0000 0.0000	0.0000 0.0000	0.0000 0.0000
PERCOLATION/LEAKAGE THROUGH LAYER 8	0.0000 0.0000	0.0000 0.0000	0.0000 0.0000	0.0000 0.0000	0.0000 0.0000	0.0000 0.0000

MONTHLY SUMMARIES FOR DAILY HEADS (INCHES)

AVERAGE DAILY HEAD ON	0.005	0.004	0.004	0.004	0.004	0.004
-----------------------	-------	-------	-------	-------	-------	-------

TOP OF LAYER 6	0.003	0.003	0.003	0.003	0.003	0.003
STD. DEVIATION OF DAILY	0.000	0.000	0.000	0.000	0.000	0.000
HEAD ON TOP OF LAYER 6	0.000	0.000	0.000	0.000	0.000	0.000

ANNUAL TOTALS FOR YEAR 5

	INCHES	CU. FEET	PERCENT
PRECIPITATION	13.87	448098.156	100.00
RUNOFF	0.013	414.692	0.09
EVAPOTRANSPIRATION	13.886	448627.469	100.12
DRAINAGE COLLECTED FROM LAYER 5	0.0006	18.024	0.00
PERC./LEAKAGE THROUGH LAYER 7	0.000003	0.102	0.00
AVG. HEAD ON TOP OF LAYER 6	0.0036		
PERC./LEAKAGE THROUGH LAYER 8	0.000004	0.119	0.00
CHANGE IN WATER STORAGE	-0.030	-962.269	-0.21
SOIL WATER AT START OF YEAR	311.675	10069292.000	
SOIL WATER AT END OF YEAR	311.645	10068330.000	
SNOW WATER AT START OF YEAR	0.000	0.000	0.00
SNOW WATER AT END OF YEAR	0.000	0.000	0.00
ANNUAL WATER BUDGET BALANCE	0.0000	0.113	0.00

MONTHLY TOTALS (IN INCHES) FOR YEAR 6

JAN/JUL FEB/AUG MAR/SEP APR/OCT MAY/NOV JUN/DEC

PRECIPITATION	0.03	0.62	0.94	0.00	1.03	0.44
	0.37	1.10	0.47	1.53	1.16	0.61
RUNOFF	0.000	0.000	0.000	0.000	0.000	0.000
	0.000	0.000	0.000	0.086	0.000	0.000
EVAPOTRANSPIRATION	0.133	0.570	0.983	0.007	1.037	0.281
	0.528	1.099	0.436	1.385	0.985	0.853
LATERAL DRAINAGE COLLECTED FROM LAYER 5	0.0000	0.0000	0.0000	0.0000	0.0000	0.0000
	0.0000	0.0000	0.0000	0.0000	0.0000	0.0000
PERCOLATION/LEAKAGE THROUGH LAYER 7	0.0000	0.0000	0.0000	0.0000	0.0000	0.0000
	0.0000	0.0000	0.0000	0.0000	0.0000	0.0000
PERCOLATION/LEAKAGE THROUGH LAYER 8	0.0000	0.0000	0.0000	0.0000	0.0000	0.0000
	0.0000	0.0000	0.0000	0.0000	0.0000	0.0000

MONTHLY SUMMARIES FOR DAILY HEADS (INCHES)

AVERAGE DAILY HEAD ON TOP OF LAYER 6	0.003	0.002	0.002	0.002	0.002	0.002
	0.002	0.002	0.002	0.002	0.002	0.001
STD. DEVIATION OF DAILY HEAD ON TOP OF LAYER 6	0.000	0.000	0.000	0.000	0.000	0.000
	0.000	0.000	0.000	0.000	0.000	0.000

ANNUAL TOTALS FOR YEAR 6

	INCHES	CU. FEET	PERCENT
	-----	-----	-----
PRECIPITATION	8.30	268148.125	100.00
RUNOFF	0.086	2787.133	1.04
EVAPOTRANSPIRATION	8.297	268062.750	99.97
DRAINAGE COLLECTED FROM LAYER 5	0.0003	9.682	0.00
PERC./LEAKAGE THROUGH LAYER 7	0.000003	0.092	0.00
AVG. HEAD ON TOP OF LAYER 6	0.0019		

MONTHLY SUMMARIES FOR DAILY HEADS (INCHES)

AVERAGE DAILY HEAD ON	0.001	0.001	0.001	0.001	0.001	0.001
-----------------------	-------	-------	-------	-------	-------	-------

TOP OF LAYER 6	0.001	0.001	0.001	0.001	0.001	0.001
STD. DEVIATION OF DAILY	0.000	0.000	0.000	0.000	0.000	0.000
HEAD ON TOP OF LAYER 6	0.000	0.000	0.000	0.000	0.000	0.000

ANNUAL TOTALS FOR YEAR 7

	INCHES	CU. FEET	PERCENT
PRECIPITATION	9.78	315962.531	100.00
RUNOFF	0.001	25.364	0.01
EVAPOTRANSPIRATION	9.735	314496.125	99.54
DRAINAGE COLLECTED FROM LAYER 5	0.0002	5.183	0.00
PERC./LEAKAGE THROUGH LAYER 7	0.000003	0.087	0.00
AVG. HEAD ON TOP OF LAYER 6	0.0010		
PERC./LEAKAGE THROUGH LAYER 8	0.000004	0.133	0.00
CHANGE IN WATER STORAGE	0.044	1436.502	0.45
SOIL WATER AT START OF YEAR	311.562	10065618.000	
SOIL WATER AT END OF YEAR	311.606	10067054.000	
SNOW WATER AT START OF YEAR	0.000	0.000	0.00
SNOW WATER AT END OF YEAR	0.000	0.000	0.00
ANNUAL WATER BUDGET BALANCE	0.0000	-0.794	0.00

MONTHLY TOTALS (IN INCHES) FOR YEAR 8

JAN/JUL FEB/AUG MAR/SEP APR/OCT MAY/NOV JUN/DEC

	-----	-----	-----	-----	-----	-----
PRECIPITATION	0.42	0.09	0.00	0.22	0.40	2.78
	1.05	3.75	2.59	1.58	1.65	0.46
RUNOFF	0.000	0.000	0.000	0.000	0.000	0.000
	0.000	0.000	0.030	0.000	0.000	0.000
EVAPOTRANSPIRATION	0.473	0.073	0.026	0.106	0.505	2.793
	1.036	3.550	2.305	1.082	1.915	1.040
LATERAL DRAINAGE COLLECTED FROM LAYER 5	0.0000	0.0000	0.0000	0.0000	0.0000	0.0000
	0.0000	0.0000	0.0000	0.0000	0.0000	0.0000
PERCOLATION/LEAKAGE THROUGH LAYER 7	0.0000	0.0000	0.0000	0.0000	0.0000	0.0000
	0.0000	0.0000	0.0000	0.0000	0.0000	0.0000
PERCOLATION/LEAKAGE THROUGH LAYER 8	0.0000	0.0000	0.0000	0.0000	0.0000	0.0000
	0.0000	0.0000	0.0000	0.0000	0.0000	0.0000

MONTHLY SUMMARIES FOR DAILY HEADS (INCHES)

AVERAGE DAILY HEAD ON TOP OF LAYER 6	0.001	0.001	0.001	0.001	0.001	0.001
	0.001	0.001	0.000	0.000	0.000	0.000
STD. DEVIATION OF DAILY HEAD ON TOP OF LAYER 6	0.000	0.000	0.000	0.000	0.000	0.000
	0.000	0.000	0.000	0.000	0.000	0.000

ANNUAL TOTALS FOR YEAR 8

	INCHES	CU. FEET	PERCENT
	-----	-----	-----
PRECIPITATION	14.99	484282.000	100.00
RUNOFF	0.030	975.069	0.20
EVAPOTRANSPIRATION	14.906	481557.656	99.44
DRAINAGE COLLECTED FROM LAYER 5	0.0001	2.763	0.00
PERC./LEAKAGE THROUGH LAYER 7	0.000003	0.084	0.00
AVG. HEAD ON TOP OF LAYER 6	0.0006		

MONTHLY SUMMARIES FOR DAILY HEADS (INCHES)

AVERAGE DAILY HEAD ON	0.000	0.000	0.000	0.000	0.000	0.000
-----------------------	-------	-------	-------	-------	-------	-------

TOP OF LAYER 6	0.000	0.000	0.000	0.000	0.000	0.000
STD. DEVIATION OF DAILY	0.000	0.000	0.000	0.000	0.000	0.000
HEAD ON TOP OF LAYER 6	0.000	0.000	0.000	0.000	0.000	0.000

ANNUAL TOTALS FOR YEAR 9

	INCHES	CU. FEET	PERCENT
PRECIPITATION	12.47	402868.281	100.00
RUNOFF	0.322	10408.425	2.58
EVAPOTRANSPIRATION	12.263	396177.406	98.34
DRAINAGE COLLECTED FROM LAYER 5	0.0000	1.447	0.00
PERC./LEAKAGE THROUGH LAYER 7	0.000003	0.082	0.00
AVG. HEAD ON TOP OF LAYER 6	0.0003		
PERC./LEAKAGE THROUGH LAYER 8	0.000004	0.138	0.00
CHANGE IN WATER STORAGE	-0.115	-3718.933	-0.92
SOIL WATER AT START OF YEAR	311.660	10068800.000	
SOIL WATER AT END OF YEAR	311.545	10065081.000	
SNOW WATER AT START OF YEAR	0.000	0.000	0.00
SNOW WATER AT END OF YEAR	0.000	0.000	0.00
ANNUAL WATER BUDGET BALANCE	0.0000	-0.208	0.00

MONTHLY TOTALS (IN INCHES) FOR YEAR 10

JAN/JUL FEB/AUG MAR/SEP APR/OCT MAY/NOV JUN/DEC

PRECIPITATION	0.00	0.02	0.24	1.82	0.98	0.00
	1.73	3.20	0.57	5.06	0.00	0.30
RUNOFF	0.000	0.000	0.000	0.029	0.000	0.000
	0.005	0.000	0.000	0.425	0.000	0.000
EVAPOTRANSPIRATION	0.000	0.020	0.154	1.711	1.152	0.000
	1.724	2.632	1.139	1.833	1.166	0.637
LATERAL DRAINAGE COLLECTED FROM LAYER 5	0.0000	0.0000	0.0000	0.0000	0.0000	0.0000
	0.0000	0.0000	0.0000	0.0000	0.0000	0.0000
PERCOLATION/LEAKAGE THROUGH LAYER 7	0.0000	0.0000	0.0000	0.0000	0.0000	0.0000
	0.0000	0.0000	0.0000	0.0000	0.0000	0.0000
PERCOLATION/LEAKAGE THROUGH LAYER 8	0.0000	0.0000	0.0000	0.0000	0.0000	0.0000
	0.0000	0.0000	0.0000	0.0000	0.0000	0.0000

MONTHLY SUMMARIES FOR DAILY HEADS (INCHES)

AVERAGE DAILY HEAD ON TOP OF LAYER 6	0.000	0.000	0.000	0.000	0.000	0.000
	0.000	0.000	0.000	0.000	0.000	0.000
STD. DEVIATION OF DAILY HEAD ON TOP OF LAYER 6	0.000	0.000	0.000	0.000	0.000	0.000
	0.000	0.000	0.000	0.000	0.000	0.000

ANNUAL TOTALS FOR YEAR 10

	INCHES	CU. FEET	PERCENT
	-----	-----	-----
PRECIPITATION	13.92	449713.406	100.00
RUNOFF	0.458	14811.777	3.29
EVAPOTRANSPIRATION	12.169	393147.625	87.42
DRAINAGE COLLECTED FROM LAYER 5	0.0000	0.743	0.00
PERC./LEAKAGE THROUGH LAYER 7	0.000003	0.081	0.00
AVG. HEAD ON TOP OF LAYER 6	0.0001		

MONTHLY SUMMARIES FOR DAILY HEADS (INCHES)

AVERAGE DAILY HEAD ON	0.000	0.000	0.000	0.000	0.000	0.000
-----------------------	-------	-------	-------	-------	-------	-------

TOP OF LAYER 6	0.000	0.000	0.000	0.000	0.000	0.000
STD. DEVIATION OF DAILY	0.000	0.000	0.000	0.000	0.000	0.000
HEAD ON TOP OF LAYER 6	0.000	0.000	0.000	0.000	0.000	0.000

ANNUAL TOTALS FOR YEAR 11

	INCHES	CU. FEET	PERCENT
PRECIPITATION	13.33	430652.344	100.00
RUNOFF	0.449	14506.188	3.37
EVAPOTRANSPIRATION	12.920	417407.094	96.92
DRAINAGE COLLECTED FROM LAYER 5	0.0000	0.364	0.00
PERC./LEAKAGE THROUGH LAYER 7	0.000003	0.081	0.00
AVG. HEAD ON TOP OF LAYER 6	0.0001		
PERC./LEAKAGE THROUGH LAYER 8	0.000004	0.139	0.00
CHANGE IN WATER STORAGE	-0.039	-1262.978	-0.29
SOIL WATER AT START OF YEAR	312.837	10106836.000	
SOIL WATER AT END OF YEAR	312.798	10105573.000	
SNOW WATER AT START OF YEAR	0.000	0.000	0.00
SNOW WATER AT END OF YEAR	0.000	0.000	0.00
ANNUAL WATER BUDGET BALANCE	0.0000	1.534	0.00

MONTHLY TOTALS (IN INCHES) FOR YEAR 12

JAN/JUL FEB/AUG MAR/SEP APR/OCT MAY/NOV JUN/DEC

	-----	-----	-----	-----	-----	-----
PRECIPITATION	0.00	0.98	0.80	0.75	0.85	2.19
	0.98	1.85	2.14	1.46	1.75	0.77
RUNOFF	0.000	0.023	0.000	0.000	0.000	0.000
	0.000	0.000	0.000	0.005	0.005	0.000
EVAPOTRANSPIRATION	0.206	0.501	0.318	0.753	0.788	3.896
	0.858	1.902	2.210	1.452	1.220	1.242
LATERAL DRAINAGE COLLECTED FROM LAYER 5	0.0000	0.0000	0.0000	0.0000	0.0000	0.0000
	0.0000	0.0000	0.0000	0.0000	0.0000	0.0000
PERCOLATION/LEAKAGE THROUGH LAYER 7	0.0000	0.0000	0.0000	0.0000	0.0000	0.0000
	0.0000	0.0000	0.0000	0.0000	0.0000	0.0000
PERCOLATION/LEAKAGE THROUGH LAYER 8	0.0000	0.0000	0.0000	0.0000	0.0000	0.0000
	0.0000	0.0000	0.0000	0.0000	0.0000	0.0000

MONTHLY SUMMARIES FOR DAILY HEADS (INCHES)

AVERAGE DAILY HEAD ON TOP OF LAYER 6	0.000	0.000	0.000	0.000	0.000	0.000
	0.000	0.000	0.000	0.000	0.000	0.000
STD. DEVIATION OF DAILY HEAD ON TOP OF LAYER 6	0.000	0.000	0.000	0.000	0.000	0.000
	0.000	0.000	0.000	0.000	0.000	0.000

ANNUAL TOTALS FOR YEAR 12

	INCHES	CU. FEET	PERCENT
	-----	-----	-----
PRECIPITATION	14.52	469097.625	100.00
RUNOFF	0.033	1081.146	0.23
EVAPOTRANSPIRATION	15.345	495755.531	105.68
DRAINAGE COLLECTED FROM LAYER 5	0.0000	0.159	0.00
PERC./LEAKAGE THROUGH LAYER 7	0.000002	0.081	0.00
AVG. HEAD ON TOP OF LAYER 6	0.0000		

MONTHLY SUMMARIES FOR DAILY HEADS (INCHES)

AVERAGE DAILY HEAD ON	0.000	0.000	0.000	0.000	0.000	0.000
-----------------------	-------	-------	-------	-------	-------	-------

TOP OF LAYER 6	0.000	0.000	0.000	0.000	0.000	0.000
STD. DEVIATION OF DAILY	0.000	0.000	0.000	0.000	0.000	0.000
HEAD ON TOP OF LAYER 6	0.000	0.000	0.000	0.000	0.000	0.000

ANNUAL TOTALS FOR YEAR 13

	INCHES	CU. FEET	PERCENT
PRECIPITATION	10.47	338254.344	100.00
RUNOFF	0.043	1392.610	0.41
EVAPOTRANSPIRATION	10.340	334041.375	98.75
DRAINAGE COLLECTED FROM LAYER 5	0.0000	0.049	0.00
PERC./LEAKAGE THROUGH LAYER 7	0.000002	0.080	0.00
AVG. HEAD ON TOP OF LAYER 6	0.0000		
PERC./LEAKAGE THROUGH LAYER 8	0.000004	0.140	0.00
CHANGE IN WATER STORAGE	0.087	2820.750	0.83
SOIL WATER AT START OF YEAR	311.940	10077833.000	
SOIL WATER AT END OF YEAR	312.027	10080654.000	
SNOW WATER AT START OF YEAR	0.000	0.000	0.00
SNOW WATER AT END OF YEAR	0.000	0.000	0.00
ANNUAL WATER BUDGET BALANCE	0.0000	-0.601	0.00

MONTHLY TOTALS (IN INCHES) FOR YEAR 14

JAN/JUL FEB/AUG MAR/SEP APR/OCT MAY/NOV JUN/DEC

	-----	-----	-----	-----	-----	-----
PRECIPITATION	0.00	0.70	0.35	1.17	1.04	0.77
	1.61	1.62	0.21	1.09	0.02	0.66
RUNOFF	0.000	0.000	0.000	0.000	0.000	0.000
	0.000	0.000	0.000	0.000	0.000	0.000
EVAPOTRANSPIRATION	0.136	0.699	0.113	1.285	0.817	1.122
	1.610	1.620	0.168	1.131	0.020	0.659
LATERAL DRAINAGE COLLECTED FROM LAYER 5	0.0000	0.0000	0.0000	0.0000	0.0000	0.0000
	0.0000	0.0000	0.0000	0.0000	0.0000	0.0000
PERCOLATION/LEAKAGE THROUGH LAYER 7	0.0000	0.0000	0.0000	0.0000	0.0000	0.0000
	0.0000	0.0000	0.0000	0.0000	0.0000	0.0000
PERCOLATION/LEAKAGE THROUGH LAYER 8	0.0000	0.0000	0.0000	0.0000	0.0000	0.0000
	0.0000	0.0000	0.0000	0.0000	0.0000	0.0000

MONTHLY SUMMARIES FOR DAILY HEADS (INCHES)

AVERAGE DAILY HEAD ON TOP OF LAYER 6	0.000	0.000	0.000	0.000	0.000	0.000
	0.000	0.000	0.000	0.000	0.000	0.000
STD. DEVIATION OF DAILY HEAD ON TOP OF LAYER 6	0.000	0.000	0.000	0.000	0.000	0.000
	0.000	0.000	0.000	0.000	0.000	0.000

ANNUAL TOTALS FOR YEAR 14

	INCHES	CU. FEET	PERCENT
	-----	-----	-----
PRECIPITATION	9.24	298516.719	100.00
RUNOFF	0.000	0.000	0.00
EVAPOTRANSPIRATION	9.381	303061.625	101.52
DRAINAGE COLLECTED FROM LAYER 5	0.0000	0.002	0.00
PERC./LEAKAGE THROUGH LAYER 7	0.000001	0.019	0.00
AVG. HEAD ON TOP OF LAYER 6	0.0000		

MONTHLY SUMMARIES FOR DAILY HEADS (INCHES)

AVERAGE DAILY HEAD ON	0.000	0.000	0.000	0.000	0.000	0.000
-----------------------	-------	-------	-------	-------	-------	-------

TOP OF LAYER 6	0.000	0.000	0.000	0.000	0.000	0.000
STD. DEVIATION OF DAILY	0.000	0.000	0.000	0.000	0.000	0.000
HEAD ON TOP OF LAYER 6	0.000	0.000	0.000	0.000	0.000	0.000

ANNUAL TOTALS FOR YEAR 15

	INCHES	CU. FEET	PERCENT
PRECIPITATION	13.91	449390.344	100.00
RUNOFF	0.026	829.028	0.18
EVAPOTRANSPIRATION	13.824	446608.906	99.38
DRAINAGE COLLECTED FROM LAYER 5	0.0000	0.000	0.00
PERC./LEAKAGE THROUGH LAYER 7	0.000000	0.000	0.00
AVG. HEAD ON TOP OF LAYER 6	0.0000		
PERC./LEAKAGE THROUGH LAYER 8	0.000000	0.000	0.00
CHANGE IN WATER STORAGE	0.060	1953.130	0.43
SOIL WATER AT START OF YEAR	311.886	10076108.000	
SOIL WATER AT END OF YEAR	311.947	10078061.000	
SNOW WATER AT START OF YEAR	0.000	0.000	0.00
SNOW WATER AT END OF YEAR	0.000	0.000	0.00
ANNUAL WATER BUDGET BALANCE	0.0000	-0.722	0.00

MONTHLY TOTALS (IN INCHES) FOR YEAR 16

JAN/JUL FEB/AUG MAR/SEP APR/OCT MAY/NOV JUN/DEC

	-----	-----	-----	-----	-----	-----
PRECIPITATION	0.16	0.46	0.42	1.16	0.00	0.55
	0.76	3.29	0.46	2.49	0.00	0.20
RUNOFF	0.000	0.000	0.000	0.000	0.000	0.000
	0.000	0.000	0.000	0.022	0.000	0.000
EVAPOTRANSPIRATION	0.172	0.149	0.258	0.679	1.003	0.550
	0.707	2.896	0.907	0.805	1.385	0.422
LATERAL DRAINAGE COLLECTED FROM LAYER 5	0.0000	0.0000	0.0000	0.0000	0.0000	0.0000
	0.0000	0.0000	0.0000	0.0000	0.0000	0.0000
PERCOLATION/LEAKAGE THROUGH LAYER 7	0.0000	0.0000	0.0000	0.0000	0.0000	0.0000
	0.0000	0.0000	0.0000	0.0000	0.0000	0.0000
PERCOLATION/LEAKAGE THROUGH LAYER 8	0.0000	0.0000	0.0000	0.0000	0.0000	0.0000
	0.0000	0.0000	0.0000	0.0000	0.0000	0.0000

MONTHLY SUMMARIES FOR DAILY HEADS (INCHES)

AVERAGE DAILY HEAD ON TOP OF LAYER 6	0.000	0.000	0.000	0.000	0.000	0.000
	0.000	0.000	0.000	0.000	0.000	0.000
STD. DEVIATION OF DAILY HEAD ON TOP OF LAYER 6	0.000	0.000	0.000	0.000	0.000	0.000
	0.000	0.000	0.000	0.000	0.000	0.000

ANNUAL TOTALS FOR YEAR 16

	INCHES	CU. FEET	PERCENT
	-----	-----	-----
PRECIPITATION	9.95	321454.594	100.00
RUNOFF	0.022	698.199	0.22
EVAPOTRANSPIRATION	9.933	320919.969	99.83
DRAINAGE COLLECTED FROM LAYER 5	0.0000	0.000	0.00
PERC./LEAKAGE THROUGH LAYER 7	0.000000	0.000	0.00
AVG. HEAD ON TOP OF LAYER 6	0.0000		

MONTHLY SUMMARIES FOR DAILY HEADS (INCHES)

AVERAGE DAILY HEAD ON	0.000	0.000	0.000	0.000	0.000	0.000
-----------------------	-------	-------	-------	-------	-------	-------

TOP OF LAYER 6	0.000	0.000	0.000	0.000	0.000	0.000
STD. DEVIATION OF DAILY	0.000	0.000	0.000	0.000	0.000	0.000
HEAD ON TOP OF LAYER 6	0.000	0.000	0.000	0.000	0.000	0.000

ANNUAL TOTALS FOR YEAR 17

	INCHES	CU. FEET	PERCENT
PRECIPITATION	6.41	207087.875	100.00
RUNOFF	0.000	11.299	0.01
EVAPOTRANSPIRATION	6.256	202115.187	97.60
DRAINAGE COLLECTED FROM LAYER 5	0.0000	0.000	0.00
PERC./LEAKAGE THROUGH LAYER 7	0.000000	0.000	0.00
AVG. HEAD ON TOP OF LAYER 6	0.0000		
PERC./LEAKAGE THROUGH LAYER 8	0.000000	0.000	0.00
CHANGE IN WATER STORAGE	0.154	4961.207	2.40
SOIL WATER AT START OF YEAR	311.942	10077897.000	
SOIL WATER AT END OF YEAR	312.095	10082859.000	
SNOW WATER AT START OF YEAR	0.000	0.000	0.00
SNOW WATER AT END OF YEAR	0.000	0.000	0.00
ANNUAL WATER BUDGET BALANCE	0.0000	0.178	0.00

MONTHLY TOTALS (IN INCHES) FOR YEAR 18

JAN/JUL FEB/AUG MAR/SEP APR/OCT MAY/NOV JUN/DEC

	-----	-----	-----	-----	-----	-----
PRECIPITATION	0.67	0.19	0.03	1.94	0.00	0.08
	2.46	1.29	0.06	0.17	0.41	0.52
RUNOFF	0.000	0.000	0.000	0.045	0.000	0.000
	0.000	0.000	0.000	0.000	0.000	0.000
EVAPOTRANSPIRATION	0.873	0.191	0.030	0.789	1.111	0.080
	2.293	1.428	0.086	0.149	0.432	0.285
LATERAL DRAINAGE COLLECTED FROM LAYER 5	0.0000	0.0000	0.0000	0.0000	0.0000	0.0000
	0.0000	0.0000	0.0000	0.0000	0.0000	0.0000
PERCOLATION/LEAKAGE THROUGH LAYER 7	0.0000	0.0000	0.0000	0.0000	0.0000	0.0000
	0.0000	0.0000	0.0000	0.0000	0.0000	0.0000
PERCOLATION/LEAKAGE THROUGH LAYER 8	0.0000	0.0000	0.0000	0.0000	0.0000	0.0000
	0.0000	0.0000	0.0000	0.0000	0.0000	0.0000

MONTHLY SUMMARIES FOR DAILY HEADS (INCHES)

AVERAGE DAILY HEAD ON TOP OF LAYER 6	0.000	0.000	0.000	0.000	0.000	0.000
	0.000	0.000	0.000	0.000	0.000	0.000
STD. DEVIATION OF DAILY HEAD ON TOP OF LAYER 6	0.000	0.000	0.000	0.000	0.000	0.000
	0.000	0.000	0.000	0.000	0.000	0.000

ANNUAL TOTALS FOR YEAR 18

	INCHES	CU. FEET	PERCENT
	-----	-----	-----
PRECIPITATION	7.82	252640.766	100.00
RUNOFF	0.045	1465.350	0.58
EVAPOTRANSPIRATION	7.749	250338.141	99.09
DRAINAGE COLLECTED FROM LAYER 5	0.0000	0.000	0.00
PERC./LEAKAGE THROUGH LAYER 7	0.000000	0.000	0.00
AVG. HEAD ON TOP OF LAYER 6	0.0000		

MONTHLY SUMMARIES FOR DAILY HEADS (INCHES)

AVERAGE DAILY HEAD ON	0.000	0.000	0.000	0.000	0.000	0.000
-----------------------	-------	-------	-------	-------	-------	-------

TOP OF LAYER 6	0.000	0.000	0.000	0.000	0.000	0.000
STD. DEVIATION OF DAILY	0.000	0.000	0.000	0.000	0.000	0.000
HEAD ON TOP OF LAYER 6	0.000	0.000	0.000	0.000	0.000	0.000

ANNUAL TOTALS FOR YEAR 19

	INCHES	CU. FEET	PERCENT
PRECIPITATION	10.92	352792.469	100.00
RUNOFF	0.000	0.000	0.00
EVAPOTRANSPIRATION	11.090	358299.187	101.56
DRAINAGE COLLECTED FROM LAYER 5	0.0000	0.000	0.00
PERC./LEAKAGE THROUGH LAYER 7	0.000000	0.000	0.00
AVG. HEAD ON TOP OF LAYER 6	0.0000		
PERC./LEAKAGE THROUGH LAYER 8	0.000000	0.000	0.00
CHANGE IN WATER STORAGE	-0.170	-5506.426	-1.56
SOIL WATER AT START OF YEAR	312.121	10083696.000	
SOIL WATER AT END OF YEAR	311.951	10078189.000	
SNOW WATER AT START OF YEAR	0.000	0.000	0.00
SNOW WATER AT END OF YEAR	0.000	0.000	0.00
ANNUAL WATER BUDGET BALANCE	0.0000	-0.308	0.00

MONTHLY TOTALS (IN INCHES) FOR YEAR 20

JAN/JUL FEB/AUG MAR/SEP APR/OCT MAY/NOV JUN/DEC

PRECIPITATION	0.13	0.50	0.77	0.08	0.23	3.31
	0.96	0.33	2.27	1.41	0.09	0.23
RUNOFF	0.000	0.000	0.000	0.000	0.000	0.001
	0.000	0.000	0.068	0.007	0.000	0.000
EVAPOTRANSPIRATION	0.123	0.380	0.933	0.107	0.094	2.973
	1.357	0.313	1.311	1.751	0.719	0.191
LATERAL DRAINAGE COLLECTED FROM LAYER 5	0.0000	0.0000	0.0000	0.0000	0.0000	0.0000
	0.0000	0.0000	0.0000	0.0000	0.0000	0.0000
PERCOLATION/LEAKAGE THROUGH LAYER 7	0.0000	0.0000	0.0000	0.0000	0.0000	0.0000
	0.0000	0.0000	0.0000	0.0000	0.0000	0.0000
PERCOLATION/LEAKAGE THROUGH LAYER 8	0.0000	0.0000	0.0000	0.0000	0.0000	0.0000
	0.0000	0.0000	0.0000	0.0000	0.0000	0.0000

MONTHLY SUMMARIES FOR DAILY HEADS (INCHES)

AVERAGE DAILY HEAD ON TOP OF LAYER 6	0.000	0.000	0.000	0.000	0.000	0.000
	0.000	0.000	0.000	0.000	0.000	0.000
STD. DEVIATION OF DAILY HEAD ON TOP OF LAYER 6	0.000	0.000	0.000	0.000	0.000	0.000
	0.000	0.000	0.000	0.000	0.000	0.000

ANNUAL TOTALS FOR YEAR 20

	INCHES	CU. FEET	PERCENT
	-----	-----	-----
PRECIPITATION	10.31	333085.219	100.00
RUNOFF	0.075	2427.745	0.73
EVAPOTRANSPIRATION	10.251	331171.406	99.43
DRAINAGE COLLECTED FROM LAYER 5	0.0000	0.000	0.00
PERC./LEAKAGE THROUGH LAYER 7	0.000000	0.000	0.00
AVG. HEAD ON TOP OF LAYER 6	0.0000		

MONTHLY SUMMARIES FOR DAILY HEADS (INCHES)

AVERAGE DAILY HEAD ON	0.000	0.000	0.000	0.000	0.000	0.000
-----------------------	-------	-------	-------	-------	-------	-------

TOP OF LAYER 6	0.000	0.000	0.000	0.000	0.000	0.000
STD. DEVIATION OF DAILY	0.000	0.000	0.000	0.000	0.000	0.000
HEAD ON TOP OF LAYER 6	0.000	0.000	0.000	0.000	0.000	0.000

ANNUAL TOTALS FOR YEAR 21

	INCHES	CU. FEET	PERCENT
PRECIPITATION	12.85	415144.906	100.00
RUNOFF	0.017	546.517	0.13
EVAPOTRANSPIRATION	12.607	407284.125	98.11
DRAINAGE COLLECTED FROM LAYER 5	0.0000	0.000	0.00
PERC./LEAKAGE THROUGH LAYER 7	0.000000	0.000	0.00
AVG. HEAD ON TOP OF LAYER 6	0.0000		
PERC./LEAKAGE THROUGH LAYER 8	0.000000	0.000	0.00
CHANGE IN WATER STORAGE	0.226	7314.625	1.76
SOIL WATER AT START OF YEAR	311.935	10077675.000	
SOIL WATER AT END OF YEAR	312.161	10084989.000	
SNOW WATER AT START OF YEAR	0.000	0.000	0.00
SNOW WATER AT END OF YEAR	0.000	0.000	0.00
ANNUAL WATER BUDGET BALANCE	0.0000	-0.373	0.00

MONTHLY TOTALS (IN INCHES) FOR YEAR 22

JAN/JUL FEB/AUG MAR/SEP APR/OCT MAY/NOV JUN/DEC

PRECIPITATION	0.14	0.00	0.36	0.90	0.16	0.99
	1.31	1.01	1.72	0.77	0.02	0.30
RUNOFF	0.000	0.000	0.000	0.000	0.000	0.000
	0.000	0.000	0.000	0.000	0.000	0.000
EVAPOTRANSPIRATION	0.387	0.025	0.276	0.312	0.833	0.839
	1.461	1.010	1.027	1.452	0.028	0.050
LATERAL DRAINAGE COLLECTED FROM LAYER 5	0.0000	0.0000	0.0000	0.0000	0.0000	0.0000
	0.0000	0.0000	0.0000	0.0000	0.0000	0.0000
PERCOLATION/LEAKAGE THROUGH LAYER 7	0.0000	0.0000	0.0000	0.0000	0.0000	0.0000
	0.0000	0.0000	0.0000	0.0000	0.0000	0.0000
PERCOLATION/LEAKAGE THROUGH LAYER 8	0.0000	0.0000	0.0000	0.0000	0.0000	0.0000
	0.0000	0.0000	0.0000	0.0000	0.0000	0.0000

MONTHLY SUMMARIES FOR DAILY HEADS (INCHES)

AVERAGE DAILY HEAD ON TOP OF LAYER 6	0.000	0.000	0.000	0.000	0.000	0.000
	0.000	0.000	0.000	0.000	0.000	0.000
STD. DEVIATION OF DAILY HEAD ON TOP OF LAYER 6	0.000	0.000	0.000	0.000	0.000	0.000
	0.000	0.000	0.000	0.000	0.000	0.000

ANNUAL TOTALS FOR YEAR 22

	INCHES	CU. FEET	PERCENT
	-----	-----	-----
PRECIPITATION	7.68	248117.781	100.00
RUNOFF	0.000	0.000	0.00
EVAPOTRANSPIRATION	7.701	248801.344	100.28
DRAINAGE COLLECTED FROM LAYER 5	0.0000	0.000	0.00
PERC./LEAKAGE THROUGH LAYER 7	0.000000	0.000	0.00
AVG. HEAD ON TOP OF LAYER 6	0.0000		

PERC./LEAKAGE THROUGH LAYER	8	0.000000	0.000	0.00
CHANGE IN WATER STORAGE		-0.021	-682.728	-0.28
SOIL WATER AT START OF YEAR		312.161	10084989.000	
SOIL WATER AT END OF YEAR		311.929	10077490.000	
SNOW WATER AT START OF YEAR		0.000	0.000	0.00
SNOW WATER AT END OF YEAR		0.211	6816.266	2.75
ANNUAL WATER BUDGET BALANCE		0.0000	-0.846	0.00

MONTHLY TOTALS (IN INCHES) FOR YEAR 23

	JAN/JUL	FEB/AUG	MAR/SEP	APR/OCT	MAY/NOV	JUN/DEC
	-----	-----	-----	-----	-----	-----
PRECIPITATION	0.45	0.00	0.13	5.59	0.00	0.59
	1.79	2.69	2.45	0.91	0.63	0.25
RUNOFF	0.000	0.000	0.000	1.538	0.000	0.000
	0.007	0.025	0.000	0.000	0.000	0.000
EVAPOTRANSPIRATION	0.480	0.220	0.085	1.725	1.471	0.957
	2.280	2.665	1.899	1.459	0.631	0.251
LATERAL DRAINAGE COLLECTED FROM LAYER 5	0.0000	0.0000	0.0000	0.0000	0.0000	0.0000
	0.0000	0.0000	0.0000	0.0000	0.0000	0.0000
PERCOLATION/LEAKAGE THROUGH LAYER 7	0.0000	0.0000	0.0000	0.0000	0.0000	0.0000
	0.0000	0.0000	0.0000	0.0000	0.0000	0.0000
PERCOLATION/LEAKAGE THROUGH LAYER 8	0.0000	0.0000	0.0000	0.0000	0.0000	0.0000
	0.0000	0.0000	0.0000	0.0000	0.0000	0.0000

AVERAGE DAILY HEAD ON	0.000	0.000	0.000	0.000	0.000	0.000
-----------------------	-------	-------	-------	-------	-------	-------

TOP OF LAYER 6	0.000	0.000	0.000	0.000	0.000	0.000
STD. DEVIATION OF DAILY	0.000	0.000	0.000	0.000	0.000	0.000
HEAD ON TOP OF LAYER 6	0.000	0.000	0.000	0.000	0.000	0.000

ANNUAL TOTALS FOR YEAR 23

	INCHES	CU. FEET	PERCENT
PRECIPITATION	15.48	500112.437	100.00
RUNOFF	1.570	50711.020	10.14
EVAPOTRANSPIRATION	14.123	456258.937	91.23
DRAINAGE COLLECTED FROM LAYER 5	0.0000	0.000	0.00
PERC./LEAKAGE THROUGH LAYER 7	0.000000	0.000	0.00
AVG. HEAD ON TOP OF LAYER 6	0.0000		
PERC./LEAKAGE THROUGH LAYER 8	0.000000	0.000	0.00
CHANGE IN WATER STORAGE	-0.212	-6857.675	-1.37
SOIL WATER AT START OF YEAR	311.929	10077490.000	
SOIL WATER AT END OF YEAR	311.928	10077449.000	
SNOW WATER AT START OF YEAR	0.211	6816.266	1.36
SNOW WATER AT END OF YEAR	0.000	0.000	0.00
ANNUAL WATER BUDGET BALANCE	0.0000	0.142	0.00

MONTHLY TOTALS (IN INCHES) FOR YEAR 24

JAN/JUL FEB/AUG MAR/SEP APR/OCT MAY/NOV JUN/DEC

	-----	-----	-----	-----	-----	-----
PRECIPITATION	0.04	0.41	0.37	0.30	2.35	0.00
	1.21	4.98	1.62	0.82	0.00	0.32
RUNOFF	0.000	0.000	0.000	0.000	0.000	0.000
	0.000	0.027	0.022	0.000	0.000	0.000
EVAPOTRANSPIRATION	0.040	0.410	0.332	0.162	2.388	0.140
	1.210	4.073	2.426	0.390	0.318	0.367
LATERAL DRAINAGE COLLECTED FROM LAYER 5	0.0000	0.0000	0.0000	0.0000	0.0000	0.0000
	0.0000	0.0000	0.0000	0.0000	0.0000	0.0000
PERCOLATION/LEAKAGE THROUGH LAYER 7	0.0000	0.0000	0.0000	0.0000	0.0000	0.0000
	0.0000	0.0000	0.0000	0.0000	0.0000	0.0000
PERCOLATION/LEAKAGE THROUGH LAYER 8	0.0000	0.0000	0.0000	0.0000	0.0000	0.0000
	0.0000	0.0000	0.0000	0.0000	0.0000	0.0000

MONTHLY SUMMARIES FOR DAILY HEADS (INCHES)

AVERAGE DAILY HEAD ON TOP OF LAYER 6	0.000	0.000	0.000	0.000	0.000	0.000
	0.000	0.000	0.000	0.000	0.000	0.000
STD. DEVIATION OF DAILY HEAD ON TOP OF LAYER 6	0.000	0.000	0.000	0.000	0.000	0.000
	0.000	0.000	0.000	0.000	0.000	0.000

ANNUAL TOTALS FOR YEAR 24

	INCHES	CU. FEET	PERCENT
	-----	-----	-----
PRECIPITATION	12.42	401253.000	100.00
RUNOFF	0.049	1587.087	0.40
EVAPOTRANSPIRATION	12.254	395902.375	98.67
DRAINAGE COLLECTED FROM LAYER 5	0.0000	0.000	0.00
PERC./LEAKAGE THROUGH LAYER 7	0.000000	0.000	0.00
AVG. HEAD ON TOP OF LAYER 6	0.0000		

MONTHLY SUMMARIES FOR DAILY HEADS (INCHES)

AVERAGE DAILY HEAD ON	0.000	0.000	0.000	0.000	0.000	0.000
-----------------------	-------	-------	-------	-------	-------	-------

TOP OF LAYER 6	0.000	0.000	0.000	0.000	0.000	0.000
STD. DEVIATION OF DAILY	0.000	0.000	0.000	0.000	0.000	0.000
HEAD ON TOP OF LAYER 6	0.000	0.000	0.000	0.000	0.000	0.000

ANNUAL TOTALS FOR YEAR 25

	INCHES	CU. FEET	PERCENT
PRECIPITATION	8.43	272347.969	100.00
RUNOFF	0.057	1836.049	0.67
EVAPOTRANSPIRATION	8.478	273907.969	100.57
DRAINAGE COLLECTED FROM LAYER 5	0.0000	0.000	0.00
PERC./LEAKAGE THROUGH LAYER 7	0.000000	0.000	0.00
AVG. HEAD ON TOP OF LAYER 6	0.0000		
PERC./LEAKAGE THROUGH LAYER 8	0.000000	0.000	0.00
CHANGE IN WATER STORAGE	-0.105	-3395.547	-1.25
SOIL WATER AT START OF YEAR	312.044	10081212.000	
SOIL WATER AT END OF YEAR	311.939	10077817.000	
SNOW WATER AT START OF YEAR	0.000	0.000	0.00
SNOW WATER AT END OF YEAR	0.000	0.000	0.00
ANNUAL WATER BUDGET BALANCE	0.0000	-0.492	0.00

MONTHLY TOTALS (IN INCHES) FOR YEAR 26

JAN/JUL FEB/AUG MAR/SEP APR/OCT MAY/NOV JUN/DEC

	-----	-----	-----	-----	-----	-----
PRECIPITATION	0.14	0.86	0.35	1.56	0.66	0.03
	0.70	1.83	1.56	3.24	0.65	0.36
RUNOFF	0.000	0.000	0.000	0.000	0.000	0.000
	0.000	0.000	0.004	0.074	0.000	0.000
EVAPOTRANSPIRATION	0.032	0.686	0.430	1.763	0.358	0.342
	0.382	1.897	1.729	0.854	1.447	0.642
LATERAL DRAINAGE COLLECTED FROM LAYER 5	0.0000	0.0000	0.0000	0.0000	0.0000	0.0000
	0.0000	0.0000	0.0000	0.0000	0.0000	0.0000
PERCOLATION/LEAKAGE THROUGH LAYER 7	0.0000	0.0000	0.0000	0.0000	0.0000	0.0000
	0.0000	0.0000	0.0000	0.0000	0.0000	0.0000
PERCOLATION/LEAKAGE THROUGH LAYER 8	0.0000	0.0000	0.0000	0.0000	0.0000	0.0000
	0.0000	0.0000	0.0000	0.0000	0.0000	0.0000

MONTHLY SUMMARIES FOR DAILY HEADS (INCHES)

AVERAGE DAILY HEAD ON TOP OF LAYER 6	0.000	0.000	0.000	0.000	0.000	0.000
	0.000	0.000	0.000	0.000	0.000	0.000
STD. DEVIATION OF DAILY HEAD ON TOP OF LAYER 6	0.000	0.000	0.000	0.000	0.000	0.000
	0.000	0.000	0.000	0.000	0.000	0.000

ANNUAL TOTALS FOR YEAR 26

	INCHES	CU. FEET	PERCENT
	-----	-----	-----
PRECIPITATION	11.94	385745.562	100.00
RUNOFF	0.079	2542.806	0.66
EVAPOTRANSPIRATION	10.564	341290.625	88.48
DRAINAGE COLLECTED FROM LAYER 5	0.0000	0.000	0.00
PERC./LEAKAGE THROUGH LAYER 7	0.000000	0.000	0.00
AVG. HEAD ON TOP OF LAYER 6	0.0000		

MONTHLY SUMMARIES FOR DAILY HEADS (INCHES)

AVERAGE DAILY HEAD ON	0.000	0.000	0.000	0.000	0.000	0.000
-----------------------	-------	-------	-------	-------	-------	-------

TOP OF LAYER 6	0.000	0.000	0.000	0.000	0.000	0.000
STD. DEVIATION OF DAILY	0.000	0.000	0.000	0.000	0.000	0.000
HEAD ON TOP OF LAYER 6	0.000	0.000	0.000	0.000	0.000	0.000

ANNUAL TOTALS FOR YEAR 27

	INCHES	CU. FEET	PERCENT
PRECIPITATION	10.65	344069.531	100.00
RUNOFF	0.000	0.000	0.00
EVAPOTRANSPIRATION	11.702	378065.344	109.88
DRAINAGE COLLECTED FROM LAYER 5	0.0000	0.000	0.00
PERC./LEAKAGE THROUGH LAYER 7	0.000000	0.000	0.00
AVG. HEAD ON TOP OF LAYER 6	0.0000		
PERC./LEAKAGE THROUGH LAYER 8	0.000000	0.000	0.00
CHANGE IN WATER STORAGE	-1.052	-33996.883	-9.88
SOIL WATER AT START OF YEAR	313.236	10119729.000	
SOIL WATER AT END OF YEAR	312.184	10085732.000	
SNOW WATER AT START OF YEAR	0.000	0.000	0.00
SNOW WATER AT END OF YEAR	0.000	0.000	0.00
ANNUAL WATER BUDGET BALANCE	0.0000	1.048	0.00

MONTHLY TOTALS (IN INCHES) FOR YEAR 28

JAN/JUL FEB/AUG MAR/SEP APR/OCT MAY/NOV JUN/DEC

	-----	-----	-----	-----	-----	-----
PRECIPITATION	0.32	0.90	0.47	0.61	0.28	0.45
	0.70	2.76	1.60	2.30	0.01	0.34
RUNOFF	0.000	0.000	0.000	0.000	0.000	0.000
	0.000	0.000	0.009	0.003	0.000	0.000
EVAPOTRANSPIRATION	0.467	0.856	0.615	0.612	0.259	0.476
	0.627	2.380	2.044	0.569	1.551	0.487
LATERAL DRAINAGE COLLECTED FROM LAYER 5	0.0000	0.0000	0.0000	0.0000	0.0000	0.0000
	0.0000	0.0000	0.0000	0.0000	0.0000	0.0000
PERCOLATION/LEAKAGE THROUGH LAYER 7	0.0000	0.0000	0.0000	0.0000	0.0000	0.0000
	0.0000	0.0000	0.0000	0.0000	0.0000	0.0000
PERCOLATION/LEAKAGE THROUGH LAYER 8	0.0000	0.0000	0.0000	0.0000	0.0000	0.0000
	0.0000	0.0000	0.0000	0.0000	0.0000	0.0000

MONTHLY SUMMARIES FOR DAILY HEADS (INCHES)

AVERAGE DAILY HEAD ON TOP OF LAYER 6	0.000	0.000	0.000	0.000	0.000	0.000
	0.000	0.000	0.000	0.000	0.000	0.000
STD. DEVIATION OF DAILY HEAD ON TOP OF LAYER 6	0.000	0.000	0.000	0.000	0.000	0.000
	0.000	0.000	0.000	0.000	0.000	0.000

ANNUAL TOTALS FOR YEAR 28

	INCHES	CU. FEET	PERCENT
	-----	-----	-----
PRECIPITATION	10.74	346977.156	100.00
RUNOFF	0.013	412.834	0.12
EVAPOTRANSPIRATION	10.943	353530.656	101.89
DRAINAGE COLLECTED FROM LAYER 5	0.0000	0.000	0.00
PERC./LEAKAGE THROUGH LAYER 7	0.000000	0.000	0.00
AVG. HEAD ON TOP OF LAYER 6	0.0000		

PERC./LEAKAGE THROUGH LAYER 8	0.000000	0.000	0.00
CHANGE IN WATER STORAGE	-0.216	-6965.605	-2.01
SOIL WATER AT START OF YEAR	312.184	10085732.000	
SOIL WATER AT END OF YEAR	311.969	10078766.000	
SNOW WATER AT START OF YEAR	0.000	0.000	0.00
SNOW WATER AT END OF YEAR	0.000	0.000	0.00
ANNUAL WATER BUDGET BALANCE	0.0000	-0.745	0.00

AVERAGE MONTHLY VALUES IN INCHES FOR YEARS 1 THROUGH 28

	JAN/JUL	FEB/AUG	MAR/SEP	APR/OCT	MAY/NOV	JUN/DEC
	-----	-----	-----	-----	-----	-----
PRECIPITATION						

TOTALS	0.30 1.22	0.41 2.37	0.46 1.31	0.98 1.79	0.65 0.62	1.08 0.45
STD. DEVIATIONS	0.35 0.61	0.35 1.14	0.41 0.83	1.13 1.61	0.56 0.62	1.00 0.30
RUNOFF						

TOTALS	0.000 0.003	0.001 0.009	0.000 0.007	0.064 0.054	0.000 0.000	0.003 0.000
STD. DEVIATIONS	0.000 0.014	0.004 0.030	0.000 0.015	0.291 0.128	0.000 0.001	0.010 0.000
EVAPOTRANSPIRATION						

TOTALS	0.345 1.179	0.361 2.212	0.427 1.324	0.754 1.258	0.781 0.939	1.329 0.622
STD. DEVIATIONS	0.265 0.623	0.311 0.962	0.394 0.820	0.658 0.772	0.531 0.559	1.086 0.387

LATERAL DRAINAGE COLLECTED FROM LAYER 5

TOTALS	0.0001	0.0000	0.0001	0.0000	0.0000	0.0000
	0.0000	0.0000	0.0000	0.0000	0.0000	0.0000

STD. DEVIATIONS	0.0002	0.0001	0.0001	0.0001	0.0001	0.0001
	0.0001	0.0001	0.0001	0.0001	0.0001	0.0001

PERCOLATION/LEAKAGE THROUGH LAYER 7

TOTALS	0.0000	0.0000	0.0000	0.0000	0.0000	0.0000
	0.0000	0.0000	0.0000	0.0000	0.0000	0.0000

STD. DEVIATIONS	0.0000	0.0000	0.0000	0.0000	0.0000	0.0000
	0.0000	0.0000	0.0000	0.0000	0.0000	0.0000

PERCOLATION/LEAKAGE THROUGH LAYER 8

TOTALS	0.0000	0.0000	0.0000	0.0000	0.0000	0.0000
	0.0000	0.0000	0.0000	0.0000	0.0000	0.0000

STD. DEVIATIONS	0.0000	0.0000	0.0000	0.0000	0.0000	0.0000
	0.0000	0.0000	0.0000	0.0000	0.0000	0.0000

AVERAGES OF MONTHLY AVERAGED DAILY HEADS (INCHES)

DAILY AVERAGE HEAD ON TOP OF LAYER 6

AVERAGES	0.0043	0.0041	0.0039	0.0037	0.0035	0.0034
	0.0032	0.0030	0.0029	0.0027	0.0026	0.0025

STD. DEVIATIONS	0.0118	0.0114	0.0109	0.0103	0.0098	0.0093
	0.0088	0.0084	0.0080	0.0076	0.0072	0.0068

AVERAGE ANNUAL TOTALS & (STD. DEVIATIONS) FOR YEARS 1 THROUGH 28

	INCHES		CU. FEET	PERCENT
	-----		-----	-----
PRECIPITATION	11.65	(2.760)	376295.8	100.00
RUNOFF	0.141	(0.3121)	4549.51	1.209
EVAPOTRANSPIRATION	11.530	(2.5757)	372493.19	98.989
LATERAL DRAINAGE COLLECTED FROM LAYER 5	0.00051	(0.00142)	16.560	0.00440
PERCOLATION/LEAKAGE THROUGH LAYER 7	0.00000	(0.00000)	0.055	0.00001
AVERAGE HEAD ON TOP OF LAYER 6	0.003	(0.009)		
PERCOLATION/LEAKAGE THROUGH LAYER 8	0.00000	(0.00000)	0.052	0.00001
CHANGE IN WATER STORAGE	-0.024	(0.5978)	-763.57	-0.203

PEAK DAILY VALUES FOR YEARS 1 THROUGH 28		
	(INCHES)	(CU. FT.)
PRECIPITATION	4.09	132135.625
RUNOFF	1.538	49696.9805
DRAINAGE COLLECTED FROM LAYER 5	0.00002	0.78256
PERCOLATION/LEAKAGE THROUGH LAYER 7	0.000000	0.00095
AVERAGE HEAD ON TOP OF LAYER 6	0.057	
MAXIMUM HEAD ON TOP OF LAYER 6	0.113	
LOCATION OF MAXIMUM HEAD IN LAYER 5 (DISTANCE FROM DRAIN)	2.1 FEET	
PERCOLATION/LEAKAGE THROUGH LAYER 8	0.000000	0.00053
SNOW WATER	0.69	22384.7168
MAXIMUM VEG. SOIL WATER (VOL/VOL)		0.2149
MINIMUM VEG. SOIL WATER (VOL/VOL)		0.0850

*** Maximum heads are computed using McEnroe's equations. ***

Reference: Maximum Saturated Depth over Landfill Liner
by Bruce M. McEnroe, University of Kansas
ASCE Journal of Environmental Engineering
Vol. 119, No. 2, March 1993, pp. 262-270.

FINAL WATER STORAGE AT END OF YEAR 28

LAYER	(INCHES)	(VOL/VOL)
1	0.5204	0.0867
2	2.9788	0.0993
3	1.6201	0.1350
4	300.6665	0.1448
5	5.3280	0.2220
6	0.0000	0.0000
7	0.1875	0.7500
8	0.6672	0.1112
SNOW WATER	0.000	


```

*****
*****
**
**
**
HYDROLOGIC EVALUATION OF LANDFILL PERFORMANCE
HELP MODEL VERSION 3.07 (1 NOVEMBER 1997)
DEVELOPED BY ENVIRONMENTAL LABORATORY
USAE WATERWAYS EXPERIMENT STATION
FOR USEPA RISK REDUCTION ENGINEERING LABORATORY
**
**
**
*****
*****

```

```

PRECIPITATION DATA FILE:  c:\RAIN30.D4
TEMPERATURE DATA FILE:   C:\TEMP30.D7
SOLAR RADIATION DATA FILE: C:\SOLAR30.D13
EVAPOTRANSPIRATION DATA:  C:\EVAP30.D11
SOIL AND DESIGN DATA FILE: C:\SIM10B25.D10
OUTPUT DATA FILE:        C:\sim10b25.OUT

```

TIME: 17:28 DATE: 4/ 8/2015

```

*****
TITLE:  Sandoval County Landfill - 28 Years Closed - Poor Veg - 25%
Simulation 10B - Alternate Final Cover; 25% Sloped Area: 114 Acres
*****

```

NOTE: INITIAL MOISTURE CONTENT OF THE LAYERS AND SNOW WATER
WERE SPECIFIED BY THE USER.

LAYER 1

```

TYPE 1 - VERTICAL PERCOLATION LAYER
MATERIAL TEXTURE NUMBER 6
THICKNESS           = 6.00 INCHES
POROSITY             = 0.4530 VOL/VOL
FIELD CAPACITY       = 0.1900 VOL/VOL
WILTING POINT        = 0.0850 VOL/VOL
INITIAL SOIL WATER CONTENT = 0.0935 VOL/VOL
EFFECTIVE SAT. HYD. COND. = 0.720000011000E-03 CM/SEC
NOTE: SATURATED HYDRAULIC CONDUCTIVITY IS MULTIPLIED BY 1.60
FOR ROOT CHANNELS IN TOP HALF OF EVAPORATIVE ZONE.

```

LAYER 2

TYPE 1 - VERTICAL PERCOLATION LAYER

MATERIAL TEXTURE NUMBER 6

THICKNESS	=	30.00	INCHES
POROSITY	=	0.4530	VOL/VOL
FIELD CAPACITY	=	0.1900	VOL/VOL
WILTING POINT	=	0.0850	VOL/VOL
INITIAL SOIL WATER CONTENT	=	0.1381	VOL/VOL
EFFECTIVE SAT. HYD. COND.	=	0.720000011000E-03	CM/SEC

LAYER 3

TYPE 1 - VERTICAL PERCOLATION LAYER

MATERIAL TEXTURE NUMBER 6

THICKNESS	=	12.00	INCHES
POROSITY	=	0.4530	VOL/VOL
FIELD CAPACITY	=	0.1900	VOL/VOL
WILTING POINT	=	0.0850	VOL/VOL
INITIAL SOIL WATER CONTENT	=	0.1110	VOL/VOL
EFFECTIVE SAT. HYD. COND.	=	0.720000011000E-03	CM/SEC

LAYER 4

TYPE 1 - VERTICAL PERCOLATION LAYER

MATERIAL TEXTURE NUMBER 18

THICKNESS	=	2076.00	INCHES
POROSITY	=	0.6710	VOL/VOL
FIELD CAPACITY	=	0.2920	VOL/VOL
WILTING POINT	=	0.0770	VOL/VOL
INITIAL SOIL WATER CONTENT	=	0.1447	VOL/VOL
EFFECTIVE SAT. HYD. COND.	=	0.100000005000E-02	CM/SEC

LAYER 5

TYPE 2 - LATERAL DRAINAGE LAYER

MATERIAL TEXTURE NUMBER 0

THICKNESS	=	24.00	INCHES
POROSITY	=	0.4730	VOL/VOL
FIELD CAPACITY	=	0.2220	VOL/VOL
WILTING POINT	=	0.1040	VOL/VOL
INITIAL SOIL WATER CONTENT	=	0.2226	VOL/VOL
EFFECTIVE SAT. HYD. COND.	=	0.300000014000E-03	CM/SEC
SLOPE	=	5.00	PERCENT
DRAINAGE LENGTH	=	200.0	FEET

LAYER 6

TYPE 4 - FLEXIBLE MEMBRANE LINER

MATERIAL TEXTURE NUMBER 35

THICKNESS	=	0.06	INCHES
POROSITY	=	0.0000	VOL/VOL
FIELD CAPACITY	=	0.0000	VOL/VOL
WILTING POINT	=	0.0000	VOL/VOL
INITIAL SOIL WATER CONTENT	=	0.0000	VOL/VOL
EFFECTIVE SAT. HYD. COND.	=	0.199999996000E-12	CM/SEC
FML PINHOLE DENSITY	=	1.00	HOLES/ACRE
FML INSTALLATION DEFECTS	=	4.00	HOLES/ACRE
FML PLACEMENT QUALITY	=	3 - GOOD	

LAYER 7

TYPE 3 - BARRIER SOIL LINER

MATERIAL TEXTURE NUMBER 0

THICKNESS	=	0.25	INCHES
POROSITY	=	0.7500	VOL/VOL
FIELD CAPACITY	=	0.7470	VOL/VOL
WILTING POINT	=	0.4000	VOL/VOL
INITIAL SOIL WATER CONTENT	=	0.7500	VOL/VOL
EFFECTIVE SAT. HYD. COND.	=	0.499999997000E-08	CM/SEC

LAYER 8

TYPE 1 - VERTICAL PERCOLATION LAYER

MATERIAL TEXTURE NUMBER 0

THICKNESS	=	6.00	INCHES
POROSITY	=	0.4530	VOL/VOL
FIELD CAPACITY	=	0.1900	VOL/VOL
WILTING POINT	=	0.0850	VOL/VOL
INITIAL SOIL WATER CONTENT	=	0.1112	VOL/VOL
EFFECTIVE SAT. HYD. COND.	=	0.420000015000E-05	CM/SEC

GENERAL DESIGN AND EVAPORATIVE ZONE DATA

NOTE: SCS RUNOFF CURVE NUMBER WAS COMPUTED FROM A USER-SPECIFIED CURVE NUMBER OF 95.0, A SURFACE SLOPE OF 25.% AND A SLOPE LENGTH OF 650. FEET.

SCS RUNOFF CURVE NUMBER	=	95.20	
FRACTION OF AREA ALLOWING RUNOFF	=	100.0	PERCENT
AREA PROJECTED ON HORIZONTAL PLANE	=	114.000	ACRES
EVAPORATIVE ZONE DEPTH	=	28.0	INCHES
INITIAL WATER IN EVAPORATIVE ZONE	=	3.599	INCHES
UPPER LIMIT OF EVAPORATIVE STORAGE	=	12.684	INCHES
LOWER LIMIT OF EVAPORATIVE STORAGE	=	2.380	INCHES
INITIAL SNOW WATER	=	0.000	INCHES
INITIAL WATER IN LAYER MATERIALS	=	312.630	INCHES
TOTAL INITIAL WATER	=	312.630	INCHES
TOTAL SUBSURFACE INFLOW	=	0.00	INCHES/YEAR

EVAPOTRANSPIRATION AND WEATHER DATA

NOTE: EVAPOTRANSPIRATION DATA WAS OBTAINED FROM
ALBUQUERQUE NEW MEXICO

STATION LATITUDE	=	35.30	DEGREES
MAXIMUM LEAF AREA INDEX	=	0.80	
START OF GROWING SEASON (JULIAN DATE)	=	98	
END OF GROWING SEASON (JULIAN DATE)	=	299	
EVAPORATIVE ZONE DEPTH	=	28.0	INCHES
AVERAGE ANNUAL WIND SPEED	=	9.00	MPH
AVERAGE 1ST QUARTER RELATIVE HUMIDITY	=	48.00	%
AVERAGE 2ND QUARTER RELATIVE HUMIDITY	=	30.00	%
AVERAGE 3RD QUARTER RELATIVE HUMIDITY	=	45.00	%
AVERAGE 4TH QUARTER RELATIVE HUMIDITY	=	50.00	%

NOTE: PRECIPITATION DATA WAS SYNTHETICALLY GENERATED USING
COEFFICIENTS FOR ALBUQUERQUE NEW MEXICO

NORMAL MEAN MONTHLY PRECIPITATION (INCHES)

JAN/JUL	FEB/AUG	MAR/SEP	APR/OCT	MAY/NOV	JUN/DEC
-----	-----	-----	-----	-----	-----
0.37	0.47	0.48	0.99	0.72	0.99
1.39	2.34	1.20	1.50	0.55	0.47

NOTE: TEMPERATURE DATA WAS SYNTHETICALLY GENERATED USING
COEFFICIENTS FOR ALBUQUERQUE NEW MEXICO

NORMAL MEAN MONTHLY TEMPERATURE (DEGREES FAHRENHEIT)

JAN/JUL	FEB/AUG	MAR/SEP	APR/OCT	MAY/NOV	JUN/DEC
-----	-----	-----	-----	-----	-----
35.20	40.90	47.10	55.30	64.90	73.50
77.30	75.60	67.30	57.20	44.40	35.70

NOTE: SOLAR RADIATION DATA WAS SYNTHETICALLY GENERATED USING
COEFFICIENTS FOR ALBUQUERQUE NEW MEXICO
AND STATION LATITUDE = 35.30 DEGREES

MONTHLY TOTALS (IN INCHES) FOR YEAR 1

	JAN/JUL	FEB/AUG	MAR/SEP	APR/OCT	MAY/NOV	JUN/DEC
	-----	-----	-----	-----	-----	-----
PRECIPITATION	0.11	0.01	0.26	0.55	0.86	0.01
	0.99	3.66	1.17	1.12	1.67	0.57
RUNOFF	0.000	0.000	0.000	0.057	0.182	0.000
	0.003	0.315	0.040	0.064	0.005	0.011
EVAPOTRANSPIRATION	0.600	0.355	0.200	0.233	0.406	0.969
	0.984	2.846	1.631	1.034	1.498	0.745
LATERAL DRAINAGE COLLECTED	0.0007	0.0006	0.0007	0.0006	0.0006	0.0006

FROM LAYER 5	0.0005	0.0005	0.0005	0.0005	0.0004	0.0004
PERCOLATION/LEAKAGE THROUGH LAYER 7	0.0000	0.0000	0.0000	0.0000	0.0000	0.0000
PERCOLATION/LEAKAGE THROUGH LAYER 8	0.0000	0.0000	0.0000	0.0000	0.0000	0.0000

MONTHLY SUMMARIES FOR DAILY HEADS (INCHES)

AVERAGE DAILY HEAD ON TOP OF LAYER 6	0.055	0.053	0.051	0.048	0.046	0.043
	0.041	0.039	0.037	0.035	0.033	0.032
STD. DEVIATION OF DAILY HEAD ON TOP OF LAYER 6	0.005	0.001	0.001	0.001	0.001	0.001
	0.001	0.001	0.001	0.001	0.000	0.000

ANNUAL TOTALS FOR YEAR 1

	INCHES	CU. FEET	PERCENT
	-----	-----	-----
PRECIPITATION	10.98	4543744.000	100.00
RUNOFF	0.678	280478.125	6.17
EVAPOTRANSPIRATION	11.499	4758665.500	104.73
DRAINAGE COLLECTED FROM LAYER 5	0.0066	2738.642	0.06
PERC./LEAKAGE THROUGH LAYER 7	0.000009	3.626	0.00
AVG. HEAD ON TOP OF LAYER 6	0.0428		
PERC./LEAKAGE THROUGH LAYER 8	0.000000	0.000	0.00
CHANGE IN WATER STORAGE	-1.204	-498142.406	-10.96
SOIL WATER AT START OF YEAR	312.630	129372664.000	
SOIL WATER AT END OF YEAR	311.427	128874520.000	
SNOW WATER AT START OF YEAR	0.000	0.000	0.00
SNOW WATER AT END OF YEAR	0.000	0.000	0.00

ANNUAL WATER BUDGET BALANCE 0.0000 4.247 0.00

MONTHLY TOTALS (IN INCHES) FOR YEAR 2

	JAN/JUL	FEB/AUG	MAR/SEP	APR/OCT	MAY/NOV	JUN/DEC
PRECIPITATION	0.09 1.08	1.07 3.29	0.00 1.76	1.64 5.91	1.35 0.03	2.03 0.42
RUNOFF	0.000 0.041	0.067 0.388	0.000 0.124	0.356 1.614	0.000 0.000	0.487 0.000
EVAPOTRANSPIRATION	0.091 1.067	1.000 2.400	0.002 1.584	1.282 2.694	1.158 1.857	1.712 0.592
LATERAL DRAINAGE COLLECTED FROM LAYER 5	0.0004 0.0003	0.0003 0.0003	0.0004 0.0003	0.0003 0.0002	0.0003 0.0002	0.0003 0.0002
PERCOLATION/LEAKAGE THROUGH LAYER 7	0.0000 0.0000	0.0000 0.0000	0.0000 0.0000	0.0000 0.0000	0.0000 0.0000	0.0000 0.0000
PERCOLATION/LEAKAGE THROUGH LAYER 8	0.0000 0.0000	0.0000 0.0000	0.0000 0.0000	0.0000 0.0000	0.0000 0.0000	0.0000 0.0000

MONTHLY SUMMARIES FOR DAILY HEADS (INCHES)

AVERAGE DAILY HEAD ON TOP OF LAYER 6	0.030 0.022	0.029 0.021	0.027 0.020	0.026 0.019	0.025 0.018	0.023 0.017
STD. DEVIATION OF DAILY HEAD ON TOP OF LAYER 6	0.000 0.000	0.000 0.000	0.000 0.000	0.000 0.000	0.000 0.000	0.000 0.000

ANNUAL TOTALS FOR YEAR 2

	INCHES	CU. FEET	PERCENT
PRECIPITATION	18.67	7726020.000	100.00
RUNOFF	3.077	1273369.620	16.48
EVAPOTRANSPIRATION	15.439	6389126.000	82.70
DRAINAGE COLLECTED FROM LAYER 5	0.0036	1480.261	0.02
PERC./LEAKAGE THROUGH LAYER 7	0.000006	2.507	0.00
AVG. HEAD ON TOP OF LAYER 6	0.0231		
PERC./LEAKAGE THROUGH LAYER 8	0.000001	0.324	0.00
CHANGE IN WATER STORAGE	0.150	62032.586	0.80
SOIL WATER AT START OF YEAR	311.427	128874520.000	
SOIL WATER AT END OF YEAR	311.576	128936552.000	
SNOW WATER AT START OF YEAR	0.000	0.000	0.00
SNOW WATER AT END OF YEAR	0.000	0.000	0.00
ANNUAL WATER BUDGET BALANCE	0.0000	11.289	0.00

MONTHLY TOTALS (IN INCHES) FOR YEAR 3

	JAN/JUL	FEB/AUG	MAR/SEP	APR/OCT	MAY/NOV	JUN/DEC
PRECIPITATION	0.47 0.75	0.61 1.16	0.91 2.62	0.33 1.24	1.68 0.77	2.49 0.17
RUNOFF	0.002 0.000	0.001 0.012	0.003 0.362	0.000 0.011	0.146 0.044	0.597 0.000
EVAPOTRANSPIRATION	0.247 0.735	0.300 0.837	1.101 2.583	0.482 1.026	1.445 0.928	2.322 0.170
LATERAL DRAINAGE COLLECTED	0.0002	0.0002	0.0002	0.0002	0.0002	0.0002

FROM LAYER 5	0.0002	0.0001	0.0001	0.0001	0.0001	0.0001
PERCOLATION/LEAKAGE THROUGH LAYER 7	0.0000	0.0000	0.0000	0.0000	0.0000	0.0000
PERCOLATION/LEAKAGE THROUGH LAYER 8	0.0000	0.0000	0.0000	0.0000	0.0000	0.0000

MONTHLY SUMMARIES FOR DAILY HEADS (INCHES)

AVERAGE DAILY HEAD ON TOP OF LAYER 6	0.016	0.015	0.015	0.014	0.013	0.013
	0.012	0.011	0.011	0.010	0.010	0.009
STD. DEVIATION OF DAILY HEAD ON TOP OF LAYER 6	0.000	0.000	0.000	0.000	0.000	0.000
	0.000	0.000	0.000	0.000	0.000	0.000

ANNUAL TOTALS FOR YEAR 3

	INCHES	CU. FEET	PERCENT
	-----	-----	-----
PRECIPITATION	13.20	5462424.500	100.00
RUNOFF	1.179	487707.312	8.93
EVAPOTRANSPIRATION	12.175	5038323.500	92.24
DRAINAGE COLLECTED FROM LAYER 5	0.0019	797.797	0.01
PERC./LEAKAGE THROUGH LAYER 7	0.000005	1.871	0.00
AVG. HEAD ON TOP OF LAYER 6	0.0125		
PERC./LEAKAGE THROUGH LAYER 8	0.000002	0.951	0.00
CHANGE IN WATER STORAGE	-0.156	-64394.172	-1.18
SOIL WATER AT START OF YEAR	311.576	128936552.000	
SOIL WATER AT END OF YEAR	311.421	128872160.000	
SNOW WATER AT START OF YEAR	0.000	0.000	0.00
SNOW WATER AT END OF YEAR	0.000	0.000	0.00

ANNUAL WATER BUDGET BALANCE 0.0000 -11.274 0.00

MONTHLY TOTALS (IN INCHES) FOR YEAR 4

	JAN/JUL	FEB/AUG	MAR/SEP	APR/OCT	MAY/NOV	JUN/DEC
PRECIPITATION	0.00 3.02	0.07 2.72	0.17 1.04	0.19 3.38	0.38 0.35	1.20 0.36
RUNOFF	0.000 0.608	0.000 0.432	0.000 0.022	0.000 0.680	0.000 0.000	0.100 0.000
EVAPOTRANSPIRATION	0.001 2.386	0.070 1.997	0.170 1.319	0.190 1.806	0.380 1.056	1.100 0.435
LATERAL DRAINAGE COLLECTED FROM LAYER 5	0.0001 0.0001	0.0001 0.0001	0.0001 0.0001	0.0001 0.0001	0.0001 0.0001	0.0001 0.0001
PERCOLATION/LEAKAGE THROUGH LAYER 7	0.0000 0.0000	0.0000 0.0000	0.0000 0.0000	0.0000 0.0000	0.0000 0.0000	0.0000 0.0000
PERCOLATION/LEAKAGE THROUGH LAYER 8	0.0000 0.0000	0.0000 0.0000	0.0000 0.0000	0.0000 0.0000	0.0000 0.0000	0.0000 0.0000

MONTHLY SUMMARIES FOR DAILY HEADS (INCHES)

AVERAGE DAILY HEAD ON TOP OF LAYER 6	0.009 0.006	0.008 0.006	0.008 0.006	0.008 0.006	0.007 0.005	0.007 0.005
STD. DEVIATION OF DAILY HEAD ON TOP OF LAYER 6	0.000 0.000	0.000 0.000	0.000 0.000	0.000 0.000	0.000 0.000	0.000 0.000

ANNUAL TOTALS FOR YEAR 4

	INCHES	CU. FEET	PERCENT
PRECIPITATION	12.88	5330001.500	100.00
RUNOFF	1.843	762812.000	14.31
EVAPOTRANSPIRATION	10.912	4515450.000	84.72
DRAINAGE COLLECTED FROM LAYER 5	0.0010	430.594	0.01
PERC./LEAKAGE THROUGH LAYER 7	0.000004	1.513	0.00
AVG. HEAD ON TOP OF LAYER 6	0.0067		
PERC./LEAKAGE THROUGH LAYER 8	0.000003	1.316	0.00
CHANGE IN WATER STORAGE	0.124	51310.750	0.96
SOIL WATER AT START OF YEAR	311.421	128872160.000	
SOIL WATER AT END OF YEAR	311.545	128923472.000	
SNOW WATER AT START OF YEAR	0.000	0.000	0.00
SNOW WATER AT END OF YEAR	0.000	0.000	0.00
ANNUAL WATER BUDGET BALANCE	0.0000	-2.828	0.00

MONTHLY TOTALS (IN INCHES) FOR YEAR 5

	JAN/JUL	FEB/AUG	MAR/SEP	APR/OCT	MAY/NOV	JUN/DEC
PRECIPITATION	0.27 1.40	0.68 1.86	0.78 1.82	1.73 3.13	0.97 0.00	0.20 1.03
RUNOFF	0.000 0.000	0.013 0.135	0.020 0.332	0.332 0.577	0.132 0.000	0.000 0.000
EVAPOTRANSPIRATION	0.390	0.316	1.111	1.372	0.871	0.199

	1.220	1.905	0.721	2.555	0.759	0.974
LATERAL DRAINAGE COLLECTED	0.0001	0.0001	0.0001	0.0001	0.0001	0.0000
FROM LAYER 5	0.0000	0.0000	0.0000	0.0000	0.0000	0.0000
PERCOLATION/LEAKAGE THROUGH	0.0000	0.0000	0.0000	0.0000	0.0000	0.0000
LAYER 7	0.0000	0.0000	0.0000	0.0000	0.0000	0.0000
PERCOLATION/LEAKAGE THROUGH	0.0000	0.0000	0.0000	0.0000	0.0000	0.0000
LAYER 8	0.0000	0.0000	0.0000	0.0000	0.0000	0.0000

MONTHLY SUMMARIES FOR DAILY HEADS (INCHES)

AVERAGE DAILY HEAD ON	0.005	0.004	0.004	0.004	0.004	0.004
TOP OF LAYER 6	0.003	0.003	0.003	0.003	0.003	0.003
STD. DEVIATION OF DAILY	0.000	0.000	0.000	0.000	0.000	0.000
HEAD ON TOP OF LAYER 6	0.000	0.000	0.000	0.000	0.000	0.000

ANNUAL TOTALS FOR YEAR 5

	INCHES	CU. FEET	PERCENT
	-----	-----	-----
PRECIPITATION	13.87	5739684.500	100.00
RUNOFF	1.540	637258.812	11.10
EVAPOTRANSPIRATION	12.394	5128694.000	89.35
DRAINAGE COLLECTED FROM LAYER 5	0.0006	230.867	0.00
PERC./LEAKAGE THROUGH LAYER 7	0.000003	1.302	0.00
AVG. HEAD ON TOP OF LAYER 6	0.0036		
PERC./LEAKAGE THROUGH LAYER 8	0.000004	1.519	0.00
CHANGE IN WATER STORAGE	-0.064	-26507.818	-0.46
SOIL WATER AT START OF YEAR	311.545	128923472.000	
SOIL WATER AT END OF YEAR	311.481	128896960.000	
SNOW WATER AT START OF YEAR	0.000	0.000	0.00

SNOW WATER AT END OF YEAR	0.000	0.000	0.00
ANNUAL WATER BUDGET BALANCE	0.0000	7.067	0.00

MONTHLY TOTALS (IN INCHES) FOR YEAR 6

	JAN/JUL	FEB/AUG	MAR/SEP	APR/OCT	MAY/NOV	JUN/DEC
PRECIPITATION	0.03 0.37	0.62 1.10	0.94 0.47	0.00 1.53	1.03 1.16	0.44 0.61
RUNOFF	0.000 0.000	0.014 0.001	0.005 0.000	0.000 0.643	0.030 0.187	0.003 0.000
EVAPOTRANSPIRATION	0.088 0.301	0.587 1.159	0.948 0.430	0.007 0.933	1.004 0.866	0.437 0.698
LATERAL DRAINAGE COLLECTED FROM LAYER 5	0.0000 0.0000	0.0000 0.0000	0.0000 0.0000	0.0000 0.0000	0.0000 0.0000	0.0000 0.0000
PERCOLATION/LEAKAGE THROUGH LAYER 7	0.0000 0.0000	0.0000 0.0000	0.0000 0.0000	0.0000 0.0000	0.0000 0.0000	0.0000 0.0000
PERCOLATION/LEAKAGE THROUGH LAYER 8	0.0000 0.0000	0.0000 0.0000	0.0000 0.0000	0.0000 0.0000	0.0000 0.0000	0.0000 0.0000

MONTHLY SUMMARIES FOR DAILY HEADS (INCHES)

AVERAGE DAILY HEAD ON TOP OF LAYER 6	0.003 0.002	0.002 0.002	0.002 0.002	0.002 0.002	0.002 0.002	0.002 0.001
STD. DEVIATION OF DAILY HEAD ON TOP OF LAYER 6	0.000 0.000	0.000 0.000	0.000 0.000	0.000 0.000	0.000 0.000	0.000 0.000

ANNUAL TOTALS FOR YEAR 6

	INCHES	CU. FEET	PERCENT
PRECIPITATION	8.30	3434706.500	100.00
RUNOFF	0.881	364773.812	10.62
EVAPOTRANSPIRATION	7.456	3085344.000	89.83
DRAINAGE COLLECTED FROM LAYER 5	0.0003	124.013	0.00
PERC./LEAKAGE THROUGH LAYER 7	0.000003	1.184	0.00
AVG. HEAD ON TOP OF LAYER 6	0.0019		
PERC./LEAKAGE THROUGH LAYER 8	0.000004	1.637	0.00
CHANGE IN WATER STORAGE	-0.038	-15546.033	-0.45
SOIL WATER AT START OF YEAR	311.481	128896960.000	
SOIL WATER AT END OF YEAR	311.443	128881416.000	
SNOW WATER AT START OF YEAR	0.000	0.000	0.00
SNOW WATER AT END OF YEAR	0.000	0.000	0.00
ANNUAL WATER BUDGET BALANCE	0.0000	9.049	0.00

MONTHLY TOTALS (IN INCHES) FOR YEAR 7

	JAN/JUL	FEB/AUG	MAR/SEP	APR/OCT	MAY/NOV	JUN/DEC
PRECIPITATION	1.10 0.71	0.15 2.96	0.13 0.64	0.23 0.12	0.66 1.89	0.69 0.50
RUNOFF	0.038 0.007	0.000 0.421	0.000 0.000	0.000 0.000	0.027 0.282	0.113 0.000
EVAPOTRANSPIRATION	0.868	0.365	0.121	0.026	0.850	0.478

	0.753	2.588	0.504	0.235	0.748	1.374
LATERAL DRAINAGE COLLECTED	0.0000	0.0000	0.0000	0.0000	0.0000	0.0000
FROM LAYER 5	0.0000	0.0000	0.0000	0.0000	0.0000	0.0000
PERCOLATION/LEAKAGE THROUGH	0.0000	0.0000	0.0000	0.0000	0.0000	0.0000
LAYER 7	0.0000	0.0000	0.0000	0.0000	0.0000	0.0000
PERCOLATION/LEAKAGE THROUGH	0.0000	0.0000	0.0000	0.0000	0.0000	0.0000
LAYER 8	0.0000	0.0000	0.0000	0.0000	0.0000	0.0000

MONTHLY SUMMARIES FOR DAILY HEADS (INCHES)

AVERAGE DAILY HEAD ON	0.001	0.001	0.001	0.001	0.001	0.001
TOP OF LAYER 6	0.001	0.001	0.001	0.001	0.001	0.001
STD. DEVIATION OF DAILY	0.000	0.000	0.000	0.000	0.000	0.000
HEAD ON TOP OF LAYER 6	0.000	0.000	0.000	0.000	0.000	0.000

ANNUAL TOTALS FOR YEAR 7

	INCHES	CU. FEET	PERCENT
	-----	-----	-----
PRECIPITATION	9.78	4047160.750	100.00
RUNOFF	0.887	366889.500	9.07
EVAPOTRANSPIRATION	8.909	3686690.250	91.09
DRAINAGE COLLECTED FROM LAYER 5	0.0002	66.393	0.00
PERC./LEAKAGE THROUGH LAYER 7	0.000003	1.117	0.00
AVG. HEAD ON TOP OF LAYER 6	0.0010		
PERC./LEAKAGE THROUGH LAYER 8	0.000004	1.704	0.00
CHANGE IN WATER STORAGE	-0.016	-6478.566	-0.16
SOIL WATER AT START OF YEAR	311.443	128881416.000	
SOIL WATER AT END OF YEAR	311.428	128874936.000	
SNOW WATER AT START OF YEAR	0.000	0.000	0.00

SNOW WATER AT END OF YEAR	0.000	0.000	0.00
ANNUAL WATER BUDGET BALANCE	0.0000	-8.530	0.00

MONTHLY TOTALS (IN INCHES) FOR YEAR 8

	JAN/JUL	FEB/AUG	MAR/SEP	APR/OCT	MAY/NOV	JUN/DEC
	-----	-----	-----	-----	-----	-----
PRECIPITATION	0.42	0.09	0.00	0.22	0.40	2.78
	1.05	3.75	2.59	1.58	1.65	0.46
RUNOFF	0.012	0.000	0.000	0.000	0.000	0.259
	0.022	0.280	0.517	0.151	0.024	0.006
EVAPOTRANSPIRATION	0.394	0.084	0.025	0.109	0.496	2.537
	1.016	3.269	1.901	0.993	1.767	0.947
LATERAL DRAINAGE COLLECTED FROM LAYER 5	0.0000	0.0000	0.0000	0.0000	0.0000	0.0000
	0.0000	0.0000	0.0000	0.0000	0.0000	0.0000
PERCOLATION/LEAKAGE THROUGH LAYER 7	0.0000	0.0000	0.0000	0.0000	0.0000	0.0000
	0.0000	0.0000	0.0000	0.0000	0.0000	0.0000
PERCOLATION/LEAKAGE THROUGH LAYER 8	0.0000	0.0000	0.0000	0.0000	0.0000	0.0000
	0.0000	0.0000	0.0000	0.0000	0.0000	0.0000

MONTHLY SUMMARIES FOR DAILY HEADS (INCHES)

AVERAGE DAILY HEAD ON TOP OF LAYER 6	0.001	0.001	0.001	0.001	0.001	0.001
	0.001	0.001	0.000	0.000	0.000	0.000
STD. DEVIATION OF DAILY HEAD ON TOP OF LAYER 6	0.000	0.000	0.000	0.000	0.000	0.000
	0.000	0.000	0.000	0.000	0.000	0.000

ANNUAL TOTALS FOR YEAR 8

	INCHES	CU. FEET	PERCENT
PRECIPITATION	14.99	6203163.000	100.00
RUNOFF	1.270	525679.625	8.47
EVAPOTRANSPIRATION	13.538	5602342.000	90.31
DRAINAGE COLLECTED FROM LAYER 5	0.0001	35.392	0.00
PERC./LEAKAGE THROUGH LAYER 7	0.000003	1.081	0.00
AVG. HEAD ON TOP OF LAYER 6	0.0006		
PERC./LEAKAGE THROUGH LAYER 8	0.000004	1.748	0.00
CHANGE IN WATER STORAGE	0.181	75103.383	1.21
SOIL WATER AT START OF YEAR	311.428	128874936.000	
SOIL WATER AT END OF YEAR	311.609	128950040.000	
SNOW WATER AT START OF YEAR	0.000	0.000	0.00
SNOW WATER AT END OF YEAR	0.000	0.000	0.00
ANNUAL WATER BUDGET BALANCE	0.0000	0.943	0.00

MONTHLY TOTALS (IN INCHES) FOR YEAR 9

	JAN/JUL	FEB/AUG	MAR/SEP	APR/OCT	MAY/NOV	JUN/DEC
PRECIPITATION	0.02 0.34	0.18 3.97	0.50 0.48	2.41 2.01	0.14 0.52	1.78 0.12
RUNOFF	0.000 0.000	0.000 1.045	0.001 0.000	0.889 0.430	0.000 0.003	0.211 0.000
EVAPOTRANSPIRATION	0.205	0.144	0.535	1.521	0.104	1.610

	0.285	2.817	0.439	1.596	0.477	0.346
LATERAL DRAINAGE COLLECTED	0.0000	0.0000	0.0000	0.0000	0.0000	0.0000
FROM LAYER 5	0.0000	0.0000	0.0000	0.0000	0.0000	0.0000
PERCOLATION/LEAKAGE THROUGH	0.0000	0.0000	0.0000	0.0000	0.0000	0.0000
LAYER 7	0.0000	0.0000	0.0000	0.0000	0.0000	0.0000
PERCOLATION/LEAKAGE THROUGH	0.0000	0.0000	0.0000	0.0000	0.0000	0.0000
LAYER 8	0.0000	0.0000	0.0000	0.0000	0.0000	0.0000

MONTHLY SUMMARIES FOR DAILY HEADS (INCHES)

AVERAGE DAILY HEAD ON	0.000	0.000	0.000	0.000	0.000	0.000
TOP OF LAYER 6	0.000	0.000	0.000	0.000	0.000	0.000
STD. DEVIATION OF DAILY	0.000	0.000	0.000	0.000	0.000	0.000
HEAD ON TOP OF LAYER 6	0.000	0.000	0.000	0.000	0.000	0.000

ANNUAL TOTALS FOR YEAR 9

	INCHES	CU. FEET	PERCENT
	-----	-----	-----
PRECIPITATION	12.47	5160335.500	100.00
RUNOFF	2.578	1066972.250	20.68
EVAPOTRANSPIRATION	10.078	4170516.250	80.82
DRAINAGE COLLECTED FROM LAYER 5	0.0000	18.538	0.00
PERC./LEAKAGE THROUGH LAYER 7	0.000003	1.056	0.00
AVG. HEAD ON TOP OF LAYER 6	0.0003		
PERC./LEAKAGE THROUGH LAYER 8	0.000004	1.765	0.00
CHANGE IN WATER STORAGE	-0.186	-77161.875	-1.50
SOIL WATER AT START OF YEAR	311.609	128950040.000	
SOIL WATER AT END OF YEAR	311.423	128872880.000	
SNOW WATER AT START OF YEAR	0.000	0.000	0.00

SNOW WATER AT END OF YEAR	0.000	0.000	0.00
ANNUAL WATER BUDGET BALANCE	0.0000	-11.423	0.00

MONTHLY TOTALS (IN INCHES) FOR YEAR 10

	JAN/JUL	FEB/AUG	MAR/SEP	APR/OCT	MAY/NOV	JUN/DEC
	-----	-----	-----	-----	-----	-----
PRECIPITATION	0.00	0.02	0.24	1.82	0.98	0.00
	1.73	3.20	0.57	5.06	0.00	0.30
RUNOFF	0.000	0.000	0.000	0.501	0.104	0.000
	0.289	0.213	0.053	2.069	0.000	0.000
EVAPOTRANSPIRATION	0.000	0.020	0.173	1.268	0.996	0.000
	1.438	2.454	1.053	1.593	1.161	0.441
LATERAL DRAINAGE COLLECTED FROM LAYER 5	0.0000	0.0000	0.0000	0.0000	0.0000	0.0000
	0.0000	0.0000	0.0000	0.0000	0.0000	0.0000
PERCOLATION/LEAKAGE THROUGH LAYER 7	0.0000	0.0000	0.0000	0.0000	0.0000	0.0000
	0.0000	0.0000	0.0000	0.0000	0.0000	0.0000
PERCOLATION/LEAKAGE THROUGH LAYER 8	0.0000	0.0000	0.0000	0.0000	0.0000	0.0000
	0.0000	0.0000	0.0000	0.0000	0.0000	0.0000

MONTHLY SUMMARIES FOR DAILY HEADS (INCHES)

AVERAGE DAILY HEAD ON TOP OF LAYER 6	0.000	0.000	0.000	0.000	0.000	0.000
	0.000	0.000	0.000	0.000	0.000	0.000
STD. DEVIATION OF DAILY HEAD ON TOP OF LAYER 6	0.000	0.000	0.000	0.000	0.000	0.000
	0.000	0.000	0.000	0.000	0.000	0.000

ANNUAL TOTALS FOR YEAR 10

	INCHES	CU. FEET	PERCENT
	-----	-----	-----
PRECIPITATION	13.92	5760374.000	100.00
RUNOFF	3.229	1336256.250	23.20
EVAPOTRANSPIRATION	10.597	4385428.000	76.13
DRAINAGE COLLECTED FROM LAYER 5	0.0000	9.521	0.00
PERC./LEAKAGE THROUGH LAYER 7	0.000003	1.043	0.00
AVG. HEAD ON TOP OF LAYER 6	0.0001		
PERC./LEAKAGE THROUGH LAYER 8	0.000004	1.778	0.00
CHANGE IN WATER STORAGE	0.093	38681.965	0.67
SOIL WATER AT START OF YEAR	311.423	128872880.000	
SOIL WATER AT END OF YEAR	311.516	128911560.000	
SNOW WATER AT START OF YEAR	0.000	0.000	0.00
SNOW WATER AT END OF YEAR	0.000	0.000	0.00
ANNUAL WATER BUDGET BALANCE	0.0000	-3.307	0.00

MONTHLY TOTALS (IN INCHES) FOR YEAR 11

	JAN/JUL	FEB/AUG	MAR/SEP	APR/OCT	MAY/NOV	JUN/DEC
	-----	-----	-----	-----	-----	-----
PRECIPITATION	0.00	0.65	1.87	0.30	1.26	0.33
	0.64	2.32	0.22	5.49	0.06	0.19
RUNOFF	0.000	0.007	0.217	0.002	0.015	0.000
	0.002	0.210	0.000	2.094	0.000	0.000
EVAPOTRANSPIRATION	0.053	0.212	1.518	0.566	0.876	1.040

	0.495	2.223	0.116	2.208	1.299	0.246
LATERAL DRAINAGE COLLECTED	0.0000	0.0000	0.0000	0.0000	0.0000	0.0000
FROM LAYER 5	0.0000	0.0000	0.0000	0.0000	0.0000	0.0000
PERCOLATION/LEAKAGE THROUGH	0.0000	0.0000	0.0000	0.0000	0.0000	0.0000
LAYER 7	0.0000	0.0000	0.0000	0.0000	0.0000	0.0000
PERCOLATION/LEAKAGE THROUGH	0.0000	0.0000	0.0000	0.0000	0.0000	0.0000
LAYER 8	0.0000	0.0000	0.0000	0.0000	0.0000	0.0000

MONTHLY SUMMARIES FOR DAILY HEADS (INCHES)

AVERAGE DAILY HEAD ON	0.000	0.000	0.000	0.000	0.000	0.000
TOP OF LAYER 6	0.000	0.000	0.000	0.000	0.000	0.000
STD. DEVIATION OF DAILY	0.000	0.000	0.000	0.000	0.000	0.000
HEAD ON TOP OF LAYER 6	0.000	0.000	0.000	0.000	0.000	0.000

ANNUAL TOTALS FOR YEAR 11

	INCHES	CU. FEET	PERCENT
	-----	-----	-----
PRECIPITATION	13.33	5516221.500	100.00
RUNOFF	2.547	1053980.750	19.11
EVAPOTRANSPIRATION	10.852	4490911.000	81.41
DRAINAGE COLLECTED FROM LAYER 5	0.0000	4.659	0.00
PERC./LEAKAGE THROUGH LAYER 7	0.000003	1.036	0.00
AVG. HEAD ON TOP OF LAYER 6	0.0001		
PERC./LEAKAGE THROUGH LAYER 8	0.000004	1.785	0.00
CHANGE IN WATER STORAGE	-0.069	-28692.598	-0.52
SOIL WATER AT START OF YEAR	311.516	128911560.000	
SOIL WATER AT END OF YEAR	311.447	128882864.000	
SNOW WATER AT START OF YEAR	0.000	0.000	0.00

SNOW WATER AT END OF YEAR	0.000	0.000	0.00
ANNUAL WATER BUDGET BALANCE	0.0000	15.853	0.00

MONTHLY TOTALS (IN INCHES) FOR YEAR 12

	JAN/JUL	FEB/AUG	MAR/SEP	APR/OCT	MAY/NOV	JUN/DEC
	-----	-----	-----	-----	-----	-----
PRECIPITATION	0.00	0.98	0.80	0.75	0.85	2.19
	0.98	1.85	2.14	1.46	1.75	0.77
RUNOFF	0.000	0.023	0.006	0.024	0.083	0.213
	0.000	0.039	0.220	0.295	0.288	0.006
EVAPOTRANSPIRATION	0.002	0.458	0.799	0.772	0.613	2.601
	0.844	1.878	1.988	1.164	1.019	1.060
LATERAL DRAINAGE COLLECTED FROM LAYER 5	0.0000	0.0000	0.0000	0.0000	0.0000	0.0000
	0.0000	0.0000	0.0000	0.0000	0.0000	0.0000
PERCOLATION/LEAKAGE THROUGH LAYER 7	0.0000	0.0000	0.0000	0.0000	0.0000	0.0000
	0.0000	0.0000	0.0000	0.0000	0.0000	0.0000
PERCOLATION/LEAKAGE THROUGH LAYER 8	0.0000	0.0000	0.0000	0.0000	0.0000	0.0000
	0.0000	0.0000	0.0000	0.0000	0.0000	0.0000

MONTHLY SUMMARIES FOR DAILY HEADS (INCHES)

AVERAGE DAILY HEAD ON TOP OF LAYER 6	0.000	0.000	0.000	0.000	0.000	0.000
	0.000	0.000	0.000	0.000	0.000	0.000
STD. DEVIATION OF DAILY HEAD ON TOP OF LAYER 6	0.000	0.000	0.000	0.000	0.000	0.000
	0.000	0.000	0.000	0.000	0.000	0.000

ANNUAL TOTALS FOR YEAR 12

	INCHES	CU. FEET	PERCENT
PRECIPITATION	14.52	6008666.500	100.00
RUNOFF	1.197	495514.187	8.25
EVAPOTRANSPIRATION	13.199	5461894.000	90.90
DRAINAGE COLLECTED FROM LAYER 5	0.0000	2.042	0.00
PERC./LEAKAGE THROUGH LAYER 7	0.000002	1.034	0.00
AVG. HEAD ON TOP OF LAYER 6	0.0000		
PERC./LEAKAGE THROUGH LAYER 8	0.000004	1.794	0.00
CHANGE IN WATER STORAGE	0.124	51260.234	0.85
SOIL WATER AT START OF YEAR	311.447	128882864.000	
SOIL WATER AT END OF YEAR	311.571	128934128.000	
SNOW WATER AT START OF YEAR	0.000	0.000	0.00
SNOW WATER AT END OF YEAR	0.000	0.000	0.00
ANNUAL WATER BUDGET BALANCE	0.0000	-5.563	0.00

MONTHLY TOTALS (IN INCHES) FOR YEAR 13

	JAN/JUL	FEB/AUG	MAR/SEP	APR/OCT	MAY/NOV	JUN/DEC
PRECIPITATION	0.58 1.27	0.00 1.76	0.04 1.83	0.28 0.73	0.62 0.57	2.45 0.34
RUNOFF	0.001 0.095	0.000 0.059	0.000 0.453	0.000 0.025	0.079 0.001	0.466 0.000
EVAPOTRANSPIRATION	0.724	0.001	0.040	0.282	0.543	1.982

	1.141	1.622	1.217	0.800	0.326	0.712
LATERAL DRAINAGE COLLECTED	0.0000	0.0000	0.0000	0.0000	0.0000	0.0000
FROM LAYER 5	0.0000	0.0000	0.0000	0.0000	0.0000	0.0000
PERCOLATION/LEAKAGE THROUGH	0.0000	0.0000	0.0000	0.0000	0.0000	0.0000
LAYER 7	0.0000	0.0000	0.0000	0.0000	0.0000	0.0000
PERCOLATION/LEAKAGE THROUGH	0.0000	0.0000	0.0000	0.0000	0.0000	0.0000
LAYER 8	0.0000	0.0000	0.0000	0.0000	0.0000	0.0000

MONTHLY SUMMARIES FOR DAILY HEADS (INCHES)

AVERAGE DAILY HEAD ON	0.000	0.000	0.000	0.000	0.000	0.000
TOP OF LAYER 6	0.000	0.000	0.000	0.000	0.000	0.000
STD. DEVIATION OF DAILY	0.000	0.000	0.000	0.000	0.000	0.000
HEAD ON TOP OF LAYER 6	0.000	0.000	0.000	0.000	0.000	0.000

ANNUAL TOTALS FOR YEAR 13

	INCHES	CU. FEET	PERCENT
	-----	-----	-----
PRECIPITATION	10.47	4332696.500	100.00
RUNOFF	1.179	487751.469	11.26
EVAPOTRANSPIRATION	9.390	3885611.000	89.68
DRAINAGE COLLECTED FROM LAYER 5	0.0000	0.623	0.00
PERC./LEAKAGE THROUGH LAYER 7	0.000002	1.029	0.00
AVG. HEAD ON TOP OF LAYER 6	0.0000		
PERC./LEAKAGE THROUGH LAYER 8	0.000004	1.792	0.00
CHANGE IN WATER STORAGE	-0.098	-40664.684	-0.94
SOIL WATER AT START OF YEAR	311.571	128934128.000	
SOIL WATER AT END OF YEAR	311.472	128893464.000	
SNOW WATER AT START OF YEAR	0.000	0.000	0.00

SNOW WATER AT END OF YEAR	0.000	0.000	0.00
ANNUAL WATER BUDGET BALANCE	0.0000	-3.796	0.00

MONTHLY TOTALS (IN INCHES) FOR YEAR 14

	JAN/JUL	FEB/AUG	MAR/SEP	APR/OCT	MAY/NOV	JUN/DEC
	-----	-----	-----	-----	-----	-----
PRECIPITATION	0.00	0.70	0.35	1.17	1.04	0.77
	1.61	1.62	0.21	1.09	0.02	0.66
RUNOFF	0.000	0.000	0.001	0.129	0.040	0.008
	0.127	0.089	0.000	0.015	0.000	0.020
EVAPOTRANSPIRATION	0.046	0.699	0.183	1.073	0.792	1.107
	1.462	1.551	0.103	1.180	0.021	0.638
LATERAL DRAINAGE COLLECTED FROM LAYER 5	0.0000	0.0000	0.0000	0.0000	0.0000	0.0000
	0.0000	0.0000	0.0000	0.0000	0.0000	0.0000
PERCOLATION/LEAKAGE THROUGH LAYER 7	0.0000	0.0000	0.0000	0.0000	0.0000	0.0000
	0.0000	0.0000	0.0000	0.0000	0.0000	0.0000
PERCOLATION/LEAKAGE THROUGH LAYER 8	0.0000	0.0000	0.0000	0.0000	0.0000	0.0000
	0.0000	0.0000	0.0000	0.0000	0.0000	0.0000

MONTHLY SUMMARIES FOR DAILY HEADS (INCHES)

AVERAGE DAILY HEAD ON TOP OF LAYER 6	0.000	0.000	0.000	0.000	0.000	0.000
	0.000	0.000	0.000	0.000	0.000	0.000
STD. DEVIATION OF DAILY HEAD ON TOP OF LAYER 6	0.000	0.000	0.000	0.000	0.000	0.000
	0.000	0.000	0.000	0.000	0.000	0.000

ANNUAL TOTALS FOR YEAR 14

	INCHES	CU. FEET	PERCENT
PRECIPITATION	9.24	3823697.500	100.00
RUNOFF	0.430	177895.828	4.65
EVAPOTRANSPIRATION	8.856	3664705.750	95.84
DRAINAGE COLLECTED FROM LAYER 5	0.0000	0.020	0.00
PERC./LEAKAGE THROUGH LAYER 7	0.000001	0.249	0.00
AVG. HEAD ON TOP OF LAYER 6	0.0000		
PERC./LEAKAGE THROUGH LAYER 8	0.000001	0.439	0.00
CHANGE IN WATER STORAGE	-0.046	-18905.289	-0.49
SOIL WATER AT START OF YEAR	311.472	128893464.000	
SOIL WATER AT END OF YEAR	311.427	128874560.000	
SNOW WATER AT START OF YEAR	0.000	0.000	0.00
SNOW WATER AT END OF YEAR	0.000	0.000	0.00
ANNUAL WATER BUDGET BALANCE	0.0000	0.664	0.00

MONTHLY TOTALS (IN INCHES) FOR YEAR 15

	JAN/JUL	FEB/AUG	MAR/SEP	APR/OCT	MAY/NOV	JUN/DEC
PRECIPITATION	0.90 1.89	0.77 4.45	0.35 0.69	1.15 0.37	0.01 0.40	2.59 0.34
RUNOFF	0.011 0.039	0.032 0.795	0.000 0.000	0.328 0.000	0.000 0.000	0.395 0.000
EVAPOTRANSPIRATION	0.567	0.485	0.883	0.863	0.015	1.596

	2.235	3.505	1.031	0.393	0.283	0.401
LATERAL DRAINAGE COLLECTED	0.0000	0.0000	0.0000	0.0000	0.0000	0.0000
FROM LAYER 5	0.0000	0.0000	0.0000	0.0000	0.0000	0.0000
PERCOLATION/LEAKAGE THROUGH	0.0000	0.0000	0.0000	0.0000	0.0000	0.0000
LAYER 7	0.0000	0.0000	0.0000	0.0000	0.0000	0.0000
PERCOLATION/LEAKAGE THROUGH	0.0000	0.0000	0.0000	0.0000	0.0000	0.0000
LAYER 8	0.0000	0.0000	0.0000	0.0000	0.0000	0.0000

MONTHLY SUMMARIES FOR DAILY HEADS (INCHES)

AVERAGE DAILY HEAD ON	0.000	0.000	0.000	0.000	0.000	0.000
TOP OF LAYER 6	0.000	0.000	0.000	0.000	0.000	0.000
STD. DEVIATION OF DAILY	0.000	0.000	0.000	0.000	0.000	0.000
HEAD ON TOP OF LAYER 6	0.000	0.000	0.000	0.000	0.000	0.000

ANNUAL TOTALS FOR YEAR 15

	INCHES	CU. FEET	PERCENT
	-----	-----	-----
PRECIPITATION	13.91	5756236.000	100.00
RUNOFF	1.600	662046.375	11.50
EVAPOTRANSPIRATION	12.257	5072048.000	88.11
DRAINAGE COLLECTED FROM LAYER 5	0.0000	0.000	0.00
PERC./LEAKAGE THROUGH LAYER 7	0.000000	0.000	0.00
AVG. HEAD ON TOP OF LAYER 6	0.0000		
PERC./LEAKAGE THROUGH LAYER 8	0.000000	0.000	0.00
CHANGE IN WATER STORAGE	0.053	22138.258	0.38
SOIL WATER AT START OF YEAR	311.427	128874560.000	
SOIL WATER AT END OF YEAR	311.480	128896696.000	
SNOW WATER AT START OF YEAR	0.000	0.000	0.00

SNOW WATER AT END OF YEAR	0.000	0.000	0.00
ANNUAL WATER BUDGET BALANCE	0.0000	3.404	0.00

MONTHLY TOTALS (IN INCHES) FOR YEAR 16

	JAN/JUL	FEB/AUG	MAR/SEP	APR/OCT	MAY/NOV	JUN/DEC
PRECIPITATION	0.16 0.76	0.46 3.29	0.42 0.46	1.16 2.49	0.00 0.00	0.55 0.20
RUNOFF	0.000 0.000	0.029 0.292	0.001 0.003	0.167 0.602	0.000 0.000	0.003 0.000
EVAPOTRANSPIRATION	0.176 0.699	0.311 2.632	0.267 0.883	0.555 0.659	0.750 1.206	0.547 0.209
LATERAL DRAINAGE COLLECTED FROM LAYER 5	0.0000 0.0000	0.0000 0.0000	0.0000 0.0000	0.0000 0.0000	0.0000 0.0000	0.0000 0.0000
PERCOLATION/LEAKAGE THROUGH LAYER 7	0.0000 0.0000	0.0000 0.0000	0.0000 0.0000	0.0000 0.0000	0.0000 0.0000	0.0000 0.0000
PERCOLATION/LEAKAGE THROUGH LAYER 8	0.0000 0.0000	0.0000 0.0000	0.0000 0.0000	0.0000 0.0000	0.0000 0.0000	0.0000 0.0000

MONTHLY SUMMARIES FOR DAILY HEADS (INCHES)

AVERAGE DAILY HEAD ON TOP OF LAYER 6	0.000 0.000	0.000 0.000	0.000 0.000	0.000 0.000	0.000 0.000	0.000 0.000
STD. DEVIATION OF DAILY HEAD ON TOP OF LAYER 6	0.000 0.000	0.000 0.000	0.000 0.000	0.000 0.000	0.000 0.000	0.000 0.000

ANNUAL TOTALS FOR YEAR 16

	INCHES	CU. FEET	PERCENT
PRECIPITATION	9.95	4117508.500	100.00
RUNOFF	1.099	454665.375	11.04
EVAPOTRANSPIRATION	8.894	3680366.750	89.38
DRAINAGE COLLECTED FROM LAYER 5	0.0000	0.000	0.00
PERC./LEAKAGE THROUGH LAYER 7	0.000000	0.000	0.00
AVG. HEAD ON TOP OF LAYER 6	0.0000		
PERC./LEAKAGE THROUGH LAYER 8	0.000000	0.000	0.00
CHANGE IN WATER STORAGE	-0.042	-17516.123	-0.43
SOIL WATER AT START OF YEAR	311.480	128896696.000	
SOIL WATER AT END OF YEAR	311.438	128879176.000	
SNOW WATER AT START OF YEAR	0.000	0.000	0.00
SNOW WATER AT END OF YEAR	0.000	0.000	0.00
ANNUAL WATER BUDGET BALANCE	0.0000	-7.449	0.00

MONTHLY TOTALS (IN INCHES) FOR YEAR 17

	JAN/JUL	FEB/AUG	MAR/SEP	APR/OCT	MAY/NOV	JUN/DEC
PRECIPITATION	0.29 0.90	0.01 1.10	0.37 0.61	0.07 0.00	0.91 1.07	0.31 0.77
RUNOFF	0.000 0.000	0.000 0.010	0.000 0.017	0.000 0.000	0.225 0.070	0.000 0.000
EVAPOTRANSPIRATION	0.284	0.018	0.074	0.217	0.845	0.310

	0.494	1.228	0.860	0.000	0.314	1.053
LATERAL DRAINAGE COLLECTED	0.0000	0.0000	0.0000	0.0000	0.0000	0.0000
FROM LAYER 5	0.0000	0.0000	0.0000	0.0000	0.0000	0.0000
PERCOLATION/LEAKAGE THROUGH	0.0000	0.0000	0.0000	0.0000	0.0000	0.0000
LAYER 7	0.0000	0.0000	0.0000	0.0000	0.0000	0.0000
PERCOLATION/LEAKAGE THROUGH	0.0000	0.0000	0.0000	0.0000	0.0000	0.0000
LAYER 8	0.0000	0.0000	0.0000	0.0000	0.0000	0.0000

MONTHLY SUMMARIES FOR DAILY HEADS (INCHES)

AVERAGE DAILY HEAD ON	0.000	0.000	0.000	0.000	0.000	0.000
TOP OF LAYER 6	0.000	0.000	0.000	0.000	0.000	0.000
STD. DEVIATION OF DAILY	0.000	0.000	0.000	0.000	0.000	0.000
HEAD ON TOP OF LAYER 6	0.000	0.000	0.000	0.000	0.000	0.000

ANNUAL TOTALS FOR YEAR 17

	INCHES	CU. FEET	PERCENT
	-----	-----	-----
PRECIPITATION	6.41	2652586.250	100.00
RUNOFF	0.323	133843.375	5.05
EVAPOTRANSPIRATION	5.697	2357613.000	88.88
DRAINAGE COLLECTED FROM LAYER 5	0.0000	0.000	0.00
PERC./LEAKAGE THROUGH LAYER 7	0.000000	0.000	0.00
AVG. HEAD ON TOP OF LAYER 6	0.0000		
PERC./LEAKAGE THROUGH LAYER 8	0.000000	0.000	0.00
CHANGE IN WATER STORAGE	0.389	161130.656	6.07
SOIL WATER AT START OF YEAR	311.438	128879176.000	
SOIL WATER AT END OF YEAR	311.827	129040312.000	
SNOW WATER AT START OF YEAR	0.000	0.000	0.00

SNOW WATER AT END OF YEAR	0.000	0.000	0.00
ANNUAL WATER BUDGET BALANCE	0.0000	-0.752	0.00

MONTHLY TOTALS (IN INCHES) FOR YEAR 18

	JAN/JUL	FEB/AUG	MAR/SEP	APR/OCT	MAY/NOV	JUN/DEC
	-----	-----	-----	-----	-----	-----
PRECIPITATION	0.67	0.19	0.03	1.94	0.00	0.08
	2.46	1.29	0.06	0.17	0.41	0.52
RUNOFF	0.007	0.000	0.000	0.578	0.000	0.000
	0.153	0.004	0.000	0.000	0.001	0.000
EVAPOTRANSPIRATION	1.061	0.191	0.030	0.657	0.707	0.080
	2.115	1.478	0.060	0.157	0.422	0.262
LATERAL DRAINAGE COLLECTED FROM LAYER 5	0.0000	0.0000	0.0000	0.0000	0.0000	0.0000
	0.0000	0.0000	0.0000	0.0000	0.0000	0.0000
PERCOLATION/LEAKAGE THROUGH LAYER 7	0.0000	0.0000	0.0000	0.0000	0.0000	0.0000
	0.0000	0.0000	0.0000	0.0000	0.0000	0.0000
PERCOLATION/LEAKAGE THROUGH LAYER 8	0.0000	0.0000	0.0000	0.0000	0.0000	0.0000
	0.0000	0.0000	0.0000	0.0000	0.0000	0.0000

MONTHLY SUMMARIES FOR DAILY HEADS (INCHES)

AVERAGE DAILY HEAD ON TOP OF LAYER 6	0.000	0.000	0.000	0.000	0.000	0.000
	0.000	0.000	0.000	0.000	0.000	0.000
STD. DEVIATION OF DAILY HEAD ON TOP OF LAYER 6	0.000	0.000	0.000	0.000	0.000	0.000
	0.000	0.000	0.000	0.000	0.000	0.000

ANNUAL TOTALS FOR YEAR 18

	INCHES	CU. FEET	PERCENT
PRECIPITATION	7.82	3236072.750	100.00
RUNOFF	0.743	307466.469	9.50
EVAPOTRANSPIRATION	7.220	2987809.750	92.33
DRAINAGE COLLECTED FROM LAYER 5	0.0000	0.000	0.00
PERC./LEAKAGE THROUGH LAYER 7	0.000000	0.000	0.00
AVG. HEAD ON TOP OF LAYER 6	0.0000		
PERC./LEAKAGE THROUGH LAYER 8	0.000000	0.000	0.00
CHANGE IN WATER STORAGE	-0.143	-59203.742	-1.83
SOIL WATER AT START OF YEAR	311.827	129040312.000	
SOIL WATER AT END OF YEAR	311.684	128981104.000	
SNOW WATER AT START OF YEAR	0.000	0.000	0.00
SNOW WATER AT END OF YEAR	0.000	0.000	0.00
ANNUAL WATER BUDGET BALANCE	0.0000	0.419	0.00

MONTHLY TOTALS (IN INCHES) FOR YEAR 19

	JAN/JUL	FEB/AUG	MAR/SEP	APR/OCT	MAY/NOV	JUN/DEC
PRECIPITATION	0.00 1.61	0.77 2.21	0.76 0.94	0.38 0.97	0.31 1.33	1.22 0.42
RUNOFF	0.000 0.016	0.001 0.181	0.003 0.008	0.001 0.048	0.000 0.163	0.162 0.000
EVAPOTRANSPIRATION	0.258	0.408	1.117	0.251	0.392	1.106

	1.125	1.977	1.129	1.154	0.860	0.722
LATERAL DRAINAGE COLLECTED	0.0000	0.0000	0.0000	0.0000	0.0000	0.0000
FROM LAYER 5	0.0000	0.0000	0.0000	0.0000	0.0000	0.0000
PERCOLATION/LEAKAGE THROUGH	0.0000	0.0000	0.0000	0.0000	0.0000	0.0000
LAYER 7	0.0000	0.0000	0.0000	0.0000	0.0000	0.0000
PERCOLATION/LEAKAGE THROUGH	0.0000	0.0000	0.0000	0.0000	0.0000	0.0000
LAYER 8	0.0000	0.0000	0.0000	0.0000	0.0000	0.0000

MONTHLY SUMMARIES FOR DAILY HEADS (INCHES)

AVERAGE DAILY HEAD ON	0.000	0.000	0.000	0.000	0.000	0.000
TOP OF LAYER 6	0.000	0.000	0.000	0.000	0.000	0.000
STD. DEVIATION OF DAILY	0.000	0.000	0.000	0.000	0.000	0.000
HEAD ON TOP OF LAYER 6	0.000	0.000	0.000	0.000	0.000	0.000

ANNUAL TOTALS FOR YEAR 19

	INCHES	CU. FEET	PERCENT
	-----	-----	-----
PRECIPITATION	10.92	4518915.000	100.00
RUNOFF	0.584	241583.344	5.35
EVAPOTRANSPIRATION	10.498	4344447.000	96.14
DRAINAGE COLLECTED FROM LAYER 5	0.0000	0.000	0.00
PERC./LEAKAGE THROUGH LAYER 7	0.000000	0.000	0.00
AVG. HEAD ON TOP OF LAYER 6	0.0000		
PERC./LEAKAGE THROUGH LAYER 8	0.000000	0.000	0.00
CHANGE IN WATER STORAGE	-0.162	-67121.984	-1.49
SOIL WATER AT START OF YEAR	311.684	128981104.000	
SOIL WATER AT END OF YEAR	311.522	128913984.000	
SNOW WATER AT START OF YEAR	0.000	0.000	0.00

SNOW WATER AT END OF YEAR	0.000	0.000	0.00
ANNUAL WATER BUDGET BALANCE	0.0000	6.487	0.00

MONTHLY TOTALS (IN INCHES) FOR YEAR 20

	JAN/JUL	FEB/AUG	MAR/SEP	APR/OCT	MAY/NOV	JUN/DEC
	-----	-----	-----	-----	-----	-----
PRECIPITATION	0.13	0.50	0.77	0.08	0.23	3.31
	0.96	0.33	2.27	1.41	0.09	0.23
RUNOFF	0.000	0.001	0.000	0.000	0.000	0.525
	0.001	0.000	0.608	0.319	0.000	0.000
EVAPOTRANSPIRATION	0.163	0.358	0.896	0.158	0.099	2.580
	1.226	0.295	1.098	1.350	0.495	0.191
LATERAL DRAINAGE COLLECTED FROM LAYER 5	0.0000	0.0000	0.0000	0.0000	0.0000	0.0000
	0.0000	0.0000	0.0000	0.0000	0.0000	0.0000
PERCOLATION/LEAKAGE THROUGH LAYER 7	0.0000	0.0000	0.0000	0.0000	0.0000	0.0000
	0.0000	0.0000	0.0000	0.0000	0.0000	0.0000
PERCOLATION/LEAKAGE THROUGH LAYER 8	0.0000	0.0000	0.0000	0.0000	0.0000	0.0000
	0.0000	0.0000	0.0000	0.0000	0.0000	0.0000

MONTHLY SUMMARIES FOR DAILY HEADS (INCHES)

AVERAGE DAILY HEAD ON TOP OF LAYER 6	0.000	0.000	0.000	0.000	0.000	0.000
	0.000	0.000	0.000	0.000	0.000	0.000
STD. DEVIATION OF DAILY HEAD ON TOP OF LAYER 6	0.000	0.000	0.000	0.000	0.000	0.000
	0.000	0.000	0.000	0.000	0.000	0.000

ANNUAL TOTALS FOR YEAR 20

	INCHES	CU. FEET	PERCENT
PRECIPITATION	10.31	4266485.000	100.00
RUNOFF	1.454	601548.625	14.10
EVAPOTRANSPIRATION	8.908	3686226.750	86.40
DRAINAGE COLLECTED FROM LAYER 5	0.0000	0.000	0.00
PERC./LEAKAGE THROUGH LAYER 7	0.000000	0.000	0.00
AVG. HEAD ON TOP OF LAYER 6	0.0000		
PERC./LEAKAGE THROUGH LAYER 8	0.000000	0.000	0.00
CHANGE IN WATER STORAGE	-0.051	-21292.131	-0.50
SOIL WATER AT START OF YEAR	311.522	128913984.000	
SOIL WATER AT END OF YEAR	311.470	128892696.000	
SNOW WATER AT START OF YEAR	0.000	0.000	0.00
SNOW WATER AT END OF YEAR	0.000	0.000	0.00
ANNUAL WATER BUDGET BALANCE	0.0000	1.776	0.00

MONTHLY TOTALS (IN INCHES) FOR YEAR 21

	JAN/JUL	FEB/AUG	MAR/SEP	APR/OCT	MAY/NOV	JUN/DEC
PRECIPITATION	1.10 1.68	0.50 1.87	0.00 2.53	1.52 0.49	0.47 1.19	1.04 0.46
RUNOFF	0.017 0.246	0.003 0.193	0.000 0.588	0.199 0.000	0.001 0.117	0.182 0.001
EVAPOTRANSPIRATION	0.848	0.751	0.021	1.323	0.399	0.930

	1.249	1.303	2.426	0.539	0.905	0.393
LATERAL DRAINAGE COLLECTED	0.0000	0.0000	0.0000	0.0000	0.0000	0.0000
FROM LAYER 5	0.0000	0.0000	0.0000	0.0000	0.0000	0.0000
PERCOLATION/LEAKAGE THROUGH	0.0000	0.0000	0.0000	0.0000	0.0000	0.0000
LAYER 7	0.0000	0.0000	0.0000	0.0000	0.0000	0.0000
PERCOLATION/LEAKAGE THROUGH	0.0000	0.0000	0.0000	0.0000	0.0000	0.0000
LAYER 8	0.0000	0.0000	0.0000	0.0000	0.0000	0.0000

MONTHLY SUMMARIES FOR DAILY HEADS (INCHES)

AVERAGE DAILY HEAD ON	0.000	0.000	0.000	0.000	0.000	0.000
TOP OF LAYER 6	0.000	0.000	0.000	0.000	0.000	0.000
STD. DEVIATION OF DAILY	0.000	0.000	0.000	0.000	0.000	0.000
HEAD ON TOP OF LAYER 6	0.000	0.000	0.000	0.000	0.000	0.000

ANNUAL TOTALS FOR YEAR 21

	INCHES	CU. FEET	PERCENT
	-----	-----	-----
PRECIPITATION	12.85	5317587.000	100.00
RUNOFF	1.548	640508.125	12.05
EVAPOTRANSPIRATION	11.086	4587554.000	86.27
DRAINAGE COLLECTED FROM LAYER 5	0.0000	0.000	0.00
PERC./LEAKAGE THROUGH LAYER 7	0.000000	0.000	0.00
AVG. HEAD ON TOP OF LAYER 6	0.0000		
PERC./LEAKAGE THROUGH LAYER 8	0.000000	0.000	0.00
CHANGE IN WATER STORAGE	0.216	89525.453	1.68
SOIL WATER AT START OF YEAR	311.470	128892696.000	
SOIL WATER AT END OF YEAR	311.687	128982216.000	
SNOW WATER AT START OF YEAR	0.000	0.000	0.00

SNOW WATER AT END OF YEAR	0.000	0.000	0.00
ANNUAL WATER BUDGET BALANCE	0.0000	-0.641	0.00

MONTHLY TOTALS (IN INCHES) FOR YEAR 22

	JAN/JUL	FEB/AUG	MAR/SEP	APR/OCT	MAY/NOV	JUN/DEC
	-----	-----	-----	-----	-----	-----
PRECIPITATION	0.14	0.00	0.36	0.90	0.16	0.99
	1.31	1.01	1.72	0.77	0.02	0.30
RUNOFF	0.000	0.000	0.000	0.030	0.000	0.027
	0.001	0.041	0.082	0.110	0.000	0.000
EVAPOTRANSPIRATION	0.399	0.000	0.324	0.486	0.581	0.826
	1.445	0.970	0.975	1.316	0.024	0.050
LATERAL DRAINAGE COLLECTED FROM LAYER 5	0.0000	0.0000	0.0000	0.0000	0.0000	0.0000
	0.0000	0.0000	0.0000	0.0000	0.0000	0.0000
PERCOLATION/LEAKAGE THROUGH LAYER 7	0.0000	0.0000	0.0000	0.0000	0.0000	0.0000
	0.0000	0.0000	0.0000	0.0000	0.0000	0.0000
PERCOLATION/LEAKAGE THROUGH LAYER 8	0.0000	0.0000	0.0000	0.0000	0.0000	0.0000
	0.0000	0.0000	0.0000	0.0000	0.0000	0.0000

MONTHLY SUMMARIES FOR DAILY HEADS (INCHES)

AVERAGE DAILY HEAD ON TOP OF LAYER 6	0.000	0.000	0.000	0.000	0.000	0.000
	0.000	0.000	0.000	0.000	0.000	0.000
STD. DEVIATION OF DAILY HEAD ON TOP OF LAYER 6	0.000	0.000	0.000	0.000	0.000	0.000
	0.000	0.000	0.000	0.000	0.000	0.000

ANNUAL TOTALS FOR YEAR 22

	INCHES	CU. FEET	PERCENT
PRECIPITATION	7.68	3178138.000	100.00
RUNOFF	0.291	120556.703	3.79
EVAPOTRANSPIRATION	7.396	3060596.000	96.30
DRAINAGE COLLECTED FROM LAYER 5	0.0000	0.000	0.00
PERC./LEAKAGE THROUGH LAYER 7	0.000000	0.000	0.00
AVG. HEAD ON TOP OF LAYER 6	0.0000		
PERC./LEAKAGE THROUGH LAYER 8	0.000000	0.000	0.00
CHANGE IN WATER STORAGE	-0.007	-3011.583	-0.09
SOIL WATER AT START OF YEAR	311.687	128982216.000	
SOIL WATER AT END OF YEAR	311.469	128891896.000	
SNOW WATER AT START OF YEAR	0.000	0.000	0.00
SNOW WATER AT END OF YEAR	0.211	87309.484	2.75
ANNUAL WATER BUDGET BALANCE	0.0000	-3.305	0.00

MONTHLY TOTALS (IN INCHES) FOR YEAR 23

	JAN/JUL	FEB/AUG	MAR/SEP	APR/OCT	MAY/NOV	JUN/DEC
PRECIPITATION	0.45 1.79	0.00 2.69	0.13 2.45	5.59 0.91	0.00 0.63	0.59 0.25
RUNOFF	0.000 0.289	0.000 0.628	0.000 0.115	3.146 0.008	0.000 0.006	0.038 0.000
EVAPOTRANSPIRATION	0.455	0.245	0.089	1.476	1.012	0.092

	1.959	2.063	1.813	1.416	0.629	0.251
LATERAL DRAINAGE COLLECTED	0.0000	0.0000	0.0000	0.0000	0.0000	0.0000
FROM LAYER 5	0.0000	0.0000	0.0000	0.0000	0.0000	0.0000
PERCOLATION/LEAKAGE THROUGH	0.0000	0.0000	0.0000	0.0000	0.0000	0.0000
LAYER 7	0.0000	0.0000	0.0000	0.0000	0.0000	0.0000
PERCOLATION/LEAKAGE THROUGH	0.0000	0.0000	0.0000	0.0000	0.0000	0.0000
LAYER 8	0.0000	0.0000	0.0000	0.0000	0.0000	0.0000

MONTHLY SUMMARIES FOR DAILY HEADS (INCHES)

AVERAGE DAILY HEAD ON	0.000	0.000	0.000	0.000	0.000	0.000
TOP OF LAYER 6	0.000	0.000	0.000	0.000	0.000	0.000
STD. DEVIATION OF DAILY	0.000	0.000	0.000	0.000	0.000	0.000
HEAD ON TOP OF LAYER 6	0.000	0.000	0.000	0.000	0.000	0.000

ANNUAL TOTALS FOR YEAR 23

	INCHES	CU. FEET	PERCENT
	-----	-----	-----
PRECIPITATION	15.48	6405935.000	100.00
RUNOFF	4.229	1750120.750	27.32
EVAPOTRANSPIRATION	11.501	4759453.500	74.30
DRAINAGE COLLECTED FROM LAYER 5	0.0000	0.000	0.00
PERC./LEAKAGE THROUGH LAYER 7	0.000000	0.000	0.00
AVG. HEAD ON TOP OF LAYER 6	0.0000		
PERC./LEAKAGE THROUGH LAYER 8	0.000000	0.000	0.00
CHANGE IN WATER STORAGE	-0.250	-103651.125	-1.62
SOIL WATER AT START OF YEAR	311.469	128891896.000	
SOIL WATER AT END OF YEAR	311.429	128875552.000	
SNOW WATER AT START OF YEAR	0.211	87309.484	1.36

SNOW WATER AT END OF YEAR	0.000	0.000	0.00
ANNUAL WATER BUDGET BALANCE	0.0000	11.630	0.00

MONTHLY TOTALS (IN INCHES) FOR YEAR 24

	JAN/JUL	FEB/AUG	MAR/SEP	APR/OCT	MAY/NOV	JUN/DEC
	-----	-----	-----	-----	-----	-----
PRECIPITATION	0.04	0.41	0.37	0.30	2.35	0.00
	1.21	4.98	1.62	0.82	0.00	0.32
RUNOFF	0.000	0.000	0.000	0.002	0.194	0.000
	0.011	0.979	0.393	0.108	0.000	0.000
EVAPOTRANSPIRATION	0.040	0.329	0.282	0.261	2.123	0.240
	1.197	3.662	1.568	0.623	0.088	0.262
LATERAL DRAINAGE COLLECTED FROM LAYER 5	0.0000	0.0000	0.0000	0.0000	0.0000	0.0000
	0.0000	0.0000	0.0000	0.0000	0.0000	0.0000
PERCOLATION/LEAKAGE THROUGH LAYER 7	0.0000	0.0000	0.0000	0.0000	0.0000	0.0000
	0.0000	0.0000	0.0000	0.0000	0.0000	0.0000
PERCOLATION/LEAKAGE THROUGH LAYER 8	0.0000	0.0000	0.0000	0.0000	0.0000	0.0000
	0.0000	0.0000	0.0000	0.0000	0.0000	0.0000

MONTHLY SUMMARIES FOR DAILY HEADS (INCHES)

AVERAGE DAILY HEAD ON TOP OF LAYER 6	0.000	0.000	0.000	0.000	0.000	0.000
	0.000	0.000	0.000	0.000	0.000	0.000
STD. DEVIATION OF DAILY HEAD ON TOP OF LAYER 6	0.000	0.000	0.000	0.000	0.000	0.000
	0.000	0.000	0.000	0.000	0.000	0.000

ANNUAL TOTALS FOR YEAR 24

	INCHES	CU. FEET	PERCENT
PRECIPITATION	12.42	5139645.000	100.00
RUNOFF	1.687	697958.000	13.58
EVAPOTRANSPIRATION	10.675	4417646.000	85.95
DRAINAGE COLLECTED FROM LAYER 5	0.0000	0.000	0.00
PERC./LEAKAGE THROUGH LAYER 7	0.000000	0.000	0.00
AVG. HEAD ON TOP OF LAYER 6	0.0000		
PERC./LEAKAGE THROUGH LAYER 8	0.000000	0.000	0.00
CHANGE IN WATER STORAGE	0.058	24045.205	0.47
SOIL WATER AT START OF YEAR	311.429	128875552.000	
SOIL WATER AT END OF YEAR	311.487	128899600.000	
SNOW WATER AT START OF YEAR	0.000	0.000	0.00
SNOW WATER AT END OF YEAR	0.000	0.000	0.00
ANNUAL WATER BUDGET BALANCE	0.0000	-3.799	0.00

MONTHLY TOTALS (IN INCHES) FOR YEAR 25

	JAN/JUL	FEB/AUG	MAR/SEP	APR/OCT	MAY/NOV	JUN/DEC
PRECIPITATION	0.09 0.86	0.09 1.41	0.56 0.47	0.61 2.14	0.19 0.43	1.58 0.00
RUNOFF	0.000 0.022	0.000 0.078	0.000 0.000	0.000 0.458	0.000 0.000	0.525 0.000
EVAPOTRANSPIRATION	0.148	0.075	0.575	0.452	0.349	1.055

	0.795	1.375	0.354	1.437	0.782	0.002
LATERAL DRAINAGE COLLECTED	0.0000	0.0000	0.0000	0.0000	0.0000	0.0000
FROM LAYER 5	0.0000	0.0000	0.0000	0.0000	0.0000	0.0000
PERCOLATION/LEAKAGE THROUGH	0.0000	0.0000	0.0000	0.0000	0.0000	0.0000
LAYER 7	0.0000	0.0000	0.0000	0.0000	0.0000	0.0000
PERCOLATION/LEAKAGE THROUGH	0.0000	0.0000	0.0000	0.0000	0.0000	0.0000
LAYER 8	0.0000	0.0000	0.0000	0.0000	0.0000	0.0000

MONTHLY SUMMARIES FOR DAILY HEADS (INCHES)

AVERAGE DAILY HEAD ON	0.000	0.000	0.000	0.000	0.000	0.000
TOP OF LAYER 6	0.000	0.000	0.000	0.000	0.000	0.000
STD. DEVIATION OF DAILY	0.000	0.000	0.000	0.000	0.000	0.000
HEAD ON TOP OF LAYER 6	0.000	0.000	0.000	0.000	0.000	0.000

ANNUAL TOTALS FOR YEAR 25

	INCHES	CU. FEET	PERCENT
	-----	-----	-----
PRECIPITATION	8.43	3488502.250	100.00
RUNOFF	1.083	448111.000	12.85
EVAPOTRANSPIRATION	7.399	3061939.750	87.77
DRAINAGE COLLECTED FROM LAYER 5	0.0000	0.000	0.00
PERC./LEAKAGE THROUGH LAYER 7	0.000000	0.000	0.00
AVG. HEAD ON TOP OF LAYER 6	0.0000		
PERC./LEAKAGE THROUGH LAYER 8	0.000000	0.000	0.00
CHANGE IN WATER STORAGE	-0.052	-21544.705	-0.62
SOIL WATER AT START OF YEAR	311.487	128899600.000	
SOIL WATER AT END OF YEAR	311.435	128878056.000	
SNOW WATER AT START OF YEAR	0.000	0.000	0.00

SNOW WATER AT END OF YEAR	0.000	0.000	0.00
ANNUAL WATER BUDGET BALANCE	0.0000	-3.651	0.00

MONTHLY TOTALS (IN INCHES) FOR YEAR 26

	JAN/JUL	FEB/AUG	MAR/SEP	APR/OCT	MAY/NOV	JUN/DEC
	-----	-----	-----	-----	-----	-----
PRECIPITATION	0.14	0.86	0.35	1.56	0.66	0.03
	0.70	1.83	1.56	3.24	0.65	0.36
RUNOFF	0.000	0.015	0.000	0.096	0.000	0.000
	0.012	0.050	0.307	1.012	0.000	0.000
EVAPOTRANSPIRATION	0.048	0.745	0.370	1.639	0.590	0.103
	0.375	1.844	1.433	0.651	1.111	0.757
LATERAL DRAINAGE COLLECTED FROM LAYER 5	0.0000	0.0000	0.0000	0.0000	0.0000	0.0000
	0.0000	0.0000	0.0000	0.0000	0.0000	0.0000
PERCOLATION/LEAKAGE THROUGH LAYER 7	0.0000	0.0000	0.0000	0.0000	0.0000	0.0000
	0.0000	0.0000	0.0000	0.0000	0.0000	0.0000
PERCOLATION/LEAKAGE THROUGH LAYER 8	0.0000	0.0000	0.0000	0.0000	0.0000	0.0000
	0.0000	0.0000	0.0000	0.0000	0.0000	0.0000

MONTHLY SUMMARIES FOR DAILY HEADS (INCHES)

AVERAGE DAILY HEAD ON TOP OF LAYER 6	0.000	0.000	0.000	0.000	0.000	0.000
	0.000	0.000	0.000	0.000	0.000	0.000
STD. DEVIATION OF DAILY HEAD ON TOP OF LAYER 6	0.000	0.000	0.000	0.000	0.000	0.000
	0.000	0.000	0.000	0.000	0.000	0.000

ANNUAL TOTALS FOR YEAR 26

	INCHES	CU. FEET	PERCENT
PRECIPITATION	11.94	4941010.500	100.00
RUNOFF	1.492	617501.312	12.50
EVAPOTRANSPIRATION	9.666	4000189.000	80.96
DRAINAGE COLLECTED FROM LAYER 5	0.0000	0.000	0.00
PERC./LEAKAGE THROUGH LAYER 7	0.000000	0.000	0.00
AVG. HEAD ON TOP OF LAYER 6	0.0000		
PERC./LEAKAGE THROUGH LAYER 8	0.000000	0.000	0.00
CHANGE IN WATER STORAGE	0.781	323322.125	6.54
SOIL WATER AT START OF YEAR	311.435	128878056.000	
SOIL WATER AT END OF YEAR	312.216	129201376.000	
SNOW WATER AT START OF YEAR	0.000	0.000	0.00
SNOW WATER AT END OF YEAR	0.000	0.000	0.00
ANNUAL WATER BUDGET BALANCE	0.0000	-1.924	0.00

MONTHLY TOTALS (IN INCHES) FOR YEAR 27

	JAN/JUL	FEB/AUG	MAR/SEP	APR/OCT	MAY/NOV	JUN/DEC
PRECIPITATION	0.97 1.44	0.32 1.95	0.92 2.26	0.00 0.11	0.40 0.81	0.00 1.47
RUNOFF	0.000 0.035	0.000 0.119	0.000 0.056	0.000 0.000	0.015 0.003	0.000 0.073
EVAPOTRANSPIRATION	0.885	0.986	0.655	0.321	0.303	0.231

	0.710	2.527	1.262	0.986	0.790	0.829
LATERAL DRAINAGE COLLECTED	0.0000	0.0000	0.0000	0.0000	0.0000	0.0000
FROM LAYER 5	0.0000	0.0000	0.0000	0.0000	0.0000	0.0000
PERCOLATION/LEAKAGE THROUGH	0.0000	0.0000	0.0000	0.0000	0.0000	0.0000
LAYER 7	0.0000	0.0000	0.0000	0.0000	0.0000	0.0000
PERCOLATION/LEAKAGE THROUGH	0.0000	0.0000	0.0000	0.0000	0.0000	0.0000
LAYER 8	0.0000	0.0000	0.0000	0.0000	0.0000	0.0000

MONTHLY SUMMARIES FOR DAILY HEADS (INCHES)

AVERAGE DAILY HEAD ON	0.000	0.000	0.000	0.000	0.000	0.000
TOP OF LAYER 6	0.000	0.000	0.000	0.000	0.000	0.000
STD. DEVIATION OF DAILY	0.000	0.000	0.000	0.000	0.000	0.000
HEAD ON TOP OF LAYER 6	0.000	0.000	0.000	0.000	0.000	0.000

ANNUAL TOTALS FOR YEAR 27

	INCHES	CU. FEET	PERCENT
	-----	-----	-----
PRECIPITATION	10.65	4407183.000	100.00
RUNOFF	0.301	124446.953	2.82
EVAPOTRANSPIRATION	10.485	4338741.000	98.45
DRAINAGE COLLECTED FROM LAYER 5	0.0000	0.000	0.00
PERC./LEAKAGE THROUGH LAYER 7	0.000000	0.000	0.00
AVG. HEAD ON TOP OF LAYER 6	0.0000		
PERC./LEAKAGE THROUGH LAYER 8	0.000000	0.000	0.00
CHANGE IN WATER STORAGE	-0.135	-56008.656	-1.27
SOIL WATER AT START OF YEAR	312.216	129201376.000	
SOIL WATER AT END OF YEAR	312.081	129145368.000	
SNOW WATER AT START OF YEAR	0.000	0.000	0.00

SNOW WATER AT END OF YEAR	0.000	0.000	0.00
ANNUAL WATER BUDGET BALANCE	0.0000	3.404	0.00

MONTHLY TOTALS (IN INCHES) FOR YEAR 28

	JAN/JUL	FEB/AUG	MAR/SEP	APR/OCT	MAY/NOV	JUN/DEC
	-----	-----	-----	-----	-----	-----
PRECIPITATION	0.32	0.90	0.47	0.61	0.28	0.45
	0.70	2.76	1.60	2.30	0.01	0.34
RUNOFF	0.000	0.034	0.000	0.030	0.000	0.003
	0.003	0.191	0.334	0.338	0.000	0.000
EVAPOTRANSPIRATION	0.900	0.595	0.806	0.582	0.267	0.463
	0.611	2.035	1.886	0.475	0.908	0.771
LATERAL DRAINAGE COLLECTED FROM LAYER 5	0.0000	0.0000	0.0000	0.0000	0.0000	0.0000
	0.0000	0.0000	0.0000	0.0000	0.0000	0.0000
PERCOLATION/LEAKAGE THROUGH LAYER 7	0.0000	0.0000	0.0000	0.0000	0.0000	0.0000
	0.0000	0.0000	0.0000	0.0000	0.0000	0.0000
PERCOLATION/LEAKAGE THROUGH LAYER 8	0.0000	0.0000	0.0000	0.0000	0.0000	0.0000
	0.0000	0.0000	0.0000	0.0000	0.0000	0.0000

MONTHLY SUMMARIES FOR DAILY HEADS (INCHES)

AVERAGE DAILY HEAD ON TOP OF LAYER 6	0.000	0.000	0.000	0.000	0.000	0.000
	0.000	0.000	0.000	0.000	0.000	0.000
STD. DEVIATION OF DAILY HEAD ON TOP OF LAYER 6	0.000	0.000	0.000	0.000	0.000	0.000
	0.000	0.000	0.000	0.000	0.000	0.000

ANNUAL TOTALS FOR YEAR 28

	INCHES	CU. FEET	PERCENT
	-----	-----	-----
PRECIPITATION	10.74	4444426.500	100.00
RUNOFF	0.934	386358.500	8.69
EVAPOTRANSPIRATION	10.299	4261924.500	95.89
DRAINAGE COLLECTED FROM LAYER 5	0.0000	0.000	0.00
PERC./LEAKAGE THROUGH LAYER 7	0.000000	0.000	0.00
AVG. HEAD ON TOP OF LAYER 6	0.0000		
PERC./LEAKAGE THROUGH LAYER 8	0.000000	0.000	0.00
CHANGE IN WATER STORAGE	-0.493	-203853.828	-4.59
SOIL WATER AT START OF YEAR	312.081	129145368.000	
SOIL WATER AT END OF YEAR	311.588	128941512.000	
SNOW WATER AT START OF YEAR	0.000	0.000	0.00
SNOW WATER AT END OF YEAR	0.000	0.000	0.00
ANNUAL WATER BUDGET BALANCE	0.0000	-2.565	0.00

AVERAGE MONTHLY VALUES IN INCHES FOR YEARS 1 THROUGH 28

	JAN/JUL	FEB/AUG	MAR/SEP	APR/OCT	MAY/NOV	JUN/DEC
	-----	-----	-----	-----	-----	-----
PRECIPITATION						

TOTALS	0.30 1.22	0.41 2.37	0.46 1.31	0.98 1.79	0.65 0.62	1.08 0.45
STD. DEVIATIONS	0.35 0.61	0.35 1.14	0.41 0.83	1.13 1.61	0.56 0.62	1.00 0.30

RUNOFF

TOTALS	0.003	0.009	0.009	0.245	0.046	0.154
	0.072	0.257	0.166	0.417	0.043	0.004
STD. DEVIATIONS	0.008	0.016	0.041	0.609	0.069	0.201
	0.137	0.289	0.203	0.601	0.085	0.014

EVAPOTRANSPIRATION

TOTALS	0.355	0.361	0.476	0.658	0.677	1.009
	1.084	2.016	1.156	1.106	0.807	0.555
STD. DEVIATIONS	0.328	0.286	0.432	0.509	0.443	0.823
	0.567	0.808	0.680	0.668	0.477	0.346

LATERAL DRAINAGE COLLECTED FROM LAYER 5

TOTALS	0.0001	0.0000	0.0001	0.0000	0.0000	0.0000
	0.0000	0.0000	0.0000	0.0000	0.0000	0.0000
STD. DEVIATIONS	0.0002	0.0001	0.0001	0.0001	0.0001	0.0001
	0.0001	0.0001	0.0001	0.0001	0.0001	0.0001

PERCOLATION/LEAKAGE THROUGH LAYER 7

TOTALS	0.0000	0.0000	0.0000	0.0000	0.0000	0.0000
	0.0000	0.0000	0.0000	0.0000	0.0000	0.0000
STD. DEVIATIONS	0.0000	0.0000	0.0000	0.0000	0.0000	0.0000
	0.0000	0.0000	0.0000	0.0000	0.0000	0.0000

PERCOLATION/LEAKAGE THROUGH LAYER 8

TOTALS	0.0000	0.0000	0.0000	0.0000	0.0000	0.0000
	0.0000	0.0000	0.0000	0.0000	0.0000	0.0000
STD. DEVIATIONS	0.0000	0.0000	0.0000	0.0000	0.0000	0.0000
	0.0000	0.0000	0.0000	0.0000	0.0000	0.0000

AVERAGES OF MONTHLY AVERAGED DAILY HEADS (INCHES)

DAILY AVERAGE HEAD ON TOP OF LAYER 6

AVERAGES	0.0043	0.0041	0.0039	0.0037	0.0035	0.0034
	0.0032	0.0030	0.0029	0.0027	0.0026	0.0025
STD. DEVIATIONS	0.0118	0.0114	0.0109	0.0103	0.0098	0.0093
	0.0088	0.0084	0.0080	0.0076	0.0072	0.0068

AVERAGE ANNUAL TOTALS & (STD. DEVIATIONS) FOR YEARS 1 THROUGH 28

	INCHES		CU. FEET	PERCENT
PRECIPITATION	11.65 (2.760)		4819969.0	100.00
RUNOFF	1.424 (0.9521)		589430.50	12.229
EVAPOTRANSPIRATION	10.260 (2.1627)		4245724.00	88.086
LATERAL DRAINAGE COLLECTED FROM LAYER 5	0.00051 (0.00142)		212.120	0.00440
PERCOLATION/LEAKAGE THROUGH LAYER 7	0.00000 (0.00000)		0.702	0.00001
AVERAGE HEAD ON TOP OF LAYER 6	0.003 (0.009)			
PERCOLATION/LEAKAGE THROUGH LAYER 8	0.00000 (0.00000)		0.663	0.00001
CHANGE IN WATER STORAGE	-0.037 (0.3208)		-15398.10	-0.319

PEAK DAILY VALUES FOR YEARS	1 THROUGH	28
	(INCHES)	(CU. FT.)
PRECIPITATION	4.09	1692523.870
RUNOFF	2.964	1226554.2500
DRAINAGE COLLECTED FROM LAYER 5	0.00002	10.02380
PERCOLATION/LEAKAGE THROUGH LAYER 7	0.000000	0.01213
AVERAGE HEAD ON TOP OF LAYER 6	0.057	
MAXIMUM HEAD ON TOP OF LAYER 6	0.113	
LOCATION OF MAXIMUM HEAD IN LAYER 5 (DISTANCE FROM DRAIN)	2.1 FEET	
PERCOLATION/LEAKAGE THROUGH LAYER 8	0.000000	0.00684
SNOW WATER	0.69	286725.6250
MAXIMUM VEG. SOIL WATER (VOL/VOL)		0.1628
MINIMUM VEG. SOIL WATER (VOL/VOL)		0.0850

*** Maximum heads are computed using McEnroe's equations. ***

Reference: Maximum Saturated Depth over Landfill Liner
by Bruce M. McEnroe, University of Kansas
ASCE Journal of Environmental Engineering
Vol. 119, No. 2, March 1993, pp. 262-270.

FINAL WATER STORAGE AT END OF YEAR 28

LAYER	(INCHES)	(VOL/VOL)
1	0.5100	0.0850
2	3.0164	0.1005
3	1.4821	0.1235
4	300.3972	0.1447
5	5.3280	0.2220
6	0.0000	0.0000
7	0.1875	0.7500
8	0.6672	0.1112
SNOW WATER	0.000	

**APPLICATION FOR PERMIT RENEWAL AND MODIFICATION
SANDOVAL COUNTY LANDFILL**

**VOLUME III: LANDFILL ENGINEERING CALCULATIONS
SECTION 10: HELP MODEL**

ATTACHMENT III.10.A-7

UNIT III TEN-YEAR INTERMEDIATE COVER

```

*****
*****
**
**
**
**      HYDROLOGIC EVALUATION OF LANDFILL PERFORMANCE      **
**      HELP MODEL VERSION 3.07  (1 NOVEMBER 1997)          **
**      DEVELOPED BY ENVIRONMENTAL LABORATORY                **
**      USAE WATERWAYS EXPERIMENT STATION                   **
**      FOR USEPA RISK REDUCTION ENGINEERING LABORATORY      **
**
**
*****
*****

```

```

PRECIPITATION DATA FILE:  c:\RAIN10.D4
TEMPERATURE DATA FILE:   C:\TEMP10.D7
SOLAR RADIATION DATA FILE: C:\SOLAR10.D13
EVAPOTRANSPIRATION DATA:  C:\EVAP10.D11
SOIL AND DESIGN DATA FILE: C:\UNITIII.D10
OUTPUT DATA FILE:        C:\unitiii.OUT

```

TIME: 34: 8 DATE: 4/ 8/2015

```

*****
TITLE:  Sandoval County Landfill - Unit III Intermediate Cover Analy
*****

```

NOTE: INITIAL MOISTURE CONTENT OF THE LAYERS AND SNOW WATER
WERE SPECIFIED BY THE USER.

LAYER 1

```

TYPE 1 - VERTICAL PERCOLATION LAYER
MATERIAL TEXTURE NUMBER 6
THICKNESS           = 12.00 INCHES
POROSITY             = 0.4530 VOL/VOL
FIELD CAPACITY       = 0.1900 VOL/VOL
WILTING POINT       = 0.0850 VOL/VOL
INITIAL SOIL WATER CONTENT = 0.1111 VOL/VOL
EFFECTIVE SAT. HYD. COND. = 0.720000011000E-03 CM/SEC

```

LAYER 2

TYPE 1 - VERTICAL PERCOLATION LAYER

MATERIAL TEXTURE NUMBER 18

THICKNESS	=	1080.00	INCHES
POROSITY	=	0.6710	VOL/VOL
FIELD CAPACITY	=	0.2920	VOL/VOL
WILTING POINT	=	0.0770	VOL/VOL
INITIAL SOIL WATER CONTENT	=	0.1310	VOL/VOL
EFFECTIVE SAT. HYD. COND.	=	0.100000005000E-02	CM/SEC

LAYER 3

TYPE 2 - LATERAL DRAINAGE LAYER

MATERIAL TEXTURE NUMBER 0

THICKNESS	=	24.00	INCHES
POROSITY	=	0.4530	VOL/VOL
FIELD CAPACITY	=	0.1900	VOL/VOL
WILTING POINT	=	0.0850	VOL/VOL
INITIAL SOIL WATER CONTENT	=	0.1111	VOL/VOL
EFFECTIVE SAT. HYD. COND.	=	0.300000014000E-03	CM/SEC
SLOPE	=	2.80	PERCENT
DRAINAGE LENGTH	=	420.0	FEET

LAYER 4

TYPE 4 - FLEXIBLE MEMBRANE LINER

MATERIAL TEXTURE NUMBER 35

THICKNESS	=	0.06	INCHES
POROSITY	=	0.0000	VOL/VOL
FIELD CAPACITY	=	0.0000	VOL/VOL
WILTING POINT	=	0.0000	VOL/VOL
INITIAL SOIL WATER CONTENT	=	0.0000	VOL/VOL
EFFECTIVE SAT. HYD. COND.	=	0.199999996000E-12	CM/SEC
FML PINHOLE DENSITY	=	1.00	HOLES/ACRE
FML INSTALLATION DEFECTS	=	4.00	HOLES/ACRE
FML PLACEMENT QUALITY	=	3	- GOOD

LAYER 5

TYPE 3 - BARRIER SOIL LINER
MATERIAL TEXTURE NUMBER 0

THICKNESS	=	0.25	INCHES
POROSITY	=	0.7500	VOL/VOL
FIELD CAPACITY	=	0.7470	VOL/VOL
WILTING POINT	=	0.4000	VOL/VOL
INITIAL SOIL WATER CONTENT	=	0.7500	VOL/VOL
EFFECTIVE SAT. HYD. COND.	=	0.499999997000E-08	CM/SEC

LAYER 6

TYPE 1 - VERTICAL PERCOLATION LAYER
MATERIAL TEXTURE NUMBER 0

THICKNESS	=	6.00	INCHES
POROSITY	=	0.4530	VOL/VOL
FIELD CAPACITY	=	0.1900	VOL/VOL
WILTING POINT	=	0.0850	VOL/VOL
INITIAL SOIL WATER CONTENT	=	0.1111	VOL/VOL
EFFECTIVE SAT. HYD. COND.	=	0.420000015000E-05	CM/SEC

GENERAL DESIGN AND EVAPORATIVE ZONE DATA

NOTE: SCS RUNOFF CURVE NUMBER WAS COMPUTED FROM A USER-SPECIFIED CURVE NUMBER OF 85.0, A SURFACE SLOPE OF 5.% AND A SLOPE LENGTH OF 400. FEET.

SCS RUNOFF CURVE NUMBER	=	85.30	
FRACTION OF AREA ALLOWING RUNOFF	=	100.0	PERCENT
AREA PROJECTED ON HORIZONTAL PLANE	=	60.400	ACRES
EVAPORATIVE ZONE DEPTH	=	18.0	INCHES
INITIAL WATER IN EVAPORATIVE ZONE	=	2.119	INCHES
UPPER LIMIT OF EVAPORATIVE STORAGE	=	9.462	INCHES
LOWER LIMIT OF EVAPORATIVE STORAGE	=	1.482	INCHES
INITIAL SNOW WATER	=	0.000	INCHES
INITIAL WATER IN LAYER MATERIALS	=	146.334	INCHES
TOTAL INITIAL WATER	=	146.334	INCHES
TOTAL SUBSURFACE INFLOW	=	0.00	INCHES/YEAR

EVAPOTRANSPIRATION AND WEATHER DATA

NOTE: EVAPOTRANSPIRATION DATA WAS OBTAINED FROM
ALBUQUERQUE NEW MEXICO

STATION LATITUDE	=	35.30 DEGREES
MAXIMUM LEAF AREA INDEX	=	0.00
START OF GROWING SEASON (JULIAN DATE)	=	98
END OF GROWING SEASON (JULIAN DATE)	=	299
EVAPORATIVE ZONE DEPTH	=	18.0 INCHES
AVERAGE ANNUAL WIND SPEED	=	9.00 MPH
AVERAGE 1ST QUARTER RELATIVE HUMIDITY	=	48.00 %
AVERAGE 2ND QUARTER RELATIVE HUMIDITY	=	30.00 %
AVERAGE 3RD QUARTER RELATIVE HUMIDITY	=	45.00 %
AVERAGE 4TH QUARTER RELATIVE HUMIDITY	=	50.00 %

NOTE: PRECIPITATION DATA WAS SYNTHETICALLY GENERATED USING
COEFFICIENTS FOR ALBUQUERQUE NEW MEXICO

NORMAL MEAN MONTHLY PRECIPITATION (INCHES)

JAN/JUL	FEB/AUG	MAR/SEP	APR/OCT	MAY/NOV	JUN/DEC
-----	-----	-----	-----	-----	-----
0.37	0.47	0.48	0.99	0.72	0.99
1.39	2.34	1.20	1.50	0.55	0.47

NOTE: TEMPERATURE DATA WAS SYNTHETICALLY GENERATED USING
COEFFICIENTS FOR ALBUQUERQUE NEW MEXICO

NORMAL MEAN MONTHLY TEMPERATURE (DEGREES FAHRENHEIT)

JAN/JUL	FEB/AUG	MAR/SEP	APR/OCT	MAY/NOV	JUN/DEC
-----	-----	-----	-----	-----	-----
35.20	40.90	47.10	55.30	64.90	73.50
77.30	75.60	67.30	57.20	44.40	35.70

NOTE: SOLAR RADIATION DATA WAS SYNTHETICALLY GENERATED USING
COEFFICIENTS FOR ALBUQUERQUE NEW MEXICO
AND STATION LATITUDE = 35.30 DEGREES

MONTHLY TOTALS (IN INCHES) FOR YEAR 1

	JAN/JUL	FEB/AUG	MAR/SEP	APR/OCT	MAY/NOV	JUN/DEC
PRECIPITATION	0.11 0.99	0.01 3.66	0.26 1.17	0.55 1.12	0.86 1.67	0.01 0.57
RUNOFF	0.000 0.000	0.000 0.000	0.000 0.000	0.000 0.000	0.000 0.000	0.000 0.000
EVAPOTRANSPIRATION	0.441 0.574	0.293 3.160	0.086 2.512	0.174 0.528	0.211 1.530	0.198 0.785
LATERAL DRAINAGE COLLECTED FROM LAYER 3	0.0000 0.0000	0.0000 0.0000	0.0000 0.0000	0.0000 0.0000	0.0000 0.0000	0.0000 0.0000
PERCOLATION/LEAKAGE THROUGH LAYER 5	0.0000 0.0000	0.0000 0.0000	0.0000 0.0000	0.0000 0.0000	0.0000 0.0000	0.0000 0.0000
PERCOLATION/LEAKAGE THROUGH LAYER 6	0.0000 0.0000	0.0000 0.0000	0.0000 0.0000	0.0000 0.0000	0.0000 0.0000	0.0000 0.0000

MONTHLY SUMMARIES FOR DAILY HEADS (INCHES)

AVERAGE DAILY HEAD ON TOP OF LAYER 4	0.000 0.000	0.000 0.000	0.000 0.000	0.000 0.000	0.000 0.000	0.000 0.000
STD. DEVIATION OF DAILY HEAD ON TOP OF LAYER 4	0.000 0.000	0.000 0.000	0.000 0.000	0.000 0.000	0.000 0.000	0.000 0.000

ANNUAL TOTALS FOR YEAR 1

	INCHES	CU. FEET	PERCENT
PRECIPITATION	10.98	2407387.250	100.00
RUNOFF	0.000	0.000	0.00
EVAPOTRANSPIRATION	10.491	2300209.500	95.55
DRAINAGE COLLECTED FROM LAYER 3	0.0000	0.000	0.00

	JAN/JUL	FEB/AUG	MAR/SEP	APR/OCT	MAY/NOV	JUN/DEC
	-----	-----	-----	-----	-----	-----
PRECIPITATION	0.09	1.07	0.00	1.64	1.35	2.03
	1.08	3.29	1.76	5.91	0.03	0.42
RUNOFF	0.000	0.000	0.000	0.005	0.000	0.037
	0.000	0.034	0.000	0.525	0.000	0.000
EVAPOTRANSPIRATION	0.386	0.371	0.298	1.468	1.120	2.477
	0.821	2.832	1.576	3.036	1.913	0.559
LATERAL DRAINAGE COLLECTED FROM LAYER 3	0.0000	0.0000	0.0000	0.0000	0.0000	0.0000
	0.0000	0.0000	0.0000	0.0000	0.0000	0.0000
PERCOLATION/LEAKAGE THROUGH LAYER 5	0.0000	0.0000	0.0000	0.0000	0.0000	0.0000
	0.0000	0.0000	0.0000	0.0000	0.0000	0.0000
PERCOLATION/LEAKAGE THROUGH LAYER 6	0.0000	0.0000	0.0000	0.0000	0.0000	0.0000
	0.0000	0.0000	0.0000	0.0000	0.0000	0.0000

MONTHLY SUMMARIES FOR DAILY HEADS (INCHES)

AVERAGE DAILY HEAD ON	0.000	0.000	0.000	0.000	0.000	0.000
TOP OF LAYER 4	0.000	0.000	0.000	0.000	0.000	0.000
STD. DEVIATION OF DAILY	0.000	0.000	0.000	0.000	0.000	0.000
HEAD ON TOP OF LAYER 4	0.000	0.000	0.000	0.000	0.000	0.000

ANNUAL TOTALS FOR YEAR 2

	INCHES	CU. FEET	PERCENT
	-----	-----	-----
PRECIPITATION	18.67	4093435.500	100.00
RUNOFF	0.601	131841.516	3.22
EVAPOTRANSPIRATION	16.856	3695735.250	90.28
DRAINAGE COLLECTED FROM LAYER 3	0.0000	0.000	0.00
PERC./LEAKAGE THROUGH LAYER 5	0.000000	0.000	0.00
AVG. HEAD ON TOP OF LAYER 4	0.0000		
PERC./LEAKAGE THROUGH LAYER 6	0.000000	0.000	0.00
CHANGE IN WATER STORAGE	1.213	265855.094	6.49
SOIL WATER AT START OF YEAR	146.823	32191130.000	
SOIL WATER AT END OF YEAR	148.035	32456984.000	
SNOW WATER AT START OF YEAR	0.000	0.000	0.00
SNOW WATER AT END OF YEAR	0.000	0.000	0.00
ANNUAL WATER BUDGET BALANCE	0.0000	3.332	0.00

MONTHLY TOTALS (IN INCHES) FOR YEAR 3

	JAN/JUL	FEB/AUG	MAR/SEP	APR/OCT	MAY/NOV	JUN/DEC
PRECIPITATION	0.47 0.75	0.61 1.16	0.91 2.62	0.33 1.24	1.68 0.77	2.49 0.17
RUNOFF	0.000 0.000	0.000 0.000	0.000 0.006	0.000 0.000	0.000 0.000	0.033 0.000
EVAPOTRANSPIRATION	0.362 0.508	0.301 0.384	0.566 3.455	0.464 0.653	1.706 1.446	2.984 0.493
LATERAL DRAINAGE COLLECTED FROM LAYER 3	0.0000 0.0000	0.0000 0.0000	0.0000 0.0000	0.0000 0.0000	0.0000 0.0000	0.0000 0.0000
PERCOLATION/LEAKAGE THROUGH LAYER 5	0.0000 0.0000	0.0000 0.0000	0.0000 0.0000	0.0000 0.0000	0.0000 0.0000	0.0000 0.0000
PERCOLATION/LEAKAGE THROUGH LAYER 6	0.0000 0.0000	0.0000 0.0000	0.0000 0.0000	0.0000 0.0000	0.0000 0.0000	0.0000 0.0000

MONTHLY SUMMARIES FOR DAILY HEADS (INCHES)

AVERAGE DAILY HEAD ON TOP OF LAYER 4	0.000 0.000	0.000 0.000	0.000 0.000	0.000 0.000	0.000 0.000	0.000 0.000
STD. DEVIATION OF DAILY HEAD ON TOP OF LAYER 4	0.000 0.000	0.000 0.000	0.000 0.000	0.000 0.000	0.000 0.000	0.000 0.000

ANNUAL TOTALS FOR YEAR 3

	INCHES	CU. FEET	PERCENT
PRECIPITATION	13.20	2894126.750	100.00
RUNOFF	0.038	8427.326	0.29
EVAPOTRANSPIRATION	13.321	2920615.000	100.92

DRAINAGE COLLECTED FROM LAYER	3	0.0000	0.000	0.00
PERC./LEAKAGE THROUGH LAYER	5	0.000000	0.000	0.00
AVG. HEAD ON TOP OF LAYER	4	0.0000		
PERC./LEAKAGE THROUGH LAYER	6	0.000000	0.000	0.00
CHANGE IN WATER STORAGE		-0.159	-34917.191	-1.21
SOIL WATER AT START OF YEAR		148.035	32456984.000	
SOIL WATER AT END OF YEAR		147.876	32422068.000	
SNOW WATER AT START OF YEAR		0.000	0.000	0.00
SNOW WATER AT END OF YEAR		0.000	0.000	0.00
ANNUAL WATER BUDGET BALANCE		0.0000	1.503	0.00

MONTHLY TOTALS (IN INCHES) FOR YEAR 4

	JAN/JUL	FEB/AUG	MAR/SEP	APR/OCT	MAY/NOV	JUN/DEC
	-----	-----	-----	-----	-----	-----
PRECIPITATION	0.00	0.07	0.17	0.19	0.38	1.20
	3.02	2.72	1.04	3.38	0.35	0.36
RUNOFF	0.000	0.000	0.000	0.000	0.000	0.000
	0.145	0.008	0.000	0.120	0.000	0.000
EVAPOTRANSPIRATION	0.335	0.123	0.154	0.154	0.113	0.179
	2.326	2.739	0.993	2.314	1.566	0.565
LATERAL DRAINAGE COLLECTED FROM LAYER 3	0.0000	0.0000	0.0000	0.0000	0.0000	0.0000
	0.0000	0.0000	0.0000	0.0000	0.0000	0.0000
PERCOLATION/LEAKAGE THROUGH LAYER 5	0.0000	0.0000	0.0000	0.0000	0.0000	0.0000
	0.0000	0.0000	0.0000	0.0000	0.0000	0.0000
PERCOLATION/LEAKAGE THROUGH LAYER 6	0.0000	0.0000	0.0000	0.0000	0.0000	0.0000
	0.0000	0.0000	0.0000	0.0000	0.0000	0.0000

MONTHLY SUMMARIES FOR DAILY HEADS (INCHES)

AVERAGE DAILY HEAD ON	0.000	0.000	0.000	0.000	0.000	0.000
TOP OF LAYER 4	0.000	0.000	0.000	0.000	0.000	0.000
STD. DEVIATION OF DAILY	0.000	0.000	0.000	0.000	0.000	0.000
HEAD ON TOP OF LAYER 4	0.000	0.000	0.000	0.000	0.000	0.000

ANNUAL TOTALS FOR YEAR 4

	INCHES	CU. FEET	PERCENT
	-----	-----	-----
PRECIPITATION	12.88	2823965.750	100.00
RUNOFF	0.274	60083.098	2.13
EVAPOTRANSPIRATION	11.560	2534509.750	89.75
DRAINAGE COLLECTED FROM LAYER 3	0.0000	0.000	0.00
PERC./LEAKAGE THROUGH LAYER 5	0.000000	0.000	0.00
AVG. HEAD ON TOP OF LAYER 4	0.0000		
PERC./LEAKAGE THROUGH LAYER 6	0.000000	0.000	0.00
CHANGE IN WATER STORAGE	1.046	229375.547	8.12
SOIL WATER AT START OF YEAR	147.876	32422068.000	
SOIL WATER AT END OF YEAR	148.922	32651444.000	
SNOW WATER AT START OF YEAR	0.000	0.000	0.00
SNOW WATER AT END OF YEAR	0.000	0.000	0.00
ANNUAL WATER BUDGET BALANCE	0.0000	-2.574	0.00

MONTHLY TOTALS (IN INCHES) FOR YEAR 5

	JAN/JUL	FEB/AUG	MAR/SEP	APR/OCT	MAY/NOV	JUN/DEC
PRECIPITATION	0.27 1.40	0.68 1.86	0.78 1.82	1.73 3.13	0.97 0.00	0.20 1.03
RUNOFF	0.000 0.000	0.000 0.000	0.000 0.021	0.024 0.001	0.000 0.000	0.000 0.000
EVAPOTRANSPIRATION	0.387 1.307	0.283 2.206	0.483 0.721	2.134 3.210	0.589 1.266	0.380 0.848
LATERAL DRAINAGE COLLECTED FROM LAYER 3	0.0000 0.0000	0.0000 0.0000	0.0000 0.0000	0.0000 0.0000	0.0000 0.0000	0.0000 0.0000
PERCOLATION/LEAKAGE THROUGH LAYER 5	0.0000 0.0000	0.0000 0.0000	0.0000 0.0000	0.0000 0.0000	0.0000 0.0000	0.0000 0.0000
PERCOLATION/LEAKAGE THROUGH LAYER 6	0.0000 0.0000	0.0000 0.0000	0.0000 0.0000	0.0000 0.0000	0.0000 0.0000	0.0000 0.0000

MONTHLY SUMMARIES FOR DAILY HEADS (INCHES)

AVERAGE DAILY HEAD ON TOP OF LAYER 4	0.000 0.000	0.000 0.000	0.000 0.000	0.000 0.000	0.000 0.000	0.000 0.000
STD. DEVIATION OF DAILY HEAD ON TOP OF LAYER 4	0.000 0.000	0.000 0.000	0.000 0.000	0.000 0.000	0.000 0.000	0.000 0.000

ANNUAL TOTALS FOR YEAR 5

	INCHES	CU. FEET	PERCENT
PRECIPITATION	13.87	3041026.000	100.00
RUNOFF	0.046	10019.410	0.33
EVAPOTRANSPIRATION	13.813	3028597.250	99.59

DRAINAGE COLLECTED FROM LAYER	3	0.0000	0.000	0.00
PERC./LEAKAGE THROUGH LAYER	5	0.000000	0.000	0.00
AVG. HEAD ON TOP OF LAYER	4	0.0000		
PERC./LEAKAGE THROUGH LAYER	6	0.000000	0.000	0.00
CHANGE IN WATER STORAGE		0.011	2408.774	0.08
SOIL WATER AT START OF YEAR		148.922	32651444.000	
SOIL WATER AT END OF YEAR		148.933	32653852.000	
SNOW WATER AT START OF YEAR		0.000	0.000	0.00
SNOW WATER AT END OF YEAR		0.000	0.000	0.00
ANNUAL WATER BUDGET BALANCE		0.0000	0.422	0.00

MONTHLY TOTALS (IN INCHES) FOR YEAR 6

	JAN/JUL	FEB/AUG	MAR/SEP	APR/OCT	MAY/NOV	JUN/DEC
	-----	-----	-----	-----	-----	-----
PRECIPITATION	0.03	0.62	0.94	0.00	1.03	0.44
	0.37	1.10	0.47	1.53	1.16	0.61
RUNOFF	0.000	0.000	0.000	0.000	0.000	0.000
	0.000	0.000	0.000	0.123	0.000	0.000
EVAPOTRANSPIRATION	0.352	0.290	0.282	0.231	0.825	0.545
	0.214	1.019	0.581	1.697	1.292	0.707
LATERAL DRAINAGE COLLECTED FROM LAYER 3	0.0000	0.0000	0.0000	0.0000	0.0000	0.0000
	0.0000	0.0000	0.0000	0.0000	0.0000	0.0000
PERCOLATION/LEAKAGE THROUGH LAYER 5	0.0000	0.0000	0.0000	0.0000	0.0000	0.0000
	0.0000	0.0000	0.0000	0.0000	0.0000	0.0000
PERCOLATION/LEAKAGE THROUGH LAYER 6	0.0000	0.0000	0.0000	0.0000	0.0000	0.0000
	0.0000	0.0000	0.0000	0.0000	0.0000	0.0000

MONTHLY SUMMARIES FOR DAILY HEADS (INCHES)

AVERAGE DAILY HEAD ON	0.000	0.000	0.000	0.000	0.000	0.000
TOP OF LAYER 4	0.000	0.000	0.000	0.000	0.000	0.000
STD. DEVIATION OF DAILY	0.000	0.000	0.000	0.000	0.000	0.000
HEAD ON TOP OF LAYER 4	0.000	0.000	0.000	0.000	0.000	0.000

ANNUAL TOTALS FOR YEAR 6

	INCHES	CU. FEET	PERCENT
	-----	-----	-----
PRECIPITATION	8.30	1819791.870	100.00
RUNOFF	0.123	26970.953	1.48
EVAPOTRANSPIRATION	8.035	1761621.870	96.80
DRAINAGE COLLECTED FROM LAYER 3	0.0000	0.000	0.00
PERC./LEAKAGE THROUGH LAYER 5	0.000000	0.000	0.00
AVG. HEAD ON TOP OF LAYER 4	0.0000		
PERC./LEAKAGE THROUGH LAYER 6	0.000000	0.000	0.00
CHANGE IN WATER STORAGE	0.142	31200.320	1.71
SOIL WATER AT START OF YEAR	148.933	32653852.000	
SOIL WATER AT END OF YEAR	149.075	32685052.000	
SNOW WATER AT START OF YEAR	0.000	0.000	0.00
SNOW WATER AT END OF YEAR	0.000	0.000	0.00
ANNUAL WATER BUDGET BALANCE	0.0000	-1.253	0.00

MONTHLY TOTALS (IN INCHES) FOR YEAR 7

	JAN/JUL	FEB/AUG	MAR/SEP	APR/OCT	MAY/NOV	JUN/DEC
	-----	-----	-----	-----	-----	-----
PRECIPITATION	1.10	0.15	0.13	0.23	0.66	0.69
	0.71	2.96	0.64	0.12	1.89	0.50
RUNOFF	0.000	0.000	0.000	0.000	0.000	0.000
	0.000	0.008	0.000	0.000	0.003	0.000
EVAPOTRANSPIRATION	0.617	0.383	0.279	0.238	0.227	1.300
	0.708	2.287	0.558	0.391	1.061	1.523
LATERAL DRAINAGE COLLECTED FROM LAYER 3	0.0000	0.0000	0.0000	0.0000	0.0000	0.0000
	0.0000	0.0000	0.0000	0.0000	0.0000	0.0000
PERCOLATION/LEAKAGE THROUGH LAYER 5	0.0000	0.0000	0.0000	0.0000	0.0000	0.0000
	0.0000	0.0000	0.0000	0.0000	0.0000	0.0000
PERCOLATION/LEAKAGE THROUGH LAYER 6	0.0000	0.0000	0.0000	0.0000	0.0000	0.0000
	0.0000	0.0000	0.0000	0.0000	0.0000	0.0000

MONTHLY SUMMARIES FOR DAILY HEADS (INCHES)

AVERAGE DAILY HEAD ON TOP OF LAYER 4	0.000	0.000	0.000	0.000	0.000	0.000
	0.000	0.000	0.000	0.000	0.000	0.000
STD. DEVIATION OF DAILY HEAD ON TOP OF LAYER 4	0.000	0.000	0.000	0.000	0.000	0.000
	0.000	0.000	0.000	0.000	0.000	0.000

ANNUAL TOTALS FOR YEAR 7

	INCHES	CU. FEET	PERCENT
	-----	-----	-----
PRECIPITATION	9.78	2144285.250	100.00
RUNOFF	0.010	2200.263	0.10
EVAPOTRANSPIRATION	9.572	2098725.750	97.88

DRAINAGE COLLECTED FROM LAYER	3	0.0000	0.000	0.00
PERC./LEAKAGE THROUGH LAYER	5	0.000000	0.000	0.00
AVG. HEAD ON TOP OF LAYER	4	0.0000		
PERC./LEAKAGE THROUGH LAYER	6	0.000000	0.000	0.00
CHANGE IN WATER STORAGE		0.198	43357.937	2.02
SOIL WATER AT START OF YEAR		149.075	32685052.000	
SOIL WATER AT END OF YEAR		149.273	32728410.000	
SNOW WATER AT START OF YEAR		0.000	0.000	0.00
SNOW WATER AT END OF YEAR		0.000	0.000	0.00
ANNUAL WATER BUDGET BALANCE		0.0000	1.090	0.00

MONTHLY TOTALS (IN INCHES) FOR YEAR 8

	JAN/JUL	FEB/AUG	MAR/SEP	APR/OCT	MAY/NOV	JUN/DEC
	-----	-----	-----	-----	-----	-----
PRECIPITATION	0.42	0.09	0.00	0.22	0.40	2.78
	1.05	3.75	2.59	1.58	1.65	0.46
RUNOFF	0.000	0.000	0.000	0.000	0.000	0.000
	0.000	0.009	0.058	0.000	0.000	0.000
EVAPOTRANSPIRATION	0.504	0.342	0.298	0.255	0.222	1.875
	1.102	3.458	2.175	1.628	2.043	0.692
LATERAL DRAINAGE COLLECTED FROM LAYER 3	0.0000	0.0000	0.0000	0.0000	0.0000	0.0000
	0.0000	0.0000	0.0000	0.0000	0.0000	0.0000
PERCOLATION/LEAKAGE THROUGH LAYER 5	0.0000	0.0000	0.0000	0.0000	0.0000	0.0000
	0.0000	0.0000	0.0000	0.0000	0.0000	0.0000
PERCOLATION/LEAKAGE THROUGH LAYER 6	0.0000	0.0000	0.0000	0.0000	0.0000	0.0000
	0.0000	0.0000	0.0000	0.0000	0.0000	0.0000

MONTHLY SUMMARIES FOR DAILY HEADS (INCHES)

AVERAGE DAILY HEAD ON	0.000	0.000	0.000	0.000	0.000	0.000
TOP OF LAYER 4	0.000	0.000	0.000	0.000	0.000	0.000
STD. DEVIATION OF DAILY	0.000	0.000	0.000	0.000	0.000	0.000
HEAD ON TOP OF LAYER 4	0.000	0.000	0.000	0.000	0.000	0.000

ANNUAL TOTALS FOR YEAR 8

	INCHES	CU. FEET	PERCENT
	-----	-----	-----
PRECIPITATION	14.99	3286588.250	100.00
RUNOFF	0.067	14792.084	0.45
EVAPOTRANSPIRATION	14.595	3199945.500	97.36
DRAINAGE COLLECTED FROM LAYER 3	0.0000	0.000	0.00
PERC./LEAKAGE THROUGH LAYER 5	0.000000	0.000	0.00
AVG. HEAD ON TOP OF LAYER 4	0.0000		
PERC./LEAKAGE THROUGH LAYER 6	0.000000	0.000	0.00
CHANGE IN WATER STORAGE	0.328	71848.391	2.19
SOIL WATER AT START OF YEAR	149.273	32728410.000	
SOIL WATER AT END OF YEAR	149.601	32800258.000	
SNOW WATER AT START OF YEAR	0.000	0.000	0.00
SNOW WATER AT END OF YEAR	0.000	0.000	0.00
ANNUAL WATER BUDGET BALANCE	0.0000	2.014	0.00

MONTHLY TOTALS (IN INCHES) FOR YEAR 9

	JAN/JUL	FEB/AUG	MAR/SEP	APR/OCT	MAY/NOV	JUN/DEC
	-----	-----	-----	-----	-----	-----
PRECIPITATION	0.02	0.18	0.50	2.41	0.14	1.78
	0.34	3.97	0.48	2.01	0.52	0.12
RUNOFF	0.000	0.000	0.000	0.162	0.000	0.000
	0.000	0.209	0.000	0.011	0.000	0.000
EVAPOTRANSPIRATION	0.465	0.318	0.302	1.806	0.477	1.614
	0.510	3.069	0.816	1.801	0.569	0.484
LATERAL DRAINAGE COLLECTED FROM LAYER 3	0.0000	0.0000	0.0000	0.0000	0.0000	0.0000
	0.0000	0.0000	0.0000	0.0000	0.0000	0.0000
PERCOLATION/LEAKAGE THROUGH LAYER 5	0.0000	0.0000	0.0000	0.0000	0.0000	0.0000
	0.0000	0.0000	0.0000	0.0000	0.0000	0.0000
PERCOLATION/LEAKAGE THROUGH LAYER 6	0.0000	0.0000	0.0000	0.0000	0.0000	0.0000
	0.0000	0.0000	0.0000	0.0000	0.0000	0.0000

MONTHLY SUMMARIES FOR DAILY HEADS (INCHES)

AVERAGE DAILY HEAD ON TOP OF LAYER 4	0.000	0.000	0.000	0.000	0.000	0.000
	0.000	0.000	0.000	0.000	0.000	0.000
STD. DEVIATION OF DAILY HEAD ON TOP OF LAYER 4	0.000	0.000	0.000	0.000	0.000	0.000
	0.000	0.000	0.000	0.000	0.000	0.000

ANNUAL TOTALS FOR YEAR 9

	INCHES	CU. FEET	PERCENT
	-----	-----	-----
PRECIPITATION	12.47	2734072.500	100.00
RUNOFF	0.382	83788.273	3.06
EVAPOTRANSPIRATION	12.231	2681754.000	98.09

DRAINAGE COLLECTED FROM LAYER	3	0.0000	0.000	0.00
PERC./LEAKAGE THROUGH LAYER	5	0.000000	0.000	0.00
AVG. HEAD ON TOP OF LAYER	4	0.0000		
PERC./LEAKAGE THROUGH LAYER	6	0.000000	0.000	0.00
CHANGE IN WATER STORAGE		-0.144	-31467.961	-1.15
SOIL WATER AT START OF YEAR		149.601	32800258.000	
SOIL WATER AT END OF YEAR		149.457	32768790.000	
SNOW WATER AT START OF YEAR		0.000	0.000	0.00
SNOW WATER AT END OF YEAR		0.000	0.000	0.00
ANNUAL WATER BUDGET BALANCE		0.0000	-1.817	0.00

MONTHLY TOTALS (IN INCHES) FOR YEAR 10

	JAN/JUL	FEB/AUG	MAR/SEP	APR/OCT	MAY/NOV	JUN/DEC
	-----	-----	-----	-----	-----	-----
PRECIPITATION	0.00	0.02	0.24	1.82	0.98	0.00
	1.73	3.20	0.57	5.06	0.00	0.30
RUNOFF	0.000	0.000	0.000	0.025	0.000	0.000
	0.011	0.001	0.000	0.636	0.000	0.000
EVAPOTRANSPIRATION	0.253	0.269	0.251	0.830	0.850	0.415
	1.364	2.704	1.461	1.783	0.967	0.617
LATERAL DRAINAGE COLLECTED FROM LAYER 3	0.0000	0.0000	0.0000	0.0000	0.0000	0.0000
	0.0000	0.0000	0.0000	0.0000	0.0000	0.0000
PERCOLATION/LEAKAGE THROUGH LAYER 5	0.0000	0.0000	0.0000	0.0000	0.0000	0.0000
	0.0000	0.0000	0.0000	0.0000	0.0000	0.0000
PERCOLATION/LEAKAGE THROUGH LAYER 6	0.0000	0.0000	0.0000	0.0000	0.0000	0.0000
	0.0000	0.0000	0.0000	0.0000	0.0000	0.0000

MONTHLY SUMMARIES FOR DAILY HEADS (INCHES)

AVERAGE DAILY HEAD ON	0.000	0.000	0.000	0.000	0.000	0.000
TOP OF LAYER 4	0.000	0.000	0.000	0.000	0.000	0.000
STD. DEVIATION OF DAILY	0.000	0.000	0.000	0.000	0.000	0.000
HEAD ON TOP OF LAYER 4	0.000	0.000	0.000	0.000	0.000	0.000

ANNUAL TOTALS FOR YEAR 10

	INCHES	CU. FEET	PERCENT
	-----	-----	-----
PRECIPITATION	13.92	3051987.750	100.00
RUNOFF	0.672	147431.953	4.83
EVAPOTRANSPIRATION	11.764	2579295.750	84.51
DRAINAGE COLLECTED FROM LAYER 3	0.0000	0.000	0.00
PERC./LEAKAGE THROUGH LAYER 5	0.000000	0.000	0.00
AVG. HEAD ON TOP OF LAYER 4	0.0000		
PERC./LEAKAGE THROUGH LAYER 6	0.000000	0.000	0.00
CHANGE IN WATER STORAGE	1.484	325261.500	10.66
SOIL WATER AT START OF YEAR	149.457	32768790.000	
SOIL WATER AT END OF YEAR	150.941	33094052.000	
SNOW WATER AT START OF YEAR	0.000	0.000	0.00
SNOW WATER AT END OF YEAR	0.000	0.000	0.00
ANNUAL WATER BUDGET BALANCE	0.0000	-1.581	0.00

 AVERAGES OF MONTHLY AVERAGED DAILY HEADS (INCHES)

DAILY AVERAGE HEAD ON TOP OF LAYER 4

AVERAGES	0.0000	0.0000	0.0000	0.0000	0.0000	0.0000
	0.0000	0.0000	0.0000	0.0000	0.0000	0.0000

STD. DEVIATIONS	0.0000	0.0000	0.0000	0.0000	0.0000	0.0000
	0.0000	0.0000	0.0000	0.0000	0.0000	0.0000

AVERAGE ANNUAL TOTALS & (STD. DEVIATIONS) FOR YEARS 1 THROUGH 10

	INCHES		CU. FEET	PERCENT
	-----		-----	-----
PRECIPITATION	12.91 (2.877)		2829666.5	100.00
RUNOFF	0.221 (0.2512)		48555.49	1.716
EVAPOTRANSPIRATION	12.224 (2.5613)		2680101.00	94.714
LATERAL DRAINAGE COLLECTED FROM LAYER 3	0.00000 (0.00000)		0.000	0.00000
PERCOLATION/LEAKAGE THROUGH LAYER 5	0.00000 (0.00000)		0.000	0.00000
AVERAGE HEAD ON TOP OF LAYER 4	0.000 (0.000)			
PERCOLATION/LEAKAGE THROUGH LAYER 6	0.00000 (0.00000)		0.000	0.00000
CHANGE IN WATER STORAGE	0.461 (0.5864)		101009.95	3.570

PEAK DAILY VALUES FOR YEARS 1 THROUGH 10		
	(INCHES)	(CU. FT.)
PRECIPITATION	1.97	431926.469
RUNOFF	0.383	83915.4297
DRAINAGE COLLECTED FROM LAYER 3	0.00000	0.00000
PERCOLATION/LEAKAGE THROUGH LAYER 5	0.000000	0.00000
AVERAGE HEAD ON TOP OF LAYER 4	0.000	
MAXIMUM HEAD ON TOP OF LAYER 4	0.000	
LOCATION OF MAXIMUM HEAD IN LAYER 3 (DISTANCE FROM DRAIN)	0.0 FEET	
PERCOLATION/LEAKAGE THROUGH LAYER 6	0.000000	0.00000
SNOW WATER	0.58	127235.2270
MAXIMUM VEG. SOIL WATER (VOL/VOL)		0.3289
MINIMUM VEG. SOIL WATER (VOL/VOL)		0.0823

*** Maximum heads are computed using McEnroe's equations. ***

Reference: Maximum Saturated Depth over Landfill Liner
by Bruce M. McEnroe, University of Kansas
ASCE Journal of Environmental Engineering
Vol. 119, No. 2, March 1993, pp. 262-270.

FINAL WATER STORAGE AT END OF YEAR 10

LAYER	(INCHES)	(VOL/VOL)
1	1.0564	0.0880
2	146.2910	0.1355
3	2.7392	0.1141
4	0.0000	0.0000
5	0.1875	0.7500
6	0.6666	0.1111
SNOW WATER	0.000	

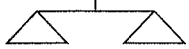
**APPLICATION FOR PERMIT RENEWAL AND MODIFICATION
SANDOVAL COUNTY LANDFILL**

**VOLUME III: LANDFILL ENGINEERING CALCULATIONS
SECTION 10: HELP MODEL**

**ATTACHMENT III.10.B
SUMMARY OF GEOTECHNICAL SOIL TEST DATA**

ATTACHMENT 1
SUMMARY OF GEOTECHNICAL TEST RESULTS
SANDOVAL COUNTY LANDFILL

Sample Number	Sample Depth (fbgs)	USCS Class	Grain Size Distribution			Uniformity Coefficient	Natural Moisture (%)	Standard Proctor		Permeability (cm/sec)
			Pass #10 (%)	Pass #40 (%)	Pass #200 (%)			Max. Dry Density (PCF)	Optimum Moisture (%)	
BH-1	10	SP	88.5	77.6	4.7	3.05	2.5			
BH-1	20	SP-SM	95.5	80.9	7.4	3.04	3.9			
BH-1	35	SP-SM	99.3	91.3	5.4	2.61	4.0			
BH-1	40	SP	98.8	92.2	3.7	2.38	2.6			
BH-2	10	SP-SM	99.9	94.0	9.4	3.17	2.8			
BH-2	20	SP								9.88 E-06
BH-2	25	SP	99.6	95.6	2.6	1.90	3.7			
BH-2	30	SP	99.7	92.4	1.5	1.87	3.5			
BH-2	40	SP	99.7	92.1	1.9	1.85	3.4			
BH-2	40-45	SP						126.3	12.5	
BH-3	10	SP	97.5	89.4	1.6	1.84	2.5			
BH-3	15	SP								2.48 E-06
BH-3	20	SP	91.9	81.9	1.4	1.90	6.8			
BH-3	30	SP	99.1	90.6	1.0	1.80	3.5			
BH-3	35	SP	97.0	72.4	0.6	1.96	3.0			
BH-3	40-45	SP						129.7	10.5	
BH-4	10	SP	96.8	91.9	2.0	1.82	3.4			
BH-4	15	SP	99.8	95.8	1.4	1.79	3.7			
BH-4	20	SP	99.7	93.8	1.5	1.80	4.9			
BH-4	40	SP	99.2	95.2	1.0	1.77	2.8			
BH-5	10	SP	95.6	87.4	0.9	1.83	3.1			
BH-5	20	SP	99.0	95.3	2.0	1.79	2.7			
BH-5	30	SP	98.5	84.8	0.4	1.82	3.0			
BH-5	35	SP	99.9	92.5	0.4	1.77	3.9			
BH-5	40-45	SP						130.6	12.8	
Stockpile		SP	76.9	45.6	0.2	3.34				2.45 E-07



DATE 01 08 15
CLIENT GORDON ENVIRONMENTAL
PROJECT Sandoval County LF

PERMIT
CONTRACT 211.14.03/01
JOB PSL: CELL 4-C
FILE 1543002

GORDON ENVIRONMENTAL, INC
213 South Camino Del Pueblo
Bernalillo, New Mexico 87004

ATTENTION: K. Gordon, PE
M. Heinsteins, PE

HYDRAULIC CONDUCTIVITY of GRANULAR SOILS
(Falling Head)

Specimen ID

Reference Reports:
1434 001

Orange-Brown SAND

CLASSIFICATION: USCS
Tested at: 101.3 lbs/ft³

% Passing # 200 Sieve :ASTM C 136

% Retained on 3/4" Sieve 0.0%

Maximum Dry Density 121.7 lbs/ft³

Optimum Moisture 8.9% of Dry Weight

% Compaction of Maximum Density 83.2%, Hydrated w/ deAired, distilled H₂O

COEFFICIENT OF PERMEABILITY, cm/sec: K 3.33×10^{-4}

Corrected Coefficient PERMEABILITY, cm/sec: K 3.16×10^{-4}
20°

ACSPOB 1015
BERNALILLO NM 87004

505-867-6585

Laboratory & Field Testing Services

ACNM-NMSHTD & NICET Certified

DATE 01 08 15

CLIENT GORDON ENVIRONMENTAL
PROJECT Sandoval County LF

PERMIT

CONTRACT 211.14.03/01

JOB PSL

FILE 1534001

GORDON ENVIRONMENTAL, INC
213 South Camino Del Pueblo
Bernalillo, New Mexico 87004ATTENTION: K. Gordon, PE
M. Heinstein, PEHYDRAULIC CONDUCTIVITY of GRANULAR SOILS
(Falling Head)

Specimen ID

Reference Reports:

1434 074

Light Brown SAND

CLASSIFICATION:

USCS

Tested at:

97.8 lbs/ft³

% Passing # 200 Sieve :ASTM C 136

% Retained on 3/4" Sieve

0.0%

maximum Dry Density

113.9 lbs/ft³

Optimum Moisture

11.6% of Dry Weight

% Compaction of Maximum Density

85.9%, Hydrated w/ deAired, distilled H₂O

COEFFICIENT OF PERMEABILITY, cm/sec: K

8.90 X 10⁻⁴

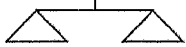
Corrected Coefficient PERMEABILITY, cm/sec: K

9.77 X 10⁻⁴

20°

ACSPOB 1015
BERNALILLO NM 87004

505-867-6585



Laboratory & Field Testing Services

ACNM-NMSHTD & NICET Certified

DATE 06 30 14
CLIENT GORDON ENVIRONMENTAL
PROJECT Sandoval County LFPERMIT
CONTRACT 211.147.03
JOB PSL
FILE 1434021GORDON ENVIRONMENTAL, INC
213 South Camino Del Pueblo
Bernalillo, New Mexico 87004ATTENTION: K. Gordon, PE
M. Heinstein, PEHYDRAULIC CONDUCTIVITY of GRANULAR SOILS
(Falling Head)

Specimen ID	Moist: Source A
Reference Reports:	Orange-Tan SAND,
1434 001	With Silt, Trace Gravel
1434 003	CLASSIFICATION: USCS
	Tested at: 99.6 lbs/ft ³

% Passing # 200 Sieve :ASTM C 136	8.1%
% Retained on 3/4" Sieve	0.0%
Maximum Dry Density	121.7 lbs/ft ³
Optimum Moisture	8.9% of Dry Weight
% Compaction of Maximum Density	81.8%, Hydrated w/ deAired, distilled H2O
COEFFICIENT OF PERMEABILITY, cm/sec: K	1.04×10^{-3}
Corrected Coefficient PERMEABILITY, cm/sec: K	8.97×10^{-4}

**APPLICATION FOR PERMIT RENEWAL AND MODIFICATION
SANDOVAL COUNTY LANDFILL**

**VOLUME III: LANDFILL ENGINEERING CALCULATIONS
SECTION 10: HELP MODEL**

ATTACHMENT III.10.C

HELP MODEL GUIDANCE DOCUMENT (NMED SWB, 1998)

Guidance Document

for

Performance Demonstration for an Alternate Cover Design
under Section 502.A.2 of the New Mexico
Solid Waste Management Regulations (20 NMAC 9.1)
Using HELP Modeling

and

Performance Demonstration for an Alternate Liner Design
under Section 306.A.2 of the New Mexico
Solid Waste Management Regulations (20 NMAC 9.1)
Using HELP Modeling

This document is for guidance only and is subject to change. However, any deviations from this document must be fully justified to the satisfaction of the Department.

Prepared by the
New Mexico Environment Department
Solid Waste Bureau
Permit Section
April 1, 1998

**Performance Demonstration for an Alternative Cover Design
under Section 502.A.2 of the New Mexico
Solid Waste Management Regulations (20 NMAC 9.1)
Using HELP Modeling**

1. Existing Solid Waste Landfills without a Liner System:

A prescriptive landfill cover system must, in accordance with Section 502.A.1, consist of an infiltration layer comprised of a minimum of 18 inches of earthen material with the required hydraulic conductivity (K) and a minimum of 6 inches of soil that is capable of sustaining native plant growth as an erosion layer (Figure 1). The cover component of 18 inches of earthen material must be equivalent to the least hydraulically conductive natural subsoils or a saturated hydraulic conductivity of no greater than 1×10^{-5} cm/sec. For example, if the hydraulic conductivity of the natural subsoils is 5×10^{-6} cm/sec, then the K of the infiltration layer material must be equivalent to these soils. *However, this example is for modeling purposes only. If the K of the underlying subsoils is less than 1×10^{-5} cm/sec (e.g., 5×10^{-6} cm/sec), then an alternative cover design must be proposed since 1×10^{-5} cm/sec is the lowest acceptable actual K for soils used in covers due to desiccation and root penetration (see example below).* If the hydraulic conductivity of the natural subsoils is greater than 1×10^{-5} cm/sec (e.g., 1×10^{-4} cm/sec), the K of the infiltration layer material must equate to the 1×10^{-5} cm/sec requirement.

If the infiltration layer meets the minimum hydraulic conductivity of 1×10^{-5} cm/sec or that of the natural subsoils and the minimum 18 inch condition then a Hydrologic Evaluation of Landfill Performance (HELP) Model simulation is not required. If an alternative cover design is proposed, it must achieve an equivalent reduction in infiltration as the infiltration layer specified in Section 502.A.1.a. Therefore, a HELP Model simulation is required to demonstrate that the design of such a cover provides equivalent reduction in infiltration as the prescriptive cover design. If the natural subsoils have a hydraulic conductivity of less than 1×10^{-5} cm/sec (e.g., 5×10^{-6} cm/sec), then the cover must achieve equivalent reduction in infiltration as that of the prescriptive cover but with an 18 inch infiltration layer with a hydraulic conductivity of 5×10^{-6} cm/sec.

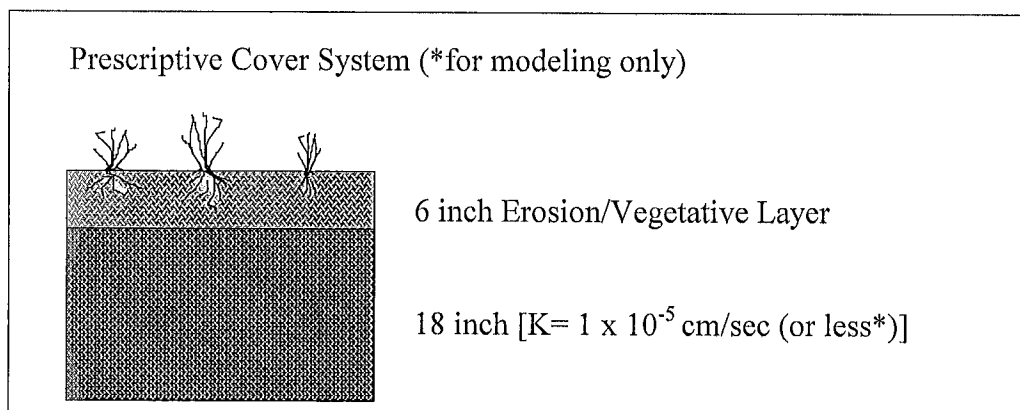


Figure 1. Prescriptive Cover System

A demonstration of equivalent reduction in infiltration is determined by using the EPA HELP Model. The HELP Model simulations need to compare the prescriptive cover and the alternative cover design (Figure 2). The simulation for the prescriptive cover must include the erosion, infiltration and intermediate cover layers. The alternative cover design simulation includes the intermediate and alternative cover layers. The two designs are to be simulated for years 1 through 5 with “poor” vegetation during the post-closure care period to demonstrate equivalency (Simulations #1 & #2). In New Mexico, it is assumed for a conservative value that the vegetation will be between “bare ground” and “fair vegetation” designated as “poor vegetation”. Precipitation (wettest 5 consecutive year period using Climatedata CD or NOAA data files: discs or manual entry), evapotranspiration, temperature (use values associated with wettest 5 consecutive years of precipitation), and solar radiation data must be site specific and identical for both alternative and prescriptive cover designs simulations. Provide justification for all input parameters in the model utilizing the attached forms. Indicate characteristics of on-site or other sources of soil proposed for the construction of cover and the parameter values in the model. It is anticipated that the entire area of the landfill or cell will be modeled. The Department recommends initializing the soil moisture content to be the value of the wilting point plus 25% of the difference between the wilting point and the field capacity [i.e., (field capacity - wilting point) x 0.25 + wilting point]. Other values deviating from this range may be used but must be fully justified. The leaf area index may be between 0.8 and 1.6 depending on the site location. The evaporative zone depth may be between 18” and 28” depending on the site location.

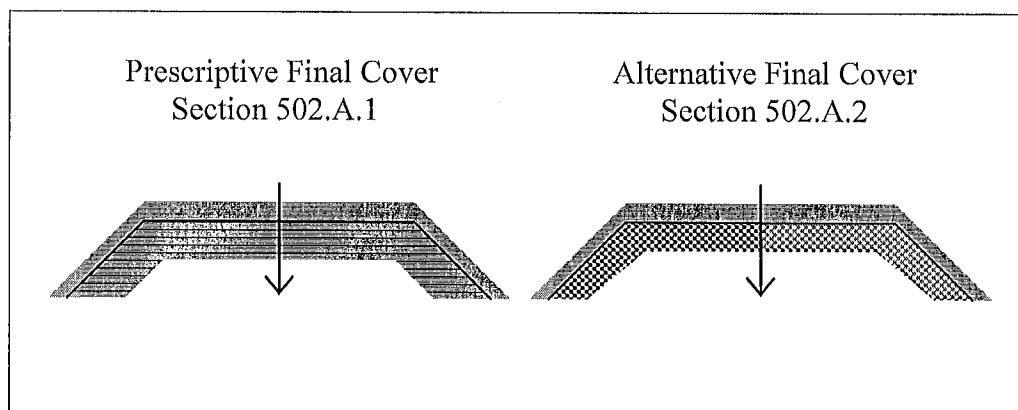


Figure 2

For example, comparing the prescriptive cover of:

- 1) 6 inches of topsoil
- 2) 18 inches of compacted soil ($K = 5 \times 10^{-6}$ cm/sec* - to meet natural subsoils $K = 5 \times 10^{-6}$)
- 3) Intermediate cover layer (optional* for modeling purposes) [*unless an intermediate cover layer is used for modeling purposes with a proposed alternative cover system (see below), then an intermediate cover layer must be used for modeling purposes]

with a proposed alternative cover system of:

- 1) 6 inches of topsoil
- 2) 30 inches of compacted ($K = 1 \times 10^{-5}$ cm/sec*)
- 3) Intermediate cover layer (optional for modeling purposes)

* $K = 5 \times 10^{-6}$ cm/sec is for modeling purposes only since 1×10^{-5} cm/sec is the lowest acceptable actual K for soils used in covers. Even if soils with $K = 5 \times 10^{-6}$ cm/sec are available for use in the cover, over time the K will increase to 1×10^{-5} cm/sec due to desiccation and root penetration.

Input Parameters for HELP Simulation #1 (Prescriptive Cover)

Weather data

City/State: The weather data should be from the nearest reporting station that has at least 40 years of data.

Latitude: The latitude must be specific for the site to use in synthesizing solar radiation data.

Evaporative zone depth: 18" to 28" corresponding with "poor" vegetation (see EPA Engineering Documentation for Version 3, Figure 5 - e.g., Clovis would be 20"; Santa Fe and Roswell would be 24"; Las Cruces, Albuquerque, and Farmington would be 28")

Maximum leaf area index: 0.8 to 1.6 corresponding with "poor" vegetation (see EPA Engineering Documentation for Version 3, Figure 3 - e.g., Clovis would be 1.6; Santa Fe and Roswell would be 1.2; Farmington would be 1.0; Las Cruces and Albuquerque would be 0.8)

Growing season start and end day: from solar radiation data (default)

Average wind speed: from solar radiation data (default)

Relative humidity: from solar radiation data (default)

Precipitation: daily precipitation from the wettest 5 consecutive years for the appropriate weather reporting station

Temperature: daily* minimum and maximum temperatures corresponding with the wettest 5 consecutive years for the appropriate weather reporting station
(*may be monthly averages if manual entry is used)

Solar radiation data: synthetically generated using coefficients for the appropriate* default (HELP) weather reporting station (*should be the closest by distance or latitude - consult with the Department if the appropriate station is not obvious)

Landfill Cover Data

Type of vegetation: Type 2 for "poor"

SCS Runoff curve #: may be generated from HELP or user specified* (*must be justified)

% of area allowing runoff: 100%; “closed”

Surface area: entire disposal area of landfill

Soil and Design Data

Source of soil characteristics: geotechnical data should be obtained from the source material.

Number of layers: There should be a layer for each type of material used (or compacted v. non-compacted)

Layer Number: (There should be a justification sheet for each layer.)

Thickness: 6” of topsoil, 18” of infiltration layer, 12” of intermediate cover layer* [*optional for modeling purposes (unless an intermediate cover layer is used for modeling purposes with a proposed alternative cover system in Simulation #2, then an intermediate cover layer must be used for modeling purposes)]

Layer type: “1” vertical percolation layer for all cover materials

Soil texture: The texture # should approximate the geotechnical characteristics (see EPA HELP User’s Guide for Version 3, Table 4).

Total porosity: If the actual porosity is not known, then the default value may be used that most closely approximates the geotechnical characteristics.

Field capacity: If the actual field capacity is not known, then the default value may be used that most closely approximates the geotechnical characteristics.

Wilting point: If the actual wilting point is not known, then the default value may be used that most closely approximates the geotechnical characteristics.

Moisture content: The moisture content should be initialized to be the value of the wilting point plus 25% of the difference between the wilting point and the field capacity [i.e., (field capacity - wilting point) x 0.25 + wilting point].

Saturated hydraulic conductivity (K): The K of the infiltration layer must be the greatest actual value (unless greater than 1×10^{-5} cm/sec*) of the underlying soil [e.g., If the actual (two tested samples - different locations) K of the underlying soil = 1×10^{-6} cm/sec and 2×10^{-6} , then model 18” of 2×10^{-6} cm/sec for the infiltration layer; *If the K of the underlying soil = 5×10^{-5} cm/sec, then model 18” of 1×10^{-5} cm/sec].

Input Parameters for HELP Simulation #2 (Proposed Alternate Cover)

Weather data (must be the same as Simulation #1)

City/State: The weather data should be from the nearest reporting station that has at least 40 years of data.

Latitude: The latitude must be specific for the site to use in synthesizing solar radiation data.

Evaporative zone depth: 18" to 28" corresponding with "poor" vegetation (see EPA Engineering Documentation for Version 3, Figure 5 - e.g., Clovis would be 20"; Santa Fe and Roswell would be 24"; Las Cruces, Albuquerque, and Farmington would be 28")

Maximum leaf area index: 0.8 to 1.6 corresponding with "poor" vegetation (see EPA Engineering Documentation for Version 3, Figure 3 - e.g., Clovis would be 1.6; Santa Fe and Roswell would be 1.2; Farmington would be 1.0; Las Cruces and Albuquerque would be 0.8)

Growing season start and end day: from solar radiation data (default)

Average wind speed: from solar radiation data (default)

Relative humidity: from solar radiation data (default)

Precipitation: daily precipitation from the wettest 5 consecutive years for the appropriate weather reporting station

Temperature: daily* minimum and maximum temperatures corresponding with the wettest 5 consecutive years for the appropriate weather reporting station
(*may be monthly averages if manual entry is used)

Solar radiation data: synthetically generated using coefficients for the appropriate* default (HELP) weather reporting station (*should be the closest by distance or latitude - consult with the Department if the appropriate station is not obvious)

Landfill Cover Data

Type of vegetation: Type 2 for "poor"

SCS Runoff curve #: may be generated from HELP or user specified* (*must be justified)

% of area allowing runoff: 100%; "closed"

Surface area: entire disposal area of landfill

Soil and Design Data

Source of soil characteristics: geotechnical data should be obtained from the source material.

Number of layers: There should be a layer for each type of material used (or compacted v. non-compacted)

Layer Number: (There should be a justification sheet for each layer.)

Thickness: 6" of topsoil, 18" to proposed thickness of infiltration layer, 12" of intermediate cover layer* (*optional for modeling purposes)

Layer type: "1" vertical percolation layer for all* cover materials including GCLs used (*consult with the Department if a FML is proposed to be used in the cover)

Soil texture: The texture # should approximate the geotechnical characteristics (see EPA HELP User's Guide for Version 3, Table 4).

Total porosity: If the actual porosity is not known, then the default value may be used that most closely approximates the geotechnical characteristics.

Field capacity: If the actual field capacity is not known, then the default value may be used that most closely approximates the geotechnical characteristics.

Wilting point: If the actual wilting point is not known, then the default value may be used that most closely approximates the geotechnical characteristics.

Moisture content: The moisture content should be initialized to be the value of the wilting point plus 25% of the difference between the wilting point and the field capacity [i.e., (field capacity - wilting point) x 0.25 + wilting point].

Saturated hydraulic conductivity (K): The K must be tested for the actual value unless the K is less than 1×10^{-5} cm/sec* (e.g., If the tested K is 5×10^{-5} cm/sec, then model the proposed thickness of the infiltration layer at 5×10^{-5} cm/sec. However, if the tested K is 2×10^{-6} , the lowest value to be modeled would be 1×10^{-5} cm/sec). * 1×10^{-5} cm/sec is the lowest acceptable K for soils used in covers due to desiccation and root penetration; unless a GCL is proposed, then the actual K may be modeled for the GCL layer (i.e., 0.24" at 3×10^{-9} cm/sec).

2. New Solid Waste Landfills:

As in the above case, the cover for the proposed landfill with a prescriptive or alternative liner must achieve an equivalent protection as the liner. If an alternative final cover is proposed for the landfill, then a demonstration must be submitted to the Bureau for approval pursuant to Section 502.A. It must be determined by this demonstration that the proposed final cover design includes an infiltration layer that achieves an equivalent reduction in infiltration as the bottom liner (Figure 3). A HELP Model simulation comparison is acceptable for this demonstration for a 5 year period with vegetation. Precipitation (wettest 5 consecutive year period using Climatedata CD or NOAA data files: discs or manual entry), evapotranspiration, temperature (use values associated with wettest 5 consecutive years of precipitation), and solar radiation data must be site specific and identical for both liner and cover design simulations. Provide justification for all input parameters in the model utilizing the attached forms. Demonstrate the relationship of the characteristics of on-site or other sources of soil proposed for the construction of cover or liner and the parameter values in the model. It is anticipated that the entire area of the landfill or cell will be modeled. The Department recommends initializing the soil moisture content to be at least the value of the wilting point plus 25% of the difference between the wilting point and the field capacity [i.e., $(\text{field capacity} - \text{wilting point}) \times 0.25 + \text{wilting point}$]. Other values deviating from this range may be used but must be fully justified.

For example, the comparison must include a HELP Model simulation for the liner and the proposed final cover systems as below (see Simulations #4 & #3, respectively).

The simulation for an alternative liner system* could include:

- 1) the drainage/protective layer of the liner with leachate collection system,
- 2) the 60-mil HDPE FML,
- 3) the 0.25 inch ($K = 3 \times 10^{-9}$) GCL (geosynthetic clay liner),
- 4) the 6 inches of compacted in situ soil used as the prepared subgrade, and
- 5) with the solid waste cell open and no runoff.

*Any alternative liner system must meet the demonstration as described in the "Performance Demonstration For An Alternative Liner Design under Section 306.A.2 of the New Mexico Solid Waste Management Regulations (20 NMAC 9.1) Using HELP Modeling".

A liner system is compared with a HELP Model simulation for a proposed final cover:

- 1) 18 inches non-compacted material (6 inches of topsoil with poor grass and 12 inches of non-compacted soil),
- 2) the 0.25 inch GCL ($K = 3 \times 10^{-9}$),
- 3) 12 inches of intermediate cover (6 inches of compacted soil and 6 inches of non-compacted soil), and
- 4) with the solid waste cell closed and final placement of the cover to include runoff.

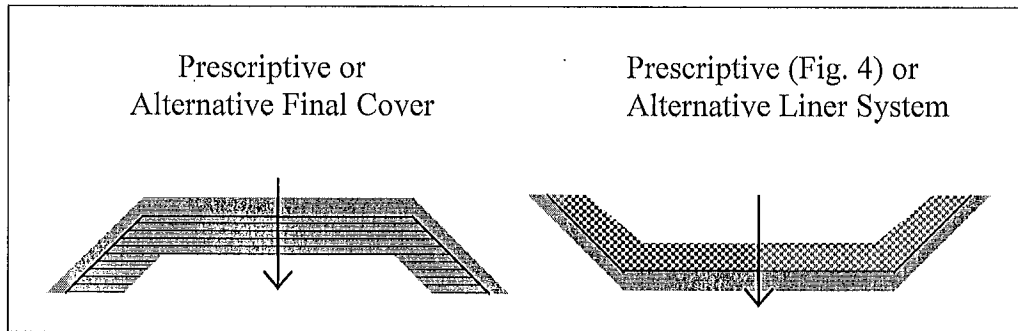


Figure 3

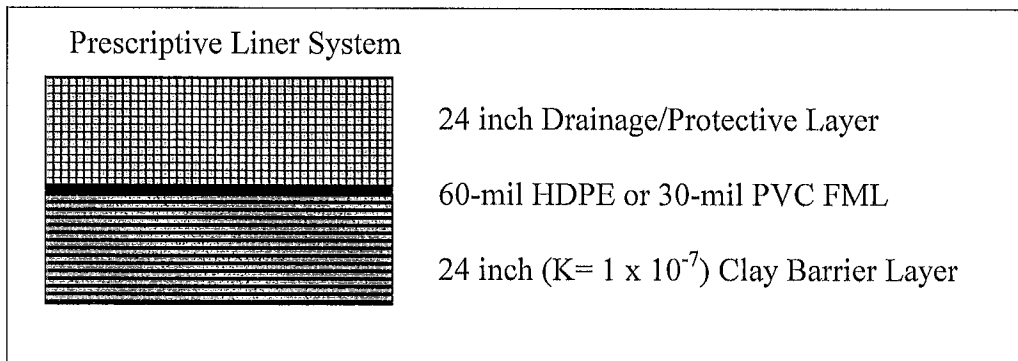


Figure 4

Input Parameters for HELP Simulation #3 (Proposed Alternate Cover)

Weather data

City/State: The weather data should be from the nearest reporting station that has at least 40 years of data.

Latitude: The latitude must be specific for the site to use in synthesizing solar radiation data.

Evaporative zone depth: 18" to 28" corresponding with "poor" vegetation (see EPA Engineering Documentation for Version 3, Figure 5 - e.g., Clovis would be 20"; Santa Fe and Roswell would be 24"; Las Cruces, Albuquerque, and Farmington would be 28")

Maximum leaf area index: 0.8 to 1.6 corresponding with "poor" vegetation (see EPA Engineering Documentation for Version 3, Figure 3 - e.g., Clovis would be 1.6; Santa Fe and Roswell would be 1.2; Farmington would be 1.0; Las Cruces and Albuquerque would be 0.8)

Growing season start and end day: from solar radiation data (default)

Average wind speed: from solar radiation data (default)

Relative humidity: from solar radiation data (default)

Precipitation: daily precipitation from the wettest 5 consecutive years for the appropriate weather reporting station

Temperature: daily* minimum and maximum temperatures corresponding with the wettest 5 consecutive years for the appropriate weather reporting station
(*may be monthly averages if manual entry is used)

Solar radiation data: synthetically generated using coefficients for the appropriate* default (HELP) weather reporting station (*should be the closest by distance or latitude - consult with the Department if the appropriate station is not obvious)

Landfill Cover Data

Type of vegetation: Type 2 for "poor"

SCS Runoff curve #: may be generated from HELP or user specified* (*must be justified)

% of area allowing runoff: 100%; "closed"

Surface area: entire disposal area of landfill or cell (leachate collection basin)

Soil and Design Data

Source of soil characteristics: geotechnical data should be obtained from the source material.

Number of layers: There should be a layer for each type of material used (or compacted v. non-compacted)

Layer Number: (There should be a justification sheet for each layer.)

Thickness: 6" of topsoil, Proposed thickness of infiltration layer or rooting medium or drainage layer, Possible GCL (0.24") or FML, subgrade thickness for GCL or FML (minimum of 6"), 12" of intermediate cover layer* (*optional for modeling purposes)

Layer type: Type "1" - vertical percolation layer for all* cover materials including GCLs used (*consult with the Department if a FML is proposed to be used in the cover)

Soil texture: The texture # should approximate the geotechnical characteristics (see EPA HELP User's Guide for Version 3, Table 4).

Total porosity: If the actual porosity is not known, then the default value may be used that most closely approximates the geotechnical characteristics.

Field capacity: If the actual field capacity is not known, then the default value may be used that most closely approximates the geotechnical characteristics.

Wilting point: If the actual wilting point is not known, then the default value may be used that most closely approximates the geotechnical characteristics.

Moisture content: The moisture content should be initialized to be the value of the wilting point plus 25% of the difference between the wilting point and the field capacity [i.e., (field capacity - wilting point) x 0.25 + wilting point].

Saturated hydraulic conductivity (K): The K must be tested for the actual value unless the K is less than 1×10^{-5} cm/sec* (e.g., If the tested K is 5×10^{-5} cm/sec, then model the proposed thickness of the infiltration layer at 5×10^{-5} cm/sec. However, if the tested K is 2×10^{-6} , the lowest value to be modeled would be 1×10^{-5} cm/sec). * 1×10^{-5} cm/sec is the lowest acceptable K for soils used in covers due to desiccation and root penetration; unless a GCL is proposed, then the actual K may be modeled for the GCL layer (i.e., 0.24" at 3×10^{-9} cm/sec).

Input Parameters for HELP Simulation #4 (Prescriptive Liner or Proposed Alternate Liner - Tier I)

Weather data (must be the same as Simulation #3)

City/State: The weather data should be from the nearest reporting station that has at least 40 years of data.

Latitude: The latitude must be specific for the site to use in synthesizing solar radiation data.

Evaporative zone depth: 12" to 18" corresponding with bare ground (see EPA Engineering Documentation for Version 3, Figure 5 - e.g., Santa Fe and Roswell would be 14"; Las Cruces, Albuquerque, and Farmington would be 18")

Maximum leaf area index: 0.0 corresponding with bare ground

Growing season start and end day: from solar radiation data (default)

Average wind speed: from solar radiation data (default)

Relative humidity: from solar radiation data (default)

Precipitation: daily precipitation from the wettest 5 consecutive years for the appropriate weather reporting station

Temperature: daily* minimum and maximum temperatures corresponding with the wettest 5 consecutive years for the appropriate weather reporting station
(*may be monthly averages if manual entry is used)

Solar radiation data: synthetically generated using coefficients for the appropriate* default (HELP) weather reporting station (*should be the closest by distance or latitude - consult with the Department if the appropriate station is not obvious)

Landfill Cover Data

Type of vegetation: Type 1 for "bare ground"

SCS Runoff curve #: may be generated from HELP or user specified* (*must be justified)

% of area allowing runoff: 0%; "open"

Surface area: entire disposal area of landfill or cell (leachate collection basin)

Soil and Design Data

Source of soil characteristics: geotechnical data should be obtained from the source material.

Number of layers: There should be a layer for each type of material used (or compacted v. non-compacted)

Layer Number: (There should be a justification sheet for each layer.)

Thickness: 24" of drainage/protection layer, possible geonet*, FML, 24" of 1×10^{-7} cm/sec clay barrier layer for prescriptive liner or GCL or other proposed thickness of clay barrier layer for an alternate liner. (*A demonstration that no more than one foot of head will be on the liner must be made for this simulation. Therefore, a geonet may be necessary if the 24" drainage layer material is incapable of transmitting leachate so 12" of head is not on the liner.)

Layer type: Type "2" for lateral drainage layer - slope (minimum of 2%) and drainage length must be designated (consult with the Department if leachate recirculation is proposed); Type "4" for geomembrane liners - geomembrane pinhole density of 1/acre, geomembrane installation defects of 4/acre and liner installation quality of "good"; Type "3" for barrier soil layers including GCLs (any soil layer underlying a geomembrane must be considered to be a barrier soil layer)

Soil texture: The texture # should approximate the geotechnical characteristics (see EPA HELP User's Guide for Version 3, Table 4).

Total porosity: If the actual porosity is not known, then the default value may be used that most closely approximates the geotechnical characteristics.

Field capacity: If the actual field capacity is not known, then the default value may be used that most closely approximates the geotechnical characteristics.

Wilting point: If the actual wilting point is not known, then the default value may be used that most closely approximates the geotechnical characteristics.

Moisture content: The moisture content should be initialized to be the value of the wilting point plus 25% of the difference between the wilting point and the field capacity [i.e., (field capacity - wilting point) \times 0.25 + wilting point].

Saturated hydraulic conductivity (K): For the 24" of drainage/protection layer use the tested K* for modeling the prescriptive liner design and for a proposed alternate liner design; for a possible geonet use the lowest value from the manufacture's specifications; for the FML use a K* value which is the greatest value from the manufacture's specifications; 24" of 1×10^{-7} cm/sec clay barrier layer for prescriptive liner or GCL (3×10^{-9} cm/sec) or other proposed soil barrier layer for an alternate liner. (*must be the same value in both Simulation #5 & #6)

**Performance Demonstration for an Alternate Liner Design
under Section 306.A.2 of the New Mexico
Solid Waste Management Regulations (20 NMAC 9.1)
Using HELP Modeling**

1. Permit applicants proposing an alternate liner in accordance with Section 306.A.2 must demonstrate the liner "... provides equivalent protection as the composite liner ... and ensures concentration values listed in Section 1110 will not be exceeded in the uppermost aquifer ... ". This requires that a two tier demonstration be made:

Tier 1 - the alternative liner provides equivalent protection, and

Tier 2 - the alternate liner ensures the uppermost aquifer will be protected.

The first tier of this demonstration may be satisfied through mathematical modeling using the EPA Hydrologic Evaluation of Landfill Performance (HELP) model. Two computer modeling analyses must be performed - (1) an analysis of the composite liner as specified in Section 306.A.1 and (2) an analysis of the proposed alternate liner as specified in Section 306.A.2. Each of these analyses must be performed under identical hydrologic and climatologic loading conditions of five years with no solid waste in the landfill (see Simulations #5 & 6). This time period is necessary to adequately evaluate the performance of the two liners. A successful demonstration of equivalent protection has been made when the analyses show equal or less percolation/leakage through the bottom layer of the proposed alternate liner than the percolation/leakage through the bottom layer of the Section 306.A.1 composite liner (Figure 5).

The second tier of the demonstration must include HELP modeling of the actual design conditions and the entire operational development of the landfill as closely as possible by doing a succession of model simulations which consider the factors in Section 306.A.2.a. To aid in accomplishing this, each successive computer simulation must use the previous simulation's moisture content output as the input for the following simulation (Figure 6). The modeling design method must be fully described. If no leakage is indicated at the end of the second simulation (#8) and subsequent simulations (#9 & #10) continue to indicate no leakage, then a successful demonstration has been made that the uppermost aquifer will be protected as required by Section 306.A.2 and it will not be necessary to perform a fate and transport modeling.

2. Justification for all input parameters in the HELP modeling must be provided utilizing the attached forms. Demonstrate the relationship of the characteristics of the soil proposed for the construction and operation of the landfill and the parameter values used in the model. Show justification for the soil and waste moisture content parameters as well as geomembrane liner data and storm water runoff fractions. The initial moisture content of the soil should be initialized by the use in the HELP model. The Department recommends initializing the soil moisture content to be the value of the wilting point plus 25% of the difference between the wilting point and the field capacity [i.e., (field capacity - wilting point) x 0.25 + wilting point]. Other values deviating from this range may be used but must be fully justified.

3(1) First Tier of the Demonstration

Two simulations must be made, one of the Section 306.A.1 specified liner and one of the proposed alternate liner, both using the same precipitation (wettest 5 consecutive year period using Climatedata or NOAA tapes), temperature (use values associated with 5 wettest consecutive years), solar radiation, and evapotranspiration data (see Simulations #5 & #6). Current historic NOAA weather data from the nearest representative weather station as published by the National Climatic Data Center in Asheville, North Carolina must be used for the precipitation and temperature files. Both simulations must be made for the landfill in the open condition with no run-off and a Leaf Area Index of zero. *Simulations:*

- #5 A simulation for the specified liner design must be performed using a 24 inch protective layer, a lateral drainage layer (which may be integral with the protective layer), an FML, and a 24 inch barrier layer of soil with a saturated hydraulic conductivity of 1×10^{-7} cm/sec. This simulation must be performed using no solid waste and for a five year period.
- #6 A simulation for the proposed alternate liner design must be performed using a 24 inch protective layer, a lateral drainage layer (which may be integral with the protective layer), and the other proposed liner layer (the bottom layer must be modeled as a barrier layer). This simulation must be performed using no solid waste and for a five year period.

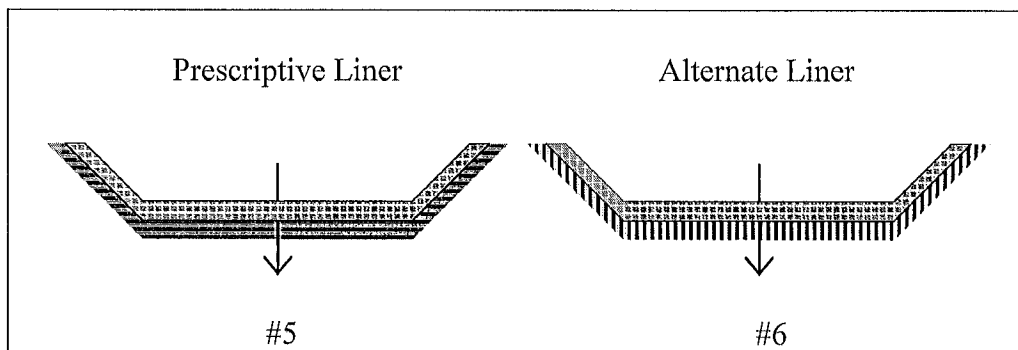


Figure 5

Compare the average annual percolation from the bottom layer of the two simulations. If the percolation is equivalent, a successful demonstration has been made for the first tier.

Input Parameters for HELP Simulation #5* (Prescriptive Liner - Tier I)

same as Simulation #4 with prescriptive liner design

Input Parameters for HELP Simulation #6* (Proposed Alternate Liner - Tier I)

same as Simulation #4 with proposed alternate liner design

*One of these simulations will also serve for the alternate cover design equivalency demonstration.

3(2) Second Tier of the Demonstration

Four simulations encompassing the entire life cycle of the facility to model actual design conditions and operational development as closely as possible must be performed (see Simulations #7, #8, #9 & #10). This is accomplished through a succession of four model simulations: one simulation of the open landfill, a second with the landfill partially filled with solid waste, a third with the landfill in the closed condition with bare ground, and a fourth with the landfill in the closed condition with “poor” vegetation. *Simulations:*

- #7 The initial simulation must model the open landfill at start-up when the landfill contains no solid waste. The time period should extend for the anticipated duration of this condition (a minimum of two years).
- #8 A succeeding simulation to model conditions of the partially filled landfill for a five year period*. This would incorporate daily and intermediate covers. (*This period may vary in accordance with anticipated operations.)
- #9 Model the landfill in the closed condition with bare ground (a minimum of a two years).
- #10 Finally, perform a simulation to model the landfill in the closed condition with poor vegetation for remainder of the post-closure care period (a minimum of 28 years).

If the simulations indicate no leakage after the third simulation (#9) and the subsequent simulation (#10), then the simulations have served to demonstrate the concentration values delineated in Section 1110 of the Regulations will not be exceeded in the uppermost aquifer at the relative point of compliance. Therefore, a successful demonstration has been made for the second tier.

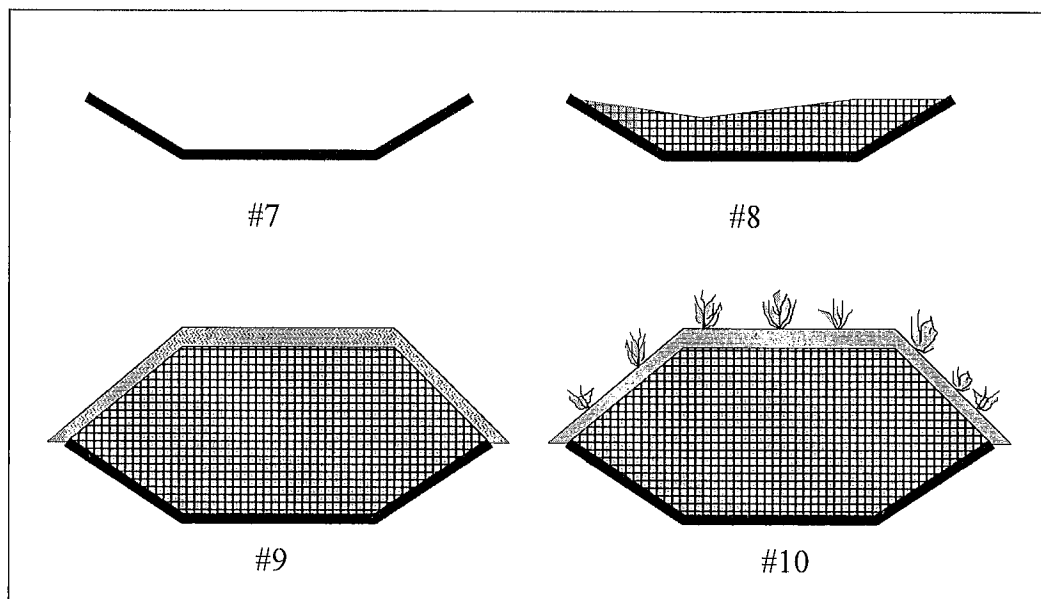


Figure 6

Input Parameters for HELP Simulation #7 (Proposed Alternate Liner - Tier II)

Weather data (must be the same as Simulation #3)

City/State: The weather data should be from the nearest reporting station that has at least 40 years of data.

Latitude: The latitude must be specific for the site to use in synthesizing solar radiation data.

Evaporative zone depth: 12" to 18" corresponding with bare ground (see EPA Engineering Documentation for Version 3, Figure 5 - e.g., Santa Fe and Roswell would be 14"; Las Cruces, Albuquerque, and Farmington would be 18")

Maximum leaf area index: 0.0 corresponding with bare ground

Growing season start and end day: from solar radiation data (default)

Average wind speed: from solar radiation data (default)

Relative humidity: from solar radiation data (default)

Precipitation: daily precipitation from 2 consecutive years for the appropriate weather reporting station

Temperature: daily* minimum and maximum temperatures corresponding with 2 consecutive years for the appropriate weather reporting station

(*may be monthly averages if manual entry is used)

Solar radiation data: synthetically generated using coefficients for the appropriate* default (HELP) weather reporting station (*should be the closest by distance or latitude - consult with the Department if the appropriate station is not obvious)

Landfill Cover Data

Type of vegetation: Type 1 for "bare ground"

SCS Runoff curve #: may be generated from HELP or user specified* (*must be justified)

% of area allowing runoff: 0%; "open"

Surface area: entire disposal area of landfill or cell (leachate collection basin)

Soil and Design Data

Source of soil characteristics: geotechnical data should be obtained from the source material.

Number of layers: There should be a layer for each type of material used (or compacted v. non-compacted)

Layer Number: (There should be a justification sheet for each layer.)

Thickness: 24" of drainage/protection layer, possible geonet, FML, 24" of 1×10^{-7} cm/sec clay barrier layer for prescriptive liner or GCL or other proposed thickness of clay barrier layer for an alternate liner.

Layer type: Type "2" for lateral drainage layer - slope (minimum of 2%) and drainage length must be designated (consult with the Department if leachate recirculation is proposed); Type "4" for geomembrane liners - geomembrane pinhole density of 1/acre, geomembrane installation defects of 4/acre and liner installation quality of "good"; Type "3" for barrier soil layers including GCLs (any soil layer underlying a geomembrane must be considered to be a barrier soil layer)

Soil texture: The texture # should approximate the geotechnical characteristics (see EPA HELP User's Guide for Version 3, Table 4).

Total porosity: If the actual porosity is not known, then the default value may be used that most closely approximates the geotechnical characteristics.

Field capacity: If the actual field capacity is not known, then the default value may be used that most closely approximates the geotechnical characteristics.

Wilting point: If the actual wilting point is not known, then the default value may be used that most closely approximates the geotechnical characteristics.

Moisture content: The moisture content should be initialized to be the value of the wilting point plus 25% of the difference between the wilting point and the field capacity [i.e., (field capacity - wilting point) \times 0.25 + wilting point].

Saturated hydraulic conductivity (K): For the 24" of drainage/protection layer use the tested K for modeling the proposed alternate liner design; for a possible geonet use the lowest value from the manufacture's specifications; for the FML use a K value which is the greatest value from the manufacture's specifications; GCL (3×10^{-9} cm/sec) or other proposed soil barrier layer for an alternate liner.

Input Parameters for HELP Simulation #8 (Proposed Alternate Liner - Tier II)

Weather data (must be the same as Simulation #3)

City/State: The weather data should be from the nearest reporting station that has at least 40 years of data.

Latitude: The latitude must be specific for the site to use in synthesizing solar radiation data.

Evaporative zone depth: 12" to 18" corresponding with bare ground (see EPA Engineering Documentation for Version 3, Figure 5 - e.g., Santa Fe and Roswell would be 14"; Las Cruces, Albuquerque, and Farmington would be 18")

Maximum leaf area index: 0.0 corresponding with bare ground

Growing season start and end day: from solar radiation data (default)

Average wind speed: from solar radiation data (default)

Relative humidity: from solar radiation data (default)

Precipitation: daily precipitation from 2 to 5* consecutive years for the appropriate weather reporting station (*may vary with landfill operations)

Temperature: daily* minimum and maximum temperatures corresponding with 2 to 5 years (same years as precipitation) for the appropriate weather reporting station
(*may be monthly averages if manual entry is used)

Solar radiation data: synthetically generated using coefficients for the appropriate* default (HELP) weather reporting station (*should be the closest by distance or latitude - consult with the Department if the appropriate station is not obvious)

Landfill Cover Data

Type of vegetation: bare ground

SCS Runoff curve #: may be generated from HELP or user specified* (*must be justified)

% of area allowing runoff: 0%; "open"

Surface area: entire disposal area of landfill or cell (leachate collection basin)

Soil and Design Data

Source of soil characteristics: geotechnical data should be obtained from the source material.

Number of layers: There should be a layer for each type of material used (or compacted v. non-compacted)

Layer Number: (There should be a justification sheet for each layer.)

Thickness: 240" of solid waste (this thickness may vary depending on landfill operations); 24" of drainage/protection layer; possible geonet*; FML; 24" of 1×10^{-7} cm/sec clay barrier layer for prescriptive liner or GCL or other proposed thickness of clay barrier layer for an alternate liner.

Layer type: Type "1", vertical percolation layer, must be used for solid waste. Type "2" for lateral drainage layer - slope (minimum of 2%) and drainage length must be designated (consult with the Department if leachate recirculation is proposed); Type "4" for geomembrane liners - geomembrane pinhole density of 1/acre, geomembrane installation defects of 4/acre and liner installation quality of "good"; Type "3" for barrier soil layers including GCLs (any soil layer underlying a geomembrane must be considered to be a barrier soil layer)

Soil texture: The texture # should approximate the geotechnical characteristics (see EPA HELP User's Guide for Version 3, Table 4).

Total porosity: If the actual porosity is not known, then the default value may be used that most closely approximates the geotechnical characteristics.

Field capacity: If the actual field capacity is not known, then the default value may be used that most closely approximates the geotechnical characteristics.

Wilting point: If the actual wilting point is not known, then the default value may be used that most closely approximates the geotechnical characteristics.

Moisture content: The moisture content must be initialized to be the value of the previous simulation's (from Simulation #7) moisture content output as the input for the following simulation (Simulation #8). For compacted municipal solid waste with a HELP soil texture number of "18" use 20%* by volume/volume (which is greater than per mass basis - see EPA HELP User's Guide for Version 3 for conversion) (*a lower value may be used if justified)

Saturated hydraulic conductivity (K): For compacted municipal solid waste with a HELP soil texture number of "18" will have a K of 1×10^{-3} cm/sec. For the 24" of drainage/protection layer use the tested K for modeling the proposed alternate liner design; for a possible geonet use the lowest value from the manufacture's specifications; for the FML use a K value which is the greatest value from the manufacture's specifications; GCL (3×10^{-9} cm/sec) or other proposed soil barrier layer for an alternate liner.

Input Parameters for HELP Simulation #9 (Proposed Alternate Liner - Tier II)

Weather data

City/State: The weather data should be from the nearest reporting station that has at least 40 years of data.

Latitude: The latitude must be specific for the site to use in synthesizing solar radiation data.

Evaporative zone depth: 12" to 18" corresponding with bare ground (see EPA Engineering Documentation for Version 3, Figure 5 - e.g., Santa Fe and Roswell would be 14"; Las Cruces, Albuquerque, and Farmington would be 18")

Maximum leaf area index: 0.0 corresponding with bare ground

Growing season start and end day: from solar radiation data (default)

Average wind speed: from solar radiation data (default)

Relative humidity: from solar radiation data (default)

Precipitation: daily precipitation from 2 consecutive years for the appropriate weather reporting station

Temperature: daily* minimum and maximum temperatures corresponding with 2 consecutive years for the appropriate weather reporting station
(*may be monthly averages if manual entry is used)

Solar radiation data: synthetically generated using coefficients for the appropriate* default (HELP) weather reporting station (*should be the closest by distance or latitude - consult with the Department if the appropriate station is not obvious)

Landfill Cover Data

Type of vegetation: Type 1 for "bare ground"

SCS Runoff curve #: may be generated from HELP or user specified* (*must be justified)

% of area allowing runoff: 100%; "closed"

Surface area: entire disposal area of landfill or cell (leachate collection basin)

Soil and Design Data

Source of soil characteristics: geotechnical data should be obtained from the source material.

Number of layers: There should be a layer for each type of material used (or compacted v. non-compacted)

Layer Number: (There should be a justification sheet for each layer.)

Thickness: 6" of topsoil, Proposed thickness of infiltration layer or rooting medium or drainage layer, Possible GCL (0.24") or FML, subgrade thickness for GCL or FML (minimum of 6"), 12" of intermediate cover layer* (*optional for modeling); Proposed thickness of solid waste (this thickness will vary depending on landfill design); 24" of drainage/protection layer; possible geonet*; FML; 24" of 1×10^{-7} cm/sec clay barrier layer for prescriptive liner or GCL or other proposed thickness of clay barrier layer for an alternate liner.

Layer type: Type "1" - vertical percolation layer for all* cover materials including GCLs used in the cover (*consult with the Department if a FML is proposed to be used in the cover). Type "1", vertical percolation layer, must be used for solid waste. Type "2" for lateral drainage layer - slope (minimum of 2%) and drainage length must be designated (consult with the Department if leachate recirculation is proposed); Type "4" for geomembrane liners - geomembrane pinhole density of 1/acre, geomembrane installation defects of 4/acre and liner installation quality of "good"; Type "3" for barrier soil layers including GCLs (any soil layer underlying a geomembrane must be considered to be a barrier soil layer)

Soil texture: The texture # should approximate the geotechnical characteristics (see EPA HELP User's Guide for Version 3, Table 4).

Total porosity: If the actual porosity is not known, then the default value may be used that most closely approximates the geotechnical characteristics.

Field capacity: If the actual field capacity is not known, then the default value may be used that most closely approximates the geotechnical characteristics.

Wilting point: If the actual wilting point is not known, then the default value may be used that most closely approximates the geotechnical characteristics.

Moisture content: The moisture content must be initialized to be the value of the previous simulation's (from Simulation #8) moisture content output as the input for the following simulation (Simulation #9).

Saturated hydraulic conductivity (K): The K must be tested for the actual value unless the K is less than 1×10^{-5} cm/sec* (e.g., If the tested K is 5×10^{-5} cm/sec, then model the proposed thickness of the infiltration layer at 5×10^{-5} cm/sec. However, if the tested K is 2×10^{-6} , the lowest value to be modeled would be 1×10^{-5} cm/sec). * 1×10^{-5} cm/sec is the lowest acceptable K for soils used in covers due to desiccation and root penetration; unless a GCL is proposed, then the actual K may be modeled for the GCL layer (i.e., 0.24" at 3×10^{-9} cm/sec). For compacted municipal solid waste with a HELP soil texture number of "18" will have a K of 1×10^{-3} cm/sec. For the 24" of drainage/protection layer use the tested K for modeling the proposed alternate liner design; for a possible geonet use the lowest value from the manufacture's specifications; for the FML use a K value which is the greatest value from the manufacture's specifications; GCL (3×10^{-9} cm/sec) or other proposed soil barrier layer for an alternate liner.

Input Parameters for HELP Simulation #10 (Proposed Alternate Liner - Tier II)

Weather data

City/State: The weather data should be from the nearest reporting station that has at least 40 years of data.

Latitude: The latitude must be specific for the site to use in synthesizing solar radiation data.

Evaporative zone depth: 18" to 28" corresponding with "poor" vegetation (see EPA Engineering Documentation for Version 3, Figure 5 - e.g., Clovis would be 20"; Santa Fe and Roswell would be 24"; Las Cruces, Albuquerque, and Farmington would be 28")

Maximum leaf area index: 0.8 to 1.6 corresponding with "poor" vegetation (see EPA Engineering Documentation for Version 3, Figure 3 - e.g., Clovis would be 1.6; Santa Fe and Roswell would be 1.2; Farmington would be 1.0; Las Cruces and Albuquerque would be 0.8)

Growing season start and end day: from solar radiation data (default)

Average wind speed: from solar radiation data (default)

Relative humidity: from solar radiation data (default)

Precipitation: daily precipitation from 28 consecutive years for the appropriate weather reporting station

Temperature: daily* minimum and maximum temperatures corresponding with 28 consecutive years for the appropriate weather reporting station
(*may be monthly averages if manual entry is used)

Solar radiation data: synthetically generated using coefficients for the appropriate* default (HELP) weather reporting station (*should be the closest by distance or latitude - consult with the Department if the appropriate station is not obvious)

Landfill Cover Data

Type of vegetation: Type 2 for "poor"

SCS Runoff curve #: may be generated from HELP or user specified* (*must be justified)

% of area allowing runoff: 100%; "closed"

Surface area: entire disposal area of landfill or cell (leachate collection basin)

Soil and Design Data

Source of soil characteristics: geotechnical data should be obtained from the source material.

Number of layers: There should be a layer for each type of material used (or compacted v. non-compacted)

Layer Number: (There should be a justification sheet for each layer.)

Thickness: 6" of topsoil, Proposed thickness of infiltration layer or rooting medium or drainage layer, Possible GCL (0.24") or FML, subgrade thickness for GCL or FML (minimum of 6"), 12" of intermediate cover layer* (*optional for modeling); Proposed thickness of solid waste (this thickness will vary depending on landfill design); 24" of drainage/protection layer; possible geonet*; FML; 24" of 1×10^{-7} cm/sec clay barrier layer for prescriptive liner or GCL or other proposed thickness of clay barrier layer for an alternate liner.

Layer type: Type "1" - vertical percolation layer for all* cover materials including GCLs used (*consult with the Department if a FML is proposed to be used in the cover). Type "1", vertical percolation layer, must be used for solid waste. Type "2" for lateral drainage layer - slope (minimum of 2%) and drainage length must be designated (consult with the Department if leachate recirculation is proposed); Type "4" for geomembrane liners - geomembrane pinhole density of 1/acre, geomembrane installation defects of 4/acre and liner installation quality of "good"; Type "3" for barrier soil layers including GCLs (any soil layer underlying a geomembrane must be considered to be a barrier soil layer)

Soil texture: The texture # should approximate the geotechnical characteristics (see EPA HELP User's Guide for Version 3, Table 4).

Total porosity: If the actual porosity is not known, then the default value may be used that most closely approximates the geotechnical characteristics.

Field capacity: If the actual field capacity is not known, then the default value may be used that most closely approximates the geotechnical characteristics.

Wilting point: If the actual wilting point is not known, then the default value may be used that most closely approximates the geotechnical characteristics.

Moisture content: The moisture content must be initialized to be the value of the previous simulation's (from Simulation #9) moisture content output as the input for the following simulation (Simulation #10).

Saturated hydraulic conductivity (K): The K must be tested for the actual value unless the K is less than 1×10^{-5} cm/sec* (e.g., If the tested K is 5×10^{-5} cm/sec, then model the proposed thickness of the infiltration layer at 5×10^{-5} cm/sec. However, if the tested K is 2×10^{-6} , the lowest value to be modeled would be 1×10^{-5} cm/sec). * 1×10^{-5} cm/sec is the lowest acceptable K for soils used in covers due to desiccation and root penetration; unless a GCL is proposed, then the actual K may be modeled for the GCL layer (i.e., 0.24" at 3×10^{-9} cm/sec). For compacted municipal solid waste with a HELP soil texture number of "18" will have a K of 1×10^{-3} cm/sec. For the 24" of drainage/protection layer use the tested K for modeling the proposed alternate liner design; for a possible geonet use the lowest value from the manufacture's specifications; for the FML use a K value which is the greatest value from the manufacture's specifications; GCL (3×10^{-9} cm/sec) or other proposed soil barrier layer for an alternate liner.

Equivalency Demonstrations

Typical “New” Landfill:

Alternate Cover Design Equivalency Demonstration (two simulations)

Simulation #3 & (either Simulation #5 or #6)

Average Annual Percolation from bottom layer of Simulation #3 must be less than or equal to (equivalent*) the Average Annual Percolation from the bottom layer of Simulation #5 or #6 (depending on the proposed liner design).

Alternate Liner Design Equivalency Demonstration

Tier I (two simulations) - Simulation #5 & Simulation #6

Average Annual Percolation from bottom layer of Simulation #6 must be less than or equal to (equivalent*) the Average Annual Percolation from the bottom layer of Simulation #5.

Tier II (four simulations) - Simulations #7, #8, #9, #10

Average Annual Percolation from bottom layer of Simulation #7 must decrease to zero for Simulations #9 & #10.

For closing an “old” (no liner system) landfill:

Alternate Cover Design Equivalency Demonstration (two simulations)

Simulation #1 & Simulation #2

Average Annual Percolation from bottom layer of Simulation #2 must be less than or equal to (equivalent*) the Average Annual Percolation from the bottom layer of Simulation #1

Submit hardcopies of all output files and submit all input files on 3.5” diskette.

*If the two Average Annual Percolation values are within 0.00001” of each other, then the demonstration is successful since these values are practically equal (the definition of equivalent) and well within modeling uncertainty.

**APPLICATION FOR PERMIT RENEWAL AND MODIFICATION
SANDOVAL COUNTY LANDFILL**

**VOLUME III: LANDFILL ENGINEERING CALCULATIONS
SECTION 10: HELP MODEL**

ATTACHMENT III.10.D

HELP MODEL INPUT AND OUTPUT FILES: CD-ROM